ISSN 1018-5593

European Commission

nuclear science and technology

Community's research and development programme on radioactive waste management and storage

Shared-cost action (1990-94)

Annual progress report, 1994

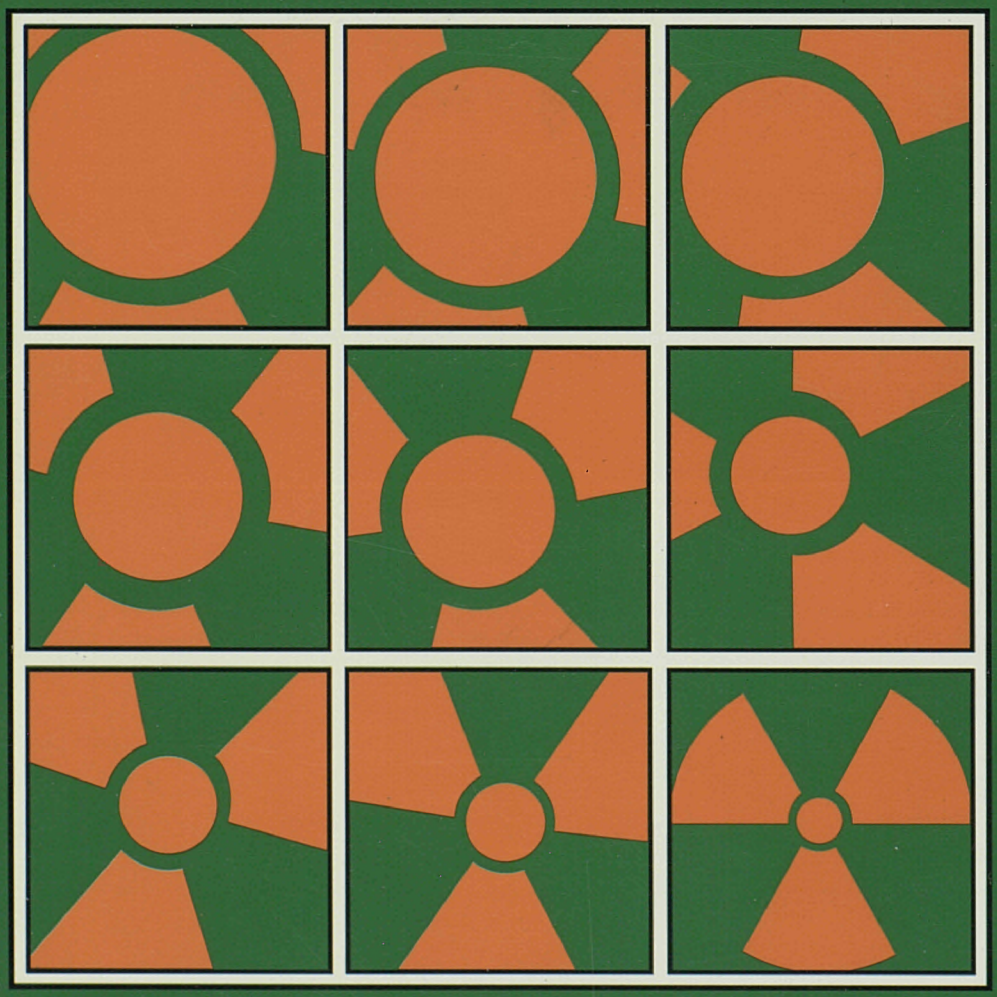

Report

EUR 16548 EN

European Commission

nuclear science and technology

Community's research and development programme on radioactive waste management and storage

Shared-cost action (1990-94)

Annual progress report, 1994

Directorate-General
Science, Research and Development

1995

EUR 16548 EN

LEGAL NOTICE

Cataloguing data can be found at the end of this publication

Luxembourg: Office for Official Publications of the European Communities, 1995

ISBN 92-827-4632-1

Printed in Luxembourg

CONTENTS

FOREWORD

This report covers the progress of research work and activities started and developed during 1993 in the framework of the five-year programme (1990-1994) of the European Atomic Energy Community on **"Management and Storage of Radioactive Waste"**. This R&D programme has been adopted by decision 89/664/EURATOM of the Council of the Ministers of the European Union on 15 December 1989.

The Council Decision, together with the technical content and the indicative Community financial contributions for the individual sections of the programme, has been published in the Official Journal of the E.C., Nr. L395, 30.12.1989, p. 28-32.

The initial total amount of funding allocated to the programme of 79.6 million ECU over the five-year period, has been reduced to 76.5 million ECU.

The programme is subdivided in :

Part A : **Waste management and associated R & D projects**
- A1: Studies of management systems (Task 1)
- A2: Waste treatment (Task 2)
- A3: Safety of the multi-barrier system of geological disposal (Task 3, Task 4 and Task 5)

Part B : **Construction and/or operation of underground facilities**

A call for research proposals has been launched (O.J. of E.C. Nr. C55/4, 7 March 1990) to implement the programme through shared-cost research contracts with public organisations or private firms established in the Member States. Multipartner projects have been encouraged.

Contract negotiations for the selected research proposals lead to the signature of 120 contracts for both Part A and Part B of the Programme. The number of research projects running in 1994 is 94.

The European Commission is responsible for implementing and managing the programme and is assisted in this task by the Management and Coordination Advisory Committee "Nuclear Fission energy - Fuel cycle/processing and storage of waste" (see the annexed list of the Members of the Committee).

In addition to shared-cost research contracts, the programme also includes study contracts, awards of training and mobility grants, as well as international co-operation agreements with states outside the European Union.

The co-operation among various teams within the Member States has considerably been promoted by the numerous multi-partner research projects.

The presentation and discussion of the work carried out during periodical progress meetings of working groups of the various projects assures the exchange of information within contractors and representatives of public and private institutions in the Community which are interested in the specific research area.

In this report, the objectives, the working programme and a synopsis of progress and results obtained for each contract in 1994 are presented as prepared by the contractors, under the responsibility of the project leader(s). Several projects have been extended to 1995. The overall results and conclusions of the whole five-year programme 1990-94 are planned to be presented and discussed during the fourth International Conference on "Radioactive Waste Management and Disposal" organized by the European Commission in Luxembourg on 25-29 March 1996.

From 1995 onward, the most of the R&D pursued under the EAEC Programme on "Management and Storage of Radioactive Waste" will be carried out under the specific RTD programme "Nuclear Fission Safety of the EURATOM Framework Programme 1994-1998.

The European Commission wishes to express its gratitude to all scientists who have contributed to this report.

N. CADELLI
Head of the Programme
"Management and Storage of Radioactive Waste"

MEMBERS OF THE MANAGEMENT AND COORDINATION ADVISORY COMMITTEE
NUCLEAR FISSION ENERGY
FUEL CYCLE/PROCESSING AND STORAGE OF WASTE [1]

(during 1994)

BELGIUM	Th.	VAN RENTERGEM
	G.	DEDEURWAERDER
DENMARK	K.	BRODERSEN
	S.	HOE
FRANCE	J.	LEFEVRE
	P.	RIEUTORD
GERMANY	M.	BLOSER
	H.G.	RIOTTE
GREECE	S.	AMARANTOS
IRELAND	C.	HONE
	F.	TURVEY
ITALY	G.	GROSSI
	F.	MORSELLI
LUXEMBOURG	C.	BACK
NETHERLANDS	H.	CORNELISSEN
	J.W.A.	VAN ENST (Chairperson)
PORTUGAL	A. J.	DA CONCEICAO SILVA
	C.	RAMALHO CARLOS
SPAIN	J. L.	ROJAS DE DIEGO
	M.	RODRIGUEZ PARRA
UNITED KINKDOM	R.L.	JACKSON
	P.J.	HUBBARD
COMMISSION	H.J.	ALLGEIER
	J.	VAN GEEL
	T.	Mc MENAMIN (Secretary)

[1] This Committee was established by the Council Decision of 29 June 1984 dealing with structures and procedures for the management and coordination of Community research, development and demonstration activities (OJ N° L 177, 4.7.1984, p. 25).

PART A

WASTE MANAGEMENT AND ASSOCIATED R&D PROJECTS

A1 : STUDIES OF MANAGEMENT SYSTEMS

A2 : WASTE TREATMENT

A3 : SAFETY OF THE MULTI-BARRIER SYSTEM OF GEOLOGICAL DISPOSAL

A1: STUDIES OF MANAGEMENT SYSTEMS

Task 1

"Studies of Management Systems"

* List of contract
* Introduction to Task 1

Topic 1	:	System studies
Topic 2	:	Harmonisation of radioactive waste management practises and policies
Topic 3	:	Comparative assessment of disposal practices in various management schemes for toxic and radioactive waste
Topic 4	:	Information
Topic 5	:	Transmutation studies

TASK 1 - LIST OF CONTRACTS

Topic 1 : System studies

Contract

FI2W-CT92-0119 Study of the retrievability of radioactive waste from a deep underground disposal facility.

Topic 2 : Harmonisation of radioactive waste management practices and policies

FI2W-CT90-0060 Assessment and proposal for activity limits for release of very low-level radioactive waste to landfills.

Topic 3 : Comparative assessment of disposal practices in various management schemes for toxic and radioactive waste.

FI2W-CT90-0042 Comparison of safety assessment methods for toxic and radioactive wastes.

FI2W-CT90-0061 Disposal of radioactive waste and toxic waste in underground repositories.

Topic 4 : Information of the public

FI2W-CT90-0036 Study of a communication strategy aimed at achieving a possible better understanding of the consequence of radioactive waste management in a well defined group of public.

FI2W-CT90-0043 Information of the public in the field of decommissioning waste. Study of strategies and means for specific information.

FI2W-CT90-0074 The evolution and implementation of a public information strategy on radioactive waste management.

TASK 1 - LIST OF CONTRACTS

Topic 5 : Transmutation studies

FI2W-CT91-0103	Transmutation of long-lived radionuclides by advanced converters.
FI2W-CT91-0104	Participation in a CEC strategy study on nuclear waste transmutation.
FI2W-CT91-0106	Potentialities and costs of partition and transmutation of long-lived radionuclides.

INTRODUCTION TO TASK 1 - STUDIES OF MANAGEMENT SYSTEMS

A. Objective

The system studies concern the evaluation of various scenarios for the management of different types of waste. Harmonisation work mainly involves the development of common waste management criteria and schemes. Waste from dismantling operations and spent fuel where these are considered as waste are included as well as the development of analytical models for minimising transport of waste. An additional topic is the evaluation of the possibilities offered by transmutation to reduce the inventory of long-lived radionuclides. Information of the public in all fields of radioactive waste management and disposal is a further topic.

B. Research performed under previous programmes

System studies have been performed by comparing various management schemes for particular categories of wastes or groups of waste streams; the comparisons were based on evaluation of costs and radiological consequences to workers and the public. The management alternatives were studied for:

- solid plutonium contaminated waste,
- alkaline liquid wash waste from fuel reprocessing and zircaloy-hulls,
- reactor waste (waste from normal operation of light-water reactors),
- waste management implications of direct spent fuel disposal and disposal after reprocessing.

Activities in the field of harmonisation of practises covered a review on "Objectives, standards and criteria of radioactive waste disposal in the European Community", the development of criteria for exemption from regulatory control for radioactive waste not linked to the nuclear fuel cycle, and first approaches to waste equivalence.

C. Present programme (1990-1994)

Studies are performed under five headings corresponding to specific research topics.

Topic 1 : System studies

The system studies are based on the comparison of possible management schemes, with the definition of waste inventories at origin, an analysis of the subsequent steps in the possible management routes (treatment, transport, interim storage and disposal), evaluation of costs and determination of radiological consequences. The sensitivity of each scenario to modifications in waste quantities, release limits, and waste acceptance criteria is also evaluated.
The main waste streams concerned are radioactive waste arising from decommissioning of nuclear installations, tailings from uranium-treatment, spent fuel declared as being waste and very low level waste candidate to being exempted from regulatory control.

Topic 2 : Harmonisation of radioactive waste management practices and policies

The main field of activity is the development of the scientific basis for developing criteria for exemption of particular waste streams from regulatory control. Particular disposal routed considered are incineration and disposal at industrial waste burial sites.

Topic 3 : Comparative assessment of disposal practices in various management schemes for toxic and radioactive waste

Studies are performed which compare radioactive waste management schemes to management practises for waste streams involving radioactive isotopes in material not linked to the nuclear fuel cycle and toxic waste mixed with radioactive elements. Particular attention is paid to disposal of toxic and mixed waste in salt formations.

Topic 4 : Information of the public

Studies on strategies allowing efficient information to be given to the public, and on how a good degree of penetration through various media may be reached are in progress. An exhibition targeted at school children (aged up to 18) and using the latest interactive multi-media techniques was developed to be installed in Science Museums and Information centres for the public. Development of information materials (booklets, visual, aids, etc.) is also part of the activities.

Topic 5 : Transmutation studies

After having established the inventory of long-lived radionuclides produced for a given reactor capacity in considering the spent fuel as a waste, the possibilities of reducing the inventory of long-lived actinides and fission products by partitioning and transmutation are calculated. The conventional routes are irradiation in thermal reactors with MOX-fuel and a mix of light-water-reactors and fast reactors, with long-lived radionuclides added in a homogeneous or heterogeneous way.

Title:	Study of the retrievability of radioactive waste from a deep underground disposal facility
Contractor:	ECN
Contract no:	FI2W-CT92-0119
Duration of contract:	July 1992 to March 1994
Period covered:	January 1994 to December 1994
Project leader:	J. Prij

A. OBJECTIVES AND SCOPE

Retrievability of radioactive waste emplaced in a deep repository in a geological formation has received increasing attention during recent years. Most of the Member States of the European Union, however, have not, up to date, included provisions for retrievability in their regulatory framework or in recommendations for disposal of waste. Other countries, like the United States, ask for an access to conditioned waste to be guaranteed for some decades.

Retrievability of suitably packaged waste may only be guarantied during the period that the waste packages remain intact and the position of the package is known. As those conditions can only be met for a few centuries, provisions for retrievability make sense only for up to some hundreds of years.
During these few centuries, retrievability may be realised by keeping the access to the waste packages open, by maintaining in operational condition the access shafts and the main galleries. A second possibility is to dispose the waste in a suitable overpack and abandon the repository after backfilling, closing, and sealing. In this case the waste must be re-mined from the surface. Although this re-mining will be very costly it is obvious that there will be a point in time, where the cost of keeping the repository in operating condition will be higher than those of re-mining from the surface to reach the waste packages in a closed repository.
The objective of this study is to determine this break-even point for several storage options.

B. WORK PROGRAMME

Present state of the retrievability option
Existing information on retrievability of radioactive waste will be collected in EC-Member States and other countries having a nuclear energy production programme.

Overview of expected modifications because of opting for retrievability
This overview will examine aspects concerning design and fabrication of waste packages, design of the repository, operation and maintenance of the repository and associated equipment, surveillance and control of the installation, and maintaining a documentation system when changing from final disposal to retrievability.
For these factors an estimate of additional costs and occupational exposure will be attempted. Evaluations about radiation protection and long term safety to the environment will be made without carrying out detailed performance assessment calculations.

Detailed evaluations for a reference disposal scenario
A detailed evaluation under realistic conditions will be made in performing a comparison between the costs of retrieval of the waste from a suitable deep underground repository

(including the annual costs of keeping the repository open) and the costs of re-mining the waste from a final deep underground repository (including the costs of closing and sealing).

The **assumptions** and **boundary conditions** are:

- The study is restricted to HAW (high level radioactive waste). The quantity of HAW is based on 20 GW installed nuclear power (in standard LWR NPP's) operating for a period of 30 years.
- Two types of waste management strategies will be considered, direct disposal of all spent fuel and disposal of the HAW from reprocessing all the spent fuel
- One loading sequence of the waste into the repository will be considered.
- The disposal concepts will be chosen based on current state of the mining and disposal techniques.
- Three types of host rock will be considered: clay, granite and rock salt.
- One retrieving and one re-mining strategy will be selected.
- The waste will be stored in a suitable overpack, capable of keeping radiation level at the outside small enough for human presence in the vicinity of the waste and capable of withstanding the rock pressure in the repository.

The **activities** to be carried out are:

- select feasible **final disposal** and **retrievable storage** concepts for each of the three host rock formations,
- assess the feasibility of the selected options: concise safety evaluations will be performed concerning radiation protection and long term safety to the environment,
- select a feasible **retrieval** and **re-mining** concept for each of the three host rock formations,
- assess the feasibility of retrieval for the concepts chosen with respect to maximum temperatures and stability of the mine-building after retrieval,
- determine the total costs of each option selected:
  - for the retrievable options the total costs are the annual costs to guarantee the retrievability, and the costs of the retrieval.
  - for the final disposal concepts selected the total costs are the costs of closing and the costs of re-mining.
- evaluate the costs in present day value and determine for each of the host rocks the break-even point at which re-mining is more favourable from an economical point of view. This evaluation will be based on the present-day society and present day estimates of the economical parameters such as interest rates.

C. PROGRESS OF WORK AND OBTAINED RESULTS

State of advancement

The project has been completed and the final report has been prepared.

Progress and results

Since both options of storage of the waste require the container to be liberated from the surrounding backfill under elevated temperature conditions, an extensive temperature analysis

has been performed of the individual container and of the complete repository. It appears that the maximum temperature at the container surface reaches 160 °C for storage in clay. This temperature will be reached some 10 years after storage. For storage in granite the maximum temperature will be 123 °C and will be reached after 20 years of storage. For storage in rock salt, the maximum temperature of 117 °C will be reached after about 20 years. The extreme temperatures always occur for storage of vitrified waste. No attempt has been made to investigate the existing criteria for mining at elevated temperatures. However, ore production mining at rock temperatures up to 120 °C has been reported. Apart from local hot areas the rock temperature is below this temperature and therefore it is very unlikely that the temperature will be a major obstacle for proper retrieval.
The aspects of safety regarding the repository operation and regarding the complete fuel cycle, as well as the long term safety of the stored waste, and the chemical interaction between the container and the surrounding rock, which may lead to the formation of corrosion gases, have not explicitly been treated in this study.
The storage and removal of the heat generating waste and the related thermal expansion or contraction of the rock may cause instability phenomena in the underground or collapse of the galleries. For a repository in clay this stability is not a major problem due to the presence of a concrete lining in all underground excavations. For granite and rock salt an assessment of the stability has been performed and it appears that in only relatively small regions around the waste cracks may form or instability may occur. The extent of this damage is such that support measures as used in normal mining practice are sufficient to guarantee the safety of the retrieval operation.
The cost for construction of the repository, re-mining the waste from a closed and sealed repository, and the annual operating cost for the different options is in 1994 money terms:

Cost in millions of Netherlands Guilders (1994)

	Spent fuel			Vitrified waste		
	clay	granite	salt	clay	granite	salt
Repository construction	730	511	618	546	417	507
Re-mining	518	595	622	424	451	529
Annual care and maintenance	1.3	2.4	1.8	1.3	2.4	1.8

These numbers are based on normal ore production mining practice and it has been assumed that the overpack of the waste is such that no additional precautions for radiation protection or safety are required.
The cost of the overpack, which is estimated at 2000 million of NLG, will contribute significantly to the total cost of the waste cycle. However, it does not influence the position of the break-even point, and therefore it is not incorporated in the cost for the repository.
The method of financing the storage of the waste has not been a subject in this study. The moment of decision for closing and sealing of the repository on one side and keeping the repository in operating condition on the other side is assumed to be when all the waste has been stored. The break-even point has been defined as that point in time where the net present value of the expenditure for both options at the moment of decision is equal.
The position of the break-even points is strongly dependent on the real return rate. Therefore the period from the decision point to the break-even point is represented as function of the

real return rate for the selected host rock types. For a real return rate of 5 percent, the break even point for storage in clay, Figure 1, is in the order of 35 to 40 years, for storage in granite, Figure 2, in the order of 22 to 25 years and for storage in rock salt, Figure 3, about 45 years.

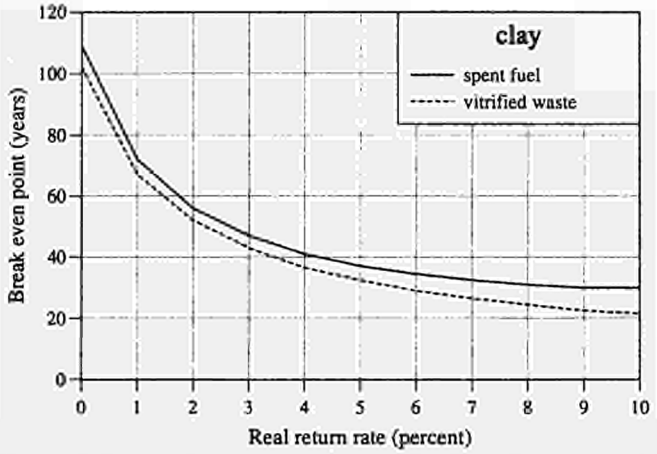

Figure 1 *Effect of the real return rate on the break even point for storage in clay.*

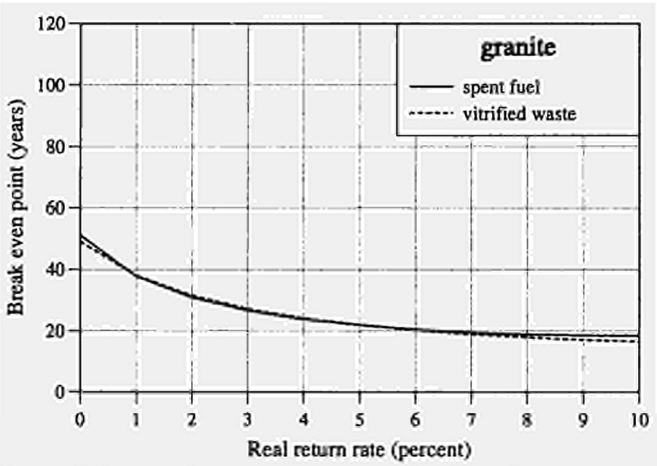

Figure 2 *Effect of the real return rate on the break even point for storage in granite.*

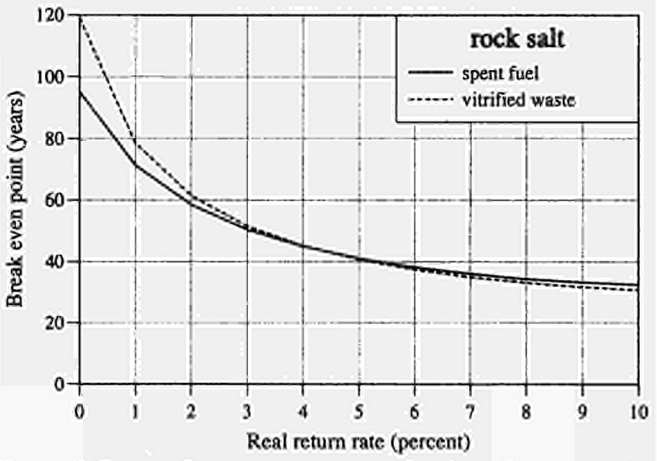

Figure 3 *Effect of the real return rate on the break even point for storage in rock salt.*

Title	**Assessment and proposal for activity limits for release of very low-level radioactive waste to landfills**
Contractor	CEA/IPSN, France and ONDRAF, Belgium
Contract N°	FI2W-CT90-0060
Duration of contract	April 1991 - July 1995
Period covered	1 January 1994 - 31 December 1994
Project leader	J.M. PERES (CEA/IPSN, coordinator)

A. OBJECTIVES AND SCOPE

In the frame of studies dealing with low level waste destinations, the project aims to establish acceptance criteria for municipal and industrial landfill.

Correspondances between levels of exposure and levels of radioactivity will be established.

From this work, it will be possible to derive activity concentration and surface activity levels for acceptance criteria to landfill disposal.

A complementary study will investigate the implications of disposal management in a specific landfill which receives only very low level radioactive waste.

B. WORK PROGRAMME

The initial program included :

-Phase 1 : Analysis of landfill disposal practices of industrial and municipal waste. A particular attention was paid to the regulatory context and to the conditions encountered in the different installations.

Phase 2 : Development of a radioprotection code CERISE, in order to establish the relations between exposure and radioactivity of waste, including a data bank of dose conversion factors.

Evaluation of the exposure of workers and public resulting from the water pathway using the code GEOLE (geosphere) and the code ABRICOT (biosphere).

Phase 3 : Establishment of the correspondance between exposure and activity concentration in the one hand or surface activity in the other hand.

Proposal of levels of radioactivity for the waste acceptance in the different types of landfill and for different dose criteria.

Final report.

The additional program includes :

-Review of the existing information of the volumes and radionuclides content in very low level radioactive waste,

-Review of operating data of a landfill including working conditions,

-Evaluation of radiological impact in the case of landfill disposal of very low level radioactive waste,

-Discussion of monitoring procedures.

The aim of this particular development is to highlight, with an exemple, the feasability on a safety point of view, of this type of management.

C. PROGRESS OF WORK AND OBTAINED RESULTS

State of advancement

The first part of the program (phase 1,2,3) has been published under EUR 15483 FR. The english translation of this document is in progress.

Progress and results

.The work carried out include :

- Review of the different waste types (concrete, metal, heat insulator, technological waste...) in the range from 1Bq/g to 100Bq/g.
- Site definition and disposal concept.

The landfill site is assumed to be a generic site. In french context, a site capacity of about 250 000 m3 corresponding to very low level waste generated until 2050.

Nowadays, no specified site is selected for this type of waste. The site is defined as a "saturated sandy-argilaceous formation"

- Review of main scenarios to be considered : landfill site workers, disturbance of the site after closure, radionuclide transfer via groundwater
- Selection of input parameters to be used in computer codes,.is underway.
- Waste acceptance and monitoring procedures have been determined.

List of publications

Ph.GUETAT (CEA/IPSN), L.BAEKELANDT (ONDRAF)
CECcontract N° FI2W-CT90 00 60. Annual Progress Report 1993 (EUR 15853)

J.M.ASSELINEAU, Ph. GUETAT, P.RENAUD (CEA/IPSN) L.BAEKELANDT, B.SKA (ONDRAF).
Propositions de niveaux d'activité pour l'enfouissement de déchets en décharges contrôlées en France et en Belgique. EUR 15483 FR.

Title:	Comparison of Safety Assessment Methods for Toxic and Radioactive Wastes
Contractor:	Intera Information Technologies Ltd.
Contract No.:	FI2W-CT90-0042
Duration of Contract:	March 1991 - December 1994
Period Covered:	January 1994 - December 1994
Project Leader	Richard Little (Intera) and Carlos Torres (IMA/CIEMAT)

A. OBJECTIVES AND SCOPE

The need for safety assessments of waste disposal stems not only from the increasing implementation of regulations requiring the assessment of environmental effects but also from the more general need to justify decisions on protection requirements. Just as waste disposal has become more technologically based, through the application of more highly engineered design concepts and through more rigorous and specific limitations on the types and quantities of the waste disposed, so too must the assessment procedure become more sophisticated. It is the overall aim of this study to improve the predictive modelling capacity for post-disposal safety assessments of land-based disposal facilities through the development and testing of a comprehensive yet practicable assessment framework.

Within this project the disposal of toxic, radioactive and mixed hazardous wastes is considered. The term "toxic wastes" is interpreted broadly to include any kind of liquid or solid non-radioactive waste which could give rise to some detrimental environmental effects, post-disposal. The associated work programme is being undertaken jointly by Intera Information Technologies, Environmental Division, United Kingdom, and Instituto de Medio Ambiente of Centro de Investigaciones Energéticas Medioambientales y Tecnológicas (IMA/CIEMAT), Spain.

B. WORK PROGRAMME

B.1. To review the different waste types and to compare and contrast concepts and methods adopted for their land based disposal.

B.2. To review the kinds of criteria adopted for authorising disposals, in so far as they relate to post-disposal environmental impact.

B.3. To review the different assessment methods which have been used to assess post-disposal environmental impacts and to evaluate the advantages and disadvantages of alternative assessment methods.

B.4. To identify the types of post-disposal impact which might arise and use a scenario analysis, according to a well defined procedure, to determine how such impacts may arise.

B.5. To develop and enhance a practicable framework for assessment of post-disposal safety for disposal of wastes to land-based facilities taking full account of existing methodological developments.

B.6. To test the application of the framework on a representative set of example disposals. Illustrations will reflect realistic problems of environmental assessment.

C. PROGRESS OF WORK AND OBTAINED RESULTS

State of advancement

During 1994 the extension to the project, which involved the further development and testing of the Safety Assessment Comparison (SACO) framework (Figure 1), has been completed.

Progress and results

C.1 Enhancing the Assessment Framework (B.5.)

In Phases 2 and 3 of the initial project, the SACO methodology was developed and tested. In light of this work, the aim of Phase 4 was to develop and enhance the SACO methodology further. The following tasks were undertaken and have been reported in /1/, /2/, /3/.

- **Task 1** - Generic information, which could be used to support the SACO methodology, especially Steps 1, 2, 3 and 8, in cases where site-specific data are scarce, were identified and collated. Such information related to technical data on: the wastes (eg contaminant concentrations in different waste types, solubilities of contaminants under different Eh and pH conditions, waste densities, waste porosities, and waste hydraulic conductivities); the disposal facilities (eg hydraulic conductivities, porosities and life expectancies of engineered barriers); the geosphere (eg hydraulic conductivities, porosities, dispersivities and contaminant sorption coefficients for different geological media); the biosphere (eg contaminant sorption coefficients for different surface environments, sediment and water transfers, human and animal intake/activity data, and subchronic and chronic contaminant toxicity levels for humans); regulatory and other criteria which affect assessment objectives (eg performance of engineering barriers, Environmental Quality Standards for contaminant concentrations in media such as groundwater and surface water, and dose/risk levels for humans).

- **Task 2** - Procedures to aid scenario analysis in Steps 5 and 6 of the SACO methodology were developed and enhanced. For example, the simple scoping calculations used under Phase 2 to make preliminary assessments of the impacts of waste disposals on groundwater were extended to allow the screening of other scenarios, such as human intrusion and gas generation.

- **Task 3** - Version 1.0 of the SACO assessment code was reviewed and Version 2.0 produced. The code application was made more user friendly, the representation of processes considered in the code enhanced, and certain new features from the original list of processes identified under Phase 2 of the original project were incorporated. Key enhancements were:

    - modularisation of the code to allow independent running of the geosphere and biosphere components of the code;
    - development of links to software packages such as SPSS and Lotus;
    - development of simplified source term models;
    - improved flexibility of the biosphere model;
    - porting of the code to UNIX platforms;
    - improvements to SACO input and output files resulting from the above enhancements and the need to make SACO more user friendly.

C.2 Testing the Enhanced Assessment Framework (B.6.)

The aim of Phase 5 was to continue the SACO test programme using data from shallow and deep disposal systems, and uranium mill tailings. In particular, the following tasks were undertaken and have been reported in /4/, /5/.

- **Task 1** - Collation of site-specific data from appropriate sources for the assessment of the SACO methodology (generic data were be collated under Task 1 of Phase 4). During Phase 3, budgetary and temporal restrictions meant that it was not possible to apply the SACO methodology to real sites in entirely realistic situations. For Phase 5, where possible, the methodology was applied to real examples from the disposal of toxic and radioactive waste. In addition, tests based upon data from international intercomparison exercises were continued to be used. Such tests allowed the comparison of results from the SACO assessment code with those from other assessment codes.

- **Task 2** - Testing of the SACO methodology. The data collected in Task 1 of Phases 4 and 5 were used to test the SACO methodology and assessment code, especially the modifications made in Phase 4.

The tests undertaken during Phase 5 are summarised in Table I and below.

- Shallow Disposal - The disposal of radioactive and toxic waste to shallow facilities was considered. The radioactive disposal case was based primarily on the continuing Near-Surface Radioactive Waste Disposal Safety Assessment Reliability Study (NSARS) programme /6/, /7/, whilst data based on a site in the United Kingdom (UK) were used for the disposal of toxic waste /8/,/9/.

- Deep Disposal - The disposal of radioactive waste to an engineered deep facility was considered. The facility, geosphere and biosphere were based on the granite option of the study concerned with the Performance Assessment of Geological Isolation Systems for Radioactive Waste (PAGIS) /10/, /11/.

- Uranium Mill Tailings - Disposals to mill tailings of wastes which pose a radioactive hazard is assessed. Data from the real site considered in the V2.1 and V2.2 scenarios of the Uranium Mill Tailings Working Group of the Biosphere Model Validation (BIOMOVS) study were used for the test case /12/, /13/.

Illustrative results from the application of the SACO framework are given in Figures 2-4.

The testing of the SACO framework during Phases 3 and 5 of the project has shown that:

- it is applicable to all waste types;

- it is applicable to shallow and deep disposal facilities;

- it is applicable to varying levels of data availability;

- it has a range of possible end points, including barrier performance, environmental quality standards, and human health risks;

- it allows the comparison of the long term environmental impacts of different disposal options and waste types.

It is concluded that the overall aim of this study, to improve the predictive modelling capacity for post-disposal safety assessments of land-based disposal facilities through the development and testing of a comprehensive yet practicable assessment framework, has been achieved.

Indeed, the framework is now being used in a CEC funded investigation into the derivation of illustrative disposal limits for the toxic, non-radioactive component of low level and exemptible radioactive wastes /14/.

List of publications

LITTLE, R.H., TORRES, C., TOWLER, P.A., SIMÓN, I. and AGÜERO A., The Analysis of the Long Term Environmental Impact of Landfills using the Safety Assessment Comparison (SACO) Methodology. Paper to be presented at SARDINIA '95, the Fifth International Landfill Symposium, Sardinia, 2 - 6 October 1995.

TOWLER, P.A., SIMÓN, I., CLARK, K.J. and WATKINS, B.M., Application of the Safety Assessment Comparison Methodology (SACO) to Deep Disposal Systems for Radioactive and Toxic Wastes. Paper to be presented at SARDINIA '95, the Fifth International Landfill Symposium, Sardinia, 2 - 6 October 1995.

LITTLE, R.H. and TORRES, C., The Development of a Methodology for the Safety Assessment of Radioactive and Toxic Waste Disposals. Paper presented at the 16th USDoE Low-Level Radioactive Waste Management Conference, Phoenix, 13-15 December 1994.

SIMÓN, I., TORRES, C., AGÜERO A. and LITTLE, R.H., Evaluacion de un Almacenamiento Superficial de Residuos Radiactivos y Toxicos con la Metodologia SACO. Paper presented at the Fifth Congress of the Spanish Radioloigical Protection Society, Santiago de Compostela, 26-29 April 1994.

AGÜERO A., SIMÓN, I. And TORRES, C., Evaluacion Ambiental de Diques de Esteriles de Uranio con la Metodologia SACO Participacion en Ejercicios Internacionales. Paper presented at the Fifth Congress of the Spanish Radioloigical Protection Society, Santiago de Compostela, 26-29 April 1994.

SMITH, G.M., LITTLE, R .H., TORRES, C. and SIMÓN, I., Coherent and Consistent Decision Making for Mixed Hazardous Waste Management: The Application of Quantitative Assessment Techniques. Waste Management 94. Tuscon, 27 February – 3 March 1994, Proceedings Vol 2, pp 1173-1177.

LITTLE, R.H., GROGAN, H.A, SMITH, G.M. and TORRES, C., Land Disposal Practices in Europe and North America. J. Inst. Water and Env. Man. 7, 354-362.

LITTLE, R.H., TORRES, C., CHARLES, D., GROGAN, H.A., SIMÓN, I., SMITH, G.M., SUMERLING, T.J. and WATKINS, B.M., Post-Disposal Safety Assessment of Toxic and Radioactive Waste: Waste Types, Disposal Practices, Disposal Criteria, Assessment Methods, and Post-disposal Impacts. EUR 14627 (1993).

LITTLE, R.H., TORRES, C., SIMÓN, I. and SMITH, G.M., Quantitative Assessment and Its Relevance to Waste Disposal. International Conference on Environmental Pollution, Sitges (Barcelona), 28 September - 1 October 1993. Proceedings Vol 2, pp 525-532.

TORRES, C., SIMÓN, I., AGÜERO A., LITTLE, R.H. and SMITH, G.M., Metodologia (SACO) para la Evaluacion Comparativa de la Seguridad de los Sistemas para la Disposicion Final de los Residuos Toxicos y Radiactivos. 19th Annual Reunion of Spain Nuclear Society, Caceres, 6-8 October 1993. Proceedings pp 390-392.

TORRES, C., SIMÓN, I., LITTLE, R.H., SMITH, G.M. and AGÜERO A., Safety Assessment Comparison Assessment Methodology for Toxic and Radioactive Wastes (SACO Version 1.0). International Conference on Nuclear Waste Management and Environmental Remediation, Prague, Czech Republic, 5-11 September 1993. Proceedings Vol 3, pp 589-598.

References

/1/ INTERA and IMA/CIEMAT, Intera Report IE2732-11 (Version 1.0) (1995)
/2/ INTERA and IMA/CIEMAT, Intera Report IE2732-12 (Version 1.0) (1995)
/3/ INTERA and IMA/CIEMAT, Intera Report IE2732-13 (Version 1.0) (1995)
/4/ INTERA and IMA/CIEMAT, Intera Report IE2732-14 (Version 1.0) (1995)
/5/ INTERA and IMA/CIEMAT, Intera Report IE2732-15 (Version 1.0) (1995)
/6/ IAEA, Co-ordinated Research Programme on the Safety Assessment of Near-surface Radioactive Waste Disposal Facilities (NSARS). Specifications for Test Case 2A (1992).
/7/ IAEA, Co-ordinated Research Programme on the Safety Assessment of Near-surface Radioactive Waste Disposal Facilities (NSARS). Specification for Test Case 2B (1993).
/8/ PALMER, C. and YOUNG, P.J., Protecting Water Resources from the Effects of Landfill Sites: Foxhall Landfill Site. J. Inst. of Water and Env. Man., 5, 682--696.
/9/ PALMER, C. and YOUNG, P.J., Leachate Contamination from Closed Landfills - Predicting the Impacts. In New Developments in Landfill. Proceedings of the 1992 Harwell Waste Management Symposium. UK Atomic Energy Authority, AEA Environment and Energy, pp 65--82.
/10/ CADELLI, N., COTTONE, G., ORLOWSKI, S., BERTOZZI, G., GIRARDI, F. and SALTELLI, A., PAGIS (Performance Assessment of Geological Isolation Systems for Radioactive Waste) Summary. EUR 11775 EN (1988).
/11/ VAN KOTE, F., PERES, J.M., OLIVIER, M., LEWI, J., ASSOULINE, M. and MEJON-GOULA, M.J., PAGIS (Performance Assessment of Geological Isolation Systems for Radioactive Waste): Enfouissement dans des Formations Granitiques. EUR11777 FR (1988).
/12/ BIOMOVS, BIOMOVS II Uranium Mill Tailings Working Group Scenario Description Version 2.1 (Final-Revised), November 1994. SSI, Stockholm (1994).
/13/ BIOMOVS, BIOMOVS II Uranium Mill Tailings Working Group Scenario Description Version 2.2, February 1995. SSI, Stockholm (1995).
/14/ CLARK, K.J., SCHALLER, K.H., LITTLE, R.H., MAUL, P.R., TOWLER, P.A., and WATKINS, B.M., An Illustration of the Application of Radioactive Waste Disposal Assessment Methods to Mixed Waste Disposals. Paper to be presented at the Third Biennial Mixed Waste Symposium, Baltimore, 7 - 11 August 1995.

Table I: Phase 5 test cases

	Test Case 1		Test Case 2	Test Case 3
	SHALLOW DISPOSAL SYSTEM		DEEP DISPOSAL SYSTEM	URANIUM MILL TAILINGS
	Toxic Waste	Radioactive Waste		
DISPOSAL FACILITY	UK site	NSARS Level 2B	PAGIS Granite	BIOMOVS UMT V2.1 and V2.2
WASTE TYPE	UK site	NSARS Level 2B	PAGIS Granite	BIOMOVS UMT V2.1 & V 2.2
GEOSPHERE	UK site	NSARS Level 2A	PAGIS Granite	BIOMOVS UMT V2.1 & V 2.2
BIOSPHERE	UK site	BIOMOVS Complementary Studies	PAGIS Granite	BIOMOVS UMT V2.1 & V 2.2

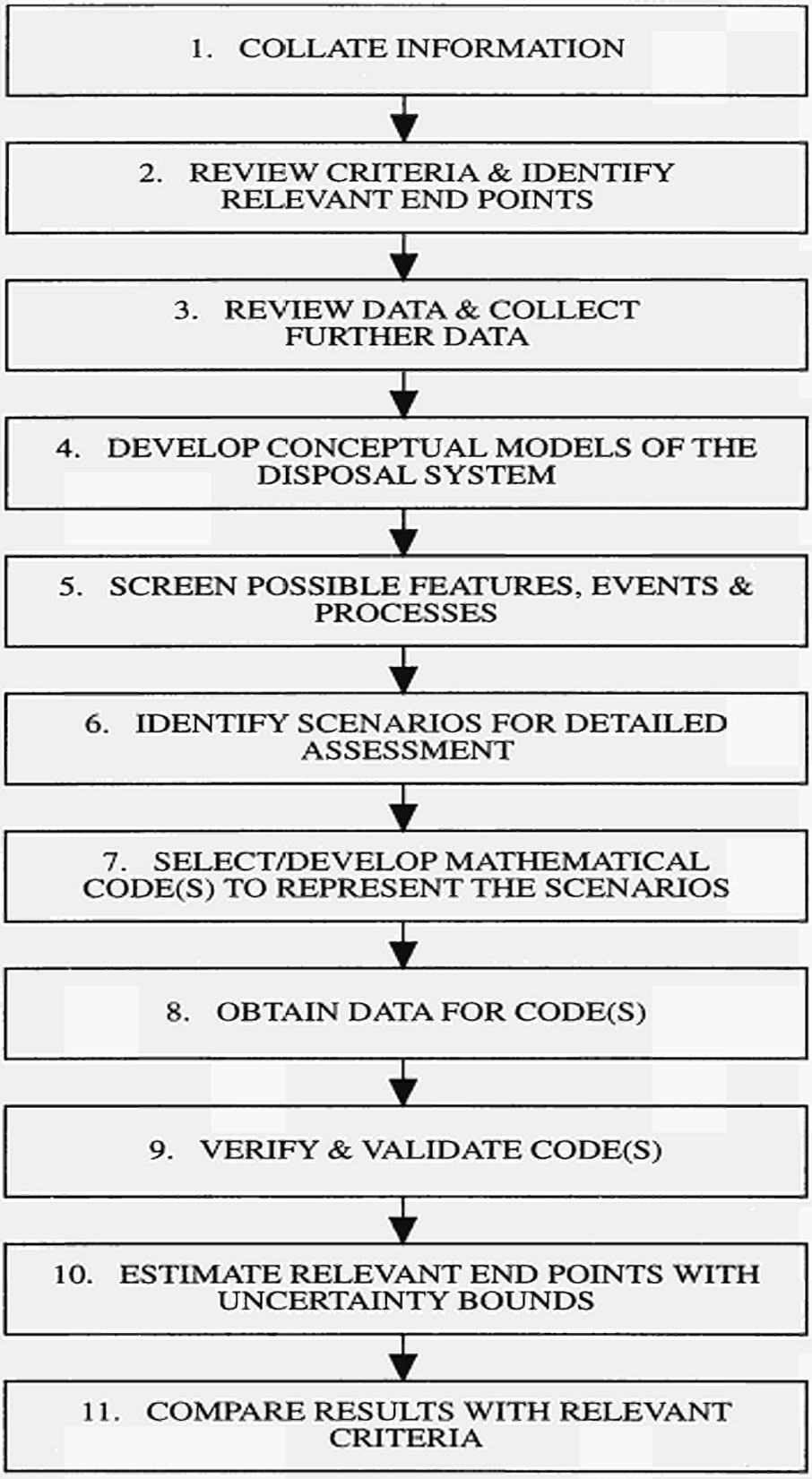

Figure 1: The SACO assessment framework

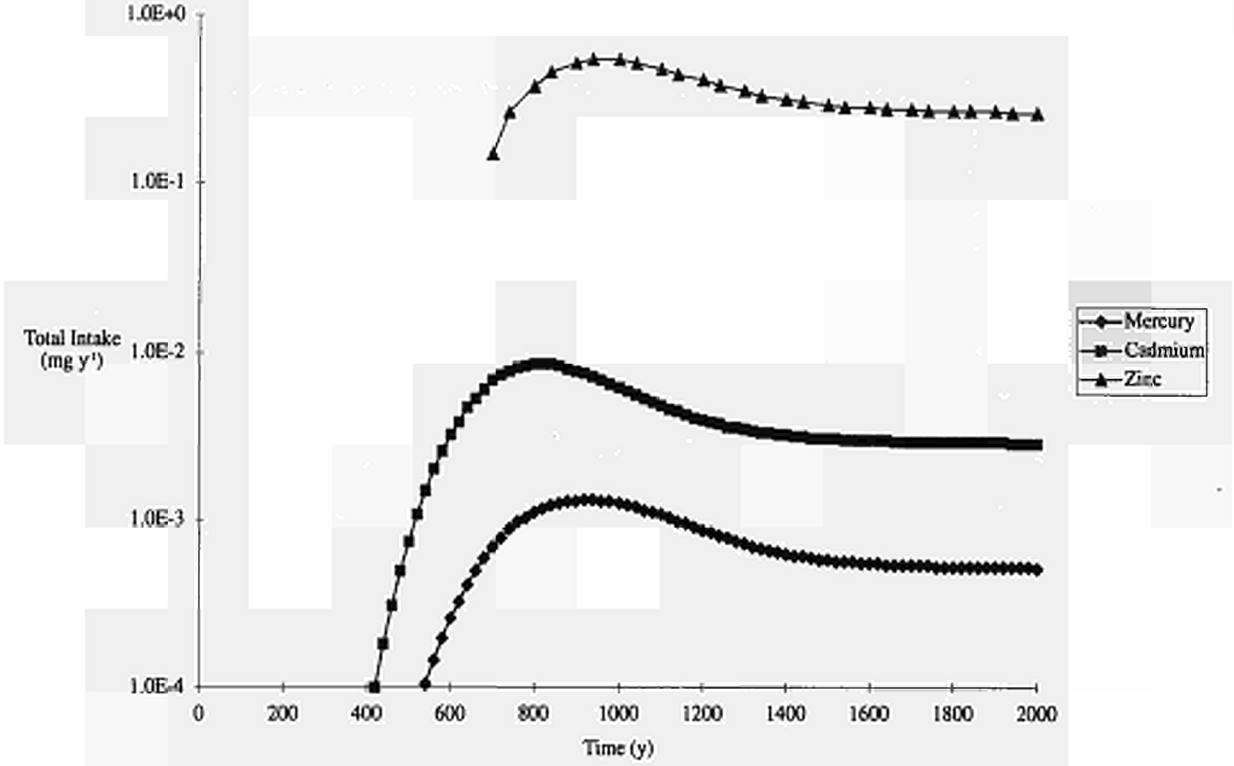

Figure 2: Heavy metal intakes from the shallow toxic waste disposal test case

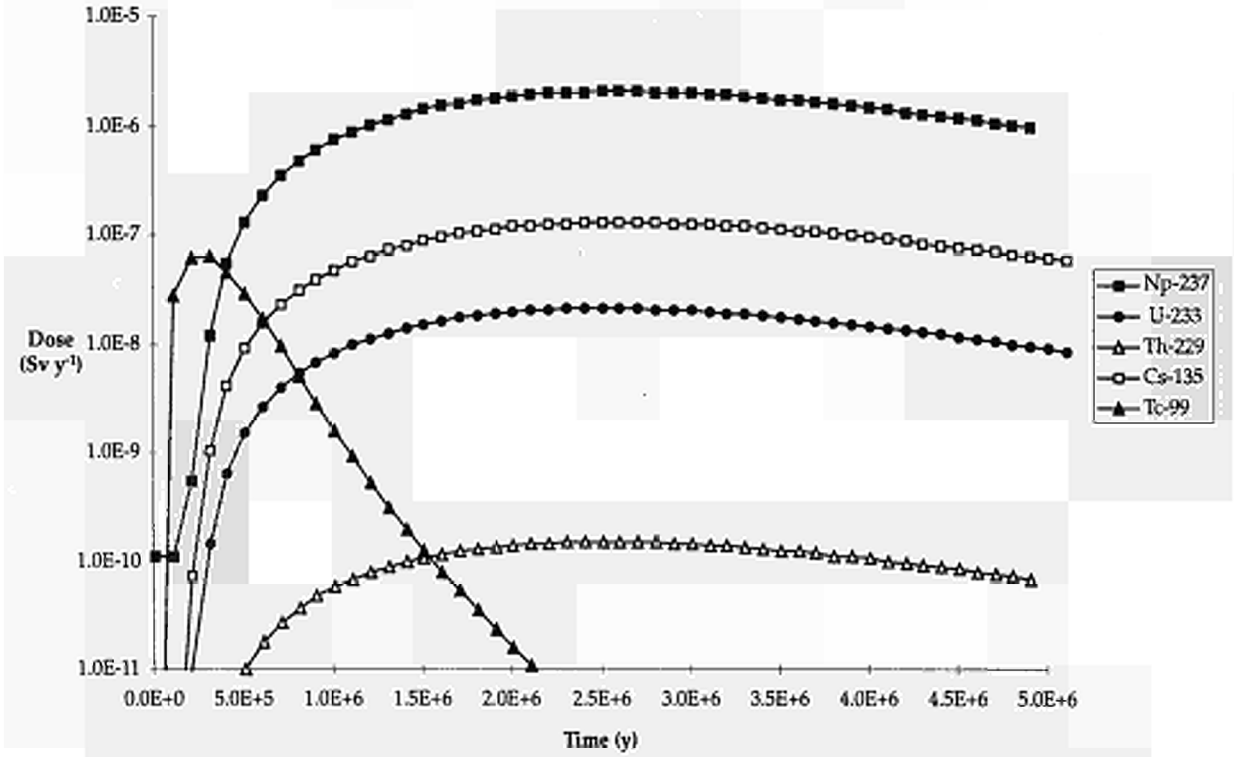

Figure 3: Doses from the deep radioactive waste disposal test case

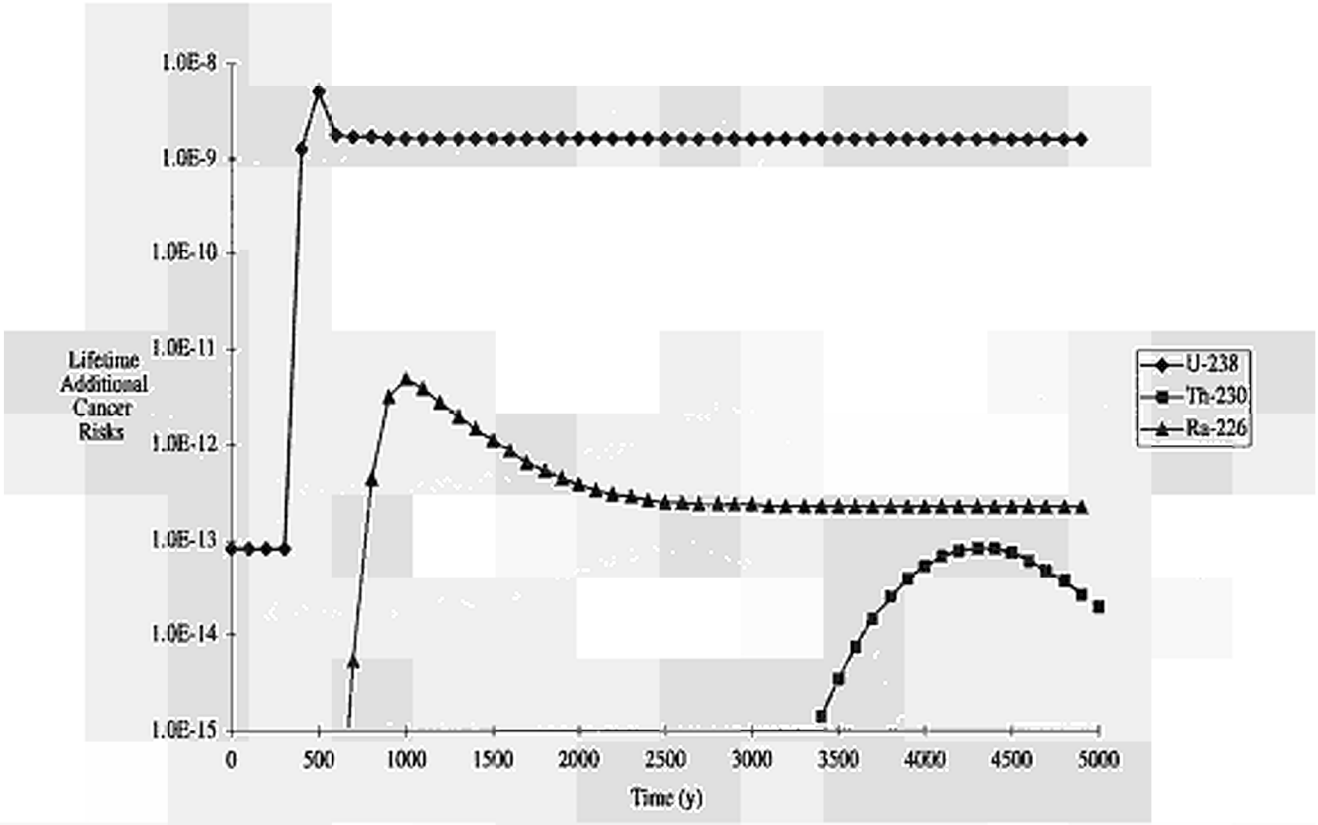

Figure 4: Risks from the uranium mill tailings test case

Title:	Disposal of Radioactive Waste and Toxic Waste in Underground Repositories
Contractor:	GSF-Forschungszentrum für Umwelt und Gesundheit, GmbH; Stichting Energieonderzoek Centrum Nederland (ECN)
Contract No:	FI2W-CT90-0061
Duration of contract:	March 1991 - June 1994
Period covered:	January 1994 - June 1994
Project Leaders:	Th. Brasser (GSF - Coordinator); A. van Dalen (ECN)

A. OBJECTIVES AND SCOPE

The initial objective of a mutual research project between GSF and ECN is to delineate the statutory boundary conditions pertaining to an underground emplacement of hazardous wastes. At the same time the wastes of relevance to disposal are to be characterized according to type, composition, origin, toxicity, and volume, while taking the particularities of the situation in both countries into due consideration. Assumed potential hazards to the environment emanating from disposal are to be assessed on the basis of these data. The current strategies for an underground storage of hazardous wastes are described and compared with the concepts for the final disposal of radioactive wastes. Reference is taken to the special R&D topics of final disposal, such as the selection of the host rock, investigation of the geomechanical and hydrogeological situation, transport methods, backfilling and sealing techniques as well as the more complex subjects, such as the spreading of toxic agents and the safety analysis. This mutual project is to combine the basic knowledge of the repository concepts for the disposal of radioactive and hazardous wastes.

B. WORK PROGRAMME

B.1 Consideration of legal stipulations for the underground disposal of toxic wastes, based on the aims, requirements, techniques and safety concepts of radioactive waste disposal.

B.2 Description of the types of waste, their composition, origin, toxicity and assessment of their potential hazards to the environment emanating from the emplacement.

B.3 Description of strategies for underground disposal of toxic wastes and comparison with the concepts for radioactive waste disposal.

B.4 Compilation of special requirements on the disposal of toxic wastes in deep geological formations, summarizing those results which can be generally adopted from the R&D work in the field of radioactive waste disposal.

C. PROGRESS OF WORK AND OBTAINED RESULTS

With the completion of the study in June 1994 the final report has been submitted to the Commission. Its main results are compiled in the following.

In the **Federal Republic of Germany** the concept of nonretrievable and, in the postoperational phase, surveillance-free disposal in deep geological formations is being pursued in conjunction with the disposal *of radioactive wastes*. This concept has been implemented for some thirty years in the form of R&D programmes, technical development projects, and site investigations.

The approval procedure is currently in progress for a final repository for non heat-*producing radioactive wastes* in the former Konrad iron ore mine. A further final repository - especially for heat-generating, high radioactive wastes - is currently undergoing exploration in the Gorleben salt dome. Since 1st July 1990, the "Final Repository *for Radioactive Wastes* at Morsleben" (ERAM), has held the legal status of a national final repository in conformance with the Law Relating to Nuclear Energy. Site approval had already been granted to the former German Democratic Republic in 1972, and approval was granted for sustained operation in 1981 and 1986. In the Asse research mine, techniques and methods of investigation for the disposal of *radioactive wastes* are under development.

In the **Netherlands** the disposal *of radioactive wastes* in salt formations has been under investigation for about twenty years. The final report on the initial phase of the **Netherlands** research programme on geological disposal of radioactive wastes in salt formations (OPLA) has recently been published. Since in situ investigations have hitherto not been feasible in the **Netherlands**, the research programme of the GSF in the experimental Asse mine has become the object of close cooperation and participation. A three-year follow-up programme for OPLA is currently in preparation.

Underground deposition of *chemical-toxic wastes*, partially with the proviso of retrievability, is already in progress for particular types of wastes in various mines in the **Federal Republic of Germany**. On the one hand, such measures are implemented in compliance with the laws relating to waste disposal; on the other hand, mining law may also be applicable under certain conditions, for instance, in conjunction with the underground re-utilization of residues as backfilling materials. Since 1991 a "Technical Regulation Relating to Storage, Chemical/Physical, Biological Treatment, Incineration, and Deposition of Hazardous Wastes" (TA Abfall) has become effective as a supplement to the Waste Disposal Act; underground deposition in salt rock is thereby treated with a series of regulations, too. Besides the existing facilities a number of conceptions and pending approval procedures are currently in progress.

In the **Netherlands** a growing tendency in favour of underground deposition of certain categories of *chemical-toxic wastes* can be observed at present. If a waste disposal concept of this kind can be realized, however, it will be feasible only with a guarantee of waste retrievability from a present-day standpoint.

For large-scale industrial implementation of concepts for the underground deposition *of chemical-toxic wastes*, the examination of results obtained in the field of *radioactive wastes* for applicability in individual cases and, if appropriate, further waste-specific research and development projects are recommended.

For the **Netherlands** section of the joint research project the consequences of the retrievability requirement are the object of special consideration. This implies that the associated projects are based exclusively on the mine concept. In contrast, final repository concepts for both mines and caverns are being pursued in the **Federal Republic of Germany**.

Within the scope of the joint research project by GSF and ECN, the general legal conditions for underground deposition of *chemical-toxic wastes* are first determined - on the basis of the objectives, requirements, techniques, and safety concepts in connection with the disposal of *radioactive wastes* (chapter 1). Subsequently, the types of wastes relevant to underground deposition are classified in accordance with type, composition, and quantity, and the differences between the situation in the **Federal Republic of Germany** and that in the **Netherlands** are described (chapter 2). On this basis the present concepts for underground deposition of *chemical-toxic wastes* are indicated and compared with the concepts for the disposal *of radioactive wastes* (chapter 3). These concepts are referred to the major R&D objectives in the field of *radioactive waste* disposal, such as selection of the host rock, investigation of the geomechanical and hydrogeological conditions, transport, backfilling, and sealing techniques, as well as the complex topics of pollutant propagation and safety analysis (chapter 4). This joint venture should provide a summary of fundamental understanding of final repository concepts *for radioactive wastes*, on the one hand, and *chemical-toxic wastes*, on the other hand. On the basis of the clearly defined relationship between final repository costs and recycling, general economic aspects of underground deposition are also presented.

The study has been conducted by both contractual partners, GSF (for the area of the **Federal Republic of Germany**) and ECN (for the area of the **Netherlands**). The two institutions have been cooperating for quite some time in the field of *radioactive waste* disposal, both bilaterally and within the scope of programmes of the European Union. The present project is designed for D - NL information transfer on a broad basis, which can later be extended to further member countries of the European Union.

The Commission of the European Union has supported the performance of the present study within the framework of its R&D programme, "Disposal of *Radioactive Wastes*", coordinated the work within the scope of this programme, and participated in financing.

C.1 Legal principles

The legal principles for underground deposition in the **Federal Republic of Germany** as well as in the **Netherlands** are first summarized. Existing laws, ordinances, guidelines, bodies of regulations, etc., as well as those in planning or preparation, are thereby taken as basis, and a distinction is made between *radioactive* and *chemical-toxic wastes*. By means of a comparison, different trial solutions or features in common, especially with respect to the basic objectives and safety criteria, are indicated.

As a matter of principle, the disposal of *radioactive wastes* in the **Federal Republik of Germany** is governed by nuclear energy law, and the disposal of *chemical-toxic wastes* by waste disposal law. This subdivision of waste disposal into two legal fields is ultimately based on the founding agreements of the European Community. In 1957 the member countries of the European Community concluded the Euratom Agreement with the aim of providing the conditions for the peaceful use of nuclear energy on a European level. On the basis of this agreement, guidelines and ordinances

have subsequently been enacted by the Community, especially for protecting the population and employees against ionizing radiation. Regulatory instructions for such tasks as the disposal of *radioactive wastes* are not included in EC law; these are determined by the laws of the respective member countries. This was implemented in German federal law concerning *radioactive waste* with the enactment of the Atomic Act and the Radiation Protection Ordinance. Since 1974 a technical concept for the disposal of these wastes has been available to the German Federal Government.

The development of laws relating to wastes, including the legal basis for waste disposal (that is, e.g. for *chemical-toxic wastes*), has proceded quite differently. The fundamental system of contracts at the European level is the Agreement on the Establishment of the European Economic Community concluded in 1957. In **German** federal law, legal regulations relating to waste disposal were not proposed until long after this time, particularly because of the question of competency between the German Federal Government and the Federal States. In 1971, the German Federal Government passed a draught law relating to the disposal of waste materials. In contrast, a modern waste disposal law has existed only since 1986. The Law Relating to the Avoidance, Recycling and Disposal of Wastes will become effective in 1996 at the earliest. A Technical Regulation (TA Abfall), which has existed since 1991, is among other points an administrative specification for ensuring environmentally compatible waste disposal in the **Federal Republic of Germany** in the future. It comprises regulations for storage, chemical/physical and biological treatment, incineration, and disposal of *chemical-toxic wastes*. A further Technical Regulation relating to municipial wastes (TA Siedlungsabfall) includes requirements on recycling, treatment, and disposal of those wastes in accordance with the state of the art, as necessary for avoiding impairment of general well-being.

The legal regulations pertaining to the disposal of *radioactive wastes* and those pertaining to the disposal of *chemical-toxic wastes* are thus based on mutually independent fields of law. The disposal of *radioactive wastes* is governed by nuclear energy law, whereas the disposal of *chemical-toxic wastes* is governed by the waste act. In spite of these differences in the development of nuclear energy law and waste disposal law all the way to differences in the selection of the terms and designations in the laws and ordinances, essential agreements are evident in the implementation of the concepts. Project evaluation and examination of environmental compatibility are specified in both fields of law. Residues which cannot be recycled at the present state of technology or for economic reasons require disposal as wastes in an orderly manner. Limiting values for appraising environmental compatibility are anchored in the Law Relating to Nuclear Energy; in the case of *chemical-toxic waste* disposal, however, reference must be made to other legal fields in environmental law. The Water Resources Act is applicable in both fields of law and constitutes a part of the project evaluation procedure or results in independent water rights proceedings.

Since the abandonment of *radioactive waste* processing on an industrial scale in the **Federal Republic of Germany**, the disposal concept is based on final deposition in mines. The disposal of chemical-toxic wastes in underground repositories is likewise anchored in the waste act; however, it represents only one disposal possibility among others, but the concepts are comparable. In both cases the basic objective is the protection of man and his environment, that is, the biosphere. Analyses of wastes, sites, and long-term safety of a repository system must demonstrate that this method of disposal is unobjectionable.

Waste disposal which endangers the environment, regardless of whether the wastes concerned are radioactive or nonradioactive, is equally liable to prosecution in accordance with the Penal Code.

In the **Netherlands** the last few years the legislator published laws and regulations and revised older laws in order to have a systematic view on regulation of the environment. The General Law on Environment Mangement has to cover all parts describing and regulating influences of human activities on the environment. Concerning wastes produced in society the most urgent subject was regulated first the last year: the law on landfill disposal in relation to soil protection. Related to the degree of isolation of the landfill from the environment non-chemical and low toxic *chemical waste* may be disposed.

The important part of the system of environmental hazardous (*chemical-toxic*) *waste*, the new name after repeal of the Chemical Waste Act, is the leachability of toxic compounds. The system of waste classification for disposal purposes based on leachability is used in practise for nearby a decade, but the introduction into the legislation is still not made.

Legislation for deep underground disposal is not available in the **Netherlands**; the Mine Law allows only to bring down materials in direct relation to the mining. For the technical and economical conditions of waste disposal in a salt formation the legal conditions are important. The evolution in legislation for Environment Management has been used in this report to formulate the main conditions for deep underground disposal:

- waste disposal becomes a private enterprise, economic profit is a consequence,
- in principle the wastes disposed underground are retrievable,
- competent authorities have to control the obeyance of the legal conditions,
- at the end of the operational phase or end of the license the mine has to be closed with the guarantee of safety to the environment.

No decision has been taken for the final disposal of *radioactive waste*, agreed in an interim storage for 50 to 100 years.

C.2 Characterization of wastes

The types of wastes in question for underground deposition or disposal in compliance with the present regulations are classified with respect to type, composition, and quantity. In the case of *radioactive wastes* the existing data for the final repositories in operation or in the planning stage can be employed in the **Federal Republic of Germany**. Since much less knowledge is available in the case of *chemical-toxic wastes*, exemplary analyses are performed on relevant types of wastes for better classification of these wastes, since the appraisal of the long-term behaviour of wastes in an underground repository requires thorough knowledge of all components of the wastes as well as their potential behaviour upon release under the conditions of deposition. This applies to *radioactive wastes* as well as *chemical-toxic wastes*.

Radioactive wastes are - in the **Federal Republic of Germany** - subject to surveillance by federal governmental authorities from their origin until final deposition; this applies to the raw *radioactive wastes* such as those arising in nuclear facilities, as well as conditioned wastes from reprocessing plants. The radionulcide inventory of *radioactive wastes* with negligible heat generation, which do not originate from nuclear installations, but rather from the field of research and development or from applications of radioisotopes in commerce, industry, or medicine, is extensively known and can be determined without difficulty if necessary. The criteria, such as the specification of limiting values and

classification with respect to types of wastes, are established largely in accordance with national regulations. An international specification in analogy with the IAEO Classification is the objective of current endeavours.

The mass content of radioactive nuclides as referred to the accompanying materials *in radioactive wastes* is very low, especially for wastes with negligible heat generation as well as for conditioned wastes. The radionuclides are associated with a high mass content of accompanying materials which, as a rule, are known (conditioning products, among other items) and whose toxicity is low or zero.

Chemical-toxic wastes are subject to surveillance by the authorities of the German Federal States, in most cases only after declaration as wastes or as residues. The characterization of wastes first requires reference to the description by the waste proprietor; in addition, however, waste analyses must be performed by the waste producer or disposer. The analyses are then performed in conformance with known codes of practice or standard methods. But in many cases the usual or specified methods of analysis do not allow a complete characterization of wastes. Consequently, the best-suited analytical technique must first be assigned to each type of waste; as a rule, more detailed analyses are then necessary for improving the overall balance. Furthermore, no universally applicable bodies of regulations exist for the qualitative classification of the concentration ranges determined for components of waste materials. Upon investigation of the leaching behaviour under conditions of deposition, even wastes with identical waste code numbers exhibit decidedly different characteristics. Hence, the assignment of waste materials to an underground repository - as well as of residues for underground backfilling measures - is feasible only conditionally on the basis of waste disposal instructions (such as TA Abfall); instead, the assignment must be site-specific and waste-specific.

In the **Netherlands** *radioactive wastes* are considered unsuitable for aboveground disposal, the classification is based on the interim storage. Shielding of radiation and removal of decay heat are the main items for the classification. The data collection of *radioactive wastes* received and to be accepted in the near future is related to the actual nuclear power of the two power stations, and the wastes from radioactive material users.

For *chemical waste* classification the description is given of the leach procedure resulting in low toxic *chemical waste* and non-chemical waste suitable for landfill disposal. Provisional definitions for *high toxic* and *medium toxic chemical waste* are: not suitable for aboveground disposal, and disposal in a facility showing no or negligible release to the environment respectively.

The data collection of *chemical wastes* in the **Netherlands** published yearly is according to this system (C-1, C-2, and C-3 wastes). The declaration of the wastes according to the Chemical Waste Act is considered fairly accurate and complete. Some large volume wastes not included in the data collection are problematic because other useful destinations have not been found e.g. jarosite from zinc, and gypsum from phosphate fertilizer production.

There is at the moment no consensus about deep underground disposal, so no indication of wastes suitable for an underground facility is available. A selection for this study has been taken from the C-1, C-2, and ashes from incinerators to arrive at a suitable amount for technical and economical reasons. In spite of all actions to prevent waste production and to process or (re)use waste for acceptable purposes, the government admits that inevitable some untreatable waste remains and has to be disposed of.

C.3 Final repository concepts

The concepts hitherto available or in preparation, as well as the previous practice of underground disposal of *radioactive wastes*, or deposition of *chemical-toxic wastes*, are summarized. This indicates a concentration on salt deposits, which are considered predominantly for waste disposal purposes in the **Federal Republic of Germany**, and exclusively for this purpose in the **Netherlands**. Moreover, the mine concept is considered specially from the standpoint of retrievability in the **Netherlands**.

The objective of protection relating to the final deposition of *radioactive wastes* or the deposition of *chemical-toxic* has received a comparable formulation in the **Federal Republic of Germany**. Thus, the formulation of the objective of protection in the "Safety Criteria for the Final Deposition of *Radioactive Wastes* in a Mine" is as follows: "The final deposition of *radioactive wastes* in mines shall ensure the protection of man and environment against damage by ionizing radiation from these wastes. For achieving this objective, certain requirements shall be satisfied." In the TA Abfall, "Special Requirements on Underground Repositories in Salt Rock", the following principle is formulated: "In the deposition of wastes in underground facilities in salt rock, the wastes shall be permanently isolated from the biosphere."

The successive priority of avoidance, recycling, deposition, or final deposition, that is, the demand that no wastes be produced if at all possible, and that unavoidable wastes be recycled, is anchored in nuclear energy law as well as in the waste act. If neither of these options - avoidance or recycling - is feasible, the objective of protection just mentioned requires deposition of *chemical-toxic wastes* or the final deposition of *radioactive wastes*. The requirements on final deposition of *radioactive wastes* as well as the deposition of *chemical-toxic wastes* mutually concur as far as essential features are concerned. In both approval procedures for construction and operation, an examination of the environmental compatibility as well as a project evaluation procedure with public participation are prerequisites. In both cases also the concrete location must be investigated.

A conceptual component for the disposal of *radioactive wastes* as well as *chemical-toxic wastes* is underground deposition. Exclusively mined underground cavities are intended for the final deposition *of radioactive wastes*, and shall be operated as final repository mines (e.g. chambers, drifts, and under some circumstances large boreholes). In addition to mines, caverns are available for the deposition of *chemical-toxic wastes*, especially for bulk wastes. The so-called salt concept, that is, the construction of a final repository in salt rock (for instance, Zechstein salt), is thereby pursued with priority. In principle, however, other formations may also serve as host rock. An example is the former Konrad iron ore mine, which is intended for use as a final repository for low and medium *radioactive wastes*.

The conditioning of raw *radioactive wastes* is an important component step in the disposal of these wastes. Conditioning represents a further technical barrier which imparts the necessary consistency to the wastes and decidedly decreases the release of activity in the event of leaching. In the case of conditioning of *chemical-toxic wastes* for deposition in underground repositories, questions of transport engineering or stability are of primary importance. For the final deposition of *radioactive wastes*, a number of different containers are prescribed. These containers provide handling assistance during transport as well as additional safety by virtue of their shielding effect. In accordance with the TA Abfall, the use of

containers is not mandatory for the deposition of *chemical-toxic wastes;* however, containers are probably necessary for handling in a final repository mine and are therefore demanded by operators in several cases as a rule.

Wastes are transported through a shaft into the mine. In a final repository, the wastes are transported by means of special vehicles. They are transported into a cavern by bulk conveyance or hydraulic conveyance. The deposition techniques for waste containers are independent of the type of waste. Well known and proved methods include the stacking and tipping techniques. Containerless deposition is at present envisaged only for the disposal of *chemical-toxic wastes* in caverns. After the shut-down of an underground repository, sealing measures are necessary; these measures always include plugging of the shaft. Moreover, residual cavities possibly present in the area surrounding the wastes should be backfilled, and dams must be constructed in the underground tunnel system.

Based on recent historical data (1992) in the **Netherlands** an annual toxic waste quantity in excess of 180,000 tons is deposited at various sites (excluding some 300,000 tons of contaminated soil). For the purpose of this study an annual amount of 165,500 tons has been assumed to be available at a considerable length of time for underground storage. This storage has been planned in a salt dome in a retrievable manner which influences design parameters. The mine has been developed using a highly mechanised method in order to obtain a continuous operation.

Based on a system of defining cost centres and activities, a bottom-up approach to determine the cost of the mine has been employed. Recent costs for storage have been used to obtain probable revenue. These have been transferred on a proper time scale with the aid of a project planning program from which ultimately a cash flow could be derived. The value of the mine and its internal rate of return follow from the cash flow. The net present value of the project at a discount rate of 15 per cent amounts to a negative Nlg 111 million in January 1995 money terms. The internal rate of return of the project is 8.6 per cent. Although the operating margin of the mine is high (75 per cent) the long lead time of 10 years has a major influence on the return of the project. Which internal rate of return is acceptable to this project is a matter of judgement. Compared with what is common in the mineral industries and regarding the risk of this project a minimum return of 15 per cent is required. Therefore it can be concluded that the project within these constraints is not financially attractive.

It is clear from the analysis that to construct a mine for 30000 tons of C1 and C2 waste only will reduce the net present value and the internal rate of return and is therefore less attractive. To combine the storage of *chemical-toxic waste* with low and middle *radioactive waste* will probably enhance the return of the project. This will be the case when the increased investment during the construction of the mine (in e.g. separate storage halls and waste treatment facilities) and increased operating costs (in e.g. underground storage requirements and safety arrangements) will be small compared to the increase in revenue of storing nuclear waste.

Especially the aspects of nature and quantity of *chemical-toxic waste* and its suitability for underground storage as well as requirements of the retrievability concept are recommended for further analysis in order to increase the knowledge and understanding of underground storage of *chemical-toxic waste* in the **Netherlands**.

C.4 R&D transfer

The major research and development projects hitherto executed, currently implemented, or in preparation in the field of *radioactive waste* disposal are classified with respect to their objectives, results, and possible relevance to the underground deposition of *chemical-toxic wastes*. Furthermore, special emphasis is placed on those topics from research on final repositories for *radioactive wastes* which may be of importance for the future conception and realization of underground deposition of *chemical-toxic wastes*. A requirement for research and development on underground deposition of *chemical-toxic wastes* which results from this comparison is formulated and explained. Finally, the possibilities of information transfer from the radioactive to the *chemical-toxic* field are indicated; hence, the results of the study may also be of interest to countries of the European Union without, or with only minor utilization of nuclear energy.

Research and development projects on the final deposition of *radioactive wastes* have been in progress in the **Federal Republic of Germany** for more than thirty years. In this work special emphasis has been placed on waste characterization, release behaviour, conditioning, final repository engineering, safety of final repositories, as well as site-specific investigations and associated matters. The performance and coordination of the investigations were concentrated in the field of activity of major research institutions as well as universities and industry.

In the field of deposition of *chemical-toxic wastes* research and development projects have been in progress on a large scale only for a few years. The major subjects of research are comparable with those for the final deposition of *radioactive wastes*. The present demand for research is especially high in the fields of waste characterization and release behaviour as well as the associated matters of geotechnical stability, safety during the operational phase, as well as long-term safety.

On the basis of the previous research in the field of final deposition of *radioactive wastes*, R&D transfer is feasible in nearly all major fields of research. Consequently, the decided separation between the final deposition of *radioactive wastes* and the deposition of *chemical-toxic wastes* is no longer present in the field of research policy. In some major fields of research, the formulation of the research demand is referred in the same manner to both *radioactive* and *chemical-toxic wastes* but, the extent of the necessary projects for the final deposition of *radioactive wastes* or *chemical-toxic wastes* will differ.

For waste disposal in a salt formation of both *radioactive waste* and *chemical-toxic waste* no existing facility is available in the **Netherlands**. In this way the problems are the same, thus the main parts of efforts already produced to calculate the conditions for a safe disposal of *radioactive waste* can be applied to *chemical-toxic waste* disposal. The equivalent of heat producing high active nuclear waste is not present in the chemical waste collection, meaning that disposal in deep boreholes for *chemical-toxic waste* is not needed. The engineering of the disposal facility in a saltdome is in principle about the same for both types of wastes. In both cases the concepts for disposal in rooms are preferred because of the retrievability condition. The extent of retrieval of wastes from an underground facility is not clear: all wastes or the most hazardous only.

For *radioactive waste* it has been decided in the **Netherlands** that above ground disposal is not suitable, for *chemical-toxic waste* such a decision has only been taken for high toxic C-1 wastes. The amount of C-1 wastes is by far too small (500-1000 tons per year) to think about a mined deep underground disposal. The much higher amount of wastes used in this study originates from economic reasoning to have incentives for mining by a private company.

The safety assessment studied for non-heat producing *radioactive waste* in the PACOMA contract is very useful to study *chemical-toxic waste* analog. The processes used for the description of the effects in the host rock and surroundings are the same. The studies on the effects of mixed wastes are important for the risk calculations of the chemical components.

The economics of waste disposal underground will have a large influence on the decision to perform the action of mining or not: the enterprise has to be a private one, and thus have a net profit. The conditions for underground disposal have still to be formulated; a law permitting waste disposal in the deep underground is not existing in the **Netherlands**. For *radioactive waste* the decision of how and where to dispose has been postponed for 50 to 100 years, for *chemical-toxic waste* such an action is not possible in view of the number of large interim storage facilities to be build.

Both an interim storage and a disposal mine construction means a large effort on public information to accomplish within a reasonable time the task to have the facility operational. The experiences in the nuclear field are not encouraging but of primary importance. The public reaction, the economics of waste disposal, and the legislation to be formulated are interdependent.

Title:	Study of a communication strategy aimed at achieving a possible better understanding of the consequence of radioactive waste management in well-defined group of public
Contractor:	ONDRAF/NIRAS, Belgium
Contract n°:	FI2W-CT90-0036
Duration of contract:	April 1991 - December 1994
Period covered:	January - December 1994
Project leader:	V. Vanhove

A. OBJECTIVES AND SCOPE

Starting from the hypothesis that the information of the public on radioactive waste management is confronted with prejudice and ignorance, the study tries to establish whether it is possible, by working out and disseminating an argumentation that is well adjusted to a specific target group, to reduce obstacles to information and to induce the public to understand and accept the approach of ONDRAF/NIRAS.
Phase 1 of the project (ended in June 1993) was aimed at working out and disseminating an argumentation well adjusted to 15-to-18 year old students, in order to reduce the obstacles to information and induce them to understand and accept our approach of radioactive waste management.
Phase 2 (July 1993 to the end of 1994) comprised the following actions:

a. the finalization of the prototype brochures and their official launching at national level, beginning of 1994;
b. an evaluation test prior to transmitting the information;
c. the announcement and distribution/launching of the educational package in the schools (15-to-18 year old students);
d. the development of a feedback system intended to evaluate the global project.

B. WORKING PROGRAMME

The programme of Phase 2 include three steps:

1. Introduction and pretest (July - December 1993)
Finalization of the pedagogical material (brochures, guided visits to the Information center in Dessel (province of Antwerp) on radioactive waste) and distribution of this material at a local level, training of the guides, working out and accomplishment of the pretests, announcement and preliminary information about the "Teaching project on radioactive waste" at a national level, development of the project evaluation system.

2. Operational phase and intermediate evaluation (January - December 1994)
Follow-up of the announcement of the "Teaching project on radioactive waste" at a national level, distribution of the pedagogical material, organization of visits to the Information center on radioactive waste, processing of the evaluation documents, announcement of the agenda for the school year 1994-1995.

3. Final operational phase and global evaluation (January - December 1994)
Follow-up of the operational actions and drawing-up of the final evaluation report.

C. PROGRESS OF WORK AND RESULTS OBTAINED

1. Announcement of the information project

The information project - which consists of two parts, on the one hand the information package and on the other hand the guided visit to Isotopolis, the Information center on radioactive waste in Dessel -, was officially launched in all subsidized secondary schools in Belgium on 1 January 1994. The official start was preceded by a national mailing action (in November and December 1993), addressed to the school boards in order to make the project known. This mailing comprised an explanatory letter, an information leaflet on the project and a poster for the teacher rooms or classes (copy enclosed).
In September 1994, at the beginning of the new school year, a reminder was sent to the schools with a view to planning the school trips and excursions.
In October 1994 the invitation was sent for the first reconnaissance visit for teachers, organized on 4 November 1994.
No less than 165 (?) teachers (135 Dutch - and 30 French-speaking) thus got acquainted with the information project of ONDRAF/NIRAS.
In order to make the project more widely known in educational circles, an advertisement was placed in "Scholen waarhenn, editie 1994-1995", a publication containing tips for school trips and excursions.

2. Guidance of the visits to Isotopolis

2.1. Job description

The job of the guides consists essentially in guiding and informing the visitors to Isotopolis. They work on a freelance basis for time periods of minimum 4 hours.

2.2. Profile of the guides

Preference was given to active people or people wishing to remain active after interrupting their career. Unexperienced people were not considered a target group, the risk of pulling out being too great. Moreover, the guides had to reside preferably in the Antwerp, Limburg and Brabant regions.
As for their personality, emphasis was laid on an open mind and the willingness to transmit the matter objectively to other people. Discipline was therefore also required.

The criteria according to which the candidates for the job of freelance guide were evaluated were :
* appearance / attitude
* charisma
* linguistic skills : polished speech, fluency, structured approach, accurate interaction, listening skill
* assertiveness
* social skills : interactive skills, team spirit

* motivation
* inquisitiveness
* willingness and ability to maintain objectivity

2.3. Recruitment and selection

In order to guide the visitors in Isotopolis, it was decided to appeal to self-employed freelance guides. Recruitment and selection of these collaborators were entrusted to an external recruiting agency (G. De Cock in Geel).

2.3.1. Recruitment campaign

In order to recruit new collaborators, it was decided to place an advertisement in the local newspapers in an area of 30 kilometers around Mol, and to send mailings to school boards in the provinces of Limburg, Antwerp and the region of Leuven announcing the vacancies (advertisement enclosed). This was done in June 1994. Moreover, an advertisement was broadcast by the regional TV channel "TV Kempen" (see appendix).

2.3.2. Selection

In order to screen the candidates, it was decided to opt for a two-phase procedure, more particularly a first screening on the basis of written applications, followed by a second screening based on daily sessions, during which the selected candidates were submitted in the morning to a group session and in the afternoon to an individual test. Every day, a group of maximum 10 candidates were invited. In the morning, group sessions were organized during which the candidates were submitted to a presentation exercise. During these sessions, group discussions were held and a limited number of personality tests were organized during which the required personality criteria and skills were screened. On the basis of the results of the morning session, several candidates were selected for an individual interview in the afternoon. A written report on the candidates thus selected was prepared and sent to ONDRAF/NIRAS.
The appropriate candidates were selected on 6 and 7 July 1994 and on 2 August 1994. Especially teachers from secondary education (only of Dutch origin) appeared to be interested in the job.

2.3.3. Reactions

In total, around 60 candidatures were received, about 40 of which were declared admissible. 5 % of the candidatures originated from early retired persons from the Mol-Dessel region (SCK/CEN, FBFC, Belgonucleaire). Approximately 22 % of the candidatures came from job seeking students or recently qualified students. These candidatures were declared inadmissible. The remaining 72 % originated from teachers of secondary education.
Finally 18 candidates (16 Dutch- and 2 French-speaking) were selected and admitted for training. They were notified in writing.

2.4. Training programme

A training programme, focused on both the technical and pedagogical aspects of the job, was organized in August and September 1994.
The basic programme consisted of two parts : on the one hand, a pedagogical training intended to prepare the candidates for public interaction, presentation techniques, etc. and on the other hand, a technical training intended to make them acquainted with the necessary technical background information. The basic programme is completed by permanent training on a monthly basis.
During the month of August 1994, technical training was organized. Pedagogical training was organized as close as possible to the start of the visits, i.e. in September.
All documentation material used during these training sessions, was compiled in a syllabus which was made available to each guide and will be completed according to the evolution of the management activities.

2.4.1. Technical training programme

The technical training programme was structured around various subaspects of radioactive waste management. It was conceived as a basic programme that can be studied in depth later on. The themes dealt with were :

* radioactivity and radiation protection (theory and practice)
* radioactive waste management (visit to the processing and storage facilities of Belgoprocess in Dessel)
* disposal (information session and visit to the underground laboratory HADES)

2.4.2. Pedagogical training programme

This programme comprised three phases :

* Phase 1 : preparatory practice session (body language and overall presentation), including more details on the information strategy and project
* Phase 2 : try-outs, i.e. practical testing of the prototype speeches on the various modules in Isotopolis
* Phase 3 : intermediate evaluation

In order to make the trainings as efficient as possible, it was decided to work with small groups of maximum eight persons. The programme was outlined on the basis of two groups of Dutch- and one group of French-speaking visitors.

Besides the overall selection criteria, specific assessment criteria were applied, more particularly :

* regarding structuring, completeness, clear and logical structure in accordance with the text of ONDRAF/NIRAS
* regarding linguistic usage and style
* speaking technique
* non-verbal behaviour
* contact with the public
* didactical approach
* conformity with the fixed time-limits

By October 1994, the guides were ready for their hob and started functioning in their new environment.

2.5. Extension visit Isotopolis

By the end of 1994, the visit to Isotopolis was extended with a short visit to the processing facility CILVA and the storage building for conditioned low-level waste on the Belgoprocess site, in the immediate vicinity of Isotopolis. A closed camera circuit and a technical replica enable the visitors of CILVA to from a realistic picture of the various stages of solid low-level waste processing. The storage of the conditioned low-level waste drums can be observed through two lead glass windows, which leaves a significant visual impact.

2.6. Number of visits

In 1994, 5 000 students from higher secondary education (around 140 schools) visited Isotopolis (details : see appendix).

2.7. Evaluation of the visits

During a first qualitative evaluation of the information project in 1993, the project was generally described as a good initiative. The whole project - composed of the information package "Wet jij wat er in België met radioactieve afvalstoffen gebeurt?" and Isotopolis - received 8,4 marks out of 10 from the people interrogated. The same result was obtained in 1994. 95 % of the young visitors found the subject and the exposition very interesting. 97 % of them affirm to have acquired more knowledge and insight in the matter.

Thanks to the concrete and visual information it provides, Isotopolis is considered to be the most pleasant part of the information project. The combination "information package + Isotopolis", however, obtains the best result as far as the educational aspect and the completeness of the information are concerned.

In 1994, the evaluation of the visits was further systematized by means of a questionnaire distributed after the visit and by organizing a school competition, to which a cheque of 50,000 BEF per region (one for Flanders

and one for the Walloon provinces and German-speaking Belgium) was attached. This competition was organized for the first time during the school year 1994-1995.
An overall review of the evaluation of the information project over a longer period is being prepared for the end 1995.

APPENDIX : Number of visits

The project was announced by direct mail to 1200 secondary schools in Belgium in December 1993.

During the period from 1 January to 31 December 1994, 138 schools participated in a guided visit to the information centre ISOTOPOLIS.
The North of Belgium was represented with 122 schools, totalling 4387 students. For the French speaking part of the country 16 schools and 594 students were counted.
The number of visits per month increased steadily from January on (9 schools) to May (31 schools), declining towards the summer holidays and with regular visits in the autumn period (10-15 schools per month).

The location of the information centre in Dessel has an impact on the geographical origin of the schools that apply for a guided visit. For the North, one third (42) of the schools came from the Antwerp province while the farthest province of West-Flanders participated with 7 schools. This sensibility is less important for the South where the differences are less outspoken.

As to the orientation of the classes, some disciplines showed a higher interest for the subject than others. As could be expected, the science oriented classes were better represented than others. This means that science, physics, chemistry teachers found it more interesting to include this visit in their programme.

Teachers and students all received a full information package after the visit and were asked to express their personal evaluation of the project.

Title :	Information of the public in the field of decommissioning waste. Study of strategies and means for specific information
Contractor:	CEA Saclay - DCC/UDIN
Contract N°:	FI2W-CT90-0043
Duration of contract:	June 1991 - May 1994
Period covered:	
Project leader:	F. Lambert

A OBJECTIVES AND SCOPE

DCC/UDIN is the nuclear installations dismantling unit of CEA and manages most of its waste. The nature and importance of the waste justifies public information. UDIN is in good position to yield technical and economical information.

The first step of the work consists in searching and defining a good media dissertation and producing a pilot operation of communication.
The results expected will form a practical contribution to solve sociological problems issued by waste management, whether they are hazardous or not.
The economical benefits expected from this information will be tied to human analysis, positive and intelligent, in solving conflicts related to waste management in the European Community.

To answer public needs for information, several partners were selected :

- University of Paris-Orsay to translate technical information into common ("popular") language.
- A group of sociologists explore and explain the fears and hopes of the public.
- A movie maker skilled in technical, didactic and TV films.

B WORK PROGRAMME

The programme of the study is approximately structured according to the following steps :

B1 : Selection of partners, define basis of discourse and iconographic data; evaluation of application to actual dismantling plants (e.g : G2-G3, Rapsodie).

B2 : Analysis of similar actions evolving in other fields; investigation of results, definition of the basis of the discourse.

B3 : Investigation of different fields; selection of targeted public; acceptance of such a public; approach and motivation of (media) "atypique" persons and evaluation of their reactions to the proposal discourse.

B4 : Methodology of pilot operation : study of original communication charter; meetings with support producers.

B5 : Development of adaptation operations and validation of the elaborated processes.

B6 : Final Report with global recommendations. Drafting of Annexes according to the discourse and transposable actions.

C PROGRESS OF THE WORK AND OBTAINED RESULTS

The status of progress has not been forwarded to the Commission for 1994.

Title	The evolution and implementation of a public information strategy on radioactive waste managment
Contractors	GCI Group, 1 Chelsea Manor Gardens, London, SW3 5PN
Contract N°	FI2W-CT90-0074
Duration of contract	July 1991 - June 1995
Period covered	January - December 1994
Project leader	M. McAvoy, R. Gilbert

A. OBJECTIVES AND SCOPE

The study concerns creating better public understanding of how radioactive waste is managed throughout the European Union. The programme objectives can be summarised as follows:

- To encourage a better understanding of how radioactive waste is managed across the EU and recognition of the role that DG XII plays.

- To encourage the exchange of information on communication practice between national radioactive waste agencies in Europe.

- To develop a series of authoritative communication tools for use by national radioactive waste management agencies.

Mass communication with the public across the EU has not be considered either appropriate or feasible. Resources have been directed at opinion formers and communication materials have been channelled through national waste agencies, utilising their established infrastructures.

B. WORK PROGRAMME

The 1994 programme of activities has been concerned with the development of an educational programme based on a multimedia interactive exhibition. The overall aim is to increase understanding amongst school children of the issues relating to nuclear waste.

Why an interactive exhibition?

Research - The starting point

Research conducted by GCI Group showed that:

- A great deal of educational materials for schools fail to meet the needs of school children
- Radiation is a difficult scientific concept
- The subject of radioactive waste management is not covered in most European country school curriculae
- The issue of radioactive waste management is not addressed in a socio/economic and environmental context.

The resultant educational strategy developed for DG XII by GCI has been to circumvent curricula limitations by developing and constructing a state-of-the-art exhibit to be positioned in European science museums to provide a balanced information resource on the radioactive waste issue.

1994 activity has been focused on the development, production and launch of the interactive exhibition - "The Challenge".

The exhibition is based on a detailed multi-media software programme using video footage, still photographs, text and touch screen technology to ensure full interaction with the participant. The exhibition is also accompanied by three "hands on" display panels.

The topic areas to be covered in the program were carefully researched, a comprehensive computer script developed and the content finalised in conjunction with DG XII. The script is divided into three key areas:

1. radioactivity
2. current waste management practice
3. options for long term future disposal

GCI sourced all visual material used in the exhibition, including video footage from a variety of nuclear industry sources. All aspects of the design and build stage of the exhibition were managed by GCI, in addition to close supervision of the accompanying software program development.

GCI also ensured that the exhibition contents received a thorough evaluation from educational experts to ensure that the exhibition fully meets the needs of both children and teachers. The exhibition contents was also evaluated by an independent nuclear expert to confirm its scientific accuracy.

C. RESULTS

With the aim of achieving maximum flexibility, the exhibit is:-

- **Fully adaptable to all sites:** versions of the exhibit range from 65m² to a single computer terminal; fully adaptable to all European languages (currently available in English, French and German)

- **Multimedia:** incorporating text, video, still photography, touch screen software, "hands on" interactive modules, exhibition panels, sound and light effects.

- **Attractive** to children: the design incorporates video arcade appeal with computer game technology, is customised to "speak" to each child; the design is based on the principle that "science is fun", a scientifically difficult subject is made vivid and enjoyable.

- **Measurement:** the interactive nature of the exhibition ensures that the user is constantly inputting opinions and answering questions. This data is captured by the software programme and analysis of the results will provide useful guidance on young people's attitudes to the issue and an indication of the success of the exhibit as a whole.

Edinburgh International Science Festival

The exhibition was launched at the Edinburgh International Science Festival in March/April 1994. The Edinburgh International Science Festival is the largest and prestigious science festival of its kind in Europe and is visited by over 50,000 children in the four week period.

Although a detailed analysis of the exhibition's use still needs to take place, it is clear that the exhibition was visited by a considerable number of school children and that the average stay time appears to be in the region of 12 minutes - a considerable amount of time for an exhibition of this kind. The exhibition was visited by Princess Anne and the exhibition organisers confirmed the exhibit's popularity and emphasised its important contribution to the overall success of the year's Science Festival.

Current Status

The exhibition is currently at the Isotopolis visitor centre, near Dessel in Belgium, operated by the Belgian radioactive waste agency ONDRAF/NIRAS, playing an important role in their educational programme.

Title :	Transmutation of long-lived radionuclides by advanced converters
Contractor:	Siemens AG Power Generation Group (KWU)
Contract N°:	FI2W-CT91-0103
Duration of contract:	1 October 1991 - 31 December 1994
Period covered:	1 January 1994 - 31 December 1994
Project leader:	Dr. Udo Wehmann

A Objectives and Scope

The study will analyze the possibilities, limits and technological development steps needed for the transmutation of actinides and long-lived fission products in unconventional advanced reactors and other advanced transmutation devices. The notation "advanced reactor" means fast reactors with unconventional fuel of faster neutron spectrum or smaller units, which mainly would be constructed for transmutation. The other transmutation devices are accelerator driven spallation machines and fusion reactors.

This study is one part of a coordinated partitioning-transmutation study of a group of organisation: CEA, AEA Technology, Belgonucléaire, ECN Petten and Siemens.

B Work Programme

1. Minor actinide transmutation in large fast reactors with MOX and metal fuel, fast spectrum and high axial leakage.
2. Minor Actinide transmutation in fast reactors with small power units.
3. Burning of plutonium in fast reactors and high temperature reactors.
4. Transmutation of fission products in fast reactors.
5. Influence of Lanthanide admixture to the fuel of fast reactors.
6. Transmutation capabilities of spallation machines and fusion reactors.
7. Preparation of the final report.

C Progress of Work and Obtained Results

C1 State of Advancement

The contract ended at the end of 1994. The work programme has been finished and the final report has been prepared.

C2 Progress and Results

In the following the main results and conclusions outlined in the final report will be given.

The main part of the work on transmutation of long-lived radionuclides dealt with the potential of fast reactors to transmute the actinides and the long-lived fission products Tc-99, I-129 and Cs-135. In addition to that, studies were performed on the possibilities to burn plutonium in fast reactors and high temperature reactors, and the transmutation capabilities of spallation systems were investigated on the basis of a literature study.

Concerning the capabilities of fast reactors to transmute the Minor Actinides (MA) the following points can be made:

- The concepts of homogeneous and heterogeneous recycling of MA have similar transmutation efficiencies: 30 to 35 % of the initial MA content are transmuted during a subassembly life-time of 6 years. Therefore multiple recycling will be necessary for a quantitative reduction of the MA masses.

- Small cores are less efficient than larger cores because of their lower neutron flux level. But they have the advantage to limit the positive sodium void effect, which is increasing with increasing MA content, to acceptable values.

- An upper limit of 5 % is recommended for the homogeneous recycling which limits the deterioration of the sodium void effect and the Doppler effect to an acceptable level.

- Special attention has to be paid to the build-up of Pu-238 in the fuel which reaches about 7 % of the total Pu in case of 5 % MA content. This requires efficient measures for shielding and cooling during refabrication.

- The concept of heterogeneous recycling is recommended for further investigation since it limits the number of MA containing subassemblies to a small amount (about 5 % of all fuel subassemblies) and since it avoids the strong deterioration of the sodium void effect and the Doppler effect. The content of Pu-238 is however extremely high in this concept so that special shielding and cooling measures are necessary for the refabrication route.

The comparison of oxide and metal fueled fast reactors with respect to their transmutation efficiency has shown no clear advantage for one of the concepts. Due to the larger MA mass in the fresh metal fuel, which results from its higher fuel density, the transmuted mass per year is about 20 % higher than for oxide fuel. But the relative changes per year are slightly larger in the oxide fuel and the transmutation half-times are consequently slightly smaller, both being close to 11 years. The further reduced Doppler coefficient of the metal fuel cores is certainly an advantage in unprotected loss-of-flow and loss-of-heat-sink accidents, but the power coeffi-

cient becomes very small in these cores so that the power increase in case of unprotected transient overpower accidents is by a factor 2 to 3 larger than in oxide cores. Therefore detailed safety studies are necessary to judge about the feasibility of MA admixture to the metal fueled cores.

The influence of the Lanthanides (LA) , which are difficult to be separated from the MA, on the core properties of fast reactors has been studied. It was shown that their influence is similar to that of the MA. Therefore the 5 % limit mentioned above for the MA content has to be extended to the contents of MA plus LA. In order to reserve most of these 5 % for the MA, very efficient techniques for the separation of the Lanthanides have to be developed.

The transmutation of the long-lived fission products Tc-99, I-129 and Cs-135 in fast reactors has been investigated on in-core and peripheral positions and by varying the content of moderators in order to increase the capture cross-section of these isotopes. The main results are:

- The cross-section of Cs-135 is too small even in case of optimum moderation so that there is no chance to transmute this isotope in a fast reactor.

- The transmutation rates of Tc-99 and I-129 can be enhanced by the choice of an optimum moderator content (about 10 % $ZrH_{1.8}$ on in-core positions and about 20 % on peripheral positions), but the transmutation half-times are too large in both cases. They are in the range of 40 to 60 years on peripheral positions and of 20 to 40 years on in-core positions. Since for an effective reduction of the fission product inventories at least 5 half-times would be necessary, irradiation times of more than 100 years would be required.

Taking all these results together leads to the conclusion, that fission product transmutation in fast reactors does not make sense.

The burning of plutonium has been investigated for the fast reactor and the high temperature reactor. It has been shown that the fast reactor with the present state of knowledge of reprocessing can burn about 55 kg/TWh. Assuming that the problem of solubility of the fuel during reprocessing can be solved for Pu-enrichments of up to 45 %, the rate can be extended to 80 kg/TWh. This corresponds to the LWR production of 3.5 GWe.
The capabilities of the high temperature reactor (HTR) are similare to those of the fast reactor in terms of kg/TWh. But for the HTR these values correspond to much larger relative changes which means that the plutonium is burning down much stronger during one residence time (by about 75%). But if the mass of plutonium shall be reduced quantitatively, some further recyclings would be necessary also in the HTR.

The literature study on different spallation systems (ATW of Los Alamos, PHENIX of BNL, JAERI system) and their intercomparison has shown that they are very efficient transmutation devices. But there are several aspects which need clarification before a feasibility statement can be made. They mainly concern the feasibility of the intense high-energy accelerator beam in non-pulsed operation, the verification of the claimed safety advantage of the subcritical system and the solution of the material problems linked with the irradiation by high energy particles.

C3 List of Publications

U.Strehlen, U. K. Wehmann
Influence of Lanthanides on fast reactor core parameters
CEC Progress meeting on "Partitioning and Transmutation Studies", Brussels, March 29, 1994

U. K. Wehmann
Potential of fast reactors for transmutation of Actinides and long-lived fission products
3rd OECD International Information Exchange Meeting on Actinide and Fission Product Partitioning and Transmutation, Cadarache, December 12-14, 1994

Title	Participation in a CEC strategy study on nuclear waste transmutation
Contractors	ECN (NL); Belgonucléaire (B)
Contract N°	FI2W-CT91-0104
Duration of contract	November 1991 - March 1995
Period covered	January 1994 - December 1994
Project leader	K. Abrahams (ECN, coordinator); S. Pilate (Belgonucléaire)

A. OBJECTIVES AND SCOPE

This contract has first of all as an objective the improvement of the nuclear data base for inventory calculations, which are needed in strategy studies on nuclear waste transmutation. A second contribution to the CEC strategy study will be in the form of a paper on: "Transmutation of long-lived fission products as a means of reducing the leakage dose risk of stored nuclear waste". In this way the Netherlands Energy Research Foundation ECN intends to contribute to international evaluations of recycling options for the nuclear waste problem. Its program RAS for the study of "Recycling Actinides and Fission Products" is focused on studies on strategies and scenarios, on reactor physics research, on small scale demonstrations of possibilities for transmutation, and on the nuclear parameters, which are relevant to this.

Since November 1993 Belgonucleaire has joined these efforts of ECN as sub-contractor. In an associated study Belgonucleaire identifies the possibilities as well as the constraints and limitations for a programme of recycling waste products in PWR reactors of current design with MOX fuel. This study subdivides into three parts, related respectively to the physics of recycling actinides, to the impact on fuel fabrication, and to the physics of recycling fission products. The present contract is in turn placed in the frame of broader CEC strategy studies on nuclear waste transmutation, together with contracts to CEA, Siemens, and UKAEA.

B. WORK PROGRAMME

2.1 Preparation of a nuclear data base for actinides and fission products, which is needed for the experimental verification of technological aspects of transmutation

2.2 Preparation of derived data in order to assess the ORIGEN nuclear data library for transmutation studies.

2.3 Performing sample burn-up calculations for several scenarios with the updated ORIGEN nuclear data library.

2.4 Investigation of possibilities of transmutation of long-lived fission products, and Physics of fission products recycling (associated study by Belgonucleaire)

2.5 Extended feasibility study for the transmutation of fission products

2.6 Physics of actinide recycling (associated study by Belgonucleaire)

2.7 Impact on fuel fabrication (associated study by Belgonucleaire)

C. PROGRESS OF WORK AND OBTAINED RESULTS

State of advancement

All Community contracts mentioned under A regard possibilities to reduce the long-term radio-toxicity of nuclear waste. The ECN work is focused on the preparation of common data sets and standardized libraries for relevant nuclear data as well as on a study of possibilities for transmutation of long-lived fission products. The original contract expired November 1993, but it was extended to allow more time for in-depth studies of fission product transmutation and for an extension of the work on validation of the working libraries. At the same date Belgonucleaire was associated to the ECN contract with studies on usage of MOX fuel for transmuting plutonium and americium.

Multiple (successive) recycling of Am and Pu in the form of a homogeneous extended MOX fuel $(UPuAm)O_2$ has been considered. Attention has been paid to the composition and the reactivity on voiding in a PWR in case of once, twice, and three times recycling. With compositions resulting from these calculations the dose rates has been derived for some critical stages of fuel fabrication and the necessary extra shielding as well as the margins to criticality have been evaluated. Recycling the long-lived fission products Tc-99 and I-129 in target pins in PWRs. Calculations by Belgonucleaire have been performed in close cooperation with ECN.

Work programme 2.3 (Sample burnup calculations)

MOX Benchmark BN-ECN

In order to assess the capability of the WIMS86 library for transmutation studies on MOX fuel, a burnup benchmark on MOX fuel has been defined by Belgo-Nucléaire (BN). ECN contributed to this benchmark, and performed calculations with the SAS6 burnup driver code with cross sections from a library based on the JEF2.2 file. BN performed calculations with the WIMS code system with cross sections from the WIMS86 library. The reactivity of MOX fuel and one-group cross sections have been compared as a function of burnup, as well as the nuclide densities at discharge burnup of 45 GWd/tHM. The ECN contribution to this benchmark has been reported in reference 1. The results of BN and ECN have been gathered by BN, and reported in the BN memo 9402961/220. From this benchmark, it followed that the predicted reactivity of the MOX fuel is higher when the JEF2.2 library is used then when the WIMS86 library is used. The differences vary from 900 pcm at begin of life to 1800 pcm at discharge (45 GWd/tHM). These differences are mainly due to differences in cross sections: the neutron capture cross sections of Pu-239, Pu-241 and Pu-242 have lower values in the JEF2.2 library, while the fission cross sections of Pu-239 and Pu-241 have higher values. Furthermore, it turned out that for Pu-242 in the WIMS86 library, only cross sections at infinite dilution are given. As a result of these differences, the Pu-242 concentration at discharge is about 20% lower when calculated with the WIMS86 library. The concentrations of the activation products of Pu-242 (like Am-243 and the Cm isotopes) calculated with the WIMS86 library are about 20 to 30% higher than the concentrations calculated with the JEF2.2 library.

The results of this benchmark should be interpreted with care, because differences can also be due to the calculational methods. As a result of this benchmark, it is advised to use the WIMS86 library with care when calculations on MOX fuel have to be performed.

However, it is also proposed to further assess the accuracy of the plutonium cross sections in the JEF2.2 file in order to be sure that these cross sections are accurate and correct.

Transmutation of Americium in thermal neutron flux

In a previous phase of the contract, new cross-section data libraries for transmutation studies were made, which can be used by fuel depletion codes like ORIGEN-S. This work has been described in reference 2. In 1994, sample calculations on transmutation of americium in thermal reactors were made using these new libraries. Extensive results can be found in references 3 and 4. Transmutation of americium in thermal reactors can be advantageous for two reasons: reduction of the possible dose to the population due to leakage of americium and its daughter products from underground disposal sites, and reduction of the total radiotoxic inventory of underground disposal sites.

When americium, which mainly consists of Am-241, is irradiated in a thermal neutron flux, almost all americium is transmuted to Am-242 (90%) and Am-242m (10%). The latter component is easily fissioned in a thermal neutron flux, because Am-242m has a high fission cross section and a long half life. The production of Am-242, however, leads to Cm-242, which decays to Pu-238 with a half life of 163 days. When Pu-238 captures another neutron, fissile plutonium isotopes are produced which can subsequently be fissioned. Due to the half life of Cm-242 of 163 days, americium has to be irradiated in a reactor for quite a long time to let the Cm-242 decay to Pu-238. Furthermore, the thermal neutron flux should be relative high to produce quickly fissile plutonium isotopes, directly after the Cm-242 has decayed to Pu-238. It is shown that when americium is irradiated for about three years in a high thermal neutron flux of 10^{14} $cm^{-2}s^{-1}$, a considerable reduction of the actinide mass is achieved. Then, about 70% of the initial actinide mass has been fissioned. The reduction of the radiotoxicity is less spectacular, because a part of the initial americium is transmuted to Cm-244, which is difficult to fission, and which is very radiotoxic. However, between 100 and 2,000 years of storage, the radiotoxicity of the americium sample is reduced with about a factor of ten, when the sample is irradiated for three years in the above mentioned thermal neutron flux.

A calculational study has been performed on irradiation of an americium sample in the Petten High Flux Reactor (HFR), to show the applicability of this transmutation scheme. It is shown that the initial americium density in the target should be low (about 0.4 g cm^{-3}) to limit the fission power in the sample and to enhance the transmutation of the americium. These results are also reported in reference 4, and in reference 5.

Work programme 2.4 (Transmutation of long-live fission products, ECN)

Transmutation of Tc-99 in various reactor types has been considered. The reactor types considered were a Heavy Water Reactor (HWR) like CANDU, a Liquid Metal-cooled Fast Breeder Reactor (LMFBR) like Superphénix, and a Light Water Reactor (LWR). Short descriptions of the results will be given here, more extensive results are given in ref.[6].

For the first reactor, a CANDU reactor with a power of 935 MWe was used as a reference design. Three options have been considered: transmutation of Tc-99 in the centre fuel pin in each fuel bundle, transmutation of Tc-99 in the outer fuel ring of some fuel bundles, and transmutation of Tc-99 in the moderator between the fuel bundles. The Tc-99 core loading in all cases was equal to 4.1 tonnes. The third option turned out to be the best one for transmutation of Tc-99 in an HWR, because the thermal neutron flux is highest in the

moderator between the fuel bundles. If 4.1 tonnes of Tc-99 is put in target pins in the moderator between the fuel bundles, the transmutation rate is 115 kg/a, which implies a transmutation half life of about 25 years.

The fast reactor (for which the Superphénix reactor with power of about 1200 MWe was used as a reference) turned out to be more promising. For this reactor, transmutation of Tc-99 in the inner core has been considered with the Tc-99 target pins put either in a moderated subassembly or in a non-moderated subassembly.

The first option (transmutation in a moderated subassembly) gives a relatively high transmutation rate of 122 kg/a with a transmutational half life of about 15 years when 2.7 tonnes of Tc-99 are loaded in the core. A disadvantage of this option is the effect of power peaking in adjacent fuel pins, which has to be addressed at (e.g. by decreasing the plutonium fuel enrichment in fuel pins adjacent to the moderated subassembly).

The second option (transmutation in a non-moderated subassembly) leads to a transmutation rate of about 101 kg/a when the Tc-99 core loading equals 2.7 tonnes. This implies a transmutation half life of about 18 years. The advantage of this option is the absence of any power peaking effects in adjacent fuel pins. However, its transmutation capability is slightly less than that of the first option.

Finally, transmutation of Tc-99 in an LWR has been considered. For this purpose, a 900 MWe PWR was chosen as a reference reactor, fuelled with either UO_2 fuel or with 1/4 MOX fuel and 3/4 UO_2 fuel. Target pins made of Tc-99 mixed in a neutron inert matrix were supposed to be positioned in the control guide tubes of the reactor. In the first case (UO_2 fuel), the Tc-99 pins were supposed to be positioned in all control guide tubes, in the second case (1/4 MOX fuel) only in the control guide tubes of the MOX fuel.

The first case turns out to be much better than the second one, which is caused by the softer neutron spectrum in UO_2 fuel compared to the relative hard neutron spectrum in MOX fuel. The transmutation rate of Tc-99 with a density of 10.5 g cm^{-3} reaches about 92 kg/a when 7.6 tonnes of Tc-99 are loaded in the core. This implies a transmutation half life of 57 years. When the density of Tc-99 decreases, the transmutation rate decreases due to the lower Tc-99 core loading, but also the transmutational half life decreases. With a Tc-99 density of 1 g cm^{-3}, the transmutational rate of Tc-99 becomes about 24 kg/a with a core loading of 730 kg of Tc-99. This implies a transmutational half life of 21 years.

For Tc-99 loaded in the control guide tubes of the MOX fuel, the transmutation rate of Tc-99 with density of 10.5 g cm^{-3} reaches about 17 kg/a with a core loading of 1.9 tonnes of Tc-99. This implies a transmutational half life of 77 years. When the Tc-99 density is reduced to 1 g cm^{-3}, the transmutation rate becomes 4 kg/a with a core loading of 180 kg and a transmutational half life of 31 years.

From the above mentioned results can be concluded that it will be very difficult to transmute Tc-99 in large quantities (> 100 kg/a) in a reactor with a power of about 1000 MWe with a transmutational half life less than 20 years. In all cases the Tc-99 core loading has to be very large (several tonnes), compared to the Tc-99 production of a 1000 MWe PWR, which is about 20 kg. This means that transmutation of Tc-99 in fission reactors will be very difficult to achieve in practice.

Work programme 2.4 (Recycling of Tc-99 and I-129 in PWRs, Belgonucleaire))

It has been studied wether existing PWRs can be used to transmute the long lived fission products (LLFPS) Tc-99 and I-129. Two methods of recycling have been investigated:

- Heterogeneous recycling, with the LLFP placed into target rods without fuel. These rods are then placed into the guide tubes of a standard PWR assembly.

- Homogeneous recycling, with the LLFP mixed homogeneously through all the fuel of the PWR assembly.

The fissile content of the fuel (UO_2 or MOX) has not been changed in case of heterogeneous recycling. For this special case clusters of targets were assumed to be removable. In the case of homogeneous recycling the cycle length has been kept constant by changing the fissile content of the fuel.

Calculations have been done on a macrocell, which represents four quarters of different assemblies of the core. One of these receives the fission products. The transmutation rate has been calculated by simulating an irradiation of four cycles of the assemblies that contain the LLFPs. Other parameters like the incidence on the power and on the form factor of the host assembly have been investigated. Safety characteristics of the host assembly were acceptable, but the transmutation rates are very low. In case of homogeneous recycling in UO_2 fuel, the more efficient way showed a transmutation rate of 4.5 % per year for Tc-99 and 2.1 % per year for I-129.

Work programme 2.5 (Extended feasibility study of fission product transmutation)

Transmutation scenarios have been judged in a comparison of benefits for transmutation of actinides and fission products, as based on the following criteria:

1) Exploitation of the full energy content of the actinides should reduce fuel costs and streams of waste from mining as well as from spent fuel.
2) Future proliferation risks could be eliminated by actinide transmutation as otherwise some of the untreated actinide waste might transforms itself into a manageable form of partly fissile matter by decay of short-lived products, and disposal sites might become attractive actinide mines.
3) Dose-risks by leakage of mobile elements like Rn-222 and the metalloid fission products technetium and iodine could be reduced and this argument applies for actinides as well as for fission products.

Because transmutation of fission products is mainly motivated by the wish to reduce dose-risks, a thorough study has been made of the third criterium mentioned above. As long as the integrity of a disposal site is guaranteed, *long-lived fission products will determine the leakage-risks* (products of toxicity and mobility). For an unperturbed granite repository [7] table 1 shows the risk due to spent LWR fuel in a once through scenario [8]. It is seen from this table that the unspent uranium would give the main residual actinide contribution, and that Tc and I-129 dominate dose-risks. Diffusion of anions of iodine and per-technate in ground water is more rapid than flow of the ground water itself, as is now again being realized.

TABLE 1: TIME-INTEGRATED LEAKAGE-DOSE DUE TO SPENT LWR FUEL
(direct storage of spent fuel, due to nuclear generation of one GW(e) year)

Period :	One million years	Hundred million years
Nuclides :		
Tc-99	98 %	46 %
I -129	2 %	1 %
Cs-135		24 %
U -235		6 %
U -238		14 %
Np-237		5 %
Pu-239		4 %
man Sv *)	9000	20 000

*) Collective dose for the global population. The average yearly individual dose may be obtained by dividing by the affected number of people and the indicated period.

Any collective dose rate could be compared with the natural rate from radon, and even for the most relevant long-lived fission product Tc-99 the collective dose-risk is marginal. If it can be assumed that in due time the Tc will distribute itself evenly in time and space over the world, a value around 10^{-12} Sv/year would be the magnitude of the personal average dose-rate due to electro-nuclear production of one GW(e) year. This value corresponds to about one part per billion in terms of natural radon dose-rates.

Arguments on the collective leakage-dose should be treated with some caution. First of all it is questionable whether the risk should be ranked as in table 1 (a collective integrated dose from leakage out of a repository). If one would for example rank according to the highest possible individual dose, the I-129 risk could dominate for repositories of clay [9] or rock salt [8]. Local dose-risks are almost entirely due to uptake of iodine in the thyroid. This gland usually contains about 10 mg of iodine, and risks could be made marginal by diluting the I-129 isotopically with natural iodine. It further has been shown (see fig.1) that - in contrast to table 1 - leakage doses may be dominated by U-234 in recycling scenarios.

Reductions of collective dose-risks, which are far below the natural dose-risks seem at first sight to be of less relevance. In proper disposal scenarios the world- and time-integrated collective dose from fission products is less than 10 000 man Sv for each GWe year, and thereby less than a fraction 10^{-9} of the natural dose risk. Resistance against the dumping of low-level nuclear waste into the ocean has shown that there are incentives to reduce the dose even below such marginally small values. These incentives seem hardly motivated by the wish to reduce dose risks to human beings, and in this respect it is illuminating to recall the argument on the dose risk from the fission product I-129, for which other people argue that "isotopic dilution with natural iodine should reduce the highest individual doses". As long as no agreement exists on existence of safe thresholds for dose-risks, priorities are a matter of taste, and are therefore subject to changes. As storage of actinides hardly complies with present public demands for waste disposal, any acceptable end-scenario should be terminated by the fission of the most dangerous actinide

waste. This could only be achieved by means of an extended use of fast reactors, which however also yield increasing amounts of potential radon-emitters in the waste such as U-234, Pu-238, or Cm-242. It has not yet been shown that the present scenarios for reduction of the actinides fulfil the third criterium mentioned upfront of this chapter. Release of potential radon emitters in the waste should be guarded against in any scenario, and it might be conceivable to recycle the spent uranium (REPU) together with the other actinides. The scenario in which it is most likely that all the uranium will be recycled, is the Th/U breeding cycle. Only if the major dose-risks from radon could be controlled, transmutation of Tc-99 and I-129 could become worthwhile.

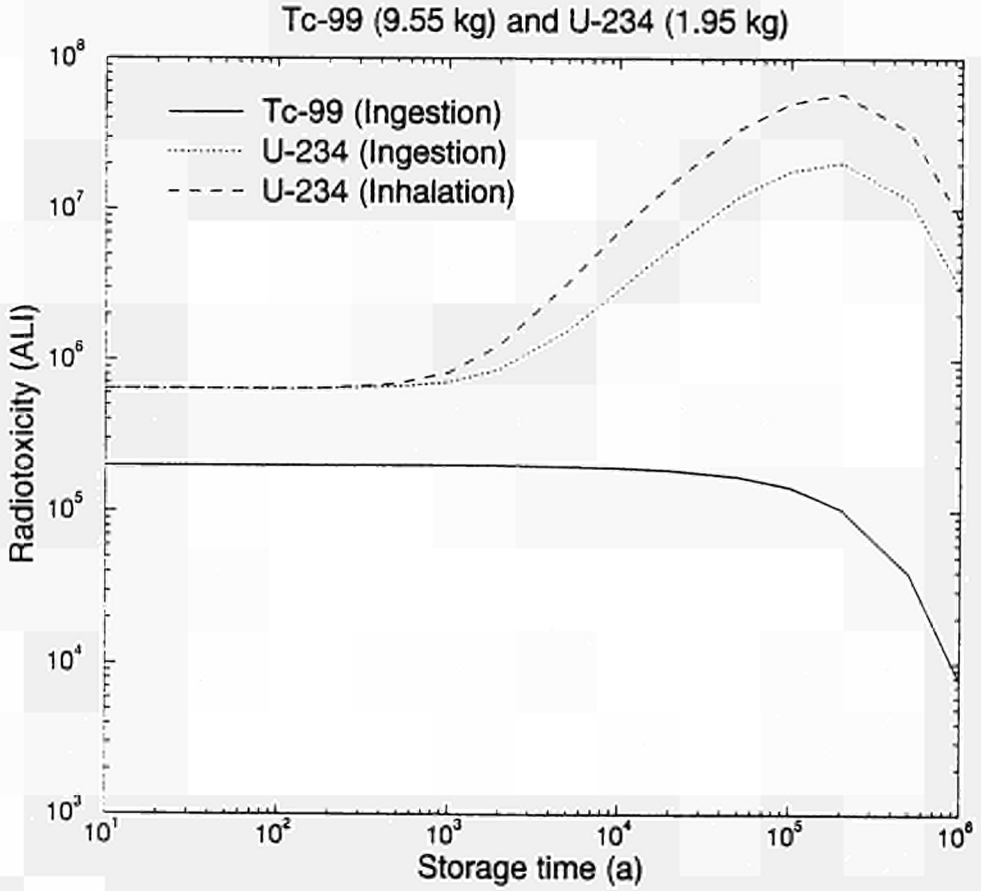

Fig.1: The radio-toxicity of Tc compared to that of U-234 and its daughters. The amount of material (9.6 kg of Tc-99 and 2 kg of U-234) is related to the yearly release of the Dutch reactor at Borssele (0.5 GW(e)).

Figure 1 shows for comparison the radio-toxicity of the Tc and the U-234, as these are released yearly by the Dutch reactor at Borssele (0.5 GW(e)). It should be noted that the dose-risk follows the radio-toxicity as given in the figure 1 if it is multiplied by the fraction of the material, which will reach the human biosphere. This might amplify the relative hazard of the U-234 considerably, as the geo-chemical mobility of radon is higher than that of technetium, and the reprocessed uranium (REPU) will only be subjected to shallow land burial in present scenarios. Therefore it is clear that the U-234 and its radon emanation leads to a much higher dose-risk than the corresponding amount of technetium, especially after a few thousand years when the extremely mobile radon-gas will be liberated by the radium, which has been formed in the mean time.

Due to the fact that U-234 will in the long run lead to mobile Rn-222 one could for example double the local dose due to emanations for a few hundred thousand years by spilling only a few hundred milligrams of U-234 or one of its precursors into the soil over a surface of only a few square kilometres. This isotope of uranium, which also occurs naturally (with an isotopic abundance of 0.0055 %) is responsible for most of the present radiation dose to mankind. Its most dangerous daughter Ra-226 has a half life of 1600 year, and about 60 t of radium in the soil emanates almost 6 litre of radon each day, which builds up an equilibrium value of about 20 litre of radon in the total biosphere of our planet. This tiny amount nevertheless contributes for about 60 % to the total radiation dose, which averages to about 10^{-3} Sv per person yearly and this leads to an estimate of the collective dose of the order of $5 * 10^6$ man Sv/year. It would be environmentally very unwanted if the present amount of U-234 would increase, and it might very well be that build-up of U-234 in the soil gives a much higher dose than the so much feared build-up of heavier actinides. *Criteria on the reduction of dose risks* will disfavour transmutation scenarios in which the waste will be contaminated with U-234 or with one of its precursors, unless a gas-tight disposal method would be applied that prevents radon emanation from the waste to reach the atmosphere.

Work programme 2.6 (Recycling of plutonium and Americium recycling as MOX fuel in PWRs, Belgonucleaire)

The actual nuclear design of a standard MOX assembly uses Pu, which has been recovered from spent UO_2 fuel with a burn-up of 45 GWd/t. This assembly has an average of about 7.8 % (in weight) of (Pu + Am) content and it has three zones of different enrichment. Actual zoning ratios are defined as the (Pu + Am) content of the zone divided by the average (Pu + Am) content. These ratios are 1.12 / 0.75 / 0.51 for the three zones respectively. The americium, which is associated with the plutonium is the Am-241, which has been formed by the decay of Pu-241 during the time elapsed between reprocessing and reloading in the reactor (the refabrication time).

Two extensions of this standard recycling have been investigated in order to burn an extra amount of americium:

- Pu with addition of 1 % Am ("doped Am")
- Pu with all Am recovered from the UO_2 spent fuel ("natural Am")

First the implications on the nuclear design of MOX assemblies have been investigated:

- overenrichment of the MOX assembly
- new zoning ratios
- influence on the assembly power and on the assembly form factor
- mass balance of major and minor actinides.

The case with addition of 1 % has been found unacceptable due to:

- too high (Pu + Am) content, leading to positive void coefficient with additional risk of release of fission gas during the end of the irradiation.
- too high quantity of Pu-238 after irradiation (the limit of 5 % was exceeded, which is a constraint put by the reprocessing)

Next the reduction of the long term toxicity has been evaluated:

> The reduction of the long term toxicity of the waste generated per unit of electricity generated, was estimated to be 20 % after 1000 years and 30 % after 10 000 years for the case "Pu + natural Am".

Finally a comparison has been made between this homogeneous Am recycling (MOX) with the heterogeneous recycling of Am in target pins (without fuel) placed in MOX assemblies: The reduction rates were found to be slightly better for homogeneous recycling but the rates are still of the same order of magnitude (about 60 % after four cycles)

Work programme 2.7 (impact on fuel fabrication, Belgonucleaire)

In this study Belgonucleaire examines the implications of recovering americium at fuel reprocessing and also examines the recycling of both the americium and plutonium as MOX fuel in light water reactors. This option is compared to the reference strategy of recycling recovered Pu only. For both strategies multiple recycling steps have been envisaged. The necessary fissile content of the MOX fuel as well as the material balance and the isotopic vector of Pu as well as for Am have been calculated for both the strategies and for three successive recycling steps. Safety aspects for the MOX-Pu recycling indicate that two recycling steps seem acceptable, whereas in the case of MOX-(Pu + Am) only one recycling step can be made due to the increase of fissile material content.

Fabrication implications:
In point of view of radiological aspects the primary blending has been retained as the most typical case. Neutron and gamma-dose rates have been calculated at a distance of 30 cm from the external wall of the glove box in which the blending device is supposed to be contained.

At the critical stage of fabrication the dose rates increase only slightly from the first recycling step of Pu to the second step. This can be explained by the dilution of the MOX spent fuel with UO_2 spent fuel between the two successive recycling steps. Change towards a combined Pu + Am strategy will however multiply the dose rates with a factor 4.5, and additional shielding is required. Although some extra shielding costs are a consequence if one would like to bring the dose rates to the same level, this extrapolation of the standard MOX fabrication seems feasible.

References

[1] J.L. Kloosterman, *ECN Contribution to a Burnup Benchmark on MOX Fuel*, ECN memo NFA-CT-94-04, Mar 1994.

[2] J.L. Kloosterman, *New Working Libraries for Transmutation Studies*, Paper presented at the GLOBAL'93, Conference, Seattle, Washington, USA, Sep 1993. Also ECN report ECN-RX-93-074, Jun 1993.

[3] J.L. Kloosterman, *Incentives for Transmutation of Americium in Thermal Reactors*, ECN report ECN-R-94-022, Oct 1994.

[4] J.L. Kloosterman and W.J.M. de Kruijf, *Transmutation of Americium in Thermal*

Reactors, Paper presented at the Third International Information Exchange Meeting on Actinide and Fission Product Partitioning and Transmutation, Cadarache, France, Dec 12-14, 1994.
Also ECN report ECN-RX-94-116, Dec 1994.

[5] W.J.M de Kruijf, *Calculational Study on Irradiation of Americium Fuel Samples in the Petten High Flux Reactor*, ECN report ECN-R-94-027, Feb 1995.

[6] J.L. Kloosterman and J.M. Li, *Transmutation of Tc-99 in Fission Reactors*, Paper presented at the Third International Information Exchange Meeting on Actinide and Fission Product Partitioning and Transmutation, Cadarache, France, Dec 12-14, 1994. Also ECN report ECN-RX-94-119, Dec 1994.

[7] S.F. Mobbs et al ('91) "Comparison of Waste Management Aspects of Spent Fuel Disposal and Reprocessing: Post-Disposal Radiological Impact", EUR 13561 EN,

[8]. K. Abrahams: "Transmutation of Long-Lived Fission Products", ECN-RX-94-003, IAEA Technical Committee Meeting on: Safety and environmental aspects of partitioning and transmutation of actinides and fission products, Vienna, 29-11-93,

[9]. L.H. Baetsle: Proc. of the Information Exchange Meeting on Act. and Fiss. Product Separation and Transmutation, Mito City, Japan, OECD 37290 (1991) 299,

List of publications 1994

[1] A.J. Janssen, "Transmutation of Fission Products in Reactors and Accelerator-Driven Systems; some critical remarks", ECN-RX-94-001

[2] K. Abrahams, Transmutation of long-lived Fission Products, ECN-RX-94-003

[3] K. Abrahams et al "Transmutation of Nuclear Waste" ECN-R-94-025

[4] K. Abrahams, W.M.P. Franken, J.H. Bultman, J.A. Heil, and A.J. Koning, "Specific Contributions of the Dutch Programme "RAS" towards Accelerator-Based Transmutation", Contribution to the International Conference on Accelerator-Driven Transmutation Technologies and Applications" in Las Vegas (July 94)

[5] K. Abrahams, "Motivation for transmuting long-lived radioactive products", reported at the "3rd International Information Exchange Meeting on Actinide and Fission Product Partitioning and Transmutation" (NEA-OECD, Cadarache, 1994)

[6] J.L. Kloosterman and W.J.M. de Kruijf, "Transmutation of Americium in Thermal Reactors", (ibid), and ECN-RX-94-116,

[7] J.L. Kloosterman and J.M. Li, "Transmutation of Tc-99 in thermal fission reactors",

[8] Th. Maldague, S. Pilate and A.F. Renard, "Impact of plutonium and americium recycling in PWR on MOX fuel fabrication" (ibid).

Title:	**Potentialities and costs of partition and transmutation of long-lived radionuclides**
Contractors:	**CEA, F; AEA Technology, UK**
Contract No:	**F12W-CT91-0106**
Duration of contract:	**October 91 - September 95**
Period covered:	**January 94 - December 94**
Project leaders:	**D. Lelièvre (CEA, Co-ordinator); R.P. Bush (AEA Technology)**

A. OBJECTIVES AND SCOPE

The study intends to analyse, on a purely conceptual point of view, the potential of a radioactive waste management strategy implementing partitioning and transmutation of the long-lived radionuclides (P&T), and to assess the technological requirements and the cost of this strategy. The achievement of these objectives is mainly based on the comparison of scenarios simulating the overall operation of a nuclear industry, reactors and related fuel cycle facilities, for a given identical electrical production and a time of operation of the system of one century.

The scenarios taken into account are characterised by:

- the types of reactors operated (PWR with UOX fuel only; PWR with Pu recycling in MOX; PWR and FR with Pu recycling in MOX),
- the reprocessing level of the irradiated fuel (no reprocessing, present reprocessing, enhanced reprocessing using techniques available at present, enhanced reprocessing using more prospective techniques).

For each of them, the evolution of the long-lived radionuclides inventory (mass and activity) is assessed. The potential long-term radiotoxicity of the resulting wastes is then evaluated for times between 10 and 10^7 years. An assessment of the fuel cycle costs of these scenarios is made.

In other respects, the accurate study of special technical aspects induced by a P&T strategy (lanthanides incineration, fuel and targets fabrication, enhanced reprocessing plant) is to be performed. An assessment of the secondary wastes that arise from the fuel cycle operations, itemised by reprocessing processes, is also intended in this work..

Two partners contribute to the study : CEA for the major part of the programme (building and assessments of scenarios) as main contracting party, AEA Technology for different systems aspects (secondary wastes, behaviour and routing of several radionuclides) as associated contracting party.

B. WORK PROGRAMME

The programme of the study is structured according the following tasks:

B. 1 Determination of reference scenarios on the basis of the use of today's reprocessing and computation of their features and potentialities in relation with the above criteria.

B. 2 Determination of new operations and related facilities induced by a P&T implementation on the basis of the first level of enhanced reprocessing and computation of their features and potentialities in relation with the above criteria.

B. 3 Rough determinations on new operations and related facilities induced by a P&T implementation on the basis of the second level of enhanced reprocessing and computation of their features and potentialities in relation with the above criteria except costs assessment

C. PROGRESS OF WORK AND RESULTS

The year 1994 has been essentially dedicated to the performance of task B3, i.e. the study of RP2 P&T scenario, in which techniques of enhanced partitioning of radionuclides unavailable at present are used.

In other respects, an amendment to the initial contract has been concluded in the end of 1993, with the intention of bringing additional results to task B2. These complements dealt with :

- the determination of the quantity of rare earth acceptable in reactor cores burning americium and curium,
- the definition of a process and the outline of a plant for the fabrication of MOX fuel with neptunium and targets with americium,
- the definition of a process, the sizing and the costs assessment of a fuel and targets reprocessing plant, allowing the recycling of uranium, plutonium, neptunium, americium, technetium and iodine and the storage of curium for its radioactive decrease to plutonium,
- the definition and the computation of the features of a set of reactors associated with this plant,
- complementary studies, not considered initially, on previously studied scenarios.

Finally, a second amendment to the initial contract has been concluded in the middle of 1994 to complement the initial study with a comparative study of several possible reprocessing processes for a P&T strategy. It is based on a systems study of these processes and, if needed, of the related fuel and targets fabrication processes. This study is carried out by AEA Technology as associated contractor.

1. Scenario RP2

Summary description

In this scenario, the reduction of potential radiotoxicity, caused by minor actinides (Np, Am and Cm) and by fission products (I, Tc), using dedicated reactors is researched. This is assumed to be possible from year 2030 on. Curium 244 is not transmuted immediately but stored so that it turns into plutonium 240 which will be transmuted then.

This transmutations are possible in CAPRA type fast reactors. In these reactors, of 1,500 MW nominal electrical power, the fuel, MOX type with high plutonium content (45%), is irradiated at 250 GWd/t. Neptunium is recycled in homogeneous mode in the MOX fuel. Americium is recycled in heterogeneous mode in inert matrix (MgO) targets placed around the core. Iodine and technetium are also recycled in heterogeneous mode in targets (CeI_3 and metal Tc) placed above and under the core.

The separation yields at reprocessing are assumed better than 99.9% for uranium and plutonium, 99.5% for minor actinides and 90% for iodine and technetium.

Losses at fuel pellets and targets fabrication are taken equal to 0.01%.

Material balance

Cumulative losses at reprocessing amount, at the end of the scenario, to about 210 tons of uranium and 7 tons of plutonium. They are reduced by a factor of 2.5 and 4 respectively, compared with those of scenarios RP1.

The quantities of minor actinides remaining in the wastes are 7 tons of neptunium, 11 tons of americium and 10 tons of curium. They mainly consist in the quantities existing before enhanced P&T techniques are implemented.

Stored curium amounts to 45 tons in the considered period. It increases at a rate of 1.5 tons per year. In the end of the scenario 44% of this curium has turned into plutonium.

The quantities of technetium and of iodine remaining in the wastes are 90 tons and 30 tons respectively. They mainly consist in the quantities existing before enhanced P&T techniques are implemented.

Stored depleted uranium amounts to nearly 1 million of tons, showing a trend to stabilisation similar to that observed in previously studied scenarios using fast reactors.

Finally, after 70 years of enhanced P&T (2,030 - 2,100), the mains statements are that :

- equilibrium state is not reached;
- uranium annual losses decrease by a factor of 6 from 5 to 0.8 tons;
- plutonium annual losses decrease by a factor of 5 from 0.3 to 0.06 tons;
- minor actinides quantities remaining in the wastes are insignificant;
- stored curium amount continues to increase at a rate of 1.5 tons per year, which might be very near of the maximum rate. Further implementation of recycling of the plutonium resulting of this storage should lead to stabilise this amount.
- stored depleted uranium amount also tends to stabilise.

Radiotoxicity balance

Two inventories have been calculated :

- a « waste » inventory taking into account radionuclides that have not been recycled in the end of the scenario and that are not supposed to be in its foreseeable continuation;
- a « cycle » inventory taking into account radionuclides present in the fuel cycle at the end of the scenario. As previously said this is not an equilibrium state inventory.

The « waste » inventory shows an immediate reduction by a factor of 10 of radiotoxicity in comparison with the open cycle scenario. This reduction increases during the first century following the end of the scenario to reach a factor of 35, a value around which it stabilises over the considered period (till 10^7 years).

The « cycle » inventory shows an immediate radiotoxicity equivalent to that of the open cycle and then a reduction by a factor of 2 during the first century following the end of the scenario. Then this ratio fluctuates about this value.

2. Impact of rare earths on americium and curium transmutation in fast and pressurised water reactors

Position of the problem

Rare earths (or lanthanides) separation from americium and curium is very difficult in today's reprocessing processes. Depending on the fuel from which these elements are extracted, the mass ratio of rare earth to the mentioned actinides varies from 2 in MOX fuel to 20 in UOX fuel. Now P&T strategies consider their transmutation in reactors, either FR or PWR. This study intends to determine whether simultaneous presence of rare earths and of americium or curium is possible and to what extent.

Transmutation in fast reactors

To answer this question, numeric simulations of the operation of an EFR core, adapted to minor actinides burning have been performed. Two types of load have been considered : homogeneous mode and heterogeneous mode.

The homogeneous mode

In the homogeneous mode, americium and possible linked elements replace UO_2 in the standard core. Computations were performed for the standard core, for a core burning « clean » americium with 3% of americium, then for cores burning americium from reprocessing (with curium and rare earths) with the same content of americium. Three levels of lanthanides separation performance were assumed (decontamination factors of 60, 30 and 12) respectively). These configurations do not affect the power nor the operation of the reactor.

The material balance of these computations shows :

- an important volume occupied by the rare earths' oxides and a consequently important reduction of the uranium load;
- an increasing plutonium consumption with the ratio of rare earth in the core;
- an americium transmutation nearly independent of the presence of rare earths, near 35% for a 1,700 EFPD;
- a rather high net curium production (2,7 kg/ TWh_e), nearly independent of the presence of rare earths;
- a low rare earth consumption.

The computations on the core's reactivity shows :

- a low initial reactivity decreasing with the rare earths ratio;
- an increasing loss of reactivity with the rare earths ratio, that makes a 1,700 EFPD reactor cycle impossible for UOX reprocessing decontamination factors under 15;
- a degradation of void sodium effect and of Doppler effect, caused by the presence of minors actinides and emphasised by the rare earths.

To recycle minor actinides from reprocessed UOX fuel, a minimum decontamination factor of 30 seems necessary. This factor can be divided by 10 for reprocessed MOX fuel.

The heterogeneous mode

The elements to be transmuted are placed in the first row of the reactor's radial blanket.

Computations are performed for « clean » americium oxide mixed with magnesium oxide and for americium from reprocessed UOX and MOX fuels (with curium and rare earths). In the case of UOX fuel, four levels of lanthanides separation performance are assumed (decontamination factors of 50, 25, 10 and 1) whereas only one (decontamination factor of 1) is assumed for MOX fuel. Rare earths are used as targets' matrix, a portion of MgO is added so that the initial mass of heavy nuclides stays the same as that of « clean » americium. Nevertheless, this is not possible in the of low decontamination factors.

The computations show that :

- rare earths are not a neutron poison in fast spectrum;
- due to the volume occupied by rare earths, americium consumption is limited by the quantity initially loaded for UOX fuel reprocessing decontamination factors under 10;
- the americium consumption weakly decreases with the rare earths ratio;

On other respects, a limitation of rare earth proportion in the targets could appear from their poor ability at matrix making.

To recycle minor actinides from reprocessed UOX fuel a decontamination factor of 10 in relation to lanthanides must be achieved. If rare earths cannot be used as matrix a factor of 30 to 50 may be necessary. In any case, it can be divided by 10 for MOX initial fuel.

Transmutation in pressurised water reactors

Numeric simulations of the operation of N4 reactor's cores, adapted to minor actinides burning, have been performed too. Only homogeneous mode was studied.

Computations were performed for cores with moderator ratios ranging from 2 to 4, loaded with americium from reprocessed fuel (UOX and MOX), with different level of reprocessing performance.

These computations show that :

- a high moderator ratio (more than 3) and a good decontamination factor (more than 1000 for UOX) are necessary to efficiently incinerate minor actinides;
- in the standard case (moderator ratio of 2), a minimum decontamination factor of americium from reprocessed UOX fuel of 100 (10 for MOX fuel) is needed to reduce the net balance of unloaded minor actinides by a factor of 2;
- in an over moderated reactor, a minimum decontamination factor of 330 for UOX fuel and 32 for MOX fuel is needed to achieve a net reduction of the minor actinides amounts;
- the higher is the decontamination factor, the less favourable is the void effect.

A compromise must be found between reactivity and transmutation efficiency.

3. Enhanced fuel and targets reprocessing plant

The study of scenario RP2 showed that one can outline a reprocessing process capable of separating U, Pu, Np, Am, Cm, Tc et I, on the basis of already qualified knowledge or soon to be so. Thus a conceptual design and a preliminary costs assessment of a plant operating this process could be performed. This new study, agreed by the CEC, is carried out in the framework of an amendment to the initial contract.

The plant size has been determined under the same hypothesis as the scenario RP2's reprocessing plant, i.e. with a capacity of 800 tHM/year. The related reactors set comprises N4 type PWRs, loaded with UOX or MOX fuel, and CAPRA type FRs. Three reactors population were considered.

The plutonium content of the PWR's MOX fuel can amount to 15%. The CAPRA FRs are loaded with a mixture of uranium, plutonium (45%) and neptunium (5%) oxides. Technetium is loaded in metallic form in their lower axial blanket. Iodine is loaded in the form of CeI_3 in their upper axial blanket. Americium is loaded in a mixture of AmO_2 and of MgO in their radial blanket.

The enhanced fuel and targets reprocessing plant (EFTRP) allows the recycling of the above mentioned radionuclides and the storage of curium so that it decays to plutonium. This plutonium will be recovered after a period of 100 years, at the end of which it stands for 85% of the stored material, and recycled. The EFTRP reprocesses the fuels and targets previously described to deliver as output uranium as uranyl nitrate, the other actinides in the form of oxide powder, technetium in metallic form, iodine in the form of cerium iodide, vitrified fission products and the metal of cladding hulls melted into ingots. The expected reprocessing yields are 99.9% for uranium and plutonium, 95% for the other radionuclides. Two variants are considered : the first one have in view the delivery of a mixed oxide of plutonium and neptunium, the second one the incomplete separation of lanthanides from americium.

Equilibrium cycle computations were performed and allowed to determine the input streams and to check the system's ability to eliminate all the produced radionuclides. It appears that this is effective for all the considered reactors populations except for technetium and americium in the case of the least provided with CAPRA reactors.

The tonnage of the different fuels and targets to be treated in the EFTRP varies greatly, depending on the reactors' population. However the streams of all chemical elements in the main part of the treatment are quite similar. The size of the headend workshops is the only variable parameter. The envelope sizing was chosen for the study.

The design of the process flowsheets and the assessment of the main streams were performed. The sizing and the costs assessment of resulting workshops were committed to the society SGN. The main flowsheet is derived of the PUREX process.

The fuels and the targets are stored five years before reprocessing. This storage takes place in ponds, except for targets of cerium iodide, dry stored.

The cerium iodide targets are processed to eliminate xenon formed by transmutation of iodine and then combined with the iodine trapped during the dissolution of the other fuels and targets.

Except the cerium iodide targets, the fuels and targets are dismantled, sheared and dissolved in concentrated nitric acid to deliver liquors with a 3N acidity. Iodine is trapped during the dissolution. The liquors are mixed, clarified and undergo successive extraction-stripping cycles necessary to obtain the expected separation.

At the first cycle, a monoamide solvent is used. This cycle allows, in addition of the usual fission products separation, to recover separately technetium, in the form of pertechnetic acid. This acid is neutralised with ammoniac. The resulting ammonium pertechnetate is recovered by evaporation and then reduced into the wished metallic state by hydrogen and high temperature treatment. The plutonium / uranium+plutonium separation is performed at the end of the first cycle by redox and acidity adjusting .

A variant allowing the coextraction of neptunium and plutonium at this cycle was also studied.

At the second cycle, a monoamide solvent is still used. Neptunium is recovered separately by acidity adjustment of stripping solution. The neptunium nitrate solution is concentrated and transformed in oxide by the oxalate process. Uranium is concentrated into uranyl nitrate without any further purification.

Plutonium undergoes another purification cycle, with still a monoamide solvent, it is then converted into oxide by the oxalate process.

The first extraction cycle raffinates undergo a complementary cycle using a diamide solvent (DIAMEX process). This cycle allows the separation of americium, curium and lanthanides from the other fission products. Americium is then separated from the mixture by an electrochemical process (SESAME process). Finally, curium is separated from the lanthanides during an extraction cycle using TPTZ as solvent. Americium and curium are converted in oxides by the oxalate process.

A simplification variant of this separation was studied in the case in which a high purity of americium is not necessary for its transmutation.

Fission products are vitrified. The metal of hulls is melted into ingots. Solvents and reagents used are totally incinerable. The effluents can therefore be concentrated and vitrified with fission products.

4. Systems aspects of partitioning and transmutation (AEA Technology)

The reprocessing processes, the study of which is proposed, are :

- the CTH process developed by Chalmers University, Gothenburg, Sweden;
- the TRPO process developed in the Peoples Republic of China;
- the TRUEX process developed in the USA;
- a typical non-aqueous process, selected from the literature;
- the DIAMEX process being developed in France.

The study on the three first processes is an extension of a work previously undertaken at AEA Technology, the study on the two last ones is a new work.

For each of these processes, the study intends to :

- identify and quantify the secondary waste streams that arise from P&T cycle plants, and if necessary propose a treatment for them;
- describe their specific plant requirements, in comparison with a reference cycle without P&T and to asses their costs;
- study the behaviour et and routing of several long lived radionuclides such as neptunium, technetium, palladium, iodine and carbon 14.

In the year 1994, the studies has focused on the two last mentioned processes (non aqueous and DIAMEX), essentially on the secondary waste point of view.

A non aqueous process

A flowsheet has been formulated for treating high level liquid waste. This liquid waste is assumed to be similar to the highly active raffinate from the THORP plant. One of its major component is gadolinium, used in the first cycle of the fuel reprocessing plant as neutron absorber.

The studied process consists of a three steps sequence :

- the headend treatment, in which an evaporation of the treated liquid is performed, followed by a conversion in chloride form, followed by a dissolution in molten salt;
- the salt extraction and stripping, used to do the major separation of actinides and rare earths and other fission products;
- the electrorefining, used to purify the actinide fraction from remaining fission products.

Except for the headend conversion process, the description of these steps is based on the work done at the USA Argonne National Laboratory (ANL) as part of the programme on the Integral Fast Reactor.

The different steps of this process will generate secondary wastes.

In the headend, gas scrubbing will be required on the evaporator and conversion process. Although relatively low temperatures are used, radioactive species, such as ruthenium or any present iodine, will no doubt be present in the off-gases. The filters and scrub treatment will give secondary waste of similar type and volume to that in a vitrification plant. The aqueous distillates would be treated in the same way, i.e., returned to the low level liquid waste treatment part of the reprocessing plant.

In the salt extraction/strip step, a zeolite column is used to extract caesium and strontium of the molten salt before its recycling. This column will become a waste, estimated at 0.4 l / ton of uranium treated. Treatment of the electrolyte salt would add only a small volume to this (about 3.5 ml / ton of uranium). As regards salt replacing, the rate at which it should take place is not known. At ANL the salt waste is to be immobilised in zeolite, which is reported to have a very high leach resistance in water. The high cadmium alloys used in this step have a significant vapour pressure at the temperature of operation. This will lead to deposits in vent pipes and in the cover gas system. The amount of radioactive species associated with this is not known but the removal of the deposits will give rise to some secondary waste even if the cadmium is returned to the process.

The electrorefining step uses electrodes of molten cadmium contained in ceramic crucibles. These electrodes are periodically removed off the molten salt to recover the actinides (cathode) and the technetium (anode). Due to these handling and to the temperature changes undergone at the same time, the crucible will inevitably break. This will give rise to a low volume of low level actinides contaminated waste; say one 3 l of MgO or BeO crucible per 5 tons of uranium equivalent processed.

The DIAMEX process

This process is under development in the CEA. This development is reported to the CEC in the framework of task 2 of the research programme on radioactive waste management. Besides, it is supposed to be developed and integrated in the conception of the EFTRP designed by the CEA in the framework of this contract (see above).

The DIAMEX process is used in complement of the PUREX process in P&T strategies aiming at the elimination of americium and curium. These actinides are present in the high level liquid stream, with the fission products after the first extraction cycle of the PUREX process. It is therefore on this stream that DIAMEX process is to be applied. It can be considered as a key step of the separation of the above mentioned actinides, prior to their transmutation. The process principle consists of extracting trivalent actinides in a liquid-liquid extraction using diamide molecules. Determinate the most appropriate extractant is one of the major objectives of the R&D on this process.

Beyond their ability to extract trivalent actinides, diamide extractants display the property of being totally incinerable, for they only contain carbon, hydrogen, oxygen and nitrogen (« CHON » principle). Their major drawback is that they simultaneously extract trivalent actinides and lanthanides. The latter appearing in a molar ratio of 50 in the solution to be treated, and taken into account the preliminary results on incineration of americium with rare earths in reactors, it is very likely that a complementary step of separation of lanthanides from actinides should be added to the DIAMEX separation itself. This step will generate a secondary waste stream. An evaluation of this is planned.

Furthermore, the DIAMEX process requires that its input solution (the high level liquid stream) were first decontaminated of technetium and neptunium. This introduces supplementary treatments, known but not applied nowadays on industrial plants. These treatments are likely to give rise to a secondary waste stream.

Finally, ruthenium shows a great affinity for diamides. It probably results in an accumulation of this element in the solvent. Any clean up method of this solvent will create a secondary waste stream. One possible solution to the problem of ruthenium accumulation in the solvent is its removal by oxidation to volatile RuO_4 before DIAMEX separation. Anyhow, off-gas scrubbing would then create a waste stream containing ruthenium.

At a lower level, several other metals as iron, zirconium, molybdenum, will have to be treated specifically and those treatments will generate secondary wastes.

A2: WASTE TREATMENT

Task 2

"Treatment of Radioactive Waste"

* List of contract
* Introduction to Task 2

Topic 1	:	Minimization of radioactive discharges
Topic 2	:	Reduction of waste volumes to be disposed of
Topic 3	:	Waste de-categorisation and actions at the source
Topic 4 *	:	Spent fuel conditioning for disposal
Topic 5	:	Potentialities of transmutation of long-lived radionuclides

* No activity running on this topic

TASK 2 - LIST OF CONTRACTS

Topic 1 : Minimization of radioactive discharges

FI2W-CT90-0054 Improvement in the performance of the conventional treatment of liquid effuents by co-precipitation.

Topic 2 : Reduction of waste volumes to be disposed of

FI2W-CT90-0053 Wet oxidation of organic containing wastes.

FI2W-CT90-0057 Advanced processes for the treatment of low level liquid wastes at a pilot plant scale.

FI2W-CT91-0095 Process design and feasibility study for incineration under pressure, condensation and effluent treatment of radioactive waste.

FI2W-CT91-0100 Melting of incinerator ashes using a microwave furnace.

Topics 3 : Waste de-categorisation and actions at the source

FI2W-CT90-0062 New macrocyclic extractants for radioactive waste treatment : Ionizable crown ethers and functionalized calixarenes.

Topic 5 : Potentialities of transmutation of long-lived radionuclides

FI2W-CT90-0047 Partition of radioactive wastes.

FI2W-CT90-0056 Advanced management of nuclear radioactive wastes : comparative evaluation of processes for enhanced separation of very long-lived radioactive species.

FI2W-CT91-0112 High-level liquid waste partioning by means of completely incinerable extractants.

INTRODUCTION TO TASK 2: TREATMENT OF RADIOACTIVE WASTE

A. Objectives

Improvement of radwaste management schemes by means of new treatment processes allowing :

* the minimization of radioactive discharges into the environment;
* the reduction of the waste volumes to be disposed of;
* the de-categorisation of waste packages in terms of disposal routes;
* the removal of long-lived radionuclides from high level waste for partitioning and/or transmutation purposes.

B. Research topics investigated within the programme 1985-1989

Investigations were carried out on volume reduction techniques for liquid waste from reactor operation, spent fuel reprocessing and from research centres. The work was focused on ultrafiltration techniques, electrochemical ion-exchange and chemical precipitation coupled with centrifugation.
Research work was devoted to the waste de-categorisation for making easier conditioning, transport and disposal operations of a number of alpha and MLW, particularly on :

- treatment flow-sheets relying on solvent extraction;
- chemical precipitation and inorganic ion-exchange techniques;
- exhaustive decontamination of solid alpha waste by leaching with electrogenerated Ag(II).

New immobilisation matrices (modified sulphur cement, ceramics and new cement formulations) have been investigated for various wastes like incinerator ashes, ion-exchange resins, sludges, dissolver residues.
Actions taken at the source of production (MOX fuel fabrication plant) for reducing alpha waste arisings also played an important part in this programme. Quality assurance schemes for waste products in conditioning facilities for cementation, drying and compaction were elaborated and critical parameters for disposal criteria selected.

C. The present programme 1990-1994

At the beginning, Task 2 comprised 13 research contracts, four of them being multinational. In 1994, the work has been progressing for 9 contracts, three of them being completed and one cancelled. The following topics have been covered:

Topic 1 : minimization of radioactive discharges

- Setting up of a downstream treatment processes for low level liquid effluents at the La Hague reprocessing plant (CEA Cadarache).
- Radium recovery from uranium tailings (LNETI).

Topic 2 : Reduction of waste volumes to be disposed of

- Recovery of boron from PWR low level liquid waste by electrodialysis, reverse-osmosis, distillation, ion-exchange and electrochemical ion-exchange as alternative treatments (Laborelec, AEA Harwell and CEN/SCK).
- Volume reduction of alpha-bearing incinerator ashes by a melting process using a microwave furnace (CEA-Valhrô).
- Ion-exchange resins destruction by H_2O_2 (AEA-Winfrith) and by incineration with oxygen under pressure (Bertin, CEA-Cadarache and INITEC).

Topic 3 : Waste de-categorisation and actions at the source

- De-categorisation of medium-level reprocessing concentrates by using "tailor-made" macrocyclic extractants (calixarenes and crown-ethers). This multipartner project associates CEA-Cadarache with the Universities of Barcelona, Belfast, Mainz, Parma, Strasbourg and Twente.

Topic 4 : Conditioning of spent fuels in view of their direct disposal

There are no activities running on this topic.

Topic 5 : Potentialities of transmutation of long-lived radionuclides

- Development and testing of enhanced treatment scheme for separation of long-lived radionuclides from high level liquid waste. This co-ordinated research programme is being carried out by CEA-FAR, FZK (former KfK) and ENEA Saluggia.

Title	Improvement in the performance of the conventional treatment of Liquid Effluents by Co-Precipitation
Contractor	CEA-DCC (F)
Contract N°	FI2W/CT90/0054
Duration of contract	May 1991 - April 1995
Period covered	January - December 1994
Project leader	FREDERICI Véronique

A. OBJECTIVES AND SCOPE

The capacity of treatment of the COGEMA irradiated fuel reprocessing plant at The Hague is to be progressively increased from 400 to 1600 tons a year. The regulations concerning the release of radioactive effluents into the sea remain unchanged, i. e. they authorize :

- 45000 Ci (1665.10^3 GBq) for all radioelements (except tritium) including 6000 Ci (222.10^3 GBq) for Sr90 and Cs137;
- 45 Ci (1700 GBq) for α emitters.

The efficiency of radioactive liquid effluent chemical treatment should therefore be improved.

At present, the Liquid Effluent Treatment Plant (so called STE3) implements a process involving a chemical co-precipitation for low activity (act.$\beta < 5$ Ci/m^3) and medium activity (act.$\beta < 300$ Ci/m^3) radioactive effluents and a neutralization, followed by filtering for any effluents suspected of the slightest radioactivity (act.$\alpha < 10^{-4}$ Ci/m^3, act.$\beta < 10^{-2}$ Ci/m^3).

In association with the treatment plant (STE3) operators who presently supply radioactive effluents, we propose to implement complementary treatments in a hot laboratory, using for example mineral exchangers, organic extractants and chemical precipitation, the application of which, in the STE3 plant at The Hague, should entail only minor modifications to the existing process.

B. WORK PROGRAMME

The work programme consists of :

10/91 to 10/93

- the caracterization of the chemical forms of the radioelements to be removed,
- the insolubilization of these radioelements by means of mineral exchangers in powder form (oxydes, sulfates, phosphates, ...), of supported organic extractants (active carbon, silica) and of precipitation treatments.

10/93 to 10/94

- the study of the separation of the insolubilized activity by means of the most appropriate processes (tangential filtering, centrifugation or columns used singly or in series).

10/94 to 5/95

- the carrying out of tests on a radioactive pilot device and final report.

C. PROGRESS OF WORK AND OBTAINED RESULTS

- State of advancement

The evolution of the radioactive liquid effluents discharged into the channel by the STE 3/La Hague shows a reduction of 30% of the active effluents and of 50% of the suspect effluents (so called "V"), but the distribution stays almost unchanged : 27% of 90Sr, 23% of 127Sb, 17% of 106Ru and 3% of 137CS. To reduce the released activity, we focused therefore our attention to these radionuclides. Moreover, V effluents should be investigated as they account for 21% of the discharged alpha activity, although they represent only 6% of β activity. With complementary treatments implementation in view, our goal is to obtain a decontamination factor of the order of 10.

During the previous period (1993), we studied the fixation of the two radionuclides (Sr 90 and Sb 125) in a column filled with sodium titanate pellets. This method was also effective to treat 3,2 liters of effluent contaminated by strontium with only 3,2 ml of sodium titanate pellets. We also investigated the fate of the contaminated pellets. The first possibility is their embedding by ceramisation. The second alternative we have chosen is the elution of the pellets by nitric acid 0,1 M which was effective. We studied in the same manner the Sb removal. But, even by decreasing the pH and the flow-rate, bad results (DF equal to 3 instead of 10) were attributed to the contact time between the effluent and the pellets, which is still too low.

During this period, we put emphasis on the Ru 106 removal which was not successful until now. Then, we proposed a treatment allowing the effluent decontamination for Sr 90, Sb 125 and Ru 106. As it includes a solid/liquid separation, we investigate a membrane process for TiO_2 (G3 form) microfiltration.

PROGRESS AND RESULTS

1. RUTHENIUM REMOVAL

Until now, DF hadn't exceeded 3 . After we shown that active carbons, like CNB 200 from PICA, allowed to remove Ru 106 molecular forms, we tried to eliminate anionic forms in neutral or slightly basic conditions by means of anionic exchangers, or cationic forms in acidic conditions by cationic exchangers. But, these experiments were unsuccessful.

We also decided to modify Ru 106 forms using reductive agents, such as SBH (sodium borohydrure), associated to compounds able to remove Ru106 new forms. This is the reason why we studied metallic copper obtained by Cu^{2+} reduction. According to the copper quantity, DF are close to 20, even for various effluents. To a less extent, it also possible to use a quaternary ammonium exchanger we previously put under sulfur form, but DF is lower (between 5 and 10).

2. TREATMENT

At this step, we can consider that the contract objective is reached, as we obtain a DF over 10 for the radionuclides (Sr 90, Sb 125 and Ru 106). We have now to define a treatment which can be applied to the A effluents after STE 3 :

— pH effluent adjusted to 12 and addition of 1% of TiO_2 for Sr 90 removal, solid/liquid separation,

— pH effluent adjusted to 5 and addition of 1% of TiO_2 for Sb 125 removal, solid/liquid separation,

— pH effluent adjusted to 2 and addition of Cu^{2+} 100 mg/l and SBH 500 mg/l for Ru 106 removal, solid/liquid separation.

This treatment can vary according to the radionuclides activity and distribution. By now, it seems essential to study the solid/liquid separation.

3. MICROFILTRATION PROCESS

Titanium oxyde G3 is a powder with a granulometry distribution around 18 μm. As there is a bad settling, the alternative for the solid/liquid separation is a membrane process. The TiO_2 microfiltration can be performed on a mineral membrane Carbosep M20 from Tech-Sep. This study was achieved on an industrial-scale device. The first experiment consisted on being sure that the membrane is in well-known conditions by acidic then basic washing.

Membrane fouling depends on microfiltration parameters. It is important to determine the maximum transfert pressure ΔP_m as a function of the mean flux density J. With a two step experiment, we conclude that the best conditions were $\Delta P_m = 0.7$ bar for a pump flow equal to 350 l/h.

We also considered the microfiltration of a TiO_2 solution at pH 6.5. The volume concentration factor was equal to 12. During this experiment, no fouling membrane occured.

4. FUTURE WORK PROGRAM

We have to convey the previous conditions of solid/liquid separation on a laboratory-scale device which can be used for contaminated effluents. The methodology should be the same. Thus, when the good parameters (Q_N,ΔP_m) is found, we shall consider the active effluent concentration first at pH 12 to remove strontium and alpha emitters, then at pH 4 or 5 for antimony. These experiments must allow a treatment of the effluents with DF close to 100. We also consider a treatment at pH 8 which includes only one step, but with lower DF. At the end, we may investigate another step for ruthenium with copper and SBH at pH 2 before adding sodium hydroxyde to neutralize the effluent.

LIST OF PUBLICATIONS

No publications other than progress reports dealing with the work under contract.

Title	**WET OXIDATION OF ORGANIC CONTAINING WASTES**
Contractor	AEA Technology - Harwell
Contract N°	FI2W/CT90/0053
Duration of contract	March 1991 - May 1995
Period covered	January - December 1994
Project leader	Dr. N.S. Holt

A. OBJECTIVES AND SCOPE

A wet oxidation process for the removal of organics from low and intermediate level radioactive wastes has been developed in parallel by AEA Technology for the treatment of reactor sludges from the Winfrith Steam Generating Heavy Water Reactor, and by Nuclear Electric for the treatment of spent organic ion exchange resins from their nuclear power stations.

The process, which is based on catalysed reaction with hydrogen peroxide, has already been subject to experimental investigations using non-radioactive pilot scale plant. Batches of simulated waste material with an ion exchange resin content of up to 50 kg per batch have been treated.

The main objective of this programme is to demonstrate the feasibility of wet oxidation treatment on a range of real radioactive wastes by the design, construction and operation of an active mobile pilot plant (50 - 100 kg / day capacity).

The key organic wastes identified as candidates for possible investigation include :

- Ion exchange resins from power reactor operation
- Decontamination liquors and resins
- Mixed reactor sludges from WSGHWR
- Solvents and scintillants
- Cellulose containing soft wastes

B. WORK PROGRAMME

The programme consists of the following tasks :

Task 2.2	Analysis of literature data and assessment of candidate wastes in UK and EU contexts
Task 2.3	Evaluation of previous experimental results
Task 2.4	Completion of small scale wet oxidation experiments
Task 2.5	Appraisal of alternative plant concepts
Task 2.6	Evaluation of complete treatment schemes

Task 2.7 Design, construction and operation of a mobile active wet oxidation pilot plant
Task 2.8 Drawing-up of process flowsheets
Task 2.9 Analysis of safety and economic aspects

C. PROGRESS OF WORK AND OBTAINED RESULTS

State of Advancement

By the end of 1993, the mobile wet oxidation facility had been delivered to AEA Technology's Winfrith site, and non-active commissioning trials completed.

During 1994, a programme of tests with non-radioactive wastes and simulants has been carried out. Safety authorisation to proceed with active trials has been received, and a programme of active tests commenced with PWR ion exchange resins. Residues from non-active tests have been successfully incorporated into a cement matrix producing a wasteform with good physical properties.

Progress and Results

Task 2.2 Analysis of Literature Data

Task completed 1992. The findings of a comprehensive literature survey on wet oxidation research were presented. Wastes containing organic ion exchange resins were confirmed as the most suitable candidates for wet oxidation treatment.

Task 2.3 Evaluation of Previous Experimental Results

Task completed 1992. The studies of AEA Technology and Nuclear Electric relating to wet oxidation prior to this programme were reviewed.

Task 2.4 Completion of Wet Oxidation Experiments

Task completed 1993. These small scale trials were used to assess the susceptibility of differing waste types to wet oxidation, and to provide information on the optimum reaction conditions to be used.

Task 2.5 Appraisal of Alternative Plant Concepts

Completed in 1992. Semi-continuous addition of waste throughout an extended reaction period emerged as the preferred option.

Task 2.6 Evaluation of Complete Treatment Schemes

Tests have been carried out to assess the suitability of cement encapsulation as a conditioning method for the primary residue produced by the treatment of ion exchange resins in the wet oxidation plant. At 20 litre scale, a cemented product was produced at a dry waste loading of 16.6 wt % . This mix formulation, using 9:1 Blast furnace slag / ordinary Portland cement (BFS/OPC), demonstrated acceptable mixing characteristics and compressive strength development with time. After 90 days the wasteform possessed a compressive strength of 19.1 N mm^{-2} which under UK product evaluation guidelines would indicate acceptable physical properties for disposal.

Task 2.7 Design, Construction and Operation of a Mobile Active Wet Oxidation Pilot Plant

Following non-active commissioning of the plant at Winfrith during 1993 a programme of both non-active and active tests has been carried out during 1994.

I) NON-RADIOACTIVE TESTS

Mixed bed ion exchange resins (condensate polishing)

This non-radioactive real waste has been generated as a result of condensate polishing and steam boiler blowdown cleanup at a UK Magnox power station. It consists of a mixture of Ambersep IR252 and IRA900 loaded with morpholine, chloride, sulphates and organic acids. The resins are of the polystyrene / divinylbenzene type with a macroreticular structure supporting the sulphonic acid and quaternary ammonium ion exchange sites.

A total of 520 litres of this waste has been processed by the wet oxidation plant, during four semi-continuous test runs. The residue after oxidation consisted of a mixture of insoluble calcium and other metal sulphates, calcium hydroxide and residual organic material, as a slurry in a weakly ammoniated aqueous phase. Residual organic material represented between 1% and 5% of the total organic carbon (TOC) originally present in the untreated resin, with a mean value for the entire campaign of 4%. The corresponding mean carbon removal factor for this waste type is therefore 96%.

The hydrogen peroxide requirement for treatment of this ion exchange resin waste was 1.5 te, equivalent to 2.9 te of 50% hydrogen peroxide per cubic metre of resin. Results for the individual runs are summarised in Table 1 below.

Original Resin Volume (litres)	Total Solids after WETOX	Total Carbon Removed	Peroxide used (te / m^3)	Volume reduction (dry product)	Volume Reduction ($40^{W}/_{W}$ wet product)	Reaction time
103	23 kg	99.2%	2.7	87%	60%	10 hrs
125	18 kg	98%	2.9	92%	74%	12 hrs
125	18 kg	97%	2.7	92%	74%	11.5 hrs
165	40 kg	96%	3.2	86%	57%	18 hrs

Table 1. Summary of results from mixed bed ion-exchange resin treatment (non-active)

Steam generator decontamination liquor simulant

This simulant consisted of a mixture of 340g $CuSO_4.5H_2O$ and 860g $FeSO_4.7H_2O$, together with 11.1 kg of EDTA (acid form). This mixture was diluted with 100 litres of water and 6.5 litres of ammonia solution (35%) added with stirring. The resultant solution was made to 152 litres with water. The pH of the solution was measured at pH 8.

The results obtained from treatment of 116 litres of this material, which is similar to effluent from decontamination operations at PWR stations in the USA, are given below. The efficacy of treatment with regard to total carbon removal is clearly demonstrated. However, if large quantities of decontamination effluents were to be processed, the semi-continuous reaction system may be less appropriate as the throughput is limited by the rate at which distillate may be produced by the combination of steam heating and reaction exotherm. The latter parameter is lowered relative to ion exchange resin treatment due to the lower organic content of the decontamination liquor simulant.

Table 2 Results of Decontamination Liquor treatment

Feed Volume	Total solids in residue	% Total carbon removal	Peroxide used (te/m^3)	Reaction Time
116 litres	10 kg	99.1	0.48	3 hrs

Simulated WSGHWR sludge waste

This material consists mainly of powdered polystyrene ion exchange resin, with calcium hydroxide and a complex mixture of decontamination liquor products in minor proportions. 200 litres of a 14 wt % slurry of this simulant waste was treated in the wet oxidation plant. After addition of 194 kg of hydrogen peroxide solution (50 wt %), 95% of the original TOC had been removed from the waste simulant. The reaction time for treatment was 7.5 hours.

II) ACTIVE OPERATIONS (HOT TESTING)

PWR Mixed bed resins (cooling pond water cleaning)

In the last month of 1994 two runs each with a resin volume of ~120 litres have been completed from a batch of mixed bed resin with a specific activity of $190MBq/m^3$. Although the radiation fields were low, useful measurements have been made around the transfer area and the plant itself at identified locations which has enabled comparison with the dose budget estimates in the safety case. These have confirmed that the actual values are significantly lower than those estimated from calculations, on average by a factor of 2.

Regarding the operability of the plant, some differences in the behaviour of the active resin were noted compared with the equivalent inactive simulant runs. These were manifested in a greater tendency for frothing, particularly in the early stages of the reaction. The system was able to adequately control this, although this did result in a more extended reaction time due to the need to maintain a reduced peroxide addition rate. As a result of some difficulties at the start of the second active run with transfer of resin using the existing hopper and transfer pump, a new waste feed system has now been installed with utilises a large peristaltic action pump. This provides for direct transfer of resin from the supply drums to the reaction vessel, bypassing the feed hopper.

The data available so far on the two completed active runs has confirmed similar organic removal efficiencies to those achieved in the previous inactive operations. The carryover of particulate activity into the off-gas has been below the level of detection. Results of more detailed activity measurements on samples of distillate and scrubber liquor are awaited.

Task 2.8 Drawing up of Flowsheets

This task is awaiting data from the active mobile plant operations, and will be progressed in 1995.

Task 2.9 Analysis of Safety and Economic Aspects

Safety approval has been gained for operation of the plant, at its present Winfrith location, with radioactive waste activities up to 12 GBq/te. No safety related incidents have occurred during the plant operations carried out to date.

List of Publications

/1/ TWISSELL, M.A., "Wet oxidation of organic containing wastes - Sixth semestrial report", AEA ES Report CPDD(94)P226 (1994)

/2/ TWISSELL, M.A., "Wet oxidation of organic containing wastes - Seventh semestrial report", AEA ES Report CPDD(94)P335 (1994)

/3/ TWISSELL, M.A., "Wet oxidation mobile active pilot plant - PreOperational Safety Report", AEA ES Report CPDD(94)P261 (1994)

/4/ TWISSELL, M.A., HEBDITCH, D.J., HOLT, N.S., "Design and Testing of a Mobile Pilot Plant for Organic Radwaste Treatment by Wet Oxidation", Proc.IChemE Research Event -1995, 237-239

Title : **Advanced processes for the treatment of low level liquid wastes at a pilot plant scale**

Contractors : LABORELEC (B) - SKC-MOL (B) - AEA-Harwell (UK) - LNETI (P)
Contract n° : FI2W - CT90 - 0057
Duration of contract : from April 1/1991 to 31/12/1994
Period covered : 1994
Project leader : Coordinator R. ROOFTHOOFT
SCK P. DE REGGE
AEA A. TURNER
LNETI J.P. GALVAO

A. OBJECTIVES AND SCOPE

The objectives of the programme are :

a) Eliminate boron from low level liquid waste of PWR plants.
Five processes will be evaluated (electrodialysis, reverse osmosis, distillation, ion-exchange and electrochemical ion-exchange).

b) Demonstrate the capabilities, reliability and cost-effectiveness of these processes for the treatment of real PWR wastes over realistic time scales at representative throughputs.
As a part of this, it is a key goal to achieve low activity discharge levels (< 2 MBq/m^3) and high waste volume reduction factors (> 500) in a cost-effective way.
An additional goal will be to obtain purified boric acid with less than 1 ppm Cl^- and a B-recovery of more than 75 %.

c) Evaluate electrochemical ion-exchange (EIx) on wastes from a nuclear research center (Harwell) in comparison with the flocculation/sand filtration process currently used for the removal of Cs, Co and α-emitters.

d) Evaluate electrochemical ion-exchange and reserve osmosis for the removal of Ra and other heavy metals from uranium mine tailing wastes in comparison with flocculation.

B. WORK PROGRAMME

First the composition of the waste streams will be identified. To select the optimal equipment batch experiments are carried out on simulant wastes. On the basis of these, bench-top experiments will be realized, firstly with simulant and then with genuine waste. On basis of the obtained information one or more pilot plants will be designed and built. They will be used for testing on real waste :
- at Doel or Tihange PWR-stations
- at Harwell research laboratories
- on the Portuguese site Sacavem for uranium mine tailing wastes

The processes which will be evaluated are
1) electrodialysis
2) reverse osmosis
3) distillation
4) ion exchange
5) electrochemical ion exchange

C. PROGRESS OF WORK AND OBTAINED RESULTS

C.1 State of advancement

All tests except evaporation under pressure have been concluded by the end of December 1995.
Pilot plants have been tested in Doel (PWR), Sacavem (mine tailingwaste) and Harwell (research centre).
The SCK pilot plant has been delayed due to safety requirements and the final testing has been postponed to 1995.
The final report will be written when all results (including SCK-testplant) are obtained.

C.2 Progress and results

a) Electrodialysis (ED)

Several tests have been performed both on recoverable and non recoverable waste solutions.
Working in a once-through system, the efficiency is too low to recycle the water in the main circuits of the plant. This is also due to the fact that the number of ED-stacks in the pilot plant is limited. Normally a reduction of the salinity by a factor 2 can be expected in each stack. The limit of conductivity is also determined by the current efficiency which decreases with the conductivity.
Working in recirculation it is possible to reach conductivities of 10 or even 5 µS/cm in the produced water. However this mode of operation decreases the apparent throughput of the system and is still limited by the decreasing current efficiency.
In all cases examined the boron losses are very low and the activity in the product water is below 2 MBq/m³ which allows a discharge to the river.
The brine can than be evaporated in the normal waste system with an important volume reduction factor which is no longer fixed by the concentration of borates.
Fouling problems have been found and made cleaning processes necessary.

b) Electrical Ion Exchange (EIX) on PWR-waste

The pilot plant has been operated either as cation EIX, as cation-anion EIX or as anion EIX.
The purpose of the different treatments is
- CEIX : decrease pH to reduce the ionisation of borates
- CAEIX : purify the solution from anions and cations
- AEIX : remove boron selectively and reconcentrate it afterwards.

This mode of operation has given following results
- sodium removal and pH adjustment is efficiently achieved by CEIX
- active Cs, some Mn and Co removal is achieved by CEIX
- some Co and Mn removal is achieved by AEIX
- boron removal is achieved by AEIX

In a 21 hours run in CAEIX mode the activity was reduced from 5,5 to 0,2 MBq/m³.
Very little change was found in chloride concentrations. As a result high chloride concentrations were also found in the 6000 ppm B concentrate.
At long AEIX treatment times the concentration of boric acid exceeded the saturation limit and precipitation occurred causing severe blockages in the anion concentrate pipes.

This problem has been overcome by increasing the rate of anion concentrate removal. Recoveries of more than 97 % of the boron have been achieved.

c) EIX on waste from Harwell

The waste solution feeding the EIX has already been treated by flocculation and filtration but is still slightly active.
CAEIX effectively resulted in the solution being partially desalted.
Due to long storage time, there was a significant buildup of algae in the storage tank and this resulted in fouling of the membranes. A coarse fibre bound cartridge filter has been installed which reduced successfully the solids to below 10 ppm.

d) Evaporation under pressure

The pilot plant has been installed at Doel Nuclear Power Plant after successful completion of precommissioning tests in Mol (SCK-CEN).
During this tests a distribution coefficient for boron of 0,016 has been measured. The volume reduction factor was 44,4 and the boron recovery 24,9 %. These low values are due to the limited operation time (96 hours). Theoretically 95 respectively 99 % of recovery can be reached in 405 respectively 624 hours.

e) Electrode manufacture for EIX

Low current density experiments have shown that the new materials studied reach an electrode lifetime in excess of 4 years.
Oxalic acid has been used to reduce chlorine evolution.

f) Uranium mine tailing waste

Reverse osmosis membranes with different cut-off have been tested. The modules were of the spiral wound type.
The membrane is protected by prefiltration on sand and by a cartridge filter.
A volume reduction factor (VRF) of 10 has been obtained with a nanofiltration membrane.
A thin film composite membrane has given a VRF of 3,2 with a water recovery of 70 %.
EIX was also evaluated but only RO seems to be technologically applicable.
Calculations on investment and operating costs have been performed and give the following results

- investment	172.000	-	195.000 ECU
- operation	67.000	-	78.000 ECU/year.

Title	Process design and feasibility study for incineration under pressure, condensation and effluent treatment of radioactive waste	
Contractors	BERTIN & Cie (F), CEA-Cadarache (F) and INITEC (SP)	
Contract N°	F12W-CT91-0095	
Duration of contract	From July 1991 to June 1994	
Period covered	January 1994 - December 1994	
Project leader	C. LEONARD	BERTIN & Cie, Coordinator
	J.F. DOZOL	CEA
	S. ALAMO	INITEC

A. OBJECTIVES AND SCOPE

The main objective of this research is the evaluation of the technical feasibility of the combustion of a range of organic wastes containing radioactive elements, by means of under pressure oxygen, using a new type of incinerator relying on the recent technical developments achieved within the MESMA (Autonomous Energy Module) project.

In particular, the study will have to demonstrate that this new type of incinerator enables a quantitative destruction of organic wastes while only releasing inactive-gases (in terms of radioactivity and chemical toxicity).

The work to be performed is focused on the study of the adaptation of a closed loop for pressurized combustion operating at 60 bar - including the setting-up of a suitable off-gas treatment - to incinerate organic waste and mainly spent ion-exchange resins.

BERTIN has to adapt the waste incineration process. In particular, a test bench for spent ion-exchange resins incineration has to be achieved. The CEA will review the possible waste to be processed, and will perform laboratory incineration and treatment trials.

INITEC participates in the design of the incineration test bench and the trials.

B. WORK PROGRAMME

According to the additional clause of the contract, the work programme has been modified and comprises five distinct steps.

1. Identification of radioactive waste which could be incinerated : different organic wastes will be analysed. The choice will take into account the incineration characteristics as well as the interest of removing organic elements from the waste (amount produced, existing solution of removal, ...).

2. Drawing-up of process flow-sheets for incineration of spent ion-exchange resins. The best process and its main operating parameters will be defined.

3. Treatment and conditioning study of secondary waste generated during the incineration process : ashes, dust, liquids and gases (uncondensable gases and the release of under pressure storage tanks).

4. Bench-scale tests : after achievement of a specific test bench, various incineration and treatment trials will be performed to confirm the hypothesis made for the drawing-up of process flow-sheets.

5. Technical evaluation : based on the results of bench-scale tests, this last step will permit to conclude upon the feasibility of the process.

C. PROGRESS OF WORK AND OBTAINED RESULTS

State of advancement

Work carried out over the last year was planned to complete the work programme. However, difficulties occurred during the pressurized incineration tests which made impossible to obtain significant results. A new furnace is currently designed and complementary under pressure trials will be performed as soon as this new furnace will be operational.

Progress and results

C.1. Incineration tests at atmospheric pressure

During the preliminary trials, three kinds of problems were encountered :

- diffusion of metallic vapours (Li, B, ...) through the ceramic pipe of the furnace inducing electrical short circuits when the furnace temperature reached about 800°C. So, due to this too low temperature level, combustion was not completed : soot formation, CO > 500 ppm, carbon percentage in ashes > 7 %
- plugging of the CO_2/O_2 feeding system by the melting of metallic ashes
- high fluctuation of the resin flowrate.

After some significant modifications of the test bench, a temperature of 1 000-1 100°C has been reached. Main results measured were :

* combustion efficiency
  - resin destruction efficiency : > 99,8 % (based on carbon balance)
  - CO content in combustion gases : < 30 ppm
  - no soot formation.

* behaviour of metals and simulated radioelements
  - Co, Mn, Sb, Li, B : main part of these elements contained in the resin was collected in a refractory crucible located at the bottom of the furnace (metallic ashes). The other fraction, volatilized during combustion, was recovered by the quench
  - Cs : caesium is very volatile. So, about 90 % was volatilized and recovered by the quench.

* gas scrubbing
  A recovering efficiency of sulphur oxides by the quench more than 97 % was obtained : SO2 content in the outlet gases was around 20 ppm-80 ppm.

* liquid composition
  In addition to metallic dust (condensation of metallic vapours), the quench and bubble scrubber liquids contain :
  - some traces of dissolved radioelements
  - sodium nitrates
  - sodium sulphates
  - eventually carbonates (depending on operating parameters).

C2. Liquid treatment

In order to decontaminate the liquid, many treatments have been tested. Four of them allow high decontamination factors :

Mn_{54}	:	>	500
Co_{60}	:	>	90
Cs_{137}	:	>	100
Sb_{125}	:	>	50

The volume of contaminated sludge resulting of these decontamination treatments represents about 7 %-8 % of the initial liquid. These sludges were composed of :

- liquid (water + sodium sulfates and nitrates) : 80 %
- radioelement hydroxides, zeolites : 20 %

C3. Incineration test under pressure

Due to defective working of a cooling circuit, the resin feeding system was destroyed. Furthermore, high thermal losses were observed during under pressure operation. So, temperature of the furnace was not high enough to be consistent with combustion. The resin feeding system is now operational and a new furnace is under setting up.

C4. Flowsheet of a 10 kg/h pilot

Based on results of atmospheric incineration trials and liquid treatment tests, the flowsheet of a 10 kg/h pilot was defined. Incineration of 10 kg/h (14 l/h) of active ion exchange resins by mean of oxygen will lead to three phasis :

- an active solid phasis, composed of metallic ashes (boron and lithium oxides, radioelements) : 0.2 l/h
- an inactive gaseous phasis, composed of about 90 % CO_2 and 10 % oxygen, with traces of CO (< 30 ppm), NO_x (< 20 ppm) and SO2 (< 80 ppm)
- an active liquid phasis (10 l/h) which results of the combustion water condensation and which contained neutralization salts (essentially sodium sulfates), radioelements (principally caesium) and condensed metallic oxides. Treatment of this phasis generates about 10 % (~ 1 l/h) of active sludge.

The volume of secondary active waste corresponds to around 1/12 of the initial resin volume.

Title :	**MELTING OF INCINERATOR ASHES USING A MICROWAVE FURNACE**
Contractor:	CEA DCC/DRDD/SCD (F)
Contract N°:	FI2W-CT91-0100
Duration of contract:	July 1991 - July 1995
Period covered:	January - December 1994
Project leader:	J.J. Vincent

A. OBJECTIVES AND SCOPE

The purpose of this investigation is to design, build and test an inactive prototype microwave melting facility for incineration ashes, with a capacity not exceeding a few kilograms per hour.

The microwave melting technique will significantly reduce the ash disposal volume while ensuring chemical and mechanical stability comparable to that of the most favorable radioactive waste containment matrices. This technique is also particularly well suited for the treatment and conditioning of radioactive ashes, which are produced in relatively small quantities (about 10 m^3 per year) based on projections for the French MELOX mixed UO_2-PuO_2 oxide fuel fabrication plant.

B. WORK PROGRAMME

B.1 Bibliographic review.
- Interrogation of data bases covering microwave melting (existing processes, operating conditions, dielectric properties of materials).

B.2 Laboratory study.
- Specification and development of a glass composition for ash incorporation compatible with certain constraints:
- moderate melting temperature (1100°C),
- satisfactory microwave susceptibility,
- suitable glass leaching resistance.

B.3 Selection of a melting device.
- Generator power and frequency.
- Melter type: casting furnace or expendable crucible furnace.
- Energy transmission mode: monomode or multimode.
- Crucible structure: cooled metal or refractory material.
- Glass casting mode: batch or continuous.
- Microwave cavity design.

B.4 Design and construction of the melting facility.

B.5 Testing and development.

B.6 Technical and economic assessment.

C. PROGRESS OF WORK AND OBTAINED RESULTS

State of Advancement

Task B1 (*bibliographic review*) was completed in 1993.

Task B2 (*laboratory studies*) was completed in 1993.

Task B3 (*selection of a melting device*). The solution was defined in 1992. The water-cooled metal melter, heated by a monomode generator operating at 915 MHz was the only avenue investigated in 1994.

Task B4 (*design and construction of the melting facility*) was completed in 1993.

Task B5 (*testing and development*) was the primary focus of the work performed in 1994. In addition to vitrification tests, the investigation was intended to comprehend and characterize the electromagnetic phenomena involved in the ash melting cavity, with the ultimate objective of improving the system energy efficiency (impedance matching in the cavity) and/or minimizing the thermal heterogeneities in the glass melt (preventing standing waves).

Progress and Results

Task B5 – Testing and Development

- ***Melting tests with the 915 MHz Applicator***

Acceptance testing of the 915 MHz melter with a 20 kW generator at the end of 1993 showed that additional measurement provisions were required to characterize the system performance. A detection crystal coupled with a milliwattmeter was therefore installed at the water load outlet immediately after the circulator to measure the incident and reflected power.

Ash containment glass melting tests were then carried out to determine the nominal capacity of the 915 MHz melter with the 20 kW generator. The results indicated that the melter was not uniformly heated, and that the glass melt in the applicator was characterized longitudinally by alternating hot orange-yellow and cool dark red zones. Reflected power measurements also showed that the short-circuit piston did not satisfactorily tune the cavity: the efficiency never exceeded 50%, i.e. the ratio of the reflected power to the incident power was 0.5. Under these conditions, with a 20 kW incident power rating, no more than 10 kW were actually absorbed by the melt. Considering the area of the glass, this is far too low to heat the glass to its process temperature. This was confirmed by optical pyrometer readings that indicated a temperature of 950°C in the "hot" layers of the melt, and by repeated plugging of the casting nozzle due to insufficiently heated glass.

These findings underscored the importance of understanding and characterizing the electromagnetic phenomena that control melter operation. The CEA/DCC/DRDD/SCD therefore decided to concentrate on this area with the hope of mastering the inherent drawbacks of the heating system.

- ***Characterization of the Unheated Electromagnetic Cavity***

Standing wave conditions in the cavity are determined by the position and nature of the terminal load, a short-circuit piston in this case. Maxwell's equations indicate that in a cavity with a short-circuit boundary condition, the electric field is nil at the wall and in quadrature with the magnetic

field (the electric and magnetic fields propagate in perpendicular planes). Determining the wavelength in the wave guide relative to the piston position d thus indicates the precise distribution of the electric and magnetic fields in the cavity.

In a lossless waveguide, the reflection coefficient Γ as a function of the piston displacement d is given by the complex expression:

$$\Gamma(d) = \Gamma_0 e^{-j\frac{4\pi d}{\lambda g}}$$ where λg is the guided wavelength.

A network analyzer, a waveguide/coaxial transition and an experimental setup were used to determine $\Gamma(d)$, characterized by its amplitude and azimuth or argument. Plotting Arg $\Gamma(d) = f(d)$ yields a set of points for which a least-squares linear regression provides a straight line relation of the type:

$$Y = AX + B$$

where Y : Arg $\Gamma(d)$
X : d
A : $-4\pi/\lambda g$.

Evaluating A, yields an accurate determination of λg, and therefore the exact positions of the electric field nodes and antinodes in the applicator.

Three cavity configurations were tested to measure λg: the empty melter and the melter containing 1.5 cm or 3 cm of water:

- For the empty melter, $\lambda g = 40.92$ cm and $\Gamma = 1$ irrespective of the piston position.
- With 1.5 cm of water in the melter, $\lambda g = 39.74$ cm and Γ ranges from 0.77 to 0.9.
- With 3 cm of water in the melter, $\lambda g = 38.17$ cm and Γ ranges from 0.59 to 0.73.

The field distributions are now known in the three test configurations; the guided wavelength is relatively unaffected by the presence or absence of water in the cavity. The results show that the short-circuit piston is unable to tune the resonance cavity ($\Gamma = 0$) as initially intended. In fact, its main function appears to be to position the field lines accurately in the melt.

- ***Characterization of the Heated Electromagnetic Cavity***

Characterizing the electromagnetic cavity at room temperature using water to simulate the glass melt was a necessary step, but a number of questions remained unanswered:

- Is the electric field distribution obtained in the presence of water representative of melter operation with molten glass?
- What are the optimum locations for the hot spots? Do they coincide with nodes or antinodes of the electric field?

Only melter characterization at normal operating temperatures could answer these questions. As the use of a network analyzer was impossible under these conditions, a novel method was devised: the measured parameter was not the electric field, but the thermal result of its action on the melt, i.e. the temperature (Figure 1).

Placing an optical pyrometer above the feed port or the off-gas port and plotting the temperature variation according to the piston position d yielded a sine curve on which the minima and maxima were separated by $\lambda g/4$, and the distance between successive maxima was $\lambda g/2$. The guided

wavelength in the heated melter ($\lambda g = 38$ cm) was therefore equivalent to the value measured with water at room temperature.

The thermal heterogeneities in the glass melt were also measured: temperature differences always exceeding 500°C were recorded between two extremes only 9 cm apart. The thermal gradients therefore reach $60°C \cdot cm^{-1}$.

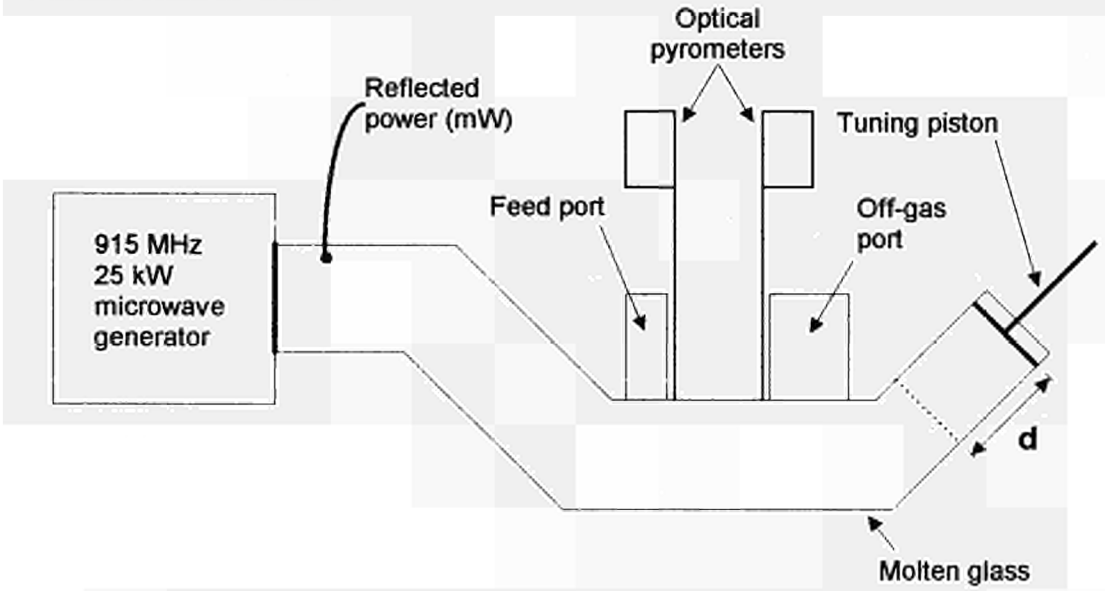

Figure 1. Pr, Γ and T versus d measurements on melter in operation

In addition, the electric field was measured at room temperature at the off-gas exhaust port with the 915 MHz melter containing water (Figure 2). The measurement line was a coaxial cable from which the outer shield was stripped over 1 cm at one end to form a probe inserted into the waveguide at right angles to the large dimension. A detection crystal supplying a galvanometer was connected to the other end of the coaxial cable. A 915 MHz generator supplied an electromagnetic signal of a few microwatts inside the waveguide.

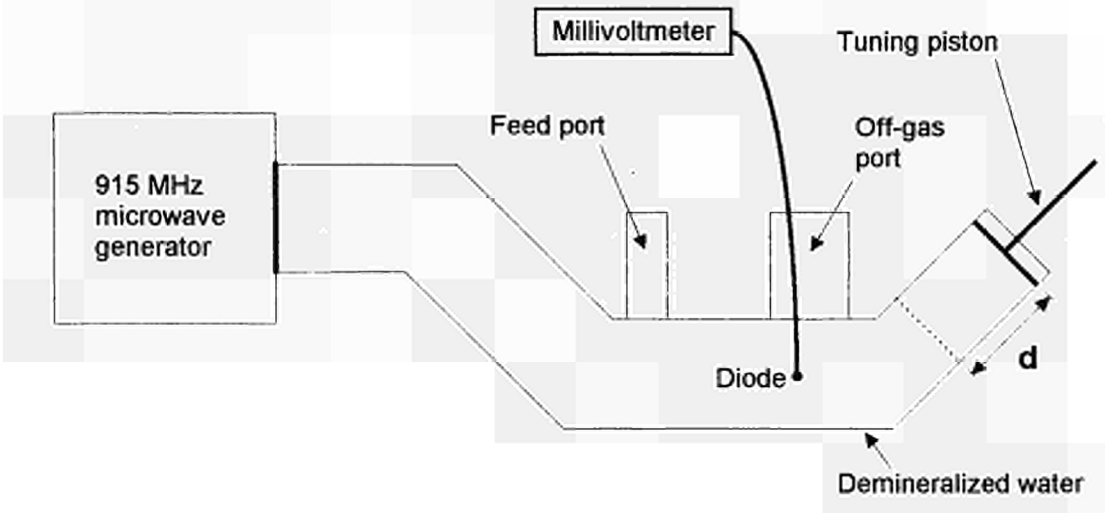

Figure 2. Electric field measurement on unheated melter

The results of these measurements were plotted together with the temperatures measured at the off-gas port in the heated melter (Figure 3): heating (temperature) is in phase quadrature with the electric field. Contrary to our initial expectations, microwave heating in the cavity is therefore inductive (resulting from the magnetic field) and not due to dielectric relaxation (resulting from the electric field).

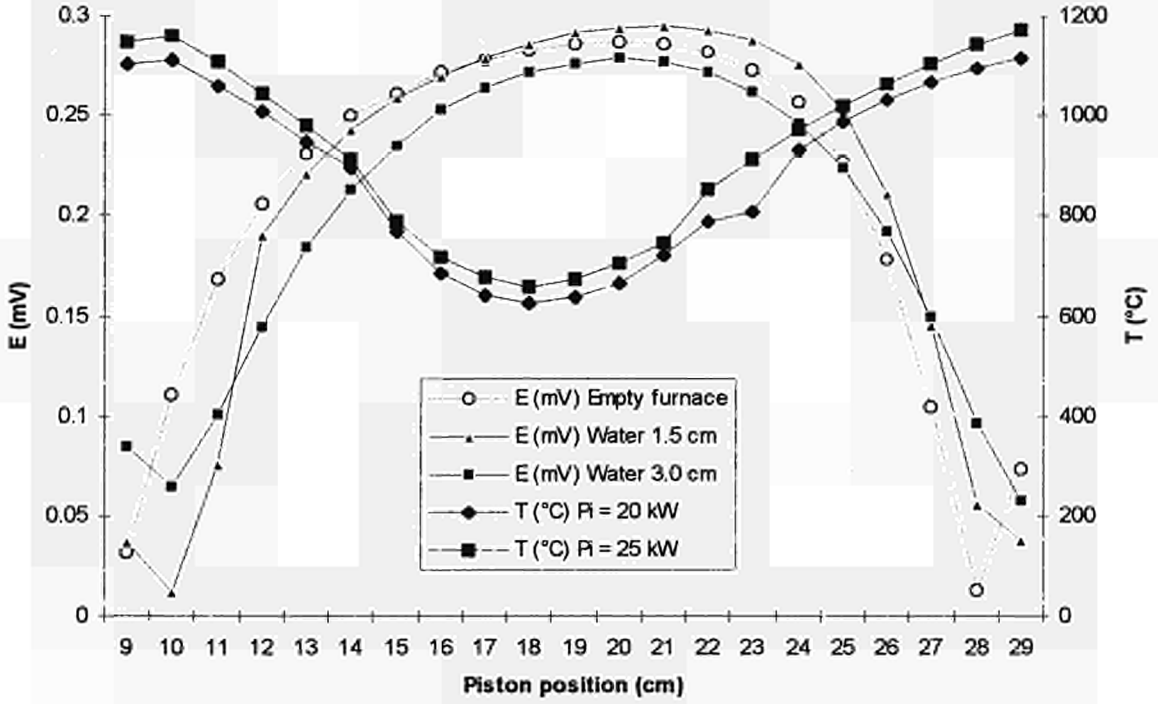

Figure 3. Temperature versus electric field at the off-gas port

- ***Impedance Matching Tests***

The results obtained showed that it is indispensable to increase the energy dissipation in the glass melt. Two options may be explored:

- Constant impedance matching with a higher power rating. A 60 kW generator was ordered by the SCD to investigate this possibility.
- Constant incident power with improved impedance matching. Tests were undertaken at room temperature using the network analyzer to develop an impedance matching valve. The results showed that it was possible to obtain resonance (total dissipation of the incident energy in the melt) for a given piston position. Qualification of this work at higher power and temperature values is scheduled for 1995.

Title	**NEW MACROCYCLIC EXTRACTANTS FOR RADIOACTIVE WASTE TREATMENT : IONIZABLE CROWN ETHERS AND FUNCTIONALIZED CALIXARENES**
Contractors	CEA/Cadarache - University of Barcelona - University of Belfast - University of Mains - University of Parma - University of Twente - EHIC Strasbourg - University of Strasbourg
Contract N°	FI2W-CT90-0062
Duration of contract	September 1991 - August 1995
Period covered	January 1994 - December 1994
Project leader	J.F. DOZOL (Coordinator) - F. LOPEZ CALAHORRA - M.A. McKERVEY - V. BOEHMER -R. UNGARO - D. REINHOUDT - M.J. SCHWING - G. WIPFF

A. OBJECTIVES AND SCOPE

The principal aim of this research consists in perfecting the schemes of decontamination of real liquid wastes : medium level reprocessing concentrate and more generally liquid wastes arising from reprocessing plants.

The objective of this research is to selectively remove actinides, cesium and strontium from high salinity wastes arising from reprocessing operations in order to minimize the volume of wastes to be disposed of in a geological formation.

It is intended to investigate the potential of new classes of organic extractants under development in different university laboratories.

The extracting properties of these compounds will be studied and the most effective products will be tested on simulated and real wastes.

B. WORK PROGRAMME

The four Universities (Barcelona, Belfast, Mainz, Parma) working on the synthesis and basic research of calixarenes devote their efforts to prepare selective extractants.

CEA tests after the screening carried out at EHIC Strasbourg the extractants prepared by the various universities involved in the project.

The University of Twente tests the potentiel of synthesized macrocycles for the transport of cations via S.L.M and, if necessary, modifies the structure of the macrocycles in order to improve the stability of the membrane and the transport of cations through the membrane.

From January molecular modeling studies are carried out by the Universities of Strasbourg and Twente and CEA, X-ray data useful for the modeling are provided by the University of Parma.

C. PROGRESS OF WORK AND OBTAINED RESULTS

1- State of advancement

Since the beginning of the contract more than 90 macrocycles have been synthesized by the several Universities involved in the project and screened at the EHIC Strasbourg. About 50 were tested at Cadarache with nuclides in simulated liquid waste.

2- Progress and results obtained in the various laboratories

2.1- European Higher Institute of Chemistry of Strasbourg

2.1.1- Extraction of Th(IV) and Eu(III) by phosphine oxide calixarenes

a) Compounds from Belfast

Twelve calixarenes (n=4,5,6,8), substituted by phosphine oxide functions at the lower rim, have been tested with thorium and europium as well as the related acyclic compound tris-diphenylphosphine oxide. All the compounds are better than T.O.P.O. and C.M.P.O., the hexamers being always the best extractants. The extraction levels are drastically increased by p-dealkylation, but decreased by the replacement of the phenyl residue on the phosphine oxide function by n-butyl. The values of the slopes of the linear plots log D vs. log C_L are all around 2. As with T.O.P.O., the extracting power decreases with increasing nitric acid concentration.

b) Compounds from Parma

Nine calixarenes (n=4,6), obtained by overall or selective functionalization with phosphine oxide functions, have been studied with thorium nitrate. Three of them are calix[4]crowns. The best compound is the di-ethoxy(diphenylphosphine oxide)-calix[4]-crown-5, whereas the similar compound whithout the crown part is much less efficient. For the calix[4] diphosphine oxides, the longer the functional chain, the less efficient is the ligand, whereas the contrary holds for the calix[6] triphosphine oxides.

c) Compounds from Mainz

Six tetraalkoxycalix[4]arenes, substituted at the upper rim by "CMPO-like" groups have been tested for thorium and europium. In equimolar concentrations of metal and ligand (10^{-4} M), the extraction of thorium nitrate is higher than 50% and shows no significant dependence on the length of the alkoxy chain. The weaker extraction of europium allowed a log-log plot analysis : a slope of 2 was found.

d) Comparison of the compounds tested

All the calixarenes are much better extractants for Th(IV) and Eu(III) than CMPO and TOPO. For $C_M = 10^{-4}$ M and $C_L = 10^{-3}$ M, the extracting power decreases in the following order :
Mainz compounds (%E = 100) > p-deak.[6]phosphine oxide (Belfast) (%E = 95) > p-dealk. [8]phosphine oxide (Belfast) (%E = 88) > p-dealk.[4]phosphine oxide (Belfast) (%E = 80). Calixarenes from Parma are less efficient (%E ≤ 5) in the same conditions. This sequence is in agreement with that established at Cadarache on simulated waste.

2.1.2- Extraction and complexation of alkali and alkaline earth cations by the para-dealkylated calix[6]arene hexa diethyl amide from Belfast.

As the p-dealkylation had shown a decrease of the Na^+ extraction and complexation in the ester series, a dealkylated calix[6] hexadiethylamide has been synthesized in order to see whether the Sr^{2+}/Na^+ could be improved. The results of complexation and extraction shown an increase of the Sr^{2+}/Na^+ selectivity which becomes better than that of DC18C6.

2.2- C.E.A. Cadarache

Three classes of calixarenes were particularly studied in 1994 :

• deterbutylated and terbutylated calix[n] arene ethoxy diphenyl phosphine oxide (n=4,6,8) synthesized by the University of Belfast.
• alkyl diphenyl phosphinoxidoacetamide calix[4]arene prepared by the University of Mainz.
• calix[4]arene butoxy dipheny phosphine oxide and calix crown 6 butoxy diphenyl phosphine oxide.
For extraction of actinides by the calixarenes synthesized at Belfast, the size of calixarenes is optimized with the hexamer. The performances also depend on the upper rim substituent, unfortunately the dealkylated calixarene is not enough soluble in NPHE to be compared with its alkylated analogue. The calix[6]arene is pointed out as the best one in the case of transport of Np and Pu through S.L.M however no significant transport of Am is observed although the stripping distributed coefficients are satisfactory.
All the compounds prepared at Mainz exhibit high extracting power toward actinides whatever the length of the linear alkyl chain branched on the lower rim, their solubility in NPHE is low ; nevertheless this low concentration is sufficient to display highly better results than those obtained with CMPO which is our reference, studied in the same conditions. The S.L.M transport experiments confirm the exceptional performances of these compounds : quantitative transports of Am and Pu are achieved with these products.
Calix[6]arene butoxy diphenyl phosphine oxide and calix[4]crown 6 butoxy diphenyl phosphine oxide synthesized at Parma exhibit a good extracting power and a high transport rate through S.L.M for plutonium.

2.3- University of Twente

2.3.1- Transport of cesium

Calix[4]arene-crown-6 derivatives 1-4 synthesized by the groups of Parma and Twente, showed enormous affinity for cesium over sodium ions. For practical applications, it is necessary to remove all cesium ions from the waste solution, this means transport of cesium ions against a concentration gradient. When a secondary salt with the same anion and a low extraction constant is present in large excess, the anion gradient acts as a "pump" for the primary salt. The properties of carriers 1-4, calix[4]arene crown 6 with respectively groups : i-propyl, n-propyl, n-octyl and NPOE, having high affinity for cesium and showing no significant sodium transport, are ideal for removing traces of cesium salts out of a solution with a high sodium concentration.
Using 0.01 M carrier solutions of 1-4 in NPOE, from a mixture of 10^{-3} M $CsNO_3$/ 1M $NaNO_3$, within 4 days 71-87 % of the cesium was transported.
The Cs^+/Na^+ ratios obtained in the receiving phase varied from 7650 (4) to 13650 (2).
The flux increased with increasing carrier concentration, carrier 4, designed to be highly soluble in NPOE, showed the highest cesium flux when 18 weight % of 4 (0.16 M) in NPOE was used. At even higher carrier concentrations, the flux decreases, probably because the viscosity in the membrane becomes too high. To compare 2-4, a carrier concentration of 0.05 M was chosen (1 did not completely dissolve in NPOE at this concentration) : virtually all cesium was removed from the source phase within 4 days. The Cs^+/Na^+ ratios varied from 2200 to almost 3800. Using conditions to simulate the saline mixture present in medium level nuclear waste solutions (10^{-3} M $CsNO_3$, 4 M $NaNO_3$, 1 M HNO_3) and again a carrier concentration of 0.05 M in NPOE, virtually all cesium was removed from the source phase, even within 24 h. The Cs^+/Na^+ ratios varied from 400-500.

2.3.2- Transport of lanthanides

The use of polarography proved to be very convenient, because this method allowed the direct detection of the complexed Eu^{3+} (to the stripping agent). Furthermore, optimization of the transport conditions showed that 1-hydroxyethyl-diphosphonic acid acts more efficient at an initial pH of 4.0 in the receiving phase. The compounds tested so far (calix[4]arenes with phosphinoxide groups at the lower rim, developed by the groups of Parma and Belfast) were not very efficient in transport of europium. Recently however, the group of Mainz developed very promising calix[4]arenes which have CMPO-like functional groups at the upper rim, and these compounds will be used in the near future as carriers for Eu^{3+}.

2.4- University of Belfast

The work carried out during 1994 was concerned primarily with completing the entire range of calixarene phosphine oxides of the general formula (calix-O-$CH_2CH_2POPh_2)_n$, n=4,5,6 and 8, for both the p-tert-butyl series and the dealkylated series. Gram quantities of these compounds have been made

available and extensive screening of their extraction efficiency for europium(III) and thorium(IV) have been completed in Strasbourg. All compounds, with the exception of the pentamers have also been screened in Cadarache. Work on the synthesis of phosphine oxides with alkyl residues on phosphorus was also started. The extension of phosphine oxide chemistry to include calixarene derivatives with shorter spacers has also been undertaken, the targets being derivatives of the type (calix-O-$CH_2PPh_2)_n$,. Preliminary studies have been conducted with the tetramer derivatives. Our synthetic work has been extended in two other directions. Firstly, we have begun the synthesis of calixarene phosphine oxides with mixed functionality, the intention here being to modulate their extracting ability towards lanthanides and actinides by introducing amide and carboxylic acid functions. Secondly, we have initiated a study of phosphine oxides which do not possess the calixarene substructure. The objective of this study is to determine the structural and conformational parameters essential for lanthanide and actinide complexation and thus enable optimal structures to be designed in the future. One such compound, 1,3,5-$C_6H_3(OCH_2CH_2POPh_2)_3$, has been synthesized and is currently under study in Strasbourg.

2.5- University of Mainz

End of 1993 the first examples of calix[4]arene ethers, substituted in p-position (at the "upper rim") by the CMPO-like structural element NH-CO-CH_2-PO-$(C_6H_5)_2$ (CMPO-calixarenes) had been prepared and early in 1994 it became clear by the extraction, complexation and transport studies carried out in Cadarache and Strasbourg, that these compounds are much better extractants for actinides than the "classical" CMPO (octyl-phenyl-N,N-diisobutyl-carbamoylmethyl phosphine oxide). Since the analogous phenolethers with a NH-CO-CH_2-PO-$(C_6H_5)_2$ substituent showed no activity at all, it was also clear, that these excellent properties must be due to the cooperative action of several of these groups attached to the calixarene skeleton.
The synthetic work carried out in Mainz was therefore more or less concentrated on the preparation of various CMPO-calixarenes, and other subjects will not be covered in this short survey. The following points were especially addressed :

2.5.1- Improvement of the synthesis

Since the Arbusov reaction of -NH-CO-CH_2-Br groups with diphenylphosphinicacid esters (which is possible with single phenols) was not successful in the case of calixarenes, we tried the attachment of (CO-CH_2-PO-$(C_6H_5)_2$) groups using various acylating agents. The acidchloride decomposes during its preparation. Reaction with the anhydride or coupling with the free acid, using dicyclohexylcarbodiimide, gave products which were difficult to purify. The p-nitrophenylester (p-NO_2-C_6H_4-O-CO-CH_2-PO-$(C_6H_5)_2$), accessible in four steps from $(C_6H_5)_2$ PCl, finally proved to be the best choice. The whole synthesis now includes the following steps :
- O-alkylation of t-butyl calix[4]arene to form a tetraether in the cone-conformation;
- Ipso-nitration to replace the t-butyl by nitro groups;
- Reduction of nitro groups to amino groups by catalytic hydrogenation;
- Aminolysis to form the (NH-CO-CH_2-PO-$(C_6H_5)_2$ groups.

2.5.2- Improvement of the solubility

Although CMPO-calixarenes are more effective than CMPO even in concentrations as low as 10^{-4} M, an improvement of their solubility in organic solvents was desirable. Therefore calix[4]arene derivatives with various alkyl ether groups were synthesized (linear C_6H_{11}, $C_{10}H_{21}$, $C_{12}H_{25}$, $C_{14}H_{29}$, $C_{16}H_{31}$, $C_{19}H_{37}$, branched C_8H_{17}) including compounds with different ether residues.

2.5.3- Elucidation of the complex structure

To gain a better understanding of the requirements for an effective complexation of actinides the following synthetic approaches were undertaken :

- CMPO-calix[4]arenes derived from 1,3-dialkoxy-2, 4-dimethoxy calix[4]arenes, which can assume also the partial cone or 1,3- alternate conformation, while the tetraalkoxy calix[4]arenes (due to the longer alkyl groups) are fixed in the cone-conformation.
- CMPO-calix[5]arenes fixed in the cone-conformation, to establish the influence of the ring size.
- Linear dimers and trimers with analogous structural elements, to establish the "macrocyclic effect".
- Calix[4]arenes bearing only two or three CMPO-structures (just in preparation), to find out how many CMPO-functions are involved in a complex.

2.6- University of Parma

The activity of Parma group in 1994 has been mainly devoted to the problem of removal of actinide ions, exploiting phosphorous containing calixarene ligands. In particular, calix[4] and calix[6]arenes selectively functionalized at the lower rim with phosphine oxide [-P(Ph_2)O] chelating groups have been synthesized. The first problem which has been tackled was to optimize the introduction of the phosphorous groups on calixarenes. The two steps synthesis which consists in the reaction of potassium diphenylphosphide on a calixarene bearing alkyl-bromide chains followed by oxidation of the resulting phosphine to phosphine oxide gives usually low yields of products. This prompted us to develop an alternative route which consists in the direct reaction with ethyl diphenyl phosphinite.
In this way we could therefore synthesize a series of calix[4]- and calix [6]arenes bearing phosphine oxide groups linked to the macrocycle through ethoxy or butoxy chains in order to better evaluate the role of the distance between the chelating groups and the calix.
Bis(diphenylphosphine oxide)calix[4]arenes,with different conformational properties have been prepared in order to exploit possible cation-p interactions on actinide complexation.
Conformationally mobile 1,3-dimethoxy, together with 1,3-dialkoxycalix[4]arenes fixed in the 1,3-alternate or cone structure have been sent to Strasbourg and Cadarache for complexations studies.
Calix[4]arenes with poliethereal bridges of different length in 1,3 positions, bis(diphenylphosphine oxide)calix[4]arene-crown-5 and -crown-6 were prepared to enhance selectivity in complexation. The size of the calixbackbone was increased using 1,3,5-trimethoxy-p-tert-butylcalix|6]arene and other selectively functionalized calix[6]arenes as starting material.

2.7- University of Barcelona

In previous reports we presented the syntheses of several ionizable crown ethers containing sulfonic groups. The results reported by the Strasbourg group about the complexing abilities of such compounds show that its behaviour is similar or worse than the conventional non-ionizable crown ethers. The results, together with the very difficult preparation, isolation, purification, and its completely inadequate solubility, convinced us to leave the study of these compounds, at least by the moment.
To solve the former problems we have devoted a big effort in the preparation and study of polymeric ionizable crown ethers, as was foreseen in the Project. The idea was to prepare such systems by polymerization of suitable monomeric vinylbenzocrown ethers, directly or previously complexed to modulate the size of the internal cavities and channels into the polymeric structures, together with other monomeric molecules containing acidic groups and with or without cross-linking agents. As expected, the preparation, purification and manipulation problems disappeared, and the ten different systems prepared exhibit good complexing characteristic and some selectivity in front of cesium and strontium in different conditions of solvent and pH. In the case of some linear (no cross-linked) low molecular weight polymeric systems, their solubility in hydrophobic solvents like chloroform converts them into good candidates to be used as extraction agents. In any case, at the moment the results have been good but insufficient and this is a study that deserves much more work.
The new trend was to modify the distearoyldibenzo-18-crown-6, previously prepared by us, or the dialcohol obtained by reduction, to introduce strong acidic groups.
The results were negative, the yields in the desired products were almost zero in any condition and the isolation and purification impossible because of the very small amounts obtained.

We have also tried the introduction of phosphoric groups from the same type of substrate. The introduction of alkyl group R would have the purpose of modulate the lipophillicity of the resulting system, specially when R = H or CH_3. In any case, the final result has always been negative : it has been impossible to isolate the desired compound, the first step, introduction of $PO(OEt)_2$ group, being specially difficult.
In the last case the idea was to use the epoxide to introduce alkyl groups in order to modify the solubility of the resulting systems in water or organic solvents.
Despite the lack of success in these last reactions we are continuing to study it, but as such unfruitful work is showing unexpected difficulties, probably due to the low electrophillicity of the carbonyl groups linked to the benzo-crown system or steric problems, we have started alternative ways with the idea of moving away the reactive center from the aromatic ring.

2.8- Molecular modeling : University of Strasbourg

Within this contract, we extended studies performed at MSM on the Na^+/Cs^+ binding by calix[4]arene crown ether derivatives, and related ionophores of interest. The computational tools are Molecular Dynamics and free energy perturbation FEP simulations, using an explicit representation of the solvent.

2.8.1- Modeling complexation of M^+ by dimethoxy-calix[4]crowns : Na^+/Cs^+ selectivity in pure aqueous/non aqueous solvents with counter-ion effects

Three forms (cone, partial cone, 1,3-alternate) were compared, with X=H/t-butyl, for the crown-6 and crown-5 hosts. Studies concerned mostly the force field and methodological assessment of these results (M^+, aromatic residues) obtained previously.
We confirmed that intrinsically, in the gas phase and pure chloroform solution, the binding sequence is $Na^+ > K^+ > Rb^+ > Cs^+$. In water, the binding selectivity depends on the conformation of the host : the cone conformation of calix[4]-crown-6 prefers Na^+ over Cs^+ ; 1,3-alternate prefers Cs^+. The partial cone displays no clear preference. In methanol and in acetonitrile, we predict very similar trends as in water. This has been confirmed by MD FEP studies on the calix[4]-bis-crown-5 and bis-crown-6 analogues simulated at MSM.
The importance of picrate counter-ion (Pic-) on structures and selectivities of H-calix[4]-crown-6 and the bis-crown analogues in water and in $CHCl_3$ was also studied.
We modeled the extraction selectivity of M^+ from water to $CHCl_3$ and predicted that calix[4]-crown-6 1,3-alternate extracts Cs^+ better than Na^+ ; while the cone extracts better Na^+. Our simulations confirm the high ionophoricity of 1,3 alternate form and explain why.

2.8.2- Modeling ionophores at the water-chloroform interface

We initiated the simulation of a series of ionophores at this interface, represented explicitly : 18-crown 6, cryptand 222, t-butyl-calix[4]tetraamide, $(OR)_2$-calix[4]crown 6 and calix[4]-bis-crown-6. Initially equally shared by the two solvents, they tend to move to the organic phase, but remain "anchored" at the interface. Studies on the M^{n+} complexes, with and without Pic^- counter-ion were also initiated and are in progress.

2.8.3- Other related studies involve

•The binding selectivity for M^{2+} complexation (Mg^{2+}, Ca^{2+}, Sr^{2+}, Ba^{2+}) in water by calixarenes. Comparison of simulated X-ray structures from Parma,
•Conformation of CMPO-like calix[4]arene M^{n+} complexes,
•Simulations of complexed CMPO, TPTZ and analogues in solution.

2.9- Molecular modeling : CEA Cadarache

Our goal is to study by Molecular Dynamics and Free Energy Perturbation techniques the relative stability and selectivity of the complexes between alkali cations and some calix[4]arenes-crown-6, synthesized in Parma, that show a good selectivity for cesium towards sodium.

In a first time, we focused on the study of the influence of the force field and of the software used for the simulations. In order to be able to compare the results of our simulations with those of Pr. Wipff's team in Strasbourg, we chose to begin with the 1,3 alternate dimethoxy-calix[4]arene-crown 6, as a test compound. These calculations were performed in vacuo with two softwares (*SYBYL* from Tripos Associates and *AMBER* from the University of San Francisco) and two force fields : Tripos FF, standard force field in *SYBYL* that we had to implement in *AMBER*, and Kollman all-atoms FF, widely used in *AMBER* and available in *SYBYL*. The same set of point charges, calculated with AM1 semiempirical method, was used for these simulations.
In spite of some differences in the values of energy and on the conformations generated, and whatever were the force field or the software used, we concluded that in vacuo, the intrinsic affinity of the calixarene for alkali cations followed the order :

$$Na^+ > K^+ > Rb^+ > Cs^+$$

This selectivity order does not take into account the influence of the environment, that can be studied qualitatively by MD simulations in a solvent box, neither the energy of desolvation of the cation which is involved in free energy calculations in an explicit solvent.
The relative free energy of binding calculated in water by the *AMBER* software with Tripos FF showed the importance of the desolvation energy of the cations to explain selectivity and then we calculated the following selectivity order :

$$Cs^+ > Rb^+ > K^+ \geq Na^+$$

Our results are in a qualitative agreement with those obtained in MSM, for 1,3 alternate dimethoxy-calix[4]arene-crown-6, with different force field conditions than ours.
Then, we chose our simulations conditions and we worked on an other compound, the diisopropoxy derivative, in the cone and 1,3 alternate conformations. MD simulations and relative free energy of binding were done in vacuo and in water for both compounds. In this case too, our results are in a qualitative agreement with the experimental results or the simulations performed in MSM. Our current simulations focus on the improvement of the accuracy of the calculations to get closer to the stability constants determined by complexation experiments.

2.10- Molecular modeling : University of Twente

The tetraester tetrahomodioxacalix[4]arene 1, is a calix[4]arene whose ring has been enlarged by the introduction of two oxygen atoms and two methylene groups. The tetrahomodioxacalix[4]arene has larger complexing capabilities towards the alkaline-earth cations, in particular Ca^{2+}, Sr^{2+} and Ba^{2+}, than towards the alkali cations. The extraction capabilities of 1 towards the alkali-earth metal ions are not very large, but they are comparable with the extraction capabilities of 1 towards Na^+.
Because of these properties, we have decided to investigate the complexing capabilities and the selectivity behaviour of 1 towards Na^+ and Sr^{2+} by means of Monte Carlo techniques. We perform Absolute Free Energies of Binding calculations via the "Double Annihilation technique" where the association constant of each complex in solution is calculated in two steps : in the first step, the cation bound to the ligand is annihilated, in the second step, the free cation is annihilated. On the basis of room temperature NMR studies, 1 may exist in many conformers in solution amongst which the 1,2-alternate and the cone conformers are the most stable ones and, in turn, the 1,2-alternate conformer is more stable than the cone conformer. Our preliminary results for Li^+ show that we can reproduce association constants which are in very good agreements with the experimental values.
Further, we are investigating the effect of the substituent on the complexing capabilities of 1 towards Na^+ and Sr^{2+}. We are, consequently, calculating the Absolute Free Energies of Binding of the tetraester and the tetraamide derivatives. The work is in progress. The Monte Carlo simulations are performed by means of the *BOSS* program of W.L. Jorgensen on a *CRAY YMP C98*.

2.11- Molecular modeling : University of Parma

The major contribution of the Parma group to the modeling part of the project is to provide structural data (in the solid state and in solution) on the complexes between calixarenes ligands and cesium and strontium salts. The attention has been first devoted to complexes of cesium salts and 1,3-dialkoxycalix[4]arene crown-6, either conformationally mobile or fixed in 1,3-alternate conformation. The X-ray crystal structures of two cesium picrate complexes have been solved by single crystal diffraction methods. Both show the cesium ion encapsulated in a binding pocket constituted by six oxygen atoms of the crowns ether and by two aromatic rings of the rotated aromatic nuclei.

The Cs-C (aromatic) contacts, which range from 3. 486(8) to 3.69(1) Å, compare very well with other systems, where cesium-arene interaction have been documented. Evidence for cation-arene interaction in methanol solution have been also obtained by ^{1}H NMR studies.

Several crystalline complexes between calixarene ligands and strontium salts have been prepared. The X-ray crystal structures of the $SrPic_2$ complexces of a p-tertbutylcalix[4]arene-diamide and a p-tertbutylcalix[4]arene-tetramide have been solved. The first one shows the strontium cation bound to four oxygen atoms of the calixarene and to two amide carbonyl groups. Both picrate anions and a water molecule are also coordinated by the strontium cation. The Sr-O distances range between 2.489(6) to 2.585(5) Å.

In the $SrPic_2$ complex of the tetramide the strontium cation is encapsulated between four oxygen atoms of the calixarene and the four carbonyl groups of the amide. The picrate anions are not bound to the strontium cation and are dispersed in the crystal lattice. The Sr-O distances range between 2.489(6) to 2.585(5) Å. Evidence that the partial cone structure is preferred for the complexation of strontium cation by conformationally mobile 1,3-dimethoxycalix[4]arene crown ethers in $CDCl_3$ solution has been obtained by ^{1}H NMR. The X-ray crystal structures of other calixarene ligands and strontium salts are currently under investigation.

Title	**Partitioning of Radioactive Wastes**
Contractor	Forschungszentrum Karlsruhe (D)
Contract N°	FI2W-CT90-0047
Duration of contract	March, 1991 - September, 1995
Period covered	January, 1994 - December, 1994
Project leader	Z. Kolarik

A. OBJECTIVES AND SCOPE

- Separation of long-lived actinides and fission products would reduce the radiotoxicity of Purex process high-level wastes. This would lower the costs and risks of final waste disposal.

- The aim of the work is to obtain distribution data, which are applicable to the development of a solvent extraction process for the separation of plutonium, neptunium, americium, curium and technetium from the highly active Purex waste solution (HAW). The target decontamination factors are 50000 for Am and Cm, 1000 for Pu and 100 for Np.

- Application of solvent extraction for treatment of highly radioactive materials is well developed. Existing knowledge of the chemistry and engineering of the method can serve as a starting point for the project work.

B. WORK PROGRAMME

1. Search for extractants or complexants which make it possible to separate transplutonides from fission lanthanides by solvent extraction.

2. Measurement of distribution and, eventually, kinetic data for selected transplutonides and lanthanides, and the working out of a proposal of a flowsheet.

C. *PROGRESS OF WORK AND OBTAINED RESULTS*

State of advancement

The experimental work was devoted to the search for solvent extraction systems, in which transplutonides could be separated from fission product lanthanides. Selective extraction of transplutonides(III) over lanthanides(III) was the preferential mode of the separation. Am(III) and Eu(III) were used as representatives of the transplutonide and lanthanide groups respectively. Cations M^{3+} of the elements to be separated were extracted in the form of simple complexes MA_3 or of solvated complexes $MA_3 \cdot B$, with A being the anion of a monoacidic extractant and B being the molecule of a solvating extractant. After having demonstrated /1/ the unsatisfactory separation efficiency of =PSSH and =PSOH acidic extractants combined with phosphoryl solvating extractants, we concentrated on the investigation of extractants including in their molecule nitrogen "soft" donor atoms. 2-Pyridinyl derivatives of Schiff bases and benzimidazole were studied as neutral solvating extractants, and 2-(2-pyridinylazo)-1-naphthol was studied as an acidic extractant. Am/Eu separation factors up to ~50 were attained.

Progress and results

Separation of transplutonides(III) from lanthanides(III)

In this stage of development, the principal aim of the work was the finding of such a configuration of donors atoms in the extractant molecule, which would be sufficiently selective for transplutonides(III) with respect to lanthanides(III). Stability of the extractant and its aqueous solubility played here a secondary role. Once a favourable configuration has been found, it can be attempted to be incorporated into a lipophilic compound with a sufficient chemical and radiation stability. We have sought molecules in which the positioning of nitrogen donor atoms allows the formation of two or more five- or six-membered chelate rings. At least some of the nitrogen atoms in such molecules must be located in aromatic-type heterocyclic rings, where they are not highly basic. In this way a strong competition of hydrogen ions with extracted metal ions can be avoided.

Schiff bases derived from aromatic or aliphatic 1,2-diamines and 2-pyridinecarbaldehyde are potentially tetradentate neutral complexants. Reaction of one mol 1,2-benzenediamine or 4-methyl-1,2-benzenediamine with 2 mols 2-pyridinecarbaldehyde gives the corresponding double Schiff bases as intermediate products only. At prolonged reaction time and, especially, at elevated temperature under the access of air the Schiff bases strongly tend to be dehydrogenated to benzimidazole derivatives. Of the latter, the potentially bidentate complexants 2-(2-pyridinyl)benzimidazole (PyPhHcy) and 4(5)-methyl-2-(2-pyridinyl)benzimidazole (PyToHcy) can easily be isolated from the reaction mixture. In contrast to work described in /2/, we were not able to obtain the double Schiff base in the reaction of 1,2-benzenediamine with 2-pyridinecarbaldehyde. When 3-methyl-1,2-benzenediamine was

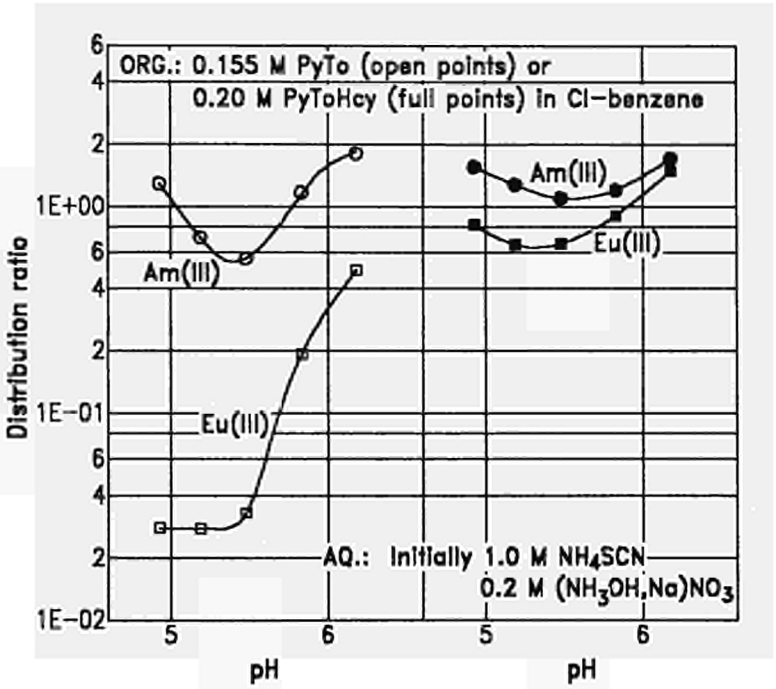

Figure 1. Extraction of Am(III) and Eu(III) thiocyanates with solvating nitrogen donor extractants: PyTo is 3-methyl-N,N′-bis(2-pyridinylmethylidene)-1,2-benzenediamine and PyToHcy is 4(5)-methyl-2-(2-pyridinyl)benzimidazole. Hydroxylamine buffer, 23°C.

reacted in ethanol at 30 - 80°C for 2 h, a coumpound which most probably was 3-methyl-N,N′-bis(2-pyridinylmethylidene)-1,2-benzenediamine (PyTo) could be isolated from the reaction mixture by solid-liquid extraction with hot petroleum ether (60 - 80°C fraction).

As an example, Figure 1 shows the extractant properties of PyTo and PyToHcy in chlorobenzene diluent for Am(III) and Eu(III). The Schiff base PyTo exhibits good selectivity for Am(III), attaining an Am/Eu separation factor of 46 at pH 4.9 (formation of a third liquid phase deprived us from measurements at lower pH values). Measurement of the extractant concentration dependency of the distribution ratio revealed that the extracted Am(III) and Eu(III) thiocyanates were solvated each by one extractant molecule.

The selectivity of the PyTo extractant, unfortunately, does not appear to be a general property of the given configuration of nitrogen donor atoms in the extractant molecule. The extraction with an analogous extractant, N,N′-bis(6-methyl-2-pyridinylmethylidene)-1,2-ethanediamine (0.060 M in a 5/3 mixture of chlorobenzene and 1-butanol), from 1.5 M NH_4SCN containing 0.2 M hydroxylamine buffer was much less selective. The distribution ratios of Am(III) and Eu(III) at pH 5.3 - 5.7 were 0.7 and 0.14 respectively, yielding an Am/Eu separation factor of 5.

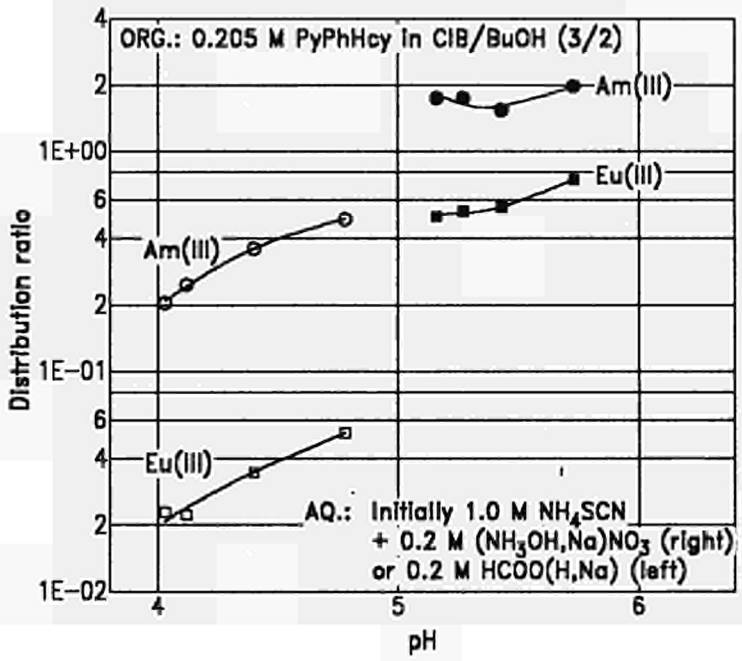

Figure 2. Extraction of Am(III) and Eu(III) thiocyanates with a solvating nitrogen donor extractant: PyPhHcy is 2-(2-pyridinyl)benzimidazole, ClB is chlorobenzene, and BuOH is 1-butanol. Hydroxylamine buffer, 23°C.

It is seen in Figure 1 that the benzimidazole extractant PyToHcy in chlorobenzene diluent is much less selective for Am(III) over Eu(III) than the Schiff base extractant. Extraction from hydroxylamine buffered solutions gives an Am/Eu separation factor which decreases from 1.8 at pH 4.9 to 1.1 at pH 6.2. The analogous 2-(2-pyridinyl)benzimidazole extractant, indeed in a mixed chlorobenzene/1-butanol diluent (3/2), is somewhat more but not yet satisfactorily selective. As seen in Figure 2, the separation factor in the extraction from hydroxylamine buffered solutions decreases from 3.5 at pH 5.2 to 2.7 at pH 5.7. However, the selectivity of the PyPhHcy extractant can be improved by varying the ionic medium in the aqueous phase, e.g. to attaining an Am/Eu separation factor of ~10 in the extraction from formate buffered solutions (see Figure 2).

2-(2-Pyridinylazo)-1-naphthol (PAN) was studied as an acidic extractant, bonding extracted metal ions through expectedly two nitrogen and one oxygen atoms. Figure 3 shows that in a mixed chlorobenzene/1-butanol diluent it exhibits some selectivity for Am(III) over Eu(III). In the extraction from 1 M NH_4Cl at pH 5.7, the Am/Eu separation factor increases from 3.45 at 0.0096 M PAN to 6.25 at 0.048 M PAN. Addition of 0.028 to 0.156 M 2-(2-pyridinyl)benzimidazole to 0.0216 M PAN increases the extraction efficiency, but not the Am/Eu separation factor which remains unchanged (~5).

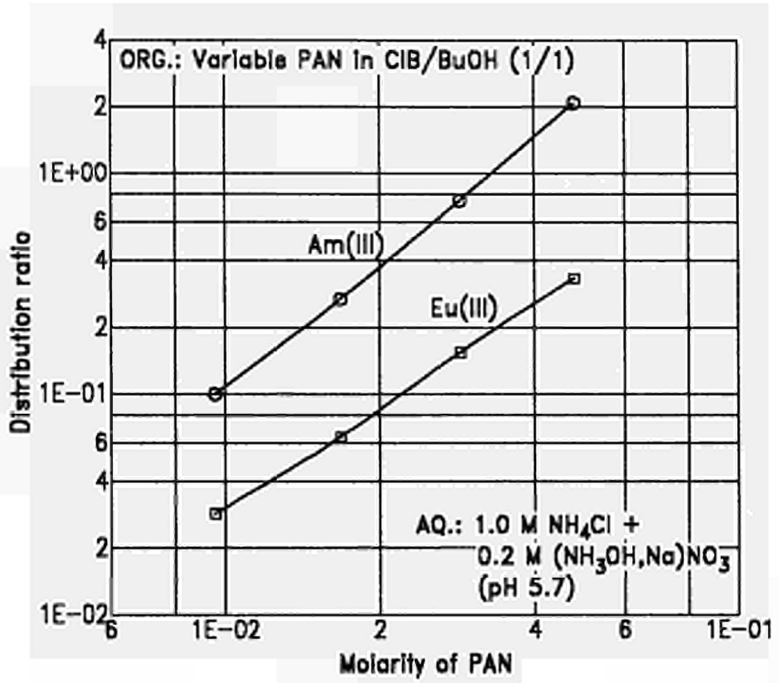

Figure 3. Extraction of Am(III) and Eu(III) with an acidic nitrogen donor extractant: PAN is 2-(2-pyridinylazo)-1-naphthol, ClB is chlorobenzene, and BuOH is 1-butanol. Hydroxylamine buffer, 23°C.

References

/1/ COMMISSION OF THE EUROPEAN COMMUNITIES, *Annual progress report 1993 on the community's research and development programme on radioactive waste management and storage, shared-cost action (1990-1994)*, EUR-15853 (1994), pp. 165-9.

/2/ KASSELOURI, S., GAROUFIS, A., KALKANIS, G., PERLEPES, S. P., and HADJILIADIS, N., *Transition Met. Chem. (London)* **18**, 531 (1993).

Title:	"Advanced Management of Nuclear Radioactive Wastes: Comparative Evaluation of Processes for Enhanced Separation of Very Long-Life Radioactive Species"
Contractor:	E. N. E. A. - Italy
Contract No:	FI2W-CT90-0056
Duration of contract:	March 91 - September 95
Period covered:	March 91 - December 94
Project leader:	Roberto Nannicini (E.N.E.A.- Ispra)

A. OBJECTIVES

The study concerns the separation of Long Lived Radionuclides (LLR) from a High Level Liquid Waste (HLLW) of a defined composition, in view of their transmutation.
A process flowsheet based on solvent extractions and back-extractions is selected and experimentally tested, with the following aims:
-verify the process effectiveness in the separation of Tc, Np, Pu, Am isotopes from the HLLW. Cs and Cm separation is not considered because: (i) ^{135}Cs transmutation is not practically achievable if no selective separation from the other Cs isotopes is performed; (ii) Cm chemical behaviour can be reasonably considered similar to that of Am
-verify the process effectiveness in the Am / trivalent lanthanides partitioning
The following process specifications are assumed:
-recovery of Am > 99.9%
-tolerable lanthanides amount in the subsequent burning operation < 5%.

B. WORK PROGRAMME

The programme of the study is structured according to the following tasks:

B.1 Lab-scale experimental investigation of the selected flowsheet
B.2 Optimization of the process operating parameters by using a computer code
B.3 Verification of the code outputs by using mixer-settler batteries

C. PROGRESS OF WORK AND RESULTS

C.1 Lab-scale experimental investigation of the selected flowsheet

The selected process flowsheet (Fig. 1) is based on the extraction of the LLR by means of a phosphine oxide (CMPO: n-octyl (phenyl)-N,N-diisobutyl carbamoyl methyl phosphine oxide, or Ph_2Bu_2: diphenyl-N,N-dibutyl carbamoyl methyl phosphine oxide) followed by three subsequent back-extractions.
By the first one, which is performed with diluted nitric acid, americium and the trivalent lanthanides are stripped from the loaded solvent. In the second one, Pu, Np and Tc are stripped by diluted HNO_3 / HF, while the third one is focused to the solvent regeneration and clean-up by Na_2CO_3: uranium is stripped in this section.
DTPA (diethylentriaminepentaacetic acid) is added to the first stripped solution in order to form a complex with Am; after adjusting to pH=3, the Am / lanthanides partitioning is performed by extracting the lanthanides with HDEHP (di-(2-ethyl)-hexyl phosphoric acid).
Concerning Ph_2Bu_2, the selection of a proper diluent is of a great importance. Due to the presence of two aromatic rings, the formation of a third phase was observed when common aliphatic diluents (such as n-dodecane) were used.
Figure 2 shows the experimental distribution ratios in CMPO obtained for Am, Eu and La by performing "cold" and "hot" tests. At $[HNO_3]$=2.5 M, Am is quite effectively extracted (D Am > 10), but the lanthanides coextraction cannot be avoided (D Eu > 7).
The distribution ratios of some fission products such as Zr and Mo can be lowered by adding small amounts of oxalic acid to the aqueous initial solution.
The disproportionation of Np (V) into Np (IV) and Np (VI) by means of $NaNO_2$ (or other agent) is being investigated with the aim to maximize Np extraction in the phosphine oxide.
Am and the lanthanides are totally stripped by diluted nitric acid; Pu is stripped too if oxalic acid is added to the aqueous phase before extraction.
This is probably due to the fact that oxalic acid is also extracted (by TBP which is present in the extracting solvent: CMPO/TBP/n-dodecane), thus making easier the Pu back extraction in diluted HNO_3 by the formation of $Pu/(COOH)_2$ complexes.
In the Am / lanthanides partitioning section, the Eu / Am separation factor was about 7 when technical grade HDEHP was employed, while a very high separation factor (about 90) was obtained by employing high-purity HDEHP.
Nevertheless, it appears to be difficult to avoid the formation of precipitates while adjusting to pH=3.

C.2 Optimisation of the process operating parameters by using a computer code

A suitable computer code allows to simulate the stationary and dynamic behaviour of mixer-settler batteries for a maximum of 5 components, taking into account their mutual influence.
By using the experimental distribution ratios as input data, it was possible to optimize the operating parameters (flow rates, number of stages, etc.) of the mixer-settler batteries to be employed in all the process sections, in order to satisfy the specifications.
Figure 3 shows the concentration of Am in the organic phase vs the number of the stage in the extraction / scrubbing battery at steady condition.
A proper selection of the flow rates allowed to reach a good separation between Am and La in the extraction / scrubbing battery.
In the Am / lanthanides partitioning section, a battery of 6 extraction stages + 6 scrubbing stages permitted to extract more than 99.9% of Eu, while more than 99.98% of Am remained in the aqueous phase.

C.3 Verification of the code outputs by using mixer-settler batteries

The code outputs are being verified by using mixer-settler batteries.
To this purpose two mixer-settler batteries have been installed at the ENEA laboratories in Saluggia and tested from a fluid-dynamic point of view, verifying their good performance.
They are now used in 'cold' tests by employing a 'UP3' simulated solution.

Fig. 1. Selected Process Flowsheet

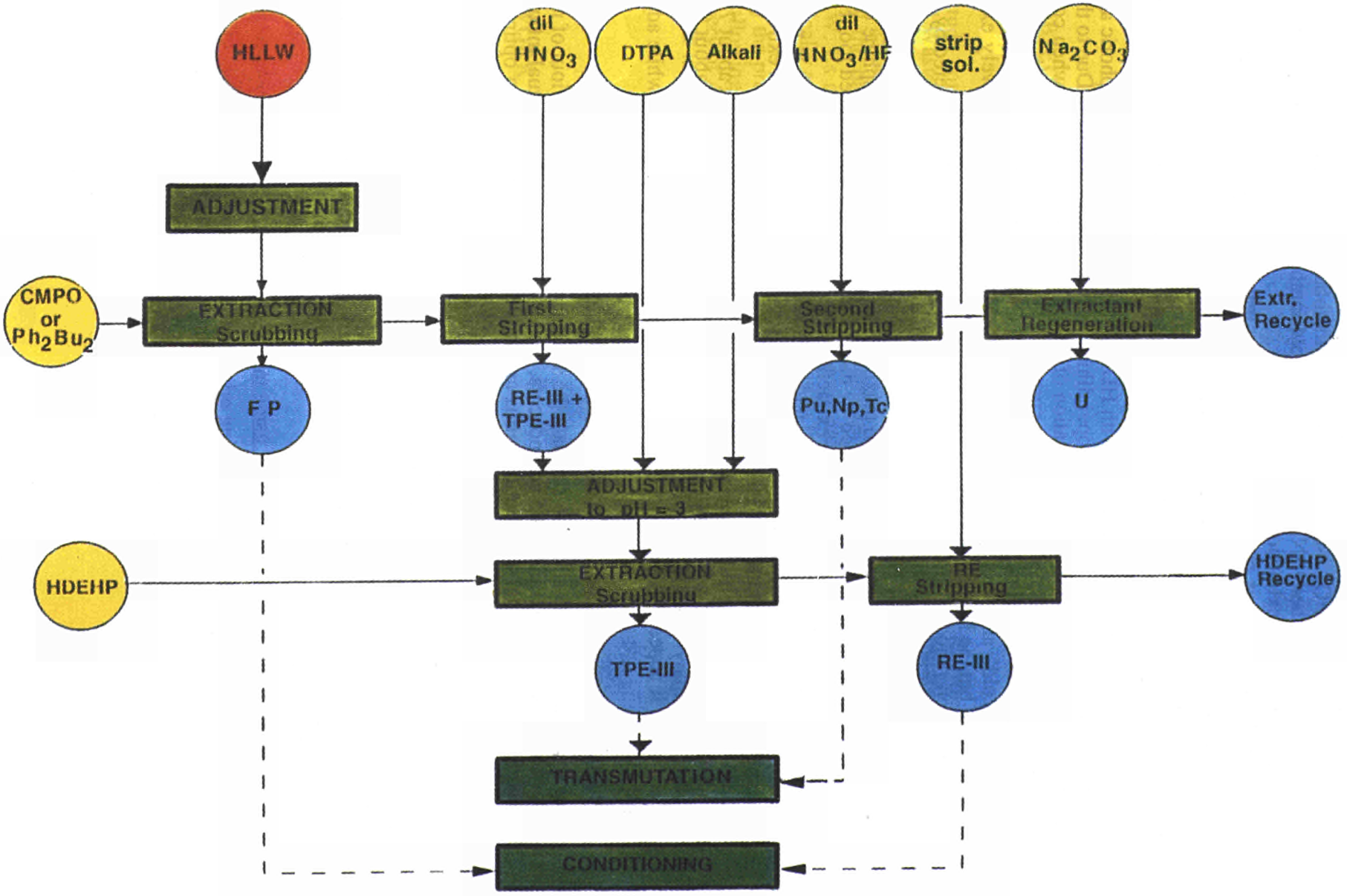

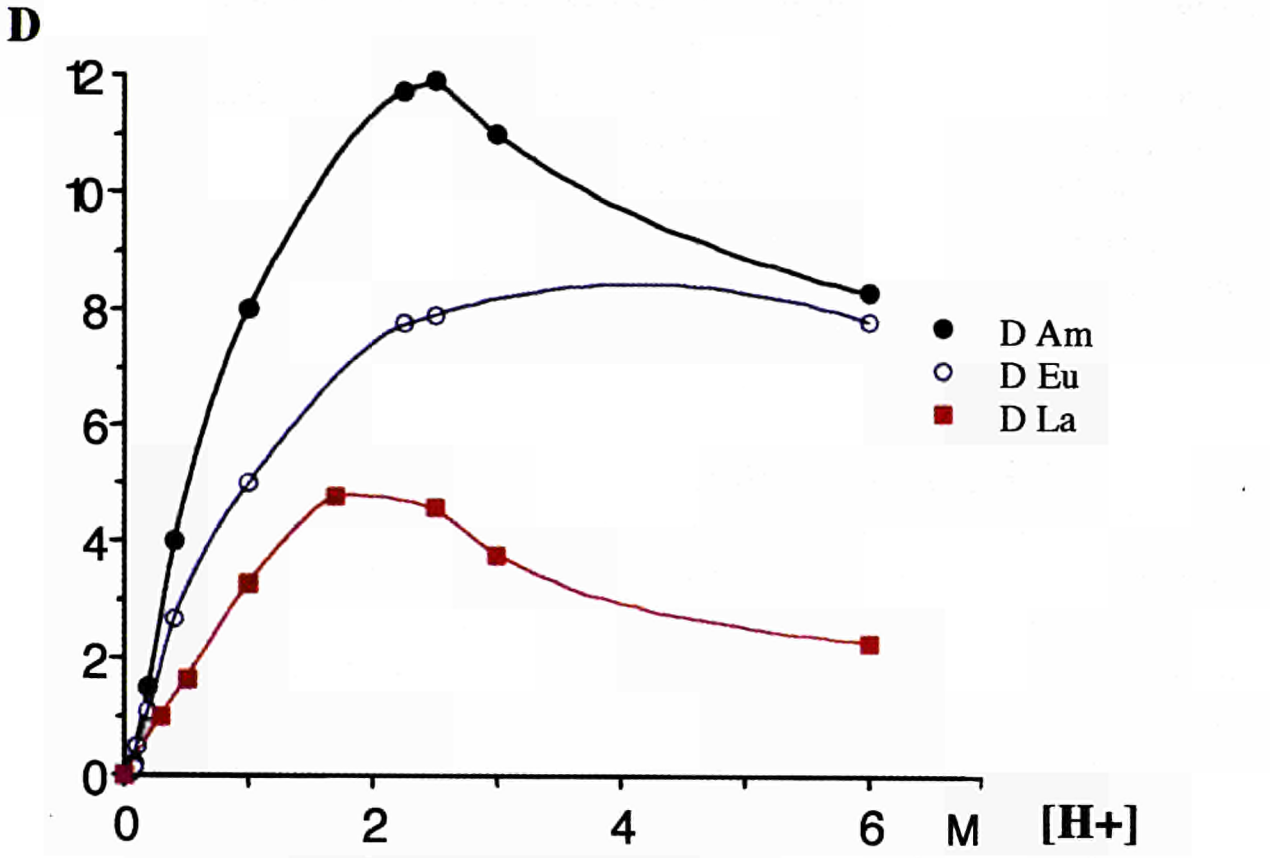

Fig. 2. Experimentally Found Am, Eu, La Distribution Coefficients

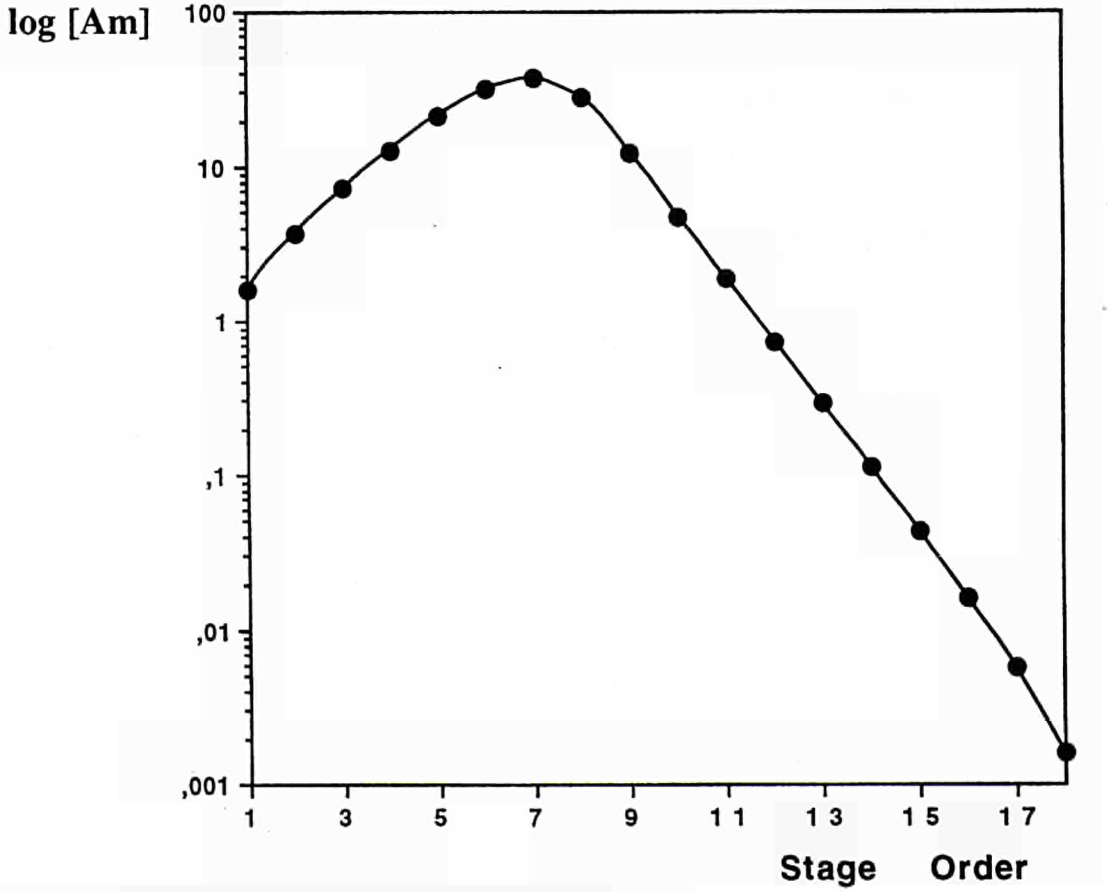

Fig. 3. Stage by Stage Am Concentrations Deduced by the Computer Code

Title	**High-level liquid waste partitioning by means of completely incinerable extractants**
Contractor	CEA-Fontenay-aux-Roses ; University of Reading
Contract N°	F12W-CT91-0112
Duration of Contract	October 1991-September 1995
Period covered	January-December 1994.
Projects leaders	Dr. C. MADIC (CEA, Coordinator) Dr. M.J. HUDSON (University of Reading)

A. OBJECTIVES AND SCOPE

The main objective of this research is to demonstrate the suitability of new types of diamides and triazine-based compounds for the removal of actinides from high level liquid waste and the subsequent purification of minor actinides from rare earths respectively. Other types of extracting agents will be also considered for the same purposes.

In terms of decontamination performance, these extractants must demonstrate properties at least equivalent to bifunctional organophosphorus extractants (like CMPO) for actinide removal, and to the combination of HDEHP and DTPA for the separation of lanthanides from trivalent actinides. These requirements are added to the requirement of complete incinerability to avoid secondary wastes.

This project, which is closely coordinated with research currently underway at KfK and Saluggia, should result in the preparation of flowsheets for HLLW partitioning and hot testings of these flowsheets.

B. WORK PROGRAMME

The study will include the following steps :

B.1. Synthesis of new organic extractants (diamides, triazine-based, hydroxamic acids).

B.2. Determination of their extracting properties and extraction performance on simulated HLLW.

B.3. Quantification of long term extractant stability to chemical attack and irradiation.

B.4. Preparation of possible partitioning flowsheets based on results from B.2.

B.5. Verification at least of two flowsheets through counter-current experiments with simulated HLLW, in order to validate the decontamination and separation performance of the extractants for partitioning experiments with real HLLW.

B.6. Scale-up of the preparation procedure for diamides, triazines and other extractants.

B.7. Definition and verification of solvent regeneration treatments.

B.8. Cooperation with laboratories working on HLLW partitioning in connection with Task N°2 of the EC programme.

C. *PROGRESS OF WORK AND RESULTS OBTAINED*

State of progress

This research programme introduced many interesting results in 1994. The most interesting and promising results are as follows :

Synthesis of extractants *(B.1.)* :

Diamides

New interesting malondiamides possessing cyclohexano groups were synthetised at Reading using the new efficient method based on malonyl esters.

Podant diamides and one oxalamide, with the formulas : $[RR'NCO]_2(CH_2)_n$, with n= 8 ; 10 and 12 ; and $[RR'NCO]_2$, respectively, were prepared at Fontenay-aux-Roses.

A new type of diamide possessing an amino bridge between the two amidic groups was prepared by PANCHIM (France).

TPTZ derivatives

A few grams of tritertiarybutylpyridyltriazine (TtBPTZ) were successfully obtained at Reading using the new high pressure synthesis route previously developed.

Determination of extractant properties *(B.2.)*

Diamides

The extracting properties of the diamides prepared at Reading, and possessing cyclohexano groups, were evaluated using inactive metallic salts. The structural properties of these molecules were also evaluated.

Third phase formation when extracting solutes like nitric acid, U(VI) and Nd(III) nitrates, was studied for two diamides, possessing a long central chain in their formulas. For these diamides, the third phase boundaries are far higher than those corresponding to the reference diamide of the DIAMEX process (DMDBTDMA).

The extracting properties of the podant diamides and oxalamide were studied. While these molecules exhibit interesting extracting properties for U(VI), they do not display any affinity for actinide(III) nitrates.

TPTZ derivatives :

The extracting properties of TtBPTZ, used in synergistic combination with αbromocapric acid, were found to be far better than those exhibited by TPTZ, or TMPTZ, studied previously. This certainly represents a major advance in this field.

Interesting structures were identified of crystals prepared after reaction between protonated forms of TtBPTZ and some anions.

Extractant characterization and stability *(B.3)* :

Diamide

The characterization of DMDBTDMA, the reference diamide of the DIAMEX process, was undertaken, and the relevant analytical methods developed. It was found that extractant batches prepared by PANCHIM were purer than those from IRCHA. Preliminary investigations of the radiolytic stability of DMDBTDMA were carried out. They showed that the molecule is reasonably stable under a radiation field.

Preparation of flowsheets *(B.4)* :

Diamide

In order to test various flowsheets of the DIAMEX process, a study was carried out of the hydraulic behavior of the solvent, composed of a solution of DMDBTDMA in TPH (aliphatic dliuent). It was shown that after purification of DMDBTDMA on alumina B chromatographic columns, the hydraulic behaviour of the solvent is suitable for counter-current mixer-settlers tests.

Progress and results

***B.1.* Synthesis of new extractants**

Diamides

The new route developed at Reading and used to synthesize of malonamides is based on the use of malonyl esters as the starting molecules. This new route appears to be useful for the preparation of industrial quantities of diamides. Using this method, several new malondiamides, possessing cyclohexano groups as substituents of the amidic nitrogens, were prepared at Reading. The formulas of these molecules are $[RR'NCO]_2CHR''$, with R"= tetradecyl, R'=cyclohexano, and R = methyl, ethyl or isopropyl groups.

Six other malonamides prepared by PANCHIM (France) were received at Fontenay-aux-Roses.

New diamides were synthesised at Fontenay-aux-Roses by Laurence NIGOND-BERTHON. The general formula of these molecules is $[RR'NCO]_2[CH_2]_n$.

Molecules for which n= 0 (oxalamide), 8 (sebaçamides), 10 and 12 were prepared.

A new molecule possessing two amidic groups linked by an amino bridge, with the formula $[CH_3C_4H_9NCO]_2NC_{14}H_{29}$, was prepared by PANCHIM.

Alkylated TPTZ

Using the high pressure synthetic route, previously developed for TPTZ and its trimethyl derivative (TMPTZ), several grams of tritertiobutylpyridyltriazine (TtBPTZ) were successfully prepared. The purified TtBPTZ was found to be quite stable. It was fully characterised by NMR spectroscopy.

B.2. Determination of the extracting properties of the new molecules

Diamides

The extracting properties of the newly prepared malondiamides were studied. It was found that the affinity of these molecules for Ln(III) (as representative of An(III) and Ln(III) mixtures) was significant. Concerning the extraction mechanism, it apppears that ion-pair formation can be observed as well as solvate formation. The crystal structures of some of the new malonamides were determined. The two amidic groups were found in the *trans* position. Thus, for the bidendate solvation of metal ions this requires the rotation of a part of the diamide molecule about a C-C bond.

Major study was carried out on third phase formation during the extraction of macro-amounts of solutes, such as nitric acid or U(VI) and Nd(III) nitrates. These properties were studied for two diamides : dimethyldibutyloctadecylmalonamide (DMDBODMA) and dimethyldibutylhexadecylethoxymalonamide (DMDBHDEMA). The third phase boundaries (TPB) exhibited by these two malondiamides are far higher than those of DMDBTDMA, the reference diamide of the DIAMEX process. These TPBs were found to be highly dependent of the concentration of the diamide and of the aqueous nitric acid. This suggests the involvement of a micellar mechanism in the extraction of these solutes.

A preliminary study was carried out. on the extracting properties of the new diamides (podants and oxalamide) These molecules exhibit significant affinities for U(VI) nitrate. From solvent saturation studies, it was shown that the two carbonyl groups of the podant diamides are bound to U(VI) in a *trans* position. The extracting properties exhibited by these molecules (podants and oxalamide) for An(III) and Ln(III) nitrates are negligible. Consequently, no further studies will be devoted to these extractants.

Alkylated TPTZ derivative

The properties of the newly synthetised TtBPTZ were studied. At Reading, the crystal structures of some solid compounds obtained by the reaction between the protonated forms of the TtBPTZ and some anions, such as PF_6^- and NO_3^-, were determined. It is quite clear that the protonated TtBPTZ molecule is able to form ion-pairs with anions. These structural determinations could be an important step in establishing the nature of the mechanism of An(III) nitrate extraction, which could either involve ion-pairs or a coordinative mechanism.

The preliminary results corresponding to the separation Am(III)/Eu(III), obtained at the CEN-FAR, are of great importance. It was shown that, when used in synergistic mixture with α–bromocapric acid, TtBPTZ exhibits far better properties than those corresponding to TPTZ or TMPTZ, previously studied. This certainly represents a

major advance in the field of the An(III)/Ln(III) separations. Using TtBPTZ, the distribution coefficients of Am(III) were often found to be greater than 1, even for a 0,15 mol/L nitric acid aqueous solution. Moreover, it appears that the separation factor $SF_{Am/Eu}$ is slightly better for TtBPTZ than for TPTZ or TMPTZ. More efforts are urgently required for the study of this very important molecule. A patent is being filed on its use for the An(III)/Ln(III) separation.

B.3. Extractant characterization and stability

Diamides

The different batches of DMDBTDMA, the reference diamide of the DIAMEX process, prepared by the companies IRCHA and PANCHIM, were characterized using several analytical methods, including gas chromatography, alone or coupled with Fourier Transform Infra Red spectroscopy (FTIR), and Mass Spectrometry (MS). Analytical measurements were also made on DMDBTDMA samples previously purified on alumina B chromatographic columns. The main conclusions of these studies are :

° DMDBTDMA prepared by PANCHIM exhibits a slightly better purity than the batch prepared by IRCHA,

° chromatographic treatment on alumina B is effective : DMDBTDMA purity close to 100% was found after treatment (PANCHIM batch).

Moreover, the hydraulic behaviour of the solvent prepared with purified DMDBDMA is far better than that of the solvent made with crude DMDBTDMA (see below).

Initial radiolytic tests of DMDBTDMA were carried out in the absence or presence of aqueous nitric acid solutions. The radiolytic resistance of the molecule was found to be good, but the presence of nitric acid promotes its decomposition. It can be stated that DMDBDMA could be a good extractant for the treatment of high level liquid wastes (HLLW).

B.4. Preparation of flowsheets

DIAMEX

For the preparation of the flowsheet tests, it is important to address technical problems, such as the hydraulic behaviour of the solvent in mixer-settlers in the different steps of the process : °extraction, ° scrubbing, ° stripping and ° solvent clean-up. As some problems of this nature arose during the performance of the hot tests of the DIAMEX process carried out in June 1993, it was considered urgent to address these difficulties. Several batches of DMDBTDMA were studied, prepared by the companies IRCHA and PANCHIM, before and after treatment on alumina B chromatographic columns. Settling tests were performed with solvents prepared by dilution of the various DMDBTDMA samples in TPH (aliphatic diluent), in different conditions corresponding to the various steps of a DIAMEX extraction cycle (extraction,

scrubbing). It was found that the PANCHIM DMDBTDMA was far better than that prepared by IRCHA, and that the chromatographic treatment is effective for removing the impurities (unidentified in 1994) responsible for the poor settling behaviour of the solvents.

At the end of the study, good hydraulic behavior of the solvent was obtained, allowing the use of a CYRNO type 21-stages mixer-settlers battery, even when the solvent is in contact with 0,1 mol/L aqueous nitric acid solution.

B.8. Cooperation with EC laboratories

Cooperation is to be established with Dr. J.P. GLATZ from TUI (Karlsruhe, Germany), to study the retention behaviour of actinide species in the DIAMEX solvent according to its radiolysis. A post-doctoral position was accordingly proposed to Denis LESAGE, a French scientist now finishing his Ph. D. at Saclay (France).

Part A3

Task 3

"Characterisation and Qualification of Waste Forms, Packages and their Environment"

* List of contracts
* Introduction to Task 3

Topic 1 Waste form characterisation and performance

Topic 2 Containment and barrier properties of the near-field (including modelling)

Topic 3 Radionuclide assay : development of standard methods and equipment for specific applications

Topic 4 Quality control of waste conditioning

TASK 3 - LIST OF CONTRACTS

Topic 1 Waste form characterisation and performance

FI2W-CT90-0012	Retention of Pu, Am, Np and Tc in the corrosion of Cogema glass R7T7 in salt solutions.
FI2W-CT90-0020	Consequences of gas production in geological repositories (PEGASE).
FI2W-CT90-0025 + 0007	Characteristics of bitumenized radioactive wastes.
FI2W-CT90-0026	Natural analogues of bitumen matrices in a deep repository.
FI2W-CT90-0027	Aqueous corrosion of nuclear glasses: influence of disposal conditions.
FI2W-CT90-0028	Effect of insoluble active dissolution fines on fission product glasses.
FI2W-CT90-0031	The corrosion of nuclear waste glasses in a clay environment: mechanisms and modelling.
FI2W-CT90-0032	Basic leaching for pure Beta long-lived emitters in radioactive wastes.
FI2W-CT90-0055	Chemistry of the reaction of fabricated and high burnup spent UO_2 fuel with saline brines.
FI2W-CT90-0077	Container properties´ ensuring safety : gas emission, biodegradation, corrosion.
FI2W-CT90-0094	Gas generation in supercompacted waste products.
FI2W-CT90-0099	Impact of additives and waste streams constituents on the immobilisation potential of cementitious materials.
FI2W-CT93-0124	Some aspects of leaching mechanisms of ions incorporated in cement or polymer.

TASK 3 - LIST OF CONTRACTS

Topic 2 Containment and barrier properties of the near-field (including modelling).

FI2W-CT90-0030	Corrosion of selected packaging materials for disposal of heat-generating radioactive wastes.
FI2W-CT90-0035	Theoretical and experimental study of degradation mechanisms of cement in the repository environment.
FI2W-CT90-0040	The performance of cementitious barriers in repositories.
FI2W-CT91-0096	Completion of the corrosion programme in Boom clay (in situ experiments).

Topic 3 Radionuclide assay : development of standard methods and equipment for specific applications.

FI2W-CT90-0010	Determination of fissile material by neutron transport interrogation.
FI2W-CT90-0034 + 0109	Inventory and characterisation of important radionuclides for safety storage and disposal. Correlation with key nuclides easy to measure in typical waste streams.

Topic 4 Quality control of waste conditioning.

FI2W-CT90-0009	Construction and testing of a computer tomography assembly for routine operation.
FI2W-CT90-0019	Test process control during treatment of low and medium radioactive waste in practice.
FI2W-CT90-0021	Establishment of non-destructive or partially destructive test procedures for determining the characteristics of waste containers.
FI2W-CT90-0023	Non-destructive examination of nuclear radioactive waste packages by advanced radiometric methods.
FI2W-CT91-0107	High Energy Accelerator Tomography

INTRODUCTION TO TASK 3 - CHARACTERISATION AND QUALIFICATION OF WASTE FORMS, PACKAGES AND THEIR ENVIRONMENT

A. Objectives

- Determination of the relevant properties and performances of waste forms and their environment (Characterisation)
- Development and validation of models and data bases describing the long-term evolution of disposed waste (Modelling)
- Improvement of the control of radioactivity in the waste and the quality of waste products/packages.

B. Research topics dealt with the 1985-1989 Programme

In the previous programme, the following main research actions were pursued:

- Characterisation of low and medium level wastes:
  Eleven waste forms were selected for joint investigation and specified as reference formulations for conditioned LLW and MLW. Many of the characteristics of these waste forms relevant to the long-term safety in different disposal environments were determined with simulates and, as far as available, with real waste specimen.

- Testing and evaluation of high active and special alpha-bearing waste forms:
  During the period 1985-1989 the development of new candidate waste forms for the High Level Liquid Waste Stream was reduced in favour of extended testing and evaluation of the industrial reference borosilicate formulations. Corrosion, nuclide leaching, radiation damage and thermal stability were investigated in laboratory test series with inactive and spiked simulates.

- Study of container and buffer/backfill materials:
  The coordinated action on container corrosion launched in the second programme was concluded: corrosion rates and mechanisms of carbon steel, Ti-Pd and Hastelloy were determined under representative conditions.
  A variety of argillaceous and cement-based buffer materials were tested to determine suitable formulations for the various repository options.

- Development of a standard waste hostrock interaction test:
  The Repository Systems Simulation Test which permits the testing of HLW glass formulations in conditions representative of geological disposal was developed and validated in a Round-Robin campaign by 14 laboratories.

- Development of methods for the Quality Assurance of Waste Packages:
  Non-destructive test methods such as computer tomography and active neutron interrogation techniques for assaying alpha emitters as well as techniques and procedures for sampling solidified waste were the most important items of a wide range of R & D projects.

C. Present programme (1990-1994)

1. Waste form characterisation and performance

- Characterization of heterogeneous waste forms
- Effects of radiation, corrosion, biodegradation, etc. on waste form stability
- Gas generation by corrosion, radiolysis and biodegradation
- Effect on inclusions on waste form crystallisation and stability
- Chemistry of reaction of spent fuel with saline brines
- Mechanisms of nuclide release under repository conditions

2. Containment and barrier properties of the near-field

- Effect of microbial activity on the near-field
- Theorical and experimental study of degradation mechanism of cement in the repository environment
- Modelling and testing of the hydration of backfill and sealing materials
- Corrosion of selected packaging materials for disposal of heat generating radioactive waste

3. Radionuclide Assay: development of standard methods and equipment for specific application

- Establishment of a European basis for the determination of relevant nuclide concentrations in industrial LLW and MLW: Study of existing methods and compilation of data bases, evaluation of currently used scaling factors and correlation.
- Development of equipment and methods for the assaying of LLW and MLW including the validation of scaling correlations for relevant emitters.
- Development of methods for measuring(checking)the nuclide inventory of conditioned TRU-wastes

4. Quality control of waste conditioning

Research actions to develop methods permitting the measurement and certification of compliance with quality requirements/criteria. Subjects being addressed include:

- Establishment of sampling procedures and techniques
- Verification of chemical composition
- Detection of unwanted or undeclared substances
- Detection/measurement of waste/matrix interaction, gas generation and release, container corrosion and swelling
- Measurement of physical properties of waste products and packaging
- Homogeneity, thermal stability, etc.

D. Programme implementation

The above topics and areas of research has been tackled under 28 contracts, the majority of which are multi partner and trans-european. Further details on projects running in 1994 are provided in the summary reports presented hereafter.

Title	Retention of Pu, Am, Np and Tc in the Corrosion of COGEMA* Glass R7T7 in Salt solutions.
Contractors	Forschungszentrum Karlsruhe GmbH, Institut für Nukleare Entsorgungstechnik (INE)
Contract N°	FI2W-CT90-0012
Duration of contract	March 1991 - February 1995
Period covered	1 January 1994 - 31 December 1994
Project leader	B. Grambow (Coordinator) (W. Lutze)
	L. Kahl, E. Bohnert, A. Schramm, P. Dressler, V. Toth, H. Geckeis

A. Objectives and Scope

High-level radioactive waste from the reprocessing of German spent fuel is vitrified at La Hague. Glass blocks will be returned to Germany and must be disposed in the deep underground eventually. The repository is expected to be located in the Gorleben salt dome. The repository constitutes a system of technical and natural barriers (multibarrier system) against the release of radionuclides. The glass is the most central technical barrier. A detailed understanding of glass performance must be obtained for all conceivable accidental conditions, in particular contact with water. The respective results shall be used to describe source terms in the framework of safety analyses.

The subject of this investigation is to study the chemical durability of the highly radioactive French borosilicate glass R7T7 in one of the three German "standard" salt solutions as a function of time and temperature. This work complements previous investigations on the durability of a very similar but non-radioactive CEA glass by measuring the release behavior of Pu, Am, Np and Tc.

B: Work programme

1. Installation of the hot cells
2. Modification of analytical techniques for radiochemical separation of Tc, Pu, Am and Np from concentrated salt solutions
3. Equipment for corrosion tests: Tantalum lined autoclaves
4. Corrosion test conditions: Powdered glass shall be corroded in salt solutions (T=110,150,190°C; S/V 10000 m^{-1}) for 45 to 1000 days (duplicate tests).
5. Solution analyses: Solution sampling at test termination and determination of pH, B, Si and Tc,Pu, Am and Np. Measurement of filtered and ultrafiltered samples.
6. Analyses of the corrosion layers to search for host phases for actinoids and Tc

*We were advised by CEA Marcoule to use a different designation for the glass. The glass investigated here was fabricated by CEA Marcoule closely simulating the chemical composition of the glass produced by COGEMA at La Hague in their vitrification plants. In the text, the glass from Marcoule is designated CEA R7T7.

C. Progress of work and obtained results

State of advancement

During the reference periode high active glass samples were corroded in highly concentrated halite saturated $Mg(Ca)Cl_2$ -solutions under Ar-atmosphere at 110, 150 and 190°C. The experiments were performed at high ratios of sample surface area to solution volume (S/V) to ensure silica saturation almost from the start of the tests. All experiments are now terminated. Radiochemical analyses is close to completion. Tc analyses are still to be done. For the 450 day leachates, also the oxidation state of Plutonium in solution has been determined. Comparison of results from active glass closely resemble respective previous results published for the inactive R7T7 glass.

I. Results of glass corrosion tests.

The results of this work and those from previous experiments with non-radioactive R7T7 glass [1,2,3] are used to characterize the behavior of actinides and Tc during glass corrosion and to compare the corrosion behavior of inactive and radioactive samples of two glasses with very similar chemical compositions.

Determination of Pu-oxidation states

Table I shows the results of the Pu oxidation state measurements. Higher Pu oxidation states, Pu(V,VI), were most abundant in leachates from experiments at 110°C. Leachates from experiments at 190°C contained Pu(III) and Pu(IV) and no Pu(VI). These results may not reflect exactly the distribution of Pu oxidation states at 110°, 150°, and 190°C. Oxidation states may have changed upon cooling, acidification, and storage of the samples. However, transitions between Pu(IV,V,VI) oxidation states are slow because destruction or formation of oxo bonds is involved. At low Pu concentrations disequilibria between Pu oxidation states may be maintained for several months [4].

Table I: Determination of oxidation states of Pu in the leachates (450 day corrosion experiments)

Temperature glass sample	Pu(III) %	Pu(IV) %	Pu(V+VI) %
110°C	2	0.2	97.8
110°C	0	8	92
150°C	10	22	68
150°C	0	4	96
190°C	43	57	0
190°C	80	20	0

pH-evolution

Figure 1 shows the evolution of pH in the leachate at 190°C. Most data are from previous work with inactive glass [1,2,3]. The figure shows that except of one case the pH values of leachates from corrosion experiments with the radioactive glass are in excellent agreement with those from experiments with the inactive glass. Acidification of the leachate during glass dissolution results from the formation of solid alteration products, in particular of Mg-silicates such as saponite [5].

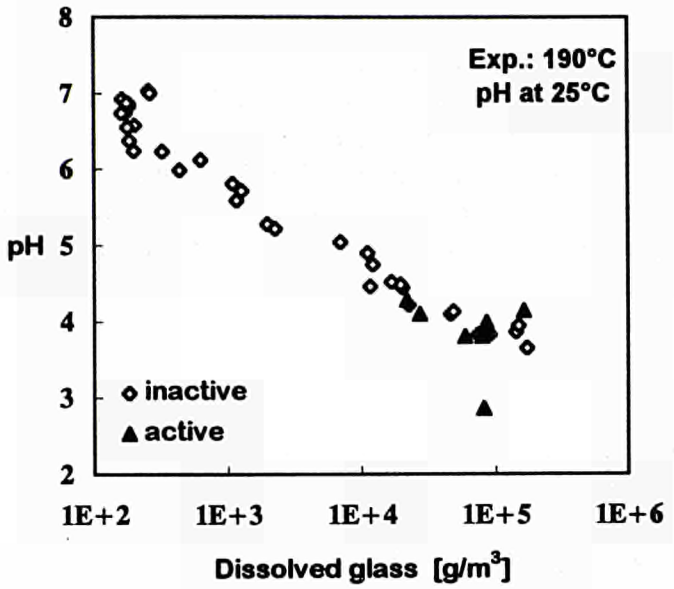

Figure 1: Evolution of pH during corrosion of active and inactive CEA-R7T7 glass in Halite saturated Mg(Ca)Cl_2-solution at 190°C

Radionuclide retention

Radionuclide specific results of the corrosion experiments with the radioactive glass are shown in figures 2 to 4 as a function of reaction progress ξ. The reaction progress measures the corroded mass of the glass per solution volume as calculated from solution concentrations of soluble elements, e.g., boron, divided by their concentrations in the glass ("normalized concentration").

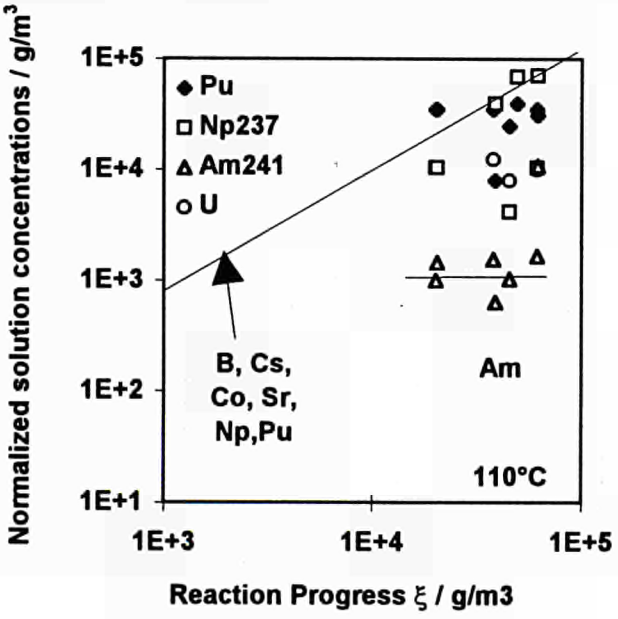

Figure 2,: Release of radionuclides from high active CEA-R7T7 glass in $MgCl_2$- solution at 110°C .

Figures 2, 3, and 4 show normalized concentrations of various radionuclides in the leachates as a function of reaction progress (log-log scales) at 110°, 150° and 190°C,

respectively. The upper curve in each figure with a slope of one represents the extent of glass dissolution. Easily soluble elements such as boron or the alkali earth elements (neutral to acid conditions!) fall on this curve. Data lower than this curve indicate retention by sorption or by formation of secondary alteration products: 90% retention on a curve one logarithmic unit lower; 99% retention, when 2 log units lower etc.. The data for Pu and Am indicate that fractions of these glass constituents are retained to various degrees during glass corrosion whereas Np and Tc are released congruently with the soluble elements from the glass.

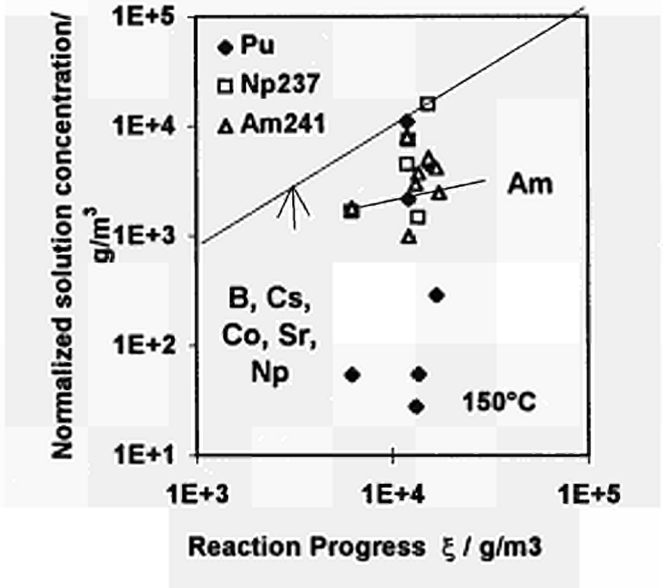

Figure 3,: Release of radionuclides from high active CEA-R7T7 glass in $MgCl_2$- solution at 150°C .

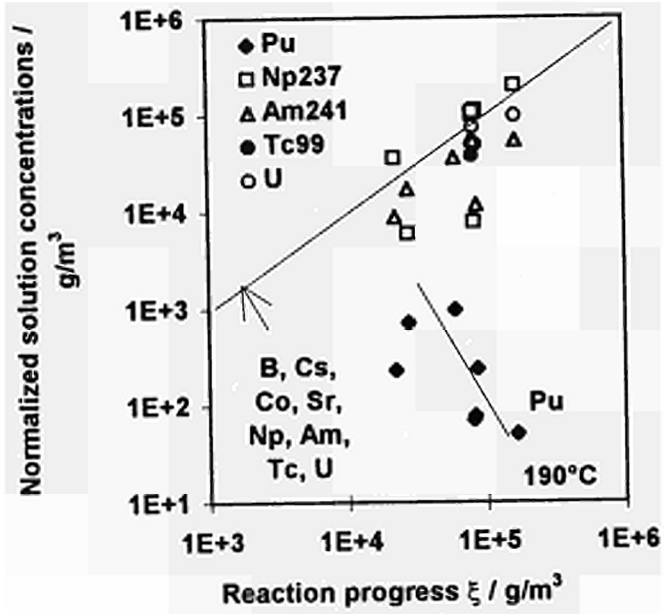

Figure 4,: Release of radionuclides from high active CEA-R7T7 glass in $MgCl_2$- solution at 190°C .

Figures 2, 3, and 4 show that there is a specific effect of temperature on the concentration of Np, Pu, Am, and Tc in the leachates. Since acidification of the salt solution during glass corrosion increases with temperature, leachates with the lowest pH are encountered at 190°C, and the effect of temperature on actinide concentrations may in reality be a pH effect or both. At 190°C, neither Np, Am nor Tc are retained to a significant extent by corrosion products or sorption on the tantalum walls and these elements are released at almost the same rate as boron. Hence, the release of Np, Am and Tc from the glass is controlled by the kinetics of glass dissolution. The decreasing rather than increasing concentrations of Pu with time and increasing reaction progress ξ (decreasing pH) are surprising and may be associated with the complex redox chemistry of Pu. The radionuclide concentrations show a quite different picture at 110°C (fig. 4). With time and increasing ξ values, Pu concentrations approach the curve of congruent glass dissolution. Am concentrations indicate a high but decreasing retention of this element with increasing ξ. At 150°C, the behavior of Pu and Am is comparable and is in between that at 110° and 190°C. Retention of Am at 110°C may be explained by the formation of Ca,REE,Am-molybdate (powellite solid solutions). These phases are known to limit concentrations of rare earth elements in solution [6]. A powellite-type phase was detected in the autoclave at 110°C. Investigations of solid reaction products at 190°C are in progress but until now, no powellite was observed. In contrast, with the inactive glasses, powellite was detected in leachates from experiments at 190°C [7] but recent experiments have indicated that powellite crystallization may takes place upon slow cooling [8].Pu(IV) and Pu(III) may occur as colloids in solution. Pu mobility is highest with the highest oxidation states of Pu, observed at the lowest temperature (table II, figure 2). At 190°C (figure 4), Pu concentrations are relatively low, as expected from the presence of Pu(IV) that forms insoluble Pu(hydr)oxide. The changes in Pu oxidation states are not yet well understood. Pu was found in the leachates as Pu(V,VI) but also as Pu(III). The reason for Pu reduction to Pu(III) could be related to an oxidation of the autoclave's tantalum surface which would be facilitated with increasing temperature. This explanation is supported by results of glass corrosion experiments where iron powder was added. Concentrations of Np and Tc were found to be about 100 times lower and Pu higher than in the parallel experiment without iron. Pu was released to the same extent as Am, Eu and Cm, indicating behavior of a trivalent element. The presence of iron probably results in the reduction of Np (V) and Tc(VII) to sparingly soluble Np(IV) and Tc(IV) and of insoluble Pu(IV) to more soluble Pu(III) (acid conditions) while iron was oxidized [9]. However, more experiments are necessary to provide an unambiguous explanation of the concentration changes of these elements in the leachates.

Time dependence of reaction

Dissolution rate data for the waste form matrix can be important in assessing the mobilization potential of soluble radionuclides. Empirical rate data, however, cannot be extrapolated to time periods of geological disposal if the reaction mechanisms are not fully and quantitatively understood. Nevertheless, empirical rate data for a given set of environmental constraints can be used to gain an understanding of the overall mechanism and can be used in its comparison with other rate-controlling processes. In particular, reaction rate data of the radioactive glass, presently under investigation may be compared with data for the inactive glass. The present experimental program does not aim at revealing new insight into the glass corrosion mechanisms. Instead it is attempted to study radionuclide behavior at high reaction progress values (at high S/V values). The reaction rate data from this study, nevertheless, may be sufficient to identify, if present, differences in the mechanism of active and inactive glass.

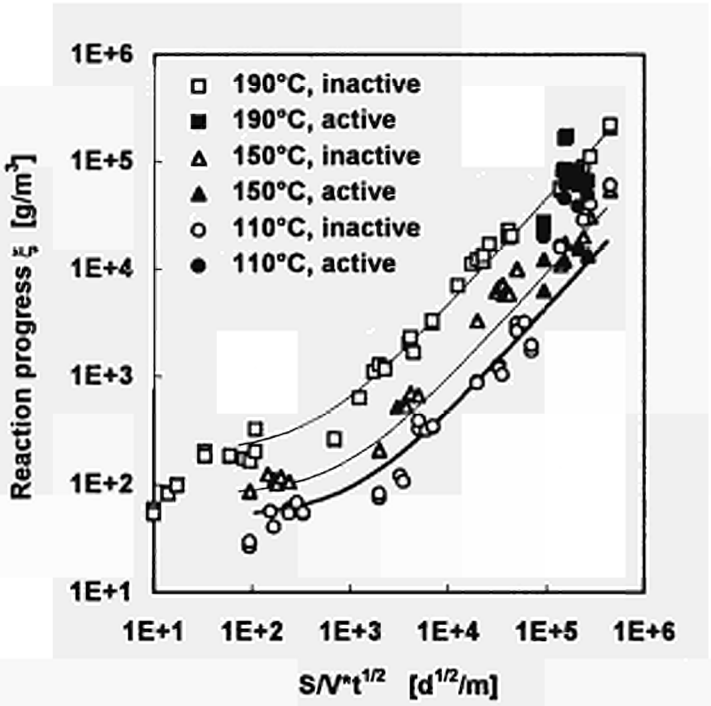

Fig. 5: Time and temperature dependence of CEA-R7T7 glass corrosion in Halite saturated $Mg(Ca)Cl_2$-solution.

The time dependence of glass corrosion (reaction progress) is shown in figure 5. Data of the active glass are compared with data of inactive corrosion experiments, executed at different S/V ratios and for different periods of time [1,2,3]. All data were plotted in one diagram (fig. 5) using an $S/V.t^{1/2}$ scale. A linear variation of reaction progress with the product $S/V.t^{1/2}$ is obtained, once silica saturation is established in solution. There is no difference between the kinetic data obtained from experiments with the inactive and radioactive glass, suggesting that the corrosion mechanism is the same. Hence, the abundant information on the time dependence of the reaction of the inactive R7T7 glass and the empirical rate law derived from these data [3] can be used to describe the behavior of the active glass. The square root of time dependency indicates glass corrosion control by a diffusion process [3]. The empirical rate law for a combination of first order dissolution with a long-term diffusion process is given in integrated form by the equation (1 or 2) [3]:

$$NC_i = Min\left(NC_{Si,sat}\left(1-\exp\left(-\frac{k_+(S/V)t}{NC_{Si,sat}}\right)\right) + \underbrace{2\rho(S/V)\sqrt{(t-t_{sat})}\sqrt{\frac{D_{eff}}{\pi}}}_{t>t_{sat}};\ NC_{i,sat}(\xi)\right) \quad (1)$$

$$NL_i = Min\left(\underbrace{NL_{Si,sat}\left(1-\exp\left(-\frac{k_+(S/V)t}{NC_{i,sat}}\right)\right)}_{\lim(t_\infty)\Rightarrow NL_{Si,sat}} + 2\rho\sqrt{\frac{D_{eff}(t-t_{sat})}{\pi}};\ NL_{i,sat}(\xi)\right) \quad (2)$$

NC_i or NL_i are the normalized concentration or normalized mass loss (normalization to surface area and glass composition) of a given glass constituent i, Min(a;b) gives the minimum of the expressions a and b, $NC_{i,sat}$ and $NL_{i,sat}$ are the normalized concentration or

the normalized mass loss of the element i at saturation which may be a function of ξ, t is time, t_{sat} is the time at which 95% of silica saturation is reached, k_+ is the normalized forward reaction rate, ρ is the density of the glass and D_{eff} is the apparent diffusion coefficient in the glass phase. The exponential part of the integrated rate law, as given in Eqs 1 or 2 is only valid for low silica containing groundwaters and for conditions where saturation of silica in solution is not hindered by secondary phase formation or by sorption or release of silica of other near field materials.

The rate law and its S/V dependence is consistent with those for binary and ternary glasses, i.e., initial (inter) -diffusion controlled alkali ion exchange and subsequent rate control by matrix dissolution but goes a step beyond in order to describe glass corrosion under conditions of long-term contact with limited quantities of water. For nuclear waste borosilicate glasses the processes in the short term are of little interest. Typically, measurements begin after 10 to 30 days of corrosion and cover, in some cases, periods of several years. Steady state of glass matrix dissolution and diffusion is reached within less than a day and reaction rates are controlled by surface reaction. Hence, an initial (inter-) diffusion controlled ion exchange process is not relevant and is not represented in Eqs. 1 or 2. Matrix dissolution is a zero order surface reaction in an open system. In a closed system it becomes a first order surface reaction and is controlled by the reaction affinity with reference to a yet empirical silica saturation concentration in solution. Long-Term glass matrix dissolution in a silica saturated solution is assumed to be controlled by water diffusion into the glass matrix [3]. In other words, the overall corrosion process begins with a solid state diffusion process: H_2O or H_3O^+ diffuses into the glass and alkali ions and other glass constituents mobilized by network hydrolysis move in the opposite direction. As the rate slows down with increasing penetration depth, the competing (parallel) process, matrix dissolution, becomes rate controlling. The rate of matrix dissolution decreases as silica saturation is attained and diffusion of water takes over again and controls the long-term rate. There is experimental evidence to support the hypothesis of a long-term diffusion process with water being the critical species. Lodding et al. [10] and Godon et a. [11] conducted SIMS measurements on inactive CEA glass R7T7 corroded for several years in concentrated salt solutions at 90°C and found a concentration profile of a hydrogen species (H_2O or H_3O^+) in the glass beneath the surface layer and a matching alkali (Li) profile in the opposite direction. Not only network modifying elements such as Li are mobilized but also network forming elements such as boron. The curves in figure 5 were calculated with the help of Eq. (1) and the respective experimental data. D_{eff} was not known and had to be used as a fit parameter. The resulting values are close to effective diffusion coefficients of H_2O in glass [3]. However, D_{eff} could be derived from SIMS concentration profiles, in which case verification of the empirical rate law would be based entirely on experimental data. There is fair agreement between the data and the calculated curves except for 110 and 150°C at high values of $S/Vt^{1/2}$. Here the reaction progress is higher at 110° than at 150°C. This was considered an artifact and not discussed in [3] when the rate law was first published and compared with experiments. However, the phenomenon has now been confirmed with the radioactive glass (see fig. 5) and must be considers real. An obvious explanation would be that a secondary phase forms at 110°C consuming silica. This would lower the silica concentration in solution and increase the corrosion rate. Further work is necessary before this effect can be understood. It is interesting to note that this behavior occurs only in brine 2. In another Mg-rich solution, designated brine 1 [1] the normal temperature dependency is found at all reaction progress values. Brine 1 contains less SO_4 and more Ca than brine 2. May be high Ca-concentrations are responsible for this effect.

CONCLUSIONS ON REPOSITORY RELEVANCE

The rate law described above can only be used for the formulation of a source term for glass performance in a repository, if its validity in presence of other engineered and natural barrier materials has been tested. Nevertheless, certain findings of our work are directly applicable to repository relevant conditions. Concentrations of actinides and Tc in the leachates are determined by their oxidation states which depend on the composition of the system, in particular on the presence of reducing components such as container materials (Fe, ..). Due to limited retention of Tc, Np, Pu and Am in the experiments in the absence of container materials, we can take no credit from secondary phase formation (solubility, coprecipitation) and the rate law for glass matrix dissolution must be used to estimate the long-term release of these elements, provided that the effect of the canister is neglected.

Since active and inactive glass have the same time and temperature dependence of corrosion, radiation damage or radiolysis are not expected to change the reaction kinetics. It has been shown in the literature [12] that inactive glass produced under laboratory conditions behaves almost identical to industrial scale full size glass canisters if exposed to the same experimental conditions. Hence, kinetic data of the inactive and active laboratory glass are directly applicable to full size radioactive glass canisters. The kinetic rate law (Eq.2) implies that the extent of long-term glass corrosion (mass of corroded glass per canister) is directly proportional to total surface area of a fractured glass canister. For t >>tsat, the extent of glass corrosion is independent on the volume of the intruding brines (2. term in Eq. 2), even though activity release of solubility limited radionuclides (NCi,sat, NLi,sat) strongly depend on solution volume. This strongly facilitates long-term extrapolations of glass behavior in a repository in salt formations, as the volumina of intruding brines are generally not known and estimations are highly dependent on assumptions and scenaria, which are difficult to validate.

References

1. Lutze, W. Müller, R. and Montserrat, W., Mat. Res. Soc. Proc. 127, 81 (1989)
2. Lutze, W. Müller, R. and Montserrat, W., Mat. Res. Soc. Proc. 112, 575 (1988)
3. Grambow, B., W. Lutze, R. Müller; Mater. Res. Soc. Symp. Proc. Vol. 257, p. 143 (1992)
4. Capdevilla, P. Vitorge and E. Giffaut, Radiochimica Acta 58/59, pp 45-52 (1992)
5. Grambow, R. Müller, Mat. Res. Soc. Symp. Proc. Vol. 176 [1990]
6. Grambow, B., R. Müller, A. Rother, W. Lutze, Rad. Chim. Acta 52/53, 501 (1991)
7. Rother A., W. Lutze, P. Schubert-Bischoff,. Mater. Res. Soc. Symp. Proc. Vol. 257, 57 (1992)
8. Bernothat,W. pers. commun.
9. Grambow, MRS Bulletin, Dec. 1994
10. Lodding, A.R., D.E. Clark, G.G. Wicks,"Leachabilities of International Waste Glasses in WIPP", EUR-15629-EM (1994)
11. Godon, N. D. Beaufort, E.Vernaz,"R7T7 glass alteration after 5 years in the WIPP". EUR-15629-EM (1994)
12. Bickford, D.F., D.J. Pellarin, Mat. Res. Soc. Symp. Proc. 84, 509 (1987)

Title	Consequences of gas production in geological repositories (PEGASE)
Contractors	ANDRA (F); ENRESA (E); GRS (D)
Contract N°	FI2W-CT90-0020
Duration of contract	August 1991 - April 1995
Period covered	January - December 1994
Project leader	S. VOINIS (ANDRA, Coordinator), F. PLAS (ANDRA), M.A. CUNADO (ENRESA) W. MULLER, D. THELLEN, H. KANNEN (GRS)

A. OBJECTIVES AND SCOPES

This project intends to model the overall impact of gas production in the nearfield and in particular on the groundwater flow, the durability of engineered barriers and on the radionuclide migration. The wastes forms will include spent fuel, vitrified wastes, medium level waste. The different rock formations envisaged are granite rock and salt. This project is divided in four stages:

1. Description of processes.
2. Analyse of gas transport mechanisms.
3. Modelling of the system.
4. Calculations in specific disposal conditions.

B. WORK PROGRAMME

B.1. Description of processes

This step consist in identifying the mechanisms for gas formation in the different waste repositories considered in the project scenarios from bibliographic or experimental studies and to establish the common data for the development of the models and for calculations. Analytical laws will be defined through this study to be integrated in the future modelling.

B.2. Analyse of gas transport mechanisms

The transport concerns the near-field and the host-rock. A listing of the main phenomena have to be identified and studied.

B.3. Modelling of the system

The modelling is based on specific developments or on already existing models for the different repository conditions considered by each participant.

B.4. Calculations

The calculations are performed for the repository conditions defined by the participants. The aim of these calculations is to verify that engineered barriers and wastes matrix are still playing their safety role in the presence of gas. The other aim is to discuss the results and their consequences on the future research.

C. PROGRESS OF WORK AND OBTAINED RESULTS

C.1. Task one

C.1.1 Data reference and bibliographic synthesis

On the basis of an exchange of informations, working group 1 (ANDRA/ENRESA/GRS) created for task 1 has finished two reports :

- Data reference : the characteristics of wastes, concepts are described in this chapter. See progress report 1
- Bibliographic synthesis : a compilation of the description concerning the potential gas formation mechanisms is finished. See progress report 3

This synthesis has been used for the establishment of the gas formation codes.

C.1.2. Gas formation codes

The description of gas generation mechanisms is presented in the progress report 4 of July 1994.

1..GASFORM:

In the following, the results for canister surface and volumetric gas production corresponding to a quadruple case (including ENRESA, ANDRA, GRS-1 and GRS-2 scenarios) performed with GASFORM are presented.

The canister surface gas production in the ENRESA scenario is due mainly to the steel corrosion with a little contribution of zircalloy corrosion (about 5 %) and an insignificant contribution of internal radiolysis (0,04 %) and radioactive decay (0,05 %).

At approximately 4200 years the ENRESA container is consumed and the steel corrosion finishes ; since the zircalloy corrosion has finished before due to zircalloy consumption and the internal radiolysis and radioactive decay are insignificant compared to steel corrosion, the integrated production becomes stable.

In the ANDRA case the integrated production becomes stable at an earlier time than in the ENRESA case since the steel available for corrosion is much lower.

It can be observed that the production rate is also lower. The reason for this is twofold : firstly, the ANDRA scenario does not include zircalloy and secondly, the steel corrosion rate is lower than in the ENRESA case due to the temperature, pH and Eh conditions. However the contribution of internal radiolysis and radioactive decay to the total canister surface gas production, though still of very little significance (0,1 %) because of the direct dependence on the alpha activity of the waste, is greater than in the ENRESA case.

In GRS cases the corrosion rate is assumed to be equal to 5.10^{-2} (GRS-1) and 1.10^{-2} (GRS-2) mm/a at 100°C. This value is corrected to take into account the decrease of corrosion rate with a lower temperature. In any case, the corrosion rate is much lower than the internally calculated values in ENRESA and ANDRA cases, thus the container life is greater.

The corrosion rate in GRS-2 is lower, than in GRS-1 but the container life is greater because there is more steel available; at the end of the GRS-1 curve it can be observed a little increase, it is due to the production by radioactive decay and internal radiolysis whose contribution to the gas production is grater than in the case of GRS-2 because of its higher disintegration constant.

The curved effect of GRS's lines is due to the quickly heat transfer from the waste to the container surface which makes the corrosion rate to decrease brusquely when 90 % of this transfer process is completed in the first years from disposal. From then on the corrosion rate states practically constant.

Concerning the volumetric gas production, in the ENRESA case more than 80 % of the integrated production at 1.10^6 years is due to microbial degradation, this mechanism is not present in the other three scenarios, since microbial degradation begins when bacteria have become adapted to the medium; this is the reason for the lower rate of ENRESA at the beginning.

It can be observed that when microbial degradation is finished because of the consumption of organic matter, the ENRESA rate (only due to external radiolysis) is much lower than the ANDRA and GRS-1 rates.

The external radiolysis in the GRS-2 case is not important because of the low gamma activity.

The ANDRA and GRS-1 external radiolysis rates are higher than the corres-ponding of ENRESA due to their higher gamma activity and thinner container; the GRS-1 rate is higher than the ANDRA rate because of the lower shielding capacity of its backfilling.

GRS's and ANDRA curves are similar because only the external radiolysis mechanism contributes to the volumetric gas production, and the gas generated from this mechanism is almost proportional to the gamma activity of the waste as the two following phenomena :

a) Decrease of generation rate due to the consumption of gamma activity by internal radiolysis.
b) Increase of generation rate due to the increase of the energy flux.

Which occur when the container consumption progresses are approximately compensated each by the other.

2. GABI :

GABI is a programm for calculating time dependent gas sources in repositories for low-mdeium or highactive waste. These calculations include the most important processs for gas generation. The precision of the modelling of each process depends on the amount of prooved informaton and experimental data which was found. Another aspect for this precision was the importance of each process for the gas generation.

The importance of the individual processes for the gas generation depends on the kind of waste and has been demonstrated by various sensitivity studies. It has been found out that in most cases radiolysis is the dominating gas generating process for HLW, while corrosion and radiolysis are comparable when calculating a case for MLW. The influence of radiolysis is hadly recognizable for a case with LLW while microbial degradation may in some cases be more important than the corrosion is. The modelling of microbial degradation is based on simplified assumptions as there are not enough prooved experimantal data on this mechanism. This makes it very hard to give detailled inormation about the gas generation by microbial degradation compared to the gas generation by corrosion.

The programming of GABI is arranged very claerly by using a single module for each process and for each important function. This fact made the program very large and it required a very long time on programming. On the other hand the modularity made it easy to verify the single modules. The program has been checked by calculating many cases for each process with other professional programs to verify all the modules used in the code. After these calculations, the cooperation between modules and the mass- and waterbalance were checked. Saved cases are stored in the subdirectory a Data base and a file named by the user with the extension. INP is generated automatically. The user can find all the important input information in this file so that it is possible to recognize input-errors even if the calculation is done. In the end, we spent almost time on quality assurance as on a programming. In addition the source-code is documented very well so that it's easy to understand the structure of GABI and to modify single processes or to add new ones.

C.2. Gas transport

Methodology of work

A physical analysis of two-phase transport in porous media has been carried out. Several codes have been studied and the codes PHOENICS and TOUGH2 have been selected for the further investigations.The codes PHOENICS and TOUGH2 take into account the main phenomena of two-phase flow. Darcy's law with relative permeabilities forms the basis for the physical modeling. Both codes have been modified for the further investigations. The mathematical model of PHOENICS has been modified in two ways. First the two-phase algorithm originally provided by PHOENICS cannot be used because interphase friction is not playing an essential role in two-phase transport in porous media. Secondly the Scalar Equation Method (SEM) provided by PHOENICS has been modified. Even with these modifications the problem was only solved fot two phase flow in porous media with a number of simplified assumptions requiering extremely high CPU-time. Therefore the application of the PHOENICS code for two phase flow in porous media is not recommended.

To study the influence of gas generation on fluid transport, the output of GABI and GASFORM can be converted to an input table of time dependent gas generation rates for TOUGH2 as a first step. Due to the fact that the gas generation rate depends strongly on the water content in the backfill material, the time dependent gas generation rates from GABI are coupled in a second step with the calculated liquid saturation from TOUGH2, according to the following expression :

$$\Gamma = SL * G_{GABI} \qquad (1)$$

with SL = Liquid saturation (in $cm^3_{liquid}/cm^3_{pore\ volume}$).
G_{GABI} = Pre-calculated gas generation rate according to GABI (in kg H_2/s) with 100 % liquid saturation.
Γ = Gas generation rate according to TOUGH2 (in kg H_2/s).

A first phase of coupling between GASFORM and TOUGH2 has been performed for drift or borehole concepts. Some adaptations have been made on TOUGH2 and on its exploration.

.Conclusions of the isothermal calculations

A configuration for isothermal conditions has been used for parametric studies concerning domain specific parameters. The results lead to the following conclsions concerning the modelling of the geometry :

-The configuration is appropriate to describe the gas flow in the drift assuming isothermal conditions, when the difference of the permeabilities of the domains "plug" and "salt" is sufficiently high, eg. larger than two orders;

-upstreamweaghting is required for transient two phase flows wuth propagating phase

fronts;
-the gas saturation profile depends strongly on the capillary pressure and on the void volumes of the drift and the plug;
-domain specific capillary pressures are dominating parameters with respect to gas transport to the different parts of he geometry.

The qualitative evolution of the pressure build-up ad the gas and liquid release due to gas production can be summarized as follows :
-gas generation results in an initial pressure build-up due to gas phase formation with a maximum pressure when the gas phase begins to pass though the plug and a long-term pressure drop due to gas release through the plug;
-the maximum pressure build-up depends strongly on the plug permeablity and is reached after only some years;
- the gas transport takes place in the upper part of he drift;
- the liquid release depends strongly on the plug permeability and decreases with time after the maximum pressure build-up has been reached.

Statements concerning the quantitative dependencies have to be assessed with caution, because the calculations are based on a large number of assumptions and specifications, in particular related to the domain specific parameters and the design of the plug.
As the saturation profile depends strongly on domain specific parameters e.g porosity, permeability and capillary pressure, a site specification program is essential to characerize these values.
Furthermore it has been demonstrated, that it s essential to perform the calculations with realistic gas generation rates since conservative assumptions could lead to exterm results; e.g pressure build-up.

Conclusion of the nonisothermal calculations

A configuraton for nonisothermal calculations has been developped and tested against the configuration used for isothermal calculations. The agreement of the two results is good, although the configuration for isothermal calculation is able to describe the upper part of the drift and the plug in more detail.
The consideration of the heat balance aquantion results in higher CPU times even when no temperature gradients are present. The CPUtime grows even more in he presence of high temperature gradients, as it has been shown in the calculations with heat sources.
A method has been developed for consideration of time dependent heat and gas sources. This method is based on the assumptions of a maximum surface temperature and an initial heat production curve. It consists of an iterative procedure for the consideration of the mutual dependencies of fluid flow, temperature and gas production.
This method has been applied as an example to POLLUX-8DWR-BE containers in a drift. The results of the simulations indicate following characteristics:
- the pressure curve is characterized by initial pressure build-up due to a temperature increase in the drift and a succeeding pressure drop due to the liquid release from the plug;
- the temperature curve reaches a maximum after 150 years and then decreases to a nearly constant value.

It has been proven that the significant initial pressure build-up is very sensitive on the chosen scenario, in particular on the initial gas content in the drift.

Conclusion on sensitivity analysis in granit :

The results of the sensitivity analysis made in granit for 1D/2D configurations and permeability/thermal and coupling parameters will be presented in the final report. The most important recommandations for future work are :

- more sensitivity study on numerical aspect to look at divergence problems;
- sensitivity analysis in 1D configuration on mesh aspect;
- adaptation of TOUGH2 on 3 components (water, air, H_2),
- experimental validation on the Kr and Pcap laws in the hardrock and backfilling material.

Title :	Characteristics of bitumized radioactive wastes
Contractor:	CEA/DOC (Cadarache et Saclay), SCK/MOL, NIRAS-ONDRAF, RISO NATIONAL LABORATORY
Contract N°:	FI2W-C£T90-0025 + 0007
Contract duration:	March 1992 - February 1996
Project leader:	M.Brunel
Task Leaders:	MM. Van Iseghem, De Goeyse, Nomine, Brodersen

A. OBJECTIVES AND SCOPE

The objective of this study is to investigate the leaching behaviour of the bitumen encapsulation of representative and homogeneous reprocessing sludges or concentrates wastes under geological disposal conditions.
The influence of the bitumen matrix and the type of waste treated will be closely examinated.
The present study will include realistic disposal scenarios and comparison of Eurobitum and M80/100, M40/50 and MR90/40 will be possible in regards to efficiency confinement of radioactivity.
The tests that should enable us to evaluate encapsulation stability are steady leaching tests in different media conditions constituted by water (CEA Cadarache and SACLAY), by a cement/clay mixture and clay/clay water mixture (SCK Mol and CEA SACLAY) with different size samples from a few cm^3 to the full size bitumen block.
Understanding of water uptake in and release of dissolved materials when bitumenized materials are disposed of under saturated as well as unsaturated conditions and quantification of swelling pressure and leaching phenomena are improved by RISO NATIONAL LABORATORY.
The small size samples of bitumenized coprecipitation sludges will be prepared by CEA Cadarache.

B. WORK PROGRAMME

B.1. Sampling

Samples are taken from an inactive and an active drum or are fabricated in suitably equipped shielded cell. The size of the samples is between 20 cm^3 and 200 l.

B.2. Inactive leaching tests

Tests are carried out by SCK Mol Laboratory in a cement/clay mixture and a clay/clay water mixture, at 23°C and 40°C, for duration until 480 days. Emphasis will be on leaching kinetics of inactive waste constituents.

B.3. Active leaching tests

Tests are carried out in similar conditions as B.2 (media, temperature, duration) by SCK Mol for the small samples (20 cm^3) and by CEA SACLAY for 200 l, 20 l, 2 l and 0,2 l samples. Leaching tests in water will be performed on 0,4 l samples in static and uncontinuous conditions by CEA Cadarache and on 200 l, 20 l, 2 l and 0,2 l for CEA SACLAY. Emphasis will be on leaching processes and kinetics of the active waste constituents.

B.4. Migration of water and ions through membranes of bitumized products

Uptake of water into bitumenized waste is important for the understanding of the long-terw behaviour of the material. Diffusion of tritiated water and ^{134}Cs ions is studied using membranes made from pure bitumen, bitumen mixed with crystals of soluble salts such as $NaNO_3$ or with insoluble sludge particles, for example $BaSO_4$. the measurements of the amounts of diffused materials are supplemented by measurement of the electrical conductivity over the membrane. This gives additional information about the migration mechanisms and the quality of the membranes.

B.5. Swelling and swelling pressure

Unrestricted swelling, water uptake and Na-leaching from samples of bitumenized materials containing soluble salts are followed using a weighing technique and chemical analyses of the leachants. The materials are simplified versions of typocal waste products. This makes it possible to investigate the influence of single parameters such as bitumen type, salt content, crystal size, presence of sludge particules, etc.
Pressure development due to water uptake in confined samples of similar materials is also investigated using a technique where swelling caused by water penetrating through a cement mortar barrier results in replacement of mercury from a bottom reservoir up in a long capillary tube.

B.6. Model describing water uptake and leaching

A research model describing the water uptake in bituminized materials containing soluble salts has been developed. The dynamics of the swelling and the generation of an internal solution-filled pore structure are modelled on teh micro-scale. Some simplifying assumptions about geometry of the system, etc. are made. The water is supposed to be transported as vapour through the bitumen films surrounding the crystals. Diffusivities for tritiated water obtained in the above-mentioned membrane experiments are utilized.

C. PROGRESS OF WORK AND OBTAINED RESULTS

The status of progress has not been forwarded to the Commission for 1993 and for 1994.

Title :	Natural analogue of bitumen matrices in a deep repository
Contractor:	CEA/DCC/DESD Cadarache, CREGU-CNRS Nancy
Contract N°:	FI2W-CT90-0026
Duration of contract:	June 1991 - November 1995
Period covered:	
Project leader:	P. Holliger (CEA Cadarache, coordinator); P. Landais (CREGU-CNRS); O. Ruau (CREGU); C. Menet-Dressayre (CEA)

A. OBJECTIVES AND SCOPE

The objective of this research programme is the investigation of the effects of radiation on the chemical changes in the structure of organic matter (OM), specifically in the Oklo U-ore deposit and its associated natural fission reactors. Studies have shown that sedimentary organic matter associated with uranium may be altered by irradiation related to (i) the natural decay of ^{238}U and (ii) the ^{235}U fission process. Such modifications must be studied by a non-destructive, in-situ technique because of the technical difficulties related to the extraction and the isolation of the organic matter. Specular reflectance Fourier transform micro infrared spectroscopy (micro FTIR) appears to be an efficient tool for microscale studies (Rochdi and Landais, 1990, Landais and al., submitted). It provides information on oxygenated, aliphatic and aromatic species abundance ratios for 200 X 200 microns large regions of organic matter on polished section samples. The morphology and texture of bitumens and mineral inclusions are first observed by optical microscopy in order to select specific areas for subsequent analysis by micro FTIR (Holliger and Landais, 1993a, 1993b). The combination of petrographic, spectroscopic and isotopic ($^{13}C/^{12}C$) studies allows the different types of organic matter from the different zones of the Oklo basin to be distinguished. New organic matter-rich samples from the core of Reactor Zone 9 (RZ.9)are now prepared. The aim is to compare the structure of OM from two different zones of nuclear criticality (RZ.9 and RZ.10) in order to discriminate different types of OM and/or functioning of the reactors (temperature, water as moderator,...). Finally, ion bombardment with varied ions of appropriate mass and energy was performed on samples from the reactor core and outside the reactor in order to detect some structural modifications of the OM.

B. WORK PROGRAMME

B.1.1 Sampling and petrographic observations (by using electron microscope and reflected light microscope)

B.1.2 In-situ characterization of the organic matter, by using specular reflectance Fourier transform micro infrared spectroscopy

B.2.1 Characterization of the OM and uraninite from nuclear reactor 10 : uranium and fission products containments (isotope data and ion microprobe cartography).

B.3.1 Experimental study of radiation effects: Pb and He implantation experiments on the Oklo samples

C. PROGRESS OF WORK AND RESULTS OBTAINED

Status of progress has not been forwarded to the Commission for 1994.

Title	Aqueous corrosion of nuclear glasses: influence of disposal conditions
Contractors	CEA-CE Valrhô, DRDD/SCD
Contract N°	FI2W-CT90-0027
Duration of contract	April 1991 - March 1995
Period covered	January - December 1994
Project leader	N. Jacquet-Francillon

A. OBJECTIVES AND SCOPE

Geological disposal of vitrified high-level waste packages will expose the containment glass to multiple complex chemical reactions (involving the host rock, the engineered barrier materials and the nuclear glass) due to the presence of the water vector in the repository environment. The presence of environmental or local site materials affects (increases or decreases) the glass matrix corrosion rates and the degree of radionuclide containment. It is therefore essential to characterize and quantify the potential reaction mechanisms in a geological disposal complex. The investigation begins at laboratory scale; the experimental approach also allows the development of a nuclear glass dissolution model applicable to actual repository conditions.

Three major avenues of research will be investigated in a programme combining an experimental approach and modeling of relational processes: ❶ basic research on aqueous corrosion of nuclear glass; ❷ the effect of the host rock on R7T7 glass alteration; and ❸ the development of models describing glass behavior in repository conditions.

B. WORK PROGRAMME

B.1 Basic research on aqueous corrosion of nuclear glass

1. The effect of glass composition on the initial dissolution rate, the solubility limit and equilibrium pH, and the role of new phases on glass dissolution kinetics will be investigated by varying the concentrations of the following components: MgO, SiO_2, Al_2O_3, B_2O_3 and fission product oxides.
2. Role of exterior ions: metallic cations (Al, Fe, Zn, Pb and Mg) and canister corrosion products; effect of the ionic strength.
3. Investigation of the interface gel layer: physical and chemical properties, thermodynamic properties and stability.

B.2 Influence of the disposal site

1. Equilibrium limits with various host materials: granite, clay (ref 448 and 802), schist and salt.
2. Parameter experiments at 90°C in the presence of schist (different types and grain sizes), clay, granite or salt (clear halite and cloudy halite).
3. Integral experiments with granite, clay and schist.

B.3 Development of a glass behavior model

1. Mechanistic model
2. Geochemical model (thermodynamics and kinetics of R7T7 glass dissolution, interactions between R7T7 glass and corrosion products, interactions between R7T7 glass and host materials: granite, clay or schist).

C. PROGRESS OF WORK AND OBTAINED RESULTS

Task B1: Basic Research on Aqueous Corrosion of Nuclear Glass

Effect of Glass Composition

The effects of MgO and SiO_2 on the aqueous corrosion stability of the glass were discussed in the 1991 Annual report [1]. The effects of the Na_2O, B_2O_3, Al_2O_3 and fission product oxide concentrations on glass corrosion were investigated through experiments with monolithes at low glass surface-area-to solution-volume (*SA/V*=10 m^{-1}) and with glass powders at high S/V ratios (20 000 m^{-1}). 20 glass compositions were determined by the mean of a statistical design.The range of compositions is as follow :

30% (in wt. %) < SiO2 < 70%
2% < Al2O2 < 20%
7% < B2O3 < 20%
9% Na2O+Li2O < 24%
2.5% < Fe2O3+NiO+Cr2O3+P2O5 < 10%
5% < P.F oxides + Actinide Oxides + ZrO2 < 25%

This part of the work is widely discussed in the 1994 Annual report.

Role of External Ions

• *Effect of Metallic Cations*

The effects of metallic cations (Al, Fe, Zn, Pb and Mg) on the corrosion kinetics of R7T7 glass were the subjects of the 1994 semiannual report [2].

– Tests were conducted at low *SA/V* ratios under static conditions at imposed pH values (acidic media at pH 2.9 and basic media at pH 8.9), using a single cell from which all solution samples were taken. The initial solution was double-distilled water to which metallic cations were added in variable concentrations. The highly diluted test medium corresponded to a very slight degree of reaction progress, allowing us to investigate the effects of the cations and anions on the initial glass dissolution rate R_0.

At concentrations of 2.5×10^{-3} M, B, Na, Ca, K, Cl^-, NO_3^-, CO_3^{2-}, SO_4^{2-} do not induce major variations in the initial dissolution rate in basic media. In acid media, at concentrations of 2.5×10^{-3} M SO_4^{2-} and NO_3^- ions tended to slightly increase the initial rate respectively by a factor of 3 and 1.4 , while $H_2PO_4^-$ ion caused the rate to diminish by a factor of 4. At concentrations of 2.5×10^{-4} M, F ions increased the initial rate by a factor of 4. At concentrations of 2.5×10^{-3} M, F ions increased the initial rate by a factor of 30.

– Tests were also conducted at high *SA/V* ratios using glass powder with flowing solution. The inflowing solution contained H_4SiO_4 at 90% of the saturation value with respect to the glass, as well as variable concentrations of metallic cations (Al, Fe, Zn). The high degree of reaction progress allowed us to assess the effect of cations on the glass dissolution rate under near-saturation conditions. The results clearly showded the kinetically limiting properties of aluminum

• *Effect of Canister Corrosion Products*

A number of the R7T7 glass dissolution experiments in the presence of corrosion products from the NS24 (PC) steel canister have been completed and the alteration solutions analyzed. The test results were discussed in the 1992 Semiannual Report [3].

The experiments on the effects of simple oxides and hydroxides (Fe, Ni, Cr and Ti) have been completed, as have the tests to assess the effects of the temperature (50°C and 70°C) and the presence of "siliceous" additives (smectite, bentonite and silica gel). The test results are now being interpreted, and will be published in a later report.

• *Effect of Ionic Strength*

The effect of the ionic strength on the initial corrosion rate is now being investigated. R7T7 glass corrosion experiments were conducted with the following brine solutions: NaCl, Na_2SO_4, $MgCl_2$, $MgSO_4$, $CaCl_2$ and $CaSO_4$. The results will be discussed in the next report.

Investigation of the Interface Gel

The R7T7 glass alteration gels are currently being analyzed.

Task B2: Influence of the Disposal Site

Equilibrium limits with various host materials

Experiments to determine the equilibrium limits of R7T7 glass in the presence of 5 environmental materials (granite, two clays, schist and salt) were conducted at 90°C with an *SA/V* ratio of 5800 m^{-1} for durations of 7 days to 1 year. All the experiments have been completed and the results have been analyzed (they will be presented in a later report).

The first results show that each medium imposes a different pH, different elemental concentrations in solution, and different degrees of glass corrosion. Although the two clay media were the most aggressive with respect to R7T7 glass during the first six months, very low corrosion rates were reached after one year in all the test media.

At the present time, no direct relation has been established between the pH, the Si concentrations and the glass corrosion rates.

Parameter experiments at 90°C

• *Alteration in the Presence of Schist*

The results of this investigation were discussed in the 1992 Annual Report [4].

• *Alteration in the Presence of Clay*

R7T7 glass alteration in two natural clays sampled from deep underground sites was studied for 1, 2, 3 and 6 months at 90°C. The clay was ultracentrifuged after the test to recover the leachate and perform elemental determinations and pH measurements. The results of this investigation will be presented in a later report.

• *Alteration in the Presence of Granite*

The results of this investigation were discussed in the 1992 Annual Report [4].

• *Alteration the Presence of Salt*

R7T7 glass corrosion tests are currently in progress with two types of salt, at temperatures of 90°C and 150°C, at an *SA/V* ratio of 70 m^{-1} for durations of 7, 14, 28, 42, 56, 70, 84, 91, 120 and 180 days and for 1 and 2 years. Only the 1 and 2-year tests have not yet been completed. The alteration solutions have been analyzed and the crystallized phases identified by X-ray diffraction.

Integral Experiments

The "TAV 6" experiment simulating a granite repository environment has been in progress for over 9 years. Glass alteration remains very slight, and is controlled by the pseudo-flow due to the solution sampling procedure. Four integral clay tests were initiated in 1992: two of them will be terminated after 6 months, and the others after 2 years. Two integral schist tests were also initiated in 1992 for periods of 6 months and 2 years.

Several integral "TAV"[1] experiments are included in this task to simulate different repository environments:

- Granite: the ongoing TAV 6 experiment was initiated over 10 years ago, in September 1983.
- Clay: 4 TAV experiments (TAV 21 to 24) were initiated in November 1992 with clays from two different formations encountered at different depths (448 m and 802 m) in the same borehole. The disposal concept selected for these tests was discussed in the 1992 Annual Report. Two of these tests were terminated after 8 months, and the other two are scheduled to be terminated after 24 months.
- Schist: a TAV experiment was initiated in November 1992, and a second will begin in January 1994.

The results of the TAV tests will be presented at a later date, when all the experimental findings are available.

Task B3: Development of a Glass Behavior Model

Mechanistic Model

This model was discussed in the 1993 Semiannual Report [5]. The effect of the major parameters were quantified by simulations at 90°C using the LIXIVER code. The pH affects the glass solubility C* and thus has only a very limited influence at values below 9. The apparent silicon diffusion coefficient in the alteration film proved to be the most sensitive parameter taken into account by the LIXIVER code: very slight D variations result in very different calculated element concentrations.

A comparison between the calculated and experimental results showed that it was impossible to fit the short-term values (up to 90 days) using only a single diffusion coefficient for the entire experimental period.

---

[1] *TAV: a French acronym for "Glass Alteration Test"*

Geochemical Model

The results of geochemical modeling (thermodynamic and kinetic constrains) with the KINDIS code of R7T7 glass at 90°C in water in contact with different clays, and in contact with flowing water, were presented in detail in the 1993 Annual Report [6].

List of Publications

1. T. ADVOCAT P. JOLLIVET, N. GODON and E. VERNAZ, *Effect of Geological Repository Parameters on Aqueous Corrosion of Nuclear Glass,* CEC Contract FI 2W CT 90 0027. Annual report 1991, CEA document SCD/92.01 (1992).

2. S. GIN, N. GODON, T. ADVOCAT P. JOLLIVET and E. VERNAZ, *Effect of Geological Repository Parameters on Aqueous Corrosion of Nuclear Glass,* CEC Contract FI 2W CT 90 0027. semiannual report 1994, CEA document SCD/94-24 (1994).

3. N. GODON, T. ADVOCAT P. JOLLIVET, F. DELAGE, S. GIN, and E. VERNAZ, *Effect of Geological Repository Parameters on Aqueous Corrosion of Nuclear Glass,* CEC Contract FI 2W CT 90 0027. semiannual report 1992, CEA document SCD/92-29 (1992).

4. N. GODON, T. ADVOCAT P. JOLLIVET,F. DELAGE, S. GIN and E. VERNAZ, *Effect of Geological Repository Parameters on Aqueous Corrosion of Nuclear Glass,* CEC Contract FI 2W CT 90 0027. Annual report 1992, CEA document SCD/93-01 (1993).

5. P. JOLLIVET, F. DELAGE, T. ADVOCAT, N. GODON and E. VERNAZ, *Effect of Geological Repository Parameters on Aqueous Corrosion of Nuclear Glass,* CEC Contract FI 2W CT 90 0027. Semiannual report: January-June 1993, CEA document SCD/93-22 (1993).

6. T. ADVOCAT P. JOLLIVET, N. GODON and E. VERNAZ, *Effect of Geological Repository Parameters on Aqueous Corrosion of Nuclear Glass,* CEC Contract FI 2W CT 90 0027. Annual report 1993, CEA document SCD/94-02 (1994).

Title	Effect of Insoluble Active Dissolution Fines on Fission Product Glasses
Contractors	CEA - CE Valrhô, SCD
Contract N°	FI2W-CT90-0028
Duration of contract	March 1991 - February 1995
Period covered	January - December 1994
Project leader	N. Jacquet-Francillon

A. OBJECTIVES AND SCOPE

Insoluble particles, known as fines, present in fission product solutions consist of cladding fragments or undissolved fission products, notably platinoids. At La Hague, these fines are vitrified with the fission product solution in the T7 facility. Platinoids are found in soluble or insoluble form with other particles. Regardless of their initial state, the platinoid elements ruthenium, rhodium and palladium are insoluble in the glass.

As a result, the amorphous glass mass contains heterogeneous inclusions comprising notably highly radioactive Ru and Rh, with substantial thermal power. It is therefore necessary to ascertain whether the SON 68 18 17 L1C2A2Z1 reference glass composition is a suitable containment matrix for these active insoluble dissolution fines. The experimental programme will include the fabrication and characterization of glass rods containing actual active fines.

B. WORK PROGRAMME

B.1 Development of an analysis method for glass containing dissolution fines.
B.2 Development of a nondestructive gamma-scanning method to measure the radionuclide distribution and the true activity.
B.3 Fabrication of glass rods containing actual active fines; quantification of the fines, and notably the platinoids, in the glass.
B.4 Preparation of test specimens after gamma scanning.
B.5 Measurement of glass containment properties at room temperature and at 90°C; determination of glass alterability at 90°C.
B.6 Leaching of test specimens at 100°C in Soxhlet devices.
B.7 Characterization of glass microhomogeneity.
B.8 Repeat steps B.4 through B.7 on glass samples submitted to a heat treatment cycle.

C. PROGRESS OF WORK AND OBTAINED RESULTS

PROGRESS AND RESULTS

A glass composition designated A130, containing fines from dissolution of fuel irradiated in the Advanced Prototype Boiler (CAP) at Cadarache, was produced in the Vulcain cell. The principal characterization tests specified in the contract have been completed on the sample.

- A 28-day dynamic leach test in Soxhlet mode was carried out on the A130 glass sample and on a nonradioactive R7T7 glass sample.
  The results obtained for the mobile elements (B, Li, Na, Mo) showed that the normalized mass loss for the A130 glass was comparable to that of the nonradioactive R7T7 reference glass.

A second glass composition designated A131, containing fines from reprocessing fuel from PHENIX fast breeder reactor at Marcoule, was also produced in the Vulcain cell. This sample is currently being characterized.

- In the as cast specimen we find platinoids in their usual form : ruthenium in the form of ruthenium oxide and palladium in the form of palladium metal together with tellurium and rodhium, and chromites due to corrosion of the melting pot.
  The average crytallization density of the glass is 0,62 % with majority development of the chromite phase.

- After heat treatment at 780°C, the same phases were observed in the heat treated glass as in an inactive heat treated specimens : platinoids in their usual forms, chromites, calcium molybdate crystals, crystals enriched in Si, O, Ca, Nd, P and crystals enriched in Si, Ca, Ni, Fe, Nd, O.
  The crystallization density increased from less than 1 % in the as-cast sample to 4,7 % after heat treatment because of the development of the Si, Ca, Ni, Fe, Nd, O phase..

Title	The corrosion of nuclear waste glasses in a clay environment : mechanisms and modelling
Contractors	NIRAS/ONDRAF (B) and SCK/CEN (B)
Contract N°	FI2W-CT90-0031
Duration of contract	March 1991 - February 1995
Period covered	January - December 1994
Project leader	R. Gens (NIRAS/ONDRAF, coordinator); P. Van Iseghem (SCK/CEN)

A. OBJECTIVES AND SCOPE

The present project is the third part of a programme which started in 1981. This programme studies the performance of various simulated HLW-glasses in one of the reference repository environments, the Boom clay, with the aim to elucidate corrosion mechanisms in clay media and to propose a source term for the radionuclide release into the nearfield. The objective of the present project is to enlarge the already existing database by the use of corrosion accelerating test conditions (accelerated tests) and more complex media (integrated tests) and to model the long term interaction between glass and clay environment, which is the final goal of the project. In the accelerated tests, SA/V (glass surface area to solution volume) and temperature are used as the corrosion accelerating parameters. To obtain a high SA/V the glass is powdered. In the integrated tests glass corrosion is studied in the presence of canister/overpack corrosion products and backfill.

Two glasses are investigated: the Cogéma R7T7 reference borosilicate glass SON68, and the DWK/Pamela reference high Al_2O_3 borosilicate glass SM539

The SCK•CEN (Mol, Belgium) was appointed for the practical execution of the programme.

B. WORK PROGRAMME

B.1. Inactive accelerated tests: powdered samples of glasses SON68 and SM539 are exposed to distilled water (DW), synthetic interstitial claywater (SIC) and a mixture of 500 g Boom clay and 25 g Fe_2O_3 per liter synthetic interstitial claywater (called "CCSICM + CP"). The SA/V values are 500, 2500 and 10000 m^{-1}, the experimental temperatures are 40, 90 and 150°C. The maximum test duration is 720 days.

B.2. Active accelerated tests: grains of glasses SON68 and SM539 are exposed to the same media as sub (B.1.). The glasses were doped with either Pu/^{134}Cs/^{90}Sr or ^{237}Np/^{99}Tc/^{55}Fe/^{241}Am. The SA/V value is approximately 400 m^{-1}. The experimental temperature is 90°C. The maximum test duration is 360 days.

B.3. Inactive integrated tests: a first series of powdered samples of glasses SON68 and SM539 is exposed to a mixture of 250 g Ca-bentonite, 250 g Boom clay and 25 g Fe_2O_3 per liter synthetic interstitial claywater. A second series of powdered glasses

is exposed to a mixture of 397 g Boom clay, 21 g Cibelcor P40 cement and 21 g Fe_2O_3 per liter synthetic interstitial claywater. The SA/V values are 500 and 2500 m^{-1}. The experimental temperatures are 40, 90 and 150°C. The maximum test duration is 720 days.

B.4. Active integrated tests: grains of glasses SON68 and SM539 are exposed to a mixture of 250 g Ca-bentonite, 250 g Boom clay and 25 g Fe_2O_3 per liter synthetic interstitial claywater. The glasses are doped with the same radionuclides as for the active accelerated tests. SA/V, temperature and test durations are also the same as sub (B.2.).

B.5. Modelling of the dissolution behaviour of the glass matrices in the studied clay disposal surroundings.

B.6. Diffusion experiments to study the migration experiments of ^{32}Si labelled silicate in Boom clay: these experiments aim to provide values for the critical parameters, necessary to understand the diffusion behaviour of silicate in Boom clay. This part of the work programme was not foreseen in the original work programme.

Table I shows an overview of the 1991 - 1995 test programme.

Table I : Overview of the corrosion tests of the 1991-1995 programme

Test Conditions	Accelerated tests		Integrated tests	
	Inactive	Active	Inactive	Active
Temp (°C)	40 90 150	90	40 90 150	90
Media	DW SIC CCSICM+CP	SIC CCSICM+CP	BC+SIC+CP+BF1 BC+SIC+CP+BF2	BC+SIC+CP+BF1
SA/V (m^{-1})	500 2500 10000	400	500 2500	400
Duration (days)	20[1,2] 28[1,3] 90 180[1] 360 720[3]	90 180 360	20[1,2] 28[1,3] 90 180[1] 360 720[3]	90 180 360

DW : distilled water
SIC : synthetic interstitial claywater
CCSICM: concentrated clay - synthetic interstitial claywater mixture
BC : Boom clay
CP : corrosion product (Fe_2O_3)
BF1 : backfill bentonite
BF2 : backfill cement
(1) : not at 40°C
(2) : not at 90°C
(3) : not at 150°C

C. *PROGRESS OF WORK AND OBTAINED RESULTS*

State of advancement

C.1. In the course of 1994, the remaining tests have been finished and the chemical analyses of the leachants have been performed. The results have been interpreted. Most tests of 360 and 720 days in SIC and in CCSICM+CP at 90°C were however restarted in the course of the first semester, because of an unacceptable evaporation of water from the test containers.

C.2. For the tests with glasses doped with Pu, ^{134}Cs and ^{90}Sr (finished already in 1993), the radiochemical analyses have been completed with the measurement of a number of container walls. The results have been interpreted. The tests with glasses doped with ^{237}Np, ^{99}Tc, ^{241}Am and ^{55}Fe have been finished in 1994. Part of the results was available by the end of 1994. The results have not yet been interpreted. The SA/V ratio of 400 m^{-1} has been verified experimentally, and the procedures for the analysis of the clay have been qualified.

C.3. In the past year, the remaining tests have been finished. The results of the chemical analyses of the leachants have become available for nearly all tests. The available results have been interpreted. A selection of tests of 360 and 720 days at 90°C has been restarted in the course of the first semester, because of an unacceptable evaporation of water from the test containers.

C.4. see section C.2.

C.5. After a thorough literature review, we extended a model, proposed by Pescatore [1], for the dissolution of glass adjacent to clay, with a moving boundary between the glass and the clay. This model was solved analytically. We also developped a numerical code, based on a stochastic algorithm, to solve this and similar models. This stochastic code was also used for solving another model we proposed for describing the dissolution of glass in water. Apart from this, we are developping a completely new model to describe the dissolution of glass in water. This new model adds a time dependence on existing thermodynamic models, that describe glass dissolution.

C.6. Four flow-through diffusion tests with ^{32}Si have been started. By the end of 1994, they were still in progress. Partial results have become available.

Progress and results

C.1. The boron and lithium concentrations in the leachants have been plotted as a function of the scaling factors SA/V.t and $SA/V.t^{0.5}$ for the tests in DW and in SIC (SA is the surface area of the glass sample, V is the leachate volume, and t is the test duration). For the tests at 40°C, this had not been done before. For the tests at 90°C and at 150°C, the plots have been completed with the new data. The plots suggest

that the long term corrosion is diffusion controlled in some cases, but not always. In the other cases, glass is dissolving faster than following the diffusion kinetics. The results are summarized in Table II.

Table II: Corrosion rate determining mechanisms for the dissolution of glass SON68 and SM539 in the various media (diff.cont. = diffusion controlled dissolution)

Glass type	Test temperature	DW	SIC	CCSICM+CP
SON68	40°C 90°C 150°C	? diff.cont. no diff.cont. (?)	no diff.cont. no diff.cont. diff.cont.	no diff.cont. (?) ? no diff.cont.
SM539	40°C 90°C 150°C	no diff.cont. diff.cont. diff.cont. (temp.)	no diff.cont. diff.cont. diff.cont. (temp.)	no diff.cont. ? no diff.cont.

The indication "?" means that the results were not or little conclusive; "temp." means that the observed mechanism was temporary.

C.2. The retention factors (this is the sample mass loss, divided by the normalised radionuclide loss) found for glasses SM539 and SON68 in CCSICM at 100 m^{-1} (previous test programme) are roughly confirmed at higher SA/V in CCSICM+CP. For glass SM539, the retention factor in the present programme is about 4 to 5 for Pu, 1 to 3 for Cs and between 1 and 2 for Sr. For glass SON68, the retention factor is about 10 for Pu, about 1.5 for Cs and between 0.5 and 2 for Sr.

C.3. The recent results confirm some trends that were observed previously in the bentonite mixture. In general the solution pH is lower for the mixture of bentonite and Boom clay than for the mixture with only Boom clay (CCSICM+CP). The results give contradictory information about the influence of the bentonite on the glass dissolution. The influence appears to depend on the corrosion indicator that is used (sample mass loss, boron-, lithium- or molybdenum concentration of the leachant), and on the test temperature. There are indications that the corrosion rate is not limited by any diffusion barrier in the bentonite mixture. In the presence of cement, the corrosion indicators suggest in most cases that the investigated glasses are less dissolved than in the bentonite mixture or in the Boom clay mixture. The retarding effect is probably temporary.

C.4. The conclusions in the previous annual report are confirmed:
The Pu concentration in solution tends to be smaller than when no bentonite is present (CCSICM+CP) until 180 days, but the difference is small after 360 days, as a result of a strong increase of the Pu concentration in the bentonite containing

mixture. The Am concentrations in solution and the ratio of the mobile leached Am over the total leached Am are lower in the bentonite mixture than in CCSICM+CP. This may be an indication for a higher sorption capacity of the bentonite mixture for Am. The total released activities are not much influenced by the addition of bentonite.

C.5. We added a moving boundary to a model of Pescatore [1], describing the dissolution of glass adjacent to clay. This model was solved analytically but also by means of a newly developped numerical code. Both the analytical solution and the numerically obtained solution coincide very well. This proves the validity of the code. The code is sufficiently general, to use it also for other diffusion problems. Numerical research shows that the amount of dissolved silica is not very sensitive to the parameter describing the movement of the boundary. Since the difference between the Pescatore model and our model is the introduction of this parameter, we did not fit the experimental data again. Other physical quantities (like for instance the position of the boundary) depend strongly on this new parameter, but were not determined experimentally. We used our code to solve a new model to describe the dissolution of glass in water. This model is very similar to the Grambow model [2]. The main difference is that we obtain an exact solution of the diffusion equation, while Grambow uses only an approximate solution (he assumes that the concentration profile of silica in the gel layer is linear). The model still has to be applied to real glasses.
We also started developping a completely new model describing the dissolution of glass in water. This new model is based on an existing thermodynamic model for the dissolution of glass. At the present, thermodynamic models are not capable of modelling the time dependence of the dissolution process. Our new model adds time dependence to a thermodynamic model. The capabilities of this new model exceed those of existing models. For instance, the new model can be used to predict local elemental concentrations in the glass reaction layer (e.g. silicon). Our new model is also capable of modelling the dependence of the dissolution rate on the composition of the glass. First results reproduce the experimental results rather well.

C.6. Against all theoretical expectations, a slight silica sorption is observed on the Boom clay. An average ηR value of 14.4 ± 4.3 is estimated from a first fitting of presently available experimental data. The mean resulting retardation factor (R) is 36.1 ± 10.8, which corresponds to a distribution coefficient K_d of 8.3 ± 2.5 (ml/g). The monomeric silica species (*i.e.*, neutral $Si(OH)_4$ or anionic $SiO(OH)_3^-$) present in the interstitial water at *in situ* pH (8-10) should in principle not be sorbed onto the negatively charged surface of clay. The total dissolved silica concentration measured in the Boom clay is $2\ 10^{-4}$ M (silica solubility controlled by chalcedony, log S = -3.71). This concentration is too low to have a significant silica polymerization. However, the silicate anion may form complexes with aluminium hydroxide groups present on the clay minerals surface, favoring its sorption. The sorption mechanism could be due to the ligand exchange between a silicate anion and an OH^- bound to an Al^{3+}. Silica may sorb by forming a hydroxy-aluminosilicate

(HAS) complex onto the surface of clay minerals. Kaolinite [$Al_2Si_2O_5(OH)_4$] is the mineral phase controlling the aluminium solubility in the Boom clay. So it is one of the best candidates, along with the free Al-OH groups of the clay minerals frayed edges to explain the silica sorption onto the Boom clay.

References

[1] C. Pescatore. The dependence of waste form leaching on migration parameters in the host medium, accepted for publication in Radiochimica Acta.

[2] B. Grambow. Nuclear waste glass dissolution: mechanisms, model and application. Report to the JSS project 87-02, phase IV, edited by SKB (Sweden).

Title :	Basic Leaching Tests for Pure Beta Long-lived Emitters in Radioactive Wastes
Contractor:	CEA Cadarache
Contract N°:	FI2W-CT90-0032
Duration of contract:	1 May 1991 - 30 April 1995
Period covered:	
Project leader:	C. Riglet (CEA Cadarache)

A. OBJECTIVES AND SCOPE

The technical solution under study to store long-lived radioactive wastes consists in:
- embedding the wastes in suitable confining matrixes (glass, cement, bitumen);
- and burying the coats in stable geological sites in which the radioactivity will decrease naturally.

The evaluation of the confining capability of the matrixes used - determined by implementing leaching tests - will enable us to assess the reliability of the process. Safety studies indicate that the long-term risk mainly stems from long-lived radionuclides.

In this context, the research contract is related to a basic leaching study of pure ß and α long-lived emitters in real and simulated wastes, in order to collect basic information about these radionuclides which are critical for the safety analysis of disposal. No reliable data are available at present for these species.

B. WORK PROGRAMME

B.1. (CEA - CIEMAT)
- Working organization
- Setting-up of a working programme
- Harmonization of the leaching procedures

B.2. (CEA)
- Definition and manufacturing of the samples
- Implementation of the leaching experiments
- Collection of the data and interpretation

B.3. (CIEMAT)
- Selection of the types of wastes, the cement formulae and of the elements to be taken into account
- Implementation of the leaching experiments with simulated wastes
- Optimization of the analytical procedures
- Collection of the data and interpretation

B.4. (CIEMAT)
- Implementation of the leaching experiments with real resins
- Collection of the data and interpretation

B.5. (CEA - CIEMAT)
- Interpretation of the data
- Comparative study of the various experiments
- Final evaluation

C. PROGRESS OF WORK AND RESULTS OBTAINED

Status of progress has not been forwarded to the Commission for 1994.

Title	Chemistry of the Reaction of Fabricated and High Burnup Spent UO_2 Fuel with Saline Brines
Contractors	Forschungszentrum Karlsruhe GmbH - INE; ENRESA - Dep. Ingenieria; UPC
Contract N°	FI2W-CT90-0055
Duration of contract	May 1991 - February 1995
Period covered	January - December 1994
Project leader	B. Grambow (INE, coordinator); A.Loida, N. Müller, H. Geckeis (INE); J. Cago (ENRESA); I. Casas, J. de Pablo, J. Giménez, M.E. Torrero (UPC)

A. Objectives and Scope

The research program aims at characterization and qualification of the chemical durability of unprocessed high burnup UO_2 fuel as a barrier against radionuclide release for disposal sites in salt formations. The reaction behavior of the fuel with saline brines is going to be studied as a function of time, temperature, redox potential, and surface area in order to give insight into the corrosion mechanisms and sources of radionuclide release. Additionally, the solubility of unirradiated UO_2 in salt brines is studied for comparison with the reaction behavior of the irradiated material in order to identify radiolysis and burnup effects and in particular to identify and quantify solubility effects in the degradation of the fuel matrix. Eventually, the ongoing work will provide a basis for modeling, bridging over the gap between experimental results and performance assessment for long-term storage of the fuel in a repository in salt formations in case of brine intrusion.

B. Work Program

I. General preparations, analytical techniques, and sample preparations

II. Characterization of the durability of spent UO_2-fuel in saturated NaCl brines

III. Solubility tests with unirradiated UO_2

IV. Modeling of the reaction behavior of spent fuel with salt brines

C. PROGRESS OF WORK AND OBTAINED RESULTS

State of advancement

High burnup spent fuel samples (single mm-sized fragments, cm-sized pellets, µm-sized powders) were corroded in non buffered NaCl solutions (initial pH ca. 7) under Ar-atmosphere, in some cases in the presence of metallic iron powder (effect of the corroding canister) under static conditions. The accumulated corrosion time has reached now about 750±5 days (tests with powders 657 days, test at 150°C: 173 d), and tests were terminated. At the end of the tests, fission and radiolysis gases, leachates and container surfaces were analyzed.

Dissolution (solubility) tests with unirradiated UO_2 in different salt brines have been carried out at various redox potentials, with and without iron or simulated radiolysis products being present.

Progress and results

I. Characterization of the durability of spent UO_2-fuel in saturated NaCl brines

Corrosion tests comprise (1) "washing" steps, where the Cs gap inventory should be removed by exposing the fuel to the leachant (95% saturated NaCl or deionized water) under Ar atmosphere for two periods of one month and afterwards replacing the total solution volume by fresh leachant. Subsequently (2) static corrosion of the fuel samples is initiated. Aliquots of the solution are sampled periodically under Ar atmosphere.

II. 1. A Radionuclide release into the aqueous phase.

The results from dissolution of spent fuel fragment F 3, pellet K 10 and powder P 1 in 95% saturated NaCl solutions are given in Fig. 1, expressed as fraction of inventories in the aqueous phase (FIAP). The cumulative Cs releases ("gap release") from pellet sized fuel/cladding segments and from individual fragments are similar (about 2-3% of the total inventory). With powdered fuel, all grain boundaries are expected to be exposed to the solution and the major Cs release occurs within few minutes of ultrasonic cleaning. Cumulative release is about 3.5% of the inventory, of which at maximum 1.5% (=3.5% - 2% gap inventory) may be attributed to release from grain boundaries. The released quantities of matrix bound radionuclides Sb125, Eu154, Am241, Pu239/240, Sr90, Ru106 and Ce144 are in most cases between $3*10^{-4}$ and $3*10^{-6}$. Release of Sr90, Tc99, Np237 and Sb125 occurred with their inventory ratios, hence, release of these nuclides is controlled by the degradation (oxidation, dissolution) of the fuel matrix. Even at low reaction progress in the absence of saturation (solubility) effects, (experiments with single mm sized fragments in large solution volumes) the solution concentrations of U, Pu, Am, and REE were significantly lower than anticipated from the extent of fuel matrix dissolution.

Results from analyzing ultrafiltered and microfiltered solution samples were the same for Ag, Sr, Sb, and Cs and differ slightly for actinides, Ru and rare earth elements probably resulting from colloid formation. Colloid formation was not enhanced in the presence of fuel powder or of iron. The highest solution concentrations of various radionuclides were observed in the tests with fuel powders (Sr 10^{-6} m, Pu 10^{-7} m, Am 10^{-7} m, Np 10^{-8} m, Tc 10^{-7} m). In general, concentrations are controlled by of inventories and by a combination of sorption, precipitation and coprecipitation phenomena.

The effect of temperature is shown in Fig. 2, where results from tests at room temperature (pellet K 10) are plotted together with data from a test (pellet K 13) carried under out at 150°C. At 150°C the release of Cs and Sr was found to be rather similar to the tests at room. Pu release fractions decreased with time at both temperatures, at 150°C, however this decrease was observed earlier. The temperature independent reaction behavior shows that the rate limiting step in spent fuel dissolution mechanism is not a thermally activated process.

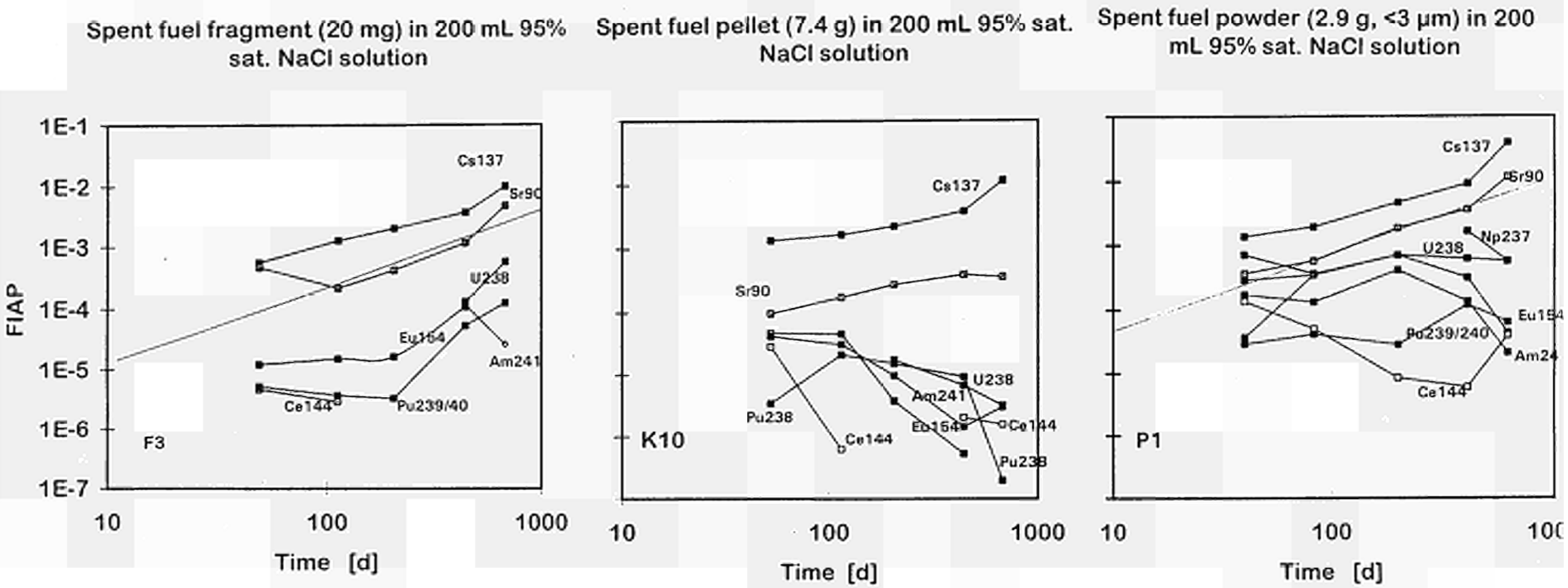

Fig. 1: Fraction of inventories of various radionuclides in the aqueous phase (FIAP), obtained after exposure of spent fuel samples for 750±5, respectively 649 days to 200 mL 95% saturated NaCl solution. Note: Samples were washed twice in the leachant for periods of 1 month each. Data from wash solutions are not included in the Figures (see annual report 1992). F 3: Spent fuel fragment (20 mg), K10: Spent fuel pellet (7.4 g), zircalloy cladding remained attached, P 1: Spent fuel powder (2.9g, particle size < 3µm), zicralloy cladding was added.

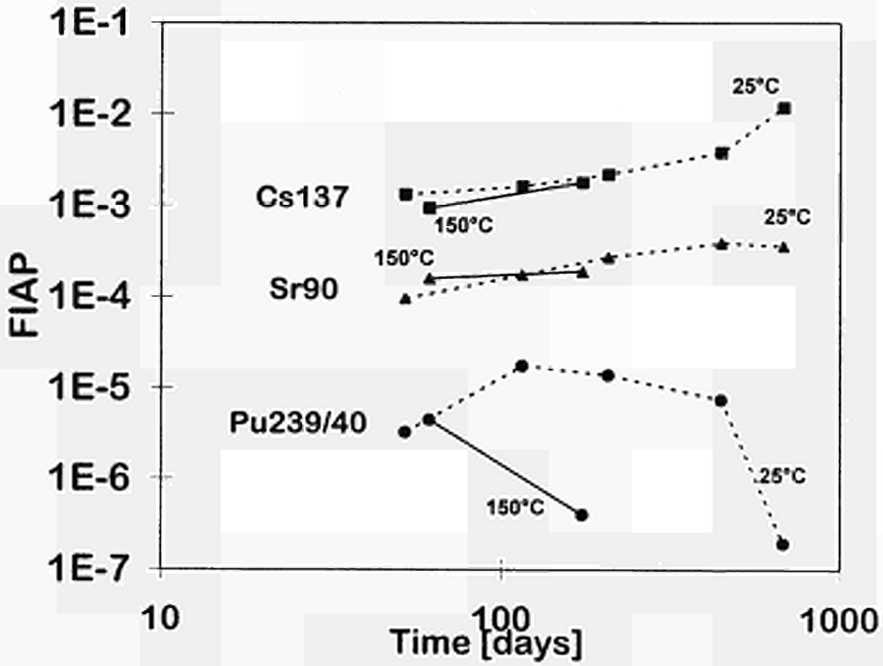

Fig. 2: Release of Cs137, Sr90 and Pu239/40 in the dissolution process of the fuel pellet K 10 (7 g) in 200 mL 95% saturated NaCl solution at room temperature in comparison with results from corrosion of fuel pellet K 13 at 150°C. Fraction of inventories of various radionuclides in the aqueous phase (FIAP)

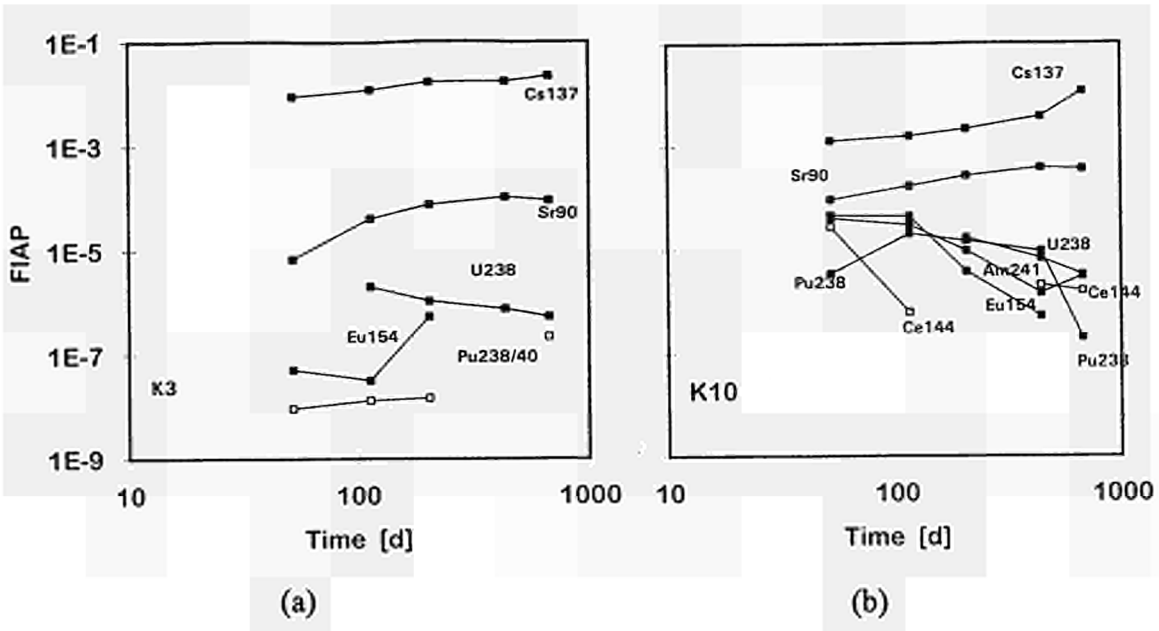

Fig. 3: Effect of the presence of iron (8.5 g powder, grain size < 10 µm) on the dissolution process of a fuel pellet K 3 (7 g) in 200 mL 95% saturated NaCl solution (a) in comparison with results from corrosion of fuel pellet K 10 without the addition of iron(b). Fraction of inventories of various radionuclides in the aqueous phase (FIAP)

Release of radionuclides from corrosion of the spent fuel pellet K 3, in the presence of 8,5 g metallic iron is shown together with data from pellet K 10 without iron in Fig 3 a,b. The presence of iron effectively reduces the solution concentration of all radionuclides, except of Cs and fission gases (see II.2). The decrease in radionuclide mobility may indicate increased stability of the fuel matrix at the lower redox potential. However, low concentration of other fission products and of actinides may alternatively be a result of sorption on iron. More work is necessary, before the effect of iron can be understood.

II. 1. B Sorption of radionuclides at container wall.

Sorption of radionuclides at the container wall (Ti) was analyzed by acid stripping the container after short ultrasonic cleaning in deionized water. Both deionized water and acid strip solution were analyzed. Table I shows the percentages of the radionuclide inventory of the altered fuel mass (calculated from Sr90 release to solution and vessel) which are sorbed on the reaction vessel, in solution and on the fuel sample. Only small quantities of radionuclides are sorbed on the container wall and a significant amount in particular of tri-tetra- and hexavalent actinides remain on the fuel sample.

Table I: Percentages at test termination of radionuclide inventories of the altered fuel masses (Sr90 based) sorbed on the reaction vessel (Ti), in solution and on the fuel sample or the cladding (experiments with pellets). Radionuclide fraction remaining on sample deduced from solution and vessel analyses. (* Sr and Cs data on sample are not deducible as Cs release is larger than Cs inventory of altered fuel mass and altered fuel mass value is based on Sr data)

leachant	DI-water			NaCl solution		
pH	7			9		
	vessel	solution	sample	vessel	solution	sample
Cs137	0.02	99.98	0.0*	0.02	99.98	0.0*
Sr90	6.3	93.7	0.0*	13.5	86.5	0.0*
Pu238/239/240	4.7	0.2	95.1	7.0	1.8	91.2
Am241	11.1	0.4	88.5	5.4	0.3	94.3
Cm244	5.2	0.2	94.6	15	0.15	84.9
U238	3.7	0.1	96.2	6.1	1.5	92.4

II. 2 Radiolysis and reaction rates

Specific formation rates of radiolysis gases are given in Table II, together with fuel alteration rates calculated from Sr release. Most autoclaves were extremely tight as indicated by the quantity of less than 0.2 vol% of N_2 after about 200 days of testing. However, autoclaves with fuel powder were not tight: about 10 to 50% of the atmosphere has been exchanged with air. In these tests oxygen production cannot be analyzed and only lower limits of hydrogen generation may be estimated from the analyzed H_2 content of the remaining atmosphere.

The formation of the radiolysis gases, oxygen and hydrogen, was observed, in quantities proportional to the spent fuel sample mass. Even with powdered fuel (grain size about 3 μm) gas generation is not enhanced, despite α-radiation contributes much more to radiolysis (escape depth in fuel about 5 μm). We conclude that the radiolysis gases are produced by γ- and not by α-radiation. In the presence of iron, only traces of oxygen were observed in the gas phase, indicating that oxygen uptake by iron corrosion effectively removes oxygen formed by radiolysis.

The data in Table II show that fuel dissolution rates are of similar order of magnitude than the rates of radiolysis gas production. This similarity may indicate control of dissolution kinetics by radiolytical production of oxidants, i.e. the rate of formation of the total amount of oxidative radiolytic species may become equal to their consumption rate by fuel oxidation/dissolution. Limitation in the production of oxidative species may explain the observed decrease in surface area normalized reaction rates with increasing S/V ratio: In first approximation (γ-dose is higher than α-dose!) the generation rates of radiolysis products depend only on fuel mass (H_2 production rates are similar for fuel powder and fuel pellets in the same solution, see Table II) but the consumption rate by oxidation/dissolution depends on surface area. For fuel pellets in NaCl solutions, the generation rate of oxidative radiolytic species appears to remain faster than the rate of their consumption by oxidative fuel dissolution (Table II), whereas, by using fine grained fuel powder, the high sample surface area leads to much faster consumption of oxidative radiolysis products and fuel corrosion rates approaches the estimated H_2 gas generation rates. For scale up of experimental observations to relevant geometric disposal configurations, the interdependency of S/V, head space in the autoclaves and radiolysis effects must be considered.

Table II: Specific generation rates of radiolysis gases during spent fuel dissolution (ca. 200 mL solution, 250 mL head space) and comparison with corresponding Sr90 based spent fuel alteration rates. HM = heavy metal, DIW = deionized water, NaCl = 95% sat. NaCl solution, Fe = iron powder added. ? = air influx. In the presence of Fe, hydrogen generation rates mainly reflect iron corrosion rates.

sample	medium	sample mass [g_{HM}]	test duration [d]	gas sample interval [d]	gas generation rate [mol/(g_{HM}.d)] H_2	O_2	fuel alteration [$mol_{UO2}/(g_{HM}d)$]
pellet K1	DIW	6.45	412	213	1.4e-7	9.4e-8	3.8e-8
pellet K1	DIW	6.45	650	220	5.4e-8	5.6e-8	3.8e-8
pellet K2	DIW	6.35	412	213	1.8e-7	1.1e-7	4.7e-8
pellet K10	NaCl	6.49	389	183	2.2e-7	8.8e-8	1.3e-8
pellet K10	NaCl	6.49	650	220	1.6e-7	8.4e-8	1.3e-8
pellet K9	NaCl	6.49	389	183	2.0e-7	8.0e-8	1.3e-8
powder P1	NaCl	2.5	414	213	2.7e-7	<1.5e-7	8.8e-8
powder P1	NaCl	2.5	650	220	3.0e-7	?	8.8e-8
powder P2	NaCl	2.5	414	213	2.1e-7	?	2.8e-7
pellet K3	NaCl/Fe	6.19	345	139	8.0e-7	<1e-8	3.6e-9
pellet K3	NaCl/Fe	6.19	650	220	1.5e-6	5.3e-10	3.6e-9
pellet K4	NaCl/Fe	6.0	267	60	8.4e-7	<1e-7	2.7e-9

II.3 Behavior of potentially solubility limited radionuclides

In order to rationalize solubility effects, the solution concentrations of radioelements, such as Pu and Am may be compared with the solubility of potentially precipitating phases. Fig. 4 a shows the Pu concentrations encountered in spent fuel dissolution tests in NaCl solutions as a function of pH together with certain curves calculated for certain bounding cases. Pu-concentrations decrease with pH. Hypothetical maximum concentrations of Pu were calculated from the extend of matrix dissolution, using Sr data as reference and assuming that Pu is dissolved congruently without being involved in secondary reactions such as sorption, resorption, precipitation or coprecipitation. Measured solution concentrations remain about a factor 100 lower than these values, clearly indicating that initially dissolved Pu is removed from solution by secondary reactions. As discussed above, sorption on the Ti-liner or on the sample itself is a possible explanation of low Pu concentrations.

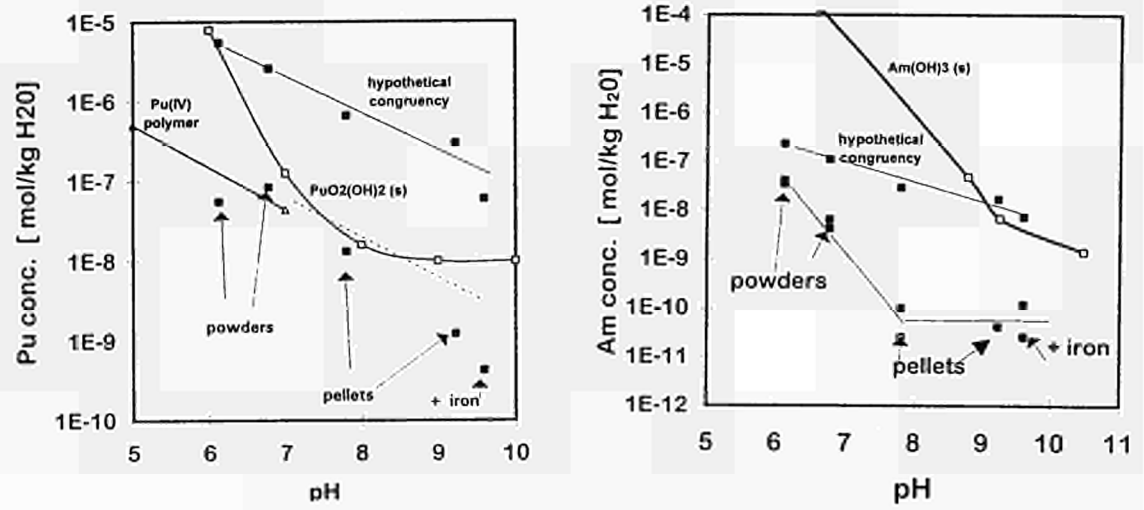

Fig 4: (a) Pu concentrations observed in spent fuel dissolution tests in NaCl solutions as a function of pH. Comparison with congruent dissolution hypothesis, with calculated solubility of $PuO_2(OH)_2$ and with solubility of Pu(IV)polymer. (b) Am concentrations in static spent fuel dissolution tests in NaCl solutions as a function of pH, compared with congruent dissolution hypothesis and with the solubility of $Am(OH)_3$

Measured Am and Eu concentrations are shown in Fig.4 b. Eu and Am concentrations are allways similar. Hypothetical maximum solution concentrations of Am were calculated (included in Fig. 4 b) with the assumption of congruent fuel matrix dissolution (using Sr as an indicator) by neglecting all secondary reactions which remove Am from solution (sorption, precipitation formation of secondary phases, etc.). Measured solution concentrations are orders of magnitude below this maximum values, indicating that Am is effectively removed from solution. One of the reasons for this observation is the possible formation of solid solutions by coprecipitation. The content of other trivalent cations in spent fuel (Nd, La, Pr, Sm..) is about 25 times higher than that of Am or Eu. It is rather unlikely that individual $Am(OH)_3$ phases will form. Instead, one expects the formation of solid solutions of the general type $(REE;AN)(OH)_3$.

III. Solubility tests with unirradiated UO_2

In these experiments, unirradiated crystalline UO_2, is axposed to aqueous solutions. Most experiments have been carried out using 1 mm as particle size. However, fine powder and pellets were also used.

The specific surface areas of the solids were determined by the BET method, using a mixture of 0.1% krypton by volume in helium as adsorbate. Values for each solid were: pellet (0.000192 m^2g^{-1}); 1 mm particle size (0.0016 m^2g^{-1}) and fine powder less than 10 μm (0.27 m^2g^{-1}).

In all the experiments, we determined the uranium concentration by the SCINTREX laser fluorescence technique [Robbins 1979] according to a method previously developed [de Pablo et al 1992] to avoid chloride and magnesium interferences.

III.1 Influence of the redox conditions

Reducing conditions were obtained by using a hydrogen flux and a palladium catalyst. Oxidizing conditions were achieved with a mixture of O_2 and N_2, with an oxygen partial pressure of 0.21 atm. The redox potential was measured by means of a platinum wire electrode. In figure 5, the total uranium concentration in solution under reducing conditions for both brines has been plotted as a function of contact time.

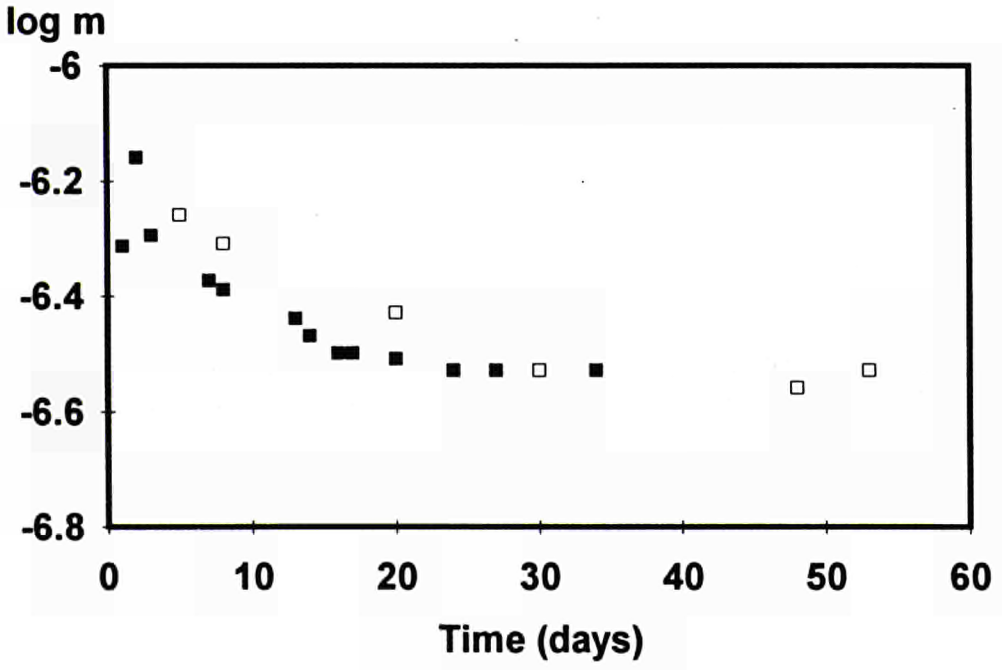

Figure 5. Dissolution of UO_2 under reducing conditions. ■ in NaCl-brine ; □ in $MgCl_2$-brine.

After this initial dissolution, the uranium concentration decreases down to a constant value which only shows slight differences depending on the brine. In the NaCl-brine, the uranium conc. is 2.8 10^{-7}molkg^{-1} and in the $MgCl_2$-brine is 3.1 10^{-7} mol kg^{-1}. These constant values seem to indicate that the uranium concentration is controlled by the solubility of a solid phase. At redox potentials (E_h) of 0 to 60 mV measured we can assume that the stable solid phase is UO_2 [Grenthe et al 1992].

For oxidizing conditions, the corresponding results are shown in figure 6. In $MgCl_2$-brine uranium concentration continues to slowly increases throughout the experiment (100 days) which indicates that the kinetics of dissolution control this concentration. In NaCl-brine, after 10 days, uranium concentrations remain constant, this result points to the possibility that this concentration would correspond to the solubility of a secondary solid phase. XPS results have shown that the solid put in contact with the $MgCl_2$-brine had a final composition of $UO_{2.1}$ while the one put in contact with the NaCl-brine brine had a final composition of $UO_{2.4}$. In NaCl-brine, the solid surface is more oxidized probably due to the precipitation of a U(VI)-solid phase.

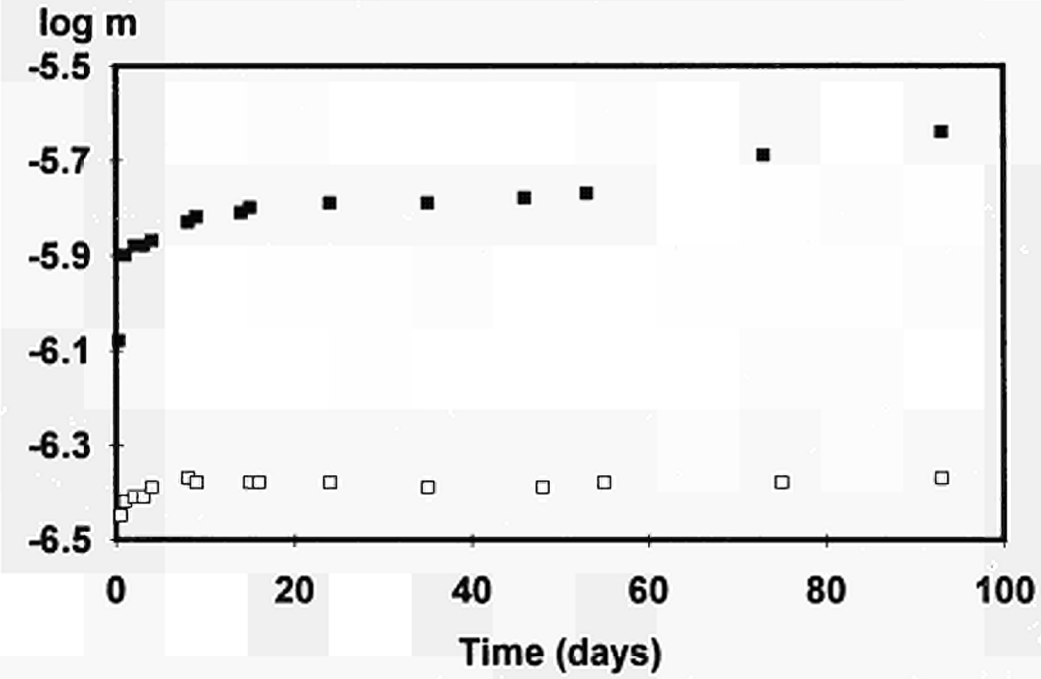

Figure 6. Uranium concentration (molality) vs time under oxidizing conditions (21% O_2/N_2). ■ in $MgCl_2$-brine ; □ in NaCl-brine.

III.2 Influence of oxidants: H_2O_2 and ClO^-

Dissolution rates of UO_2 in 95% saturated NaCl solution in the presence of various concentrations of H_2O_2 and ClO^- were determined. Comparison of results in presence of H_2O_2 with rate data given in the literature (see figure 7) show good agreement, despite the much lower ionic strenght used in the literature data.

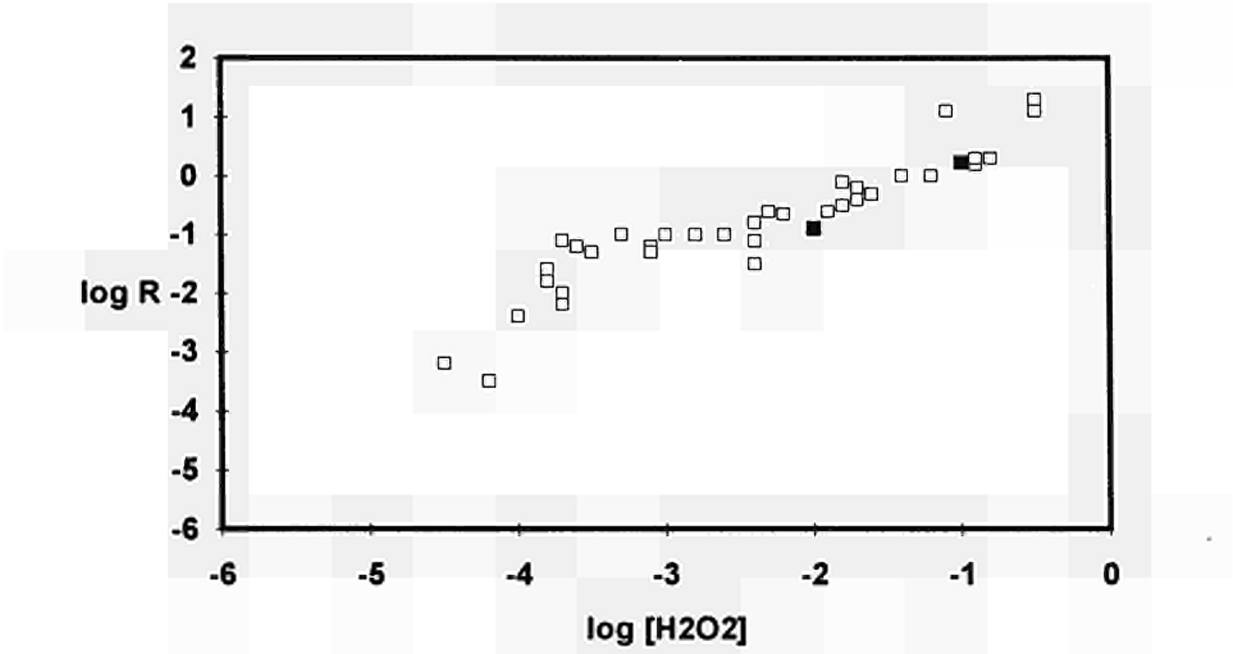

Figure 7: Dissolution rate ($\mu g\ d^{-1}\ cm^{-2}$) versus H_2O_2 concentration. ■ this work; □ from reference [Shoesmith and Sunder 1992].

Dissolution rates as a function of the concentration of various oxidants are shown in Figure 8 The same general behavior can be observed independent on the oxidant considered. A slope equal to 1 can be assumed, as it is shown in figure 8. Therefore, the following general relationship can be written:

$$\log r = \log k + \log [ox.]$$

this equation (with a slope = 1) seems to indicate that the oxidation of the UO_2 (s) is the slowest step of the overall process which would include the oxidation and the dissolution.

II. 3. Influence of Iron

Two experiments were carried out, as leachant we used 95% NaCl and nitrogen was continuously bubbling through the experimental vessel. The particle size of the solid was 1 mm and the UO_2 weight and pH in both vessels were the same. In one vessel, we introduced 9 g of iron (particle size less than 10 μm), this experiment is identified in text as F2 and the experiment without iron as F1. Uranium concentrations were $\approx 4\ 10^{-8}$ mol/L in both experiments. This value is similar to that obtained bubbling hydrogen and using a Pd catalyst [Torrero et al 1991]. This fact indicates that anoxic conditions (N_2) and reducing conditions (H_2 or Fe) are enough in this kind of experiments to avoid the oxidation of the solid. All these experiments can be explained taking into account the UO_2 solubility.

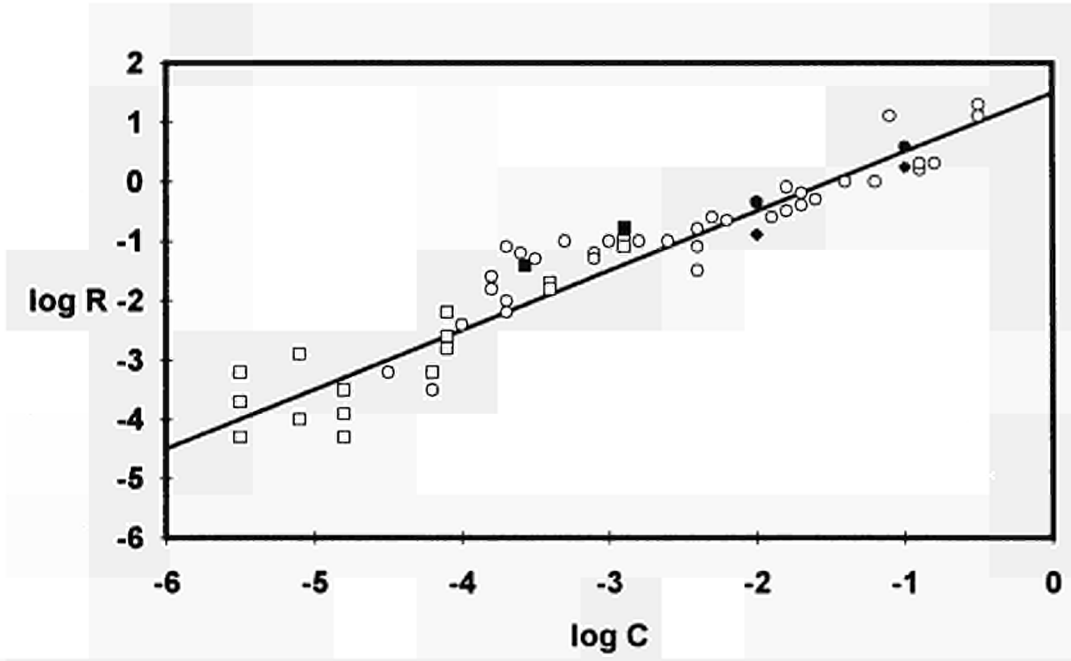

Figure 8: Dissolution rates as a function of oxidant concentration. ● ClO^- (this work); ◆ H_2O_2 (this work); ■ O_2 (Annual Report 1992); ○ H_2O_2 (Shoesmith and Sunder 1992) and □ O_2 (Shoesmith and Sunder 1992).

II.4 CONCLUSIONS

1.- Under reducing conditions, the uranium concentration behavior is independent on the brine composition and is probably controlled by UO_2 solubility at these conditions.
2.- Under oxidizing conditions, different initial dissolution rates are obtained in both brines due to their different pH. A second dissolution rate is obtained in Q-brine but not in the NaCl-brine possibly due to the precipitation of a secondary solid phase in this brine.
3.- The initial dissolution rate increases proportionally to the concentration of oxidants in solution following this equation:

$$R = k\,[\text{Oxidant}]$$

The initial dissolution rate does not depend on the S/V ratio used in this study. Results in diluted solutions are similar to those obtained in this work.
4.- The presence of iron reduces the redox potential of the solution and the results are similar to the ones obtained in nitrogen and/or hydrogen. No adsorption of uranium into the Fe powder has been observed.

REFERENCES

Casas I., J. Giménez, V. Martí, M.E. Torrero and J. de Pablo, Radiochim. Acta 66/67 (1994) 23
de Pablo J., L. Duro, J. Giménez, J. Havel, M.E. Torrero and I. Casas, Anal. Chim. Acta 264 (1992) 115
Grambow B., A. Loida, P. Dressler, N. Müller, R. Reger, B. Schweigel, J.A. Gago, I. Casas, J. de Pablo, J. Giménez and M.E. Torrero, Contract FI2W0055, Annual Report 1992
Grambow B., A. Loida, P. Dressler, H. Geckeis, P. Diaz, J.A. Gago, I. Casas, J. de Pablo, J. Giménez and M.E. Torrero, Contract FI2W0055 Annual Report 1993
Grenthe I., J. Fuger, R. Konings, R. Lemire, A. Muller, C. Nguyen-Trung and H. Wanner, *Chemical Thermodynamics of Uranium*, (Wanner and Forest Eds.) OECD/NEA 1992
Robbins J.C, Can. Inst. Min. Mat. Bull. 5/61 (1978) 2
Shoesmith D. and S. Sunder, J. Nucl. Mater. 190 (1992) 20
Torrero M.E., I. Casas, M. Aguilar, J. de Pablo, J. Giménez and J. Bruno, Mat. Res. Soc. Symp. Proc. 212 (1991) 229

Title :	Container properties ensuring safety :gas emission, biodegradation, corrosion.
Contractor :	DCC/Dir CEA Saclay
Co-contractor :	AEA Technology Harwell
Contract N°:	FI2W-CT91-0077
Contract duration :	October 1991 - October 1994
Period covered :	January 1994 -December 1994
Project Leader :	P. LESSART/ DESD/SEP/SEATN CEA Cadarache

A. OBJECTIVES AND SCOPE

The knowledge of possible evolution of conditioned waste during intermediate storage, handling and deep repository is necessary to warrant the safety of workers and to define the conditions for storage and disposal.

These conditions can depend on production of gases and of chemical compounds able to promote degradation or biodeterioration phenomena.

The origin of gas production can be :

- the waste itself, producing radon and gases from alpha and gamma radiolysis,
- the chemical or micro biological corrosion of embedding matrix and structural material,
- the radiolysis of organic compounds included in the waste.

Living micro-organisms can also produce complexing agents and organic or inorganic acids able to promote corrosion and to modify the oxydo-reduction conditions and the pH of the repository.

A part of this project is concerned with assessing the effects of alkali tolerant micro-organisms on a cement based matrix.

B. WORK PROGRAMME

Four laboratories are collaborating for this contract, one of them being from AEA Technology Harwell and the others from DSD CEA Cadarache.

Programme 01 : biocorrosion of cement and bitumen used as embedding matrix. Acid and gas production. Physico-chemical modifications of the material.

Programme 02 : gas production by an genuine concrete conditioned waste with high content of radon producers.

Programme 03 : effects of organic complexing agents in concrete and bitumen conditioned wastes on the gamma radiolysis gas production .

Programme 04 : the aim is to determine the form in which the microbial cells attach to the alkaline surface and the extend to which this change the physical and chemical properties of the cement. This will provide data to assist in setting design criteria for cement based materials used to condition the pore water chemistry in a radwaste repository.

C. PROGRESS WORK AND OBTAINED RESULTS

Programme 01 Biocorrosion of cement and bitumen. Acid and gas production.

M.F. LIBERT: DESD/SEP/SEATN CEA Cadarache FRANCE

As a conclusion of a bibliographical study, micro-organisms exist in a deep repository before man intrusion, and, furthermore, after intrusion. All the elements necessary for microbial life exist in a nuclear waste repository. During repository evolving after setting-up and sealing, oxygen concentration decreases and even if at the beginning only aerobic microbes may develop modifying the physico-chemical characteristics of the repository, after a long term, anaerobic conditions become probable.

Programme 01 a : Biocorrosion of bitumen

The aim of this work is the study of gas production in anaerobic conditions by microorganisms able to growth in the environment of a deep repository.
Bitumen is a complex mixture of different heavy hydrocarbons that can be susceptible of biodeterioration because of its organic content.
In the absence of oxygen, degradation of organic matter can be achieved by microorganisms using nitrates or sulfates as electron acceptor instead of oxygen
Samples of soils polluted by hydrocarbons were used for enrichment of natural anaerobic microbial strains. Medium used contains sulfate or nitrate depending on the metabolism of the bacteria we are looking for.
The only carbon source added in the medium is bitumen as a powder in order to obtain a large accessible surface of substrate material.
The bacteria obtained under these conditions will be then studied as quantitative gas production
Due to the presence of nitrates in bitumen embedded wastes (about 60 mg/g of bitumen for a STE 3 type bitumen enbedded waste), in a first step, we have choosen, a denitrifying bacteria known in our laboratory, *Pseudomonas aeruginosa.* This bacteria is able to reduce nitrates completely to gaseous products (the process is called denitrification) at the expense of organic matter such as bitumen.
Bacteria able to reduce sulfates as electron acceptor in presence of bitumen or embedded wastes bitumen, are now under experimentation.

Programme 01b: Biocorrosion of cement

The aim of this work is to study the cement deterioration induced by mineral or organic acids produced by alkali tolerant micro-organisms. In France, concretes planned to be used as embedding matrices are based on CPA 45 and CLC 55 cement.
The main point to notice is that each cement sample in presence of fungi (producing organic acids) exhibit a high amount of leached calcium (or Al, or Si) to compare to the same cements in presence of *Thiobacillus* (producing inorganic acids, H_2SO_4)

For example : CPA + fungi = 60% of leached Ca
CPA + *Thiobacillus* = 7% of leached Ca

Our hypothesis is:
- in the case of *Thiobacillus* the formation of ettringite or gypse at the external surface of the cement prevent any leaching of the chemical elements.
- in the case of fungi: organic acids have complexing properties of elements such as Ca, leading to a continuous leaching of these elements.
We have to confirm these informations with the chemical analysis of the cement and X rays diffractions.

Programme 02 : Actual waste packages: Gas emission

J. PERFETTINI, D. GREC, F. ROUQUETTE:
DESD/SESD/SEC . CEA Cadarache FRANCE

Among the different kinds of radioactive waste packages likely to be stored, there are the drums containing radium-bearing waste, the natural evolution of wich goes with the emission of gases. These gases are volatile radionuclides, such as radon, or non radioactive gases, induced by the radiolysis of the water or other materials present in the drum. The aim of this study is to make a qualitative and quantitative evaluation of these gases. This requires the knowledge of the chemical and radioactive composition of the waste, and specific analytical methods.

The selected radwaste drum has been submitted to accurate non-destructive tests for its characterization: radiography and tomography for determining the waste density and heterogeneity: γ spectrometry for the radiochemical determination. The radiography and tomography allowed the sedimentation of the solid phase to be proven with an accumulation of a liquid phase (its volumic mass is about 1.0 $g.cm^{-3}$) in the top of the waste, which can generate radiolytic gases.

The γ spectrometry shown the presence of ^{226}Ra, ^{208}Tl and ^{228}Ra in the waste. ^{226}Ra and ^{228}Ra are the precursors of two radon isotopes: ^{222}Rn and ^{220}Rn that can be released in the gaseous phase;

The device necessary for the study of the radon release has been manufactured. It consists of a container made of stainless steel and gas tight (in wich the waste drum is put), and a set of pipes, valves and connectors that allow the container to be coupled with a sampling capacity in which vacuum can be produced. The sampling capacity is filled up with a part of a drum atmosphere after mixing it, and the ^{222}Rn measurement is carried out by α scintillation.

The quantity of radon released has been determined after replacement of the free volume atmosphere over the waste by air, immediately or a long time after this. These measures allow the radon leak rate to be determinated, wich depends on the mean run time for the gas in the solid phase and on a retention factor.

It appears that both terms depend on the experimental conditions that would be better monitored in further experiments: temperature, pressure, use of inert gas as initial atmosphere. The non radioactive gas (due to the water radiolysis) would be analysed also, in order to exhaustively characterise the gaseous phase.

Programme 03 : Actuel waste packages: Gas emission

S. CAMARO: DESD/SEP/SETED CEA Cadarache FRANCE

Bitumen and cement are two of the materials retained for conditioning the nuclear waste of Low and Medium Activity (Types A and B).

Characteristics of all these wasteforms may be more or less modified under internal self-irradiation caused by the encapsulated radionuclides.

The irradiation-induced degradation can be promoted by the presence of organic compounds, even at very low level of concentration.

TBP and EDTA are two of these : TBP, used as solvent in the extraction of actinides in the Purex process, can be present in the bituminisates; EDTA, used in decontamination processes, may be encountered in cement-based wasteform.

The purpose of this study, performed in the PEGASUS project framework, was to investigate the influence of both these organic compounds on the behavior of the respective matrices under g-rays action.

Prior to irradiation, samples were characterized physically and chemically, in order to distinguish the effect proper to the organic compounds additives from those induced by irradiation.

The main effect induced by TBP addition in bitumen is a fluidization for content larger than 0.4 %. A reverse effect is evidenced for sample containing only 0.4 %.

The main effect induced by EDTA addition in cement is a set retarding for concentrations up to 1.5 %. Above this concentration, a "false" set seems to occur, explained by the formation of a calcic EDTA hydrate with plugging properties.

Under irradiation γ (^{60}Co), the radiolytic gases production for bitumen is increased in the presence of TBP, in conformity with the additive law ($G_{TBP} >> G_{Bitume}$). Nevertheless, the fluidizing effect caused by TBP lowers the swelling ability.

The production of radiolysis gases for cement is increased in the presence of EDTA. But this enhancement does not vary linearly with EDTA content, due to the evolution of the EDTA state with the acid content. Moreover, the addition of EDTA at low content such as 2.5 % leads to a cement mixture that is evoluting with time. So the radiolysis yield depends on the "cure" time.

Programme 04 : Biofilms attached to concrete

Undertaken by Biotechnology Services, AEA Technology, Harwell, United Kingdom
Norma O'Kelly, Sandy Arcus, Graham Holtom, Terry McGenity*, Thanh Trinh and Alan Resevear (Task leader)

* University of Leicester

A OBJECTIVES AND SCOPE

The aim is to determine the form in which the microbial cells attach to the alkaline surface and the extent to which this changes the physical and chemical properties of the cement.

B. WORK PROGRAMME

04-1. Use Electron Microscopy to examine attached biofilms on concrete.
04-2. Monitor interaction of organic materials with the concrete surface.
04-3. Measure diffusion of solutes through the biofilm.
04-4. Study influence of concrete type on the attachment of organisms.

The following objectives have been achieved:

- Anaerobic, alkali tolerant organisms from natural sources have been grown on the surface of porous cementitious matrices of the type used in ILW/LLW repositories;
- bioreactors for developing a biofilm of alkali-tolerant organisms have been built and inoculated with mixed consortia from naturally alkaline sites;
- aqueous solutions containing alkaline degradation products of cellulose are sufficient to maintain the attached microorganisms;
- Scanning Electron Microscopy have been refined to examine biofilms on the surfaces of plastic and porous cement;
- electrical methods of monitoring changes in the porosity and surface coating of cement matrices have been evaluated; conductivity, potential difference and electro-endosmosis can be used to detect changes;
- the biofilm on the surface of a porous matrix will prevent free transfer of gas but the film is delicate and is easily ruptured by a differential pressure of 2 bar;
- the diffusivity of molecules wich are representative sources of nitrogen and carbon to growing cells have been determined in the porous concrete matrix;
- inorganic nitrogen sources diffuse relatively freely than the larger organic compounds although both sources of nutrient will pass through the pores; and
- the nature of the underlying surface does not significantly affect the growing biofilm, although carbonation of the cement matrix nearest the biofilm is evident.

The overall conclusions of this study are as follows.

- Natural microbial populations exposed to alkaline liquids will form biofilms on the surface of most materials.
- Attachment to highly alkaline surfaces such as cement is slower than to inert plastic surfaces but a complete coating can be generated in less than 3 months exposure to a solution containing small amounts of nutrient.

- The alkaline degradation products of cellulose are utilised as a nutrient source by the naturally occurring mixed population of soil micro-organism forming a biofilm.
- The carbon source will be converted to carbon dioxide and carbonate the surface of concrete.
- Simple nitrogen and carbon sources can diffuse through the concrete matrix and be consumed as nutrients by microorganisms in a biofilm.
- Microorganisms will probably grow most prolifically on the outer surface of porous concrete, coating the interface at cracks and junctions.
- The organisms will directly or indirectly, cause blockage of some pores, particularly at the surface of a concrete block.
- The build up of the biofilm can be monitored by electrochemical methods and by electron microscopy.
- The biofilm and associated materials will block pores in grout and generate a black pressure of gas but this film may be disrupted by differential pressures of about 2 bar.

Title :	Gas Generation in Supercompacted Waste Products
Contractor:	Forschungszentrum Jülich (KFA)
Contract N°:	FI2W-CT91-0094
Duration of contract:	1 October 1991 - 31 August 1995
Period covered:	January - December 1994
Project leader:	R. Odoj
Executants:	H. Heimbach, H.J. Steinmetz, W. Wolf

A. OBJECTIVES AND SCOPE

On the basis of a long term cooperation contract between the Research Centre Jülich (KFA) and the German Federal Office for Radiation Protection (BfS) the Quality Control Office for Radioactive Waste (in german: Produktkontrollstelle für radioaktive Abfälle = PKS) was founded. Its main tasks are qualification and control of conditioning processes of radwaste products and radioanalytical/radiochemical analysis of material contained in waste packages prior to disposal into underground waste storages. Gas analysis as to be carried out for ensuring, that the release rates of radioactive respectively chemically reactive gases (for instance hydrogen) into the environment or the atmosphere of a waste disposal mine are not exceeded.
Within the scope of this research programme methods are evaluated for the exclusion of excessive hydrogen generation by supercompacted waste pellets and for reducing overpressure inside waste packages by hydrogen absorption.

B. WORK PROGRAMME

In Fig. 1, the time schedule for the programme, the seven main tasks are listed as follows.

2.1 Time dependent measurements on gas formation in supercompacted pellets
2.2 Heating of pellets under various conditions (p, T, t)
2.3 Measurements on generation after thermal treatment
2.4 Testing filters for hydrogen absorption (physical reaction)
2.5 Evaluation and tests of materials reacting with hydrogen (chemical reaction)
2.6 Proposal of technical procedures to avoid hydrogen overpressure
2.7 Discussion and final report

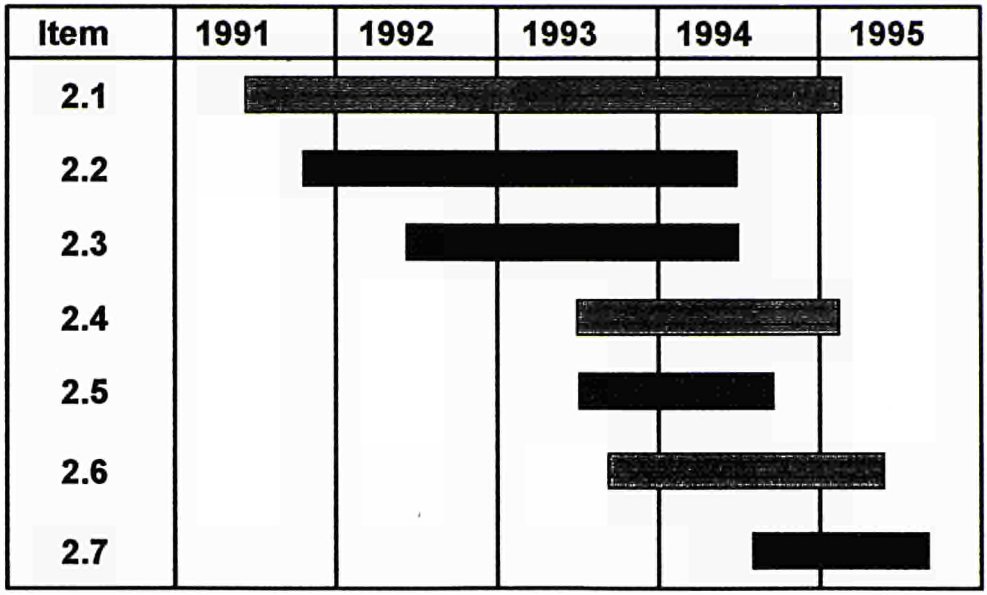

Fig. 1 Time schedule of the KFA-project „Gas generation in supercompacted waste products".

The foreseen end of the programme on 31.01.95 was shifted to the 31.08.95. At present concluding work to the tasks 2.2.-3and 2.7is carried out Experiments to the tasks 2.1 and 2.4-6 are still on going.

C. PROGRESS OF WORK AND OBTAINED RESULTS

C.1 Measurements of gas generation at various experimental conditions

The measurements on release rates of hydrogen from supercompacted radioactive or inactive pellets of different composition stored in 200-1-drums at 25°C and 70°C have been completed. The experimental results have been documented in our previous reports. Concluding investigations will determine the influence of drum or container leakrates onto hydrogen release measurements under real operating conditions.

In order to exclude the build-up of hazardous concentrations of hydrogen inside radwaste drums or containers the maximum concentration arising must be judged from measurements to be taken before storage.

The control measurements of gas release from drums resp. containers are more or less influenced by variations in their leakrate. In order to improve upon the quality of the measurements leaktight seal or an extra overpack might be used, which would be both time consuming and rather costly. It should therefore be attempted to develop a method by which the gas generation can be evaluated on the basis of a correlation between a simply measurable leak rate and the hydrogen content of the respective drum or container. Therefore in an longterm experiment hydrogen build-up and hydrogen loss were measured on a real waste container filled with drums. The experimental set-up is schematically given in Fig. 2. Hydrogen generation is

simulated by feeding a variable amount of H_2 from a gas bottle into the container and the leakrate is adjusted by use of a valve.
This experiment is still in progress. On the basis of the experimental results a method for the calculation of build-up rates and maximum concentrations will be evaluated in order to facilitate the check-up of drums and containers for storage.

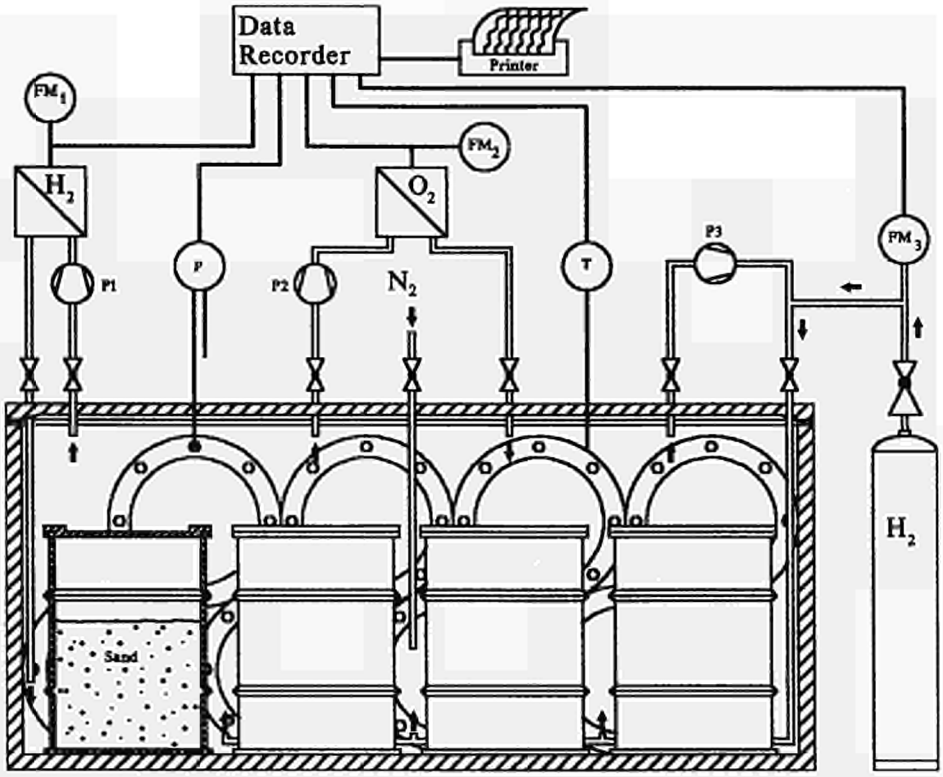

Legend: P_1-P_3 pump; FM_1-FM_3 flow meter; P pressure gauge; T temperature gauge
H_2, O_2 contents meter

Fig. 2 Experimental set-up for hydrogen release measurements under real operating conditions

C.2 Proposal of technical procedures for hydrogen absorption

A first experimental set-up for the removal of hydrogen from waste drums was constructed on the basis of successful laboratory experiments on hydrogen removal by means of catalytical recombination of hydrogen and atmospheric oxygen (physical

reaction, Eq. 1) and/or oxidation of hydrogen by a (water-forming) reaction with silver(oxide)-activated manganese dioxide (chemical reaction, Eq. 2).

$$\text{Eq.1} \quad 2\,H_2 + O_2 \xrightarrow{[\text{Catalyst}]} 2\,H_2O + 484\ \text{kJ/mol}$$

(Catalytical recombination or „cold burning" of hydrogen on platinum or palladium doped metal grids)

$$\text{Eq.2} \quad H_2 + MnO_2 \xrightarrow{[Ag_2O]} H_2O + MnO$$

(Simplified equation of a multi-step surface reaction)

Fig. 3 shows a schematic drawing of an experimental arrangement for laboratory and field investigations. The device, called *hydrogen absorption unit* in the following text, contains catalytically active grids plated with the noble metals palladium or platinum and/or activated manganese dioxide.

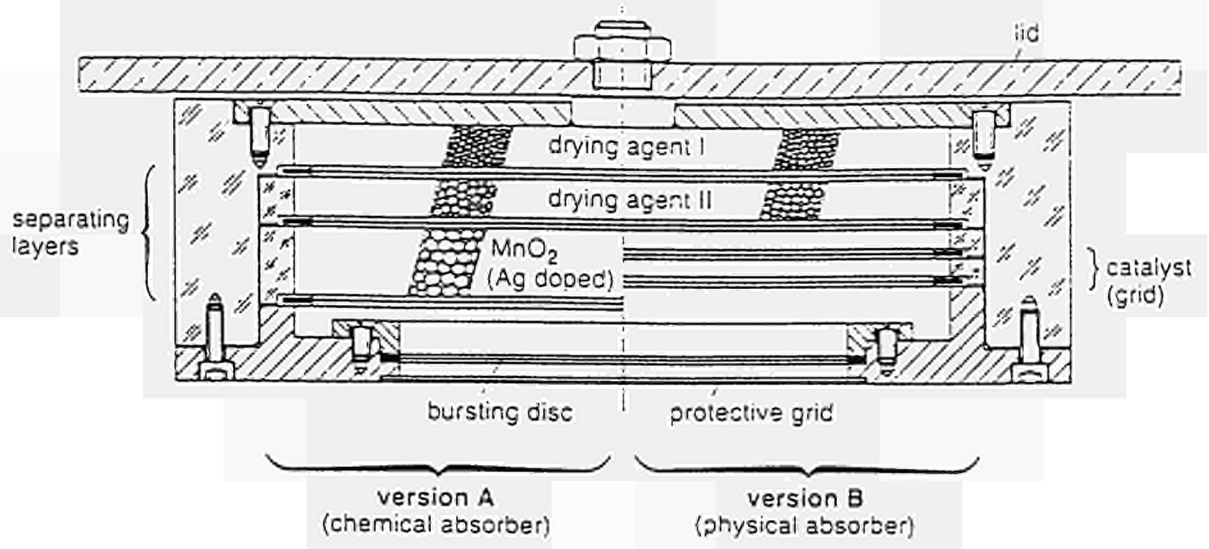

Fig. 3 Drawing of absorption unit

The hydrogen absorption unit is hermetically sealed by a bursting disk (rupture pressure NP + 200 mbar) in order to protect the absorption material from poisonous chemicals from the drum atmosphere until it is actually needed. At present in still on going experiments the technical layout of the hydrogen absorption unit is being optimized. As shown in Fig. 4 the hydrogen absorption unit is installed inside a 200-l-drum on an adjustable support.

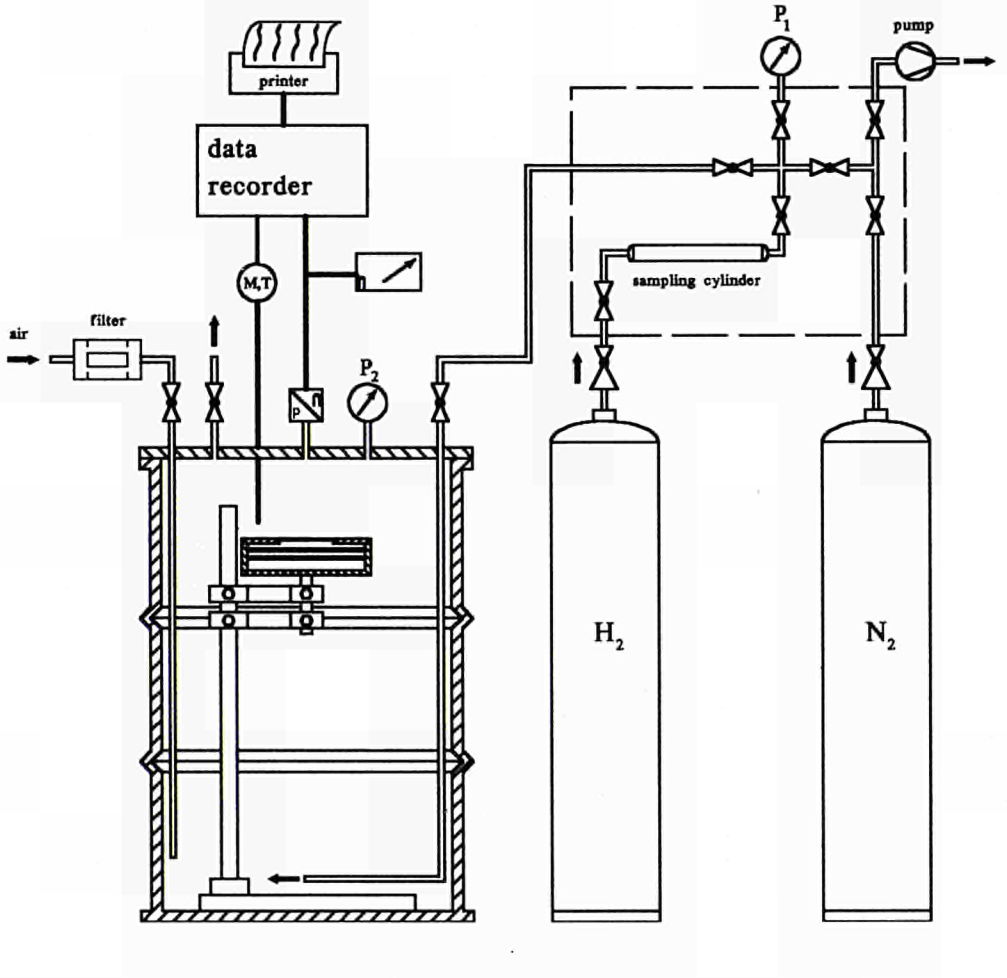

Fig. 4 Experimental set-up for testing the hydrogen absorption unit.

Hydrogen overpressure can be produced inside the drum via a gas pipe. In addition, this inlet pipe is also used to purge the drum with nitrogen at the beginning of an experiment if necessary. Through a second pipe air, cleaned by a charcoal filter, is admitted to the

drum. The pressure build up depends on the amount of hydrogen gas introduced, which is determined by use of a sampling cylinder. For the determination of the leak rate pressure can be lowered inside the drum by a vacuum pump. As hydrogen is converted to water by both the physical and the chemical method, in addition to the pressure inside the drum the humidity of its atmosphere is measured as well. This is done by pressure and humidity gauges. The experimental data are continously monitored by a data recorder. A further pressure gauge is installed to have a quick information about the overall pressure at the beginning of each experiment. The pressure equilibration after each experiment is achieved by a opening valve mounted on the lid of the drum. In the experiments carried out so far the hydrogen removal by catalysts - with and without preceeding thermal activation - as well as manganese dioxide in various experimental conditions has been investigated.

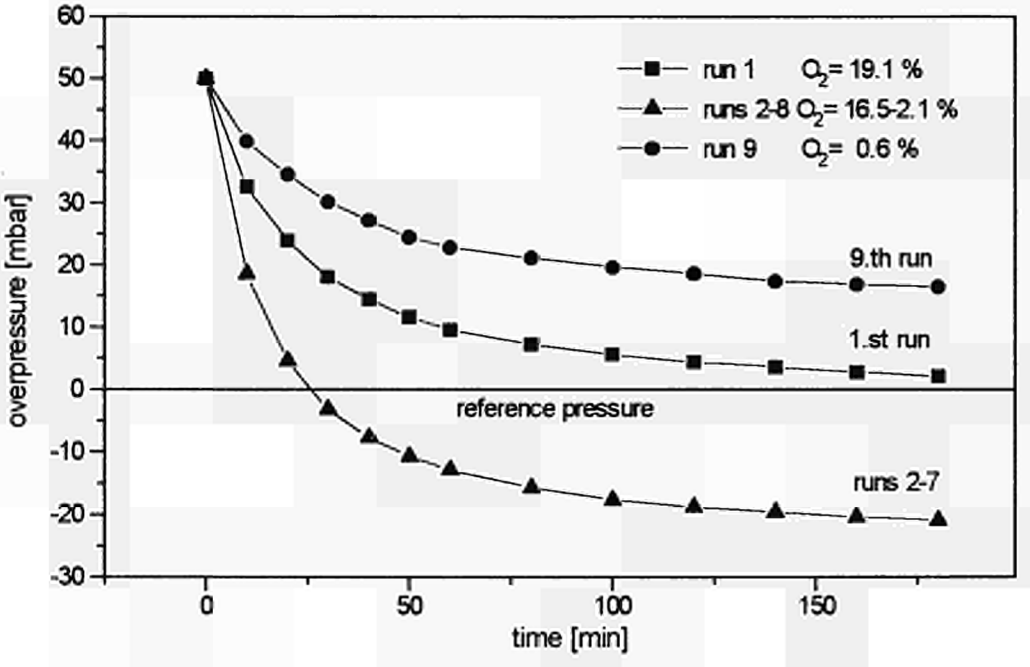

Fig. 5 Hydrogen removal by Pd-catalyst during repeated H_2 injections.

By repeated additions of constant quantities of hydrogen (constant hydrogen overpressure) the rate of pressure decrease was determined as function of decreasing oxygen content in the drum atmosphere. Fig. 5 shows the experimental results of serveral runs normalized to 50 mbar for a palladium catalyst at room temperature. With the exception of the first and last experiments (runs 1 and 9) a constant decrease of the pressure versus time was registered. The higher reaction rates of runs 2-8 may be explained with an increase in temperature of the catalyst in the first experiment due to recombination heat transfer. Even though the oxygen content in the drum atmosphere fell from 19.1 to 2.1% volume, the activity of the catalyst remained constant. This result is in accordance with equation Eq.3 under the assumption of a surplus catalyst surface.

Eq.1 $r(t) = k\ c(O_2)\ c(H_2)^2$

r(t): reaction rate; k: rate constant, $c(O_2,H_2)$: concentrations

Therefore a further reduction of the experimental set-up in size without influencing its efficiency seems to be possible. Thus the construction of a rather small cartridge prototype should be feasible. From the last experiment it can be derived that the palladium catalysed recombination reaction will strongly slow down with oxygen concentations lower than 2% volume. With the platinum catalyst in the same experiment conversion of hydrogen only occurred with activated grids. In Fig. 6 as a comparison between activated/non activated palladium and platinum catalysts the specific gas reduction rates (in mbar per time and area of the catalyst surface) are given.

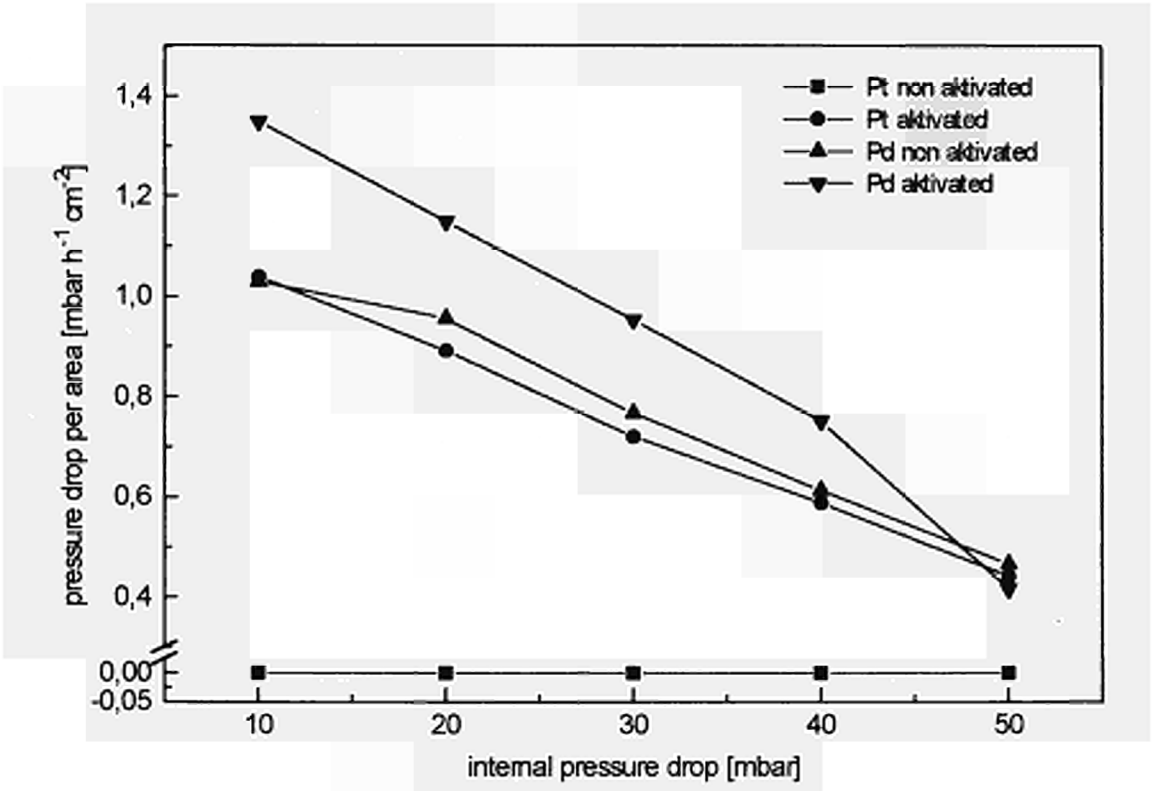

Fig. 6 Comparision of palladium and platinum catalysts.

Under real operating conditions the rapid catalytic process (oxygen content > 2% volume) will be combined with the rather slow chemical oxidation using manganese dioxide (oxygen content < 2% volume). Experiments have been carried out with chemical absorbers. In Fig. 7 the efficiency of the chemical and the catalytical H_2-degradation in a 200-l-waste drum at 50 mbar of hydrogen overpressure is compared.

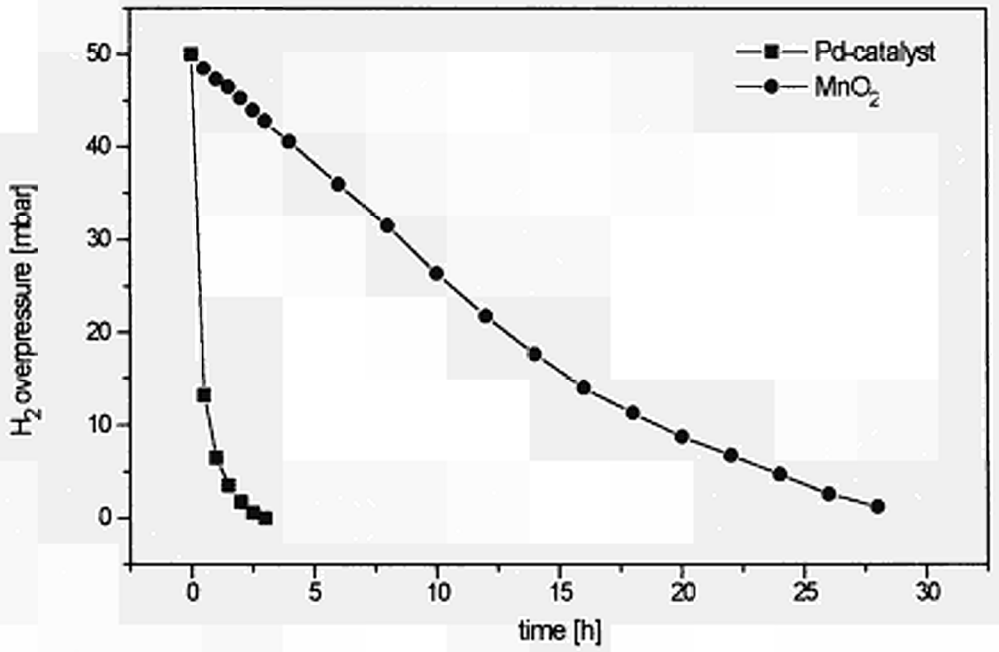

Fig. 7 Efficiency of chemical (MnO_2) and catalytical (Pd) H_2-degradation in waste drums.

D. Conclusions

- For the effective removal of harzardous hydrogen overpressures in waste drums or containers hydrogen absorption device has been developed and tested.
- The device may be reduced in size to a cartridge like prototype.
- The catalytical recombination of H_2 and O_2 is possible even at room temerature and very low O_2 concentrations down to 2% volume.
- In the absence of oxygen manganese dioxide may be used as the absorber.

Title	**Impact of Additives and Waste Stream Constituents on the Immobilisation Potential of Cementitious Materials**
Contractors	University of Aberdeen (UK); Free University of Berlin (D); AEA Windscale (UK)
Contract N°	FI2W-CT90-0099
Duration of contract	October 1991 - September 1995
Period covered	1 January 1994 - 31 December 1994
Project leader	Prof. F.P. Glasser (UA, Co-ordinator), Prof. G. Marx (FUB) Dr. R. Hibbert\Dr. A. Tyson (AEA)

A. OBJECTIVE AND SCOPE

The objective of this tri-coordinated research programme is to determine the interactions between waste and cementitious materials, in real waste forms, and also to explain the sorption phenomena of transuranics and relate laboratory data to the performance of realistic cemented waste forms within a repository.

The studies will be used to strengthen the links between empirical studies e.g. leaching, and more fundamental aspects. They will also be used to determine the impact of waste itself, both active and non-active, on the properties and performance of the encapsulating cement.

Various techniques will be used in the measurement of the aqueous phase and solid phase compositions of cement and blended cement, using inactive controls as well as formulations containing real wastes. Separation factors will be calculated for various isotopes in the above systems. The sorption processes for certain transuranics will be determined on pure cement phases and the role of certain organic complexing agents will be determined. The impact of selected inorganic ions on cement performance at longer ages will also be measured. The above experiments will be carried out at three isotherms: ambient (~ 22°C), 55°C and 80°C.

B. WORK PROGRAMME

B.1 Preparation of blended cements incorporating radioisotopes and process chemicals.

B.2 Trial runs at elevated temperatures on pore fluid expression device.

B.3 Pore fluid extraction of the samples prepared under B.1 and measurement of radioisotope sorption for the various cement blends.

B.4 Determine the effect of organic additives/real wastes on the sorption potential of the various cement blends.

B.5 Synthesis and characterisation of phase pure cement hydrates for sorption studies.

B.6 Measure the sorption of Eu(III) or Am(III), U(VI), Th(IV), Np(V) and Pu(VI) on synthetic cement hydrates, ettringite, C-S-H, tobermorite and hydrotalcite. The effect of organic additives on the sorption capacity will be determined.

B.7 Study the specific nuclide interactions (Ni, Cs, Cl and I) with cementitious materials.

B.8 Study the impact of chloride, carbonate and sulfate on cement performance.

B.9 Study the impact of organic additives/process chemicals on cement performance.

B.10 Verification of mineralogy of phase pure cement hydrates used in B.6.

C. PROGRESS OF WORK AND RESULTS OBTAINED

State of Advancement

Tasks B.1, B.2 and B.5 were completed in the in the time period 1992-1993. Tasks B.3 and B.4 have been completed in the period under review. All other tasks are currently still being worked on. We have been granted an extension in order to complete tasks B.6 to B.10. A large number of experiments have been completed on Task B.6, approximately 80 sorption measurements have been completed with 30 currently in progress. Progress has also been made in describing, mathematically, the sorption process and a number of constants for the various systems have been determined. The sorption characteristics are described by Freundlich and Langmuir isotherms. In task B.7 the work on Ni is finished and the work on Cs and Cl is essentially complete and a literature survey has begun on iodine. Work on task B.8 is progressing and several phases have been identified as important degradation products. Task B.9 is progressing with the majority of work centred on EDTA and the work on citric and oxalic acids is essentially complete. Work continues on B.10 and characterisation is done when the samples become available.

Progress and Results

C.1 Sorption Experiments on Real Cements Containing Waste Materials

The main component of the Windscale work is the extraction and analysis of pore fluids from cements by means of a high force hydraulic press which has been specially adapted for active work at temperatures up to 80°C.

This work programme consists of three main areas:

1. Cement blends containing tracers.
2. Cement blends containing tracers and selected ILW simulants and process chemicals.
3. Cement blends containing real wastes.

The Windscale work is now complete and a final report is in preparation. During 1994 the following work has been carried out:

- Pressing of test blocks containing Pu and neat cellulose followed by radiochemical analysis of the extracted pore fluids. (Part of the work under area 2 above.)
- Pressing of inactive test blocks containing neat cellulose followed by total organic carbon analysis of the extracted pore fluids. (Part of the work under area 2 above.)
- Pressing of test blocks containing real graphite waste. (Work under area 3 above.)

Results and Discussion

Plutonium Analyses on Extracts from Test Blocks Containing 'Chemical' Cellulose

Cellulose powder obtained from a chemical supplier was chosen for extended trials of Pu solubility in pore-fluid because 1993 work had shown an enhancement of Pu solubility with this form of cellulose at high loading. No enhancement had been detected in comparable tests using degraded cellulose, iso-saccharinic acid and a simulated PCM (plutonium contaminated material).

Two different types of block penetration methodology have been investigated. The first method was a one-stage block preparation with direct incorporation of Pu in the mix-water; the so-called "normal method".

The following sets of "normal method" experiments were carried out:

(i) Cellulose loadings of 1%, 3%, 6%, 8% and 11% (wt.) cured for 28 days.

(ii) Cellulose loadings of 3 and 13% cured for one, two, three, four and five months.

Simulated UK repository borehole water was used as the mix water. All curing was carried out under anaerobic conditions at 80°C. 230 kBq of Pu was incorporated into each block. This was equivalent to an initial plutonium concentration of 1×10^{-5} M.

In the 28 day cure tests (i) an enhancement of Pu pore fluid concentration was only seen at cellulose loadings of 8% and 11% (see Table 1); Pu levels in these tests were increased by three to four orders of magnitude compared to blocks containing no cellulose. At cellulose incorporation of 1% to 6% the enhancement was no more than twenty-fold.

Longer trials showed that at 3% cellulose loading no increase in Pu pore fluid concentration was observed for curing times from two to five months (see Table 2); a small decrease in Pu concentration with curing time actually being indicated. With 13% loading Pu pore fluid concentrations increased steadily with curing time up to four months; again an increase of three to four orders of magnitude was shown over the 'no cellulose' blocks.

The second method of specimen preparation, the so-called "reconstitution method", was carried out in three stages:

(a) An inactive block containing cellulose was prepared and cured for 28 days.

(b) The block was then crushed to a coarse powder and dried at 80°C for a week.

(c) The crushed cement was packed into a cylindrical container in contact with simulated borehole water containing Pu and cured for a further 28 days.

The "reconstitution method" tests gave similar trends to the 28 day cured "normal method" tests. The reconstitution Pu levels were, however, some one hundred times higher at the 0% and 1% cellulose loadings (see Table 1). These differences are not unexpected, since the Pu may not have had access to all the sorption sites available in the original cement mix.

TOC Analyses on Extracts from Parallel Tests Containing Cellulose but no Pu

These tests paralleled the "normal method" tests referred to above. Two sets of inactive blocks were prepared consisting of:

(i) a set of blocks with cellulose loadings of 1%, 3%, 6%, 8% and 11% cured for 28 days;

(ii) a set of blocks with cellulose loadings of 3% and 13% cured for one, two, three, four and five months. (No pore fluid could be extracted from the 3% cellulose test after five months curing.)

The extracted pore fluids were analysed for total organic carbon (TOC) content.

In 28 day tests the level of TOC in the pore fluid increased smoothly with increasing cellulose loading (Table 3). The amount of cellulose degraded in these tests was estimated at only 3% - 6%, assuming all the organic carbon in solution arises from cellulosic degradation products.

Although showing much more variability the TOC analyses over one to five months showed broadly similar trends to the plutonium analyses. At 13% cellulose loading the TOC content of the pore fluid increased up to three months curing but then started to decline. At 3% cellulose loading the TOC content decreased slightly with increasing curing time.

Pore Extracts from Cemented CAGR Graphite Wastes

Four 3:1 BFS/OPC blocks containing real CAGR (Commercial Advanced Gas Reactor) graphite waste were prepared and pressed. (3:1 BFS/OPC has been proposed as an encapsulation matrix for some UK graphite waste.) Two blocks were prepared with 'AnalaR'

mix water and the other two with the borehole water simulant used in previous work. The graphite was taken in the form of 70 g cores, from CAGR sleeves. Approximately 45 g of crushed graphite, taken from a different core for each test, was incorporated into each 150 g test block. Assay samples of crushed graphite were retained and analysed for H-3, C-14 and gamma content using liquid scintillation counting and gamma spectroscopy. The extracted pore fluid was analysed similarly.

The major isotopes identified in the graphite were H-3, C-14, Co-60 and Cs-134. The pore fluid concentrations of these isotopes was very low in all the tests carried out. Only a very small fraction (< 0.3%) of the total activity in the graphite is released into the pore fluid. In the case of H-3 and Cs-134, which have high solubilities and sorb poorly, this indicates effective retention within the matrix of the graphite. Similar results were obtained whether the mix water was the saline borehole simulant or 'AnalaR' water.

C.2 Sorption Experiments on Phase Pure Cement Hydrates

In this time period several systems, listed in table 4, were investigated by FG Radiochemistry at the FU Berlin.

Table 4 shows that the systems studied at higher temperatures were of great importance. It must be kept in mind that only hydrotalcite does not change at higher temperatures, even when it is under the influence of Q-brine, all the other phases studied undergo a phase change. Although the structure of hydrotalcite does not change there is a chemical change in that some hydroxyl ions are substituted by chloride ions. The data obtained fit Freundlich's equation, the relevant constants are given in Table 4.

The data of the systems listed in Table 5 do not fit this equation. The experiments were carried out in the same way as described in the proceeding reports.

Discussion of the results

Applying Langmuir's equation the expression $a_s = a_\infty \frac{\sum b_i c_i}{1+\sum b_i c_i}$ (1) was used instead of $a_s = a_\infty \sum \frac{b_i c_i}{1+b_i c_i}$ (2) in former times. The new expression is directly obtained when deriving Langmuir's equation from kinetics. The data calculated by using equation (1) must not be correct since in all cases only one ionic species had to be taken into consideration, due to the relevant speciation. The summation can be cancelled in these special cases and both equations become identical. Only under conditions where more than one ionic species must be taken into account equation (2) is superior to (1). Even (2) does not correctly represent the adsorption phenomena under investigation because it neglects the ionic species, the solvent consists of as competing particles. These can be taken into account by labelling the Na^+ and Cl^-. By applying synchroton radiation should be preferred in this case, permitting an insight into the whole system and even allowing the relevant compositions to be determined directly at the surface of the specific sorbent.

The curves obtained from the results are shown in Figure 1. The dashed lines represent theoretical curves which describe the whole adsorption process neglecting all precipitation due to restricted solubility. The full lines on the other hand represent the adsorption behaviour of uranium on hydrotalcite measured when saturation of uranium is reached in the relevant media at higher concentrations of the sorbate. It must be emphasised that the results can only be discussed in detail after obtaining all the data for the other systems under investigation.

C.3 Specific Nuclide Interactions with Cementitious Materials

The work on Ni was completed in the last reporting period and most of the work has centred on Cs and Cl. The greatest amount of work has been on Cs sorption on calcium aluminium silicate gels (C-A-S-H gels). Different methods were used to synthesise the gels with varying success. A direct reaction of CaO, SiO_2 and $AlOOH{\cdot}xH_2O$ was chosen as it did not have problems of contamination with other reagents. This method had a problem in that although gels were formed quite quickly, the level of aluminium substitution in the gels was low and variable. Sorption experiments were carried out on aliquots of these gels after one months reaction time at 25°C. Although the results were difficult to interpret, generally, the sorption for gels with no aluminium is less than for gels with aluminium, for example, C-S-H (C/S=1.5) + Al showed a higher sorption capacity than for C-S-H (C/S=1.4); R_D for C-S-H gel was 4.5 and 9.1, 47.0 for 2% and 5%Al(target) gels respectively. The results were very variable and this is probably because the level of aluminium incorporation was low and extremely variable. The samples will be left to age at 25 and 55°C for several months and the sorption experiments will be repeated.

The interaction of chloride with hydrotalcite and AFm was investigated. In the sorption experiment with AFm, the AFm converted to ettringite and no sorption of chloride was detected. Hydrotalcite did show a significant uptake of chloride; the results are given in Table 6. The hydrate (0.5g) was contacted with 100 ml of solution containing 0, 15, 150 and 1500 ppm chloride for 14 days at 25°C. This phase has high R_D values especially at the low loading of 15 ppm. However, at higher loadings the R_D is very much lower, showing that this phase has only a limited number of sorption sites for chloride.

A literature survey has begun on iodine so that the likely speciation of iodine can be determined and likely host phases responsible for sorption.

C.4 Study the Impact of Chloride, Carbonate and Sulfate on Cement Performance

The effect of sulfate and chloride of cement hydrates, especially the aluminate phases, was determined by investigating the system $CaO\text{-}Al_2O_3\text{-}CaCl_2\text{-}CaSO_4\text{-}H_2O$. C_3A was synthesised at Aberdeen and then mixed with varying proportions of $CaSO_4{\cdot}2H_2O$ and $CaCl_2{\cdot}2H_2O$ as an aqueous slurry for 5 weeks at 25°C. Six preparations were made, the Cl to SO_4 proportions being 100:0, 80:20, 60:40, 50:50, 40:60, 20:80 and 0:100. Three separate salts were identified by powder X-ray diffraction, Friedel's salt, $3CaO{\cdot}Al_2O_3{\cdot}CaCl_2{\cdot}10H_2O$, "Kuzel's" salt $6CaO{\cdot}2Al_2O_3{\cdot}CaSO_4{\cdot}CaCl_2{\cdot}24H_2O$ and monosulfate (AFm) $3CaO{\cdot}Al_2O_3{\cdot}CaSO_4{\cdot}12H_2O$. This shows that there is not a complete solid solution between monosulfate and Friedel's salt, "Kuzel's" salt is intermediate in composition. The dried samples were investigated by analytical electron microscopy (AEM) in order to determine the degree of solid solution between the two end members of the Friedel's salt and monosulfate phases. This showed that there was a complete spread of results from Friedel's salt to "Kuzel's" salt and from "Kuzel's" salt to monosulfate. This has important consequences for computer based modelling studies for solubility and stability. The stability/compatibility "Kuzel's salt" with C_4AH_{13} is about to begin, this will give describe the relationship between $3CaO{\cdot}Al_2O_3{\cdot}CaCl_2{\cdot}10H_2O$, $3CaO{\cdot}Al_2O_3{\cdot}CaSO_4{\cdot}12H_2O$, $3CaO{\cdot}Al_2O_3{\cdot}Ca(OH)_2{\cdot}12H_2O$, $6CaO{\cdot}2Al_2O_3{\cdot}CaSO_4{\cdot}CaCl_2{\cdot}24H_2O$.

A phase pure sample of $6CaO{\cdot}2Al_2O_3{\cdot}CaSO_4{\cdot}CaCl_2{\cdot}24H_2O$ has been synthesised and its solubility will be measured after equilibrium has been reached.

A literature survey was carried out to look for other potential degradation products of Portland cement attacked by either sulfate, carbonate or chloride. Novack and Colville /1/ describe the presence of birunite $8.5(CaSiO_3){\cdot}9.5(CaCO_3){\cdot}CaSO_4{\cdot}15H_2O$ a mineral which occurs with a mixture of other sulfate attack products, gypsum, ettringite and thaumasite.

These minerals were found on mature concrete subject to wetting from soil water. Birunite was also found at the hyperalkaline groundwater site at Maqarin on the Jordanian/Syrian border. /2/ It was found in a cocktail of secondary minerals formed in the metamorphic zone and spring discharges. It was found alongside C-S-H, crystalline calcium silicate hydrates, thaumasite and several other products.

Since birunite may be an important long term phase it was decided to try and synthesise it. Several syntheses are currently underway.

C.5 Impact of Organic additives/Process Chemicals on Cement Performance

The hydration and interaction of OPC in the presence of some organic acids have been investigated. Work to date has been centred on citric acid, oxalic acid and EDTA (as the disodium salt). These organics are of interest because they appear in process waste streams. Importance is therefore being attached to these soluble organic species because they may interfere with cement hydration and complex with long-lived radionuclides, increasing solubilities and reducing sorption.

The results indicate that citric acid has a more powerful retarding effect than EDTA or oxalic acid. An addition of 0.15 wt.% citric acid increases the setting time of an OPC paste by 10 hours. Some retarding tendency is evident using oxalic acid, but the effect is small compared to citric acid or EDTA, even at higher molar concentrations. This retarding effect may cause difficulties for the encapsulation process but can be easily overcome the addition of sodium hydroxide.

Cement slurries containing citric acid or oxalic acid were prepared with OPC to a w/c = 0.4. Several concentrations of citric acid and oxalic acid were studied. These samples were mixed for a known period and then filtered by suction filtration. The results show that citrate concentrations drop rapidly within the first minutes of hydration. Thereafter the rate of citrate decrease slows and by 24 hours it was less than 1 ppm. The results for oxalate show that, after the first minute of hydration, oxalate concentrations drop to less than 1 ppm even when initial concentrations of 70,000 ppm oxalate have been added. This is due to the immediate precipitation of insoluble calcium oxalate, $Ca(COO)_2 \cdot H_2O$

C.6 Verification of Mineralogy of Phase Pure Cement Hydrates from Task B.6

Some samples have been received from FUB throughout the contract and these get characterised as and when they become available. For this reporting period no samples have been given for characterisation.

References

/1/ Novack, G.A. and Colville, A.A., *Cem. Conc. Res.*, **19**, 1-6 (1989)

/2/ A natural analogue study of the hyperalkaline groundwaters. I. Source term description and thermodynamic database testing, Nagra Technical Report 91-10, Wettingen, Switzerland.

Cement Nomenclature:- C = CaO A = Al_2O_3 S = SiO_2 H = H_2O M = MgO $\bar{S}$ = SO_3

Abbreviations:- OPC - Ordinary Portland Cement BFS - Blast Furnace Slag
PFA - Pulverised Fly Ash

Report prepared by A. Kindness 2/3/95

Table 1 Pu Pore Fluid Concentrations for Backfill at Different Cellulose Loading('Borehole' Mix-Water, Anaerobic Curing at 80°C for 28 Days)

wt % Loading Cellulose	Pu Concentration (M)	
	Normal	Reconstitution
0	3.6×10^{-10}	5.0×10^{-8}
1	5.2×10^{-9}	3.0×10^{-7}
3	4.1×10^{-9}	
6	8.7×10^{-9}	
8	1.0×10^{-6}	
11	4.4×10^{-6}	8.0×10^{-6}

Table 2 Effect of Curing time on Average Pu Pore Fluid Concentrations for Backfill with Added Cellulose (Borehole 'Mix' Water, Anaerobic Curing at 80°C)

	Pu Concentration	
Time (Months)	3% Cellulose	13% Cellulose
1	4.1×10^{-9}	1.2×10^{-7}
2	3.5×10^{-9}	6.6×10^{-7}
3	2.9×10^{-9}	1.1×10^{-6}
4	1.9×10^{-9}	3.9×10^{-6}
5	2.3×10^{-9}	6.8×10^{-7}

Table 3 TOC Content of Pore Fluids from Backfill Mixes at Different Cellulose Loadings

% Cellulose in Backfill	Fluid TOC Content (ppm)*
Backfill/0% cellulose	390
Backfill/1% cellulose	1200
Backfill/3% cellulose	1770
Backfill/6% cellulose	4350
Backfill/8% cellulose	6440
Backfill/11% cellulose	6610

Notes: All cement blocks prepared with borehole water and cured at 80°C for 28 days.
* Assuming all organic carbon in pore solution arises from cellulose degradation.
TOC - Total organic carbon.

Table 4 Summary of Sorption Experiments Which Fit Freundlich's Equation

Nuclide	Cement Component	Solvent	Temperature	N_f	K_f
Europium	Hydrotalcite	bidist. Water	25°C	3.8 ± 0.9	6.0E35 ± 6.0E34
Europium	Hydrotalcite	Water with EDTA	25°C	0.7 ± 0.1	0.2 ± 0.03
Europium	Hydrotalcite	Water with EDTA	55°C	0.1 ± 0.04	3.2E05 ± 4.7E04
Europium	Ettringite	sat. NaCl with EDTA	25°C	0.4 ± 0.2	1.3E-03 ± 9.2E-04
Europium	C-S-H-gel	Water with EDTA	25°C	0.4 ± 0.04	2.3E-03 ± 3.5E-04
Europium	C-S-H-gel	Water with EDTA	55°C	0.5 ± 0.2	1.1E-02 ± 3.4E-03
Europium	C-S-H-gel	sat. NaCl with EDTA	25°C	0.7 ± 0.3	0.2 ± 9.7E-02
Europium	C-S-H-gel	sat. NaCl with EDTA	55°C	0.9 ± 0.3	64.6 ± 26.8
Europium	C-S-H-gel	bidist. Water	25°C	4.0 ± 0.5	1.7E38 ± 3.4E37
Europium	Tobermorite	Water with EDTA	25°C	0.9 ± 0.2	4.6 ± 1.2
Europium	Tobermorite	Water with EDTA	55°C	0.4 ± 0.1	5.3E03 ± 9.5E02
Europium	Tobermorite	sat. NaCl with EDTA	25°C	0.4 ± 0.1	1.8E03 ± 6.2E02
Europium	Tobermorite	sat. NaCl with EDTA	55°C	0.5 ± 0.1	4.7E-03 ± 1.5E-03
Thorium	Hydrotalcite	Water with EDTA	25°C	0.8 ± 0.1	4.0E-02 ± 1.2E-02
Thorium	C-S-H-gel	Water with EDTA	25°C	1.3 ± 0.1	1.6E03 ± 1.8E02
Thorium	Hydrotalcite	bidist. Water	55°C	1.2 ± 0.1	8.9E03 ± 4.45E03
Thorium	Ettringite	bidist. Water	55°C	1.3 ± 0.1	5.8E03 ± 5.8E02
Thorium	Tobermorite	bidist. Water	55°C	4.1 ± 1.1	1.1E37 ± 1.7E37
Thorium	C-S-H-gel	bidist. Water	55°C	1.2 ± 0.3	2.5E04 ± 2.8E04
Uranium	Hydrotalcite	bidist. Water	55°C	3.1 ± 0.4	2.6E13 ± 5.2E12
Uranium	Hydrotalcite	bidist. Water	85°C	3.0 ± 1.1	1.4E11 ± 9.8E10
Uranium	Tobermorite	Water with EDTA	55°C	0.7 ± 0.1	6.3E-02±1.5E-02
Uranium	Tobermorite	bidist. Water	85°C	0.4 ± 0.2	1.7E03 ± 5.1E02
Uranium	C-S-H-gel	bidist. Water	85°C	1.6 ± 0.6	1.9E05 ± 9.5E04
Uranium	Hydrotalcite	Water with EDTA	85°C	2.1 ± 0.4	2.2E11 ± 6.6E10
Uranium	Tobermorite	Water with EDTA	85°C	0.4 ± 0.2	1.7E-03 ± 5.1E-04
Neptunium	Ettringite	Water with EDTA	25°C	0.6 ± 0.2	1.3E-03 ± 5.2E-04
Neptunium	Tobermorite	Water with EDTA	25°C	0.4 ± 0.1	2.1E-03 ± 8.4E-04
Neptunium	Hydrotalcite	sat. NaCl	25°C	1.0 ± 0.3	2.8 ± 0.3
Neptunium	C-S-H-gel	Water with EDTA	25°C	0.3 ± 0.1	1.1E-03 ± 1.1E-04
Plutonium	Hydrotalcite	Water with EDTA	25°C	0.3 ± 0.3	3.6E-06 ± 2.5E-06
Plutonium	Hydrotalcite	sat. NaCl with EDTA	25°C	0.8 ± 0.1	5.4E-03 ± 2.4E-03
Plutonium	Tobermorite	bidist. Water	25°C	0.4 ± 0.3	5.0E-05 ± 6.7E-05
Plutonium	Tobermorite	Water with EDTA	25°C	0.9 ± 0.1	2.6 ± 1.2

Table 5 Sorption Experiments Which Do Not Fit Freundlich's Equation

Nuclide	Cement Component	Solvent	Temperature
Uranium	Ettringite	bidist. Water with EDTA	25°C
Uranium	C-S-H-gel	bidist. Water with EDTA	25°C
Uranium	Ettringite	bidist. Water with EDTA	55°C
Uranium	C-S-H-gel	bidist. Water with EDTA	55°C
Uranium	C-S-H-gel	bidist. Water with EDTA	85°C
Plutonium	Hydrotalcite	bidist. Water	25°C
Plutonium	Hydrotalcite	sat. NaCl solution	25°C
Plutonium	Ettringite	bidist. Water	25°C
Plutonium	Ettringite	bidist. Water with EDTA	25°C
Plutonium	C-S-H-gel	bidist. Water with EDTA	25°C
Plutonium	C-S-H-gel	bidist. Water	25°C

Table 6 Sorption of Chloride on Hydrotalcite

Sample	Hydrotalcite			
weight of hydrate	0.5g			
volume of solution	100 ml			
initial Cl (ppm)	blank	15	150	1500
After 14 days (ppm)	1.2	0.6	75.0	1260
R_D (ml/g)	-	4800	200	38.1

Figure 1 Sorption of Uranium on Hydrotalcite Showing Effect of Different Solutions

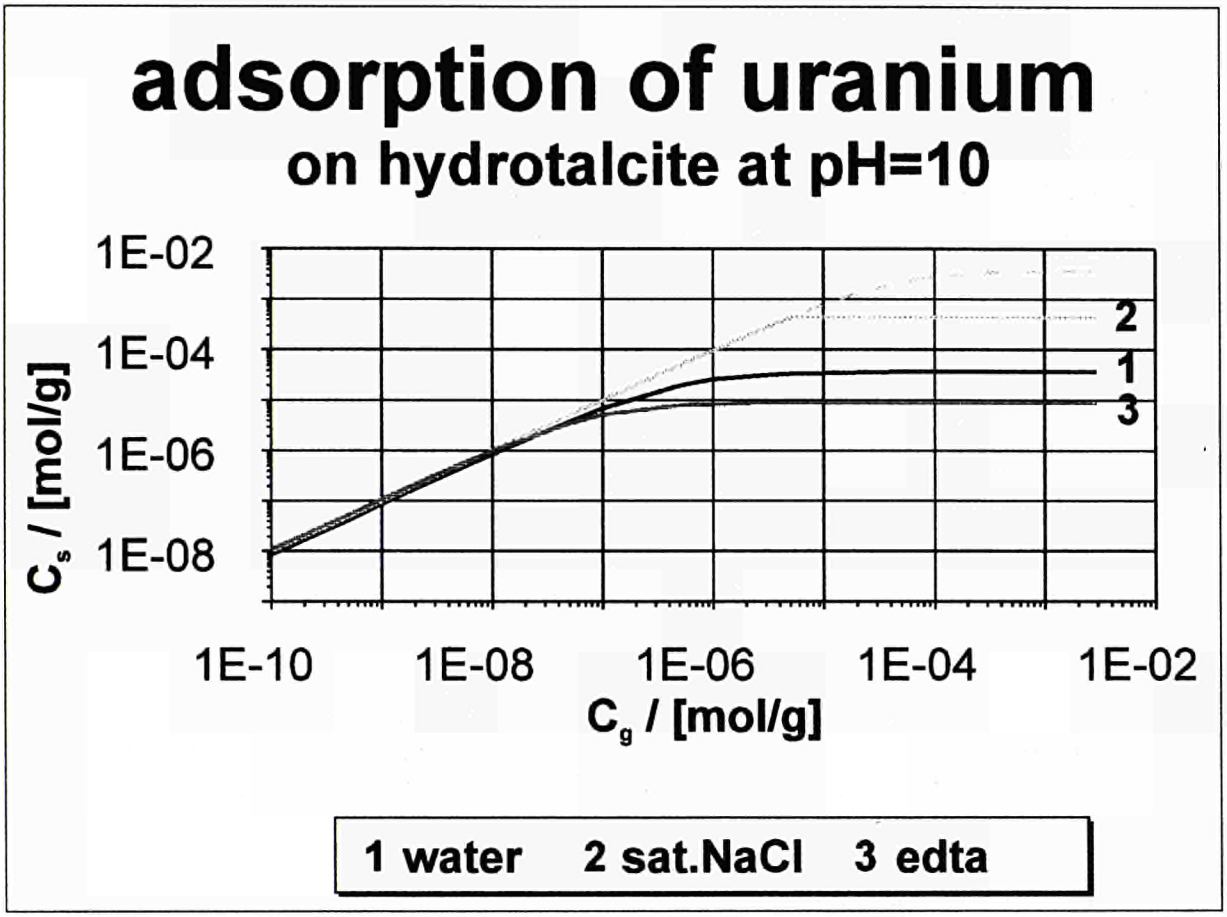

Title: **Some Aspects of Leaching Mechanisms of Ions Incorporated in Cement or Polymer**

Contractor: NCSR "Demokritos"

Contract No.: FI2W-CT93-0124

Duration of Contract: from 1 March 1993 to February 1995

Period covered: January 1- December 31, 1994

Project Leaders: S.G. Amarantos and J.H. Petropoulos

A. OBJECTIVES AND SCOPE

The present work aims at further elucidation of some mechanisms which govern the elution, by water, of some important ions from solids simulating solidified low or medium level radioactive wastes.

The distribution of Sr ion in the cement matrix after a long period of leaching as well as the physicochemical state of water within the pores in this matrix is under investigation.

In the work concerning polymers the experimental study of the sorption and diffusion behavior of a model polymer-NaCl-H_2O system will permit more detailed application and testing of the theoretical approach describing the elution of salts of both high and low solubility embedded in hydrophobic matrices, taking into account the concurrent imbibition of water.

B. WORK PROGRAMME

B.1 Cement

B.1.1 Distribution of Sr.

B.1.1.1 Experiments with specimens containing inactive Sr in the form of $SrSO_4$.

B.1.1.2 Experiments with specimens containing Sr-90 in the form of $Sr(NO_3)_2$.

B.1.2 Physicochemical state of water.

B.1.2.1 Thermogravimetric and differential scanning calorimetry measurements.

B.1.2.2 Porosimetry measurements.

B.2 Polymer

B.2.1 Sorption and diffusion experiments with NaCl in polymer films and parallel measurements of the rate of water sorption.

B.2.2 Equilibrium water uptake by polymer films at different relative humidities and salt content.

B.2.3 Study of ion transport using Na-22 and Cl-36 tracers.

B.3 Modelling and Interpretation of results

C. PROGRESS OF WORK AND RESULTS OBTAINED

State of advancement

The distribution of non-eluted strontium along the diffusion axis in cement specimens subjected to leaching under full or minimum exposure to atmospheric CO_2 was studied. The Sr was incorporated in the form of Sr-90 with or without added $Sr(NO_3)_2$. The results showed that the embedded Sr exists in the cement matrix in strongly and less strongly immobilized forms. The presence of atmospheric CO_2 results in enhancement of the Sr surface concentration because of its precipitation as $SrCO_3$.

Significant information about the physicochemical state of water within the pores of the cement matrix ("free" or "bound" water) was obtained by thermogravimetric measurements of hydrated samples and was found to be in general accord with conclusions drawn from low temperature differential scanning calorimetry. Porosity measurements are to be performed soon.

Further sorption and diffusion experiments with NaCl in polymer films were carried out. Elution results of films equilibrated in concentrated NaCl solutions showed evidence of a marked acceleration of the elution process attributable to the concurrent influx of water. Measurements of the rate of water sorption by neat polymer films were also performed. Equilibrium water vapour sorption results on neat films were complemented with data on NaCl-containing films, which showed markedly higher water uptake in accord with expectation. Sorption and diffusion experiments using NaCl solutions containing Na-22 and Cl-36 tracers were performed. No significant difference between anion and cation partition coefficients was observed. Desorption of Na-22 or Cl-36 in all concentrations studied conformed to Fickian kinetics.

Progress and Results

1. Cement specimens

B.1.1.2 Distribution of Sr along the diffusion axis of specimens containing Sr-90

Four series (E,F,G,H) of cylindrical specimens (diameter ≅height≅4 cm) initially containing 740 KBq of Sr-90 in the form of $Sr(NO_3)_2$ with added $NaNO_3$ (8% by wt) were used; specimens of series G and H contained, in addition, $Sr(NO_3)_2$ (0.15% by wt). They had been subjected to leaching (with only one flat surface exposed to leachant) by stagnant distilled water renewed periodically at 30°C, under "full" (series E,G) or "minimum" (series F,H) exposure to atmospheric CO_2 /1/. After six years of leaching, the fractional amount of radioactivity eluted was 1.3-1.8% for the former and 2.6-4.6% for the latter case.

For distribution studies the specimens were ground up progressively normal to the diffusion axis to a distance of ~10 mm from the eluted surface. The radioactivity remaining in each powdered cement layer was measured /2/. The remaining $NaNO_3$ in a blank cement specimen with the same leaching treatment was also studied. The distribution of Sr-90 in the cement specimens of series E,F and G,H is presented in Figs 1 and 2 respectively, where C is the measured radioactivity in a layer of the specimen located at distance x from the surface exposed to leachant (x=0) and C_o is the radioactivity initially incorporated. In the cases of minimum exposure to CO_2 (open points), the flattening of the concentration profiles near the surface shows that a high proportion of Sr (~80% for the specimens of series F and ~60% for those of series H) is strongly immobilized; accordingly, the leached percentage in the latter case was higher, as measured in the leachates. The amount of Sr over 60 or 80% must also be largely immobilized because its elution proceeded very slowly compared with that of Na (see

Fig. 1). The presence of CO_2 resulted in a considerable reduction of the leaching rate and a surface accumulation of Sr due to its precipitation as $SrCO_3$.

B.1.2.1 Thermogravimetric and differential scanning calorimetry measurements

The water loss of cement, exposed to a current of dry N_2, as a function of increasing temperature was investigated by thermogravimetric analysis (TGA). This technique yields information on the physicochemical state of water within the pores of the cement matrix as it provides a direct measurement of imbibed water which is "free" or bound to the cement substrate. Thermogravimetric studies were performed on samples taken from cemented specimens used in previous static elution experiments (with one flat surface of the specimen exposed to stagnant water) at 30 or 70°C /1/. The said samples were taken from, or far from, the exposed surface of the specimen and were "fully" or partially hydrated (by exposure to Relative Humidity, RH 100% or lower RH respectively) and heated from room temperature to 250°C in the TGA apparatus using a N_2 flow rate of 50 ml/min. A particle size of 105-149 µm and a heating rate of 5°C/min were chosen for all TGA measurements.

Representative TGA and DTG (derivative TG) plots of samples which had been equilibrated at various RH are presented in Fig. 3, where the weight (W) of the sample is shown in the upper curves and the rate of the weight loss at any point of the TGA curve is given by the DTA curves (lower plots). All DTG curves of Fig. 3 exhibit two distinct peaks. The first one can be related to "free" water present in large pores, while that located in narrow pores or at pore walls (physically "bound" water) gives rise to the second peak. From curves A', B' and C' it is clear, that as the water content of the sample is reduced (by equilibrating at lower humidities), the area of the first peak attributed to free water decreases much more markedly than the second peak. In the case of the specimen leached at 70°C (curves E,E') the fraction of free water is much higher and a shift of both peaks to lower temperatures is indicative of the presence of wider pores in agreement with conclusions drawn from previous mercury porosimetry results /1/. Quantitative results from TGA curves are presented in Table I, where the fraction of "free" water content is compared with the equivalent fraction of imbibed "bulk" water, f_{WB}, estimated by DSC /1/ in equivalent samples with the same water content. As indicated in Table I, the former results differ from the latter in absolute value (because of the different assumptions involved in the estimation of these values), but agree, as far as the relative variation of these values is concerned, which is the important point here.

2. Polymer specimens

B.2.1 Sorption and diffusion experiments with NaCl in polymer films and parallel measurements of the rate of water sorption

Previous equilibrium sorption experiments using cellulose acetate films (120 µm thick) at concentrations c=0.05 or 0.12 g/cm^3 of salt solution have been extended to a concentration of 0.25 g/cm^3. After equilibration films were subjected to elution by distilled water with stirring at 25°C. The values of the partition coefficients for the concentration studied here, were generally higher than those determined for the lower concentrations, while the water content of the film in equilibrium with c=0.25 g/cm^3 was found to be substantially less than that observed in the case of less concentrated solutions. NaCl elution tests were performed with parallel measurement of the rate of the water uptake. In Fig. 4, the salt elution and the concurrent water uptake of a film equilibrated at c=0.25 g/cm^3 is presented. $\Sigma a_n/A_o$ represents the fraction of salt desorbed or water taken up by the film (Σa_n: total amount of salt desorbed or of water taken up at time t, A_o: the original

amount of salt or the final equilibrium amount of water after full depletion of salt). The S shape of elution curve B indicates an acceleration of the elution process due to influx of water. The corresponding water uptake (curve B_1) exceeds the final equilibrium value and then passes through a maximum followed by a slow approach to the aforesaid equilibrium. Curve A which represents a typical elution curve of a film equilibrated in a salt solution of $c \leq 0.12$ g/cm^3 is shown for comparison.

Measurements of the rate of water absorption by neat polymer films were also performed, by immersing the latter in water and weighing at various time intervals. Films were previously, either dried by evacuation or partially hydrated by equilibrating at constant RH. Curve W of Fig. 4 represents the water uptake by a neat film (partially hydrated by equilibrating at RH=70%) where a slow approach to equilibrium is also observed.

The effect of ageing of the polymer matrix after successive equilibrations with salt solutions followed by elution tests was also investigated. Sorption parameters (partition coefficients and water content of the matrix) were not markedly affected when c=0.05 g/cm^3; a relatively small increase was noticeable when c=0.12 g/cm^3; while a marked increase was observed when c=0.25 g/cm^3, indicating that some structural changes (more intense at higher c) are induced by this cyclic absorption-desorption treatment.

B.2.2 Equilibrium water uptake by polymer films at different relative humidities and salt content

Further water vapor sorption experiments were performed at 25°C with neat or salt-loaded films. Loading of the film with salt was effected by equilibration with 0.25 g/cm^3 NaCl solution, resulting in a salt content of 12 mg/g of polymer. The film samples were first dried by evacuation, and then equilibrated with atmospheres of progressively higher or lower humidity. The water vapor sorption isotherms are presented in Figure 5 where the water regaion C_W is given on a dry polymer basis. A hysteresis effect which is more intense in the case of neat films, is observed. The higher equilibrium values of water sorption for the salt-loaded films are obviously associated with the presence of the osmotically active salt. Upon contact with water vapor activities equal to or higher than 0.84 (i.e. the water activity of the 0.25 g/cm^3 salt solution) the films tend progressively to whiten. If the water activity in the vapor phase is subsequently reduced to values lower than the above RH value, the film becomes transparent once again. At RH > 96% water droplets appeared on the polymer surface thus making further measurements impossible.

B.2.3 Study of ion transport using Na-22 and Cl-36 tracers

Sorption and diffusion of Na^+ and Cl^- separately was studied by equilibrating cellulose acetate films with salt solutions containing Na-22 or Cl-36 tracers, followed by elution of the tracer by inactive NaCl solutions of the same concentration as the equilibrating solution. The partition and diffusion coefficients of each ion separately were estimated. Some representative results are presented in Table II. In the range of concentrations studied, values of K_p for Na^+ and Cl^- (estimated from the ratio of the activity absorbed by the polymer to that of the equilibrating solution) did not differ significantly. The relatively small increase of K_p with c is in keeping with results previously determined from inactive NaCl sorption measurements /2/. Diffusion of Na-22 (curve B* of Fig. 4) and Cl-36 followed Fickian kinetics even in the case of films equilibrated and desorbed in the 0.25 g/cm^3 salt solution as no simultaneous influx of

water into the polymer occurs under these conditions. The diffusion coefficient of Cl^- was found to be higher than that of Na^+ in all cases, as also observed by others (e.g. /3/).

REFERENCES

/1/ AMARANTOS, S G., PAPADOKOSTAKI, K.G. and PETROPOULOS, J.H., Report No. EUR 13543 EN(1991).

/2/ AMARANTOS, S G., PAPADOKOSTAKI, K.G. and PETROPOULOS, J.H., Intermediate Report (January-June 1994), CEC-NCSR "Demokritos". Contract No. FI2W-CT93-0124 (July 1994).

/3/ CHAUDRY, M.A. and MEARES, P., ACS Symposium series, No. 153 (vol. 1), 101 (1981).

TABLE I. RESULTS OF TGA MEASUREMENTS ON SAMPLES TAKEN FROM LEACHED SPECIMENS AND EQUILIBRATED AT DIFFERENT RELATIVE HUMIDITIES

Specimen No.	Leaching period (days)	Leaching temp. (^oC)	RH (%)	"Free" water content % wt (dry cement basis)	Total water content % wt (dry cement basis)	Fraction of "free" water	f_{WB}
1-interior	50	30	100	11.9	19.9	0.59	0.21
			78	6.9	14.1	0.49	0.10
			55	4.7	11.3	0.41	0.044
2-interior	900	30	100	12.0	20.3	0.59	0.21
2-surface			100	14.4	23.0	0.62	0.31
3-surface	180	70	100	17.9	24.9	0.72	0.50

TABLE II. PARTITION COEFFICIENT (K_p) AND DIFFUSION COEFFICIENT (D) OF Na^+ AND Cl^-

c (g/cm^3)	K_p		D x 10^9 (cm^2/s)	
	Na^+	Cl^-	Na^+	Cl^-
0.05	0.0383	0.0363	1.0	3.2
0.12	0.0493	0.0504	1.1	-
0.25	0.0586	0.0636	0.9	1.6

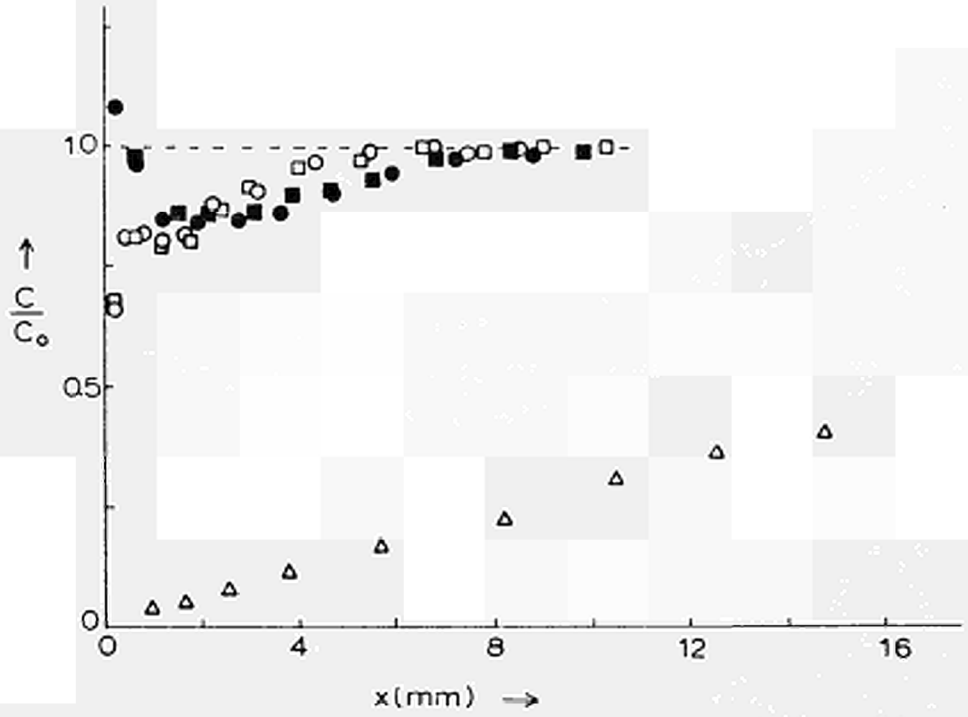

Fig. 1 Distribution of non-eluted Sr-90 (o,□,●,■) in four cement specimens of series E (●,■) or F(□,o) after six years of leaching at 30°C and distribution of non-eluted Na (Δ) in a blank specimen with the same original $NaNO_3$ content (8% wt) and the same leaching treatment.

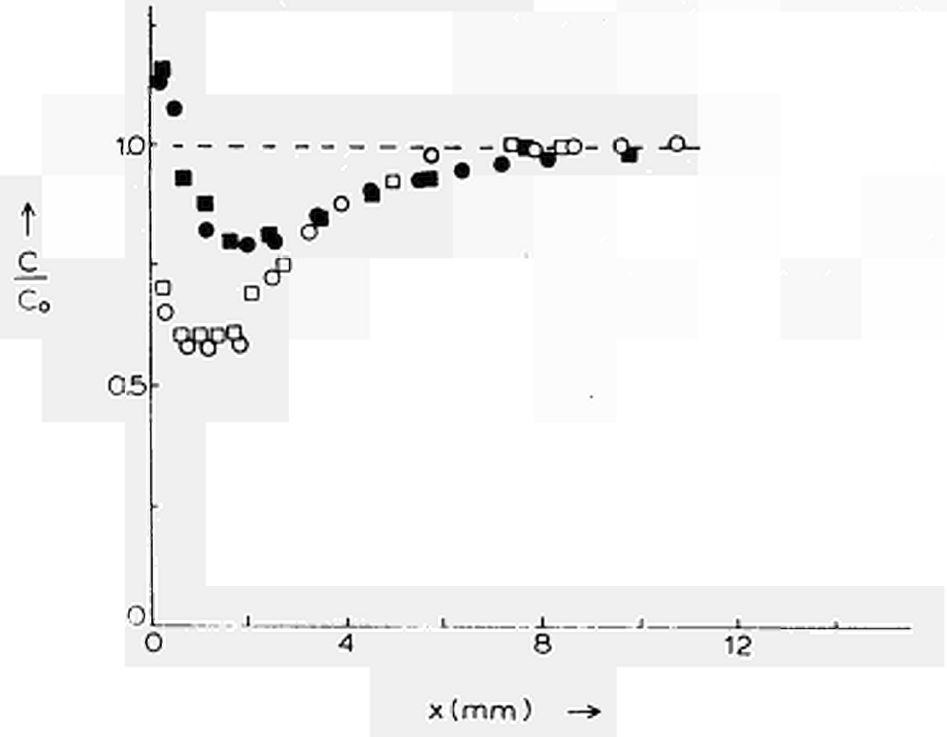

Fig. 2 Distribution of non-eluted Sr-90 in four cement specimens of series G(●,■) or H (o,□) after six years of leaching at 30°C.

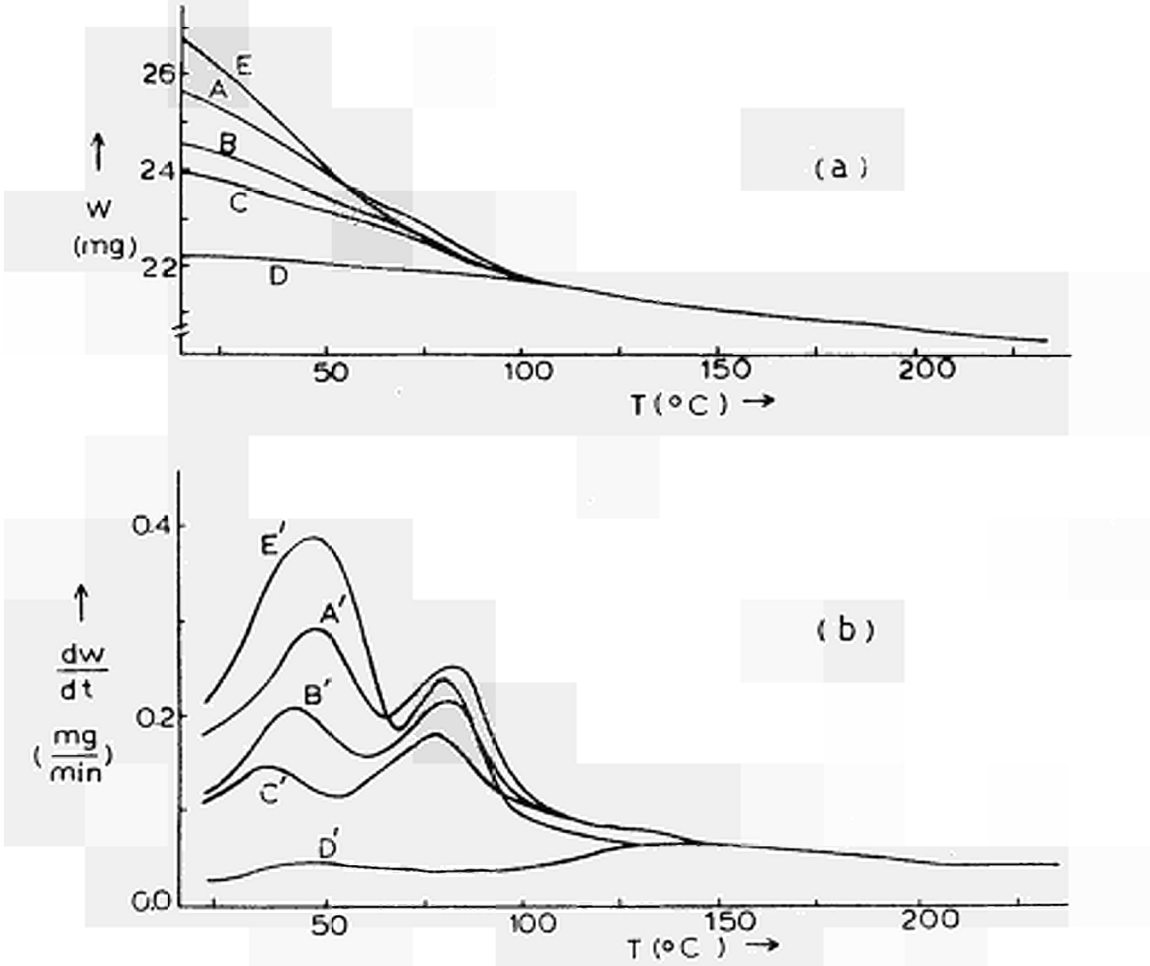

Fig. 3 (a) TGA and (b) DTG plots of cement samples taken from specimen No 1(A,B,C) or 3 (curve E) of Table I and equilibrated at RH=100% (curves A,A' and E,E'), 78% (curves B,B') or 55% (curves C,C'). Curves D,D' refer to a cement sample dried in an oven at 105°C for two hours.

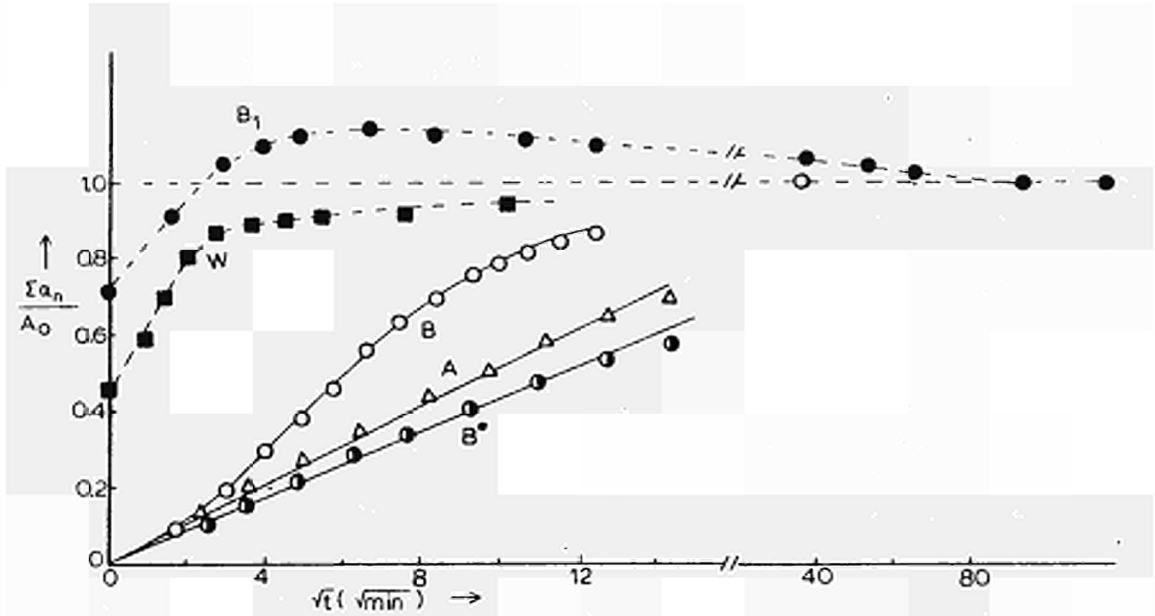

Fig. 4 A,B: Elution of NaCl from films equilibrated with 0.05 (Δ) or 0.25 (o) g/cm^3 NaCl solutions.
B*: Desorption of Na-22 from a film equilibrated with a NaCl solution (0.25 g/cm^3) and desorbed in a solution of the same concentration.
B_1: Water uptake during salt elution of case B.
W: Water uptake by a neat polymer film.

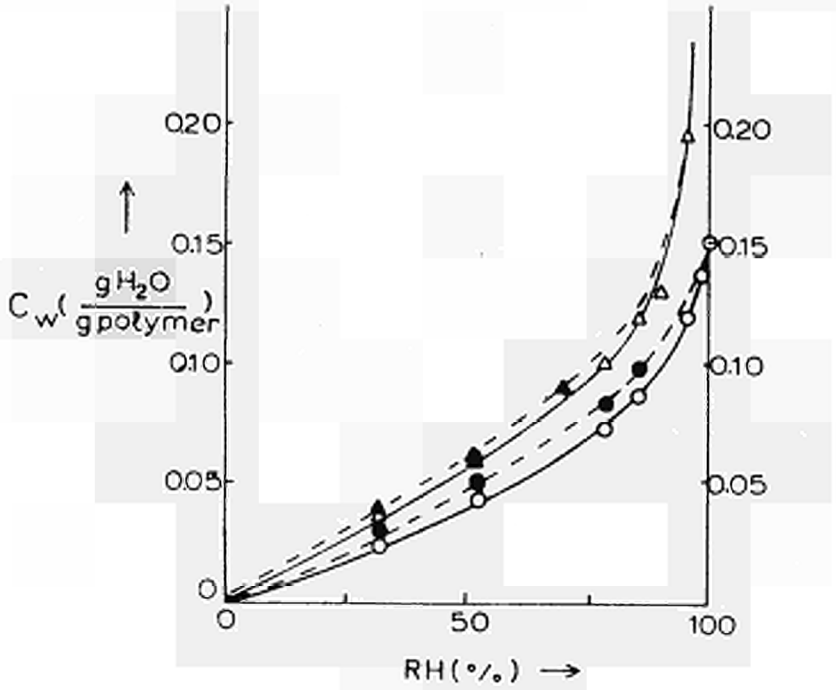

Fig. 5 Water regain of a neat (o,●) or salt-loaded (Δ,▲) polymer film equilibrated at various RH by absorption (o,Δ) or desorption (●,▲).

Title	Corrosion of Selected Packaging Materials for Disposal of Heat-Generating Radioactive Wastes
Contractors	Forschungszentrum Karlsruhe; ENRESA Madrid
Contract N°	FI2W-CT90-0030
Duration of contract	January 1991 - December 1994
Period covered	January 1994 - December 1994
Project leader	E. Smailos

A. OBJECTIVES AND SCOPE

In previous corrosion studies, carbon steels and the alloy Ti 99.8-Pd were identified as promising materials for heat-generating nuclear waste packagings acting as a barrier in a rock-salt repository. To characterize the corrosion behaviour of these materials in more detail, a research programme including laboratory-scale and in-situ corrosion studies has been undertaken jointly by KfK and ENRESA/INASMET. Besides carbon steels and Ti 99.8-Pd, also Hastelloy C4 and some Fe-base materials will be examined in order to complete the results available to date.

The research programme has two objectives:

- Investigation of the influence of essential parameters on the corrosion behaviour of the materials in disposal relevant salt brines. These parameters are: temperature, gamma radiation and selected characteristics of packaging manufacturing (KfK).
- Investigation of the resistance of carbon steels to stress corrosion cracking in an $MgCl_2$-rich brine at various temperatures and strain rates by means of the slow strain rate technique (ENRESA).

B. WORK PROGRAMME

B.2.1 Corrosion studies on the unalloyed fine-grained steel in three salt brines (two $MgCl_2$-rich, one NaCl-rich) at 150°C and gamma dose rates of 1 Gy/h and 10 Gy/h (laboratory-scale immersion tests, KfK).

B.2.2 Corrosion studies of two low-alloyed steels (TSt E 460, 15 MnNi 6.3) in three salt brines at 150°C (laboratory-scale immersion tests, KfK).

B.2.3 In-situ corrosion studies on specimens of Fe-base materials, Ti 99.8-Pd and Hastelloy C4 in rock salt at rock temperature (reference experiments, KfK).

B.2.4 In-situ corrosion studies on tubes of carbon steel, Ti 99.8-Pd and Hastelloy C4 provided with selected container manufacturing characteristics in rock salt/brines at 90°C-200°C (KfK).

B.2.5 Statistical analysis of corrosion data (KfK).

B.2.6 Stress corrosion cracking studies on unalloyed and low-alloyed steels (fine-grained steel, TSt E 460, 15 MnNi 6.3) in an $MgCl_2$-rich brine at various temperatures (25°C, 90°C, 170°C) and slow strain rates (10^{-4} - 10^{-7} s^{-1}) (ENRESA / INASMET).

C. PROGRESS OF WORK AND RESULTS OBTAINED

State of advancement

In the period under review, the long-term corrosion behavior of the preselected unalloyed fine-grained steel TStE 355 was investigated at 170°C in the vapor phase of a disposal relevant $MgCl_2$-rich brine. Experiments were conducted both in pure brine and in brines containing salt impurities, such as sulfides in concentrations of $6x10^{-4}$ - $6x10^{-3}$ M/l. Moreover, the stress corrosion cracking studies on three selected carbon steels (one unalloyed, two low alloyed) in the $MgCl_2$-rich brine at slow strain rates ($(10^{-4}$-10^{-7} $s^{-1})$ and various temperatures were completed by examination of the steels at 25°C.

PROGRESS AND RESULTS

B.2.1 Corrosion studies on the unalloyed TStE 355 steel in brines (KfK contribution)

The preselected TStE 355 carbon steel (0.17 wt.% C; 0.44 wt.% Si; 1.49 wt% Mn; bal. Fe) was examined for general and local corrosion in the vapor phase of an $MgCl_2$-rich brine at 170°C. Such experiments simulate conditions after intrusion of limited amounts of brine into the lower part of the HLW boreholes and location of the up to 300 m stacked containers in the vapor phase of the brine. In addition to the investigations in pure brine, experiments were conducted in sulfide containing brines in order to examine the influence of this salt impurity on corrosion.

The $MgCl_2$-rich brine (Q-brine, pH (25°C)=4.6) used as corrosion medium had the following composition in wt.%:

26.8 $MgCl_2$; 4.7 KCl; 1.4 NaCl; 1.4 $MgSO_4$; 65.7 H_2O.

For the experiments in the presence of sulfides, Na_2Sx9H_2O was added to the brine at concentrations of $6x10^{-4}$ M/l, $3x10^{-3}$ M/l, and $6x10^{-3}$ M/l, respectively. The experiments were performed in stainless steel pressure vessels with corrosion-resistant PTFE inserts (250 ml volume), and lasted up to 320 days. All specimens were evaluated for general and local corrosion by gravimetry, measurements of pit depth, surface profilometry and metallography.

The regression analysis of the time-dependent thickness reduction of the steel at 170°C in the vapor phase of the brines shows that a linear equation fits the experimental data well. This is in good agreement with previous results obtained for steel specimens in the liquid phase of these brines [1]. The results of the linear regression analysis of the thickness reduction of the steel in the various brines are compiled in Tab. I. For comparison, the corrosion results in the liquid phase of the brines determined in earlier work [1] are also given in Tab.I.

In the vapor phase of the Na_2S-free brine, the linear corrosion rate of the steel is about 10 µm/a and, hence, significantly lower than that in the liquid phase (about 200 µm/a). By Na_2S additions of $6x10^{-4}$ - $6x10^{-3}$ M/l to the brine, the vapor-phase corrosion rate is increased to about 20-40 µm/a. However, the values remain clearly lower than those in the liquid phase (about 192-317 µm/a). Both in the liquid and in the vapor phase of the brines, the maximum corrosion rate occurred at a Na_2S concentration of $3x10^{-3}$ M/l. At the higher Na_2S concentration of $6x10^{-3}$ M/l the corrosion rates decreased. This effect may probably be attributed to the formation of a denser corrosion layer at the higher Na_2S concentration, as was observed in the metallographic examinations.

Tenacious black corrosion products were present on all the steel specimens following exposure to the water vapor-saturated gas phase of the brines with and without Na_2S. X-ray diffraction and Mössbauer-spectroscopic analyses have shown that the corrosion products primarily consisted of Fe_3O_4 (magnetite). In addition, α-Fe_2O_3 (hematite) and α/β-FeOOH were identified. The formation of

higher oxidation-state oxides such as Fe_2O_3 or FeOOH was due to the fact that oxygen was present during the tests. The presence of tenacious corrosion products of Fe_3O_4 in the specimens is consistent with the observed low rates of general corrosion in the vapor phase of the brines.

In previous corrosion studies on fine-grained steel in the liquid phase of $MgCl_2$-rich brines [1,2],a magnesium-containing ferrous hydroxide, $(Fe,Mg)(OH)_2$, of amakinite structure was identified as the primary corrosion product, without evidence of Fe_3O_4. It appears that Mg^{2+}, when present at high concentrations in the brine, inhibits the normal formation of Fe_3O_4 from a $Fe(OH)_2$ precursor. The higher corrosion rates observed in the liquid phase of the brines, compared to the vapor phase, suggest that $(Fe,Mg)(OH)_2$ is less protective than Fe_3O_4. A further reason for the high liquid-phase corrosion is considered to be the high HCl concentration of the brine. This could be explained by the high Cl^- concentration and the hydrolysis of Mg^{2+}. The formation of $(Fe,Mg)(OH)_2$ in $MgCl_2$-rich salt brines and the increase of the corrosion rate of steels with magnesium concentration have also been reported by Westerman et al. [3].

The contribution of oxygen to corrosion should be low, because the limited amount of oxygen (about 15 mg) available in the closed experimental equipment will be consumed after a relatively short time due to the reaction with iron.

It is evident from the metallographic examinations and the surface profiles of specimens exposed to the vapor phase of the brines that the steel is resistant to pitting corrosion in the sense of an active-passive corrosion element. As in the liquid phase, a non-uniform general corrosion of a maximum depth of 80-100 µm was observed in all brines with and without Na_2S. However, with increasing test duration this uneven corrosion attack spread over the specimen surface rather than penetrated into the metal and the penetration rate decreased. Therefore, the gravimetrically determined general corrosion rates (about 10-43 µm/a) are of decisive importance for long-term predictions of the container lifetime in the vapor phase of the $MgCl_2$-rich Q-brine. In general it can be stated that the corrosion rates of the steel in the vapor phase of the test brines imply corrosion allowances that are technically acceptable for thick-walled containers. According to the results available at 170°C in the vapor phase of $MgCl_2$-rich brines, corrosion allowances of about 3 mm in sulfide-free brine and 6-12 mm in sulfide-containing brines are needed for containers made of TStE 355 steel with a service life of e.g. 300 years. Such values are clearly lower than those calculated for liquid-phase corrosion (about 55 mm).

B.2.6 Stress corrosion cracking studies on carbon steels (ENRESA / INASMET contribution)

Further stress corrosion cracking studies were performed on three preselected carbon steels in the $MgCl_2$-rich Q-brine (brine 1) at 25°C and slow strain rates of 10^{-4}-10^{-7} s^{-1}. The steels investigated were: the low alloyed steels TStE 460 and 15 MnNi 6.3 and the unalloyed fine-grained steel TStE 355. The steels had the following composition in wt.%:

TStE 460 : 0.18 C; 0.34 Si; 1.5 Mn; 0.51 Ni; 0.15 V; bal. Fe
15 MnNi6.3 : 0.17 C; 0.22 Si; 1.59 Mn; 0.79 Ni; bal. Fe
TStE 355 : 0.16 C; 0.41 Si; 1.5 Mn; bal. Fe.

The parent materials for TStE 355 and TStE 460 were hot-rolled and annealed plates, and for 15 MnNi 6.3 forged and annealed disks. The experiments were performed in Hastelloy C-276 autoclaves at an argon pressure of 13 MPa. In order to be able to interpret the results obtained in the brine, additional comparative investigations were conducted in argon as the inert medium. For the experiments round specimens of 6 mm diameter, finished with 1,000 grade emery paper were used.

Load, position, time and temperature data were logged by the microprocessor that controls the slow strain rate machine. After each test the elongation (E), reduction of area (R.A.), energy, yield strength (Y.S.), maximum load, and true stress at fracture were calculated. To evaluate the resistance of the steels to stress corrosion cracking, metallographic and scanning electron microscopic (SEM) examinations of the fracture specimen surfaces were performed in addition to the tensile experiments.

The results of the slow strain rate tests obtained for the three steels in argon and Q-brine at 25°C and strain rates of 10^{-4}-10^{-7} s^{-1} are shown in Figs. 1 and 2. All values are the average of at least two experiments. The values of the yield strength, maximum load and energy in Q-brine are very close to those in argon. However, the values of the elongation, reduction of area and true stress fracture in Q-brine are lower than those in argon, especially at the two slowest strain rates of 10^{-6} and 10^{-7} s^{-1}. Nevertheless, the loss of ductility of the steels at 25°C in Q-brine is not significant and much lower than that observed at the higher test temperatures of 90°C and 170°C [4,5,6].

In the metallographic examinations of steel specimens tested in argon and Q-brine, so signs of sensitivity to stress corrosion cracking, such as secondary cracks were observed under any of the test conditions. In case of the forged 15MnNi 6.3 steel, small areas of non-uniform general corrosion due to the local breaking of the corrosion surface layer were observed, particularly at the strain rate of 10^{-5} s^{-1}. The scanning electron microscopic (SEM) examinations show a ductile fracture surface for the steel specimens tested both in argon and Q-brine. Only at the slowest strain rate of 10^{-7} s^{-1}, some small brittle areas were observed for the steels after testing in Q-brine. This slight loss of ductility is likely due to the embrittling effect of the hydrogen produced during corrosion of the steels, as already discussed in previous work [4]. However, this effect is no significant.

REFERENCES

[1] SMAILOS, E., SCHWARZKOPF, W., KIENZLER, B., KÖSTER R., "Corrosion of Carbon-Steel Containers for Heat-Generating Nuclear Waste in Brine Environments Relevant for a Rock-Salt Repository," Mat. Res. Soc. Symp. Proc., C.G. Sombret, ed., Vol. 257, 399 (1992).

[2] SMAILOS, E., KÖSTER, R.,"Corrosion of HLW Packaging Materials in Disposal Relevant Salt Brines," Proc. of the Third International Conference on High Level Radioactive Waste Management, Las Vegas, Nevada, April 12-16, 1992, Vol. 2, p. 1676.

[3] WESTERMAN, R.E., HABERMAN, J.H., PITMAN, S.G., PULSIPHER, B.A., SIGALLA, L.A., "Corrosion and Environmental-Mechanical Characterization of Iron-Base Nuclear Waste Package Structural Barrier Materials", PNL Report 5426, Pacific Northwest Laboratories (1986).

[4] SMAILOS, E., FIEHN, B., GAGO, J.A., AZKARATE, I., "General Corrosion and Stress Corrosion Cracking Studies on Carbon Steels for Application in Nuclear Waste Disposal Containers," KfK 5166 (1993).

[5] SMAILOS, E., SCHWARZKOPF, W., GAGO, J.A., AZKARATE, I. "Corrosion Studies on Selected Packaging Materials for Disposal of Heat-Generating Radioactive Wastes in Rock - Salt Formations," KfK 5011 (1992).

[6] SMAILOS, E., FIEHN, B., GAGO, J.A., AZKARATE, I., "Corrosion Studies on Selected Metallic Materials for Application in Nuclear Waste Disposal Containers," KfK 5309 (1994)

List of publications in 1994

SMAILOS, E., "Corrosion of High-Level Waste Packaging Materials in Disposal Relevant Brines", Nuclear Technology, 104 (1993) pp. 343-350.

SCHWARZKOPF, W., SMAILOS E., KÖSTER, R., "In-situ Corrosion Studies on Selected Packaging Materials for Disposal of Heat-Generating Nuclear Wastes in Rock Salt Formations", In-Situ Testing of Radioactive Waste Forms and Engineered Barriers: Proc. of a Workshop, Corsendonk, Belgium, October 13-16, 1992, EUR-15629 (1994).

ROTHFUCHS, T., SCHWARZKOPF, W., SMAILOS, E., "Overview of HLW In-Situ Tests at the Asse Salt Mine", In-Situ Testing of Radioactive Waste Forms and Engineered Barriers: Proc. of a Workshop, Corsendonk, Belgium, October 13-16, 1992, EUR-15629 (1994).

SMAILOS, E., FIEHN, B., GAGO, J.A., AZKARATE, I., "Corrosion Studies on Selected Metallic Materials for Application in Nuclear Waste Disposal Containers", KfK-5309 (1994)

Table I. Results of linear regression analyses for the thickness reduction ($\Delta S = A + B \cdot t$) of the fine-grained steel in the test brines at 170°C

Brine	Phase	Number of specimens	A (µm)	Standard error of A (µm)	B (µm/a)	Standard error of B (µm/a)
Q-brine	V	12	5.8	2.1	10.2	3.6
	L	14	24.5	8.4	199.4	15.0
Q-brine + 6x10^{-4} M/l Na_2S	V	10	7.6	3.2	18.2	5.8
	L	8	42.8	4.9	192.5	8.0
Q-brine + 3x10^{-3} M/l Na_2S	V	12	-2.8	3.0	43.5	5.1
	L	8	22.4	24.9	317.4	40.9
Q-brine + 6x10^{-3} M/l Na_2S	V	12	4.8	3.4	20.1	5.8
	L	8	44.9	14.0	203.0	23.0

V = vapor; L = liquid; test duration: 60-322 days

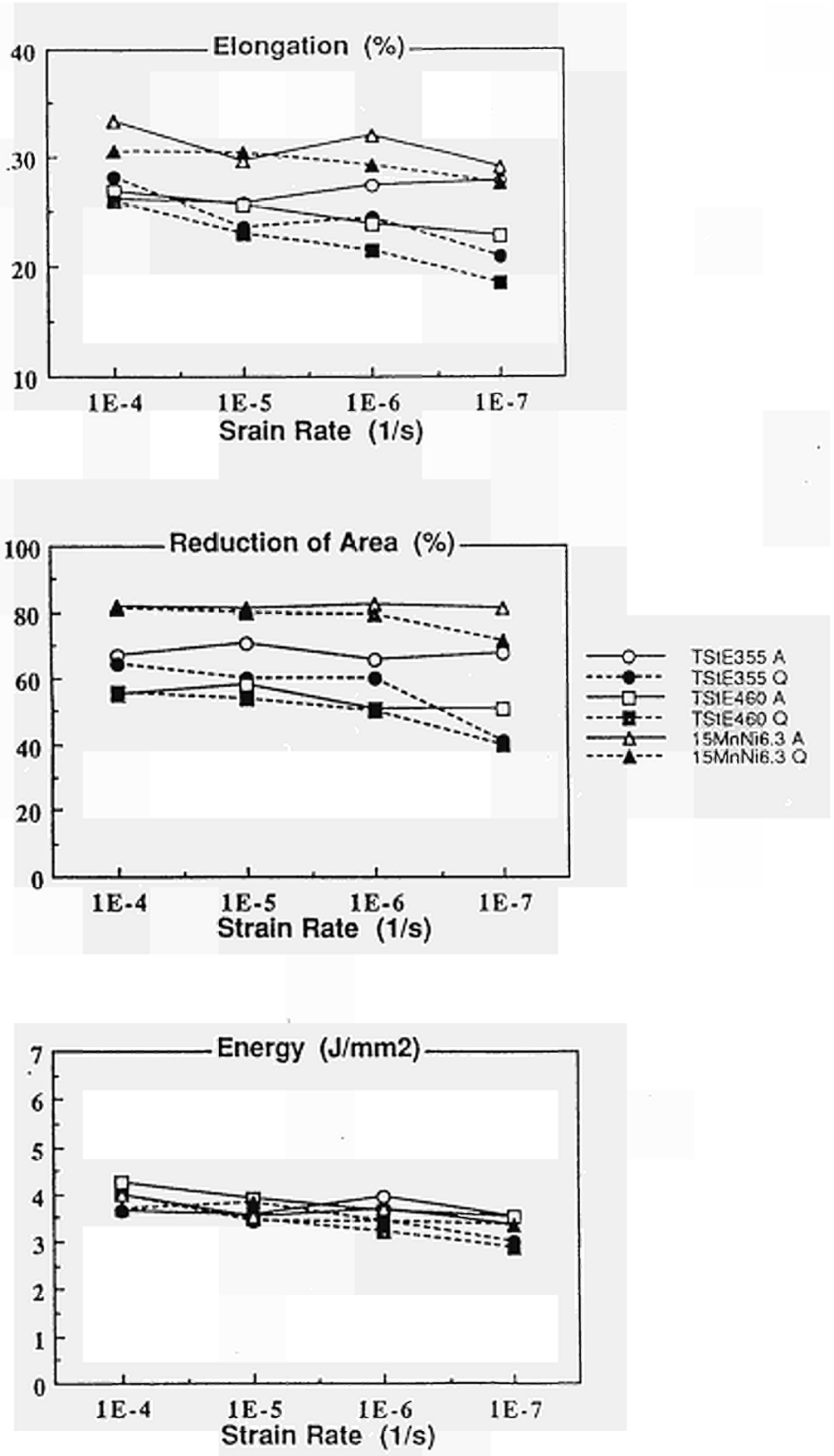

Fig. 1: Elongation, reduction of area and energy versus strain rate for the steels TStE 355, TStE 460 and 15MnNi 6.3 tested at 25°C and 13 MPa in argon and Q-brine

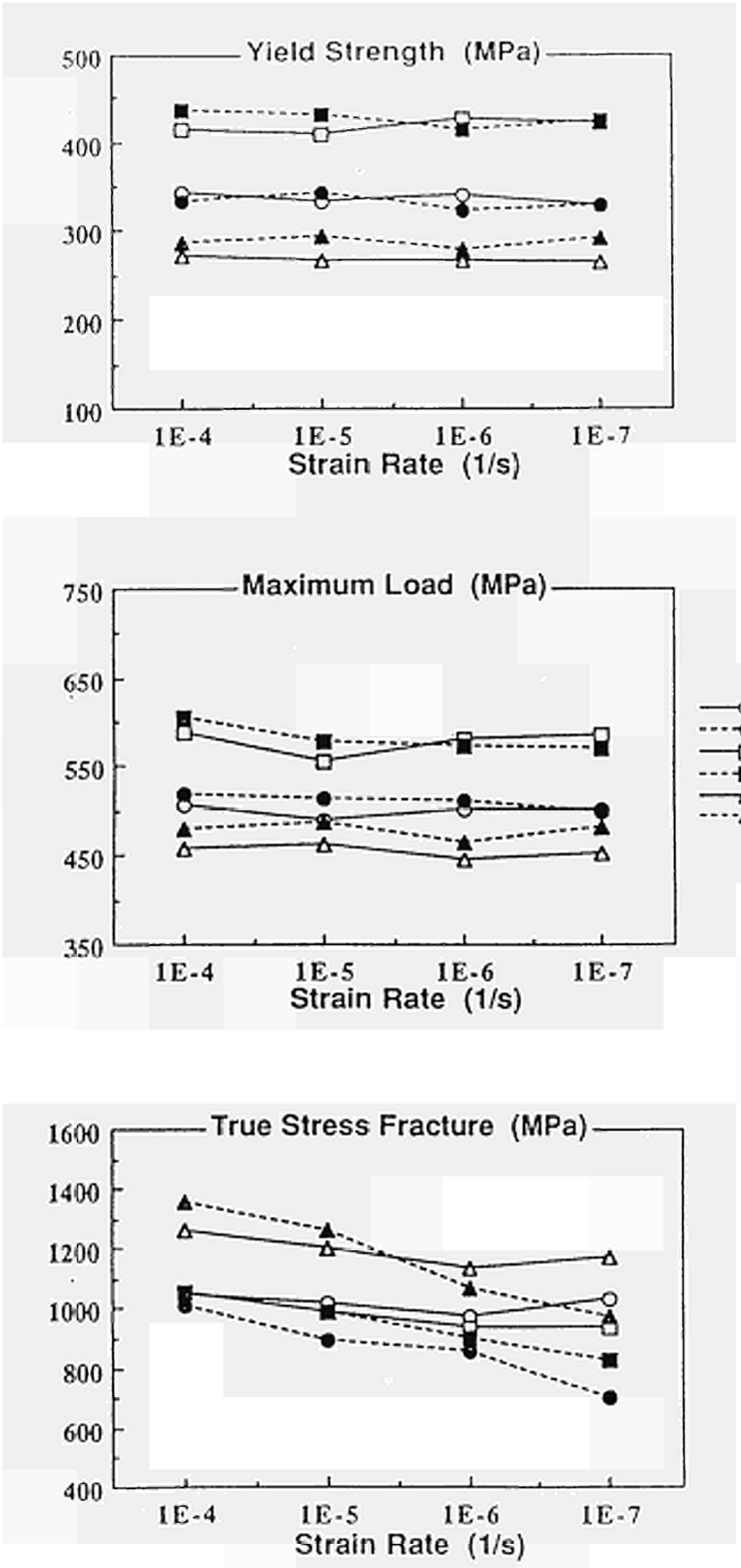

Fig. 2: Yield strength, maximum load and true stress fracture versus strain rate for the steels TStE 355, TStE 460 and 15MnNi 6.3 tested at 25°C and 13 MPa in argon and Q-brine

Title :	Theoretical and experimental study of degradation mechanisms of cement in the repository environment
Contractor:	CEA-Saclay/DCC/DESD/SESD
Contract N°:	FI2W-CT90-0035
Duration of contract:	January 1991 - November 1995
Period covered:	February 1994 - December 1994
Project leader:	Mme REVERTEGAT (Mr. ADENOT, since November 1994) - CEA, coordinator
	F. Adenot, E. Revertegat, C. Richet and L. Wu (CEA)
	D. Damidot, S.A. Stronch and F.P. Glasser (Aberdeen University)

A. Objectives and Scope

The object of the research program supported by CEC contract number F12W-CT90.0035 is to estimate the long-term corrosion of concrete used for waste disposal and to determine the mechanisms involved. Therefore we are developing a corrosion model based on the different mechanisms involved, in which it will be possible to introduce storage conditions specific to each site (type of corrosive solution, cement composition, storage temperature...).

B. Work programme

1. Investigation about degradation mechanisms involved when the cement paste is corroded by a solution containing aggressive ions :

- study of phases diagrams to determine which phases may coexist and acquisition of the thermodynamic data necessary to solve the model in the different possible cases (study of equilibria as functions of aggressive ions and temperature)
- study of degradation processes of cement pastes submitted to various aggressive environments (chlorides, sulphates, carbonates).

2. Testing of the local equilibrium hypothesis (by checking that the kinetics is effectively governed by diffusion)

3. Modelling of cement paste degradation :

- mathematics writing of the model equations built on the physico-chemical laws
- numerical resolution of the model by a microcomputer program : in a first step, a simplified algorithm is developed in order to validate the model equations
- model validation

C. Progress of work

Thermodynamic studies of complex groundwaters

Work has concentrated on utilising the data gathered and routines developed at earlier stages to investigate systems of particular importance to the chemical conditioning action of cements in the repository environment. The selected calculations concern the interaction of calcium aluminates with complex saline groundwaters.

At present, the method used allows us to determine the solid and aqueous compositions at equilibrium conditions. However, the kinetics, or rate of attainment, of equilibrium cannot currently be predicted by computation and must instead be subject to reasonable assumptions. Within the period covered by this report, results have been obtained from study of the interaction of the $CaO-Al_2O_3-H_2O$ system with $CaSO_4$-, $CaCO_3$- and $CaCl_2$- containing groundwaters, concentrating on simultaneous attacks. The systems investigated are $CaO-Al_2O_3-CaSO_4-CaCO_3-H_2O$, $CaO-Al_2O_3-CaSO_4-CaCl_2-H_2O$, $CaO-Al_2O_3-CaCO_3-CaCl_2-H_2O$ and $CaO-Al_2O_3-CaSO_4-CaCO_3-CaCl_2-H_2O$, all at 25°C. Results show that a total of twelve stable solids phases may persist at equilibrium conditions. These are the $CaO-Al_2O_3-H_2O$ phases portlandite ($Ca(OH)_2$), hydrogarnet (C_3AH_6) and gibbsite ($Al(OH)_3$), the sulfate phases gypsum ($CaSO_4.2H_2O$) and ettringite (AFt, $3CaO.Al_2O_3.3CaSO_4.32H_2O$), the carbonate phases calcite ($CaCO_3$), calcium hemicarboaluminate ($h\overline{C}A$, $3CaO.Al_2O_3.0.5CaCO_3.0.5Ca(OH)_2.10.5H_2O$) and calcium monocarboaluminate ($m\overline{C}A$, $3CaO.Al_2O_3.CaCO_3.10H_2O$) and the chloride phases $CaCl_2.6H_2O$, $3CaO.CaCl_2.15H_2O$, $CaO.CaCl_2.2H_2O$ and Friedel's Salt (F.S., $3CaO.Al_2O_3.CaCl_2.10H_2O$).

Selected Solution Compositions for the Isothermally Invariant Points in the $CaO-Al_2O_3-CaSO_4-CaCO_3-H_2O$ System at 25°C. Concentrations in mol/kg

Solids in equilibrium with aq.	[Ca]	[Al]	[SO_4]	[CO_3]	pH
CH + ett. + C_3AH_6 + $h\overline{C}A$	2.19e-2	7.59e-6	7.60e-6	1.62e-6	12.52
AH_3 + ett. + C_3AH_6 + $m\overline{C}A$	5.62e-3	3.47e-4	1.03e-5	3.13e-6	11.97
CH + $h\overline{C}A$ + $m\overline{C}A$ + ett.	2.19e-2	5.74e-6	9.15e-6	4.95e-6	12.52
$C\overline{C}$ + CH + $m\overline{C}A$ + ett.	2.19e-2	4.85e-6	1.02e-5	6.93e-6	12.52
AH_3 + $C\overline{C}$ + ett. + $m\overline{C}A$	5.02e-3	3.10e-4	1.46e-5	7.82e-6	11.92
gypsum + AH_3 + $C\overline{C}$ + ett	1.53e-2	7.03e-6	1.52e-2	8.39e-6	10.25

Initially, within the relevant parts of the $CaO-Al_2O_3-CaSO_4-CaCO_3-H_2O$ system at 25°C, $Ca(OH)_2$ maintains a pH of approximately 12.5. However, once $Ca(OH)_2$ is leached, the pH is still well buffered by the AFt and AFm type phases ($h\overline{C}A$, $m\overline{C}A$ and F.S.) even in the presence of increasing salinity. As $Ca(OH)_2$ is destabilised, the AFm and AFt phases assume the buffering action and the pH remains at 11.9 - 12.0. It is only after these phases become unstable that the pH drops significantly. This has important implications for the use of cement as a chemical barrier in waste immobilisation, as transuranics appear to have enhanced solubilities below pH~10.5.

Calculations also show that within the $Ca(OH)_2-CaCO_3-H_2O$ system, the pH decreases progressively at 25°, 50° and 85°C. However, the additional impact of NaCl on the system with increasing temperature is slight. It is useful to study these systems under the influence of sea water concentrations of NaCl because saline waters will be present at several European disposal sites.

Future work is targeted at investigating the effect of $CaSO_4$, $CaCO_3$ and $CaCl_2$ on the CaO-SiO_2-H_2O system, and on further investigation into the effect of NaCl on the CaO-Al_2O_3-H_2O and CaO-SiO_2-H_2O systems.

Degradation processes of cement pastes

Experiments were carried out on cement paste disks, made of Portland and blended cements (water/cement = 0.38) exposed to various aggressive environments at ambient temperature (pH 8.5 without corrosive ions* , pH 8.5 with $[CO_2] \sim 0.01$ mmol/l, pH 8.5 with $[Cl^-] = 20$ g/l or $[NaCl] = 0.56$ mol/l, pH 8.5 with $[SO_4^{2-}] = 10$ g/l or $[Na_2SO_4] = 0.10$ mol/l).

All these degradation experiments have been achieved except those in presence of carbonates which are still being performed.

At each date (3, 6, 12, 18, 24, 30 and 36 months), the following analyses have been carried out on samples: porosity by mercury intrusion, corroded thickness by X-ray diffraction, diffusion coefficient of tritiated water.

The measurement of the diffusion coefficient of tritiated water takes a long time. This year, we gathered the results for the main types of aggressive solutions at the different degradation periods. Thanks to these diffusion coefficients, we can estimate the diffusion coefficient in the corroded zone for each configuration. These coefficients are quite important for the understanding of the kinetics of degradation: the model shows that this diffusion coefficient controls the kinetics of degradation.

We also followed the kinetics of cement paste cylinders degradation by measuring the amount of leached ions (cf. figure 1)

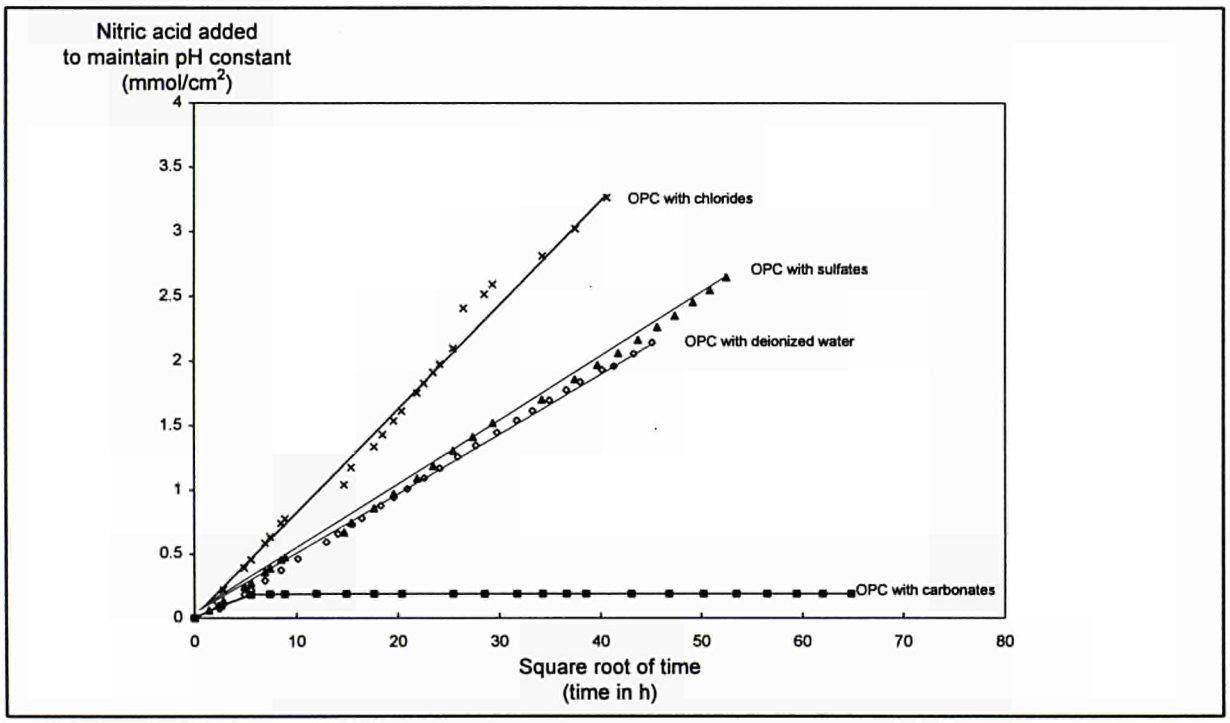

Figure 1: Nitric acid added as a function of the square root of time
OPC paste immersed in different aggressive solutions at pH = 8.5

* The reference experiment without aggressive ions could not be performed : there was some traces of carbonates in the aggressive solution.

The results obtained on OPC cement pastes and pastes made of clinker, blastfurmace slag and fly ash, in accordance with the results obtained by analysing the solid phase, show that the paste immersed with carbonates is the slowest to be corroded whereas the one immersed with chlorides is the fastest to be corroded. Between these two opposites stand the paste immersed without aggressive ions and the paste immersed with sulfates, the latter being slightly slower).
The carbonates from the corrosive solution provoke the development of carbonated phases, among which calcite. These phases, by filling pores, slow down significantly the migration of cement ions and therefore its corrosion.
The chlorides penetrate quite rapidly into the samples. By destabilizing portlandite and CSH, they speed up the corrosion.
The sulfates provoke the development of gypsum, which at a first stage slows down the corrosion. But this phase inflates and in the long term splits the samples. Nevertheless, this phase has difficulties to develop: therefore the degradation is very slightly slowed down.

The monitoring of leaching kinetics and the analysis of the leached solid phases show that the kinetics is controlled by diffusion and that the pore solution is in local equilibrium with the solid phases at every point of the cement paste.
Considering these experimental results, we have established a corrosion model and developed an algorithm to solve this model. It is validated in an ordinary case (cement paste with deionized water as the corrosive solution).

Title	The Performance of Cementitious Barriers in Repositories
Contractors	AEA Industrial Technology (co-ordinator); Risø National Laboratory; BAM; NRI
Contract N°	FI2W-CT90-0040
Duration of contract	1 May 1991 - 31 April 1995
Period covered	1 January 1994 - 31 December 1994
Project leader	Dr. A.W. Harris

OBJECTIVES AND SCOPE

Cementitious materials are likely to be used in waste disposal facilities to help retain radionuclides by acting as chemical and physical barriers to migration. Current source term calculations are based on the homogeneous repository assumption. This is unlikely to be true in reality since cementitious materials will crack, leading to inhomogeneities in mass transport and chemistry. The impact of these inhomogeneities will depend upon reactions with groundwater that can lead to the healing of cracks, to the benefit of the physical barrier performance, and sealing of concrete surfaces, to the detriment of chemical performance.

Validated models and supporting data for the physical and chemical barrier performance of cementitious materials will be developed and used to examine the simpler models employed in safety assessments. The mechanisms of crack healing within cementitious materials under repository conditions will be investigated. An assessment of the impact of cracks and inhomogeneities on the source term will be made. The reference repository will be based on the designs provided by Nirex and hence will be realistic.

WORK PROGRAMME

Task 1 - Healing of Cracks by Cementitious Materials

- Sub-task 1.1 - Experiments on crack healing
- Sub-task 1.2 - Modelling of crack healing

Task 2 - Cement-groundwater Interactions

- Sub-task 2.1 - Diffusive cement-groundwater interactions
- Sub-task 2.2 - Perfusive cement-groundwater interactions
- Sub-task 2.3 - Modelling cement-groundwater interactions

Task 3 - Barrier Properties of the Inhomogeneous Repository

- Sub-task 3.1 - Chemistry varying with position and time
- Sub-task 3.2 - Effect of fissures on the source term
- Sub-task 3.3 - Validation of source term model

Task 4 - Development and Application of Radon Emanation Technique

- Sub-task 4.1 - Initial experimental work
- Sub-task 4.2 - Upgrading of experimental facilities
- Sub-task 4.3 - Upgraded experiments

PROGRESS OF WORK AND OBTAINED RESULTS

State of Advancement

The scope of the original contract has been extended to incorporate Task 4 (Development and Application of Radon Emanation Technique). This work is being carried-out under the auspices of the PECO programme at NRI Rez in the Czech Republic. The timescale of the original Tasks 1-3 was extended to accommodate this additional work and these tasks were completed at the end of 1994. Task 4 is due to be completed at the end of April 1995.

During 1994 the development of a model of the chemistry within a cracked repository under Task 3 has been completed. A series of scoping runs have been performed to ascertain the potential effect of cracking on repository performance.

Task 4 has commenced. The task is currently behind schedule due to delays in the approval of the contract. Sub-task 4.1 has commenced and the initial experiments have been set-up and carried-out. The programme is approximately four months behind schedule.

Progress and results

Task 1 - Crack Healing

Sub-task 1.1 - Experiments on crack healing
During the current half-year period, the work programme scheduled under the original contract has been completed. The extension of the contract to include the contribution from NRI Rez has required further experimental work. Some crack filling experiments have been carried out in the period, using the experimental techniques developed previously.

Results from experiments Crack-9 and Crack-10 are now available. Experiment Crack-9 comprises four specimens in which the potassium inventory was enhanced through the addition of potassium hydroxide or potassium nitrate to the cement mortar during manufacture. This experiment is intended to provide information about the influence of alkali metals on crack healing. In addition, the diffusion of nitrate ions was investigated.

The Crack-10 experiment comprises two specimens of rapid hardening Portland cement and two specimens of the usual sulphate resistant Portland cement. Three of the specimens included an additional side crack and all specimens were exposed to tap water. It was apparent that crystals precipitated in the side cracks from tap water have an increased capability for healing such cracks. This effect apparently eliminates the tendency for increased crack healing of the main crack previously observed for such systems when a synthetic calcium bicarbonate solution was employed.

An additional experiment is also be carried-out to investigate the behaviour of deionised, carbon dioxide free water in various specimens of granulated, hardened cement pastes using radiotracers.

Sub-task 1.2 - Modelling of crack healing
Considerable effort has been devoted to the modelling of crack healing during the current period. The modelling has been considerably improved, although at the cost of a significant increase in the calculation times required. This has thus far prevented the modelling of successive columns of cement paste along the crack. The diffusion of radon is currently being included into the existing models to facilitate the interpretation of the experimental results obtained in the work performed at NRI Rez. A detailed description of the model of crack healing will be issued as a Risø Laboratory report.

Task 2 - Cement-groundwater Interactions

This Task has been completed and there are no additional results to be reported.

Task 3 - Barrier Properties of the Inhomogeneous Repository

Sub-task 3.1 - Chemistry varying with position and time

The CHEQFRAC code has been developed and tested. A verification exercise has been carried-out through a comparison with the predictions of the analytical solution for the simple model of chemistry in a crack [1]. Further verification has been obtained by comparison with other appropriate models [2]. The code is now considered to be adequately verified.

Sub-task 3.2 - Effect of fissures on the source term

The CHEQFRAC model has been used to predict the evolution of the pH in a repository backfilled with cracked Nirex reference backfill. Initial calculations were carried-out to illustrate the effect of the flow velocity on the pH profile within a crack. Demineralised water flow in a crack 20 mm wide and 1 m in length was simulated. A crack spacing of 1 m was assumed and the backfill was assumed to have an diffusion coefficient of 4×10^{-11} m^2 s^{-1} and a fractional porosity of 0.44.

The predicted pH profiles demonstrate that an increase in the flow velocity by an order of magnitude results in a decrease in the pH at a given point by about one pH unit. In all cases, a pseudo-steady state has been achieved. The calcium content of the backfill in any of the CHEQFRAC cells has not been depleted to the extent that the calcium hydroxide has been exhausted. An assumption of a constant discharge means that any variation in the crack aperture area, for example if the crack width varies, will alter the velocity of the groundwater through the cracks. It is generally assumed that the groundwater specific discharge is primarily determined by the geological environment and therefore this assumption is reasonable. In this case, the flow velocity is inversely proportional to the crack width. The model predicts that changes in the crack width, for a constant discharge, have no effect on the pH buffering of the water in the crack since the increased dilution in a wider crack is balanced by the reduction in the flow velocity.

A more detailed study was performed using a range of parameters intended to be typical of a deep repository. The effects of varying the thickness and diffusion parameters for precipitated reaction layers have been investigated. For these simulations, it was assumed that the entire discharge of groundwater through the backfilled part of the repository would be partitioned into the cracks. The repository cross-section is assumed to be a 20 m square with an array of parallel cracks at 1 m spacing and a typical width of 5 mm. The crack aperture area was assumed to be approximately 2.5 m^2. The crack length is assumed to be 0.5 m. This value was intended to represent a typical distance between backfilled waste packages or between a waste package and the edge of a repository.

The total discharge for a "high flow" case of 10^{-5} m^3 s^{-1} is equivalent to a groundwater specific discharge of 2.5×10^{-8} m s^{-1} and is intended to represent the flow in the vicinity of transmissive feature in the geology. The consideration of a value of the discharge which is an order of magnitude lower than the "high flow" case would represent a more typical value of the discharge. At a lower flow velocity, the pH at the end of the crack is about 12.5, approximately that expected for the static dissolution of calcium hydroxide. However, at the higher flow rate the pH is reduced to about 12, demonstrating that the dissolution of calcium hydroxide is not reaching saturation.

Previous experimental measurements of the properties of reaction layers indicated that the intrinsic diffusion coefficients of such layers for radiotracer migration may be about one or two

orders of magnitude lower than that of unaltered backfill. Consequently, simulations have been performed for 1 mm thick reaction layers with intrinsic diffusion coefficients either one or two orders of magnitude lower than the intrinsic diffusion coefficient assumed for the backfill (layer 1 and layer 2 respectively).

At the slower flow velocity, the effect of layer 1 on the pH at the end of the crack is negligible, the pH is still about 12.5. However, the more protective reaction layer (layer 2) results in a reduction in the pH at the end of the crack to about 10.7 at the slower flow rate. The effect at the higher flow rate is more pronounced, with layer 1 giving a reduction in the pH at the end of the crack from about 12 to less than 10. The effect of layer 2 at the higher flow rate was not simulated. It is apparent that the effects of the reaction layers are significantly enhanced as the flow velocity increases, as might be expected.

Unfortunately, the application of the CHEQFRAC model is limited to shorter timescales by the availability of computing resources. However, the analytical model can be used to investigate the potential behaviour of a cracked repository over any timescale [1].

This model has been applied to the same repository parameters as an illustrative example. The ratio of the critical time (the time required for calcium hydroxide buffering to cease) for cracked and uncracked repository are shown in Table 1. This table indicates that some values of the ratio of the critical times exceed unity. This implies that the performance of the cracked repository may exceed that of a homogeneous repository and is promoted by the presence of a large number of cracks. For very small crack spacings the model of the performance of the cracked repository is not valid. At the extreme of a very large number of cracks, the cracked repository becomes indistinguishable from a homogeneous repository. Values of the ratio in Table 1 which exceed unity actually imply that the repository will perform as if it were homogeneous.

The calculated performance of a cracked repository using the analytical model is sensitive to the value of the intrinsic diffusion coefficient for the backfill. The diffusion parameters of cementitious materials are relatively sensitive to the nature of the material, the intrinsic diffusion coefficient varying from less than 10^{-13} m^2 s^{-1} for structural concretes containing blast furnace slag or pulverised fuel ash to greater than 10^{-11} m^2 s^{-1} for porous materials such as backfill.

It is apparent that the effect of cracks is most significant for higher groundwater flow rates and large crack spacings. In the case of the repository described above with a single crack and a specific discharge of 10^{-9} m s^{-1}, the time elapsed prior to a significant reduction in the pH is only about 2000 years.

Overall, the application of the analytical model demonstrates that the presence of cracks can lead to an effective reduction in the time period for which the groundwater leaving the repository is buffered to a high pH. This is equivalent to a reduction in the effective buffering capacity of the backfill. This is due to the depletion of buffering phases from a zone adjacent to each crack such that, after an appropriate elapsed time, interaction between undepleted backfill and the groundwater is effectively prevented by the timescale required for the migration of calcium and hydroxyl ions through the depleted zone.

Sub-task 3.3 - Validation of source term model

Further consideration has been given to the validation of the model of chemistry within a crack. The initial validation experiments seemed to be inconsistent with the predictions of the model. This has been attributed to a failure to achieve equilibrium due to the necessary small-scale and short timescale (rapid flow) necessary for laboratory experiments. It has been concluded that appropriate validation experiments may not be possible on a laboratory scale and therefore no further experiments have been performed under the current programme.

Task 4 - Development and Application of Radon Emanation Technique

Sub-task 4.1 - Initial experimental work

Radon-220 has been identified as a suitable radiotracer for the characterisation of reaction layers. The source of the radon is a layer of thorium-228 introduced onto the specimen surface. The experimental apparatus is intended to allow the examination of the properties of the reaction layers formed on the surfaces of cement specimens. The design and construction of the apparatus makes use of experience at both NRI Rez and Risø Laboratory.

The apparatus intended for use in the preliminary experiments consists of a cylindrical vessel (measuring 6 cm by 1.8 cm diameter) in which a specimen is placed. The vessel is filled with a potentially reactive solution (for example a bicarbonate solution). The flow of the solution is controlled by a peristaltic pump, set to give a flow rate of 3.5 ml hr^{-1}. A carrier gas is also bubbled through the solution at a flow rate of 40 ml hr^{-1}. This gas is used to carry any radon atoms released into solution. The radon concentration in the dried carrier gas will be determined using a semiconductor detector. The carrier gas flow rate is intended to optimise the detection of radon.

A crack surface is simulated by the surface of a rod of concrete measuring 1.2 cm in diameter and 2 cm in length. The concrete studied in the initial experiments was prepared from a mixture of a Danish sulphate resistant Portland cement and sand with a water-cement ratio of 0.38. The geometric surface area of the specimen as 7.5 cm^2. This is about 10 % of the surface area of the cracks studied under Task 1. The surface was labelled by contact with a thorium-228 solution in acetone one month before use.

The theory of emanation methods suggests that the rate of radon release from the labelled solid reflects changes in the surface area and morphology [3]. For a constant concentration of thorium, an increase in radon emanation will occur for an increase in surface area. A decrease in the emanation rate occurs if the area decreases or if a radon impermeable layer forms. Taking these considerations into account, the following measurements will be made;

- concentration of radon in solution (alpha counting);
- total activity of the parent radionuclide (thorium-228) in the rod before and after exposure to the solution (gamma counting);
- determination of the concentrations of Ca, K and Na in solution.

A series of initial experiments have been performed to assess the sensitivity of the technique. The solutions employed were 0.01 M hydrochloric and nitric acids and 1.25 mM calcium bicarbonate, together with distilled water. The timescale employed was seven days in each case. The observed quantities of radon-220 decreased with time for both the calcium bicarbonate and nitric acid. The decrease in the gamma activity was determined and is reported in Table 2, together with the calcium concentrations at the end of the experiments.

The largest decrease in the gamma activity was found to occur for the nitric acid solution. This correlates with the highest calcium concentration. This suggests that the parent radionuclides are partially transferred into solution during the dissolution of the surface. The decrease in the radon-220 concentration observed is probably due to loss of the parent radionuclide. In the case of the bicarbonate solution it is likely that insufficient calcium carbonate was formed to affect the radon emanation.

Further experiments were performed to continue the investigation of the formation of surface reaction layers by interaction with calcium bicarbonate solutions. The experiments made use of the cement described above and the surfaces were once again labelled with thorium-228 and radium-224 one month prior to use. A solution flow rate of 4 ml hr^{-1} was used. The experiments are summarised in Table 3. The concentrations of calcium, potassium, sodium and bicarbonate and the solution pH were measured for the solutions after contact.

The removal of radon from the solution after contact with the specimen was monitored continuously. A typical result, that for the 1.9 mM calcium bicarbonate solution, is shown in Figure 1. An initial increase in the quantity of radon in solution reflected the desorption of radon from the specimen. The radon in solution subsequently decreased with elapsed time, reflecting the loss of radon due to both elution and radioactive decay.

During the experiments, the precipitation of calcium carbonate was observed. This was attributed to the stripping of carbon dioxide from the calcium bicarbonate solution. Consequently, it was decided that gaseous carbon dioxide should be used as the carrier gas in the next set of experiments.

The experimental apparatus was revised to allow the simulation of an actual crack. The simulated crack replaced the rod specimens used previously. The simulated crack aperture was 0.1 mm and the crack width was 43 mm. The length of the specimen was 90 mm. This gave a total crack surface area of 75 cm^2. The cementitious materials studied were sulphate resistant cements of both Danish and Czech origin. The crack surfaces were labelled in the same fashion as described above.

The apparatus was operated in a pulsed fashion to allow the exchange of the entire volume of the solution in the crack. The solutions used were 0.90, 1.05 and 2.03 mM calcium bicarbonate. The radon was stripped out of the solution using carbon dioxide and was monitored continuously. The results for the 2.03 mM solution are shown in Figure 2.

The radon measurements suggest that the radium-224 concentration in solution initially increased with elapsed time. This was expected as the solubility products of radium carbonate (assumed to be similar to barium carbonate) and calcium carbonate are similar. The results also suggest that a shift takes place in the radioactive equilibrium after contact of the labelled surfaces with the solution. This is due to the differing behaviour of Ra^{2+} and Th^{4+} at the solution pH of about 7-8. The thorium ions are absorbed by the crack surface whereas radium ions are apparently mobile in the solution. Thorium ions were not detected in the solution after exposure in the crack.

The interpretation of the radon measurements is continuing. This includes the development of models of the behaviour of radon in the system. This interpretation will make use of the solution analyses obtained during the experiments.

Sub-task 4.2 - Upgrading of experimental facilities

The experimental apparatus will be updated with the intention of improving the dynamic response of the radon release measurements. The volume of the gas separator chamber will be reduced to facilitate this improvement. The material used to cover the outer surfaces of the specimens will be considered to determine whether improvements can be obtained through the use of a different, less radon-permeable material.

References

/1/ ATKINSON, A., Nirex Safety Study Report NSS/R287 (1991) (draft).

/2/ CHAMBERS, A.V and SMITH, A.C., paper presented at Scientific Basis for Nuclear Waste Management XVII (1993).

/3/ BALEK, V. and TOLGYESSY, J., "Emanation Thermal Analysis", Elsevier (1984).

Table 1 Calculated ratio of critical time for cracked repository to buffering timescale for a homogeneous repository. The assumed values of the diffusion coefficient and repository dimension are 4×10^{-11} m^2 s^{-1} and 20 m respectively.

	$J = 10^{-9}$ m s^{-1}	$J = 10^{-12}$ m s^{-1}
"Single" crack (S = 20 m)	0.0013	1.3
Many cracks (S = 1 m)	0.51	510

Table 2 Results of the seven day radon emanation experiments.

	$[Ca_T]$ / mg dm^{-3}	Decrease in γ
Distilled water	6.05	8.0 %
0.01 M HCl	90.24	37 %
0.01 M HNO_3	114.8	43 %
1.25 mM Bicarbonate	10.24	21 %

Table 3 Experimental conditions and results for experiments using calcium bicarbonate solutions.

	$[Ca_T]$ / mg dm^{-3}	Time / days	Carrier gas	Decrease in γ
Tapwater	43.9	21	Air	33.3 %
1.6 mM $Ca(HCO_3)_2$	64	14	Air	18.2 %
1.9 mM $Ca(HCO_3)_2$	76	21	Air	23.9 %
2.5 mM $Ca(HCO_3)_2$	100	14	Air	32.0 %
2.5 mM $Ca(HCO_3)_2$	100	14	Nitrogen	12.6 %

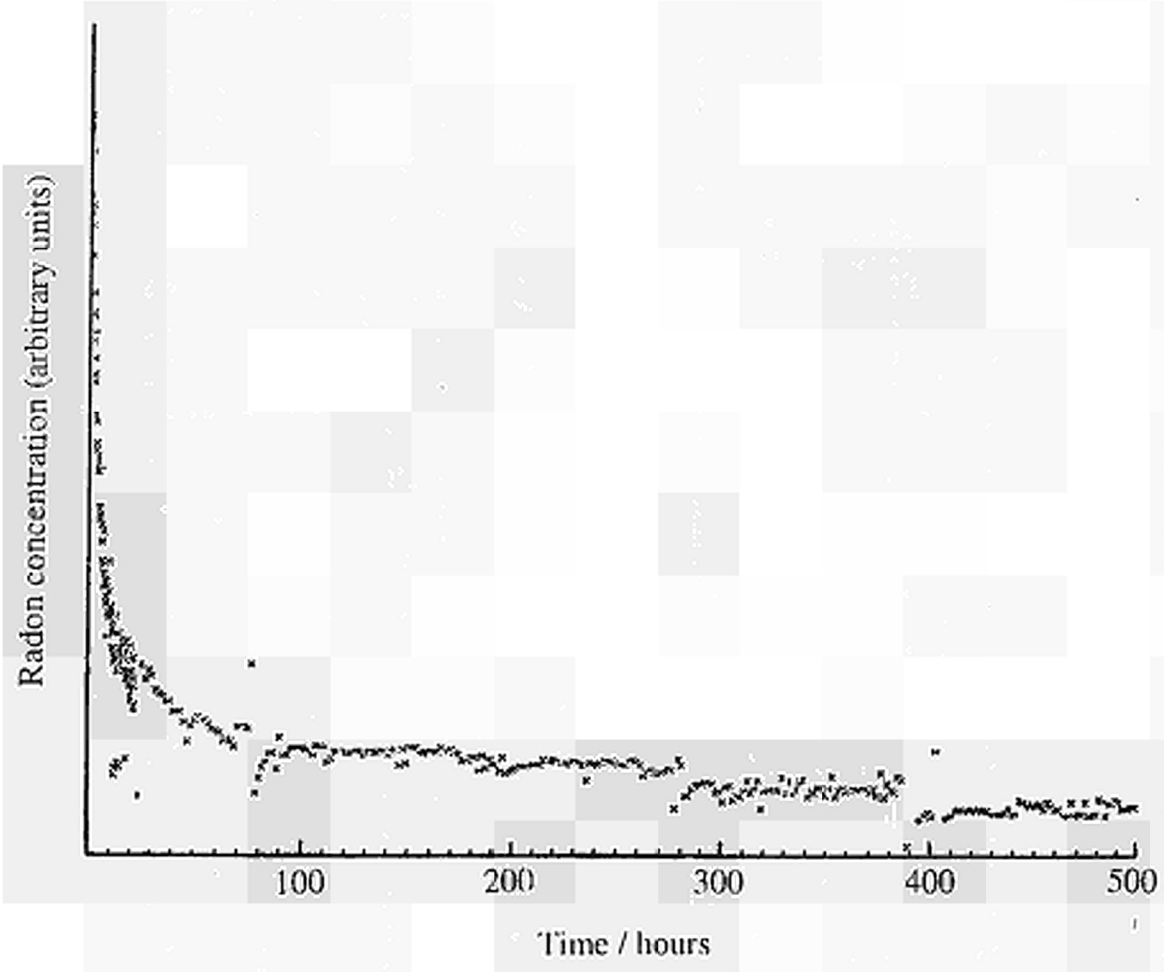

Figure 1 Time variation in radon concentration for rod specimen exposed to 1.9 mM calcium bicarbonate solution. Solution flow rate of 4 ml hr^{-1}.

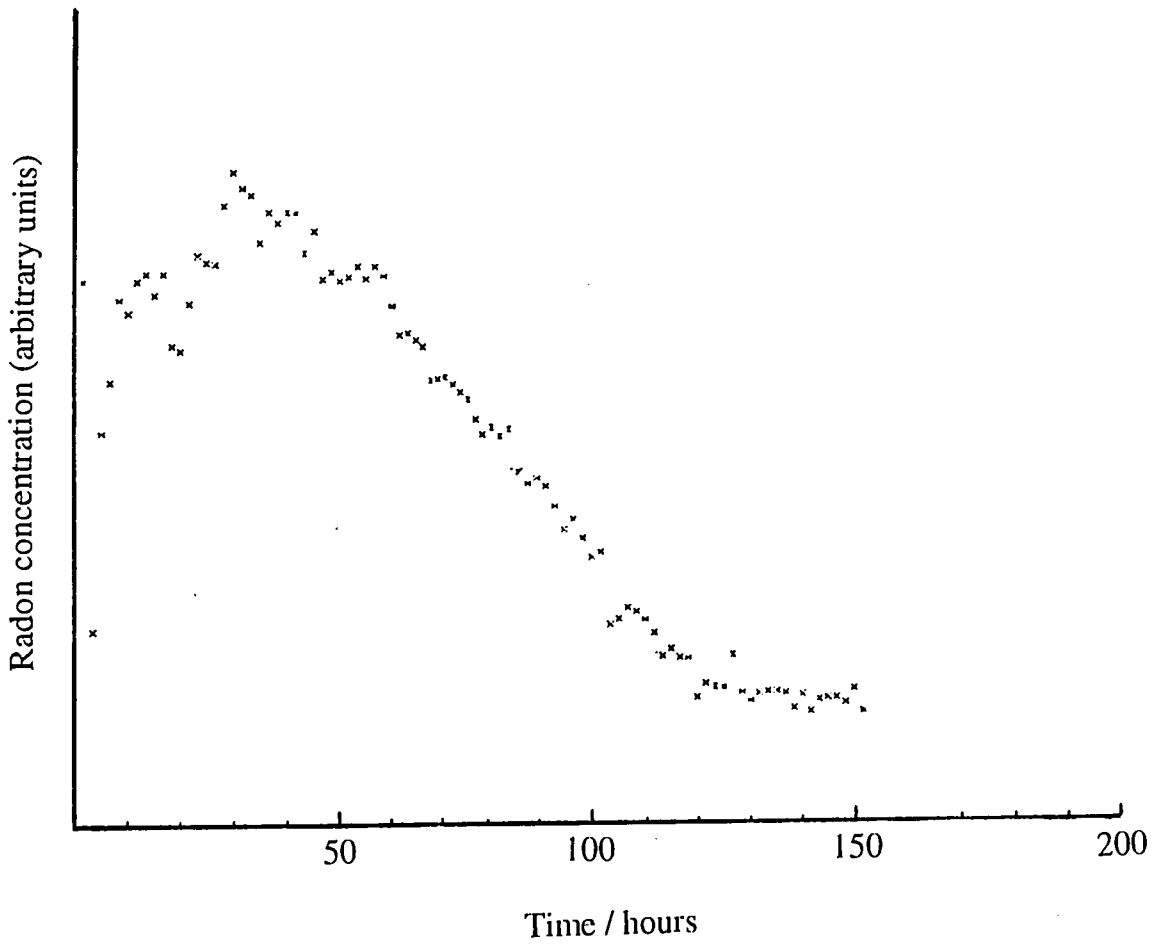

Figure 2 Time variation in radon concentration for 0.1 mm cracked specimen exposed to 2.03 mM calcium carbonate solution. Solution flow rate of 4 ml hr^{-1}.

Title:	**Completion of the Corrosion Programme in Boom Clay - in situ experiments**
Contractor:	ONDRAF/NIRAS, Brussels, Belgium
Contract No:	FI2W/CT91/0096
Duration of contract:	July 1991 - December 1994
Period covered:	January 1994 - December 1994
Project Leader NIRAS:	J. Van Miegroet
Project Leader SCK•CEN:	P. Van Iseghem

A. OBJECTIVES AND SCOPE

SCK•CEN has developed, in the early 80's and on request of the Belgian authorities (NIRAS/ONDRAF), a screening programme on the corrosion behaviour of various candidate overpack materials and conditioned waste form samples in the underground repository conditions.
SCK•CEN uses the underground laboratory, also known as the HADES facility, located in the Boom clay layer at a depth of about 225 metres below ground level, to assess through a variety of in situ experiments the possibility of Boom clay as a disposal environment. These experiments place the overpack and waste form samples either in 'direct contact with clay' (type I test tubes), in a 'humid clay atmosphere' (type II test tubes) or in a 'concrete saturated clay atmosphere' (type III test tubes). The various candidate overpack samples under investigation are all metals or their corresponding alloys (low carbon steel, stainless steel, Ni- and Ti-alloys). The waste form samples tested are mainly waste glasses. A smaller number of bitumen and cement waste form samples are considered as well.
A total of twelve corrosion tubes were installed during the period 1985 - 1994. The aim of the present research programme is the completion of the corrosion experiments initiated in the previous programme and the beginning and completion of the operation of the new installed corrosion tubes.
The main objective of this work programme is to establish a first estimate of the corrosion allowance required for the safe confinement for periods up to 500 years through the evaluation of medium term interactions (periods up to 7.5 years) between the overpack and waste form samples on the one hand and the host formation on the other hand.
The experimental work is performed by SCK•CEN.

B. WORK PROGRAMME

1. Monitoring and controlling of the ongoing corrosion experiments.
2. Design, construction and installation of the new corrosion loops.
3. Analysis of the overpack and waste form samples and of the surrounding clay.

C. PROGRESS OF WORK AND OBTAINED RESULTS

State of advancement

The section loaded with the waste form samples of tube 3, overcored at the end of 1993, was dismantled and the waste form samples, including two glasses doped with Pu, ^{134}Cs and ^{90}Sr were retrieved for further analyses. All samples had been in direct contact with Boom clay for 7.5 yeras at 90°C.
The overpack samples, the waste form samples and the clay cores adjacent to the waste form samples of tube 3 were analysed.
The first of the type III corrosion tubes, tube 9, has been overcored after a total exposure time of about 5 years (the tube has been working at 90°C for only 3.5 years). The overpack samples, mounted on the inside of the tube (interaction with a concrete equilibrated clay atmosphere), and the waste form samples, mounted on the outside of the tube (interaction with Boom clay), have been retrieved.
Tubes 5b, 8b and 10 were connected to the output measuring unit. And a Teflon® holder, containing 38 overpack samples and 18 waste form samples, was mounted on the inside of tube 8b.

Progress and results

Tube 5b was installed in situ on September 1, 1993. During 1994, the connectors were placed on the heating elements and the thermocouples. Afterwards the thermocouples were coupled to the automatic read-out system. And on June 14, 1994 the heating elements were connected to their output. The temperature of the tube reached its target value (90°C) on July 6, 1994.

A Teflon® holder, containing 38 overpack and 18 waste form samples, was mounted on the inside of tube 8b on May 6, 1994. A new automatic drainage system was installed and the system is working under helium since May 25, 1994. The thermocouples were placed on the tube and were linked to the automatic read-out system. The temperature at the inside of the tube is 19°C.

The final connections of tube 10 have been performed: the thermocouples were placed on the tube; the connectors were placed on the thermocouples and the thermocouples were linked to the automatic read-out system.

The first of the type III tubes, tube no. 9, was successfully overcored on November 11, 1994. The overpack and waste form samples were retrieved. Analyses of the overpack and waste form samples, together with the adjacent clay cores, are scheduled for early 1995.

During 1994, we have started the surface analyses of the corroded metallic samples of tube 3. The surface analyses of the C-steel and the stainless steel (AISI 316 and 1803 MoT) samples have been completed. The other metallic samples that were mounted on tube 3 will be analysed early 1995.
The individual relative mass losses were measured and the individual average corrosion rates and overall thickness reductions of the various metal and alloy samples loaded on tube 3 were calculated. The overpack samples C-steel, AISI 316 and 1803 MoT of tube 3 have been analysed:

surface analyses and analyses of embedded cross sections have been completed by means of stereomicroscopy, optical microscopy and scanning electron microscopy (SEM). Also, the elemental composition of the corrosion layers have been determined by means of electron dispersive spectrometry (EDS).
A preliminary visual examination of the corroded metal and alloy samples indicate that only carbon steel shows severe signs of corrosion attack. This observation is confirmed by the mass loss measurements. The mass loss measurements show that only carbon steel exhibits significant overall thickness reductions in direct contact with clay at 90°C. Maximum thickness reductions of 35 μm were calculated for the corroded C-steel samples. The so-called corrosion-resistant materials (stainless steels, Ni- and Ti-alloys) do not corrode in contact with clay as shown in Figure 1.
Surface analyses of the C-steel samples reveal the following aspects:
- the type of corrosion that causes the deterioration of the carbon steel samples is pitting corrosion. Figure 2 shows a global view (optical microscopy) of the pitted surface of the inner side of a chemically cleaned carbon steel sample.
- although overall thickness reductions of 35 μm were calculated, maximum pit depths up to 140 μm were measured.
- the inner side of the samples (direct contact between the samples and the inner stainless steel carrier tube) are corroded more severely than the outer side (direct contact between the samples and Boom clay).
- the surface morphology of the corroded samples between the inner and outer side of the rings is totally different: the surface of the inner side of the samples show small and deep pits, whereas the surface of the outer side presents wide and shallow pits.
- the welds seem less resistant to corrosion attack.

Several types of analyses were performed on the waste form samples loaded on tube 3 which was retrieved at the end of 1993:
(1) mass loss measurements of all 64 samples,
(2) SEM-EDXA analyses of the surface of the corroded glasses SON58 and SON68 (French origin), SM58 and SAN60 (German origin),
(3) EPMA X-ray and SIMS profiling of the reaction layers on these glasses, and
(4) radiochemical analyses of the clay cores adjacent to the glasses doped with Pu, U, Cs and Sr.

The mass losses reveal average dissolution depths between 10 and 200 μm per year (90°C, direct contact with Boom clay) for the glasses, depending on the glass composition. The mass loss data are in agreement with the data from laboratory simulation tests. On the other hand, Pu incorporated in two glass samples leached during the in situ interaction did not migrate further than 4 mm in the Boom clay. The various surface analyses showed thick reaction layers formed, on top of which secondary phases can form (see figure 3). SIMS profiling moreover reveals that two glasses (SON68 and SM58) mainly dissolve congruently, and two other glasses (SAN60 and SON58) interact by a combination of congruent dissolution and selective diffusion controlled leaching.

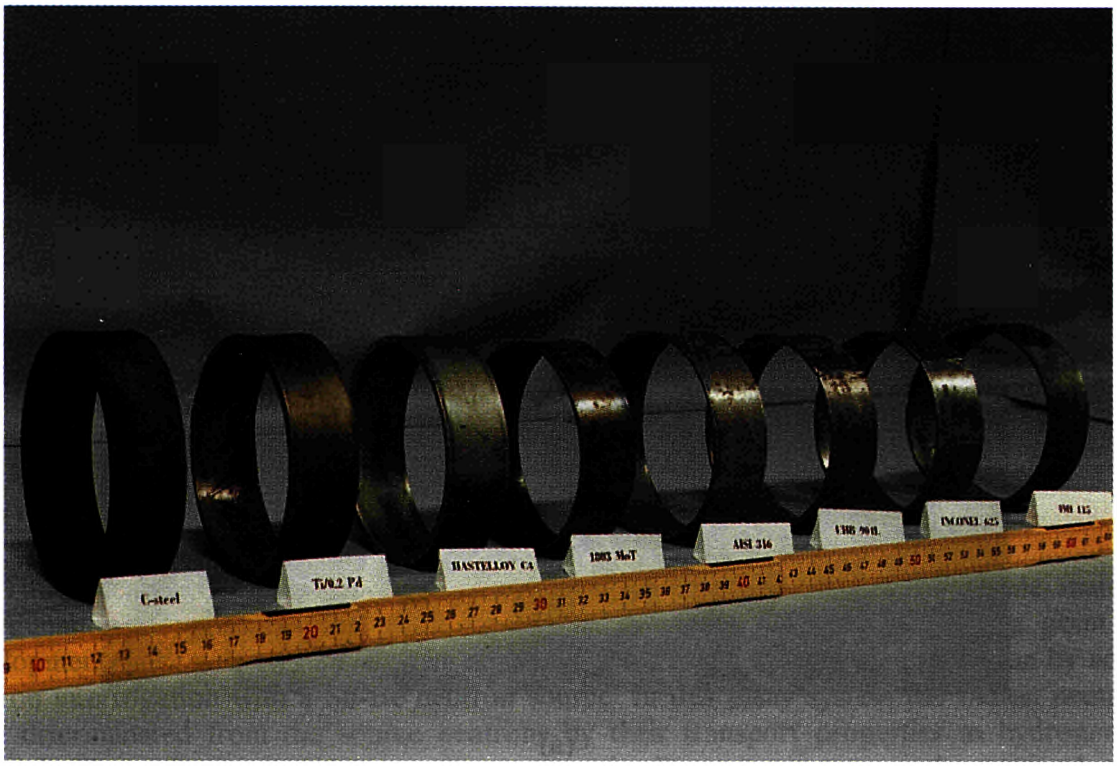

Figure 1: Line-up of all the different types of metal and alloy samples loaded on tube 3 after 7.5 years exposure to Boom clay at 90°C. Visual inspection indicate that only C-steel (metal ring on the left side of the picture) is prone to corrosion attack.

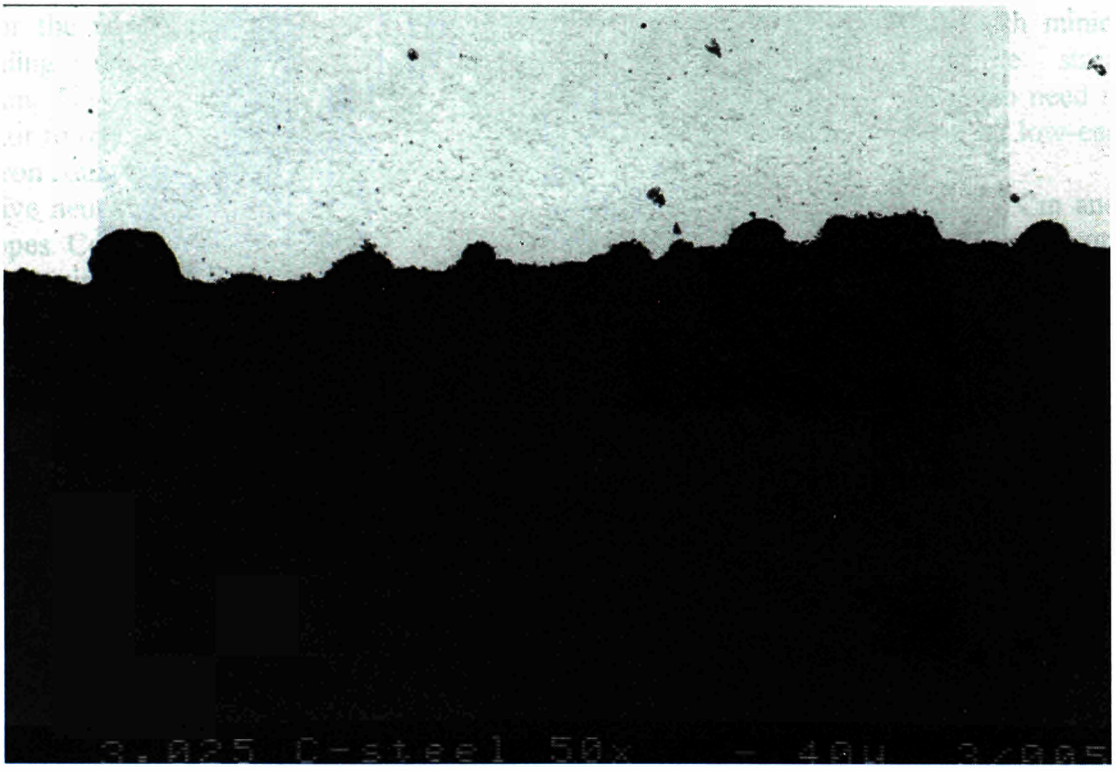

Figure 2: Global view (optical microscopy of the rough surface of the inner side of a chemically cleaned C-steel sample (unetched and polished cross section) showing many small and deep pits.

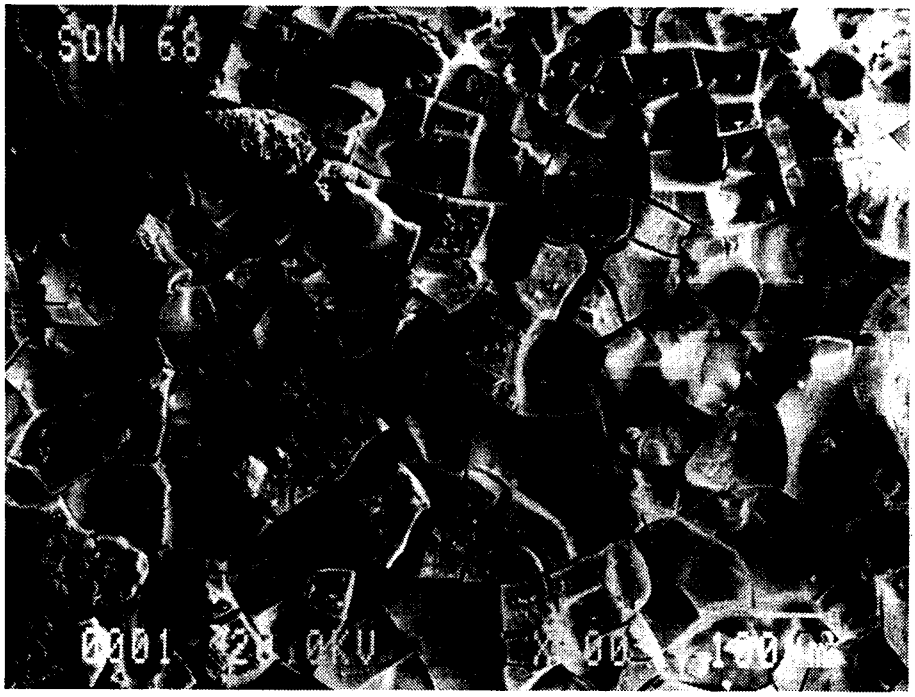

(a)

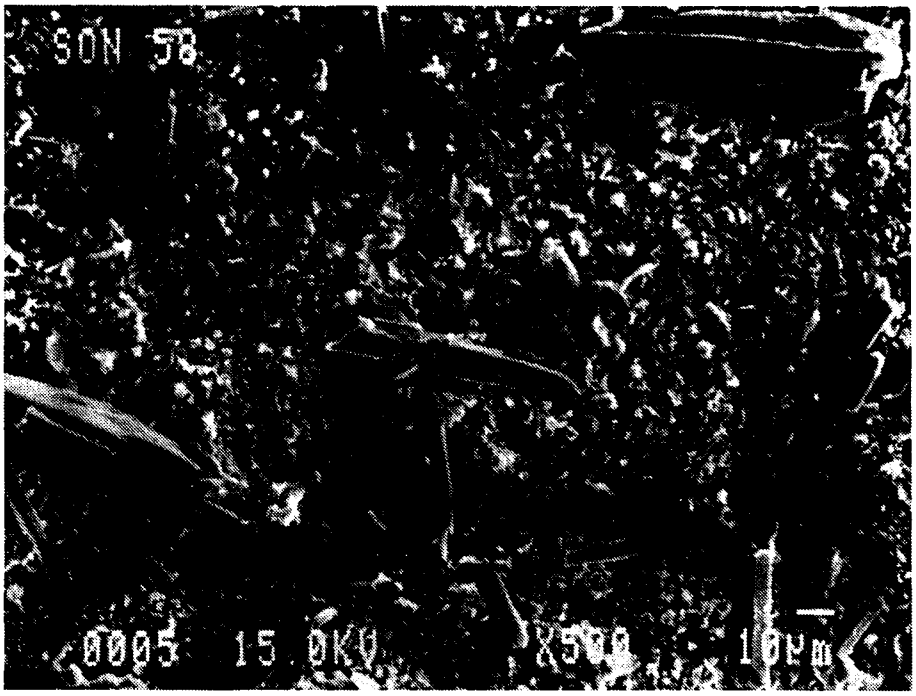

(b)

Figure 3: Scanning electron micrograph of the surface of two glasses exposed to Boom clay for 7.5 years at 90°C.
(a) glass SON68: a thick layer of about 60 μm is formed, consisting mainly of aluminium, silicon and zirconium;
(b) glass SON58: this glass shows the strongest corrosion, and various secondary phases can be identified on the surface (e.g. [Ca,S]-needles on the photograph).

Title:	**Determination of Fissile Material by Neutron Transport Interrogation**
Contractors:	Forschungszentrum Jülich (KFA) SCK/CEN Mol
Contract No.:	FI2W-CT90-0010
Duration of contract:	1 November 1991 to 31 October 1995
Period covered:	1 January 1994 to 31 December 1994
Project leader:	R. Odoj (KFA)
Experiments:	P. Filß, G. Caspary, J. Kühne (KFA)
Calculations:	R. Mandoki, M. Bruggeman, P. Van Iseghem (SCK/CEN-MOL)

A. OBJECTIVES AND SCOPE

This research is concerned with non-destructive assay techniques for fissile material determination in waste material mainly contained in waste drums. The starting point for development work was an assay system at the KFA for fissile material determination by active neutron interrogation with a Sb-Be neutron source. In this assay system the fission neutrons were discriminated from the source neutrons by their transport properties in hydrogenous material. The neutron count rate was composed of a source term and a second term proportional to the fissionable nuclides ^{233}U, ^{235}U, ^{239}Pu, ^{241}Pu.
Neutron transport calculations at CEN/SCK Mol are intended to achieve a theoretical understanding and an improvement of the assay system with different neutron sources by modelling the neutron transport properties in the waste drum and the assay system. A replacement of the Sb-Be neutron source by other low energy neutron sources, such as Am-Li, or the accelerator reaction Li (p, n) Be, will lead to an assay system with minimum shielding requirements and in the case of Am-Li constant source strength (^{241}Am, $T_{1/2}$ = 432.6a, ^{124}Sb, $T_{1/2}$ = 60.3d). As an additional advantage there is no need for a reactor to reactivate the Sb. The replacement of the Sb-Be neutron source by other low-energy neutron sources is therefore an important objective of this research.
Passive neutron emission mainly results from spontaneous fission in ^{238}Pu, ^{240}Pu, Cm and Cf isotopes. Counting these neutrons provides information about the presence of these transuranic elements in the waste matrix. Effective recording and evaluation of these neutrons is an objective of this research. The aim of the final assay system is an easy-to-use and reliable instrument for the estimation or determination of the fissile material content of various packages, mainly waste drums.

B. WORK PROGRAMME

B.1 Checking and optimizing of the Sb-Be system by comparison with neutron transport calculations.

B.2 Active neutron interrogation with other neutron sources, in particular Am-Li and Li (p,n) Be, and comparison with neutron transport calculations.

B.3 Modification of the system for passive neutron counting capabilities.

B.4 Test and performance of the active/passive neutron assay system with actual samples, mainly drums with waste from the nuclear fuel cycle.

C. PROGRESS OF WORK AND IMPORTANT RESULTS

In 1994 the development of the passive neutron system was finished. The enlargement of the neutron counter led to a higher counting sensitivity in the top and bottom part of the drum.
The work on the active NDA system was concerned with the replacement of the Sb-Be source for various reasons, mainly the high γ-dose rate during operation. Therefore measurements and calculations were performed to acquire a survey of available neutron sources. The Li(p,n)Be reaction is assumed to be the most promising neutron source for active neutron interrogation, because of the relatively low neutron energy compared to other sources (exept Sb-Be). An active assay system for small samples on the basis of the Li(p,n)Be reaction was designed and completed to run at the linac in the KFA Institut für Festkörperforschung.

C.1 Performance of the Passive Neutron System

For the sake of simplicity, the general layout of the passive assay system is repeated in **Figure 1**. The waste drum is simulated by a drum filled with concrete and containing cylindrical bore-holes (1 to 4) for the deposition of samples (as for example Pu or Cf).

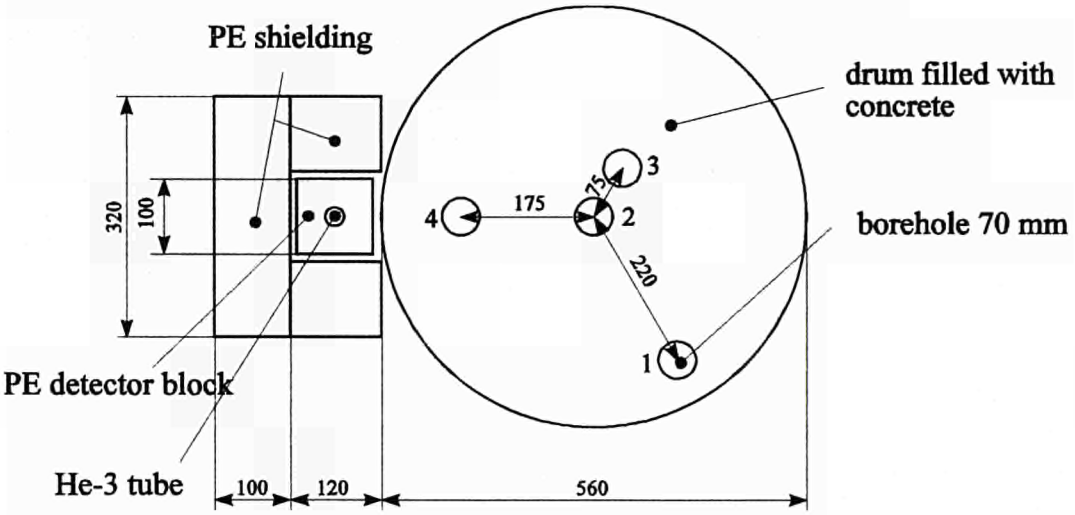

Figure 1: Cross-sectional view of the passive neutron system.

It was noticed on the basis of Table II in the preceding report that the drop of the count rate from neutron sources near the upper and lower edge of a drum was not satisfactory. Therefore the moderator of the neutron counter was enlarged to 1.3 m and equipped with two He-3 tubes throughout its length. The longer neutron counter led to an increased counting sensitivity of the bottom and top part of the drum. Table I shows count rates of 1 g Pu in different axial and radial positions of the drum.
The count rates from the bottom and top region are 77 % of the central region as compared to 57 % previously.
If the extreme bottom and top positions are omitted in Table I, the measured count rate only varies by a factor of 2 depending mainly on the radial position.

Table I

Count rate (net) from 1 g Pu point source in different positions of a waste drum.
Concrete filling in the drum 77 cm.

Axial Position	Rotating drum Net count rates in s^{-1} (background 0.13 s^{-1} subtracted)			
	Tube 2	Tube 3	Tube 4	Tube 1
bottom	0.42	0.47	0.65	0.85
1/4	0.55	0.57	0.80	1.01
1/2	0.55	0.64	0.97	1.11
3/4	0.55	0.65	0.95	1.19
top of filling	0.41	0.51	0.77	0.98

To investigate the dependencies of the count rate on different matrix densities, another drum was used containing four layers of different densities (from 1 g/cm³ to 4 g/cm³). A ^{252}Cf source was used for the measurement. Furthermore, a ^{60}Co γ-source was also measured in the centreposition of the drum to compare the count rate variations.
The results are presented in Table II.

Table II

The radial dependency of count rates in concrete layers of different density for ^{252}Cf neutrons and ^{60}Co gammas.

Density in g/cm³	^{252}Cf neutrons					^{60}Co
	Concrete layer in mm; count rate Z in s^{-1}					
	275	195	135	80	25	275
	Z	Z	Z	Z	Z	Z
1.0	19.362	22.785	25.406	30.783	38.469	528.0
2.0	17.013	21.394	25.780	35.890	46.644	116.0
3.0	10.640	14.099	18.621	28.363	40.606	27.3
4.0	8.857	11.854	15.230	23.154	34.234	8.5

The neutron count rates vary by a factor of 2 in the radial direction in the layer with a density of 1 g/cm³ and by a factor of 4 in the 4 g/cm³ layer. In the central position they vary by a factor of 2 in the axial direction due to the different densities. This is the worst case. In comparison, the variation of the ^{60}Co γ-count rate is a factor of 60. This is a clear advantage for passive neutron counting in the case of waste specimens of high density and large dimensions.

C.2 Active Neutron System

The active neutron assay systems had been successfully operated with the low-energy Sb-Be photoneutron source. The Am-Li source was in principle suitable but the available neutron count rates were low and the detection limits, based on the 2σ criterion, were high.

Sb-Be neutrons are not available because the DIDO research reactor is currently not ready for ^{124}Sb activation. Therefore a general survey of possible low-energy neutron sources was carried out /3,4,5/. To illustrate the features of available neutron sources, the spectra are sketched in Figure 1.

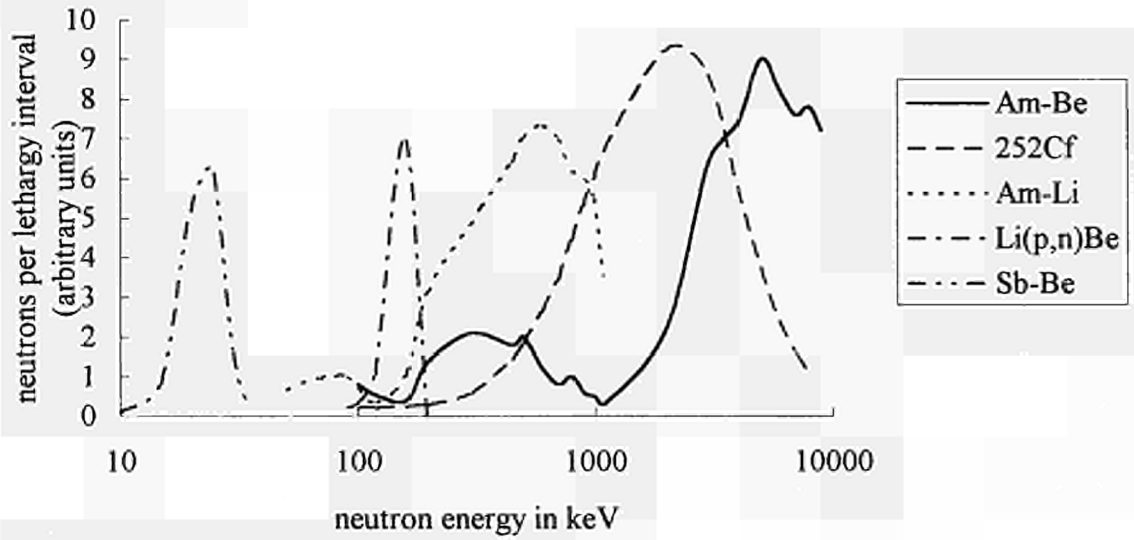

Figure 2. Spectra of possible neutron sources.

Intensive studies of the suitability of the Am-Li and ^{252}Cf neutron sources by transport calculations were performed to examine whether a moderation of the neutrons from these sources could soften the spectrum for a better separation of source and fission neutrons /1/. In the case of ^{252}Cf the results demonstrated the shortcomings of this source. Although the penetration of the waste was deeper no advantage could be observed in the separation. The same is valid for the Am-Be source, because the energies are even higher than in the case of ^{252}Cf. The Am-Li spectrum (endothermic reaction) is much lower in energy compared to the Am-Be spectrum but its high energy tailing reaches up to 2 MeV. These high-energetic neutrons are not easily separated from the fission neutrons and are probably responsible for the high source neutron term with the Am-Li assay system.

Neutrons from the Li (p, n) Be reaction at the target of the accelerator with E_p = 1.95 MeV are nearly monoenergetic in the forward direction. The actual neutron energy can be varied with proton energy. E_p = 1.95 MeV was frequently used in the later experiments. The neutron energy and intensity are furthermore dependent on the angle relative to the proton beam.

The consideration of these five neutron spectra led to the conclusion that the Li(p,n)Be source is a promising alternative to the Sb-Be neutron source. The neutron energy is still reasonably low and has a sharp cutoff to higher energies. The neutron energy and intensity in the backward direction are significantly lower. On the basis of this conclusion the basic layout of /6/ together with the outcome of the previous progress reports was modified for use at an accelerator target. This is shown in Figure 3.

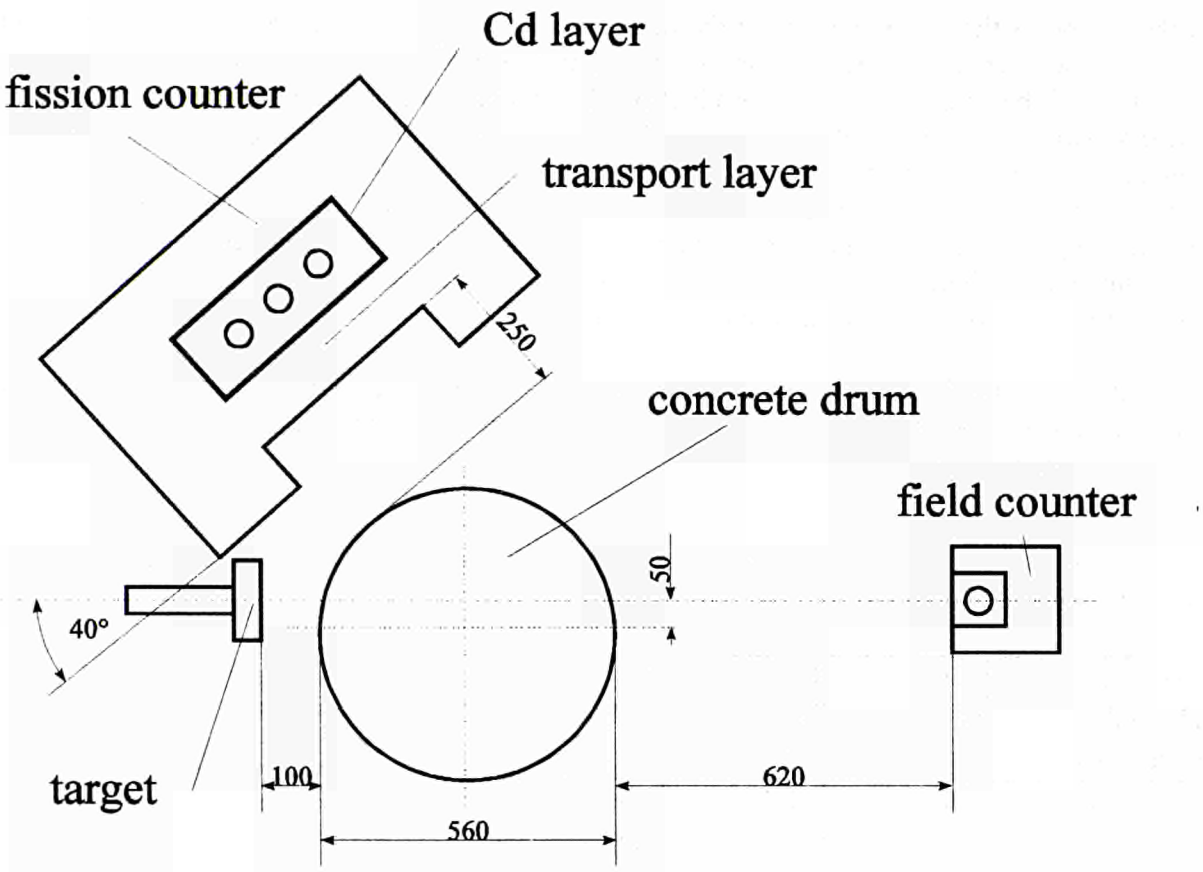

Figure 3: Cross-sectional view of assay system at an accelerator target.

A LiF target of 0.20 mg/cm^2 thickness (~ 20 keV) was used as the neutron source. $UO_2 (NO_3)_2$ solutions (natural uranium) were used as fissile material samples.

The amount of fissile material per sample was relatively low compared with the previous tests in Jülich.
At first (Table III), the neutron source strength, the proton energy scale and the target thickness were tested. The measuring geometry corresponds to (Figure 3) without the drum between the target and field counter.

Table III

Neutron generation at the accelerator near the threshold of the Li (p,n) Be reaction
Gamma dose rate at 1 m distance in forward direction: 60 µSv/h; neutron dose rate200 µSv/h.

E_p	Neutron count rate in s^{-1} at	
in MeV	Source counter	Fission counter
1.875	0.4	
1.878	648	
1.880	5307	
1.890	12229	0.1
1.900	15698	
1.920	10973	
1.950	8092	

Table III shows the steep increase of the neutron count rate at the threshold of 1.88 MeV. The start of the decrease in the neutron count rate in the forward direction is combined with the opening of the angle of neutron production. Later experiments with samples in the neutron field showed E_p = 1.90 MeV ($E_{n,\,forward}$ = 85 keV) or E_p = 1.95 MeV ($E_{n,\,forward}$ = 160 keV) as the preferential accelerator and neutron energies.
In Table IV the first experiment for fissile material detection is reported. It shows the count rate C_s of the source counter and the count rate C_F of the fission counter according to Figure 3. 250 ml polyethylene bottles with different contents of uranium were placed directly in the irradiation position (without the concrete drum).

This time the accelerator was operated at E_p = 1.9 MeV. The fission counter was equipped with a transport layer of 150 mm PE. The distance between sample and detector was slightly reduced compared to Figure 3.

Table IV

Increase of the count rate of the fission counter due to increasing uranium content.
E_p = 1.90 MeV, E_n = 85 keV

Sample 250 ml water with	^{235}U in mg	C_s in s-1	C_f in s-1
0 g Unat	0.0	1072	0.52
1 g Unat	7.2	1139	0.63
2 g Unat	14.4	1209	0.71
5 g Unat	36.0	1278	0.88
10 g Unat	72.0	1199	1.31
25 g Unat	180.0	1161	1.94
50 g Unat	360.0	1161	3.06
25 g Cu	0.0	1047	0.50

The fission counter in this setup (150 mm PE) has a background count rate of 0.52 s^{-1}. This count rate mainly results from the scattering of neutrons in the sample (water bottle). At 1000 s measuring time the 2 σ fluctuation of the background is 2 σ = 46 /1000s = 0.046 s^{-1}. Although the source count rate is fairly constant, the fission count rate increases with increasing fissile content.

The additive contribution of the uranium content according to Table IV is nearly linear. 50 g U_{nat} leads to an increase of C_F by 2541/1000s. 0.9 g U_{nat} or 6.5 mg ^{235}U would increase the background level by its 2 σ level and for a measuring time of 1000 s. The detection limit is 6.5 mg ^{235}U or 0.9 g U_{nat} in this geometry. This value should be compared with the performance of the Am-Li system mentioned in /2/, Table III, line A. On the basis of the 2 σ criterion the limit of detection was 260 mg ^{235}U there. The compared Am-Li system was furthermore very narrowly designed and not suitable for large drums.
At first attempt a 40-fold improved detection limit was obtained with this accelerator neutron source in a geometrical setup (Figure 3), which is better suited for large-scale waste drums. The neutron count rates are higher than with the Am-Li neutron source of 10^{11} Bq ^{241}Am.
In the following experiment the neutron energy was increased to E_n = 160 keV (E_p = 1.95 MeV). This gives higher source strength. At the same time the transport layer of the fission counter was increased from 150 mm to 200 mm for improved discrimination between fission

neutrons and source neutrons. In this experiment the waste drum used in the passive system (**Figure 1**) and density see ref. /2/ was placed into the neutron field. The neutron count rate (mainly thermal) was directly measured in the tubes provided for the positioning of samples. The following Figure 4 shows the variation of the neutron count rate with increasing depth in the test drum in the forward direction.
The proton energy was E_p = 1.95 MeV, the neutron energy E_n = 160 keV.

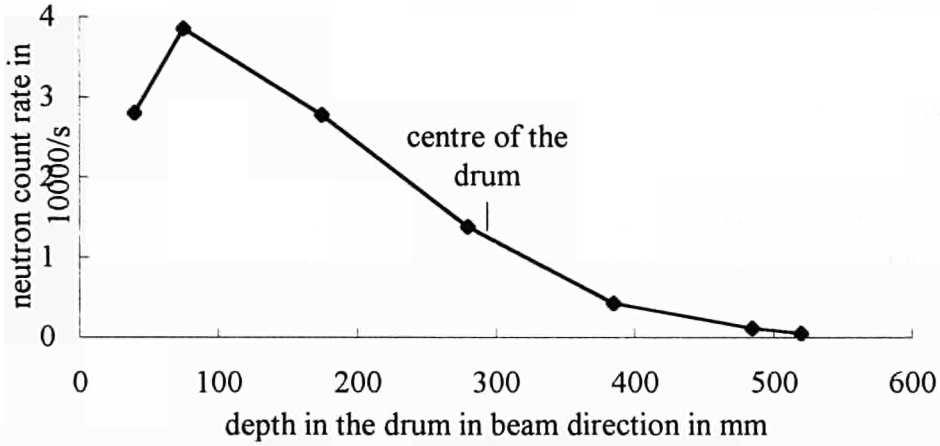

Figure 4: Measured neutron count rate in holes over the depth of the drum.
E_p = 1.95 MeV, forward direction, E_n = 160 keV

The neutron count rate is probably proportional to the thermal neutron flux. Its course is somewhat astonishing. The neutron count rate first increases behind the drum surface. This is mainly due to the lack of reflector material outside the surface of the drum. In the middle of the drum the count rate is still 1/3 of its maximum value and then decreases steeply behind the centre. From the previous calculations a more exponential course was expected. From the measured course it can be deduced that a useful high neutron flux for interrogation is maintained from the entrance position at the target to the centre of the drum. Thereafter a fissile material measurement in the drum was started.
Table V reports experimental results from the first test run for fissile material detection in various positions of a rotating drum.

Table V:
Measuring time 1000 s.
Detection of fissile material in the rotating drum
forward direction E_n = 160 keV
E_p = 1.95 MeV, transport layer 200 mm PE

Sample and position	Behind the surface	Fission counter	Source counter
empty		$0.24 \pm 0.03\ s^{-1}$	$479\ s^{-1}$
50 g U_{nat}	40 mm	$0.38\ s^{-1}$	$473\ s^{-1}$
50 g U_{nat}	75 mm	$0.31\ s^{-1}$	$476\ s^{-1}$
50 g U_{nat}	175 mm	$0.27\ s^{-1}$	$451\ s^{-1}$
50 g U_{nat}	280 mm	$0.22\ s^{-1}$	$439\ s^{-1}$

At a measuring time of 1000 s the detection of 50 g U_{nat} (360 mg ^{235}U) was possible from positions near the surface to 175 mm behind the surface. A detection in the centre was not possible with this measuring time and neutron flux for statistical reasons. In view of the low fissile content of the sample (360 mg ^{235}U) the result is acceptable. Compared to the experiments with the Sb-Be neutron source reported in /6/ Table III the obtained fission count rates are comparable:

- Li (p,n) Be neutrons, Table V
  average net fission count rate $C_F = 0{,}06\ s^{-1}/0.360\ g$
  $= 0.17\ s^{-1}\ g^{-1}$
- Sb-Be neutrons /6/, Table III
  average net fission count rate $C_F = 0.76\ s^{-1}/15\ g$
  $= 0.05\ s^{-1}\ g^{-1}$

The results with the accelerator neutrons are thus by far superior to the results with the radioactive Am-Li source and comparable to the Sb-Be results. Future experiments with increased fissile material load, and other improvements, will probably enable detection in the central part of a cemented drum.

C 3: Design of an active system for small samples

To investigate the typical properties of the Li(p,n)Be reaction, an active assay system was designed and completed for operation at the linac in KFA-IFF. Because the irradiation room at the IFF linac is restricted, samples to be measured are limited to a volume of about 1 l. The general layout is given in Figure 5.

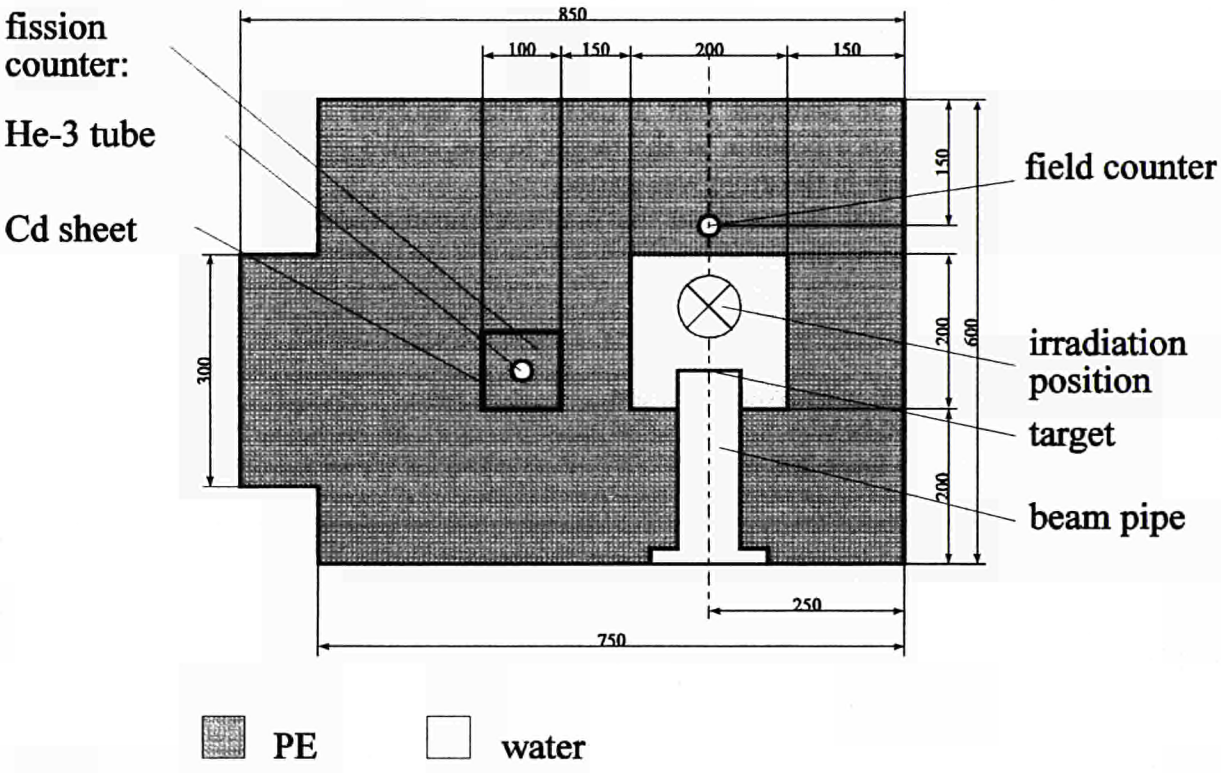

Figure 5

Cross-sectional view of the active system for small samples.

The system is completely confined by a PE shielding and surrounded by concrete the walls (500 mm) of the irradiation room (not shown in Figure 5). It mainly consists of the target mounting, the irradiation position placed in a water tank, a field counter in beam direction behind the sample position (^{3}He tube) and the fission counter.
The target is electrically insulated and equipped for measuring the target current to provide an estimation of neutron and heat production at the target. Before the beam hits the target it has to pass through an aperture consisting of four sectors to electrically determine the beam direction and to ensure that the beam hits the target with its whole width.
The fission counter consists of a ^{3}He tube embedded in a 100 mm PE block, which is surrounded by a 0.5 mm Cd sheet.
The system is designed to place the fission counter in any position in the shielding in order to vary the transport layer thickness and to evaluate the neutron flux anywhere in the system.

It is planned to investigate the following topics with this system:

- Detection capabilities and limits in comparison to the active systems of large dimensions.
- Estimation of the dependence of the separation of source and fission neutrons on the angle between the beam axis and the axis of the fission counter and sample position.
- Estimation of the dependence of the separation on the transport layer thickness at different source neutron energies.
- Self-absorption effects of thick samples.

First measurements with this system were carried out in February 1995.

D. CONCLUSIONS

The passive neutron interrogation system has been improved to obtain a reduced variation of the detection efficiency over the drum.
The use of high-density concrete as a matrix material does not influence the neutron count rate by far as much as for gamma radiation.

The active neutron assay system has been successfully operated at a proton accelerator with the Li (p,n) Be reaction near the threshold (1.88 MeV) for neutron production. The gamma dose rate of this source is several decades below that of the Sb-Be source. Handling is therefore easier. The features of this neutron source are very favourable. They provide detection capabilities for fissile material similar to those of the Sb-Be neutron source. The detection limits are between 7 and 150 mg ^{235}U depending on the matrix material and the depth in the drum. Even with concrete as the matrix material, the results are promising.
The combination of the accelerator neutron source with our detector system led to a versatile and easy-to-handle detection system for fissile material in waste matrices.
An active system for small-sized samples has been developed for further investigation of the features of the Li(p,n)be reaction as a neutron source for active neutron interrogation. This system will start operation soon.

E. REFERENCES

/1/ Mandoki, R.; Bruggeman, U.; Van Iseghem, P.;
Determination of fissile material by neutron interrogation: Design study by means of the MCNP Monte-Carlo Transport Code. SCK/CEN Annual Report 1993, R-2996, restricted

/2/ Odoj, R.; Filß, P., et al.
Determination of Fissile Material by Neutron Transport Interrogation. Annual report to the CEC for the period 1 Jan. 1993 to 31 Dec. 1993

/3/ Wirtz, K.; Beckurts, K.H.;
Elementare Neutronenphysik
Springer-Verlag (1958)

/4/ Marion, J.B; Fowler, J.L.
Fast Neutron Physics, Part I
Interscience Publisher, Inc. New York (1962)

/5/ Werle H.
Spektrumsmessungen radioaktiver Neutronenquellen im Energiebereich von 10 keV bis 10 MeV mit Protonenrückstoß-Proportionlzählvolumen
KfK, INR-4/70-25 (1970)

/6/ Filß, P.
Spalturanbestimmung in Abfallfässern und Lagerkannen für bestrahlte Brennelementkugeln durch Interrogation mit Neutronen einer Sb-Be-Quelle und Nachweis der prompten Spaltneutronen Jül-2027 (1985)

Title: **Inventory and Characterization of Important Radionuclides for Safety of Storage and Disposal. Correlation with Key Nuclides that are Easy to Measure in Typical Waste Streams.**

Contractors: CEA Cadarache, GRS-Cologne, ONDRAF/NIRAS, ENEA-Saluggia, ENRESA, AEA-Dounreay.
Contracts No: FI2W-CT90-0034 and FI2W-CT91-0109
Duration of contracts: from May 1991 to September 1995
Period covered:
Project leaders: A. Raymond, CEA-Cadarache (co-ordinator for contract n° FI2W-CT90-0034) - W. Müller, GRS-Cologne (co-ordinator for contract n° FI2W-CT91-0109) -
R. Gens, ONDRAF/NIRAS - M. Gili, ENEA-Saluggia - A. Morales, ENRESA - A. Yates, AEA-Dounreay.

A. OBJECTIVES AND SCOPE

This contribution to the characterization and the inventory of radionuclides important for the safety of storage and disposal has three main objectives:
- checking and standardisation of operational destructive and non-destructive analytical methods with application to the main waste streams of the participating institutions,
- development of some alternative analytical methods for long-lived radionuclides,
- computation of correlation factors for critical radionuclides to easily measurable key nuclides, through the analysis of the main waste streams of the contractors.

Only low- or intermediate-level wastes originating from both power plants or fuel reprocessing plants are considered in the framework of these contracts.

Samples of each selected waste stream are analysed for both easy-to-measure and critical radionuclides as determined by the national safety assessment of each contractor.

B. WORK PROGRAMME

B.1: Organization - Coordination
- review of the initial situation of the participants.
- list of information to be collected and studied.
- final choice of the list of samples and of radionuclides to be analysed.
- setting up of a working organization.

B.2: Development of analytical methods
- improvement of the current procedures for long-lived radionuclides.

- search for alternative methods as compared to those based on radiation detection.
- development of special procedures for the recovery of radionuclides from solid, low-level technological wastes.
- drafting of some common analytical methods.

B.3: Measurement of wastes from nuclear power plants (CEA, ONDRAF/NIRAS, ENRESA, GRS)
- collection of available results from previous measurements.
- waste sampling and analysis for the radioactive content.
- collection of the necessary relevant information.
- transfer of the corresponding results into the data bank.
- assessment of the results and discussion of possible further improvements concerning the number and the representativity of samples.

B.4: Measurement of wastes from fuel reprocessing plants (ENEA, AEA Technology)
- construction of a non-destructive measurement system for gamma-emitters (ENEA).
- preparation of simulated waste drums.
- tests of the measuring equipments with simulated wastes.
- intercomparison of the tests results (AEA and ENEA).
- destructive and non-destructive measurement campaigns on reprocessing wastes.
- assessment of the results and discussion of possible further improvements.

B.5: data evaluation and processing (GRS)
- evaluation of available results from previous measurements.
- continuous evaluation of the results relevant to this programme.
- implementation of data banks for wastes from both fuel reprocessing and nuclear power plants.
- development of statistical tools for evaluation of results.
- development of individual evaluation codes for each participant.
- testing and optimisation of codes for routine applications.

C. PROGRESS OF WORK AND OBTAINED RESULTS

Status of progress has not been forwarded to the Commission for 1994.

Title	**Construction and Testing of a Computer Tomography Assembly for Routine Operation**
Contractors	Forschungszentrum Jülich (KFA), FRG
Contract N°	FI2W-CT90-0009
Duration of contract	1 September 1991 - 31 August 1995
Period covered	1 January 1994 - 31 December 1994
Project leader	Dr. Reinhard Odoj Dipl.-Ing. Peter Eifler

A. OBJECTIVES AND SCOPE

The disposal of barrels containing radioactive waste material into an underground repository has to meet certain requirements of governmental regulations, one of which is the specification of the radionuclide inventory. This can be achieved by tomographic analysis of the waste containers. If a cemented matrix of relatively high density is used to condition the waste, a considerable fraction of the inner radiation is absorbed in the barrel itself. This has to be taken into account in an effort to obtain reliable results using the technique of emission tomography to quantitatively determine the specific and total activity of the waste drum. The analysis becomes even more difficult if the activity and the density of the material are distributed inhomogeneously within the barrel, or if e.g. the barrel contains canisters of unknown kind, number and size.

The preliminary objective is the measurement of the density distribution of shielded structures and heterogeneous fillings inside the drum by using a transmission tomographic method, followed by the analysis of the activity distribution of the radionuclides contained in the drum by applying the technique of emission tomography. This work including the design of a future waste tomography assay system exclusively focuses on 200 liter drums containing Low-Level-Waste (LLW) with a maximum surface dose rate of 2 mSv/h. The contents of the drums is either cemented (high density) or compacted (generally low density) with an unknown matrix. Since the inner absorption of cemented waste is generally much higher than the inner absorption of super-compacted waste, the tomographic measurements described in this paper are performed on a cemented matrix. This ensures, that the tomography assembly is capable to assay nuclear waste of almost any density, i.e. waste barrels of arbitrary contents.

B. WORK PROGRAM

B1. Design and construction of an advanced tomography assay system for nuclear waste barrels with four major capabilities:

- fast γ-scanning (GS)
- digital radiography (DR)
- transmission computerized tomography (TCT)
- emission computerized tomography (ECT)

B2. Software and hardware requirements:

- development of tomography software for transmission (TCT) and emission (ECT) tomography
- design of technical equipment in order to synchronize mechanical movement, count rate measurements and absorption data transfer to the computer
- visualization of the density and activity distribution and determination of the total activity of the waste drum

B3. Comparative test measurements:

- on dummies with different materials for testing purposes
- on typical waste drums with inner shieldings

C. PROGRESS OF WORK AND OBTAINED RESULTS

State of advancement

The initial work program was aimed at the measurement and the calculation of the density distribution of the contents of nuclear waste drums by a transmission tomography technique. The density analysis would provide information about inner shieldings and heterogeneous fillings of the waste drum. This information would be used to correct the emission data of the γ-scanning technique to calculate the total activity of the drum correctly. Not only did the work on the transmission tomography technique come to a high standard but also could the technique of emission tomography be developed to a great extent. The emission tomography technique enables to quantitatively determine the activity distribution of all detectable radioisotopes within the drum. During the period described in this report several LLW-drums have been examined by transmission as well as emission tomography. Considering the progress of work it is reasonable to modify the course of the remaining work program. It is intended not to remodel an existing γ-scanner with tomography capabilities but to construct an entirely new assay system. The new advanced tomography assay system will have extensive tomography capabilities (transmission and emission tomography), will perform γ-scanning and digital radiography, and is designed for fast assays of the waste drums. The assay system will be mobile to ensure flexible operation. A Monte-Carlo-simulation performed during this period and described in this report underlined the possibility that TCT and ECT methods can operate simultaneously.

Progress and results

The setup of the TCT/ECT-system (currently in operation at the KFA) is shown by fig. 1. The photography shows the major components of the tomography assembly: γ-source, turn-table, linear moving bench, collimator, Ge-detector and two vertical moving devices in order to examine different cross sections at different vertical positions of the drum. The experimental setup and its

mechanical equipment is designed to analyze 200 l waste drums. To ensure high precision of the drum positioning two stepping motors are used for the translation-rotational movement.

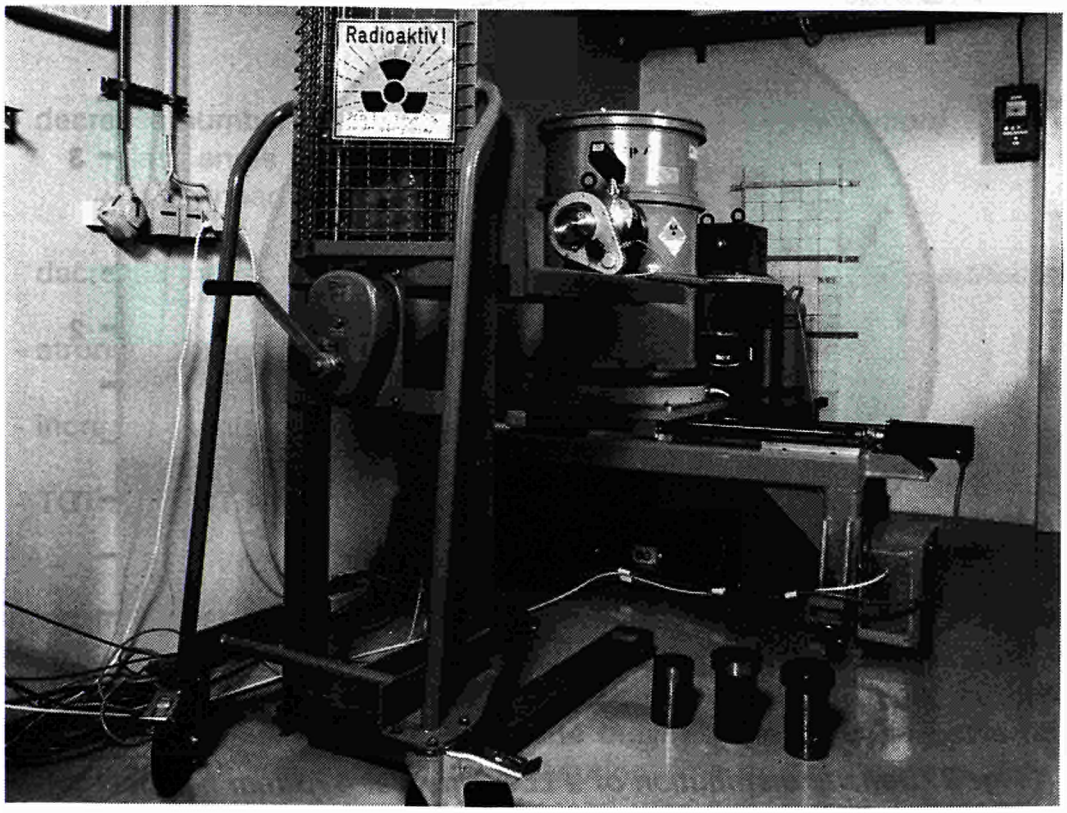

Fig. 1: TCT/ECT-assembly with radioactive LLW-drum

Fig. 2 shows the density distribution of a 200 l waste barrel of approx. 450 kg in weight. The density distribution was obtained by performing transmission tomography on the drum and by reconstructing the density by an ART-algorithm (**A**lgebraic **R**econstruction **T**echnique). The drum contains an inner canister surrounded by a thick cemented filling. The inner canister's contents is cemented material, which is distributed quite inhomogeneously showing a few, well defined, cracks. A hole of 6 cm diameter caused by a preliminary destructive assay can also be recognized. It is quite likely, that the inner canister contains radioactive material and that the outer cemented region is used for shielding purposes and will probably not contain any radioisotopes. This assumption is confirmed by the corresponding ECT-image (fig. 3). The image shows the ^{60}Co-activity distribution of the same drum at the same vertical position. All of the radioactivity is contained within the inner part of the drum, whereas the outer region is basically just a shielding. The reconstruction was carried out by a special ART-algorithm using density correction. The ECT activity image also shows the above-mentioned hole, which obviously cannot contain any radioisotopes. This activity hole would not have been found if the reconstruction algorithm had not used density correction of the emission data. The activity scale of the image is not yet calibrated, but this will be done as a future step.

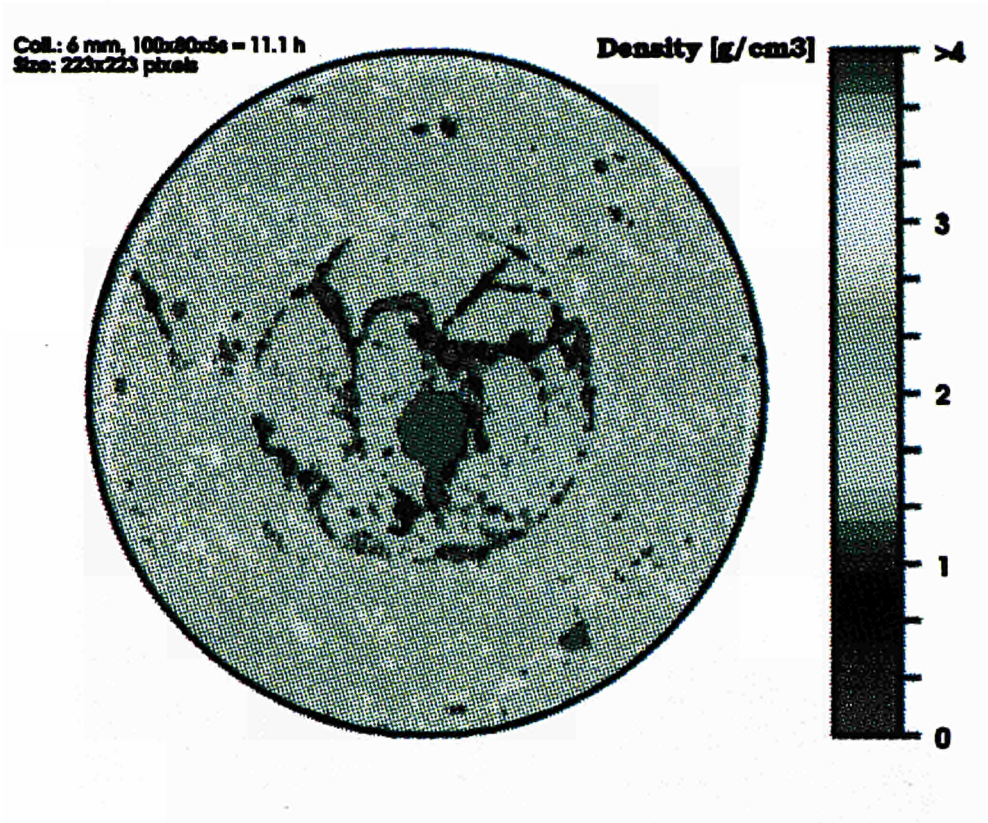

Fig. 2: Density distribution of a LLW-drum at 473 mm height

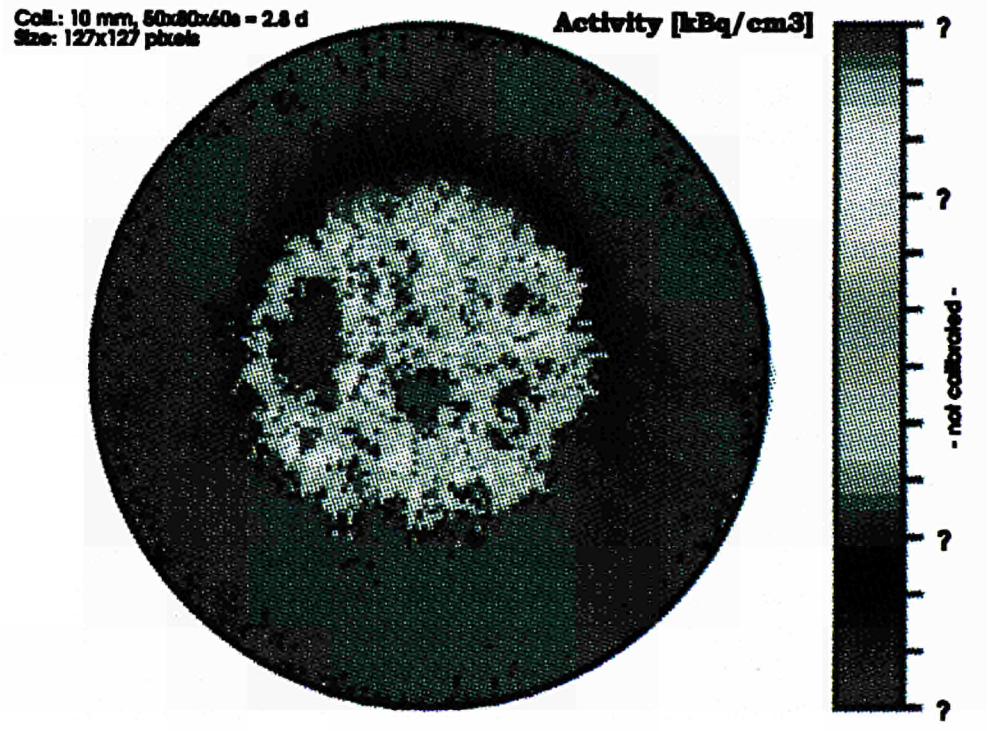

Fig. 3: ^{60}Co-activity distribution of the LLW-drum of fig. 2

In nuclear waste management it is very important to be capable of performing a fast tomography assay on the waste drums. In this respect there are several aspects, which should be very closely considered when designing a tomography assay system for nuclear waste:

- decrease number of measuring steps *(worse resolution)*
  - less angle positions
  - less linear scan steps
- decrease measuring time per step *(worse statistics, more artifacts)*
- stronger source and faster detectors *(expensive)*
- increase number of detectors *(expensive)*
- TCT and ECT simultaneously

Performing transmission tomography in a reasonable short time is not much of a problem. But analyzing the drum using the ECT-technique is, in general, very much time consuming. The question arises whether high resolution applications are necessary in nuclear waste business. In order to get a better understanding of the influence of the measuring time on the image quality the measuring time per step during an ECT-assay was set to only 1 second. The activity distribution was reconstructed and is shown by fig. 4. Fig. 4 illustrates the ^{60}Co-distribution of the drum previously shown in figs. 2 and 3. The reconstruction still gives a quite reasonable image. It is still possible to recognize that the radioactivity is contained in an inner canister. The activity hole is also visible. The ECT-measurement used a collimator of 30 mm, 1 second of measuring time, 80 angle positions and 50 scan steps per angle position. The whole ECT-procedure took about 1.1 hours, keeping in mind, that only one detector was used. The surface dose rate of the drum at this particular horizontal cross-section was approx. 300 μSv/h.

One of the aspects to accelerate tomography is to perform TCT and ECT simultaneously. It should be possible to carry out TCT and ECT measurements at the same time, even though the TCT γ-particles are very much scattered in the drum matrix. To get a better understanding of the behavior of a combined TCT and ECT geometry a Monte-Carlo simulation was performed on the setup shown in fig. 5.

The simulation was carried out by a FORTRAN computer code called MCNP. The likelihood that γ-rays will scatter or interact within the waste is many times greater than it is for them to travel through unperturbed. It is questionable if the detector shielding is sufficient enough to keep the scattered TCT γ-rays from contributing to the ECT detector readings.

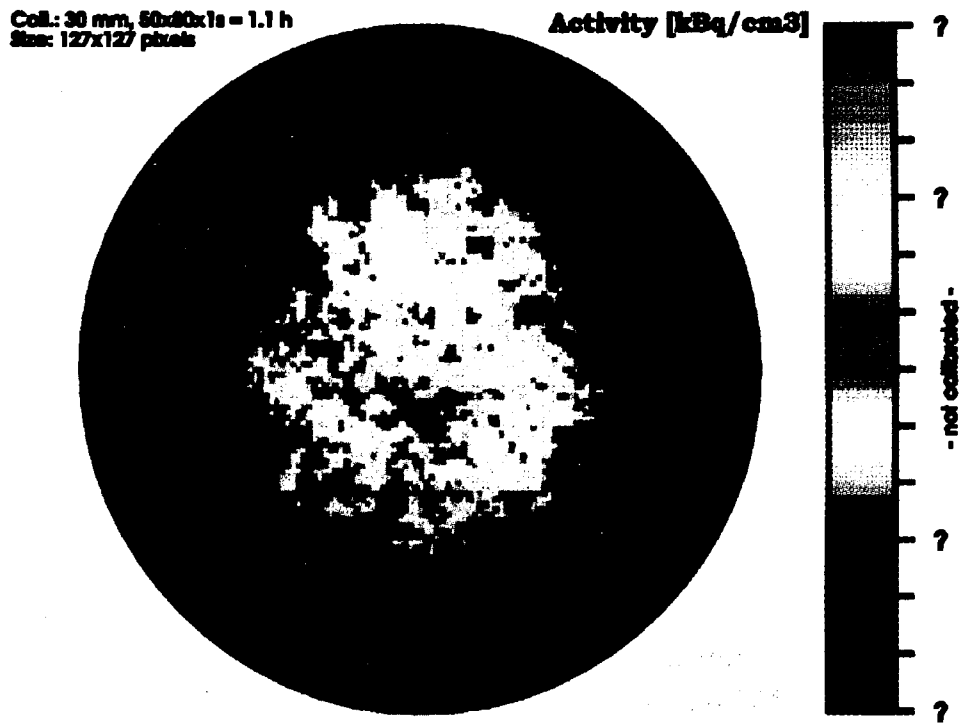

Fig. 4: Accelerated ECT of the LLW-drum shown in fig. 3

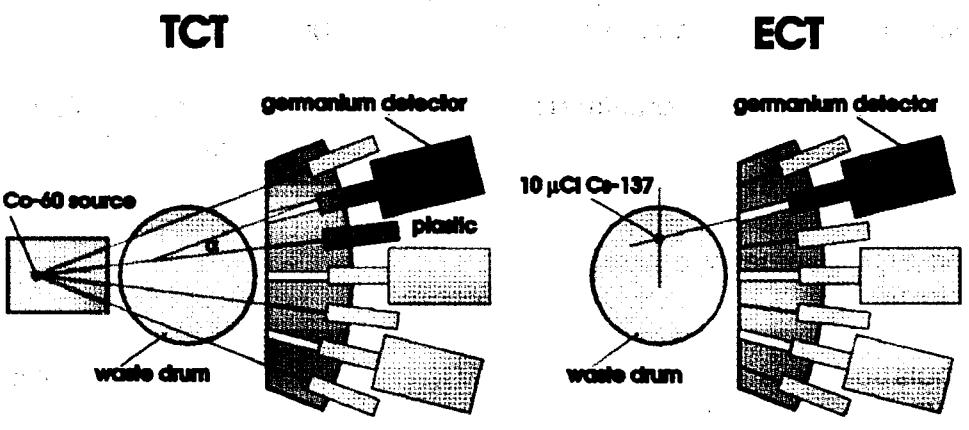

Fig. 5: Geometries of the Monte-Carlo simulation

To answer the question if the γ-rays of the external source (7 Ci) would adversely affect the readings in the germanium detectors, separate TCT and ECT simulations had to be run (fig. 5). Several assumptions were made when inputting the geometry into the computer code. First, the cylindrical source was assumed to be an isotropic point source. Second, since only the effect of the geometry was desired, all detectors were modeled as germanium to avoid introducing a detector material variable. (NOTE: Regardless if a different material was used in modeling, all references made to the plastic detectors identify them as the TCT- detectors.) For the ECT simulation, a 10 μCi source of 662 keV gammas was modeled for the nuclide ^{137}Cs. The source was placed in the midpoint of the waste drum along the axis of the collimator for the Ge-detector at +14°.

Summing of the TCT and ECT simulation data resulted in the combined TCT&ECT-spectrum of the Ge-detector shown in fig. 6. The two slightly back-shifted peaks with less energy than the two well-known photo peaks of ^{60}Co are caused by compton scattering in the drum matrix. In compton scattering, the incoming γ-ray photon is deflected through an angle α with respect to its original direction (see fig. 5) [G. Knoll 1989]. The scattered photon will appear in the Ge-spectrum as a photo peak of less than its original energy. Since the angle α is known to be approx. 12° the energy of the scattered photon can be calculated by:

$$h\nu' = \frac{h\nu}{1 + \frac{h\nu}{m_0 c^2}(1 - \cos\alpha)} = 1.26 \text{ MeV}$$

$h\nu$ = 1.332 MeV (upper peak)
m_0c^2 = 0.511 MeV

For the relatively small activity of 10 μCi of the ^{137}Cs-radioisotope the 662 keV γ-peak is easily visible. The 7 Ci ^{60}Co certainly has an effect on the background noise, however, proper background elimination and peak area determinations should yield only the desired ECT source contribution. The TCT results were obtained from a simulation run which followed 500 million source particles.

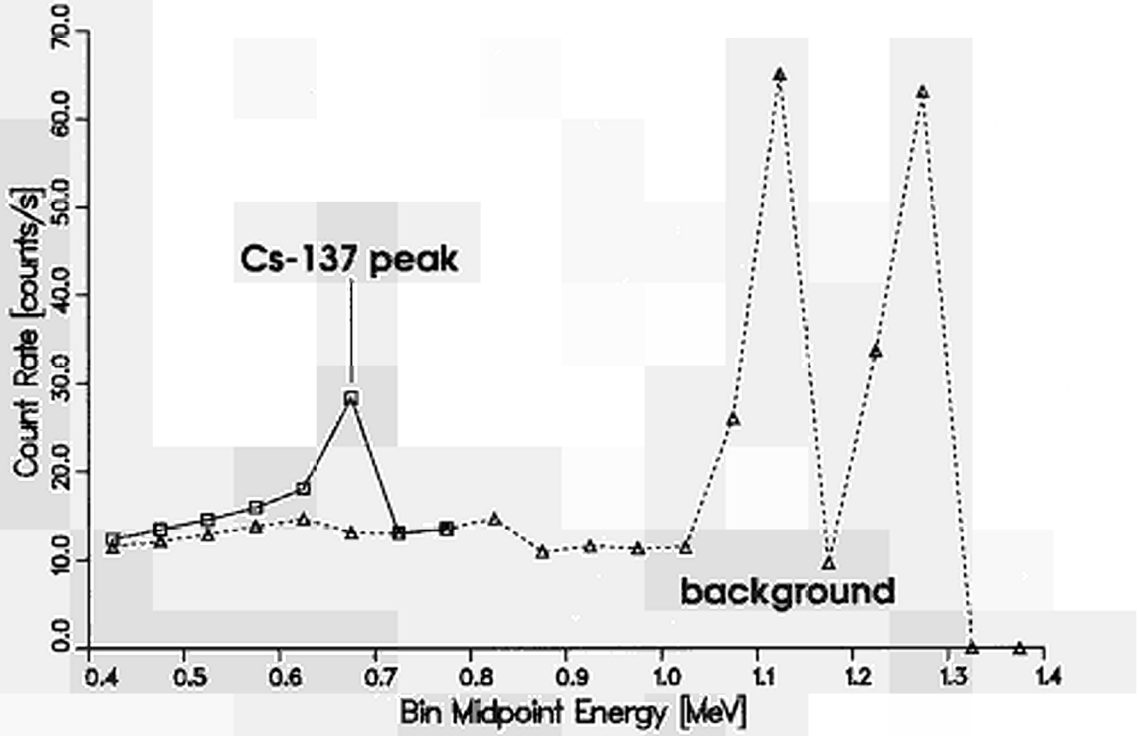

Fig. 6: Combined TCT&ECT-spectrum of the Ge-detector

List of publications

[G. Knoll 1989] Glenn F. Knoll, Radiation Detection and Measurement, 2. Edition, John Wiley & Sons, 1989.

Title	Test process control during treatment of low and medium radioactive waste in practise
Contractors	KEMA Nederland B.V., KFA Jülich, Laborelec
Contract N°	FI2W-CT90-0019
Duration of contract	January 1991 - December 1994
Period covered	January 1994 - December 1994
Project leader	H.A.W. Cornelissen, KEMA Nederland B.V. Arnhem; R. Odoj, (KFA-Jülich); R. Roofthooft (Laborelec)

A. OBJECTIVES AND SCOPE

Adequate management of radioactive waste that will be formed during operation of nuclear power stations, is an absolute necessity to warrant the protection of man and environment. Therefore, the total waste treatment process from waste release up to interim/final storage has to be controlled. Continuous process control is preferable above verification just before storage because of its higher reliability, traceability and the possibility for corrections of the system.

This research project refers to the development of test methods which are necessary to control the process of conditioning of radioactive waste. The emphasis lies upon measurement techniques and operations.

On the basis of the international exchange of information between the partners recommendations will be formulated with respect to standard testing methods and procedures where specific quality systems can be based on.

There is also a close cooperation with CEA/CEN and Taylor Woodrow.

B. WORK PROGRAMMA

Subject 1: Process descriptions of waste treatment
Subject 2: Chemical characterization
Subject 3: Radiological qualification test methods
Subject 4: Mechanical and physical qualification tests
Subject 5: Validation of test methods and evaluation.

C. PROGRESS OF WORK AND OBTAINED RESULTS

State of advancement

During this period the laboratory examinations with regard to the chemical, mechanical/physical and radiological characterization of cement/rad waste mixtures was finished. In November 1994 a validation experiment was performed at GKN Dodewaard (The Netherlands); further some experiments were performed at Doel reactor (Belgium). The results have been evaluated now.

Progress and results

C.1 Chemical characterization

The chemical characterization with respect to the determination of the concentrations of cement poisons in aqueous slurries has been finished now. Two methods are examined, namely the photometric method and measurement by means of selective electrodes. The photometric method was performed by a portable photometer (Merck, SQ 118) and multi-element kits. It was shown that the linearity for most of the species was fairly good. Further it turned out that both the reproducibility and accuracy were very satisfying.

With regard to the restricted commercial availability examinations by means of selective electrodes could only be performed for nitrate, chloride, calcium and ammonia. The calcium determinations were interfered by alkali ions present in the artificial waste water solution. Further the pH of this solution was high, namely 11. So, the ammonia concentration of it was negligible. Therefore, the detection limit was determined (0.5 $mg.l^{-1}$).

C.2 Mechanical/Physical characterization

For the prediction of the compressive strength of the hardened cemented rad waste mixture two methods were investigated, namely the impedance - and viscosity - method.

With regard to the impedance some measurements were performed at a frequency of 100 kHz. Now these measurement were performed after 10 minutes of preparation of the cement/rad waste mixtures.

The results of the second series of samples are shown in figure 1. Now the relationship between 7- and 14-days strength were found to be exponential, which was caused by varying both the w/c-ratio and the amount of rad waste:

$S = 86.14 \exp(-0.016.Z)$ (7-days strength prediction)

$S = 99.34 \exp(-0.017.Z)$ (14-days strength prediction)

where :
S = compressive strength
Z = impedance

This is an indication that the rad waste concentration influences the bonding process during hydration.

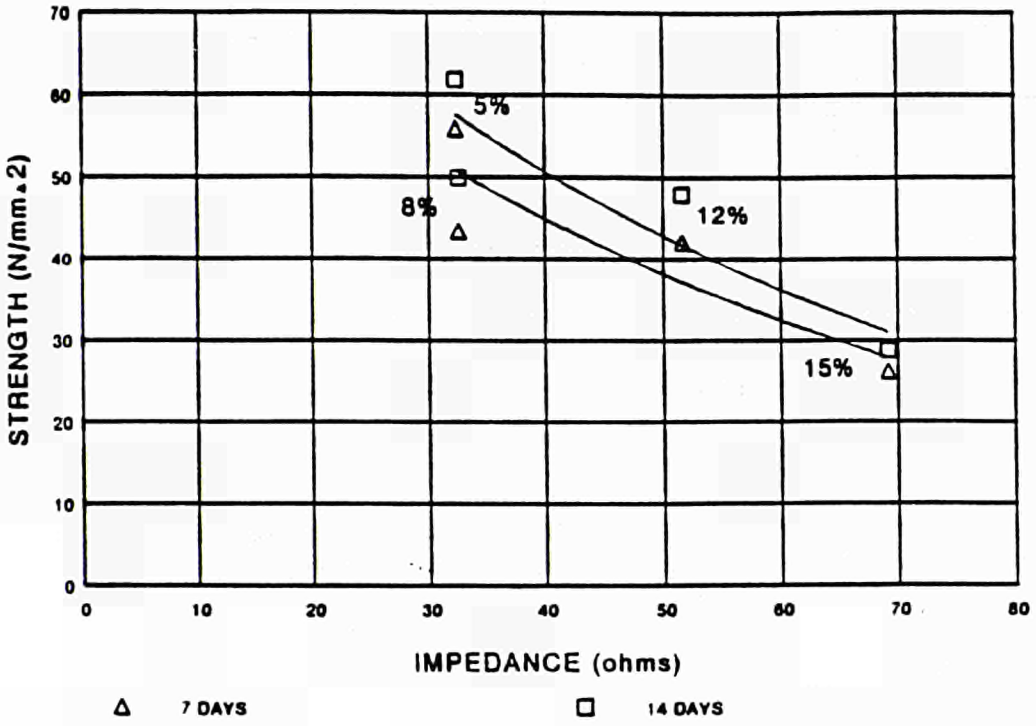

Figure 1 Impedance versus 7 and 14 days strength at various w/c ratios and rad waste concentrations. The values of these concentrations are given at the curve

The plastic viscosity was measured in a shear-rate interval between 31.85 and 191.12 sec^{-1}. If both the w/c-ratio and rad waste concentration were varied an exponential relationship of the strength and plastic viscosity was found:

S = 15.36 exp(0.45V) (7-days strength prediction)
S = 16.57 exp(o.47V) (14-days strength prediction)

where:
S = compressive strength
V = plastic viscosity.

The reliability of the results was excellent and the standard deviation was 0.323 Pa.s.

The results are given in figure 2.

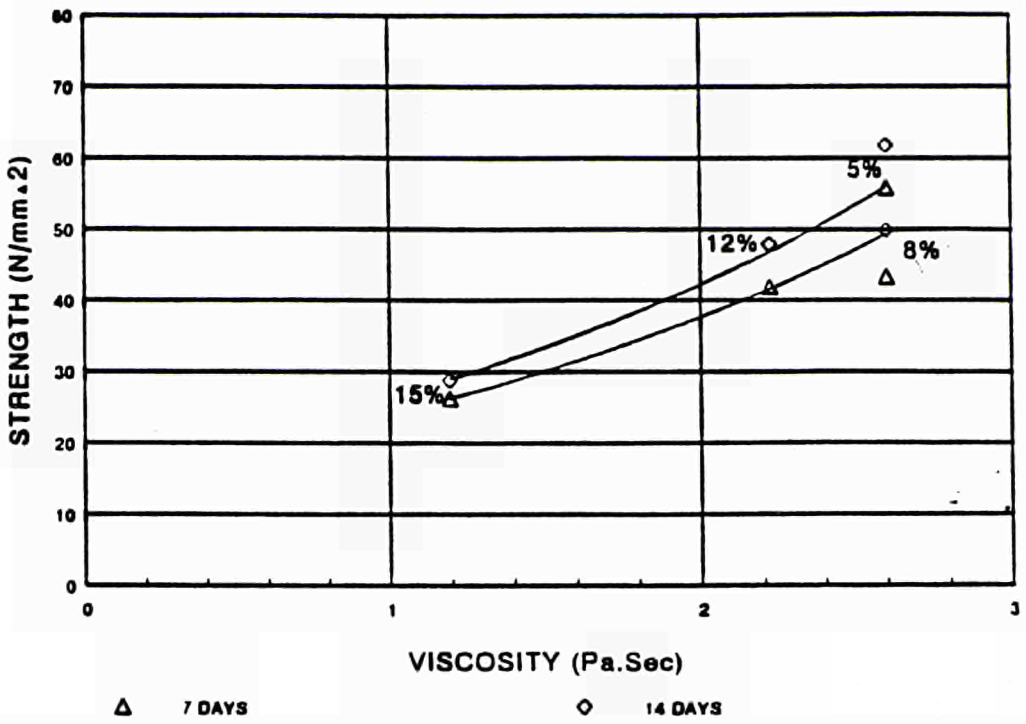

Figure 2 Viscosity versus 7 and 14 days strength at various w/c ratios and rad waste concentrations. The values of these concentrations are given at the curve

C.2 Radiological characterization

Two items were examined:

* the uniform analysis method for gamma spectra measured with incoming countrates of 2000 cps up till 500 000 cps
* the estimation of the system performance for detecting inhomogeneous immobilized radioactive waste in a 200 litre concrete package.

In figure 3 the total plot of gamma spectrum 13C5CSD6.SPE of the KEMA Test Vessel is shown.

The spectrum is measured with settings for high countrates. By careful observation of the shape of the photo peaks, one can see that the low energy tale of the photo peak increases by increasing photon energy. By analysing these peaks with commercial software it does not recognize these peaks as a single peak but treat them as **multiplets**.

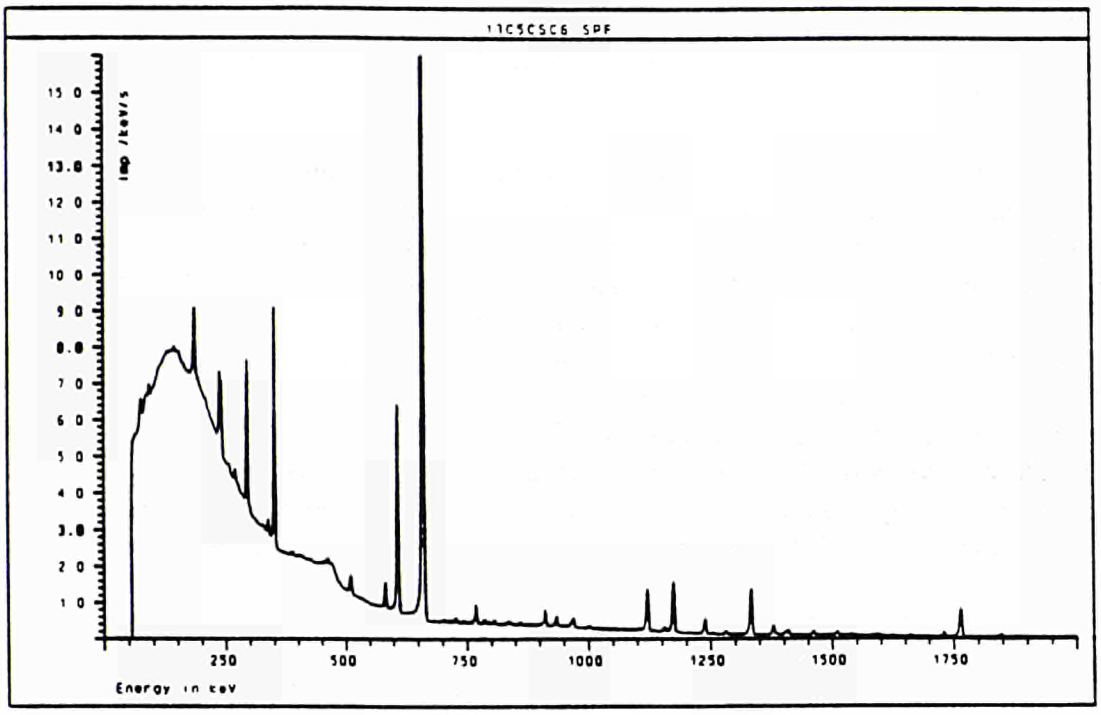

Figure 3 Gamma spectrum 13C5CSDC6.SPE of the KEMA Test Vessel with inside inhomogeneous distributed activities of ^{57}CO, ^{60}Co en ^{137}Cs. This inhomogeneity has been created by calibrated Amersham point sources.

Gamma spectroscopy specialists will judge in such cases each spectrum and skip through the reported nuclide inventory list to delete all false reported nuclides. The operator shall, due to a lack of time, easily accept the reported results by the software package.

Trained operators will have no problems with calculating the total sum of the nett area of a multiplet. However, problems will arise when deciding whether a reported part of a multiplet peak belongs to the main peak or to a second main peak from the same multiplet (see ^{214}Bi). This problem will increase by more complex spectra.

The disadvantage of this method is, that the system reports a lower nett area (technical performance) of about 15% for all energies. The great advantage of the method is, that the constant quality of the reported output is much better and easier to understand for non specialists.

The following conclusions can be drawn:

* the chance, that a wrong waste package nuclide inventory is reported, is less ny using solely main photo peaks of a multiplet analysis, then by summing all parts of the multiplet
* when this method of activity calculation is accepted, one accepts automatically that the system does not measure with the best efficiency (laboratory technical performance)

* operators will report nuclide inventories of waste packages with a better constant quality, when the system is not adjusted with "laboratory settings" but with "high countrate settings".

The quality assurance for online detection of inhomogeneous distributed immobilized waste packages depends on the sensitivity of a system to detect inhomogeneity. The performance parameter, which describes this detection limit, is called the "Minimum inhomogeneous Distributed Activity Standard deviation (MIDAS)". The value of this parameter for a certain system depends on:

* the detection geometry of the waste package (e.g. 200 litre with a density of 2300 kg/m^3) and detector (bare or with a collimator)
* the energy of the emitted photons (e.g. 661 keV and 1332 keV)
* the standard deviation of the specific radioactivity of the nuclides. This standard deviation is usually less then 5% and depends on the reported activity from a laboratory analysis of a little amount of the raw waste before it is immobilized.

The first two items are determined by the calibration of the HpGe waste system. The standard deviation of the efficiency of a waste system for all energies can be lass than 5%. This means that the standard deviation of the nuclide specific radioactivity can also be less then 5%. The third item depends on the calibration of the laboratory system. For this system an equal or even better accuracy performance can be reached.

The detection uncertainties of both systems gives an estimated overall uncertainty of about 7%. The best specification of MIDAS is equal to the estimated overall uncertainty of 7%. In practice the value of MIDAS deviation will be greater than 7%. The assessment of the value of MIDAS leads to the conclusion, that when **more than 10%** of the major nuclides have been distributed inhomogeneous, the waste system must be able to detect this inhomogeneity.

C.4 Validation experiments

C.4.1 General

The validation experiment was performed at GKN Dodewaard (the Netherlands) in November 1994. For the tests a 200 litres drum of the rad waste campaign was instrumented and monitored. The selected test methods for on-line quality control were assessed.

Additional tests were performed at the Doel PWR (Belgium) especially focused to the prediction of mechanical properties of the cemented rad waste and the verification by means of "hot" compressive tests on test cubes.

C.4.2 Chemical tests

The objective was to determine the concentrations of the various cement poisons in an aqueous radioactive waste mixture from the Dodewaard power plant by means of the two methods already studied at laboratory scale, namely photometry (KFA Jülich) and selected electrodes (KEMA).

Therefore, the solution was diluted and then divided into two equal parts. The first part has been sent to KFA Jülich for the determination of the species by photometry and the second part is has been sent to KEMA for the determination of nitrate, chloride and ammonia by selected electrodes.

C.4.3 Radiological tests

The objective is to determine online if the radioactive waste is immobilized inhomogeneous and to determine the nuclide inventory. Therefore, the next experiments with the proto type system and developed procedure will be performed at several concrete packages. These packages will contain an estimated activity of $3.7\ 10^{10}$ Bq (1 Ci) of ^{60}Co.

The following experiments are proposed and will be performed when possible:

- one 200 litre package will be monitored during the hardening process of the concrete. This experiment gives information about the dynamics of the immobilized radioactivity during the hardening process. The detector will be positioned at the top centre of the packages
- two 200 litre packages will be measured with the detector at top and side centre of the package. These experiments will indicate if it is possible to measure online the inhomogeneity of a waste package
  Remark: these measurements will take place after the cemented waste is hardened. This is necessary for reducing the dose of the involved persons
- one 1000 litre container will be measured with the detector at top and side centre of the package. In this concrete container will be a 200 litre waste package with homogeneous immobilized radioactive liquid waste but also with an unknown inhomogeneity of ^{60}Co. This inhomogeneity will be caused by contaminated/irradiated iron parts from the nuclear power plant.

C.4.3 Mechanical tests

The objective is to characterize the properties of the fresh and hardened, cemented rad waste for predicting the compressive strength after 28 days of hardening.

Laboratory tests showed that the viscosity of the fresh mixture as well as the development of temperature and electrical resistance (impedance) correlated well with the strength of the hardened conditioned rad waste. The validation tests will therefore include these three testing methods.

In Dodewaard, two 200 litres drums will be prepared to fix two thermocouples and the two electrodes for the impedance measurements.

The composition of the rad waste and the mix proportions of the cementated waste of both drums will be reported.

Temperature measurements will take place during the first 24 hours after mixing on both drums simultaneously. The impedance measurement, during about one hour after casting, will be performed on the drums one by one.

During mixing the electrical energy consumption of the mixer will be recorded. This is a measure for the viscosity.

In the KEMA laboratory simulation mixtures (but not radioactive) will be prepared containing the same materials as the two drums. The 28 days compressive strength will be determined on standard prisms (40x40x160 mm). Viscosity and impedance will be measured as well. For temperature measurements the mass will be too small.

In Doel also energy consumption of cementated waste will be recorded during a rad waste campaign in the autumn of 1994. During hardening, temperature development and impedance will be monitored as well. The equipment will be supplied by KEMA. Then the 28 days compressive strength of the actual "hot" cementated waste will be measured.

Title :	Establishment of non destructive or partially destructive test procedures for determining the characteristics of wastes containers
Contractor:	CEA Cadarache
Contract N°:	FI2W-CT90-0021
Duration of contract:	1 October 1991 - 30 September 1995
Period covered:	
Project leader:	J. MISRAKI; Co-author: R. BOSSY

A. OBJECTIVES AND SCOPES

In the frame of the low and medium wastes package's characterization, this programme proposes to establish, examination procedures, leaning on acquired experiences about real packages.
One of the main objectives is to limit very hardest the destructive examinations, the non destructive examinations having the advantage not to cause secondary wastes.

B. WORK PROGRAMME

B1: Sampling methods for analysis (alpha, beta, gamma)
B2: Gamma scanning on packages
B3: Microorganism actions on embedded wastes
B4: Water content measurement in embedded wastes
B5: Radiolysis gas measurement
B6: Thermoluminescent dosimetry

C. PROGRESS OF WORK AND RESULTS OBTAINED

The status of progress has not been forwarded to the Commission for 1994.

Title:	Non-Destructive Examination of Nuclear Radioactive Waste Packages by Advanced Radiometric Methods
Contractors:	BAM Berlin, TU Munich, CEA CEN-Valrho
Contract N°:	FI2W-CT90-0023
Duration of contract:	from 1.9.1991 to 31.12.1995
Period covered:	1.1.1994 to 31.12.1994
Project Leaders:	Dr. P. Reimers (BAM, Coordinator), C. Lierse (TUM) E. Vernaz (CEN)

A. *OBJECTIVES AND SCOPE*

NONDESTRUCTIVE EXAMINATION OF NUCLEAR WASTE PACKAGES BY ADVANCED RADIOMETRIC METHODS

The radiometric methods to be applied to the nondestructive examination of nuclear waste packages are computerized tomography (CT), digital radiography (DR), and microtomography (MCT). CT with Co-60 and linac radiation is established at BAM since more than five years. A new scanner particularly designed for waste drums was installed at TU Munich during the first months of 1992. It will be used for the work of this contract.

Computerized tomography (CT) offers the possibility to get information about the internal structure of waste containers. Often it is sufficient to make CT-measurements on selected parts of a package. Therefore, a fast method to get a survey image of the total package is very useful. As shown in the work before (CEC Report 1985-1989), digital radiography is such a NDT-method. The disadvantage is that with a one detector system the measuring time is much higher than for a CT measurement. DR with a CT-multidetector system gives a distortion of the geometry of the object. Part of this contract is the development of a new data acquisition programme that fulfills the following conditions:

- Measuring time lower than 10 min for a 200 l drum
- Correct geometrical projection and intensity calibration, probably by software correction
- Wide energy range (400 kV X-ray, Co-60, LINAC-12 MeV)

For high energy computed tomography (HECT) a new detector will be designed with improved dynamic range and fast read out time. After design and construction of the complete detector array the performance test will deliver information about spatial resolution, density resolution and limits of data readout time.

Three methods will be developed to improve the information from DR measurements:

- difference image formation
- filtering processes
- interactive image processing.

The objective of the CEN-VALRHO work is the improved quality assurance of vitrified HLW packages. The purpose of this investigation is to develop a nondestructive tomographic examination method for vitrified waste packages.

The principal defects that occur during the fabrication of glass blocks are:

- cracks and cavities which increase the surface area exposed to leaching water

- molybdic inclusions which are water soluble.

The goal is to qualify and quantify those defects by a tomographic method.
The tomographic examination method will also be applied to estimate the water penetration into the glass block inside its canister, and the glass surface area actually in contact with the water. The consolidation effect of annealing the glass block to limit the degree of fracturation will be assessed using the same method.
The tomographic interpretations will be qualified by glass leach testing.

The objective of the work at TUM is the selection and application of destructive and nondestructive inspection methods for all kinds of LLW packagesc. It includes the use of computed tomography, digital radiography, gamma scanning, passive neutron counting and destructive testing (sampling methods).

B. WORK PROGRAMME

The work programme comprises three main tasks correlated to the three partners:
BAM - digital radiography (DR), computerized tomography (CT), and micro computerized tomography (MCT)
CEA - quality control of HLW-glass blocks
TUM - quality control of LLW-containers

The nondestructive investigation work of BAM focuses on three groups of waste subjects: drums, glass canisters, and waste samples.
The work programme comprises the following topics:
- CT investigation of real LLW and MLW packages
- Study of fissuration of HLW glass blocks
- Evaluation of crack length and geometry by image processing
- Study of representative sampling procedures
- Micro-computerized tomography of core samples

The work programme of CEN-VALRHO has the following topics:
- fabrication of nonradioactive glass blocks
- definition of the tomographic examination procedure and the detection limits
- definition of the image analysis procedure using a "Pericolor" system, measurement of the length of the cracks on the images and estimation of the total internal surface to calculate the fracturation ratio
- quantification of the molybdic phase percentage
- experimental validation of the tomographic interpretation using the leaching method developed in the CEC contract n° FI 1W 182.

The contribution of the "Institut für Radiochemie, Technische Universität München "(TUM), consists of the selection of 200 l drums with different categories of low level radioactive waste as they are produced in nuclear power plants or nuclear research centres. Furthermore they use computerized transmission tomography (TCT) and emission computerized tomography (ECT) for providing reliable information about the internal structure and composition of these waste containers. They also work on destructive sampling techniques followed by preparation procedures suitable for subsequent chemical and radiochemical analyses, and on the derivation of rules

for representative sampling based on the collected tomographic informations.
The time table for these tasks was updated and completed. The work at TUM was started at 1st March 1992, and will be finished until 31st December 1995. In addition to the tomographic measurements, the applications of gamma-scanning techniques and passive neutron counting were included in the work programme to extend the nondestructive tools and to provide additional data for an adequate characterization of the radioactive waste.

C. *PROGRESS OF WORK AND OBTAINED RESULTS*

State of advancement

According to the time schedule two of four drums with low level radioactive waste, which were measured extensively by non destructive methods at TU Munich and BAM, were selected for a destructive testing procedure. Three sealed canisters fabricated by CEN-Valrho with vitrified glass are characterized by CT. The fracturation of the glass blocks was calculated from these measurements.

Progress and results

C.1 Emission computerized tomography

The spatial distribution of the activity in a radioactive waste package can be measured with single photon emission computerized tomography (ECT). Here "single photon" illustrates that only photons from a gamma decay of the radionuclides contained in the waste are detected, in contrast to positron emission tomography (PET) where the annihilation of a positron-electron pair is detected by a pair of photons. In principle, ECT data sets are measured and reconstructed the same way as TCT data. However, one has to take care of collimating problems and of the attenuation of the gamma photons on their way through the material.
We investigated a 50 l barrel of bituminized intermediate level waste (ILW) with a total activity of 3.9 GBq ^{60}Co and 68.9 Gbq ^{137}Cs. The ECT data were measured with a collimated GeLi gamma detector. A conventional MCA and two window discriminators were used to identify and extract the signals of either radionuclide separately, so that both of them could be measured at once.
First results consist of three digital emission radiographs and four ECT data sets. Images of the activity distribution were obtained by a standard filtered backprojection algorithm.
Efforts have been made to develop an iterative procedure to correct the images for self attenuation. This development is not yet finished.

C.2 Evaluation of the internal surface

Three complementary investigation methods implemented to assess the degree of fracturation of a glass block were used to obtain results which have to be correlated. These methods are:

- A nondestructive tomographic method based on stereological rules developed at BAM.

- A measurement of the weight distribution of all the fragments constituting a fractured glass block performed at CEN-Valrhô.

- Water leach tests - static and dynamic - to estimate the degree of fracturation based on the proportionality between the leached surface area and the leachate concentration of mobile elements released from the glass performed several times at CEN-Valrhô.

The tomographic measurement was performed on three sealed canisters with vitrified simulated waste fabricated by CEN-Valrhô. The goal is the nondestructive determination of the surface of the glass block before leaching experiments are done. At first an overview of each canister was taken by digital radiography and after this ten tomographic slices were measured in a distance of 10 cm. Due to some technical problems with the LINAC these measurements were performed at first with a Co-60 radiation source.

For a determination of the surface area of the vitrified waste the evaluation of the crack lenght is essential. The total surface of a glass block consists on the surface of the cylinder F_C, the upper and lower end plate F_{EU} and F_{EL} the surface of the individual pieces F_R and the surface of large voids like the head lunker F_L.

$$F_{total} = F_R + F_C + F_{EU} + F_{EL} + F_L \ [m^2] \qquad \text{(Eq. 1)}$$

Based on a statistic method [5] there is a relationship between the ratio of a surface and the volume in which it is comprimized and the ratio of the lenght of a known number of test lines and their points of intersections with this surface.

Applying the above discussed method (Eq. 1) for the calculation of the total surface gives the following result for three canisters:

Canister	A	B	C
F_{total} [m^2]	9.18	4.77	11.08

In the next period it is foreseen to compare these results with water leach tests.

C.3 Progress at TUM

Selection of radioactive waste drums for destructive testing

On the basis of all results obtained by extensive non-destructive inspections two drums were selected for the destructive testing procedure:

- Drum EG 2, a 200 l drum with cemented evaporator bottoms from a nuclear power plant
- Drum EG 4, a 200 l drum with cemented mixed waste from a research institute

Drum EG 2 was chosen due to the fact that an undeclared inner canister was clearly identified by digital radiography (DR) and transmission computerized tomography

(TCT). The results of gamma scanning (GS) showed that the total radioactive material (mainly Co-60 and Cs-137) is expected to be concentrated in this inner canister. The destructive sampling of drum EG 2 was carried out by a core drilling system in a special glove box. Five core samples were drilled out. The radiochemical analysis of the drilled core samples is still going on.

Drum EG 4 was selected due to an inner container as well, this one being much smaller than that in EG 2. The gamma spectrum gave evidence for the presence of significant amounts of Am-241 and Np-237. Since the main gamma line of U-237 could also be detected in the gamma spectrum , the presence of plutonium was proved. It is therefore intented to perform passive neutron measurements of drum EG 4 prior to destructive testing in order to verify the presence of plutonium by detecting α,n and spontaneous fission neutrons and to test the possibility of localizing this nuclides by an array of ^{3}He detectors.

Title	High energy accelerator tomography (HEAT)
Contractors	AEA Technology, Harwell Laboratory UK; BAM, Berlin, Germany
Contract N°	FI2W-CT91-0107
Duration of contract	1 January 1992 - 30 November 1995
Period covered	1 January 1994 - 31 December 1994
Project leader	Dr. Martyn Sené (Harwell) & Dr. Bernhard Illerhaus (BAM)

A. OBJECTIVES AND SCOPE

The **H**igh **E**nergy **A**ccelerator **T**omography (HEAT) project is a collaboration between AEA Technology, Harwell, UK and BAM, Berlin, Germany. The primary goal of the project is the development through design, testing and demonstration of a non-destructive technique for the generation of tomographic images of highly radioactive objects such as glass monoliths of high level radioactive waste. The technique is based on the measurement of gamma-ray transmissions with electron bremsstrahlung from an electron linear accelerator as the photon source. The novel aspect of the technique is the use of Cerenkov counters for the detection of the transmitted gamma-rays. Such detectors have a gamma-ray energy response that exhibits a low energy threshold and a non-linear response up to gamma-ray energies of several MeV. The use of detectors with such a response has three potential advantages in the context of computed tomography of highly radioactive objects. Firstly the intrinsically low sensitivity of the detectors to the low energy portion of the bremsstrahlung spectrum should reduce the beam hardening effects which result from the rapid attenuation of this portion of the spectrum by waste packages. Secondly, it should provide discrimination against the low-energy background from the objects significantly improving the signal to background ratio in measurements. Finally, the discrimination against background should also relax the detector shielding requirements.

The project builds on the tomography expertise developed over a number of years at BAM and the expertise in detector design and operation in AEA Technology.

B. WORK PROGRAMME

There are three main phases in the development of the HEAT technique, each corresponding to a period of 1 year:

1. The design construction and testing of Cerenkov counters, collimators and a bremsstrahlung converter.
2. The optimisation of counter performance for tomographic measurements.
3. The demonstration of HEAT on simulated waste.

These three phases are further subdivided into a total of 11 work packages:

WP1. Design of Cerenkov detectors.
WP2. Construction of Cerenkov detectors.
WP3. Testing of Cerenkov detectors.
WP4. Design and manufacture of collimators and bremsstrahlung converter.
WP5. Tomography tests at BAM
WP6. Detector Modifications to optimise performance.

WP7. Modifications to BAM CT system for implementation of HEAT.
WP8. Construction of full detector array and installation at BAM.
WP9. Demonstration of HEAT at BAM with simulated waste.
WP10. Assessment of technique and final report.
WP11. Co-ordination of project.

C. PROGRESS OF WORK AND OBTAINED RESULTS

This report is concerned with work carried out during 1994.
During phase 2 of the programme, carried out during 1993, modifications to the detector design were made and the new detectors were used in tomography tests of representative materials on the BAM Linac. These tests, reported in full in the Annual Report for 1993, confirmed the suitability of the detectors for tomography measurements and demonstrated the operation of the new BAM data acquisition system. Indeed it was possible to obtain a preliminary image of a simulated HLW glass monolith.
Unfortunately, towards the end of 1993 the BAM linac developed a serious fault. Despite considerable effort by the BAM staff, it has not yet proved possible to rectify the fault. Tests of replacement components for the Linac, which it is hoped will rectify the fault, are at present underway. As a result of this the final tests of the detector design have not been completed, although a decision has been made on the basis of previous measurements that the Aerogel detectors will be used. Construction of the full detector array (WP8) is progressing, but final assembly of 10 detectors awaits repair of the BAM linac.
There has also been progress with completion of detailed design of the modified data acquisition electronics, with particular attention being paid to noise reduction, and with construction of 10 channels for the BAM tomography system (WP7). Once again, however, a full test of these elements and final integration of the system with the linac await its repair.
In addition the collimator assembly, designed and manufactured in the previous phases of the project, has been commissioned in preparation for measurements with the Cerenkov detectors.
As a result of the delays introduced by the linac faults an application was made for an extension in time to the present contract. This has now been granted and so the final Phase of the programme is now scheduled for completion by 30-Nov-95.

C.1 Modifications to BAM linac

The primary electron accelerating component of the BAM linac is a standing microwave section with a length of ~1.8m. The microwaves which excite the waveguide and hence accelerate the electron beam are pulsed with a repetition rate of 250 pulses per second (pps) and a pulse width of ~4μs. The accelerated electron beam is incident on a bremsstrahlung radiator located at the end of the accelerating section. The compact device specifically designed for industrial radiography provides a bremsstrahlung γ-ray beam with an end-point energy of 12MeV and a high dose rate of 4000Gy/min/m.
Unfortunately the convenience of the compact design carries with it a requirement for combination of a travelling wave feed-wave guide section from the microwave generator (a magnetron) with the standing wave accelerating section (see figure 1). Any mismatch between these two sections results in the reflection of a portion

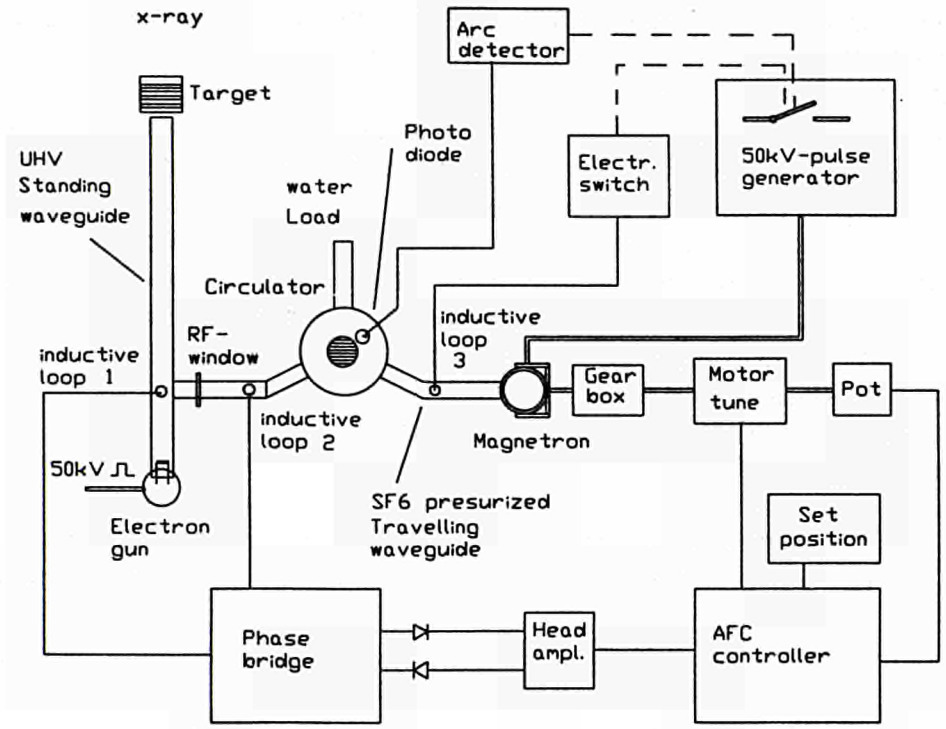

Figure 1: Block diagram of main components of BAM linac.

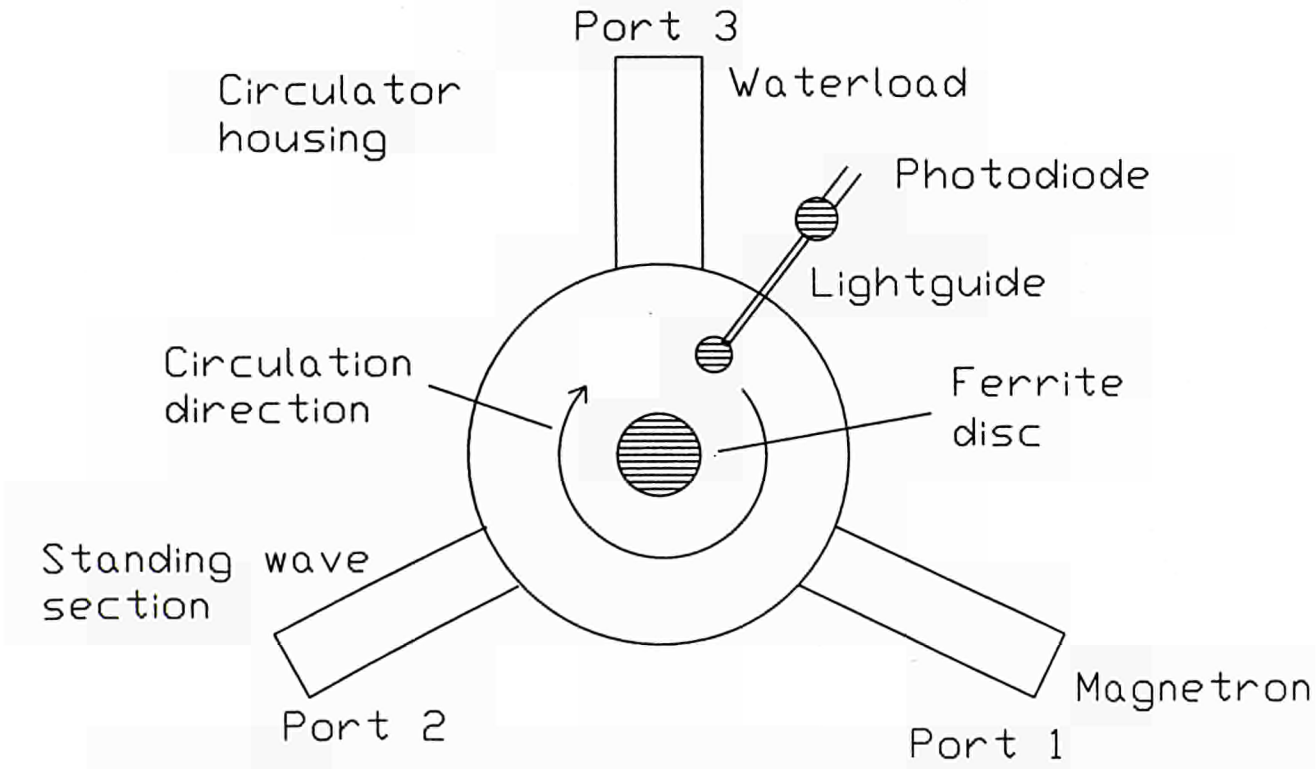

Figure 2: Schematic diagram of the operation of the three port circulator (RF directional coupler)

of the 3MW peak microwave power delivered from of the magnetron. Unattenuated such reflected power would rapidly destroy the magnetron.
To avoid this the linac is provided with a three port circulator (RF directional coupler) which directs the reflected power to a water-cooled microwave load (see figures 1 and 2). It is this crucial component of the BAM linac that has been at the heart of the problems experienced over the period since late 1993.
Failure of such a device operating with a pulsed linac can occur as a result of either peak power or mean power effects. Both failure modes have been observed in the BAM linac. In addition to damaging the ferrite material used in the circulator construction the arcing caused by peak power breakdown can dissociate molecules of the pressurised SF_6 gas, which fills the waveguides, producing hydrofluoric acid which in turn causes oxidation of the surface of all the waveguides and parts of the magnetron.
Mean power failure occurs as a result of insufficient thermal conduction between the ferrite discs in the circulator and the main body of the device. Large thermal gradients are then set up which can eventually result in cracking of the ferrite discs.
In order to overcome these problems a new circulator with an improved design was obtained. This operates with a higher DC magnetic field in a different resonance mode of the ferrite with a higher critical field. Attention has also been paid in the design of this device to the thermal conductivity between the ferrite discs at the heart of the device and a water cooled mounting plate. The circulator was delivered and initially tested using a special test rig rather than in the Linac itself.
The new circulator was delivered with a fixed waterload at port 3 (see figure 1). The output port 2 was connected via a flexible waveguide to an additional waterload supplied by BAM which contains instrumentation to measure the dumped energy. The tests were carried out with an enhanced magnetron, which is calculated to generate a radiation output of 50 Gy/min/qcm/m. These off-line tests indicated that the circulator was performing according to specification. This included the operation of built in photodiode arc-detector (see figures 1 and 2) which could be used to avoid peak power breakdown.
Following these tests the circulator was installed in the Linac housing, connecting port 3 to the standing wave section. Unfortunately, in this configuration the sensitivity of the arc-detector was such as to preclude any running as it immediately interrupted power to the magnetron. After disconnecting the arc detector the full output power of the magnetron was reached for a short time, but this was accompanied by severe breakdown in the RF waveguide system. Following the test the ferrite discs in the cirulator exhibited clear evidence of overheating and damage due to arcing. The circulator has therfore been returned to the manufacturer who have further developed their circulator design. This new design is guaranteed by the company to provide better performance and is deliverable from stock. However, in order to install the new design in the Linac some modifications to the waveguides must be made. Before this is done the new circulator is to be tested outside the Linac.
In order to complete the project contingency plans have now been made in case the BAM Linac is not operational within the next few months. Negotiations have been completed for the rent of a smaller radiography Linac ("Minac") to carry out the final measurements with the Cerenkov detectors.

C.2 Modifications to BAM data acquisition system

The four most important design parameters of the new BAM data acquisition system were:

1. The system must accept signals from photodiodes (scintillation detectors) and photomultipliers (Cerenkov detectors).
2. The system should integrate the signal produced by the 4μs Linac pulse with at least a 15 bit resolution.
3. The data processing system should be able to accept signals from at least 10 detectors.
4. Background and switching noise should be minimised.

The signal processing circuitry designed to satisfy these requirements is shown in figure 3. Apart from the gate generating electronics (pulse transformer, pulse former and inverter) which is common to all detectors this electronics is repeated for each detector channel.

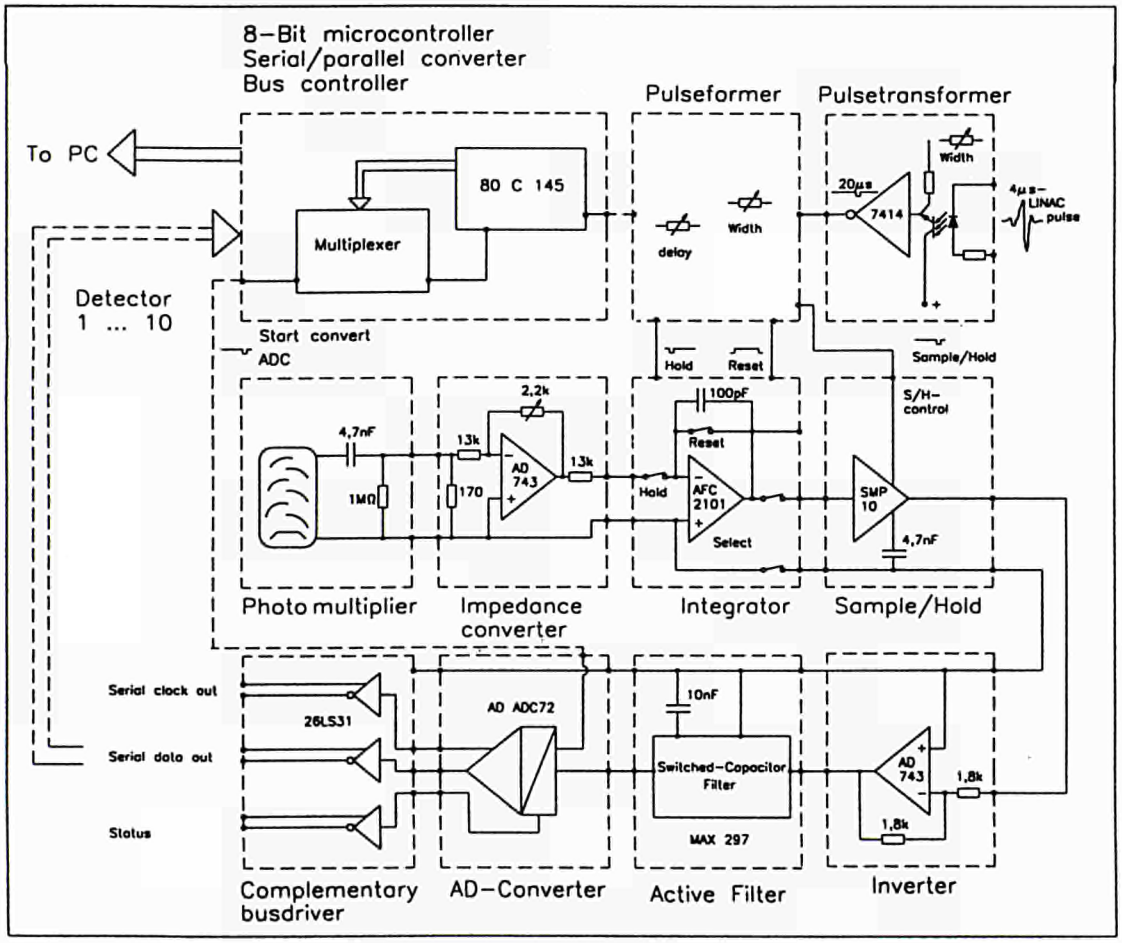

Figure 3: Block diagram of signal processing circuitry.

The main improvements to this system during the period of this report have been the installation of an improved ADC and filter system and the provision of cooling for the most sensitive parts of the detector electronics - all concerned with reducing the background and switching noise of the system to an absolute minimum.

The ADC used now is an Analogue Devices ADC71JD. This has a real 16 bit range obviating the need to use an additional sign bit as before. This ADC also digitises signals in the range 0 - 10V as compared to the previous range of 0 - 2.5V. An additional feature of this chip is that it has an on-board clock.
The most crucial advantage of this new system is that the ADC and its on-board clock do not run continuously but are triggered by a separate line, thus minimising interference between the ADC clock and the analogue signal processing. Between Linac pulses the integrator is grounded. During the pulse integration takes place. At the end of the Linac pulse all nine sample and hold circuits are triggered. Only at this stage is each ADC activated by a "start convert" signal, one after the other. The microprocessor controlled signal system has been changed to include the extra lines and drivers for this triggering function.
The analogue active filter used in the previous version of the electronics has now been replaced with a switched digital filter.
Following these modifications the detector signal processing and data acquisition system was tested with an Aerogel detector. The dark noise from the detector photomultiplier contributed 0.5mV to the signal at the ADC input. Once digitised the noise from the detectors corresponded to a fluctuation of the order of 3 (cf. maximum range of 65536).
To further test the new electronics the system was connected to another photomultiplier, the photocathode of which was illuminated by an LED. The light pulses from the photodiode were made to match the length of the linac pulse (4μs) and were varied in magnitude so as to produce signals across the whole measuring range of the ADC. When the signal from the LED corresponded to a digitised value of ~65000 the fluctuations due to noise covered a range of only ~10. Although this test does not exactly reproduce the linac conditions it does enable comparison with previous versions of the detector electronics. These results show an improvement of a factor of ~20 over the previous version of the signal processing electronics.
The part of the data acquisition electronics in which most of the noise seen in the final signal is generated is the first operational amplifier and the AFC2101 integrator. This noise can be minimised by cooling and ensuring thermal stability of these components. To achieve this the part of the new detector/electronics housing containing these two components is electrically isolated and the components mounted on small water cooled metal plates connected to each other with small brass pipes. Water for cooling is provided by a thermally stabilised water cooler unit connected to the detector housing with plastic pipes (to ensure electrical isolation and thus avoid earth loops). The housing temperature will be set in the temperature range 15-20°C depending on the humidity in the linac hall. Too low a temperature will encourage condensation on the water cooled plates. At present fabrication of the cooled housing in the BAM mechanical workshop is nearing completion.

C.3 Detector modifications and construction

As reported in the 1993 annual report, of the two prototype detectors tested in phase I and 2 of the programme (based on water and Aerogel as the Cerenkov medium), the Aerogel detector with its significantly higher γ–ray energy threshold offers the best performance for the present application.

Final detailed design modifications to the Aerogel detector have been carried out to the light guide between the Cerenkov medium and the photomultiplier (see figure 4). The purpose of this component is to transport the Cerenkov light from the Aerogel with minimum losses to the photomultiplier photocathode. In this arrangement the photomultiplier is offset from its original position so that the direct collimated γ-ray beam, travelling along the central axis of the Cerenkov medium, does not strike any part of the photocathode. The simplest geometry which allows close packing of the modified detectors in a detector array is as shown schematically in figure 4.

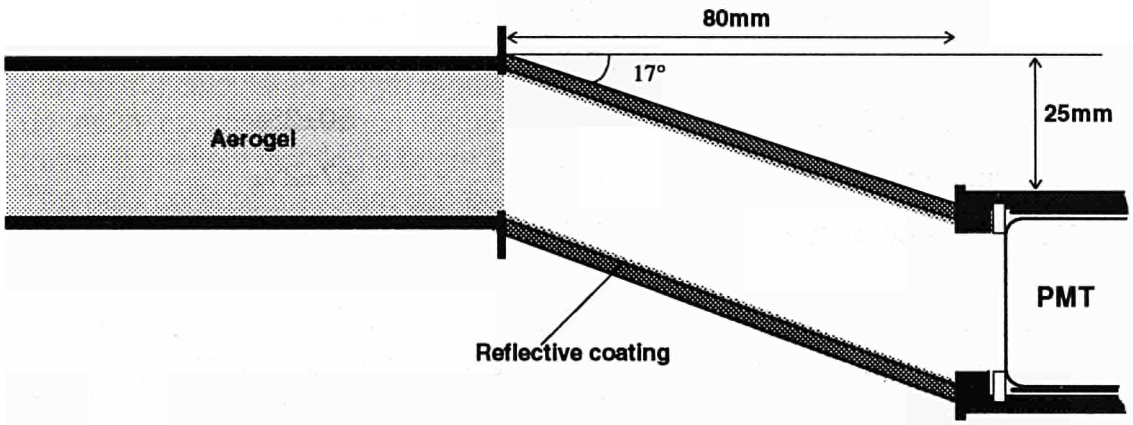

Figure 4: Schematic diagram of light guide from Cerenkov medium to photomultiplier.

Two problems were encountered with these light guides in the tests carried out in phase 2 of the programme. The first was the mechanical problem of obtaining a smooth enough surface along the whole length of the stainless steel guide, particularly in the region of the welds between the main cylindrical section and the flanges which mated with the photomultiplier and Aerogel housings. The second problem was the quality and suitability of the chrome plated reflective surface added to the guide after fabrication. Comparison of the magnitude of the signal from the detector with and without the guide indicated a light collection efficiency of ~30-35%. This is significantly below the value of 50-60% expected from Monte Carlo calculations of the expected light transmission. One possible explanation of this discrepancy is that the reflection coefficient of the chrome plating was lower than expected. This in turn could be due either to false assumptions about the spectrum of light from the Aerogel used in the calculations or to a poor quality chrome coating.
To overcome the first problems the mechanical design of the light guide has been modified so as to make it easier to weld the mating flanges on and also to smooth off the internal surface of the guide in this region.
In order to investigate the light collection efficiency of the guide off-line tests have been carried out using a blue LED placed behind a light diffuser in a light tight enclosure. The magnitude of the signal in a PMT induced by the LED when the

photocathode viewed the diffused LED directly was compared with the case when it viewed the LED via the light guide in order to give the light collection efficiency of the light guide. Measurements were made for a separation between the LED and the PMT of 3.5cm and 35cm for both the original light guide, with a chrome plated inner surface and a modified light guide with no coating but which has its stainless steel inner surface polished. In addition tests were carried out on a light guide with an evaporated layer of aluminium on its inner surface. Aluminium has potentially a much higher reflection coefficient. This was not tried in the original light guide when there was the possibility of using water as the Cerenkov medium as this would have tarnished the aluminium surface and hence rapidly degraded its optical properties. The measured light collection efficiencies are tabulated below.

Measured light collection efficiencies

	D= 3.5 cm	D = 35 cm
Chrome plated guide	34±2%	50±2%
Aluminium plated guide	34±2%	57±2%
Polished steel guide	32±2%	58±2%

These measurements showed no significant difference between the three light guides when the LED is close to the entrance to the guide indicating that the chrome and aluminium coatings are not giving any added benefit to the light collection efficiency of the guide. Indeed the uncoated guide seems to be an improvement on the older design for the case when the LED is relatively distant from the entrance to the guide (and hence most reflections are at grazing angle). Due to the high scattering cross section of the Aerogel for Cerenkov light the close geometry is the more reasonable representation of the situation in the actual detector where light will emerge from the end of the Aerogel block into a large solid angle with little or no anisotropy. The agreement between the light collection efficiency of the guide measured with the LED and deduced from the measurements with the linac (see above) supports this. Clearly under these circumstances the difference between the plain stainless steel and coated guides is negligible, hence the plain design is to be adopted.
At present preparations are under way for construction of a full set of 10 detectors. The Silica Aerogel has been delivered, as have the photomultiplier tubes, their base chains and shielded housings. Manufacture of the detector housings and light guides is nearing completion. The photomultipliers and their base chains have been tested and their gain curves measured. Final assembly of the detector array awaits repair of the BAM Linac.

C4. Collimator testing

In preparation for measurements with the Cerenkov detector array the collimator system designed and manufactured in previous phases of the project, and described in detail in the annual report for 1992, has been commissioned.

The width of each of the 9 collimator slits is controlled by a seperate line from the steering unit, located in the control room and connected to the collimator assembly via 25m long cables. Using this unit it is possible to open and close all nine collimators simultaneously to the same width from 0 to 9mm.
To guarantee an equal opening of all collimators, even for small widths, each system is supplied with separate inductive end point switches. The zero point of each was determined by shining a laser diode light through the closing slit: The transmitted light was detected and the slit closure point set when the amplitude of the transmitted light fell to zero.
To adjust the collimators to the focus of the Linac each collimator is supplied with an adjusting unit at each end of the assembly. The final adjustments are carried out with a laser diode system with the linac fixed in its final position. A 50cm long, 0.8mm wide and 6mm high slit, fixed to the CT scanner table, collimates a laser diode. The position of the slit can be made to coincide with that of the turning point of the table to an accuracy of better than 0.05mm. The table is then turned in one degree steps and moved the calculated length required to bring the slit into the correct position for lining up each collimator. When correctly adjusted, the slightly opened collimators will transmit the light yielding a bright and symmetric pattern on a screen.
The new collimator system can be used with either the old crystal diode and $CdWO_4$ detector system or the new Cerenkov detector array. For the Cerenkov detector setup the lead shielding from the previous collimator system needs to be reconfigured to ensure that the detector and collimator heights coincide. The need for extra lead shielding around the photomultipliers will be assessed when the whole system is assembled.

C.5 Software modifications

The standard reconstruction software used with the BAM CT scanner assumes a small detector opening, comparable with the size of the radiation source, thus asuming that the pencil beam of radiation has the same width throughout the wholeobject. The new collimator system was designed to allow the time required for measurement of barrels and glass containers to be reduced, if required, by increasing the collimator slit width and therefore increasing the transmitted radiation intensity. In the parallel RADWAS project at BAM reconstruction programs for emission CT have been developed for collimator openings much larger than those normally used in transmission CT. These calculate the correct pencil beam width at each point and its partial contribution to different pixels in the object. This part of the ECT software has been combined with the standard reconstruction techniques to enable such wide collimator measurements to be made in TCT. This should reduce the measurement time with minimum reduction of image resolution. More details of these modifications can be found in the 1994 annual report for contract FI2W-CT90-0023.

C.6 Future Work

Once the problems with the BAM linac have been overcome it is intended that the 10 detectors would be rapidly assembled and transported to BAM where the full detector assembly consisting of collimators, detectors and data acquisition system will be commissioned and integrated with the CT scanner system.
Once commissioned the system will be used to make detailed measurements of a simulated HLW glass monolith, particularly paying attention to the spatial and

density resolution and the magnitude of beam hardening effects. The glass monolith has been supplied by CEA/CEN Valrho and has the same outer dimensions as a commonly used high active waste cylinder and is filled with simulated waste glass. Embedded in the object are glass samples of various densities and a variable width steel slit system. These will enable the density and spatial resolution of tomographic images to be assessed.
The discrimination of the detector system against background radiation will be determined using the 2Ci ^{192}Ir high intensity X-ray tube previously used for low energy CT at BAM. A new 55Ci ^{60}Co source has also been obtained and has been delivered to BAM. To simulate the high levels of radioactivity expected in HLW, the sources will be inserted into the glass block and/or placed close to the detector collimator system.
These measurements will be compared with measurements made with conventional $CdWO_4$ scintillation detectors.

Part A

Task 4

"Disposal of radioactive waste: Research to back up the development of underground repositories"

* List of contracts
* Introduction to Task 4

Topic 1 Research related to sites and their characterisation

Topic 2 Research on gas flow

Topic 3 Radionuclide migration in the geosphere

Topic 4 Modelling in the presence of uncertainty and management of data in non-homogeneous systems

Review studies

TASK 4 - LIST OF CONTRACTS

Topic 1 : Research related to sites and their characterisation

FI2W-CT90-0046	Simulation of the effect of long-term climatic change on groundwater flow and the safety of geological disposal sites
FI2W-CT90-0049	Experiment of groundwater flow in a fracture for the validation of chemistry/hydromechanical transport coupled models for fractured media
FI2W-CT90-0050	Experiments in 600m borehole in the Asse II salt mine
FI2W-CT90-0051	Evaluation of a self-consistent approach to fractured crystalline rock characterisation
FI2W-CT91-0063	INTERCLAY II - A coordinated benchmark exercise on the rheology of clays
FI2W-CT91-0072	Sealing of boreholes in crystalline rocks
FI2W-CT91-0075	Paleoclimatological revision of climate evolution and environment in western mediterranean regions
FI2W-CT91-0092	Geochemical validation of solute residence times: review and comparison for various geological environments
FI2W-CT91-0111	Decovalex Project: modelling of THM behaviour for granite rocks
FI2W-CT91-0113	Participation to the international project for development of coupled models and their validation against experiments in nuclear waste isolation (DECOVALEX).
FI2W-CT91-0115	Underground laboratory at Tournemire: groundwater flow tests in clayish material

Topic 2 : Research on gas flow

FI2W-CT90-0048	Development of HLW-borehole sealing

TASK 4 - LIST OF CONTRACTS

FI2W-CT91-0064	The refinement of soil gas analysis as a geological investigative technique
FI2W-CT91-0076	MEGAS: modelling and experiments on gas migration in repository host rocks
FI2W-CT91-0093	Gas pressure build-up in radioactive waste disposal and mechanical effects
FI2W-CT91-0101	Salt permeability in-situ test (Amélie Mine - France)
FI2W-CT93-0125	EVEGAS, European Validation Exercise of Gas migration model through porous media

Topic 3 : Radionuclide migration in the geosphere

FI2W-CT90-0039	Continuation of the migration experiments in Boom clay (laboratory and in-situ)
FI2W-CT90-0065	CHEMVAL-2. A coordinated research initiative for evaluating and enhancing chemical models used in radiological risk assessment
FI2W-CT91-0071	OKLO-Natural analogue for transfer processes in a geological repository
FI2W--CT91-0079	Development of a model for radionuclide transport by colloids in the geosphere
FI2W-CT91-0080	Characterization and validation of natural radionuclide migration processes under real conditions on the fissured granitic environment(El Berrocal)
FI2W-CT91-0081	Fundamental studies on the interaction of humic substances
FI2W-CT91-0082	Rock matrix diffusion as a mechanism for radionuclide retardation: natural radioelement migration in relation to the microfractography and petrophysics of fractured crystalline rock
FI2W-CT91-0083	Effects of humic substances on the migration of radionuclides: complexation of actinides with humic substances
FI2W-CT91-0084	Colloid migration in groundwaters: geochemical interactions of radionuclides with natural colloids

TASK 4 - LIST OF CONTRACTS

FI2W-CT91-0085 The role of colloids in the migration of radioelements

FI2W-CT91-0097 The role of colloids in the transport of radionuclides in geological media

FI2W-CT92-0121 Analysis of the geo-environmental conditions as morphological evolution factors of the sand clay series of Tiber basin and the Dunarobba forest preservation

FI2W-CT92-0122 CHEMVAL 2: Thermodynamic database

FI2W-CT94-0130 The "Entre-Sambre-et-Meuse" cryptokarsts area as Belgian natural analogues

Topic 4 Modelling in the presence of uncertainty and management of data in non homogenous systems

FI2W-CT91-0088 The treatment of uncertainty in groundwater flow and solute transport modelling

FI2W-CT91-0089 Uncertainties in the modelling of migration

FI2W-CT91-0090 Unbiased guess as a concept to cope with fuzzy and random parameters in geochemical modelling

Review Studies :

FI2W-CT94-0126 Thermal, mechanical and hydrogeological properties of host rocks for deep geological disposal of radioactive wastes

FI2W-CT94-0128 Radionuclide transport through the geosphere into the biosphere. Review study of the project "MIRAGE"

INTRODUCTION TO TASK 4 - DISPOSAL OF RADIOACTIVE WASTE: RESEARCH TO BACK UP THE DEVELOPMENT OF UNDERGROUND REPOSITORIES

A. Objectives

The overall goal of this Task is to provide the theorical and experimental basis as well as data bases, concepts and/or models for understanding and testing the behaviour of potential host rocks (sedimentary, crystalline rocks, and evaporites) as natural isolation barriers in order to contribute to performance safety assessment of radioactive waste repositories in deep geological structures. The evaluation of the feasibility and safety of some design aspects of the construction and operation of underground repositories in different rock formations (clay, salt and granite) is also an objective of this work.

B. Research performed under the programme 1985-1989

The research areas covered were:

* development of measuring techniques for the detection and characterisation of fractures and faults in indurated clays;
* laboratory and in-situ tests to study the rheological behaviour of various host rocks, and benchmark exercises on the verification and partly "validation" of calculation tools for salt (project COSA) and clay (project INTERCLAY pilot phase);
* assessment of mechanical performance of metal containers (project COMPAS);
* mock-up and in-situ tests for emplacement and characterisation of candidate buffer and backfilling materials;
* radionuclide migration in the geosphere (project MIRAGE) including subprojects such as on the role of organic compounds, complexes and colloids (CoCo activities), on geochemical benchmark codes including the development of the thermodynamic database (CHEMVAL), and Natural Analogue studies (Natural Analogue Working Group, NAWG);
* study of the applicability of the fuzzy set theory for taking account of uncertainties in model parameters.

C. The present programme 1990-1994

The work to be carried out is subdivided into four topics:

Topic 1 : Research related to sites and their characterisation

This topic mainly deals with the calibration and intercomparison of adequate techniques for assuring relevant properties of groundwater chemistry and groundwater flow in fractured rock on selected reference sites, whereby investigations are undertaken

* in the underground laboratory at Tournemire (F) to evaluate the water flow through impermeable argillaceous formation by geological, hydrogeological and geotechnical investigations.
* at the Sellafield site (UK) to describe water flow and solute transport through

fractured rock at the site and assess the feasibility of obtaining fracture flow data by suitable methods.

Studies are also carried out concerning:

* Rheology of clay, granite and salt, (i) to improve the understanding of large-scale rock mass behaviour through adequate laboratory or in-situ tests, (ii) to develop and test suitable calculation tools and (iii) to predict their material behaviour. Benchmark exercises are undertaken within the project INTERCLAY (rheology of clay) and the project DECOVALEX (on the thermo-hydro-mechanical properties of fractured crystalline rock)
* Geoforecasting studies to predict future climate changes and simulation of effects of climate change on groundwater flow conditions in the Netherlands during the last 500.000 years as well as Paleoclimatological revision during the last 2 million years in the Western Mediterranean regions.

Topic 2 : Research on gas flow

Various research efforts in the field of gas generation, gas release and migration through host rocks (in particular clay and salt) were grouped together in a coordinated project PEGASUS (Project on the Effects of GAS in Underground Storage facilities for radioactive waste). Within the framework of the PEGASUS project, a benchmark exercise has been launched on two phase flow modelling through low permeable porous media called EVEGAS (European Validation on GAS flow)

Topic 3 : Radionuclide migration in the geosphere

Research under this topic concentrates on methodological aspects, theoretical studies, laboratory and field experiments and modelling work grouped together in international projects and subprojects already started in the 3rd programme like:

* studies of the role of colloids, organic substances and complexes (CoCo activities)
* migration experiments in clay
* Natural Analogues: study of migration processes for the understanding of long-term behaviour of geological isolation systems (Oklo study, El Berrocal study, Dunarobba forest study and Entre-Sambre-et-Meuse area (carst study)
* geochemical modelling of radionuclide migration and extension of the thermodynamic data base for use in transport models (CHEMVAL)

Topic 4 : Modelling in the presence of uncertainties and management of data in non-homogeneous systems

The overall objective of this topic is to study alternative methodologies and concepts for the modelling and handling of data in the presence of uncertainty in radionuclide transport modelling, whereas advanced studies are focused on:

* investigation of methodologies of the treatment of uncertainty with reference to modelling studies (e.g. fuzzy sets, expert judgement, information theory, etc.)
* treatment of uncertainties in radionuclide transport modelling
* methods of handling non-homogeneities (e.g. dispersion) at different scales in transport models.

Title: **Simulation of the effects of long term climatic change on groundwater flow and the safety of geological disposal sites**

Contractor	:	University of Edinburgh (EDIN), Rijksinstituut voor Volksgezondheid en Milieuhygiene (RIVM), Rijks Geologische Dienst (RGD), Université de Paris-Sud, Université de Louvain-la-Neuve
Contract N°	:	FI2W-CT90-0046
Duration of contract	:	March 91 - February 95
Period covered	:	January - December 1994
Project leader	:	G.S. Boulton (University of Edinburgh - Coordinator), T. Leijnse (RIVM), E.F.M. de Mulder (RGD), C. Marlin (Université de Paris-Sud), A. Berger(Louvain-la-Neuve)

A. OBJECTIVES AND SCOPE

The project seeks to evaluate the role of climate change in controlling the flux of groundwater through zones which might be chosen as locations for deep disposal of radioactive waste, and to estimate potential future fluxes and their impacts in the area of the Netherlands and adjacent regions. The scope of the programme is as follows:

i) *Development of a generic large-scale model of subglacial groundwater flow.* This comprised an ice sheet model driven by a climate function related to Milankovitch insolation fluctuations; a sub-model designed to estimate the flux of meltwater across the ice/bed interface; determination of effective pressure fields in subglacial bedrock; a time dependent groundwater flow model.

ii) *A geological model of the hydrology of the Netherlands and appropriate adjacent areas.* This was to include palaeoclimatic and palaeoenvironmental reconstructions for the region.

iii) *Application of the model to a transect running through the Netherlands.* The model was to be applied to situations along the transect where tests of the model can be made using geochemical, geotechnical and other approaches.

iv) *Development of a local sub-model to investigate the consequences of subglacial groundwater flow to subrosion of salt-domes.*

v) *Development of an approach to evaluation of future trends.*

B. WORK PROGRAMME

i) Development of the ice sheet model. (Completed)
ii) Development of the subglacial groundwater flow model. (Completed)
iii) Testing the groundwater flow model. (Completed)
iv) Development of a subrosion model. (Completed)
v) Testing the subrosion model. (Some progress made)
vi) Hydrogeological model construction. (Completed)
vii) Reconstruction of patterns of past climatic change and extrapolation of future change as the climate drive for the glacier/groundwater models. (Completed)
viii) Simulation of past subglacial groundwater flow and its impacts. (Completed)
ix) Prediction of future subglacial groundwater fluxes. (Completed)

C. PROGRESS OF WORK AND RESULTS OBTAINED

1.) INTRODUCTION

The major effort in the last 6 months of the project has been to synthesise the work, to produce a major report for the CEC, to prepare a book for publication and to submit papers to international journals. All this has been achieved. A major 200pp report has been submitted to the CEC. Arragements with a publisher for publication of this report have been made. Six substantial papers have been submitted to international journals and accepted since submission of the last report. More will follow.

In the following sub-sections, the principle elements of the work are briefly summarised.

2.) THE ICE SHEET MODEL (Boulton, Hulton, EDIN)

The time dependent coupled behaviour of ice sheets is described mathematically by equations which relate ice sheet form to its internal velocity distribution, to the temperature field both in the ice sheet and in the underlying lithosphere and the isostatic response of the bedrock. Variation of the ice sheet is driven by prescribed temperature and mass balance on its surface, by the geothermal heat flux and by friction at its base and by fluctuations of sea level at any marine margin.

3) THE GROUNDWATER FLOW MODELS (Leijnse, RIVM)

Groundwater flow models used in this study are either 2-dimensional vertical transects or pseudo 3-dimensional vertically integrated. The formulation of the governing equations is done by integrating the general 3-dimensional equations in one direction, making the necessary assumptions. Once the 2-dimensional or pseudo 3-dimensional equations are given, the approximate numerical solution of these equations, both in terms of groundwater heads and groundwater velocities, follows from the application of well known methods, in this case the Galerkin finite element method.

4.) HYDROGEOLOGICAL GEOMETRY OF THE SOUTHERN AND SOUTH-WESTERN SECTOR OF THE EUROPEAN ICE SHEET DOMAIN (van Gijssel, RGD)

A supraregional hydrogeological model for Northwest Europe has been compiled in order to provide a geometrical framework for large-scale (subglacial) groundwater flow models. The model comprises a general subdivision of the Cenozoic and Mesozoic subsurface of the Northwest European Basin into 3 hydrogeological units :

1. the unconsolidated Quaternary and (Upper) Tertiary predominantly sandy deposits, a multilayered aquifer. Locally (Lower) Tertiary and Cretaceous sandy deposits are included.

2. the semi-pervious clay beds of (Lower) Tertiary age.

3. the consolidated Mesozoic deposits consisting of Upper Cretaceous (and Danian) chalk (permeable when fissured) and low permeable and semi-pervious Lower Cretaceous,

Jurassic and Triassic deposits, in which regionally some important aquifers are present.

The base of the supraregional model consists of the relatively impervious deposits of Palaeozoic and Precambrian age, including the rock salt of the Permian Zechstein Group. The spatial distribution and thickness of the units to a large extent are influenced by block faulting and salt tectonics.

The large-scale 3 layer model is the result of a compilation of various geological and structural review maps, which are based on regional lithostratigraphical data. These are presented as a digital set of contour maps (original scale 1:1,500,000) of the top of each hydrogeological unit, together with a description of their characteristics.

An explanation is given to the contour maps (annexes 4.1 - 4.4), the general structural and lithological trends as well as the variations in hydrogeological properties such as permeability and porosity.

5.) ENVIRONMENTS IN TIME : RECONSTRUCTION OF MID- AND LATE QUATERNARY CLIMATE AND ENVIRONMENTAL CHANGE IN EUROPE

(van Gijssel, RGD; Boulton and Dalgleish, EDIN))

In order to be able to simulate time-dependent recharge to the aquifer systems of north-west Europe, we need firstly to have a geological narrative of environmental history. Unfortunately, the stratigraphic record on continental surfaces is a very limited representation of the full pattern of environmental variation in time and space. We need to develop approaches to interpolation in time and space which will yield a full time/space picture which is compatible with the geological record.

In order to do this, we firstly review the nature of the sedimentary building blocks of which the European terrestrial stratigraphy is constructed as a means of using understanding the duration and extent of sedimentary specific environments to synthesise lithostratigraphic sequences and the duration and extent of their components. Evidence for their age is reviewed.

A statistical hindcasting method is then used (see ch. 13) to infer the sequence of palaeotemperature and precipitation in Europe over the last 700,000 years based on statistical correlations between the pollen-derived climate records from French Maar lakes, the deep ocean isotope record and Milankovitch insolation variables. This is used to drive an ice sheet model and used to assess the extent of ice sheets in Europe which would be produced by the hindcast records. This is then compared with the lithostratigraphic analysis and conclusions about age and extent of different envoronments drawn. A synthesis compatible with models and data is one in which the Weichselian glacial stage is equivalent to ocean isotope stage 2-5, the Saalian stage is equivalent to stage 6 and the Elsterian stage is equivalent to stage 12. A major glacial event is simulated in stage 16, which may be represented by the Servack and Don tills of western Russia.

6.) SPATIAL VARIATION OF THE EUROPEAN ICE SHEET (Boulton, Punkari, EDIN)

In simulating the powerful glacial forcing of groundwater flow in Europe, it is important to establish not only the timing, duration and extent of glaciation but the also the direction of glacial forcing, equivalent to the the direction of ice flow. We have assumed a general similarity in the gross patterns of ice sheet flow during successive late Quaternary glaciations. We have therefore assumed that patterns of ice flow during the last, Weichselian, glaciation are a general key to earlier patterns.

Patterns of successive glacial lineations, reflecting the orientations of drumlins, mega-flutes, eskers and moraines have been identified on satellite images, digitised and incorporated in a GIS system. These have then been used to infer a time-dependent pattern ice sheet flow in Europe through the last glacial cycle.

7.) SIMULATING QUATERNARY ICE SHEET FLUCTUATION IN EUROPE (Hulton and Boulton, EDIN)

A numerical model is used to simulate ice sheet behaviour in Europe through the last glacial cycle. It is used in two modes, a forward mode in which the model is driven by a proxy palaeoclimate record and the output compared with a geological reconstruction of ice sheet fluctuation; and in an inverse mode, in which we determine the climate function which would be required to simulate geologically-reconstructed ice sheet fluctuations.

From these simulations it is concluded that extra-glacial climates may be poor predictors of ice sheet surface climates, that climatic transitions during the glacial period may have been much more rapid and the intensity of warming during early the Holocene was much greater than hitherto supposed. Stronger climate forcing is required to drive ice sheet expansion when sliding occurs at the bed compared with a non-sliding bed. Sliding ice sheets grow more slowly and decay more rapidly than non-sliding ice sheets with the same climate forcing.

8.) GROUNDWATER FLOW BENEATH ICE SHEETS. PART 1 - FLOWLINE MODEL (Boulton and Caban, EDIN)

Ice sheets melting basally will inject water into subglacial permeable beds under a maximum head equivalent to the total ice pressure. Melting beneath the European ice sheet is simulated for the last two glacial cycles and the consequences for groundwater flow computed along an ice sheet flowline stretching from the low permeability basement rocks of Sweden to the thick Mesozoic and Cenozoic aquifers of the Netherlands and Germany.

It is concluded that these large aquifers had a sufficient transmissivity to drain all subglacial meltwater; that groundwater heads, potential gradients and fluxes during glacial periods were very much larger than during interglacials; that proglacial permafrost played an important role in sustaining fluid overpressures in the ice sheet terminal zone; that during glacial periods major pressure pulses were driven through aquifer systems and that groundwater systems were completely reorganised.

9.) GROUNDWATER FLOW BENEATH ICE SHEETS. PART II - THE VERTICALLY INTEGRATED MODEL (van Weert and Leijnse, RIVM)

In a number of West European countries salt domes are considered as possible sites for the disposal of radioactive waste. A possible threat for the safety of repositories in this geological barrier may be the dissolution of the rock salt by groundwater (subrosion).

It is thought that increased groundwater pressures and velocities in the aquifers of Northwest Europe during the Pleistocene glaciations may have favoured dissolution and transport of rock salt. A large-scale (areal) hydrological model study has been carried out to investigate the geohydrological responses to glacial climate conditions. The conceptual basis and physical framework for this numerical model has come from a supraregional hydrogeological model of the Cenozoic and Mesozoic subsurface in Northwest Europe. Three different layers are distinguished above the relatively impervious base of Palaeozoic and Precambrian rocks.

Surface boundary conditions to simulate groundwater flow pressures and velocities related to ice sheet expansions into the Northwest European lowlands, have been deduced from indicative palaeo-environmental and palaeogeographical reconstructions for the last three glacial cycles. Boundary conditions for basal melt rates are taken from ice sheet model simulations driven by a climate function inferred from o.i. stage 6, i.e. the Saalian glaciation.

Results of the large-scale model study point to downglacier, highly pressurised groundwater flow in the aquifers underlying the ice sheet and in the ice-marginal permafrost areas. Drainage of this water mainly occurs in proglacial lakes and river systems, where permafrost is absent or discontinuous, and the ice-marginal North Sea. Hydraulic potentials and (horizontal) groundwater velocities increase as the aquifer transmissivity is reduced, occurring for example when ice advances to the margins of the upper aquifer in Germany and the Netherlands.

The draining capacity of the upper Quaternary aquifer in the North Sea Basin is sufficient to discharge the released meltwater in a northwestward direction to open sea. A different drainage pattern however may develop when the Fennoscandian and British ice sheets are confluent and have advanced into the southern North Sea area, a situation similar to the Elsterian glacial stage.

10.) MODEL TESTING USING PATTERNS OF PRE-CONSOLIDATION (Boulton and Dobbie, EDIN)

A theory of subglacial consolidation is developed which shows how the meltwater flux beneath an ice sheet leaves a consolidation signature from which many glacier-dynamic and glacier-hydrologic properties can be inferred. Examples of application of the theory are shown from the Peelo clays of the Netherlands and the tills of eastern England, in which basal melting rates, groundwater fluxes and heads and ice surface profiles are inferred from measured vertical patterns of preconsolidation. measured preconsolidation pressures at the base of the Peelo Clays are in the range 2000-3000 kPa (Boulton and Dobbie, 1993). Predicted values, derived from ice sheet simulations (chapter 8), generated by a maximum subglacial

melting rate of about 25 mm/yr, are about 1000 kPa. If the melting rate were reduced by 1/2, the predicted effective pressure would be about 2000 kPa. We are impressed by the closeness of simulated and measured values, and suggest this to be a non-trivial test.

11.) ESKERS AS A MEANS OF TESTING MELTING MODELS (Boulton and Punkari, EDIN)

A new compilation of the distribution of eskers in the area of north-west Europe occupied by ice sheets during the late Pleistocene shows systematic trends in esker frequency. The distribution and frequency of eskers is shown to be strongly correlated with the transmissivity of subglacial rocks. Eskers do not occur, for example, above thick aquifers of high transmissivity. Their absence in many such cases cannot be attributed to the existence of deformable beds.

A theory is presented which suggests how the discharge of basal meltwater will be distributed between groundwater flow and flow at or near the ice/bed interface and how the distribution of eskers will be related to the basal melting rate and the transmissivity of the subglacial bed. When applied to the area occupied by the European ice sheet, its predictions match qualitatively with the observed esker distribution. In order to produce a good quantitative fit between theory and observation, a basal melting rate of between 5 and 60 millimetres per year would be required at different stages of the evolution of the ice sheet. It is deduced that large quantities of surface meltwater did not reach the ice sheet bed except within a very narrow marginal zone.

12.) GEOCHEMISTRY OF PORE WATERS IN TERTIARY CLAYS AT MÜHLENRADE, SCHLESWIG-HOLSTEIN/GERMANY (Marlin and Ginidis, PARIS-SUD)

A borehole made in north Germany within the maximal advance of the Weichselian ice-sheet have been investigated in order to examine the geochemical signature of the pore water in a thick low-permeability level.

The isotopic measurements show significant differences between the water-table values similar to the meteoric one's and the interstitial solutions. Glacial and periglacial are possibly still present in the profile but diffusion has partly obliterated the signal.

13.) NONLINEAR REGRESSION MODELLING AS A BASIS FOR CLIMATIC HINDCASTING AND FORECASTING (Dalgleish, EDIN)

We have applied the nonlinear regression technique known as Additivity and Variance Stabilisation (AVAS) to a variety of palaeoclimatic time series. AVAS estimates a smooth, nonlinear transform for each variable, under the assumption of an additive model. The Earth's orbital parameters and insolation variations have been used as regression variables. Use of the modified orbital variables from the ACLIN model of Kukla et al (1981) enabled us to reproduce the past climate well, including the deglaciations. The ACLIN variables include obliquity lagged 6 ka. Precession results consistently suggest linearity, with warm climate corresponding with vernal equinox, in contrast with the ACLIN results. Obliquity is also linear,

with a possible threshold at 24.1 degrees, with high tilt correlating with warm climate. The relationship between eccentricity and climate is more difficult to interpret. Analysis of the contribution of each variable shows that the deglaciations are characterised by periods of increasing obliquity and perihelion approaching the vernal equinox, but not by any systematic change in eccentricity. By approximating the transforms we can obtain a future prediction, with a glacial maximum at 60 ka ap, and a subsequent obliquity forced deglaciation.

D. NEW RESULTS DURING THE FINAL PERIOD OF THE PROGRAMME - DETERMINISTIC MODELLING OF FUTURE CHANGE

by
Marie France Loutre
(Louvain la Neuve)

The group of Professor A.Berger joined the programme during the final year. In response to this and to permit their work to be synthesised with the rest of the programme, the programme was extended. The new results obtained during this final period are summarised in this section.

a) Introduction

A two dimensional, sectorally-averaged model of the northern hemisphere climate system which links atmosphere, the ocean mixed layer, sea ice, ice sheets and the underlying lithosphere has been used to investigate possible future changes. A first experiment starts from the modern condition and uses a future scenario of CO_2 forcing derived from the statistical forecasting technique presented in chapter 13.. A second experiment assumes that the Greenland ice sheet melts competely during the next century as a consequence of strong "greenhouse" warming. In the first experiment, the next glacial maximum occurs at 154ka AP. In the second, conditions converge with those of the first after 70ka.

b) The climate model

The LLN climate model is a two-dimensional (latitude-altitude) sectorially averaged model of the northern hemisphere which links the atmosphere, the ocean mixed layer, the sea-ice, the ice sheets and their underlying lithosphere. The atmospheric dynamics is represented by a zonally averaged quasi-geostrophic model. The vertical profile of the upper ocean is computed by an integral mixed-layer model which takes into account the meridional convergence of heat. Parameterisations allow to take into account sub-grid scale mechanisms eliminated by the zonal average. In each latitudinal belt the surface is divided into at most five oceanic or continental types. The climate model is asynchronously coupled to the model of three main northern hemisphere ice sheets and their underlying bedrock. Some limitation of the model must however be stated (Gallée, et al., 1991, 1992) related to the representation of topography, cloudiness and deep-sea circulation.

Simulation of the present climate shows that the model is able to reproduce the main characteristics of the general circulation and, in particular the surface wind field. The seasonal cycles of oceanic mixed layer, sea ice and

snow cover are also well reproduced (Gallée, et al., 1991). Moreover orbital variations alone can induce, in such a model, feedbacks sufficient to generate the low frequency part of the climatic variations over the last glacial-interglacial cycle (Berger, et al., 1990a and 1990b; Gallée, et al., 1992). A similar experiment over the last 200 ka using both the astronomical forcing and the CO_2 reconstruction from Shackleton, et al. (1992) has demonstrated the ability of the LLN model to simulate the 100 ka cycle in agreement with SPECMAP reconstruction (Gallée, et al., 1993).

c) Description of the experiments

Determining the possible future climatic changes becomes an important matter, for example in the safety assessments for nuclear repository sites. The 2-D climate model is used here to give a hint for answering such a question. A first experiment has been designed starting at the present time with the present-day ice sheets configuration. It is run for the next 200 kyr using isolation and CO_2 as external forcings. Insolation is computed according to Berger (1978) and CO_2 concentration is given by Dalgleish and Boulton (1994) (Figure 14.1).

In order to test the sensitivity of the future climate to the possible impact of man's activities, it was then assumed that the Greenland ice sheet would totally melt within the next century. A second experiment is thus carried out over the next 200 kyr with this initial condition and the same external forcings as in the first experiment.

d) Results

i) First Experiment

The long-term variations of the simulated ice volume of the Eurasian ice sheet and of the total Northern hemisphere ice volume are displayed in Figures 14.2 and 14.3. Total northern hemisphere ice volume is progressively increasing with more important advances at 23, 65 and 102 kyr AP and with a marked retreat at 120 kyr AP. The next glacial maximum is reached at 154 kyr AP with a total ice amount close to the one simulated at the last glacial maximum (i.e. 46.3 x 10^6 km^3 of ice). This next glacial maximum is followed by the total melting of the ice sheets at 165 kyr AP.

Similar ice volume changes in the timing and in the relative amplitude can be seen for the Eurasian ice sheet. This ice sheet is totally melted between 160 and 171 kyr AP and it nearly disappears between 116 and 123 kyr AP, with less than 0.05 x 10^6 km^3 left. On the contrary the maximum amount of ice for this ice sheet is of 14.8 x 10^6 km^3 at 153 kyr AP. In the model the Eurasian ice sheet cannot extend beyond the 40 - 75 °N zone. Moreover Figure 14.4 shows that it remains most of the time north of 60 °N. Most precisely it extends south of 60 °N only between 60 and 70 kyr AP, 100 and 114 kyr AP, and after 172 kyr AP; it reaches latitudes south of 55 °N only once at about 155 kyr AP. Its height remains lower than 3000 m except at the next glacial maximum when it reaches more than 3300 m. As a consequence, the bedrock depression related to these ice sheet load can reach about 2000 m. Similarly the North American ice sheets are represented by a single ice sheet which cannot be wider than the continent and extends at most from 30 - 80 °N. In particular in this

experiment it hardly extends further south than 55 °N at 150-155 ka AP and it reaches altitudes higher than 3000 m.

Simultaneously to these ice-sheet volume, height and extend changes, temperature is also experiencing long-term variations. The hemispherically averaged annual mean surface temperature is decreasing with a slow cooling trend of about 0.01 ° kyr-1 between the present-day simulated hemispherically averaged annual mean surface temperature 6 °C and it decreases down to 12.1 °C at 148 kyr AP. Its variations are closely following the ice volume variations over the next 200 kyr.

In the latitude bands 50 - 55 °N the averaged annual mean surface temperature is generally comprehended between 2.5 - 4.5 °C (Figure 14.7). But it reaches higher values for example at the present-time (5.1 °C) and lower values (1.3 °C at the next glacial maximum for example). The continental annual mean temperature in the same latitude band (Figure 14.10) undergoes temperature change of the same amplitude than the averaged surface temperature but it is smaller, between 2.4 °C (t=0) and -1.7 °C (t=152 kyr AP). This continental annual mean temperature remains below 0 from 60 to 68 kyr AP, from 95 to 113 kyr AP, from 135 to 157 kyr AP, and from 177 to 194 kyr AP. But the seasonal contrast is very important as in January the zonal mean temperature of the continent vary between -18 °C and -25 °C (with a mean of -21.5 °C) while this temperature is comprehended between 24 °C and 15 °C (with a mean of 18.8 °C) in July. When reduced to sea level these temperatures are to be reduced by about 2.5 °C, 10 °C and 8 °C in annual mean, in January and in July respectively.

In the latitude bands 60 - 65 °N the averaged annual mean surface temperature decrease between a glacial and an interglacial is very important (Figure 14.8). It reaches 11.4 °C between present-time and 153 kyr AP. The variations of the surface temperature (Figure 14.11) at this latitude band is mainly related to continental temperature changes due to albedo modifications.

The variation of the temperature related to climatic changes is less important in the lower latitudes. Indeed some feedbacks and processes are particularly important at high latitudes. For example, the albedo temperature feedback plays an important role through the change of snow and sea ice cover as well as taiga / tundra shifts.

In the 20 - 25 °N latitudinal belt the averaged annual mean surface temperature is comprehended between 21.5 °C and 23.6 °C and the averaged annual mean temperature of the continent varies between 21.2 °C and 23.5 °C. The seasonal variability is less important than at 50 - 55 °N. The mean value is about 14 °C in January and 30 °C in July, i.e. only 16 °C more. Moreover the amplitude of the signal is also less important than in the 50 - 55 °N latitudinal belt : at the maximum 4 °C in January and 7 °C in July, which can be at least partially explained by the fact that at these times of the year and latitude the temperatures are closely following the insolation which amplitude is slightly less important in January than in July. When reduced to sea level these temperatures are lowered by about 6 °C, 3 °C and 5 °C for the annual mean, January and July respectively.

The ice sheet surface temperatures at the zonal mean height in annual mean as well as in January is closely following the variation of the ice sheet volume for Eurasian as well as North American ice sheet. However, during summer (July) temperature is experiencing very rapid changes such as between 140 and 150 ka AP for example, mainly for the North

American ice sheet. The temperature is varying by a few degrees and is coming back to its initial value in a few thousand years. This phenomenon mainly occurs at the end of the growing phase of the ice sheet.

ii) Second experiment

The major result of this experiment is that the climate system keeps memory of its boundary conditions for about 70 kyr. Indeed after 70 kyr AP the simulated variable are nearly exactly the same in the two experiments starting with different initial boundary conditions.

The ice sheets are not going to significantly reappear in the northern hemisphere before 50 kyr AP (Figure 14.2 and 14.3). The next glacial stage is delayed by 2 kyr and is less extensive (17.5 x 10^6 km^3 instead of 21.1 x 10^6 km^3). This confirms results already obtained with a former version of the model (Berger, et al., 1991). As far as temperature is concerned climate is slightly warmer in the second experiment : the most important hemispheric annually averaged temperature difference between the two experiments is less than 0.7 °C (Figure 14.6). However, more important differences occur in temperature and polar regions (Figure 14.7 and 14.8). For example, this annual mean temperature difference is about 2 °C in the 60 - 65 °N latitude band. Moreover the continental surface temperature are following the same pattern with an annually averaged difference of about 0.75 °C (Figure 14.9). This difference reaches 2.8 °C in the 60 - 65 °N latitude band (Figure 14.11).

e) Conclusion

According to these simulations and the given CO_2 concentration the long term cooling trend which began 6 kyr ago will continue until the next full glacial maximum at 154 kyr AP. Over this time span some interglacial stage occur but the next full interglacial with a complete melting of the ice sheets is delayed until 165 kyr AP. Moreover the sensitivity test to the present-day northern hemisphere ice volume shows that the possible impacts of the greenhouse warming on the Greenland ice sheet over the next centuries could be significant on the geological time scale, at least over the next 70 kyr.

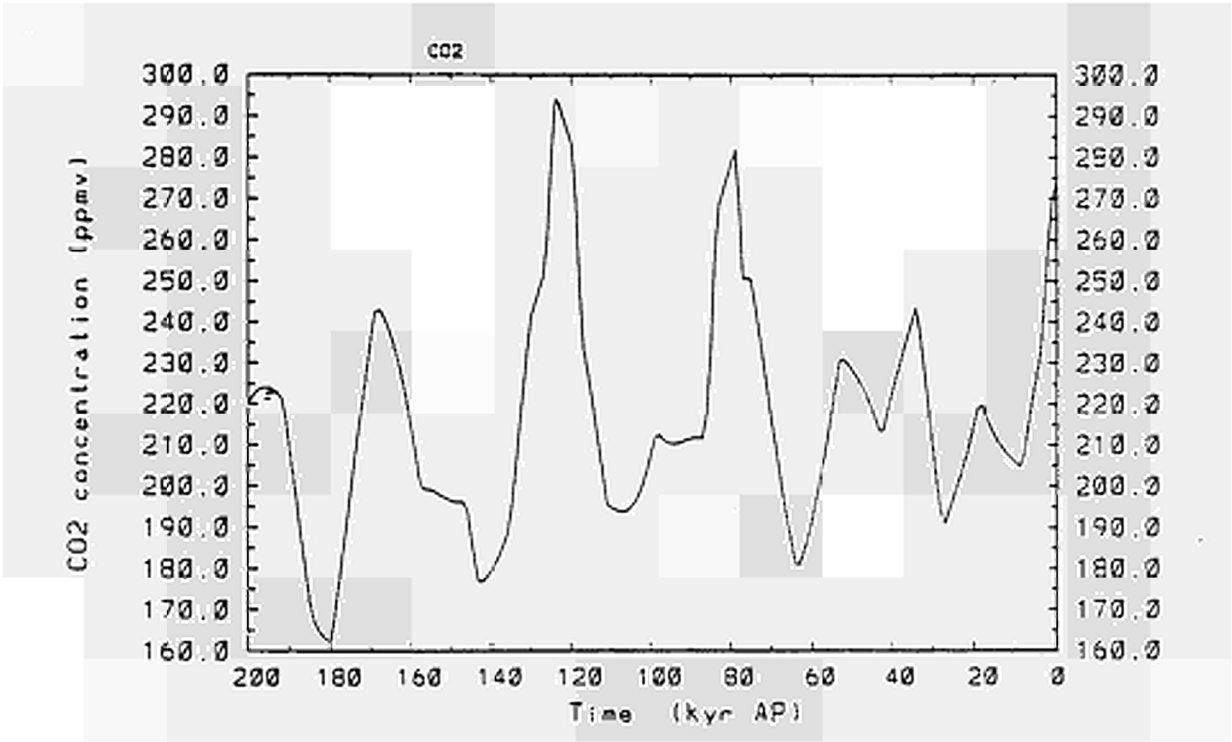

Fig. 14.1 CO_2 forcing for the next 200 kyr.

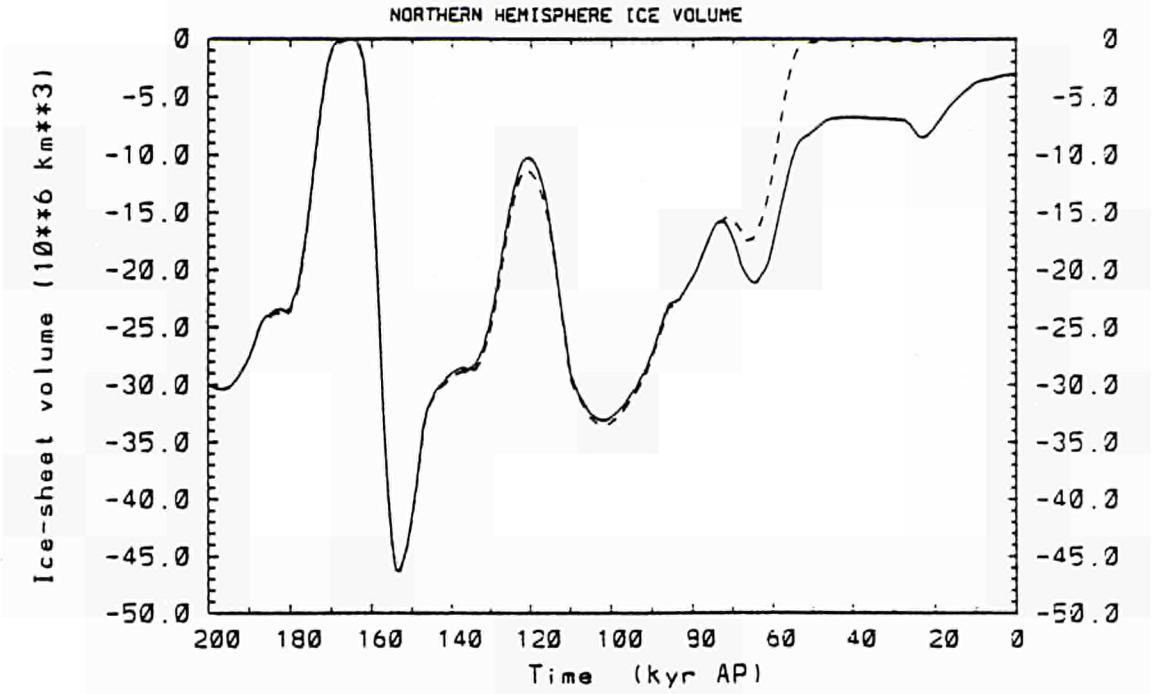

Fig. 14.2 Variations over the next 200 kyr of the simulated total northern hemisphere ice volume with the present-day boundary conditions today (full line) and assuming no Greenland ice sheet today (dashed line).

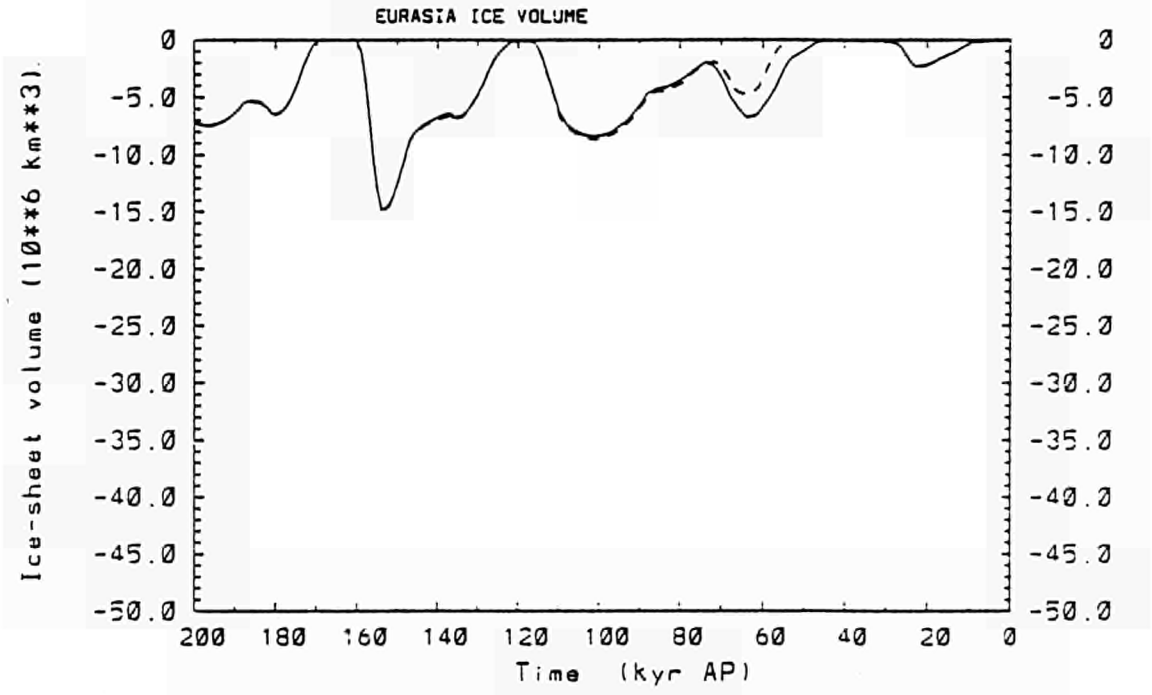

Fig. 14.3 Variations over the next 200 kyr of the simulated Eurasian ice-sheet volume with the present-day boundary conditions today (full line) and assuming no Greenland ice sheet today (dashed line).

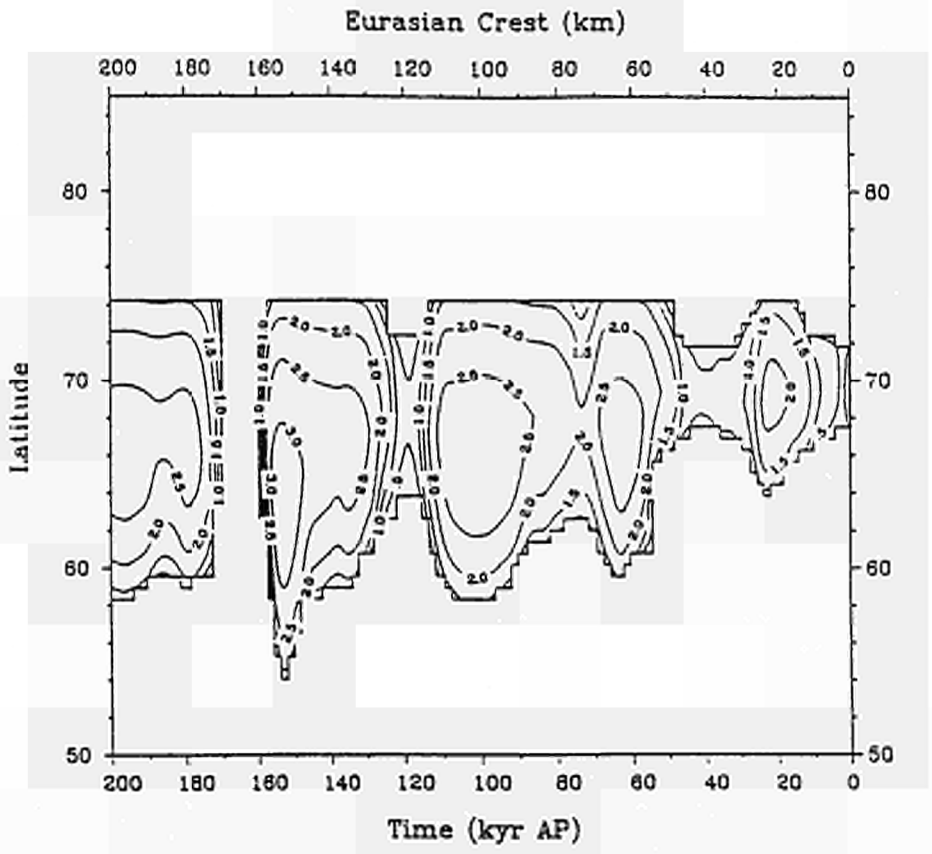

Fig. 14.4 Variations over the next 200 kyr of the latitudinal extent of the Eurasian ice sheet crest elevation above present sea level with the present-day boundary conditions today.

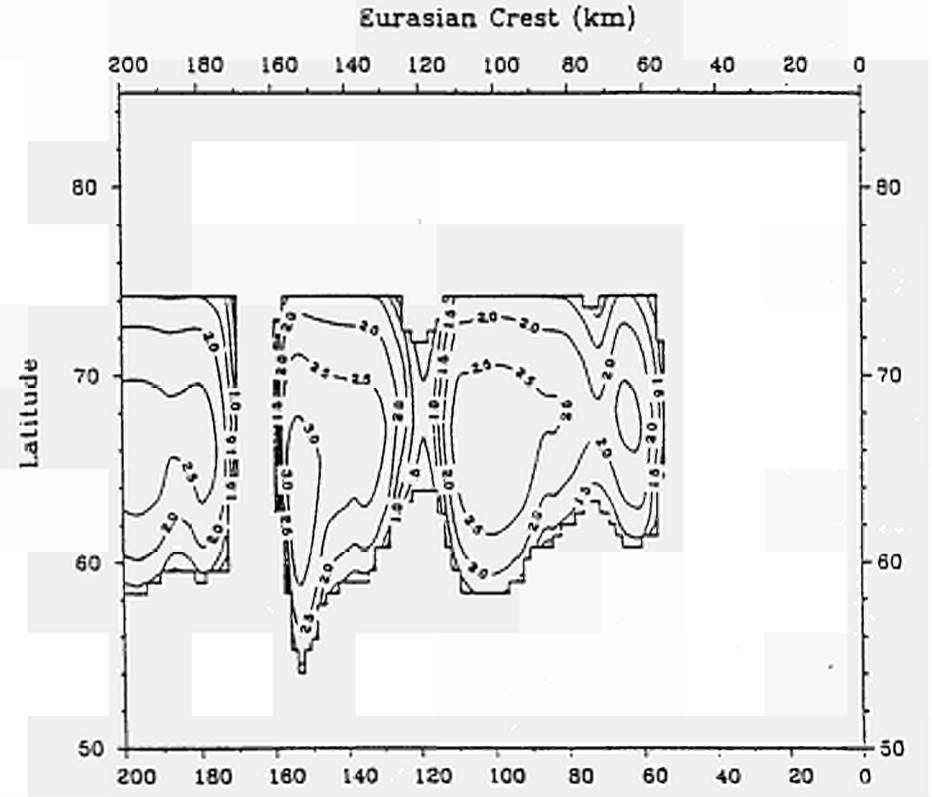

Fig. 14.5 Variations over the next 200 kyr of the latitudinal extent of the Eurasian ice sheet crest elevation above present sea level assuming no Greenland ice sheet today.

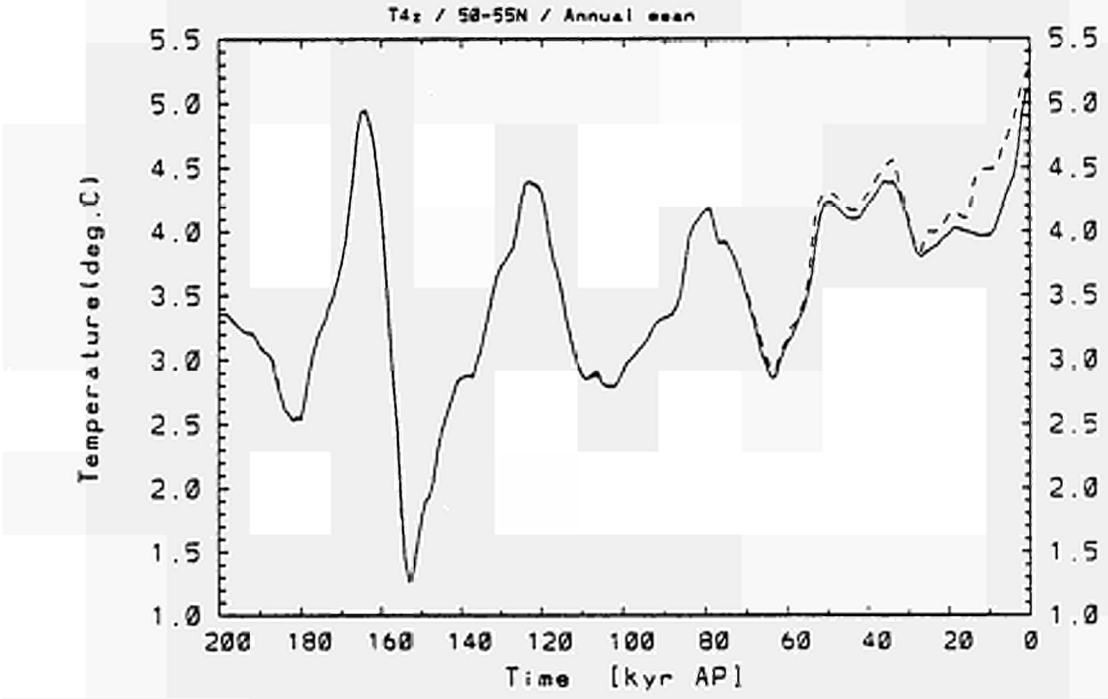

Fig. 14.7 Variations over the next 200 kyr of the simulated annual mean surface temperature in the 50 - 55 °N latitude band with the present-day boundary conditions today (full line) and assuming no Greenland ice sheet today (dashed line).

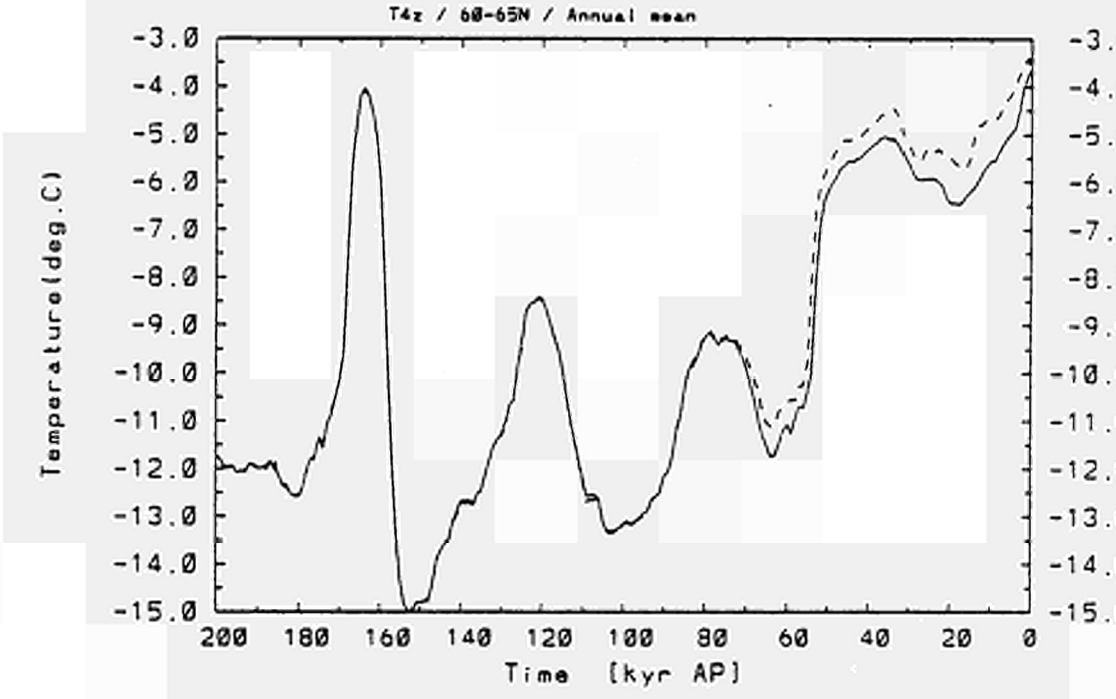

Fig. 14.8 Variations over the next 200 kyr of the simulated annual mean surface temperature in the 60 - 65 °N latitude band with the present-day boundary conditions today (full line) and assuming no Greenland ice sheet today (dashed line).

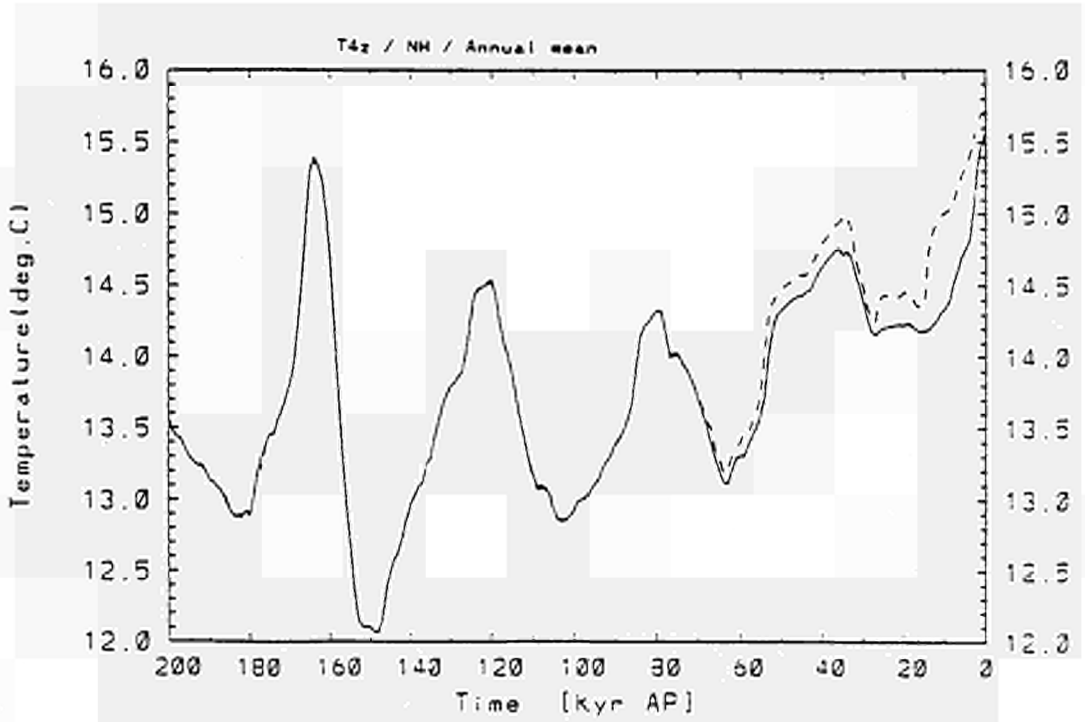

Fig. 14.6 Variations over the next 200 kyr of the simulated hemispherically averaged annual mean surface temperature with the present-day boundary conditions today(full line) and assuming no Greenland ice sheet today (dashed line).

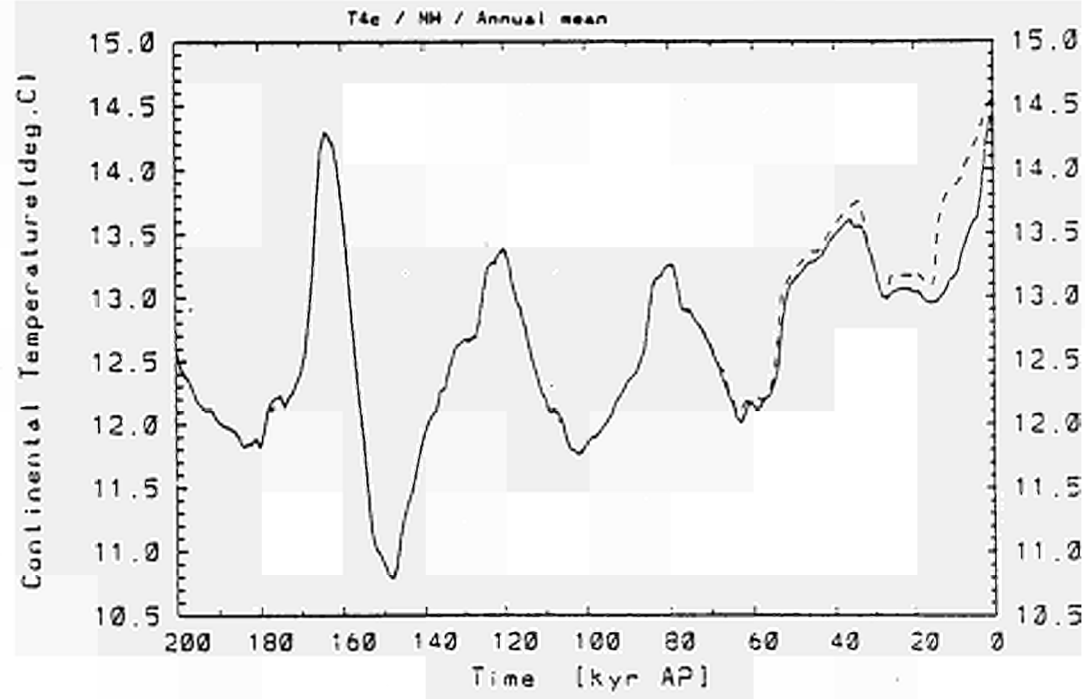

Fig. 14.9 Variations over the next 200 kyr of the simulated hemispherically averaged annual mean continent temperature with the present-day boundary conditions today (full line) and assuming no Greenland ice sheet today (dashed line).

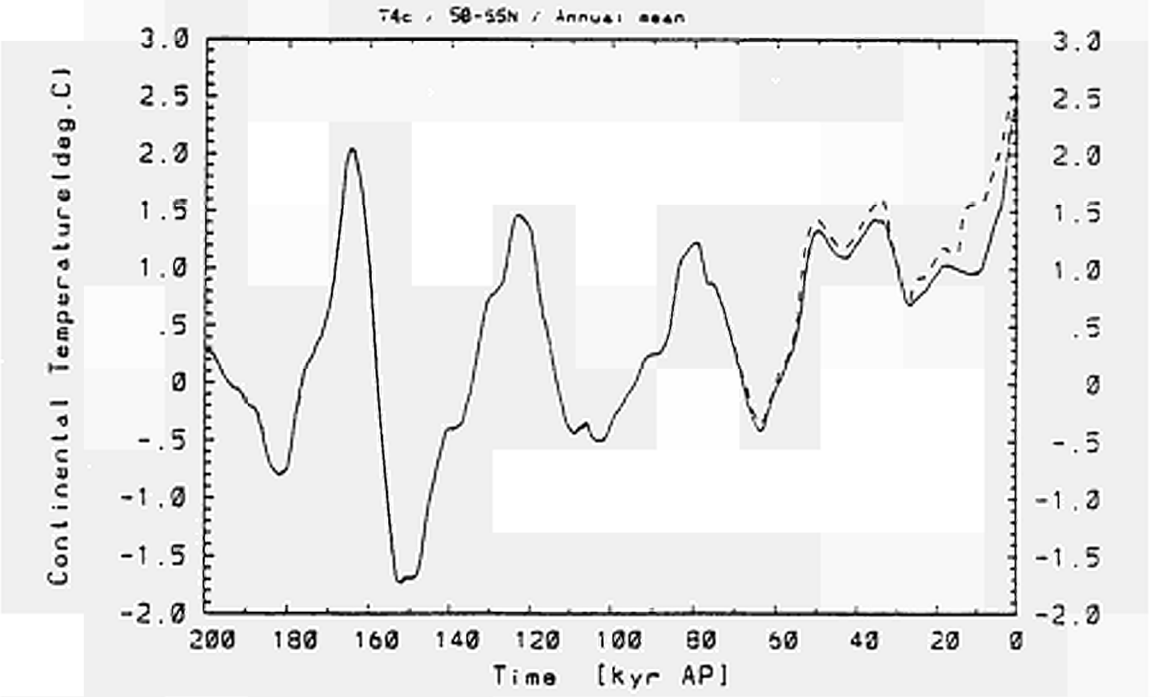

Fig. 14.10 Variations over the next 200 kyr of the simulated annual mean continent temperature in the 50 - 55 °N latitude band with the present-day boundary conditions today (full line) and assuming no Greenland ice sheet today (dashed line).

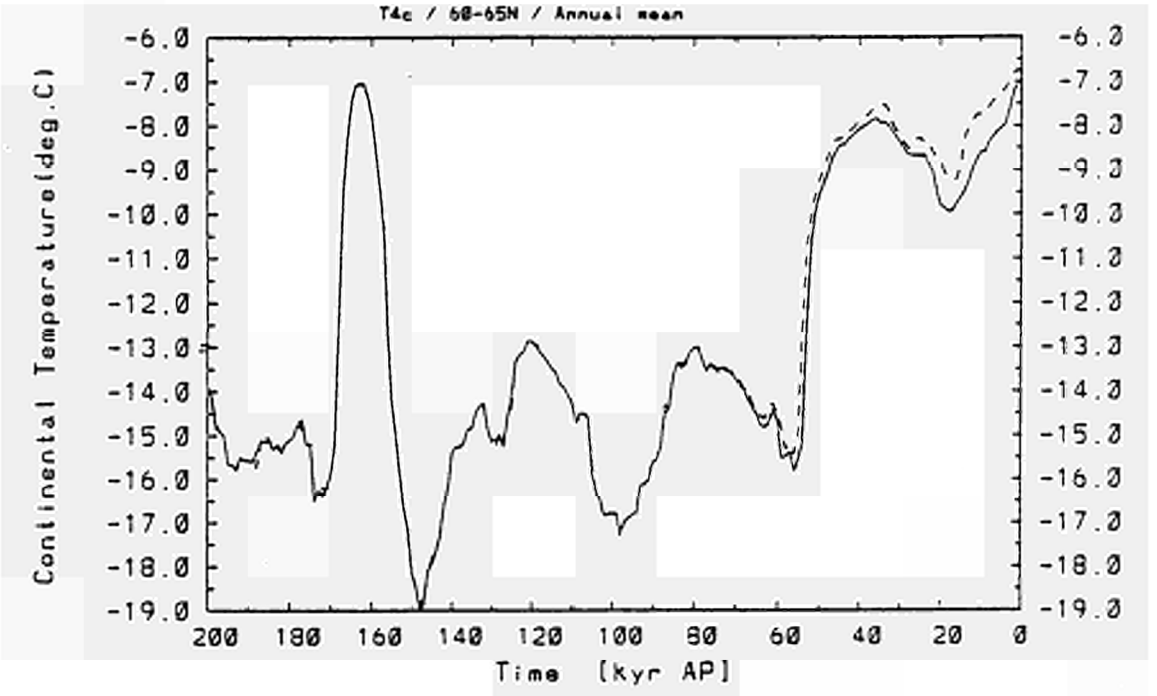

Fig. 14.11 Variations over the next 200 kyr of the simulated annual mean continent temperature in the 60 - 65 °N latitude band with the present-day boundary conditions today (full line) and assuming no Greenland ice sheet today (dashed line).

Title	Experiment of groundwater flow in a fracture for the validation of chemistry/hydromechanical transport of coupled models for fractured media
Contractors	BRGM
Contract N°	FI2W-CT90-0049
Duration of contract	1 January 1991 - 30 June 1995
Period covered	1 January 1994 - 31 December 1994
Project leader	S. GENTIER (BRGM)

A. OBJECTIVES AND SCOPE

This project is a circumstantial study in laboratory concerning the relationship between the morphology, the flow and the chemical reactions water-rock in the fracture. The objective is the achievement of an experiment designed for the validation of chemistry-hydromechanical transport of coupled models which integrate explicitly the morphology of the voids of the fracture and its variations.

The morphology of a natural fracture in a granite will be studied from profiles recorded on each side of the fracture and from the casting of the voids. The flow channels will be determined from the morphology of the voids and from radial flow experiments. The petrology of each side of the fracture will be analysed. All these data will permit the choice of some profiles on the sides of the fracture about which the micro-roughness will be recorded as a witness of the initial topography.

After this preliminar phase, radial flow tests will be performed on the fracture. The tests will be realized at various levels of normal stress and in temperature. During the tests, the chemistry of the water entering and exiting of the fracture will be determined. Moreover, during the tests, mechanical, hydraulical and thermal data will be recorded. At the end of each experiment, the micro-roughness of each side of the fracture will be examined again to see if there are dissolutions or precipitations on some parts of the fracture. These results will be correlated with chemical balance of the test.

B. WORK PROGRAMME

The scheduled successive phases for the achievement of the works are :

B.1 Design and fitting of the prototype.
B.2 Testing of the equipment and qualification tests.
B.3 Choice of the sample and initial caracterization of the fracture (macro-roughness, micro-roughness, map of the voids, mineralogy).
B.4 Tests of percolation (2 tests according to the necessary duration for each percolation).
B.5 Caracterization of the morphology after percolations.
B.6 Presentation and interpretation of the results.

C. PROGRESS OF WORK AND OBTAINED RESULTS

State of advancement

By the end of this year, the state of advancement is the following :

- The initial characterization of the micro-roughness is achieved. A complete sytem to ensure precise positioning of the sample on the micro-profilometer has been designed and built.
- The hydromechanical characterization has been performed before percolations to define the hydromechanical conditions for the percolation (flow, stress) and to indentify the main channels.
- After a series of tests to verify the functionning of all the equipments, a first percolation has been conducted.
- The profiles of micro-roughness recorded before the percolation have been rerecorded after the first percolation.

Progress and results

C.1 Hydraulical characterization

In order to determine the hydraulic and mechanical conditions of the first percolation and to assess the manner in which the flow passes along the fracture plane, injection tests using dyed water were carried out on the concrete replicas of the fracture walls. These tests showed that the flow is heterogeneous in the fracture plane. For a stress of 15 MPa, most of the flow occurs in sectors 4 and 1, with sector 3 playing an intermediate role and sector 2 being only slightly involved in the flow. These data helped to define the profile sampling pattern for the micro-roughness analysis.

C.2 Morphological characterization

After to have designed and built a complete system to ensure precise positioning of the sample on the micro-profilometer, twenty eight profiles were recorded on each wall, their position being in part determined by the results of the initial mineralogical and hydraulic characterization of the fracture (production zones). These profiles are 70 mm long on the upper wall and 55 mm long on the lower wall (presence of the central injection hole). The instrument used to record the profiles has a resolution of 0,25 μm along the direction of translation and 0,6 μm along the vertical axis.

C.3 The first percolation

The test conditions were as follows :
- Normal stress ; 6 MPa,
- Flowrate : 0.7 ml/min, i.e. 42 ml/h,
- Temperature : 21 to 23° C (ambiant temperature),
- Fluid injected : hydrofluoric acid at 10^{-3} M/l.

The fluid is recovered in four sectors around the cylindrical sample. Four successive injections of the acid fluid (called tests) have been performed with the same conditions separated by water rinsing and constituted the first percolation.

In each of the four tests, the injection pressure stabilized between 0.9 and 1.2 MPa. The pressure curve for the first test is very regular, but those for the other three tests are less regular. These fluctuations could be due to flow instabilities within the fracture. These first results indicate that the flow paths are modified during percolation. To summarize, sector 2 was productive during the first two tests but seems to have become obstructed during test 3 when sectors 3 and 4 opened up and maintained the flow during test 4 with, however, a slight closing of sector 4. Sector 1 appears to have been unproductive troughout all the tests (apart from a short-lived productivity during test 3).

For the chemical aspect, samples (minimum 5 cm^3) of the exiting fluids were analysed for six major elements : sodium, potassium, magnesium, calcium, aluminium and silicon. The analyses were made by atomic absorption flame spectrometry. Silica is determined by colorimetry.
As no advanded geochemical interpretation has yet been undertaken, only the results of these premiminary tests can be presented. They have been plotted on three main types of diagram showing :
- the cumulative number of moles for each liberated elements versus time,
- the cumulative mass of each element normalized to the fluid mass produced versus time,
- the cumulative number of moles for the elements taken in pairs (binary diagram).
Only some examples ot the two last types of diagram are commented and presented here.

Evolution of the cumulative mass for each element normalized to the fluid mass produced versus time

These diagrams are established for each of the recovery sectors and for each of the four tests carried out. With all the tests, only sectors 2, 3 ans 4 were sufficiently productive to enable a chemical analysis of the percolate. They were plotted in order to ascertain the quantity of elements independently of the fluid mass. The results are expressed as a concentration (g/l).

The diagrams corresponding to sector 2 (figure 1) show a rapid increase of in released concentrations within the first 100 minutes for all the elements. This increase was followed by a slow decrease, after which the concentrations tend to stabilize. This stabilization reflects a quasi-static state in which the velocity of fluid circulation and velocity of mineral dissolution maintain a same ratio. With long-duration tests it should be possible to determine whether or not this stability is lasting. One notes an anomalous behaviour for aluminium and strong concentration differences between tests 1 and 2 for all the elements.

In sector 3, for many of the elements, such as potassium, sodium, calcium and magnesium, the concentration increase was clearly less rapid than in sector 2. Moreover, only the potassium and silica concentrations tended to stabilize. Fairly curiously, the aluminium and silica concentrations show an identical evolution to that observed for most of the elements in sector 2.

In sector 4, as with the preceding sector, the concentration increase for each element was generally slower than in sector 2. Moreover, only potassium, sodium and aluminium show concentrations that tended to stabilize.

Evolution of the cumulative number of moles for the elements taken in pairs (binary diagram)

Some of these diagrams (figure 2) are given here only for information insofar as no advanced geochemical interpretation has yet been carried out. They were drawn up for a definite purpose and, as far as possible, to serve as a basis for identifying the host minerals of each of the chemical elements liberated in the medium.

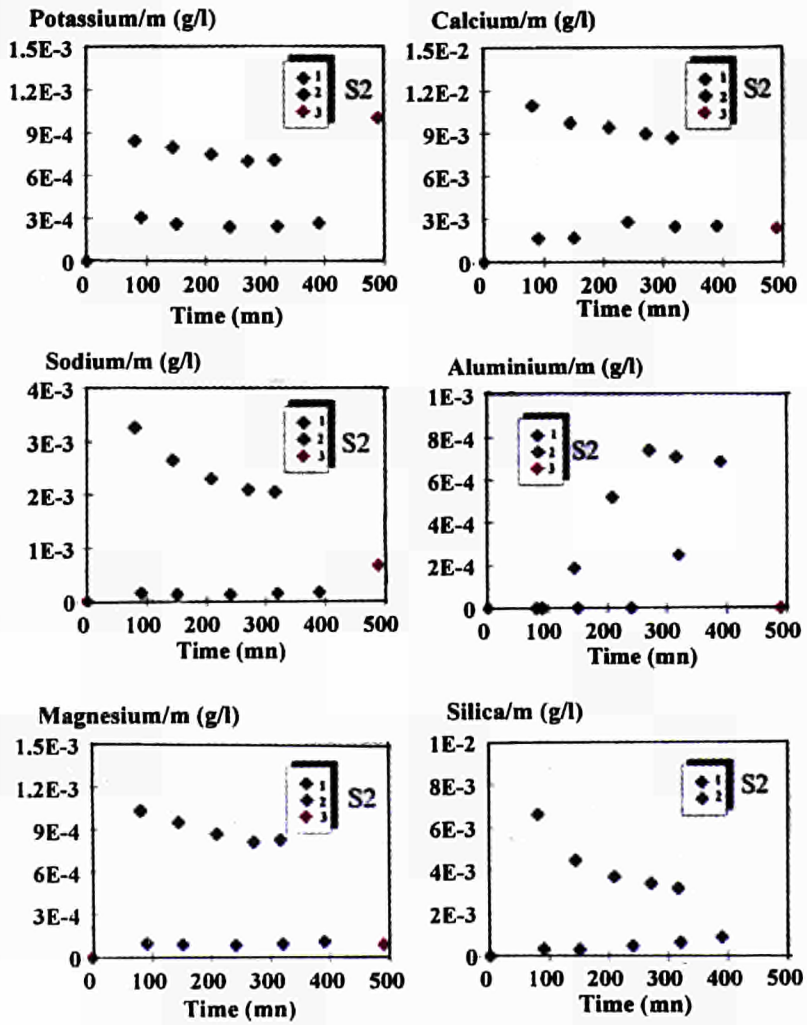

Figure 1: Cumulative mass of each element normalized to the total mass of the released fluid (m) for the tests 1, 2 and 3 (sector 2).

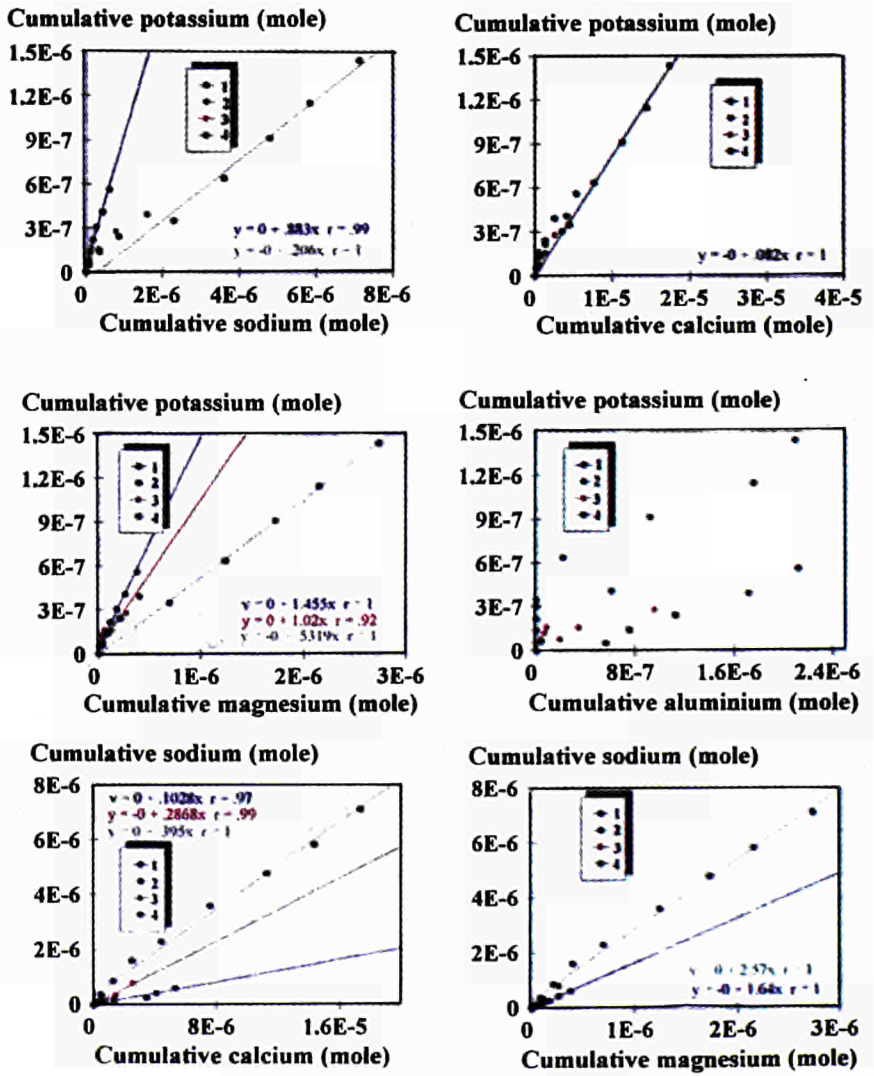

Figure 2: Examples of diagrams showing the evolution of element pairs for the four tests.

For the time being we shall limit ourselves solely to the following two observations :
- the linearity of most of the element pair ratios for all the tests (K^+-Na^+; K^+-Mg^{2+}; Na^+-Ca^{2+}; K^+-Ca^{2+}; Na^+-Mg^{2+}; etc...)
- the presence of two distinct evolutions between test 1 and test 2. For the moment, and in the absence of other proof, this result is attributed to a dissolution of different host minerals. It should be noted that the evolution obtained during tests 3 and 4 often appears intermediate between those of tests 1 and 2 (K^+-Na^+; K^+-Mg^{2+}; Na^+-Ca^{2+}; etc...)

Only through hydrofluoric acid dissolution tests on each of the granite minerals individually and through a detailed mineralogical study of the walls after percolation can we proceed further than the present observations. It must, however, be noted that we shall very likely encounter interpretation problems with respect to the elements that are present in several host minerals, i.e. aluminium and silica, in particular, because they are contained by most of the minerals involved.

C.4 Conclusion

From a purely technical standpoint, the designed test equipment appears to be fully operative and enabled a complete sequence of the different phases to be carried out, from surface characterization of the walls (micro-roughness, macro-roughness) to recovery of the percolate on which major-element analysis indicates that chemical phenomena affect the fracture and modify the flow channels.

A few important observations for the continuation of the study can be made :
- the evolution of the geochemical phenomena and their kinetics will be very sensitive to variations in the hydromechanical parameters;
- the influence of "rinsing" with demineralized water could not be quantified, but is certainly not negligible. Il could, in particular, cause a rise in the pH and thus favour a precipitation of aluminium hydroxides which would disturb the flow channels.
- the solution coming into contact with different zones containing variable quantities of certain minerals (biotites, feldspars) could explain the important variations noted both during a single test and between two tests. This hypothesis could be verified by measuring the surface distribution of each mineral species on the fracture plane.

Title	Experiments in a 600 m borehole in the Asse II salt mine.
Contractors	ECN - Petten
Contract N°	FI2W-CT90-0050
Duration of contract	January 1991 - December 1994
Period covered	January 1994 - December 1994
Project leader	J.J. Heijdra

A. OBJECTIVES AND SCOPE

In order to assess the safety of disposal of radioactive waste in salt formations, models for the thermo-mechanical behaviour of rock salt that have been developed in previous programmes have to be verified by in-situ experiments. It has been proven by the COSA project that computations based on laboratory scale experiments do not accurately predict the in-situ measurements.

In this research programme the following in-situ measurements are to be carried out in the Asse II salt mine in Germany with measuring equipment developed in a previous programme under contract number FI1W/0084:

1. Determination of in-situ elastic behaviour of salt and convergence measurements at the bottom of the borehole with different pressures. The measurements will be carried out with the Variable Pressure Device (VPD) in the available 300 m hole.
2. Free convergence measurements of the salt wall at five depths in a borehole, i.e. at different salt pressures as soon as a 600 m deep borehole becomes available.

The experimental results obtained will be available to predict the behaviour of salt deposits and will give essential information to be used in safety assessment of disposal facilities for radioactive waste in rock salt, especially in the field of elastic behaviour and pressure dependency of creep.

B. WORK PROGRAMME

The tasks which need to be performed during the contract period are:

1. Maintenance of installed equipment:
   Including the maintenance of the hardware and software required for remote instrument control and data transmission between the Asse salt mine and the ECN in Petten.
2. Execution of the experimental programme:
   The VPD measurements require that parameters (pressures) are changed and thus require local operation. The convergence measuring devices have to be installed in the borehole before measuring and removed afterwards.
3. Data collection and interpretation of the results:
   The automatically collected experimental data will be validated and interpreted.
4. Evaluation of experimental results:
   Consequences for the models used for the description of thermo-mechanical behaviour of rock salt resulting from the measurements will be evaluated taking into account the measurements performed in previous programmes.

C. PROGRESS OF WORK AND OBTAINED RESULTS

State of advancement

By the end of march 1994 a new borehole with a depth of 484 m from the 750 m level became available. After removal of the drill strings and drill head, removal of the drilling rig and installation and testing of the convergence measuring devices, convergence measurements have been started by the end of July 1994. With an interruption due to failure of the data collection system, the measurements are continued up to the present.

Based on the measurements of the modulus of elasticity by means of the variable pressure device, a revised set of parameters has been determined for the description of the time dependent material behaviour of rocksalt as used by ECN.

The final report is in preparation and will be submitted in the first quarter of 1995.

Progress and results

Based on the revised value of the modulus of elasticity and the measurements in the first ECN 300 m borehole dating from 1989, revised parameters for the secondary creep law:

$$\dot{\varepsilon}_{eq} = A\sigma^n e^{\frac{-Q}{RT}}$$

have been derived.

The complete set of parameters for the revised constitutive model of ECN is given in the following table:

Table 1. *Revised set of constitutive parameters from in situ tests of ECN*

E = 22.4 GPa; υ = 0.3; $\alpha = 4\ 10^{-5}\ K^{-1}$
$A = 6.17\ 10^{-2}\ MPa^{-6}\ day^{-1}$; n = 6.0; Q = 54.0 kJ/mole

In the newly drilled 500 m borehole the convergence and temperature has been measured at four vertical locations, determined by the measuring cable. The depth below the surface of these measuring stations was: 880 m, 1030 m, 1130 m, and 1230 m. The raw measured diameters are given in Figure 1.

It can be seen, especially for the bottom convergence unit, that the measured curves are not yet parallel in the first months. As in the former measurements in the 300 m hole the convergence measuring devices have to become set and to flatten out initial roughness of the wall before an accurate measurement result can be obtained. It also can be noted that the initial diameter for the individual units is not the same.

When these preliminary results are compared to the theoretical predictions based on the primary rock pressure, large discrepancies exist. For the units higher in the borehole this can be expected due to the disturbance of the rock pressure from the old production mine rooms. For the lower positions the distance to the disturbing production rooms is sufficiently large and the rock pressure will not deviate much from the primary rock pressure. In order to estimate the deviation at the measuring locations, the pressure has been determined that gives the best fit of the theoretical value and the measured value. Because the initial diameter of

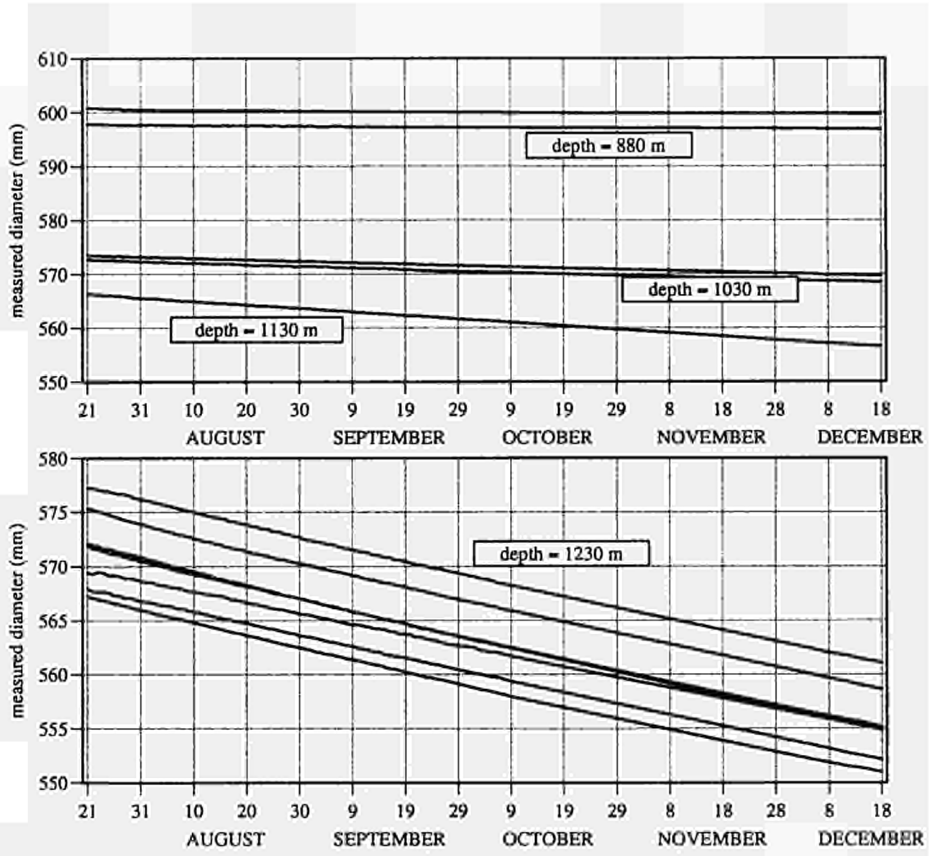

Figure 1. *Measured diameters in the new 500 m borehole.*

the borehole is not a priori known, due to wall roughness and dwelling of the drill head, this initial diameter has also been used as an optimising parameter. The measured temperatures which remain constant during the period of measurement are given in Table 2, together with the primary rock pressure and the pressure which gives the best fit between theoretical and measured convergence.

Table 2. *Temperatures and calculated pressures from the 500 m borehole.*

depth (m)	temperature (°C)	Primary rock pressure (MPa)	Calculated rock pressure (MPa)
880	*38.4**	18.65	14.4
1030	42.3	21.83	20.7
1130	44.0	23.94	24.7
1230	44.8	26.06	27.2

* At location 880 m the temperature measurements are unreliable and hence for this position the temperature has been determined by means of interpolation of other temperature data

The convergence signal used for this fitting procedure is the average of the available signals at each location. This convergence is represented in Figure 2 together with the theoretical prediction based on the primary rock pressure and the theoretical prediction based in the "best fit" pressure. The abscissa value in this graph is the time from the creation of the hole. Since the borehole has been drilled in a relatively long period, the starting point for each depth location is different and has been determined as the actual time when the drilling progressed to the relevant depth.

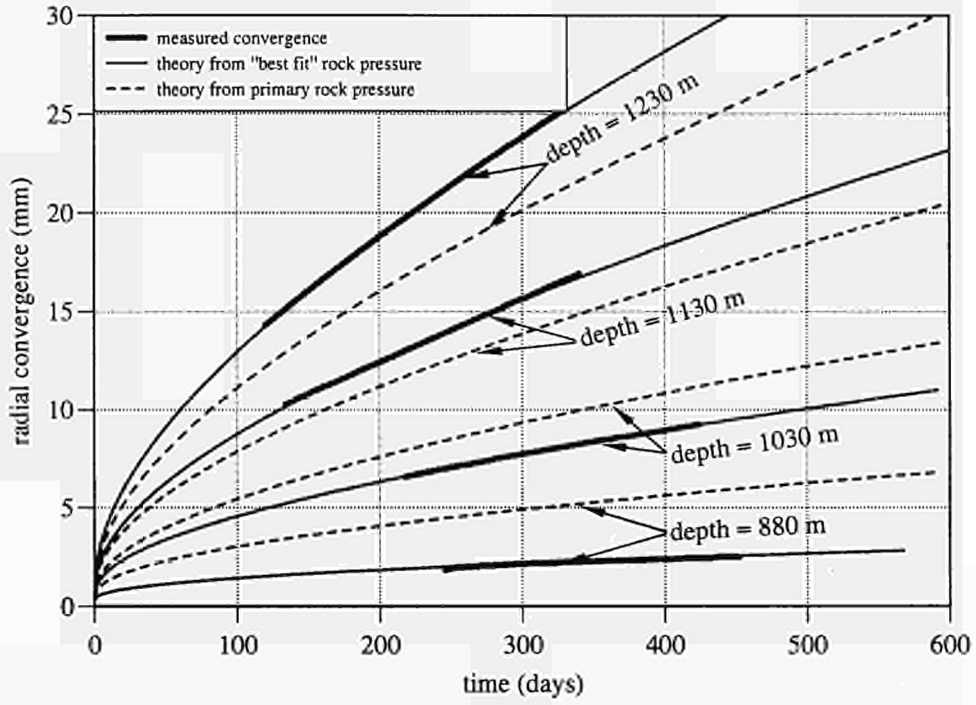

Figure 2. *Measured convergence in the new 500 m borehole.*

It can be seen that for the lower two stations the primary rock pressure leads to an under-estimate of the convergence, and hence the best fit pressure is higher. For the two units closest to the gallery the primary rock pressure leads to a higher convergence than the measured one.

In Figure 3 the measurements are represented with the normalized with the above determined "best fit" pressure, together with the theoretical normalized convergence.

Conclusions

The bottom of the 500 m borehole is far away from the rooms created in the production mining phase of the Asse salt mine. There is no reason why the pressure there should deviate from the lithostatic pressure. Since the pressure determined with the new creep model exceeds this lithostatic pressure by one MPa, this may lead to the conclusion that the new model needs to be reconsidered. The most probable source of inaccuracies is the pressure of 22 MPa assumed at the location of the 1989 measurements. If a lower value for this pressure is found, based on the new 500 m measurements, a higher creep rate will be found.

This higher creep rate can also account for a fraction of the discrepancies found between

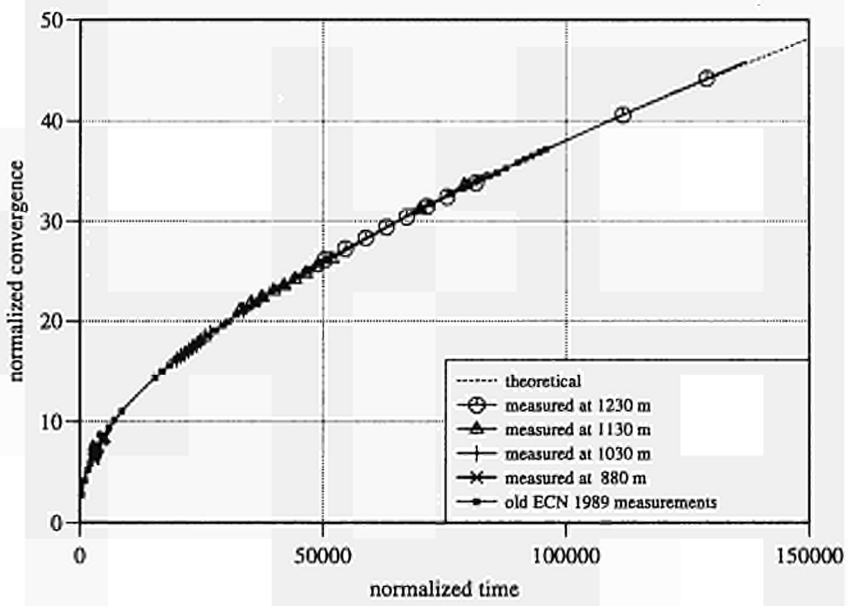

Figure 3. *Measurements from the new 500 m borehole and theoretical convergence in normalized form.*

measurements and calculations of pressures and deformations in the HAW test field. However, because the measurements period is relatively short and the convergence units need time to become set in the borehole, no firm conclusions can be drawn yet.

Especially from Figure 3, the advantage of measuring at greater depth can be seen. In the period of measurements the normalised time period covered with measured data considerably increased, compared to the 1989 measurements which where the longest available up to now.

List of publications

Hamilton, L.F.M., Prij, J., Jockwer, N., 1993(I): *Drilling surveillance and geomechanical experiments in deep boreholes in salt.* Commission of the European Communities, Report EUR 14235 EN.

Hamilton, L.F.M., Prij, J., Benneker, P.B.J.M., 1993(II): *In situ measurements of the mechanical response of rock-salt on variable pressure load.* Commission of the European Communities, Report EUR 14440 EN.

Heijdra, J.J., Prij, J., 1992. *Convergence measurements in a 300 m deep borehole in rock salt.* ECN-C--92-016.

Heijdra, J.J., Prij, J., 1995. *Geomechanical measurements in the 600 m borehole project. Final report for contract FI2W-CT90-0050.* ECN-C--95-013.

Title	Evaluation of a self-consistent approach to fractured crystalline rock characterization
Contractors	Golder Associates (UK) Ltd
Contract N°	FI2W-CT90-0051
Duration of contract	June 1991 - May 1994
Period covered	January 1994 - May 1994
Project leader	M. Brightman

A. OBJECTIVES AND SCOPE

The aims of the project are:

(i) to assess the errors in predictions of a nuclide migration in fractured crystalline rocks resulting from the application of inappropriate interpretation techniques;

(ii) to assess the impact of the "partial flow dimension" approach on the results derived from hydrogeological testing; and

(iii) to develop a methodology for constructing fracture network models to incorporate field flow dimensional information directly.

B. WORK PROGRAMME

The project has been subdivided into the following five tasks:

(1) to provide a literature review of the impact of the application of "partial flow dimension" interpretation on hydrogeological tests in fractured crystalline rocks;

(2) to evaluate, present and assess the effect of "dimensional" interpretation on some existing data sets;

(3) to simulate "dimensional" results within a fracture network model;

(4) to assess the available methods by which "dimensional" results would be incorporated explicitly into a fracture network model; and

(5) to demonstrate the effect of cylindrical flow assumptions on the output from a transport version of the fracture network model, when compared to results analyzed using the actual "partial flow dimension".

C. PROGRESS OF WORK AND OBTAINED RESULTS

State of Advancement

All the tasks except part of Task (4) have been completed by October 1993 and have been documented in our previous progress reports. All parts of Task (4) have been completed by June 1994. A draft final report has been prepared and is undergoing internal review prior to submission to the CEC.

Progress and Results

C.1 Dimensional Behaviour and Multi-Fracture Configurations

In 1994, the main task was to understand dimensional behaviour of multi-fracture systems in a well test. This work included two parts:

(1) numerical simulations of synthetic well tests in simple fracture system configurations which contain only a few fractures, so that the simulated results can be easily understood.

(2) re-analyzing synthetic well tests results in the two randomly generated fracture networks one contains over 500 fractures and another over 1000.

Six different simple fracture network configurations, as shown in Figure 1, were used to study the relationship between a fracture network and its dimensional responses. This approach is referred to as a "library of responses". A realistic fracture network to represent fractured rocks would be much more complex and it is unlikely that there is a unique relation between a complex network and a dimensional behaviour. Many different fracture networks may produce very similar dimensional behaviour. The purpose of this part of study is to determine the common "properties" of networks which produce similar dimensional behaviour.

In a well test conducted in fractured rocks, the induced pressure signal usually spreads from fewer fractures (which are directly connected to the testing section) to larger cluster(s) of fractures (which are further away from testing section). During this process, the flow dimension is likely to change from early time to late time, as demonstrated in our previous progress reports. Therefore, a composite model to account for the dimension changes has been developed and implemented in FlowDim (for the details of the well test interpretation package FlowDim, refer to the final report). The composite model is based on solving the following partial differential equation system:

$$\frac{T_1}{r^{n_1-1}}\frac{\partial}{\partial r}\left[r^{n_1-1}\frac{\partial h_1}{\partial r}\right] = S_1\frac{\partial h_1}{\partial t} \qquad r_w \le r \le r_f \text{ (inner zone)}$$

and

$$\frac{T_2}{r^{n_2-1}}\frac{\partial}{\partial r}\left[r^{n_2-1}\frac{\partial h_2}{\partial r}\right] = S_2\frac{\partial h_2}{\partial t} \qquad r_f \le r \le \infty \text{ (outer zone)}$$

where, r is the distance from a testing section; r_w is wellbore radius; r_f is the distance of the two zones' interface from a testing section; t is time from start of testing; T_i, S_i, n_i, $h_i(r,t)$ are transmissivity, storativity, flow dimension and pressure head response in inner zone (i = 1) and outer zone (i = 2) respectively.

The generalized composite type curves for different flow dimensions are obtained from different boundary conditions of constant rate or constant pressure tests for both source and observation sections. Sets of type curves are included in the final report. Since there are more parameters (up to 8) in a composite model, manual matching with FlowDim is not efficient and a non-linear regression algorithm has been implemented in FlowDim.

Over 20 synthetic test simulations with different simple fracture network configurations have been carried out. Figures 2 and 3 show two examples of them. Explanations are given in each figure individually.

Another important finding of this study is to quantify and understand space filling properties in a fracture network. The two larger randomly generated fracture networks reported in the second progress report, have been re-analyzed using the composite model. Better understanding of both flow dimension and space filling in fracture networks has been achieved as a consequence.

C.2 Alternatives to incorporate flow dimension into discrete fracture network modelling

After gaining understanding of flow dimension and space-filling in describing the flow geometry of fractured crystalline rocks, the next stage is to incorporate this flow dimension information into the flow simulator using the discrete fracture network modelling approach. There are essentially three ways in which measured hydraulic properties of fractured rock can be used in discrete fracture network models:

1) **Forward modelling**: A conceptual network is generated and the hydraulic test results are simulated. This process is repeated until a good match between the simulated and real test results is found.
2) **Library of Responses**: Responses of relatively simple fracture geometries are generated by simulation. In this way a "library" of typical responses to known geometries is generated. Real test results are then interpreted using the library to guide the analyst in recognizing different possible fracture geometries.
3) **Stochastic Conditioning**: Using a stochastic inversion process such as POCS (projection onto convex sets), the hydraulic and geometric properties are used to condition fracture networks as they are generated. The hydraulic and geometric properties of the network are assumed to be fractal (at least within the range of interest).

Forward modelling is conceptually the most straightforward, and is how fracture network modelling has been carried out in the nuclear waste industry so far. However, it can be time consuming and inefficient as it is something of a trial and error process. It also requires a "good" initial guess of the properties (geometrical and hydrogeological) as well as the conceptual model. The library of responses approach aims to guide the modeller to construct a limited range of alternative model configurations consistent with existing data. This should lead to more rapid problem solving. Stochastic conditioning is the most natural method to proceed with fracture network modelling, as it follows the sequence of measuring properties and then using them as input into numerical models of performance. However, the ability to condition fracture networks to appropriate stochastic parameters is limited at this time. Details of the methods to implement these approaches are presented in the final report.

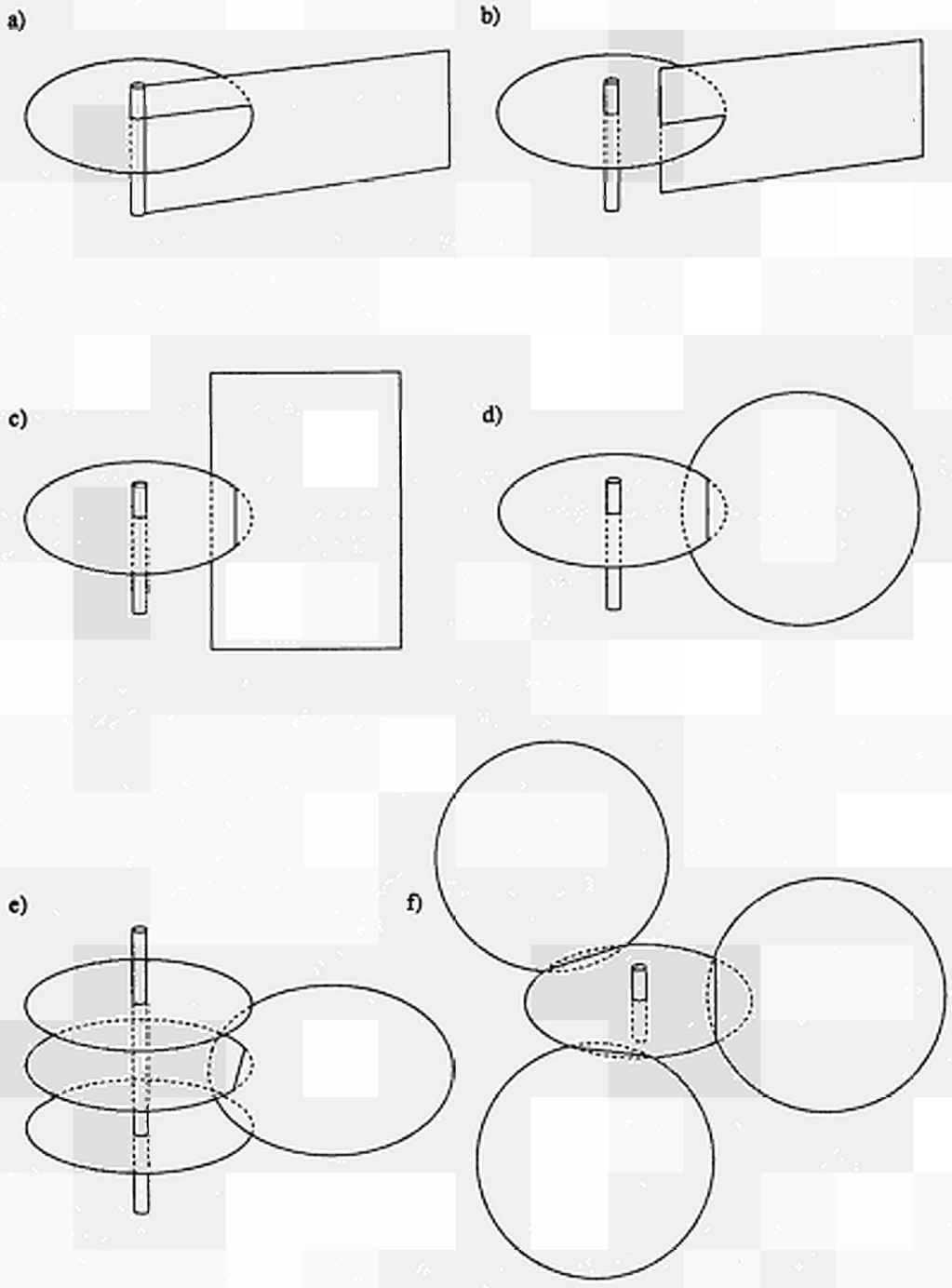

Figure 1 Simplified fracture configuration for study of relationship between fracture network and its dimensional behaviour

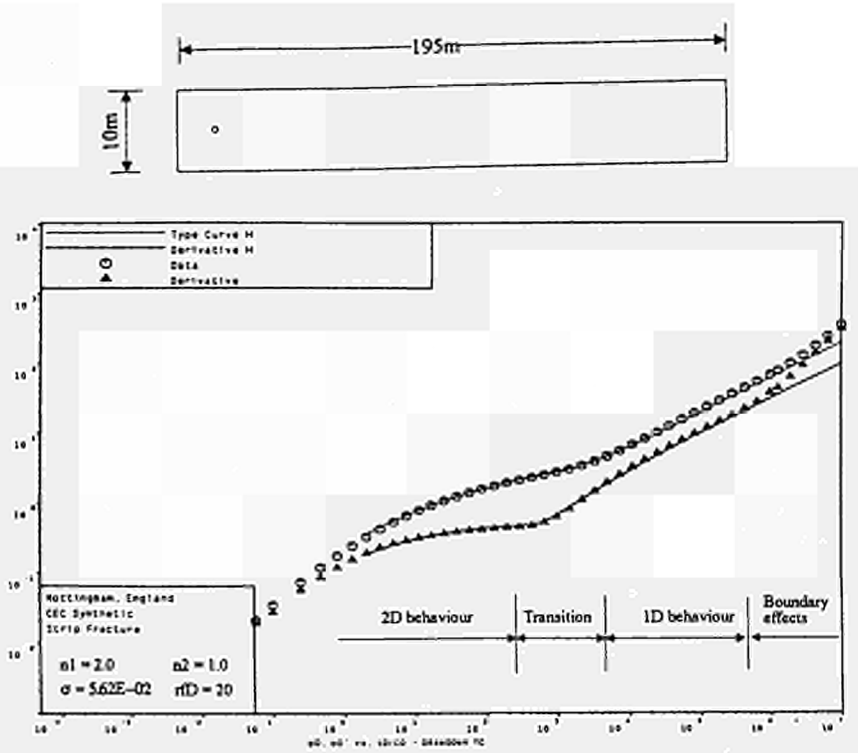

Figure 2 One horizontal strip fracture with a testing section located close to one end, which produces composite behaviour (from 2D to 1D). Very good matching has been achieved using FlowDim.

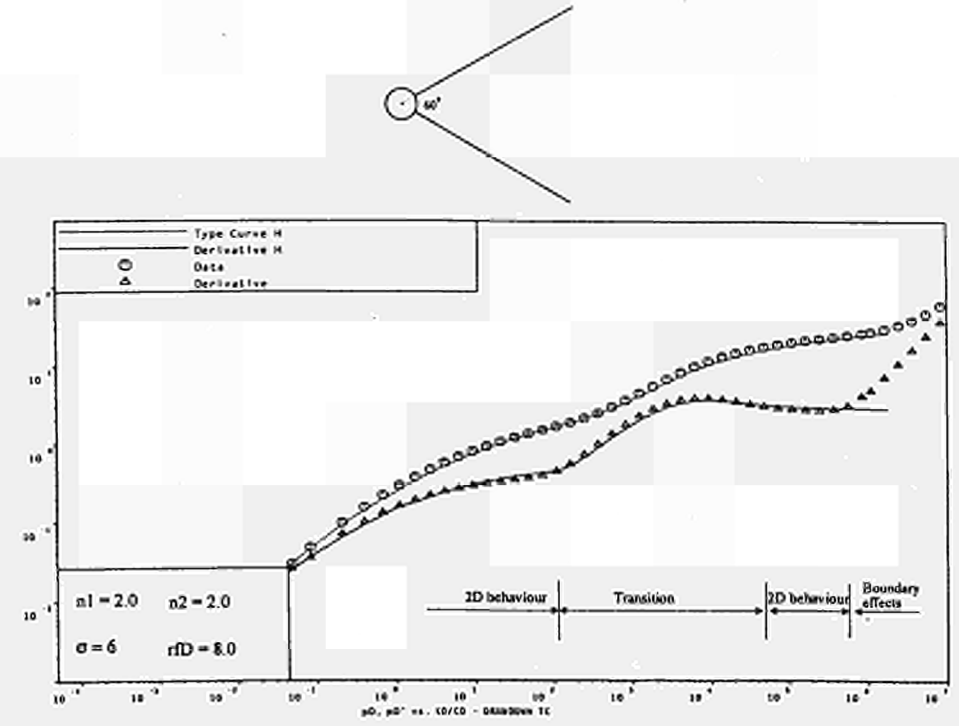

Figure 3 Only one sixth of the circumference of a circular horizontal fracture is available for flow in the outer zone. Very good matching using FlowDim is achieved using a composite model with both zones' dimensions as 2.0. The matched $\sigma = 6$ clearly demonstrated the meaning of this parameter.

Title	**INTERCLAY II - A Coordinated Benchmark Exercise on the Rheology of Clays**
Contractors	WS Atkins Science & Technology and other partners (see Table 1 below)
Contract N°	FI2W-CT91-0063
Duration of contract	June 1991 - August 1994
Period covered	January 1994 - August 1994
Project leader	N.C. Knowles

A. Objectives and Scope

INTERCLAY II was a coordinated benchmark exercise dealing with the numerical prediction of the rheology of clays. Its broad objectives was to improve confidence in predictions of the geomechanical behaviour of clay in situations relevant to the underground disposal of radioactive waste. Thirteen organisations participated (Table 1). A small Steering Committee comprising WS Atkins, GCG and SCK provide the technical leadership.

Coordinator	WS Atkins	UK	)
	GCG	UK	) Steering Committee
	SCK/CEN	B	)
	BRGM	F	
	CEA	F	
	EMP	F	
	ETSIM	S	
	G.3S	F	
	GEODESIGN	B	
	ISMES	I	
	LGC	B	
	BNFL	UK	) Observer
	ENRESA	S	) Observer

Table I - INTERCLAY 11 Participants

B. Work Programme

Three principal stages were defined:

In Stage 1, the basic ability of popularly used models and the computer codes which contain them were briefly reviewed. The review comprised a comparison of the theoretical capabilities of the codes and their performance on 4 simple, somewhat hypothetical problems.

In Stage 2, laboratory tests on reconstituted clays provided the basis for two computational benchmark problems. Participants were asked to replicate the measured laboratory behaviour as far as possible.

In Stage 3, 'in-situ' behaviour was modelled. Sources of well validated in situ behaviour are relatively scarce and a specially designed heater test was performed at SCK's Mol research facility. Precise details of the actual in situ behaviour was withheld from participants so that their predictions were 'blind'.

In each stage, the work programme was broadly as follows:

1. The coordinator prepared discussion documents in cooperation with the Steering Committee and circulated them to the participants for comment.
2. Participants in plenary meetings discussed and agreed details of suitable benchmark problems to be solved.
3. The coordinator prepared and circulated detailed specifications of agreed problems.
4. The participants solved the specified benchmark problems to the best of their ability using appropriate codes. The Coordinator collected and compiled the results and other data from participants and prepared draft reports.
5. Results and overall progress were assessed in plenary meetings at intervals of approximately 6 months.
6. The Coordinator prepared and issued final definitive reports taking account of participants' comments.

C. Progress of Work

The chronological progress in terms of key events is set out in Table II. Two day plenary meetings of all participants were held in Epsom (4/5 July 1991)/1/, Mol (20/21 January 1992) /2/, Fontainebleau (7/8 September 1992) /3/, Bergamo (29/30 March 1993) /4/, Madrid (17/19 November 1993) /5/, Orleans (21/22 April 1994) /6/, and Palaiseau (27/28 June 1994) /7/. The final meeting was held in conjunction with the HADES project group meeting. The Steering Committee met periodically and in addition maintained regular contact by telephone and fax, in order to progress necessary activities.

The project has now been completed and the achievements of each stage are outlined below:

In **Stage 1**, four benchmark problems have been successfully addressed. All are hypothetical problems and serve as verification tests of the computer codes used ("verification" in this sense is defined as demonstrating that the mathematical formulation of the problem is correctly implemented and solved by the program. It says nothing about whether the mathematical formulation correctly replicates the real physical situation). The four benchmarks were:

1.1 an axisymmetric 1-D approximation of a cylindrical (i.e. tunnel) excavation under isothermal and isotropic conditions /7/.

1.2 a two-dimensional, axisymmetric approximation of the progressive excavation of a cylindrical tunnel in clay, again under isotropic and isothermal conditions /7/. (The approximations implied in 1.1 and 1.2 are relevant to deep repositories in clay - e.g. Mol).

1.3 a plane-strain representation of the somewhat idealised construction operation and post-closure stages of a shallow 'lined trench' repository founded on clay /8/. (This was based on the Drigg LLW disposal facility operated by BNFL in the UK).

1.4 problem 1.1 extended to include a centrally located heat source /8/.

In all cases interest centred on the ability of the various conceptual models (and the codes in which they are implemented) to predict steady state behaviour. To provide a proper basis on which to assess these verification problems the "physics" was fully defined - i.e. the loading, boundary conditions, material models and the numerical values of the parameters were all given. It was intended that the only variation between the participants' models would be code-specific (e.g. in the detail of the numerical discretisation or solution procedures used). Various popularly used constitutive models were defined in terms of both effective and total stress with data parameters selected to provide equivalent behaviour wherever possible. (The data relates to Boom clay for benchmark 1.1, 1.2 and 1.4 and to the Drigg site for 1.3, although in the latter case it was found that despite extensive geotechnical surveys the existing information was not in a form suitable for numerical models). The broad technical capabilities of the codes used by the various participants were also reviewed in this stage and an attempt was made to collate authoritative sources of data for Boom clay /8/.

The results of Stage 1 /9/ broadly demonstrated that verification of computer codes is no longer a major issue (i.e. all codes were capable of predicting the same behaviour, given identical descriptions of the problem). Some differences were observed but these have been satisfactorily resolved following discussion and subsequent investigation. (In this respect two further smaller scale problems were posed to investigate aspects of problems 1.3 and 1.4).

In **Stage 2**, two benchmarks based on laboratory-scale tests were tackled. The ideal basis for such benchmarks was defined as a set of laboratory tests in which the behaviour is fully quantified, self-consistent and moreover unfamiliar to participants, but in practise these requirements could not be met. A search, carried out concurrently with Stage 1, highlighted the paucity of any authoritative source of suitable tests.

Benchmark 2.1 was based around tests on kaolin carried out at Cambridge University some years ago /10,11/. Three sets of heated triaxial tests on cylindrical samples were available, the first two of which were undrained and the third drained. Experimental results were available for temperature and pore pressure at two locations within the sample. As few additional material data were available, participants were asked to calculate the temperature and pore pressure changes at the two locations observed in the first two experiments. They were then asked to 'back-fit' their constitutive models to achieve adequate agreement with these experimental results and subsequently predict the results for Experiment 3. Thus they were to use the first two experiments to 'validate' their models prior to calculating the response of Experiment 3 thereby retaining an element of 'blind prediction'.

Benchmark 2.2, was based on experimental work commissioned by the INTERCLAY II project performed at ISMES in Bergamo, Italy /12,13/. The experiments comprised a series of heated hollow cylinder tests supported by triaxial tests on Boom clay from the -223 level at Mol. As in Benchmark 2.1, some element of blind prediction was included in the specification: participants were asked to predict

the results of the hollow cylinder tests based on the triaxial test data. They were then issued with the results for the hollow cylinder tests to enable 'back fitting' and some investigation of the effects of parametric variations.

The increased complexity of the Stage 2 benchmarks, compared with Stage 1 was reflected in the scatter in the results, which although still within acceptable bounds, highlights the need for further work to fully understand the differences. The inevitably small scale of the laboratory tests also tends to exaggerate effects such as non-homogeneity of material (relative to in-situ measurements). It is clear that in developing and tuning constitutive models, the stress path followed in the supporting laboratory tests needs to be designed with sound appreciation of the effects of anisotropy.

The **Stage 3** benchmarks used the ATLAS in-situ heater tests at the Mol facility in belgium. These tests were designed specifically for the project and comprised a 20m long, 190mm diameter, horizontal lined borehole containing electrical resistance heaters with two smaller diameter boreholes, containing pressure and temperature sensors, in the same horizontal plane. Design and installation were satisfactorily completed by July 1992 /14/, although some sensors were inadvertently damaged during installation.

Over 12 months was then allowed for the clay mass to respond to the excavation disturbance, before heating was started in July 1993. Participants were asked to model the drilling of the central borehole and emplacement of the liner, using their own judgement to decide the level of detail necessary /15/. They were then to introduce the heating phase and to predict the response of the clay to the disturbance.

A number of methods were used to model the initial conditions, the excavation of the borehole and the convergence of the clay. Accordingly, the resulting initial response to the excavation varied between participants. In comparison, the predictions to the response to heating were similar for all the models, and the predictions of temperature change showed good agreement, both between participants and with the measured values.

Pore pressure predictions were obviously affected by the flow boundary conditions imposed at the borehole surface. The majority of participants specified zero flow during heating, but in some cases where convergence of the clay onto the liner had not been achieved before heating started, fully or partially drained conditions had been imposed. The pore pressures were in reasonable agreement with the experimental values at the end of the experiment, but the pore pressure change due to the effect of heating was generally under-predicted. These results are consistent with those observed in Stages 1 and 2: the major differences between the results appear to be in the initial unloading, as a result of the different approach used to model the excavation.

Throughout the project, difficulty was experienced in obtaining meaningful data in a form suitable for the various models, highlighting the need for data requirements to be noted when designing characterisation tests. It is important to appreciate the range of applicability of the tests and to understand their limitations. A further issue

is the effect of uncertainty due to natural variations in the geotechnical properties on the reliability of computer predictions; while it may be possible at the present state of the art to formulate a methodology to validate predictions given 'certain' data, practical means to allow for uncertainties in data are largely undeveloped. Further work is necessary both in developing suitable methodologies and in defining the role of supporting laboratory tests for calibration.

The project also highlights the need to recognise the opportunity for human error and to devise means of controlling it. The experience from this exercise is that in most cases, 'errors' were not discovered until the results were compared against the experimental results and those of the other participants. Errors were primarily due to misinterpretations of the benchmark specifications as a result of either incomplete definition of the required parameters or misinterpretation of their meaning. The differences were 'corrected following initial comparisons, but the experience is a salutary demonstration of the difficulty of communicating a precise specification of engineering situations and the opportunity for human error that therefore exists.

References

/1/ INTERCLAY 11 Minutes of plenary meeting, Epsom, 4/5 July 1991, WS Atkins Engineering Sciences.

/2/ INTERCLAY 11 Minutes of plenary meeting, Mol 20/21 January 1992, WS Atkins Engineering Sciences.

/3/ INTERCLAY 11 Minutes of plenary meeting, Fontainebleau, 7/8 September 1992, WS Atkins Science & Technology.

/4/ INTERCLAY 11 Minutes of plenary meeting, Bergamo, 29/30 March 1993, WS Atkins Science & Technology.

/5/ INTERCLAY 11 Minutes of plenary meeting, Madrid 17/19 November 1993, WS Atkins Science & Technology

/6/ INTERCLAY 11 Minutes of plenary meeting, Orleans, 21/22 April 1994, WS Atkins Science & Technology.

/7/ INTERCLAY 11 Minutes of plenary meeting, Palaiseau, 27/28 June 1994, WS Atkins Science & Technology.

/8/ INTERCLAY 11 - Properties of Boom Clay - Bibliography GCG (London), August 1992.

/9/ CEC INTERCLAY 11 project - Report on Stage 1, WS Atkins Science & Technology, January 1993 (To be published as an EUR Series Report).

/10/ Savvidou, C. and Britto, A.M., 'Thermally Induced Effects in Saturated Clay', Proceedings of the International Workshop on thermo-mechanical of Clays and Clay Barriers #, Seriate (Bergamo), Italy, October 20-22, 1993.

/11/ INTERCLAY 11 - Specification of Benchmark 2.1, October 1992, WS Atkins Science & Technology.

/12/ Baldi, G., Borsetto, M. and Pellegrini, R., 'Medium Scale Laboratory Tests for the Interpretation of the Thermo-mechanical Properties of Clays', Proceedings of the International Workshop on Thermo-mechanics of Clays and Clay Barriers, Seriate (Bergamo), Italy, October 20-22, 1993.

/13/ INTERCLAY 11 - Specification of Benchmark 2.2., May 1993, WS Atkins Science & Technology.

/14/ CEC Benchmark INTERCLAY 11 - Installation Report of the ATLAS Equipment, November 1992, SCK/CEN.

/15/ INTERCLAY 11 - Specification of Benchmark 3.1, December 1993, WS Atkins Science & Technology.

Table II Summary of Interclay II Key Events

Date	Event	Purpose
June, 1991	Steering Committee Meeting, Braunschweig	Discussion of possibilities for Benchmarks 1.1 - 1.4
July, 1991	Plenary Meeting, Epsom	Selection of Benchmarks
August, 1991	Draft Specification for Benchmarks 1.1 and 1.2 issued	
September, 1991	Specification frozen - results required 31/12/91	
January, 1992	Plenary Meeting, Mol	Discussion of Benchmark results. Specification of Benchmarks 1.3 and 1.4
February, 1992	Draft specification for Benchmarks 1.3 and 1.4 issued	
March, 1992	Specification frozen - results required 31/7/92	
June, 1992	Installation of ATLAS Tests at Mol completed	
September, 1992	Plenary Meeting, Fontainebleau	Discussion of Benchmark results. Specification of Benchmark 2.1. Experimental tests for Benchmark 2.2 commissioned at ISMES
October, 1992	Specification of further work on 1.3 and 1.4 issued. Specification for Benchmark 2.1 issued	
November, 1992	Specification frozen - results required 31/12 92	
March, 1993	Plenary Meeting, Bergamo	Discussion of Benchmark results. Specification of Benchmark 2.2. Discussion of Stage 1 report.
May, 1993	Specification for Benchmark 2.2 issued	
May, 1993	Specification frozen - results required 14/7/93	
July, 1993	Heating phase of ATLAS tests started	
November, 1993	Plenary Meeting, Madrid	Discussion of Benchmark results. Specification of Benchmarks 3.1 and 3.2
December, 1993	Specification for Benchmarks 3.1 and 3.2 issued - results required 21/3/94	
April, 1994	Plenary Meeting, Orleans	Discussion of Benchmark results.
June, 1994	Final Plenary Meeting, Palaiseau	Discussion of Benchmark results and project achievements

Title	SEALING OF BOREHOLES IN CRYSTALLINE ROCKS
Contractors	BRGM, SIF BACHY, MOTT MACDONALD
Contract N°	FI2W-CT91-0072
Duration of contract	1 October 1991 - 30 September 1995
Period covered	1994
Project leader	J.-F. OUVRY (BRGM - Coordinator); F. DUFOURNET-BOURGEOIS (SIF BACHY); J.P. BEVERIDGE (MOTT MACDONALD)

A. OBJECTIVES OF THE PROJECT

The objective of the study is the theoretical design and practical implementation of an in situ borehole-sealing technique that is applicable to fractured crystalline rock. The sealing, or backfilling, of boreholes in or around sites for the disposal of radioactive waste is usually done with compacted bentonite, bentonite slurry or cement slurry. It is proposed to design a special product that combines a bitumen emulsion with clay and other substances. A fracture identified in crystalline rock will be selected for injection testing. The fracture aperture, measured in drill cores, will be studied in the laboratory and the data will be processed statistically. Tests with water will enable the study of the hydraulic behaviour of the fracture, before and after slurry injection, to define the efficiency of the method.

The contract combines the competence of several partners, including BRGM (F), the SIF BACHY Company (F) and MOTT MACDONALD Civil Company (UK).

B. WORK PROGRAMME

- Literature survey and assessment of earlier work.
- Laboratory tests for optimizing the grout concentration.
- In situ tests of the fracture (geophysics, water injection) and laboratory work (definition of the fracture space on core samples).
- Grout injection into the fracture, geophysical estimation of its penetrability, and evaluation of the injection by means of sample studies and water tests.

C. PROGRESS OF WORK AND OBTAINED RESULTS

State of progress

By October 1994, the progress of the work phases that began in October 1991 was as follows:

- The literature survey concerning the concept of resealing boreholes in the context of an underground laboratory is completed.

- Research into the components of the mineral and hydrocarbon phases of the sealant was continued; laboratory analysis of the various preselected materials make it possible to define the components and their relative proportions for the experimental grout. During this phase, a laboratory device was developed for testing the injectability of the selected mixtures.

- At the experimental site, the fractures were sampled and studied morphologically. At the same time a series of in situ water tests was carried out to determine the hydraulic behaviour of the rock, and a geophysical radar (Georadar) reconnaissance provided additional information on the in situ rock structure.

- The selected grout was tested during an in situ injection programme at the experimental site.

- Coring was carried out to sample the injected grout 28 days.after its placement

- The cores were studied under the scanning electron microscope of BRGM.

Progress and results

Methodology (concept of borehole sealing)

The literature survey showed that numerous laboratory studies and in situ pilot tests carried out over the last ten years have determined the conditions for use and drawbacks of different sealing materials and methods (First Progress Report, CEC Contract No. F12W - CT 910072, 1992).

The materials and methods of borehole sealing must be adapted to the rock types intersected by the boreholes. For example, where the borehole cuts non-fractured rock with a very low potential for fluid circulation, one method of plugging is the use of dry compacted bentonite. Conversely, where the borehole cuts fractured crystalline rock with a high potential for fluid circulation, bentonite plugs are likely to be eroded (CEC Final Report EUR 1409 3FR - Plugging fractures and boreholes in fractured geological formations, 1992).

Intervals of fractured crystalline rock cut by a borehole require a sealant that will plug the fractures in the borehole walls as well as the borehole itself (Figure 1). The injected grout must fill the aperture between the fracture walls so as to diminish fluid circulation towards the borehole.

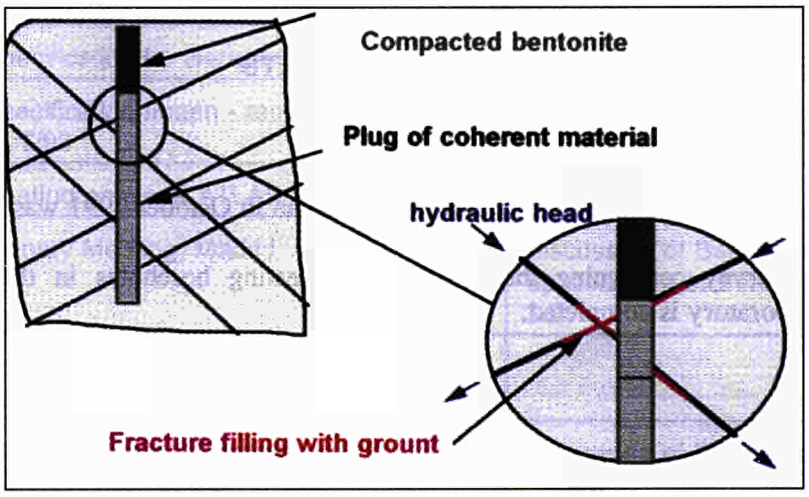

Figure 1 -Concept of adapted borehole sealing

Characterization of the fractured crystalline rock to be treated

Reconstruction of the initial characteristics of a rock mass (i.e. before its disturbance by reconnaissance drilling) requires a detailed geological and structural knowledge of the rock body. This is obtained through petrographic and structural studies on oriented borehole cores, complemented by geophysical well logging, from which the plotted joints and fractures are subdivided into families (or sets), each one characterized by its strike and its dip.

Morphology, continuous length, spacing, thickness, and possibly type of infill and percentage of voids, can then be determined for each fracture set. Although these parameters are not always easily quantifiable, their systematic study is essential for any borehole in a sealing borehole project.

Fractured crystalline rocks are commonly areas of water circulation, which occurs through the fracture networks and in particular through open and interconnected fractures. One method of satisfactorily determining the characteristics of the fracturing is through downhole water tests. Indeed, this is the only way of determining a parameter as important as the hydraulic aperture of fractures.

In order to complete the characterization of fractured rock masses, BRGM has developed laboratory techniques by which it is possible to quantify the aperture between two walls of a fracture. This is done by a method of moulding, whereby the voids between the two walls of the fracture are filled with a coloured silica resin. The mould is then studied by light transmission and the image digitized with a camera. On the resultant image, which comprises grey levels, the darkest zones correspond to the largest voids (Figure 2); Figure 3 shows the distribution, after processing, of void heights obtained for a sampled fracture from an experimental site.

The fracture used for the present study was characterized hydraulically in the borehole and gave a downhole unit absorption value of about 1.4 10^{-7} $m^3.s.^{-1}.m^{-1}$ at 4 MPa.

Selection of an injection grout to plug fractures in crystalline rock

Selection of the basic components for the grout was based on several parameters, predominant among which are particle size (with regard to grout penetration of small cracks) and durability of the component properties.
The components of the selected grout are:

- *Hydraulic binder*

  The hydraulic binder used for formulating the grout is an ultrafine slag cement, such as Spinor A cement from Ciments d'Origny, France. Its composition is given in Table 1 and its particle size distribution is shown in Figure 4.

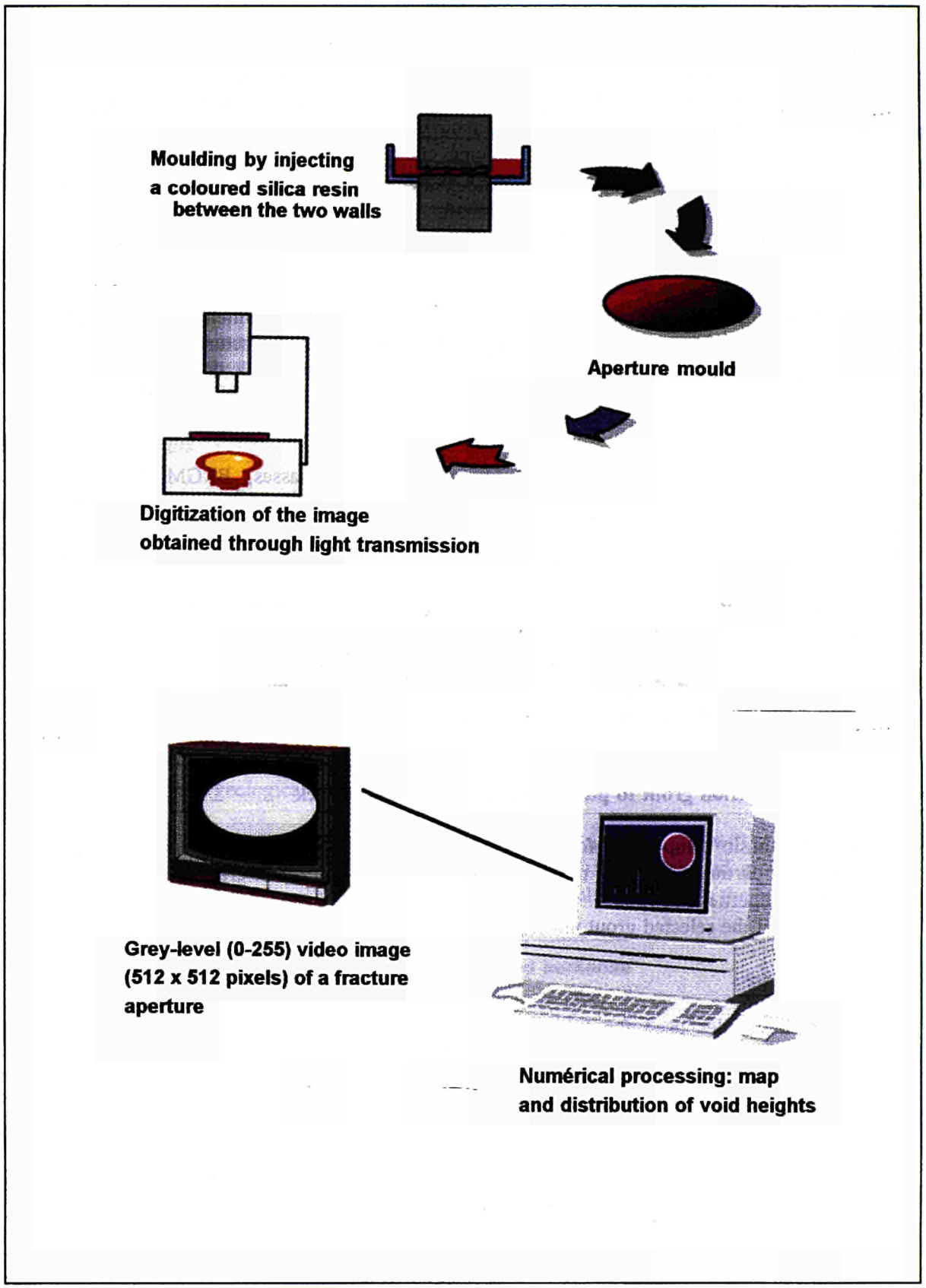

Figure 2 - Diagrams showing the principle of studying the aperture between the walls of a fracture

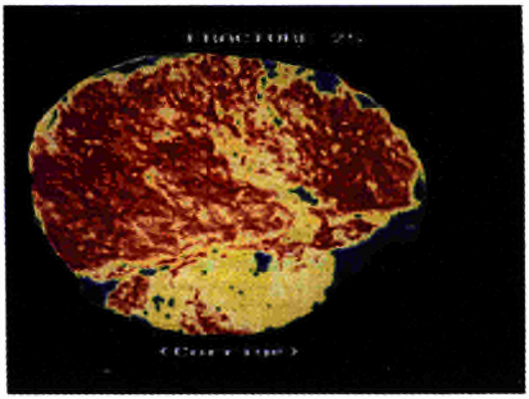

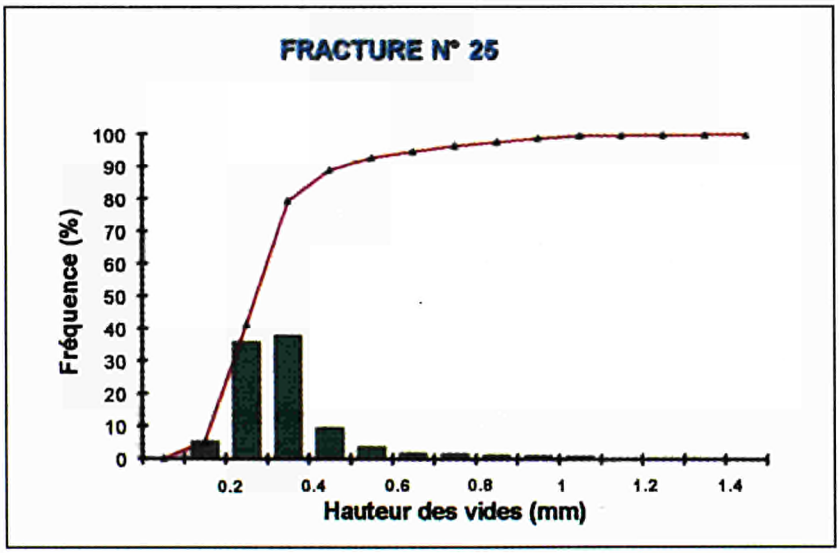

Figure 3 - Processing void heights in a fracture.

Table 1 - Chemical composition (%) of Spinor A cement

Component	Percentage
SiO_2	28.0
Al_2O_3	7.0
Fe_2O_3	1.5
CaO	45.0
MgO	5.0
K_2O	0.5
SO_3	6.0
TiO_2	0.5
MnO	0.5
Na_20	1.0
LOI*	3.0

* LOI: loss on ignition

- *Clay*

The FoCa clay is a studied calcic bentonite used by ANDRA. Its mineralogical composition is given in Table 2 and its particle size distribution is shown in Figure 4. As the most common fracture width is around 0.3-0.5 mm, the clay component was first smoothed in the laboratory to give a product with a median particle diameter of 3.5 μm and a maximum particle diameter of 10 μm (as against 4.6 and 28 μm respectively before smoothing).

Table 2 - Mineralogical composition of the FoCa clay

Component	Percentage
Clay Phase	
Interstratified smectite (50%) - china clay	81.0
Free kaolin	5.0
Other phase	
Quartz	5.3
Goethite	6.6
Calcite	1.2

- *Hydrocarbon phase*

The hydrocarbon phase is a bitumen emulsion with a globule diameter smaller than 10 μm and a particle size distribution as shown in Figure 5.

The purpose of the hydrocarbon phase is to improve the hardening properties of the grout, notably its breaking strength, permeability and capacity to adhere to the fracture walls. Several bitumen emulsions were tested, in particular for their polarity (anionic or cationic) and breaking ability (choice and amount of surfactants); they all gave a similar globule size.

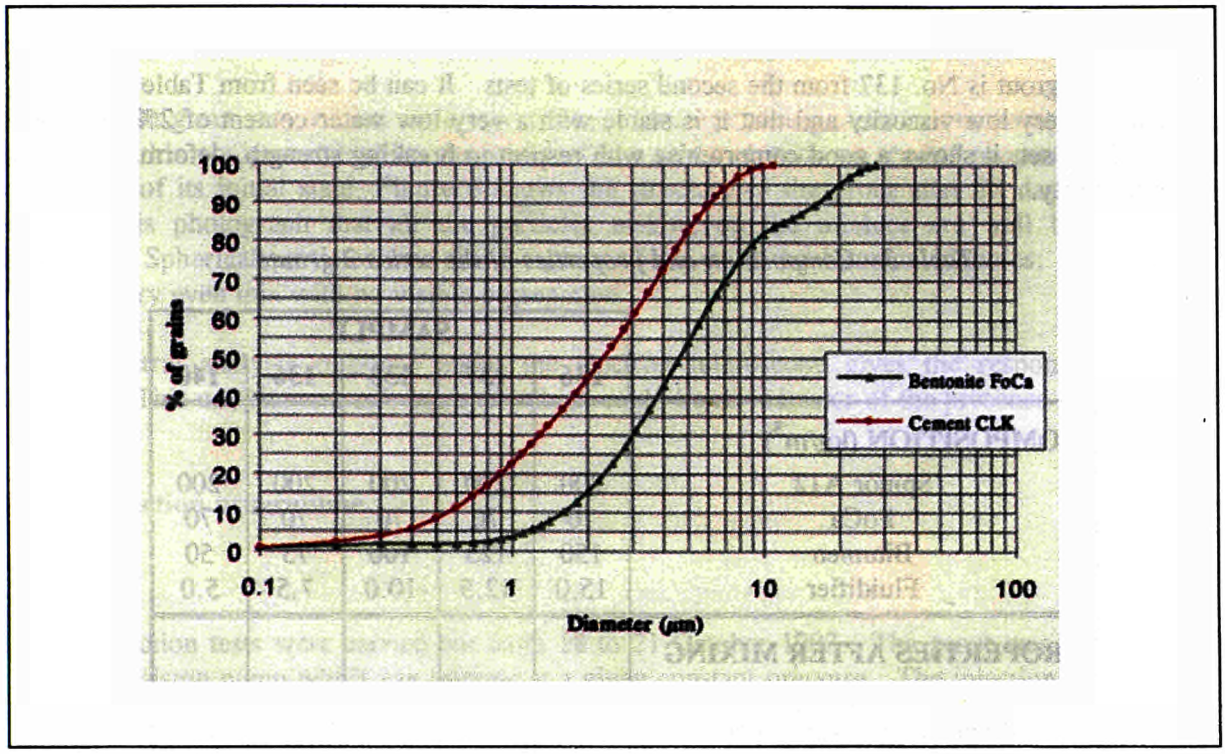

Figure 4 - Particle size distribution of the selected clay and cement components

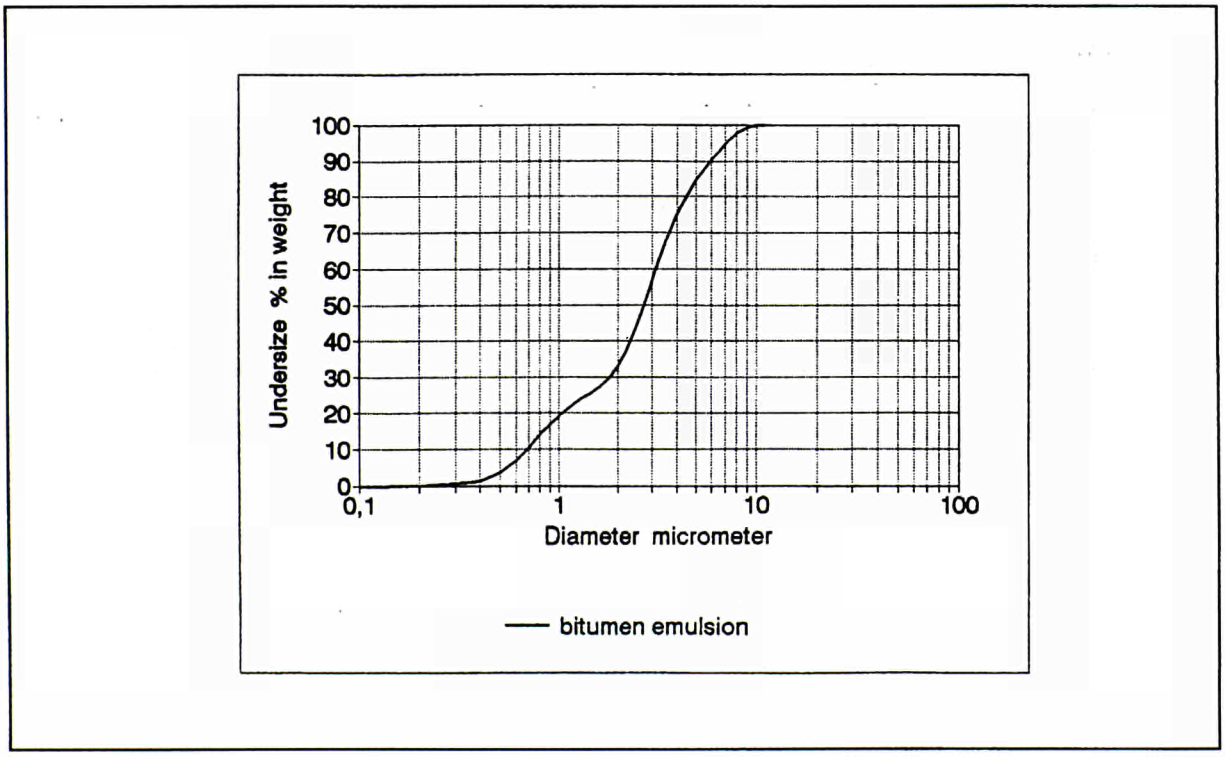

Figure 5 - Particle size distribution of the selected bitumen

- *Fluidifier (thinner)*

  A fluidifier was added.

The selected grout is No. 137 from the second series of tests. It can be seen from Table 3 that this grout has a very low viscosity and that it is stable with a very low water content of 2% after two hours. Once set, it shows a good compromise with respect to breaking strength, deformability and impermeability.

Table 3 - Composition and properties of the series 2 grouts

	SAMPLE				
	136	**137**	**138**	**136**	**140**
COMPOSITION (kg/m^3)					
Spinor A12	200	200	200	200	200
FoCa	70	70	70	70	70
Bitumen	150	125	100	75	50
Fluidifier	15.0	12.5	10.0	7.5	5.0
PROPERTIES AFTER MIXING					
Marsh viscosity (s)	31	31	30	29	29
Bingham viscosity (mPas)	5.7	5.0	4.3	4.3	4.1
Yield point (Pa)	0.4	0.4	0.4	0.4	0.4
Free water: 2h (%)	1	2	2	2	3
Filtration: 30' (ml)	64	100	132	194	330
PROPERTIES AFTER SETTING					
Cohesion (g/cm^2)					
4 h	11.7	11.7	11.7	11.7	11.7
1 day	220	245	228	206	108
2 days	828	820	767	750	690
3 days	1625	1586	1480	1230	1021
UCS (MPa)					
7 days	0.54	0.33	0.47	0.37	0.41
14 days	0.99	0.82	0.78	0.63	0.38
28 days	1.13	0.94	0.65	0.57	0.79
49 days	1.19	1.10	1.15	1.01	0.84

The mechanical tests which were carried out show an unconfined compressive strength of 1.10 MPa and a breaking strain of 10% after 49 days of setting. Its permeability, measured after 28 days, is 2.9 10^{-10} m/s.

The resultant grout was studied under a variable pressure scanning electron microscope of BRGM; the use of this equipment enables the study of wet material with no special preparation; this no modificate of its initial state. Figure 6 shows the structure of the grout after 28 days. It can be seen in this photograph that all the particles making up the mixture are well below 10 μm diameter. Spherical particles can also be seen which could be bitumen globules. The texture shows a very even mix with no visible segregation.

X-ray spectral analysis response under the electron microscope gives the response shown in Figure 7. This one shows a sulphur peak which could be an indicator of the presence of bitumen.

In situ injection programme

Principle:

In situ injection tests were carried out from 18 to 21 October 1993. The grout was injected by a pneumatic piston pump which can operate at a given constant pressure. The injection pressure and flow rates were continuously measured at the well head, and the surrounding boreholes were equipped with sensors to record possible over-pressure caused by the injection.

The grout was prepared in a laboratory type "manufacturing unit".

Injection of the central borehole (S2) fractures

Before injecting the grout, each one of the boreholes was cleaned and saturated with circulating water for about 12 hours at 0.6 MPa pressure.

During a first trial, the section of the borehole intersecting fractures F24, F25, F26 and F27 was isolated with a double packer then injected. The injection pressure was fixed at about 2 MPa in the first instance and later at 4 MPa. The total volume of grout injected in the section was 14.5 l.

In a second trial, the double packer was replaced by a simple packer and the borehole injected in sections of 1 m.

Finally after removal of the packer equipment the borehole was cleaned with water.

Injection of the surrounding boreholes S1, S3 and S4

These three boreholes were injected using the same method as for borehole S2, i.e. at 1 m intervals with a single packer. Then the boreholes have been cleaned with water using asteel pipe lowered in the borehole.

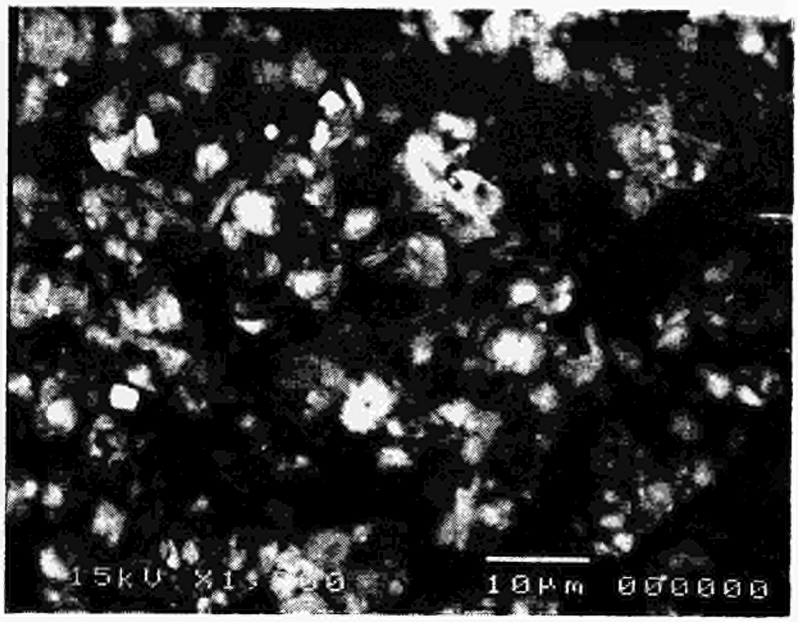

Figure 6 - Grout dispersion seen under the variable pressure SEM

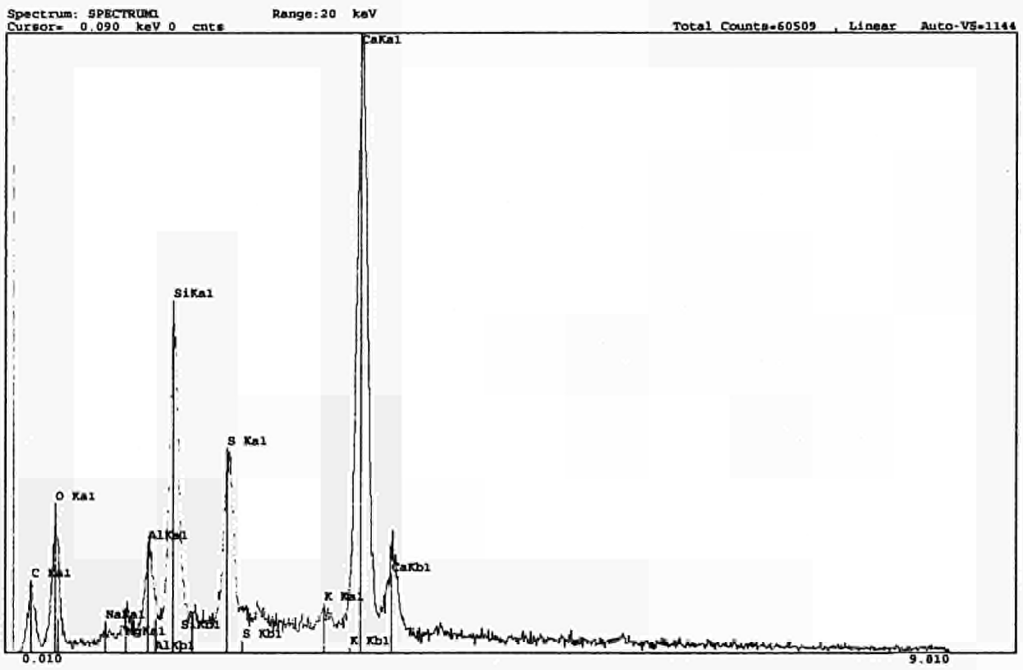

Figure 7 - X-ray spectral analysis under the variable pressure SEM

In situ permeability measurements

In situ permeability water tests were carried out in the boreholes two months later. The downhole unit absorption after treatment was, for a 0.70 m section in hole S2, 7.3 10^{-12} $m^3.s.^{-1}.m^{-1}$.

This is to be compared with an absorption of 1.5 10^{-7} $m^3.s.^{-1}.m^{-1}$ obtained before treatment.

Coring the injected rock

The injected granite was cored (116mm) at the end of March 1994. Two holes were drilled with a separation of 17 cm and 27 cm with respect to the central borehole S2. No particular precaution was taken during the coring, which was done using a diamond bit and drilling fluid.

Study of the sampled fractures shows grout lining the walls. This indicates that the grout is resistant to the drilling fluid and sticks well to the fracture walls

Study of the fracture injection by Georadar

Georadar uses the reflection of electromagnetic waves to investigate the upper levels of the subsurface. A transmitter sends brief impulses (a few nanoseconds) of electromagnetic energy into the ground, and these are reflected by anomalies such as a contact between two materials of different composition or the presence of a fracture. The signal is then captured by a receiver, amplified, developed and finally transformed into an electric current.

An on-site Georadar programme was carried out in order to provide a complete tomographic survey within the area delimited by the four boreholes. The transmitter and receiver were placed in two different boreholes, then progressively moved one at a time within the boreholes.

Interpretation of a second tomographic survey made after the on site injection proved difficult and the results are so far not conclusive regarding the objectives, i.e. monitoring the penetration of the grout and evaluation of the injection.

List of Publications

DUFOURNET-BOURGEOIS F., OUVRY J.F., Traitment des forages de reconnaissance autour ou au droit d'un site potentiel de stockage. Symposium International GEOCONFINE, 8-11 June 1993, Arnould, Barres and Corne (eds.), A.A. Balkema.

DUFOURNET-BOURGEOIS F., OUVRY, J.F., Sealing of exploration boreholes in and around a potential radioactive waste disposal site. First workshop on design and construction of deep repositories. 30-31 March 1993, Bäckblon and Svemar (eds.), Swedish Nuclear Fuel and Waste Management Co., SKB.

GANDAIS M., DUFOURNET-BOURGEOIS F., ESNAUT A., OUVRY J.F., Scellement de forages sur les sites de stockages de dechets radioactifs. First International Congress on Environmental Geotechnics, Edmonton, Canada, 10-15 July 1994.

Title	Paleoclimatological Revision of Climate Evolution and the Environment in Western Mediterranean Regions.
Contractors	ENRESA
Contract N°	FI2W-CT91-0075
Duration of contract	June 1991 - May 1995
Period covered	January - December 1994
Project leader	C. Bajos, P. Peaudecerf and D. Barettino

A. OBJECTIVES AND SCOPE

To evaluate the security of a high-level waste repository it is necessary to determine how future climate changes will affect the safety of the repository. The magnitude and likelihood of these changes can be inferred from the study of past climate changes. However, to date, little data has been available about past climate evolution in Spain and other Western Mediterranean countries. This project is concerned with the study of climate changes which have occurred over the last 2 million years in the Western Mediterranean regions, which will be of importance for developing scenarios for the safety analysis of a high level repository in Spain. Even though the techniques to be used in the study will provide information with different time scales, special emphasis will be placed on climate changes over the last 1000 years.

The project is being carried out by ENRESA as the main contractor and BRGM as an associate contractor. Work on climate evolution in Spain has been subcontracted to the Instituto Tecnológico y Minero de España (ITGE). BRGM is responsible for the review of past climate data from Southern France, Italy and the North of Morocco and for the development of scenarios.

B. WORK PROGRAMME

The project has been subdivided into the following tasks:

Task 1) a) Synthesis of the environment in Spain over the last two million years: D. Barettino (ITGE) and T. Torres (ETSIMM).

b) Paleoenvironmental evolution during the Quaternary in the context of Europe and Western Mediterranean regions: B. Defaut, P. Peaudecerf (BRGM).

Task 2) Paleoclimatic and environmental study of Quaternary deposits in the River Tajo Valley. A. Pérez (CSIC) and D. Barettino (ITGE).

Task 3) Study and dating of travertines in Spain as a paleoclimatic and paleoenvironmental index. T. Torres (ETSIMM) and D. Barettino (ITGE).

Task 4) Climatic reconstruction of the last thousand years in Spain on the basis of dendrochronological series: J. Creus (CSIC), L. A. Fernández (INIA) and D. Barettino (ITGE).

Task 5) Paleoenvironmental reconstruction and construction of future evolution scenarios. P. Peaudecerf, G. Farjanel, M. Garcín (BRGM).

C. PROGRESS OF WORK

State of advancement.

All tasks have progressed according to the attached time table (Figure 1) and no delays are foreseen. Task 1 ended in 1993. Task 2 is near completion. Field work has finished and all laboratory results have been received and analysed. Currently, the task 2 leader is writing up the final report. Task 3 has ended and final reports have been received. Tasks 4 and 5 are progressing as originally planned. A new task, to integrate the information obtained from the different tasks, was initiated during the last semester of 1994.

Progress and results.

Task 2: Paleoclimatic and environmental study of Quaternary deposits in the Tajo Valley.

Erosion was the dominant process in the centre of the Iberian Península during the Quaternary. It has formed a complex system of terraces and glacis in the major river valleys of the Iberian Península. The geomorphology of these systems is relatively well known, but important gaps still exist regarding their chronology and their paleoenvironmental significance. Of all the major Spanish valleys, the Tajo Valley , with its well preserved terraces with fossils, archaeological sites and buried soils, was considered a suitable site to obtain climatic and environmental information. At the scale of the Iberian Península, the results obtained in the Tajo Valley will be of great use because of the evolutionary similarity between this valley and other major valleys in the Península.

The ultimate objective of this task is to establish the relationship between the terraces along the Tajo Valley and the isotopic states of oxygen. This could later be used to establish paleoclimatic correlations with the rest of Europe.

Several fossils and a polarity change found in these deposits have been used to date some terraces and to establish correlations between them in two different areas. Some fossils found, mainly mammals and pollen, have provided useful information about the environmental conditions dominating the Tajo Valley during the Quaternary.

Task 3: Study and dating of travertines in Spain as a paleoclimatic and paleoenvironmental index.

The objective of this task is to investigate the possibilities of using quaternary continental carbonate deposits as paleoclimatic and paleoenvironmental indicators. These deposits were selected because they are very abundant and widely distributed throughout the Iberian Península. However, the type of environmental information they provide differs from one type of carbonate deposit to the other. For instance, the isotopic composition of travertine depends on several factors that are difficult to control and which may introduce large uncertainties in the paleotemperatures deduced from them. In addition, travertines are not usually preserved during cold periods when fluvial incision is prevalent. However, they often contain fossil remains, such as pollen, gasteropods and vertebrates that can be useful climate indicators. On the other hand, the paleoclimatic information

obtained from speleothem is less problematic because their isotopic composition is affected by fewer variables.

The research centred on five field sites that meet most of the following criteria:well preserved deposits of different origin with long stratigraphic records, fossil remains and situated in different climatic areas throughout the Península.

The information collected at the sites with travertine deposits has made it possible to date all the travertine terraces found and to reconstruct the paleoenvironmental evolution of the sites. This will be used to calculate incision rates and erosion. Pollen and isotope studies carried out in the sediments of a small lake in Northern Spain suggest that stable isotopes in travertines could be used as paleoclimatic indicators. Isotope analises in speleothems indicate progressive cooling since the Middle Pleistocene, with short intervals of higher temperatures.

Task 4) Climatic reconstruction of the last thousand years in Spain on the basis of dendrochronological series.

Field sampling has been completed. Thirty-seven chronologies (i.e. each tree ring has been matched with the corresponding year of formation) have been obtained. They have been grouped in seven zones to increase the reliability of climatic retropredictions. These areas are as follows:

- Galician zone (5 chronologies).
- Central Range (10 chronologies).
- North-western Iberian Range (4 chronologies).
- South-western Iberian Range (3 chronologies).
- Serranía de Cuenca (4 chronologies).
- Western Pyrenees (4 chronologies).
- Eastern Betica Ranges (6 chronologies).

To reconstruct past climatic variables it is necessary, in addition to establishing chronologies for each area, to collect climatic information from existing weather stations. This objective has also been completed during 1994. Only those weather stations with rainfall and temperature records longer than 40 years have been selected.

Several climatic variables have already been reconstructed seven weather stations, whose location can be seen in Figure 1. The variables and periods reconstructed at each station are described below.

Navacerrada.

- Temperature in February, March and April from 1770 to 1986.
- Temperature in July, August and September from 1683 to 1986.
- Rainfall in July and August from 1680 to 1986.
- Rainfall in August, September and October from 1773 to 1986.
- Total rainfall from 1770 to 1986.

Avila.

- Temperature in September and October from 1770 to 1986.

Segovia.

- Temperature in September and October from 1770 to 1986.

Madrid.

- Temperature in February and March from 1771 to 1986.
- Rainfall in September and October from 1770 to 1986.

Uña.

- Rainfall in July, August and September from 1700 to 1986.

Puebla de Brollón.

- Temperature in September from 1757 to 1992.
- Mean temperature from 1733 to 1992.

Santiago - Labacolla.

- Temperature in April from 1757 to 1992.
- Rainfall in April from 1757 to 1992.

Carballino.

- Temperature in May from 1757 to 1992.
- Temperature in April from 1650 to 1992.

Ginzo de Limia.

- Rainfall in April from 1757 to 1992.
- Rainfall in May from 1757 to 1992.

Task 5) Paleoenvironmental reconstruction and construction of future evolution scenarios.

The first objective, the reconstitution of a site representative of conditions in Spain, during the last glaciation in now finished. A report, in French, is available upon request. The reconstitution has been carried out with the code "Prospect" developed by BRGM. The work has involved the identification of all the relevant geological processes that have acted at this site over the last 120.000 years and their quantification whenever possible.

The site chosen is located in the Tajo Basin, near the Jarama River. The basin was formed during the late Cretaceous and filled up with fluvial, lacustre and palustre sediments during the Tertiary. The Quaternary began with the deposition of piedmont deposits, known as Raña, followed by fluvial dissection, which created a system of terraces, glacis and alluvial fans typical of most Spanish valleys. Some

of the rivers at the site seem to be controlled by a fault system that may have been active during the Quaternary. A hypothetical repository is located in the Tertiary sediments at a depth of 500 m below the surface of the ground.

Figure 2 shows schematically the conceptual model developed for the site. That is, the processes considered to have affected the site and the links established between them.

The simulated causes of site evolution are sea level fluctuations caused by freezing and melting of glaciers worldwide, annual mean global temperature, regional vertical movements and differential vertical displacement caused by a hypothetical fault. The parameters that quantify these processes are represented by the uppermost nodes, or entry nodes, in Figure 2. Their magnitude and rate of change are input to the model at the beginning of the simulation.

The rest of the nodes in Figure 2, are no-entry nodes, and represent parameters that are calculated by the code. Their values at any given time depend on the entry node values and the links established between the nodes.

The causal links established between the parameters depend on whether the parameter is a variable (i.e. a site characteristic such as temperature) or a phenomenon (i.e. primary cause of evolution with time). Deriv represents the impact of a phenomenon on a variable. CDeriv represents the impact of a phenomenon on a variable under certain conditions. M+ or M- is used when a change in a variable causes proportional changes in another variable. CM+ is similar to M+ but with certain conditions. CDcl indicates the link established if a variable reaches a critical value that my trigger a phenomenon. IDecl is similar to CDecl, but a value is assigned to the phenomenon. Equa is used when the value of a variable is the result of a mathematical relation between many variables.

During simulation, entry node values and their evolution over the last 120.000 years are propagated through the conceptual scheme described above. The model is calibrated when the results obtained compare well with present field conditions.

The best simulation was achieved when vertical movements were introduced in the entry nodes. This made it possible to simulate tilt blocks which are believed to have caused the migration of the Jarama River. The results show that over the last 120.000 years the Jarama has eroded 15 m of river bed deposits and created 3 terraces of 1 to 2 metres in thickness. The temperature at the simulated site would not allow permafrost formation.

In addition, work has progressed in the construction of future evolution scenarios at the paleosite for the next 100000 years. It is assumed that the geological and climatological conditions during the next 100000 years will be comparable in amplitude and sequence to those experienced during the most recent Quaternary. It is also assumed that the stress field at the paleosite will not change greatly during the next 100000 years, since the site is not expected to be subjected to glacial isostasy or major changes due to plate tectonics. The rest of the information needed for the future evolution of the paleosite is the same as for calibration. Some preliminary results and schematic reconstitutions are presented in Figure 3.

Final Reports:

APARICIO, M.T., 1.994 "Molúscos Fósiles del Pleistoceno de las Terrazas del Río Tajo en Toledo". CSIC.

GALLARDO, J.y PEREZ, A., 1.994 "Edafosecuencia en la Cuenca Media (Talavera de la Reina) del Valle del Tajo: Indicadores Paleoclimáticos". CSIC.

GARCIN, M. et al., Septembre 1994 "Modélisation du Paléosite du Jarama". BRGM. N 1092

RUIZ, B. y MARTIN, T., 1.994 "Análisis Polínico en Depósitos de Terrazas y Facies Asociadas en Toledo". CSIC.

SESE, C. y SOTO, E., 1.994 "Interpretación Paleoecológica y Paleoclimática de los Mamiferos del Pleistoceno de las Terrazas del Valle del Tajo, en Toledo y Fuentidueña de Tajo". CSIC.

TORRES, T. et al., 1.994 Area "F". Travertinos Lacustres de las Lagunas de Ruidera (Ciudad Real - Albacete).

TORRES, T. et al., 1.994 Area "C". Travertinos Fluviolacustres de Río Blanco (Soria). ETSIMM.

TORRES, T. et al., 1.994 Area "D". Travertinos Lacustres de Banyoles (Gerona). ETSIMM.

TORRES, T. et al., 1.994 Area "E". Travertinos Fluviales de Jorox (Málaga). ETSIMM.

TORRES, T. et al., 1.994 Area "B". Travertinos fluviales de Priego (Cuenca). ETSIMM.

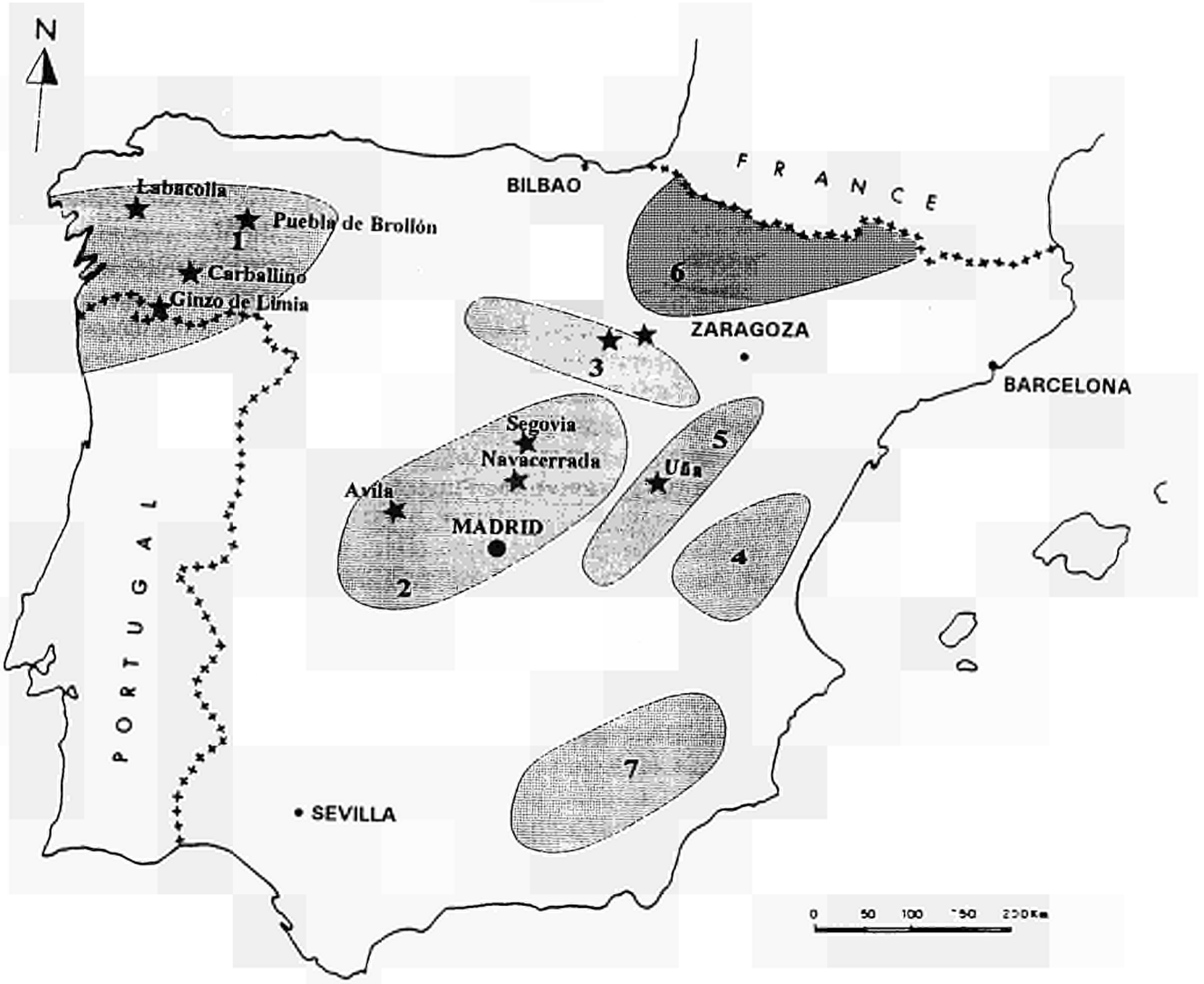

* Weather stations with climatic reconstruction.

Figure 1. **Climatic areas for tree-ring studies. 1. Galicia. 2. Central Range. 3. North-western Iberian Range. 4. South-western Range. 5. Serranía de Cuenca. 6. Western Pyrenees. 7. Eastern Betica Ranges.**

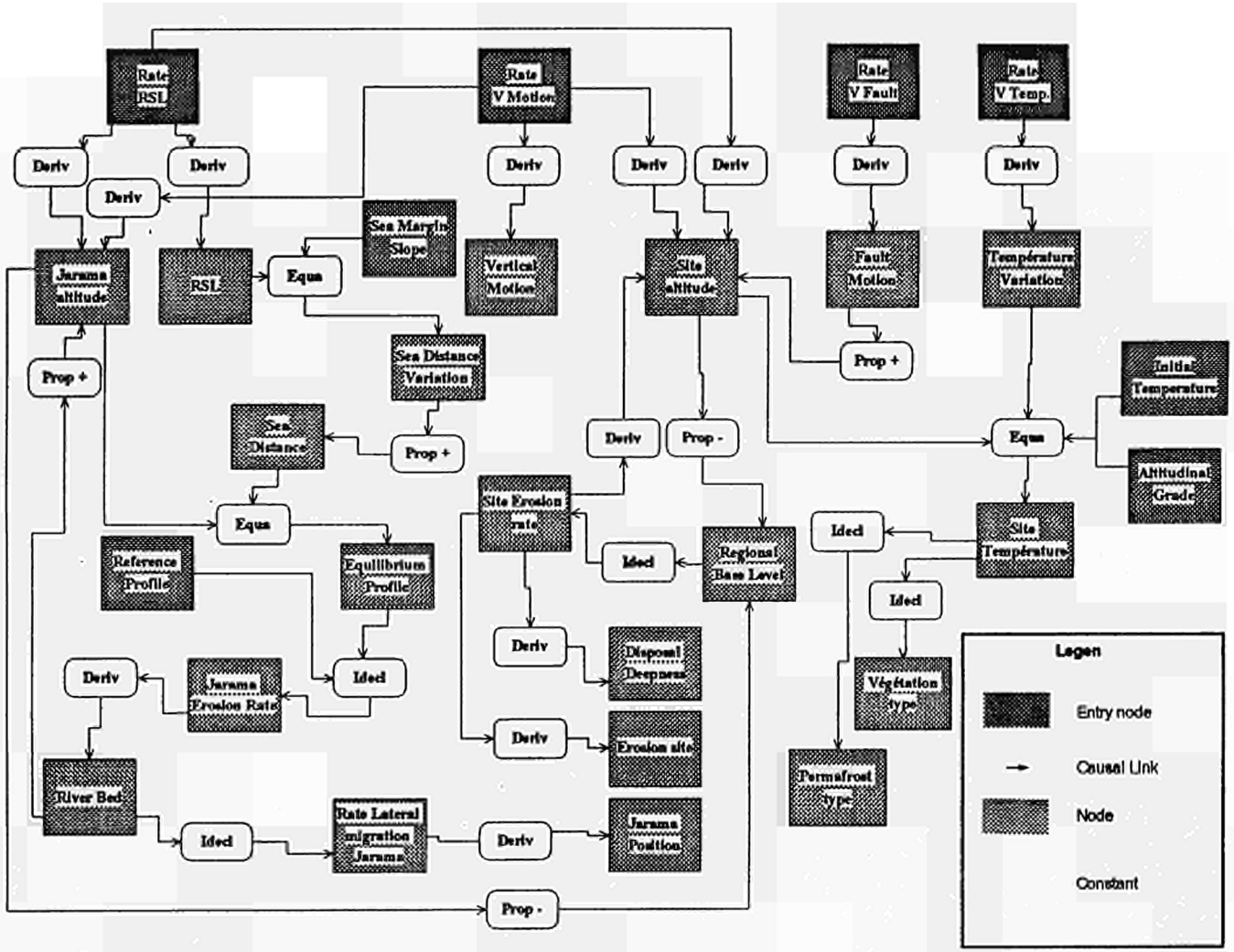

Figure 2. Processes and relationships considered in the paleoenvironmental reconstitution of the Jarama River Site.

5000 AP

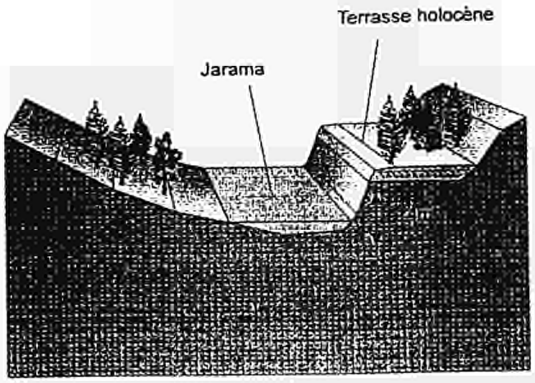

Site temperature about 4.25°C,
taiga type vegetation,
Jarama River bed: 4 m below present level,
0,5 m erosion at site.

37 500 AP

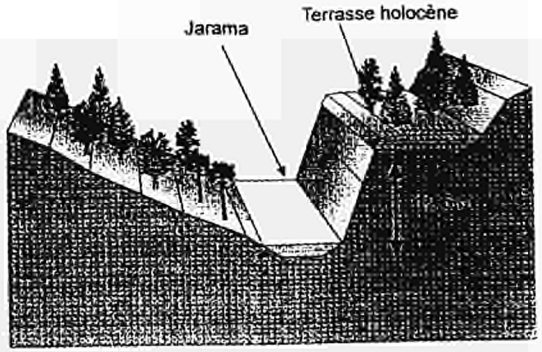

Site temperature 5.5°C,
mixed forest,
Jarama River bed: 12,5 m below present level,
3,9 m erosion at site,
sea level: -75 m.

90 000 AP

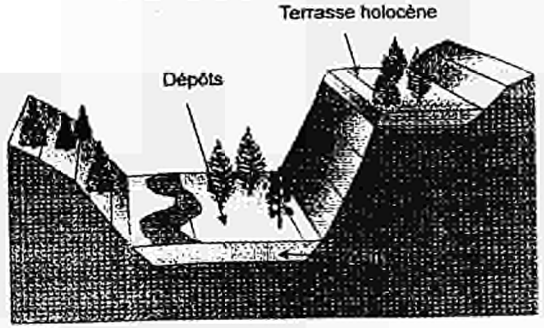

Site temperature 4.7 °C,
taiga type vegetation,
2m sediment accumulation,
Jarama River migrates 70 to 80 m,
sea level: -65 m.

30 000 AP

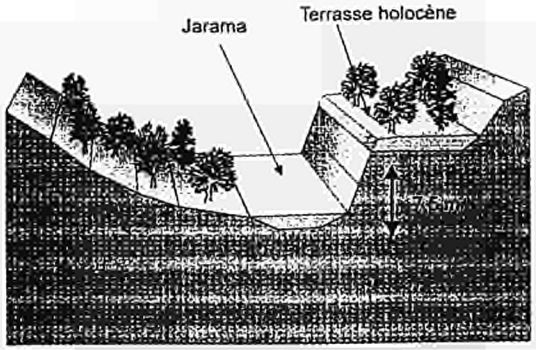

Site temperature about 10.5°C,
subxerophytic vegetation (oaks),
Jarama River bed: 7,5 m below present level,
3 m erosion at site,
Sea level: -70 m.

60 000 AP

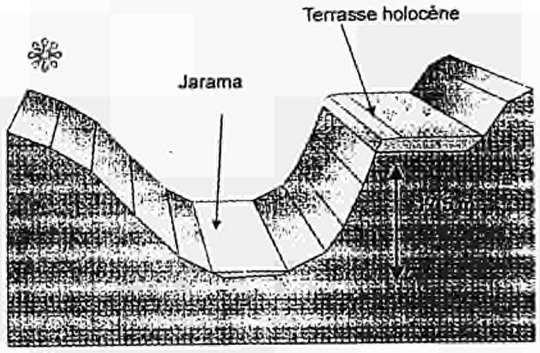

Site temperature -2°C,
tundra type vegetation,
Jarama River bed: 17,5 m below present level,
6 m erosion at site,
Sea level: -150 m.

100 000 AP

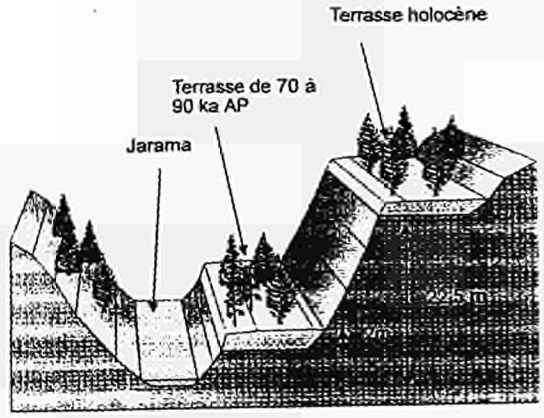

Site temperature 4°C,
Taiga type vegetation,
Jarama River bed: 22,5 m below present level,
10 m erosion at site

Figure 3. Site evolution for the next 100.000 years.

Title :	Geochemical validation of solute residence times : review and comparison for various geological environments
Contractor:	United Kingdom Nirex Limited and NERC.BGS
Contract N°:	FI2W-CT91-0092
Duration of contract:	1 April 1992 - 31 March 1995
Period covered:	
Project leader:	Dr P J Hooker (UK Nirex - Coordinator) Dr R Metcalfe (NERC.BGS)

A. OBJECTIVES AND SCOPE

The scope of the project is to assess the uses of geochemical and isotopic techniques in the estimation of groundwater movements over the long time-scales appropriate to the disposal of radioactive waste in various and "reference hydrogeological environments. The objectives are:

- to compile relevant geochemical data for various European hydrogeological environments from different sources;
- to review the validity of these data under the various hydrogeological and geochemical conditions and their consistency with hydrodynamic information. The review will highlight the contrasts between the geological and hydrological histories of the various European locations (e.g. structure, tectonics, permeabilities, climate etc);
- to assess the concept of "reference" hydrogeological environments to illustrate principles, features and limitations of groundwater residence time estimations;
- to identify specific data needs, "gaps" and uncertainties.

B. WORK PROGRAMME

1. Review of the literature for methods and data for estimating solute and groundwater residence times in various hydrogeological environments.
2. Discussions and collaboration with appropriate European research groups concerned with radioactive waste repository investigations and groundwater tracer techniques.
3. Gaining new data from measurements in European laboratories on samples from (a) investigations being carried out by UK Nirex Ltd., if available, and (b) other appropriate groundwater systems.
4. Reporting on the different stages of work as they are completed. The expected reports comprise two review reports, a progress report on new data and a final report.

C. PROGRESS OF WORK AND OBTAINED RESULTS

The status of progress has not been forwarded to the Commission for 1994.

Title:	DECOVALEX Project: modelling of thermo-hydro-mechanical behaviour for granite rocks
Contractor:	IPSN/CEA
Contract n°:	FI.2W-CT91-0111
Duration of contract:	January 1992 June 1995
Period covered:	January 1994 - December 1994
Project Leader:	J.C. GROS (IPSN)

A. OBJECTIVES AND SCOPE

DECOVALEX (DEvelopment of COupled models and their VALidation against EXperiments in nuclear waste isolation) is an international co-operative research project to support the development of mathematical models of coupled thermal, hydrological and mechanical (THM) processes in hard rocks and their validation against laboratory and field experiments.

This project has launched in 1991 by the Swedish Nuclear Power Inspectorate (SKI), and include nine Funding Organizations representing nine countries and one Funding Party (CEC). The Funding Organizations support fourteen Research Teams working in parallel on three Bench Mark Test and six Test Case problems.

Models and codes are used to study the so-called Bench Mark Test (BMT), and Test Case problems (TC). Bench Mark Tests are defined as theoretical initial-boundary value problems of a generic nature, and Test Cases are laboratory or in situ experiments of part or full aspects of coupled THM processes in hard rocks.

The DECOVALEX Project was started in 1991 and was divided into three phases of one year each.

The Institut de Protection et de Sûreté Nucléaire (IPSN) as Funding Organization and the Commission of the European Community (CEC) as Funding Party, financially supported the research team of the Ecole des Mines de Paris (EMP) to study the following problems:

- Bench-Mark Test 1 (BMT.1) : far-field THM model;
- Test Case 2 (TC.2) : Fanay-Augères THM field test;
- Test Case 6 (TC.6) : borehole injection test.

Results presented in this report concern the Test Case 2 (TC.2), phase III carried out in 1994.

B. WORK PROGRAMME

The Test Case 2 proposed by IPSN, (J.C. Gros, 1992) was to compare the results of 3D computer simulations obtained by different conceptual approaches, (equivalent continuous porous medium, discret and discontinuous approaches) and with those of thermal and mechanical measurements carried out during the Fanay-Augères T.H.M. field test. This test was managed and conducted by the IPSN from 1985 to 1988 in the framework of a shared contract with the Commission of the European Communities (contract n° 127-80-7 WASF, and agreement n° 1).

B.1 Brief description of the Test Case 2

The experimental device was located in granite, at a depth of 100 m. The dimensions of the rock tested were 10 m x 10 m x 5 m,. The fractures network recorded at the surface of the experimental floor is represented in figure 1, (from S. Derlich, 1990). Only the six most conductive fractures represented by thicker lines in figure 1, were taken into account in TC.2.

The thermal experiment was carried out in two phases :

- a 51 days phase of heating to a temperature 80 °C,
- a 74 days phase of cooling until the initial temperature was reached.

The heat source is located at a depth of 3 m from the floor's surface. Total power was 1 000 W, and the upper temperature limit was 80 °C.

Due to the medium's desaturation, the programme of hydraulic measurement initially planned was considerably reduced.

The data of this test case are :
- fractures network of the experimental floor,
- stresses state in rock mass,
- mechanical parameters of rock matrix and some fractures,
- thermal parameters of granite,
- hydraulic parameters of the most conductive fractures,
- chronological account of temperatures in terms of time,
- chronological account of displacements in terms of time.

B.2 Computer codes used

The computer codes used by the various DECOVALEX project teams may be grouped into two categories, according to type of approach :
- codes based on a continuous approach, with or without joints using the Finite Element Method (FEM);
- codes based on a distinct approach, in which the medium is made up of blocks which may be rigid or deformable, and separated by joint-elements simulating the rock's discontinuities, and using the Distinct Element Method (DEM).

The two codes CHALEF 3 D and VIPLEF 3 D used by the IPSN research team, based on the Finite Element Method, were developed by the Ecole des Mines de Paris, (Centre de Géotechnique et d' Exploitation du Sous-sol).

Two basic assumptions were made for these codes :
- all the water flows take place only in the fractures. Flows in the porosity of the blocks are neglected.
- all the heat flows take place only in the blocks

CHALEF 3 D allowed the resolution of heat conduction in steady state and in transient state in 3 dimensions. The principal unknown is the chronological account of the scalar field of temperatures T(x,t). The thermal parameters, (conductivity and specific heat) are function of temperature.

VIPLEF 3 D allowed the calculation of the displacements and stresses occurring at any moments in 3 D structures made up of linear or non-linear elastic, elastoplastic or elastoviscoplastic materials with or whithout instantaneous plasticity.
This code takes into account thermal dilatations, pore pressures and the temperature influence on the rheological characteristics.

C. PROGRESS OF WORK AND OBTAINED RESULTS

State of advancement

As mentioned in the last annual progress report (1993), difficulties occurred for modeling the test case n° 2 by the discrete approach.

The contract is extended by 6 months for completion by 30 June 1995, (supplementary agreement n° 1 to contract n° FI. 2W-CT 91-0111). This agreement is devoted to complete the report of the test case n° 2 (TC.2) and to treat the test case n° 6 (TC.6): borehole injection test.

Progress and results

The final report of the TC.2 was completed in March 1995.

The aim of the study is to compare the simulation of a continuous medium behaviour (A. Rejeb, 1992) with a new simulation of a rock mass crossed by six major fractures which is a more realistic approach.

The modelling of the thermo-mechanical behaviour using a continuous medium was carried out as part of contract between the IPSN and the CEC before the DECOVALEX project,

(contract n° FI.1W/0246-F). The modelling consisted in 2 D and 3 D simulations using CHEF and VIPLEF codes, (A. Rejeb, 1992 ; A. Rejeb & G. Vouille, 1994).

In this new simulation by discrete approach, calculations of temperatures, displacements and stresses were carried out in 3 dimensions by the Finite Element Method (FEM) with CHALEF 3 D and VIPLEF 3 D codes. The main difficulty for the calculations is the tridimensional aspect of the problem which is independent of the resolution method used.

- Realization of the mesh

The mesh of the 3 D model was realized in two stages :
- the mesh of the rock mass (whithout the fractures) was made with the XMAILLE automatic code developed by the Ecole des Mines de Paris , (O. Stab, 1992);
- the tetrahedral mesh including special surfacic elements was used to represent the discontinuities of the medium (joint elements).

The final mesh is made up of 4 739 nodes and 16 771 elements (13 324 tetrahedra for the rock mass and 3 447 triangular joints for the discontinuities).

- Thermal results

For thermal results, heat transfer in the fractured granite was confirmed conform to Fourier's law. As a general rule, the discrete model slightly overestimates the temperatures near to the source, (G. Vouille et al, 1995). Agreement between the calculations and the measurements improved with distance from the heat source.
This observation was indicate by A. Rejeb (1992) in the simulation by a continuous medium, and it would arise from the difference between the thermal parameters of the rock mass and those measured on samples in laboratory which are not representative of the medium.

- Mechanical results

On mechanical point of view, the study has shown clearly that the presence of fractures is in favour to the thermal dilatation of blocks crossed by the 5 heat sources, (Figure 2).
Generally, the introduction of six fractures in the model, allowed better to description (qualitative at least) of the opening and the throw of fractures, (G. Vouille et al., 1995).
The modelling with fractures gives better results than the continuous medium for vertical deformations of the block, between the heat source and the experimental floor surface, (Figure 3).

For the longitudinal and transversal extensometers however, the results of the calculation with the fractures appear more erratic when compared to the experimental results than the calculation with the continuous medium. In fact, the opening of the experimental floor fractures contribute to reduce the extensions measured on the blocks.

The results obtained with the fractured medium shows that this model is unable to take into account the irreversible behaviour of surface extensometers during the cooling phase. This behaviour is due to the chosen model which does not include any irreversibility: in fact, a fracture which has been opened does not support any stress as long as it does not close of the same quantity. This representation is inaccurate to take into account the shear displacement of this fracture which can induce an irreversibility.
This analysis cannot explain some aspects of the fractures mechanical behaviour. So, a parametric analysis would allow to know these mechanical behaviours.

A comparison between various approaches, (continuous, continuous with special joint-element, discontinuous), and experimental results of the Fanay-Augères T.H.M. field test will be begun in 1995.

REFERENCES

DERLICH S. (1990): Etude des possibilités de stockage dans les formations géologiques: l'expérience Thermo-Hydro-Mécanique (T.H.M.) - Rapport final, (contrat CCE n° 127-80-7 WASF, et avenant n° 1), Sciences et Techniques Nucléaires, EUR 13 115 FR.

GROS J.C. (1992): DECOVALEX - Phase III / Test Case 2: Fanay-Augères T.H.M. Field Test. Rapport SERGD n° 92/43.

REJEB A. (1992): Comportement thermomécanique du granite - Application au stockage des déchets radioactifs. Thèse de Doctorat de l' Ecole des Mines de Paris, 23/06/1992.

REJEB A., VOUILLE G. (1994): Expérience Thermo-Hydro-Mécanique de Fanay-Tenelles. Interprétation des résultats expérimentaux et validation de modèles thermomécaniques - Rapport final, (contrat CCE n° FI.1W/0246), Sciences et Techniques Nucléaires, EUR 14 962 FR.

STAB O., (1992): Maillage automatique tridimensionnel par opérations booléennes. Thèse de Doctorat de l' Ecole des Mines de Paris, décembre 1992.

VOUILLE G., TIJANI S.M., HUMBERT B., (1995): Projet DECOVALEX - Test Case n° 2. Modélisation thermomécanique tridimensionnelle de l'expérience T.H.M. de Fanay-Augères, Ecole des Mines de Paris (CGES) - Rapport 10.02.95.RR.01, (Rapport interne).

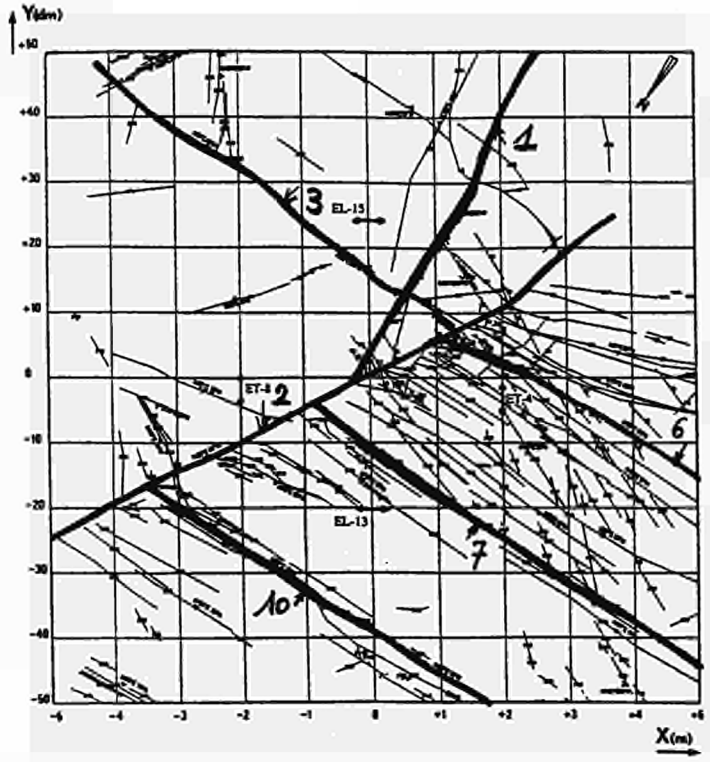

Figure 1: Test Case 2 - Network of fractures at the surface of the experimental floor (only the six fractures drawn in thicker lines were used in the model, (from S. Derlich, 1990)

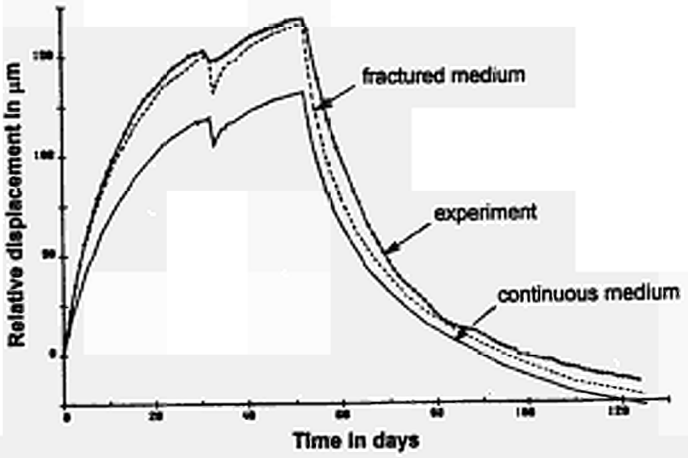

Figure 2: Comparison between calculations and extensometer EF-13 measurements in borehole F.1, at 1 m from the heat source, (from G. Vouille et al, 1995)

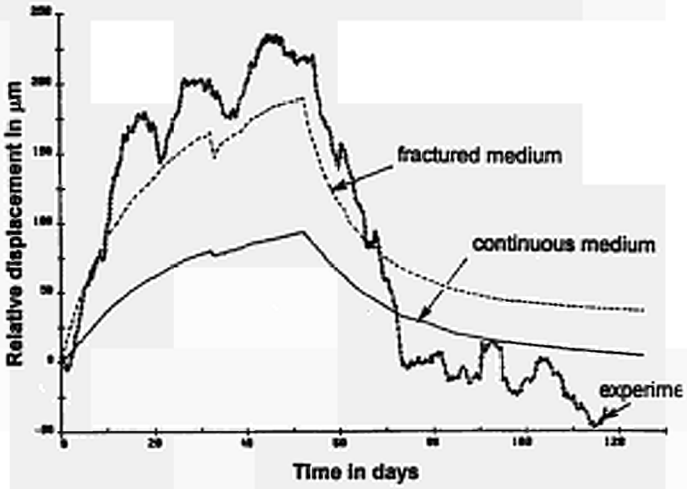

Figure 3: Comparison between calculations and laser V cell n° 4, at the surface of the experimental floor, (from G. Vouille et al., 1995)

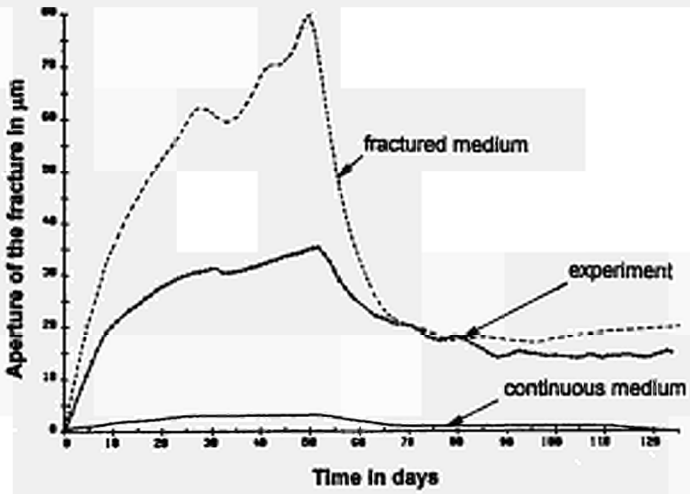

Figure 4: Comparison between calculations and extensometer EF-1 on the major fracture n° 1, (from G. Vouille et al., 1995)

Title	Participation to the International cooperative project for the DEvelopment of COupled models and their VALidation against EXperiments in nuclear waste isolation - "DECOVALEX"
Contractors	(1) Agence Nationale pour la gestion des Déchets RAdioactifs (ANDRA) - France (2) Commissariat à l'Energie Atomique (CEA) Direction des réacteurs Nucléaires - Département de Mécanique et Technologie - Service d'Etudes Mécaniques et Thermiques - France (3) INERIS Groupe Géotechnique et Atmosphère Industrielle - Laboratoire de Mécanique des Terrains - Ecole des Mines de Nancy - France (4) United Kingdom Atomic Energy Authority (AEA) Theorical Studies Department - AEA Decommissioning and Radwaste - Harwell Laboratories - United Kingdom
Contract N°	FI2W-CT91-0113
Duration of contract	October 1991 - September 1994
Period covered	1994
Project leader	F. PLAS (ANDRA: coordinator), M. DURIN (CEA), H. BAROUDI (INERIS), A.H. HERBERT (AEA D&R)

A/OBJECTIVES AND SCOPE

Hydro-Thermo-Mechanical processes in jointed rock is very difficult task to treat but may be of importance in nuclear waste performance assessment. This called for an international cooperation in peer review for code developers, to develop a data base and to provide bench-mark tests and test cases of THM processes. DECOVALEX was initiated by the Royal Institut of Technology of Stockholm (KTH) and the Swedish Nuclear Power Inspectorate (SKI) as an international coordinated project for three years (1991-1994) dealing with the study of coupled hydro-thermo-mechanical modeling processes in fracturated rock and associated computer codes /1//2/. The objectives of DECOVALEX are listed below:

- To support the development of codes for THM modeling.
- To investigate and apply suitable algorithmes for THM modeling.
- To investigate the capabilities of different codes to describe recent laboratory experiments and to perform code verification.
- To compare theory and model calculations with results on recent field experiments.

The aim of the CEC contract FI2W-CT-91-113 is the participation of European research teams to the international DECOVALEX project. In order to increase the understanding of the various coupled THM processes in fractured hard rocks, three laboratories developing specific modeling concept are collaborating for this contract with the coordination of ANDRA:

- **CEA/DMT** using the **equivalent porous media** modeling concept with **CASTEM/TRIO codes,**
- **INERIS** using the **discrete block network** modeling approach with **UDEC and 3DEC code,**
- **AEA D&R** using the **discrete fracture network** modeling approach with **NAPSAC code.**

B. WORK PROGRAM

The DECOVALEX programme is developped according to three main phases:

Phase I : October 1991 to # March 1993
Phase II : # March 1993 to October 1993
Phase III : November 1993 to October 1994

Bench Mark Tests and Test Cases were defined for each phase as shown in the table 1 and table 2 /3//4//5//6//7/. The contributions of the CEA/DMT, INERIS and AEA R&D are indicated in the table 3.

Problem	Physical Processes
BMT1	Coupled T-H-M processes in fractured rocks with two orthogonal sets of persistent fractures. Domain size 3000 x 1000 m, 2-D far-field problem
BMT2	Coupled T-H-M processes in fractured rocks with four discrete fractures. Domain size 0.75 x 0.5 m, 2-D near-field problem
BMT3	Coupled T-H-M processes in fractured rocks with a realistic fracture network from Stripa Mineof 6580 fractures, Domain size 50 x 50 m, 2-D near-field problem
TC1	Coupled shear - flow test of a single rock joint, 2-D problem.
TC1:2	Same set up as TC1 with different joint properties
TC2	Fanay-Augères (France) experiment of coupled T-H-M processes in fractured rocks; 3-D problem. Domain size 10 x 10 x 5 m
TC3	Large scale experiment (Big-Ben) of coupled T-H-M processes in engineered buffer materials
TC4	Triaxial experiment of coupled normal stress-flow processes
TC5	Coupled shear-flow experiments of a single rock joint on a direct shear machine, 2-D problem
TC6	In situ Borehole injection experiment at 150 m depth in fractured rock

Table 1 - Physical processes in BMT and TC problem of the DECOVALEX project

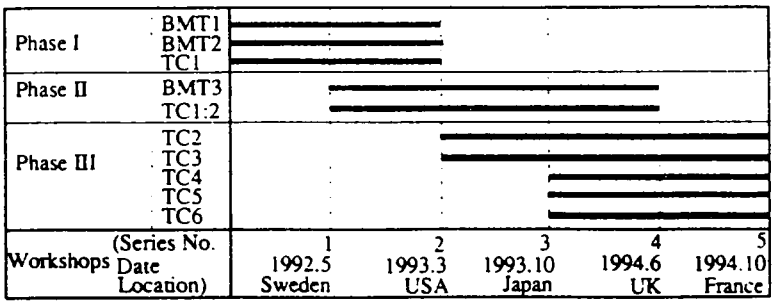

Table 2 - Phases of DECOVALEX project, BMT and TC problems and workshop series

Research teams	DECOVALEX exercices
CEA/DMT	**BMT1 - BMT3**
INERIS	**BMT1 - TC1 - BMT3 - TC2**
AEA R&D	**BMT3**

Table 3 - DECOVALEX BMT and TC problems treated by CEA/DMT, INERIS and AEA R&D

C. PROGRESS OF THE WORK AND OBTAINED RESULTS

State of advancement

As planned, the main activities of the research teams were focussed on the problems of the DECOVALEX phase III and/or the synthesis of the problems of the DECOVALEX phases II and I /2//8/. So CEA/DMT mainly worked on a synthesis of the BMT1 and finished the modeling of the BMT3 that was already gone forward in 1993. The participation of INERIS to the BMT3 was closed in 1993: it was impossible to model the thermal sequence with UDEC because of the high Hydro-mechanical coupling. So INERIS decided to model the TC2 "Fanay Augères". AEA R&D finished its works on the BMT3 and began a synthesis of this problem.

Two workshops were taking place in 1994: the 4th one on June at Oxford /7//10/, hosted by NIREX and the 5th one on October at Paris, hosted by ANDRA /9//11/. This 5th DECOVALEX workshop can be considered as the end of DECOVALEX for the research teams. However it was decided to publish the overall works and results of DECOVALEX in a special book (Elsevier Editions). That's why the research teams will be mobilised as authors or contributors of the different book chapters, until mid-1995.

The possible continuation of the DECOVALEX project was also discussed at Paris. Two main projects were presented: the first one proposed by PNC concerns a T-H-M test in Kamaishi mine, the second one proposed by NIREX concerns the modelling of the Hydro-mechanical response of the geological media during the excavation of the access shaft of the futur Sellafield underground laboratory. Two task force groups were created in order to evaluate each proposal. Their conclusions will be discussed during the last DECOVALEX steering Committee in march at Washington (USA) hosted by NRC.

Progress and results

CEA/DMT performed a synthesis of the BMT1 /12//13/ called " Discrete and Continuum approaches to simulate the thermo-hydro-mechanical couplings in a large fractured rock mass". The following general conclusions can be drawn :

- Provided meshes are fine enough temperature fields are well predicted by all the research teams.

- There is a reasonable agreement between discrete and discontinuum approaches on the overall displacement and stress fields (figure 1). The continuum method leads to lower stress variations. The patterns of the local deformation in the zone located above the repository, are rather different for the two identical approches. This cause significant differences on joints opening profiles. For the continuum approaches, this fact can be partly explained by the non linear material models used for the equivalent medium.

- The hydraulical results (heads and flux) are very different, both quantitatively and qualitatively (figure 2). The disagreements seem to decrease with the distance from the repository. The origin should not be the type of approach but the highly non-linear flow laws used by both continuum approach and discontinuum approach.

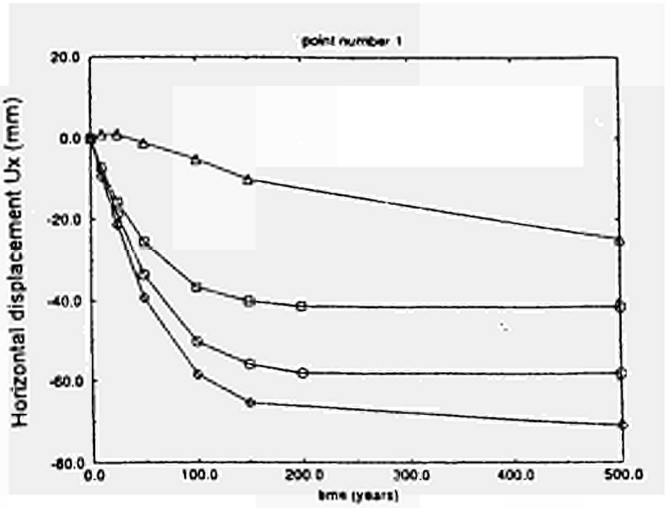

Figure 1 - BMT1: Comparison of the horizontal Displacement at point 1

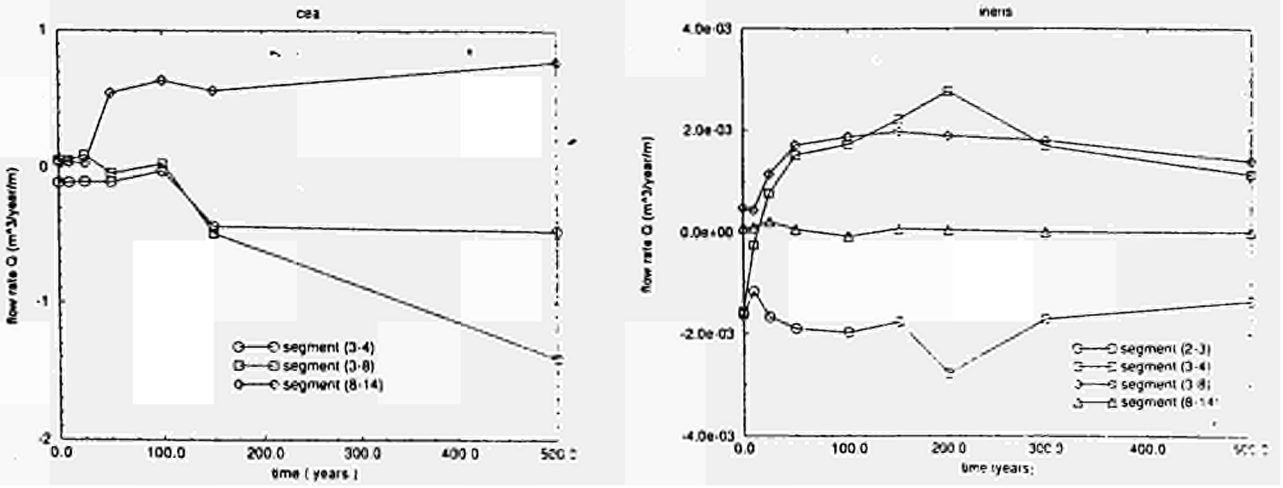

Figure 2 - BMT1 : Flow rates across segments (2-3), (3-4), (3-8), (8-14) obtained by INERIS and CEA

INERIS perfomed the TC2 "Fanay Augères THM test" with the 3DEC code. Simplifications of the fracture set were needed: six fractures and three fractured zones were distinguished (figure 3). The main conclusions of the modelling are the following:

- With 3DEC the temperatures are calculated by using an analytical solution. This cause an importante overestimation of the temperatures near the thermal source. Then a difference of 3°celsius is found on the floor because the thermal convection with the air of the chamber isn't taken into account.

- The deformations obtained with 3DEC are qualitatively in agreement with the experimental results (figure 4). But quantitatively the results of 3DEC are overestimated or underestimated; The main reasons seem to be :

- Overestimation of the thermal field near the thermal source
- Overestimation of the mechanical properties of the different fractured zones due to the simplification
- Underestimation of the (normal or tangential) stiffness modulus of some fractures.

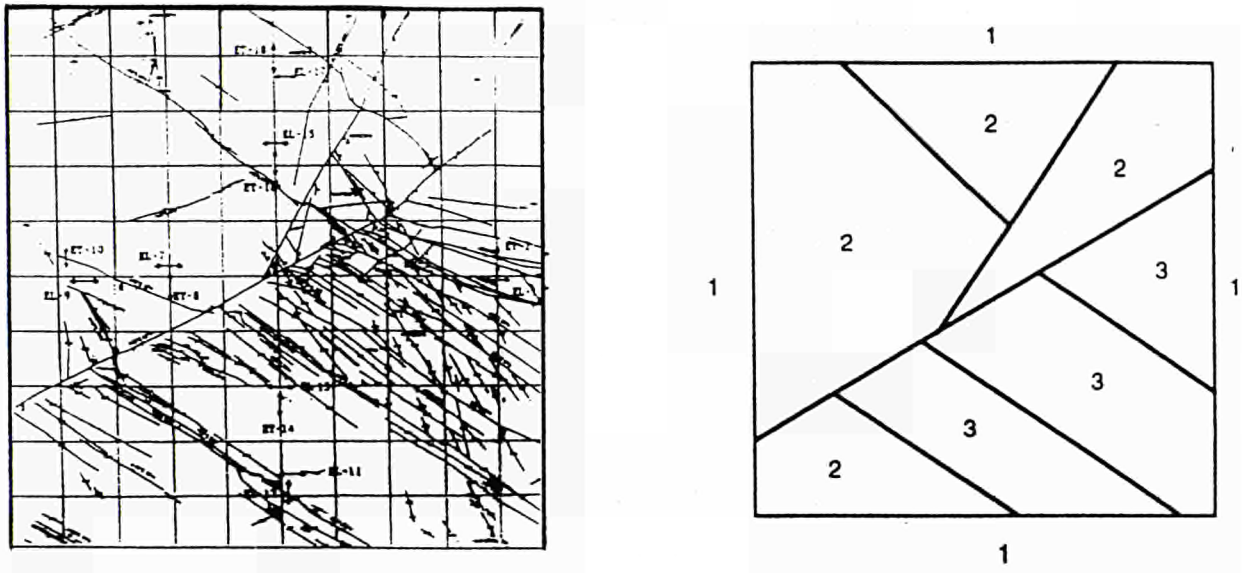

initial fracture network

Simplified fracture network

Figure 3 - TC2 : fracture network used by INERIS

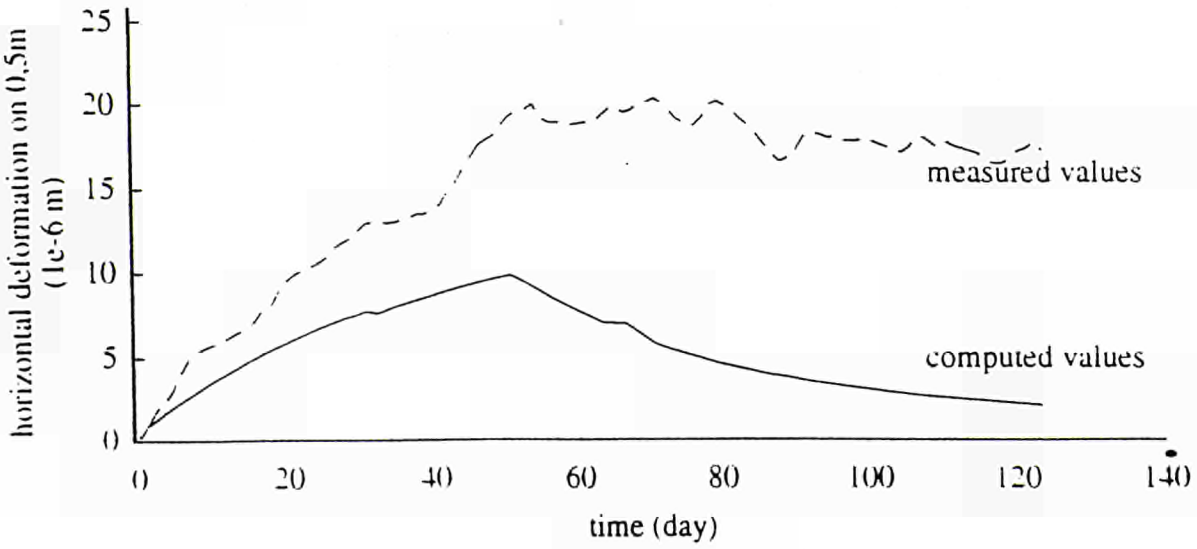

Figure 4 - TC2 : Comparison modelling-experiment of the electrical surface extensometer EL11

The modeling of the BMT3 was performed by 8 research teams (table 4).

	CEA/DMT	KHP	ITASCA	CNWRA	INERIS	NGI	VTT	AEA
Code	CASTEM TRIO	THAMES	FLAC	UDEC	UDEC	UDEC	UDEC	NAPSAC
Coupling	T > > H,M M > > H	Fully coupled	T > > M M< > H	T> >H,M M> >H	T> >H,M M> >H	T> >H,M M> >H	T> >H,M M> >H	H M> >H

Table 4 - Research teams involved in the BMT3

The main conclusions of the comparison are following:

- The agreement on the thermal field is good.The agreement is also fairly good for the displacement, considering the array of different approaches. By the way, the agreement on the stresses may also be considered as acceptable. The differents occur in the hydraulical field (head and flux) as shown on figure 5. The cause is supposed to be a combination of the approach and the use of highly non-linear hydro-mechanical laws but the problem is still opened.

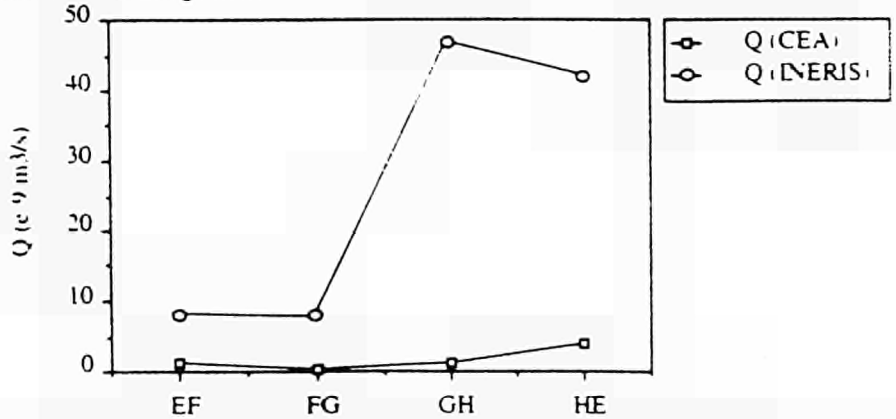

Figure 5 - Comparizon of the CEA and INERIS water flux across different sections at time t = 1 during the sequence 3

- The homogeneization schemes used for BMT3 are very different and result in different REVs and tensors of strain and permeability. The existance of a REV and its relation with the size of mesh have not been resolved. A possible solution proposed with UDEC is to use a mixed scheme in which an inner, small scale region containing the tunnel and the heat source, is modelised by a discrete approach with an explicit representation of fractures, surrounded by a continuum media. The key problem is to ensure the continuity of the hydro-mechanical fields at the interface.

For the nuclear waste management (performance assessment, safety assessment), one of the practical problems is to define what is acceptable in terms of mechanic and hydraulic, also taking into account the capability to discribe the fracture set and to evaluate its hydro-mechanical properties.

- The specific difficulties of the discontinuum approaches are first to collecte the overall data on the fracture set (distribution, geometry, aperture, hydro-mechanical properties) and second the limitation by the required computer time and storage capacity that increase dramatically with increase of fracture number and domain size.

List of references

/1/ DECOVALEX Memorandum - 1st meeting of Steering Committee at Hotel Mercure, Paris, France - October 28, 1991.

/2/ DECOVALEX - Mathematical Models of Coupled T-H-M Processes for Nuclear Waste Repositories - Report of Phase I -
L. Jing, J. Rutqvist, O. Stephansson, C-F. Tsang, F. Kautsky
SKI Technical Report 93:31

/3/ DECOVALEX Memorandum - 3rd meeting of Steering Committee at Laurence Berkeley Laboratory,San Francisco, USA - March 10, 1993

/4/ DECOVALEX Memorandum - 4st meeting of Steering Committee at PNC Head Office, Tokio, Japan - October 29, 1993

/5/ DECOVALEX Memorandum - 2nd workshop at Laurence Berkeley Laboratory, San Francisco, USA - March 8-10, 1993

/6/ DECOVALEX Memorandum - 3rd workshop at PNC Tokai Works, Mito, Japan - October 26-28, 1993

/7/ DECOVALEX Memorandum - 4th workshop, Oxford May 30 - June 1 , 1994, hosted by MIREX, United Kingdom

/8/ DECOVALEX - Mathematical Models of Coupled T-H-M Processes for Nuclear Waste Repositories - Report of Phase II -
L. Jing, J. Rutqvist, O. Stephansson, C-F. Tsang, F. Kautsky
SKI Technical Report 94:16

/9/ DECOVALEX Memorandum - 5th workshop, Paris October 17 - 20, 1994, Hosted by ANDRA at INSTM, France

/10/ DECOVALEX Memorandum - 5st meeting of Steering Committee at NIREX Head Office, Oxford, United Kingdom - June 2, 1994

/11/ DECOVALEX Memorandum - 6st meeting of Steering Committee at ANDRA Head Office, Fontenay Aux Roses, France - October 21, 1994

/12/ DECOVALEX - 2nd Progress Report - CEC Contract n°FI2W-CT91-113, Rapport ANDRA 694 RP AND 92.003, May 1993

/13/ DECOVALEX - 3rd Progress Report - CEC Contract n°FI2W-CT91-113, October 1993

Title	Underground laboratory at Tournemire : groundwater flow tests in clayish material
Contractors	CEA/IPSN
Contract N°	FI2W-CT91-0115
Duration of contract	January 1992 - December 1995
Period covered	January - December 1994
Project leader	Jean-Yves BOISSON

A. OBJECTIVES AND SCOPE

In the framework of its research programme concerning the safety studies of waste geological disposal, the French Institut de Protection et de Sûtreté Nucléaire (CEA/IPSN) is developing in situ researches concerning the confining properties of geological formations. IPSN is studying at the Tournemire site, a geological formation constituted by indurated claystones of Toarcian (upper Lias). This site has been selected because of its geological simplicity and also because a former railway tunnel gives access to the centre of the Toarcian formation. This tunnel crosses a 200 m thick toarcian clay formation; the overlying limestone layers are 270 meters thick, so the geotechnical and hydrogeological conditions can be considered as representative of those of a deep repository.

The research program concerns hydrogeological properties of clay in order to determine the characteristics of fluid transfers through the clay formation and more particularly, it intends to develop new methods for the investigation of very low permeability medium and to perform modelling of fluids transfers.

B. WORK PROGRAMME

The Tournemire program includes:

- General geological and hydrogeological investigations of the site;
- Drilling operations in the tunnel for geological purposes, in situ hydrogeological testing and sampling of material for laboratory studies
- Detailed geological studies, including important structural studies relative to paleohydrogeological understanding;
- Development of long term in situ hydrogeological testing;
- Laboratory studies of core samples for petrophysic identifications, diffusive properties, different fluid potentials and associated fluxes measurements;
- Development of important isotopic studies of the intestitial fluid and solid phase (matrix and fractures);
- Modelling of fluid transfers through the argillaceous material.

C. PROGRESS OF WORK AND OBTAINED RESULTS

State of advancement

Six boreholes were drilled from the tunnel to the bottom and to the top of the Toarcian formation. These works have allow to get a very good knowledge of the geological environment around the tunnel.

In addition to analysis formerly performed to reach a better characterisation of such media, cores produced by two of these boreholes were sampled to study the isotopic contents of the pore water. Due to the very low water content (1 to 3% wt) of the rock and to its high degree of induration. it was impossible to utilise squeezing technique for the extraction of water. Thus, water was recovered by distillation under vacuum to measure its stable isotope contents.

Taking into account that transfers into this formation, if they exist, should be essentially diffusive, it has been necessary to precise the characteristics values of diffusion coefficients from these argilites. With this respect, mass transfer studies of deminaralized water through two types of clay sample taken from the CD borehole of the Tournemire site have been carried out.

A new research programme thanks to detailed laboratory studies aiming to a better understanding of fluids transfers through these formations of the agilites Tournemire type has been developed in 1994. The first stage of this programme was a coring campaign of height boreholes from the tunnel so as to provide excellent quality samples. This has been performed for this purpose and has been achieved at the end of 1994.

Progress and results

C.1 Isotopic studies from interstitial pore water

Four types of pore water can be distinguished from their stable isotope contents (^{18}Oet ^{2}H) : (i) meteoric water which is isotopically similar to that of the overlying aalenian karstic aquifer, (ii) meteoric water whose isotope contents are modified, probably due to exchange with host rock, (iii) water enriched in heavy isotopes possibly due to an evaporation processes close to the tunnel and, (iv) water rich in heavy isotopes which could contain a part of residual connate water. With the exception of the third type, whose occurrence seems caused by the presence of the tunnel, these water types seem "randomly" distributed with depth. This "randomly" distribution could be probably controlled by variations of the accessibility to rock porosity. This point has to be clarified.

C.2 Isotopic studies from calcite filling in fractures

In addition to the study on pore water, isotopic measurements were made on the secondary calcite that filled the fractures crossed by the boreholes. Variations of the stable isotopes contents (^{13}C and ^{18}O) of these calcite cannot be explained by temperature effects only. They imply that several different types of water have circulated in the fractures. A hypothesis to explain the distributions with

depth of ^{13}C and Iron contents in fracture minerals would involve both upward and downward circulation.

All the secondary calcite are ^{14}C free. Their $^{234}U/^{238}U$ ratio are close to one, but they mostly reflect the contribution of a detrital fraction and cannot be used to estimate the age of the calcite. However, the very high $^{230}Th/^{234}U$ ratio measured on a sample taken at the bottom of the profile, probably indicates a secondary sink of ^{234}U. This suggest that water circulation would have occurred in the fractures at the lower part of the toarcian formation, more recently than 300 000 years ago.

C.3 Characterisation of diffusive transfers at laboratory

These studies have allow the characterisation of diffusive transfers, and those under an hydraulic head of 1,5 MPa (15 bars) applied at the upper part of the sample, which have been submitted before to an axial mechanical stress of 4,7 Mpa. Two kinds of sample have been studied : sample coming from the upper Toracian (argilite with low content of $CaCO_3$), and sample from the mean Toarcian (argilite with high $CaCO_3$ content).

After 90 days of diffusion tests with demineralized tritiated water, experimental curves give the following results :

- for sample ($10,6.10^{-3} \leq$ thickness $\leq 10,7.\ 10^{-3}$ m) from upper Toarcien :
  - $3,06.\ 10^{-12} \leq$ diffusion coefficient De $\leq 4,07\ 10^{-12}$ m^2/s
  - $2,10.\ 10^{-5} <$ flux in steady state Qd $\leq 3,26.\ 10^{-5}$ m^3.m^{-2}/day
  - $9,6 <$ porosity $\leq 10,2$ %
- for sample ($10,6.\ 10^{-3} \leq$ thickness $\leq 11,0.\ 10^{-3}$ m) from mean Toarcien :
  - $3,10.\ 10^{-12} \leq$ diffusion coefficient De $\leq 3,39.\ 10^{-12}$ m^2/s
  - $2,50.\ 10^{-5} <$ flux in steady state Qd $\leq 2,63.\ 10^{-5}$ m^3.m^{-2}/day
  - $8,5 \leq$ porosity $< 9,3$ %

After 60 days of permeation tests with demineralized tritiated water (hydraulic head of 1,5 MPa), following the diffusion tests, experimental curves give the following results :

- for sample ($10,6.10^{-3} \leq$ thickness $\leq 10,7.\ 10^{-3}$ m) from upper Toarcien :
  - $1,89.\ 10^{-14} \leq$ permeation coefficient $K_p \leq 3,37.\ 10^{-14}$ m/s
  - $2,27.\ 10^{-5} \leq$ flux in steady state Qp $\leq 4,12.\ 10^{-5}$ m^3.m^{-2}/jour
  - $1,40.\ 10^{-15} \leq$ permeability coefficient K $\leq 1,05.\ 10^{-15}$ m/s
- for sample ($10,6.\ 10^{-3} \leq$ thickness $\leq 11,0.\ 10^{-3}$ m) from mean Toarcien :
  - $2,16.\ 10^{-14} \leq$ permeation coefficient $K_p \leq 3,33.\ 10^{-14}$ m/s
  - $2,63.\ 10^{-5} \leq$ flux in steady state Qp $\leq 3,93.\ 10^{-5}$ m^3.m^{-2}/jour
  - $8,49.\ 10^{-15} \leq$ permeability coefficient K $\leq 1,06.\ 10^{-15}$ m/s

These results show clearly that towards demineralized water transfer via diffusion or permeation, there is no very significative difference in the physical behaviour between sample from mean torcian and upper torcian.

Moreover, tests performed with hydraulic head (1,5 Mpa) show that water or humidity transfers are essentially diffusive (cf figure 1).

C.4 New fluid transfers research programme

A new research programme aiming to a better understanding of fluids transfers through these formations of the agilites Tournemire type has been developed in 1994. It consists of :

- a programme of fundamental studies and laboratory measurements for a complete characterisation of the material about its possibility of fluid transfer (diffusive transfer, different water potentials (chemical, suction...)) into the clay;
- a wide isotopic measurement programme on the whole formation surrounding the tunnel (natural isotopes, new technics for the fluid phase extraction, great amount of sample to characterise transfers both at the geological time scale and at the time scale corresponding to the perturbation due to the presence of the tunnel itself);
- development of long time hydraulic tests into boreholes, specifically conceived for the case of clay rocks of very low permeability.

The two first points suppose the obtention of a very precise and high quality sampling phase of the formation all around the tunnel. A coring campaign of height boreholes from the tunnel have been performed for this purpose and have been achieved at the end of 1994. The characteristics and position of these boreholes around the tunnel can be seen on the figure 2. It also indicates the importance of the sampling network for laboratory investigations.

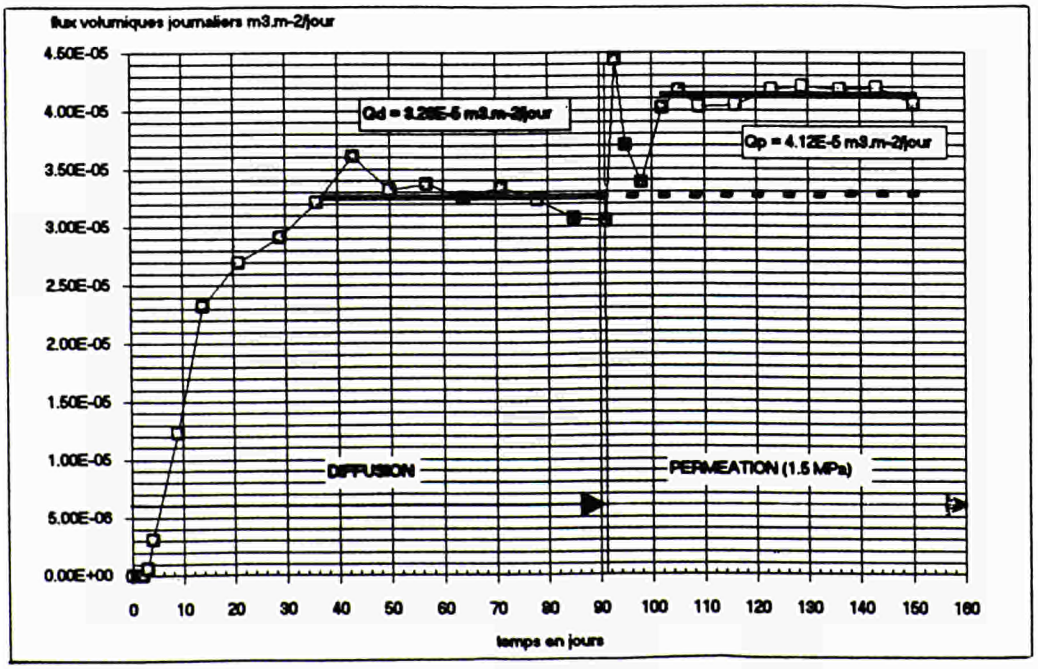

figure 1 : volumic fluxes per day through Tournemire argilite (sample n° 7A)

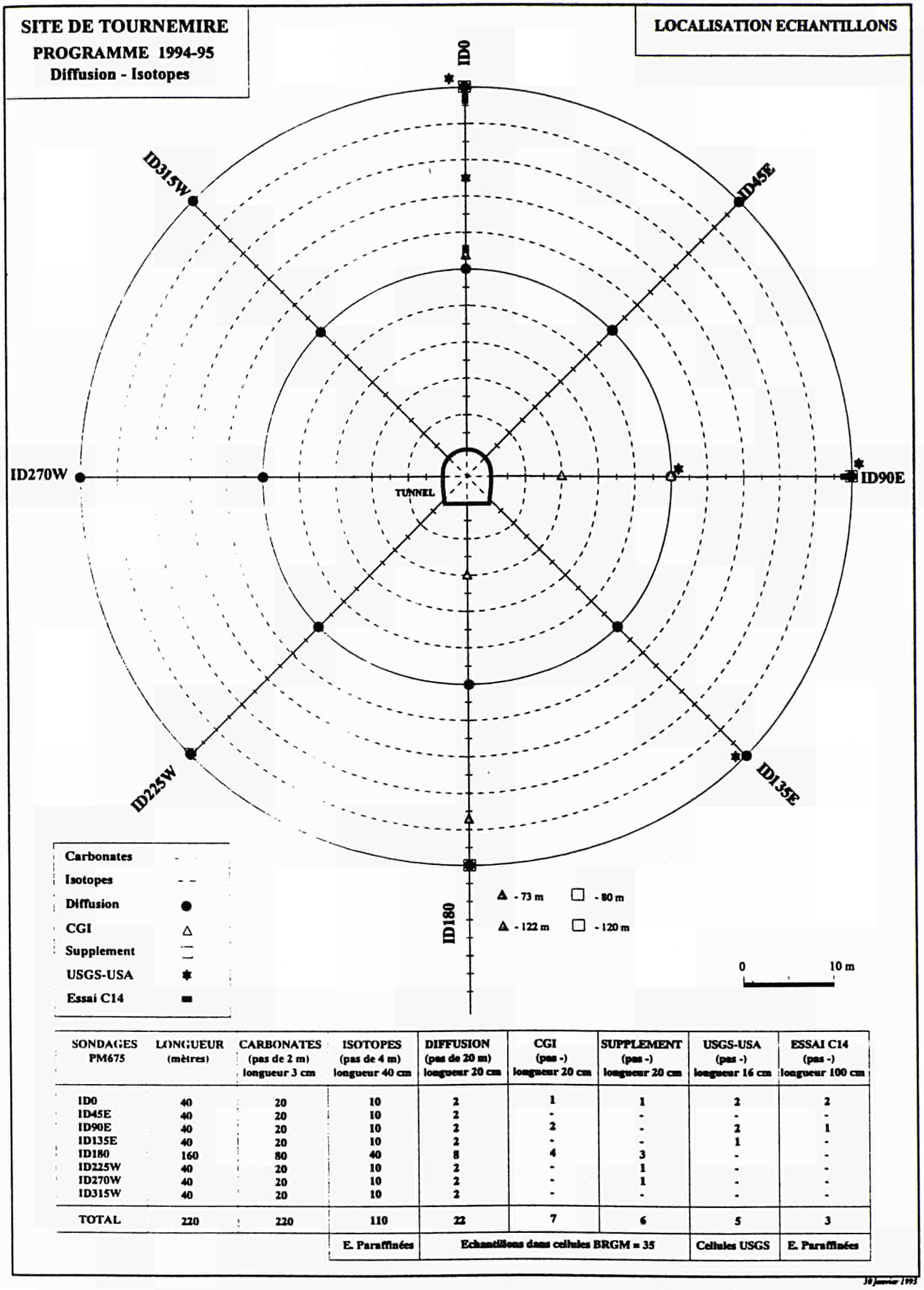

SONDAGES PM675	LONGUEUR (mètres)	CARBONATES (pas de 2 m) longueur 3 cm	ISOTOPES (pas de 4 m) longueur 40 cm	DIFFUSION (pas de 20 m) longueur 20 cm	CGI (pas -) longueur 20 cm	SUPPLEMENT (pas -) longueur 20 cm	USGS-USA (pas -) longueur 16 cm	ESSAI C14 (pas -) longueur 100 cm
ID0	40	20	10	2	1	1	2	2
ID45E	40	20	10	2	-	-	-	-
ID90E	40	20	10	2	2	-	2	1
ID135E	40	20	10	2	-	-	1	-
ID180	160	80	40	8	4	3	-	-
ID225W	40	20	10	2	-	1	-	-
ID270W	40	20	10	2	-	1	-	-
ID315W	40	20	10	2	-	-	-	-
TOTAL	220	220	110	22	7	6	5	3
			E. Paraffinées	Echantillons dans cellules BRGM = 35			Cellules USGS	E. Paraffinées

30 Janvier 1995

figure 2 : New fluid transfers research programme : boreholes configuration around the tunnel and samples localisation

Title	Development of borehole seals for high-level radioactive waste (The Debora-project)
Contractors	GSF-Institut für Tieflagerung (IfT), Braunschweig, Germany Stichting Energieonderzoek Centrum Nederland (ECN), Petten, The Netherlands
Contract N°	FI2W-CT90-0048
Duration of contract	January 1991 - December 1994
Period covered	January 1994 - December 1994
Project leader	T. Rothfuchs, J. Prij

A. OBJECTIVES AND SCOPE

The overall objective of a nuclear repository is to protect man and his environment against ionizing radiation from radioactive waste emplaced in this underground repository.

According to section 45 of the German Radiation Protection Ordinance the individual dose to man, caused by radionuclides passing out of the repository, is to be limited to 0.3 mSv/year. In order to achieve this objective within the multiple barrier system of the repository, suitable sealing systems like borehole seals, drift seals and shaft seals are to be developed.

The objective of the DEBORA-project is the "Development of Borehole Seals for High-Level Radioactive Waste".

The DEBORA-project consists of two phases. During the first phase (1991 - 1994) a test plan for a subsequent in situ verification test will be developed in form of a desk study. This study will include an evaluation of literature, a performance of model calculations, and discussions of experts to identify the requirements for and the tasks of HAW-borehole seals under normal repository conditions. Altered repository conditions will be considered at a later stage of the project.

During the second phase, to be started in 1995, in situ tests will be performed and the sealing techniques elaborated during the first phase will be verified.

B. WORK PROGRAMME

B.1 Compilation of the technical boundary conditions important for the design of HAW-borehole seals
B.2 Definition of the tasks of HAW-borehole seals
B.3 Analysis of events affecting the design of the borehole seal
B.4 Performance of model calculations
B.5 Elaboration of sealing techniques
B.6 Development of an in situ test plan

C. PROGRESS OF WORK AND OBTAINED RESULTS

State of advancement

After the completion of items 1 and 2 of the work programme (see APR 1991 and APR 1992) emphasis was given to the analysis of events affecting the design of HAW borehole seals. This work comprises the evaluation of literature and, as far as possible, the performance of model calculations in order to estimate the conditions of state in and around borehole seals. In this regard fluids which will be released into the borehole and their generation mechanisms have been summarized. Corrosion of steel as packaging material has been studied in the literature and the amount of hydrogen resulting from corrosion and from radiolysis of released fluids have been estimated in order to obtain input data for the calculation of the borehole gas pressure.

Concerning the elaboration of sealing techniques (item 5) literature studies were performed in regard of the selection of suitable sealing materials.

Progress and results

1. Compilation of the technical boundary conditions important for the design of HAW-borehole seals

A compilation of the technical boundary conditions was already reported in (GSF-ECN, 1992). According to the german disposal concept data about the geometrical arrangement of a HAW repository and about the waste canisters were compiled.

2. Definition of the tasks of HAW-borehole seals

The work performed in this regard consisted in a review and compilation of legal requirements to be considered inside and outside a nuclear repository. The respective information was reported in (GSF-ECN, 1992).

3. Analysis of events affecting the design of the borehole seal

In the past years the importance of the waste emplacement tempo, the release of fluids from the rock mass and the generation of fluids by corrosion of the waste canisters and by radiolysis of fluids was analysed.

Furthermore, different materials have been analyzed in regard of their suitability as sealing materials. Crushed salt was identified as the most suitable sealing material.

Crushed salt will not only be used to seal the borehole but it is also used in the annulus between the canister stack and the borehole wall for the required distribution of the canister weight loads. In this sense the borehole will be sealed in the annulus as well as in the empty space above the canister stack, the borehole seal region.

The initial permeability of crushed salt is high (ca. 10^{-12} m^2) but as a consequence of the thermally induced salt convergence it finally reaches very small values which are comparable to those of the undisturbed surrounding rock mass (10^{-21} - 10^{-22} m^2). Because of this behaviour the high initial amounts of fluids released into the borehole shortly after waste emplacement can escape from the borehole thereby avoiding the development of high gas pressures in the borehole. The long term

permeability, however, is low and limits a possible escape of radionuclides on the one hand and a inrush of brine from the repository on the other hand.

Model calculations have been performed in the report period to estimate the maximum occuring borehole gas pressure under consideration of the time dependent decrease of the permeability of the crushed salt.

4. Performance of model calculations

The numerical calculations for the estimation of the borehole gas pressure were performed by Golder Associates (1994) for GSF with the finite difference computer code ECLIPSE (Intera, 1993). In the calculations a simultaneous Darcy-gas-flow through the borehole seal consisting of salt grit, through the salt grit in the annulus between the waste canister stack and the borehole wall, through disturbed zones around the disposal borehole and the disposal drift and through the undisturbed rock salt was considered.

The cross section of the disposal drift was assumed to be 6 x 6 m and the widths of the disturbed zones around the disposal drift could be modelled as being 2.0, 5.0 or 10.0 or 20.0 m, respectively. Around the borehole a disturbed zone with an extension of 0.5, 1.0 or 1.5 m could be modelled.

The single elements in the disposal borehole were assumed to have the following measures:

- disposal borehole: radius = 0.3 m, depth: 300 m
- borehole seal: radius = 0.3 m, length: 30 m
- canister stack: radius = 0.215 m, length: 270 m
- salt grit: width of the annulus = 0.085 m.

The calculations were performed under consideration of a predetermined gas generation rate inside the borehole and selected combinations of rock salt and salt grit parameter values.

Two gas sources were considered in the calculations. First, the gas released from the pore space of the rock mass into the borehole and second, the hydrogen produced by corrosion of the waste canisters.

The hydrogen production inside a HAW-borehole that results from fluid release from the rock mass and the corresponding corrosion of the waste canisters (Spies et al., 1993) was already shown in (GSF-ECN, 1993). The data given are based on a canister corrosion rate of 60 μm/year. This rate was reported by Smailos et al. (1992) as being representative for the corrosion rate of a Pollux canister fabricated of fine-grained steel TStE355.

The extension of the disturbed zones around the disposal drift and the borehole were assumed to be 2.0 and 0.5 m, respectively and the value of the permeability k of the disturbed zone was varied between 10^{-16} and $10^{-20}m^2$. Three values of the permeability of the undisturbed rock mass were considered, 10^{-21} m^2, 10^{-22} m^2 and 0.0 m^2. For the permeability of the salt grit in the ring annulus two constant values of 10^{-12} m^2 and 10^{-18} m^2 as well as time dependent values have been considered. Also for the permeability of the borehole seal constant values as well as time dependent values have been considered.

The time dependent values of the permeability were determined on the basis of time dependent values of the porosity of the salt grit which is compacted with time. The compaction of the salt grit and the resulting

porosity was calculated by van den Horn and Prij (1994). The permeability data were determined from the porosity data with the following equation (GSF-IfT, 1991)

$$k = fp \cdot c \cdot \phi^q$$

with

k = permeability [m^2]
ϕ = porosity [-]
fp = factor representing higher permeabilities because of settlement effects in the salt grit
c,q = constants, determined in experiments

and on the basis of experimental data already reported in (GSF-ECN, 1992).

The Figure 1 shows as an example the results of the predictive calculations of the development of the borehole gas pressure for various seal permeabilities. A comparison of the different results allows the following conclusions:

* The maximum borehole gas pressure amounts to approximately 3 MPa and the maximum gas release rate at the gallery is 2.2 m^3/day for k_{seal} = 10^{-15} m^2 and occurs only temporarily approximately three years after sealing of the borehole. It is $2 \cdot 10^{-3}$ m^3/day for k_{seal} = 10^{-19} m^2 and it occurs in this case approximately 30 years after sealing of the borehole.

In conclusion it can be stated that the most sensitive parameters for the development of the gas pressure inside a HAW-disposal borehole besides the gas sources are the permeabilities of the seal and of the disturbed zones around the disposal borehole.

The calculated maximum borehole gas pressure of approximately 3 MPa seems to be acceptable. The gas release rates into the disposal gallery are rather low and do not create real problems, e. g. in regard of the development of dangerous hydrogen concentrations in a repository during the operation as well as during the post operation phase.

The validity of the law used for the calculation of the salt grit compaction and the validity of the law of Darcy for the calculation of the gas flow in low permeable media, however, are to be proved by appropriate laboratory or in-situ-tests.

5. Elaboration of sealing techniques

During the course of the desk studies the material properties of several candidate sealing materials as for instance bentonite, asphalt and bitumen and salt grit have been analyzed in regard of their suitability for sealing HAW emplacement boreholes. The results were already reported in (GSF-ECN, 1992), (GSF-ECN, 1993) and (GSF-ECN, 1994).

6. Development of an in situ test plan

In the recent years theoretical work together with laboratory investigations were started in regard of the development of constitutive models on the compaction behaviour of the crushed salt. Most of the constitutive laws presented in recently published literature can be written in the following form:

$$\dot{e}_v = A \cdot f(T) \cdot (p/p_o)^n \cdot g(\varphi)$$

with

e_v	=	compaction (Vo-V)/Vo)
Vo	=	initial volume of the crushed salt
A	=	structural parameter
T	=	absolute temperature
p	=	hydrostatic pressure
p_o	=	reference pressure
φ	=	porosity
n	=	material parameter

So far no in situ-experiments suitable for the necessary validation of the models have been performed. The DEBORA II project including respective in situ-experiments will therefore be started in 1995.

As already pointed out crushed salt will not only be used to seal the borehole but it is also used in the annulus between the canister stack and the borehole wall for required distribution of the canister weight loads. In this sense the borehole will be sealed in the annulus as well as in the empty space above the canister stack, the borehole seal region.

The compaction of the crushed salt is determined by the convergence of the rock mass. In the upper part of the borehole above the canister stack the convergence is less dependent on the heat release of the waste canisters than in the lower part where high temperatures do exist. The compaction behaviour and the permeability of crushed salt are therefore to be investigated in the annulus between the waste canisters and the rock mass as well as in the upper part of a borehole above the canister stack which requires two separate experiments.

Figure 2 shows the design of the planned experiment 1 for the investigation of the crushed salt compaction in the annulus. The experiment is suitable to investigate the model of crushed salt compaction and the resulting permeability of the compacted salt over a comparably wide parameter range.

Figure 3 shows another experiment designed to investigate the compaction of crushed salt in the borhole seal part above the canister stack. The experiment can be performed in a 15 m deep borehole with a 5 m high dump of crushed salt. In order to achieve the necessary degree of compaction within one to two years some additional heaters are required in peripheral boreholes.

In order to minimize the costs of the in situ experiments they are thought to be performed in empty boreholes in the HAW-test field at the 800 m level in the Asse salt mine.

Within the report period first model calculations have been performed for the necessary design of the experiments. In a first step thermomechanical calculations were performed to estimate the achievable compaction of crushed salt in the experiment 1. The power of the heater placed in the borehole liner was assumed to be 3500 watts/6 m. Maximum temperatures of about 100 °C in the backfill material and a maximum radial stress of about 14.5 MPa at the borehole wall at the heated midheight were predicted. The induced convergence of the borehole leads to a decrease of the backfill porosity as shown in Fig. 4.

Essential parameters for the prediction of gas flow in the ring annulus and the borehole seal are the permeability and the porosity in the backfill material during compaction. The experiment 1 is therefore designed

to provide a one-dimensional flow system which allows a straight forward calculation of these parameters from the measurements.

The flow domain consists of backfill material in the ring annulus over a height of about 6.00 meters. Nitrogen will be injected at the bottom and collected at the top again. Pressure and mass flux will be measured at both ends of the flow system. It is intended to apply an instantanious pressure increase at the inflow boundary and then to keep the pressure constant. In this case a pressure wave will go through the flow system until it reaches the outflow boundary. Only then a mass flow over the outflow boundary can be measured. After that, pressure and mass flow converge to steady-state conditions. The whole process will be called a "flow experiment" further on.

The minimum value for the backfill porosity is fairly high in comparison to the porosity of the undisturbed rock which is believed to be about 0.1 %. In addition to that permeability depends exponentially on the porosity. The resulting permeability constrast is greater than eight orders of magnitude between salt grit and undisturbed rock during the DEBORA experiment. This confirms the validity of the assumption of a one-dimensional gas flow.

But due to stress redistribution after drilling there may be a disturbed zone around the borehole which shows a higher permeability than the undisturbed rock. Up to now no reliable method exists to estimate the range of this disturbed zone or the extent of the structure changes. However, the 1-d flow assumption would have to bequestioned for a very large increase of permeability only.

Permeability is calculated easiest from steady-state mass flow. But steady-state conditions can never be reached mathematically in a flow system as described above . Only a state of sufficient convergence can be defined. For this reason a critical value of the ratio r between outflow and inflow is chosen to define steady-state conditions. Accuracy of the measure equipment will probably not allow a value greater than r=0.99 .

The pressure puls cannot physically be applied to the flow system as it is done in a mathematical model. Gas flows already into the system before the final input pressure can be reached. Nevertheless it is intended to simulate flow using a step function for the pressure at the inflow boundary. Therefore the time necessary to build up the required pressure should be small compared to the time which is needed to reach steady-state conditions in the above defined sense.

Basis of the calculation of permeability and porosity from measurements is the continuity equation into which Darcys generalized flow law and the ideal gas equation are substituted. From this equation it is easy to calculate permeability and porosity in two steps. Permeabilty can be calculated iteratively using the measured steady-state mass flux and the pressure at the boundaries. Evaluation of the porosity has to be done by fitting the transient mass-flux curves of the numerical model to the measured fluxes. It is thereby assumed that gas temperature and dynamic viscosity are constant during a flow experiment.

To get a feeling for the technical requirements of the flow experiments some numerical simulations were performed. One point of interest was the required amount of steady-state mass-flux under the expected conditions. This flux is a function of the permeability and the pressure gradient which can be converted to porosity and the pressure difference. The results of the parameter variations are summarized in Fig. 5.

The curves in Fig. 5 show the exponential dependency of the mass flux on the porosity. Due to the non-linearities in the continuity equation it depends exponentially on the pressure difference as well.

In Fig. 6 the time coresponding to r=0.99 is drawn against the porosity. It shows that calculation of the porosity from a flow experiment is not feasable significantly above a value of 10 % because several minutes should pass at least until steady-state conditions are reached.

References

GSF-ECN, 1992: DEBORA-Project, Progress Report July - December 1991, Joint Report of GSF-Institut für Tieflagerung and Energy Research Foundation Netherlands - ECN, Abteilungsbericht IfT 2/92

GSF-ECN, 1993: The DEBORA-Project, Progress Report January - June 1993, Joint Report of GSF-Institut für Tieflagerung and Energy Research Foundation Netherlands - ECN, Abteilungsbericht IfT 4/93

GSF-ECN, 1994: The DEBORA-Project, Progress Report July - December 1993, Joint Report of GSF-Institut für Tieflagerung and Energy Research Foundation Netherlands - ECN, Abteilungsbericht IfT 3/94

GSF-IfT, 1991: Systemanalyse Mischkonzept, Technischer Anhang 7, Analyse der Langzeitsicherheit von Endlagerkonzepten für wärmeerzeugende radioaktive Abfälle, GSF-Institut für Tieflagerung

Golder Associates GmbH Celle, 1994: Modellierung des Entgasungsprozesses über die Saumzone und einen Bohrungsverschluß im Zusammenhang mit der Einlagerung wärmeerzeugender hochradioaktiver Abfälle in Bohrlöchern, GSF-Contract No. 31/140190/93

Hermann, A.G., Knipping, B., 1993: Waste Disposal and Evaporites - Contributions to Long-Term Safety, Springer Verlag, Berlin Heidelberg

Intera, 1993: ECLIPSE 100 User's Reference Manual 92A, Intera Petroleum Production Division, Abingdon, England

PTB, 1989: Interner Arbeitsbericht, Physikalisch-Technische-Bundesanstalt, Braunschweig.

Smailos, E., Schwarzkopf, W., Kienzler, B., Köster, R., 1992: Corrosion of Carbon-Steel Containers for Heat-Generating Nuclear Waste in Brine Environments Relevant for a Rock-Salt Repository, Mat. Res. Soc. Symp. Vol. 257, 399-406

Spies, Th., van den Horn, B. A., Prij, J., Müller, K., Rothfuchs, T., 1993: Sealing of HAW-Boreholes in Salt Formations, In: Proc. 3rd Pegasus Progr. Meeting, June 3-4, 1993, Köln, Commission of the European Communities, EUR 15734 EN

Van den Horn, B. A., Prij, J., 1994: Thermomechanical Analysis of a Backfilled Borehole, Netherlands Energy Research Foundation ECN, Petten, ECN-C-93-045

Van den Horn, B. A., Prij, J., 1994: Three-Dimensional Finite Element Analysis of a Gallery with a Borehole, ECN-Report ECN-C-94-031

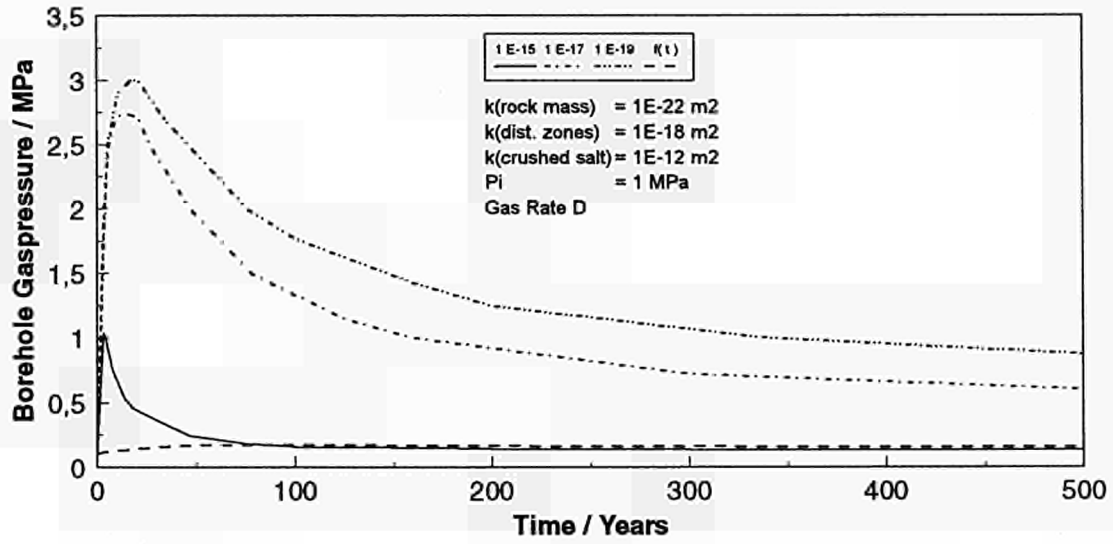

Fig. 1: Borehole Gas Pressure Development 30.5 m below the Disposal Drift (at the Lower End of the Borehole Seal)

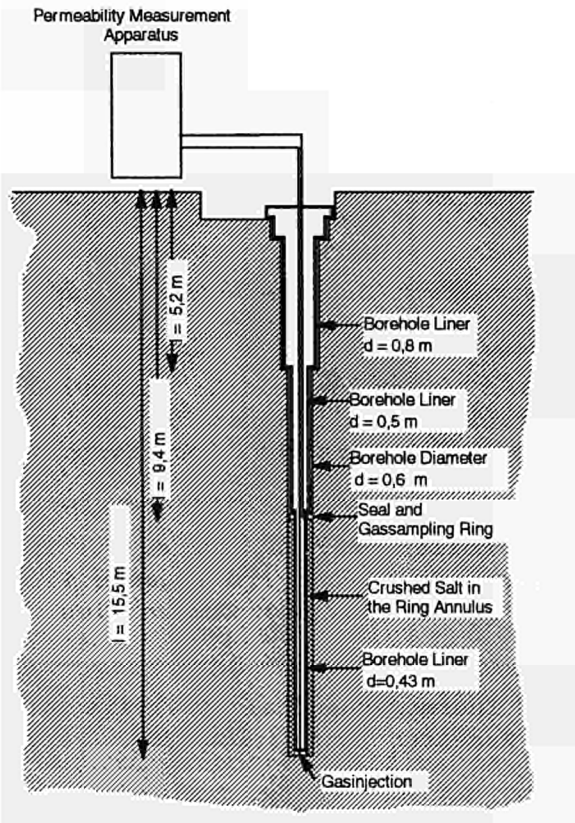

Fig. 2: Layout of the DEBORA Experiment 1

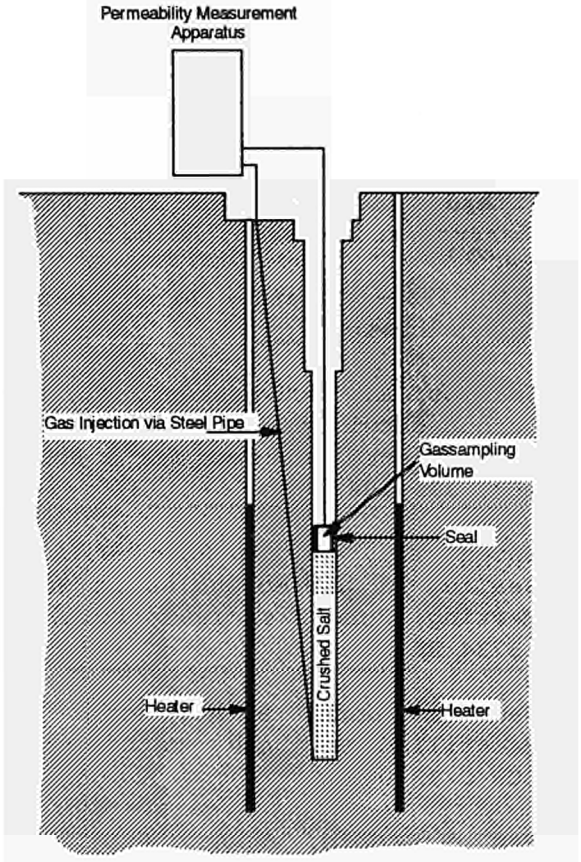

Fig. 3: Layout of the DEBORA Experiment 2

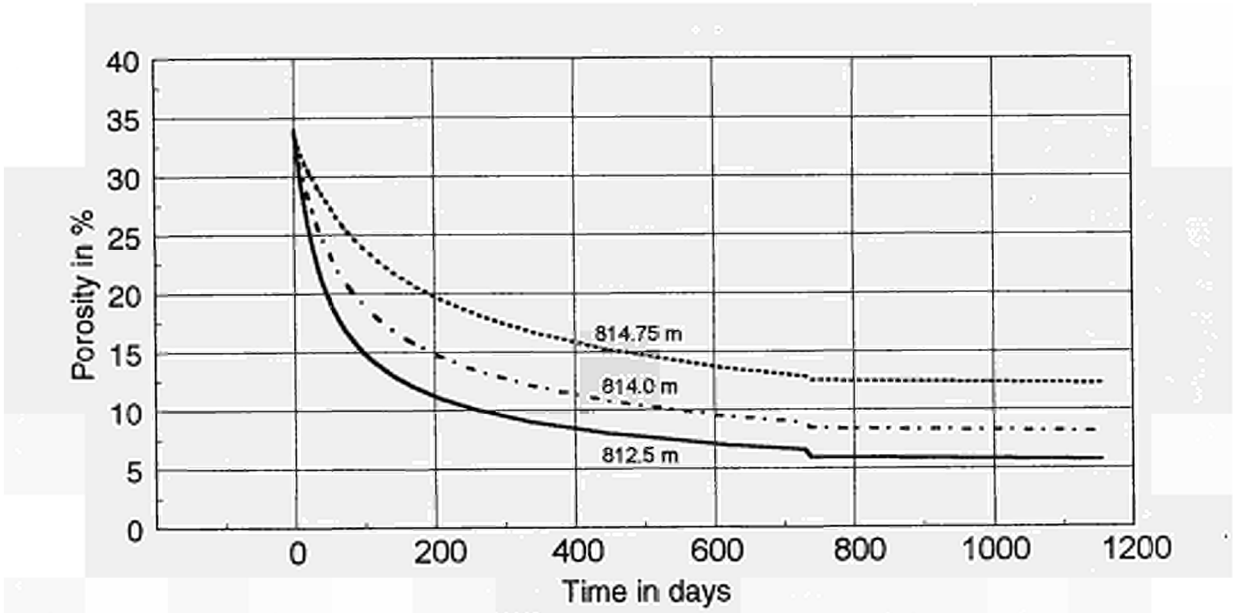

Fig. 4: Calculated Decrease of the Porosity in the DEBORA Experiment 1

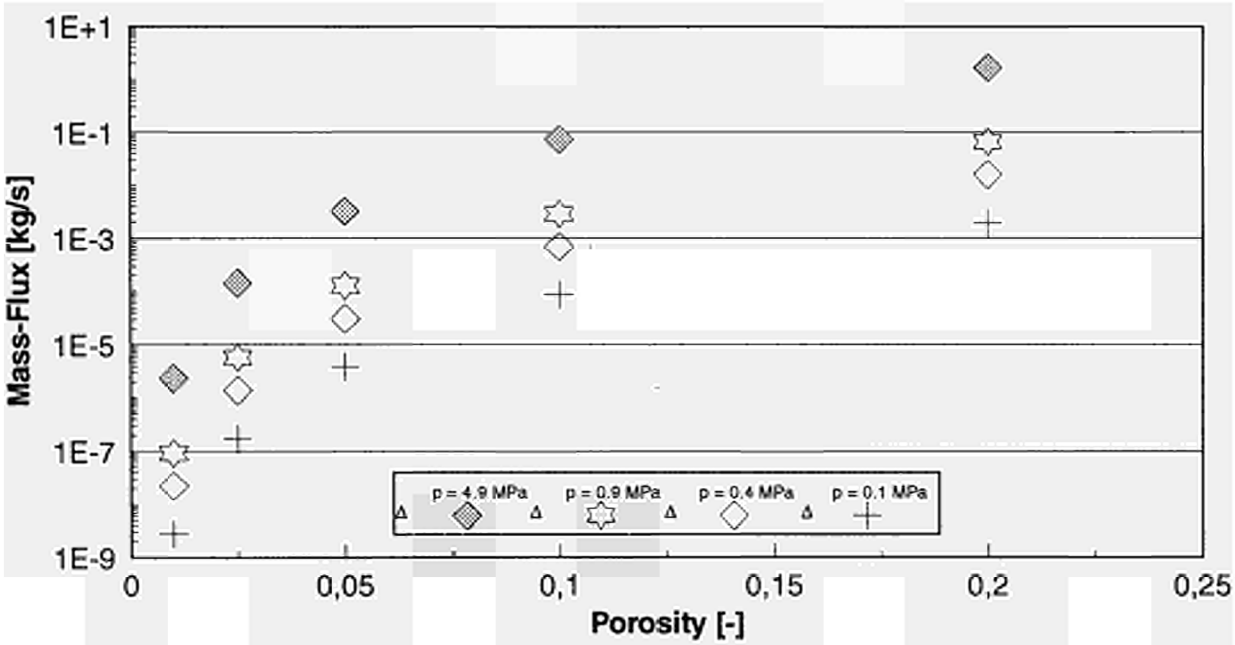

Fig. 5: Steady-state Mass-Flux as a Function of Porosity and Pressure difference in the DEBORA Experiment 1

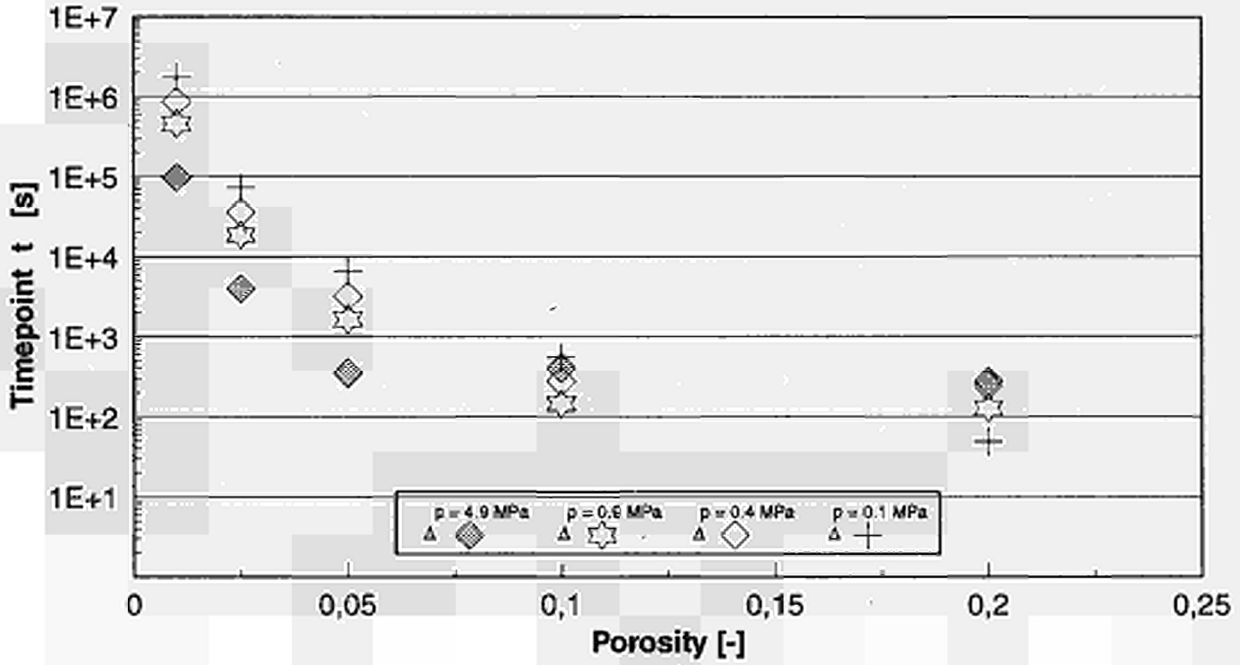

Fig. 6: Time Passed until Ratio r Equals 0.99 as a Function of the Porosity in the DEBORA Experiment 1

Title: **The refinement of soil gas analysis as a geological investigative technique**
Contractor: Università "La Sapienza", Rome (Italy)
Contract N$_i$: FI2W-CT91-0064
Duration of contract: from April 1991 to June 1995
Period covered: November 1993 to October 1994
Project Leader: S. Lombardi

A. OBJECTIVES AND SCOPE

The present research project consists of a multidisciplinary study aimed at refining a set of geological investigation methods for the assessment of the safety of sites for operation such as radioactive waste repositories, with high potential for environmental hazard.
The studies are based on the integration of sampling and analyses of soil gases with other investigation techniques. Previous soil gas surveys performed by the participants have demonstrated that the soil gas method has great potential for tracing buried faults and fractures in clayey terrains and has a great flexibility. It is possible in fact to carry out surveys along profiles and/or according regular grids at different scales, i.e. with sampling densities in the range of one to a hundred samples per square kilometre.
The main objectives of the research are:
- the implementation of the analytical and sampling techniques of the soil gas method;
- the study of soil gases as fault tracers and of gas migration within soil and fractured zones by means of in situ tests;
-the comparison (and calibration) of the soil gas approach with other methods in order to test both the soil gas method and different lithotypes as natural barriers to gas migration;
-the creation of a data base in order to give mathematical models on gas generation and migration. The co-participants in the research with Rome University are: ISMES, Italy; Exeter University, U.K., and INTERA Sciences, U.K., as subcontractor of Rome University.

B. WORK PROGRAMME

The present work has been subdivided into seven tasks:

Task 1- Selecting areas in Italian subsiding sedimentary basins as test sites for the soil-gas and geophysical surveys. Laboratory equipment testing and setting up.
Task 2 - Sampling and analysis of soil gas (Rome and Exeter Universities).
Task 3 - Comparison between Rome and Exeter soil gas data.
Task 4 - Study of soil gas variations with depth, using shallow boreholes ranging from 5 to 10 meters (Rome University).
Task 5 - Execution of in situ tests by injection of gases into the soil and subsequent sampling and analysis (Rome University).
Task 6 - Geomorphological and structural research as support to the study of fracture and fault systems (Rome University). Geophysical, geotechnical and pedological studies in order to identify the main geological features and to characterise the soil and subsoil of the study areas (ISMES).
Task 7 - Statistical and mathematical analysis of the distribution of soil gases upon the data collected in the surveys conducted by Rome and Exeter Universities. This task will be carried out with the help of Intera Sciences.

C. PROGRESS OF WORK AND OBTAINED RESULTS

State of advancement

In 1994 all tasks of the work programme have been completed. The research focused on a further development of tasks 2, 5, 6 and 7, and on performing task 4. The soil gas data-base has been completed (1222 samples have been collected and analysed) and further informations have been obtained by a second gas injection test.

In particular the following works have been performed:

- regional soil-gas survey in the Siena Basin (Rome University); this final work is aimed at assessing gas leakage distribution throughout the basin extension, in correspondence with both regional faults and unfractured clayey deposits;
- analysis of He and CO_2 concentration in soil-air versus depth (Rome University);
- a second gas injection test to study the gas ($He+CO_2$) movement through faulted clayey rocks (Rome and Exeter Universities); the study has been developed to assess controls of local hydrogeology upon gas migration;
- a further geotechnical analysis to assess the main characteristics of the clayey rocks at the gas injection site (ISMES);
- application on soil-gas data (from the Siena Basin) of a quantitative methodology to interpret fault structures (INTERA).

Progress and results

ROME UNIVERSITY (G. Etiope, S. Lombardi)

Regional soil-gas survey in the Siena Basin

The Siena Basin has been selected as research site for soil-gas analysis since it provides a geological scenario that may be considered as natural analogue of underground gas-bearing repository. In fact the basin is characterized by the occurrence, below a thick clay cover, of high pressure gas domains (linked to low enthalpy geothermal fluids). In the previous reports the results of detailed soil gas surveys, performed in correspondence with local tectonic discontinuities, were described. In this report soil-gas data collected at regional scale (1 sample per square kilometer), throughout the basin, are introduced.

Soil-gas statistics are listed in the following table. Distribution of values above the mean plus 1/2 standard deviation is highlighted on contour line maps obtained by computer processed "kriging" interpolation method (Fig. 1a-c).

Tab.I - Descriptive statistics of He, Rn and CO_2 data in the Siena Basin (regional survey: 1 sample /km^2)

GAS	*Mean*	*Std.Dev.*	*Min.Val.*	*Max.Val*	*Number*
ΔHe (ppb)	8	163	-632	626	249
^{222}Rn (Bq/l)	20	15.93	0	90.3	249
CO_2 (%)	1.31	3.22	0.03	46	249
CO_2 (%) *	1.13	1.53	0.03	15.89	248

* Data computed discarding the maximum value (46%) found close to Acqua Borra thermal spring

The regional survey highlighted the gas-bearing feature of the fault systems bounding and crossing the basin. The "Rapolano fault system", in the eastern edge of the basin, provides a very permeable way out for deep seated fluids (gas and water). However, the system known as "Arbia Line" is the most interesting one since it crosses transversally (with orientation N45E) the basin cutting hundreds meters of clayey cover. Soil-gas analyses pointed out that endogenetic gases use both these tectonic discontinuities as preferential gas leak route:

-He concentrations reach levels highly above the atmospheric content.

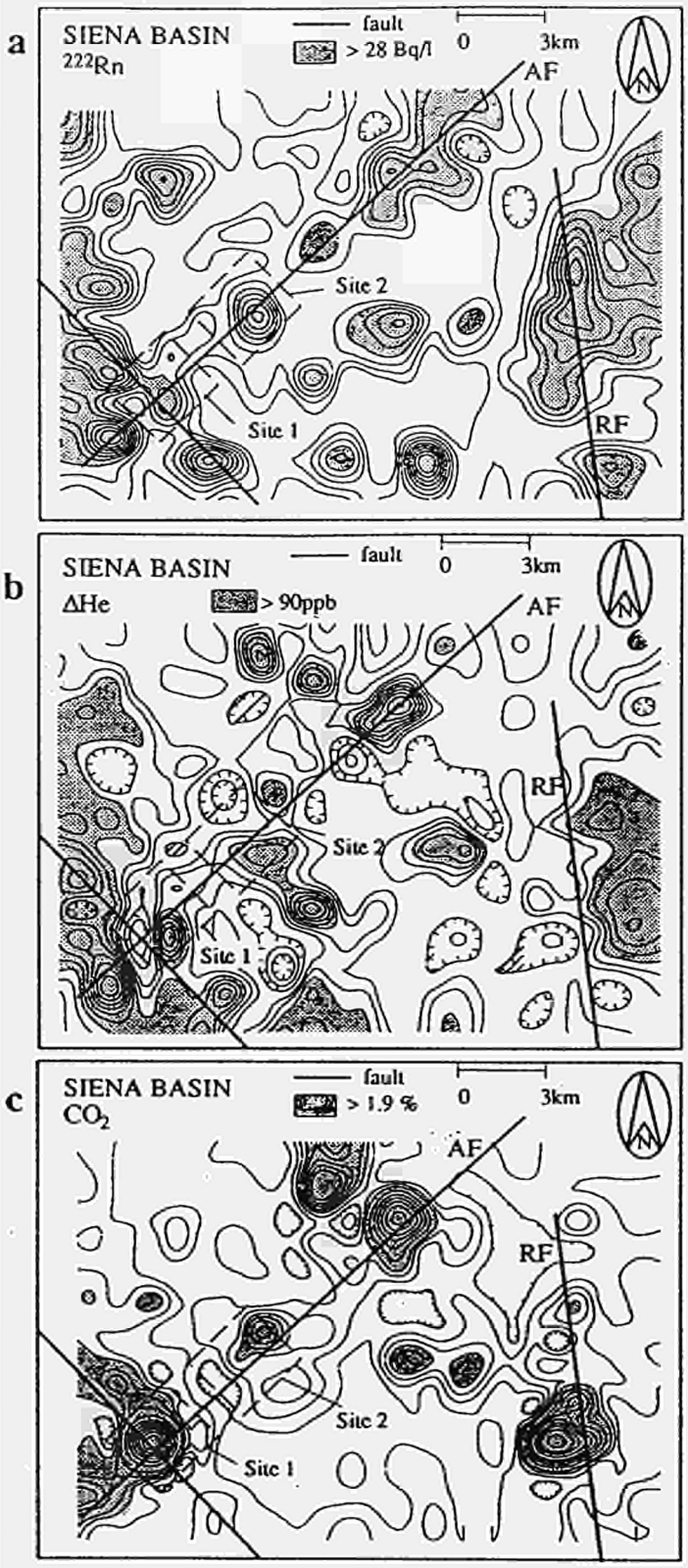

Fig. 1. Rn (a), He (b) and CO_2 (c) soil gas regional distribution in the Siena basin

AF: Arbia Fault; RF: Rapolano Fault

-Rn values in some points are highly above the maximum levels that may be supported by the very low U content of the clays [1]. Only an advective gas upflow from the subsoil can account for the observed Rn anomalies.
-CO_2 reached values up to three orders of magnitude above the atmospheric content;
-Statistically derived contourlines of Rn and CO_2 anomalies showed similar location, shape and directions. A Rn-CO_2 coupling evidence appears even by point-to-point analysis. Probably, Rn is transported from the subsoil, through fault-linked pathways, by carrier gases of which CO_2 could be one of the major components.
Basically, soil-gas anomalies did not occur homogeneously throughout the fault lines: anomalous zones often alternate with the lack of any gas signal. Keeping in mind the probability that gas anomalies were not always detected because of bias errors, we suppose that faults in clay are not totally permeable to gases throughout their extension.

Concluding remarks

Regional soil-gas surveys pointed out the occurrence of gas leakage connected to faults, both in the margin and in the middle of the Siena basin, regardless of the clay thickness.
Terrestrial gases ascending from high pressure gas domains linked to geothermal reservoirs cross the clayey formations in the fractured zones. Fractures in clays do not self-seal totally but in most of zones clays behave as a brittle, and consequently gas permeable, medium. Far from faulted zones no significant gas leakage occurs.

ROME UNIVERSITY (G. Ciotoli, S. Lombardi)

Study of soil gas variation with depth

In July 1994 a set of fixed soil gas probes at different depths (5, 3 and 1.5 m) was placed at Pieve Pacina (Castelnuovo Berardenga) in the Siena Basin. The probes are made of the same mould of the portable probes. Soil-gas sampling was carried out daily to examine naturally variation of soil gas concentration with depth. Unfortunately the probe 5 m deep intercepted a shallow water table and therefore gas sampling was not possible. The set of probes was located perpendicularly across the fault recognized by previous seismic surveys (Fig.2).
Soil-gas samples were analysed for He and CO_2 on site in the Rome University's mobile laboratory equipped with a mass spectrometer for mass 4 and a gas chromatograph (Tab.II).

Tab. II - ΔHe (ppb) and CO_2 (%) values at different depth in the period 10 July - 3 August 1994.

Date/ Depth	10/7	11/7	12/7	15/7	16/7	18/7	19/7	20/7	21/7	22/7	23/7	24/7	25/7	26/7	27/7	28/7	03/8
-0.5m	54	158	-321	190	41	-335	-494	-298	447	222	280	307	237	84	122	3631	
-1.5m	307	0	552	3796	81	-193	567	-30	596	336	323	495	482	168	247		
-3.0m	1000	-158	4969	5534	163	304	900	237	1193	2579	652	709	475	167	562	1102	

Date/ Depth	10/7	11/7	12/7	15/7	16/7	18/7	19/7	20/7	21/7	22/7	23/7	24/7	25/7	26/7	27/7	28/7	03/8
-0.5m	9.45	10.05	6.15	5.47	7.85	5.8	8.1	5.35	7.3	6.85	3.05	6.75	6.0	10.6	6.7	10.25	8.46
-1.5m	9.04	9.55	6.32	11.65	11	11.2	8.55	9.85	9.88	11.35	13.0	11.95	11.45	11.55	7.8	11.5	12.08
-3.0m	8.11	8.75	5.91	11.55	10.65	12.05	10.5	10.75	10.8	12.10	13.7	13.82	12.5	13.15	11.35	12.55	13.8

Data show that helium and carbon dioxide concentrations generally increase with depth, trending toward a saturation value. 14 samples out of 16 for He and 14 out of 17 for CO_2 displayed the highest concentrations at 3 m. It is worth to note that ΔHe values increase positively with depth and at depth of 3.0 m only one value was negative (on 11th July). Moreover data show a lower increase of CO_2 concentration between 1.5 and 3.0 m than

between 0.5 and 1.5 m , coherently to what reported by Hinkle, 1994 [2]. Further results will be discussed in the final report. However, the interpretation of gas anomalies can be difficult because soil-gas are affected by both meteorological and environmental conditions. In conclusion, the measure of meteorological parameters (i.e. atmospheric temperature and pressure, rainfall), as well as pedological and hydrogeological ones could constitute a task for a possible extent of the research.

ROME AND EXETER UNIVERSITIES (G. Ciotoli, G.A. Duddridge, G. Etiope, P. Grainger, M. Guerra, S. Lombardi)

Second gas injection test in the Siena Basin's clays

In July 1994 a second gas injection test was performed at Pieve Pacina (Castelnuovo Berardenga) in the Siena Basin. In this second test helium and carbon dioxide were injected within a saturated and fractured sandy-clayey sequence. This work was aimed at the following objectives:

- to confirm the helium soil gas distribution (channelling phenomenon) obtained in the first injection test (1993);
- to study and compare the behaviour of the two gases injected;
- to examine lateral displacement of gas versus vertical one after the injection and to obtain information about the relative effectiveness of gas migration as free-phase or dissolved in groundwater. To this aim a 70 m deep borehole and a 15 m deep piezometer were drilled to collect and analyse gases dissolved in groundwater and to evaluate the main hydrochemical parameters (pH, conductivity, alkalinity). Moreover the drilling of the borehole and of the piezometer yielded a better definition of the stratigraphic sequence and of the hydrogeological features of the area.

Background survey

As in the first injection test, prior to the gas injection, a He and CO_2 soil gas survey was performed to establish background values in the field. The background survey was conducted on 11 and 12 July 1994. Helium was analysed on site by Exeter University's mobile laboratory with a Leybold UL400 mass spectrometer, carbon dioxide was also analysed on site by Rome University's mobile laboratory using a Perkin-Elmer sigma 3B gas chromatograph. A sampling grid was pegged out and labelled using the same strategy of 1993 test. Its geometry and orientation as well as piezometer and boreholes location are shown in Fig.2

The background survey showed that the maximum value of ΔHe was found to be 911 ppb at site 4/5. However the mean values of ΔHe in soil gases was assessed at 100 ppb. This result matches well with 1993 background figures. Carbon dioxide reached a maximum at site 5/1 (9.72%), the other values being of the same order of magnitude of 1993 survey.

Gas injection procedure

The gas injection arrangements have been sketched in the 7th report. They consisted of two gas cylinders fed via a gauge panel to the gas injection point at the bottom of a packered borehole. The packer was of the single type as used in the 1993 experiment. The packer was lowered to a position above the screened borehole section. The main valves are indicated on the diagram, but extra ones were provided so that the control panel could be removed and isolated from the injection lines after gas injection. Also the up line pressure gauge had an arrangement so that it could be used to monitor the packer pressure.

The packer was inflated up to a pressure of 5 bars using an air compressor. Gas cylinders of He and CO_2 were arranged so that either could be selected as the injection gas. It had been considered important in the experiment for both He and CO_2 to be injected under the same pressure conditions. The alternating input of the two gases was used when it was realized that simultaneous injection was the least satisfactory solution due to mixing problems. Calculations showed that it would take longer to inject CO_2 and in each repeat cycle He was injected for 2

minutes and CO_2 for a little over 11 minutes. During gas injection control was made using the cylinder head regulator and the control gauge panel used for monitoring and recording pressure and flow values. However, with the rapid changeover of gases and the constant need to adjust regulators to prevent over pressurisation and drops in pressure, due most probably to the irregular dissolving of CO_2 in the groundwater, an accurate trace of the injection progress was impossible. This problem prevented the injection of He and CO_2 at the same pressure.

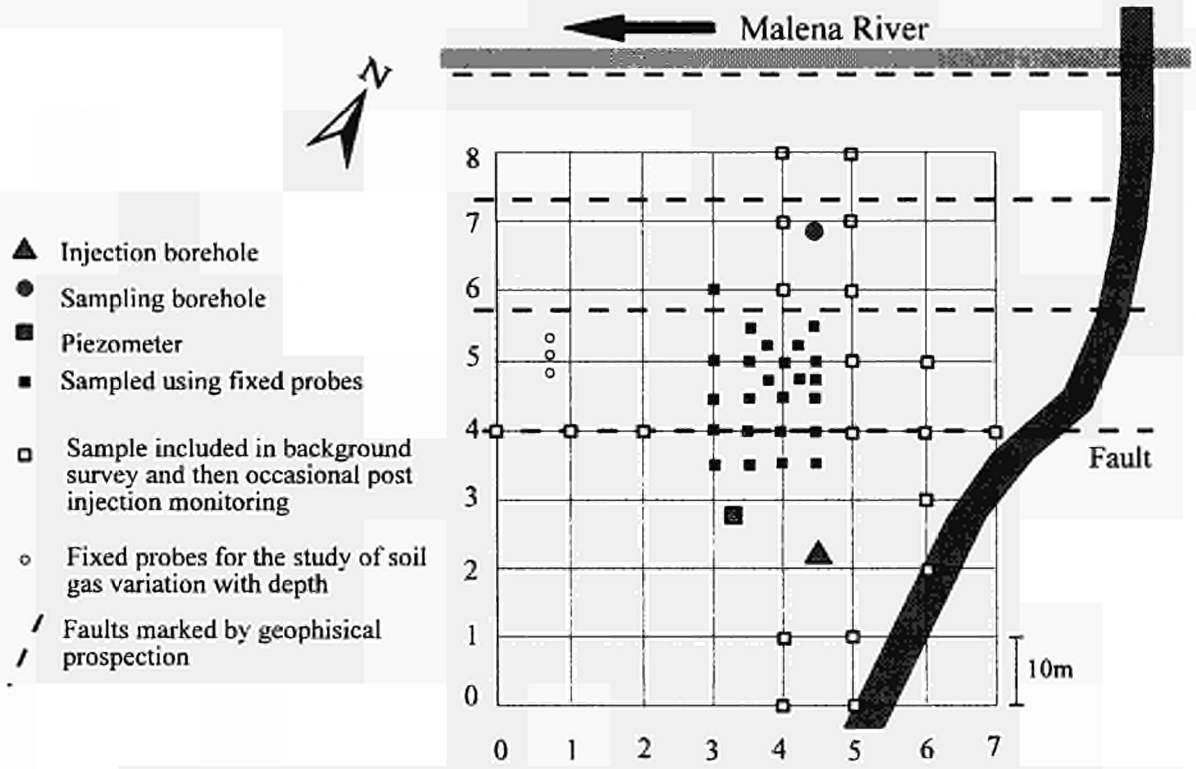

Figure 2. Map of monitoring area at Pieve Pacina (Castelnuovo Berardenga, Siena Basin). Probes for the study of soil gas variation with depth are shown too.

Monitoring and results from the injected gases

The soil gas monitoring survey began just after the injection. Samples were collected once a day; occasionally same points were sampled twice a day. The day after the injection a sharp increase of helium (2,276 ppb) was observed at site 4/4.5. During the following days ΔHe higher values were confined to a small, central area. In fact, the most anomalous concentrations were found at site 4.25/4.75 (14,355 ppm), 4/4.5 (5,349 ppm), and 4/5 (up to 1,899 ppm). Outer points maintained at background levels. Consequently it was decided to concentrate sampling resources on monitoring the high value points. Only from time to time during the subsequent days peripheral points were tested to check that there was no gas leakage.

Figure 3 shows ΔHe and CO_2 concentrations vs. time for points with higher ΔHe. Peak values of He can be seen to occur in the period 7 to 10 days. In many of the selected cases there is a clear transition from background concentrations to gas rise. During this time, in the same area where higher ΔHe anomalies were found, it was noted an increasing trend of CO_2 The maximum observed post injection value was 5.3% at site 5/6, two days after the injection. Because of the great background noise typical of naturally occurring CO_2 in soil, it is difficult to discriminate the arrival of injected CO_2 at the surface. Both He and CO_2 space distribution during July-September is shown in Fig. 4. Helium diagrams demonstrated a centralised zone of high gas concentration dispersing over days to remove surrounding background values and

then dissipating completely by September. CO_2 shows no clear centre of emission as there is for He, but the higher values (more than 4%) occur approximately in the same period of Helium.

In order to examine lateral displacement of gas in the aquifer versus vertical migration, samples of groundwater were taken once a day from the piezometer and the vertical borehole. The main chemical-physical parameters (pH, conductivity, alkalinity) have been measured, as well as dissolved He and CO_2. Gases have been extracted from groundwater *in situ* by vigorous shaking and then analysed by spectrometry (helium) and gas chromatography (carbon dioxide). Sampling and analyses are still in progress.

Conclusion

The experiment has confirmed the results of the 1993 test in showing that injected He will follow a specific narrow channelway to the surface and then spread laterally in the soil horizon. The centre of emission was within the same area as in 1993. The process of injecting CO_2 at the same time as He proved difficult in terms of gaining accurate injection readings and maintaining similar injection zone pressures. In this respect a redesign and renewal of the injection equipment is recommended for any further experiments of this type to provide separate injection lines for each gas and an injection zone pressure transducer. Interpretation of gas anomalies in groundwater requires the understanding of hydrological setting of the studied area. Field test are in progress and a complete discussion and conclusion will be given in the final report.

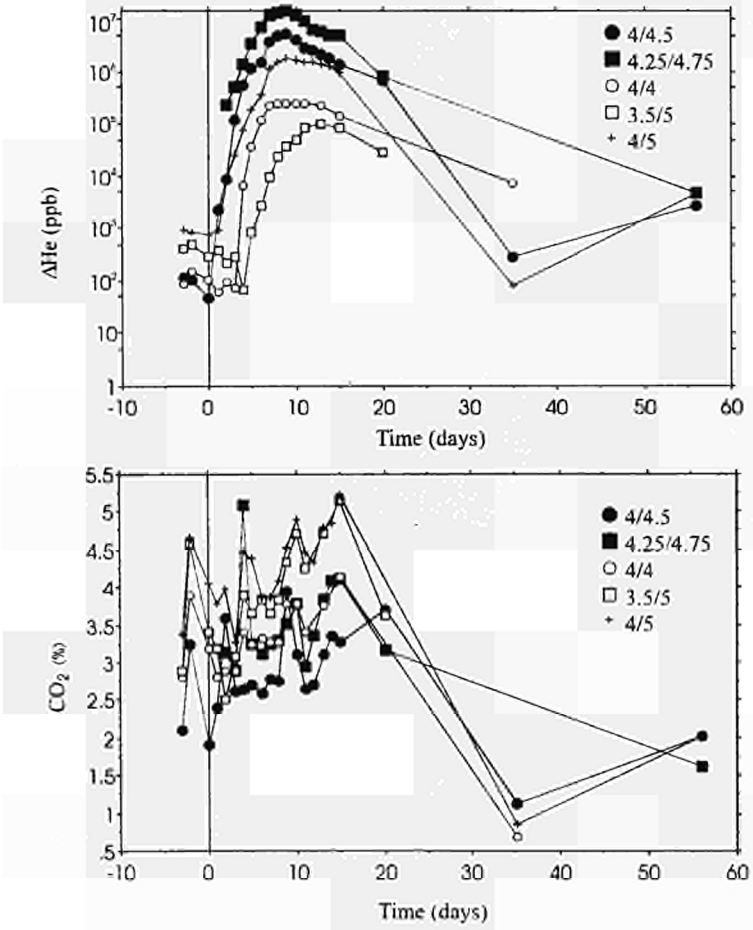

Figure 3. Soil gas ΔHe and CO2 variation during the second injection test.

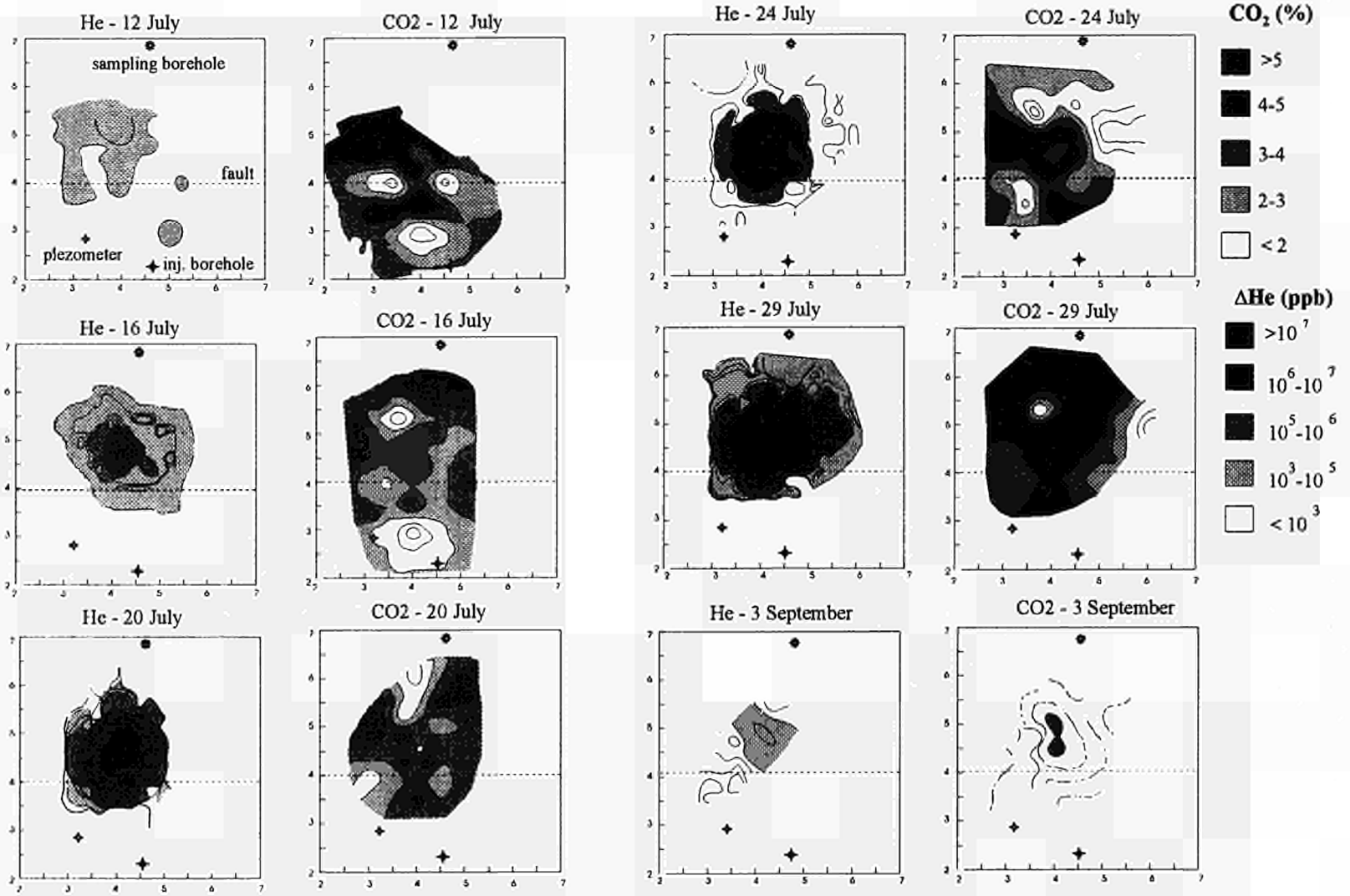

Fig. 4 - He e CO2 distribution post injection test at Pieve Pacina (Castelnuovo Berardenga)

ISMES(V. Chiantore)

Geotechnical laboratory analysis of drilling cores from the injection test site

Five semi-undisturbed sandy-clayey samples, coming from drilling at the injection test site (Siena Basin) have been analysed for classification (granulometry, moisture content, bulk density, specific gravity) and permeability tests (Tab.III). Such data are going to be compared with hydrogeological parameters obtained by field tests, performed by Rome University, still in progress.

Tab. III - Summary of classification and permeability data of samples from the injection test site

Sample	depth (m)	w (%)	g (kN/m^3)	Sand-Silt-Clay (%)	Spec Gr	Void ratio	K (cm/s)
1	34.30-34.60	17	21.54	7/56/37	2.76	0.46	1.9E-9
2	40-40.32	16	21.59	7/59/34	2.74	0.45	2.7E-9
3	45-45.30	17	20.69	34/47/19	2.72	0.48	1.1 E-7
4	45.60-45.90	19	20.62	33/50/17	2.73	0.50	2.2 E-7
5	59.20-59.50	16	20.95	11/56/33	2.74	0.46	4.8 E-9

INTERA (M.D. Impey)

Automatic identification of soil-gas anomalies and regional faultlines in the Siena Basin

A quantitative methodology to analyse soil-gas data, in order to provide an interpretation of regional fault structures, has been developed (see previous reports). The methodology is based on generating a fractal interpolation of soil-gas data which has the same heterogeneity as the data. This interpolation is then searched for positive gas anomalies, and straight lines are fitted through sets of anomalies. Since faults tend to be linear and positive anomalies lie at points along faults, the fitted lines are ranked, by reference to a number of properties, in order to identify the "optimal" interpretation. This ranking is based on quantitative criteria, which may be controlled to reflect "soft" geological information. Details of the methodology and an example of its applications on survey data from the Siena Basin will be show in the final report.

References

[1] ETIOPE G., LOMBARDI S. (1994): ^{222}Rn soil gas in sedimentary basin in central Italy: its implications in the radiation protection zoning. Rad. Protect. Dosim. (in press).

[2] M. E. HINKLE (1994): Environmental conditions affecting concentrations of He CO2, O2, and N2 in soil gases. Applied Geochemistry, 9, 53-63.

Title	MEGAS : Modelling and Experiments on GAS migration in repository host rocks
Contractors	SCK/CEN (B), INTERA (UK), BGS (UK), ISMES (I)
Contract N°	FI2W-CT91-0076
Duration of contract	1 March 1991 - 31 May 1995
Period covered	1 January 1994 - 31 December 1994
Project leader	G. Volckaert (SCK, coordinator), M. Impey (Intera), S. Horseman (BGS), V. Fioravante (Ismes)

A. OBJECTIVES AND SCOPE

For the option of a deep geological disposal facility several potential sources of gases were identified : i.e. the anaerobic corrosion of iron, degradation of organic materials, the gas present as such in the waste packages. Of those gases hydrogen is certainly the gas which can be released in the potentially largest amount. For the safety evaluation of a repository, it is necessary to know the effects of gasses on the host rock.

The primary objective of the MEGAS project is to understand the consequences of gas generation in a clay host rock. The final objective of this project will be to validate a gas migration model and to confirm our understanding using an in situ gas injection experiment.

B. WORK PROGRAMME

1. Chemical reaction and diffusion experiments

The reaction capacity of hydrogen with Boom clay observed in previous experiments will be further investigated by determining the intrinsic reaction rate, the reaction capacity and the diffusion coefficient.

2. Geotechnical experiments : uniaxial

In these experiments the gas permeability (two-phase flow) and the gas breakthrough pressure will be determined.

3. Geotechnical experiments : triaxial

The goal of these experiments will be to define the conditions under which preferential pathways for gas migration might develop and to examine bubble growth and migration. Triaxial experiments will also be performed at elevated temperature.

4. In situ experiments

These will be performed in the HADES underground research facility (Mol, Belgium).

5. Modelling

The following approaches will be utilized : modelling the dynamics of bubble flow and modelling two phase flow. The laboratory experiments will be used to validate and, possibly, calibrate a basic two phase flow model.

Within this project INTERA will perform the main modelling work. The SCK/CEN will be responsible for the gas reaction, diffusion, uniaxial flow and in situ experiments. BGS will perform geotechnically based triaxial gas flow experiments. ISMES will perform experiments at higher temperature.

C. *PROGRESS OF WORK AND OBTAINED RESULTS*

State of advancement

1. Chemical reaction and diffusion experiments

A last Boom clay slurry hydrogen reaction has been carried out in the upgraded reactor vessel. Some chemical and biological analysis were performed afterwards.

Two through-diffusion tests were performed in the through-diffusion cells, developped to solve the problem of a hydrogen diffusion leak in the former in-diffusion cells. These were the last experiments planned in the frame of the contract.

2. Geotechnical experiments : uniaxial

A set of three additional gas breakthrough experiments has been performed. In these experiments, the Boom clay cores were placed in an oedometer and confined under a constant vertical stress. Three gas breakthrough experiments on larger clay cores are in preparation. These experiments required the construction of isostatic cells, which are now available. The clay cores were taken in the test drift in September and a first experiment has already been started.

3. Geotechnical experiments : triaxial

Two experiments have been performed in the flow-through apparatus. One of these experiments was a multi-stage hydraulic conductivity test. The other one was designed to study the hydraulic transport properties of the clay, in relation to the compaction stress state.

4. In situ experiments

Hydraulic tests are carried out in the multi screen piezometer installed in 1986 at the bottom of the shaft. The purpose of these tests, performed in the deepest piezonest's screen, is to assess the influence of geomechanical parameters on hydraulic properties of the Boom clay under in situ conditions.

The gas injection experiment in the new in situ experimental set-up has been carried out. Similar hydraulic tests as in the vertical piezonest are now performed in the gas injection screen.

5. Modelling

Because of the doubt concerning the validity of Darcy's law for the modelling of gas migration in low permeability media, an alternative modelling approach has been studied. One solution would be to use a capillary bundle model where a network of capillary tubes provides an idealized topological representation of the available pathways for gas migration in the medium.

Progress and results

1 Chemical reaction and diffusion experiments (CEN•SCK)

The last chemical reaction experiment has been completed after almost one year of operation. Figure 1 shows the hydrogen pressure decrease versus time. A rapid dissolution of hydrogen is followed by a slow constant hydrogen consumption (10^{-8} mole H_2. d^{-1}. $gclay^{-1}$), which can be assimilated to a first order reaction. After a few months, the reaction rate suddenly increased to stop abruptly one month later. The presence of bacteria was the most probable explanation for this phenomenon, so we decided to realize microbial analysis in addition to the already planned chemical analysis. The chemical analysis of the gas phase revealed large amounts of methane (31.05 %) and nitrogen (59.65 %). Hydrogen had completely disappeared (0.11 % of the gas phase). This can obviously be attributed to the presence of methanogenic bacteria, which were detected by the microbial analysis (14 bacteria. $gclay^{-1}$). This is certainly an underestimation of the real population, because methanogenic bacteria quickly die when exposed to air, as happened during the sampling. Sulphate-reducing bacteria were also detected (32.5 bacteria. $gclay^{-1}$), and

can be largely responsible for the reduction of the sulphate ions in the liquid phase of the slurry (from 7.92 mg. l^{-1} before the experiment to 0.15 mg. l^{-1} after the experiment) and the apparition of thiosulphate ion traces. The pH remained unchanged, while the Eh decreased from -300mV to -450mV versus the hydrogen standard electrode. Another important observation is the increase of the total organic carbon content in the liquid phase during the experiment (from 597 mg. l^{-1} before the experiment to 728 mg. l^{-1} after the experiment).

Two through-diffusion tests have been carried out. The principle of these experiments is to put a hydrogen source at constant pressure in contact with the top face of a clay plug, and to monitor the increase in pressure versus time at the bottom face, where the vacuum was previously realized. Unfortunately, an initial carbon dioxide degassing which occurs at this face just after the vacuum is installed prevents us from obtaining reliable results. Due to a very strong correlation between the parameter ηR (product of diffusional porosity with the retardation factor) and the parameter D (diffusion coefficient), only their product ηRD can be derived with enough confidence. When comparing the obtained ηRD values for both in-diffusion and through-diffusion experiments, we see that they vary within one order of magnitude i.e. from 6.8×10^{-7} to 9.6×10^{-6} $cm^2.s^{-1}$.

2 Geotechnical experiments: uniaxial (CEN•SCK)

Three more gas breakthrough experiments on small clay cores (ϕ is 38 mm, length is about 40 mm) are finished. In these experiments, the cores are placed in an oedometer and confined under a constant vertical stress equivalent to the total in situ stress at the level of the underground laboratory. This is a way to control the effective stress conditions inside the clay sample. The observations made during these experiments confirm that gas migration in a low permeability medium, such as Boom clay, is non Darcian. In all experiments, breakthrough occurred at an almost zero effective stress. The gas flow rate through the clay sample was so high that it could not be attributed to a two-phase flow migration mechanism. This flow rate decreased as the pressure at the outlet face increased, and it finally reached an equilibrium. Figure 2 shows an example of an observed gas flow-rate evolution for sample 23B8K2. To diminish the scale effect due to the heterogeneity of the Boom clay, a set of three gas breakthough experiments on large clay cores (ϕ is 80 or 100 mm, length is about 300 mm) are in preparation. A total of seven clay cores have been taken in the test drift of the experimental gallery. Two different techniques were used: three samples were taken with a core drilling machine, and four other samples by pushing a stainless steel tube with cutting edges into the clay layer. Three isostatic cells were built, which will contain the large clay cores. An isostatic confining pressure of 4.5 MPa will be applied. The experimental setup for one isostatic cell is shown on Fig. 3. The clay consolidation will be monitored with a magnetic displacement transducer. To measure the water outflow, and to impose a constant water pressure equal to the in situ value at the outlet, a syringe pump will be used for the three systems. The gas injection at the inlet will be performed with the same kind of apparatus or an equivalent system.

3 Geotechnical experiments: triaxial (BGS)

The British Geological Survey has completed two long term experimental histories during 1994. The test T3S2 sampled parallel to the bedding, ran for 4 months and began (after sample consolidation) with a multi-stage hydraulic conductivity test. This consisted of an ascending and descending flow history with flow rates between 10 and 30 $\mu l.hr^{-1}$. At each stage, the hydraulic conductivity was calculated at steady-state conditions. Due to significant pyritic inclusions, the resulting relationship between the effective stress and the flow-rate was less pronounced than

previously recorded. The effect of these incipient features was most evident during the course of the gas injection phase. After an initial period of pressurisation, the gas pressure was held constant at the upstream face of the core. Classic breakthrough conditions were then observed when pumping resumed, shortly followed by an extended steady-state period and a shut-in observation. Re-pressurisation and a second breakthrough sequence were recorded at which point pumping ceased and a hydraulic pulse test began. Basic geotechnical parameters were calculated and the core photographed before storage. Test T3S3 sampled perpendicular to bedding ran for 8 months and was designed to study the hydraulic transport properties of the clay, in relation to the compaction stress state. Hydraulic conductivity measurements were made at various points in *stress space* as the sample was first moved back down its swelling rebound line, then on the VCL (virgin consolidation line) and finally back up a new swelling line. Hydraulic conductivity and specific storage contours were then calculated for the flow path in void ratio and effective stress space from both the consolidation and the flow test data. The sample was then moved back down the new rebound line and further conductivity measurements made. The analysis of this test and final conclusions will be presented when the testing procedure is complete.

4 In situ experiments (CEN•SCK)

It was decided to carry out hydraulic tests in E4, the multi screen piezometer installed at the bottom of the shaft. The purpose of these tests is to assess the coupling between hydraulic and mechanical effects i.e. to determine the correlation between the hydraulic conductivity and the effective stress and to test the "self-healing" capacity of the clay layer after a gas flow occurred by the creation of preferential pathways. Water will therefore be injected, or withdrawn, at different pressures with a syringe pump, and the variation of the mean hydraulic conductivity will be calculated. It is foreseen to operate these test in two different screens. A first choice has been made for a screen which did not show any pressure variation during the gas injection experiment of 1993. The results will be compared to those obtained from a second hydraulic test, performed in the gas injection screen. Some preliminary results shown on Fig. 4 and obtained from the tests performed in the unperturbated medium indicate a linear relationship between hydraulic conductivity and effective stress, up to about 0.6 MPa above the initial local pore water pressure. Above this pressure value, corresponding to the breakthrough pressure observed during the gas injection experiment, a discontinuity in the relationship is perceived i.e. the hydraulic conductivity is about fifty percent higher than expected. This can be an indication that the zero effective stress situation has been created.

A gas injection experiment has been performed in the new in situ gas injection setup E5. Helium has been injected in the filter that was used to perform the preceding hydraulic test. Starting from the initial pore water pressure value, we increased the gas pressure with a weekly increment of 0.1 MPa until the occurrence of a breakthrough was established. This breakthrough was detected after fourty-four days at a gas pressure of 2.36 MPa, i.e. 0.69 MPa above the original local pore water pressure. After the gas pressure was increased to 2.38 MPa, the formation of a preferential pathway between filters 20 (the injection filter) and 19 was established. This phenomenon occurred at the same gas overpressure than that observed during the gas injection in E4. The pathway extended later to filter 18 and 21, both located on the injection piezonest, after the gas injection pressure was increased to 2.53 MPa. The pressure evolution in filters 18, 19, 20 and 21 is shown on Fig. 5.

It was decided to perform hydraulic tests in the gas injection screen immediately after the gas injection experiment. The tests are similar to those carried out in E4, but the water injection is here performed with the gas injection device. The water flow-rate is monitored with the magnetic displacement transducer and the pore water pressure in the neighbour filters is measured with

pressure transducers.

5 Two-phase flow modelling (INTERA)

Given the current debate about the validity of the Darcy two-phas flow models to simulate gas migration in very low permeability media, such as Boom clay, alternative modelling approaches have been examined. One alternative is to use a capillary bundle approach. In these models an ensemble of capillary tubes provides an idealized, topological representation of the available pathways for gas migration in a medium. The ensemble consists of capillaries with different radii, with the radii distributed according to a probability distribution function, which may be determined from analysis of data from gas migration experiments [1]. Such models have been used to simulate the saturation and desaturation of bentonite layers, and can model the hysteresis behaviour dependent on wether saturation is increasing or decreasing [2].
Consider a single capillary of given length and radius, with gas at a given pressure at one end and water at a given pressure at the other. The water pressure at the gas/water interface is equal to the difference of the gas pressure and the capillary pressure. This means that the pressure drop along the water column is known. Assuming the water flow is unidirectional, the total water flux through the capillary can be computed by solving the steady-state Navier-Stokes equations. Applying a pseudo steady-state approximation means that these equations can be applied to describe the water flux arising from the motion of a gas/water interface along a capillary. The interface velocity is given by the flux value averaged over the cross-section of the path-leg in which the interface is situated. The total migration of gas through the bundle of capillaries is simulated by computing individually the position of the gas/water interface. Quantities such as the water saturation level at a given distance along the capillary bundle can then be computed by summing the contributions from all capillaries in which the gas/water interface position is less than this distance along the capillary bundle.

6 Conclusion

The reaction capacity of undisturbed clay towards hydrogen is negligible. Though, the presence of methanogen and sulfate-reducing bacteria could induce a consumption of the produced hydrogen. This is a favourable issue concerning the gas migration in the host rock of a waste repository.
The gas injection experiments peformed in laboratory and in situ confirm that gas will only migrate, in significant quantities, by the formation of preferential pathways once the effective stress is annihilated. Preliminary in situ hydraulic tests confirm this hydro-mechanical behaviour of Boom clay, but more experimental data are necessary to quantify the link between hydraulic and geomechanical parameters of Boom clay.
Due to its lower local effective stress distribution, the excavation disturbed zone is expected to concentrate the major pathways. The addition of a swelling backfill material is required to reduce this effect by increasing locally the effective stress distribution. So, further gas migration experiments and hydraulic tests on backfill material will be needed.
Further modelling work is needed. The two-phase flow code TOPAZ will most probably be abandoned in favour of a capillary bundle model. The experimental data collected from the gas breakthrough experiments realized on large clay cores will serve to verify and validate the model.

7 References

[1] M.D. Impey and H. Takase
Scoping calculations for gas migration in the Rokkasho-mura shallow land burial Phase II facility.
ID3577-6 Version 1, September 1993

[2] P. Grindrod, M. D. Impey, S. Saddique and H. Takase
Saturation and gas migration within clay buffers.
High Level Radioactive Waste Management
Proceedings of the fifth annual international conference
Las Vegas, Nevada, 22 to 26 May 1994

List of publications

[1] G. Volckaert, K. Bateman, V. Fioravante, M. Impey, K. Worgan
MEGAS - Modelling and experiments on gas migration in repository host rocks
Semestrial Progress Report 1993, first semester
Contract no. FI2W-CT91-0076
Ed.: SCK•CEN R2976, 1994

[2] L. Ortiz, G. Volckaert, P. De Cannière, M. Put, J. Harrington, S. Horseman, V. Fioravante, M. Impey, K. Worgan
MEGAS - Modelling and experiments on gas migration in repository host rocks
Pegasus meeting 26 to 27 May 1994, University of Exeter

[3] L. Ortiz, G. Volckaert, M. Put, M. Impey
The MEGAS E5 experiment: a large 3-D in situ gas injection experiment for model validation
Proceedings of GEOVAL '94 : An international symposium on validation through model testing with experiments, Paris, 11 to 14 October 1994, OECD

[4] S. Horseman and J. Harrington
Migration of repository gases in an overconsolidated clay
British Geological Survey technical report, WE/94/7

[5] G. Volckaert , M. Put , L. Ortiz , P. De Cannière , S. Horseman , J. Harrington , V. Fioravante , M. Impey and K. Worgan
MEGAS - Modelling and experiments on gas migration in repository host rocks
Annual progress report, XII/423/93-EN

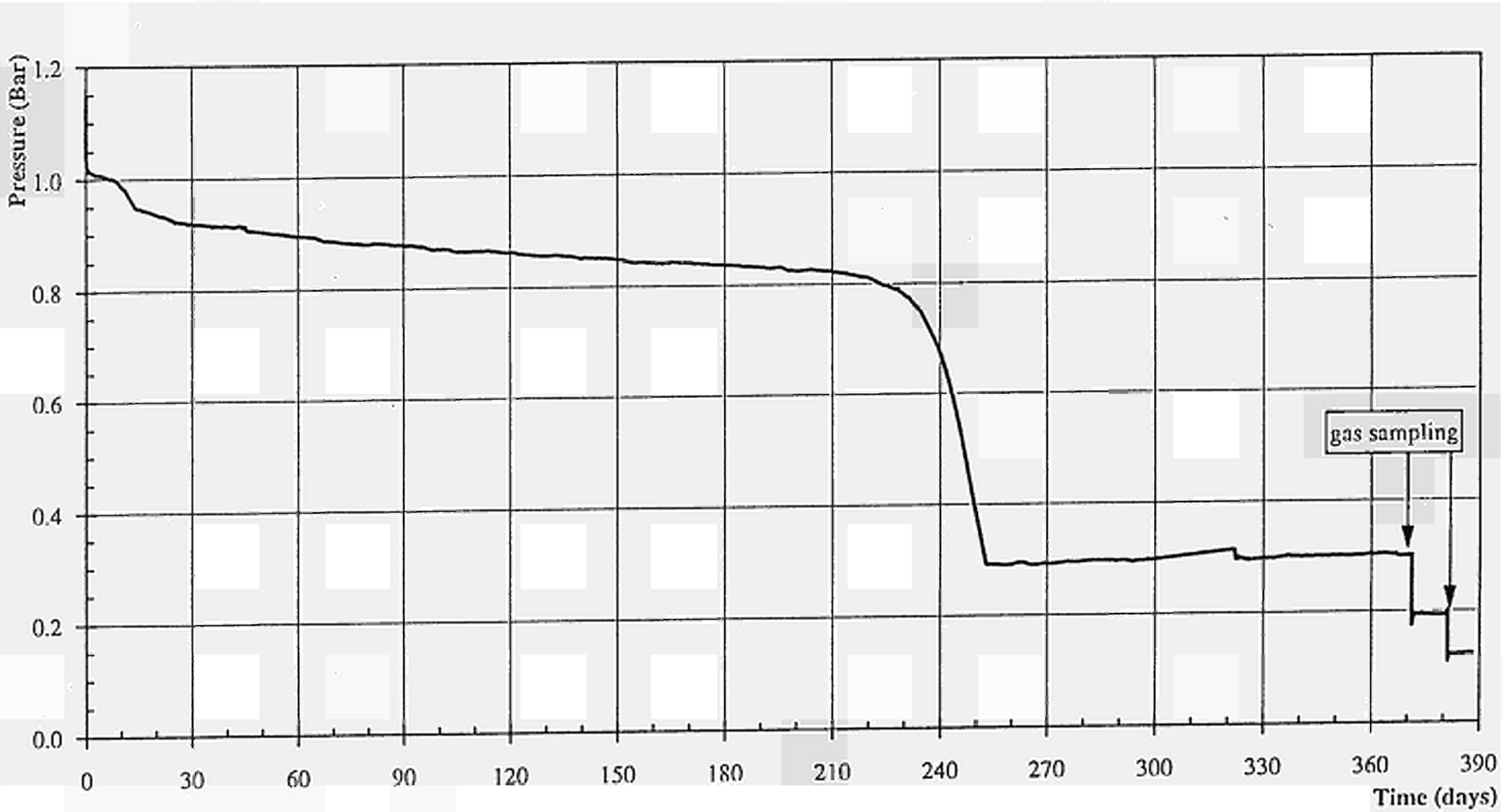

Figure 1 Evolution of the gas pressure in the experiment Megas N° 11 (reaction E1 between Boom clay and hydrogen) as a function of time. Pressure corrected at 25 °C.

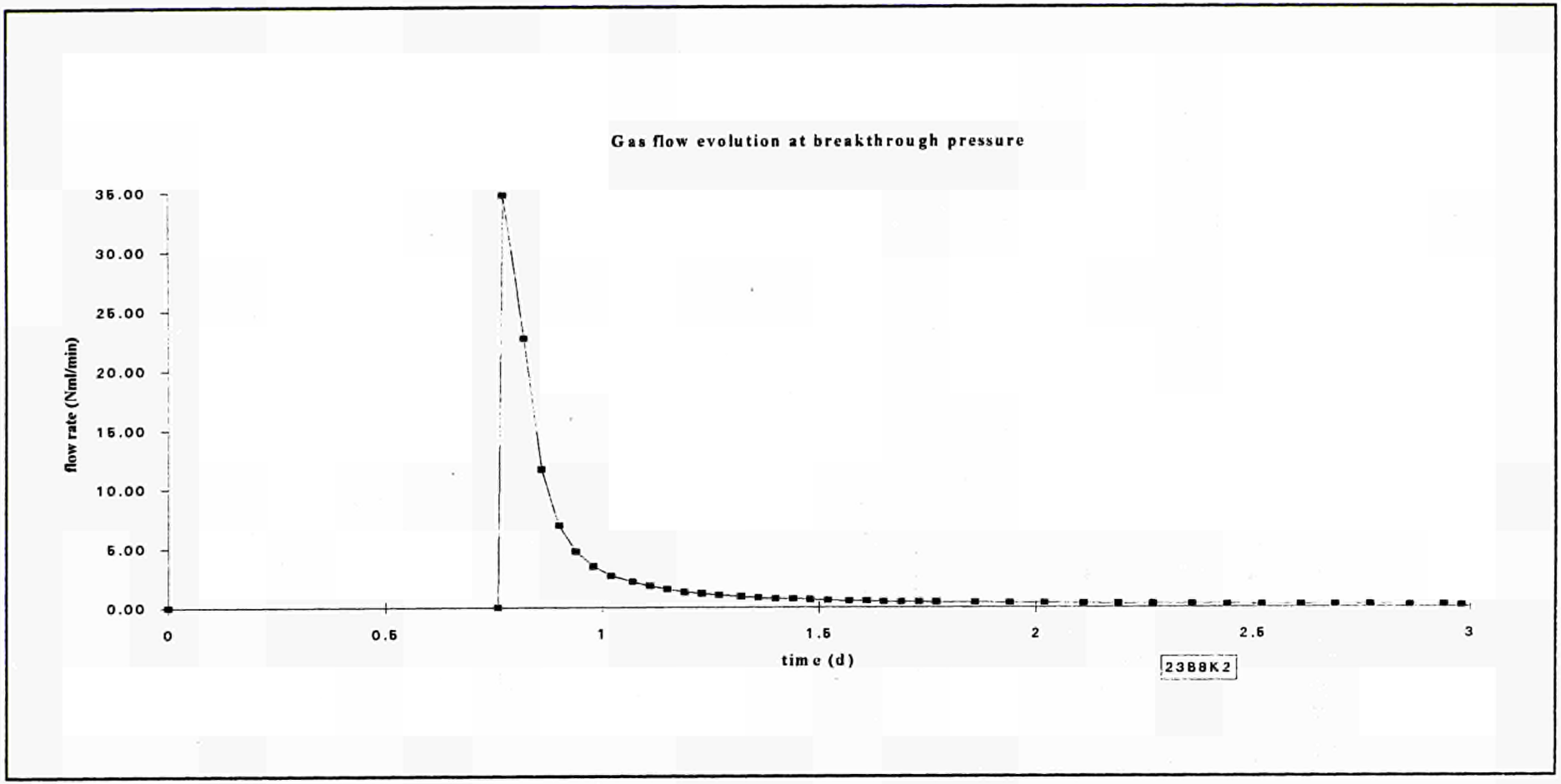

Figure 2 Gas flow-rate evolution at breakthrough pressure in clay sample 23B8K2

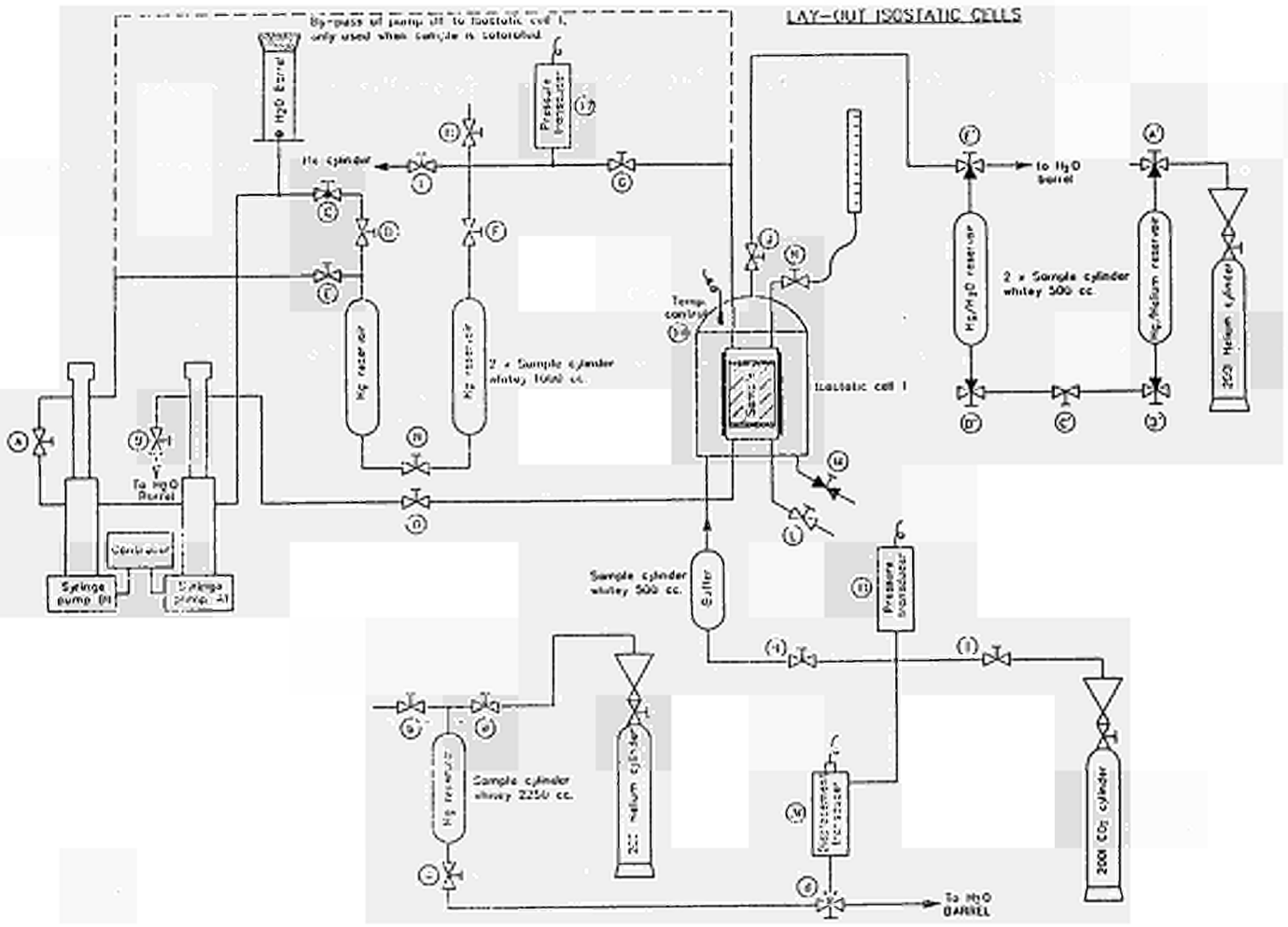

Figure 3 Sample feed system for the isostatic cell no. 1

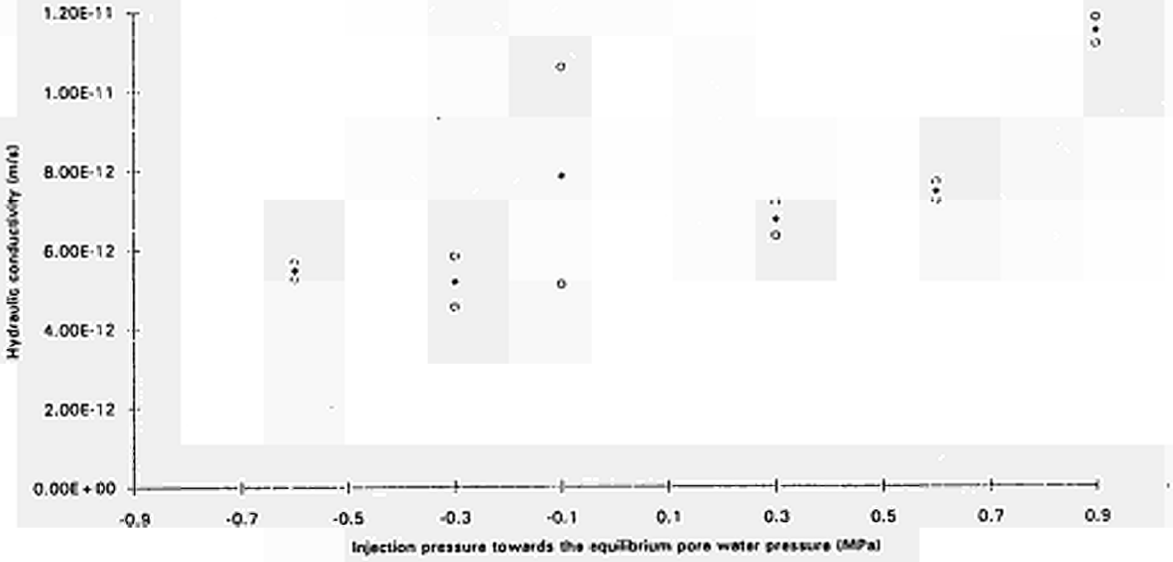

Figure 4 Calculated mean hydraulic conductivity and standard deviation in E4, as a function of the injection pressure given relatively to the local initial pore water pressure

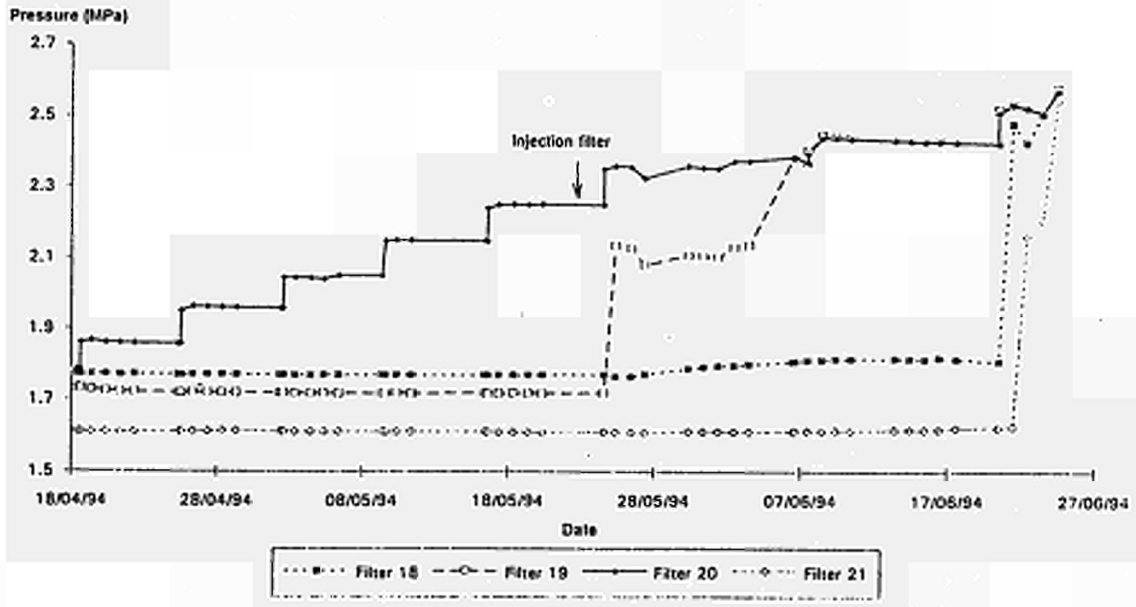

Figure 5 Pressure evolution in filters 18, 19, 20 and 21 of the central piezonest during the gas injection experiment realized in E5

Title	**Gas Pressure Build-up in Radioactive Waste Disposal and Mechanical Effects**
Contractor	GEOSTOCK, France
Contract N°	FI2W-CT91-0093
Duration of contract	July 1991 - December 1994
Period covered	January 1994 - December 1994
Project leader	T. Manai

A. OBJECTIVES AND SCOPE

The specific aim of this study is to evaluate the consequences of gas generation from a radioactive waste repository. The evaluation will be carried out in terms of gas migration in the backfill and host rock and in terms of mechanical effects.
The phenomenology of the physical process involved in gas transport will be reviewed, then some selected numerical codes taking into account two-phase flow will be presented. The gas pressure build-up will be simulated for different designs of repository and different host rock characteristics using numerical two-phase flow models such as the reservoir simulations used in the oil industry.
The mechanical modelling using new theoretical developments for fracture initiation and propagation through bifurcation theories will be carried out with the co-operation of the French Petroleum Institute (IFP).

B. WORK PROGRAMME

The work is divided into Work Packages (WP):

WP1 Phenomenology review: inventory of two-phase flow phenomenology applied to gas migration from a radioactive waste repository.
WP2 Laboratory experiment: limited number of investigations on representative host rock core samples.
WP3 Two-phase flow modelling.
WP4 Mechanical modelling developments: theoretical work for the elaboration of a new criterion for fracture initiation and propagation.
WP5 Gas generation risk.
WP6 Final report and conclusions.

C. PROGRAMME OF WORK AND OBTAINED RESULTS

State of Advancement

The main activity over the last year was devoted to designing and performing the experimental tests and analysing the gas generation risk by simulating gas migration from a different types of radioactive waste disposal.
The situation is as follows:

WP1	*Completed 1991*
WP2	*Completed mid-1994*
WP3	*First part completed 1991*
WP4	*2D modelling completed 1992*
	3D modelling completed 1993
WP5	*Completed (1994)*
WP6	to be completed .

Progress and results

C1. Laboratory Experiment(WP2)

C1.1.Experimental Methodology and Procedure

In order to obtain data on various types of host rock, it was found necessary to undertake laboratory tests on representative samples. The study was approached on the basis of standard experimental procedures in widespread use in the oil industry and involved the following steps:

i)In the absence of test specimens of the specific rocks, a set of specimens was selected to cover the permeability range 10-2mD to 10-4mD as an approximation, in terms of permeability, to the petrophysical properties of potential host rocks.

ii) Capillary pressures were measured with an air/mercury fluid system as the air was entering and being expelled from the specimens, to determine inter alia the displacement pressures.

iii) Displacement pressure was measured with a water/helium system on one of the specimens, in order to reproduce conditions similar to those encountered in alpha-type radioactive waste repositories.

The analytical procedures for all these steps are briefly summarised in Table1.

TABLE 1. *Laboratory Test Procedures*

SPECIMEN SELECTION

Measure Air Permeability

1)Dry specimen between 40°C and 70°C.
2)Set up specimen in Hasler cell at 20bar pressure.
3)Measure gas permeability (Kg at increasing gas flows (Qg)

Measure Porosity and Void Ratio

4)Helium densimeter test.

AIR/MERCURY CAPILLARY PRESSURES

1)Place dry specimen in cell and evacuate to 10-3 torr for 2 hours.
2)Set cell horizontal and measure pressure and volume of mercury injected.

DISPLACEMENT PRESSURE

1)Set up specimen in isotropic-stress cell.
2)Apply constant 80 bar stress with cell vertical.
3)Measure helium driving pressure and displaced water (if any).

C1.2. Discussion of Results

Sample Selection

The rock specimens had to be similar to the host rock around the projected repository, especially in

terms of permeability. Ten specimens were first selected and their permeabilities to air at constant pressure was determined. The final list contained three specimens, a carbonate rock (Specimen 2), a marl (Specimen 3) and a marly limestone (Specimen 6).
These samples were chosen chiefly to cover the whole range of permeabilities of concern in the study. Additional standard determinations were also made on all three specimens, such as dry weight, total volume and total volume of solid material in order to determine density, porosity and pore volume. Table2 lists the leading features of the specimens used for capillary pressure measurements.

Table 2. *Properties of Three Specimens*

Specimen	Permeability mD	Density g/cm^3	Porosity (%)	Pore Volume cm^3
2	6.0E-2	2.69	11.30	8.206
3	6.3E-4	2.71	0.80	0.509
6	1.E-3	2.71	4.36	2.574

Air/Mercury Capillary Pressure

The method of measuring capillary pressures was based on injecting mercury into the specimen (Purcell's method). There were two main reasons for this choice:

1) The equivalence between water/air and water/hydrogen interface surface tensions at 20°C make for convenient conversion to the water/air system.

2) The method is much easier to operate in the laboratory than other methods.

Using this method, the technique was to inject mercury (outward air flow curve) up to a pressure of close to 350bar, then to withdraw it (inward air flow curve) by dropping the pressure back to its initial value. Once the capillary pressure curves had been obtained for the air/mercury system, they were converted to find water/hydrogen system values. The conversion was based on the ratio between mercury/air and water/air interface surface tensions.
The standard capillary pressure curves for inward and outward air movements and illustrates the different behaviour of the three specimens. The displacement pressure can be derived from such curves, i.e. the pressure at which mercury (in the present tests) begins to displace the air from the pores of the specimen.
For the carbonate rock (Specimen 2), the outward air flow capillary pressure curve can be schematically subdivided into three phases:

1)The initial portion in which the percent mercury saturation is very low, up to a pressure of around 0.4bar.

2)The central portion of the curve, featuring three breaks in slope (at 10%, 32% and 80% mercury saturation). The displacement pressure corresponds to the second break where the mercury has not yet displaced the air from the specimen but has simply occupied the superficial pores unoccupied by the vapour.

3)The end of the curve is an asymptote to maximum (100%) saturation.

With the marl (Specimen 3), the outward air flow capillary pressure can also be broken down into three distinct phases:

1)The first part of the curve up to 1.7bar approx. while mercury saturation is less than 0.3%.

2)The central, erratic part of the curve, up to about 22% mercury saturation.

3)The more or less straight terminal part which is distinctly less steep than the mid-curve portion.

The break between the central and terminal portions represents the displacement pressure.
The outward air flow capillary pressure curve for the marly limestone (Specimen 6) also displays three parts:

1)Initial portion up to 0.7bar approx., at low mercury saturation.

2)Central near-vertical portion up to 150bar pressure when mercury saturation is slightly more than 2%. This represents the displacement pressure for the air/mercury system.

3)Terminal portion rising steadily from 150bar to 350bar and mercury saturation of up to 70% of the pore space.

These outward air flow capillary pressure curves should be viewed beside the pore size distribution

curves and the idea of pore interconnection, since the above observations can be explained by:

-a high proportion of small pores in Specimen 6, requiring a high pressure for the mercury to penetrate, and

-a more balanced mix of pore sizes in Specimen 3 and, more markedly, Specimen 2, which explains the ease with which the mercury penetrated the pores.

Table 3 lists measured displacement pressures for the air/mercury system and calculated displacement pressures for a water/air system based on the ratio between interface surface tensions (which is 6.59).

Table 3. *Displacement Pressures for Specimens Tested*

Specimen	Water/Air Displacement Pressure (bar)	Air/mercury Displacement Pressure (bar)
2	9.1	60
3	18.2	120
6	22.8	150

The inward air flow capillary pressure curves for the three specimens show that, as would be expected, the rock captures some of the mercury with more than 50% being irrecoverable except from the marly limestone (Specimen 6).

Permeability/Displacement Pressure Correlation

In order to assess the consistency between displacement pressure/permeability correlations from the laboratory tests and the calibration equation put forward in Report GK/RDD-92/024, i.e. (cf. C.K. Thomas, D.L. Katz and M.R. Tek, SPE Journal, June 1968) (Pc)T = 7.37 (1/K)0.43

It should be noted that the water permeability values used for plotting this curve were derived from measured air permeabilities, using the following conversion formula (cf. Klinkenberg effect)

Kw = Ka / [1 + (b/Pm)]

in which b = 0.77 Kw-0.39 (approximate constant J for a gas/solid system ...)

Pm is the mean pressure of gas flowing through a porous material (in atm) Kw and Ka are in mD.

C1.3Proposed Gas Migration Modelling

In the gas migration modelling, the gases from the radioactive waste repository are assumed to have formed already, so that it ignores the many potential gas formation mechanisms. The modelling concerns itself only with the migration of the newly-formed gases into the rock.

For successfully running the model and solving the equations, the flow equations in particular, it is necessary to know a certain number of constitutive equations for the material(s) involved. In the case of gas migration from an alpha-type radioactive waste repository, we must know the relative permeability and capillary pressure equations. The laboratory determinations described above will thus provide a valuable data set for the gas migration model.

Table 4 summarises the properties of the three gases selected for test. These properties, together with the capillary pressure Vs saturation curves and relative permeability Vs saturation values (Table 5) will provide input for the next step of modelling the gas migration process.

Table 4. *Test Specimen Properties Permeabilities from BEICIP*

Specimen	air Permeability mD	Water/Air Displacement Pressure (bar)	Water/Air Displacement Pressure (Psi)
2	6.0E-2	9.1	132
3	6.3E-4	18.2	264
6	1.E-3	22.8	331

Table 5. ***Water and Gas Relative Permeabilities Vs Percent Saturation with Water***

Specimen	Swi (%)	Sgc	Pore Index I
Clay	10	3	5.55
Sandstone	30	6	1
2	3.16	43.93	5
3	(10)	47.42	5.5
6	(15)	67.06	5.5

Sgc Critical gas saturation (or residual saturation)
Swi Irrecoverable liquid saturation
Sw Water saturation
I Pore Index

C2 Risk Analysis of gas migration

C2.1.Introduction

On the basis of two repository designs, three types of host rocks, and two gas rate histories, twelve problems have been simulated using a two-phase flow numerical model. In all these problems, the same initial conditions have been applied and the simulation have been run over a period of 100,000 years starting at the beginning of gas release.

Simulation results consist of saturation maps, which give grid-block gas saturations at some relevant time-steps (e.g., at gas rate changes), and gas pressure curves which give the gas pressure at each time step in some relevant grid-blocks (e.g., inside the storage cavities).

C2.2 Case study definition

Each case study is based on a repository type, a set of host-rock petrophysical properties, and a gas rate scenario. With two possible types of repository, three available sets of petrophysical properties, and two different gas rate scenarios, a total of twelve case studies have been simulated.

C2.3 Repository and domain descriptions

C2.3.1 First type of repository

The first type of repository consists of an infinite number of parallel storage galleries of infinite length. All galleries are located at the same depth (top at a depth of 500 m) and the gallery spacing is regular. A field wide horizontal aquifer is considered 200 m above the galleries (depth of 300 m), an infinite domain being assumed below.

The gallery sections are approximated by square sections of 10×10 m^2 and the gallery spacing (from side to side) is 25 m. The waste canisters fill 60% of the gallery section, backfill materials (sand) occupying the other 40%.

All flows being in vertical plans perpendicular to the galleries, such a three-dimensional (3D) problem can be modelled as an equivalent two-dimensional (2D) one in which a vertical domain cross-section, perpendicular to the galleries, only needs to be represented. In addition, vectical symmetry plans allow limiting the 2D space to a finite domain involving half a gallery section.

C2.3.2- Second type of repository

The second type of repository involves *passage galleries* along which regurlarly spaced vertical storage cavities are hollowed out. An infinite number of passage galleries of infinite length is considered. All galleries are located at the same depth (top at a depth of 500 m) and the gallery spacing is regular.
A field wide horizontal aquifer is assumed 200 m above the galleries (depth of 300 m), the domain being infinite downwards.
The gallery sections are approximated by rectangular sections of 4×6 m^2 and the gallery spacing (from side to side) is 41 m. The storage cavities are modelled as vertical rectangular boxes 35 m height with a square section of 1.3×1.3 m^2. Caps 10 m long are at the top of the cavities. The cap material is supposed to have host-rock's petrophysical properties (especially the same low intrinsic permeability). The remaining 25 meters of cavities are filled in equally with waste canisters and backfill materials (sands).

Vertical symmetry plans parallel and perpendicular to galleries allow limiting the study to a finite domain involving half a gallery section and a quarter of a cavity section.

C2.4 - Rock petrophysical properties

C2.4.1 Data's origin
See the above description

C2.4.1.1 - First rock sample (#2)

The first rock sample is a carbonate. It shows the highest permeability (6 10^{-2} mD) and porosity (11.3 %), and the lowest gas threshold pressure (9.1 bar). It is therefore the most suitable rock type for gas flow, and probably the least appropriate one for radioactive waste repository purposes.

C2.4.1.2 Second rock sample (#3)

The second rock sample is a marl. Unlike sample #2, it shows the smallest permeability (6.3 10^{-4} mD) and porosity (0.8 %). While a low permeability leads to small gas flows, a very low porosity, as this is the case here, means very small pore volumes and thus abilities for rapid gas displacements which may not be suitable. The gas threshold pressure, however, is more than twice bigger than sample #2's one (19.7 bar).

C2.4.1.3 Third rock sample (#6)

The third rock sample is a marly limestone which shows some intermediate rock properties with an intrinsic permeability of 10^{-3} mD and a porosity of 4.4 %. The gas threshold pressure, however, is the highest one (22.8 bar).

C2.5- Backfill material properties

In both types of repositories, galleries and cavities are filled in with either waste canisters and backfill materials, or backfill materials only. At the exception of the cavity caps in the second type of repository, all backfill materials are supposed to be sands. The following basic sand properties are considered.

•Intrinsic permeability = 100 mD
•Porosity = 18 %
• Gas/water capillary pressure = 0 bar (for all water saturation values)
•Critical gas saturation = 0
• Relative permeabilities = linear functions of water saturation
• Irreducible water saturation (fraction) = 0.01
•Compressibility = 10^{-3} bar

As for cavity caps, we assume the backfill materials to be re-compacted host-rock with same petrophysical properties.

C2.6 Fluid properties

The two fluids here considered are water and hydrogen gas (H_2). PVT, viscosity, and gas solubility tables are used.

C2.7 Sources of gas

The gas release originates from two major mechanisms. One is the steel corrosion of canisters; the other one is the radiolysis of water by nuclear radiation. The evaluation of gas rates is far beyond the scope of the present study. The following gas rates were therefore widely inspired from the bibliography.

Two gas rate scenarios are considered for each type of repository.

C.2.7.1First type of repository

•**First gas rate** scenario; rates are per unit length of storage gallery:

from 0 to 1 year, $Q = 8.3\ 10^{-2}$ Nm^3/day
from 1 to 50 years, $Q = 2.0\ 10^{-2}$ Nm^3/day
from 50 to 10,000 years, $Q = 1.1\ 10^{-2}$ Nm^3/day

•**Second gas rate** scenario; rates are per unit length of storage gallery:

from 0 to 10 years, $Q = 8.3\ 10^{-2}$ Nm^3/day
from 10 to 50 years, $Q = 2.0\ 10^{-2}$ Nm^3/day
from 50 to 10,000 years, $Q = 1.1\ 10^{-2}$ Nm^3/day

C.2.7.2Second type of repository

•First gas rate scenario; rates are per storage cavity:

from 0 to 1 year, $Q = 2.7\ 10^{-2}$ Nm^3/day
from 1 to 50 years, $Q = 5.1\ 10^{-3}$ Nm^3/day
from 50 to 10,000 years, $Q = 2.1\ 10^{-3}$ Nm^3/day

•Second gas rate scenario; rates are per storage cavity:

from 0 to 10 years, $Q = 2.7\ 10^{-2}$ Nm^3/day
from 10 to 50 years, $Q = 5.1\ 10^{-3}$ Nm^3/day
from 50 to 10,000 years, $Q = 2.1\ 10^{-3}$ Nm^3/day

C2.8Two-phase flow simulations

C2.8.1 Presentation of the flow simulator

GENESYS has been used as a two-phase flow simulator (two phases and two components). The simulations are based on a standard (control-volume) finite-difference approach and block-centred grid systems (i.e., gas and water pressures are computed at grid-block centers).

As this was required, GENESYS takes into account relative permeability and capillary pressure functions, fluid PVT functions, and a gas solubility function.

C2.8.2 Boundary conditions

The same boundary conditions apply to all case studies. They consist of no-flow boundary conditions (Neumann conditions) assigned to the domain's boundaries.

Between 0 and 300 m depth, however, a high permeability aquifer, with high porosity, is re-presented, which allows simulating a constant water pressure condition at a depth of 300 m.

A high porosity layer also has been introduced far enough below the storage cavities. Such a layer, which has a same low permeability as the host-rock, aimed at simulating an infinite domain downwards.

All gas sources are located inside storage cavities.

C2.8.3 Initial conditions

We assume that the whole field, including the host-rock and the backfill materials, is fully saturated with water.

In all case-studies, a "two-aquifer" system had to be used to define suitable initial conditions. One of the aquifer is comprised of the galleries and cavities. The other one includes the host-rock domain and the (real) top aquifer.

The initial condition applying to the first aquifer is an hydrostatic condition with the atmospheric pressure set at the topmost point of the aquifer (i.e., at a depth of 500 m).

The initial condition on the second aquifer is an hydrostatic condition too, but with the atmospheric pressure set at the surface (i.e., at a depth of 0 m).

C2.9 SIMULATION RESULTS FOR THE FIRST TYPE OF REPOSITORY

Which simulation results ?

Our interest will more particularly bear on the following points.

1. Time at which the storage galleries are fulled of gas.
2. Time at which gas starts flowing through the host-rock (i.e., gas saturation over the critical gas saturation).
3. If the gas reaches the top aquifer and at what time this happens.
4. Pressure build-up in cavities and pressure difference between gas in and water out of the cavities.

Gas saturation maps have been edited at 1 (or 10 years for the second gas rate scenario), 50, 1 000, 2 500, 5 000, 7 500, 10 000, 50 000, and 100 000 years.

Besides pressure values versus time, such graphes allow determining when storage cavities start to be full of gas. Indeed, in most case studies, within cavity gas pressure and near cavity water pressure tend to become equal after some few months or years and remain quite close as long as the storage cavity is filling in with gas. When the cavity is full of gas, **a rapid increase(Gas Pressure Build-up)** of within cavity gas pressure then occurs to overcome the host-rock's gas threshold pressure and to allow gas flowing out of the cavity through the host-rock.

Six case studies have been simulated for the first type of repository.

C2.10 SIMULATION RESULTS FOR THE SECOND TYPE OF REPOSITORY

Which simulation results ?

Our interest will more particularly bears on the following points.

1. Time at which the storage cavities are fulled of gas.
2. Time at which gas starts flowing through the host-rock (gas saturation over the critical gas saturation).
3. Time at which gas reaches the passage galleries.
4. If gas reaches the top aquifer and, if so, time at which this happens.
5. Pressure build-up in storage cavities and pressure difference between gas in and water out of the cavities.

Gas saturation maps have been edited at 1 (or 10 years for the second gas rate scenario), 50, 1 000, 2 500, 5 000, 7 500, 10 000, 50 000, and 100 000 years.

Six case studies also have been simulated for the second type of repository.

C2.11 ANALYSIS OF SIMULATION RESULTS

From the twelve gas release problems which have been simulated, conclusions can be drawn regarding the possible influence of rock petrophysical properties, gas rates, or repository concepts on gas migration and gas pressure build-ups. The main conclusions are discussed in the present section.

C2.11.1Influences of the repository type

The simulation results are quite different from one repository type to an other.

On the one hand, all the simulations involving the first type of repository show that gas reaches the top aquifer before 1 000 or 2 500 years. Although such a result is relevant only for the rock petrophysical properties and gas rate scenarios here considered, it remains unacceptable and rises the problem of suitability of this type of repository for radioactive waste purposes.

On the other hand, the second type of repository gives much better results in terms of both pressure build-ups and gas migration. The most favourable cases, for which gas never reaches the top aquifer and remains confined under a depth of 460 m, are obtained when the petrophysical properties of the third sample (#6) are assigned to the host-rock.

Actually, the main difference between the two repository concepts lies in passage galleries which are involved in the second type of repository. Although such galleries have no purpose but that of waste canister transport facility, they influence quite a lot water and gas flows in such a way which makes the second type of repository more suitable regarding gas migration and pressure build-up. Three relevant aspects of passage galleries allow understanding their propitious effects.

1.Being located in between storage cavities and the top aquifer, the galleries lie on (natural) gas streamlines and thus can easily drain gas.
2.The high porosity and permeability of the backfill material and its very low gas threshold pressure make the galleries suitable as gas storage tanks.
3.In addition, the galleries being very close to (canister) storage cavities, they tend to slow down and break the pressure build-ups of both water near cavities and gas in cavities.

C2.11.2Influences of rock petrophysical properties

As this was above discussed, host-rock petrophysical properties are essential since they condition flows around the cavity. From the twelve simulated problems, favourable rock properties can be derived. If the objective is to limit as much as possible gas migration (i.e., avoiding gas flowing too far from cavities), some or all of the following conditions should be met.

1. Very low intrinsic permeability (for lowering flows)
2. High porosity (for lowering flow velocities[1])
3. High gas threshold pressure (for better confining gas in cavity)
4. Flattened relative permeability curves (for lowering **gas** flows)

Note, however, that the above conditions 1, 3, and 4 usually lead to higher gas pressure build-ups which might be unsuitable in some cases (for example, for rock stability reasons).

C2.11.3 Influences of gas rate scenario

As boundary conditions, within cavity gas rates are of paramount importance. Unfortunately, they result from complex physical (e.g., water radiation) and chemical (e.g., steel corrosion) phenomena which cannot really be controlled. Practically, in order to modify the gas rates, one can either prefer a different type of canisters (e.g., smaller volume or area, smaller steel thickness), use a different type of radioactive wastes (e.g., re-compacted wastes), or change the cavity dimensions or the number of canisters (i.e., increasing or decreasing the relative volume occupied by canisters in cavity). By so doing, gas rates can be changed, but the problem to be simulated also becomes different.
In the present study, the sensitivity analysis to gas rates has been evaluated by changing the duration of the first high rate period which is of one year in the first scenario, and of 10 years in the second scenario. Beside the times required to fill up cavities with gas, the main differences from one case to an other were related to **gas and water pressure build-ups**. **No noticeable differences were observed on gas saturation maps**.
The latter result does not mean that gas rates are of secondary importance compared to the repository design or to rock petrophysical properties. It just tells us that the initial gas rates (say, during some few years) have few effects on long term (say, several thousands of years) gas saturation distributions.
A good evaluation of gas rates and gas rate changes with time, therefore, remains essential to simulate the right flow problem.

REFERENCES

[1] THOMAS, L K, KATE, D L, Threshold Pressure Phenomenon in Porous Media; SPE, June 1968
[2] BROOKS, R H, COREY, A T, Properties of Porous Media Affecting Fluid Flow; Jour. Irrigation & Drainage Div., Proc ASCE, June 1966
[3] LEVERETT, M C, Capillary Behaviour in Porous Solids; Tulso Meeting, Oct 1940
[4] KATZ, D L: Properties of Reservoir Rock (Chap 2), McGraw Hill, NY, 1959
[5] BREITENBACH, E A, THURNAV, D H, Van POOTEN; SPE 2019

Title :	Salt Permeability in-situ test (Amélie Mine - France)
Contractors :	ANDRA and G.3S
Contract N° :	FI2W-CT91-0101
Duration of contract:	March 1992 - August 1995
Period covered:	January 1994 - December 1994
Project leader:	J.F. LAURENS (ANDRA), A. COURNUT (ANDRA)

A. OBJECTIVES AND SCOPE

The purpose of the in situ test that is performed in the MDPA Amelie Mine is to measure the gas permeability of a rock salt bed previously submitted to a brine percolation.

This is of major importance for predicting the behaviour of gases present in the repository (gas coming from radiolysis, corrosion, bacteriological activity, trapped air...).

As the measured quantities will be very low, the choice of experimental parameters should allow to eliminate, minimize or quantify all the indesirable effects in order to facilitate data interpretation.

The scientific interpretation of the results will be made by G.3S.

B. WORK PROGRAM

The initial work program was :

1 - Pre-feasibility tests in order to validate the experimental device (tightness of the borehole system, accuracy of the measurements, etc...).

2 - Pilot test in borehole n° 1, with brine, increasing the pressure till fracture occurs in the rocksalt.

3 - Test in borehole n° 2 including :

- measurement of gas permeability;
- injection of brine and measurement of brine permeability;
- emptying of the borehole and measurement of gas permeability.

After cost evaluation of the pre-feasibility tests, it has been decided to reduce the work program in 93 in order to remain within the financial limits of the contract.

The pilot test to find the point of fracturing the rocksalt was cancelled. Only one borehole will be used for the entire test program.

C. PROGRESS OF WORK AND RESULTS OBTAINED

The following steps were achieved in 1993 :

- Specifications of the test site and of the experimental device defined;
- Technical procedures of the test written;
- Test site prepared and borehole done in the Amélie Mine (September to December);
- All parts of the experimental device ordered.

During the first half of the year 1994, the injection system for gas and brine as well as packers were tested in laboratory.

The entire system was installed and tested at the test site in July 94. After a few adjustments, the first experiment started in October 94.

1. SPECIFICATIONS OF THE TEST SITE

1.1 Dimension of the test site

The test site is located in an existing gallery named "voie au mur JOSEPH". Its dimensions are :

length	:	4.0	m
width	:	2.0	m
height	:	3.35	m

It includes all the experimental devices and the borehole.

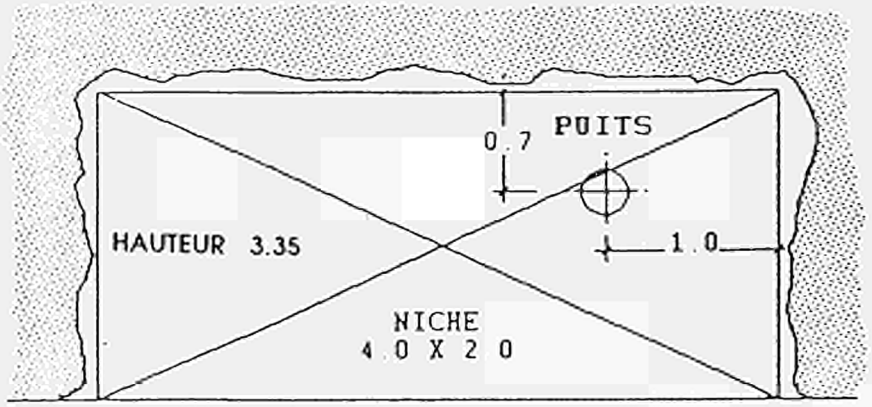

EXISTING GALLERY NAMED
"VOIE AU MUR JOSEPH"

1.2 Borehole specifications

The borehole length is 17.5 m. Its diameter 146 mm in the lower part. Only the last 6 meters are cored.

At the top of the borehole a casing is sealed to the rock. The quality of the borehole wall must be very good in order to ensure a perfect gas and brine tightness of the packers system. This point was verified by endoscopy.

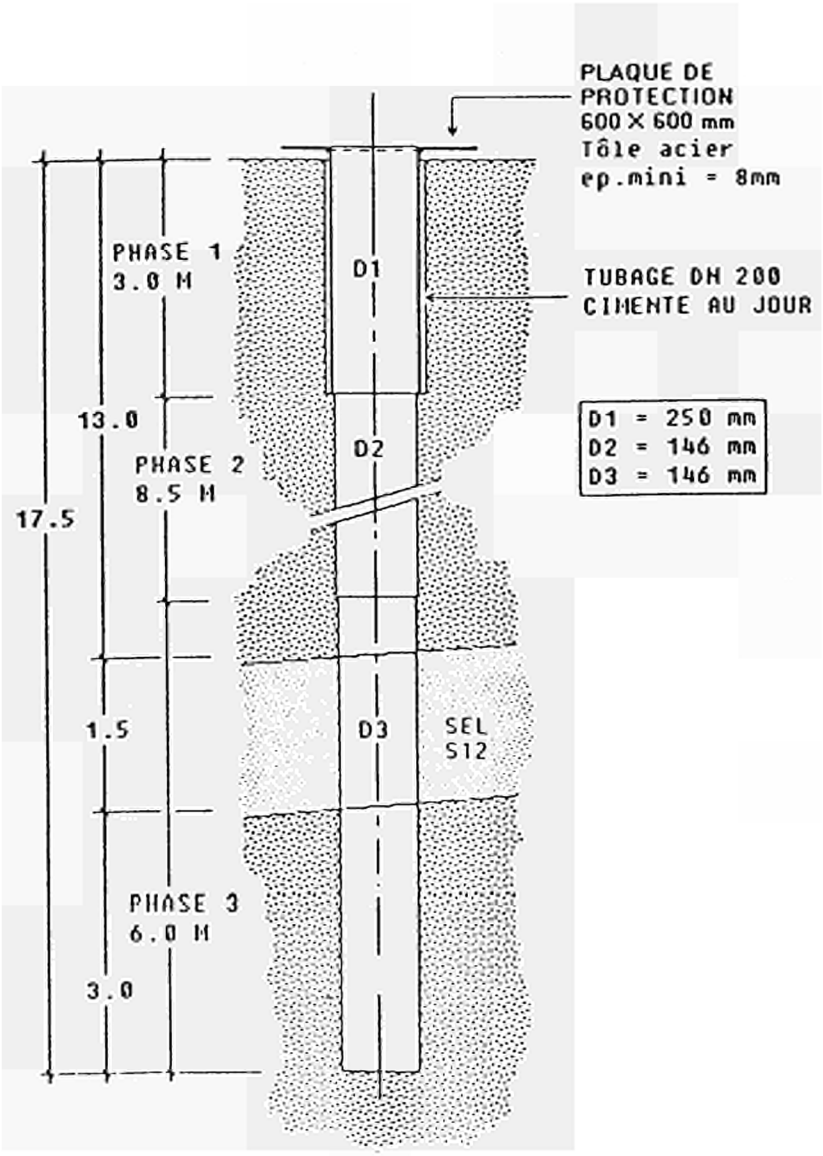

2. SPECIFICATIONS OF THE EXPERIMENTAL DEVICE

2.1 Shutter system

The length of the experimental chamber was defined after the endoscopy of the borehole (= 0.75 m). Two double packers systems are used to insure the tightness of the chamber.

Each system is 1 m long including two inflatable packers 0.2 m long separated by a 0.6 m long chamber that was injected with a special polymeric resin.

Eight injection or control pipes connect this system to the top of the borehole.

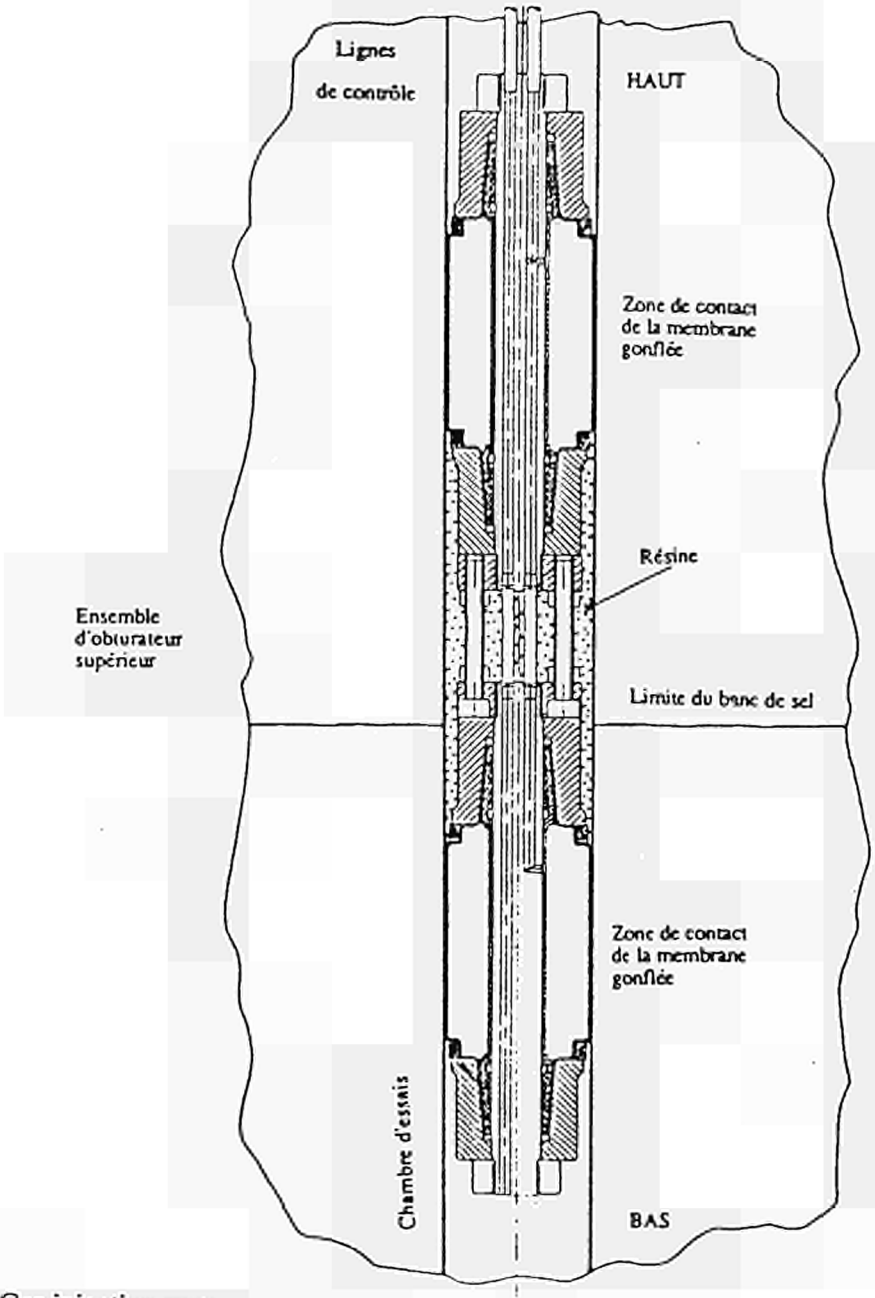

2.2 Gas injection system

A reference pressure is given by a device using a dead weight. The difference between the pressure of the chamber and the reference pressure allows gas injection until equilibrium is reached. The amount of injected gas is calculated according to the loss of pressure in a buffer bottle. The precision of the pressure is 0.01 Mpa.

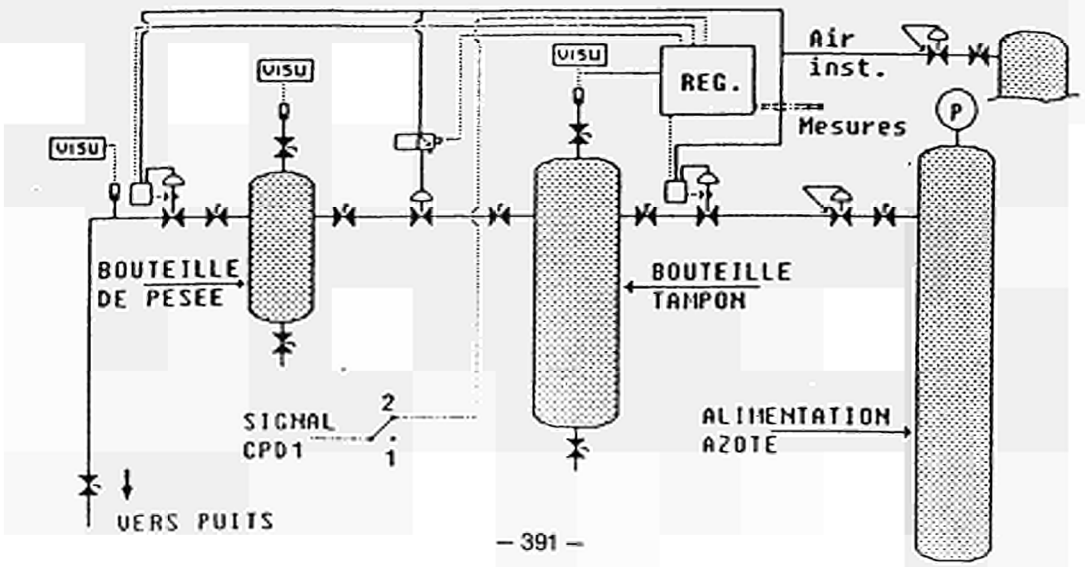

2.3 Brine injection system

The injector is a piston whose movement is driven continuously by the difference of pressure between the reference and the chamber. The maximum brine flux is 500 mm^3 / mn, the minimum 0.1 mm^3 / mn.

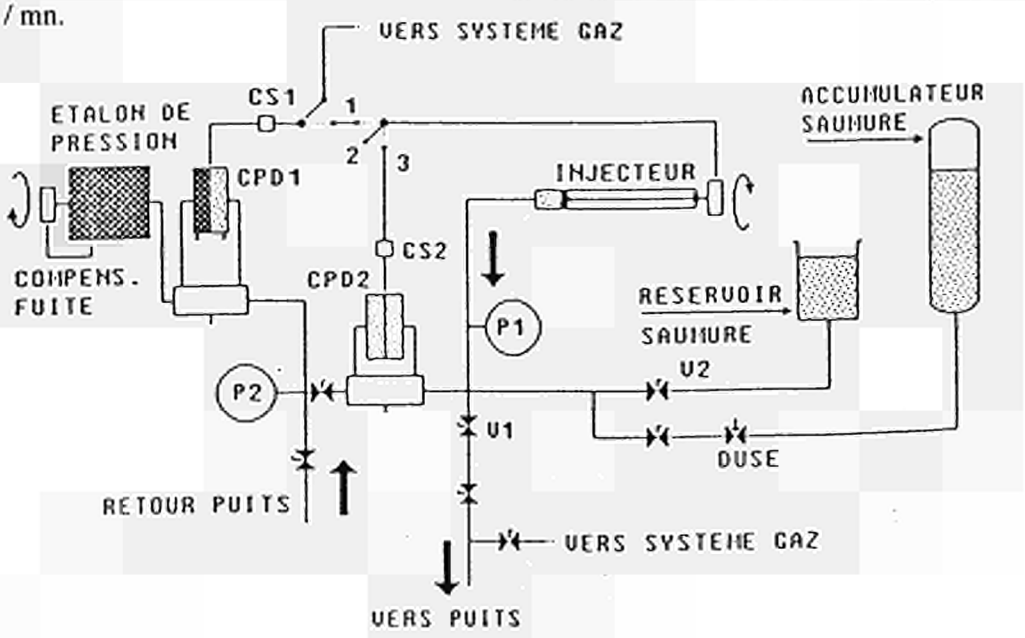

2.4 Thermal regulation system

The entire injection system (surface and borehole) function at the temperature of the chamber (= 36°C) in order to prevent undesirable effects (cristallization, creeping...).

For this purpose, a ventilation system with two fans and electric heaters was built.

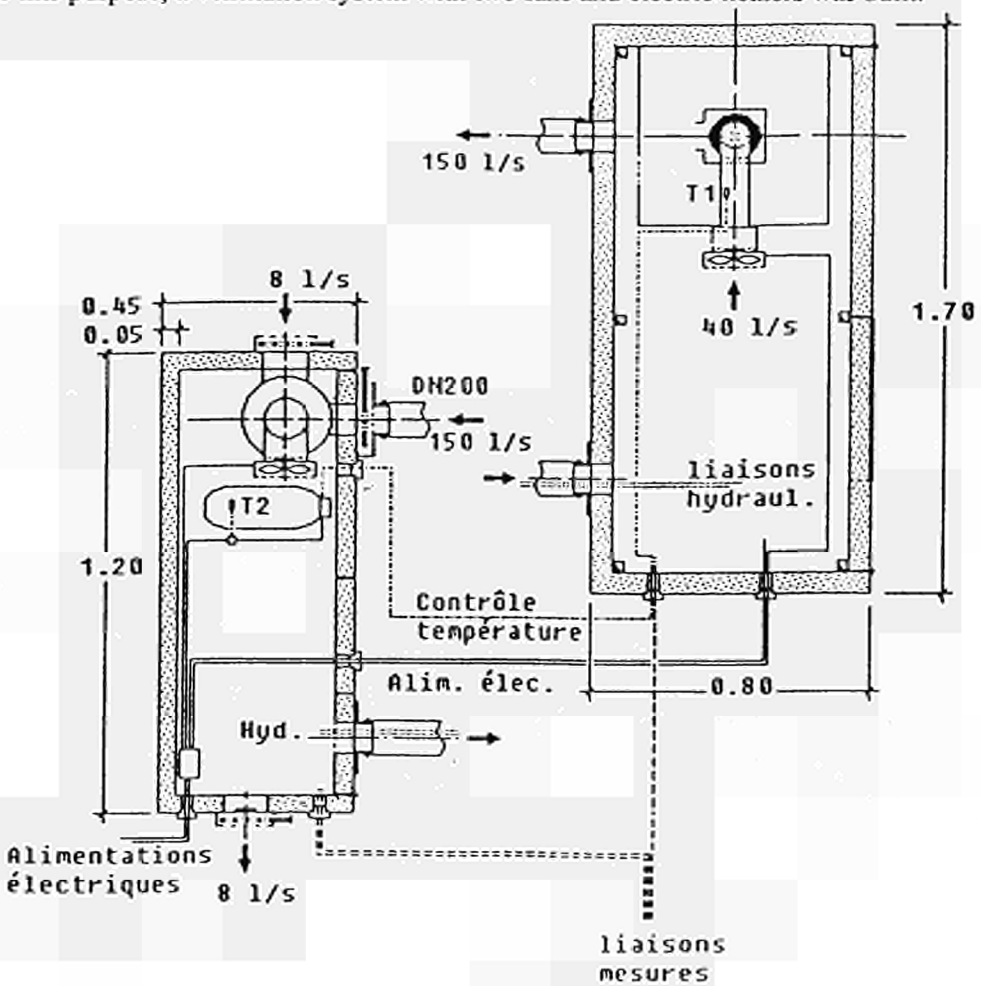

2.5 Data acquisition system

Test data is collected by a data logger connected to the SELTICA system (already used for "SEL BROYE" and "CPPS" tests) that sends them daily to G.3S in Palaiseau near Paris.

3. WORK DONE

After the necessary tests and adjustments of the system several phases of the experiment were achieved :

- two injections of gas at the pressure of 40 bars then 60 bars were conducted with a total duration of 42 days in November and December 1994;
- one injection of brine at 20 bars started mid December 1994.

Two phases of injection of gas showed the pressure of the gas in the chamber evolved between 39.92 and 40.05 bars for the first phase of the experiment (gas at a pressure of 40 bars) and between 59.9 and 60.05 bars for the second phase of the experiment (gas at pressure of 60 bars).

The interpretation of the results is in progress.

Publication

COSENZA P., BAZARGAN B., GHOREYCHI M.
Essai in situ de la perméabilité du sel au gaz et à la saumure. Rapport de suivi 1994.
ANDRA internal report n° 624 RP G.3S 94-003.

Title	EVEGAS (European Validation Exercise of GAS migration model through porous media
Contractors	GEOSTOCK (F); Bertin & Compagnies (F); ANDRA (F); CIMNE (E); ARMINES (F); INTERA (UK); CEN (B); SIMOCO (UK); GRS (D)
Contract N°	FI2W-CT93-0125
Duration of contract	January 1994 - December 1995
Period covered	January 1994 - December 1994
Project leader	T. MANAI (GEOSTOCK)

A. OBJECTIVES AND SCOPES

The EVEGAS project aims at the verification and validation of numerical codes suitable for simulating gas flow phenomenon in low permeability porous media.
Physical phenomena involved in gas generation and gas flow are numerous, often complex, and may not be very well described.
The existing numerical codes cannot represent all the occurring possible phenomena, but allow a good trade-off between simplicity and representativity of such phenomena.
Two phase flow (Gas and Water) appear to be the most consequential phenomena in gas migration and pressure sizing.
The project is organised in three major steps:

1)A simple problem with analytical solutions

This is a necessary first step which allows assessing the accuracy of numerical solutions in function of given parameters. Such a quantitative evaluation of the numerical codes, will be useful to interpret deviations that might occur in simulating more realistic test cases.

2)A few problems based on laboratory or in-situ experiments

Such tests will aim access to the following information:

- the accuracy of the numerical solutions (**assuming the existing of good and representative experimental data**).

3)A 3-D repository scenario involving the following aspects

- a repository design
- a source of gas
- rock characteristics
- fluid characteristics.

B. WORK PROGRAM

The project is divided into five work packages (denoted WP) each of them involving one or several tasks.
The first work package (WP1) is dedicated to the analysis of selected numerical codes. Such analysis will be of paramount importance in describing test cases.
It includes examination of the problems that can be simulated and of the numerical schemes and solving methods used.
The next work packages (WP2, WP3, WP4) are related to the three levels of test cases. Each work packages includes four tasks as follows:

- T1: general and detailed specification (GDS) of the test cases
- T2: general and detailed definition (GDD) of the test cases
- T3: simulation of the test cases by participants
- T4: analysis of results and reporting.

C. PROGRESS OF WORKS AND RESULTS

State of advancement

The last year was dedicated to the following work packages and tasks :

-Code analysis (WP1)
-First level test cases specification and definition (WP2T1, WP2T2)
-First level test cases simulation by participants (WP2T3)
-First level test cases simulation results analysis and reporting (WP2T4)
-Second level test cases specification and definition (WP3T1, WP3T2)

WP1,WP2T1,WP2T2,WP2T3,WP2T4,WP3T1 and WP3T2 was accomplished

Progress and results

C1. CODE ANALYSIS(WP1)
C1.1.Comments

C.1.1.1.Codes objectives

The six considered codes have been initially designed for different purposes, and then extended in order to take into account new problems. This initial design or main scope appears in the documentation, and also explains that a number of features only appear into one or two of them.

This paragraph presents the vocation of the codes, but this should not be interpreted as limitations of the ability of each of them to treat the problems addressed to in the EVEGAS project.
Only the two codes SUNIDJ and BRIGHT are dedicated to the problem under concern, namely gas migration related to radioactive waste disposal, and they are also the most recent among the six analysed codes.
For SUNIDJ the problem is that of the migration of a gas (H_2) produced at one location (point or finite volume) of a porous medium saturated by a liquid, and with the assumption that the overall problem is an isothermal one.
It can be noticed that this code explicitly tries to apply petroleum engineering based approaches to solve this actual problem.
For BRIGHT the point dealt with, is that of the sealing joints of repository wells dug in salty formations. As the joints are filled by compacted salt aggregates, the problem is to ensure that no migration may occur, neither toward the atmosphere nor toward the surrounding water, due to some thermal (not gas) release at the repository location.
GENESYS and ECLIPSE have been initially designed to study gaseous and liquid petroleum production, with some emphasis put on phase changes, miscibility phenomena, and on the fractured nature of the porous media. They of course consider multispecies and heat transport.
TOUGHII and PROFLOW are generic codes, i.e. not really dedicated to some specific problem, the former, whose name is an acronym of "Transport of Unsaturated Groundwater and Heat" has been mainly used for hydrogeology studies including some phase changes and multispecies considerations, the latter, as also indicated by its name, aims general fluids transports in porous media.
The high degree of generality of a code like PORFLOW, makes it a multipurpose tool which can deal with various physical problems, with the drawback that the description of the problem remains to be done.
In the same way, the codes issuing from petroleum engineering, and which as such have been highly developed, are now also multipurpose tools (for example even gas-storage problems can be treated by option modules), having their own language.

C1.1.2.Entrance levels

This paragraph presents at which level of the modelisation process, is defined the documentation of each code, as indeed a code results from the modelisation of a class of problems.

The terms of the problem consist, firstly in the description of the whole set of taken into account phenomena, this defining the physical modelisation or set of physical hypotheses, and secondly in the set of questions concerning the studied process.
This is ***the first entrance level*** of a given problem.
BRIGHT is the only code to start from this first level, this making easier the search of the used physical hypotheses. SUNIDJ partly starts from this level but the asked questions, i.e. the quantities to be defined, are not clearly presented.
Once the physical problem is well and completely posed, it has to be translated mathematically; this leads to express equations: definition equations for the quantities, equations translating the used general physical principles, and some equations representing specific phenomena.
This is ***the second entrance level.***
At this level, the equations are written directly together with the boundary conditions (BC) and the system state equations at some initial time (IC). This implies that a first selection has been made among the various quantities, to define those which are considered as unknowns and those which are considered as parameters. By many aspects SUNIDJ is defined at this level.
In order to go towards the problem resolution, the former equations, BC and IC are most often mathematically transformed by substitution, addition and so on, to achieve a restricted set of equations and principal unknowns completed by compatible BC and IC, and to which are joined secondary equations and unknowns.
This is ***the third entrance level***, at this third level, the objective is to solve a mathematically well posed problem rather than to deal with physical interpretation.
Three of the studied codes use this entrance level:

- this level is natural for PORFLOW with respect to its generic vocation
- and as regards TOUGHII and GENESYS, it is probably because they are under development for a longer time and that the two first levels must have been published earlier.

Finally, as the equations are solved numerically, they have to be discretized, and often linearized, in a way which takes into account algorithms and computers constraints.
This is ***the fourth entrance level***, which is the only one used in the supplied ECLIPSE's documentation.

C1.1.3.Main physical hypotheses

The analysed codes are related to:

- flows, therefore to fluids displacements and to migrations when relative displacements occur
- in a porous unsaturated medium, therefore containing somewhere a minimum amount of at least two fluids
- with mass and thermal transfers
- with time dependency
- in a limited spatial domain.

In this spatial domain, Newtonian mechanics and ordinary thermodynamical principles are applied, hence the necessary conservation of mass, momentum and energy.
These quite general hypotheses are as hidden as are those which concern the macroscopic continuity of the media, which is necessary to define thermodynamical quantities, or the continuity of movements which allow to define partial and total derivatives. In a way or another, all the codes deal with multiphase flows.
The studied flowing fluids either are each considered as a specific fluid like in PORFLOW, or can be most often considered as fluids having two phases (liquid and vapour).
It must be noticed that for petroleum engineering originated codes, only the main fluid can have two phases.
As these flows take place in a porous material, there are indeed three phases.
All the codes consider at least one solid phase (porous material), and at least two different fluids, therefore they are multispecies.
All the codes can also treat imbibition and drainage problems with at least one wetting fluid (or phase) and at least one non-wetting fluid (or phase).

But for BRIGHT, which studies the complete medium i.e. the porous material plus the fluids, the porous material is assumed to be perfectly rigid, with usually isotropic and locally homogeneous properties.
PORFLOW, GENESYS and ECLIPSE have options for some non-isotropic properties like permeabilities.
The heterogeneity linked to fractured porous material can be taken into account by GENESYS and ECLIPSE.
The mass transfers are taken into account for phase changes, and species displacements.
The thermal transfers generally occur via the solid phase, but can also concern the primary fluid, though it is limited by the hypothesis of local thermal equilibrium.

Two exceptions must be outlined:

- on one side SUNIDJ considers no thermal transfer
- at the opposite side BRIGHT studies the local thermo-hydro-mechanics interdependencies.

For all the codes, at least the principal unknowns are assumed to vary in space and time, therefore all of them can treat unsteady problems.
The spatial domain is rather poorly defined, it is more or less assumed to be infinite, with specific areas for gas sources (but for BRIGHT), or for liquid sources (but for BRIGHT and SUNIDJ), or for thermal sources (but for SUNIDJ).

C1.1.4.Hypotheses related to the porous medium

A porous medium is characterised by:

- a geometrical quantity (porosity)
- a behaviour law with respect to local constraints (rheological law)
- and a quantity which defines the interactions between solid and fluid phases (permeability).

This last quantity implies the selection of a law of flow in the porous medium.

It can be noticed that other characterisations of the porous medium could have been done, like those based on fractal approaches.
Only BRIGHT offers a geometrical model for the porosity; an idealised geometry of salt grains and open pores is characterised by three parameters, the total porosity of the open pores is computed locally, and can vary in time and space.
Generally, the porosity is defined by a single parameter, constant in time, and which may vary in space inside the studied domain.
In order to have this scalar quantity everywhere defined, the concepts of homogenisation, representative elementary volume or effective quantity, are used. All these concepts consist in computing a local mean value, which will be all the more precise as the medium will be homogeneous.
Petroleum engineering originated codes also define a **dual porosity in order to represent (to model) the fractures**, therefore at each point two porosities are defined, and through an option these can be used to build an average value or pseudo-porosity.
The porous medium is generally assumed to be rigid; BRIGHT is the only code to really take into account the deformability of the medium with respect to local constraints, temperature and geometrical definition of the medium.
The permeability concept can only be defined with respect to the law of flow in porous medium, generally Darcy's law. But as this law is used independently for each fluid or phase, this requires to introduce concepts of intrinsic permeability (related to the porous medium alone) and of relative permeabilities (related to the different fluids or phases).
It must be pointed out that for very little porous media, the independent use of Darcy's law for each fluid may be doubtful, as some effects like Knundsen's ones are not described, though they may be important in this case.
The intrinsic permeability is usually represented by a scalar quantity, which is an average over values in several directions or values in the vicinity. In fact it is an effective permeability.

For PORFLOW the permeabilities can be defined with respect to the three main directions, and for ECLIPSE one permeability is considered along the main flow direction, and another one is considered orthogonal to it.
ECLIPSE and GENESYS consider one permeability for the matrix and another one for the fractures, with an option to deduce from them an average value, which defines an effective intrinsic permeability.
The relative permeabilities are assumed to be functions of the saturations in all the codes, with several available selections for these functions which can be derived from arrays of value or from empirical laws. These relative permeabilities are usually the one of the main source of non-linearity in the equations.
For example, in TOUGHII, some available functions are: linear law, power law, Brook-Corey's curves, Grant's curves, functions of Flatt-Klikoff, Sandia, Vermia...
The associated phenomena such as residual saturation of the wetting phase, hysteresis are also dealt with but the way it is done is not documented.
The Klinkenberg, i.e. the dependency of the relative permeability with respect to the local pressure level, may also be taken into account in all the codes.
The global permeabilities (intrinsic permeability x relative permeability) are therefore also dependent of the saturations and of the capillary pressure.
This capillary pressure, which is well defined only in the case of one solid phase, one non-wetting phase and one single wetting phase, is a function of the characteristics of the porous medium (porosity), of the permeabilities and of the saturations.
As for relative permeabilities, several empirical laws can be used to define the capillary pressure.
For example, in TOUGHII, some available laws are: linear law, Dickens's function, Trust model, functions of Milly, Leverett, Sandia, or Brooks-Corey's relationships.
It must be outlined that, everything related to relative permeabilities and capillary pressures, in a porous medium with numerous fluid components, is still to be studied, and therefore that only a priori models can be used for such cases. Moreover available data concern almost exclusively, either the couple water-air or the couple liquid-gas for the petroleum.
And last, it can be noticed that the saturation vapour pressure of a fluid is not the same in a free open space that in a porous medium. **This effect is taken into account by TOUGHII (Kelvin's law) and by BRIGHT.**

C2.FIRST LEVEL TEST CASES(WP2T1,WP2T2)

C2.1.Objectives

The prediction of gas migration in the context of radioactive waste disposal requires to take into account quite a lot of simultaneous phenomena, such as interactions of gas with liquids, thermal transfers, capillary pressure effects..., all of these phenomena occurring in a more or less known porous media, which may present gradients of properties.
In order to have realistic predictions of gas migration, it is essential to have a good physical knowledge of all these phenomena, and it is also essential to use numerical schemes able to deal with the mathematical modelling of these phenomena, with the maximum accuracy and with as small side-effects as possible.
For example when physical diffusion is an important phenomenon, it is essential that the so-called numerical diffusion is negligible with respect to the physical one.
On another hand, to be effective, the numerical prediction has to use reasonable computing resources on current computers, and in fact computational modelling is always a trade-off between available resources and some desired accuracy.
Therefore, to establish these compromises users have to get some insight of how the accuracy evolves as a function of the used computational resources.

C2.2.Detailed objectives

Once the physical model has been established, i.e. the set of equations is defined, the user which faces an existing tool can only act on the following features:

- mesh definition
- time step choice
- numerical scheme selection if several of them are available.

It is the objective of these tests specifications to get some insight of how costs, accuracy and side-effects evolve with respect to these features, avoiding the intrinsic difficulties of physical modelling which has to be addressed by another set of test cases.

C2.3.Test cases selection

C2.3.1.Numerical difficulties

To select significant test cases, one has to consider the main numerical difficulties related to gas migration modelling, which apart from boundaries conditions, are:

- no linearities related to relative permeabilities and capillary pressure evolutions with respect to saturations
- large gradients like in the vicinity of saturation fronts
- coupling of equations.

Another difficulty, at least for finite differences approximations, is the fact that, for fully 3-D flows, it is impossible to have meshes aligned with the flow characteristics, and that this leads to a loss of accuracy called axes effects.
It must also be stressed that, in order to have reasonable computational costs, it is necessary to use implicit solvers which use to smear solutions (numerical diffusion) especially in the case of non-linear equations.
Significant test cases have to address these difficulties.

C2.3.2.Constraints

The constraints which have been taken into account to select these level one test cases are:

- compatibility with all the numerical tools used in the project
- no physical modelling difficulties
- availability of analytical solutions in order to have a firm basis for accuracy assessment.

C2.3.3.Selection

The basic test case which has been selected, is the 1-D immiscible displacement of one fluid by another one with the following assumptions:

- uniform and constant densities
- uniform permeability
- analytical properties.

This case is well known as the **Buckley Leverett** case and it exhibits several interesting features:

- as far as the capillary pressure is neglected there is an analytical transient solution
- there is a discontinuity of the saturation profile, i.e. an infinite gradient.

In order to address the objectives presented in § 2.2, computations will be performed on several 2-D meshes with several time steps.

C3 Result simulation analysis(WP3T4)

C3.1 Mesh size effect

This effect is to be analysed by comparing the results of the cases:

- 1.01 (dx = L/10)
- 1.02 (dx = L/20)
- 1.03 (dx = L/40),

or

- 1.08 (dx = L/10)
- 1.09 (dx = L/20)
- 1.10 (dx = L/40).

C3.2 Irregular mesh effect

This effect is to be analysed by comparing the results of the cases:

- 1.03 (dx = L/40)
- 1.04 (dx = L/10 for $x < 0.4$ L and dx = L/40 for $x > 0.4$ L),

or

- 1.10 (dx = L/40)
- 1.11 (dx = L/10 for $x < 0.4$ L and dx = L/40 for $x > 0.4$ L).

For the chosen parameters, the saturation front is located in the region $x > 0.4$ L where the mesh spacing is L/40.

C3.3 Mesh orientation effect

This effect is to be analysed by comparing the results of the cases:

- 1.02 (dx = L/20)
- 1.05 (dx = L/20 ,the mesh lines at 45 degrees from the front propagation direction)

or

- 1.08 (dx = L/20)
- 1.12 (dx = L/20 with the mesh lines at 45 degrees from the front propagation direction).

C3.4 Time step effect

This effect is to be analysed by comparing the results of the cases:

- 1.02 (dx = L/20 dt = t0/15)
- 1.06 (dx = L/20 dt = t0/30)
- 1.07 (dx = L/20 dt = t0/60),

or

- 1.08 (dx = L/20 dt = t0/15)
- 1.13 (dx = L/20 dt = t0/30)
- 1.14 (dx = L/20 dt = t0/60).

The value of t0 is such that the front is approximately located at x = 0.6 L, and is the reference time at which all the results are analysed.

C3.5 Capillary pressure effect

This effect is to be analysed by comparing the results of the cases 1.01 to 1.07 with the results of the cases 1.08 to 1.14.

C3.6. Criteria

C3.6.1 Front location

The front location can be classically defined by three points:

- the point where a value close to the front top is reached
- the point where a value close to the front foot is reached
- the point where the mid height value is reached.

The later definition, has been chosen as it doesn't depend too much on the front spreading. It is built from the supplied results by linear interpolation.

C3.6.2 Front spreading

As numerical models use discretised representations, the saturation front spreading has been defined by the number of cells on which it is spread, and also by the distance between the points corresponding to saturation levels
s1 and s2 defined by :

$$\begin{cases} S_1 = S^f_{min} + 0.1(S^f_{max} - S^f_{min}) \\ S_2 = S^f_{min} + 0.9(S^f_{max} - S^f_{min}) \end{cases}$$

where S^f_{min} is the minimum (initial) saturation, and S^f_{max} the saturation value at the front.

C3.6.3 CPU evolution

The tests have been performed on different computers having different architectures, moreover as the objective related to this criterion is mainly to define whether the CPU cost is proportional to the number of nodes or grows faster, the raw CPU cost have been normalised by the CPU cost of the test case 1.01, for each software.

C3.6.4 Memory evolution

The memory requirements are not very much dependant on the computers, so the memory sizes are absolute values.

C3.7. Presentation of the results

C3.7.1 Status of cases

The table below shows the status of the cases with the following conventions:

- •D stands for Done
- •F stands for done but obviously False
- •C stands for done but not converged.

TOUGH corresponds to the use of TOUGH by ANDRA and TOUGH.b by GRS.

Tableau 1.

case	TOUGH	TOUGH.b	ECLIPSE	SUNIDJ	PORFLOW	GENESYS	BRIGHT
1.01	D	D	D	D	F	D	N
1.02	D	D	D	D	F	D	N
1.03	D	F	D	D	F	D	N
1.04	D	D	D	D	F	D	N
1.05	N	N	N	N	N	N	N
1.06	D	D	D	D	F	D	N
1.07	D	D	D	D	F	D	N
1.08	D	D	D	D	F	D	D
1.09	D	D	D	D	F	D	D
1.10	D	N	D	D	F	D	D
1.11	D	D	D	C	F	D	D
1.12	N	N	N	N	N	N	D
1.13	D	N	N	D	F	D	D
1.14	D	D	D	D	F	D	D

C3.7.2 Comments on the cases

As it can be seen from table 1, there are no results for the case 1.05 and only one for the case 1.12, so these cases are not taken into account for the analysis.

Generally speaking the specified time steps have not been used as such, they have instead been used as maximum time steps together with some automatic time step control, and it seems that these 'maximum' time steps have not been reached in any test cases.

C3.7.2.1 TOUGH

It has appeared that TOUGH cannot deal with arbitrary fluids and properties in fact it can only take into account predefined standard fluids like air and water together with their usual properties, and moreover only one single liquid phase can be computed at a time.

These restrictions of use have lead to the definition of specific physical values input, compatible with the objectives of the test cases, but inducing different results. For the analysis, the main difference is that for the basic cases the saturation front height is about 0.1 and is about 0.95 for the test performed using TOUGH, and also that there are no gradients near the input side at the opposite of the basic case.

The specific input parameters are:

- permeability 3.10^{-12} m^2
- water viscosity 1.10^{-3} $kg/m.s$
- air viscosity 1.810^{-5} $kg/m.s$
- filtration velocity 1.10^{-8} m/s

These features must be kept in mind, when looking at the results.

C.3.7.2.2 TOUGH.b

See previous paragraph for the test cases definition. The case 1.03 is obviously false, probably because of a bad input value. For unknown reasons there are two missing cases : 1.10 and 1.13.

C.3.7.2.3 ECLIPSE

For unknown reasons one case is missing : 1.13. The cases with capillary pressure (1.08 to 1.14) look strange, this may be due to some mistake in the boundary conditions.

C3.7.2.4 SUNIDJ

Some computations have been performed several times, using different numerical options, especially some test cases have been performed using one or two (left and right) saturation value per node. Only the cases with two saturations per node have been analysed.
The case 1.11 failed to converge for unknown numerical reasons.

C.3.7.2.5 PORFLOW

All the cases are obviously false because there is no front in the computational domain, this may be due to some mistake in the input values.

C3.7.2.6 GENESYS

No remarks.

C3.7.2.7 BRIGHT

The cases without capillary pressure (or with a neglectible one) have not been done.
The cases with capillary pressure have been done using an initial water saturation value which is not neglectible, i.e. 0.03 for a front height of about 0.1. The corresponding theoretical saturation profile has been taken into account for the analysis.

C3.8. Analysis

For this global analysis, the cases which can be considered as false are not taken into account.

C3.8.1 Front location

The front is rather well located for most cases. For the cases without capillary pressure the discrepancy between the numerical values and the theoretical ones are always smaller than half a cell.

For the cases with capillary pressure the discrepancy between the numerical values and the theoretical ones are larger ,but for TOUGH (and TOUGH.b) for which the results are almost identical to those without capillary pressure because of its specific test cases definition. The effect of mesh size can mostly be seen for cases 1.08 1.09 and 1.10, for which it is clear that the finer the mesh the better the results.

The influence of a coarse upstream mesh can be seen by comparing the results of the case 1.04 (resp 1.11) with those of the case 1.03 (resp 1.10). All these cases having the same fine spatial discretization in the neighbourhood of the front (x > 400), the discrepancies only come from the fact that the front has been travelling in a coarse mesh before arriving in the fine one.

C3.8.2 Front spreading

All the numerical tools spread the front over approximately 2 to 3 cells,this being a classical range.

- the first order improvement of the results versus the spatial discretization (cases 1.01 1.02 1.03 and cases 1.08 1.09 1.10)
- the relatively small influence of a coarse upstream mesh.

C3.8.3 CPU evolution

The CPU cost evolution is classically $C = N^P$,where C is the CPU cost, N the number of cells and p an exponent.

Table 2

Software	Exponent P
TOUGH	1
SUNIDJ	3
ECLIPSE	1
PORFLOW	1
GENESYS	2
BRIGHT	2.5

It must be noticed that these values combine the direct effect of computing more nodes, and the induced effect of computing more time steps because usually the finer the mesh the smaller the time step.

When the exponent value is 1., it means that the number of time steps remains unchanged.

C3.8.4 Memory requirements

The memory evolution, is classically $C = N^q$,where M is the memory requirement, N the number of cells and q an exponent.

the values of q **are all close to 1.**, this means that the memory requirements are proportional to the number of cells, i.e. that there is no matrix storage.

C3.8.5 Time steps

As explained in paragraph 4, automatic time step control has been used for almost all cases.

The main conclusion which can be derived from the results is that all the used time steps are all smaller than the specified ones. More precisely, the fact that the results of cases 1.02 1.06 and 1.07 (or 1.09 1.13 and 1.14) are identical implies that the effective time steps are smaller than the specified minimum one.

The minimum specified time step (150 days) corresponds to a displacement of 0.88 m ,i.e. 1/28 the cell size for these cases.

C3.9 Analysis of the softwares

This paragraph presents some provisional conclusions about the use of the tested softwares.

TOUGH and GENESYS produced satisfactory results for all cases, taking in mind the restrictions presented in paragraph 4.2.1 for TOUGH.

ECLIPSE and SUNIDJ produced satisfactory results only for the cases without capillary pressure. For the cases with capillary pressure, it is not possible to know whether their bad results come from mistakes in input data or from the numerical approach.

BRIGHT produced some satisfactory results only for the cases with capillary pressure (with some numerical instability in the vicinity of the front for one case), it would be interesting to know its behaviour for cases with a neglectible capillary pressure.

PORFLOW did not produce any results comparable with the reference solution, hopefully because of mistakes on input data. The only remarks that can be done are that the results are relatively dispersed, and that there are non neglectible numerical instabilities for all the cases with capillary pressure.

It can be noticed that GENESYS and ECLIPSE predict saturation values higher than the theoretical ones in a quite large domain upstream the front and also at the front location.

C4 Second level test case definition and specification (WP3T1,WP3T2)

EVEGAS second level test cases based on laboratory experimental result. A heterogeneous plug made by eight rocks samples (whose length is L_i from different rocks) is maintained in a vertical position and was saturated with water at the initial time and the bottom plug pressure is maintained at 20 bar. The air was injected downward at the plug top at a constant flow rate (150 cm^3/h). The produced gas and water at the plug bottom are monitored by a flash device. The whole experiment apparatus is maintained at a constant temperature (20 °C).

The aim of the second test cases is to simulate the laboratory experiment ,at the above described conditions and configuration, in order to predict water production versus time and water saturation profiles and pressure profiles at some relevant times. Some data related to computing aspect are required.

This second level test cases in the frame of the EVEGAS project should contribute to get information on the predictive numerical model capabilities faced experimental result.

Title	Continuation of the migration experiments in Boom clay (laboratory and in situ)
Contractors	ONDRAF/NIRAS, B; CEN/SCK, B
Contract N°	FI2W-CT90-0039
Duration of contract	September 1991 - August 1995
Period covered	January 1994 - December 1994
Project leader	De Preter P. (ONDRAF/NIRAS, Coordinator) B. Neerdael (CEN/SCK)

A. OBJECTIVES AND SCOPE

As the PAGIS |1| and PACOMA |2| safety studies have indicated, the migration of the critical radionuclides in the Boom clay is one of the key factors in the overall HLW disposal concept in Belgium. For this reason this programme aims at identifying the relevant migration mechanisms and at quantifying the migration parameters for these radionuclides.
The programme, a continuation of ongoing research, involves both percolation and diffusion experiments in the laboratory and in situ (underground lab).
The experimental work is performed by CEN/SCK.

B. WORK PROGRAMME

1. Migration experiments in the laboratory.
   For a selected list of critical (^{14}C, ^{99}Tc, ^{129}I, ^{135}Cs, ^{237}Np) and possibly critical radionuclides (^{79}Se, ^{93}Zr, ^{107}Pd, U-, Am- and Cm-isotopes) as well as for dissolved organic molecules migration experiments in clay cores will be executed.

2. In situ migration experiments.
   In situ migration tests with HTO (tritiated water) and ^{134}Cs were started previously and are regularly monitored.
   Additional tests with Am, Tc and HTO are planned.

C. PROGRESS OF WORK AND OBTAINED RESULTS

State of advancement

1. Laboratory experiments

For the non-retarded species HTO, I^-, Br^-, HCO_3^- and low molecular weight organic molecules the geometric factor G has been calculated from earlier performed migration tests. Different values are obtained for the horizontal and vertical direction.
The measured apparent diffusion coefficients D for the strongly retarded Eu have been further interpreted by assuming a quantitative Eu-complexation by the organic molecules.
The effect of the ionic strength on the HTO and I^- diffusion accessible porosities has been studied.

2. In situ experiments

Additional experimental results have become available for the three large scale in situ migration tests : two with $^{125}I^-$ and one with HTO. The experimental results are compared to model calculations.
An in situ percolation experiment with ^{134}Cs has been terminated and the obtained migration date are presented.

Progress and results

1. Laboratory experiments

For the non-retarded species HTO, I^-, Br^-, HCO_3^- and the low molecular weight organic molecules sucrose and lactose the geometric factor G has been calculated from the previous migration experiments on the Boom clay. For the different species comparable geometric factors are found. However, slightly different values are obtained on undisturbed horizontal and vertical clay cores : $\pm$ 0.15 and $\pm$ 0.10 respectively. This finding evidences the anisotropy of the Boom clay for diffusive and advective transport. A broader range of G-values is mesasured on reconsolidated clay pastes (0.08 - 0.27). Figure 1 gives the geometric factors as a function of consolidation pressure for I^-, HTO, HCO_3^-, sucrose and lactose for the clay paste experiments.

From the four impulse type diffusion experiments with Eu, which were ended in 1993, only the apparent diffusion coefficient D could be derived (see Annual Progress Report 1993). As it is reasonable to assume that Eu migration in the Boom clay will be determined by the mobile organic molecules, the effective diffusion coefficients obtained for the low molecular weight organic molecules |3| can be used to calculate the corresponding ηR values for Eu |4|. The results are given in Table 1. For these organic molecules η = 0.05 and R values of $\pm$ 2.0 15^5 are calculated for Eu. This corresponds to a K_d of about 6 $m^3.kg^{-1}$.

In order to quantify the effect of the ionic strength on the diffusion accessible porosity of I^- and HTO, their migration in three clay cores equilibrated with 1.0 N NaCl was studied. The results are summarized in Table 2. The rather surprising observation is that the HTO porosities remain ± 2 times higher than the I^- porosities, which is unexpected on the basis of double layer theory. No explanation can be given at the moment.

2. In situ experiments

The updated results for the three large scale in situ migration experiments with HTO and I^- are given in the Figures 2-4.
For HTO the agreement between the HTO concentrations measured in the porewater, and the model predictions is excellent, even for migration distances of 2 meters. No satisfying agreement is observed for the two I^- in situ tests. Possible explanations for the difference will be checked in the future.

An in situ percolation experiment with ^{134}Cs has been ended after a total migration time of nearly 7 years. In this experiment two clay cores sandwiching a ^{134}Cs labelled filter paper have been emplaced in a borehole. Due to the hydraulic gradient towards the underground laboratory the pore water continuously percolated through the clay cores. The measured migration profile is given in Figure 5. The following diffusion parameter values were obtained : $D = 1.0\ 10^{-13}\ m^2 s^{-1}$ and $\eta R = 1086$.

List of publications

Put M.J. and De Cannière P. (1994)
"Migration behaviour of ^{14}C labelled bicarbonate, HTO and ^{131}I in Boom clay".
Radiochimica Acta 66/67, 385-388.

References

|1| PAGIS - Disposal in clay formations (Ed. by J. Marivoet), CEC report EUR 11776 EN (1988).

|2| PACOMA - Performance assessment of the geological disposal of medium-level and alpha waste in a clay formation in Belgium (J. Marivoet and Th. Zeevaert), CEC report EUR 13042 EN (1991).

|3| Henrion P.N., Put M.J. and Van Gompel M. (1991). The influence of compaction on the diffusion of non-sorbed species in the Boom clay.
Radioactive Waste Management and the Nuclear Fuel Cycle, 16 (1) 1-14.

|4| De Preter P., De Cannière P., Moors H. and Put M., (1994). In situ and laboratory migration experiments for the Boom clay.
Paper presented at the CEC-meeting "Migration of radionuclides in the geosphere" Brussels, 15-17 November 1994.

Table 1 : Results of the type C1 diffusion experiments with ^{152}Eu on clay pastes.

P_{con} [@] (MPa)	Run time (y)	D ($m^2.s^{-1}$)	$\eta.R.D$ [#] ($m^2.s^{-1}$)	R [#] (-)	K_d [#] ($m^3.kg^{-1}$)
0.8	4.15	$1.6\ 10^{-15}$	$1.5\ 10^{-11}$	$1.8\ 10^{5}$	5.7
4.5	4.36	$6.2\ 10^{-16}$	$5.9\ 10^{-12}$	$1.9\ 10^{5}$	6.0
4.5	4.49	$6.3\ 10^{-16}$	$5.9\ 10^{-12}$	$1.9\ 10^{5}$	5.9
7.0	4.39	$2.6\ 10^{-16}$	$3.2\ 10^{-12}$	$2.5\ 10^{5}$	7.7

[@] Consolidation pressure

[#] estimated value

Table 2 : Results of the type D2 percolation experiments with $^{131}I^-$ and HTO on clay cores at 1 M NaCl

Core orientation (P_{con} - MPa)[@]	Species	$\eta.R$ [#] (-)	D ($m^2.s^{-1}$)	$\eta.R.D$ ($m^2.s^{-1}$)	G [$] (-)
Vertical	I-	0.28	$1.5\ 10^{-10}$	$4.2\ 10^{-11}$	0.075
(4.65)	HTO	0.51	$1.8\ 10^{-10}$	$9.2\ 10^{-11}$	0.078
Horizontal	I-	0.35	$4.6\ 10^{-10}$	$1.6\ 10^{-10}$	0.23
(4.65)	HTO	0.63	$3.6\ 10^{-10}$	$2.3\ 10^{-10}$	0.16
Vertical	I-	0.35	$1.4\ 10^{-10}$	$4.9\ 10^{-11}$	0.070
(-)	HTO	0.64	$1.6\ 10^{-10}$	$1.0\ 10^{-10}$	0.068

[@] Consolidation pressure

[#] We assume that these species are not retarded or R = 1.

[$] $D_{aq}(I^-) = 2.00\ 10^{-9}\ m^2.s^{-1}$; $D_{aq}(H_2O) = 2.26\ 10^{-9}\ m^2.s^{-1}$.

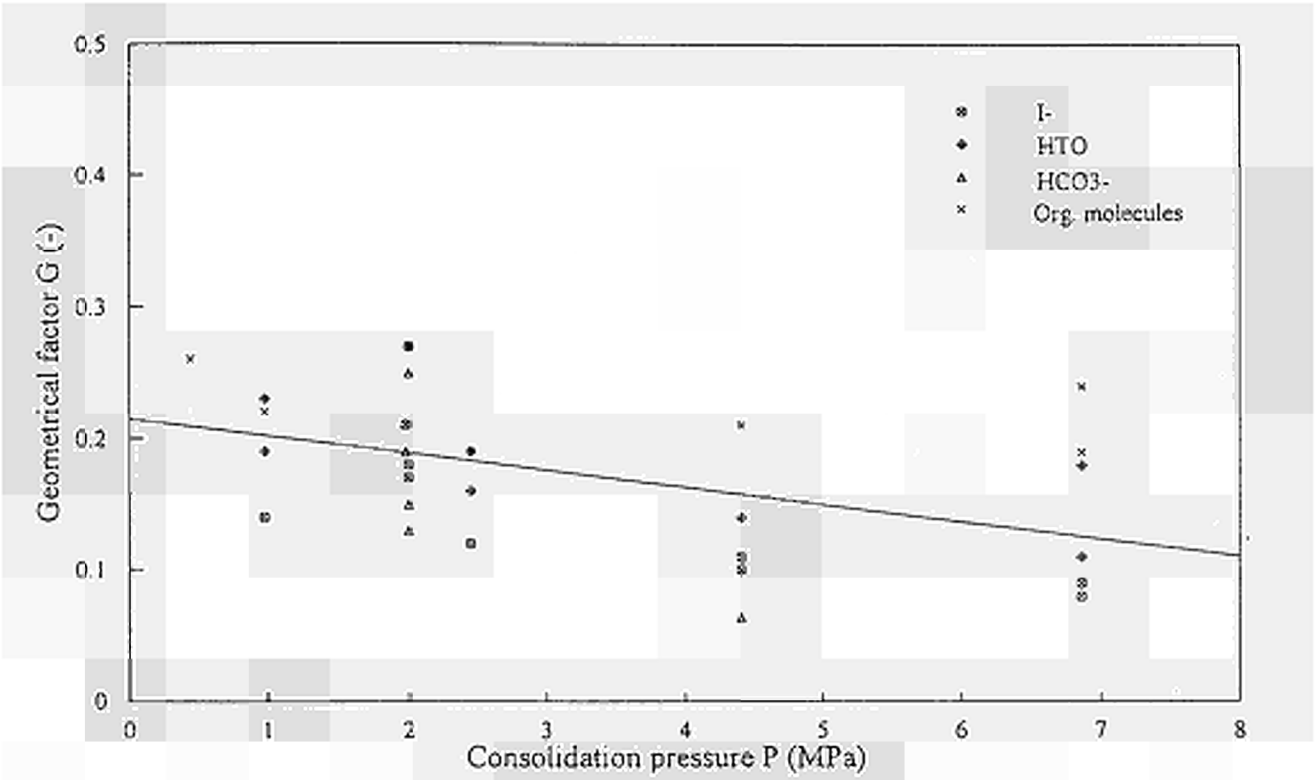

Figure 1: The geometrical factor G measured on reconsolidated Boom clay pastes for non-sorbed species (I^-, HTO, HCO_3^-, lactose and sucrose) as a function of consolidation pressure.

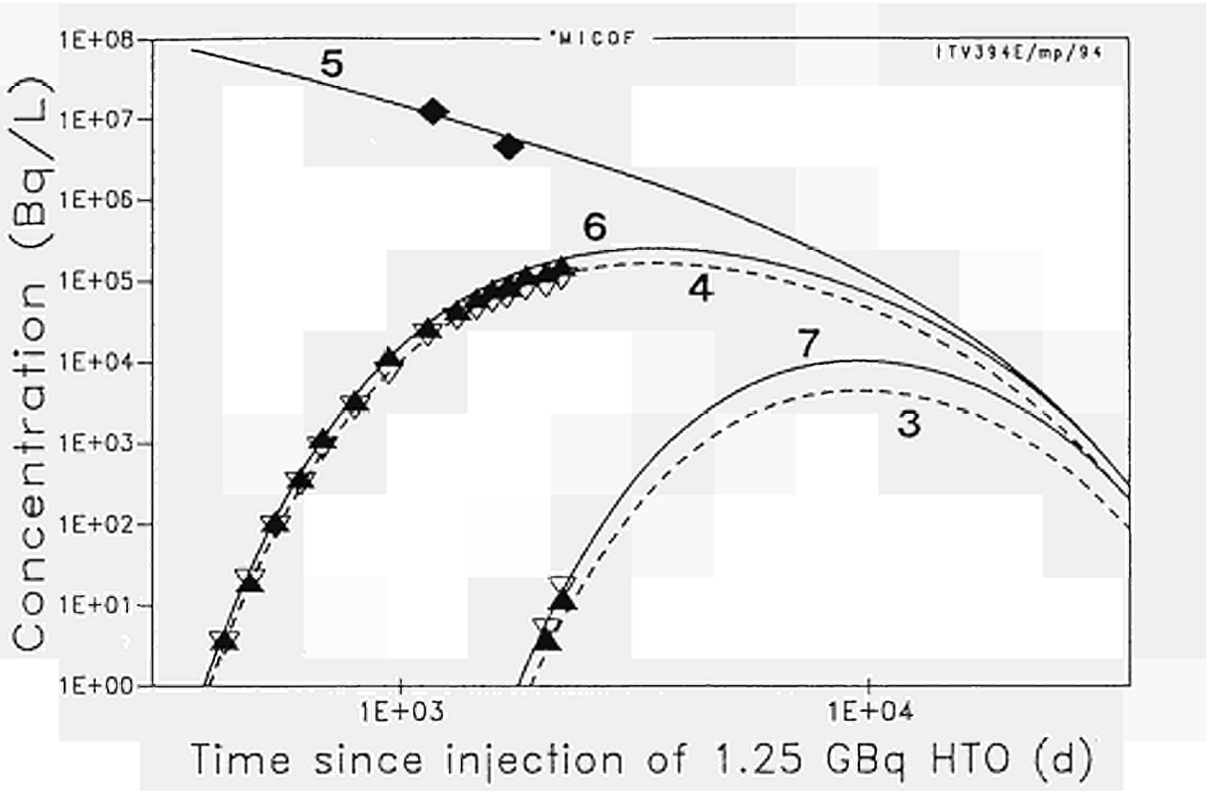

Figure 2: HTO concentration evolution in the Boom clay interstitial liquid for the filters 3 to 7. Symbols refer to experimental measurements and curves to model predictions. Results are given for the injection filter nr. 5 and for the filters at 1 m (nr. 4 and 6) and 2 m (nr. 3 and 7) from the injection filter.

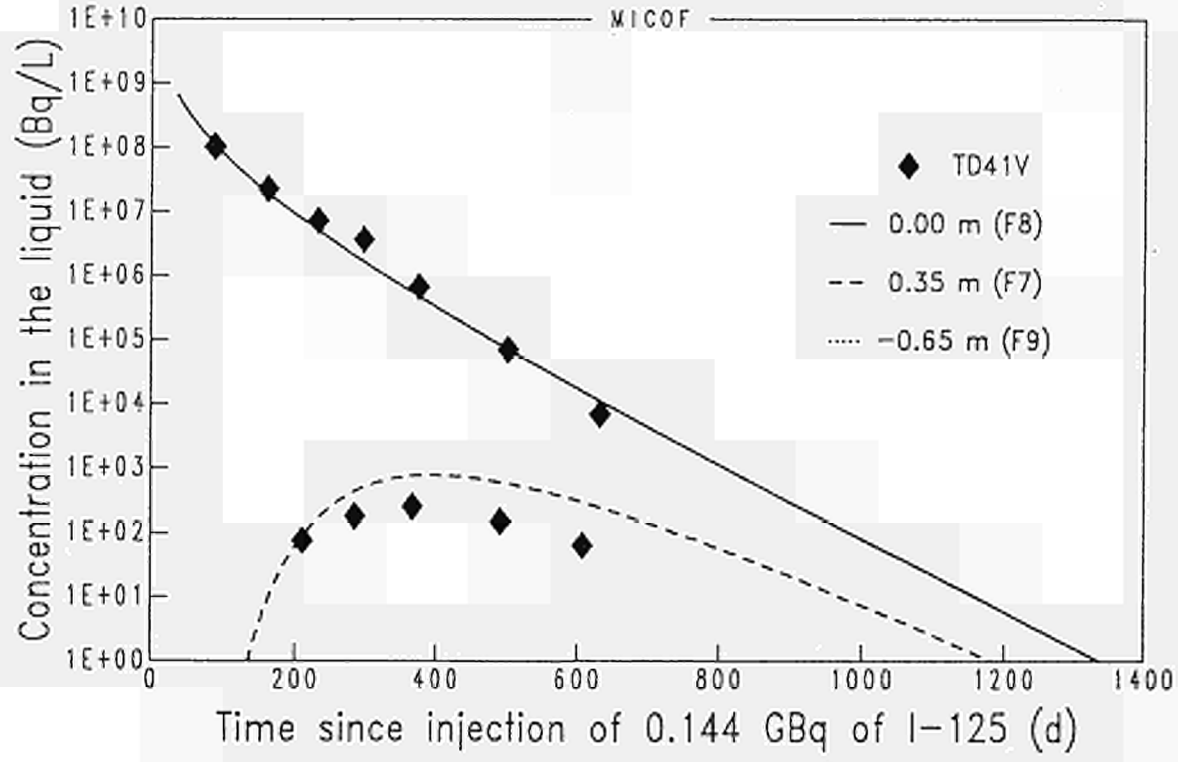

Figure 3: ^{125}I concentration evolution for the injection filter (nr. 8) and filter nr. 7 (at 0.35 m) of the vertically oriented piezonest. Symbols refer to experimental measurements and curves to model predictions.

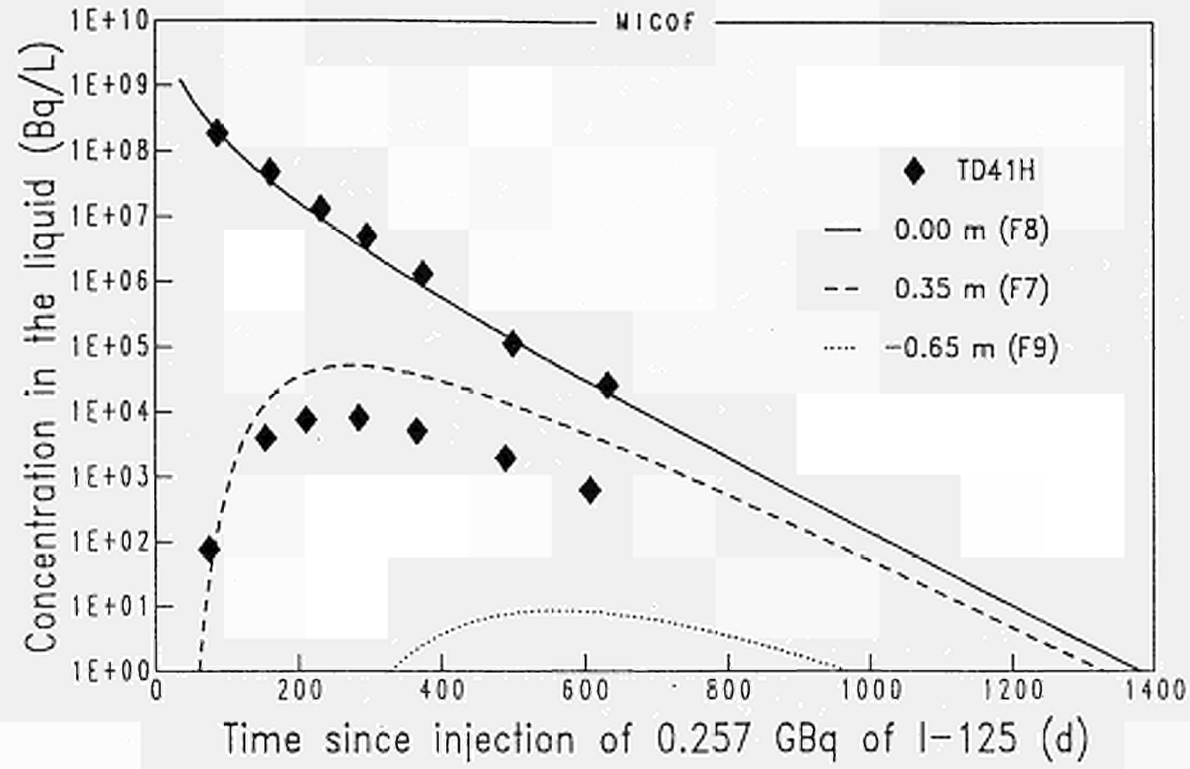

Figure 4: ^{125}I concentration evolution for the injection filter (nr. 8), filter nr. 7 (at 0.35 m) and filter nr. 9 (at 0.65 m) of the horizontally oriented piezonest. Symbols refer to experimental measurements and curves to model predictions.

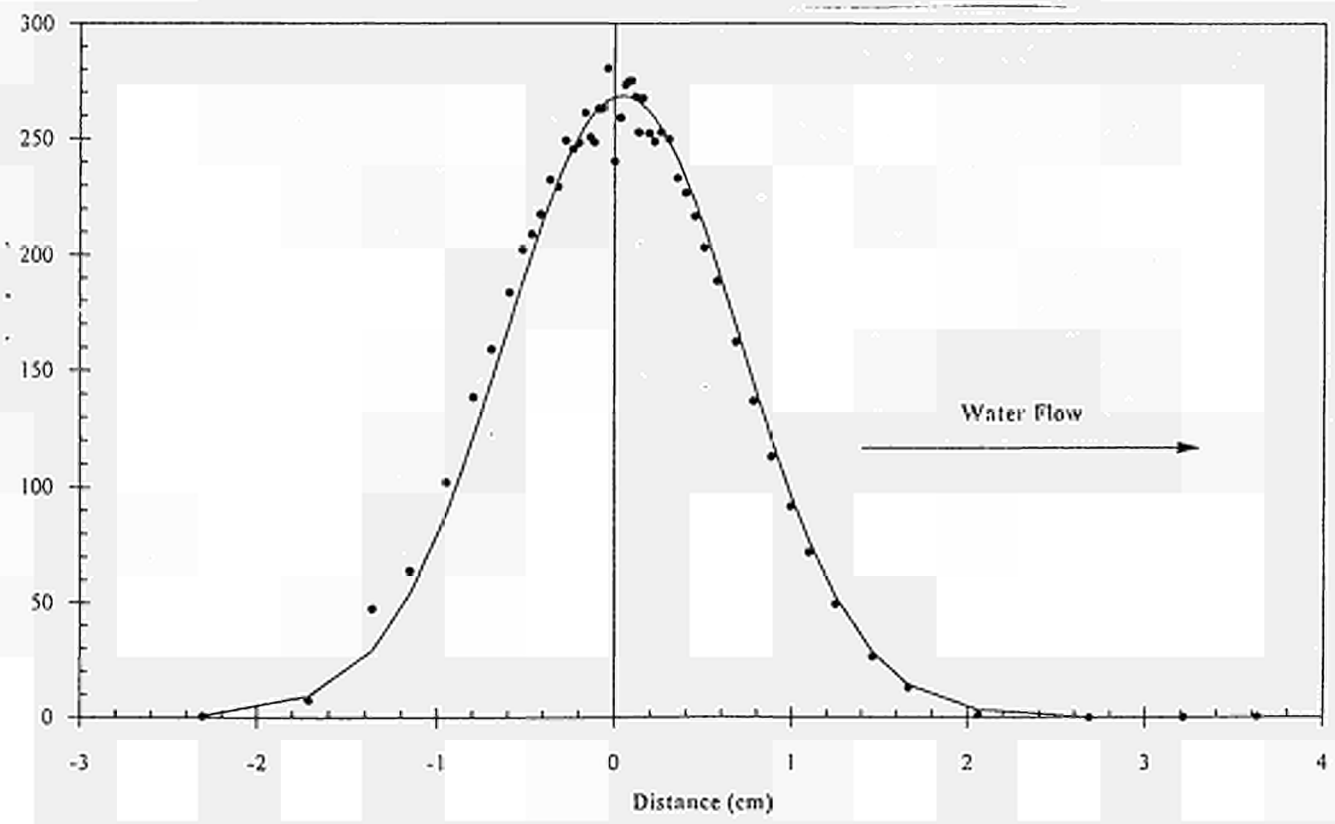

Figure 5: Migration profile for ^{134}Cs obtained in the in situ percolation experiment. The Darcy velocity of the percolating solution is 2.2 10^{-9} $m.s^{-1}$. The ^{134}Cs source (labelled filter) paper was placed at x = 0.

Title	CHEMVAL 2: A coordinated research initiative for evaluating and enhancing chemical models used in radiological risk assessment
Contractors	WS Atkins Environment, Epsom, (UK); NRC-BGS (UK); AEA (UK); ANDRA (F); CEA-IPSN (F); Univ Loughborough (UK); MBT (E); GSF (D)
Contract N°	FI2W-CT91-0065
Duration of contract	May 1991 - October 1994
Period covered	January 1994 - October 1994
Project leader	D. Read (Coordinator, WS Atkins); R. Fabriol, T. Merceron (BRGM/ANDRA); H. Lang (GSF-IfH); P. Warwick, D. Read (LUT/WS Atkins); C. Tweed, M. Crawford (AEA Harwell); J. Bruno (MBT/ENRESA); Ph. Jamet, D. Stammose (EMP/CEA)

A. OBJECTIVES AND SCOPE

The international CHEMVAL Project, initiated in 1987, has been assessing the validity of computer-based models used to describe the geochemistry of radioactive waste disposal systems. The original project [1,2,3] was concerned, primarily, with the verification of equilibrium models, though a number of attempts were made at a *priori* predictive validation. CHEMVAL 2 aimed to build on this earlier study by targeting specific areas shown to be of particular concern in radiological assessment.

B. WORK PROGRAMME

Twenty organisations in ten countries currently participate in CHEMVAL and, of these, seven have direct responsibilities for technical coordination, as outlined below:

a) Temperature Effects:	BRGM/ANDRA, France (R. Fabriol, T. Merceron)
b) Ionic Strength Effects:	GSF-IfH, Germany (H. Lang)
c) Organic Complexation:	LUT/WS Atkins, UK (P. Warwick, D. Read)
d) Sorption Processes:	AEA Harwell/BGS, UK (C. Tweed, M. Crawford)
e) Co-Precipitation:	MBT/ENRESA, Spain (J. Bruno)
f) Coupled Modelling:	EMP/CEA (Ph. Jamet, D. Stammose)

Stage 1 - Definition and initiation of programme, production of status reviews;

Stage 2 - Execution of research programmes for each technical area encompassing data review, model development, code verification, and model validation;

Stage 3 - Comparison with experimental studies and final reporting.

C. PROGRESS OF WORK AND OBTAINED RESULTS

State of advancement

During 1994, the tasks identified in the CHEMVAL2 status review [4] and the programme of experimental and numerical investigations have been completed. The results presented at the 5th Plenary Meeting (Barcelona) have been analysed and issued as progress report [5]. Draft final reports were circulated at the 1994 MIRAGE meeting in Brussels and are now being finalised.

In addition the need for continued development and maintenance of a standardised thermodynamic database, both within this project, and for studies of radioactive waste management in general, has been recognised and was undertaken in parallel with the CHEMVAL2 programme under the related CEC Contract F12W/CT92/0122.

Progress and Results

The structure of the CHEMVAL2 Project is shown in Figure 1. WS Atkins together with the two main funding organisations, CEC and HMIP, provide a secretariat acting as contact point for the technical coordinators. The role of WS Atkins encompasses organisation of meetings, preparation of reports and dissemination of data in addition to modelling and review activities. Progress within each research area is summarised below.

a) Temperature Effects

Owing to the incompleteness of data describing the heat capacity of many species as a function of temperature, a modified form of the classic van't Hoff relationship has been adopted to account for temperature induced changes in equilibrium stability constants. The activity coefficients of ions in solution also vary with temperature and a modification of the Davies Equation [6] was proposed by BRGM/ANDRA to account for this. The expression incorporates a fourth order polynomial for the Davies 'A' parameter enabling calculations to be made in the range 0-200°C.

In order to implement and test these ideas, modifications were made to existing codes and comparisons undertaken against a set of verification tests performed by participants using alternative numerical methods. The test cases included data from the Dogger limestone reservoir of the Paris Basin [7] and a New Zealand geothermal field [8]. In summary the methodology appears to work well below 100°C but breaks down progressively at higher temperatures. This is particularly the case for carbonate-rich systems where the dependence of stability constants on heat capacity can no longer be assumed to be negligible.

To date, enthalpy values have been obtained for more than 50% of the aqueous and 80% of the solid species present in the CHEMVAL Database (V4.0). These have been incorporated into the database for release as Version 6.0 [9].

b) Ionic Strength Effects

The CHEMVAL thermodynamic database as developed up to the release of Version 5.0 in May 1994 accounts for the activity coefficient (γ) using a modified form of the Davies Equation [6] and is intended for applications where the total salinity does not exceed 0.3 mol dm^{-3}. In order to extend simulations to more saline waters, a work programme was adopted [4] with the following objectives:-

i) to compare alternative procedures for γ correction using a series of standard test cases;

ii) to implement a viable method for γ correction allowing equilibrium calculations for waters ranging to ≈2 molal within tolerable error limits.

As with the elevated temperature programme described previously, a practical method was required which could be applied consistently to a range of different conditions. Thus, for reasons of data availability, the Specific Interaction Theory (SIT), advocated by Grenthe et al. [10], was preferred over the approach of Pitzer and co-workers [11]. Comparison of the various correction methods available clearly demonstrated the suitability of SIT (Figure 2) and, subsequently, considerable effort has been expended in re-casting the CHEMVAL Database (V5.0) using the relationship:-

$$\log \gamma_i = -A\, z_i^2((I^{1/2} / (1+ 1.5 \cdot I^{1/2})) + \sum_k \varepsilon_{ik} M_k \qquad (1)$$

where ε_{ik} is the specific interaction coefficient accounting for short range interaction between the *i*th and the *k*th ion, and I, z_i, and A have their usual meaning.

Approximately 200 published interaction coefficients have now been collated and the database has been re-evaluated accordingly. As the database contains in excess of 1,300 aqueous species, however, a protocol has been developed to guide users where the necessary constants are lacking. This database will be issued concurrently with the general Version 6.0.

c) Organic Complexation

The problems associated with quantifying complexation of trace elements by high molecular weight organic matter were highlighted during the original CHEMVAL Project [2]. The theoretical basis for most extant models is weak and few if any have

a real predictive capability. CHEMVAL2 has sought to develop a practical modelling tool which may be used in conjunction with conventional inorganic speciation models. Comparative evaluation of models has focused on a simple mixed ligand binding model [12], a statistical approach based on a continuous distribution of formation constants [13], and electrostatic double layer methods [14,15]. The work of [14] and [15] had to be reconciled with the requirements of inorganic speciation calculations, in some cases necessitating the development of new codes [16].

Each model was assessed against both literature data and the results of bespoke experiments performed at LUT. The experimental data were obtained using High Performance Size Exclusion Chromatography (HPSEC) for the binding of Ni onto humic material.

Prediction of the amount of metal bound to humic and fulvic acids is primarily dependent on the formulation of the binding equations, the actual constants used and the assumed site densities on the organic molecule. All of the models employed are able to fit the experimental data, though it has not yet been demonstated that any has a real and generic predictive capability. Overall, it was concluded that the electrostatic approach as formulated by Tipping and co-workers [14] offers the most advantages, primarily for reasons of data availability. This model was incorporated, therefore, into the PHREEQE code [16,17] and distributed among the CHEMVAL participants.

d) Sorption Processes

The objectives of work on sorption processes within CHEMAL2 are to compare the various models which have been incorporated into geochemical speciation codes and to assess their usefulness for simulating observed behaviour in the laboratory and in the field. Participants were provided with information on the amount of metal sorbed to selected substrates at fixed values of pH, ionic strength and metal concentration. They were then asked to calibrate their preferred model before interpolating and extrapolating the simulations as a function of the primary controlling variables. In the case of uptake onto mono-mineralic surfaces (Co, Am, U, Ni onto silica; Am onto alumina) reasonable predictions were obtained for four of the five cases, the exception (Am–silica) reflecting the highly irregular data set. No obvious conclusions could be drawn, however, concerning the relative performance of the models in a predictive sense. The fact that most models are capable of reproducing the supplied data sets suggests that further work is needed to constrain the degree of freedom in modelling assumptions.

Two alternative conventions to simulating adsorption were identified; these differ in whether or not the activity coefficients of binding species are included explicitly

during calculation of the surface concentrations. Sorption constants derived for a particular reaction depend on the convention adopted and caution must be exercised when extracting and employing literature data.

The testing of sorption models for natural systems focused on bespoke experiments conducted by BGS of Ni uptake onto sandstone from NW England. Experimental data were reproduced with reasonable accuracy using a triple layer model [18] by assuming that Fe-oxides dominate surface behaviour (Figure 3). Much more work is required to demonstrate that such simplifying assumptions may be applied more widely.

e) Co-Precipitation

Solubility limits based on equilibrium precipitation–dissolution of idealised stoichiometric phases are used to establish source term concentrations for radiological assessment and also to estimate maximum concentrations of radioelements in geologic media. Calculations based on pure solid phases may be grossly in error, however, as trace elements in nature tend to occur as substituted 'impurities' in mineral phases.

From a phenomenological point of view two different distribution laws have been used to describe the partitioning between coprecipitates and the aqueous phase at equilibrium. If equilibrium is attained between the bulk of the solid solution and the aqueous phase the system follows what is known as the Berthelot-Nernst homogeneous distribution law:-

$$([A] / [B])_{aq} = D\,(\{A\} / \{B\})_{solid} \qquad (2)$$

When equilibrium is reached only between the surface of the solid and the aqueous phase, the distribution of components follows the so-called Doerner-Hoskins logarithmic law:-

$$\log ([A] / [B])_{aq} = \lambda\,(\{A\} / \{B\})_{solid\ surface} \qquad (3)$$

At a low percentage of enrichment of the host solid phase by the foreign ion, the values of D and λ tend to converge [19]. Also, since at low enrichment of the host solid phase (<5%), the activity of the host remains essentially unchanged, the activity of the trace metal (T) can be related to its molar fraction in the solid solution. Consequently, the conditional solubility product of the trace metal solid in the co-precipitate can be expressed as [4]:-

$$K_{sp(co\text{-}precipitated\ T)} = K_{sp(pure\ T\ phase)} \cdot \chi_{T(OH).n} \qquad (4)$$

This gives an operational way of approaching trace metal co-precipitation within geochemical modelling by relating the conditional stability constant to the individual thermodynamic properties of the trace metal oxide as well as to the amount of trace metal coprecipitated.

This approach has been tested against field data from the Poços de Caldas natural analogue site in Brazil where uranium levels in groundwaters are thought to reflect equilibrium with uranium–iron oxyhydroxide coprecipitates [20]. More exhaustive testing of the U–Fe system has been possible on the laboratory scale following experimental work performed at the Polytechnical University of Catalonia (UPC). Spectroscopic analysis of the co-precipitated solid provided conclusive evidence of U incorporation within the Fe oxide lattice as opposed to scavenging by purely surface phenomena. Examination of kinetic data indicates at least a two step process in which rapid surface uptake is followed by microscopic rearrangement and firm fixation upon ageing. The application of the simple conditional constant approach to U partitioning, based on the solubility of schoepite ($UO_2(OH)_2$), was shown to give satisfactory results at up to 3% uranium enrichment.

f) Coupled Chemical-Transport Processes

Significant developments carried out to coupled codes following the completion of the first CHEMVAL Project [3] have allowed more exhaustive verification and true *a priori* simulations of both laboratory experiments and field systems. Experiments designed specifically for testing such models have been performed at AEA Winfrith (UK) and CEA Grenoble (France) dealing with, respectively:-

- uranium transport through intact sandstone cores, and
- transport of caesium and strontium through a packed, clay-rich alluvial sand column.

The Winfrith case actually comprises eight separate floods aimed at quantifying the effects of metal concentration, competing ions, organic complexants (EDTA) and surface characteristics on uranium transport. The reversibility of uranium adsorption and the kinetics of the desorption process were also studied. Results obtained to date indicate that the bulk of uranium transported through the column is in reversible equilibrium with mineral surfaces and uptake can be quantified, therefore, using a surface complexation model with an electrostatic double layer description of the surface reactions. The surface was found to have a high but finite capacity for uranium and, once saturated, provided no barrier to migration. More than 90% of the uranium sorbed was readily recovered during down-flooding with the remainder much more strongly bound (Figure 4).

D. CONCLUSIONS

Research carried out within the CHEMVAL2 Project has greatly enhanced the ability of participating groups to simulate geochemical reactions under conditions other than steady state. Accounting for the effects of temperature and salinity present analogous problems in many respects as both are primarily constrained by data availability rather than by lack of conceptual understanding. The database initiatives started within CHEMVAL2 represent substantial progress but do not, by any means constitute a final solution. Importantly, however, the methods chosen can be extended to other components and to more extreme conditions without modification. No universally acceptable approach has been found in the case of metal binding by high molecular weight natural organics (humics) or surface adsorption. On the balance of evidence within this study, a preference has been expressed for electrostatic models in both cases and data are currently being collated to allow more exhaustive testing. The relatively simple conditional solubility approach to simulating coprecipitation has been shown to work well for the systems studied and has the added advantage of requiring no additional data. Finally, coupled chemical transport investigations, albeit on small-scale laboratory columns, have engendered confidence in the ability of extant models to predict contaminant migration behaviour within known limits. Extrapolation of these findings to the field, however, will undoubtedly prove to be much more problematic.

E. ACKNOWLEDGEMENTS

The CHEMVAL2 Project is supported under the 4th CEC Research and Development Programme on the Management and Storage of Radioactive Waste (1990-1994. Funding from the UK DoE/HMIP is also gratefullly acknowledged. The results of this work may be used in the formulation of UK Government Policy, but views expressed in this work do not necessarily represent UK Government Policy. Particular thanks are expressed to H. von Maravic (CEC) and R. Yearsley (HMIP), the following staff at WS Atkins: J. Thomas, D. Bennett and M. Tyrer, and all the CHEMVAL2 participants.

F. REFERENCES

[1] READ, D., BROYD, T.W., CHEMVAL Project. Report on Stage 1: Verification of Speciation Models. CEC Report EUR 12237EN. 364 p. (1989).

[2] READ, D. (Ed.), CHEMVAL Project. Report on Stage 2: Application of Speciation Models to Laboratory and Field Data Sets. CEC Report EUR 13124EN. 229 p. (1990).

[3] READ, D. (Ed.), CHEMVAL Project. Report on Stages 3 and 4: Testing of Coupled Chemical Transport Models. CEC Report EUR 13675EN. 234 p. (1991).

[4] READ, D. (Ed.), CHEMVAL2 Project. Status Review of CHEMVAL2 Technical Areas, June 1992. Report UK DoE/HMIP/RR/93.014, 236 p. (1992).

[5] READ, D. (Ed.), CHEMVAL2 Project. 5th Progress Report Covering the Period May 1993 - April 1994.

[6] DAVIES, C.W., Ion Association. Butterworths, London (1962).

[7] ROJAS, J., Caracterisation et modelisation du reservoir geothermic du Dogger Basin, Parisien, France. BRGM Report R30269 IRGSGN89 (1989).

[8] BRUTON, C.J., GLASSLEY, W.E., BOURCIER, W.L., Field Based Test of Geochemical Modelling Codes: New Zealand Hydrothermal Systems. Mat. Res. Soc. Symp. Proc., 333: 617-24.

[9] FALCK, W.E., PAUL, L., CHEMVAL2 Project. Final Report on the Thermodynamic Database Project. CEC Report EUR (in prep.).

[10] GRENTHE, I., FUGER, J., KONINGS, R.J.M., LEMIRE, R.J., MULLER, A.B., NGUYEN-TRUNG, C., WANNER, H., Chemical Thermodynamics of Uranium, Chemical Thermodynamics 1, North Holland, Amsterdam etc. (1992).

[11] PITZER, K.S., Thermodynamics of Electrolytes. I. Theoretical Basis and General Equations. J. Chem. Phys., 77, 268-77.

[12] SPOSITO, G., MATTIGOD, S.V., GEOCHEM: A Computer Program for the Calculation of Chemical Equilibria in Soil Solutions and other Natural Water Systems. Dept. Soil Environ. Sci. Rep., Kearney Found. Soil Sci., Univ. Calif.

[13] PERDUE, E.M., LYTLE, C.R., A Critical Examination of Metal-Ligand Complexation Models: Application to Defined Multi-Ligand Mixtures. In: CHRISTMAN, R.F., GJESSING, E.T. (Eds.), Aquatic and Terrestrial Humic Materials, Ann Arbor (1983).

[14] TIPPING, E., HURLEY, M.A., A Unifying Model of Cation Binding by Humic Substances. Geochim. Cosmochim. Acta, 56: 3627-41.

[15] FALCK, W.E., Two Modified Versions of the Speciation Code PHREEQE for Modelling Macromolecule-Proton/Cation Interaction. CEC Report EUR13202EN (1989).

[16] CRAWFORD, M.B., PHREEQEV: The Incorporation of a Version of Model V for Organic Complexation in Aqueous Solutions into the Speciation Code PHREEQE. Comp. Geosci., (in press).

[17] PARKHURST, D.L., THORSTENSON, D.C., PLUMMER, L.N. PHREEQE: A Computer Program for Geochemical Calculations. USGS Report USGS/WRI 80-96 (1985).

[18] DAVIS, J.A., JAMES, R.O., LECKIE, J.O., Surface Ionization and Complexation at the Oxide/Water Interface. I. Computation of Electrical Double Layer Properties in Simple Electrolytes. J. Coll. Interface Sci., 63(3), 480-99 (1978).

[19] STUMM, W., MORGAN, J.J., Aquatic Chemistry. 780 p., New York, J. Wiley (1981).

[20] BRUNO, J., CROSS, J.E., EIKENBERG,J., McKINLEY, I.G., READ, D., SANDINO, A., SELLIN, P., Testing of Geochemical Models in the Poços de Caldas Analogue Study. NAGRA Rep. NTB 90-29 (1990).

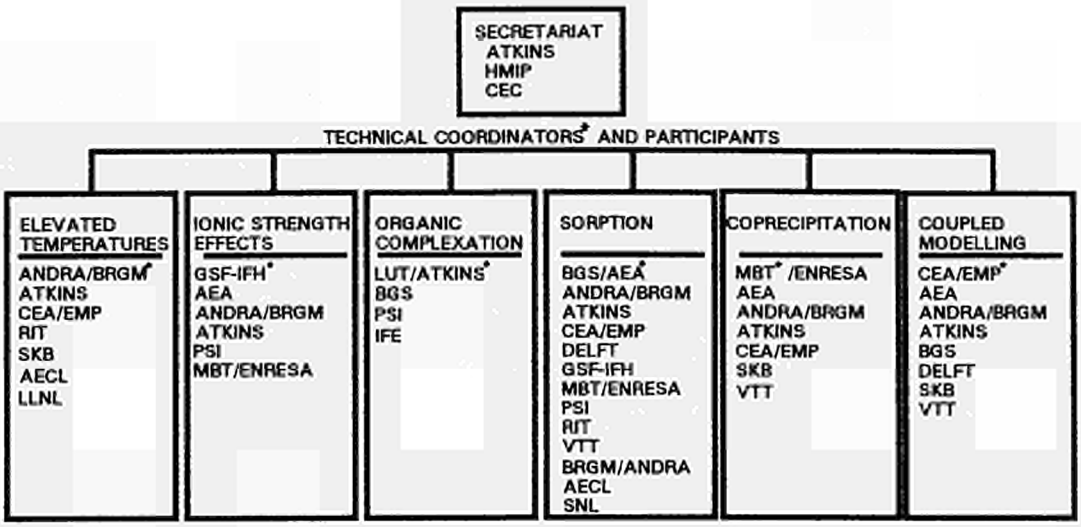

Figure 1: Organisation of the CHEMVAL2 Project

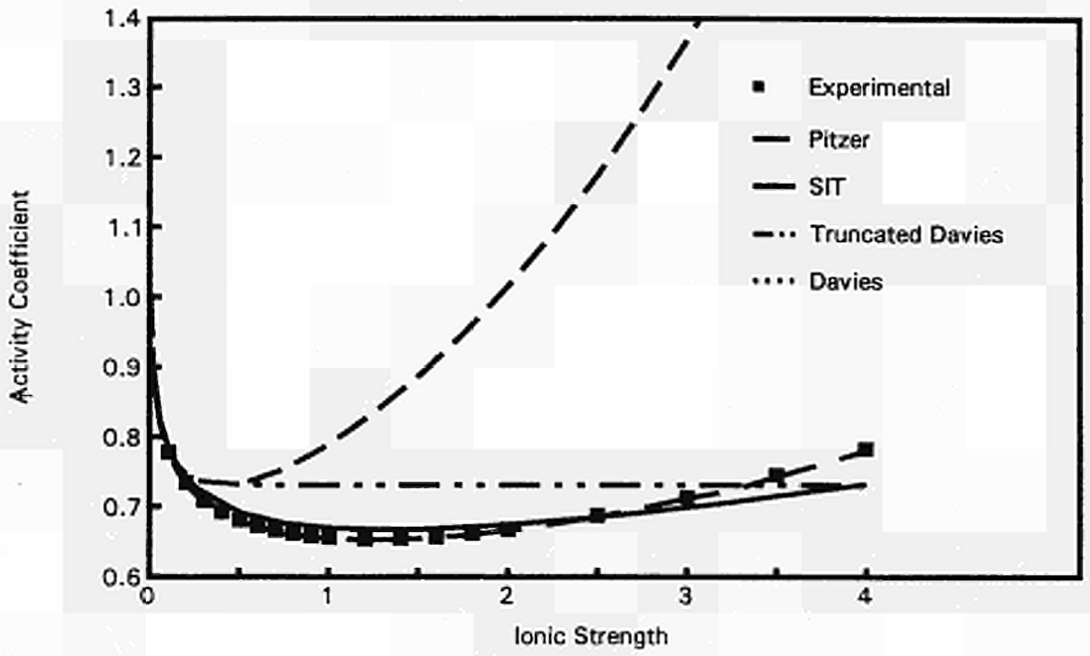

Figure 2: Comparison of activity correction methods: NaCl-solution.

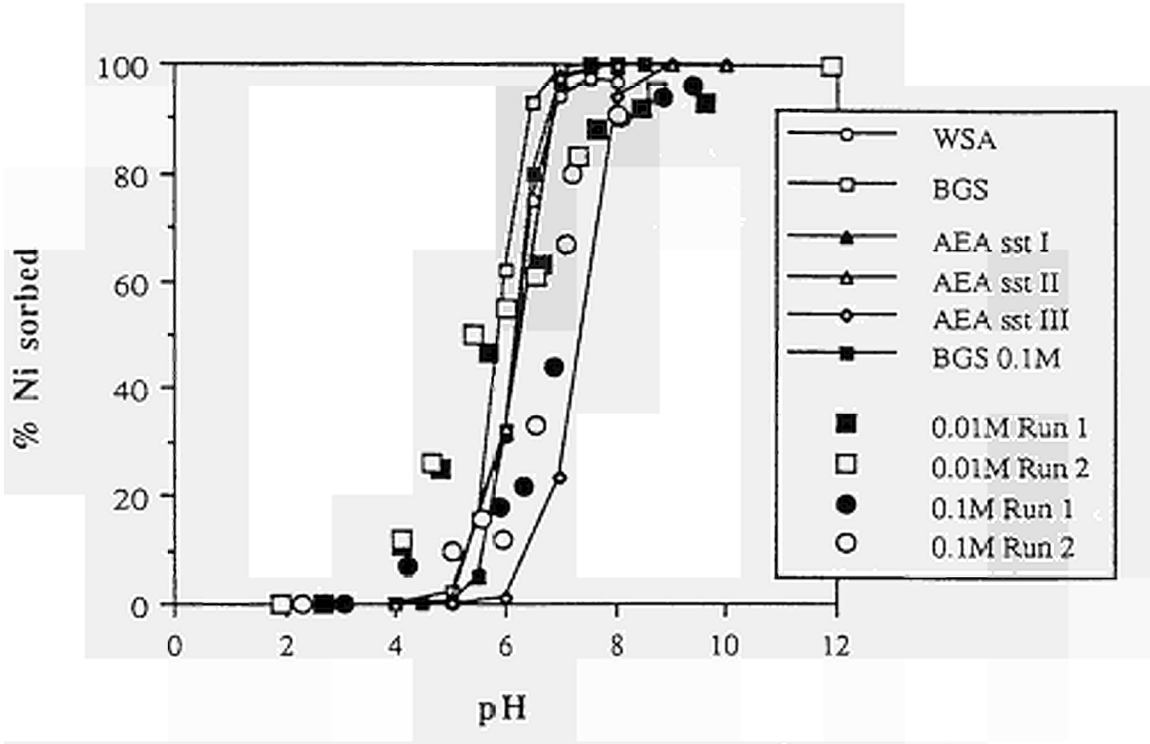

Figure 3: Modelling of Ni-sorption onto St. Bees Sandstone

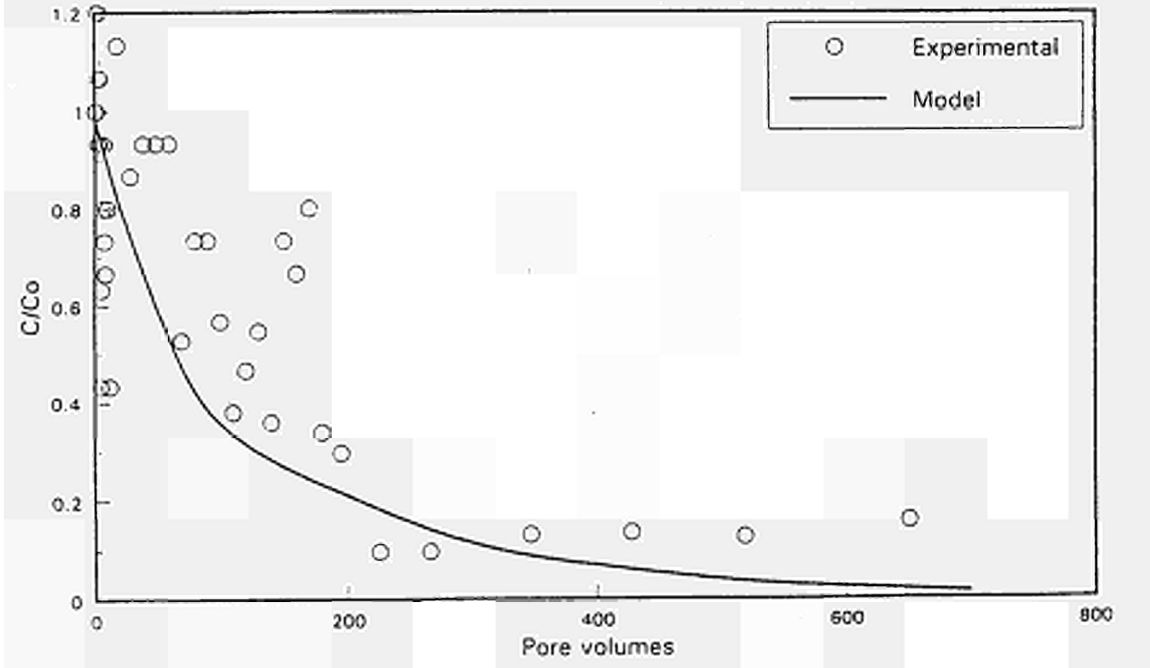

Figure 4: U-transport through Clashach Sandstone: Down-flooding.

Title	Oklo, natural analogue for transfer processes in a geological repository
Contractors	CEA/IPSN, CNRS/CGS, CREGU
Contract N°	FI2W-CT90-0071
Duration of contract	January 1991 - June 1995
Period covered	January 1994 - December 1994
Project leader	General : P.-L. Blanc (IPSN/DPEI), Source term : Ph. Holliger (DCC/DESD), Ancient migrations : F. Gauthier-Lafaye (CNRS/CGS), Recent migrations : E. Ledoux (EMP), P. Toulhoat & D. Louvat (DCC/DESD), Integrated modelling : E. Ledoux

A.- OBJECTIVE AND SCOPE

The nuclear phenomenon of Oklo (Gabon) is the only natural case of fission products being stored in a geological environment for a significant period of time (two billion years). Therefore, the Oklo uranium deposit is a good example for the study of natural analogy with deep radioactive waste disposal, specially radionuclide mass transfer processes to the surface. However the peculiarities of this uranium ore deposit imply a thorough assessment of the radionuclides and daughters as well as ancient and recent geochemistry and hydrodynamics.

B.- WORK PROGRAM

This program involved several different tasks :

1.- *In situ* SAMPLING, in close collaboration with the mining company (COMUF, Mounana, Gabon). To this part of the program was added the collecting of new data on the general setting of the Oklo mining area and deposits.

2.- Study and characterisation of the SOURCE TERM (mostly in CEA laboratories).

3.- Studies on the geochemical systems ruling the migrations have been in turn be divided into : studies on the ancient migrations, contemporaneous to the rock diagenesis, to the nuclear reactions and to the general geological history of the basin, and on the recent to present migrations (tertiary to present?).

3.A.- The studies of the ANCIENT MIGRATIONS encompassed several subjects, and implied collaboration between CEA laboratories and other institutions :

3.A.a.- CEA laboratories (DCC/DESD) cooperated with other institutions in the program to assess the petrography and elemental chemistry of the deposits.

3.A.b.- The retention properties of the clays towards radionuclides have been the main topic of the investigations of the CGS (CNRS, Strasbourg).

3.A.c.- The contribution of CREGU (Nancy) has been to investigate the thermal history of the deposits in and around the reactor zones. The CRPG (CNRS, Nancy) collaborated with them to the modelling of heat transfer.

3.A.d.- The reconstruction of the chemical characteristics of the hydrothermal fluids which left their chemical imprint in tracer mineral when they were circulated through the deposits has been conducted by the EMP (Fontainebleau).

3.B.- The study of the RECENT MIGRATIONS also implied collaborations between CEA laboratories and other institutions :

3.B.a.- The CIG (EMP, Fontainebleau) has been responsible for the understanding of the hydrogeological conditions.

3.B.b.- DCC/ DESD has taken charge of the hydrochemistry.
(Conterra A.B. on behalf of SKB (Sweden) has been involved in part 3.B., particularly on the Bangombé area.)

4 - MODELLING : The final integrated hydrodynamical-geochemical modelling is the responsibility of EMP on behalf of CEA/ IPSN.

C.- PROGRESS OF WORK AND RESULTS OBTAINED

State of advancement

We can summarise the present state of the program as follows :

TASK 1, FIELD SAMPLING, is now finished : the last opportunities for solid rock sampling were provided by an hydrogeology & hydrochemistry field missions in July, 1994 : important results may be integrated in the last reports as annexes, or more likely in a second phase of the Oklo project.

TASK 2, SOURCE TERM studies : the analytical phase has now been finished for one year. A general balance of fissiogenic materials has been obtained for RZ 10, the best preserved. The final report of this task is now under edition.

TASK 3.A, ANCIENT MIGRATIONS : in the case of this task also, the analytical phase has been finished for one year. The wealth of data collected on the general petrography and geochemistry of the reactor zones, on the reactor-clay, on the reconstruction of the fluids and on the fluid inclusions has now been synthesised in a final report now under edition.

TASK 3.B, RECENT MIGRATIONS, is very much linked to TASK 4, INTEGRATED MODELLING. The water samples needed for the hydrochemical and isotopic analyses have mainly been collected in 1993. Though a complete description and understanding of groundwater chemical evolution in Okelobondo and Bangombé conceming major elements behaviour, redox control and uranium behaviour has been obtained, the final interpretations of the data and the final report on the hydrochemistry have not been obtained as yet. Thus the integration of the hydrochemistry data into the hydrodynamical model has been delayed. The EC allowed us a six month delay for the completion of the modelling exercise.

Progress and results

1 - FIELD SURVEY, SAMPLING, AND GEOLOGICAL SETTING :

The last-discovered fission reactors in Oklo showed some oddities by comparison to those previously studied. (RZs 1 to 9) which had been worked out before this program was initiated. RZ 15, to the North, came to the same end and was not studied, but work was in full course in RZs 10 & 13, thus accessible, and several others, though recognised, were not worked yet, in Okélobondo (OK 84^{bis}) and in Bangombé (Ba 145 &-^{bis}, c^a 30 km S-E from Oklo). RZ 16 was discovered in the course of the program, in April, 1991. The opportunities to compare, not just new results to parameters obtained years ago, but also to apply simultaneously new techniques or methods to samples from different RZs and deep environments, have been very stimulating in producing new hypotheses and interpretations.

2 - THE SOURCE TERM :

The source-term characterisation consists into U and FP isotope measurements, in order to calculate the nuclear parameters for each RZ, and the amount of radionuclides & daughters retention in the reactor core, *i.e.* their (very) near-field geochemical behaviour.

Most of the isotope data were obtained by Secondary Ions Mass Spectrometry, allowing :

.- on the one hand, to obtain complete punctual mass spectrums between 1 & 280, gathering all the elements and atom associations (mainly simple and double oxides such as UO_2), the major interest being in the mass range of the FP, between 80 & 180 ;

.- on the other hand, by scanning polished rock surfaces 100 to 400µm in diameter for the masses of interest, to obtain images allowing comparisons of the distribution of different elements or isotopes in the sample.

DATING THE SPONTANEOUS FISSION REACTIONS :

The U/ Pb age of crystalline uraninites from RZ 10, preserved in organic matter, is 1.968±55 Gy, in accordance with the 1.950 Gy calculated from the U to Nd and U to Th fission balance.

By contrast, galenas from the core of RZ 13, have given a $^{207}Pb/^{206}Pb$ age of 870 ±40 My, in accordance with the U/Pb age obtained on massive uraninites from the same levels, which is 850 ± 50 My. This is interpreted as dating the rearrangement of the crystalline lattice of these uraninites during the contact metamorphism caused by the intrusion of a Dolerite dyke cutting East-West.across the bearings.

The global mean $^{235}U/^{238}U$ isotopic ratio at the time of the spontaneous fission reactions has been estimated : 1.95 Gy ago it was 3.68 %, i.e. five times higher than the present global value of 0.7254 %.

NUCLEAR PARAMETERS :

These nuclear parameters come from results obtained on samples from several reactor zones: 2, 7-9, 10, 13, Okélobondo and Bangombé :

.- On reactor core whole rock samples, the ^{235}U depletion range between 0.463 % et 0.678 %.

.- Fluences are between 1.36 et 0.225 x 10^{21} n/cm^2.

.- The number of fissions, per ^{238}U atom present today, range between 0.5 et 3.5 %.

.- The apparent age, calculated from the abundance of U, Nd & Sm is between 1.8 and 2.2 Gy (the true age being 2 Gy). These elements remained into position with reference to each other.

.- On the contrary, the U migration is spectacular in the Okélobondo area (sample OK 84bis) where the Nd & Sm apparent age is 5 Gy, corresponding to a 95 % loss of initial U in the clay facies.

.- In the Ba 145 RZ, the present thickness of the core (only 5 cm) does no longer account for criticality at any time in the history of the bearings, thus evidencing U loss.

RADIOLYSIS :

Water radiolysis has been evidenced at the edge of RZ 10 core : free O_2 & H_2 were found in fluid inclusions in quartz crystals. Locally oxidising conditions are confirmed by small amounts of minium (Pb_3O_4) and hematite : H_2 is inert at low temperatures, but O_2 remains very reactive. However metallic lead, galena and coffinite show that overall a reducing environment has been maintained in the core of the RZs, probably as a result of buffering of the redox conditions by the organic matter.

TOPOGRAPHY OF REACTOR ZONE 10 :

Topographical and geological data both from mining drifts and boreholes in RZ 10 have been fed to an " Earth vision " computer software by the Eosys company, in order to obtain a 3-D description of the RZ, showing the volume distribution of the core facies, and curves of equal ^{235}U ratio. This 3-D modelling also allows an evaluation of the total U consumed and of the energy dissipated by the nuclear fission reactions :

Overall, the reactor zone 10 core facies amounts to a south-east to north-west lens, or tongue, with a rough length of 40m, 10 to 15m width and a 0.5 to 3m thickness.

The reactor core volume for various depletion rates, as obtained from the balance so calculated, can be found in the following budget.

$^{235}U/^{238}U$	ROCK VOLUME
< 0.7 %	5500 m^3
< 0.675 %	1400 m^3
< 0.650 %	310 m^3
< 0.600 %	80 m^3
< 0.575 %	12 m^3

This gives a high estimate of 90 kg for the weight of ^{235}U missing at present, *i.e.* 650 kg consumed at the time by the nuclear reactions.

3.A.- THE GEOCHEMICAL SYSTEMS : ANCIENT MIGRATIONS

3.A.a.- PETROGRAPHY AND ELEMENTAL CHEMISTRY

Rock facies, in and around the deep reactor zones are similar to those known from the previously studied reactor zones, but they exhibit some peculiar features, such as a high mechanical coherency, related to the absence of supergene weathering. The same differences are now found with the shallow Bangombé "Ba 145" zone.

The sandstones surrounding the reactors were deposited as layers (or lenses) with thickness ranging from a few centimetres to the meter. The grains ranges from fine sand to conglomerate. Ferrous chlorite and illite are present, and calcite may be present as fissure infillings.

The "reactor-clay" facies generally surrounds the reactor proper. Magnesian chlorite is interspersed with corroded quartz grains and less-soluble primary minerals (zircon, sphene, uranium oxides). Secondary minerals (coffinite, cryptocristalline zircon, sphene & apatite) develop at their expense. Organic matter is generally present in close vicinity to the reactor-clay and reactor-core facies. In Bangombé, ferralitic alteration is superimposed, and red (ferrous) oxydes are present at every level.

The main mineral phases in the "reactor-core" facies are uraninite and magnesian chlorite. In the shallow Ba 145 reactor, hematite and iron hydroxides are present together with titanium oxides,

separated from uraninite by a rim of illite.

All these facies can be run through by fissures, with a width ranging from micrometers to a few millimetres. They are generally filled with fibrous calcite (probably dissolved at Bangombé).

3.A.b.-FISSION PRODUCTS MIGRATION :

The conclusions expressed in 1978 & 1991 by R. Naudet remain globally valid, but they must be somehow attenuated. It now appears that U & PF (including the lanthanides) migrations are rather a rule.

The conclusions which can be drawn on radioelements mobility as studied in the new RZs are summed up in the following table.

RADIOELEMENT/ FISSION PRODUCTS	BEARING PHASES IN REACTOR 10 WALLS
Uranium	Uraninite, clays, apatite
Plutonium (^{235}U enrichment)	Clays, apatite
Thorium	Heavy minerals (?)
Rare Earth Elements	Uraninite, clays, apatite
Platinum metals	(?)
Zirconium	Heavy minerals (?), oxides (?)
Antimony & silver	Sulphides
Lead	Sulphides, metallic lead

Uranium : Anomalous U is found in the walls of the RZs, 10 cm to 1m from the core facies, in clays or in sandstones. Several migration phases took place, as the U shows a different isotope ratio according to its position, into the crystal structure of the minerals or only adsorbed at their surface. At the edges of RZ 10, an enrichment in fissiogenic REE has been caused by alteration conducting to U loss.

Plutonium & other transuranic elements : In RZ 10, it has been shown that Pu migrated either during or soon after the fission reactions, during the crystallisation of the reactor clays. It is difficult to estimate with accuracy the amount of Pu having actually migrated from the various RZs.

Thorium : This is a very stable element, well correlated to U in the core of the RZs. The anomalies observed in the walls of RZ 10 evidence a mobility of ^{236}U, before its transmutation into ^{232}Th.

The Rare Earth Elements : As a rule, the spectrum of the REE content in the sandstones and clays close (< 50cm) to the core facies is very similar to the ^{235}U fission production. When dissociated, they reveal a mobilisation of U by comparison with the REE. The clays have retained the REE which migrated while the RZs were active. The heavy to intermediate REE have been more mobile than the light REE. Such a conclusion had already been formulated on RZ 2.

The platinum elements : Metallic aggregates, containing fission platinum elements Ru, Rh & Pd (associated to Pb, As & S) and Te inclusions (associated to As, S, & Bi) separate from platinum metals, have been discovered in silica and at joints of UO_2 grains having undergone fission. In this case, ^{209}Bi marks the good containment of ^{237}Np. These grains are homologous of insoluble nodules observed in modern spent fuel, and this is one of the strong point of the analogy with man-made waste disposal . The ^{99}Ru/^{101}Ru isotope ratios demonstrate that these aggregates are contemporaneous to the fission reactions, and that ^{99}Tc, father to ^{99}Ru, was trapped there. The distributions of Ru, Rh & Pd in the reactor clays are in accordance with their respective fission yield, showing their fissiogenic origin and their mobility from the core to the walls in RZ 10. Isotope analyses show a mobility of Pd by comparison to Rh & Ru. This conclusion is at variance with results obtained on RZs 1 to 8, where Ru, trapped in sulphides, had been evidenced at a migration distance of 1,5 m from the RZs, or even to some 10 meters. Pd & Rh were considered as more stable.

Zirconium : Fissiogenic Zr, characterised by its ^{91}Zr/^{90}Zr ratio, has been detected, together with natural Zr, in the walls close to the core of RZ 10. A slight negative anomaly in ^{91}Zr, daughter to ^{91}Y, reveals an early migration of this element from the RZ core.

The Alkalies and alkaline-earth elements : Significant isotopic anomalies of Rb, Sr & Ba have been reported once, in RZ 10 core : as they are very soluble, they were in most cases easily mobilised by the reactor fluids and replaced at the end of the reactions by elements with a normal isotopic composition.

3.A.c & d.- THERMAL HISTORY OF RZ 10 AND RECONSTRUCTION OF THE ANCIENT FLUIDS :

Microthermometric measurements have been done on the fluid inclusions of authigenic quartz, apatite and calcite crystals. The observed evolution shows a decrease in temperature away from the RZ. Furthermore, the fluids show an increase in salinity reflecting the importance of the phenomena of mineral dissolution during the fission reactions. In quartz, the reactor fluid, of a low salinity, was heated up to more than 400 °C. Apatite recorded a lower temperature, but an increased salinity, while finally in calcite, the temperature was of about 120 °C, with a strong salinity.

During hydrothermal circulation, mineral precipitation occurred at the cheeks of open fractures (vein linings), or as isolated crystals in the rocks. Authigenic minerals play a role as traps for dissolved species, efficiently concentrating some elements, according to the mineral considered. Apatite and sulphides (galena and pyrite) are geochemical traps for REE, for Ag , As & Sb, and for Mo, respectively.

The correspondence between thermal and chemical observations is good, and four hydrothermal circulation stages have been inferred :

.- The initial fluid, reworking the sedimentary metallic stock from the FA sandstones, shows no relation with the RZs ;

.- The fluid related with the nuclear reactions, 1.97 Gy ago, seems to have had a very light elemental load, except FP, according to the REE content of the associated apatites ;

.- Another fluid apparently contributed to the dilution of the fluids which escaped from the RZs ;

.- a very late hydrothermal stage is related to the dolerite intrusion, about 850 My ago.

The modelling of the heat transfers associated to the reactions has been revisited, and shows that before the reactions, the fluid circulation in the bearings were in accordance with what is known for basins undergoing subsidence and burial. The nuclear reactions did not change considerably the hydrodynamical regime around the RZs. The main heat dissipating process was not convection, but conduction. The intense weathering of rocks in and around the RZs was caused by the increase in temperature alone, and by the very long time factor, which allowed quantitatively important transfers.

3.B.- THE PRESENT MASS-TRANSFERS

The aim of the far-field studies was to assert & to model the groundwater circulation, which may transport elements produced in the RZs.

3.B.a.- HYDROGEOLOGY

A drilling & sampling program, set down in 1991-1992 after a preliminary modelling, was conducted from September, 1992 to August, 1994. Two sites are investigated:

.- a deep RZ in Okélobondo allows the study of elemental transfers at a 500 m scale, through a highly heterogeneous sedimentary sequence ; the area is submitted to an upward (discharging) groundwater flow from deep geological formations, increasing the odds to sample waters having been in contact with a RZ ;

.- the almost outcropping RZ at Bangombé, in a well-defined flow system, in a less heterogeneous geological situation, but undergoing active surface alteration.

A good understanding of the hydrodynamical conditions on both site has been reached : piezometric levels (hydraulic heads) in Okélobondo are about 375 m in the discharge area, and about 435 m in the recharge area. Data in the surficial piezometers are in accordance with the preliminary modelling, while the deeper ones show the influence of the mining activities ; At Bangombé, piezometric observations show that, upstream from the experimental trench, the free water table is about 15 m below ground surface, while it is just level with the surface below this trench. The change in heads from the dry to the rainy season have remained minor during the observation period. On both sites hydraulic tests have been performed in order to assess the hydraulic conductivity of the stratigraphic units of concern.

The preliminary modelling had shown the need to complete the drilling program to collect new data to constrain the conceptual models. The next step will be a successive integration of the new data : physical and chemical parameters, and will be followed by the radionuclide transport modelling.

3.B.b.- HYDROGEOCHEMISTRY

Sampling campaigns for hydrochemical & isotope analyses of the waters, needed for the validation of the proposed hydrogeological model, and for the development of the hydrodynamical model, have taken place from February, 1993 to August, 1994.

The groundwaters evolution is evaluated with reference to two major phenomena :

- the progressive acquisition of solutes by water-rock interaction, and the following reequilibration with secondary minerals ;
- the lithological redox conditions, which are usually controlled by an equilibrium between Fe II (dissolved) and Fe III.

The Oklo-Okélobondo Area : Groundwaters in the Oklo-Okélobondo area are distributed into 3 types :

- shallow waters (alterites) have a low pH & a low bicarbonate content, low total dissolved sulphur, but a high CO_2 content caused by biological activity, and a high tritium content ;
- intermediate waters (upper pelites & complexes) show intermediate pH & alkalinity, together with a high silica content due to intense leaching, a total dissolved sulphur content increasing with pH, intermediate ^3H content, and a tendency to equilibrium with carbonate minerals, in carbonate rich aquifers (dolomitic complexes) ;
- confined waters (deep pelites & Okélobondo mine) show a high pH, high alkalinity, high total dissolved sulphur, low ^3H content and a tendency towards equilibrium with secondary alumino-silicate minerals and are at equilibrium with carbonates. However the waters from the OK 84 RZ show a high ^3H content, so that the possibility of *in situ* ^3H production is under investigation, rather than recent contamination.

The redox control is anomalous, with no correlation between depth and confinement : the most reducing waters are found in organic matter bearing aquifers.

Preliminary results on the stable environmental isotopes allow a similar distribution of the Okélobondo groundwaters into three sets :

- surface waters have the highest heavy isotopes content : their main recharge is of local origin, at present,
- the deeper & more eastern waters are depleted, indicating either recharge under cooler climatic conditions or recharge from an area at a higher altitude or a longer transit time,
- samples from the "complexes" and from the western part of the area show isotopic compositions close to the global meteoric water line, and may originate either from shorter aquifer pathways from lower altitude recharge areas, or from mixing of the two end-members already defined.

The Bangombé area : In Bangombé it is also possible to discriminate between waters recharged high above on the Bangombé plateau (COMILOG open-cast workings), from shallow waters with local recharge. Under reserve of confirmation, the water transit time estimates (from total inorganic dissolved carbon ^{14}C data) from the Bangombé plateau range from 6300 ± 1700 years to 9300 ± 1300 years according to the hydrological circuit adopted. The buffering of the redox conditions by organic matter appears intense in the RZ there, slowing down U re-mobilisation.

Investigations for a natural, specific RZs Tracer : Ever since the beginning of the program, the $^{235}U/^{238}U$ isotope ratio was under consideration as a natural tracer for the RZs, because U is rather soluble in the weakly reducing waters in Oklo, and because it is the most specific geochemical signature for the fission RZs.

Prior to U isotopic analysis, samples were rigorously selected according to hydrological & geochemical criteria (degree of groundwater evolution, flowpathes...), Significant results have been obtained. In order to avoid analytical mass fractionation effects, critical for accurate isotopic measurements, the " Total Consumption Method ", (in which all ions produced during ion emission at different current levels are integrated), was applied.

At Bangombé, a strong anomaly is found in the water soaking the RZ (BAX 03 : 0,00683) ; faintly marked in the overlying pelites (BAX 04 : 0,007201), it does not extend to the underlying sandstones (BAX 02 : 0,007232, measurement is not significant), confirming the discharging flow diagram.

Sample OKH2-An comes from a new drill-hole, set in the immediate vicinity of the OK84 RZ : the measurement (0,00715) is in accordance with what was expected.

Sample OK2, in which a strong anomaly (0.006872) is noted, comes from a short slightly up-going drill-hole, in a crosscut in " fût G " (up- & downcast gallery) in Okélobondo. This drill hole cuts through the mineralised layer and a crushed zone, in which is circulated a confined water, close to global equilibrium. Isotopic anomalies have not been reconfirmed as yet in this area, though two " ghost " RZs have been postulated somewhat to the north, at a higher level, and an unconfirmed anomalous measurement has been recorded from a surface exploratory borehole close to the place.

The practical use of the $^{235}U/^{238}U$ ratio as a tracer of far-field U migration from the RZs is a result quite specific to Oklo. It should make it possible to trace, within the bearings themselves, waters which came into contact with the RZs. The proportion of U actually originating from the RZs, and the distance to which such anomalies will remain significant, has not been assessed yet. It has not been possible to exploit to its true value this remarkable tool.

4.- HYDRODYNAMIC MODELLING :

Due to its better accessibility, and to the better quality of the data obtained, the modelling of the Bangombé site has been treated as a priority. The experience derived will then be transposed as much as possible to the modelling of the more complex Okélobondo site.

BANGOMBE

2-D modelling has been performed on the semi-regional and local scales, following the geological cross-section proposed in the conceptual model, and taking into account the data obtained. This modelling has the following objectives :

- the understanding of the flow, and the estimate of the groundwater transit time along the modelled profile ;
- the study of the influence of rock heterogeneity :
- the study of permeability contrasts:
- the study of the permeability :
- to assert the consistency of the transfer of information from the regional scale model to the local scale model.

The calculation codes used are the USGS SUTRA code for the semi-regional scale modelling, done by CONTERRA AB, and the METIS code for the local scale modelling, done at the EMP. The equations describing the flow in a continuous medium are solved by Sutra according to an hybrid method combining finite elements and finite differences, and by METIS following the finite elements method. The results are the field of potentials and field of flow lines (figures 1, 2 & 3).

Model setting : The physical parameter used to constrain the model is the hydraulic conductivity, as measured in the different piezometers at the local scale, and extrapolated at the regional scale.

Hydrogeological validation : A piezometric follow-up has been done. These measurements are used to validate the hydraulic potential field and the flow lines (figures 2 & 3).

Isotopic validation : We expect from the isotope study undertaken some information which will make it possible to use natural tracers such as ^{18}O and tritium to validate the flow model. The tritium and ^{18}O measurements would confirm the results obtained by simulating the transportation of these elements according to the hydrodynamic section proposed (figures 4 & 5).

Chemical validation : The ongoing hydrogeochemical study allows the recognition of different groundwater families, according to their chemical composition. The available analyses show a good consistency between the calculated flow lines, the behaviour of the major elements and the presence of a redox front above the reactor zone.

OKELOBONDO :

The preliminary 2-D modelling is presently revisited, and updated according to the new data obtained. Once the hydrodynamic diagrams of Bangombé and of Okélobondo validated, an integrated hydro-geo-chemical modelling, simulating the dissolved U transport from the reactor zone will be done.

5.- CONCLUSIONS : PERFORMANCE ASSESSMENT POTENTIALITIES

Chemical analogies between Oklo and deep radioactive waste disposal projects are rigorous : it is commonplace to point out to the fact that Oklo remains the only site where a complete inventory of fission products have been met with at any time.

The history of the site is several orders of magnitude longer than the duration of the confinement demonstration required. This is a serious drawback when one has to unravel the chain of events which influenced the elemental retention there. It is also an unconquerable handicap when one considers the understanding of the becoming of short-lived elements (with reference to the age of the site) :

.- the decay chain of ^{237}Np is now extinct in nature to the benefit of ^{209}Bi alone, the single natural isotope of this element : only in the very near-field is it possible to assume that excess Bi comes from initial Np.

.- ^{135}Cs has now totally decayed to ^{135}Ba. In most samples from the RZs, the alkaline-earth elements observed (Rb, Sr & Ba) are not part of the fission processes : being very soluble, they were mobilised by the reactor fluids and replaced by elements with a normal composition.

.- ^{129}I has decayed to ^{129}Xe, one of the most abundant isotope of this element. It has been evaluated that only 1 % to 0.1 ‰ of the rare gases formed during the fissions reactions remained in RZs 1 to 6. The information as to the mobilisation either of I or of Xe remains inconclusive.

The analogy between Oklo and a waste repository has been revived by the discovery of metallic inclusions with platinum metals in. The containment of ^{99}Tc has been demonstrated. It is a strong analogy between the Oklo uraninites and modern spent fuel, as well as an analogy between spontaneous fission 1.97 Gy ago and present controlled fission. Favourable to the disposal of unprocessed spent fuel, this analogy must not be considered detrimental to the disposal of reprocessed, vitrified wastes.

The analogy between native metals and canister(s) materials are poor. Occasionally observed, copper (KBS 3 concept) remains scarce in Oklo, and is not a fissiogenic (or activation) product. Iron, present everywhere in the geological environment, plays an important role in the control of the redox conditions : This is not enough to make it a proper analogue for a stainless steel canister. Lead has been shown to have been much more mobile than U or FP in RZ 13 during the dolerite dyke intrusion. Actually, it is the degree of oxidation of sulphur which may cause some problems with respect to the behaviour of Cu & Pb.

The analogy between the Oklo organic matter and the present matrix for low and medium activity wastes, though no longer very high (as the bitumens in Oklo are now closer to graphite than to liquid bitumen) is still relevant if we manage to reconstruct their role in the containment of the FP during the first hundred thousands years after the fission reactions. The part played by these bitumen as buffer of the redox conditions in the presence of radiolysis (the H_2 and O_2 species have been observed as traces, but in the free state, in fluid inclusions) is a very important result. This redox buffering by almost graphitic carbon still seems an efficient process in Bangombé. No concept for an engineered barrier relies on this phenomenon at present.

The analogies between *in situ* hydrothermal secondary clays in Oklo, contemporaneous to the fission reactions, and a man-mixed & emplaced clay sealant are not perfect either. It would not be possible, in a repository, to rely on the formation of secondary minerals to trap directly radionuclides into their crystalline lattice : however the Swedish SKB 91 exercise calculated for Pu a migration distance into the engineered barrier, which is of the same order of magnitude as the distance at which a ^{235}U enrichment (daughter to ^{239}Pu) has been evidenced. It would be interesting to confirm this result, as the only limiting factor actually identical is the half-life of the radioelement, 24,000 y approximately.

An important aspect of this program, not directly nuclear, is the real-scale test of the ability of the teams gathered within the working group, and which are actually representative of the international scientific community, to gain a full appraisal of the whole of the phenomena involved, from the nuclear reactions (even from the deposition and reconcentration of uranium in the bearings) to the weathering and final leaching of the shallowest (topographically speaking) of these reactor zones.

The abusive simplification, according to which " the Oklo phenomenon " bears the proof of the safety of any type of underground waste disposal, will certainly not be sustainable again, if it ever seriously was. In fact, the scientific credibility of the safety assessment will gain more in a correct evaluation of the (low) mobility of the REE, of U and of transuranium elements, than in denying the reality of a phenomenon, which the very extant of sedimentary ore deposits do witness.

6.- LIST OF REPORTS & PUBLICATIONS

Anonymous (1994) : Oklo, natural analogue for transfer processes in a geological repository, contract FI2W/CT0071, in Community's research and development programme on radioactive waste management and storage shared-cost action (1990-1994), annual progr. report 1993, EUR 15853 EN, pp 502-511.

BLANC, P.-L. (1994) : Oklo, natural analogue for a radioactive waste repository : a summary of results of the analytical phase. *in* Oklo WG, Proceed. 3rd joint C.E.C.-CE.A. prog. meet., Brussels, 11-12th October 1993, to be published, EUR series.

BLANC, P.-L. [éd.] (1994) : Oklo, analogue naturel de stockage de déchets radioactifs. Contrat FI 2W-CT91-0071, Rapport d'avancement au 31 décembre 1992, SERGD 93/ 56 GEST, 284 p. & ann.

BROS, R., F. Gauthier-Lafaye, J. Samuel & P. Stille (1994) : Mineralogy and isotope geochemistry of clays associated with reactors at Oklo (reactor 10) and Bagombé. *in* Oklo WG, Proceed. 3rd joint C.E.C.-CE.A. prog. meet., Brussels, 11-12th October 1993, to be published, EUR series.

DYMKOV Y., P. Holliger, M. Pagel, A. Gorshkov & A. Artyukhina (1995) : A La-Ce-Sr-aluminous hydroxy-phosphate of the goyazite-florencite series in the nuclear reactor zone 13, Oklo uranium deposit (Gabon)- to be published by Mineralia Deposita.

EBERLY P., J. Janeczek & R.C. Ewing (1994) : Petrographic analysis of samples from the Uranium deposit at Oklo, Republic of Gabon. 4th Internat. Conf. " Migration 93 " ,Charlestown.

ESCALIER DES ORRES, P. (1994) : Implications of the Oklo studies to be used in repository assessment. *in* Oklo WG, Proceed. 3rd joint C.E.C.-CE.A. prog. meet., Brussels, 11-12th October 1993, to be published, EUR series.

GAUTHIER-LAFAYE, F. (1994) : Géologie des réacteurs, étude des épontes et des transferts anciens. Contrat FI 2W-CT91-0071, Rapport final, CNRS/CGS- IPSN, 1ère part. 106 p., ann. & fig 94 p., 2ème part. 106 p. dont tab. & fig, septembre 1994.

GURBAN, I., E. Ledoux, J. Smellie & A. Winberg (1994) : Hydrogeology and modelling at Okélobondo and Bagombé sites. 15 p., 7 fig. *in* Oklo WG, Proceed. 3rd joint C.E.C.-CE.A. prog. meet., Brussels, 11-12th October 1993, to be published, EUR series.

GURBAN, I., E. Ledoux & A. Winberg (1994) : Caractérisation et modélisation des migrations à distance des zones de réaction : synthèse des investigations hydrogéologiques réalisées sur les sites d'Okélobondo et Bagombé. Rapport final EMP-CIG-Armines/ IPSN, contrat CCE FI 2 W- CT91-0071, septembre 1994.

HIDAKA H. & Ph. HOLLIGER (1994) : REE geochemistry of Oklo and Bagombé natural reactors. *in* Oklo WG, Proceed. 3rd joint C.E.C.-CE.A. prog. meet., Brussels, 11-12th October 1993, to be published, EUR series.

HIDAKA H., T. Sugiyama, M. Ebihara & Ph. Holliger (1994) : Isotopic evidence of 90 Sr inferred from excess 90 Zr in the Oklo natural fission reactors : Implication for geochemical behaviour of fissiogenic Rb, Sr, Cs and Ba. Earth and Planet. Sci. Lett., 122, 173-182.

HIDAKA H., K. Takahashi & P. Holliger (sous presse), Migration of fission products into micro-minerals of the Oklo natural reactors, soumis à Radiochimica Acta.

HOLLIGER, Ph. (1994) : Source term characterisation : main isotopic features and modelling of reactor zones 10 and 13. *in* Oklo WG, Proceed. 3rd joint C.E.C.-CE.A. prog. meet., Brussels, 11-12th October 1993, to be published, EUR series.

HOLLIGER, Ph. (1995) : Oklo, analogue naturel de stockage de déchets radioactifs. Terme source : caractérisation isotopique, paramètres nucléaires et modélisation. Rapport final DESD-SESD/ IPSN, contrat CCE FI 2 W- CT91-0071, 70 p.+ ann., 31 fig, 16 Pl., janvier 1995.

JAKUBICK A.T., J.A. O'Neil & R. Gnoyke (1994) : Vacuum extraction of hydrogen isotopes from Oklo samples. *in* Oklo WG, Proceed. 3rd joint C.E.C.-CE.A. prog. meet., Brussels, 11-12th October 1993, to be published, EUR series.

JANECZEK J. & R.C.EWING (1994) : Mineralogy of the Bangombé reactor zone, Gabon : Report of preliminary results. *in* Oklo WG, Proceed. 3rd joint C.E.C.-CE.A. prog. meet., Brussels, 11-12th October 1993, to be published, EUR series.

KARLSSON F. (1994) : Oklo P. -A. issues. *in* Oklo WG, Proceed. 3rd joint C.E.C.-CE.A. prog. meet.,

Brussels, 11-12th October 1993, to be published, EUR series.
LAAKSSOHARJU M. (1994) : Colloid material. *in* Oklo WG, Proceed. 3rd joint C.E.C.-CE.A. prog. meet., Brussels, 11-12th October 1993, to be published, EUR series.
MARAVIC, H. von, Ed., (1994) : Oklo Working Group Proceedings, 3rd joint CEC-CEA prog. meet., Brussels, 11-12th October, 1993, to be published, EUR-series.
MENET-DRESSAYRE C & M.-T. MENAGER (1994) : Migration élémentaire autour des réacteurs nucléaires d'Oklo (Gabon) - Implications pour le stockage de déchets nucléaires de haute activité. *in* Oklo WG, Proceed. 3rd joint C.E.C.-CE.A. prog. meet., Brussels, 11-12th October 1993, to be published, EUR series.
MOULIN, V. & J.-P. VILAREM (1994) : Analysis of colloïds from Oklo/ Okélobondo and Bangombé waters. *in* Oklo WG, Proceed. 3rd joint C.E.C.-CE.A. prog. meet., Brussels, 11-12th October 1993, to be published, EUR series.
NAGY, B., (1994) : Gabon's natural reactors : Nature shows how to contain radioactive waste. Nuclear Engineering international, February 1994, pp.30-31.
NAGY, B., (1994) : Heterogeneous composition and texture of the Oklo and Bangombé natural fission reactors. *in* Oklo WG, Proceed. 3rd joint C.E.C.-CE.A. prog. meet., Brussels, 11-12th October 1993, to be published, EUR series.
PEDERSEN K. (1994) : Microbial studies. *in* Oklo WG, Proceed. 3rd joint C.E.C.-CE.A. prog. meet., Brussels, 11-12th October 1993, to be published, EUR series.
PETTERSSON C. (1994) : Organic material. *in* Oklo WG, Proceed. 3rd joint C.E.C.-CE.A. prog. meet., Brussels, 11-12th October 1993, to be published, EUR series.
PEYCELON H. (1995) : Oklo, analogue naturel. Reconstitution des circulations fluides anciennes par la géochimie des éléments traces : du champ proche au champ lointain. Thèse de doctorat Ecole des Mines de Paris, 11 janvier 1995, 105 p. plus annexes.
PIBOULE, M., J. Amossé & E. Moiny(1994) Compte-rendu d'activités Inst. Dolomieu, Univ. Grenoble : Rapport final Oklo., Partie 1, 22 p., partie 2, 25 p. +tab. & fig, 5 ann.
RAIMBAULT L. & H. PEYCELON (1994) : From near to far field : An attempt to reconstruct ancient fluid circulations around Oklo fossil reactors. *in* Oklo WG, Proceed. 3rd joint C.E.C.-CE.A. prog. meet., Brussels, 11-12th October 1993, to be published, EUR series.
ROYER, J.-J. & C. LE CARLIER DE VESLUD (1994) : Modelling heat and fluid transfers during natural nuclear reaction in the Oklo uranium deposit (Gabon). *in* Oklo WG, Proceed. 3rd joint C.E.C.-CE.A. prog. meet., Brussels, 11-12th October 1993, to be published, EUR series.
SAVARY V. & M. PAGEL (1994) : Redox conditions and thermal history in reactors 10 and 16. *in* Oklo WG, Proceed. 3rd joint C.E.C.-CE.A. prog. meet., Brussels, 11-12th October 1993, to be published, EUR series.
SAVARY V., M. Pagel & Ph. Holliger (1994) - Histoire thermique de zones de réactions nucléaires d'Oklo (Gabon) - Résumé, Réunion des Sciences de la Terre, Nancy, Avril 1994.
SERE V., J. Carpena et J.-R. Kienast (1994) - Du zircon néoformé lors des réactions nucléaires d'Oklo - Résumé, Réunion des Sciences de la Terre, Nancy, Avril 1994.
SUNDER S., N.H. Miller & A.M. Duclos (1994) : Geochemistry of samples from the natural fission reactors in the Oklo uranium deposits : an XPS andXRD study. *in* Oklo WG, Proceed. 3rd joint C.E.C.-CE.A. prog. meet., Brussels, 11-12th October 1993, to be published, EUR series.
TOULHOAT P., D Louvat, J.-P. Gallien, P. L'Hénoret & R. Guérin (1994) : Hydrogeochemical studies at Oklo/Okélobondo and Bangombé sites. *in* Oklo WG, Proceed. 3rd joint C.E.C.-CE.A. prog. meet., Brussels, 11-12th October 1993, to be published, EUR series.

Title	Development of a Model for Radionuclide Transport by Colloids in the Geosphere
Contractors	ARMINES-EMP/INTAKTA/RIVM/CNRS-LSGC/ENRESA
Contract N°	FI2W-CT91-0079
Duration of contract	October 1991 - September 1995
Period covered	1 January 1994 - 31 December 1994
Project leader	E. Ledoux (ARMINES/EMP, co-ordinator)

A. OBJECTIVES AND SCOPE

The main objective of the joint research programme is to develop mathematical models which describe and predict the migration behaviour of radionuclides in a groundwater system in presence of colloids. Laboratory experiments within this research programme support the model development and are used to test the validity of the mathematical concepts under well-controlled conditions. The models will be used for long-time performance assessment and calibration with field experiments forms part of the final goal.

B. WORK PROGRAMME

The following list resumes the major topics of the research programme:

- → development of lumped parameter models based on global concepts and a macroscopic scale;
- → planning and elaboration of laboratory experiments under well-controlled conditions and with simple materials, followed by experiments with natural materials at laboratory (column) scale as well as at field scale;
- → development of phenomenological models, involving radionuclide chemistry, colloid chemistry, colloid medium interaction, pore-scale processes and hydrodynamic phenomena;
- → establishment of a database, specific for the models developed;
- → performance assessment modelling, i.e. application of the codes to P.A. scenarios;
- → documentation of the codes and final reporting of the group's conclusions and findings.

C. PROGRESS OF THE WORK AND RESULTS OBTAINED

C.1. State of advancement

The third project year has lead to improvement of the individual contributions and to partial agreement between models and experimental results. Also, a start has been made to formulate links between the different models in order to come to a consistent model for colloid-facilitated radionuclide transport in the domain of radioactive waste disposal.

C.2. Progress and results in model development

In order to achieve the objectives, we adopted two different modelling approaches, i.e. a *macroscopic*, i.e. relatively large scale approach and a more *phenomenological* approach involving small-scale processes. Both approaches will be briefly outlined below, as well as part of the experimental results.

Macroscopic approach

The macroscopic approach is represented by three different codes: COLTRAP, TRUMP and a mixing-cell model.

COLTRAP (colloid facilitated transport of pollutants, developed by H. van de Weerd, RIVM) is one-dimensional lumped parameter finite difference model with stationary groundwater flow in which equations for flow of groundwater and transport of colloids and pollutants are simultaneously solved. At present, the model runs for one type of pollutant (i.e. one species) and one type of colloid. COLTRAP has been applied to column experiments from LSGC/CNRS (Nancy, France), making use of a fully automatic least-square inversion method to determine relevant parameters, i.e. dispersivity, retardation coefficient, fraction of equilibrium sorption sites and equilibrium rate coefficients.

TRUMP is a finite difference, one-dimensional lumped parameter transport code, originally developed to describe temperature distributions for steady state or transient conditions in a single fracture system. The model is actually applied to hypothetical scenarios in order to test the validity of the K_D approach with a surface complexation code.

The mixing-cell-in-series model allows one to associate the shape of a breakthrough curve to quantifiable, lumped parameters. A sand column is accordingly considered as a series of mixing cells comprising two zones: a mobile zone, where the transport of colloid occurs, and an immobile zone, where the mass transfer of colloid is assumed

to be diffusion controlled. This modelling approach is applied successfully on column experiments, carried out at the LSGC/CNRS (Nancy, F).

Phenomenological approach

The phenomenological modelling approach has lead to a number of different conceptual models and codes. Radionuclide, colloid and matrix chemistry have been modelled according to thermodynamic principles by code CHESS. Radionuclide interaction with medium and colloid surfaces has been modelled according to the surface complexation chemistry accounting for electrostatic surface charge development, which has been attached to speciation and hence included in the CHESS code.

Then, we developed a colloid adsorption model, which includes colloid-matrix interface as well as pore-scale processes. These different aspect, once coupled with an appropriate geosphere groundwater model, lead to the so-called phenomenological performance assessment model.

The chemical part of the model has been tested and applied to different systems, e.g. speciation of Am(III), Eu(III), Np(IV,V), Th(IV), Co(II) and U(VI) but also to systems which include colloidal or mineral surface, e.g. adsorption of the radionuclides mentioned on silica colloids or grains as a function of pH and different ionic strengths. Humic colloids -radionuclide interaction have been modelled using, among others, Aldrich humic acids, Gorleben humic and fulvic acids, Am(III) and Eu(III).

C.3. Experimental Results

Column experiments using longitudinally fractured granite have been continued by CIEMAT (Spain). Colloids generated by clay-infill materials from the El-Berrocal main gallery (mainly illite, smectite and kaolinite) have been characterized and spiked with ^{137}Cs and ^{60}Co tracers. These spiked colloids have been ultra-filtered and the filters have been analyzed by Gamma spectrometry to elucidate if there exists a preferential association between specific size-classes of colloids and the radionuclides.

Column experiments show a very sharp peak at approximately 4 fracture volumes, followed by a long tail, i.e. a slow release of radionuclides. The sharp peak is related to fast breakthrough of non-reactive colloids. The tail is related to desorption of radioactive species from retained colloids. Column experiments with latex colloids have been carried out as well. However, only extreme low colloid concentrations were eluted, to low for detection. New detection methods based on spectrofluorimeter measurements are actually being tried out.

Laboratory experiments with columns packed with natural sand from Entraigues (South of France), mainly composed of quartz and ~0.26 mass % clay material, have been carried out by the LSGC/CNRS (Nancy, France).

The porous medium is a natural sand of the south of France composed of 81% of quartz. The solution of colloids is a suspension of spherical and mono-dispersed carboxyled polystyrene beads, so called latices. In a common range of ionic concentration (10^{-4} M to 0.1 M) and pH (3 to 10), the zeta potential of the latices and the sand are largely negative; therefore the elements of the system are in repulsive conditions. The experimental set-up is a classical liquid chromatographic set-up where the concentration of particles is measured by optical density, as well as the electric conductivity and pH. A type-experiment consists of an injection of a NaCl pre-flush followed by de-mineralized water.

The influence of ionic concentration and flow rate of the injected solution is first studied for latex suspensions of 100 mg/l and 0.21 m in diameter. The experiments performed at three ionic strengths and five flow rates show that the higher the flow rate, the earlier the Breakthrough Point (BTP) time and the higher the ionic strength, the later the BTP time. Empirical correlations can be written between the BTP time (t_{BTP}) and the ionic concentration (I), e.g. $t_{BTP} = A + B \log I$ and $t_{BTP} = C \exp(-DQ)$.

The effect of colloid size has also been examined by using three different colloid diameters: 0.11, 0.21 and 0.79 μm. The retention conditions are optimized: a low flow rate (0.05 ml/mn) and a high ionic concentration (10^{-2} M NaCl). A part of the largest particles appears very quickly which seems to indicate that they follow fast streampaths. On the contrary, a large amount of small particles is captured, probably in "pockets" of the sand surface. We conclude that the smaller the diameter of the particles, the higher the retention in the medium. The size of particles seems to be very important in the behaviour of colloids with respect to a given porous medium.

The second part of the breakthrough curve is a long tail. The effect of two parameters on the tailing is studied: the flow rate and the ionic concentration.The influence of the flow rate is examined through the behaviour of latex particles of 0.21 μm in diameter at a concentration of 100 mg/l. The ionic concentration of NaCl is low: 10^{-4} M. Figure 1 shows that the first part of the curve is identical for the two flow rates until 50% of the initial concentration. Then the tails are different: the curve at 1 ml/mn is above the curve of 0.5 ml/mn. The tails join after 20 pore volumes. A similar result is obtained for a lower concentrated suspension (20 mg/l). We conclude that the higher the flow rate, the less important the retention of colloid in porous medium.

The effect of ionic concentration is studied with the same latex suspension as above

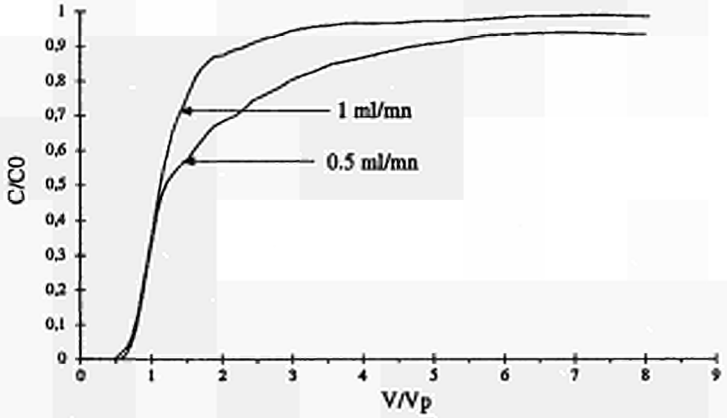

Figure 1: Influence of flow rate on the tail of the BTC.

(100 mg/l- 0.21 m). The suspension is injected at a medium flow rate (0.5 ml/mn) at two ionic NaCl concentrations, i.e. 10^{-4} and 10^{-3} mol/l. Figure 2 presents the resulting curves. The tails of the curves join at 12 pore volumes. A similar result is obtained with a lower concentrated suspension of 20 mg/l, the tails join at 4.2 pore volumes. The conclusion is that the ionic concentration has no effect on the tails of the curves.

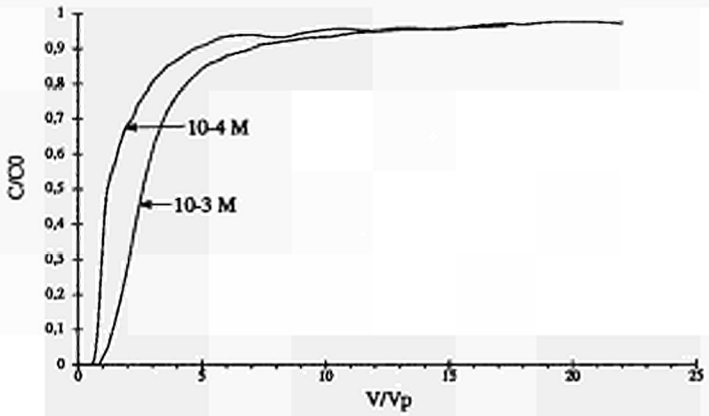

Figure 2: Influence of ionic strength on the tail of the BTC.

In conclusion, the flow rate and ionic concentration influence the retention of particles as determined by the position of the BTP. Increasing flow rate decreases the retention, increasing ionic concentration increases the retention of particles. of other parameters such as ionic strength and flow rate, as determined by the tails of the curves is more ambiguous. The size of the colloidal particles is an important parameter because the retention time can be very high if the particles are very small. Capture by filtration is important also because of the greater opportunity for particles to diffuse in the pores at the surface of the sand grains.

Title	Characterization and Validation of Natural Radionuclide Migration Processes under real conditions in a Fissured Granitic Environment
Contractors	ENRESA/CIEMAT, UPC/CIMNE, AEA, BGS and CEA/IPSN
Contract N°	FI2W-CT91-0080
Duration of contract	March 1991 - February 1995
Period covered	January 1994 - December 1994
Project leader	Pedro Hernán (ENRESA, Coordinator) Task leaders: Carmen Marín (CIEMAT), LuisPérez del Villar (CIEMAT), Jordi Guimerà (CIMNE/UPC). Contractors leaders: Pedro Rivas (CIEMAT), Jesús Carrera (UPC/CIMNE), M. Ivanovich (AEA/Harwell), Benjamin Klinck (BGS) and J.M. Fernández (CEA/DCC)

A. OBJECTIVES AND SCOPE

The objective of the project is the characterisation of natural radionuclide (U, Th, and their decay products) migration processes in a fractured granitic environment and validation of models describing these processes.

In situ studies are being developed at the "El Berrocal" site, a post-tectonic batholith, taking into account:

- The characteristics of the rock fissures and discontinuities
- The hydrodynamic and hydrogeological conditions, and
- The variation of the physico-chemical characteristics with depth.

In parallel to these in situ activities, a series of laboratory experiments are underway to study the same phenomena under controlled conditions.

Finally, the identified processes are being modelled and the models validated.

The project is managed and coordinated by ENRESA (Spain), with the technical assistance of Intera Environmental Division (United Kingdom). Participating organisations include CIEMAT (Spain), CIMNE (Spain), CEA/IPSN-Cadarache (France), AEA Technology (United Kingdom) and BGS (United Kingdom). Partial funding is provided by the CEC-Brussels. JRC/CEC-Ispra cooperates with the Project participants. The Project is scheduled to run for four years, in two two-year phases. Phase 1 was initiated on 1st March 1991, and is the subject of this contract.

B. WORK PROGRAMME

B.1 Characterization of the physical environment: Geotectonic characterisation from the surface. Underground characterisation from boreholes. Geochemical and petrographic fissural filling studies. Litho-structural model of the site.

B.2 Geochemical characterisation: Hydrogeochemistry (physicochemical and ionic phases). Groundwater colloidal phases studies (sampling, characterisation and

transport). Groundwater mixing and circulation patterns. Fissure filling characterization. Hydrothermal and weathering transformations.

B.3 **Migration studies:** Natural radionuclide distribution. Mobilization/retention processes (laboratory). In situ migration experiments.

B.4 **Hydrogeological characterisation:** Assessment of borehole conditions. Design and construct wireline straddle packer testing system. Transmissivity and head measurements. Define numerical models. Design and perform crosshole interference tests in selected fractured zones.

B.5 **Modelling studies:** Development of a computer code (flow and transport, 2-D fractures in 3-D medium). Prediction of uncertainties caused by spatial heterogeneity. Flow and solute transport in a single fracture.

C. PROGRESS OF WORK AND OBTAINED RESULTS

State of advancement

The Project is getting to an end. The activities are being undertaken on time, but in optimizing a maximum set of *in situ* data, it has been decided to go on with the field activities up to the very ending day of the contract. The global objective indicated in section A is intended to be fulfilled by means of the working groups whose names and specific sub-objectives are:

Structural WG. Development of the 3-D Structural Model of the site.

Hydrogeology WG. To develop the Groundwater Flow Model of the site, and development of Computer Codes for coupled flow and transport models.

Geochemistry WG. To establish the Geochemical Model integrating litho and hydrogeochemistry of the Site. Modelling the minor and trace elements behaviour according to the geochemical conditions of the Site.

Tracer Test WG. To study the radionuclide behaviour in the granitic media (at laboratory scale), and to design, perform and model, the mass transport in the fractured granite (at a real scale between boreholes).

Reporting and Integration WG. During 1994, a fifth group has begun to function, whose objectives are implicit in their name.

Within the reported period the main activities of the different task groups have been the use of graphic and geometrical modelling means for **structural geology** interpretation. An extensive use of isotopes, the *mise au point* of a sequential leaching method to complement uranium speciation and discriminating between adsorbed and precipitated phases, together with an intensive sampling series in borehole S-16 at (457-490 m) depth, have been the most relevant activities of the **Geochemistry Task Group.** As regards **Hydrogeology**, a conceptual and numerical modelling for the local system has been produced and the code development for coupled flow and transport model has been completed, on site, the main efforts have been addressed towards the completion of the necessary hydrogeological data

to support the tracer test between boreholes S-11, S-13 and S-2 whose performance has meant the basic issue of the **Tracer Test Task Group.**

Progress and Results

C.1 Characterisation of the Physical Environment.

During last year the extrapolation of surface data to boreholes (core visual observations and televiewer data), allowed a preliminary 3-D structural model to be established. During the reported period this model has been refined and completed with the aid of ROCKWARE, FRACMAN and EARTH VISION means. They have contributed in interpretation and visualization of the structural reality. They have also rendered, mainly the latter, an important help in illustrating the tracer test configuration. Three sources of data have been used in these studies; lineament mapping (length, direction and fracture connections), profiles field measurements from joints (aperture, dip and spacing) and televiewer data of fractures in boreholes, that provides the same kind of information as the previous one but from depth.

By means of SPOT images analysis the study region has been divided into a series of morpho-tectonic blocks, the fractures contained in each of them have been submitted to hypothesis tests CHI-square and Kolmogorov-Smirnov, to analyse the degree of similarity among the blocks.

As regards field work a detailed study of joints, based on a series of profiles N-S and E-W, has been undertaken, the measured objects have been submitted to a statistical study. The sample follows a log-normal distribution and the measured directions coincide with those of the main fractures.

A specific part of the structural work has been aimed to provide geometrical support to the tracer test performance. To this respect it has been stated that the main connections between S-13 and S-15 take place above the mineralised quartz-vein.

All these studies and some other minor ones, not cited here, need a final integration in the global structural model.

C.2 Geochemical Characterisation.

INTRODUCTION

The work performed under this activity is reported divided into five inter-related issues: Lithogeochemistry, Hydrogeochemistry, Water-rock interaction, Geochemical modelling, and Testing of down-hole probes. An important part of the effort in 1994, has rely in reporting, and in fact some of the chapters of the final Geochemistry task group report, have been already written.

LITHOGEOCHEMISTRY

Refining of the previously established lithogeochemical model has progressed in the characterisation, mineralogical and geochemical, of the different granitic phases defined in the above mentioned model. A new approach of this period of work has been the production

of chondrite normalised REE diagrams. Comparison of the so called reference granite with the rest of the phases has made possible to determine the quality of the alteration effects as regards enrichment and depletion of trace elements. Compared to the reference granite, the hydrothermally altered granite is enriched in Fe^{3+}, Mg, Ca, K, C, S and OH^- and depleted in Si, Al, Fe^{2+}, and Na. In has been also studied the geochemistry of the mineral fillings, having established a classification of a suite of elements with their associated minerals, having been used the results in the second stage of the blind predictive modelling exercise to constrain the choice of solubility limiting phases.

HYDROGEOCHEMISTRY

The main aspects, to be considered in this chapter as deduced from this year work relates to:

- sampling in S-16 and S-17 boreholes
- comparison of water chemistry variations and pumping rates
  hydrogeochemistry of springs and wells, refining of groundwaters classification and studies in colloids from borehole S-17 and S-14.
- stable isotopes contribution to global interpretation

Concerning the second of the listed topics, it is worthy to say that it represents an important issue, difficult to be considered concluded, as regards mainly the spatial coverage and associated representativity of the sample when increasing pumping rates and pumping volumes. It has been proved within this work that physico-chemical and chemical element variations occur, while Eh, pH, EC and major ions are generally constant, 9 to 10 volumes of water need to be pumped, from the packed-off sections, for the trace elements to reach steady concentrations. Only a rigid simultaneous control of groundwater heads variation together with a very close and accurate model of the paths flow network, could provide objective information on the above stated subject. This is therefore an open question worthy of further research elsewhere in fractured media. Notwithstanding this, it is expected that progress in data analyses within this project will end by furnishing further valid information.

Colloids are also an open question in the Project. It was generally found that only a small proportion of Uranium (less than 5% of the total) was being transported in colloidal form, it must be said that all the examined waters for this purpose exhibited U concentrations below 300 ppb. Only recently in the last three months it has been found a different situation with a higher concentration of uranium linked to a colloidal form, the studies are not finished yet, but it appears that the U bearing colloids correspond to allophanes, it is convenient to add that the U concentration of S-17 groundwaters at that depth (-138 to -168 m), is near to 2000 ppb. This issue is still controverted within the project and discussions on interpretation are currently active.

In very few words, stable isotopes, as regards groundwaters characterisation, have shown that no major differences noticeable by stable isotopes can be ascribed to the waters, what, in time record terms, means that they are all in the same interval of relative recent age, this statement is reached by almost any approach in the Project.

WATER-ROCK INTERACTION

The main activities associated to this heading deal with the Natural Series radionuclides disequilibrium. In obtaining reliable data to feed the SUDDEN model it has been relevant the effort devoted in validating a sequential leaching method that has led to a comparison of two approaches within the geochemistry working group.

Some modifications have been made in the SUDDEN code to make its treatment of mobile uranium isotopes more realistic. The effect of this change was to lower the calculated rock-water interaction times so they are more in agreement with the overall conceptual model of the site that suggests the waters are very young. Something already stated by mineralogical studies approach as it is that precipitation predominates over sorption, has been also given by the model. The code finally indicates that the rock-water interactions times are in the range of 20 to 3300 years.

By mean of 59 samples submitted to WATEQ4F, it has been established some complementary conclusions as regards water-rock interaction in the carbonate, silicate and uranium systems.

BLIND PREDICTIVE GEOCHEMICAL EXERCISE

In the first stage of this exercise ended during the present period, only the major chemistry was known for the different participants, the aim was to predict solubility and speciation for a set of 14 trace elements on the basis of their major chemistry and physico-chemical parameters. Results offered unrealistic predictions mainly due to unsuitability of databases as regards mineral speciation. For the second stage, four elements were eliminated. An additional information for this phase was the real mineralogical data given as a known to the participants, there was also a suggestion made to the modellers by the coordinator of the exercise in the sense of incorporating co-precipitates as potential sources. As a result of these new inputs, a better fit has been obtained in global terms. The exercise has also contributed to provide a series of database improvements.

TESTING OF DOWN-HOLE PROBES

As regards geochemistry the CHROMATOLAB probe has been used in boreholes S-14 and S-17, and measurements of pH, Eh, EC, dissolved gases, elemental concentrations and bacteria populations have been measured.

Concerning diffusion studies, FORALAB probe has been installed in S-17, using I and Sr in clay and granite mixtures from El Berrocal.

C.3 Migration Studies.

This has been a major field of activity within the reported period. As regards *in situ* experiments, two tracer tests have been run within this year. A first one between S-11 and S-12 was performed in February and March 1994. Three tracers previously essayed in the laboratories were employed; eosine, iodide and fluoresine, and breakthrough curves were obtained for the three tracers. The percentages recovered were 56% for iodide and fluoresine and 35 for eosine. The modelling of the breakthrough curves was done without matrix

diffusion or any other retention mechanism being taken into account. The peak was reasonably reproduced but there was a worst fitting in the tail.

The values obtained for dispersivity and porosity are the following:

	dispersivity	porosity
eosine	2.5 m	4.3×10^{-2} m
fluoresine	1.0 m	2.0×10^{-2} m
iodide	2.0 m	2.3×10^{-2} m

The large scale tracer test between boreholes S-2-S13-S15 has begun. There were problems with equipment when it was first installed in the boreholes but these have been solved, and the equipment shows a full robustness in its behaviour. Pumping in the packed-off sections was performed to test for pressure responses in the rest of the system. These results proved satisfactory. Dilution tests were then performed under natural and stressed conditions due to pumping. It was found that pumping increases the head gradient between the upper S13 injection and recovery intervals but it lowers the head gradient between the lower S13 injection and recovery intervals, this is because pumping acts in the opposite direction to natural flow for the lower injection interval.

In mid-December, the tracer test began with the injection of three tracers into the upper interval of borehole S13 (Gd-EDTA, D_2O and fluoresine) after which the injection interval was flushed. Later on the presence of tracer was still measured in the injection interval, so the water was pumped out and replaced with tracer-free water to avoid a long injection time. Breakthrough was recorded after 1 day and peak recovery after 4 days.

Preliminary modelling of the leading edge of the breakthrough curve using a simple homogeneous model gave the following parameter values:

- porosity, 1.2×10^3 m
- dispersivity 17 m.
- mass recovery 2.5 g.

The tail of the breakthrough curves is now being recovered. After this, a further injection will take place using all three injection intervals.

In parallel some laboratory migration experiments that use crushed El Berrocal granite (from borehole S11) and groundwaters (from borehole S2) have been undertaken. A number of dye tracers were used and HTO as non-conservative tracer for comparison. All of the dyes were retarded with respect to the HTO and the sulphaflavine showed a small degree of sorption. The cumulative recovery curves for these tests indicated only 80% recovery for eosine yellow and 100% for the other dyes.

A series of migration tests using a selenate tracer was performed at Ispra using a El Berrocal granite core section under reducing conditions. The tests were repeated using a range of flow rates and it was discovered that the higher the flow rate, the faster the breakthrough and the greater the percentage recovery. However, sorption was evident in all cases. A similar set of migration tests under oxidating conditions resulted in a much lower recovery rate. *i.e.* higher sorption. The sorption of Se within the column is thought to be due to sulphide minerals in the granite that cause a chemical reduction of the Se.

Another set of migration tests has begun using radionuclide-loaded colloids (clay particles). The interpretation of these breakthrough curves has just started and only preliminary results are available. However, it appears that peak breakthroughs are delayed for the larger colloids and that some smaller colloids do not interact with the fracture infill materials.

C.4 Hydrogeological Characterization.

During the last year of the project, many efforts have been devoted to integrate geological, hydrochemical and hydraulic information in a hydrogeological conceptual model. To prove its consistency, 3-D numerical models were developed, the latter is also treated under C.5.

HYDROGEOLOGICAL CONCEPTUAL MODEL.

In this section is presented an abstracted version of the information given by J. Guimera in its paper presented at MIRAGE 94.

The geology shows that those fractures associated to extensional stress direction, display more important openings at the site scale, as it does the relationship with the mineralized quartz dykes. Their contribution to the ground water flow and transport system gives a clear anisotropic behaviour of the hydraulic properties, being the hydraulic conductivity higher in the vertical direction. Hydrological behaviour of the uranium quartz dyke has been largely discussed since the general feeling is that the geological importance must be translated into hydraulic properties.

Flow occurs topographically downhill, by the most weathered-altered zone close to surface, and downwards across the rock massif. When recharge and ground water reach the UQD, sulfur mineral dissolution takes place and water is enriched in sulfate. To explain sulfate content south of the UQD, ground water has to intersect this structure.

Borehole hydraulic characterization, performed by using conventional straddle packer system for single borehole testing, was finished and successfully applied down to 600 m. A series of pulse, slug and constant head tests revealed that transmisivity (T) ranges from 10^{-6} to 10^{-9} m^2/s and exceptionally, 10^{-5} m^2/s. The instrumentation's lower operative threshold was 10^{-11} and it was occasionally reached.

Cross hole hydraulic tests have been directly performed isolating well characterized fracture intervals.

NUMERICAL MODELLING.

Numerical modelling attempts to quantify hydraulic tests and natural flow in 1, 2 and 3 dimensions by using analytical solutions and numerical methods (finite elements) combined with parameter estimation techniques. Tests involve space extensions that show the relevance of major and minor fractures and in such this way, they are evaluated. Single borehole tests allow to discriminate skin and fracture flow effects with different K and S than of the rock matrix.

C.5 Code Development

As regards development of TRANSIN-III code during 1994, effort was made in verifying all possibilities of the code.

Applications made for the El Berrocal Project show some numerical problems associated to tethaedrical elements. To overcome these problems trigonal prisms were selected among a series of alternatives. As regards program validation, pumping and pulse tests were performed at El Berrocal that were modelled entirely in 3·D with embedded fractures.

A second chapter within this task is the formal documentation of the program, which is always open to adjustments not only for calculation, but also for the input of the data. A final document is still in progress.

The last topic extensively treated in 1994 concerns to the programming of a good system of pre and post processors, that include executing of a series of programs that perform the following processes.

. Assessment of the system geometry, including;

- Borehole location.
- Length of packed-off sections and position of the packers.
- Fractures location, (direction and dip), and checking of intersections.
- "Layers" location.

. Generation of system geometry 2-D plottings, by means of the INTRIDI program.

. Generation a bi-dimensional mesh by means of DIB2DUMG program.

. Generation of a 3-D network with the TRIDI4 program.

C.6 Reporting.

During this year, mainly in the second half, the activity of reporting has been an important one within the global tasks of the Project, after a series of working sessions the contents of the future reports have been agreed. It has been also decided that apart from the topical report listing, a series of working group reports will be prepared previous to the final summary report.

The full list of reports intended to be published, is included here. The TR series will be only edited by ENRESA. The Commission will publish the TGR series and the Final Summary Report.

EL BERROCAL PROJECT REPORT LIST

Topical Reports.

TR-1 L. Pérez del Villar & J. Pardillo.
Lithological map of the El Berrocal Site, Spain.

TR-2 R. Campos & C. Marín.
Structural analysis of the El Berrocal Site, Spain.

TR-3 J. Pardillo.
Mineralogical and Geochemical characteristics of the El Berrocal reference granite. Spain.

TR-4 M. Pelayo.
Mineralogy, geochemistry and isotope geochemistry of the El Berrocal fracture fillings, Spain.

TR-5 P. Gómez, M. Ivanovich, E. Reyes & M.T. Crespo.
Hydrochemical and isotopic characterization of the groundwater from the El Berrocal Site, Spain.

TR-6 P. Gómez, M.J. Turrero & M. Ivanovich.
Sampling and characterization of colloids in groundwaters from the El Berrocal Site, Spain.

TR-7 M. D'Alessandro, J. Guimerà, F. Mousty / A. Yllera.
In situ migration tests with conservative groundwater tracers at the El Berrocal.

TR-8 J.M. Vinson.
Strategie d'etude et de qualification d'un site par mesure et experimentation in situ en forage.

TR-9 L. Pérez del Villar.
An approach to the calculation of the mineralogical distribution of U and Th in the fresh granite from the El Berrocal Site, Spain.

TR-10 L. Pérez del Villar.
The clays fissural filling associated with N100°-110°E fractures at the El Berrocal Site, Spain:Characterization, genesis and retention capacity of radioactive and other elements.

TR-11 L. Pérez del Villar, B. de la Cruz, J. Pardillo, J.S. Cózar & M.T. Ménager.
Mineralogical and geochemical characterization of the altered granite from the El Berrocal Site, Spain.

TR-12 M. García.
Distribution coefficient studies in separated mineral phases from the granite at the El Berrocal Site, Spain.

TR-13 M. García.
Experimental migration studies with granitic materials from the El Berrocal Site, Spain: a first approach.

TR-14 M. Ivanovich, A. Hernández, A. Chambers, L. Pérez del Villar, S. Hasler & T. Crespo.
Rock-water interaction modelling using uranium series disequilibrium concepts at the El Berrocal Site, Spain.

TR-15 D. Holmes, J. Guimerà & F. Recreo.
Hydrology, hydrogeological testing methodology, test equipment and results from boreholes at the El Berrocal Site, Spain.

TR-16 J. Carrera.
User's guide for TRANSIN-II.

TR-17 J. Carrera.
User's guide for TRANSIN-III.

TR-18 J. Carrera.
Stochastic analysis of flow and transport in a single fissure.

TR-19 Report Integration Group (W.M. Milller editor).
El Berrocal Project: Phase One Summary Report.

TR-20 M. García, A. Yllera & A. Hernández.
Column experiments using geological materials: application to radionuclide migration studies.

TR-21 J. Tamarit, M. García, J. Carrera & J. Guimerà.
Design of tracer test equipment for the El Berrocal Site, Spain.

TR-22 L. Vives, P. Tume, M. Saaltnik, J. Carrera & J. Guimerà.
Three dimensional pumping tests.

TR-24 L. Pérez del Villar.
Influence of the alteration processes on the U-Th-REE bearing minerals in the El Berrocal granite/U-quartz vein system, Spain.

TR-25 P. Grindrod, J. Carrera & D. Noy.
Modelling field tracer tests at the El Berrocal study Site, Spain.

TR-26 M. García & J. Beno.
Results from field tracer tests in boreholes S2-S13-S15 at the El Berrocal study Site, Spain.

TR-27 M. D'Alessandro, J. Guimerà & M. García.
Design, performance and interpretation of tracer tests in boreholes S11-S12 at the El Berrocal study Site, Spain.

Task Group Reports.

TGR-1 R. Campos et al.
Structural Task Group Report.

TGR-2 J. Guimerà et al.
Hydrogeology Task Group Report.

TGR-3 L. Pérez del Villar et al
Lithogeochemistry: Geochemistry Task Group Report (1).

TGR-4 P. Gómez et al.
Hydrogeochemistry: Geochemistry Task Group Report (2).

TGR-5 M. Ivanovich et al.
Rock-water interaction: Geochemistry Task Group Report (3).

TGR-6 J. Bruno et al.
Blind Predictive Modelling exercise: Geochemistry Task Group Report (4).

TGR-7 J. Guimerà et al.
Tracer Test Task Group Report.

Final Summary Report.

SR-1 Report Integration Group.
Final Summary Report.

Title	Fundamental studies on the interaction of humic substances
Contractors	National Environmental Research Institute
Contract N°	FI2W-CT91-0081
Duration of contract	1 June 1991 - 30 June 1995
Period covered	January 1994 - December 1994
Project leader	Lars Carlsen

A OBJECTIVES AND SCOPE

The overall objective of the project is to covalently label humic materials with a radionuclide (eg C-14, H-3, I-125) in order to use the labelled material during investigations of their interactions in

(a) complexation reactions with cations (eg Eu, Sn, Co, Ni) and cation competition reactions (eg with Na, Ca)

(b) sorption of humic and humic complexes onto solid surfaces and

(c) precipitation/dissolution behaviour of humic material.

The radionuclidic labelled humic material will provide information on the presence of the complexed radionuclide as well as information on the "free" humic material.

The project is carried out by a collaborate effort of the National Environmental Research Institute (DK) and Loughborough University of Technology (UK).

B WORK PROGRAMME

The project is subdivided into three phases:

Phase 1: Preparation of labelled humic materials:
a) Preparation of C-14-labelled humic material from C-14-labelled phenol or C-14-labelled methylamine.
b) Preparation of iodine-labelled humic materials.

Phase 2: Characterisation of the labelled humic material:
a) Determination of the acidity, functional group capacity and size distribution of the non-labelled and labelled humic materials.
b) Determination of the europium binding capacity of the non-labelled and labelled humic materials.

Phase 3: Studies on the aqueous and solid surface chemistry of the labelled humic material
a) Investigation and determination of the associating capacities of the labelled humic material with radionuclides of interest (eg Ni, Sn, Co).
b) Investigation of solid surface sorption using columns filled with sand.

C PROGRESS OF WORK AND OBTAINED RESULTS

State of advancement

Humic and fulvic acids are present in nearly all environmental waters and because they are known to form water soluble complexes with metals and some anthropogenic organics materials they may be important transport agents for environmental pollutants. Studies of the interactions of humic materials with these pollutants and their transport behaviour is more easily facilitated if the humic material is covalently labelled with a suitable radionuclide. During the year 1993 successful radiolabelling of humic materials with I-125, a gamma emitter and with C-14, a beta emitter and the characterisation of the radiolabelled humic material have been accomplished.

The project is sub-divided into three phases:

Phase 1: Preparation of labelled humic materials:

Phase 2: Characterisation of the labelled humic material:

Phase 3: Studies on the aqueous and solid surface chemistry of the labelled humic material:

Phases 1 and 2 are completed and Phase 3 is ongoing.

Progress and results

1. Phase 1 and Phase 2

The results from these two phases have be reported in previous annual reports and shall, as such not be included in the present report.

2. Phase 3

The work within phase 3 has been concentrated on a) migration studies elucidating the migration of radionuclides through sand columns in the presence of humic materials focussing on the role of the latter and b) the interaction between humic materials and solid surfaces, the latter being exemplified by γ-Al_2O_3.

Migration through sand columns

The transport of radiolabelled humate, and complexes of metal-radiolabelled humate, have been investigated using 15cm long glass columns packed with an environmentally interesting sand taken a site in Cumbria, UK. The columns were eluted with synthetic groundwater of similar chemical compo-

sition to that found at the site. Two types of investigations were conducted; flooding experiments in which the column was continually eluted with synthetic groundwater containing either radiolabelled humate or metal-radiolabelled humate complex or, injection experiments, in which a solution containing the radiolabelled humate or metal-radiolabelled humate complex was injected onto the column from a 1ml injection loop. For the flooding experiments a flowrate of 10 mL h^{-1} was used whereas for the injection experiments a flowrate of 40 mL h^{-1} was used. In each set of experiments, the eluant was fraction collected in order to determine the activity in each fraction and therefore permit the calculation of the percentage of radioactivity recovered from the column. The speciation of the radioactivity in each the fraction could also be determined by using size exclusion chromatography.

In previous reports we have elucidated that intact metal humates migrate through sand columns as such without retention, i.e. with the same speed as the free humic acids [1,2]. It appeared, however, that a significant amount of the metal ions as well as of the opriginal humate ligand apparently are sorbed onto the column material. Thus, in the case of freshly prepared europium humate approximately 75-80% of the europium and 40-45% of the original humate ligand were found to be sorbed onto the sand [1].

Flooding Experiments

In order further to elucidate the sorption processes apparently operating within the sand column/ground water system, a series of flooding experiments of laboratory columns of sand originating from an experimental site in Cumbria, UK using a synthetic ground water, closely resembling the original site ground water, as eluent. The studies have been carried out as sorption/desorption experiments, i.e. a certain amount of ground water spiked, and equilibrated with either HTO, I^--125 or Eu^{3+}-152 was passed through the column followed by elution with pure, i.e. unspiked ground water. The levels of radioactivity both in the the eluate as well as within the columns have been followed in order to establish the mass balanced for the single tracers.

Initially the sand column, equilibrated with the ground water, was flooded with HTO spiked ground water, HTO being the obvious conservative tracer.

The expected concentration profile was immediately noted. Thus, following passage of ca. 40 mL of the HTO spiked ground water, corresponding to the pore volume of the column, the tritium concentration is increased to a constant level of ca. 4000 cpm/mL corresponding to the tritium concentration in the spiked ground water. Following passage of 320 mL of the tritiated ground water, the eluate was changed to normal, i.e. unspiked ground water, which, after passage of ca. 40 mL caused an almost momentarily decrease in the tritium concentration level to zero, without any tailing other than the expected due to simple dispersion through the column. On this background it was concluded that the column under investigation exhibited a uniform homogeneous porous structure.

Often iodide is believed to behave as a conservative tracer in migration experiments. This is, however, by no means of necessity generally the case. Thus, the present study unambiguously disclosed that introduction of iodine into the sand column in the form of iodide lead to a significant sorption apparently due to the presence of a non-equilibrium situation in the sand column/ground water system with respect to iodide.

The concentration level following elution with approximately 40 mL af the I^- 125-spiked ground water increases to a virtually constant value of ca. 5000 cpm/mL. This value has to be compared with the $I\text{-}125^-$ concentration in the spiked ground water, which amounts to 8100 cpm/mL. Thus, the recovery of iodide between ca. 200 mL and 800 mL is about 67%.

Following flooding with 775 mL of the I^--125-spiked ground water further 400 mL of unspiked ground water were passed through the column. A rather steep decrease in the activity I-125 level was noted. However, a pronounced tailing is noted. Even following the elution with 400 mL of the unspiked ground water the concentration level had reached a value of approximately 800 cpm/mL. These results strongly indicate a significant retention of iodine within the column. This was unambiguously verified by determining the iodine concentration along the column by gamma counting of the I-125 clearly demonstrating the sorption of iodine throughout the column.

Based on the general features for europium sorption [3], a pronounced sorption of europium in the sand column was to be expected, even taking into account that part of the europium in the Eu-152-spiked ground water appears as an apparently mobile Eu-humate complex. In agreement with this, only a very minor fraction of the europium introduced to the column was eluted. In Fig. 1 the europium concentration level, measured as the activity of the eluted Eu-152, is visualized as function of eluent passed through the column. Immediately it is noted that in the case of europium a rather slow increase of the Eu-152-concentration in the effluent developed levelling out at approximately 2700 cpm/mL, which has to be compared with the Eu-concentration, equivalating 24800 cpm/mL in the incomming Eu-152-spiked ground water. Since free europium is not eluted from the sand column, the Eu-activity in the column effluent can be associated with humic acid complexed europium. Thus, since 20% of the Eu in the ground water has been estimated to be present as Eu-humic complexes, the eluted amount of europium amounts to ca. 54% of the complexed and ca. 11% of the total amount of europium originally introduced to the column.

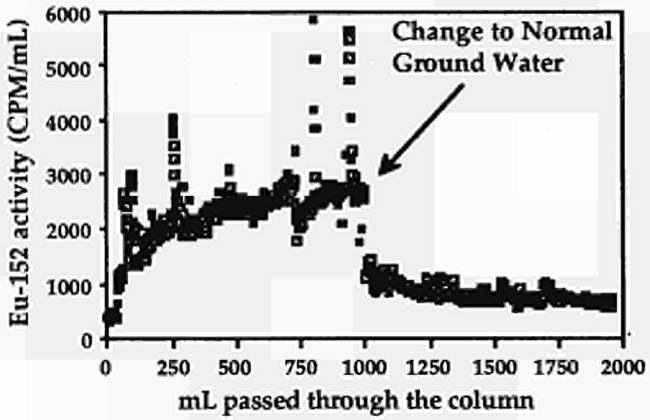

Figure 1. Europium concentration in the effluent as function of volume of ground water passed through the column

The interaction between humic acids and γ-Al_2O_3

The interaction between humic substances and mineral surfaces may play a crucial role in determining the fate of pollutants in e.g. the soil/ground water system due to significant changes in surface characteristics as a consequence of the surface coating with organic material. The interaction between humic acids and γ-Al_2O_3 has been investigated as a model system focussing on the possible reversibility of the reaction as well as on a possible size fractionation of the humic material as a consequence of a preference for sorption of selected molecular size fractions of the latter.

To determine whether humic acid molecules are sorbed to alumina across the entire range of their molecular weights or whether there is preferential sorption of only a fraction of the molecular weight range, gel permeation chromatography (GPC) using Sephadex G-25, which separates globular proteins within the range of 1.000 to 5.000 Daltons, and Sephadex G-50, which separates globular proteins within the range of 1.500 to 30.000 Daltons was used.

Figure 2a shows the normalised (for absorbance) GPC results of the humic acid containing supernatants separated on the G-25 gel. These results show that humic acids are sorbed to γ-Al_2O_3 over the whole molecular weight range but that there is a sorption preference for the lower molecular weight fractions. This is supported by Figure 2b, which shows the same solutions analyzed on the G-50 gel. Davis and Gloor [4] have found that for sorption of DOC (dissolved organic carbon) from lake water onto γ-Al_2O_3, there was a preferential sorption of the low molecular weight fraction.

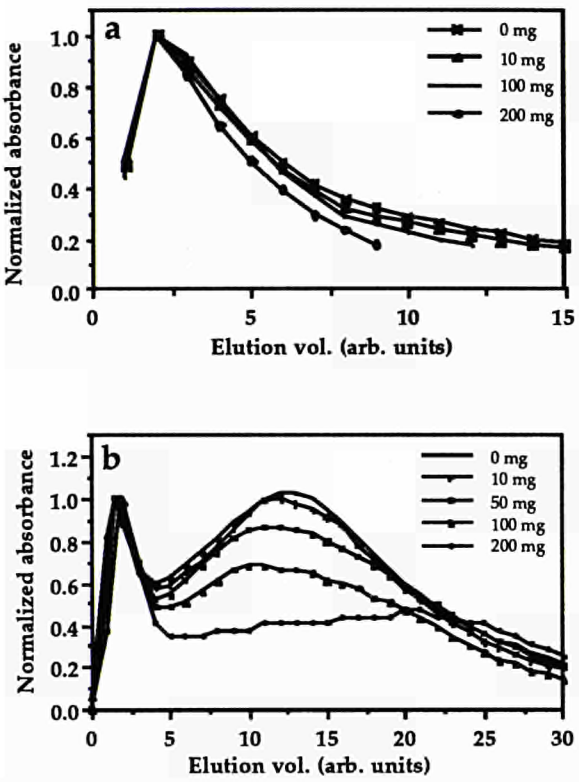

Figure 2. Normalized elution profiles of molecular weight distributions of humic acids (400 ppm) sorbed onto alumina using a Sephadex G-25 (a) and Sephadex G-50 (b) column, respectively, eluted with 0.05 M NaCl.

By measuring the light absorbance at 465 and 665 nm of humic substances, the E4/E6 ratios can be calculated. This ratio is widely used by soil scientists to characterize humic substances and is believed to be related to the molecular weight of the humic substances, the O, C and COOH content and, the total acidity [5]. A low E4/E6 ratio signifies a high molecular weight humic material of high C, low O, low COOH content and low total acidity. These observations can especially be seen by comparing fulvic acids and humic acids. Fulvic acids, generally have a higher E4/E6 ratio, are lower in molecular weight, higher in acidity and lower in C content, than humic acids. However, ususally, the molecular weight distribution of the humic material is the predominant determinant of the E4/E6 [5]. The results from the gel filtration were supported by the measurements of the E4/E6 ratios (Figure 3) of the supernatants, which shows that the ratio decreases with increasing amount of γ-Al_2O_3 to the solutions. These observations indicate that the average molecular weight distribution of the humic acid was increasing during sorption.

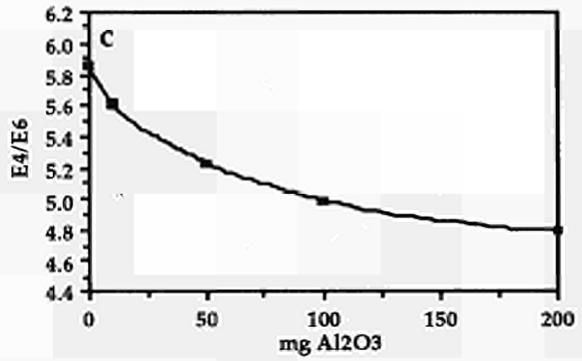

Figure 3. Sorption of Humic acids onto varying amounts of alumina. Variation in E4/E6 ratios.

The sorption, which probably involves attachment to the alumina surface by the carboxlylic groups, are virtually irreversible for pH ≤ 7. However, release of low molecular weight species from the coated surfaces was observed, possibly due to degradation of the humic material.

References

1. Carlsen, L., Lassen, P., Warwick, P., Randall, A.: Radio-labelled humic materials in migration studies, in: Scientific Basis for Nuclear Waste Management XVI (C.G. Interrante and R.T. Pabalan, eds.) Materials Research Society, Pittsburgh, 1993, pp 811- 816

2. Carlsen, L., Lassen, P., Warwick, P., Randall, A.: Radio-labelled humic- and fulvic acids: A new approach to studies on environmental fate of pollutants, in press

3. D. Haigh, J.J.W. Higgo, G.M. Williams : The effect of organics on the sorption of stontium, caesium, iodine, neptunium, uranium and europium by glacial sand, EUR 13519 EN, Commission of the European Communities, Nuclear Science of Technology, Luxembourgh, 1991

4. Davis, J. A. and Gloor, R.: Adsorption of Dissolved Organics in Lake Water by Aluminum Oxide. Effect of Molecular Weight. Environ. Sci. Technol., 15 (1981) 1223-1229.

5. Chen, Y., Senesi, N. and Schnitzer, M.: Information Provided on Humic Substances by E4/E6 Ratios. Soil Sci. Soc. Am. J., 41 (1977) 352-358

List of publications

1) P. Lassen, L. Carlsen, P. Warwick, A. Randall and R. Zhao, Radioactive labelling and characterization of humic materials, Environ. Int. 20 (1994) 127-134

2) Lars Carlsen, Pia Lassen, Peter Warwick and Amanda Randall, Radio-labelled humic- and fulvic acids: A new approach to studies on environmental fate of pollutants, in: Humic Substances in the Global Environment and Implications on Human Health, N. Senesi and T.M. Miano, eds., Elsevier, Amsterdam,1994, 1107-1112

3) Amanda Randall, Peter Warwick, Pia Lassen, Lars Carlsen and Peter Grindrod Transport of europium and iodine through sand columns in the presence of humic acids, Radiochim.Acta, 66/67 (1994) 363-368

4) Pia Lassen, Lars Carlsen and Peter Warwick, The interaction beweeen humic acids and γ-Al_2O_3, Theophrastus' Contributions to Advances studies in Geology, in press

5) Lars Carlsen, Pia Lassen, Peter Warwick and Amanda Randall, Labelled humics for studies of environmental fate of pollutants, in press

6) Amanda Randall, Pia Lassen, Peter Warwick and Lars Carlsen, Labelling of humic material by enzymatically mediated incorporation of ^{14}C-phenol, accepted for publication

7) L. Carlsen, P. Warwick, and P. Lassen, Fundamental studies on the interaction of humic substances, submitted for publication (presented at the Mirage Plenary Meeting, Brussels, nov. 1994)

Title:	Rock matrix diffusion as a mechanism for radionuclide retardation: natural radioelement migration in relation to the microfractography and petrophysics of fractured crystalline rock.
Contractors:	University of Exeter, UK; University of Oviedo, E; CEA Fontenay-aux-Roses, F; University of Liverpool, UK; University of Franche-Comté, Besançon, F; University of Oxford, UK.
Contract No.:	FI2W-CT91-0082.
Duration of contract:	01.03.91 - 31.03.95.
Period covered:	01.01.94 - 31.12.94.
Project Leaders:	M. J. Heath (Exeter), M. Montoto (Oviedo).

A. OBJECTIVES AND SCOPE

Rock matrix diffusion is an important element in radionuclide migration models: diffusion from water-conducting fractures into the rock matrix provides a potentially important mechanism for the retardation of nuclides migrating from a repository. Recent studies of crystalline rocks have shown, however, that free diffusion of nuclides from fractures into the rock matrix does not always take place and that very little of the rock adjacent to fractures may be available for diffusion.

Although mathematical models describing diffusion have been developed in the past, they have never been furnished with complete physical and chemical data from actual sites. The aims of the study are: (1) to observe evidence of past diffusion of uranium and its daughters from fractures into the rock adjacent to fractures; (2) to relate observed diffusion phenomena to the physical properties of the rock; (3) to construct physicochemical profiles across fractures and into the adjacent rock to allow complete characterisation of past diffusion and assess the potential for future diffusion; and (4) to develop a mathematical diffusion model that can be validated by reference to geological evidence and be incorporated reliably into overall radionuclide migration models.

B. WORK PROGRAMME

B.1 Determination of rock properties and examination of evidence for past diffusion in a series of rock slices at distance of up to 50 cm from hydrogeologically-active fractures;

B.2 Quantitative petrophysical analysis and the determination of key physical properties (accessible porosity, dry density, void index, kinetic water behaviour, dynamic properties);

B.3 Quantitative microstructural analysis using optical, fluorescence, acoustic and confocal laser microscopy, digital image processing and stereological techniques;

B.4 Geochemical analysis (major elements, iron chemistry, uranium and thorium, Rare Earth Elements, selected trace elements);

B.5 Uranium disequilibrium studies by alpha spectrometry;

B.6 Uranium microcartography by autoradiographic, fission track and SEM/EDX techniques;

B.7 The development of a mathematical diffusion model based upon real geological/geochemical data.

C. PROGRESS OF WORK AND OBTAINED RESULTS

State of advancement

The study is focused on the El Berrocal study site in Spain. The work undertaken during 1994 has included the following:

(1) Field sampling, sample preparation and sample distribution (Exeter/Oviedo);
(2) Petrographical and microstructural characterisation of the El Berrocal granite (Oviedo/Besançon/Oxford);
(3) Petrographical and mineralogical study of the EB8 profile (Oviedo/ Fontenay-aux-Roses);
(4) Uranium series investigations (Exeter/Harwell);
(5) Geochemistry (Exeter/Fontenay-aux-Roses);
(6) Phase separation tests (Harwell);
(7) Uranium series diffusion modelling (Liverpool).

To date, detailed physicochemical profiles have been obtained from cores EB4, EB5, EB6 and EB8, while work is still in progress on EB9 and EB11. Some additional petrophysical work has also been carried out on a seventh core (EB7).

Progress and results

C.1 Field sampling, sample preparation and sample distribution.

A total of seven cores from boreholes S-14 and S-16 have been selected for analysis (Table I; Figure 1). These cores have been chosen to enable the rock adjacent to hydrogeologically-active fractures to be studied, and are in various stages of investigation.

TABLE I.

Sample number	Borehole number	Depth (m)
EB4	S-16	37.85 - 38.24
EB5	S-14	161.07 - 161.18
EB6	S-14	119.90 - 120.50
EB7	S-14	227.60 - 227.73
EB8	S-16	327.40 - 327.65
EB9	S-16	468.50 - 468.85
EB11	S-14	215.35 - 215.45

TABLE I. Borehole core samples, El Berrocal.

Additional work has been carried out on block samples and on oriented cores, 42 mm in diameter and about 150 mm long, drilled in three different locations inside the mine adit.

C.2 Petrophysical characterisation of the El Berrocal granite

Different studies have been carried out to characterise petrophysically the rock matrix and to determine petrophysical profiles for each core in relation to distance from the fracture. Before cutting, each core has been subjected to non-destructive testing in Oviedo using ultrasonic techniques to determine any possible anisotropy in the rock matrix. Following core cutting, a series of petrophysical parameters have been determined on rock slices obtained at different distances from the fracture.

In order to understand the water dynamics through the rock matrix, a series of elemental physical properties (open porosity, void index, and water content after two days, five days and under saturation) have been determined in Oviedo, along with the following petrographic components and parameters of petrophysical significance: volume percentage of minerals (Vv), specific surface of grains (Sv grains), mineral affinity, specific surface of microcracks (Sv cracks), and microcrack orientation. The alteration state of the rock matrix has been studied in Oviedo as part of the petrophysical characterisation.

The best microstructural data have been obtained by applying different microscopy techniques to the same thin section, combining the information obtained by polarising light, fluorescence, confocal laser scanning, acoustic and scanning electron microscopy, the latter coupled with energy dispersive X-ray analysis. The petrographic components thus observed have been mapped and quantified using stereology and digital image analysis of the images obtained. Impregnated polished thin/thick slices have been prepared perpendicular to the fracture surface for microscopic studies. In the case of EB8, for example, six slices have been obtained, four of them including the fracture surface (EB8/1-0°, 45°, 90° and 135°); the two remaining slices (EB8/2-15° and 60°) being situated 34 mm from the fracture.

Confocal laser microscopy has been applied in Oviedo for a real three-dimensional fractographic analysis of the rock matrix, specifically the relationship between fissures and the rock-forming minerals, and the orientation of fissures (strike and dip). A geometrical procedure has been developed in Besançon to evaluate the dip of cracks as they are observed under fluorescence microscopy. Acoustic microscopy has been used in Oxford to quantify the weathering of feldspar crystals at grain level; the study has also attempted to evaluate possible anisotropies in small volumes of the rock matrix.

C.2.1 Non-destructive testing: ultrasonics

Non-destructive testing using ultrasonic techniques is carried out on all sample cores prior to cutting in order to detect possible anisotropies in the rock and for microstructural characterisation. The velocity of longitudinal waves (Vp) and the flight time have been measured in each core at increasing distances from the fracture surface and parallel to it. The cores are analysed in a series of 'virtual' slices at 10 mm intervals from the fracture. Four directions (45° from each other) have been measured for each 'slice'. The values for each direction have been determined in relation to distance from the fracture for cores EB4, EB5, EB6, EB8, EB9 and EB11. Results for EB4, EB5 and EB6 were described in Heath (1994). The results for cores EB8, EB9 and EB11 show no significant variation in Vp with distance from the fracture. In EB9, the measurements parallel to the fracture surface show differences in Vp of only around 4% which, in practice, shows petrophysical isotropy. In the case of core EB11 (Fig. 2), the different directions do, however, exhibit differences in Vp, suggesting some anisotropy.

C.2.2 Physical and hydric properties

Selected physical properties (open porosity, void index, water content after two days, water content after 5 days and saturation water content) have been measured following ASTM and ISRM standard methods. These physical properties have been evaluated in the different slices obtained by cutting parallel to the fracture. In the case of sample EB8 (Fig. 3), the values obtained for all these parameters are high, particularly open porosity which varies from 2.59% in the rock immediately adjacent to the fracture to 1.58% deep into the profile, while the profiles obtained clearly show a decrease in the value of each of these properties with increasing distance from the fracture.

The physical property profiles show that the nature of the variation of all of these properties with distance from the fracture is similar in core EB8, unlike cores EB5 and EB6 in which variation with distance from the fracture varies from property to property and from core to core. It seems that, in core EB8, the microfissuration is higher close to the fracture. In the case of EB9 (Table II), it can be seen that maximum open porosity values (up to 2.81%, a very high value) occur in the rock adjacent to the fracture surface. Thereafter, it decreases to fairly constant values throughout the rest of the profile. Similar behaviour is observed in the rest of the hydric parameters. It seems that the rock adjacent to the fracture surface (within 10 mm) is characterised by greater microfissuration and different petrophysical characteristics.

TABLE II.

L (mm)	V_i	W_1	W_7	W_{sat}	n_0
0-10	0.76	0.89	0.95	1.08	2.81
10-20	0.40	0.51	0.46	0.51	1.34
20-30	0.39	0.41	0.44	0.48	1.27
30-40	0.44	0.41	0.45	0.48	1.28
40-50	0.46	0.46	0.48	0.53	1.40
50-60	0.43	0.44	0.48	0.52	1.37
60-70	0.56	0.57	0.59	0.65	1.72

Table II. Physical properties of EB9 (borehole S-16, 468.50 m). L, distance from the fracture; Vi, void index (water content after 1 hour); W_1 and W_7, water content after 1 and 7 days respectively; W_{sat}, water content under saturation; n_0, open porosity.

In EB11, the open porosity and other hydric parameters increase as the fracture surface is approached though there is some variation deeper into the profile (Heath et al. 1994).

C.2.3 Alteration studies: mineral and rock deterioration indices

Because of the high degree of alteration of core EB8, as inferred from the hydric properties and microscopic observations, it was decided that a deeper study of the state of the rock matrix would be interesting. The "rock and mineral

deterioration indices" proposed for granitic rocks (Ordaz et al., 1978) have been used in order to evaluate the state of deterioration of EB8. These are petrographic indices inferred from optical polarizing microscopy of the rock-forming minerals and their individual states of alteration. The deterioration indices calculated for the rocks studied are related to certain physical and mechanical properties and to mineralogical textural aspects. In core EB8, it is intended to correlate these indices with the values obtained for the hydric properties. The information provided by the rock and mineral alteration indices have been shown to be very useful in the study of this sample and are consistent with the high values obtained for physical properties.

Mineral deterioration indices

The purpose of mineral deterioration indices is to allow numerical evaluation of the grade of degradation of granitic material. It is based on the estimation of the alteration state of the principal groups of rock-forming minerals: quartz, feldspar and mica. The deterioration levels of each mineral group are classified from 0 to 4 as the alteration increases, as shown in Table III.

TABLE III.

GRADE	DETERIORATION LEVEL OF FELDSPARS	DETERIORATION LEVEL OF QUARTZ	DETERIORATION LEVEL OF MICA
0	Apparently unaltered; without optically visible cracks.	Without optically visible cracks.	Apparently unaltered; without optically visible cracks.
1	Isolated microcracks of length less than grain size. Slight secondary alteration	Microcracks of length less than grain size.	Only altered on boundaries and/or along cleavages.
2	Interconnected microcracks of length approximately equal to grain size. Alteration areas less than 50% of grain surfaces.	Microcracks of length approximately equal to grain size. Microcracks interconnected.	Alteration on boundaries, with small spots of alteration inside the grains. Microcracks.
3	Microfissures crossing the grain. Alteration areas more than 50% of grain surface.	Microfissures crossing the grain. Incipient development of subgrains.	Alteration areas less than 50% of grain surface. Microfissures crossing the grain.
4	Extremely microfissured. Alteration areas occupying practically all the grain.	Extremely microfissured. Presence of subgrains.	Alteration areas more than 50% of grain surface. Abundant microfissures.

Table III. Proposed alteration grades for the principal rock-forming minerals.

The determination of deterioration grades is based upon the observation of thin sections under the polarizing optical microscope whereby a statistically representative measure of the grains of each mineral group can be obtained. For every grain, the grade is obtained from the established scale. The deterioration index for each mineral phase is then obtained by multiplying the different grades by the respective percentage of grains which exhibit that grade:

$$D_{(F,Q,M)}=\Sigma g_i \, P_i \, /100$$

where P_i are the different percentages of grains of a certain mineral group with deterioration grade g_i. The deterioration indices for each mineral in core EB8 are:

Feldspar $D_F = 2.97$ Quartz $D_Q = 2.27$ Mica $D_M = 1.39$

These partial indices provide a first approach to the general alteration state of the rock. Feldspars show the highest alteration index, corresponding mainly to chemical alteration with wide appearance of alteration products. Quartz shows no chemical alteration but mechanical breakdown, showing well-developed cracks crossing the grains. The two main micas (muscovite and biotite) show very different behaviour: muscovite is mainly unaltered, while biotite shows a higher degree of alteration and is often chloritized.

Rock deterioration index

Following the same approach, a 'rock deterioration index', I_d, can be defined, taking into account the mineral deterioration indices and the mineralogical modal analysis. It is defined as follows:

$$I_d=(xD_Q + yD_f + zD_M)/100$$

where x, y, and z are, respectively, the modal percentages of quartz, feldspar and mica present in the rock, and D_Q, D_F and D_M are the respective mineral deterioration indices. For example, the modal analysis of core EB8 is:

Quartz = 41.33%; Feldspar = 50.7%; Mica = 7.8%

With these data and the mineral alteration indices, the rock alteration index can be calculated as $I_d = 2.55$. This index can be considered to be an illustrative indicator of the level of alteration reached by the rock, but it should be noted that it is based on a subjective scale.

C.2.4 Confocal laser microscopy

Fluorescein-impregnated 'thin' sections, mainly 180 μm thick, have been studied under confocal laser scanning microscopy using a "LEICA CLSM". Experience has shown that, under normal instrumental conditions, microfractographic information can be obtained to a depth of 170 μm in the thin section. The results obtained so far prove the great usefulness of CLSM in characterising the microcrack network of fissured rock. This technique has been shown to be the most appropriate for observing and evaluating the open rock microfractography of El Berrocal granite; that is, the interconnected fissure network that would allow the migration of water and radionuclides through the intact rock. The CLSM has the ability to obtain 'virtual' sections of the rock at given depths (Z); thus, correlative images corresponding to different Z values in the rock section can be obtained, and other information coming from upper and lower Z values can be ignored. The images obtained have been used in the microstructural analysis of El Berrocal granite.

C.2.5 Microstructural studies

A methodology has been developed for the quantification of petrographic parameters from images obtained under confocal laser scanning microscopy. The purpose of this approach is to evaluate the petrographic parameters of interest in relation to distance from the fracture. To this end, 150 μm thick, impregnated,

artifact-free slices were prepared perpendicular to the fracture surface. Digital image processing techniques were used for analysis of the images obtained.

The following petrographic parameters have been evaluated:

- Specific surface of fissures versus mineral phase (Sv): this parameter represents the total inner area of a surface per unit rock volume and has been obtained from the image of the fissures appearing in quartz, feldspars and mica:

$$est(S_v) = \left(\frac{4}{\pi}\right) \times \frac{\sum length\ fissures}{\sum area\ (total)}$$

In the case of EB9, centimetre of rock nearest the fracture is different from the rest of the profile are different and the two zones, identified as 0-10 mm and 10-20 mm respectively, have been tested separately. The values of specific surface of fissures versus mineral phase are shown below:

	Sv (mm^{-1})		
	Total	(0-10 mm)	(10-20 mm)
Feldspar	7.13	7.46	6.79
Quartz	8.92	10.74	7.05
Mica	0.81	1.31	0.30

- Void volume (Vv): This parameter gives the distribution of voids versus fissure aperture, and is calculated by multiplying the specific surface by the aperture.

- Fractal dimension of mineral boundaries (D): the roughness of fissures and grain boundaries, which is very important in radionuclide migration processes, can be quantified using the fractal dimension of the surface profiles. The fractal character of a line expresses the dependence of the length of the line on the unit of measurement used. It is calculated by measuring the boundary length with different units. The fractal dimension of the boundary is obtained from D = 1-m (where m is the slope of the linear portion of the plot).

- Fissure orientation: histograms have been obtained for two slices from EB8 separated by 45°. In representing fissures, an angle of 0° is considered to be parallel to the fracture surface and 90° perpendicular to it.

- Linear crack density has been studied under fluorescence microscopy and is expressed by the number of fissures per millimetre. Two perpendicular directions have been considered both parallel and perpendicular to the fracture surface in two thin slices from EB8. The results obtained were:

	Linear crack density (fissures/mm)	
	EB8 (45°)	EB8 (90°)
0°	0.20	0.34
90°	0.14	0.33

Table VI shows the values of these microstructural parameters in core EB8.

Table VI.

Mineral	Sv (mm^{-1})	D	Vv(%)
Feldspar	27,54 σ=11.6	1.087	50.7
Quartz	14.29 σ=8.1	1.075	41.33
Mica	5.84 σ=2.5	1.080	7.8

Table VI. Petrographic and microstructural parameters obtained for core EB8. Sv = specific surface; D = fractal dimension; Vv = volume percentage (mineralogical modal analysis).

The directions were considered both parallel and perpendicular to the fracture surface in two thin slices from sample EB9, in which the measured Linear Crack Density was 0.45 fissures/mm.

C.2.6. Acoustic microscopy

Acoustic microscopy is exceptionally sensitive to surface cracks and at the same time shows the relation of cracks with other petrographic components. This technique has been used to quantify the weathering of feldspar crystals in El Berrocal granite at grain level. The aim of this work is to quantify the weathering of feldspar crystals at grain level in samples of granite from El Berrocal using acoustic microscopy, according to the approach outlined in a previous report (Heath et al., 1993). At an earlier stage, Rayleigh wave velocities were measured at several points in certain minerals in thin section. The Line Focus Beam Microscope (LFBM) was used in these measurements to assess the influence of crystallographic orientation on the velocity of Rayleigh waves in the mineral surface. The results showed a large angular dependence of the velocity of surface acoustic waves in feldspar grains, ranging from about 3000 to 5000 m/s. This suggested that more than one mode of surface acoustic waves may be responsible.

On the basis of this early work, it was decided to try to use the longitudinal wave velocity instead to quantify the weathering of crystals. For this, a different method of quantitative acoustic microscopy, the time-resolved technique, has been applied (the 'OXSAM'). This is similar in principle to the time-of-flight technique in NDT, but uses very short pulses to resolve echoes from the different interfaces of the specimen (the top and the bottom surface of the thin section of rock); it is then possible to deduce the elastic properties of the specimen from the amplitude and timing of the echoes. The OXSAM, with a spherical lens, can be operated in two modes: an image mode and a pulse mode. In the pulse mode the lens emits short pulses at a peak frequency of 220 MHz and a pulse length of about 5 ns. The lens acts as both transmitter and receiver. The appropriate experimental conditions (type of specimen, thickness of the rock section, frequency of the lens etc.) has first to be established since no previous applications of this method to rock materials are known. The more interesting results are from samples:

- EB4/2-90°: a 30 µm polished thin section;
- EB5/3-30°: a 130 µm polished thin section.

The first thin section was of standard thickness in petrographic studies and was used in the previous studies of acoustic microscopy under LFBM. The second section is thicker (135 µm) and is much better for the study of the microcrack network characteristics under confocal laser scanning microscopy.

The 30 µm thin sections give poor results because the reflections from the bottom are too close to those from the top. The use of a lens of 500 MHz frequency gives no better results. The first results from the 130 µm thin section (again with the 220 MHz lens) were not good: it seems that reflections from the bottom of the section were hidden by a cable echo, though changing the cable to one of different length gave no better results and it remained very difficult to identify the reflection from the bottom surface of the section. Perhaps the difficulty in identifying the signal arises from the characteristics of the sections themselves.

C.3 Petrographical and mineralogical study of the EB8 profile

The results of petrographic and mineralogical studies of a 25 mm profile from core EB8 are described here. Corresponding results from cores EB4, EB5 and EB6 were presented in Heath (1994) and discussed by Ménager et al. (1994).

C.3.1 Methodology

Samples have been prepared to enable the same thin section to be studied (1) at Fontenay-aux-Roses by scanning electron microscopy and induced fission track analysis (for petrography, mineralogy and the determination of the distribution of particulates), and (2) in Oviedo under confocal laser microscopy (for microstructural analysis). Thick (150 µm) polished sections have been prepared after impregnation with fluorescein resin. Six polished, oriented sections have been studied from profile EB8. Samples EB8/1-0°, EB8/1-45° and EB8/1-135° have been cut perpendicular to and intersecting the fracture surface. Samples EB8/2-15° and EB8/2-60° have been obtained from deeper within the profile and do not intersect the fracture.

C.3.2 Alteration of the primary paragenesis

The sample preparation technique adopted allows the degree of alteration of the primary phases in the rock to be evaluated and the microporosity of the system to be observed. In the El Berrocal granite, the alteration processes observed in the primary paragenesis affect mainly biotite and plagioclase. The degree of alteration of these phases in profile EB8 is variable and is not correlated with distance from the fracture. The rock slice 6 - 16 mm from the fracture surface shows greater plagioclase alteration than samples from the rock adjacent to the fracture. The degree of alteration of the biotites is variable within individual crystals in accordance with the distribution of pathways for the circulation of fossil or recent fluids (that is, near microfissures or near zones of high porosity due to preferential dissolution along grain boundaries). The same is observed for the alteration of accessory phases, notably uraninite, xenotime and monazite. The rock adjacent to the fracture appears to be particularly enriched in primary accessory uraniferous phases (uraninite and xenotime) and secondary coffinite immediately adjacent to the fracture. This enrichment is probably associated with processes of primary and secondary mineralisation of the granite.

C.3.3 Nature and stability of the secondary paragenesis

The principal secondary phases are phyllosilicates, carbonates and fluorides. The phyllosilicates are mainly located in the macro- and micro-fissure network and seal the microporosity of the system. They are particularly abundant in the rock immediately adjacent to the fracture and appear to be stable. Manganese-rich calcium carbonate coatings have been observed on the fracture surface. Some carbonates also occur in association with the phyllosilicates within altered zones. Secondary fluorite is observed in the microporosity of the system, particularly in altered plagioclase. These phases are particularly abundant in sections most distant from the fracture. The fluorite crystals show characteristic dissolution features associated with an episode of secondary destabilisation.

C.3.4 Characteristics and trapping capacity of the microporosity

The microporosity of the samples investigated appears to have evolved as follows: (1) the rock was conditioned at an early stage by the intensity of the microfissuration and the degree of dissolution of the primary minerals; (2) at a later stage, the effective microporosity (and, consequently, the permeability of the system) seems to have been directly associated with the nature of the secondary minerals and their long term stability. For example, the degree of interconnection between the pores in the fissures sealed by phyllosilicates is probably weak. In contrast, the interconnectivity of pores and their accessibility to circulating fluid is greater in the altered plagioclase, in which secondary dissolution is observed.

As already mentioned, the sample preparation technique employed has permitted detailed observation of the microporosity under scanning electron microscopy. These observations have allowed evaluation of the retention of particulate material in the microporosity of the granite near the fracture surface. Among these particles, microcrystals of calcite, 0.5 μm or less in size, have been identified along with spherical particles of variable dimensions, the smallest appearing to be colloidal. The quantitative analysis (by SEM+EDX) of the spherical particles has allowed Fe, Ti(Fe), Si and Si-Al particles to be distinguished. The origin of the trapped spherical particles is not clear. Two principal origins are possible: (1) generation in situ (with limited transport) or (2) filtration and trapping of imported suspended particles. Determination of the relation between suspended material and 'host' mineral has been attempted for the larger particles, which are largely observed in quartz and plagioclase.

C.3.5. Retention of uranium in secondary phases

The analysis of uranium microdistribution by induced fission track analysis has been carried out on six samples from core EB8. In the samples intersecting the fracture, a slight uranium enrichment (less than 10 ppm) is observed in the phyllosilicate fracture surface coating and in the secondary phyllosilicates sealing the microfissures close to the fracture. The observation in situ of particulates within the microporosity of a crystalline formation is new and provides a link with the data being obtained on colloid extracts from El Berrocal groundwaters.

C.4 Uranium series investigations

Uranium series disequilibrium investigations have been carried out in Exeter, supported under sub-contract by the Isotope Geoscience Laboratory, Harwell. These studies have focused on the key activity ratios $^{234}U/^{238}U$ and

$^{230}Th/^{234}U$ in a series of rock slices taken from each core. Complete profiles are now available for cores EB4, EB5, EB6 and EB8 and work is in progress on cores EB9 and EB11. The EB4, EB5 and EB6 profiles were described in Heath (1994).

The EB8 profile (Fig. 4) is similar to that of EB5 in that there is an elevated $^{234}U/^{238}U$ activity ratio (1.06) on the fracture surface with activity ratios near unity throughout the rest of the profile. This ^{234}U enrichment indicates geologically-recent uranium deposition, the chemical profile showing weak uranium enrichment at the fracture face. The $^{230}Th/^{234}U$ activity of 0.85 at the fracture surface is consistent with recent uranium deposition, but the rest of the profile is rather erratic, making interpretation difficult. Work on cores EB9 and EB11 is continuing.

C.5 Geochemistry

Major and trace element geochemistry has been determined on a series of rock slices taken from each core in Exeter and Fontenay-aux-Roses. Of particular importance are the uranium and thorium profiles and the iron chemistry. Studies of other elements were described in Heath (1994).

C.5.1 Uranium and thorium

In core EB8, there is only a weak enrichment of uranium on the fracture which is reflected in a slight ^{234}U excess. Thorium does not show any mobilisation in any of the profiles studied to date. Work on EB9 and EB11 is continuing.

C.5.2 Iron chemistry

Of particular importance in the geochemical work being undertaken is the iron chemistry, as the iron oxidation and uranium geochemistry appear to be closely correlated in some of the profiles examined. Results from EB4, in particular, showed an increase in iron oxidation in the 20 mm or so immediately adjacent to the fracture with fairly constant levels for the rest of the profile studied. There is a also slight enrichment in total iron on the fracture surface. The iron oxidation profile correlates well with the uranium profile suggesting that redox conditions exercise a strong control over uranium mobility in this shallow (38 m) core. In samples taken from greater depth, this relationship with iron oxidation is not observed, there being slight reduction on the fracture surface in core EB8 where a ^{234}U excess suggests geologically-recent uranium deposition.

C.6 Phase separation studies

Early attempts at modelling the isotopic profiles proved difficult due to the complex distribution of uranium in the rock. Uranium microcartography has shown uranium to be distributed in a variety of mineral phases and microstructural locations in the rock, and the purpose of the phase separation tests has been to attempt to separate these fractions and determine their isotopic characteristics.

C.6.1 Sequential leaching methodology

Phase separation has been carried out by the sequential leaching of samples over a 24 hour period using the reagents shown in Table V.

TABLE V.

Stage	Phase	Procedure
1	IE	1 M $MgCl_2$ at pH 7
2	AH	0.1 M $Na_4P_2O_7$ at pH 9.8
3	TAOD*	Tamm's Acid Oxalate: Ammonium oxalate + Oxalic Acid $((NH_4)_2(COO)_2)$ $((COOH)_2)$
4	CR	Coffin's Reagent (Sodium citrate + citric acid) + 5% $Na_2S_2O_4$
5	CO	Morgan's Reagent (Sodium acetate at pH 5.0)
6	RES**	$HClO_4/HF/HNO_3$

TABLE V. Phase separation scheme.

IE = ion exchangeable phase;
AH = adsorbed phase;
TAOD = amorphous Fe/Mn oxyhydroxide phase;
CR = crystalline Fe/Mn oxyhydroxide phase;
CO = carbonate phase;
RES = residue;
* = shaken in the dark;
** = total dissolution.

C.6.2. Results

Phase separations have been carried out on cores EB6 (Fig. 5) and EB11. For a broad interpretation, the uranium can be considered to have two major distributions, an immobile fraction represented by the residue and a mobile fraction represented by the leached phases. On this basis, the results show that (1) up to 80% of the uranium in the rock is held in the residue (only 51% in sample EB6.0, the 5 mm of uranium-enriched rock adjacent to the fracture face), much of which is made up of the resistate accessory minerals; and (2) this fraction is in isotopic equilibrium and does not appear to have participated in the uranium mobilisation processes of the last ~ 1 Ma. The mobile phases, in which EB6.0 is enriched, include those held in microfractures and grain boundaries. These results, along with those from the uranium microcartography, are being used to help distinguish the different uranium distributions in the rock and, thus, help to model the isotopic profiles.

C.7. Uranium diffusion modelling

The data obtained in these studies are providing the input for a mathematical diffusion model being developed in Liverpool. The intention is to model the uranium concentration and uranium isotopic activity ratios with distance from the fracture for comparison with the observed profile data in order to describe the processes observed and estimate values of the solid/solution exchange coefficient, K_d, and effective diffusivities.

C.7.1 Assumptions and modelling difficulties

The main basis of the diffusion model consists of the following elements:

(1) migration of ^{234}U and ^{238}U from a fracture into the rock matrix by diffusion;

(2) retardation of the uranium by sorption, characterised by a linear sorption (partition) coefficient which is assumed to be reversible.

The simulations of this model are based upon the observation that fracture profile data from at least some of fractures studied show enrichment of uranium at the fracture face decreasing rapidly with distance into the rock. It seems, however, that the simulated $^{234}U/^{238}U$ activity ratios do not vary with distance from the fracture in a way that matches the actual data.

From the profile data obtained, it is clear that the processes controlling uranium mobility in the near-fracture rock are many and various. It is, therefore, difficult to develop simple models that adequately explain the observed uranium distributions and isotopic ratios. Among the difficulties encountered are:

(1) High uranium concentrations are seen within a centimetre or so of the fracture wall, suggesting a high sorption exchange coefficient, K_d, for uranium; while

(2) Uranium series disequilibria ($^{234}U/^{238}U$ and $^{230}Th/^{234}U$) of varying signatures frequently extend out to several centimetres within the rock.

The model so far developed to explain the observed El Berrocal profiles features matrix diffusion, with high sorption, some scoping calculations for K_d, and a thumb sketch of the leaching of uranium back out into the fracture.

C.7.2 El Berrocal fracture profiles

The data obtained from El Berrocal cores EB4, EB5, EB6 and EB8 demonstrate the difficulty of establishing a model that is widely applicable to the many profiles that are now being obtained. Each profile has its own characteristics, having evolved in a different geochemical environment. The presence of evidence requiring apparently contradictory explanations is not uncommon, as each profile has been produced by a long and complex history. In core EB6, for example, uranium enrichment on the fracture surface appears to have been followed by leaching of uranium, the latter having produced the low $^{234}U/^{238}U$ activity ratios observed. More data and more profiles are needed before any widely applicable model can be developed. Further model development requires data from sets of similar profiles exhibiting a commonality of processes.

C.8 Discussion

The results obtained so far suggest that, although in some cases the shape of the elemental and isotopic profiles into the rock matrix from fractures is consistent with rock matrix diffusion, it is clear that other processes strongly influence radioelement migration into the rock matrix. Both shallow and deep cores have been studied and it appears that, in both the oxidising near-surface environment and under deeper, more reducing conditions, redox processes exercise a strong control over uranium mobility. In core EB4 (borehole S-16, 37.85 - 38.24 m), for example, there is a clear correlation between elemental and isotopic uranium distributions and iron oxidation (Fe_2O_3/FeO ratios). In cores EB5

(S-14, 161.07 - 161.18 m) and EB8 (S-16, 327.40 - 327.65 m), however, a ^{234}U excess at the fracture surface appears to be associated with iron reduction. In each case, the uranium mobilisation has taken place within zones of physical change adjacent to the fracture. Core EB6 (S-14, 119.90 - 120.50 m) is rather different in that there appears to be a ^{234}U loss throughout the profile, a significant observation which is being confirmed with additional analyses. Work on EB9 and EB11 is continuing.

It is clear from the work undertaken so far that there are strong mineralogical and microstructural controls of radioelement migration through the rock matrix which must be understood if the overall retardation potential is to be assessed. Of particular importance for uranium mobilisation is the mineralogical location of the element in the rock (locked into primary resistate phases or in readily-leached sites such as microfracture fillings). It is, therefore, essential that this uranium distribution is understood if the isotopic data are to be interpreted correctly.

Acknowledgements

The authors wish to thank Empresa Nacional de Residuos Radiactivos (ENRESA) and the Centro de Investigaciones Energéticas, Medioambientales y Tecnológicas (CIEMAT) for their generous help in all aspects of the project.

References

HEATH M. J. (1994). Rock matrix diffusion as a mechanism for radionuclide retardation: natural radioelement migration in relation to the microfractography and petrophysics of fractured crystalline rock. Report on Phase 1 (March 1991 - February 1993). Topical Report (Contract FI1W-CT91-0082). CEC EUR Series.

HEATH M. J. et al. (1994). Rock matrix diffusion as a mechanism for radionuclide retardation: natural radioelement migration in relation to the microfractography and petrophysics of fractured crystalline rock. 7th Progress Report to CEC (Contract FI1W-CT91-0082), December 1994.

MÉNAGER, M. T., HEATH, M. J., IVANOVICH, M., MONTJOTIN, C., BARILLON, R., CAMP. J. and HASLER, S. E. (1994). Migration of uranium from uranium-mineralised fractures into the rock matrix in granite: implications for radionuclide transport around a radioactive waste repository. Proc. 4th Int. Conf. on Chemistry and Migration Behaviour of Actinides and Fission Products in the Geosphere (Migration '93), Charleston, USA, 12-17 December 1993. Radiochimica Acta, 66/67, 475-483.

ORDAZ, J., ESBERT, R. M. and SUAREZ DEL RIO, L. M. (1978). A proposed petrographical index to define mineral and rock deterioration in granitic rocks. Proc. Symp. Deterioration and Protection of Stone Monuments, Paris. 1, pp 2-6.

PEREZ DEL VILLAR, L., DE LA CRUZ, B., PARDILLO, J., PELAYO, M., TURRERO, M. J., GOMEZ, P., and RIVAS, P. (1993). Preliminary lithogeochemical model of the "El Berrocal" site (S. Gredos, Spain). El Berrocal Project, Rept. EB-CIEMAT(93)6.

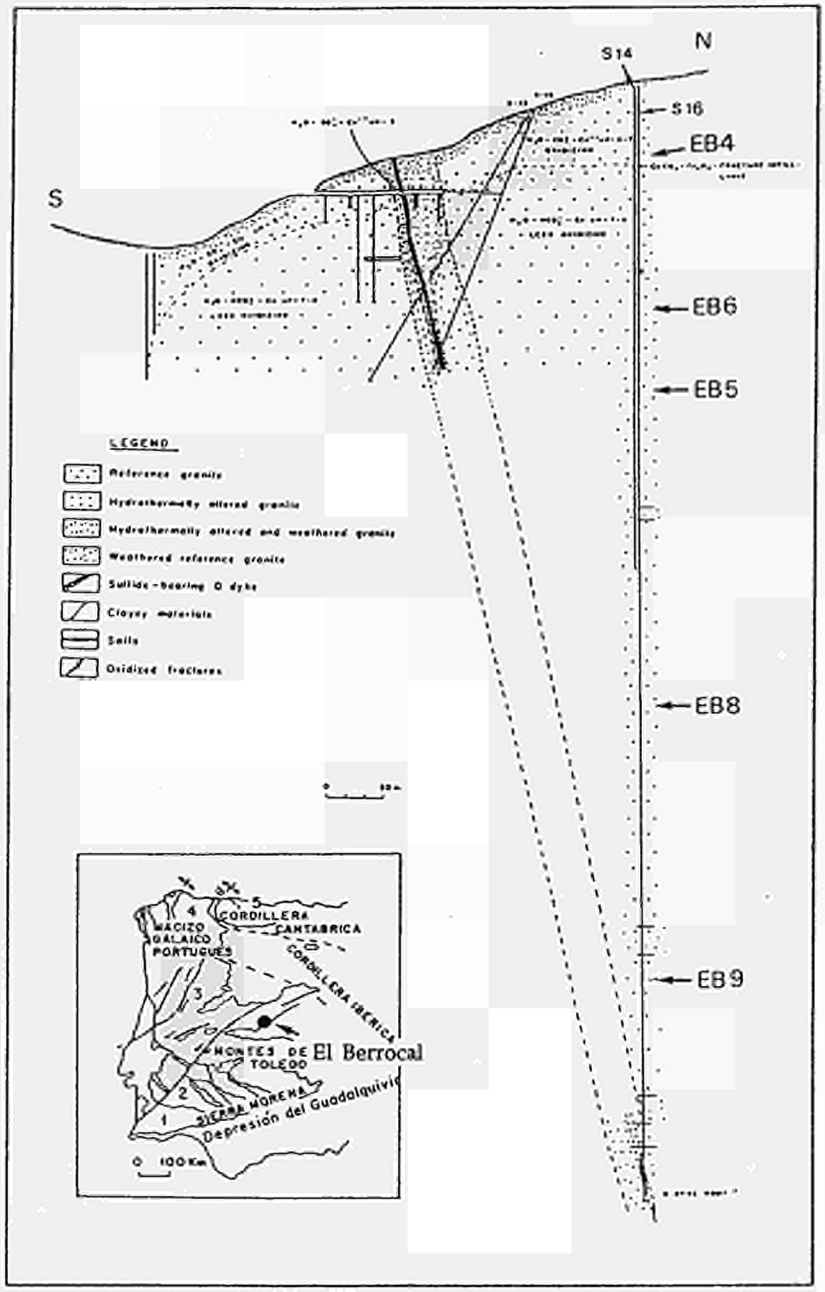

Figure 1. Location map and schematic cross-section of the El Berrocal granite showing the mineralised dyke, the different zones of the granite and the location of boreholes and samples. Modified after Pérez del Villar et al. (1993).

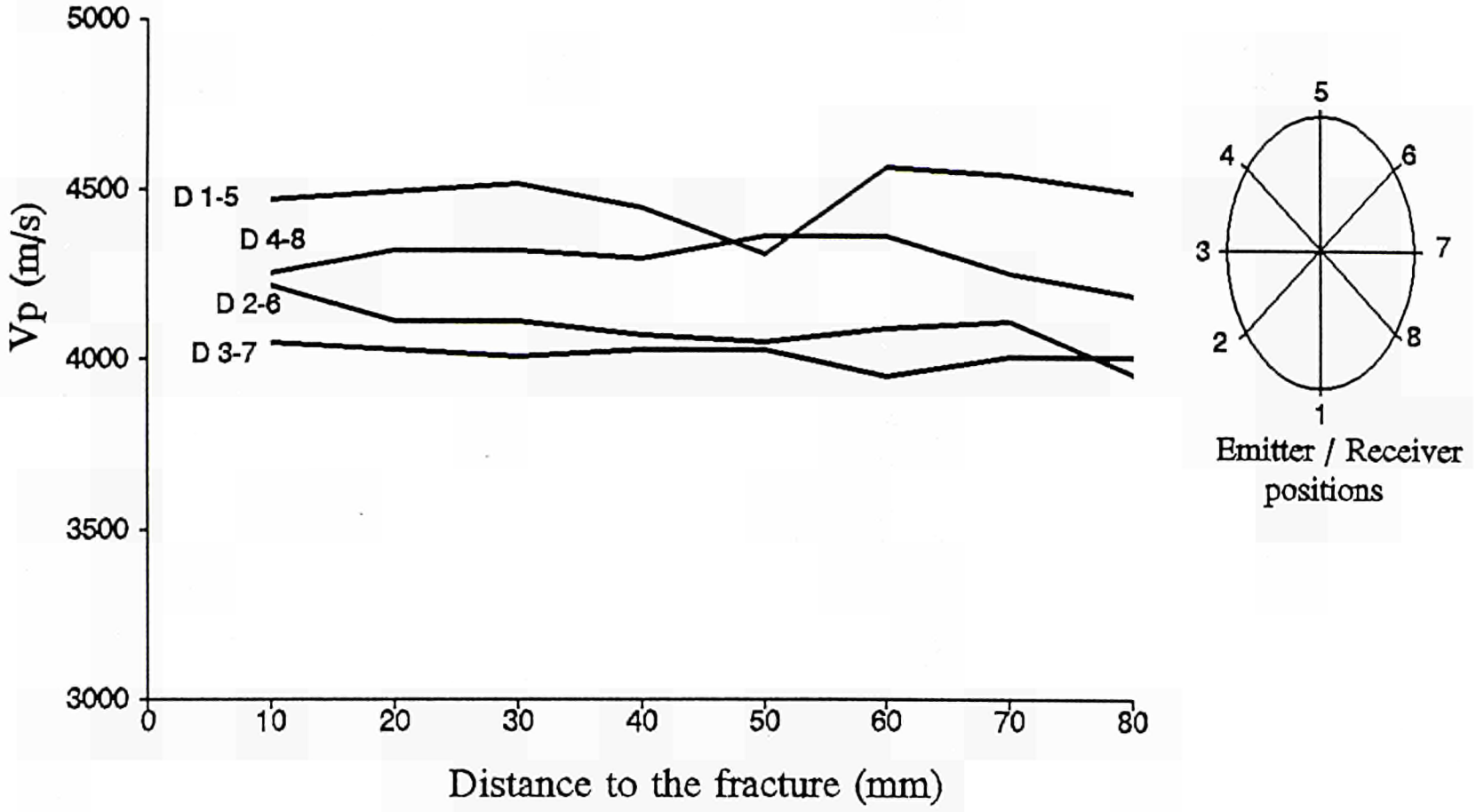

Figure 2. Variation in mean values of Vp (m/s) along the different measurement directions (see inset) in core EB11 as a function of distance from the fracture.

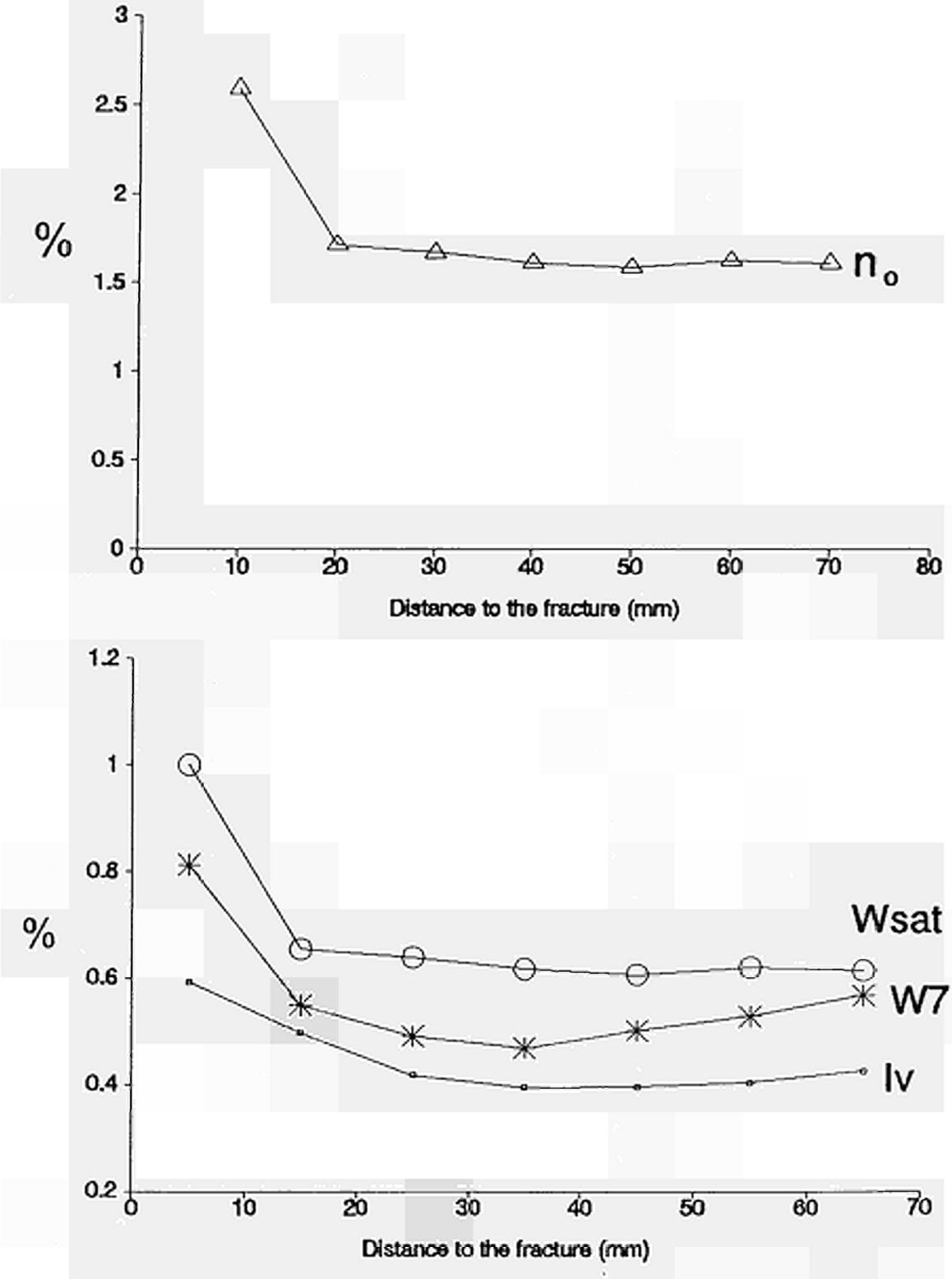

Figure 3. Variation in open porosity (n_o) (top) and hydric properties (W_{sat} = saturation water content; W_7 = water content after 7 days; Iv = void index) with distance from the fracture, core EB8.

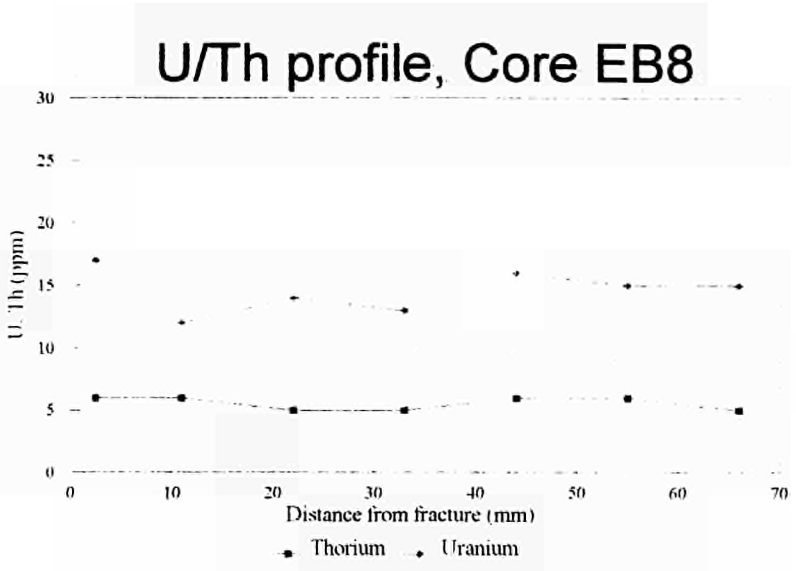

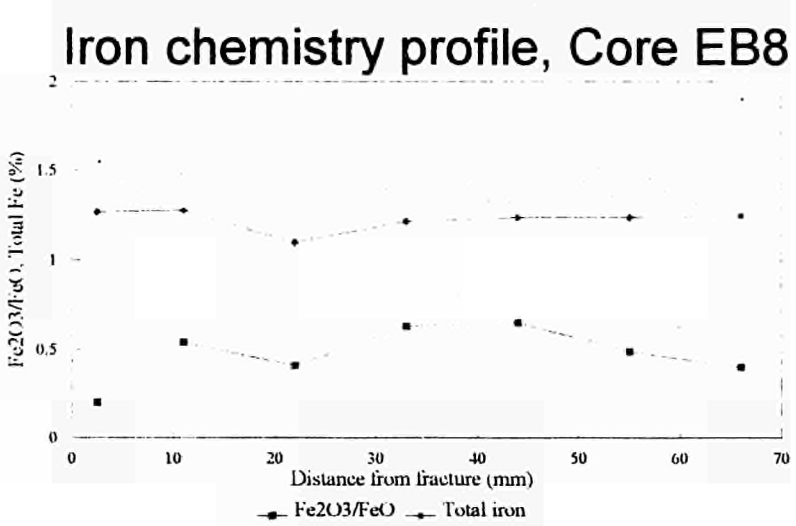

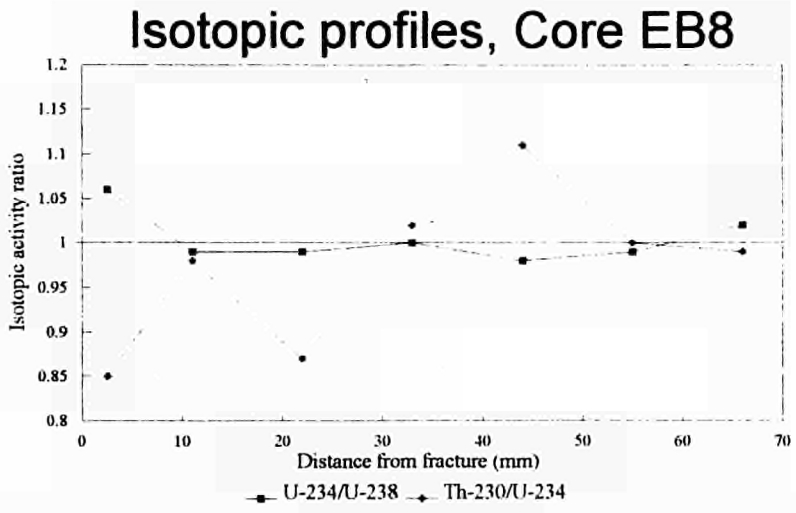

Figure 4a. Geochemical and isotopic profiles, core EB8 (Error bars are shown in Fig. 4b).

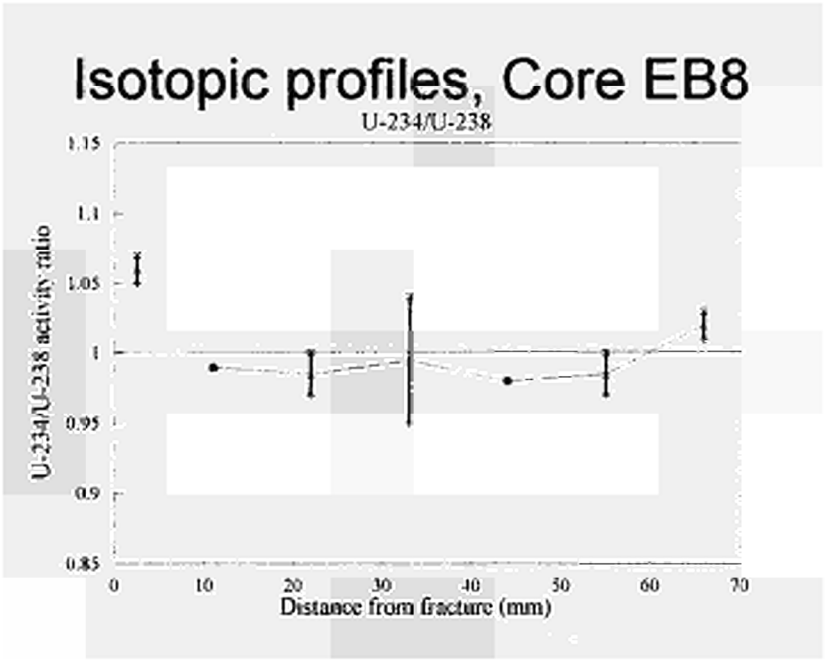

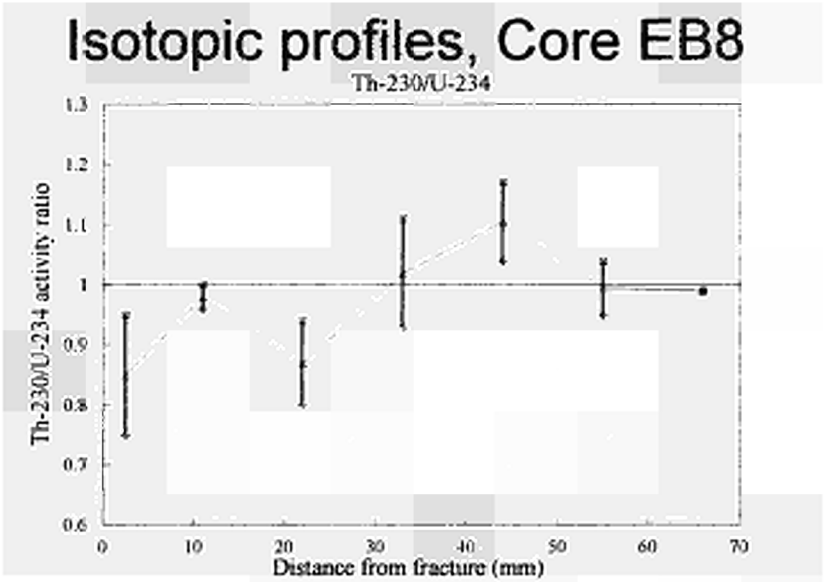

Figure 4b. Detailed isotopic profiles, core EB8 (Error bars = one standard deviation).

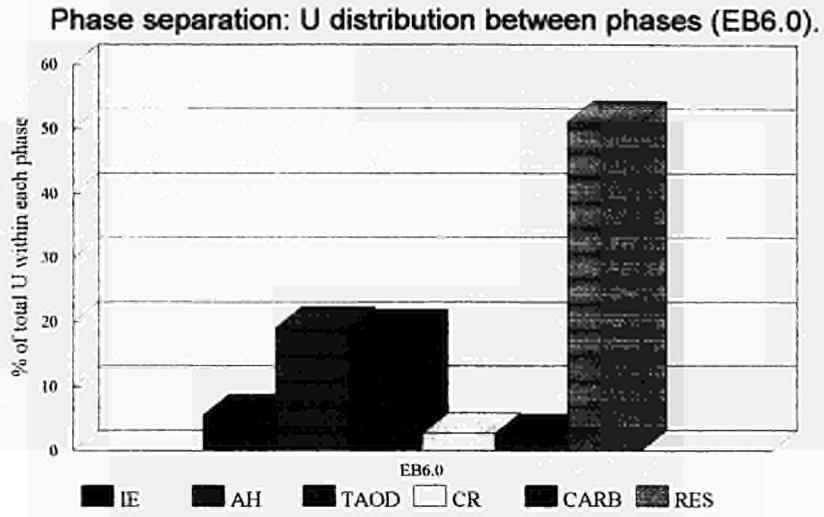

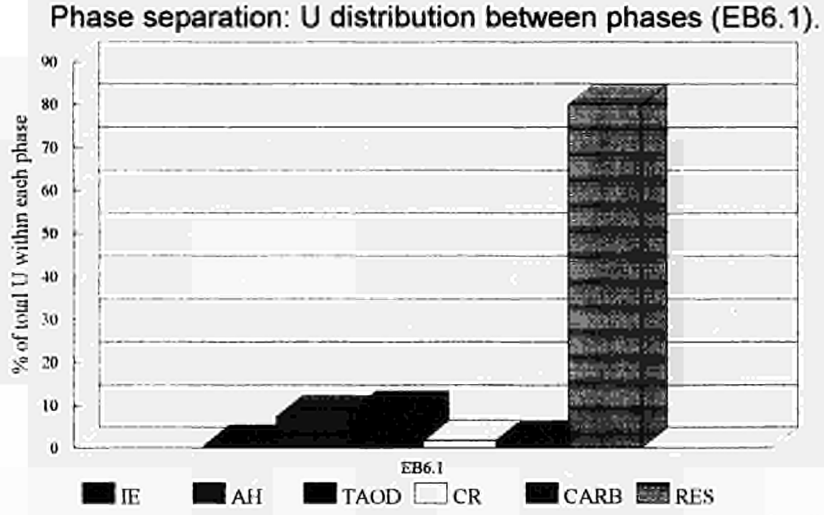

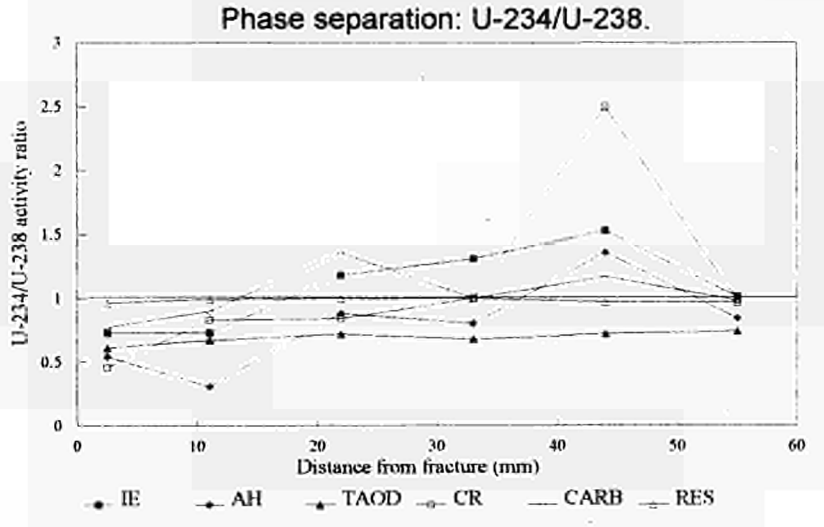

Figure 5. Results of phase separations, core EB6, showing uranium distribution between phases in samples EB6.0 and EB6.1 and $^{234}U/^{238}U$ activity ratio profiles for each phase.

Title	Effects of Humic Substance on the Migration of Radionuclides: Complexation of Actinides with Humic Substances
Contractors:	Technische Universität München, Garching, Germany (TUM); Commissariat à l'Energie Atomique, Fontenay-aux-Roses and Saclay, France (CEA-FAR/SAC); Universität Mainz, Mainz Germany (UM); Katolieke Universiteit Leuven, Heverlee, Belgium (KUL); Europea Commission, Joint Research Centre, Ispra, Italy (JRC-Ispra)
Contract N°	FI2W-CT91-0083
Duration of contract	June 1991 - June 1994
Period covered	January 1994 - June 1994
Project leader	K.R. Czewinski, J.I Kim (TUM, Coordinators); V. Moulin (CEA-FAR/SAC); N. Trautmann (UM); A. Maes (KUL); G. Bidoglio (JRC-Ispra)

A. OBJECTIVES AND SCOPE

The aim of the present research program is to study the complexation behavior of actinide ions with humic substances in natural aquifer systems and hence to quantify the effect of humic substances on the actinide migration. Aquatic humic substances commonly found in all groundwaters have a strong tendency towards complexation with actinide ions. This is one of the major geochemical reactions but at the moment least quantified. Therefore, the effect of humic substances on the actinide migration is poorly understood. In the present research program the complexation of actinide ions with humic substances will be described thermodynamically. This description will be based on a simple concept to facilitate the introduction of the resulting reaction constants into geochemical modeling of actinide migration. This program is a continuation of the activities of the COCO-group in the second phase of the CEC-MIRAGE project.

B. WORK PROGRAM

The program consists of the following three main tasks:

Task 1:	Complexation reactions of actinide ions with well characterized reference and site-specific humic and fulvic acids
Task 2:	Competition reactions with major cations in natural groundwaters
Task 3:	Validation of the complexation data in natural aquatic systems by comparison of calculation with spectroscopic experiment

C. PROGRESS OF WORK AND RESULTS OBTAINED

1 Complexation reaction of actinide ions with reference and site specific humic acids.

1.1 Humic substances

For the present study, humic and fulvic acids from three different sites and a commercial humic acid are used. They were purified, protonated and characterized previously [1-4]. The commercial product is included as a reference material for the purpose of intercomparison. These products are named as follows:

Gohy-573(HA):	Humic acid from Gorleben (FRG)
Gohy-573(FA):	Fulvic acid from Gorleben (FRG)
Fanay-Augeres(HA):	Humic Acid from Fanay Augeres (F)
Fanay-Augeres(FA):	Fulvic Acid from Fanay Augeres (F)
Boom-Clay(HA):	Humic acid from Boom Clay (B)
Boom-Clay(FA):	Fulvic acid from Boom Clay (B)
Aldrich(HA)I:	Humic acid from Aldrich Co. (Commercial)

The participating laboratories have agreed upon the introduction of additional batches of the reference humic acid, since the original amount purchased was not sufficient to meet growing experimental demands. For interpretation of the complexation behavior, the proton exchange capacity of each humic substance is critically important and are given in Table 1.

Table 1. Proton exchange capacities of the studied humic substances

	Proton exchange capacity (in meq/g)			
	TUM	CEA-FAR/SAC	KUL	JRC-Ispra
Aldrich(HA)I	5.43 ± 0.16	6.0 ± 0.5	2.7/3.9[1)]	5.24
Aldrich(HA)II	4.18 ± 0.15		4.38 ± 0.07	
Aldrich(HA)III	4.61 ± 0.11			
Gohy-573(HA)	5.38 ± 0.20	5.2/5.2	3.5/4.5[1)]	
Gohy-573(FA)	5.70 ± 0.09			
Fanay-Augeres(HA)	1.85 ± 0.05	3.4 ± 0.2		
Fanay-Augeres(FA)	6.93 ± 0.06	5.7		
Boom-Clay(HA)	4.22 ± 0.02			
Podzol-B(HA)			5.4	

1): pH=7/10

1.2 Experimental techniques

TUM

UV/Vis-spectroscopy, time resolved laser fluorescence spectroscopy (TRLFS), ultrafiltration and anion exchange chromatography are applied for the study of actinide-humate complexation. UV/Vis-spectroscopy is used for the study in the µmolar concentration range of both Am^{3+} and humic acid. The complexation is quantified by peak deconvolution of mixed bands with reference peaks of the free Am^{3+} ion and the Am-humate complex at 503.2 nm and 505.5 nm. Through TRLFS, the Cm-humate and UO_2-humate complexation is investigated in the nmolar concentration range with a low loading of humic acid. The fluorescence yield of Cm-humate is enhanced by energy transfer from humic acid molecules to metal ions. By selective excitation at different wavelength, the spectroscopic speciation of Cm^{3+} and the humate complex is optimized. Speciation by TRLFS for the uranium study is made by excitation of the uranyl ion followed by peak deconvolution of the emission bands of the non-complexed UO_2^{2+} ion and UO_2-humate. By time discrimination, the high humic acid fluorescence background is eliminated. Ultrafiltration is used for the Am-humate and UO_2-humate complexation study covering the metal ion concentration ranges of used for the two spectroscopic methods. The anion exchange chromatography is performed with Varian Analytichem Bond Elute Strong Exchanging Resin, on which the polyanionic humic acid and the uranyl humate complex are sorbed whereas the non-complexed uranyl cation remains in solution. Influence of the purification of humic acid on the complexation is also examined. The non-purified humic acid is analyzed by Inductively Coupled Plasma-Atomic Emission Spectroscopy (ICP-AES), Mono-Standard Neutron Activation Analysis (MS-NAA) for metal ion concentration, and IR-spectroscopy for humic acid structure.

CEA-FAR/SAC

TRLFS is applied for the study of the humate complexation of Cm^{3+} and UO_2^{2+} using an excitation energy at 337 nm and the EDTA and humate complexation of Dy^{3+} at 355 nm [1]. By energy transfer from EDTA to the complexed Dy^{3+} ion, the Dy-EDTA complex is selectively quantified by its emission at 576 nm. The competition effect of Ca^{2+} on Dy-humate complexation and temperature effects are also studied by this method. The UO_2^{2+} complexation is quantified through quenching of the UO_2^{2+} fluorescence at 514 nm. Life-time measurements and the position of the emission peak maximum give information on the uranium oxidation state and the quench mechanism for the UO_2-humate complex. The humate complexation of NpO_2^+ is investigated with UV/Vis-spectroscopy. The complex and the free NpO_2^+ ion are quantified from the peaks at 991 nm and 981 nm, respectively.

UM

A three step-laser-resonance-ionization mass spectroscopy system (RIMS) is used for the detection of actinides down to the femtomolar concentration range [2]. For studies in the nanomolar to micromolar concentration range, gamma spectroscopy is used for quantification of actinide ion concentrations. Separation of the non-complexed ions from their humate complex is accomplished by electrophoretic ion focusing, cation exchange, and anion exchange chromatography. The first technique is applied to separate the humic acid and metal humate species from the cationic free metal ion. This method is used for the humate complexation of NpO_2^+ and Sm^{3+} and Ca^{2+} competition experiments. For the Sm-humate complexation experiments, Biorad AG 50W X 8 cation exchanger is used to separate the free Sm^{3+} ion from the solution. Anion exchange chromatography is performed with DEAE Sephadex A-25, where the humic acid and humate complex are sorbed, while the non-complexed NpO_2^+ is left in solution. For determination of the oxidation state of neptunium, liquid-liquid extraction with thenoyltrifluoroacetone (TTA) is used.

KUL

Cation exchange and dialysis methods are used for the study of Eu-humate complexation and experiments for competition with different cations. The cation exchange technique has been used by KUL over several years [3,4]. The competition of Ca^{2+} on the Eu-humate complex is studied by this method. Dialysis operates on the separation of various Eu^{3+} species. By both experimental techniques, the influence of different competing ligands (oxalic acid, diglycolic acid, iminodiacetic acid, acetylacetone, hydroxide, and carbonate) on the complexation is studied. The dialysis technique is also applied for the study of the competition by different cations. Different dialysis membranes are tested for their applicability.

JRC-Ispra

TRLFS is used for the competition study between the trivalent lanthanide and Cr^{3+} and Tl^{3+} with humic acid. The decrease of the Eu^{3+} or Tb^{3+} fluorescence signal from the humate complex is examined as a function the non-fluorescent Cr^{3+} or Tl^{3+} concentration. The properties of the UO_2^{2+} as a function of pH is examined by TRLFS.

1.3 Results of the complexation study

TUM

The fulvate complexation of trivalent actinides is examined at pH 6 in 0.1 M $NaClO_4$. The pH effect on trivalent actinide humate complexation is studied from pH 3.0 to 6.0 at 0.1 M $NaClO_4$, while the ionic strength influence is examined at pH 6.0 and varied from 0.001 M to 5.0 M. The complexation of UO_2^{2+} to humic acid (Gohy-573) is investigated at pH 4.0 and an ionic strength of 0.1 M. The metal ion concentration is varied from the nmolar to μmolar ranges to examine the influence of the humic acid loading on the complexation behavior. No significant difference in the results is found between the three experimental methods.

The loading of humic acid by actinides varies from approximately one percent to a level of saturation to examine the effect of metal ion concentration on the humate complexation [5-9]. Taking the loading capacity into account, no influence of loading on the complexation constant is observed (Table 3). Comparing the results for the Gohy-573 humic acid with previous studies for Aldrich humic acid and Bradford humic acid [9,11,12], no significant difference in the complexation constant is found.

CEA-FAR/SAC

The complexation of Cm^{3+}, Dy^{3+}, NpO_2^+ and UO_2^{2+} with humic acid is investigated between pH 4.0 and 7.0 at constant ionic strength of 0.1 M. To investigate the influence of the ionic strength, the Cm-humate complex is also studied in 0.001 M $NaClO_4$ at pH 4.2 and 6.1. The experiment is based on measuring the total fluorescence intensity as a function of the humic acid concentration at a constant metal ion concentration. The quantification of the humate complex and free metal ion is made by analyzing the fluorescence titration curve [10]. UV-visible spectroscopy is used for the NpO_2^+ study.

The effective ligand concentration, expressed as a complexation capacity, is found to vary with pH, ionic strength and the total metal ion concentration. The complexation constants evaluated by taking the complexation capacity into account are found to be independent of pH and ionic strength. This is in agreement with the results from TUM and KUL. However, the complexation constants determined by CEA-FAR/SAC are found to vary significantly with the metal ion concentration, similar to results found by JRC-Ispra [11,12]. For the complexation reaction it is assumed that only a 1:1 complex is formed. The stability constants are presented in Table 3.

UM

The complexation of NpO_2^+ in the femtomolar concentration range with Aldrich and Gohy-573 humic acids is investigated. The humic acid concentration is varied between 20 mg/L and 200 mg/L. The pH is varied from 3.0 to 9.0 and the ionic strength from 0.001 M to 0.1 M. Over this range a 1:1 complex is found. Since the loading capacity is not evaluated due to the low metal ion concentration, the humic acid ionization fraction (α) is used. No difference in the complexation reaction between the Aldrich and Gohy-573 humic acids is found. However, the complexation strength of the Aldrich humic acid is somewhat higher (Table 3).

The Sm^{3+} complexation with Aldrich humic acid is studied at pH 3.0 to 5.0. The humic acid concentration is varied from 2 mg/L to 60 mg/L, with the Sm^{3+} concentration varied from 1 nmol/L to 10 µmol/L, and the ionic strength from 0.01 to 0.1 M. The experimental techniques are cation exchange and electrophoretic ion focusing. Over the entire experimental range a 1:1 stoichiometry is found. The stability constants are given in Table 3.

The effect of temperature on NpO_2-humate complexation shows a linear decrease of the complexation strength with increasing temperature. From 21°C to 60 °C, the relative amount of NpO_2-humate decreases from 38 % to 13 %. Under anoxic conditions (Ar-atmosphere), a pseudo-first order reduction of NpO_2^+ to Np^{4+} is observed over a time span of 120 h. The rate constants vary with pH and reach a maximum at pH 3.5.

KUL

KUL has determined the complexation constants for Eu^{3+} with Podzol and Aldrich humic acids by ion exchange and dialysis. The Eu^{3+} concentrations are $3x10^{-7}$ and $3x10^{-8}$ mol/L, while the humic acid concentration is varied between 10^{-5} and 10^{-4} mol/L, and the pH is varied from 4.0 to 10.0 in 0.1 M $NaClO_4$. In the non-hydrolyzing range (pH 4.0 - 6.0), no influence of pH on the complexation constant is found if the variation of the free ligand concentration is taken into account (Table 3).

In the presence of competing ligands, the formation of Eu-humate complexes is strongly enhanced and data are interpreted by "apparent" complexation constants for the formation of mixed complexes as examined by cation exchange and dialysis. The dialysis method makes use of the size difference among the colloidal humic acid, non-complexed metal ions, and competing ligands. Experiments are performed at ionic strength of 0.1 M with a Eu^{3+} concentration of approximately 10^{-7} mol/L. The competing ligands are acetylacetone, diglycolic acid, iminodiacetic acid, carbonate and hydroxide.

Above a certain critical concentration of a given competing ligand, an increase of the Eu interaction strength with humic acid is observed. The critical concentration decreases with increasing the interaction strength of a given ligand. The results are interpreted as a generation of mixed complexes. Experimental data with competing ligand concentration well beyond their critical concentrations are examined for the stoichiometry by analysis of the relation:

$$Eu^{3+} + HA(I) + nL \iff EuL_nHA(I) \qquad (1)$$

where L is acetylacetone, diglycolic acid, iminodiacetic acid, or carbonate. The nearest integer number for the n value is 2 (1.76±0.28). Therefore, KUL suggests to describe the ternary system Eu^{3+}, humic acid and ligand L by the following two reactions:

$$Eu^{3+} + HA(III) \iff EuHA(III) \qquad (2)$$

$$Eu^{3+} + 2L + HA(I) \iff EuL_2HA(I) \qquad (3)$$

On the common basis for the humate ligand of HA(III) the observed complexation constant $\log\beta_{exp.}$ is written as:

$$\log\beta_{exp.} = \log\beta_1 + \log\beta_{mix\ 2,1} + 2 \times \log[L] + \log 3 \qquad (4)$$

where $\log\beta_1$ refers to reaction (2), "$\log\beta_{mix\ 2,1} + 2 \times \log[L]$" refers to reaction (3) and log 3 accounts for the two different expressions of the humate ligand concentration (HA(I) and HA(III)) in reactions (2) and (3) (Table 2). It is concluded that for modeling under in situ conditions the formation of mixed complexes of metal ions with humic acid should be taken into account.

Table 2. Observed mixed humate species stability constants

Ligand	$\log\beta_{mix\ 2,1}$	standard deviation
AA^-	15.44	0.43
DGA^{2-}	16.33	0.46
IDA^{2-}	18.14	0.49
CO_3^{2-}	17.97	0.58
OH^-	18.00	0.36

AA^-: Acetylacetone; DGA^{2-}: Diglycolic acid; IDA^{2-}: Iminodiacetic acid

JRC-Ispra

The fluorescence properties of the UO_2^{2+} hydroxide system are examined in 0.1 M and 1.0 M ionic strength from pH 2 to 11.8. A variance in the decay times and relative fluorescence efficiencies with respect to the uranyl species is observed. Polynuclear complexes are found to have a higher fluorescence efficiency than the uranyl ion.

Table 3. Results from complexation studies of metal ions with humic substances

Humic Substance	Metal Ion	$[M^{Z+}]$ (mol/L)	pH	Ionic Strength (mol/L)	Laboratory	Method	log ß (L/mol)
Gohy-573 FA	Am^{3+} Cm^{3+}	10^{-6}-10^{-9}	6.0	0.1	TUM	TRLFS UF UV-Vis	5.86±0.11
Gohy-573 HA	Am^{3+} Cm^{3+}	10^{-6}-10^{-9}	3.0-6.0	0.001-5.0	TUM	TRLFS UF UV-Vis	6.26±0.12
Gohy-573 HA	UO_2^{2+}	10^{-5}-10^{-7}	4.0	0.1	TUM	TRLFS UF IE	6.16±0.13
Aldrich HA	Am^{3+} Cm^{3+} Dy^{3+}	10^{-5}-10^{-9}	4.2-6.9	0.1	CEA-FAR/SAC	TRLFS	6.1 to 9.1
Aldrich HA	NpO_2^{+}	10^{-4}	7.0	0.1	CEA-FAR/SAC	UV-Vis	4.57±0.13
Aldrich HA	UO_2^{2+}	10^{-8}	4.0-5.0	0.1	CEA-FAR/SAC	TRLFS	7.6±0.3
Aldrich HA	Sm^{3+}	10^{-5}-10^{-9}	3.0-5.0	0.01-0.1	UM	IE EIF	6.5±0.5
Aldrich HA	NpO_2^{+}	10^{-8}-10^{-12}	4.0-9.0	0.001-0.1	UM	IE EIF	4.5±0.4
Gohy-573 HA	NpO_2^{+}	10^{-8}-10^{-12}	4.0-9.0	0.001-0.1	UM	IE EIF	4.1±0.4
Aldrich HA Podzol B	Eu^{3+}	10^{-6}-10^{-8}	3.5-10.0	0.01-0.1	KUL	IE D	6.88±0.28
Gohy-573 HA	Cr^{3+}	10^{-6}	5.5	0.1	ISPRA	TRLFS	6.3

D: Dialysis
EIF: Electrophoretic Ion Focusing
IE: Ion Exchange
TRLFS: Time Resolved Laser Fluorescence Spectroscopy
UF: Ultrafiltration
UV-Vis: UV-Visible spectroscopy

2 Competition reactions with cations in natural groundwaters

CEA-FAR/SAC

The competition effect of Ca^{2+} on the Dy-humate complex is studied at pH 5.0 in 0.1 M $NaClO_4$. At Dy^{3+} and humic acid concentrations of $2x10^{-6}$ mol/L and 3.3 mg/L, respectively, the Ca^{2+} concentration is varied from zero to 34 mmol/L. At the maximum Ca^{2+} concentration, a decrease of the fluorescence signal of approximately 40% from the Dy-humate complex is observed. However, in the Ca^{2+} concentration range of natural waters ($1x10^{-5}$ to $4x10^{-3}$ mol/L) no significant effect on the Dy-humate complexation is found.

UM

The influence of divalent cations on the complexation of NpO_2^{+} and Sm^{3+} with humic acid is examined by electrophoretic ion focusing. For the NpO_2^{+} experiments, the conditions are pH 5.0 in 0.1 M $NaClO_4$ with 10^{-13} mol/L NpO_2^{+} and a humic acid concentration of 30 mg/L with

competition from Ca^{2+} and Mg^{2+}. The divalent ions show a considerable influence on the NpO_2-humate complex with no detectable difference between Ca^{2+} and Mg^{2+}. Increasing the divalent cation concentration from 10^{-6} mol/L to 10^{-3} mol/L, the concentration ratio of the complexed NpO_2^+ to the free ion decreases by a factor of 7. For the study of the Mg^{2+} effect on Sm-humate at pH 5, the Mg^{2+} concentration is varied from 10^{-8} M to 10^{-3} M, with 2 mg/L humic acid and 10^{-8} M Sm^{3+}. The effect of Mg^{2+} is observed only at high concentrations similar to the results obtained by CEA-FAR/SAC.

KUL

Studies of cation competition on the Eu-humate complexation are conducted between pH 3.0 and 6.0 at 0.1 M ionic strength with dialysis and cation exchange. Concentrations of competing cations are varied, while the Eu^{3+} concentration is in the µmole/L range and the humic acid concentrations are between $3x10^{-5}$ eq/L and $3x10^{-4}$ eq/L. Competition reactions are found to deviate from a simple ion exchange process. The results are interpreted assuming two different types of exchange sites with different interaction strength towards different complexing cations. The competition strength of the different cations studied is found to increase with the strength of their humate complexation:

$$Fe^{3+} \approx Cu^{2+} > Al^{3+} > Fe^{2+} > Ca^{2+} > [Co(NH_3)_6]^{3+} > Na^+$$

These and previous results (Table 4) verify that the competition effect is mainly governed by the relative complexation strength between the actinide ions and the competing metal ion.

JRC-Ispra

JRC-Ispra has studied the competition effect of Cr^{3+} and Tl^{3+} on Tb^{3+} and Eu^{3+} with humic acid (Gohy-573 HA) at pH 5.5 in 0.1 M $NaClO_4$. Kinetic studies show that the equilibration of Eu^{3+} and Tb^{3+} is fast, whereas the exchange equilibrium with Cr^{3+} requires approximately 24 hours. The complexation constant derived for Cr^{3+} is $\log\beta(Cr^{3+}\text{-HA}) = 6.3$, similar to Eu^{3+} and Tb^{3+}. From the Tl humate competition studies, a conditional binding constant is determined.

Table 4. Summary of the competition studies

	Competition effect of		
	Ca^{2+}, Mg^{2+} on		Cr^{3+} on
Laboratory	M^{3+}	MO_2^+	M^{3+}
CEA-FAR/SAC	minor		
UM	minor	important	
KUL	minor		
JRC-Ispra			equal strength

3 *Validation of the results in natural aquatic systems by comparison of calculation with spectroscopic experiment*

TUM

Thermodynamic data on the actinide humate complexation are generated on purified, well characterized humic and fulvic acids. Their applicability for geochemical modeling of natural aquatic systems can be limited by changes of humic acid complexation properties due to the isolation process and purification by acid, base and fluoride treatment. For this reason, TUM has investigated the complexation of Am^{3+} with humic acid from the Gorleben groundwater Gohy-573 in its natural and purified forms at pH 6.0 in 0.1 M $NaClO_4$.

Natural humic acid is isolated from the groundwater by ultracentrifugation at 600.000 g. A portion of this natural humic acid is purified according to the standard procedure of the COCO-group [4]. The original groundwater and both isolated humic acids are characterized for their inorganic impurities and IR-spectroscopic properties.

The complexation study with Am^{3+} is conducted with humic acid concentrations between 2.5×10^{-5} mol/L and 3.8×10^{-5} mol/L ([HA(III)]). The Am^{3+} concentration is varied to give Am^{3+} to HA(III) concentration ratios between approximately 0.1 and 2.0. Using the excess Am^{3+} concentration, the loading capacity of humic acid is evaluated. The loading capacities and the complexation constants do not differ from one another and agree well with previous results on the site specific COCO-group standard humic acid from the same groundwater (Gohy-573(HA)) (Table 3) [13]. The mean value of the Am^{3+} complexation constants with natural and purified humic acid is found to be:

$$\log\beta = 6.26 \pm 0.05$$

The results show that purification of humic acid has no significant influence on its complexation behavior with Am^{3+} and thus thermodynamic data from studies on purified humic acid can be applied readily for natural systems.

CEA-FAR/SAC

Speciation calculations using the evaluated stability constants for NpO_2^+, UO_2^{2+}, and Am^{3+} with humic acid are conducted. The calculations ignore the formation of polynuclear and mixed species and competition from competing cations. The ionic strength is assumed to be 0.1 M, and the humic acid concentration is determined from the complexation capacity. The calculations are made for two natural conditions; granitic and sedimentary. The granitic conditions are mine waters (low pH, high CO_2 partial pressure) and evolved granitic waters (high pH, low CO_2 partial pressure). The sedimentary conditions are Boom clay interstitial

water (bicarbonate, slightly alkaline) and a number of different conditions inherent to Gorleben. The calculations predict only the trivalent actinides are greatly effected by humic acid complexation, while Np and U are dominated by carbonate speciation. However, the inclusion of mixed complexes alters theses results.

---

[1]. Moulin, C., Decambox, P., Mauchien, Moulin, V and Theyssier, M.: On the Use of Laser-Induced Time-Resolved Spectrofluorometry for Interaction Studies Between Organic Matter and Actinides: Application to Curium, Radiochim. Acta, **52/53**, 119-25, (1991).

[2]. Ruster, W., Ames, F., Kluge, H.-J., Otten, E.-W., Rehklau, D., Scheerer, F., Herrmann, G., Muehlbeck, C., Riegel, J., Rimke, H., Sattelberger, P. and Trautmann, N.: A Resonance Ionization Mass Spectrometer as an Analytical Instrument for Trace Analysis, Nucl. Instr. Meth. Phys. Res., **A281**, 547, (1989).

[3]. Maes, A., De Brabandere, J. and Cremers, A.: A modified Schubert Method for the Measurement of the Stability of Europium Complexation in Alkaline Conditions, Radiochim. Acta, **44/45**, 51-7 (1988).

[4]. Maes, A., De Brabandere, J. and Cremers, A.: Complexation of Europium(3+) and Americium(3+) with Humic Substances, Radiochim. Acta, **52/53**, 41-7 (1991).

[5]. Buckau, G., Kim, J.I., Klenze, R., Rhee, D.S. and Wimmer, H.: A Comparative Study of the Fulvate Complexation of Trivalent Transuranium Ions, Radiochim. Acta, **57**, 105-111 (1992).

[6]. Kim, J.I., Rhee, D.S. and Buckau, G.: Complexation of Am(III) with Humic Acids of different Origin, Radiochim. Acta, **52/53**, 49-55 (1991).

[7]. Kim, J.I., Wimmer, H. and Klenze, R.: A Study of Curium(III) Humate Complexation by Time Resolved Laser Fluorescence Spectroscopy, Radiochim. Acta, **54**(1), 35-41 (1991).

[8]. Kim, J.I., Buckau, G., Bryant, E. and Klenze, R.: Complexation of Americium(III) with Humic Acid, Radiochim. Acta, **48**, 135-43 (1989).

[9]. Kim, J.I. and Sekine, T.: Complexation of Neptunium(V) with Humic Acid, Radiochim. Acta, **55**, 187-192, (1991).

[10]. Moulin, V., Tits, J., Moulin, C., Decambox, P., Mauchien, P. and de Ruty, O.: Complexation Behavior of Humic Substances Towards Actinides and Lanthanides Studied by Time-Resolved Laser Induced Spectrofluorometry. Radiochim. Acta. **58/59**, 121 (1992).

[11]. Bidoglio, G., Omenetto, N. and Robouch, P.: Kinetic Studies of Lanthanide Interactions with Humic Substances by Time Resolved Laser Fluorescence, Radiochim. Acta, **52/53**, 57-63, (1991).

[12]. Bidoglio, G., Grenthe, I., Qi, P., Robouch, P. and Omenetto, N.: Complexation of Eu and Tb with Fulvic Acids as studied by Time Resolved Laser Fluorescence, Talanta, **38(9)**, 999-1008, (1991).

[13]. Kim, J.I., Rhee, D.S. and Buckau, G.: The Complexation of Trivalent Actinide Ions with Humic and Fulvic Acids, Submitted to Radiochim. Acta.

Title	Colloid migration in groundwaters : geochemical interactions of radionuclides with natural colloids
Contractors	TUM - Institut für Radiochemie (D); AEA (UK); GSF (D); WS Atkins (UK)
Contract N°	FI2W-CT91-0084
Duration of contract	May 1991 - April 1994
Period covered	January 1994 - April 1994
Project leader	J.I. Kim, P. Zeh (TUM, coordinators)

A. OBJECTIVES AND SCOPE

The aim of the joint research programme is to determine the significance of groundwater colloids in far field radionuclide migration. The characterization, quantification and theoretical interpretation of colloid-borne transport phenomena of radionuclides in selected Gorleben aquifer systems are the main objectives of the present research programme. Gorleben aquifer systems are chosen because they are well characterized in terms of their hydrological and geological properties and because they contain substantial amounts of colloids of different chemical compositions as well as considerable quantities of chemical homologues and natural analogues of radionuclides, e.g. M(III), M(IV), M(VI), and Th and U decay series. The research tasks are investigated jointly by the four laboratories (listed below) in close coordination of experimental capacities of each laboratory.

TUM: Technische Universität München, F.R.G. (coordinator: J.I. Kim, P. Zeh)
AEA: AEA Technology, Harwell, U.K. (M. Ivanovich)
GSF: Forschungszentrum für Umwelt und Gesundheit GmbH, München, F.R.G. (P. Fritz)
Atkins: W.S. Atkins Engineering Sciences, London, U.K. (D. Read)

B. WORK PROGRAMME

1 Sampling of groundwaters, colloids and sediments under well controlled (TUM, AEA)

2 Characterization of colloids, groundwaters and sediments (TUM, AEA, GSF)

3 Generation of pseudocolloids of radionuclides ($Z \geq 3^+$): Am(Eu) for M(III), Th for M(IV), Np for M(V), U for M(VI); (TUM)

4 Transport process study by scaled column experiments (TUM, GSF)

5 Synthesis and theoretical interpretation (Atkins ES)

C. PROGRESS OF WORK AND OBTAINED RESULTS

State of advancement

For the project study, groundwater samples and sediments were collected from four boreholes that penetrate the geologically and chemically heterogeneous Gorleben aquifers. The sampled groundwaters were submitted to parallel ultrafiltration using filters of different pore sizes to estimate the size and quantity of natural colloids present. Groundwaters, colloids and sediments have been characterized for their chemical composition and physical properties. The actinide ions of M(III), M(IV) and M(VI) are found to be strongly sorbed on the aquatic colloids rich in humic substances (termed humic colloids). Sorption preferentially occurs on humic colloids with a size range between 100 nm down to about 1 nm. The sorption and desorption of the actinide ions onto and from the aquatic humic colloids is reversible with respect to the pH variation.

The results from the column experiments with trivalent ^{152}Eu and ^{241}Am and tetra/ pentavalent $^{237}Np/^{233}Pa$ indicate that in groundwater rich in humic colloids a substantial part of injected lanthanide and actinide ions appears mobile through generation of actinide pseudocolloids. The recovery of the injected lanthanide and actinide ion concentration is > 63 %, while being dependent on the groundwater flow velocity through the column. The retardation factor of the mobile portion of lanthanide and actinide ions is close to 1, indicating that the migration of the mobile lanthanide and actinide ions through the column is comparable to that of ^{3}HHO and $^{82}Br^{-}$. This may be explained by the fact that the lanthanide and actinide ions introduced in the groundwater are stabilized through sorption onto humic colloids, which migrate through the sediment column with negligible interaction. The migration behaviour ofhumic colloids through the column may be explained by size exclusion as well as anion repulsion.

Progress and results

1 Sampling of groundwaters, colloids and sediments

Groundwater and colloids were collected anaerobically (N_2 + 1% CO_2) from selected aquifer systems from the geological site foreseen for the future German nuclear waste repository at Gorleben [1]. Sediments were collected from drill cores, corresponding to sampled boreholes. The sampling procedure is explained in detail in the previous progress report [2].

2 Characterization of groundwaters, colloids and sediments

2.1 Experimental techniques

Analytical methods and laboratory techniques employed for the characterization of groundwaters, colloids and sediments are described in the progress report [2].

2.2 Chemical composition of groundwater and colloids

The physical characteristics, partly measured in the field, and the chemical compositions of groundwaters Gohy 572, Gohy 611, Gohy 573 and Gohy 2227 are found to be different according to their different aquifer conditions [1]. The salinity, given as an electrical conductivity ($\mu S\ cm^{-1}$), generally increases with the aquifer depth and, as expected, the highest salinity among the four groundwaters is found in the one (Gohy 2227) nearest to the salt dome surface. High DOC concentrations are found in Gohy 573 and Gohy 2227. These boreholes are intersecting stratigraphic intercalations of lignite within the sampled aquifers. In the investigated groundwaters no correlation between the salinity and DOC concentration is observed. DOC in the groundwaters, separated and characterized according to a known procedure [3], is observed as a composite of humic and fulvic acids which are loaded with various metal ions and behave as colloids. For this reason they are named "humic colloids". Ultrafiltration of the four groundwaters Gohy 572, Gohy 573, Gohy 611 and Gohy 2227 using a flat bed filter system with a variety of nominal filter pore sizes from 1000 nm down to about 1 nm is carried out at TUM. Analytical results of filtrates are given in the 3rd progress report [2]. Concentrations of DOC in the filtrates show a gradual decrease with decreasing the pore size of filters. At the smallest pore size of about 1 nm, between 91.2% (Gohy 2227) and 95.7% (Gohy 573) of DOC are filtered, whereas the measured values for DOC in the filtrates at 1000 nm, 450 nm and 100 nm are almost identical. From these data and according to the results obtained from the earlier work [1, 4], it is apparent that the predominant amount of humic colloids is found in the size range less than 100 nm down to about 1 nm. It is known from the earlier work [1, 4] that trace elements of higher oxidation state are, in general, preferentially associated with humic colloids. Between 87.9% - 99.6% of REE and other trace elements (Th, U, Hf, Zr) in the groundwaters Gohy 573 and Gohy 2227 are filtered at the smallest pore size of about 1 nm, suggesting that these trace elements are associated almost quantitatively with humic colloids. This is supported by U/Th studies carried out at AEA Harwell.

Colloids fractionated by ultrafiltration at different pore sizes from 400 nm down to about 1 nm are analysed by neutron activation analysis (NAA) at TUM and the analytical values are given in the 3rd progress report [2]. The divalent metal ions, Ca, Sr and Ba, are associated with humic colloids in a portion between 6% and 60%. The mole fraction of the divalent ions loaded on humic colloids changes from groundwater to groundwater, depending on their total concentration and the amount of DOC [3]. The trace metal ions of higher oxidation state ($\geq 3+$) are strongly associated with humic colloids. In groundwater Gohy 2227 the filtration at about 1 nm pore size shows an average (92.9 ± 11.5)% of these ions being bound on thus filtered colloids. Trace ions associated with humic colloids are the trivalent rare earth elements (REE; 94.4 ± 9.2)%, tetravalent Zr, Hf, Th (98.2 ± 14.5)%, pentavalent Ta (87.7 %) and hexavalent U (73.7%). The trivalent Fe follows the same tendency. In Gorleben groundwaters with a relatively large amount of humic substances, generally more than 80% of polyvalent metal ions ($Z \geq 3+$) are sorbed on colloids collected on the 1 nm filter [1, 3, 4].

2.3 Chemical and mineralogical compositions of sediments

The chemical compositions of the sediment samples from drill cores taken from the boreholes Gohy 573, Gohy 611 and Gohy 2227 show marked differences in concentrations of SiO_2, Al_2O_3, Fe_2O_3 and K_2O, which are the main components of quartz, feldspar and clay minerals. The lowermost lignite found in the borehole Gohy 573 is overlaid by relatively pure quartz-sand, whereas the lignite in the borehole Gohy 2227 is covered by sediments with a higher portion of clay (marl). In the case of the borehole Gohy 573, concentrations of lanthanides and other metal ions in the lignite are ten times higher than those of the quartz-sand. This is not the case for the borehole Gohy 2227, where the lanthanides and other elements are equally distributed between lignite and overlying sand and marl. Differences might be accounted for the different sorption behaviour of the overlying sediments owing to varying clay content. Another reason could be different sources for the lignites found in drill cores of the two boreholes Gohy 573 and Gohy 2227. The high concentrations of humic colloids in the groundwater samples Gohy 573 and Gohy 2227 are probably related to the glacial lignite intercalations.

2.4 Study of U/Th-decay series disequilibrium

A comprehensive background to radioactive decay series and the concept of radioactive disequilibrium as well as a synthesis of Gorleben U series data is given by AEA in the fifth progress report [2a].

Surface characterization of some drill core samples from boreholes Gohy 573 and Gohy 2227 have indicated that solid/solution exchange processes are taking place [2]. However, the U series disequilibrium data obtained to date by AEA are ambiguous in terms of the humic colloid provenance and the source of their natural actinide loads. Thus, for example, total sand samples $^{234}U/^{238}U$ activity ratios are all close to unity indicating little exchange with groundwaters; the lignite total sample, on the other hand, indicate U uptake. The solid phase distributions of U and Th indicate significant components of total U and Th residing in the original phase of the lignite samples in contrast to sand samples where the residual mineral phases contain most U and Th. From the U/Th isotope ratios found in the surface phases of the solids it has been inferred that active radionuclide exchange is taking place in these aquifers. The question of colloid provenance and the origin of the colloid borne actinides in the Gorleben aquifer has been adressed through the U series disequilibrium data. Although the conclusions are somewhat ambiguous, it is possible that the humic colloids present in groundwater Gohy 573 and Gohy 2227 have different isotopic histories and possibly different sources, other than local lignite [2].

3 Generation of pseudocolloids of radionuclides

Actinide ions with a variety of oxidation states (≥3+) are in general unstable in groundwater at neutral pH, besides a dioxoactinyl ion of pentavalent state [5], because of their strong tendency towards the hydrolysis reaction [6]. For this reason, they are easily sorbed on aquatic colloids through either complexation or ion exchange reaction [7, 8]. The

generation of such colloids, termed actinide "pseudocolloids", may lead to an apparent solubility of a given actinide being much higher than its thermodynamically available solubility [9]. For this reason, the generation of actinide pseudocolloids may facilitate the migration, or eventually the retardation, of these elements in a given aquifer system. Task 3 of the present study adresses the mechanisms that may lead to the generation of actinide pseudocolloids in the selected groundwaters. The main intention is to investigate how actinide pseudocolloids are generated in groundwaters rich in humic substances. The generation mechanisms of actinide pseudocolloids by sorption of actinide ions on groundwater colloids is studied at TUM with actinide ions of three important oxidation states (trivalent, tetravalent and pentavalent) [2]. Results of sorption/desorption experiments carried out so far with the trivalent ^{241}Am and ^{244}Cm and the tetravalent $^{232/234}Th$ in humic substance rich groundwaters from the Gorleben aquifers are reported in detail in the 3rd progress report of the present research programme [2]. The $^{241}Am^{3+}$, $^{244}Cm^{3+}$ and the $^{234}Th^{4+}$ ions introduced in the original groundwaters are found to be sorbed quantitatively on humic colloids. The sorption and desorption behaviour is depending on the pH.

4 Transport process in the column experiment

The aquatic transport of lanthanide and actinide ions through a sediment matrix may be retarded by various sorption reactions such as ion exchange, matrix diffusion and diffusion into micropores of the sediment [10]. Knowledge of the retardation factor and the total recovery of an injected tracer ion enables the assessment and quantitative description of its migration behaviour through a sediment-groundwater column. The column experiment is performed for ^{152}Eu (at GSF), ^{241}Am, ^{237}Np and ^{233}Pa, ^{234}Th, ^{238}Pu and ^{233}U (at TUM) in the presence of natural humic colloids. Data obtained from the column experiment are used to test either an organic complexation model and a coupled chemical transport model developed in this study [11] which may assist in predicting retardation or mobility of colloid bound lanthanide and actinide ions in aquifer systems rich in humic substances.

Hydraulic properties

Prior to the migration experiment with the lanthanide or actinide ions under investigation, the hydraulic properties of each column are characterized carefully and stable experimental conditions are maintained. The effective porosities determined by nine different experiments at both TUM and GSF [2,11] appear consistent. The mean value is found to be $n_{eff} = 0.330 \pm 0.014$.

Trivalent ions: ^{152}Eu

The breakthrough characteristics of the trivalent ^{152}Eu ion are determined at GSF and allow the assessment of the migration behaviour of trivalent actinide ions, since the europium ion can be regarded as a chemical homologe to trivalent actinide ions. The Eu tracer introduced in the groundwater (5×10^{-5} mol L^{-1}) is quantitatively sorbed on humic colloids and 70% of the ^{152}Eu concentration injected into the column is recovered. The ^{152}Eu is eluted from the column at a retardation factor of $R_f = 1.0$, indicating that 70% of

the injected ^{152}Eu concentration is transported without sorption, at the same flow rate as $^{82}Br^-$ [2, 11].

The Eu tracer experiment is continued at different flow velocities in order to examine the influence of the groundwater flow rate on the Eu migration behaviour. The filtration velocities (Table 1) are adjusted closely to or higher than groundwater velocities observed in Gorleben aquifer systems, between < 1 m a^{-1} and 48 m a^{-1} [12].

Table 1: ^{152}Eu tracer experiments at different filtration velocities

Column	Flow velocity v_f (cm s^{-1})	Flow velocity v_f (m a^{-1})	Recovery W (%)	Retardation factor R_f
EG 1-25	5.2×10^{-5}	16.4	64	0.90
EG 1-24	2.1×10^{-4}	66.2	71	0.98
EG 1-27	1.2×10^{-3}	378	92	1.02

The sorption parameters (retardation factor and recovery rate) determined for individual experiments are listed in Table 1. At the lowest flow rate of $v_f = 5.2 \times 10^{-5}$ cm s^{-1} (corresponding to 16 m a^{-1}) only 64.3 % of the injected ^{152}Eu concentration is found in eluates and the rest 35.7 % remains sorbed on the column. At a rather high velocity of $v_f = 1.2 \times 10^{-3}$ cm s^{-1} (corresponding to 378 m a^{-1}), 91.6% Eu is recovered. The fact suggests that the flow rate of groundwater has a direct influence on the recovery of a colloid borne tracer ion migrating through the column, which implies that the interactive equilibria of the Eu^{3+} between colloids and sediment are kinetically controlled in the system. The retardation factors for the mobile portion of ^{152}Eu tracer at different v_f, however, are almost identical (0.90, 0.98, 1.02). The colloid size distribution determined by ultrafiltration of the ^{152}Eu traced groundwater remains the same both in the injected water and in the eluate, in the size range between 2 nm and 100 nm in diameter, indicating little interaction of the colloids with the Pleistocene sand.

Trivalent ions: ^{241}Am

Am in the groundwater is quantitatively sorbed on humic colloids [2, 4]. The humic acid concentration in groundwater, estimated on the basis of proton exchangeable functional groups [13, 14] is approximatly 7.8×10^{-4} eq L^{-1} and the CO_3^{2-} concentration under 1 % CO_2 partial pressure at pH 7.6 is calculated to be 6.6×10^{-5} mol L^{-1}. The first complexation constants of Am(III) with the ligand anions: OH^-, CO_3^{2-} and humic acid are known to be log β = 6.3 [15], 6.22 [16] and 6.44 [17], respectively. A combination of both sets of data suggests that the predominant species in the groundwater at pH 7.6 would be the Am(III) humate or mixed ligand complexes.

In the column experiment carried out with a Am concentration of 8.7×10^{-6} mol L^{-1} 79.2 % Am injected at a flow velocity $v_f = 2.4 \times 10^{-4}$ cm s^{-1} passes through the column at a velocity similar to that of the ideal tracer (R_f = 1.12). The result suggests that the

Am^{3+} ion is stabilized by sorption onto humic colloids which suppress its interaction with the column sand. At a lower Am concentration (1.8×10^{-6} mol L^{-1}) nearly the same result is obtained with a retardation factor $R_f = 1.02$ and 67.6 % recovery. The size distribution of Am pseudocolloids is determined in the input groundwater as well as in different eluate fractions. Almost no change in size distribution of Am pseudocolloids occurs during their passage through the column. The Am pseudocolloids are found predominately in the size smaller than 200 nm.

After migration experiments the column is cut into slices (thickness = 1 cm) to attain information about the distribution of the sediment-bound Am. The Am concentration is analysed by γ-counting. The highest activity is found in the upper 6 cm of the column corresponding to approximately 50 % of the retained Am. The retardation factor calculated for 50 % of the total sorbed Am is $R_f = 3000$, indicating low mobility of the sorbed Am.

Tetravalent ions: ^{238}Pu

The column experiment (Fig. 1) carried out at TUM shows the retardation for the mobile portion of Pu with $R_f = 0.97 \pm 0.13$. This retardation indicates that the mobile Pu species migrates similar to the non-sorbing $^{82}Br^-$-tracer and the mobile Am-, Np-, Pa- and U-pseudocolloids. The total recovery of Pu is 63.7 % indicating that a large fraction of Pu is mobile. Ultrafiltration of Pu in the groundwater Gohy 2227 shows that the amount of Pu sorbed on colloids (> 1 nm) is 98.3 %. This amount is higher than the Pu recovery of 63.7 % indicating that Pu-colloids are partly sorbed on or filtered by the sediment.

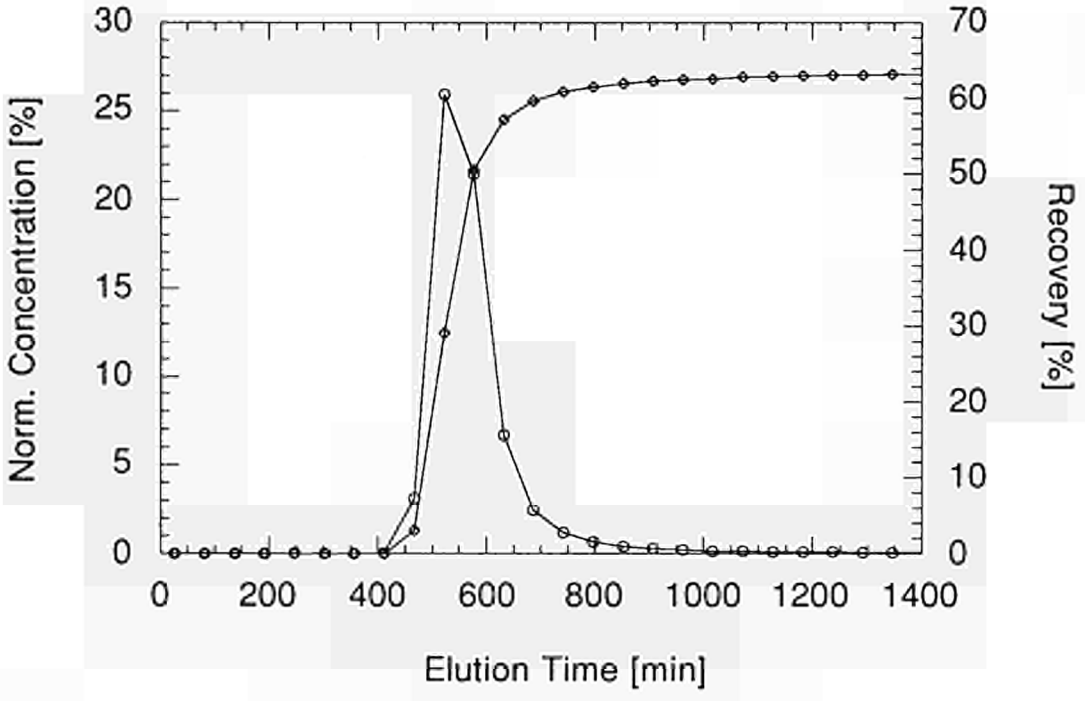

Figure 1: Pu column experiment: Breakthrough curve and recovery for $^{238}Pu(IV)$.

Tetra- and pentavalent ions: $^{237}Np/^{233}Pa$

The results of the migration experiment carried out at TUM with the pentavalent ^{237}Np ion indicate that a large portion of Np has undergone reduction to Np(IV) during equilibration with humic colloids. After an equilibration time of 20 days approximately 27% of Np in solution is still present in the pentavalent oxidation state as NpO_2^+, Np(V)-monocarbonate and Np(V)-humate. The remaining 73% found to be the tetravalent Np(IV). The neptunium reduction phenomenon is studied in detail elsewhere [18]. As expected, the tetravalent Np is strongly bound on humic colloids and its migration through the sand column is directly influenced by the mobility of humic colloids. The sorption of the NpO_2^+ ion on humic colloids, however, is shown to be negligibly small [19]. The recovery of Np in the column experiment at a flow velocity $v_f = 2.5 \times 10^{-4}$ cm s^{-1} is 63%, which is slightly lower than the values for Am and Eu. The retardation of the mobile Np is calculated to be $R_f = 0.94$. This indicates that the migration of the mobile portion is similar to that of $^{82}Br^-$.

The ^{237}Np tracer used in the migration experiment is in radioactive equilibrium with its daughter nuclide ^{233}Pa generated from α-decay. In the solution protactinium is present at a low concentration of about 6.9×10^{-12} mol L^{-1}. ^{233}Pa is found quantitatively sorbed on humic colloids. The breakthrough and recovery curves of Pa obtained from the column experiment show an almost quantitatively elution from the column. This is attributed to the stabilization of Pa in the groundwater by sorption on colloids which suppresses interaction of Pa with the sediment in the column. Contrary to Np no soluble ionic species of protactinium is formed which may interact with the sediment in the column. The retardation factor of the mobile Pa is calculated to be $R_f = 0.93$ which is almost similar to the value for Np ($R_f = 0.94$). Thus, Pa(V) passes the column in the same way as Np(IV) somewhat faster than $^{82}Br^-$.

Hexavalent ions: ^{233}U

The migration behavior of hexavalent uranium seems to distinguish from the other actinide ions. In the tracer solution, used for column experiments, a high portion of ionic species passes through the filter pore size of 1 nm. This may be explained by the fact that hexavalent uranium forms strong complexes with carbonate ions in solution. The total recovery of the injected U is rather low (9.4 %) compared to those found in the other experiments. One reason for the low recovery may be the high portion of ionic species in the U tracer solution, suggesting that ionic U species have greater interaction with the sediment and are sorbed on the sediment. The mobile U, eluted from the column is found quantitatively bound on colloids, predominantly in the size range between 1000 nm and 2 nm. This indicates that the uranium bound on humic colloids is mobile whereas the carbonate species are sorbed on the sediment. The retardation factor of $R_f = 1.10$ is observed for the mobile U, which is comparable to the values for Am, Np, Pa and Eu.

5 Synthesis and theoretical interpretation

The overall objective is to develop a model capable of simulating complexation between natural organics and heavy metals, in conjunction with transport in groundwater systems. In more detail, the aims and objectives included:

- development of a model capable of representing explicitly radionuclide uptake and transport;
- specification of data requirements and a protocol for the experimental programme;
- development of a stepwise modelling strategy for synthesis and theoretical interpretation of experimental data;
- assessment of predictive modelling capabilities from a preformance assessment (PA) perspective and development of an understanding of the conditions under which colloid mediation transport needs to be considered.

Two organic complexation models [20, 21] based on an electrostatic description of the humic surface have been selected for development. The Rigid Sphere and Surface models [20] have been enhanced and incorporated into the coupled chemical transport code, CHEMTARD [22] and an inorganic speciation code PHREEQE [23]. Although testing demonstated that incorporation was sucessfully achieved, the complexity of the system required that certain simplifying assumptions were made (e.g. local equilibrium conditions).

The highly complex nature of the column experiment involving transport and 3 different interacting phases (aqueous species, organic colloids and an inorganic rock matrix), demanded a stepwise modelling strategy to permit an understanding of the involved processes. This strategy involved:

- inorganic speciation modelling using PHREEQE in conjunction with the CHEMVAL thermodynamic database;
- speciation calculations in the presence of organics using a modified version of PHREEQE, including the Flat Surface model;
- sorption onto inorganic surfaces in the absence of organic colloids;
- chemical transport of radionuclides in the presence of organic colloids using the modified version of CHEMTARD.

The initial phase of inorganic speciation model was to identify which aqueous species were dominant under experimental conditions and hence should be concidered in sorption and organic complexation reactions. The second stage of the modelling programme, using the available binding constants, indicated that <98 % colloidal uptake would occur for all radionuclides, with the exception of uranium, prior to column injection. These results were consistent with the ultrafiltration results for Eu, Am, and Th column input solutions. For the third stage of the modelling programme (sorption onto the column matrix) the highly heterogeneous nature of the column material necessitated the assumption, that silica represents the dominant sorptive surface and that adsorption could be simulated adequately using a surface complexation model. To identify appropriate

adsorption data, exhaustive literature reviews were important. The final stage of the modelling programme involved applying the collated and derived data to model the physico-chemical transport processes using the modified version of CHEMTARD. Two different approaches were taken to modelling transport: the first approach assumed that radionuclide concentrations as aqueous species were negligible compared to the portions bound to the colloids and the column matrix. The second approach permitted complete re-equilibration at each calculation mode.

Adopting the first approach, colloid and matrix binding constants and site concentrations indicated 100 % sorption of Eu and Am to the colloids. On this basis, modelling adequatly reproduced experimental data in terms of recovery and breakthrough times. For all radionuclides, both modeling approaches gave a broader breakthrough peak and no tailing of the peak as observed in the experiment. This implies that colloids are less dispersed than calculated and the release of retained radionuclide (e.g. desorption) is slow with respect to experimental timescale.

In summary the column experiments in conjunction with modelling studies, have helped understanding of the role of colloids in actinide transport and have led to the identification of a number of outstanding uncertainties.

List of references

[1] Dearlove, J.P.L., Longworth, G., Ivanovich, M., Kim, J.I., Delakowitz, B., Zeh, P.: A Study of Groundwater-Colloids and their Geochemical Interaction with Natural Radionuclides in Gorleben Aquifer Systems, Radiochim. Acta **52/53**, 83 (1991)

[2] Kim, J.I., Delakowitz, B., Zeh, P., Probst, T., Lin, X., Ehrlicher, U., Schauer, C.: Colloid Migration in Groundwaters: Geochemical Interactions of Radionuclides with Natural Colloids, CEC-Contract FI2W/0084, 3rd Progress Report, Institut für Radiochemie, Technische Universiät München, RCM **00293** (February 1993).

[2a] Kim, J.I., Delakowitz, B., Zeh, P., Probst, T., Lin, X., Ehrlicher, U., Schauer, C.: Colloid Migration in Groundwaters: Geochemical Interactions of Radionuclides with Natural Colloids, CEC-Contract FI2W/0084, 5th Progress Report, Institut für Radiochemie, Technische Universiät München, RCM **00394** (February 1994).

[3] Buckau, G.: Komplexierung von Americium (III) mit Huminstoffen in natürlichen Grundwässern, Inaugural Dissertation, Freie Universität Berlin (1991).

[4] Kim, J.I., Zeh, P., Delakowitz, B.: Chemical Interactions of Actinide Ions with Groundwater Colloids in Gorleben Aquifer Systems, Radiochim. Acta **58/59**, 147-154 (1992).

[5] Neck, V., Kanellakopulos, B., Kim, J.I.: Solubility and Hydrolysis Behaviour of Neptunium (V), Radiochim. Acta **56**, 25 (1992).

[6] Kim, J.I.: Chemical Behaviour of Transuranic Elements in Natural Aquatic Systems, In: Handbook on the Physics and Chemistry of the Actinides, eds. A.I. Freeman and C. Keller, Elsevier Science Publ. B.V., 1986, Chap. 8.

[7] Moulin, V., Robouch, P., Vitorge, P., Allard, B.: Spectrophotometric Study of the Interaction between Americium (III) and Humic Materials, Inorg. Chim. Acta **140**, 303 (1987).

[8] Kim, J.I., Buckau, G., Rommel, H., Sohnius, B.: The Migration Behaviour of Transuranium Elements in Gorleben Aquifer Systems: Colloid Generation and Retention Process, Mat. Res. Soc. Symp. Proc. **127**, 849 (1989).

[9] Kim, J.I.: Actinide Colloid Generation in Groundwater, Radiochim. Acta **52/53**, 71 (1991).

[10] Klotz, D., Lang, H.: Experimentelle Untersuchungen zur Migration ausgewählter Radionuklide im Deckgebirge des Endlagerortes Gorleben, Untersuchungsprogramm IV. Teil III: Durchlaufsäulen-Versuche zur Bestimmung dynamischer Sorptionsdaten ausgewählter Radionuklide in Sedimenten aus den Schächten des Bergwerkes Gorleben. GSF-Bericht **20/92**, GSF-Forschungszentrum für Umwelt und Gesundheit, Neuherberg, 98 - 129 (1992).

[11] Kim, J.I., Delakowitz, B., Zeh, P., Probst, T., Lin, X., Ehrlicher, U., Schauer, C.: Colloid Migration in Groundwaters: Geochemical Interactions of Radionuclides with Natural Colloids, CEC-Contract FI2W/0084, 4th Progress Report, Institut für Radiochemie, Technische Universiät München, RCM **00793** (August 1993).

[12] Bundesamt für Strahlenschutz: Fortschreibung des Zusammenfassenden Zwischenberichtes über bisherige Ergebnisse der Standortuntersuchung Gorleben vom Mai 1983, **ET-2/90**, Bundesamt für Strahlenschutz, Fachbereich Nukleare Entsorgung und Transport, Salzgitter, 161 - 173 (1990).

[13] Kim, J. I., Buckau, G., Li, G. H., Duschner, H., Psarros, N.: Characterization of Humic and Fulvic Acids from Gorleben Groundwater, Fresenius, J. Anal. Chem. **338**, 245 (1990).

[14] Kim, J. I., Buckau, G., Klenze, R., Rhee, D. S., Wimmer, H.: Characterization and Complexation of Humic Acids, CEC-Report EUR **13181** EN, Brussels, 5 (1991).

[15] Stadler, S., Kim, J. I.: Hydrolysis Reactions of Am(III) and Am(IV), Radiochim. Acta **44/45**, 39 (1988).

[16] Meinrath, G., Kim, J. I.: The Carbonate Complexation of the Am(III) Ion, Radiochim. Acta **52/53**, 29 - 34 (1991).

[17] Kim, J. I., Rhee, D. S., Buckau, G.: Complexation of Am(III) with Humic Acids of Different Origin, Radiochim. Acta **52/53**, 49 - 55 (1991).

[18] Zeh, P., Kim, J. I.: Reduction of Neptunium(V) in Humic Rich Groundwaters, Radiochim Acta (in progress).

[19] Kim, J. I., Sekine, T.: Complexation of Np(V) with Humic Acid, Radiochim. Acta **55**, 187 (1991).

[20] Falck, W.E.: Two Modified Versions of the Speciation Code PHREEQE for Modelling Macromolecule-proton/cation Interaction. Br. Geol. Surv. Tech. Rep. **WE/89/57** (1989).

[21] Tipping, E., Hurley, M.A.: A Unifying Model of Cation Binding by Humic Substances. Geochem. Cosmochim. Acta **56**, 2627-3641 (1992).

[22] Bennett, D.G., Liew, S.K., Mawbey, C.M., Read, D.: CHEMTARD Version 3.0: Theoretical Overview. UK Dept. of Environment Report No. **DOE/HMIP/RR/92.036** (1992).

[23] Parkhurst, D.L., Thorstenson, D.C., Plummer, L.N.: PHREEQE - A Computer Program for Geochemical Calculations. US Geol. Surv., Water-Resources Investigations 80-96 (1985).

Title	The role of colloids in the migration of radioelements
Contractors	Risø National Laboratory, Denmark
Contract N°	FI2W-CT91-0085
Duration of contract	May 1991 - December 1994
Period covered	1 January 1994 - 31 December 1994
Project leader	B. Skytte Jensen

A. OBJECTIVES AND SCOPE

The objective of the present investigation is to quantify the behavior of colloids (humic acids) under varying chemical conditions. The aim is to derive thermodynamically based expressions, which may be used for modelling their interactions with pore-water constituents in natural systems.

B. WORK PROGRAMME

To collect useful information on humic acid behavior, which can support the present investigation.

To study and quantify flocculation processes, which are induced by the addition of polyvalent cations in competition with other ions present.

To follow the distribution of trace elements (R.E.) between flocculate and solution.

As a tentative model for the thermodynamic interpretation of the experimental data the humic acids will be modelled as finely dispersed ion-exchangers with a possible limited miscibility of surface phases.

C. PROGRESS OF WORK AND OBTAINED RESULTS

The experimental work, which has been presented previously, has resulted in a series of matrices containing data on concentrations of soluble humic acid, calcium, sodium, lanthanum, europium and erbium as well as pH and E4/E6 data obtained in experiments in which calcium chloride and sodium chloride were added in varying amounts.
The aim of the study is to identify mathematical expressions relating these data to the conditions imposed on the system, ultimatively to be able to derive equations useful for predictive modelling.

A priori the speciation of humic acid interacting with added salts is expected to be rather complicated both in the soluble and the flocculated state. Not alone the flocculate must be expected to possess ion-exchange properties, but because of their size, the soluble humic acids will also be expected to associate strongly with available cations in ion-exchange like reactions.

In addition to the experiments described previously, sets of investigations have been performed using a new stock-solution of humic acid, which seems to be more monodisperse, than the previously used sample.
In fig.1 are the results for residual humic acid in solution for the two stock-solutions compared.

Figure 1a,b

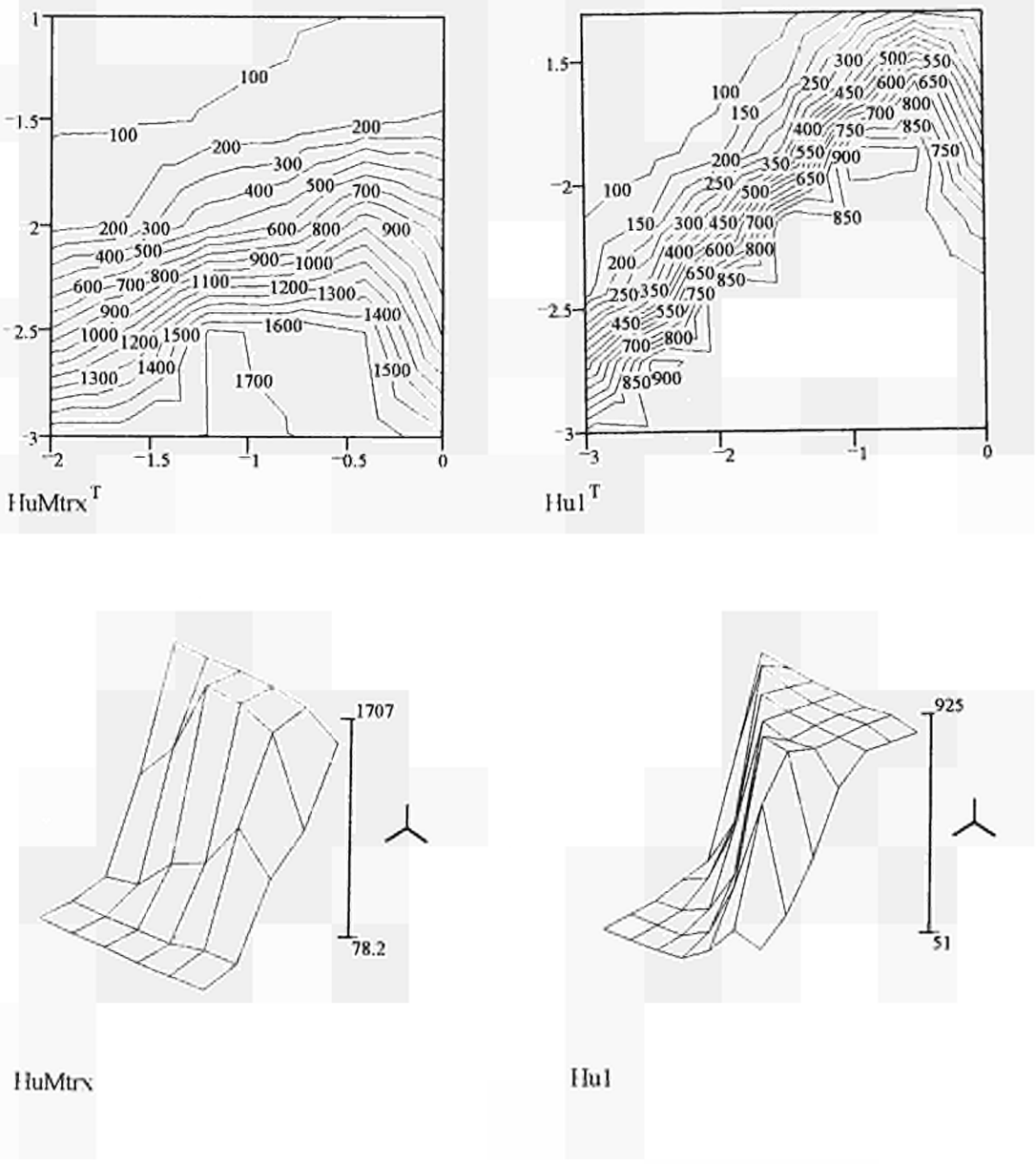

It is seen, that the two stock solutions result in similar although not identical patterns. However, if the E4/E6 ratios for the two samples are compared, the two stock-solutions show very different patterns indicating that the first sample is more polydisperse than the new sample. The consequences of this observation is discussed thoroughly in the final report.

The previously measured data for Rare-Earth behavior indicate that they are strongly adsorbed to humic acids both in solution and as flocculate. Instead of describing the binding of cations to soluble humic acid as complexformation a model involving ion-exchange to soluble species has been developed, which even allow for residual charges on the species. In this model adsorption is governed by selectivity constants, which deviate much from the complexity constants most often presented.

A standard procedure for identifying the stoichiometry of chemical reactions is to plot the logarithm of the concentration of one species against the logarithm of the concentration of a probable reactant. The limiting slopes at low concentrations will indicate the ratio between the number of moles of the reactant in the product to the monomer. In the case of the formation of a precipitate, which can be considered as an infinite polymer, the slope should be infinite at the onset of flocculation.

Figure 2a,b

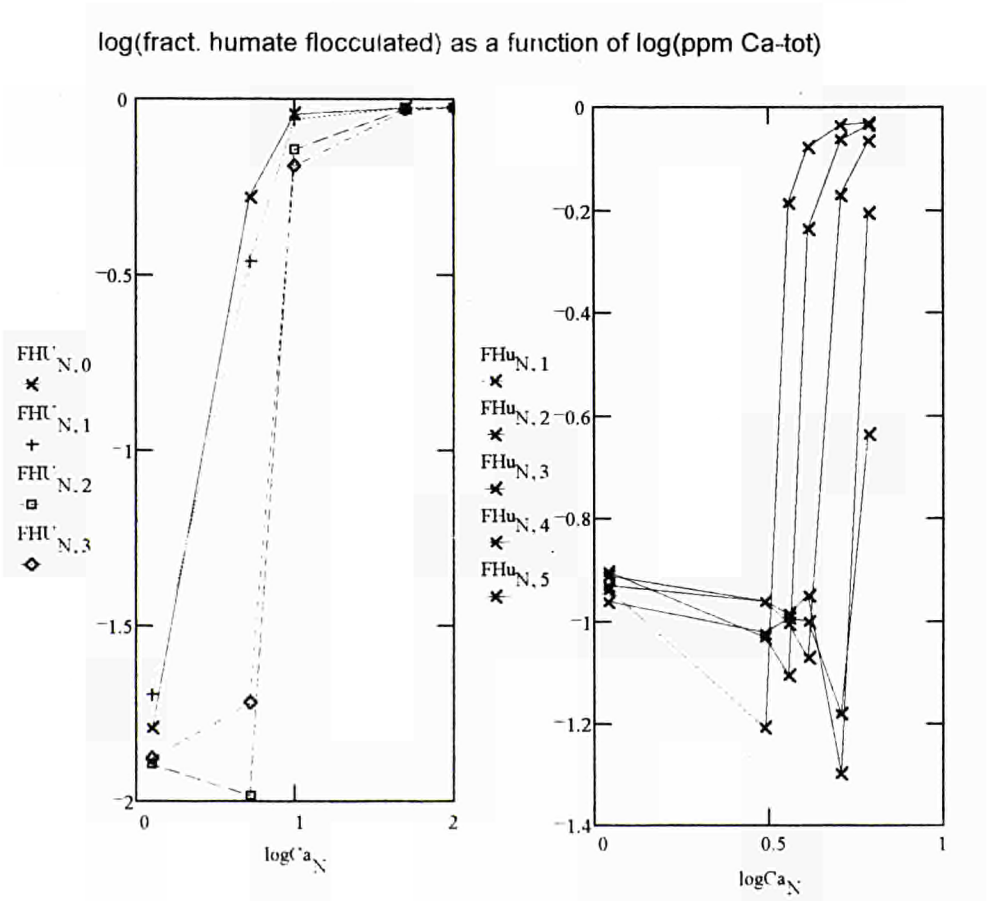

Numerous other logarithmic plots can be made demonstrating the competitive effects between sodium and calcium and the proton. They will not be shown here, but will be thoroughly discussed in the final report.

Finally a set of potentiometric titrations on a thoroughly prepared de-ionised humic acid were performed.

In these experiments titrations were performed on solutions containing different amounts of humic acids to disclose any polymerisation or de-polymerisation reactions and also under conditions, where the content of added sodium chloride were varied.

It will be shown in the final report, that a set of normalised titration curves obtained with varying concentrations of the "acid" will coincide if no polymerization or de-polymerization reactions occur. The display of several normalised titration curves made on the de-ionised humic acid in figure 3 demonstrate clearly that such reactions have to be taken into account, although it is not possible at present to decipher the data obtained.

Figure 3.

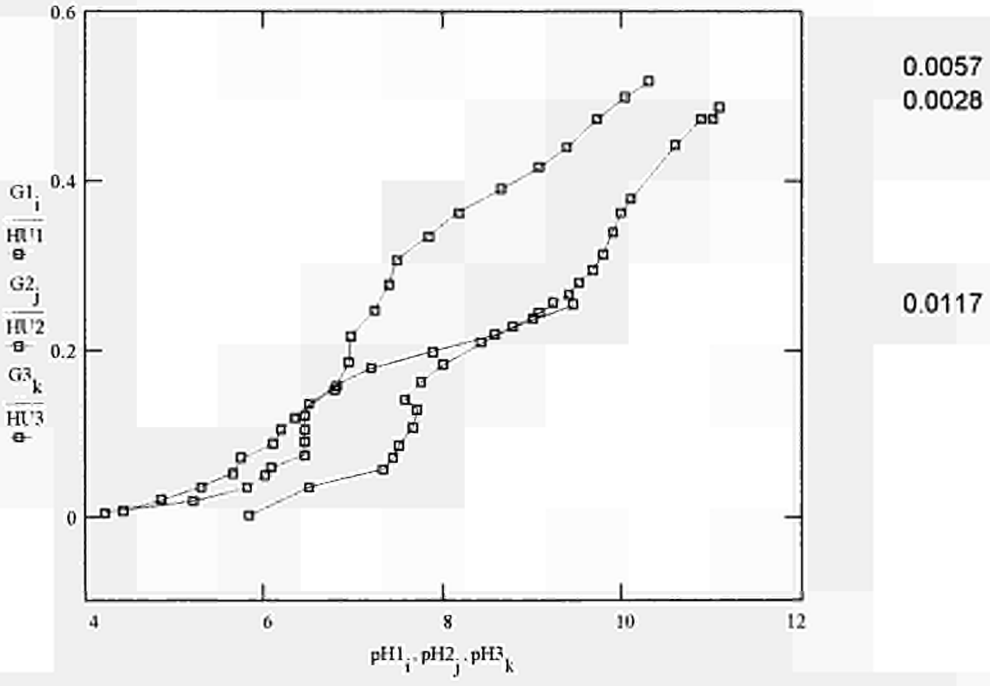

The three titration curves have been corrected for the auto protolysis of water. They have all been normalized by dividing with the amounts of humic acid being titrated, i.e. 2.8, 5.7, and 11.7 mg/10 ml.

CONCLUSIONS.

Although it is premature to elaborate on a model describing humic acid behavior, the observations made indicate, that it is governed by equilibrium reactions, and thus it should in principle be possible to do a purely thermodynamic modelling.

However, the humus system seems to be extremely complicated involving the possible formation of diverse micellar species, crosslinking by polyvalent cations and de-polymerisation by monovalent cations etc.

The main difficulty in such studies is probably, that samples of humic or fulvic acids being isolated for further study are born as mixtures of building blocks, which differ both with regard to their chemical structure and their size. Due to their amphiphilic nature they are prone to form ill-defined aggregates alone or accompagnied by impurities, which may be present.

Any modelling of humic acid behavior, which may be quite complicated even for a well-defined amphiphile, has to consider these complications at least qualitatively.

Humic acids have quite low exchange capacities, a number of 5 meqv. per gram could be typical. If it i assumed that each building block contains one exchanging site, the average moleweight would be 200. If the units are assumed to contain 10 exchanging groups, the average moleweight would be 2000 etc.

The titration curves presented in figure 3, do clearly indicate the presence of polymerisation and/or de-polymerisation reactions when humic acid is neutralised by base. The curves may perhaps be interpreted as due to the formation of diverse micellar structures as intermediates, but the possibility of very slow kinetics during some stages of neutralisation cannot be excluded either.

A computer model is being considered, which can solve equilibria, in which at least two micellar components are present simultaneously.

Title	**The role of colloids in the transport of radionuclides in geological media**
Contractors	CEA (F), CIEMAT (E), CNRS (F), GERMETRAD (F), GSF (D), INFM (I), INTERA (GB), NRI (CZ)
Contract N°	FI2W-CT91-0097
Duration of contract	October 1991 - December 1994
Period covered	January 1994 - December 1994
Project leader	V. Moulin, P.Rivas, J.C. Dran, J. Piéri, H. Lang, G. Della Mea, P. Grindrod, V. Balek

A. OBJECTIVES AND SCOPE

The main objective of this programme is to understand how colloids could influence the migration behaviour of radionuclides in geological formations. This is being achieved firstly, by identifying the *retention mechanisms* of colloids and pseudocolloids on mineral surfaces by static and dynamic experiments, and secondly by investigating the formation of pseudocolloids. These studies will provide an insight into retention mechanisms and there upon validate retardation parameters used in *transport models,* which will be developed to predict colloid transport under conditions relevant to geological disposals. Moreover, this research is focused on *model systems* (surfaces, colloids) selected from studies carried out on the El Berrocal site (Spain).

Two types of experiments are planned, depending on whether well-characterised colloidal solutions interact with mineral surfaces (as monoliths), allowing the solid-liquid phase analysis (batch tests), or powdered materials (batch and column tests). For the study of pseudocolloid formation, sorption experiments (batch tests) with radionuclides are conducted either with model inorganic colloidal suspensions or with mineral monoliths as macroscopic surfaces of colloids. Dynamic experiments are performed using well-defined packing of both synthetic and natural minerals (major constituents of granite, such as those found at "El Berrocal"). Moreover, a particular attention is devoted to the *organic coatings* (under static and dynamic conditions). These studies will provide data directly usable by migration models. These models are developed to predict colloid transport under conditions relevant to geological disposals.

B. WORK PROGRAMME

B.1. Colloid properties
B.1.1. Colloid characterisation
B.1.2. Application to a site
B.2. Sorption mechanisms
B.2.1. Pseudocolloid formation: association of radioelements with colloids
B.2.2. Interaction of colloids and pseudocolloids on mineral surfaces
B.3. Transport mechanisms
B.3.1. Transport experiments in model systems without organic coatings
B3.2. Transport experiments in model systems with organic coatings
B.4. Modelling

C. PROGRESS OF WORK AND RESULTS OBTAINED

State of advancement

The main emphasis of work in this period (Jan-Dec 94) has involved:

- the stability properties of natural colloids from El Berrocal groundwaters (more or less oxidised conditions) and artificial colloids generated from the fracture-filling materials and the barrier components (clayey suspensions);
- the interaction of actinides with colloidal suspensions through static experiments and radiochemical analysis (formation of pseudocolloids); the effect of humic substances has been particularly studied in the case of systems constituted by silica colloids and americium/uranium;
- the interaction of colloidal and pseudocolloidal suspensions with mineral surfaces through static experiments and ion beam analysis with a particular interest to the reversibility;
- the transport behaviour of radioelements and colloids within model porous media through column experiments; the influence of organic coatings has been specially investigated;
- the development of a theoretical model to account for the transport of colloids in geological media which will be validated by means of the present experimental data.

Progress and results

1. Colloid properties: Application to a site, "El Berrocal" (Spain) (CIEMAT, CEA)[1]

The stability of the colloids (natural, artificial) has been studied as a function of pH, ionic strength and Ca concentration by monitoring the size and the charge of the particles. A particular attention to the kinetics of aggregation has also been performed for each parameter. From these studies, it arises that:

- the natural waters and the clayey colloidal suspensions are instable in acidic pH,
- the natural colloids are very sensitive to the variation of ionic strength (from 0.001 to 0.1 M); in the case of the clayey suspensions and the clay barrier components there is a complete destabilisation at high ionic strength with a rapid kinetics;
- the variation of Ca concentration from 40 ppm to 400 ppm induces a rapid aggregation for the clayey suspensions.

The main conclusions obtained from these results refer that aggregation is mainly controlled by ionic strength.

2. Sorption mechanisms (CEA, CNRS, INFM, GSF, NRI)

The main aim of this working phase is to determine the retention mechanisms of colloids and pseudocolloids (association of radionuclides with colloids) on mineral surfaces which induces to study firstly the formation of pseudocolloids and secondly the interaction of model colloids (true, pseudo) with mineral surfaces. In this part, model systems are used for

- *the colloidal suspensions*: either representative of those identified in "El Berrocal" ground waters with respect to their composition, or representative of specific charges or sizes
- *the mineral surfaces*: representative of the constituents of the granitic geological barrier.

[1] This working task on the "El Berrocal site" leads to have strong interactions with another CEC contract "Matrix Rock Diffusion" (FI2W-CT91-0082) coordinated by Exeter University (Dr Heath).

Formation of peudocolloids [2] **(CEA, CNRS, GSF, INFM)**

Two complementary batch tests are performed within this task:

1) sorption experiments with fine particle suspensions and radionuclides or chemical analogues and use of radiochemical analysis of the liquid phase (CEA,GSF)
2) sorption experiments with mineral monoliths (considered as macroscopic surfaces of fine particles) and heavy elements and use of Rutherford Backscattering Spectrometry (RBS) for the analysis of the solid surface (CEA, CNRS, INFM).

This working period has been mainly devoted to the role of humic substances in the retention behaviour of cations (in particular Am(III)) on colloids. The uptake of Am(III) by silica colloids in the presence of humic and fulvic acids has been determined as a function of pH (3-9), ionic strength (0.001-0.1 M) and organic concentration (0-10 ppm). Under these conditions, humic substances are mainly in solution due to sursaturation, although some interactions occur with silica (mainly in the acidic pH range).

In the presence of humic acids, a complete decrease of Am sorption onto silica colloids is observed whatever the HA concentration, whereas *in the presence of fulvic acids*, no effect is observed at the lowest concentration (1 ppm), but at 10 ppm, a sorption delay occurs. At an ionic strength of 0.001 M (figure 2), a very low concentration of humic substances (humic or fulvic), namely 1 ppm, is enough to prevent the retention of Am(III) onto silica colloids. Up to pH 9, less than 20 % of americium is retained on the colloids whereas, above pH 9, humic acids are stronger complexing agents than fulvic acids to maintain Am(III) in solution.

For this system, a strong competition occurs between inorganic and organic colloids in favour of the organic ones, even in a large excess of inorganic colloids. It appears that humic substances prevent the formation of inorganic pseudocolloids (Am-silica colloids) due to the highly stable complexes formed between trivalent actinides and humic/fulvic acids. Under the conditions of natural waters (alkaline pH), in the presence of organic concentration representative of crystalline formations (1-10 mg/l) or sedimentary formations (several ten mg/l even hundred), trivalent actinides will be present as organic complexes (except with 1 ppm of fulvic acids at the highest ionic strength) in the presence of high concentrations of inorganic colloids such as silica.

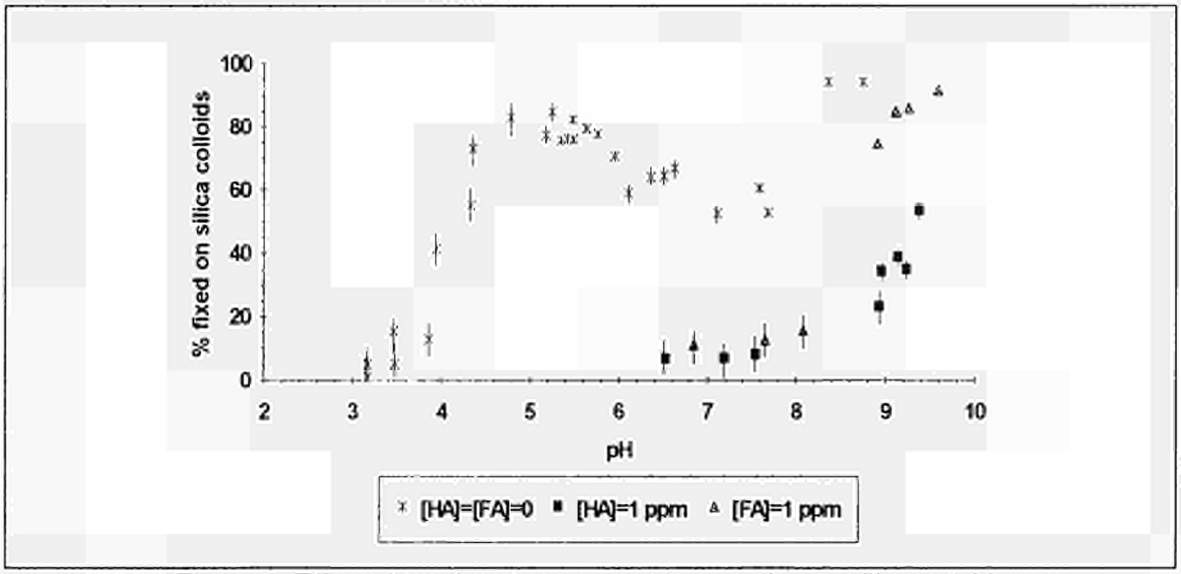

Figure 2. Effect of humic substances on Am sorption on silica colloids
$[SiO_2]$=100 ppm; $NaClO_4$ 0.001M

[2] In the framework of this working task, a collaboration with another CEC contract "Development of a model for radionuclide transport by colloids in geosphere" (FI2W-CT91-0079) coordinated by ARMINES (Dr Ledoux) becomes effective.

Interaction (retention) of colloids and pseudocolloids with mineral surfaces (CEA, CNRS,INFM, NRI)

The interaction of colloids (true or pseudo) with mineral surfaces (as monoliths) is studied by batch tests on model systems (colloids, monoliths, cations) by using Rutherford Backscattering Spectrometry (RBS) for the analysis of the surface. This technique allows to determine the quantity of the heavy element fixed (in atoms/cm^2) as well as the depth distribution.

For this working task, different items are studied:
- the influence of the characteristics of the components as the size and the charge of the colloids and the charge and the composition of mineral surfaces;
- the effect of addition order of the constituents (simultaneously or sequentially);
- the influence of physico-chemical parameters: pH, ionic strength;
- the reversibility (with respect to solution composition);

Different systems have been investigated such as i) binary systems (monolith, colloid) ii) ternary systems (monolith, colloid1, colloid2). The monoliths are either silicates (silica, albite, biotite, muscovite), oxides (hematite) or carbonates (calcite); the colloids either CeO_2 (50nm) and ThO_2 (5 nm) as model of true colloids (for radioelements), or Fe_2O_3 (hematite, 100nm), SiO_2 (80 nm) and humic substances as carrier colloids representative of those occurring in natural waters.

The main features obtained up to now are:

- colloid sorption is a surfical retention process with a very low surface coverage (less than one monolayer),
- colloid sorption is strongly dependent on the electrical charges of both constituents (monolith, colloid),
- colloid sorption is irreversible with respect to solution composition whatever the solution parameters (ionic strength, temperature, presence of a carrier colloid); the strong attachment of colloids for monoliths has also been confirmed by AFM (Atomic Force Microscopy) observations performed at AEA-Harwell (Dr M. Ivanovich, Dr C. Sofield) on silica monoliths covered by ceria colloids,
- silicate minerals present similarities towards colloid sorption and desorption,
- the role of the carrier colloid is different according to the order of the sequential addition of the reactants, in particular a decrease or an increase of retention,
- organic carrier colloids have the same behaviour as other negatively charged carrier colloids (such as silica colloids).

In the framework of the static experiments, a particular attention is devoted to the changes occurring on solid surfaces (colloid, monolith) during sorption processes through the use of the Radon Emanation Method (REM: labelling with ^{228}Th and measurement of release rate of radon) developed by the NRI (Nuclear Research Institute). This method permits to investigate rapid changes on the solids and at the interfaces and brings information on the retention dynamic (i.e. kinetics).It has been revealed through the use of this technqiue that morphology changes take place in the mineral surface layers. Results obtained contribute to a better understanding of the kinetics of the interaction between the mineral surfaces (glass beads, silica, mica) and colloids (hematite, ceria).

3. Transport mechanisms (GSF, GERMETRAD)

The main goals of this part is to determine the transport mechanisms of colloids as well as the role of colloids on the transport of radioelements through well defined materials (column experiments). For this purpose, flow-through column tests on model systems (with or without organic coatings) are carried out as a function of:
- the colloid characteristics (size, charge)
- the water chemistry (typical boundary conditions)
- the hydrodynamic factors (flow-rate).

Transport experiments in model systems in the absence of organic coatings (GSF)

These transport experiments are investigated to infer the colloid and pseudocolloid transport in porous media. They are carried out in small columns packed with stable monodisperse materials (either glass beads or quartz sand). In order to achieve the objectives, batch (determination of sorption and desorption coefficients) and column tests are performed in parallel in order to better understand the sorption and transport mechanisms of colloids (true or pseudo).

The main characteristics of these column packings (with different granulometries) have been determined, in particular their ion-exchange capacity, their surface area and their pore volume and pore size distribution (table 2). Before handling colloids and pseudocolloids, breakthrough curves of radionuclides (tracers such as ^{36}Cl; ions such as ^{85}Sr, ^{45}Ca, ^{22}Na; potential colloids such as ^{144}Ce, ^{152}Eu) have been obtained on these model columns with different mobile phases (NaCl 0.01 M, $CaCl_2$ 0.01 M, ammonium formate 0.01 M, synthetic "El Berrocal" water (borehole S1): pH 6.8; I=0.0012; cations: Ca,Mg,Na,K; anions: Cl,SO_4,HCO_3). In particular, through these flow-through column tests, the importance of isotope- and ion-exchange mechanisms has been quantified showing a very small contribution of the isotopic effects compared to the ionic exchange effects.

As the main properties of the colloidal systems are linked to their charge, the electrostatic surface charges of the colloids under investigation (ceria, silica, iron oxides) have to be determined. In addition, latex particles (fluorescent) are also used in order to stress important features. Streaming potential studies have thus been performed qualitatively and quantitatively using a special streaming current technique. Under the conditions of the synthetic groundwater, negatively charged colloids are occurring for silica and latex particles, whereas ceria colloids are found to be positively charged.

This working period has mainly be devoted to the transport behaviour of colloids and radionucldies in the presnece of carrier colloids.

Transport behaviour of colloids

The importance of *filtration effect*s in colloid transport phenomena has been underlined by performing experiments with fluorescent latex spheres (negatively charged) which have shown that no retardation (or scarcely) occurs but a very low recovery of particles (27 % to 1 % according to their sizes) exists.

For silica and ceria colloids, the effect of ionic strength has also been investigated on glass bead columns. Silica colloids are transported in the column even faster that the non-sorbing reference tracer (Cl) with a complete recovery at the lowest ionic strength, whereas the ceria colloids are strongly retarded in the column with a very low recovery (1%) (figure 3). At a higher ionic strength (0.1 M), a strong retardation of silica and ceria colloids occur with a low recovery (2 and 1% respectively).

It arises from these studies that ionic strength appears as a parameter controlling both surface electrical charges (related to sorption processes) and colloid stability (related to filtration processes) inducing different transport behaviour of colloidal entities.

Transport behaviour of pseudocolloids

The transport behaviour of radionuclides either as ionic species (Eu, Ce) or as true colloids (CeO_2) has been studied in the presence of a carrier colloid (silica) at different ionic strengthes. At low ionic strength, ceria colloids are simultaneously eluted with silica colloids (with a low recovery for both) whereas in the absence of a carrier colloid, ceria colloids are strongly retarded in the column. For the radionuclides in the presence of the carrier colloid, there is an earlier or the same breakthrough than Cl at low and high ionic strength respectively, wheras in the absence of silica colloids, Eu and Ce are retarded in the column.

These different experiments underline the importance of *electrostatic interactions* during the transport in the column.

Transport experiments in model systems in the presence of organic coatings (GERMETRAD)

The effect of organic coatings (as immobilised humic acids) on the transport of radionuclides (in the ionic, colloidal or pseudocolloidal form) is evaluated through dynamic experiments performed with columns filled with silica beads covered with humic acids. A procedure has been developed in order to link the organic molecules (through covalent bonding) on the well-defined packing particles of silica. Hence stable "humic acid columns" are realised. The procedure followed in these dynamic experiments is illustrated on figure 3.

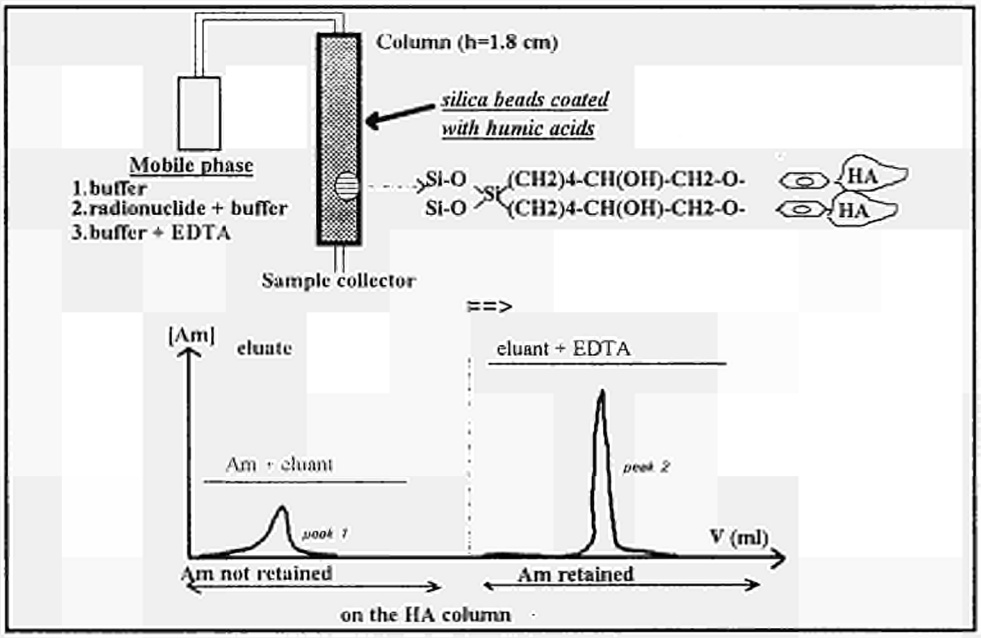

Figure 3: Schematic representation of the procedure followed in the dynamic experiment with organic coatings

This working period has mainly be devoted to the transport of colloids and pseudocolloids in the humic acid column as well as in a pure silica column in order to underline the effect of the immobilised humic acids.

Transport of colloids: CeO_2

The main features arising from the studies concerning the affinity of ceria colloids for the "humic acid" (HA)/pure silica columns at different pH and flow-rates are:

- the flow-rate has no effect on the ceria elution curves;

- the total amount of ceria fixed on the HA column increased with increasing the ceria concentration; the fraction of ceria eluted by EDTA (corresponding to the fraction retained) is always the same whatever the concentration; but there are in all cases a large fraction not eluted by EDTA corresponding to an "irreversible" fraction strongly fixed on the HA column;
- when decreasing pH (6 to 4), ceria colloids are more tightly bound to the HA column;
- ceria colloids are more strongly retained on the HA column compared to the pure silica column; the "irreversible" fraction exists in both cases;
- concerning the competition between a true colloid (ceria) and a radionuclide (Am), ceria colloids are more tightly bound to the HA column than Am.

Transport of pseudocolloids: Silica+Am(III)

The effect of pH (pH 6, 7, 8) and flow rate (from 4.5 ml/h to 27 ml/h) has been investigated on the transport of pseudocolloids (Am and silica colloids as carrier colloids). For each injection, the elution behaviour of silica and americium has been monitored. Both parameters (pH and flow-rate) have a great influence on the transport behaviour of Am present as a pseudocolloid as follows:

- at pH 6, the pseudocolloid injected on the column is dissociated (silica is eluted earlier than Am) and Am is not retained on the HA column: 80% of Am eluted whatever the flow-rate except at the lowest one where Am is fixed on the organic film; on the contrary, in the absence of silica carrier colloid and at the highest flow-rate, Am is completely retained on the HA column;
- at pH 7, americium is eluted at the same volume than the silica colloid with ~50% of recovery except at the lowest flow-rate where most of Am is retained on the HA column; moreover, silica colloids are recovered in a larger extent than at pH 6;
- at pH 8, americium and silica colloids are eluted at the same time with ~80% of recovery for both components whatever the flow-rate.

It arises from these experiments that kinetics and pH exerts a great influence on the stability and the transport behaviour of americium present as a pseudocolloid. The future work will consist in studying the transport behaviour of pseudocolloids (silica and Am) on a silica column in order to quantify the role of the organic coating and to compare all results with the elution behaviour of americium not associated with a carrier colloid.

4. Modelling (INTERA)

The modelling of colloid transport through fractured and porous media has been developed so as to provide:

- an initial review and discussion of theoretical and experimental issues from the transport modelling perspective;
- calculations of elution rates and dispersivities which could be generalised and calibrated by the experimental data;
- a consideration of the microscopic models useful in characterising dynamic processes prior to the derivation of microscopic migration parameters.

Using evidence from batch experiments (section C.2.), a model describing colloid-surface interaction has been proposed as an a alternative to one suggested by Ecole des Mines in which several assumptions are made: reversible capture, capture is instantaneous and the colloid density is required to be homogeneous in an arbitratry small δ-layer close to the surface.

Rather than the above heuristics, our alternative model has been based on asymptotics. The assumptions are: the uptake on the surface is diffusion-limited and on the time-scale of the experiment the sorption is irreversible. Thus a microscopic model for colloid transport through a single pore was produced using these assumptions and the unknown parameters were calibrated against results from batch experiments.

These ideas have been upscaled to form a macroscopic model for transport of colloids through a porous media where the adsorption is limited by the specific surface area and the

density of colloids already sorbed. This non-linear model was calibrated against a simple linear model (where sorption is unlimited and first order kinetics) and the two models were subsequently upscaled with respect to both concentration and length.

It has been found that some difficulty occurs in calibrating the models such that they agreed perfectly or small length scales and concentrations. However, it has been demonstrated that there could be large discrepancies between the two models if (keeping the other parameters fixed) if we increased one of these by a large factor.

This leads us to conclude that we must take great care when interpreting models based on "small" scale laboratory data and behaviour is sensitive to parameters which may be derived directly from batch experiments. Results produced by P. Warwick exhibit behaviour analogous to that produced by the simple linear model, giving no evidence for surface saturation. Our results suggest that this is due to the experimental set-up and that experiments must be performed on larger columns with a much slower flow ("real" world conditions) for acceptable conclusions to be made.

LIST OF PUBLICATIONS

Dran J.C., Della Mea G., Moulin V., Petit J.-C. and Rigato V. (1994) Interaction of pseudocolloids with mineral surfaces: the fate of the scavenged cation. Radiochimica Acta **66/67**, 221-227

Grindrod P., Edwards M., Higgo J. and Williams G. (1994) Analysis of colloid an tracer breakthrough curves. Fourth Intern. Conf. on the Chemistry and Migration Behaviour of Actinides and Fission Products in the Geosphere. Charleston, SC USA, December 12-17, p 797-802

Moulin V., Petit JC., Vilarem J.P., Casanova F., Dran J.C., Milcent M.C., Durand JP., Goudard F., Bioret A., Piéri J., Della Mea G., Lang H., Gomez P., Turrero M.J., Tejedor E., Rivas P., Grindrod P. (1994) The role of colloids in the transport of radionuclides in geological media. Fourth CEC semestrial report DESD 94.110 (March)

Moulin V., Labonne N., Vilarem J.P., Casanova F., Dran J.C., Pentecote S., Milcent M.C., Goudard F., Durand JP., Boulay C., Piéri J., Della Mea G., Rigato V., Lang H., Turrero M.J., Gomez P., Melon A.M., Adell A., Rivas P., Crompton S., Grindrod P., Balek V. (1994) The role of colloids in the transport of radionuclides in geological media. Fifth CEC semestrial report DESD 94.115 (August)

Turrero M.J., Gomez P., Perez del Villar L., Moulin V., Magonthier M.C. and Ménager M.T. (1995) *Relation between colloid composition and the environment of their formation: application to the El Berrocal site (Spain).* Applied Geochem. in press

Title	Analysis of the geo-environmental conditions as morphological evolution factors of the sand-clay series of the Tiberine Basin and the Dunarobba Forest preservation
Contractors	"La Sapienza" Univ., Rome, Italy, Perugia Univ., Italy, Exeter Univ.
Contract N°	FI2W-CT92-0121
Duration of contract	July 1992 - June 1995
Period covered	January 1994 - December 1994
Project leader	G. Valentini - S. Lombardi ("La Sapienza" Univ., coordinator); P. Ambrosetti (Perugia Univ. Coordinator); P. Grainger (Exeter Univ. Coordinator)

A. OBJECTIVES AND SCOPE

In the continental deposits within the Tiberine basin, very old (some My) vegetal remains often outcrop in different areas; in some stratigraphic levels they show the original characteristics, in other levels they have been transformed into lignite-like deposits.

The scope of this research is the definition of geological, hydrogeological and geochemical processes which allowed for the preservation of the unaltered wood from many tree trunks in the Dunarobba area, located near the village of Avigliano (Terni, central Italy).

B. WORK PROGRAMME

As outlined in the project proposal and in the previous reports the study is organised in three main fields.

a) reconstruction of the geological and structural setting of the sedimentary basin;

b) reconstruction of the hydrogeological setting and studies of the fluid phases (water and gas);

c) studies of the natural barriers in the Dunarobba Forest area.

In the first field, the geological and structural setting and the morphological evolution have been analysed. The data come from surface mapping in the south-western part of the Tiberine basin and from deep gravimetric, soil gas, geoelectrical and local geomechanical investigations.

Regarding the second field hydrogeological, geochemical and geophysical surveys have been carried out in order to understand the groundwater circulation and the water-rock interactions in the Dunarobba forest area. Furthermore, in order to assess the effectiveness of the Dunarobba sandy-clayey sequences (Fosso Bianco Unit) as a natural barrier to fluid migration, soil gas surveys and a gas injection test have been performed.

In the third field the spatial identification of the natural barriers limiting groundwater flow within the Dunarobba Forest area is dealt with. With particular regard to this point, detailed lithostratigraphic reconstructions and hydraulic conductivity investigations of the deposits surrounding the Dunarobba Forest are considered of great importance in relation to the diffusion of natural radionuclides. According to these goals, research on the solid phase of the clayey-sandy deposits was planned. Investigations using convergent geotechnical, mineralogical and geochemical methodologies have been performed. Further, analyses of the organic matter was conducted to qualify the preservation state of the Dunarobba Forest tree trunks.

C. PROGRESS OF WORK AND OBTAINED RESULTS

Referring to each research field, the new data acquired in the period January 1994 - December 1994 are synthesized.

C.1 Reconstruction of the geological and structural setting of the sedimentary basin

Geological and structural surveys

Based on geological surveys of the south-western branch of the Tiberine Basin, the setting of the geological formations has been established. A detailed map of the area around the

Dunarobba Forest is shown in fig. 1.

The deposits containing the tree trunks belong to the Fosso Bianco unit (lower - upper Pliocene). Local sedimentological analysis of the outcrops and drill cores from the Fossil Forest area indicates that the depositional environment was a swampy lacustrine coast. In particular silty clay, lignite and sand indicate: a) emerged swampy environments that underwent active pedogenesis and were characterized by a hydromorfic palaeosol; b) subemerged areas with stagnant or weakly aggitated waters which were prone to floods.

The assesment of the tectonic framework has been obtained by structural, gravimetric, soil gas and geoeletrical surveys. The fault system depicted in fig.1 is the comprehensive result of this work. The area is located in the northern sector along the axis of a complex horst (NW-SE strike) built by a twofold system of faults with strikes of N310-320 and N65-95. These fault systems characterize the Dunarobba area and produce a close net of discontinuities. The main surface discontinuites appear to correspond to the pre-Pliocene substratum faults delineated by gravimetric surveys. The minor surface discontinuites do not have the same correspondence.

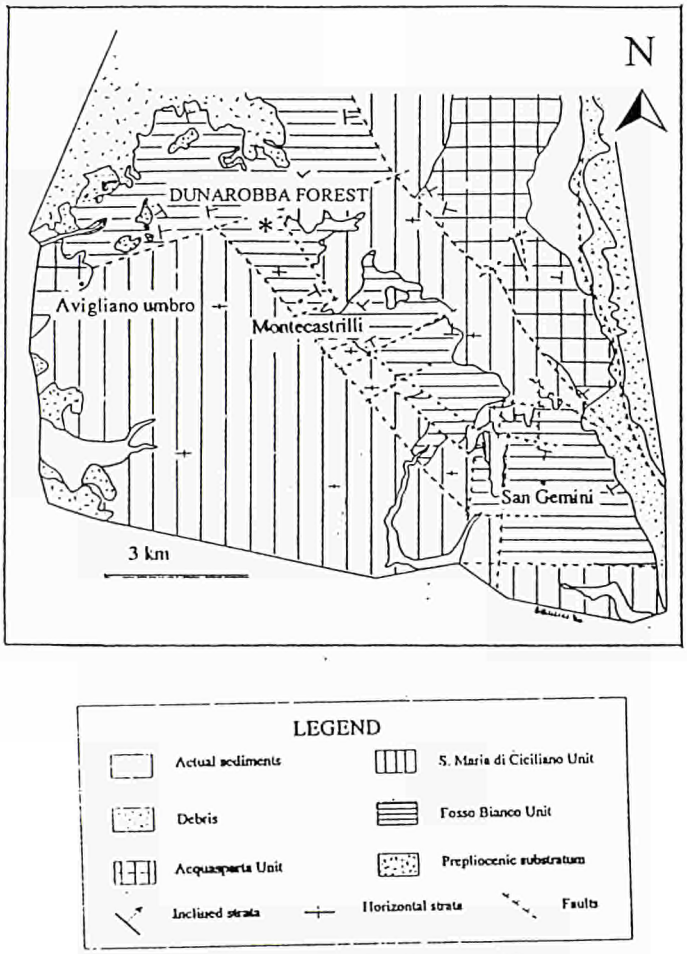

Fig. 1 - Geology of the Dunarobba area.

Based on geophysical investigations performed in the south-western branch of the Tiberine Basin and on subsurface drilling performed in a limited area (including the Dunarobba Forest), the three dimensional arrangement of the basin has been defined. This arrangement includes the depth to the calcareous substratum, the shape of the basin, margin trends and any substratum discontinuites. In the Dunarobba area, located near the western margin within a satellite-like basin, the thickness of the Pliocene clayey sequence is reduced (approximately 120 m) with respect to the central area where it exceeds 1000 m. The gravimetric surveys and

dipole - dipole geoelectric investigations confirm the horst structure recognized by geological surveys.

Soil gas detailed survey

In the summer of 1993 a regional soil-gas survey was carried out in the Medium Tiber valley to detect buried discontinuities that act as preferential routes for deep gases rising towards the surface (see previous reports). In the summer of 1994 a more detailed area of about 8 km^2, between the village of Dunarobba and Castel dell'Aquila, was selected and sampled. Soil-gas sampling was performed during a dry period, to minimize variations induced by climatic factors, with a grid density of 4 samples per square kilometer. Gas samples were analysed for CO_2, He and Rn, with the main statistics shown in the following table. Data whose values exceed the mean value plus 1/2 st. dev. are considered anomalous. For radon data the standard deviation exceeds the mean value, therefore it has been more appropriate to calculate these parameters without considering values above the 90th and below the 10th percentiles.

	Min.Val.	Max Val.	Mean	St. Dev.	Mean+1/2St. Dev.	N° Sampl.
CO2 (%)	0.02	14	2.12	2.09	3.16	200
Rn (Bq/l)	1.85	189.1	13	10	18	200
DHe (ppb)	-406	467	15	140	85	200

Tab. 1 - Soil-gas statistics.

The resulting distribution of these gases is shown in Fig.2 as contour lines obtained by using "kriging" interpolation method. The maps also show the main tectonic discontinuities reported in the figure 1.

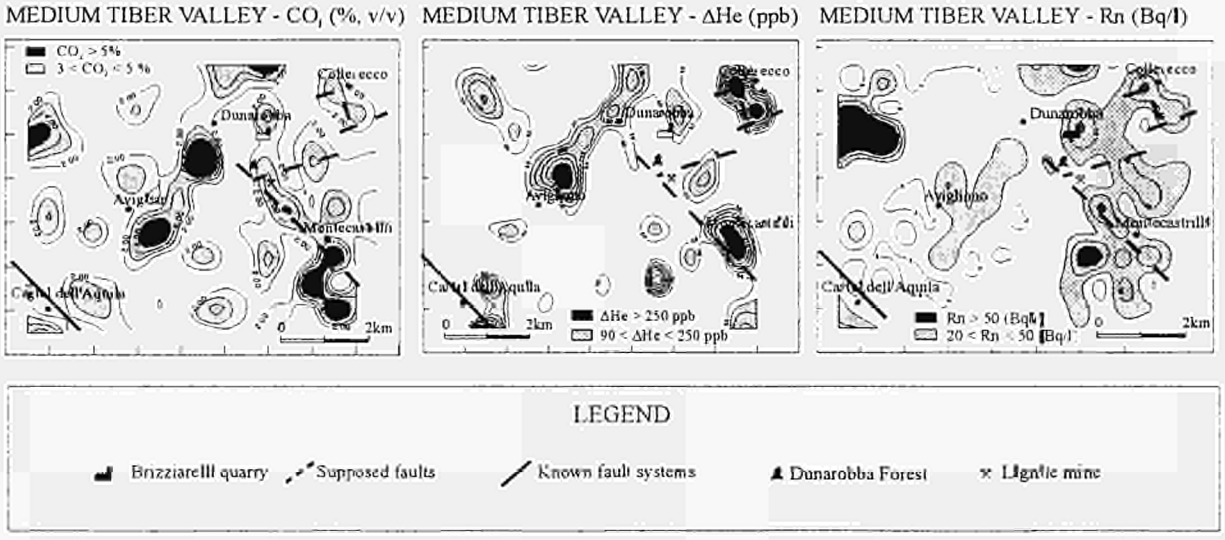

Fig.2 - Detailed soil-gas survey (CO2, He, Rn) in the medium Tiberine Basin

In the figure it is possible to observe that CO_2, He and Rn anomalies form elongated zones trending N40-45E, along the direct line connecting the built-up areas of Avigliano and Dunarobba, and N40-45W in the eastern sector of the studied area (Montecastrilli). The N40-45W anomaly coincides with an important tectonic discontinuity that divides the main outcropping lithological units. As well a gas anomaly, trending N40-45E and marked by all three gases, seems to cross the basin suggesting the presence of an important transversal tectonic element in this area. Furthermore, a Rn anomaly area is located in the western corner of the map, while at Montecastrilli and Collesecco spotty helium anomalies occur in correspondence with recognized tectonic elements.

The detailed soil-gas survey confirms the occurrence of those gas anomalies observed in the regional survey. The detailed character of this sampling yielded a better definition of the location and extent of the anomalous area linked to the supposed tectonic elements.

Self potential surveys

In agreement with the approved geophysical research program, in which the seasonal repetition of Self Potential (SP) surveys and the execution of large and small - scale geoelectrical tomographies were proposed, we have performed in 1994 an SP survey at the end of the spring season (end of June 1994) and three small-scale dipolar tomographies inside the Dunarobba Forest area. The pattern of the SP anomalies is very similar to that surveyed in the winter season (Annual Progress report 1993) while the tomographies confirm tne main lineaments already observed in the previous survey.

The dipole-dipole geolectric investigations (fig.s 3, 4) show the high-resolution small-scale tomographies within the Dunarobba Forest. The lenghts of the profiles vary from slightly more than 100 m to slightly less than 800 m for a maximum depth of investigation between 25 and 110 m. Common to all dipolar tomographies is the presence of relatively low-apparent resistivity values (typical of a clayey-sandy mixture) distributed throughout the sections, indicating a rather homogeneous deposit apart from the two anomalous signatures described below. The first anomaly refers to the tomography of fig. 3, where one observes, close to the Briziarelli kiln, a deep resistive wedge-shaped body which is interpretated as the uppermost edge of a horst-like structure. This feature was observed in the previous large-scale tomography (the apparent resistivity values are as high as 100 Ohmmeter). The second anomaly refers to the profiles of fig 3 and 4, where a series of small, relatively resistive nuclei appear, for the most part, closely correlated with the visible sequence of fossil trees and, for the remaining part, probably with fossil wood remnants within the clayey-sandy complex.

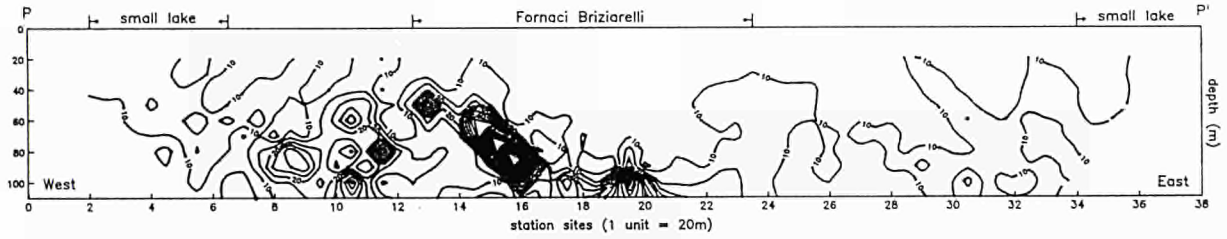

Fig. 3 - Dunarobba Forest dipole-dipole mid-range geoelectrical tomography along profile PP'. Contour lines in Ωm.

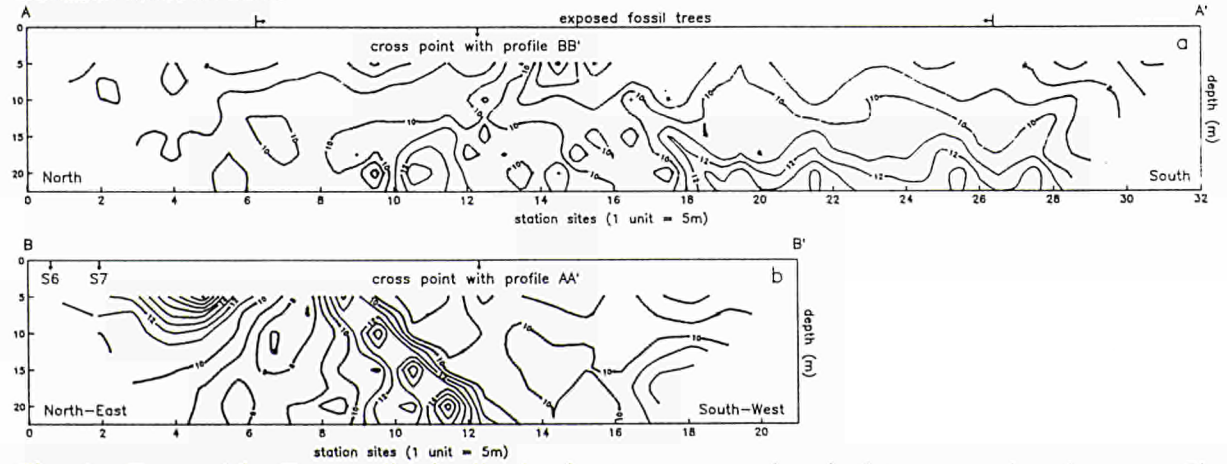

Fig. 4 - Dunarobba Forest dipole-dipole short-range geoelectrical tomography along profiles AA'(a) and BB'(b). Contour lines in Ωm.

C.2 Reconstruction of the hydrogeological setting and studies of the fluid phases (water and gas)

Hydrogeological survey

In order to understand head fluctuations and groundwater flow, hydrogeological surface mapping and piezometric measurements in equipped boreholes have been carried out.
In an area of 10 km^2 around Dunarobba Forest, a total number of 77 water points (58 wells, 17 springs and 2 lakes) has been recorded. For each of these water points the following data have been collected during four different surveys (February 1993, July 1993, October 1993 and March 1994):

- springs: flow rate, water temperature, water electrical conductivity, aqueous tritium content;
- wells: phreatic level, water temperature, water electrical conductivity, aqueous tritium.

In March 1994 we concluded one complete year of observation.

Regarding the five equipped boreholes inside the Dunarobba Forest, starting in December 1993 and for the all 1994, periodic measurements of the groundwater level, water temperature, water electrical conductivity and aqueous tritium content have been performed.

Seasonal flow patterns, phreatic levels of springs and the similarity of water temperatures allow us to hypothesize that the underground circulation in the deposit of the Tiberine Basin are controlled by a shallow aquifer system, either single or multilayered. Data collected from the Casagrande cells in the equipped boreholes show that interstitial pressure increases down to a depth of 40 m. As a result, deep waters are likely to follow two paths of circulation: an upward one, which tends to mix pore water in the upper layers and another one, which remains at depth and tends to flow deeper. Also, tritium data suggest vertical layering, since the deepest water samples are characterized by low tritium values.

The low permeability of the clayey level (C.3) in the Tiberine basin Pliocene sequence and the intense network of discontinuities in the rock mass (C.1) suggest that fluid circulation mainly occurs along faults and fractures.

Geochemical characterization of the aqueous phase

The water samples collected from the springs and wells already mentioned have been analysed for major elements as well as isotopes of the water molecule (^2H, ^3H, ^{18}O) and ^{13}C in Total Dissolved Carbon (TDC).

The waters can be classified as calcium bicarbonate waters, however, an evolution toward the chloride-nitrate pole can be recognised. In this case two different source contributions can be inferred:

- the first, is due to infiltration of meteoric water remobilizing the fertilisers which are intensively used in the area;
- the second, is linked to a lateral contribution from carbonate massifs bordering the Dunarobba district. In this case the groundwater flow takes place along fault systems, reaching deeper horizons where the waters could be enriched in chloride due to the presence of Triassic evaporitic layers and perivolcanic fluids.

The second groundwater component seems to be independent of the water cycle during the year and, at the same time, the geographical distribution of chloride seems to be related to the tectonics of the district. In fact, the chloride distribution in July 1993 shows an excellent correlation with an important fault system, NE-SW, detected by geological, geophysical and geochemical (soil gas) surveys.

The ^{18}O data show seasonal variations indicating the direct contribution of meteoric water, variations which are more evident in springs and wells linked to subsurface circulation. When plotted on a δ^2H vs $\delta^{18}O$ (Fig. 5), the samples fall on the classic meteoric water line. However, samples taken in wells PZ8 and PZ33 are depleted in ^{18}O, which could be explained by an exchange between water and an excess CO_2 in the pore space . This hypothesis finds support in the soil CO_2 anomalies and chloride distributions, inferring a tectonic control of fluid circulation in the area.

To follow water movement through the undersatured zone, isotope analyses have been

carried out on the pore water in soil samples, after extraction following the methods suggested by the IAEA (1991).

The pore water in soil samples collected during the winter of 1993 indicates the presence of non evaporated water in the deeper layers of the unsaturated zone whereas, in the shallower zones, the waters seem to be affected by a slight evaporative process. The large spread of the results (40% and 7% respectively for ^{2}H and ^{18}O) indicates the complexity of the direct recharge mechanism through the unsaturated zone. These results should be completed (and checked) by the analyses of the samples collected in the others hydrogeological surveys.

The ^{13}C values from TDC are distributed in two groups: the first one (with a mean value of -13%°) is linked to shallow groundwater; the second (-8%) is related to a contribution of deep CO_2 rising along faults.

The existence of CO_2 of deep origin has been confirmed by the isotopic composition of calcite present in the few clay samples collected at the surface in the Dunarobba area. In future, a wider ^{13}C survey of the carbonatic phase will be performed, mainly on samples collected at different depths, to attempt a reconstruction of groundwater paleocirculation.

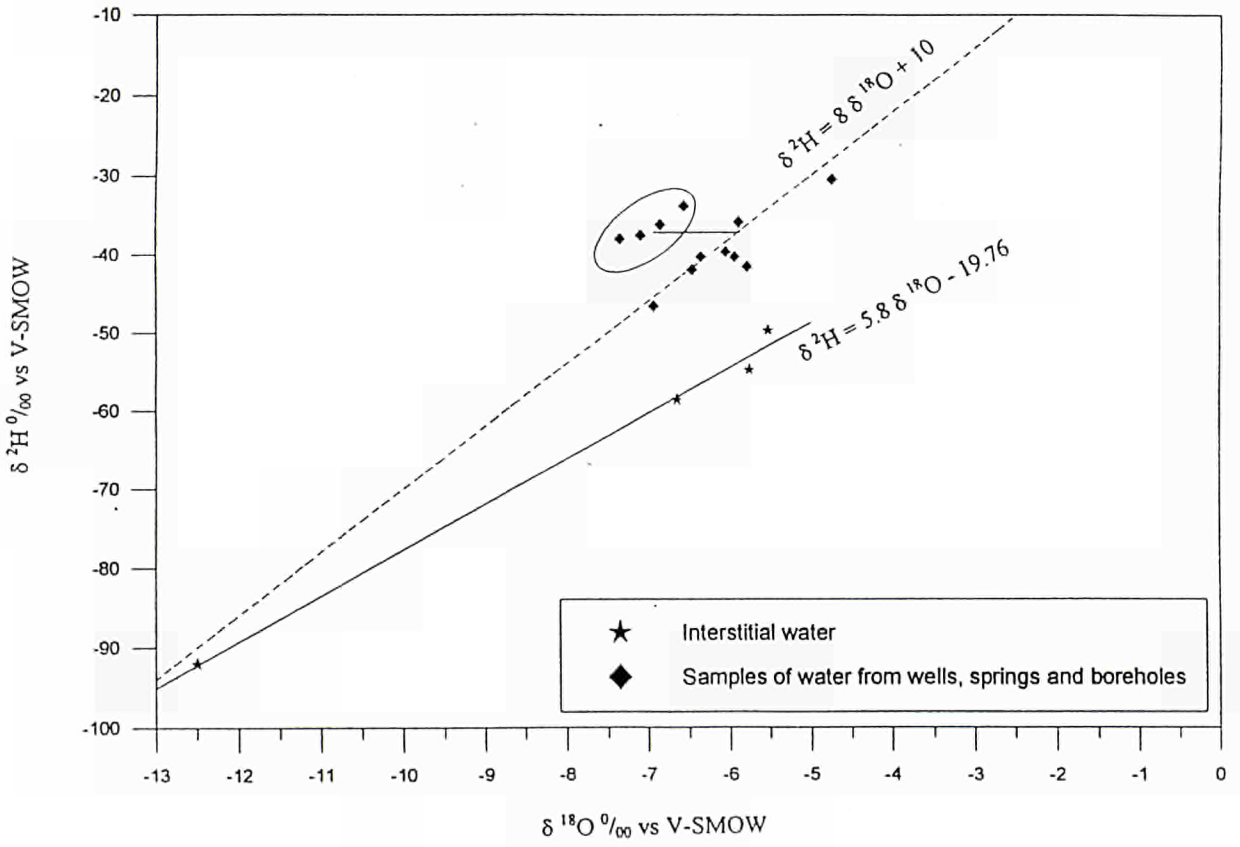

Fig. 5 - Relationship between $\delta^{2}H$ and $\delta^{18}O$ for the interstitial water and water samples from wells, springs and boreholes (first geochemical survey).

Gas injection experiment

A gas injection experiment using helium was undertaken by the Earth Resources Centre of the University of Exeter and the University of Rome to obtain information on the localised

sealing properties of the clay, to compare with the regional emission of natural helium . It was not possible to undertake the test at the Dunarobba Forest site due to the sensitivity and perceived possible damage to the site. Therefore, a site within the same clay was selected 3 km to the east, near Collesecco.

A borehole was cored vertically to a depth of 15 m and cased. The lowest 3 m section was screened and a packer set above it. A grid of 16 soil gas sampling sites was established around the borehole with a spacing of 10 m, with a further 12 sites radiating from the borehole. Soil gas samples were collected by probes at a depth of 0.5 m. Additional 2 and 4 m deep probes at four locations proved ineffective because of waterlogging. A background soil gas survey was made on 21 and 22 June 1994, with helium analyses performed on site using the ERC mobile laboratory.

The helium values (relative to atmospheric air) were generally below 100 ppb. On the first day a few values between 100 - 1000 ppb were found, but these had diminished by the second day, suggesting a very low flux of natural helium.

Helium was injected into the borehole below the packer on 23 June, at positive pressures up to 1.6 bars. A few samples taken from the grid showed an increase after only 2.5 hours, up to 3800 ppb at one point, which then dispersed within 24 hours.

Measurements close to the borehole revealed much higher values, up to 10^7 ppb only 1.5 m away from it on 27 June. Figure 6 shows the exponential decay at two of these high value sites over the next 20 days.

The results of the experiment indicate that all the injected He was dispersed to the atmosphere via permeable pathways through the clay in the vicinity of the borehole. If it is assumed that these pathways were induced by the drilling process itself, then the sealing properties of the clay have been demonstrated by the absence of He anomalies elsewhere.

However, there remains the possibility that such a preferential pathway may divert all the gas flux to it and away from any naturally occurring pathways. Possibly the high initial 1032 ppb He value indicated a pre-existing pathway, but without a background survey prior to drilling this can not now be determined.

Alternatively the presence of so much gas in the ground may always cause the creation of a vertical escape chimney. To further test the clay, He needs to be introduced deep into the ground with the minimum of disturbance. An inclined borehole, or better, a horizontal borehole from a quarry side would avoid the vertical drilling disturbance.

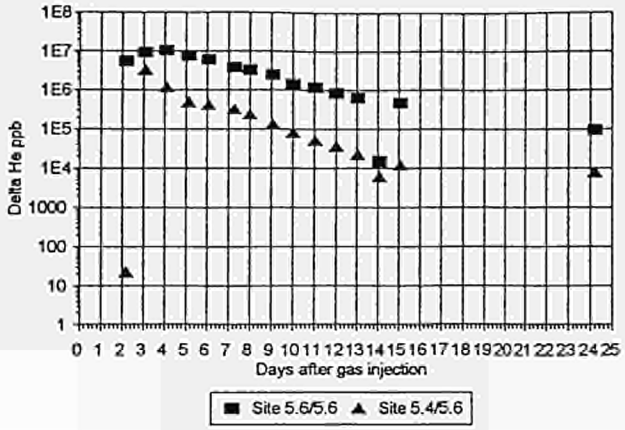

Fig. 6 - Decay of injected helium from two sample sites within three metres of the borehole.

C. 3 Studies of the natural barriers in the Dunarobba Forest area.

Lithostratigraphy of the Dunarobba sequence

Detailed lithostratigraphic reconstructions of the Pliocene terrigeneous sequence have been

performed either on outcrops and quarries inside the Dunarobba area or on vertical sequences from boreholes. In the Dunarobba Forest area starting from ground level (where the trunks outcrop) to 45 m b.g.l, the vertical sequence shows clayey-silty laminated strata with frequent sandy levels and rare gravelly horizons; these coarser levels represent 20% of the drilled sequence. The organic content is very high in some levels, with abundant wood floats and roots. The facies association is typical of a palustrine environment along a lacustrine coast. From 45 m b.g.l. to 116.5 m b.g.l. the sequence is more homogeneous and the lithotype is a laminated silty clay, with rare thin strata of clayey silt, which is frequently jointed. The facies association is of a deep lacustrine environment.

In the Dunarobba Forest area, hypothetical correlations between this and other surveyed sequences point out a complex spatial arrangement of these two different types of deposits, affected by both the depositional environment and the tectonic displacements. The spatial distribution of the deep lacustrine deposits (silty clay with rare thin strata of clayey silt) appears to be of great importance in the definition of the natural barriers because of their lower hydraulic conductivities relative to the unit which contains the wood remains (clayey-silty laminated strata with frequent sandy levels and rare gravelly horizons).

Mineralogical characterization

The claystones in which the Dunarobba Forest occur consist of a variable mixture of the following minerals: 1- a mix-layered smectite, 2- illite, 3-kaolinite, 4- a chlorite, 5- a carbonate, 6- a quartz.

Given the preliminary separation that has been carried out on all samples analyzed (leaching of the organic matter, separation of the clay size fraction, deposition on a millipore filter) the amount of non layered minerals (quartz and carbonates) is very minor in all samples.

Quartz is certainly detrital, whereas the carbonate changes in composition from pure calcite to a calcite-ankerite solid solution and may be regarded as either detrital or diagenetic (most probable).

Clay minerals are of three types:

a) homogeneous phases of constant or nearly constant composition: kaolinite, illite (this phase can be, in part, detrital muscovite);
b) complex chemical solid solutions: the chlorites which vary greatly in both their Al/Si and Mg/Fe ratios (on account of intensities of their even vs. odd basal peaks);
c) complex chemical as well as mechanical inter-layered phases: the smectites.

A preliminary analysis of clay from the gas injection borehole shows a high montmorillonite content, which would tend to enhance the sealing properties against gas migration at that site and may not be typical of the Dunarobba forest site.

Consolidation state and hydraulic conductivities

Preliminary investigations on the index parameters (granulometric composition and Atterberg limits) of samples belonging to the Fosso Bianco unit show a clear distinction between deposits of the palustrine facies associations and deposits of the lacustrine facies association. In fig. 7 the data from samples recovered from the drilling performed in the Dunarobba area are reported. The grain size distribution is less scattered in the materials of deep lacustrine origin while the samples belonging to the palustrine facies association (in which the trunks are embeded) are characterized by more variable fractions of sand, silt and clay. Furthermore, the plasticity and mineralogical activity appear higher in the deep lacustrine deposits.

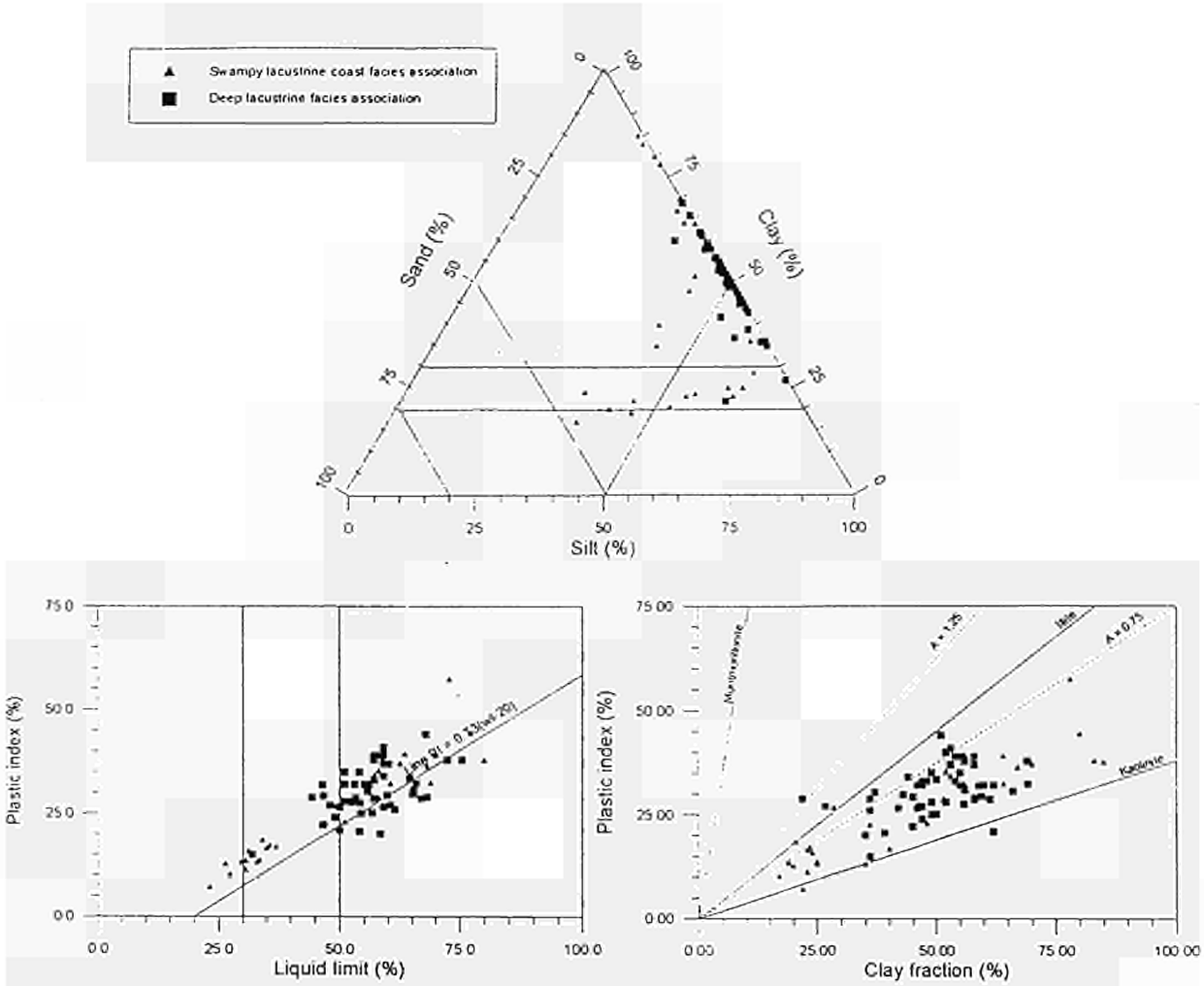

Fig. 7 - Fosso Bianco unit: grain - size chart (U.S. Bureau of Soils), plasticity chart and activity chart.

The parameters referring to the state of the materials indicate a high density. In fact samples belonging to the deposit containing the tree trunks (collected at a depth between 1.5 to 4.2 m b.g.l.) are characterized by an average total unit weight (γ_n) in the range 19.1-19.9 kN/m^3 and a void index in the range 0.57 - 0.74. The average total unit weight of the deepest samples ranges from 19.8 to 20.2 kN/m^3 and the void ratio is in the range 0.85 to 0.53; most of the γ_n values are close to the upper boundary.

The consolidation state is high as shown by oedometric tests on undisturbed samples recovered at different depths below ground level. The state of overconsolidation is demonstrated by the high ratio between yield pressure and the corresponding effective pressure for all undisturbed samples recovered at different drilling depths.(fig. 8). Studies on the causes of this overconsolidation are in progress. In particular the role of the $CaCO_3$ as cement is being analyzed; first results show a good relationship between $CaCO_3$ content and yield pressure as shown in fig. 8, where the two variables are plotted versus sample depth. In this figure a tendency to an incremental increase of yield pressure versus depth is evident; the negative deviations from this trend are related to a decrease in the $CaCO_3$ content. Some natural cementation effects on enhanced microstructure resistance have been shown by comparing the stress-strain behaviour of remoulded samples with that of samples at different $CaCO_3$ contents. More research regarding the distribution of $CaCO_3$ inside the microstructure have been planned. In addition the effect of secondary consolidation process will be evaluated.

In order to measure the hydraulic conductivity of clayey levels, oedometric tests have been performed both on undisturbed samples under natural density conditions (γ_n =20 kN/m^3 ca.) and on remoulded samples having a low density (γ_n=16 kN/m^3). The first set shows a range $2*10^{-13}$ to $2*10^{-10}$ m/s while the second set ranges between $2*10^{-12}$ and $1*10^{-9}$ m/s. Direct permeability measurements on some undisturbed clayey samples, already tested on the oedometric apparatus, have being carried out; the results of these tests confirm the values obtained by oedometric tests at low stress levels. In the sandy levels, as shown by the measurements taken in Casagrande cells located along the drillings, the permeability is approximately 10^{-4} m/s.

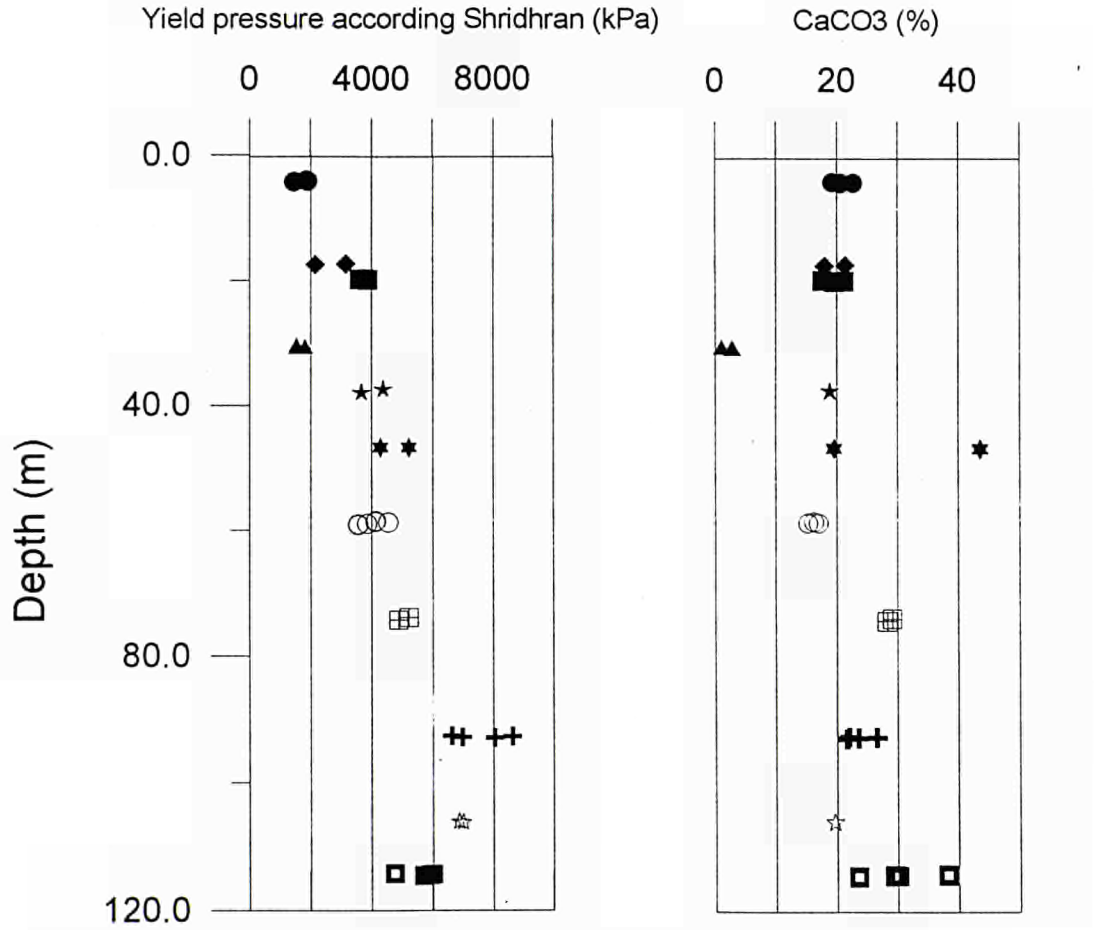

Fig. 8 - Yield pressure and carbonate content (from borehole S6, S7)

Geochemical characteristics

The $^{87}Sr/^{86}Sr$ ratios (in the soluble and insoluble fractions) of some natural clayey samples collected at different depths along the vertical sequence in the Dunarobba Forest show values significantly different from sample to sample, suggesting that each sedimentary horizon behaves as a closed geochemical system.

Radiochemical analyses of samples collected from the Dunarobba site at different distances from a tree trunk are reported in tables 2 and 3.

Borehole	distance from the trunk	Samples and depth of sampling (m)
S - 8	0,5 m	N1 from 1.0 to 1.8; N2 from 1.8 to 2.6
S - 9	1,0 m	N1 from 1.0 a 1.8; N2 from 1.8 to 2.6
S - 10	1,5 m	N1 from 1.0 a 1.8; N2 from 1.8 to 2.6
S - 11	2,5 m	N1 from 1.0 to 1.8; N2 from 1.8 to 2.6; N3 from 2.6 to 3.4
S - 12	3,5 m	N1 from 1.0 to 1.8; N2 from 1.8 to 2.6; N3 from 2.6 to 3.4
S - 13	4,5 m	N1 from 1.0 to 1.8; N2 from 1.8 to 2.6; N3 from 2.6 to 3.4

Tab. 2 - $^{87}Sr/^{86}Sr$ ratios of the carbonate and silicate fractions and % $CaCO_3$ of the analysed samples (the reported values have been corrected in relation to the age of the deposit).

U, Th, Ra and K, analysed by gamma spectrometry, show uniform values (the internal variability is about 25%).

Observing the data in table 3 it can be seen that there are no evident relationships between the organic matter content (in the table expressed as % C) and the uranium concentration. As is well known,organic matter has the ability to act as a scavenger of U from sedimentary connate waters. The above lack of a relationship between these two species infers a low degree of permeability within the same sedimentary level and between the different sedimentary horizons, as the low permeability does not allow for the extraction of U by the organic matter.

The analysed samples also indicate an evident disequilibrium between ^{226}Ra and ^{238}U for at least 6 samples. On the basis of the above considerations, this disequilibrium is likely not related to the migration and enrichment of ^{238}U in the most reducing environment. In fact there is an excess of ^{238}U, whether in samples which are enriched or very poor in organic matter. Therefore, the observed disequilibrium could be related to the migration of ^{226}Ra or ^{230}Th (parent of ^{226}Ra) .

The $^{228}Ra/^{228}Th$ ratios show a behaviour similar to that of $^{226}Ra/^{238}U$ ratios, such that in samples which show $^{228}Ra/^{228}Th$ in equilibrium, the same equilibrium is evident in the $^{226}Ra/^{238}U$ ratios. As well, for samples in which there is disequilibrium in the $^{226}Ra/^{238}U$ ratios, a clear disequilibrium is evident in the $^{228}Ra/^{228}Th$. It is possible therefore to conclude that the Th is the only chemical element responsible for these variations, in particular the radionuclides ^{228}Th and ^{230}Th formed during the recoil phenomenon .

According to some recent Italian studies, the observed disequilibrium between $^{226}Ra/^{238}U$ and $^{228}Ra/^{228}Th$ is related to the capacity of some mineralogical phase to behave as scavenger for Th and not for Ra.

It is possible to calculate the characteristic migration distance by diffusion in a porous medium for a given radionuclide by using the following equation:

$$x=(D\ t)^{1/2}$$

where x is the characteristic migration distance for a given radionuclide; D is the effective diffusion coefficient for the radionuclide in porous medium and t is the time in which the process is active (which in this case equals the mean life of the radionuclide).

Using this equation we calculated a characteristic migration distance for ^{230}Th to be about 20 m and for ^{228}Th to be 14 cm. As the analysed samples cover a distance of 6 m one can see that the entre system is in equilibrium. Therefore, the diffusive migration of the considered radionuclides into the interstitial fluids is limited to the radius of about 6 meters, due to the absorptive capacity of these clayey sediments.

As for sample DS 13 N2, it is possible to observe that all $^{234}U/^{238}U$ activity ratios are in disequilibrium (with an excess of ^{234}U) with the exception of the sub-sample collected close to the interface between organic rich sediment and clayey sediment. The excess of ^{234}U can be related to the high organic matter content (about 14%) which acted as scavenger for the uranium of the interstitial fluids.

As for the radius of diffusion of ^{234}U, we calculated a limit of about 10 cm.

Sample	U *ppm*	Th *ppm*	^{226}Ra *ppm*	K_2O %	$^{226}Ra/^{238}U$	$^{228}Ra/^{228}Th$	C %	H_2O %
S8N1	1,9 +/- *0.3*	4,8 +/- *0,1*	1,7 +/- *0,1*	1,04 +/- *0,02*	0,89 +/- *0,15*	1,10 +/- *0,08*	3,3	14,6
S8N2	2,6 +/- *0,4*	7,9 +/- *0,2*	2,5 +/- *0,1*	1,69 +/- *0,01*	0,96 +/- *0,16*	1,19 +/- *0,06*	6,7	16,8
S9N1	1,7 +/- *0,3*	6,2 +/- *0,1*	1,8 +/- *0,1*	1,20 +/- *0,02*	1,06 +/- *0,19*	1,10 +/- *0,08*	5,6	13,3
S9N2	2,2 +/- *0,3*	9,1 +/- *0,2*	2,2 +/- *0,1*	2,00 +/- *0,03*	1,00 +/- *0,14*	0,95 +/- *0,07*	2,5	14,9
S10N1	3,0 +/- *0,4*	6,4 +/- 0,1	2,2 +/- 0,1	1,54 +/- 0,02	0,74 +/-0,10	1,38 +/- *0,09*	4,1	18,1
S10N2	1,6 +/- *0,3*	6,6 +/- *0,2*	1,8 +/- *0,1*	1,30 +/- *0,02*	1,12 +/- *0,21*	0,98 +/- *0,08*	7,6	12,0
S11N1	1,4 +/- *0,3*	6,1 +/- *0,1*	1,6 +/- *0,1*	1,14 +/- *0,02*	1,14 +/- *0,26*	0,98 +/- *0,08*	4,8	14,6
S11N2	2,1 +/- *0,4*	5,2 +/- *0,1*	1,5 +/- *0,1*	1,40 +/- *0,01*	0,71 +/- *0,14*	1,22 +/- *0,06*	22, 5	25,3
S11N3	2,9 +/- *0,3*	6,4 +/- *0,2*	1,7 +/- *0,1*	1,39 +/- *0,02*	0,58 +/- *0,07*	1,31 +/- *0,08*	1,9	15,5
S12N1	2,5 +/- *0,4*	8,0 +/- *0,2*	1,7 +/- *0,1*	1,60 +/- *0,02*	0,68 +/- *0,09*	1,20 +/- *0,08*	1,6	16,4
S12N2	3,1 +/- *0,4*	7,9 +/- *0,2*	2,0 +/- *0,1*	1,71 +/- *0,02*	0,64 +/- *0,08*	1,34 +/- *0,09*	7,9	15,4
S12N3	2,8 +/- *0,3*	7,3 +/- *0,2*	2,3 +/- *0,1*	1,45 +/- *0,01*	0,82 +/- *0,10*	1,30 +/- *0,07*	8,7	15,4
S13N1	1,8 +/- *0,3*	5,0 +/- *0,1*	1,7 +/- *0,1*	1,16 +/- *0,02*	0,94 +/- *0,19*	0,91 +/-*0,08*	10, 5	15
S13N2	2,5 +/- *0,4*	5,8 +/- *0,1*	1,9 +/- *0,1*	1,33 +/- *0,02*	0,76 +/- *0,12*	1,04 +/- *0,08*	14	21,8
S13N3	2,0 +/- *0,3*	6,7 +/- *0,1*	2,5 +/- *0,1*	1,44 +/- *0,02*	1,25 +/- *0,18*	0,94 +/- *0,08*	9,5	9,9

Tab. 3 - U, Th elementary concentration, $^{226}Ra/^{238}U$ and $^{228}Ra/^{228}Th$, organic matter content (%) and % H_2O for the analysed samples

Organic matter

After many difficulties were overcome, wood samples were extracted from one tree trunk (18M) at Dunarobba (from below ground level) and sent to the subcontractor at the University of Nebraska, Lincoln, USA on the instruction of ERC, Exeter, UK. Samples of clay and wood from the interface of the same trunk were sent to ERC.

The long delay in receiving the specimens (April 1994) presented laboratory programming difficulties and the full organic analysis at Nebraska was not completed by the end of 1994.

The 20 elemental analyses show atomic H : C ratios (fig.9) ranging from 1.6 (very similar to fresh wood of similar species) down to 1.1 (more typical of buried wood in which much of the cellulose has been degraded but the lignin is moderately well preserved). The mean value of H : C is nearer the lower end of the range, at 1.3. The fact that some samples are exceedingly well preserved suggests that the alteration seen may be due to recent weathering as the samples come from approximately one metre below existing ground level. The molecular analyses and O: C data will enable more substantive conclusions.

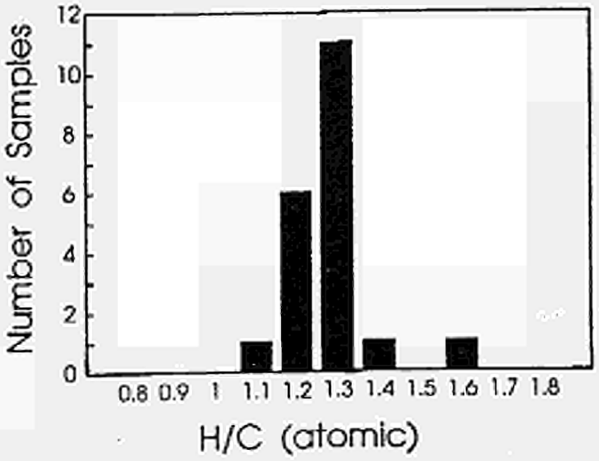

Fig. 9 - Atomic H:C ratios in wood samples.

Title	Chemval 2 - Thermodynamic database
Contractors	WS Atkins Environment
Contract N°	FI2W-CT92-0122
Duration of contract	September 1992 - December 1994
Period covered	January 1994 - December 1994
Project leader	W.E. Falck

A. OBJECTIVES AND SCOPE

The principal objective of the CHEMVAL2 database project is the production of an extended, reviewed thermodynamic data compilation applicable to geochemical modelling studies in the EC member states. The database will be fully referenced to source and emphasises radioelements and other chemical components of relevance to radioactive waste disposal.

The CHEMVAL thermodynamic database has been compiled as a result of collaborative work during the 1985-1989 CEC MIRAGE Project [1,2]. Production of a standardised database has proved invaluable for comparison of simulations performed in different laboratories and has helped to increase the confidence in models now being used in national radiological safety assessments.

The continued need for a centralised database facility is clear and encompasses:

- data review for elements not currently included in the database
- coordination and compilation of data arising from CHEMVAL2 activities and parallel research work coordinated within the CEC CoCo (Colloids and Complexes) projects.
- data management, primarily the collation and dissemination of frozen data sets.

B. WORK PROGRAMME

The work programme comprises three separate stages reflecting the various phases of the CHEMVAL2 project.

Stage 1 – agree scope of data reviews; establishment of format for database and its mode of distribution

Stage 2 – collation and review of thermodynamic data; annual issue of frozen data sets; coordination and management of less quantitative information arising from CHEMVAL2 and related projects

Stage 3 – final reporting

Database work continued throughout the contractual period up to the completion of CHEMVAL2 in December 1994.

C. *PROGRESS OF WORK AND OBTAINED RESULTS*

State of advancement

The project has advanced in line with the proposed schedule and is almost complete. The final version of the thermodynamic database is currently being prepared for release (Spring 1995) together with the final project report.

Progress and Results

In Stage 1 of the project, the following tasks were agreed upon:

a) amend errors/gaps identified in Release 4.0 [3];
review redox–equilibria of elements already contained in Release 4.0;

b) add the new elements Ni, As, Cu, Cd, and the rare earth elements;

c) add enthalpy (ΔH°) and heat capacity (C_p)data for all species as made available under the CHEMVAL2 activities dealing with 'Temperature Correction';

d) develop a database suitable for higher ionic strength solutions ($I<2$ mol dm^{-3}), employing the Specific Interaction Theory (SIT) as activity coefficient (γ) correction method;

e) management of data arising out of the main CHEMVAL and CoCo activities.

a) Amendment of errors and gaps and review of redox equilibria

Stage 2 saw the majority of errors and gaps in the earlier reviews eliminated and most of the redox equilibria reviewed. One hundred species had been marked for review [4], these were for the most part referenced to secondary data compilations only, and/or serious disagreements between CHEMVAL and other databases were found. The literature was searched for relevant primary references in order to satisfy the quality criteria adopted for the CHEMVAL database [3]. A number of aqueous species for elements already in the database were also added. A more detailed account of this work has been given in previous reports [4,5,6]

Following the final publication of the NEA-review of uranium aqueous chemistry [7], relevant data were added to the CHEMVAL database after making the necessary recalculations to ensure internal consistency. The CHEMVAL 5.0 values derived from source literature have all been replaced by those recommended in [7], and a few additional species, mainly of relevance to far-field studies, have been included.

The dBaseIV™ files, which form the reference format for the relase of the CHEMVAL database, have been amended since Release 4.0 in order to accommodate ancillary infomation necessary to construct data files for use with speciation codes, such as species valence and stoichiometric coefficients.

b) Addition of new elements

The elements Ni, Cu, Cd and As have been added to the database. These elements were chosen for their radiological significance or their involvment in the formation of solid phases with important radioelements.

The trivalent rare earth elements (REE) may serve as analogues for trivalent actinides and are, therefore, of great interest. A large body of data on REE's has been compiled, which subsequently has undergone review prior to inclusion in the database.

The CHEMVAL Thermodynamic Database Release 6.0 will contain 1291 aqueous species and 516 solid phases for 59 elements and 3 organic ligands.

c) Temperature correction

Owing to the incompleteness of data describing the heat capacity (C_p) of many species as a function of temperature, a modified form of the classic van't Hoff relationship has been adopted to account for temperature induced changes in equilibrium stability constants. The activity coefficients of ions in solution also vary with temperature and a modification of the Davies Equation [8] was proposed by BRGM/ANDRA to account for this. The expression incorporates a fourth order polynomial for the Davies 'A' parameter enabling calculations to be made in the range 0-200°C. In summary, the methodology appears to work well below 100°C but breaks down progressively at higher temperatures.

Enthalpy data for a large number of aqueous (>50%) and solid (>80%) species (based on Release 4.0) have been received from the CHEMVAL2 topic group 'Temperature Correction', and have now been included, together with their pertinent references, in preparation of Release 6.0 of the database.

d) Ionic strength correction

The CHEMVAL thermodynamic database as developed up to the release of Version 5.0 in May 1994 accounts for the activity coefficient (γ) using a modified form of the Davies Equation [8] and is intended for applications where the total salinity does not exceed 0.3 mol dm^{-3}. In order to extend simulations to more saline waters, a work programme was adopted [9] with the following objectives:-

i) to compare alternative procedures for γ correction using a series of standard test cases;

ii) to implement a viable method for γ correction allowing equilibrium calculations for waters ranging to ≈2 molal within tolerable error limits.

As with the elevated temperature programme described previously, a practical method was required which could be applied consistently to a range of different conditions. Thus, for reasons of data availability, the Specific Interaction Theory (SIT), advocated by Grenthe et al. [7], was preferred over the approach of Pitzer and co-workers [10]. Comparison of the various correction methods available clearly demonstrated the suitability of SIT (Figure 2) and, subsequently, considerable effort has been expended in re-casting the CHEMVAL Database (V5.0) using the relationship:-

$$\log \gamma_i = -A\, z_i^2((I^{1/2} / (1+ 1.5 \cdot I^{1/2})) + \sum_k \varepsilon_{ik} M_k \qquad (1)$$

where ε_{ik} is the specific interaction coefficient accounting for short range interaction between the *i*th and the *k*th ion, and I, z_i, and A have their usual meaning.

Approximately 200 published interaction coefficients have now been collated and the database has been re-cast accordingly. As the database contains roughly 1,300 aqueous species, however, a protocol has been developed to guide users where the necessary constants are lacking. This database will be issued concurrently with the general Version 6.0.

e) Management of data arising out of the main CHEMVAL and CoCo activities

In the context of the CHEMVAL activities in the field of organic complexation and sorption a considerable body of data has arisen. These are held ready for use with the models chosen during the work. In both areas the preferred model is based on electrostatic interaction. Organic complexation data have been collated or determined for use with the model proposed by Tipping and co-workers [11,12], while the data on sorption are mainly for use with implementations of the triple-layer model [13].

D. CONCLUSIONS

Research carried out within the CHEMVAL2 Project has greatly enhanced the ability of participating groups to simulate geochemical reactions. Accounting for the effects of temperature and salinity present analogous problems in many respects as both are primarily constrained by data availability rather than by lack of conceptual understanding. The database initiatives started within CHEMVAL2 represent substantial progress but do not, by any means constitute a final solution.

E. ACKNOWLEDGEMENTS

The CHEMVAL2 Project is supported under the 4th CEC Research and Development Programme on the Management and Storage of Radioactive Waste (1990-1994. Funding from the UK DoE/HMIP is also gratefullly acknowledged. The results of this work may be used in the formulation of UK Government Policy, but views expressed in this work do not necessarily represent UK Government Policy. Particular thanks are expressed to H. von Maravic (CEC) and R. Yearsley (HMIP), the following staff at WS Atkins: D. Read, J. Thomas, D. Bennett, L. Paul, D. Ross and all the CHEMVAL2 participants.

F. REFERENCES

[1] READ, D. (Ed.), CHEMVAL Project. Report on Stage 2: Application of Speciation Models to Laboratory and Field Data Sets. CEC Report EUR 13124EN. 229 p. (1990).

[2] FALCK, W.E., Critical Evaluation of the CHEMVAL Thermodynamic Database with Respect to its Contents and Relevance to Risk Assessment of Radioactive Waste Disposal beneath Sellafield and Dounreay. Rep. Fluid Processes Res. Group, Br. Geol. Surv., WE/91/6C (1991).

[3] CHANDRATILLAKE, M., FALCK, W.E., READ, D., CHEMVAL Project – Guide to the CHEMVAL Thermodynamic Database. Report to Her Majesty's Inspectorate of Pollution/DOE, DOE/HMIP/RR/92/094 (1992).

[4] FALCK, W.E., RIDGE, D.M, CHEMVAL2: Thermodynamic Database, CEC Contract No. FI2W/CT92/0122, 1st and 2nd Periodic Progress Report (September 1992 - August 1993).

[5] FALCK, W.E., CHEMVAL2: Thermodynamic Database, CEC Contract No. FI2W/CT92/0122, 3rd Periodic Progress Report (September 1993 - February 1994).

[6] FALCK, W.E., PAUL, L., CHEMVAL2: Thermodynamic Database, CEC Contract No. FI2W/CT92/0122, 4th Periodic Progress Report (March 1994 - September 1994).

[7] GRENTHE, I., FUGER, J., KONINGS, R.J.M., LEMIRE, R.J., MULLER, A.B., NGUYEN-TRUNG, C., WANNER, H., Chemical Thermodynamics of Uranium, Chemical Thermodynamics 1, North Holland, Amsterdam etc. (1992).

[8] DAVIES, C.W., Ion Association. Butterworths, London (1962).

[9] READ, D. (Ed.), CHEMVAL2 Project. Status Review of CHEMVAL2 Technical Areas, June 1992. Report UK DoE/HMIP/RR/93.014, 236 p. (1992).

[10] PITZER, K.S., Thermodynamics of Electrolytes. I. Theoretical Basis and General Equations. J. Chem. Phys., 77, 268-77.

[11] TIPPING, E., HURLEY, M.A., A Unifying Model of Cation Binding by Humic Substances. Geochim. Cosmochim. Acta, 56: 3627-41.

[12] CRAWFORD, M.B., PHREEQEV: The Incorporation of a Version of Model V for Organic Complexation in Aqueous Solutions into the Speciation Code PHREEQE. Comp. Geosci., (in press).

[13] DAVIS, J.A., JAMES, R.O., LECKIE, J.O., Surface Ionization and Complexation at the Oxide/Water Interface. I. Computation of Electrical Double Layer Properties in Simple Electrolytes. J. Coll. Interface Sci., 63(3), 480-99 (1978).

Title	The Entre-Sambre-et-Meuse cryptokarsts area as Belgian Natural Analogues
Contractors	ONDRAF, FPMs (Mons Polytechnics)
Contract N°	FI2W-CT94-0130
Duration of contract	July 1994 - June 1995
Period covered	July - December 1994
Project leader	P. Manfroy (ONDRAF/NIRAS, Coordinator); Th. De Putter (FPMs)

A. OBJECTIVES AND SCOPE.

The Entre-Sambre-et-Meuse (hereafter abbreviated to ESEM) Miocene cryptokarsts area (Southern Belgium) is regarded as a natural analogue of the Belgian project for geological disposal of high-level radioactive waste. Indeed, the host sediment of the Belgian project is clay and the ESEM natural analogue contains clay as a sedimentary infilling *and* as neoformed mineral phases (kaolinite and its hydrous counterpart, halloysite). The study focuses on two aspects involving clay and its isolation capacity.
a.- Argillaceous sediments bearing organic matter in the ESEM karsts contain well-preserved Miocene wood fragments; the potential role of overlying clay beds in this preservation is considered ;
b.- Significant anomalies in rare earth elements (REE) - which are analogues of several actinides present in the high-level waste - provide relevant information on the mobilization and trapping of these elements, with relation to clay mineralogy and neoformation processes.

The study has a two-fold scope. First, it is intended to demonstrate the efficiency of the long-term (ca 10 m.y.) isolation capacity of clay, with regard to easily hydrolizable wood components. Secondly, it focuses on the role played by clay minerals in "dynamic" processes, such as the mobilization of trace elements (including REE) during palaeoweathering.

B. WORK PROGRAMME.

The initial work programme (beginning of year 1994) covered the following tasks :

1. *Field work* was necessary to give an overview of the karst internal organization and location in the local geological context and to collect samples of organic matter bearing sediments.
- Classical geological field work as well as photographic survey of all relevant sites (including the threatened ones : sand and/or peat exploitation) had to be performed in this respect.

2. An *evaluation of the preservation state of organic matter* was planned to start immediately after sampling.
- Thin sections in vegetal remains and palynological preparations provided further information on the plant themselves as well as on their palaeoecology.

- Total organic carbon (TOC) analyses was performed on selected samples.
- Some organic geochemistry tests indicated the possible conservation of hemicellulose, cellulose and lignine in the wood remains.
- Scanning electron microscope (SEM) microphotographs were performed on selected samples.

3. The *geochemical and mineralogical study of clay* and other relevant mineral phases took place after the completion of field work and sampling.
- Mineralogical determination of clay minerals (XRD) and, possibly, SEM microphotographs were carried out on selected samples.
- Geochemical analyses on the <2μ fractions (clay) provided the major and minor elements content. Similar analyses on the sand fractions (2-64μ) were also planned.
- Trace element and REE (Ba, La, Ce, Pr, Nd, Eu, Sm, Gd, Dy, Ho, Er, Yb, Lu, Hf, Ta, W, Pb, Th, U, V, Cr, Co, Ni, Rb, Sr, Y, Zr & Nb) contents were measured on selected samples and interpreted in the light of a mineralogical identification of accessory minerals.
- γ-ray spectrometry indicated the possible trapping of radionuclides on peat and/or clay minerals.
- Preliminary contacts were made to investigate the opportunity of studying the ESEM kaolinites and halloysites by electron paramagnetic resonance (EPR).

Today, at the beginning of the year 1995, most of these analyses are completed. They yielded significant results which are briefly summarized in the following section.

C. PROGRESS OF WORK AND RESULTS OBTAINED.

C.1. Results in organic matter characterization and wood preservation.

Organic geochemistry and palynofaciological data provide relevant information on the nature and evolution of the ESEM organic rich sediments, including those in which the wood pieces are embedded.
TOC values range from only traces to values as high as 29,5%; high TOC values are sometimes associated to significantly high HI (up to 231), especially in the upper part of each organic matter-bearing layer (see discussion below). Globally, the organic matter type (as deduced from the HI/OI diagram : type 3) reflects its continental origin.

Three different palynofacies have been recognized :

- The first (PF1) is made up of nearly 100 % of black-brown debris showing irregular opacity and poorly preserved cellular and vascular structures. Such organic debris are mainly produced by intensive alternation-carbonization of fresh phytoclasts during repeated transportation cycles and/or during the early diagenesis in highly oxydizing interstitial environments. We refer to such allochtonous remains as to degradofusinite and/or semifusinite. These black remains also constitute the organic "background input" in the next two palynofacies.

- The second palynofacies (PF2) is basically composed of the same carbonized ligneous remains as PF1. However, **numerous fresh phytoclasts** are also found, where typical gymnospermous areolated punctuations are frequently recognized.

The gymnosperm branches and trunk fragments are believed to be the "autochtonous" organic matter input, originating from the immediate surroundings of the lake and embedded in the "allochtonous" (i.e. recycled) components of PF2. **Their cellulose content**, as measured with a Fibertec 1010 heat extractor and confirmed by assessing biodegradability (cellulolytic enzyme system), **is as high as 44 %** (of dry matter); hemi-celluloses are found in concentrations of about 3 to 6 % (De Putter et al., 1994).

In our opinion, the preservation of pristine wood pieces in the highly oxydized surrounding organic matter is mainly due to the fact that these wood fragments have been quickly buried in the PF2 sediments. Sedimentation rates clearly increased periodically in the lakes, as indicated by sedimentological arguments. Moreover, the thickness of sediments trapped in short time intervals (about 4,5 m/m.y.), as well as the "rythmic" increase of HI values and concomitant decrease in TOC values in the upper part of each organic matter-bearing sediment layer, also strongly support this idea.
With increasing sediment input in the lake waters, oxydation can no longer occur and cellulose is protected from further degradation (together with hemi-cellulose and other hydrolizable components). The preservation of cellulose and hemi-cellulose over long time intervals probably benefited largely from the presence of overlying clay beds (kaolinite, illite, minor smectite and I/S mixed layers). These clay beds seem indeed to have driven the downward percolating (and oxydizing) fluids laterally to the karst wall and, by doing so, prevented the wood bearing sediments from any contact with these chemically aggressive fluids.

- Finally, the third palynofacies (PF3) is mainly composed of amorphous-granulous masses resulting from an intensive biodegradation of ligneous and cuticular material (Hart et al., 1994). Few occasional fresh wood pieces are also recognized in PF3. Massive translucent ambercoloured resinous fragments with irregular cracks are abundant. Resins could be highly hydrogenated organic components and probably account for the high HI values measured in PF3 (up to 300).

As far as our studies are concerned, it is worth noting that, although the sediments pertaining to these palynofacies are geometrically close to each other, the three facies contain organic matter remains that are *quite different in terms of preservation*. The "regular" alternation of these palynofacies (and associated vegetal remains) suggests that the geological context (presence or absence of clay) and diagenetic history must account for these differences.

The above-mentioned results have been submitted for publication in a German review (De Putter *et al.* (a), submitted). Further analyses have been performed to check the presence of proteins in some samples (seeds, twigs). Results, however, indicate that the protein content of the samples are in the same range as that of the surrounding soils, with high N_3 content owing to the low pH values of these soils.

C.2. Results in REE and trace element migration and trapping.

Percolating acidic fluids involved in the deepening of the ESEM cryptokarsts have transformed the mineralogy of i) the continental sands filling the karsts and ii) the marine clays deposited in the bottom of the sinkholes. Trace element (V, Rb, Y, Zr, Nb, Ba, REE, Hf, Ta, W, Pb, U, Th) content of the karst sedimentary infilling is used to constrain the fluid/sediment interaction. As previously stated (section A), special attention is paid to the REE mobilization since these elements are involved in the problem of radwaste geological disposal, as fission products and chemical analogues to some actinides and Th.

Our study suggests that the REE contained in the heavy minerals of sands have undergone little or no migration, except for the LREE mobilized by the dissolution of accessory monazite, which are trapped in epigenetic minerals ([Ce,Pb,Co] alumino-silicates, [Ce,Mn,Pb] oxyhydroxydes and less frequent Ce-rich glauconite). As no Mn-LREE minerals were previously known, the systematics of our [Ce,Mn,Pb] oxyhydroxydes is currently investigated. They should be compared to some minerals of the (poorly known) rhabdophane group, although none of these minerals contain Mn.

On the other hand, the REE adsorbed onto the marine clays are mobilized by phosphatic complexes [$Ln(H_2PO_4)^{2+}$] and trapped a few decimeters below their starting point, in the epigenetic clays - kaolinite, halloysite - formed at the interface between the karst infilling and its carbonated substratum. Secondary monazite concomitantly precipitates and occurs in some samples as euhedral and well-graded micro-crystals associated with clay pellets.

Our study suggests that clay neoformation and REE trapping in secondary monazite were synchronous. Low p fluids, enriched in Al, Si and REE phosphatic complexes, percolated in the most permeable parts of the limestone beds of the substratum (stratification seams, fissures). As a consequence of the chemical reaction between H_3O^+ and $CaCO_3$, p slowly rises, creating geochemical conditions favouring kaolinite (high p, efficient drainage) and halloysite (high p, reduced drainage due to kaolinization) neoformation, as well as REE trapping (De Putter *et al.* (b), submitted).

With regard to the migration and trapping of trace elements (others than REE), work is still in progress; however, our preliminary results confirm that there is an efficient trapping of these elements, that were also mobilized from the chemical decomposition of the accessory minerals, on the neoformed clays. Selective trapping, however, occurs : a preferential Th concentration is observed in kaolinite, while halloysite concentrates Ba, Ni, Sr and, to a lesser extent, Cr, Pb & Co. Current data suggest that, although a direct adsorption process of the trace elements on the clay minerals cannot be ruled out, the neoformation of accessory minerals, which in turn are physically immobilized by the surrounding clay beds, is highly probable.

In a broader context, the main asset of the current geochemical study lies in the demonstration of the efficient setting of short-distance (i.e. decimetric) chemical equilibria. The whole system is believed to have quickly turned into a geochemically "closed" state, probably due to the impervious character of the epigenetic clay minerals. As the geochemical environment of the studied sites were chemically highly aggressive, we should refer to the actual short-distance

migration of REE and trace elements in the ESEM analogue as to highly conservative values, with reference to the safety assessment of high-level radwaste geological disposal projects.

Conclusions

Current work shows that the Entre-Sambre-et-Meuse cryptokarsts are highly potential natural analogues.

The good preservation of Miocene (*ca* 10 m.y.) wood fragments, which still retain significant part of their hemicellulose and cellulose content, illustrates the isolation capacity of the clayey peat in which they are embedded. Current work focuses on the preservation of other fragile organic molecules, such as proteins.

The mobilization and trapping of trace elements (especially REE) is being studied thoroughly. It appears to be controlled by accessory minerals dissolution and/or neoformation, the latter process being intimately linked to extensive halloysitization-kaolinitization. REE and trace element distribution patterns suggest that the small-scale studied systems acted as closed ones, which still increases the interest of the ESEM analogue. This research also provides new data on the migration of REE in continental sedimentary environments subjected to intense (but non-lateritic) weathering and on some aspects of the LREE mineralogy. It would, in our opinion, require a long-term study project.

Selected references

De Putter, Th., Thonart, P., Roblain, DK, Dupuis, Ch., Nicaise, D., 1994. Preservation of wood components in Miocene trees of the Entre-Sambre-et-Meuse area (Southern Belgium). Abstract volume, 6th International Workshop on Plant Taphonomy : 5.

De Putter, Th., André, L., Nicaise, D., Dupuis, Ch., (b) submitted. Trace element mobilization and trapping in the Cenozoic cryptokarsts from Southern Belgium. E.U.G.-8 Strasbourg meeting, abstract book.

De Putter, Th., Dupuis, Ch., Fairon-Demaret, M., Nicaise, D., Roblain, D., Roche, M., Thonart, P., (a) submitted. A brief sketch of the Entre-Sambre-et-Meuse (Southern Belgium) Miocene wood fragments taphocoenosis. Ns Jahrb. für Geol. und Paläont.

Title :	The treatment of uncertainty in groundwater flow and transport modelling
Contractor:	AEA Technology, Windscale, UK.
Contract N°:	FI2W-CT91-0088
Duration of contract:	1 April 1991 to 31 March 1995
Period covered:	1 January 1994 - 31 December 1994
Project leader:	Dr J D Porter

A. OBJECTIVES AND SCOPE

Analysis and understanding of the groundwater flow in the neighbourhood of a radioactive waste repository play important roles in a performance assessment. Such analyses rely on numerical modelling in order to study the flow and transport over the very long times that must be considered. Two vital issues which must then be considered are the way in which the available data are used in constructing the mathematical model of the site and the uncertainty that is implied in the results of the model by uncertainties in the model parameters and in the model itself. The two tasks in this project address these issues. The first task is concerned with the investigation of novel approaches to the construction of mathematical models of a site. The second task is concerned with the investigation of methods for the estimation of uncertainty in groundwater flow and transport calculations.

B. WORK PROGRAMME

Task 1: Site Characterisation

1.1 Site Models: Mathematical models that can be used to represent a site will be reviewed. A computer package based on a selected method will then be written.
1.2 Inverse Problem Techniques: Methods for the inverse problem will be investigated and a selected approach will be applied in conjunction with the site models developed in Task 1.1.
1.3 Effective Properties: Methods for relating measured data to model parameters will be investigated using numerical calculations, based on the site models developed in Task 1.1.

Task 2: Treatment of Uncertainty

2.1 Methods for the Treatment of Uncertainty: Methods for the estimation of uncertainty in the results of groundwater flow and transport models will be investigated.
2.2 Parameter Sensitivity: Methods for the estimation of sensitivity coefficients will be investigated. The coefficients will be used to study the topic of data worth.
2.3 Model Uncertainty: The study of this topic will build on experience of "what-if" studies and will pay particular attention to long-timescale changes in hydrogeology.

C. PROGRESS OF WORK AND OBTAINED RESULTS

State of Advancement

Task 1: Indicator geostatistical methods [1,2,3] were selected for investigation in this project and have been used to analyse the distribution of clay at the Gorleben site [4]. Indicator Kriging (i.e. interpolation of the indicator function to generate a clay distribution on a cross section of interest) has been carried out, particularly for the cross-section used as the basis for groundwater modelling in the international INTRAVAL project [4]. It has been concluded that the method only produces clay distributions with the degree of continuity seen in geological interpretations of the site data if the geostatistical analysis takes account of the stratigraphy of the system. This has been achieved using a coordinate transformation.

Tasks 2: A method of estimating the uncertainty in steady-state groundwater flow and solute transport calculations, based on the evaluation of an appropriate adjoint state [5] has been implemented in the AEA Technology groundwater flow code NAMMU [6,7] and fully tested and documented. The method allows the sensitivity of performance measures such as velocity at a point, travel time from a point, concentration and various weighted combinations of the results of flow and transport calculations to be efficiently calculated. The sensitivities can then be used in the estimation of the uncertainty in the performance measures.

Progress and Results

Task 1: Site Characterisation

This task is concerned with the investigation of methods for the construction of mathematical models of a site. Work in this area has concentrated on the application of Indicator geostatistical methods [1,2,3]. In particular, binary indicator geostatistics has been used to analyse the distribution of clay at the Gorleben site, using petrographic data from 92 boreholes [4]. An indicator function is defined which takes the value 1.0 in the part of a borehole log which contains clay and takes the value 0.0 in the rest of the log. The function therefore describes the probability of finding clay at a given location. The clay stratum has been selected for study because the clay has a much lower permeability than any of the other materials present in the model area (sands, silts, gravels) and so it can be anticipated that the distribution and continuity of the clay will have a strong influence on the groundwater flow at the site.

An experimental variogram for the indicator variable (rock type) was inferred from the data and fitted by a theoretical model. Indicator Kriging (i.e. interpolation of the indicator function to generate a clay distribution on a cross section of interest) is then performed using the model variogram. In a series of tests it was found that indicator Kriging only produces clay distributions with the degree of continuity shown in the geological interpretation of the site data if the geostatistical analysis takes account of the

stratigraphy of the system. In particular, the variogram and Kriging analyses must be performed in a coordinate system that follows the changes in the elevation of the strata. This is done by transforming the vertical coordinate in the borehole logs so that the top and bottom of selected 'marker horizons' in each borehole are mapped to constant vertical coordinate values. The discretisation of the borehole logs and the subsequent variogram analysis are then carried out in the transformed system.

A disadvantage of the transformation approach arises from the fact that it is then necessary to carry out the indicator Kriging calculations in the transformed coordinate system, i.e. Kriging is performed at a set of points defined in the transformed coordinates. The results of Kriging must then be mapped back to the original coordinates in which the data was supplied before they can be compared in detail with the geological interpretation for the site. This issue was addressed in the last year and a method of implementing the inverse transformation numerically has been designed and implemented.

The assignment of facies types in the borehole log has also been investigated. This can have a significant impact on a normal geological interpretation. The logs supplied with the original data set [4] only gave main components in each section of the boreholes. More detailed borehole logs, giving more information on the materials present (e.g. 'silty clay' or 'clayey silt') are now available. This information can be taken into account in the Kriging analysis if it is used to influence the assignment of the indicator variable. In the period covered by this report, the entire geostatistical analysis, from variogram estimation onwards was repeated twice, using different versions of the indicator data based on the more detailed information in the most recent version of the borehole logs. The results show that the reinterpretation of the borehole logs has a significant impact on the predicted continuity of the clay layers. Overall, the results demonstrate that the indicator Kriging method can quickly show the impact of different interpretations of the borehole logs and can give results that are in good agreement with a geological interpretation, where that interpretation is well founded on the borehole data.

Task 2: Treatment of Uncertainty

The aim of Task 2 is to investigate methods for the treatment of uncertainty in groundwater flow and solute transport calculations. A method of estimating the uncertainty in steady-state groundwater flow and solute transport calculations, based on the evaluation of an appropriate adjoint state [5] has been implemented in the AEA Technology groundwater flow code NAMMU [6,7] and fully tested and documented [6]. The method makes it possible to compute and display the sensitivity of many performance measures (results of interest) to particular input parameters and boundary conditions of a numerical model. Performance measures related to the groundwater flow equation that are currently supported, and an indication of their relevance are as follows:

- the specific discharge at a point. This could be used to quantify uncertainties in flow rates;

- the components of the specific discharge;

- an area-weighted velocity magnitude. This could be used to estimated the uncertainty in the groundwater flux out of a particular volume;

- pressure;

- a weighted average pressure over a set of points. This could be useful in model calibration;

- travel time along a pathline from a location of interest This could be used to estimate the uncertainties in groundwater travel times from a repository location.

In addition, the implementation of the method has been extended to the steady-state solute transport equation [8]. Available performance measures related to the solute transport equation are:

- a weighted average of solute concentration at a set of points. This could be used to estimate the uncertainties in predictions of solute concentration in a subdomain (e.g. a particular stratum);

- a weighted average difference between measured and predicted solute concentration. This could be useful in model calibration;

- a weighted average of solute fluxes at a set of points. This could be used to estimate the uncertainties in the flux out of a potential repository zone;

- integrated flux of solute through a surface. This could be used to estimate the uncertainties in the rate of discharge to the biosphere.

The implementation of the adjoint method in NAMMU thus provides the facility to estimate efficiently the sensitivity of a wide range of performance measures to the input parameters and boundary conditions of a numerical model. The solution of the adjoint equation is naturally based on the same form of discretisation as that used for the groundwater flow and transport equations. However, because the range of discretisation methods available within the NAMMU code has recently been extended [6], further work has been undertaken in order to ensure that the adjoint method could also be used with the new discretisation methods. In particular, a new type of finite element known as the 'mixed element' has been developed for use with NAMMU. These elements have computational advantages for pathline calculations and situations where precise local mass balance is important. They obtain these advantages by treating the pressures and velocities on the elements rather differently from the standard finite elements that were used in the past. Verification of the mixed element version of the adjoint routines is underway for pressure, specific discharge and travel time performance measures associated with the two-dimensional groundwater flow equation. The PACOMA example [9] is being used as a test case.

ACKNOWLEDGEMENT

This project is cofunded by the Nirex Safety Assessment Research Programme (NSARP) of UK Nirex Ltd.

REFERENCES

1. A.G. Journel, *Imaging of Spatial Uncertainty: A Non-Gaussian Approach* in Geostatistical, Sensitivity and Uncertainty Methods for Groundwater Flow and Radionuclide Transport Modelling, B.E. Buxton (Ed.), Battelle Press, 1989.

2. G. Matheron, H. Beucher, C. de Foquet and A. Galli, *Conditional Simulation of the Geometry of Fluvio-Deltaic Reservoirs,* SPE Paper 16753, 1987.

3. J.D. Porter, *Application of indicator geostatistics to the Gorleben data set,* Proceedings of the 4th International High Level Waste Management Conference, Las Vegas, B Cole (Ed.), American Nuclear Society, 1993.

4. *INTRAVAL Phase II Test Case: Saline groundwater movement in an erosion channel crossing a salt dome.* Bundesanstalt für Geowissenschaften und Rohstoffe.

5. J.L. Wilson and D.E. Metcalfe *Illustration and Verification of Adjoint Sensitivity Theory for Steady State Groundwater Flow,* Wat. Resour. Res. **21**, 1602, 1985.

6. L.J. Hartley, C.P. Jackson and S.P. Watson, *NAMMU (Release 6.2) User Guide,* AEA Report AEA-ESD-0138, 1994.

7. S.T. Morris, *NAMMU (Release 6.2) Reference Manual: NAMMU Commands,* AEA Report AEA-ESD-0144, 1994.

8. L.J Hartley, *Adjoint Sensitivity Analysis of Steady-State Solute Transport,* in Computational Methods in Water Resources X, A. Peters et. al (Ed.), Kluwer Academic Publishers, Dordrecht, 1994.

9. K.H. Winters, C.M. Clark and C.P. Jackson, *The UK Contribution to the CEC PACOMA Project: Far-field Modelling of Radioactive Waste Disposal in Clay,* Nirex Safety Studies Report NSS/R185, 1990.

Title	Uncertainties in the modelling of migration
Contractors	Risø National Laboratory, Denmark
Contract N°	FI2W-CT91-0089
Duration of contract	September 1991 - August 1994
Period covered	January - August 1994
Project leader	B. Skytte Jensen

A. OBJECTIVES AND SCOPE

The objectives of the present investigation is to estimate the uncertainties to be ascribed to the results of modelling of diffusion and convective flow in heterogeneous media.

Especially the uncertainties which are the consequences of the possible presence of unidentified heterogeneities in a given formation will be considered.

Only recently has attention been paid to the uncertainties to be ascribed to the modelling of migration, wherefore the relevant tools have not been firmly established yet.

Several approaches are possible in such studies mostly related to experimental field or the laboratory. In the present investigation, "computer-experiments" alone will be used as the tool.

B. WORK PROGRAMME

To investigate the effects of "inserting" heterogeneities in two - and three dimensional "geological formations" on both diffusion and convective flow.

To develop the relevant mass-conserving algorithms which can handle diffusion in heterogeneous media.

To study the influence of "heterogeneities"on two dimensional convective flow by means of conformal mapping.

To investigate the possibilities of describing flow in interconnected fractures in the light of the previous studies.

C. PROGRESS OF WORK AND OBTAINED RESULTS

By 2D-modelling of convective flow under diverse geometrical conditions by means of conformal mapping techniques it has been shown, that pure convective flow may show pronounced longitudinal dispersion effects, although none such is assumed to occur within the individual flowtubes.
It was also shown, that the magnitudes of the calculated dispersions depends highly on the way "samples were extracted" from the set of calculated flowtubes, indicating that similar uncertainties have to be ascribed to field data.
The calculations have been performed by means of the programs HETEFLOW and SOURCEFLOW.

By semi-quantitative arguments have been demonstrated, that transversal dispersion effects will be expected to arise by convective flow in 3-D systems.
It is obvious, that due to the often pronounced concentration gradients arising in such calculations, unavoidable diffusion reactions will in actual systems tend to level these gradients out, wherefore modelled and experimental data will not be expected to coincide closely.

An important observation from these calculations is, that the modellings of different sampling techniques give an indication of the types of uncertainties if not their magnitudes, which have to be ascribed to experimental data obtained by sampling in the field. Due to these uncertainties it will hardly be possible by calculating backwards to identify or characterize the geological structures, which have been passed by the flow. If other evidence is not available, the model used might well be grossly in error due to mere ignorance.

The flow of water through fractured rock is often modelled by analogy to the flow of electricity in a network of conductors by means of the Kirchoffs equations. This may work well for the flow of water, but to describe the flow of dissolved material the dispersion is alone "explained" by assuming different distributions of permeabilities and hold-up volumes in a large number of individual paths. This "explanation" is not supported by the present study, which also ascribes dispersion effects to the individual paths, wherefore the passage through a small number of fractures might well be described. The former model may not give meaningful dispersions in this case.
In a recent investigation the dispersions expected by flow through a series of interconnected fractures have been investigated.
The flow in a single fracture was considered being adequately modelled as the flow from a source to a sink in an infinitely large two-dimensional layer. The distance between the source and sink is assumed to be finite, and may even be very small.
In a previous report has been shown, that a plug of dissolved matter in the inlet at the source will demonstrate a pronounced "dispersion" with time, when concentrations are measured at the outlet from the sink.

The mathematical expressions describing this ideal system have been derived -or approximated satisfactory - allowing for the calculation of concentration distributions obtained after the passage of any concentration distributions entering a source-sink system.

In figure 1. are given a couple of examples of different concentration distributions as input (F_i's) and how they are changed after the passage of one, two and three identical source-sink systems connected in series.($w_{i,0}$, $w_{i,1}$ and $w_{i,2}$)

Figure 1.

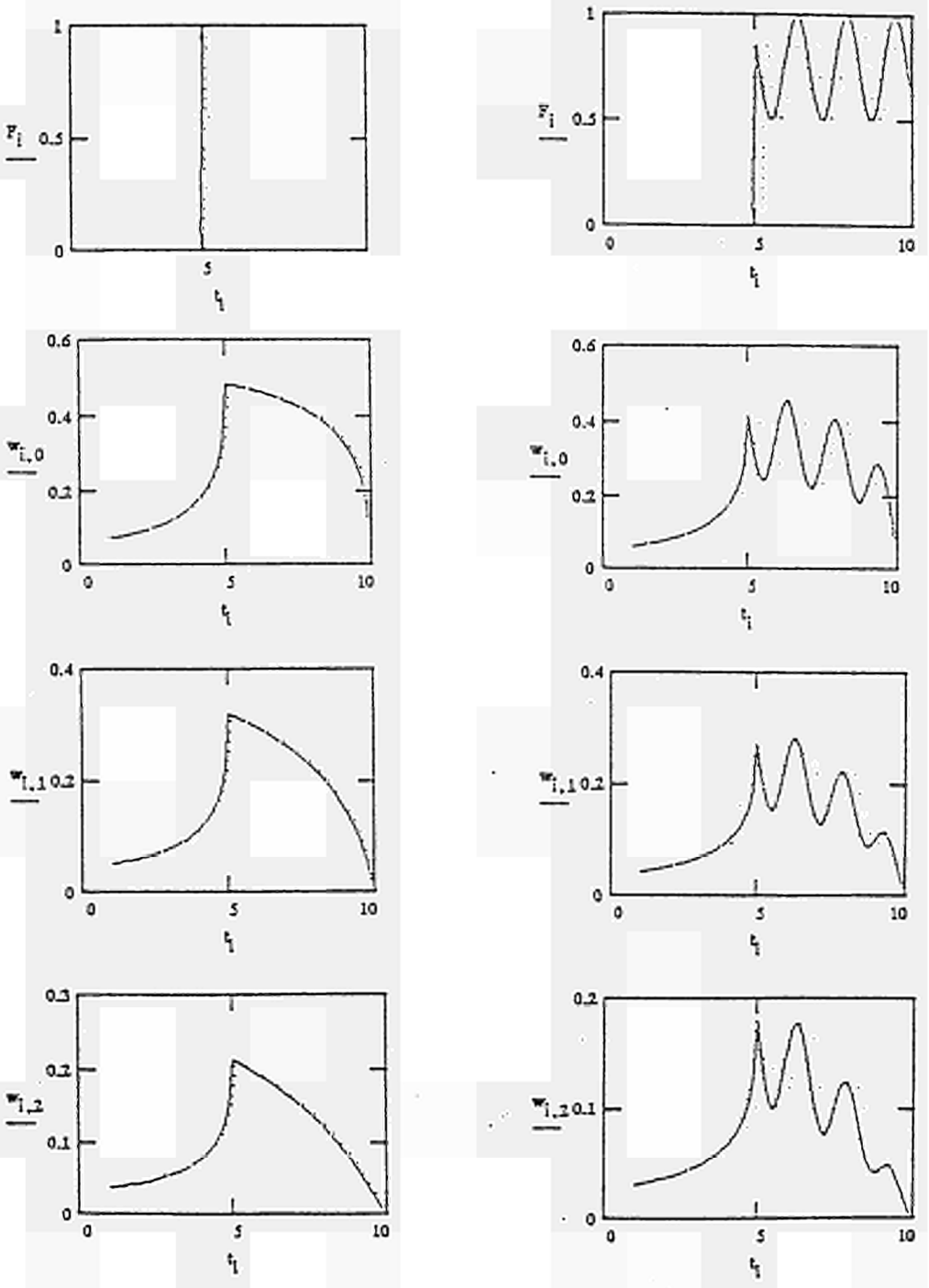

It has been shown, that in an ideal source-sink system as the one investigated, appr. half of the added amount in a plug will pass the system quite rapidly and the rest more slowly giving rise to an infinite tailing.

In actual non-infinite systems the initial phase is believed to be quite similar to that for the infinite fracture, whereas the tailing is expected to approach zero at a steeper rate.

In figure 1, presented above, has been used a "normalized" time, t_N, as the abscissa. This time has been shown to be related to the real time, t_R, by the formula:

Eqn. 1

$$t_R = L^2 * t_N$$

where L is the distance between the source and sink.

It will therefore be possible to model the effect of transport through a series of dissimilar source-sink systems in real time, even if the source-sink distances vary.

The graphs shown above demonstrate clearly, that a series of connected source-sink systems are quite effective in eliminating peak concentrations and in effectively diluting an added amount of a solute into the passing solvent.
The pattern observed is similar to that expected for non-equilibrium flow through a system with large dead-end pores.

When branching transport between several source-sink systems are possible, this effect is expected to be even more pronounced.

In the following figure 2. is given another example, in which is shown the concentrations distributions expected by passage of a plug through source-sink systems differing in the distance between the source and sink by a factor of two, when plottet versus real time, t_R.

Figure 2.

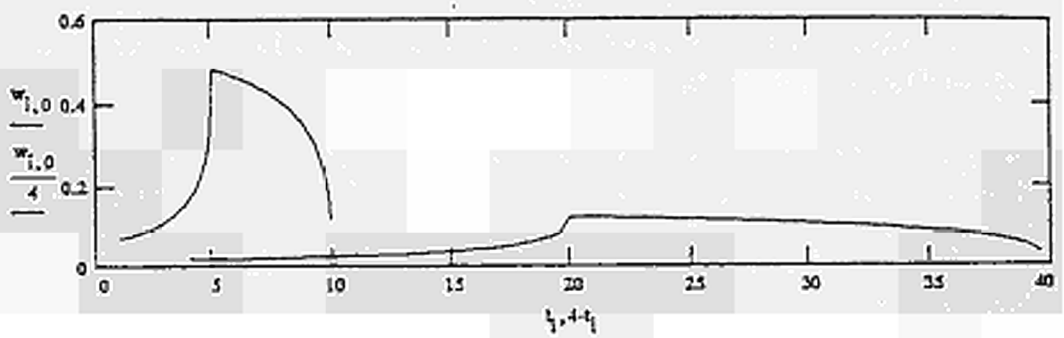

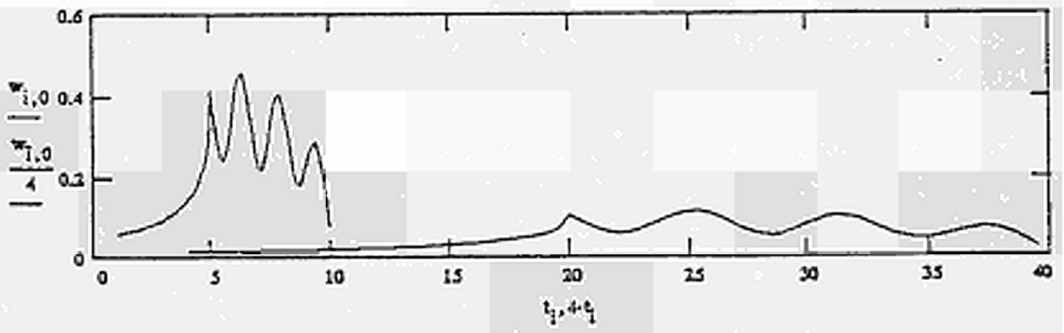

Title	Unbiased Guess as a Concept to Cope with Fuzzy and Random Parameters in Geochemical Modelling
Contractors	BRENK SYSTEMPLANUNG
Contract N°	FI2W-CT91-0090
Duration of contract	1 June 1991 - 30 September 1994
Period covered	1 January 1994 - 30 September 1994
Project leader	H.D. Brenk

A. *OBJECTIVES AND SCOPE*

Any risk analysis dealing with the transport of radionuclides from a radioactive waste repository on the basis of deterministic equations suffers from two severe problems. Firstly, all processes in reality are random in nature and, secondly, the data basis and the knowledge about the relevant processes will never be complete. The aim of the study is to investigate the applicability of fuzzy set theory in decision making and the potential of information theory in this context. Since ambiguity in the valuation of models and model parameters represents the main obstacle for a consent about the results, it seems very promising to apply a kind of maximum entropy method, the "method of unbiased guess", in order to deal with incomplete knowledge. While the incorporation of randomness into this approach is straightforward adequate methods have to be developed in order to deal with incomplete knowledge or subjective quantities (i.e. expert judgement). The main aim of the study is to propose a theoretically well-founded formalism serving this purpose. The capability of this formalism will be demonstrated on a non-trivial migration problem.

B. *WORK PROGRAM*

1. Compilation of the relevant aspects of information theory. Special emphasis is put onto the method of unbiased guess and its theoretical foundation.
2. Discussion of the problems of geochemical modelling in risk assessments with respect to uncertainty using probability density functions and the theory of fuzzy sets.
3. Development of a formalism for a consistent and unambiguous incorporation of incomplete knowledge employing the method of unbiased guess.
4. Demonstration of the applicability of the formalism using a simulated migration problem as a test case.
5. Documention
6. Project coordination

C. *PROGRESS OF WORK AND OBTAINED RESULTS*

This project was completed during 1994 and the final report has been accepted by the Commission for publication in the EUR series. The following is the summary from the final report.

Summary

This work is concerned with the problem of making assertions on propositions, which contain different kinds of uncertainties. It is shown, how the uncertainties coming from statistical data, expert knowledge and linguistic inaccuracies can be represented by probability densities, possibility distribution functions and membership functions, which define random variables, fuzzy variables and fuzzy sets. Based on these representations, two suggestions have been worked out to handle the problem of mixed uncertainties, which do not allow a purely probabilistic or possibilistic treatment. The most important result of these investigations is a sequence of inequalities between formal probabilities, possibilities, necessities and some 'mixed measures'. The inequalities are a consequence of a probability/possibility transformation derived within this project, which maps probability densities to possibility distribution functions and vice versa. Initial implementation of the corresponding numerical algorithms on a computer and the application to a very simple hypothetical geochemical transport problem were carried out. Extensive calculations of synthetical examples and realistic applications is the subject of future work.

Title: Thermal, mechanical and hydrogeological properties of host rocks for deep geological disposal of radioactive wastes

Contractors: INTERA (UK), ANTEA-BRGM (F), BGR (D), ISMES (I)

Contract N°: FI2W/CT94/0126

Duration of contract: From 01.08.94 to 31.01.95

Period covered: August 1994-December 1994

Project leaders: N. Chapman, INTERA (UK) (Coordinator); B. Côme, ANTEA-BRGM (F);M. Langer, BGR (D); F. Gera, ISMES (I)

A. OBJECTIVES AND SCOPE

The Commission of the European Communities has supported in its subsequent R&D programmes on Management and Storage of Radioactive Waste, a large number of research activities on the characterisation of potential host rocks for deep geological repositories. Such R&D programmes have been carried out also in countries non-member of the European Union. Coming to the end of its fourth five-year (1990-1994) R&D programme, the Commission would like to have carried out a review study and evaluation of the state-of-the-art on current relevant knowledge. The objective of this evaluation will be to provide the Commission with advice on the most important issues where further work is required. The review study will focus on deep geological disposal of long-lived waste in saliferous, argillaceous and crystalline rock formations.

B. WORK PROGRAMME

The following questions are to be addressed:

- Scope of the available data
- What information is still needed?
- What information is not needed?
- Where are the major uncertainties?
- How could the information be obtained?
- Are there site-specific aspects?
- How can the EC help to coordinate further work?

The findings will be presented in a report of about 150 pages target length.

C. PROGRESS OF WORK AND OBTAINED RESULTS

In conducting the review a number of linking themes emerged which could be regarded as common, non-formation specific issues which might usefully underpin the up-coming EC radioactive waste management programme:

- **Treatment of spatial variability.** Understanding of the heterogeneous nature of flow and transport systems and the geomechanical properties of geological formations at all scales has increased considerably over recent years. However, there is still a long way to go in terms of translating this information into appropriate models to predict system behaviour and towards testing these models against field experiments at scales representative of the repository system and the far-field. Rigorous methods for detecting and defining spatial variability, describing it in models, testing and validating these models and quantifying the uncertainties involved, should form a focus of work in every area of the future programme.

- **Developing and testing alternative conceptual models.** The identification of alternative conceptual models of THM processes at all scales and the development of techniques for comparing and testing them should feature in the future programme. A properly structured programme should ensure that this procedure is rigorous and well documented in an effort to avoid any gaps. A similar approach also needs to be adopted towards identifying and testing alternative models for the large-scale behaviour of potential repository sites, implying placing emphasis on comprehensive site characterisation projects (see below).

- **Treatment of uncertainty.** Translating information from field and laboratory tests aimed at quantifying THM properties of geological formations involves the propagation of various levels of uncertainty. Techniques for identifying and quantifying these uncertainties, reducing them wherever possible and ensuring that they are adequately treated and propagated through a safety assessment should be incorporated into all projects in the future programme.

- **Integrated projects at well characterised field sites.** It is believed that considerable benefits would accrue from integrating a number of experimental projects at well-characterised field sites with access available both from the surface and from underground facilities. This would enable concentration of effort, economy of resources and the widest use of the available data. Focusing the efforts of a number of teams on defining projects and measurement programmes would allow a wider range of alternative interpretational approaches to be tested and would generate larger datasets. This approach would be especially valuable in addressing the themes in the three preceding bullet points. In addition, this aspect should be well-integrated with similar suggestions from the other (geochemical) review group.

The conclusions of the reviewers in each of the three regional environments were presented at the one-and-a-half day workshop in Brussels from 12-13 January 1995. (Ref.1)

The closing discussion session concentrated on the critical issue of how the European Commission is to make the best use of its funding by focusing on a limited number of well co-ordinated projects which address key issues. Various ways of defining such a small group of projects, which integrate individual research projects into larger 'umbrella' projects, were discussed. These included focusing on:

- specific technical issues emerging from the review (e.g. gas)
- specific sites
- general themes (e.g. uncertainty).

A proposal was made to establish five umbrella projects which could integrate proposals received under the general and specific headings in the Call for Proposals Information Package.

These proposed umbrella projects are listed below.

Possible Co-ordinated Projects
TCHM* performance of clays, focused on identifying and characterising: • potential mechanisms which would cause near-field behaviour to diverge from that predicted in performance assessments • the behaviour of clays as a far-field barrier to advection and diffusion, paying particular attention to membrane effects, techniques for hydraulic characterisation of clay formations and interpretation of long-term, large-scale hydraulic behaviour.
Gas, in **all** geological environments, addressing: • pressure dissipation and migration mechanisms from a repository • the use of natural gases in establishing spatial variability in gas & hydraulic conductivity of geological formations and structures at specific sites.
Testing alternative conceptual models for groundwater flow (and, in connection with MIRAGE, transport) in heterogeneous fractured rocks, using both underground research facilities and groups of deep boreholes.
Further studies of the coupled TCHM aspects of brine migration in salt formations and, in particular, in crushed salt backfill materials.
Palaeohydrogeological ('geoprospective') studies of the stability and evolution of deep groundwater fluxes in **all** geological environments being considered for disposal purposes.

*TCHM includes the important couplings of **chemistry** with THM processes. A number of contributors to the workshop identified this as an extremely important issue which should not be overlooked in interpreting field and experimental results.

References

B. Haijtink (ed.) Testing and modelling of thermal, mechanical and hydrogeological properties of host rocks for deep geological disposal of radioactive waste. Proceedings of a workshop. Brussels 12-13 January 1995. EUR 16219 (1995)

Title: Radionuclide transport through the geosphere into the biosphere. Review study of the project MIRAGE.

Contractor: CEA-IPSN (F)

Contract N°: FI2W/CT94/0128

Duration of contract: From 01.07.94 to 31.12.94

Period covered: July-December 1994

Project leader: P. Escalier des Orres, CEA-IPSN (F) (Coordinator); J. Bruno, INTERA (E); J. Kim, FZK-INE (D); A. Maes, K.U.Leuven (B); G. de Marsily, Univ. P.&M. Curie (F); R. Wernicke, GRS (D)

A. OBJECTIVE AND SCOPE

The objectives of this review study was to come to a critical evaluation of the state-of-the-art in the different research areas of the EC coordinated project MIRAGE (MIgration of RAdionuclides through the GEosphere) which was launched by the Commission in 1983. The study focused on the research work covered under the umbrella MIRAGE such as geochemical behaviour of radionuclides in natural aquifer systems including colloids and organic materials, natural migration systems including Natural Analogue Studies, modelling of radionuclide migration including model verification and validation and finally migration and retardation experiments performed by laboratory and in-situ tests.

The review study was carried out by a team of experts from six organisations with two main goals in mind:

* to evaluate how the results obtained from the MIRAGE project contribute to performance/safety assessment of deep geological disposal of radioactive waste and
* to provide the Commission with advice on the most important issues where further work is required in the Commission 4th R&D Programme on Nuclear Fission Safety (1994-1998) and where our understanding is sufficient.

B. WORK PROGRAMME

The topics which needed to be performed within the review study were:

* Chemistry of actinides and fission products in natural aquifer systems
* Water-rock interaction, radionuclide transport modelling and data collection
* Natural analogue studies
* Geochemical modelling in the frame of the CHEMVAL project
* Contribution of the MIRAGE project to safety assessment of geological disposal.

Whereby the work has been guided by the following questions:

- Scope of the available data
- What information is still needed, in which format (qualitative/quantitative), for use in?
- How could the data, information be obtained?
- What information is not needed?
- Where are the major uncertainties?
- Are there site-specific aspects?

C. PROGRESS OF WORK AND OBTAINED RESULTS

The conclusions which have been reached at the end of the review work in the different research fields involved in the project MIRAGE can be summarised as follows:

- **BASIC MECHANISMS UNDERSTANDING**

Complexation with natural organics

The complexation of long-lived radionuclides, especially tetravalent actinides ions, with natural organics, mainly humic acids, may either enhance or delay their migration, depending on the prevalent hydrochemical conditions. This mechanism is thus one of the issues for a long term performance/safety assessment. The main line of the recommendations relies on the need for a better understanding of complexation phenomena under natural conditions, e.g. a medium high pH range [pH = 6-9] with the presence of competing ligands or migration behaviour of actinides humate complexes in various hydrogeological environments, including fractured crystalline rocks or porous sediments. The objective will be at the end, to reach a consensus on the reaction to be considered at the heart of the modelling.

Colloid generation and colloid transport

The formation of pseudocolloids of actinides or some fission products with the potentiality to facilitate the migration of the radionuclides, appears to be one of the key uncertainty in the performance/safety assessment. The main recommendation, in consistency with the previous paragraph leads to put the effort on the natural hydrogeological systems [porous aquifer medium & fractured-rock flow systems]: quantification of aquatic colloids of different origin, pseudocolloid generation, quantification of the reaction mechanisms, modelling of RN pseudocolloids migration. The recommendation does not preclude the need for migration experiments with large scale columns.

- **SITE CHARACTERISATION**

Uncertainty and spatial variability

Either for porous-aquifer or fractured-rock flow systems, an effort has to be done on the geological modelling for a better conceptualisation and representation of the rock facies [petrography and structure], the geochemical characteristics, fracturation [scales, mineral coatings]. This modelling has to include uncertainties such as stochastic models for the parameter spatial distribution or alternative conceptual models. This step is a prerequisite to predict migration conditions and the near-field evolution. Upscaling local rock properties is one of the difficulties that will have to be investigated and validated by in situ work.

- **INTEGRATED STUDIES ON SITES**

The two previous issues need to be achieved through validation on real sites. These sites should represent [regarding the EU deep geological disposal programmes] for sedimentary systems, deep clay and salt-dome environments and fractured rock environment for crystalline formations. A special attention should be dedicated to natural tracers [palaeohydrogeology methods].

Natural analogue studies should also take benefit from a comprehensive, coordinated and correlated approach involving the different disciplines such as geology, geochemistry, hydrogeology and hydrochemistry.

The reviewing on the CHEMVAL project concludes to the necessary link between testing and development of geochemical transport modelling with the natural systems studies and real sites above-mentioned. It will be in particular, the opportunity to take into account kinetics in the water-rock interactions and to address all the inherent uncertainties.

• METHODOLOGICAL RECOMMENDATIONS

Data acquisition

Data and parameters will have to be of a documented quality for use in performance and safety assessments. Uncertainties associated with data, will have to be addresses and where possible, probability density functions should be provided. More generally, well documented data sets, systematic transparency of the assumptions associated to expert judgement, and peer review will enhance confidence building.

Publication policy

The rate of peer reviewed publications in the past MIRAGE projects, as well as publications in non-radwaste literature is very low. It is of primary importance to modify the perception of EC editorial products and to encourage firmly the publications of results in internationally recognised scientific journals. The EC green reports (EUR reports) could have their editorial policy modified in order to incorporate peer reviews and to, maybe, give them a more synthetic content.

• WORKING GROUPS

The establishment of a working group of experts within the concerted actions framework of the next R&D programme is strongly recommended for the thermodynamic database relevant to geochemical modelling, in particular for actinides: compilation, evaluation and validation of the thermodynamic data, sensitivity analysis of the applicability of the existing data.

The reviewers recognise the very good work done by the "NAWG" and this structure could be an example for the management of some of the projects within the MIRAGE project.

Task 5

"Method of Evaluating the Safety of Disposal Systems"

* List of contracts
* Introduction to Task 5

Topic 1 Complements to the previous evaluations

FI2W-CT90-0016 Performance assessment of the geological disposal of spent fuel in a clay layer

Topic 2 Sensitivity studies

FI2W-CT90-0017 EVEREST : EValuation of Elements Responsible for the doses Equivalent associated with the final STorage of radioactive waste

FI2W-CT92-0123 Consideration of environmental changes in long-term radioactive waste disposal system evaluations

INTRODUCTION TO TASK 5 - METHOD OF EVALUATING THE SAFETY OF DISPOSAL SYSTEMS

A. Objectives

The methods developed hitherto shall be up-dated and the relative importance of the various radionuclide release and transport mechanisms assessed. Moreover the analysis should be extended to new types of waste so that a comprehensive safety assessment of disposal systems can be made.

B. Research performed under the 1985-1989 Programme

The projects PAGIS (Performance Assessment of Geological Isolation System for vitrified HLW) and PACOMA (Performance Assessment of Confinement of Medium-level and Alpha waste) have been completed. In addition support studies have been carried out on:
- the assessment of human intrusion into underground repository considered in PAGIS and PACOMA
- modelling the long-term evolution of geological disposal systems
- software quality assurance procedures for risk assessment codes

C. Present programme (1990-1994)

The research work covers two fields:

- Topic 1 "Complements to the previous evaluations"

  - Improved global dispersion models for Iodine-129 and Carbon-14 by NRPB-Chilton. The new models should appropriately represent possible future climatic states, which may influence the long term radiological impact from the two radionuclides.
  - Evaluation of radiological consequences from geological disposal systems in clay of UO_2 and MOx spent fuels (by CEN/SCK Mol). This study will allow to extend PAGIS evaluations to the disposal of unreprocessed spent fuel (UO_2) and recycled fuel at the end of its irradiation cycles.

- Topic 2 "Sensitivity studies"

  - EVEREST (Evaluation of the Elements Responsible of dose Equivalent associated to the final STorage of radioactive waste). This is a multi-partner project (CEA)IPSN; ANDRA; CEN/SCK; GRS and ECN) for studying the sensitivity of evaluated radiological consequences towards the elements of performance assessments (scenarios, phenomena, parameters) for deep waste repositories in granite, salt and clay at different sites.

  - State of the art analysis on environmental changes in the long-term radwaste disposal system evaluations. It should provide a complement to the evaluation of the sensitivity of the parameters related to environmental variations.

Title:	Performance Assessment of the Geological Disposal of Spent Fuel in a Clay Layer
Contractor:	Centre d'Etude de l'Energie Nucléaire - Studiecentrum voor Kernenergie SCK•CEN, B
Contract No.:	FI2W/CT90/0016
Duration of contract:	1 March 1991 - 31 March 1995
Period covered:	1 January 1994 - 31 December 1994
Project leader:	J. Marivoet

A. OBJECTIVES AND SCOPE

Hitherto the performance assessments, which have been carried out within the C.E.C.'s R&D programme on radioactive waste management like PAGIS /1/ and PACOMA /2/, considered mainly waste types which result from the reprocessing of spent fuel. However for technical reasons the recycling cannot be repeated more than three cycles and the economical justification of the reprocessing becomes debatable because of the relatively low cost of fresh uranium. It is therefore reasonable to consider the direct disposal of uranium oxide and/or mixed oxide spent fuels as a realistic option.

The main objective of the study is the evaluation of the radiological consequences of the geological disposal of spent fuel in a hypothetical repository located in the Boom clay layer at the Mol site.

B. WORK PROGRAMME

The work programme consists of the following tasks:

B.1 Data collection
- Spent fuel inventories
- Repository concept
- Near field processes and characteristics
- Far field and biosphere data

B.2 Adaptation of the methodology
B.3 Models and computer codes
B.4 Deterministic calculations
B.5 Stochastic calculations
B.6 Conclusions

C. PROGRESS OF WORK AND OBTAINED RESULTS

State of advancement

The developed near field model considers the radionuclide releases from the various components of the spent fuel. The near field and the clay migration models have been integrated into one computer code, because of the strong coupling of the radionuclide behaviour in these two compartments.

Deterministic calculations evaluated the radiological consequences of the disposal of uranium oxide and mixed oxide spent fuels with burn-up of 33 and 45 GWd/tHM. The computer codes have already been adapted for the elaboration of the stochastic calculations.

Progress and results

C.1 Models and computer codes

Rather simple mathematical models, mainly based on estimated corrosion times, are used to calculate the maximum release rates from each of the five components of the spent fuel; these components are: the gap between the fuel pellets and the hulls, the zircalloy hulls, the structural parts of the fuel assemblies, the grain boundaries of the fuel pellets and the uranium oxide matrix. Because for many radionuclides the effective release from the near field is strongly restricted by their solubility, the near field model takes into account solubility limits.

The NUCDSPF code is a modified version of the NUCDIS code /1,2/ that has been adapted for the spent fuel calculations; it allows to simulate the various release processes in the near field and the migration of radionuclides through the host clay layer.

C.2 Deterministic calculations

Deterministic calculations have been carried out to assess the radiological consequences of the disposal of spent fuel in the Boom clay layer at the Mol site.

The near field and clay compartments are modelled with the NUCDSPF code. An example of the calculated releases from the spent fuel and the resulting concentration in the near field compartment of the clay model is given in Fig. 1 for Pd-107. The Pd is released relatively fast from the grain boundary but its concentration in the near field compartment is strongly limited by its solubility.

The original NUCDIS code is used to simulate the radionuclide transport in the aquifer, because of the importance of the actinide decay chains in the case of spent fuel disposal. The biosphere conversion factors taken from the PACOMA report /2/ are applied to estimate doses from the calculated concentrations in the well water. The evolutions of the doses via the water well pathway calculated are shown in Figs. 2 and 3 respectively for the cases of disposal of spent fuel with a burn-up of 33 GWd/tHM and of MOX fuel with a burn-up of 45 GWd/tHM.

The highest dose rate via the well pathway is due to I-129 and amounts to 3.3 10^{-6} Sv/a for 33 GWd/tHM spent fuel and to 7.1 10^{-6} Sv/a for MOX spent fuel; the I-129 peak occurs after about 60,000 years. Another important radionuclide is Pa-231 which yield a dose of 1.3 10^{-7} Sv/a for both fuel types after 100 million years. Other radionuclides which yield doses higher than 10^{-10} Sv/a are Ra-226, Np-237, Th-232 and C-14.

The highest dose rate from the river pathway is also due to I-129 and amounts to respectively 1.42 10^{-9} Sv/a and 3.00 10^{-9} Sv/a. The dose rates due to other isotopes are all below 10^{-11} Sv/a.

In the calculations mentioned above, the solubility limit of an element is applied to each isotope of that element. However for the uranium decay chains more than one uranium isotope is present and the near field concentration of minor uranium isotopes can thus be much lower than the elemental solubility limit. This effect is especially important for the U-235 decay chain, because the molar fraction of U-235 is only 1.5 %. The result of the application of the distribution of the uranium solubility limit over its isotopes reduces the total dose rate at 100 million years with about a factor 7.

The deterministic performance assessment calculations show that spent fuel is a very stable waste form. The low solubility of the uranium oxide and its low conversion rate has a strong influence on the release of very soluble fission products like I-129. For this kind of radionuclides it is essential to perform a detailed modelling of the release mechanisms from the different spent fuel components and to take the conversion rate of the considered type of spent fuel into account.

The difference between the dose rates calculated for the two considered fuel types is only important for I-129 due to which MOX spent fuel leads to a two times larger dose rate than 33 GWd/ tHM uranium oxide spent fuel.

REFERENCES

/1/ Marivoet, J. and Bonne A., "PAGIS : Disposal in Clay Formations", C.E.C. Report EUR-11776 (1988)

/2/ Marivoet J. and Zeevaert T., "PACOMA : Performance Assessment of the Geological Disposal of Medium-level and Alpha Waste in a Clay Formation in Belgium", C.E.C. Report EUR-13042 (1991)

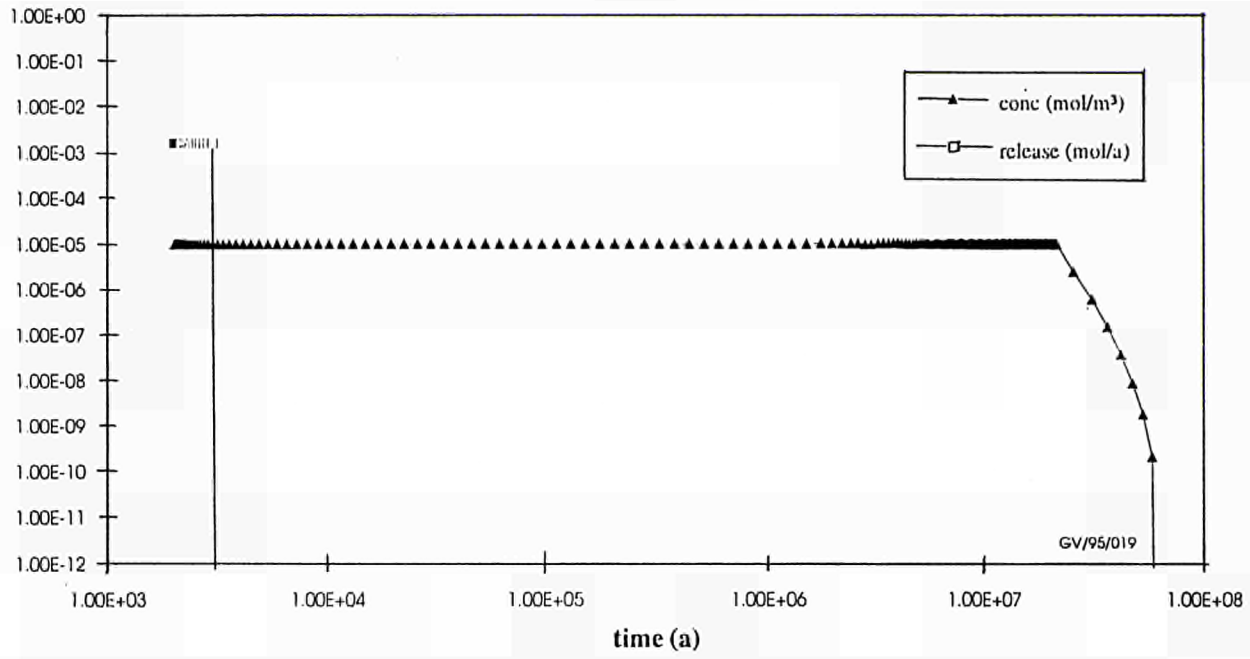

Fig. 1 Evolutions of the release of Pd-107 from the spent fuel and its concentration in the near field for MOX spent fuel

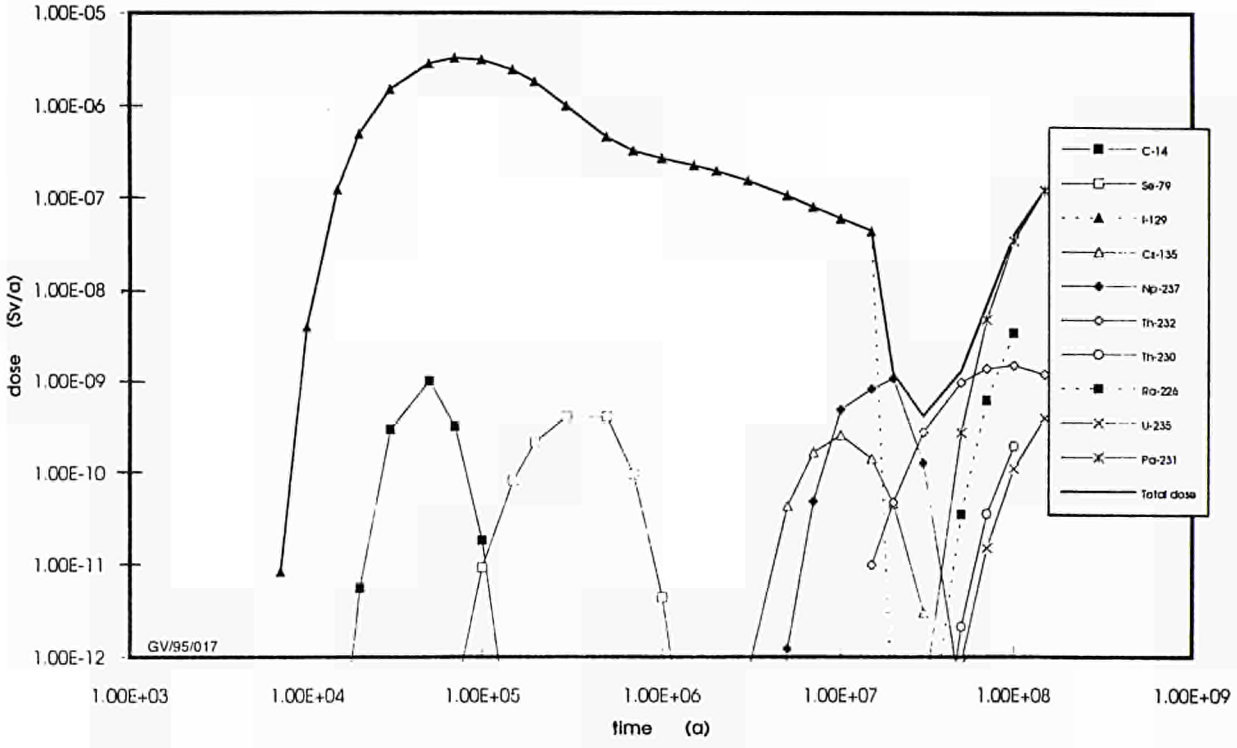

Fig. 2 Evolution of the dose rate via the water well pathway in the case of the normal evolution scenario for 33 MWd/tHM spent fuel

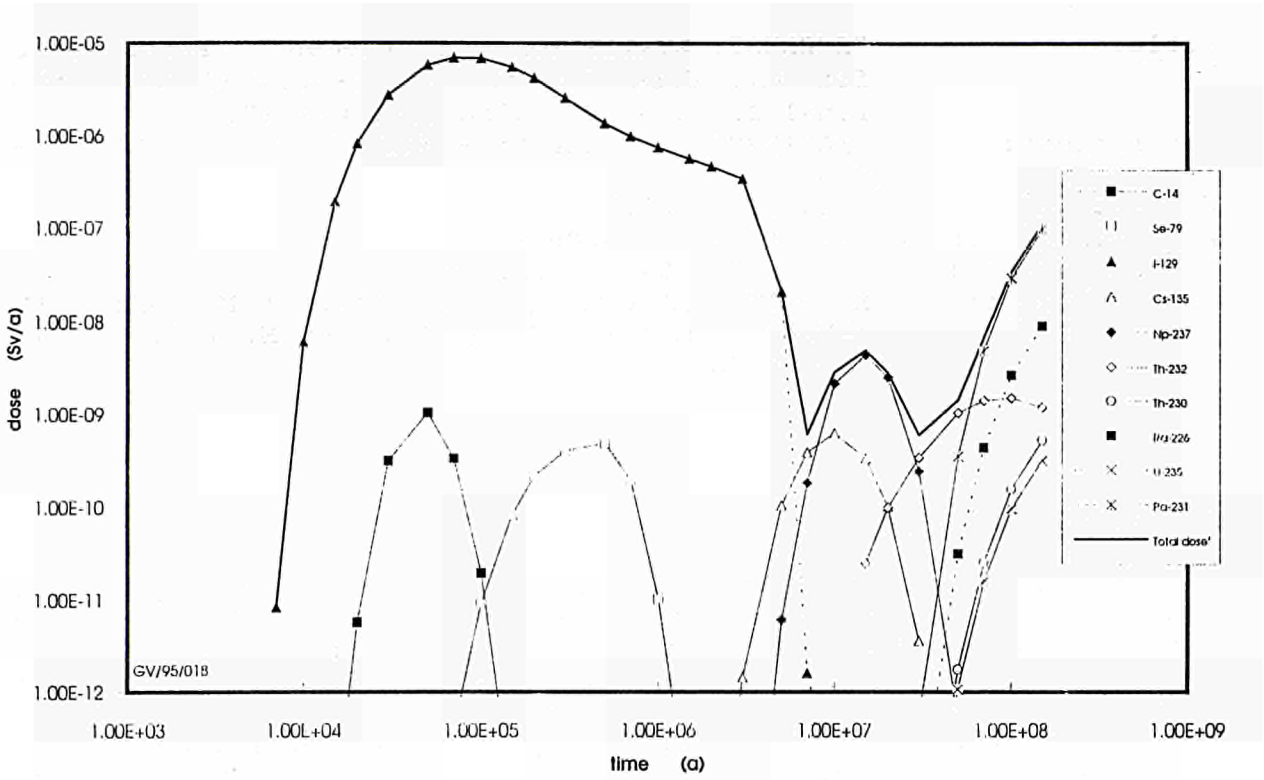

Fig. 3 Evolution of the dose rate via the water well pathway in the case of the normal evolution scenario for MOX spent fuel

Title:	"EVEREST: **EV**aluation of **E**lements **R**esponsible for the dose **E**quivalent associated with the final **ST**orage of radioactive waste".
Contractors:	CEA/IPSN* - ANDRA ** - CEN / SCK ° - ECN°° - GRS°°°
Contract n°:	FI2W CT 90-0017
Duration of contract:	01/04/91 - 30/06/95
Period covered:	from 01/01/94 to 31/12/94
Project Leaders:	M. GOMIT (CEA/IPSN, Coordinator); M. RAIMBAULT (ANDRA); M. MARIVOET (CEN/SCK); M. PRIJ (ECN); M. MARTENS (GRS)

A. OBJECTIVES AND SCOPE

The general objective is the evaluation of the sensitivity of the radiological consequences associated with deep nuclear waste disposal to the different elements in the performance assessment. The following geological formations are taken into consideration: clay, granite and salt, for HLW and MLW.
This work will be realized in four phases: 1-elaboration of the methodology, 2- model description and data collection, 3- calculations,
4- interpretation of results.

B. WORK PROGRAMME

B.I - Methodology: this phase will be divided into four steps: identification of main features controlling the radionuclide transfer to human beings, scenarios, definition of calculations to be performed and reflexion on different approaches and techniques of sensitivity analyses.
B.II - Model description and data collection: documentation and presentation of the models and codes to be used, compilation of the site data and of the other data (waste inventory, package, repository design...)
B.III - Calculations: deterministic and stochastic calculations for normal and altered selected scenarios for each site. The results obtained will be used for sensitivity analyses.
B.IV - Interpretation of the results: the final phase will lead to a hierarchized list of the most influential elements (scenarios, phenomena, RN..) for each site; this list can contribute to the definition of future orientation of the R&D programmes.

* Commissariat à l'Energie Atomique - ** Agence Nationale pour la gestion des Déchets Radioactifs - ° Centre d'Etudes pour l'énergie Nucléaire / Studiecentrum voor Kernenergie - °° Stiching Energieonderzoek Centrum Nederland - °°° Gesselschaft für Reaktorsicherheit mbH -

C. PROGRESS OF WORK AND OBTAINED RESULTS

State of advancement

During the previous part of the project, items 1 and 2 of the work programme were mainly treated. A large part of 1994 was devoted to deterministic and stochastic calculations for normal and altered selected scenarios for each site. The general plan of the final report has been prepared.

During the period covered by this report a contribution of CIEMAT-ENRESA to Chapter 4, Climatic Changes, of the EVEREST Project Final Report has taken place. The contribution is based on the CEC Contract n° FI2W-CT92-0123, "Consideration of environmental changes in long term radioactive waste disposal system evaluations". A draft final report has been submitted to the EVEREST project members.

More, in complement of the present programme, an extension to the EVEREST project has been proposed to develop some complementary aspects:

- the evaluation of the performance of various statistical techniques for sensitivity analysis (CEN/SCK);
- the sensitivity studies to alternative hydrogeological models in sedimentary contexts (CEN/SCK, IPSN);
- the probabilistic analysis of the groundwater intrusion scenario for salt (ECN);
- the deterministic and probabilistic analysis of the solution mining scenario (ECN, GSF);
- the sensitivity study of alternative repository models on nuclide release (GRS);
- the conceptual model uncertainty studies (GRS);
- the influence of the actinides and fission products partitioning on the radiological impact of HLW geological repository (IPSN).

Progress and results

B.I Methodology

. CIEMAT-ENRESA

Environmental variations and their impact on the disposal system, i.e., the elements responsible for environmental change, the empirical evidence of that environmental change and its effects on the repository performance (impacts on the geological setting, on the geosphere-biosphere interface and on the biosphere environment); the current capacity to predict environmental evolution, and the existing methods and techniques for consideration of environmental change in the safety assessment of disposal systems are the main items covered by CIEMAT-ENRESA contribution.

Of all the forcing mechanisms that have been considered, climate and tectonic changes are those having the greatest influence on radioactive waste disposal systems. This influence would operate via modification in the safety parameters of the geological barrier and also by introducing changes and adaptations in the biospheric system surrounding the repository.
The climate is a major component of the environmental variability over tens of thousands of years and there is widespread consensus that the most probable climate changes over the next few thousand years will be those represented by the climate episodes that have occurred during post-glacial times. During the next 10 000 - 60 000 years period a Würm type glaciation can be expected as foreseen by the Milankovitch theory and beyond 160 000 years more severe Riss-type glaciations may occur. As a result of this, aquifer systems could be strongly influenced by the long-term climatic evolution and alterations in the behaviour of repository systems may be caused indirectly by those climatic changes as well. In the framework of the EVEREST project, influences of the climatic changes on the repository system components behaviour (mainly on the aquifer system) have been analyzed according to both the considered climate sequences and the hydrogeological and transport codes being used.

B.II Model description and data collection

. GRS

NEARFIELD

1) Simulation of the Convergence-Diffusion Scenario (Brine Intrusion and Brine Pockets)

To simulate the convergence-diffusion scenario 80 random sample sets have been generated using the GRS-developed sofware system SUSA. From these sample sets, 80 input files for the near- and farfield have been generated. After testing the features implemented in MARNIE to improve the capability of the code to simulate this scenario, the calculation of the parameter sample sets was started.

2) Simulation of the Cavern-Convection Scenario (Human Intrusion: Solution Mined Cavern)

The data to be used in this scenario including the uncertain parameters and the associated distribution functions were compiled. 100 random sample sets were generated from which 100 input files were produced. To account for all important features arising from this scenario, new models were implemented and tested.

3) Sensitivity Studies on Convergence Models

The analysis of the 19 cases agreed by ECN, GRS and GSF was completed. The resuls calculated by GSF (with EMOS) and by GRS (with MARNIE) were compared.

4) Sensitivity Study of Alternative Repository Models on Nuclide Release (EVEREST Extension)

The three alternative models of the central-, chamber- and MLW-borehole field were generated. New models necessary to simulate the nuclide release from the repository in the three alternative models were implemented and tested. The input data of four different flow- and out-flow locations for the brine and nuclide flow in the convection-diffusion scenario were generated for each of the alternative repository models.

FARFIELD

1) Geosphere Model for the Simulation of the Convection-Diffusion Scenario and the Cavern-Convection Scenario

The hypothetical repository is located in a salt dome below the Gorleben erosion channel. The channel consists of two aquifers (the upper "Saale" and the lower "Elster" aquifers) and few silt (aquiclude) and clay (aquifuge) layers. It crosses the Elbe River and has two watershed boundaries in the South and in the North. A 2-D model of the channel was established with no flow boundary conditions at the bottom, in the South and in the North. The flow from the South to the North is governed by a given piezometric head at the top of the modelled area. The model used in the framework of the EVEREST Project is based on 2-D steady-state freshwater calculations. A nuclide source has been assumed to exist above the hypothetical repository. Nuclide transport calculations will be performed for four nuclide decay chains and 16 fission products. All geosphere calculations will be made using the finite element code NAMMU (see Annual Progress Report 1993).

100 input parameter sets were generated using Monte-Carlo techniques. In 1994, all groundwater calculations and about 60 percent of the transport calculations for the cavern-convection scenario were carried out.

2) EVEREST-Extension

Due to sparse hydrogeological data of the northern part of the channel, some qualitative properties of this part are still unknown. Several assumptions about the hydrogeological behaviour in this part can be made. The first EVEREST calculations are based on one assumption. The objective of the additional work is to study the influence of the qualitative uncertainties on the nuclide transport mentioned above.

100 groundwater and pathline calculations were carried out using randomly chosen conceptual models of the northern part of the channel in combination with the 100 parameter sets mentionned above. A subsequent sensitivity study was planned. The study was not completely successful because some of the pathlines calculated did not reach the boundary of the domain due to numerical reasons. There are two possibilities to complete the study in 1995:

a) to repeat the calculations using the new NAMMU version 6.2 which uses a mass-conservative discretisation;
b) to perform transport calculations instead of the pathline calculations.

BIOSPHERE-Model

The biosphere-model has the following features:
- The groudwater which carries the radionuclides is modelled to enter the biosphere via a farmer's well.
- The water is used for the consumption and for irrigation purposes, causing irradiation exposure by ingestion of contaminated food, by inhalation of responsible particles and by staying on contaminated ground.
- Radiation exposure will be calculated using the MINIBIOS code provided by NRPB in Harwell (UK).

The nuclide- and site-specific parameters simulating the transport of the radionuclides through the biosphere depend on climatic and cultural conditions. These parameters and the associated distribution functions have been compiled for both the current German climate and the Mediterranean climate, excluding possible ice-ages.

The calculation of the possible radiation exposure will be performed using 100 random sample sets for each of the selected nuclides and decay chains. These sample sets and the input files were produced.

B.III Calculations

. CEN/SCK

CEN/SCK completed the deterministic calculations by the analyses of two altered evolution scenarios: the exploitation and poor sealing scenarios. For the exploitation scenario, the potential consequences of the use of water pumped from the Ruisbroek-Berg aquifer are evaluated, this aquifer underlies the host clay layer. Since the water flow in this aquifer is small relatively, high radionuclide concentrations can occur. Various modelling approaches with a variable degree of complexity have been applied. Finally, a two-dimensional three-layers model, which considers the host formation, the Ruisbroek-Berg aquifer and the Asse clay, was solved with the PORFLOW computer code. The calculated dose rates are very sensitive to the value of the Darcy's velocity in the Ruisbroek-Berg aquifer.

The analysis of the poor sealing scenario, in which the consequences of an unsuccessful sealing of the access shaft and the transport galleries are evaluated, revealed that the length of the galleries between the poorly sealed shaft and the waste disposal galleries strongly influences the radionuclides fluxes released into the surrounding aquifers. A minimum length of about 50 meters seems to be sufficient to reduce the consequences of the poor sealing scenario to the level of the normal evolution scenario.

Stochastic calculations were carried out for the normal evolution and exploitation scenarios. The sensitivity studies carried out for the two considered scenarios yield similar results. For both

scenarios, the Darcy's velocity in the aquifer is the most influential parameter. Other strongly influential parameters are related to the diffusion of the radionuclides through the clay layer; these parameters are the effective thickness of the clay layer, the diffusion coefficient and retardation factors in the clay. A less influential parameter but still significant is the biosphere conversion factor.

. ECN

1) Convergence model sensitivity study

Previous studies have shown that the convergence plays an important role in the consequence analysis of the groundwater intrusion/extrusion type scenarios for repositories in rock salt formations. As the contemporary computer codes for the performance assessment: EMOS, EMOS_ECN and MARNIE are based on different models for the convergence, it was judged to be necessary to investigate the consequences of these different models. This has been investigated thoroughly and the main conclusions are:

i) The assumptions made in EMOS and MARNIE model concerning the model of convergence lead to relatively simple, robust but inflexible program. This is a big advantage as it gives the user a good feeling for the quality of the results. This is of particular advantage if large number of stochastic analyses have to be performed.
ii) The assumption made in ECN model concerning the model for convergence and compaction lead to a very flexible program with the capability of more accurate predictions, as it takes into account more physical phenomena. They, however, also lead to a more complex program in which the output is not easily understood due to the large amount of input values. This certainly is a disadvantage for stochastic analyses.

In order to have a reliable performance assessment, the models should include the important phenomena. On the other hand, keeping confidence in the results requires the models to be as simple as possible. Based on these remarks and the conclusions of the model comparison the following can be recommanded:

iii) The convergence model in EMOS and MARNIE can be significantly improved by implementation of the transient convergence.
iv) Implementation in EMOS and MARNIE of the explicit model for the compaction of backfill as present in the ECN model is not recommended because it does not lead to significantly more reliable results but give additional complications due to the determination of the backfill pressure.
v) The incorporation of the stiffness of the waste containers as present in the three code packages should be investigated further.

2) Human Intrusion Scenario of Solution Mining a Salt Exploitation Cavern (GSF)

The human intusion scenario of solution mining a cavern in the area of a former repository for radioactive waste has been discussed. Two models have been developed, describing alternative procedures of mining a cavern. In the first model (model 1), the simplifying assumption is made that during mining the height of the cavern is kept constant and the radius increases in time. In the second model (model 2) it is assumed that the radius of the cavern is kept constant, while the height of the cavern increases during mining. In reality, of course, a superposition of these two extreme procedures occurs. At the beginning of the mining process the volume increase of the cavern is more like in model 2 with a small cavern radius, while, after the cavern has reached the desired height, model 1 better fits to the mining procedure to increase the cavern radius.

During mining of the cavern in a repository area, former disposal boreholes filled with waste containers may be struck and the containers laid open fall down to the bottom of the cavern. Here, they are successively covered with a layer of insolubles. Models have been developed which allow to estimate the number of containers which are exposed to the brine above the sump and release radionuclides into the brine.
Brine extracted from the cavern is used for salt production, where about 20 % of the salt is for human consumption. During salt production, a cleaning procedure is applied to remove calcium, magnesium, sulfates and carbonates from the brine. The precipitates are given back into the cavern. During the condensation procedure to obtain cristalline salt, residual brine containing most of the potassium is pumped back into the cavern. If radionuclides are solved in the brine, a certain amount of these will also be removed from the salt during the cleaning and condensing procedures. The reduction of radionuclides remaining in the salt is taken into account by reduction factors, which are estimated from the chemical processes carried out during salt production.

Netherveless, a non-negligible inventory of radionuclides remains in the salt. Annual dose rates have been calculated, assuming that men are consuming contaminated salt. Preliminary results have been discussed. It turns out, that the dose is rather high in the case of striking disposal boreholes filled with MLW. The main reasons for this high dose are the large number of containers which are laid open, since the distance between MLW boreholes is small compared to the radius of a salt exploitation cavern, and the short mobilization time applied for MLW in a cement matrix.

. GRS

NEARFIELD

1) Cavern-Convection Scenario

The reference case of the cavern-convection scenario was calculated for a period of 10^6 years. To simulate the cavern-convection scenario, the calculation of the 100 sample sets was carried out and the sensitivity analysis of the nuclide flow from

the cavern into the geosphere at 14 selected points in time has been performed.

2) Convection-Diffusion Scenario

The first results of the simulation of the convection-diffusion scenario were already obtained. The result entity is the release of the nuclide flow from the repository into the geosphere.

. IPSN

1) Normal evolution scenario for the granite site

For the quasi 3D modelling with the MELODIE code, the granitic block is represented using the porous equivalent medium approach with an explicit description of the main fractures. The reference flow calculation has been performed at the regional and local scales for the normal evolution scenario including a Wurm type glaciation (from 25 000 to 75 000 years) with a 100 meters thick impervious permafrost at the surface of the granite site.

The extension of the regional model is roughly 900 km^2. The regional mesh has been modelled to a depth of 1500 meters. Nine main fractures have been taken into account with faults corridors centered on these main fractures. The conclusions of the regional scale calculations were that the major part of the flow takes place in the fractured zones. At the regional scale, the results flow calculations have been allowed to define a more restricted zone around the repository area called "local scale" covering 100 km^2. The calculated flowrates at the surface nodes have been led to select seven outlets. The repository is located at a depth of 500 meters.
Deterministic radionuclide transport calculations (at the local scale only) have been done up to 10^7 years both for High Level radioactive Wastes (HLW) and Medium Level radioactive Wastes (MWL) and for many radionuclides. The results of the reference case have been shown in terms of activity flowrates at the outlets and will be expressed in terms of dose equivalents in the biosphere in the final phase.

A parametric calculational approach have been defined to evaluate the sensitivity of the release rates at the geosphere/biosphere interface with respect to the hydrogeological parameters (Permeability and porosity) and to the transport parameters (Solubility limits and retardation coefficients). The combination of these three parameters have led to 27 simulations for each actinide radioactive chain and each fission product.

Steady state groundwater flow calculations have been done using TRISEC (3D code for hydrogeological modelling). The first comparisons with the MELODIE code (quasi 3D version) in terms of hydraulic heads and Darcy's velocities are satisfactory. Particle tracking calculations have been performed. Comparisons with the ANDRA's results (TRIO code) will be made.

2) Exploitation of water scenario

The exploitation water scenario is associated to the extraction of water in a well drilled in a detected fault. A well of 300 meters deep and 0,2 meter in diameter is considered. The duration of exploitation of the well is fixed to 100 years. Two different positions as close as possible to the repository and down flow in the contaminated plume are examined. Flow calculations have been performed to determine the flowrate of the well and to examine the consequences of the exploitation of water (deformation of the equipotentiel curves, modification of pore velocities in the vicinity of the well). Transport calculations have been defined to compute the radionuclide activity flowrate in the well. The sensitivity analysis relative to this scenario will be made according to the date of occurrence of the well.

3) Normal evolution scenario for the clay site

A sedimentary basin model has been completed with the NEWSAM code, encompassing the estimated natural boundaries reached during glaciations periods, as defined in the figure below.

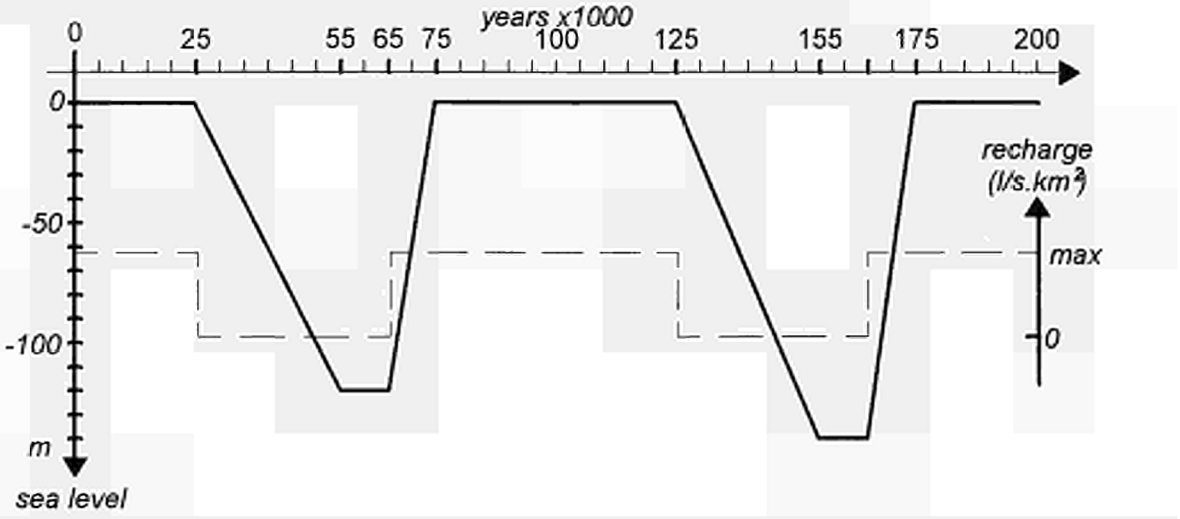

The permafrost is considered existing everywhere except in the main river basins below a given level, thus allowing recharge from aquifers below. The transient calculations show that in the host formation in the site area the piezometric heads seem almost not pertubated during the two successive glaciation periods.

To study the transport in clay and dilution in the two overlaying deep aquifers, a MELODIE quasi-3D block-shaped meshing concerning only the confined formations in the site area (covering 35 x 35 km^2) was used. Gradients in accord with the NEWSAM results were imposed on the boundaries. Four virtual outlets are defined : the downstream limits of all aquifers above and below and the top surface of the domain. Glaciation effects were not taken into account since the radionuclides stay confined in the host formation during glaciations periods.

The dilution was first studied through the behavior of an ideal tracer, considering or not vertical leakage: the average residence time of the tracer inside the domain, measured as the time to reach half the maximum concentration, ranges between 2 and 2.6 million years for the 4 outlets in the no-leakage case and ranges between 100 000 and 150 000 years for the main outlets with leakage (vertical velocity = 7.10^{-5} m/year).

Transport calculations were then done for B and C type wastes, using the same inventory, solubility limits and retardation factors than in the granite case.

B.IV Interpretation of the results

. CEN/SCK

A comparison of the parameter rankings obtained in EVEREST with the rankings obtained in the PAGIS and PACOMA studies for the Mol site shows that the Darcy's velocity in the aquifers became in EVEREST a much more influential parameter than it was in the earlier studies. This can be explained by the better knowledge of the migration parameters in the Boom clay. Indeed, the Belgian R&D programme on geological disposal of the last six years strongly focused on the migration of radionuclides in clay.
As a consequence, the values of the migration parameters of elements like iodine are fairly known and the influence of their uncertainties on the calculated doses is thus strongly reduced. On the other hand, the hydrogeological site characterisation was more or less neglected and the uncertainty in the Darcy's velocities is not decreased. The uncertainties considered in EVEREST are even larger because we now try to include the potential influence of climatic changes on the water flow in the aquifers.

Tittle	Consideration of Environmental Changes in Long-Term Radioactive Waste Disposal System Evaluations
Contractors	CIEMAT, Spain, and ENRESA, Spain
Contract Nº	FI2W-CT92-0123
Duration of contract	19 months from December the 1st, 1992 to June 30th, 1994
Period covered	December 1993 to December 1994
Project Leader	Mr. F. Recreo (CIEMAT; coordinator) Ms. C. Bajos (ENRESA)

A. OBJECTIVES AND SCOPE

The objective of the work is a state-of-the-art analysis consisting basically in a well-founded, critical discussion of the phenomena of long-term environmental changes, their basis and the existing or foreseeable scientific and technological capacity for suitable consideration in the safety evaluation of radioactive waste disposal systems.

The analysis will include also a comparative study of the different existing regulations, guidelines and observable current international tendencies on the issue of the post-closure timescales in the context of safety analysis, as well as a comparative analysis between what is indicated above and the actual consideration given to climatic changes within the EVEREST project, and will conclude with a series of suggestions for subsequent tasks, which may be recommended to the EC for development.

The project is carried out by a collaborate effort of the Nuclear Technology and the Environmental Institutes of CIEMAT, and ENRESA.

B. WORK PROGRAMME

B.1. Basis for safety evaluation of high-level radioactive waste disposal systems : Safety objectives and principles. Current situation and observable tendencies on expression of safety principles and objectives and on timescales consideration.

B.2. Environmental variation and its effect on the disposal system : Basis and elements of environmental variation. Environmental variation effects of relevance to the safety of the repository.

B.3. The human capacity to predict environmental evolution : The variability of the climate system over different timescales and its effect on geo-biospheric systems. Current capacity for evaluation and prediction; available methods and techniques : limits and levels of confidence.

B.4. Consideration of environmental change in disposal system safety evaluation : Existing methods and techniques. Approaches of different countries to consideration of environmental change.

B.5. Comparative analysis within the EVEREST project : Summary of the methods used in EVEREST for consideration of environmental changes. Qualitative comparison with the state-of-the-art previously described.

B.6. Conclusions and recomendations for subsequent development : General conclusions and recommendations regarding environmental change and repository safety. Specific conclusions and recommendations regarding EC R & D activities related to the EVEREST project.

C. PROGRESS OF WORK AND OBTAINED RESULTS

State of advancement

During the period covered by this report the intended bibliographic study has been concluded, and a draft final report has been submitted both to the EVEREST project and to the Commission by July 1994.

The descriptive sections of the work carried out during this period centre on scientific and methodological aspects of significance in the field from B.1 to B.5 (see below) : information on physical processes currently considered to be important for the Earth's both short- and long-term environmental evolution; existing techniques for reconstructing the recent (Plio-Quaternary) geological past, a comparative analysis of regulations and guidelines for high-level radioactive waste disposal systems evaluations, and a comparative analysis of the methods used in the EVEREST project for consideration of environmental changes. The review also comprises a summary of work performed by various countries around the world on the incorporation of environmental change evaluations into performance assessment of radioactive waste disposal systems.

Progress and results

C.1. Basis for safety evaluation of high-level radioactive waste disposal systems

A revision of the safety principles and objectives as well as of the safety criteria and indicators is included : individual and collective dose; individual and collective risk; radiotoxicity indicators and the comparison with natural radiation, among other safety criteria and indicators.

C.2. Environmental variation and its effect on the disposal system

The environmental system is made up of 5 subsystems : the atmosphere, the oceans, the cryosphere, the lithosphere and the biosphere. These subsystems are interrelated by way of physical, chemical and biological processes, the response time and sensitivity of each subsystem being variable.

The climate is a major component of environmental variability over tens of thousands of years. In a modern consideration [1], [2], the climate needs no astronomical variation to suffer a change of regime since its dynamics possesses intrinsically stochastic components (autovariations). [3].

The theory that variations in seasonal solar radiation intensity as a result of astronomical factors might give rise to periodic glaciations was originally put forward by the French mathematician Joseph Adhémar at the end of the 19th century. The Yugoslavian astronomer M. Milankovitch refined and formalized Adhémar's hypothesis between 1920 and 1930. Milankovitch's theory associated glacial cycles with changes in the distribution of solar irradiance as a result of variations in the geometry of the Earth's orbit, depending on three elements : obliquity, equinoctial precession, and eccentricity. Precession is a cycle with a period of 23,000 to 26,000 years; the cycle of obliquity has a duration of 41,000 years, and the cycle of the orbit (which is a double one : oscillation of the eccentricity of the ellipse and rotation of the ellipse around the Sun), has a duration of 96,000 years.

Although climate variations are the result of variations in the amount of solar radiation received and retained by the system, an important part of the environmental variation is random and caused by processes internal to the system, amplified by feedback mechanisms.

The most significant evidence backing the theory of Milankovitch came from the isotopic variation of ^{18}O / ^{16}O in foraminifers from deep submarine samples. The Milankovitch theory explains clearly the Quaternary glacial/interglacial cycles by means of three orbital cycles of 100, 41 and 23 thousand years, possibly amplified by feedback mechanisms such as ice-albedo and CO_2.

The position and extent of the continents and oceans resulting from plate tectonics and polar drift is another of the variables controlling climate change. Plate tectonics have also conditioned relief (which in turn controls atmosphere circulation) and volcanic emissions of CO_2.

Apart from the natural causes of climate change, the appearance of man and of its capacity to modify the surroundings led to the possibility for anthropogenic causes of climate pattern change, these being difficult to quantify and predict.

Variations in the atmospheric concentration of greenhouse gases is another of the variables controlling climate change. Water vapour, carbon dioxide and ozone are the three factors mainly responsible for the greenhouse effect. If

duplication of CO_2 as a result of human activity were to saturate all the bands of absortion currently having some degree of transparency, the atmosphere would tend to become a 100 % black body. The best estimates of equilibrium global temperature rise associated with a doubling of CO_2 concentrations lie in the range 1.5 - 4.5 ºC [4], [5].

Of all the forcing mechanisms that have been analyzed, climate and tectonic changes would appear to be those having the greatest influence on radioactive waste storage systems. This influence operates via modifications to the safety parameters of the geological barrier, and also by introducing changes and adaptations to the biospheric system surrounding the geological medium. The effects of climatic change are especially evident in relation to geomorphic and hydrological processes, sea level change and permafrost development. Glacial effects are of particular importance. Tectonic change is of interest primarily for its influence on permeability conditions around the repository. [6].

Although climate seems to play a fundamental role in determining groundwater flow, it may have a significantly delayed response and its effects are not simply determined. On the other hand, its time-dependent nature is difficult to quantify. The response time is dependent on several factors. Land elevation and sea level act as major boundary conditions of a groundwater system. Changes in these boundary conditions may lead to delayed response groundwater effects. [6].

There is a general consensus that the most probable climate changes over the next few thousand years will be those represented by the various climate episodes that have occurred during post-glacial time (the Holocene). [7]. Nevertheless, for the next 100,000 years the world's climate could be dominated by glaciations, as it has been over similar periods for the past million years. [8]. A realistic description of those conditions that might influence the performance of a repository during a glaciation cycle should consider an overview over the various mechanisms and processes involved in a typical glaciation cycle and an assessment of their influence on repository performance. The "glaciation scenario" covers from the present to the next interglacial, when the climatic conditions will once again return to the present conditions [8] 125,000 years AP.

Enhanced greenhouse warming is expected to cause changes that, in turn, will have implications for the climatic response to orbital forcing, such as changes in the cryosphere. Three possible patterns describing this relationship can be identified [10]: a) A relatively short (1 ka) period of greenhouse gas-induced warming followed by a switch back into the "natural" pattern of glacial/interglacial cycles. b) after a period of warming, the next glaciation will be delayed and will be less severe; c) the enhanced greenhouse warming will so weaken the positive feedback mechanisms which transform the relatively weak orbital forcing into global glacial/interglacial cycles, that the initiation of future glaciations will be prevented (the "irreversible greenhouse effect"). Goodess, Palutikof and Davies assume that the climate system will recover from the effects of enhanced greenhouse warming and

that orbital forcing will operate much as it has over the Quaternary. Based on these assumptions, it is reasonable to use the geological record of the Quaternary period as a guide to the future, beyond the point of transition. [9].

C.3. The human capacity to predict environmental evolution

The Milankovitch forcing mechanism accounts only for 60 % of the variance recorded on the 780 ka registers in the frequency window between 19 ka and 100 ka, or 85 % of the variance if the windows are four narrow bands around the orbital cycles. [10]. The rest of the variance must be result of solar variability, volcanic activity, stochastic mechanisms, etc. [9]. Variability might be separated into a deterministic part and a random part associated with fluctuations in the weather.

The study describes the calculation tools currently used for the description, modelling and quantitative prediction of future climate, its regional features and its geological and environmental effects, making a distinction between descriptive or phenomenological (ARMA, ARIMA, Markovian) models and mechanismic (EBM, RCM, GCM) models, and reviewing some specific models already available.

C.4. Consideration of environmental change in disposal system evaluation.

There are two main approaches for the description and modelling of the geo-biospheric systems, able to estimate also the uncertainty of the prediction: a) the Scenario Analysis Approach, and b) the Environmental Simulation Approach.

A different kind of problems emerges when the scientific knowledge is unable to predict, even probabilistically, what variables will be important in the distant future and the state of a variable that may be important in the far future, as it is the case with many processes of the future biospheric system controlled by humans, e.g. agronomic practices, socioeconomic factors, etc. The human intrusion in the repository introduces a similar problem of unpredictability.

The Environmental Simulation Approach gives no method to take into account this kind of processes. The Scenario Analysis Approach makes it possible to illustrate the possible effect of this kind of processes, but the completeness and representativeness of the set of scenarios is in any case undefined.

The study contains a short description of the approaches of different countries to consideration of environmental change, with a specific analysis of time dependant codes of the English Methodology (TIME-2 and TIME-4), [11], [12] the French deterministic Program CASTOR, [13] and the AEGIS (USA) geological simulation codes GSM and FFSM.[14], [15].

C.5. Comparative analysis within the EVEREST project.

In the EVEREST project, the five member organizations have chosen the systematic approach for scenario selection, ending up with a common list of scenarios to be considered throughout the project. For each geological formation the normal evolution scenario and some altered evolution scenarios have been identified. For clay and granite formations both the normal evolution scenario and the severe (Riss type) glaciation scenario are considered from a climatic change viewpoint. The normal scenario considers the influence of a Würm type glaciation, including glaciation effects such as permafrost.

Dominant primary FEPs for the normal evolution scenario in a Dutch salt formation are subrosion, diapirism and denudation, so no explicit consideration of climatic changes has been made for this normal evolution scenario in the framework of the EVEREST project. The three scenarios selected in the EVEREST project for the Gorleben site (the normal evolution scenario, the water intrusion scenario and the solution mining scenario) have been modelled according to the main release and transport mechanisms. Nevertheless, no climatic changes effects have explicitly been taken into consideration for long-term radionuclide transport calculations.

C.6. Conclusions and recomendations for subequent development.

In progress.

References to the published literature.

[1] BENZI, R., Tellus 34, 10-16 (1982).

[2] NICOLIS, C., Tellus 34, 1, 1-9 (1982).

[3] LEITH, C.E., Nature 276, 352-355 (1978).

[4] MacCRAKEN, M.C., LUTHER, F.M., Carbon Dioxide Research Division, Office of Energy Research, US Department of Energy Report DOE/ER-0237 (1985).

[5] BOLIN, B., DÖÖS, B.R.; JÄGER, J., The Greenhouse Effect, Climatic Change and Ecosystems, SCOPE 29, Wiley, New York (1986).

[6] DAMES & MOORE INTERNATIONAL, Technical Report TR-D & M-12 (1989).

[7] SCHUMM, S.A. and CHORLEY, R.J., NUREG/CR-3276 RW (1983).

[8] AHLBOM, K., ÄIKÄS, T., ERICSSON, L.O., SKB Technical Report SKB TR-91-32 (1991).

[9] GOODESS, C.M.; PALUTIKOF, J.P. and DAVIES, T.D., The Nature and Causes of Climatic Change. Assessing the Long Term Future. Belhaven Press, London (1992).

[10] IMBRIE, J. et al., Milankovitch and Climate, D. Reidel, Dordrecht, pp 269-306 (1984).

[11] DAMES & MOORE, User Document UD-D&M-1, UK Department of the Environment Report No. DOE/RW/88.088 (1988).

[12] DAMES & MOORE, Technical Report TR-D & M-18, UK Department of the Environment Report No. DOE/HMIP/RR/91.050 (1991).

[13] CANCEILL, M. et al., Bureau de Recherches Géologiques et Minières Report 84 SGN 229 STO (1984).

[14] INTERA Environmental Consultants, Inc. Technical Report, ONWI-447 (1983).

[15] INTERA Environmental Consultants, Inc. Technical Report, ONWI-436 (1983).

PART B

Construction and/or operation of underground facilities

* List of contracts

* Introduction to Part B

PART B - LIST OF CONTRACTS

CONSTRUCTION AND/OR OPERATION OF UNDERGROUND FACILITIES OPEN TO COMMUNITY JOINT ACTIVITIES

Project B1 :	**"The underground facility in the Asse Salt Mine (FRG)"**
FI2W-CT90-0002	The HAW project : test disposal of highly radioactive radiation sources in the Asse salt mine
FI2W-CT90-0068	In-situ investigation of the long-term sealing system as a component of a dam construction
FI2W-CT90-0069	Active handling experiment with neutron sources
FI2W-CT92-0120	Thermo-mechanical simulation of the near field of an emplacement borehole in a salt formations (Amélie, France) - "CPPS test"
FI2W-CT94-0127	In-situ research on compaction of and gas release in saliferous backfill (TSS-experiment)
Project B2 :	**"The underground facility HADES in the argillaceous layer under the Mol Site (B)"**
FI2W-CT90-0003	Preliminary demonstration test for disposal of high-level radioactive waste in clay: b)CERBERUS, c)Mine-by-Test
FI2W-CT91-0098	Demonstration of the in-situ application of an industrial clay-based backfill material (BACCHUS 2)
FI2W-CT91-0102 and -0033	Modelling and validation of the thermal-hydraulical-mechanical and geochemical behaviour of the clay barrier
FI2W-CT92-0117	Acquisition and regulation of water chemistry in an argillaceous medium (ARCHIMEDE)
FI2W-CT91-0116	Phenomenology of hydrical exchanges between underground atmosphere and storage host-rock (PHEBUS)
FI2W-CT94-0129	Modelling of the thermo-mechanical behaviour of clay (CACTUS test)
Project B4 :	**"Underground validation facility at Sellafield (UK)"**
FI2W-CT91-0114	Hydrological characterisation of fractured rock (Sellafield)

INTRODUCTION TO PART B : CONSTRUCTION AND/OR OPERATION OF UNDERGROUND FACILITIES OPEN TO COMMUNITY JOINT ACTIVITIES

A. Objectives

The main objective of this part of the programme is the construction and the operation of underground facilities to develop and demonstrate emplacement techniques and to validate site and design criteria of deep geological repositories. All these facilities have been declared, by the responsible bodies in the Member States on which territories the facilities are build, open to scientists of the Community for joint R&D activities.

B. Research performed under the programme 1985-1989

In the programme 1985-1989 joint research activities were already started at the Asse salt mine (FRG) and in the HADES underground facility at Mol (B). The research in the Asse salt mine concerned mainly the preparation of the HAW test whereas at Mol a Test Drift was excavated and various lining systems tested. Moreover, a combined heating/radiation experiment (CERBERUS) was started.

C. The present programme 1990-1994

Research activities at the facilities in the Asse salt mine and in the HADES facility in clay at Mol (Project B1 and B2 respectively) started during the previous programme were continued. Additional research projects have been initiated as described below. However, in December 1992 the Federal Government in Germany decided not to continue with the HAW project.
The construction of underground facilities in France (Project B3) has been delayed and the planned budget has been allocated to research activities on clay and salt, complementary to the investigations in Mol and Asse.
Site characterization work at Sellafield (UK) (Project B4) has started.

Project B1 : The underground facility at the Asse salt mine (FRG)

After the decision taken by the Federal Government in Germany in December 1992 not to continue with the HAW project, research was concentrated on the accompanying laboratory programme, consisting mainly of irradiation experiments in salt samples in the irradiation facilities at Saclay(F) and Petten(NL). The electrical heaters installed in two boreholes in the Asse mine and running since November 1988, were shut down under controlled conditions and retrieved.

Within the DAM project a multicomponent dam is being developed, and scheduled to be constructed and tested in the Asse mine for use as an engineered barrier in galleries. The CEC is participating in a subproject concerning an in-situ experiment on the tightness of a long-term sealing component consisting of salt bricks. The seal will be tested on tightness first against gas and then against brine. However due to a review of the project, no in-situ work took place during 1994.

The AHE experiment (Active Handling Experiment) with neutron sources aims at studying the effect of neutron back-scattering on the overall neutron, and neutron induced gamma-dose rates during handling of highly active material in a repository in a salt formation.

The TSS experiment concerns the demonstration of disposal of spent fuel in a gallery. The EC is participating in part of the project related to investigations on the compaction of crushed salt as backfill material and gas release.
The CPPS project, performed in the Amélie potash mine (F), concerns investigation of the thermo-mechanical behaviour of the near-field of waste emplacement boreholes in salt.

Project B2 : Experiments at the HADES underground facility at Mol (Belgium)
In the HADES underground facility in the Boom clay beneath the site of Mol, the following large projects are being carried out.
The PRACLAY project is a preliminary demonstration test for disposal of HLW canisters in horizontal mini-tunnels in clay. It is intended to feature a full scale simulation, over a length of 20 m of the cross sectional configuration of the waste environment, complete with heat generation (electrical heaters). The project was however suspended for various reasons in 1993 and no progress is reported.

The combined heating-radiation test(CERBERUS) aims at investigating the near-field effects in an argillaceous environment of a HLW canister. It uses a Co-60 radiation source of 397 TBq and two electrical heating elements each dissipating 365W.
In a mine-by test the response of the clay on the excavated Test Drift is monitored.

In the CACTUS project, the near-field thermo-hydro-mechanical behaviour of clay around boreholes with high-level waste, using electrical heaters, was investigated and is now being modelled.

The BACCHUS-2 project aims at optimizing and demonstrating an installation procedure for a clay based backfill material. The instrumentation of this experiment will be optimized in such a way that it can be used as a validation experiment for a hydromechanical model being developed.

The ARCHIMEDE project aims at the investigations of the water chemistry in clay and the PHEBUS project concerns the study of the hydrous behaviour of clay around ventilated excavations.

Project B3 : Underground facilities
The construction of underground facilities in France has been delayed. The planned budget has been allocated to research activities on clay (ARCHIMEDE and PHEBUS) and salt (CPPS) (see above B1 and B2). Furthermore the CEC is participating in the underground facility at Tournemire (see Task 4).

Project B4 : Underground facilities in the United Kingdom
The Commission is participating in some parts of the site characterisation programme carried out by UK Nirex Ltd. at Sellafield (UK).

Title	The Haw-project: Test disposal of highly radioactive radiation sources in the Asse salt mine
Contractors	GSF-IfT/Braunschweig-Germany, ECN/Petten-The Netherlands, ANDRA/Fontenay-aux-Roses-France, ENRESA/Madrid-Spain
Contract N°	FI2W-CT90-0002
Duration of contract	May 1990 - December 1994
Period covered	January - December 1994
Project leader	T. Rothfuchs, L. Vons, M. Raynal, J.C. Mayor

A. OBJECTIVES AND SCOPE

In order to improve the final concept for the disposal of high-level radioactive waste (HAW) in boreholes drilled into salt formation plans were developed a couple of years ago for a full scale testing of the complete technical system of an underground repository. To satisfy the test objectives, thirty highly radioactive radiation sources were planned to be emplaced in six boreholes located in two test galleries at the 800-m-level in the Asse salt mine. A duration of testing of approximately five years was envisaged.

Because of licensing uncertainties the German Federal Government decided on December 3rd, 1992 to stop all activities for the preparation of the test disposal immediately.

In the course of the preparation of the test disposal, however, a system, necessary for handling of the radiation sources was developed and installed in the Asse salt mine and two non-radioactive reference tests with electrical heaters were started in November 1988. These tests serve for the investigation of thermal effects in comparison to the planned radioactive tests. An accompanying scientific investigation programme performed in situ and in the laboratory comprises the estimation and observation of the thermal, radiation-induced, and mechanical interaction between the rock salt and the electrical heaters and the radiation sources, respectively. The laboratory investigations are carried out at Braunschweig (FRG), Petten (NL), Saclay (F) and Barcelona (E).

As a consequence of the premature termination of the project the working programme 1992 - 1994 was revised. The new programme for 1993 and 1994 agreed to by the project partners includes a controlled shut-down of the heater tests in 1993 and a continuation of the laboratory activities until the end of 1994.

B. WORK PROGRAMME

B.1 In-Situ-Activities

B.1.1 Controlled shut-down of the heater experiments and continuation of in-situ measurements

B.1.2 Thermomechanical analyses

B.1.3 Post test sampling

B.2 Laboratory Activities

B.2.1 Irradiations at Saclay

B.2.2 Irradiations at the HFR in Petten and modelling of radiation damage

B.2.3 Development of a measuring system for high doses

B.2.4 Gamma field and gamma spectra calculations

B.3 Desk Studies

B.3.1 Description of the mineralogical and geochemical properties of the test field

B.3.2 Evaluation of the experiences gained from the cold training with the handling system

C. PROGRESS OF WORK AND OBTAINED RESULTS

State of advancement

In May 1991 the handling system for the radiation sources was approved by the mining authorities and by the Technischer Überwachungsverein (TÜV). From November 1988 until August 1993 the two preceding electrical reference tests were operated at the test sites A1 and B1 in the test galleries A and B at the 800-m-level of the Asse mine. Corresponding thermomechanical and geochemical investigations as well as laboratory investigations on radiolysis effects in salt were performed since beginning of the project. The results obtained until the end of 1993 were reported in (CEC, 1991), (CEC, 1992) and (GSF-IfT, 1994).

Progress and results

1. In-situ-activities

1.1 Controlled shut-down of the heater experiments and continuation of the in situ-measurements

According to the results of a preceding thermomechanical analysis the two electrical heaters in the HAW test field were shut-down linearly over a period of six months. The heater power was at zero on August 26, 1993. The shut-down procedure was accompanied by the measurement of temperatures, rock stresses and rock deformation and the release of fluids into the heater boreholes. The results were already reported in (GSF-IfT, 1994).

1.2 Thermomechanical analyses

For the purpose of validation of the analysis models used, measurements and calculation results for temperatures, pressures, and deformations have been compared. The discrepancies are identified and explained qualitatively or even quantitatively (Heijdra et al., 1995).

Temperatures

For the comparison of measured and analyzed temperatures the results from the revised three-dimensional analysis as well as the axisymmetric analysis have been used. In general the temperatures close to the galleries show a distinct influence of the seasonal change in ambient outside temperature. For most temperatures the measurements before the start of the heaters are about 3 to 5 °C lower than the analysis results.

Measurements and calculations for the salt temperatures at a distance of 124 cm from the borehole show a good correspondence for higher locations and for the lower locations at this distance the effects of the heater geometry are still noticeable in the 3-D analysis.

At a distance of 424 cm from the borehole, the correspondence between measured and calculated values is good. It can be noticed that at this distance the three-dimensional analysis gives better results than the axisymmetric. Hence this radius is in the transition area between the zone where local effects such as the geometry and position of the heater dominate and the zone where global effects such as the presence of the other holes and the gallery dominate. In Fig.1 the salt temperatures for both radial distances at the elevation of the heater are represented.

Stresses

The Glötzl load cells around the heated boreholes, Fig.2, show a large scatter in the measured data. It can be seen that the presure on the cells is still building up at the moment that the heaters are switched on. After

the start of the heaters the pressure seems to build up rapidly. In the heated period the stress level of measurements and calculations is in the same range, however in the heated period the slopes of measurements and calculations are markedly different.

For the Glötzl stressmeters far from the heated boreholes the pressure does not reach a stationary value in the experimental period which agrees with the results of the analyses of the behaviour of the cell (Benneker et al., 1991). Based on extrapolation of the measurements it is to be expected that the measured pressure will exceed the calculated pressure by one or two MPa.

The Glötzl stressmeters in the pillar between the galleries, are prestressed by means of an epoxy resin injection after one year of operation. Like the cells in the unheated zone they show a tendency to be still in the phase of building up pressure. Also for these cells the extrapolation of the measurements to the final pressure leads to a higher pressure than the analysis results.

The Glötzl stressmeters in the wall of the galleries, show a behaviour comparable to those in the pillar. The measured pressure increases to a significantly higher value than the calculated predictions.

It may be said that the general tendency of the measurements points to the fact that the initial rock pressure of 11 MPa assumed at the start of the analysis in reality will be 1 or 2 MPa higher.

Displacements

Since the displacements are always relative quantities, care has been taken to correct measurements and calculated values such that relative zero occurs at the same date.

For the extension of the gallery walls the measurements show a value which is a factor 2.5 to 3.0 higher than the calculation results. For the horizontal convergence of the gallery, Fig.3 again the analysis results are roughly a factor of 2 smaller than the measurements. Also for the extensometers around the A3/B3 boreholes the measurements are a factor of 2.5 higher than the analysis results.

For the vertical convergence at the location of the A1/B1 borehole, the difference between the measurements and calculations is a constant factor of 1.6, which is noticeably smaller than for the horizontal convergence. For the extensometers in the floor the correspondence between measurements and calculations is good, although it can be seen that in the 3-D analysis the shut-off period was assumed to start at February 1st 1993, while in reality this started at the beginning of March. The change in displacement rate at the start of the shut-down phase, is more gradual in the measurements than that of the analysis.

In the vertical convergence of the gallery at the location of borehole A3 again the measurements are a factor of 2 higher than the analysis results. For the extensometers in the floor near borehole A3, extensometers close to the bottom surface, are in the same range as the analysis results, while the for the extensometers measuring deeper into the salt the analysis results again are smaller than the measurements.

It can be noted that at locations where the deformation is mainly due to thermal expansion such as the extensometers in the floor near the heated borehole, the correspondence between measurements and calculations is good. At locations where the deformation is mainly due to creep, such as the horizontal convergence of the gallery, the analysis underestimates the measurements by a factor of 2 to 2.5. As in the case of the pressure measurements, these observations again give reason to assume that the initial rock pressure was 1 or 2 MPa higher as has been assumed in the

analysis. Since the creep deformation rate depends on the equivalent stress to the power 5.5, an increase of 1 or 2 MPa may well cause a deformation which is a factor of 2 to 2.5 higher.

1.3 Post test sampling and analyses

After termination of the heater tests on August 26, 1993 the mining of the access drift for the uncovering of the heater liner B1 was started in October 1993. The drift starts from an inclined tunnel leading to the deeper parts of the mine. The end of the drift, 8 m behind the heater borehole B1 at a distance of 10 m to the heater borehole A1 was reached by the end of January 1994. Figure 4 shows the room that was left below the HAW-test field after salt and corrosion specimen sampling and instrumentation inspection.

Inspection of Measuring Instruments

During mining of the access drift several instrumentation boreholes as shown is Fig. 4 were reached by the mining machine. After uncovering the instruments were immediately visually inspected in regard of their constitution after having been in place at elevated temperature for more than five years. No corrosion could be found at the various materials during the visual inspection except for a rubber tube shown which disintrigrated to a certain extent.

Special attention was given to the grouted boreholes containing AWID flat cells because a perfect embedding is required in order to obtain reliable measuring data. The AWID stress sensors were precasted in suitable mortar consisting of crushed salt of 3 mm grain size, saturated brine and magnesit (MgO_2). After curing the precasted cells were inserted into the respective boreholes and the gap between the cemented cylinder (100 mm diameter) was filled with the same mortar. At the uncovered cells it was found that the filling mortar after curing does not show any voids and the distribution of the salt grains appears to be homogeneous. Furthermore, there is obviously a perfect contact between the borehole wall and the filling material as well as between the filling material and the precasted cement cylinder so that one could expect acceptable measuring conditions. The reasons for the fluctinations in the observed measuring data, however, are still inexplicable.

Sampling and Analysis of Salt and Corrosion Specimens

At a distance of 5 m to the liner of the borehole B1 the mining activities were interrupted and the mining machine was taken away.

Two radial core drillings producing salt cores of 110 mm diameter were drilled 12.52 m and 13.52 m below the test drift floor (see Fig. 4). 21 salt samples were taken from the 5 m long cores. Each sample was devided into three pieces. One for the gas content analysis, one for the water content analysis and one piece as a reference sample to be stored in the Asse core storing facility for eventually necessary later investigations.

The salt taken from the core sections was immediately put into gastight sealed plastic bottles to avoid an undesired escape of the volatile components.

Within the framework of the post test analyses of the salt samples it should be investigated whether the heating of the salt over almost five years led to any changes in the mineralogical composition of the salt or its fluid content. No mineralogical changes could be found but it is obvious, that comparably great salt crystals grew within the first 20 cm of the salt surrounding the heater liner. The water content of the samples

ranges between 0.02 and 0.6 wt% which is quite typical for the Staßfurt halite. Drying effects, if existing, are very small.

The salt samples taken for the analysis of the fluid content were stored in the gastight sealed plastic bottles for a period of nine months and then the gas atmosphere in the bottle was analyzed gaschromatographicly. Figure 5 shows the relative gas concentrations of H_2, CH_4 and CO_2 versus the radial distance of the sample from the heater liner. The enrichment of H_2 in the vicinity of the liner is possibly due to the corrosion of the metal specimens on the liner surface. This assumption is confirmed by the results of the corrosion analyses of these specimens (see below). The low values for CO_2 can be explained by adsorption of this gas on the salt crystal surfaces. Similar effects have also been observed earlier at other samples.

After drilling of the core boreholes the mining of the access drift was continued carefully up to a distance of 10 - 20 cm to the liner. From this point onwards two separate parallel running drifts were mined on both sides of the liner coming together again approximately 1.5 m behind the liner. In this way a salt layer of 10 - 20 cm was left south, east and west of the liner and a salt layer of 1.5 m behind the liner. The 10 - 20 cm thick salt layer was taken away with an electric hammer whereas the block behind the liner was cut with a saw into three pieces.

After the removing of the big salt blocks the corrosion specimens were accessible as desired and the uncovered liner was left in the center of the excavated room. The excavation activities were finished in early February 1994.

The metal specimens placed on the liner surface consisted of the corrosion resistant materials Ti99.8-Pd, Hastelloy C4, Nickel and Cr-Nr steel 1.4833, and the corrosion allowance TStE 355 carbon steel. The corrosion results indicate that the alloy Ti99.8-Pd is highly resistant to pitting and crevice corrosion, and its general corrosion rate is negligible low (< 0.1 µm/year). Nickel is subjected to non-uniform general corrosion and its corrosion rate (13 µm/year) is clearly higher than that of Ti99.8-Pd. The Cr-Ni steel 1.4833 investigated suffered from severe pitting corrosion and stress corrosion cracking. Therefore, the Cr-Ni steels must be excluded as materials for long-lived containers. The Ni-Cr-Mo alloy Hastelloy C4 shows a high resistance to general corrosion, but the formation of some small pits on the specimen surface was observed. For this reason there is some doubt about the suitability of Hastelloy C4 as container material.

The corrosion allowance (actively corroded) material carbon steel TStE 355 shows a good resistance to pitting and crevice corrosion, and its general corrosion rates (13 - 37 µm/year) imply corrosion allowance acceptable for thick-walled containers. In view of these results, the alloy Ti99.8-Pd and the carbon steels continue to be considered as the most promising materials for the realization of the corrosion resistant and corrosion allowance container concept, respectively.

2. Laboratory Activities

2.1 Irradiations Performed by ECN at the HFR in Petten

Within the framework of irradiation experiments performed by ECN solid natural rock salt samples from the 800-m-level of the Asse mine were gamma-irradiated at 100 °C with spent fuel elements from the High Flux Reactor (HFR) at Petten. Dose rates in the experiments varied between 200 and 20 kGy/h in monthly cycles. After irradiation the radiation induced stored energy was studied as function of total dose. Total doses up to 1200 MGy

were reached. Initially there is an approximately linear increase of stored energy with increasing total dose, which levels of at higher doses until it reaches a saturation value of about 140 J/g. The results of the stored energy measurements were compared with those obtained by other scientists for irradiated pure and K-doped NaCl single crystals.

A few parameters of the theoretical models used to describe the formation of radiation damage in rock salt were critically reviewed. It is discussed that the back reaction used in the models should be described as $\gamma = c_o \exp(-E_\gamma/kT)$ with c_o = 1E16 and E_γ = 0.4 and that for the stored energy per defect a value of 5 eV/defect should be used. With these modified parameters the models were compared with the experimental results obtained from the GIF A experiments (see Fig. 6).

In Fig.6 the measured stored energy values are also compared with the results of model calculations using the modified Jain-Lidiard model (Van Opbroek and den Hartog, 1985) and the extended Jain-Lidiard model by Soppe (Soppe, 1993). In both models some parameters were modified as based on our latest insights (Donker et al., in prep.). In Fig. 6 it can be observed that both models predict more damage than experimentally observed. The conversion factor used to ease comparison of stored energy and amount of defects is 5 eV/defect corresponding to 82.5 J/g per mol% damage as discussed in (Donker et al., in prep.)

2.2 Irradiations Performed for GSF-IfT at the HFR in Petten

In addition to the irradiation experiments of ECN ground samples of natural rock salt samples were irradiated for GSF-IfT at the HFR at Petten. Radiation doses between 10^6 and 10^8 Gy were applied, while the temperature was varied between 100°C and 250°C. The radiation-induced formation of colloidal sodium, molecular chlorine and the associated storage of energy in rock salt as well as the formation and release of gases were investigated.

In general radiation damage, i.e. colloidal sodium and molecular chlorine, increased with dose. The data indicate that maximum colloid formation occurs at around 130 °C. Above 150°C colloid formation starts to saturate with increasing dose. At 100°C about 0,7 mol% sodium were detected for 10^8 Gy but no saturation was indicated in the investigated dose range. In all cases sodium colloid accumulation was accompanied by the formation of equivalent molar amounts of chlorine gas, most of which was found to be in the bulk, but chlorine evaporation from the salt increased with temperature.

The stored energy followed the trends outlined for the molecular radiation products. A conversion factor ob about 70 J/g per mol-% colloidal sodium in rock salt was derived from the data. The influence of sulfate-containing minerals such as anhydrite and polyhalite was investigated, but the results are not yet available. The gas atmosphere in which the rock salt is irradiated does not affect the formation of radiation damage but has a significant influence on the distribution of volatile products. In synthetic air, N_2O, CO, CO_2 as well as some H_2 were detected, while in a helium atmosphere H_2, CH_4, and CO_2 but no CO or N_2O were observed. The data suggest that the radiation-induced gas formation in an emplacement borehole for vitrified high-level radioactive waste in rock salt is only moderate.

References

Benneker, P.B.J.M., Hamilton, L.F.M., 1991: Isothermal behaviour of a Gloetzl in the HAW test field. Petten, Energieonderzoek Centrum Nederland. ECN-C--91-066.

CEC, 1991: The HAW-Project: Demonstration Facility for the Disposal of High-Level Waste in Salt, Synthesis Report 1985 - 1989, Commission of the European Communities, Nuclear Science and Technology, EUR 13263 EN

CEC, 1992: The HAW-Project: Test Disposal of Highly Radioactive Canisters in the Asse Salt Mine, Fed. Rep. Germany, Activity Report May 1990 - December 1991, Commission of the European Communities, Nuclear Science and Technology, EUR 14531 EN

Donker, H., Soppe, W.J. and García Celma, A., in prep. "A Comparison of Measured and Calculated Stored Energy in Irradiated Natural Rock Salt".

GSF-IfT, 1994: The HAW-Project: Test Disposal of Highly Radioactive Sources in the Asse Salt Mine, Progress Report July - December 1993, GSF-Institut für Tieflagerung, Abteilungsbericht IfT 2/94

Heijdra, J.J., Broerse, J., Prij, J., 1995: Thermo-mechnical analyses and model validation in the HAW test field. Final Report. ECN-C--94-064

Soppe, W.J., 1993: J. Phys.: Condensed Matter 5, 3519

Van Opbroek, G. and den Hartog, H.W., 1985: "Radiation Damage of NaCl: Dose Rate Effects". J. Phys.: Sol. State Phys. 18, p. 257-268.

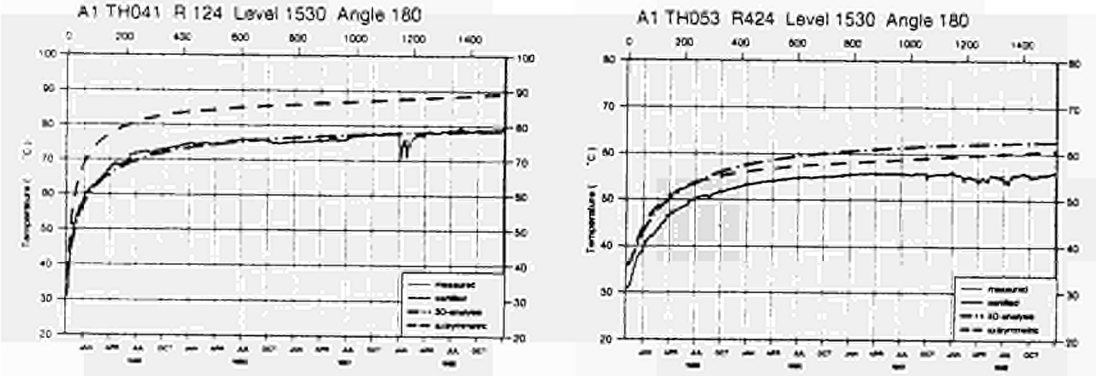

Fig. 1: Measured and calculated temperatures in the salt at 1.24 m and at 4.24 m from the borehole axis

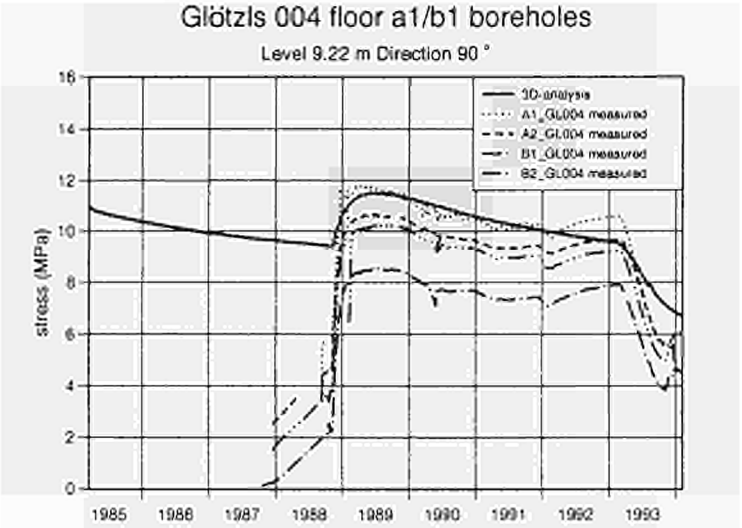

Fig. 2: Measured and calculated pressure for Glötzl loadcells in the floor near the heated boreholes

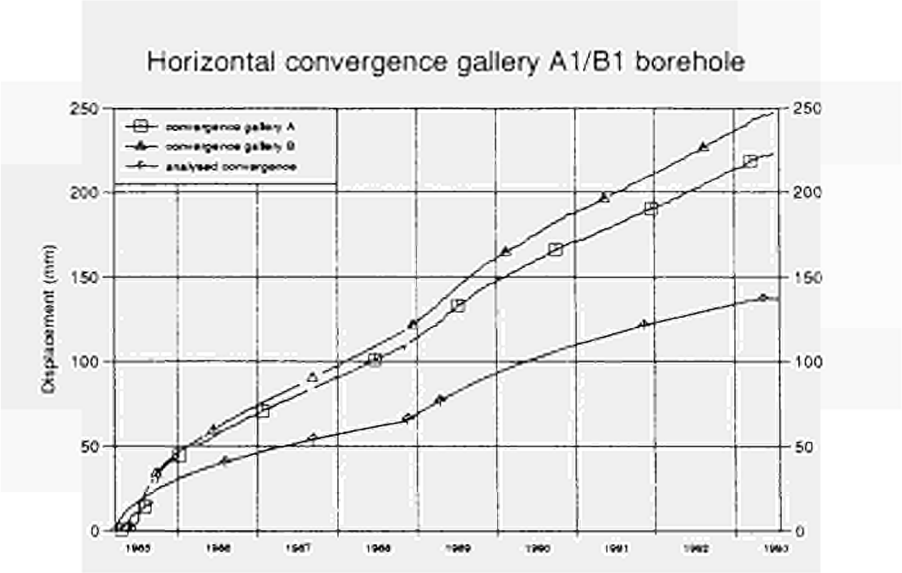

Fig. 3: Measured and calculated convergence of the gallery at the location of the heated borehole.

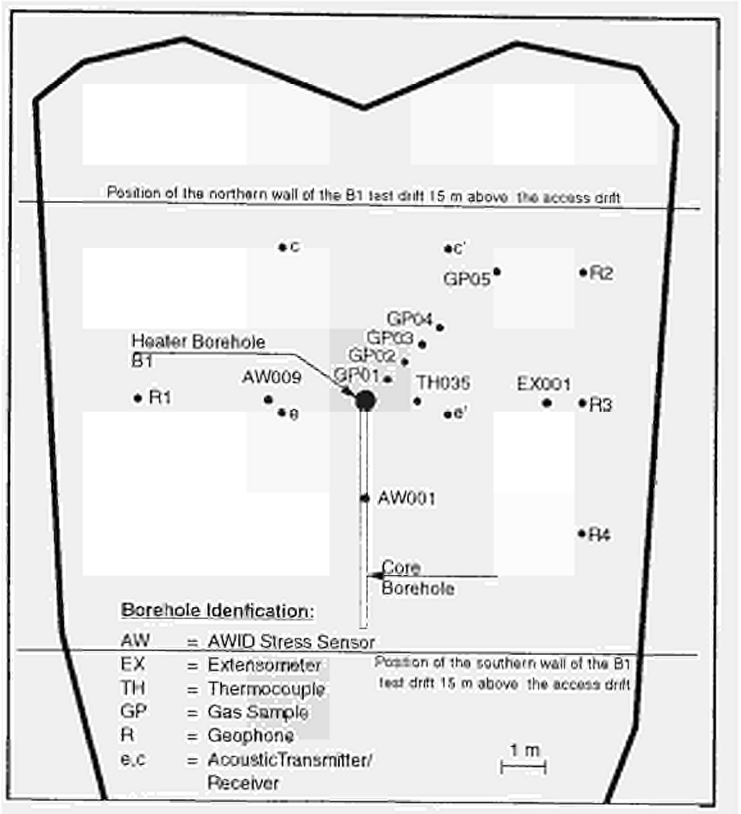

Fig. 4: Position of measurement boreholes around heater borehole B1 and contours of the room left below the HAW test field after salt and corrosion specimen sampling

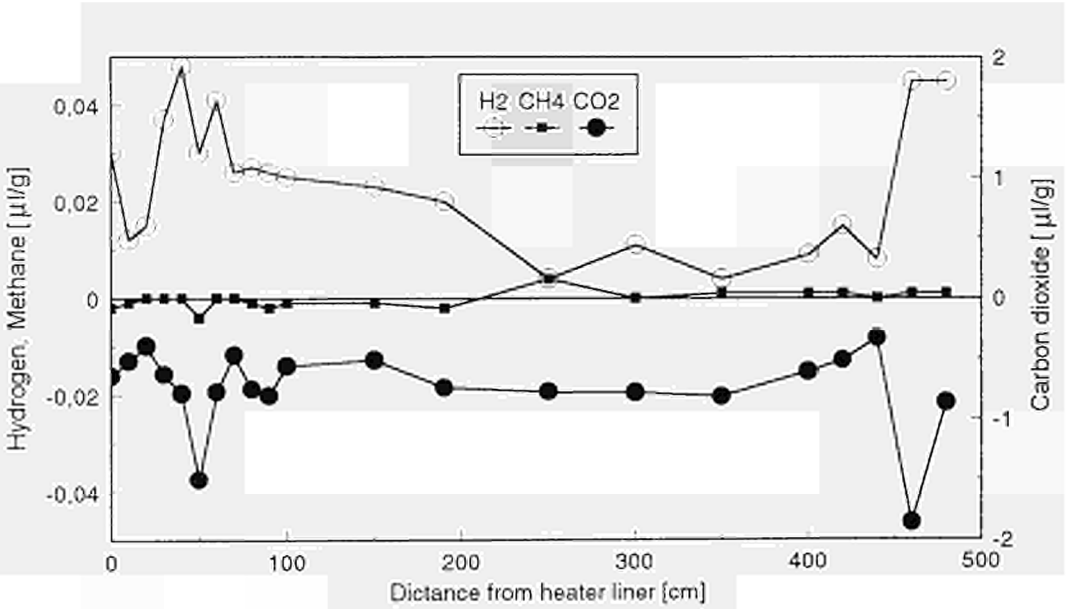

Fig. 5: Gas release/adsorption of the core samples from the radial core drilling at the heater borehole B1

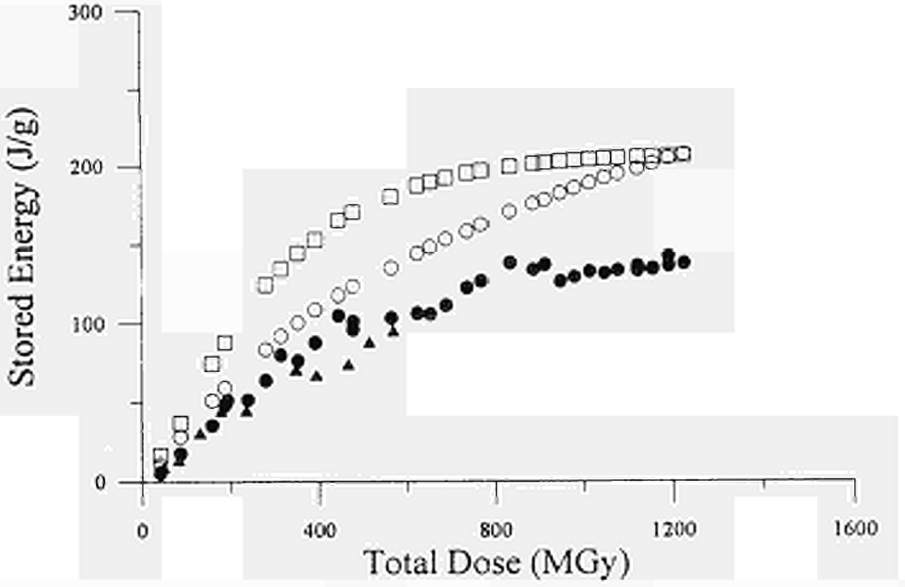

Fig. 6: Comparison of measured stored energy values on pure natural salt sample irradiated in the GIF A0 (triangles) and GIF A1 (full circles) with model calculations using the modified Jain-Lidiard model (squares) and with model calculations using the extended Jain-Lidiard model by Soppe (open circles). The model calculations have only been performed for the GIF A1 experiments.

Title:	**IN SITU INVESTIGATION OF THE LONG-TERM SEALING SYSTEM AS A COMPONENT OF A DAM CONSTRUCTION**
Contractors:	Deutsche Gesellschaft zum Bau und Betrieb von Endlagern für Abfallstoffe mbH (DBE) GSF - Forschungszentrum für Umwelt und Gesundheit GmbH Agence Nationale pour la Gestion des Déchets Radioactifs (ANDRA) Empresa Nacional de Residuos Radiactivos, S.A. (ENRESA)
Contract No:	FI2W - CT 90 - 0068
Duration of contract:	April 1, 1991 - March 31, 1995
Period covered:	January 1, 1994 - December 31, 1994
Project Coordinator:	W. Bollingerfehr, DBE
Project Leaders:	W. Bollingerfehr, DBE — J. F. Laurens, ANDRA N. Stockmann, GSF — F. Huertas, ENRESA

A. OBJECTIVES AND SCOPE

Dam constructions represent an essential component of the multibarrier safety concept for a repository for radioactive waste in salt formations. Within the scope of the dam project the long-term seal, which is responsible for the long-term safety of a dam construction is subjected to an in situ test. The main objectives of the scientific investigation programme are:

- to provide proof of the tightness of the long-term seal as a dam construction component by means of experimental investigations to obtain essential data concerning the effectiveness and
- to prognosticate its function (tightness) over long time periods (up to approximately 500 years) via model calculations.

The long-term evolution of permeability and porosity will be considered, as well as investigations of the chemical stability and the petrophysical behaviour will be performed.

The state of the art on calculations and codes for multiple-phase flow will be analyzed, and adequate mathematical models and computer codes will be developed and verified.

B. WORK PROGRAMME

According to the Technical Annex of the contract, the work programme consists of the following tasks:

for DBE and GSF

I/1. Conception, numerical preliminary investigations and detailed planning of the long-term seal test in the Asse Mine
I/2. Preliminary and parallel laboratory and in situ (borehole) tests
I/3. Instrumentation of the long-term seal construction
I/4. Performance of the large scale test long-term seal with gas and brine
I/5. Evaluation of the test results
I/6. Hydraulic modelling

for ANDRA

II/1. Physicochemical and petrophysical characterization
II/2. Evaluation of the solubility of materials
II/3. Dissolution kinetics
II/4. Laboratory batch experiments
II/5. Laboratory open system experiment
II/6. Pilot study in mine gallery (Amelie Mine)
II/7. Geochemical modelling
II/8. Petrophysical modelling
II/9. Interpretation and final modelling of the coupled system

for ENRESA:

III/1. Analysation of the state of the art on calculations and codes for multiple-phase flow

III/2. Conceiving laboratory experiments for measuring the permeability of the long-term seal against brine

III/3. Development of adequate mathematical models and computer codes for the numerical simulation of multiple-phase flow

III/4. Code verification

III/5. Interpretation of the in situ test measurements using the developed codes

C. PROGRESS OF WORK AND OBTAINED RESULTS

State of advancement

Since the beginning of 1993 the Bundesamt für Strahlenschutz (BfS) is responsible for the Dam project which is considered as final waste disposal facility related.

In 1994 DBE was asked by BfS to perform with GSF a redesign of the dam concept starting with a cheque of the project fundamentals and assumptions. The results of this first redesign step have been summarized in a report which was made available for BfS in August 1994. In December 1994 BfS finally decided not to continue the dam project due to political reasons.

In the year 1994 DBE's and GSF's main activities were focussed on the redesigning of the dam concept; meanwhile the performance of the original DBE/GSF-programme was interrupted.

ANDRA who is in charge of the investigation of the geochemical behaviour of salt briquettes and its interactions with saturated brine, completely interrupted it's work programme.

ENRESA has improved and extended the multiple-phase-flow code CODE-BRIGHT as well as it's verification. In addition, permeability experiments have been carried out.

Progress and results

1. Activities of the DBE and the GSF

DBE and GSF have performed the first redesign step of the dam concept. The planning fundamentals as well as the assumptions have been checked. A final report describing the redesigning results was compiled. In parallel to this the negotiation with BfS concerning a continuation of the in-situ activities in the Asse-Mine has been performed.

2. Activities of the ANDRA

During 1994 ANDRA stopped the planned work programme due to the interruption in the dam project.

3. Activities of the ENRESA

Developments during 1994 have been made in the following topics: Numerical modelling, simulation of compacted fill behavior in rock galleries and experimental work.

3.1 Numerical Modelling

In a previous report for the period 1991 - 1993 a detailed description of constitutive models developed for salt aggregates and the set of governing equations for coupled Thermo-Hydro-Mechanical boundary value problems was given.

They constitute the basis for program CODE-BRIGHT which has been verified (see task III.4) against several closed form solutions. CODE-BRIGHT has been improved and extended during 1994 in the following aspects:

a. integration rules have been modified in order to avoid "locking" behaviour in incompressible materials.

b. Several mew constitutive relations have been implemented. These refer to water retention relationships, relative permeability and, more significantly, the introduction of state surfaces to reproduce the volumetric behaviour of aggregates when changes in suction take place.
c. Input and output modules have been modified. In particular the program output is now compatible with general postprocessing program DRACVIU.
d. Several numerical techniques have been introduced in connection with the storage, advective, diffusive and volumetric strain terms.

3.2 Simulation of compacted fill behaviour in rock galleries

A comprehensive simulation (see task III/5) of the behaviour of a sealing dam has been carried out. Variables defining the initial state of salt aggregates are in accordance with proposals to use compacted salt bricks. The rock has been assumed to be brine saturated and the fully coupled hydromechanical problem was considered. The simulation has extended for a period of 27 years in order to reach a negligible residual porosity of the backfill (n~ 0,0001). A pressure build up in the backfill was computed when the fill becomes saturated. Then a transient flow process towards the host rock develops. Both FADT and DC mechanisms have been considered. The first one is relevant, in the example solved, in the backfill whereas the second controls the creep of the host rock. This case has shown the capabilities of the tools developed to handle the interaction between the manufactured dam and the surrounding rock.

3.3 Experimental work

A series of creep tests of edometric type in brine-saturated specimens were ended this year. On the other hand new equipment to perform creep tests in unsaturated compacted salt aggregates has been manufactured. (see task III/2).

The brine-saturated specimens have been tested for two years. Applied stresses range from 0.2 MPa to 40 MPa. Specimens of 50 mm and 30 mm diameter and 112 μm, 325 μm and 970 μm particle sizes were tested. At the same time a series of permeability measurements were carried out during the creep tests and various stress levels.

Suction measurements were also performed on salt aggregates compacted to porosities ranging from 10 % to 15 %. The specimens were made by compacting salt aggregates of 112 μm, 325 μm and 970 μm particle sizes.

Finally, the equipment to perform creep tests in unsaturated specimens was manufactured based on and edometric vessel connected to two chambers where a fixed relative humidity is established. Circulation of vapour from the chambers of the specimen allows to control the degree of saturation in the specimen while stress increments are applied to the specimen. In this case permeability measurements are carried out using the pulse method.

Title	**Active handling experiment with neutron sources**
Contractors	Deutsche Gesellschaft zum Bau und Betrieb von Endlagern für Abfallstoffe mbH (DBE) Agence Nationale pour la Gestion des Déchets Radioactifs (ANDRA) Forschungszentrum Karlsruhe GmbH (FZK)
Contract N°	FI2W-CT90-0069
Duration of contract	1 April 1991 - 30 June 1995
Period covered	1 January 1994 - 31 December 1994
Project leader	H.J. Engelmann (DBE), J.M. Hoorelbeke (ANDRA)

A. OBJECTIVES AND SCOPE

The Active Handling Experiment with Neutron Sources (AHE) is a demonstration test which will be performed by DBE and ANDRA/CEA in the Asse mine with FZK acting as coordinator. Besides the CEC, the DBE contribution is supported by the Bundesministerium für Forschung und Technologie (BMFT) under contract 02 E 8472 7.

The objective of the AHE experiment is to investigate radiological aspects of handling high level waste (either spent fuel or vitrified high level waste) in an underground repository. Neutron dose rates are measured resulting from direct radiation and from neutrons scattered by the surrounding host rock (rock salt). Computer codes and model calculations are to be verified by these experiments. Thus, an experimentally validated tool will be available for future detailed repository planning with emphasis on minimizing the radiation exposure of the operating personnel.

B. WORK PROGRAMME

According to the Technical Annex of the original contract, the overall programme consists of the following formal items

Design planning	1991/1992
Implementation planning	1992
Construction and acquisition	1992/1993
Execution and disposal	1993/1994
Evaluation and description	1994.

In the course of 1994, the duration of the contracted was extended to 30.06.95.

From a more practical point of view, the programme can be broken down into the following activities:

1. Shielding and backscattering calculations for a POLLUX cask with spent fuel and a transfer cask with vitrified high level waste
2. Design and construction of shielding casks which simulate a POLLUX cask and a transfer cask
3. Planning of test programme with shielding casks
4. Planning and design of instrumentation for experiment
5. Execution of the measurements

5.1 Above-ground measurements

5.2 Underground measurements in the ASSE mine

6. Evaluation and documentation of the results.

C. PROGRESS OF WORK AND OBTAINED RESULTS

State of advancement

The license for the active test in the Asse mine was granted November 16, 1993. Then the shielding cask and the neutron sources were ordered. At May 2nd 1994, the shielding cask was shipped to Great Britain for loading with the neutron line source.

The above ground measurements at the area of the Physikalisch Technische Bundesanstalt (PTB) were performed from June to August 1994, and the underground measurements in the Asse mine lasted from September to December 1994. The evaluation of the experimental results is still under way, but it can already be concluded, that the forecasted increase in neutron dose rate due to backscattering was actually observed in the experiments.

Progress and results

After the license for the active test in the Asse mine was granted November 16, 1993, the shielding cask, the neutron sources and some other components were ordered and manufactured. In the first part of the annual progress report, the components for the test are presented, and in the second part of the report some preliminary results of the above and underground measurements are outlined.

C 1. Manufacturing of the components

C 1.1 Shielding cask

The AHE shielding cask is designed as a Type-A-container for maximum safety during transport and conforms to the GGVS transport regulations (GGVS: Regulations and Road Transport of Dangerous Cargo). It consists of three concentric cylindrical jackets of different materials:

- container of nodular cast iron (outer cask)
- neutron moderator
- container of stainless steel (inner cask).

The outer cask and its lid (Fig. 1) is made of nodular cast iron GGG 40.3, the composition of which is given in Tab. 1. The whole body was proved on casting defects by ultrasonic tests, performed by the technical control board TÜV Nordrhein-Westfalen. The outer cask has a length of 1350 mm, a diameter of 912 mm and a weight of 5728 kg.

The neutron moderator consists of polyehtylene (Solidur) and fits between the outer and inner cask. The composition of the moderator is given in Table 2. The moderator has a length of 600 mm, an inner and outer diameter of 513 mm and 312 mm, respectively, and a weight of 71.6 kg.

The inner cask is made of stainless steel 15 MnNi63, the composition of which is given in Tab. 3. In the center of the container a borehole had been drilled, in which the line source will be placed. The inner cask has a lenght of 620 mm, a diameter of 312 mm and a weight of 400 kg. Fig. 2 is a picture of the inner stainless steel container being loaded into the outer cask made of nodular cast iron. The specification of the steel is given in Table 3.

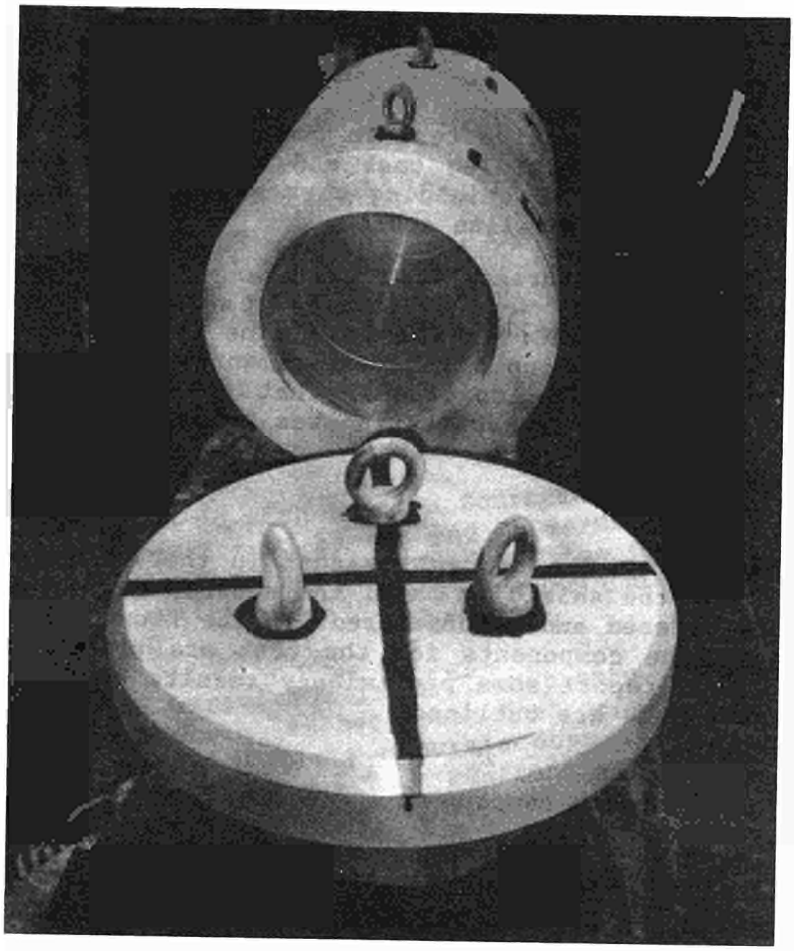

Fig. 1: Container of nodular cast iron

Tab. 1: Composition of nodular cast iron GGG40.3

Fe %	C %	Si %	Mn %	P %	S %	Mo %	Cr %
94,127	3,590	1,960	0,200	0,029	0,004	0,060	0,030

$\rho = 7{,}13\ g/cm^3$

Tab. 2: Composition of polyethylene

H %	C %
14,4	85,6

$\rho = 0{,}91\ g/cm^3$

Tab. 3: Composition of the stainless steel 15 MnNi63

Fe %	C %	Si %	M %	P %	S %	Cr %	Mo %	Ni
97,2107	0,160	0,220	1,420	0,007	0,002	0,130	0,030	0,680

Al %	V %	N %	Cu %	Nb %	Ti %	As %	Sn %
0,023	0,005	0,006	0,090	0,001	0,002	0,005	0,009

$\rho \sim 7{,}8$ g/cm^3

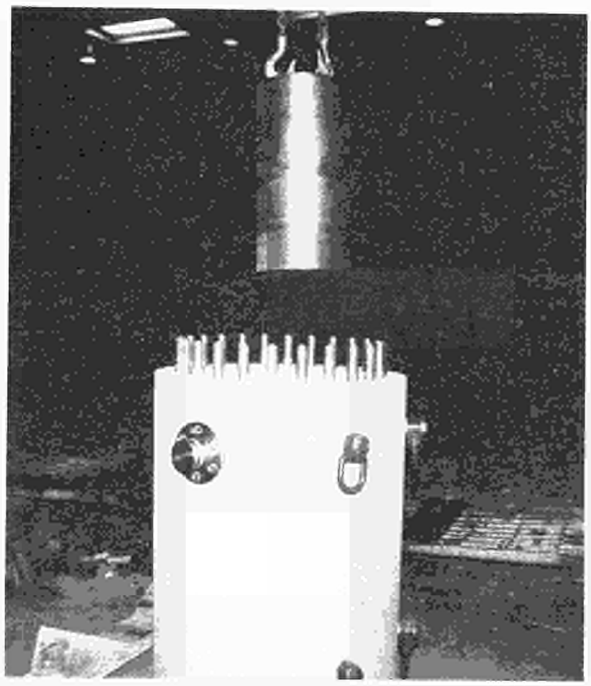

Fig. 2: Inner stainless steel container being loaded into the nodular cast iron cask

Fig. 3 is a view into the shielding cask. The borehole which accomodates the neutron line source is clearly visible in the center. The lifting-screws are only for handling the inner container and were removed thereafter.

The line source contains 40 individual neutron capsules and 20 spacers in a stainless steel tube as shown in Fig. 4. Each capsule is filled with Californium 252 which has a source strength of about 4,4 E6 n/s. The distribution of the source strength of the individual capsules over the line source is demonstrated in Fig. 5. The maximum source strength is 5.06 E6, and the minimum source strength 3.54 E6 n/s. Capsule 5769NC has been calibrated at the National Physical Laboratory at Middlesex in England and is used as reference for the source strength of the remainder capsules.

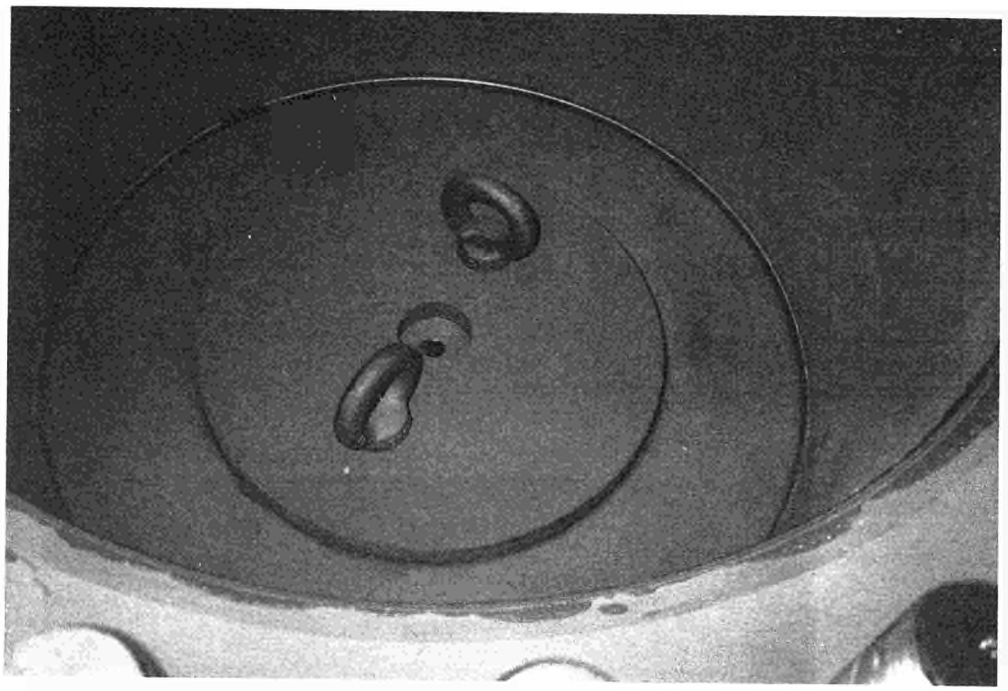

Fig. 3: View into the shielding cask

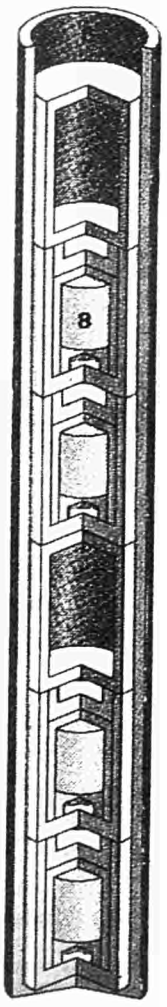

Fig. 4: Line source

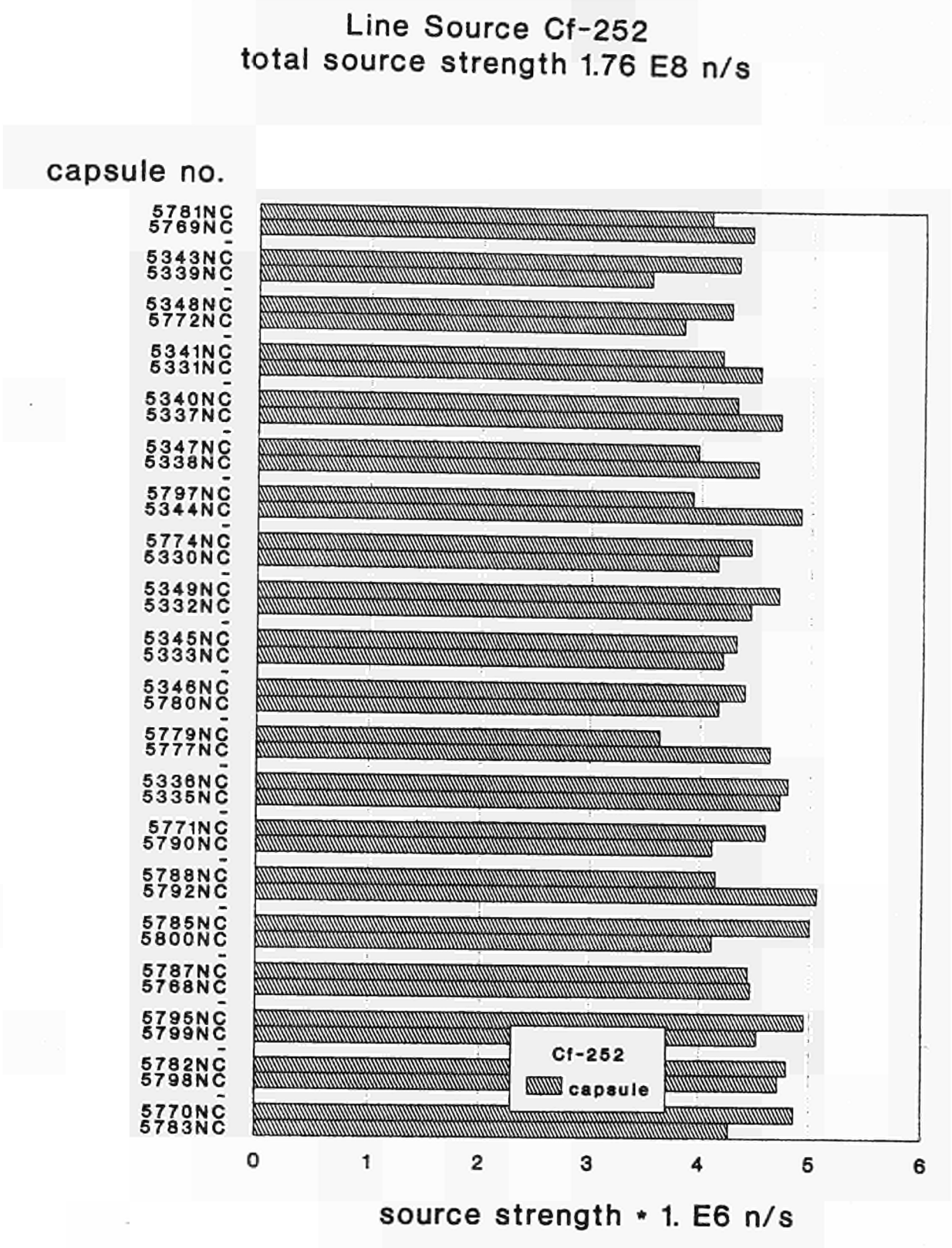

Fig. 5: Distribution of the source strength of the Cf-252 capsules

C 1.2 Bearing support

The bearing support allows to hold the shielding cask in a horizontal as well as in a vertical position above the floor. Fig. 6 shows the cask with its screwed top lid (32 screws M39) and three hexagon screws for transportation and handling. The center-line of the shielding cask lies 1.50 m above the floor. The support on the left side of the bearing support may be lowered to move the shielding cask by means of the load bents into the vertical position.

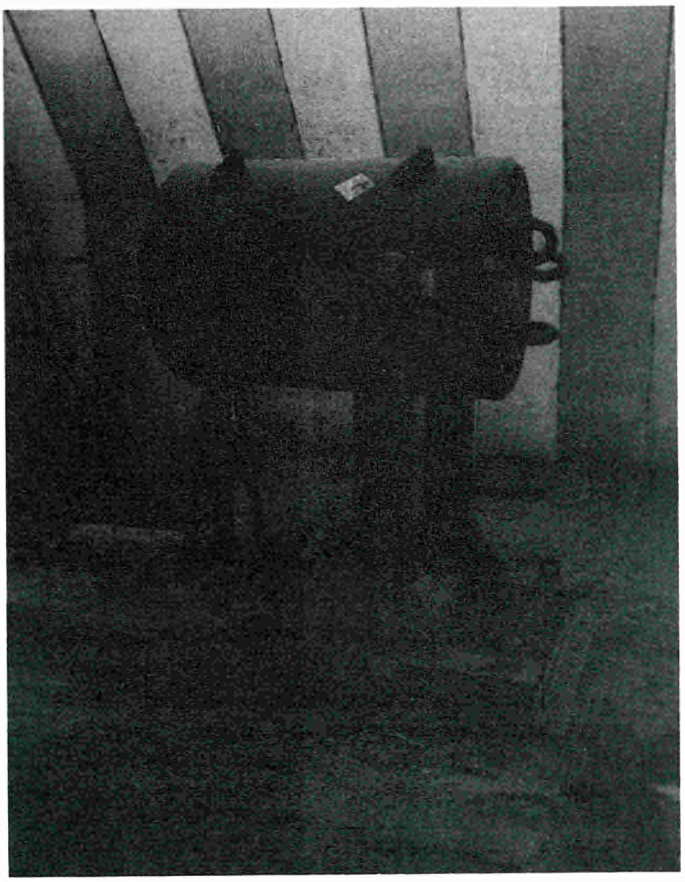

Fig. 6: Bearing support with shielding cask

In Fig. 7 the experimental configuration is shown with the shielding cask in the bearing support in a horizontal position and the trestle made of aluminium for the experimental arrangement. A rectangular supporting net for the detector is mounted above the shielding cask, which can be lifted manually up and down. To protect the experimental set-up against bad weather conditions, during the above ground tests at the PTB area, the whole experiment was covered by a tent.

C 2. Some preliminary results

The following measuring devices were used

- HANDI (University of Saarbrücken) and Harwell-REM-counters for neutron dose rate measurements
- Ionization chambers and FAG-chambers for gamma dose rate measurements
- Bonner spheres, Nuclear Enterprise (NE)-213 scintillation spectrometers and H_2-counters for neutron spectrum measurements.

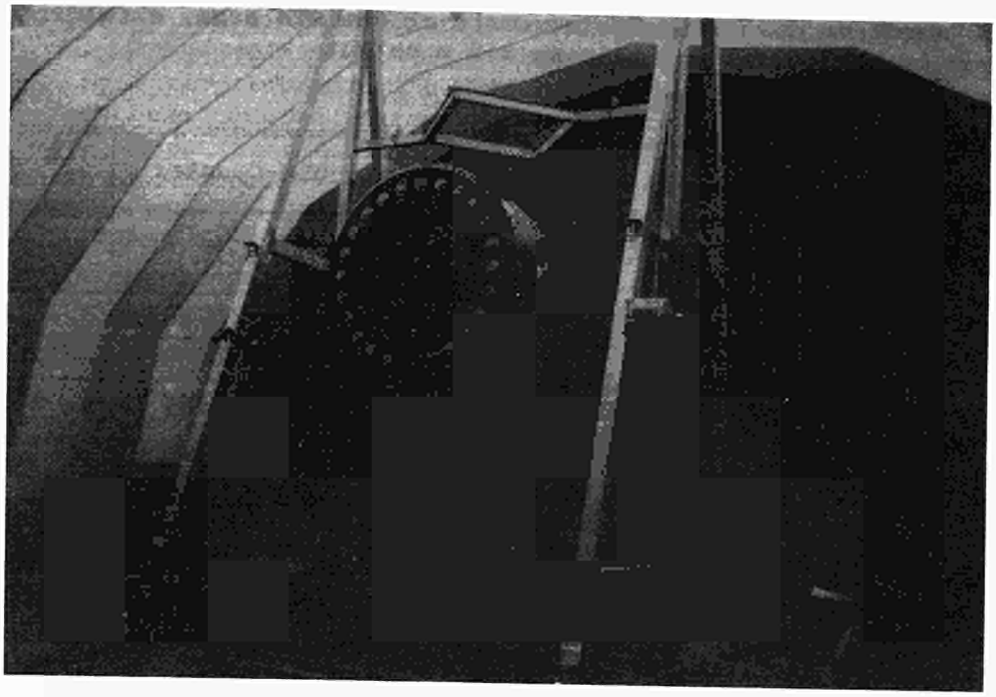

Fig. 7: Experimental configuration

Measurements at the PTB area were made in horizontal and vertical positions. The number of measurements are listed in Tab. 4.

Tab. 4: Number of above ground measurements at the PTB area

	Shielding Cask-Position	
	Horizontal	Vertical
Neutron Dose Rate:		
HANDI	24	5
Harwell-REM-Counter	15	5
Gamma Dose Rate:		
I-Chamber	16	4
FAG-Chamber	9	5
Neutron Spectra:		
Bonner Sphere	8	4
NE 213	4	1
H_2-Counter	2	1

Some results from the neutron dose rate measurements at the PTB area for the shielding cask in a horizontal position at a height of 1.5 m are given in Tab. 5. The term % means standard deviation.

Tab. 5: Neutron dose rate measurements at the PTB area, shielding cask in horizontal position at 1.5 m height

Detector position at top of cask

distance from top [m]	HANDI		Harwell-REM-Counter		HANDI/REM
	µSv/h	%	µSv/h	%	
1	29,8	±1,17	43,2	±0,53	0,690
2	10,7	±3,27	15,0	±0,89	0,712
3	5,7	±6,14	7,6	±1,26	0,750

Detector position at bottom of cask

distance from bottom [m]	HANDI		Harwell-REM-Counter		HANDI/REM
	µSv/h	%	µSv/h	%	
1	64,8	±0,54	78,37	±0,39	0,83
2	19,8	±1,77	25,13	±0,69	0,79
3	10,3	±3,40	12,67	±0,97	0,81

Detector position above cask

distance from surface [m]	HANDI		Harwell-REM-Counter		HANDI/REM
	µSv/h	%	µSv/h	%	
0,3	91,41	±0,38	113,08	±0,33	0,80
1	32,93	±1,06	41,5	±0,54	0,79

As can be seen from Tab. 5, the ratio of the measured neutron dose rates HANDI/REM is about 0.7 to 0.8 which may be due to the different thresholds of the two instruments. A difference like that can often be found when using different kinds of detectors. Calibration of the various detectors will be done by using the results from the neutron spectra measurements with the Bonner spheres which might result in some modifications of the values shown in Tab. 5.

The neutron dose rates measured along the axis of the shielding cask at 1 m distance from the surface aboveground and underground are shown in Fig. 8.

The forecasted increase in neutron dose rate due to neutron backscattering in the galleries of a disposal mine is clearly visible.

Similar results were obtained at various distances from the top of the shielding cask, see Fig. 9. As pointed out in the figure, backscattering increases the local neutron dose rate in the near field (1 to 2 m) by a factor of about 2, whereas at longer distances (3 to 5 m) the increase amounts to a factor of about 4 to 5.

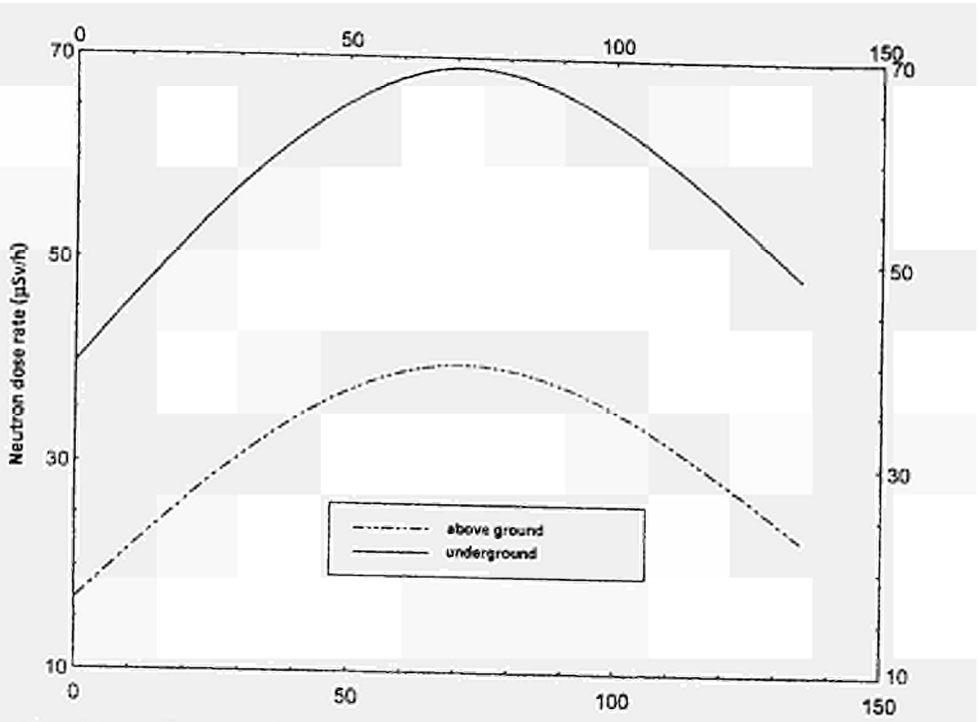

Fig. 8: **Neutron dose rates along the shielding cask at 1 m distance from the surface, measured with the Harwell-REM-Counter**

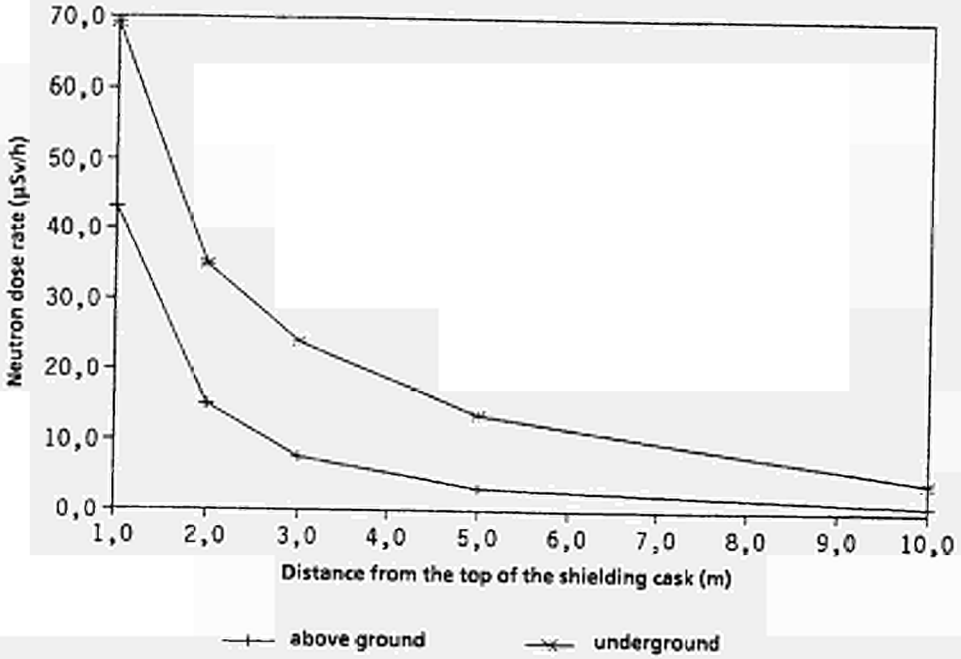

Fig. 9: **Neutron dose rates at various distances from the center of top of the shielding cask, measured with the Harwell-REM-Counter**

These preliminary results clearly indicate that backscattering has to be taken into account when evaluating the dose burden to the plant personal working in a disposal mine.

The underground measurements in the Asse mine were finished by the end of 1994. Evaluation and documentation of the results are under way.

Title:	Thermomechanical simulation of the near field of an emplacement borehole in a salt formation (Amélie Mine - France) - "C.P.P.S. TEST"
Contractors:	Agence Nationale pour la Gestion des déchets RAdioactifs (ANDRA) - France G.3S (Groupement pour l'étude des Structures Souterraines de Stockage) - France
Contract No:	FI2W-CT92-0120
Duration of contract:	April 92 - March 95
Period covered:	January 94 - December 94
Project leaders:	A.COURNUT (ANDRA), M.GHOREYCHI (G.3S)

A/ OBJECTIVES AND SCOPE

The aim of "CPPS" test is to study the near field thermomechanical behaviour in deep layered salt around a borehole waste emplacement under thermal loading. This is of major importance for predicting the behaviour of radioactive waste storage particularly as regards the temperature and the pressure that the canisters will have to withstand. The influence of marno anhydritic layers will be studied as well.

The experiment is to include three tests in separate boreholes at the Amelie Mine underground facilities, with identical heating probes but different types of thermal loadings and backfilling materials. The scientific interpretation of the results will be made by G.3S (see figure 1).

B/ WORK PROGRAM

1. CPPS ONE : Positioning of a prototype heater with an annulus between the heater and the borehole as small as possible (< 5 mm) and heating after having observed the borehole convergence.

2. CPPS TWO : Positioning of a heater with an empty annulus (2,5 cm) and heating after having observed the borehole convergency.

3. CPPS THREE : Positioning of a heater with the annulus (2,5 cm) filled with crushed salt and immediate heating.

C/ PROGRESS OF WORK AND RESULTS OBTAINED

State of advancement

CPPS 1 probe was installed in December 1991. After a period of observation of the borehole creeping, the heater was turned on in May 20th 1992. The heating power was 2.4KW. After two months the heating power was increased up to 4 KW in order to speed up the borehole creeping. The heating was shut down in February 17th 1993 after approximately nine months.

The fact that no major power cut occured during this period, will facilitate the scientific interpretation.

The CPPS 2 and 3 probes were positioned in December 1993. They include new, more accurate, pressure sensors.

The heater was turned on in March 14th 1994 on both CPPS 2 and 3, with a heating power of 2,4 KW. In June 11th 1994, the heating power was increased to 3,8 KW on the CPPS 3 only.

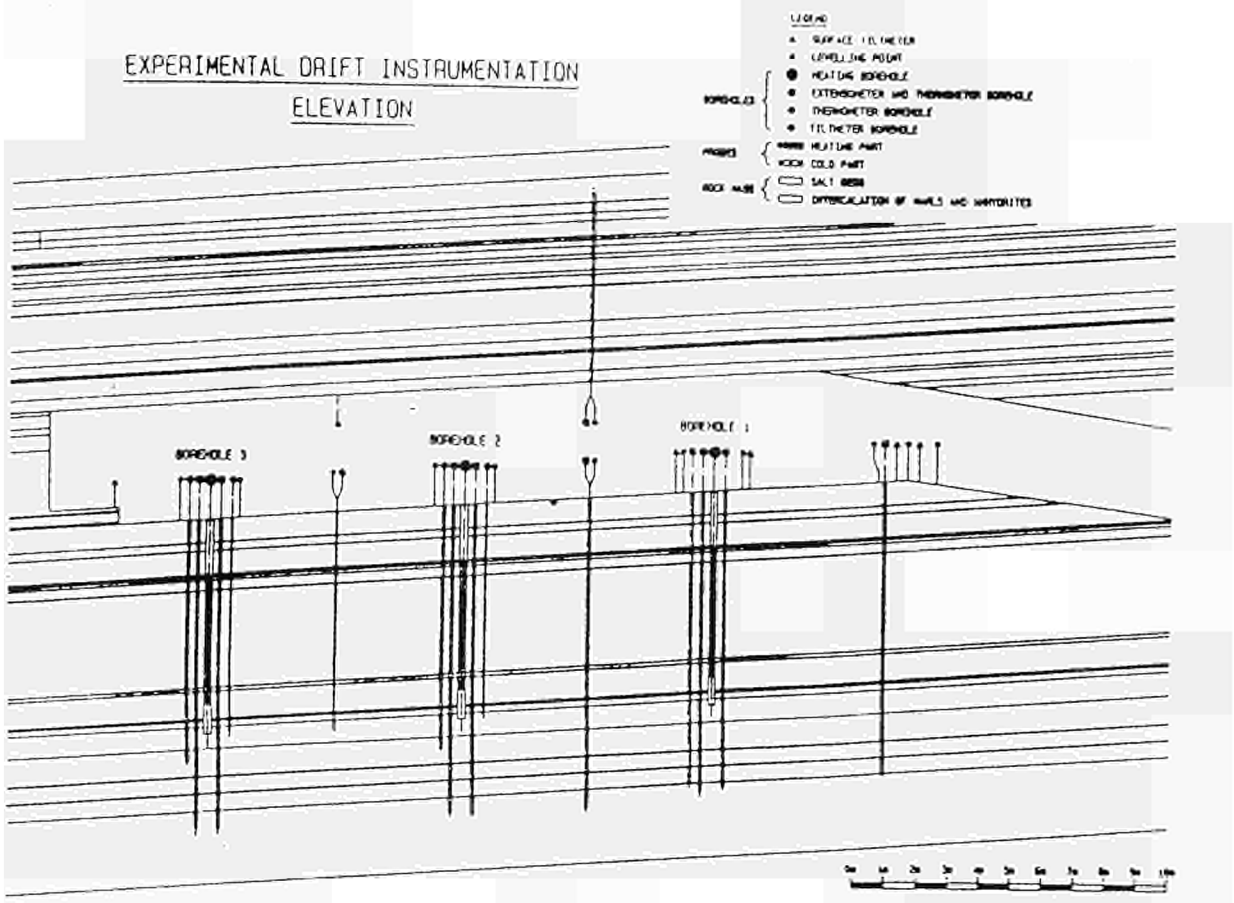

Figure 1

Progress and results

C.1 Heating power

On CPPS 1, after nearly two months at 2.4 KW, the power was increased to 4 KW. After eight months the power was reduced to 2.4 KW and stopped after approximately nine months, in February 1993.

On CPPS 2 and 3, after four months at 2,4 KW, the power was increased to 3,8 KW on CPPS3 only. The power could not be increased on CPPS 2 because of the high temperature already reached in the probe core (around 270° C).

C.2 Borehole closure (see figure 2)

On CPPS 1, at the end of the first heating stage, the closure rate was very low. Three days after the increase of power, the borehole was in contact with the probe. The stiffness of the probe was such that after the contact no deformation was observed.

On CPPS 2, after 7,5 months of heating, the convergence reached 19 mm, that is to say 7,6% of the borehole diameter. The complete closure of the space existing between the borehole wall and the probe cannot be expected within the duration of the experiment, considering the fact the heating cannot be increased without damaging the probe.

On CPPS 3, after 7,5 months of heating, the convergence reached 16,6 mm, that is to say 6,6% of the borehole diameter.

PROBE # 2

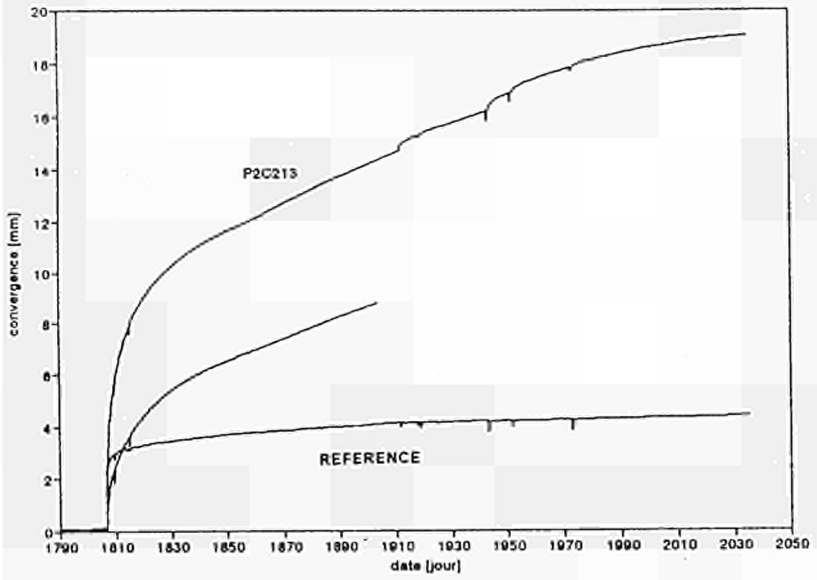

BOREHOLE CLOSURE ON CPPS 2
Figure 2

C.3 Temperature (see figure 3)

On CPPS 1, during the first stage, the maximum temperature was 120°C on the surface of the probe. During the second stage the temperature reached 200°C and more or less stabilised. At a distance of 70 cm from the axis of the probe, the temperature reached 70°C.
One month after the shut down of the heaters, the rock temperature returned to its normal value.

On CPPS 2, the following temperatures were obtained :
- in the probe core : 270°C,
- at the probe wall : 270°C,
- at the borehole wall : 180°C.

On CPPS 3, the following temperatures were obtained :
- in the probe core : respectively 150°C for a heating power of 2,4 KW and 210°C for a heating power of 3,8 KW,
- at the probe wall : respectively 140°C and 205°C,
- at the borehole wall : respectively 120°C and 180°C.

Comparison between the temperatures obtained in CPPS 2 (empty annulus) and in CPPS 3 (annulus filled with crushed salt) shows very clearly the favourable influence of the crushed salt on the temperature gradient between the probe and the borehole wall, and on the temperature in the probe core.

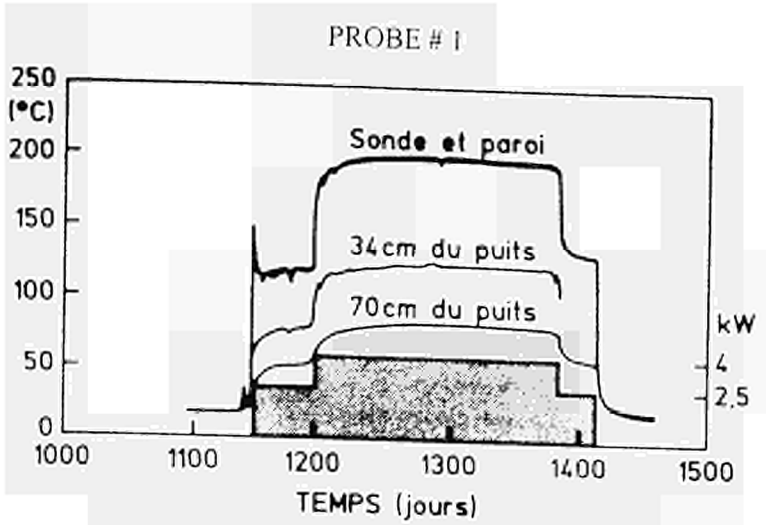

NEAR FIELD TEMPERATURE ON CPPS 1
Figure 3

C.4 Displacements in rock salt around the borehole (see figure 4)

Around CPPS 1, the displacements of the rock salt reached 9 mm at the surface and 4 mm at a depth of 3.75 meters and 1 mm at a depth of 5.50 meters.

Around CPPS 2, it reached 11,5 mm at the surface and stabilized.

Around CPPS 3, it reached 17,8 mm at the surface.

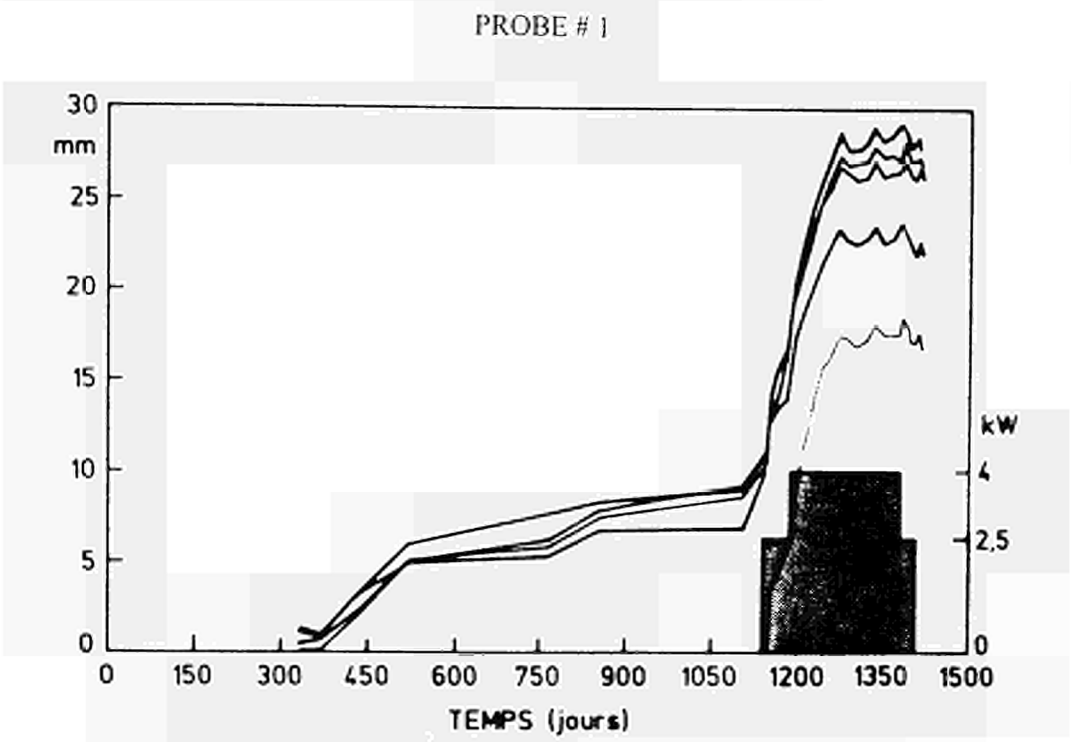

DISPLACEMENTS IN ROCK SALT AROUND BOREHOLE
Figure 4

C.5 Displacements at the floor of the gallery versus time (see figure 5)

The maximum displacement induced by the heating was approximately 20 mm.

PROBE # 1

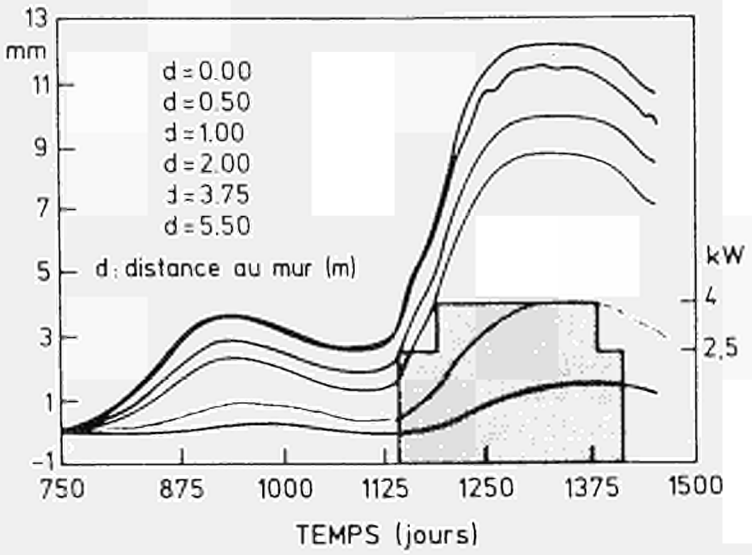

DISPLACEMENTS AT THE FLOOR OF THE GALLERY
Figure 5

C.6 Displacements at the floor of the gallery versus distance from the borehole and time (see figure 6)

The heating has significantly influenced the floor of the gallery up to 12 meters away from the borehole center.

PROBE # 1

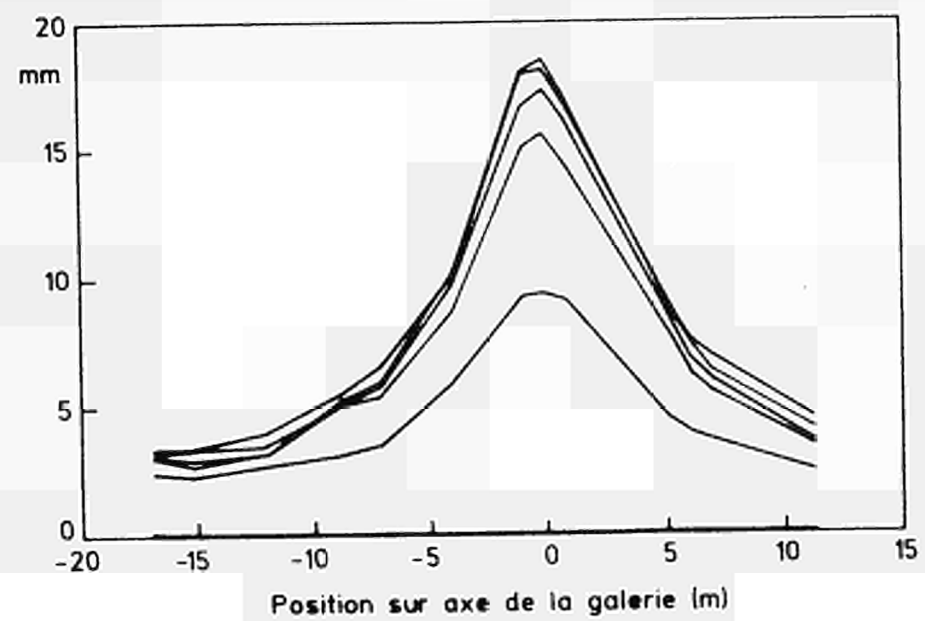

EVOLUTION OF THE DISPLACEMENTS AT THE FLOOR OF THE GALLERY
Figure 6

C.7 Dip angle of the floor around the borehole (see figure 7)

This figure shows the two heating steps. The dip angle varies according to the direction. Due to the effect of the walls of the gallery, the dip angle measured perpendicularly to the axis of the gallery is much greater than the angle measured parallely.

PROBE # 1

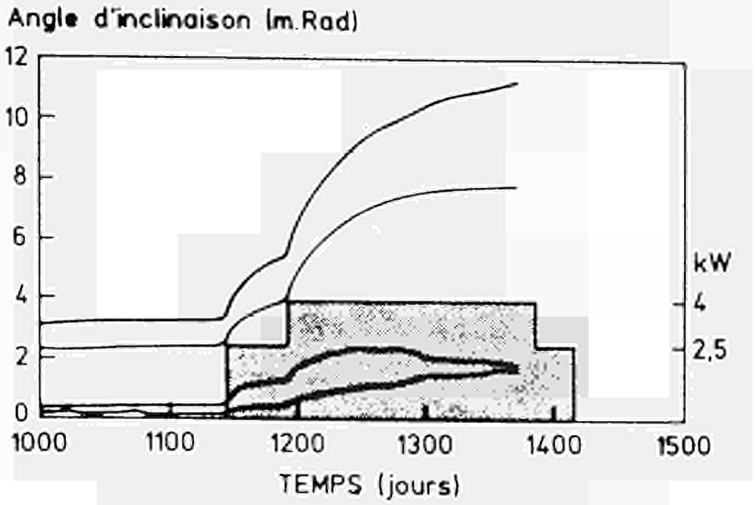

DIP ANGLE AROUND BOREHOLE
Figure 7

C.8 Pressure (see figure 8)

It seems that the pressure on the probe varies between 7 and 10 MPa.

PROBE # 1

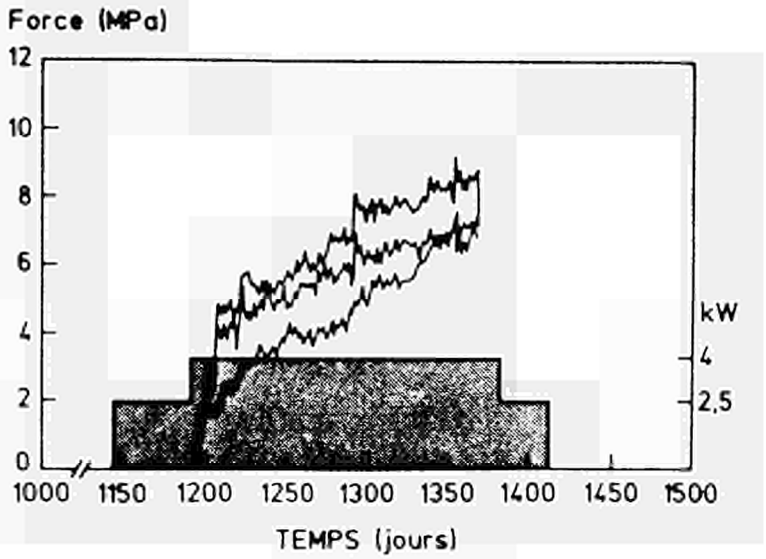

PRESSURE ON THE PROBE
Figure 8

Title:	In-situ research on compaction of and gas release in saliferous backfill (TSS experiment).
Contractor:	GSF-Institut für Tieflagerung (IfT), Braunschweig, Germany
Contract-No.:	FI2W - CT94 - 0127
Duration of contract:	August 1994 - April 1995
Period covered:	August 1994 - December 1994
Project Leader:	J. Schneefuß

A. OBJECTIVES AND SCOPE

The R&D-programme of the TSS-project concerns the final disposal of spent fuel elements of nuclear power plants. The direct disposal provides the packaging of the fuel rods in self shielding Pollux casks and their emplacement in the drifts of a repository mine in rock salt. The remaining volume of the drifts is backfilled with crushed salt immediately after the emplacement of the casks.

A large scale demonstration test is being carried out in the Asse salt mine to study the thermal and thermomechanical effects on the backfill and the surrounding rock salt in connection with this kind of storage. The test field is designed similar to a real repository. It comprises two parallel test drifts which are 3.5 m high and 4.5 m wide with a pillar of 10 m width between (Fig. 1). In each test drift three dummy casks are deposited. The dimensions, weight and heat output of the casks correspond to real Pollux casks. They are equipped with electrical heaters operated at a thermal power output of 6.4 kW each. Additionally, the test field includes several observation and access drifts, from which a large number of boreholes extend into the vicinity of the test drifts, as do boreholes from the test drifts into the ambient rock salt. The boreholes as well as the backfill and the surface of the dummy casks are equipped with various measuring gauges.

The main objectives of the test are the study of the thermomechanical interactions of heated casks, backfill and surrounding rock salt for the validation of thermal and thermomechanical computer models as well as the investigation of moisture and gas release due to heating and corrosion processes.

The project is supported by the Bundesministerium für Bildung, Wissenschaft Forschung und Technologie (BMBF) and the EC. Several partners contribute to the study (GSF-Forschungszentrum für Umwelt und Gesundheit GmbH: infrastructure; temperature, stress and deformation measurements in the backfill and the surrounding rock; backfill compaction; gas release; Bundesanstalt für Geowissenschaften und Rohstoffe (BGR): stress measurements in the rock; permeability of the backfill; numerical modeling; Deutsche Gesellschaft zum Bau und Betrieb von Endlagern für Abfallstoffe mbH (DBE): backfilling technique; designing and installation of the heater casks; testing of measuring techniques; Kernforschungszentrum Karlsruhe GmbH (KfK): coordination; corrosion studies; numerical modeling).

B. WORK PROGRAMME

B.1 Thermomechanical effects in the backfill
B.2 Gas components in the backfill

C. PROGRESS OF WORK AND OBTAINED RESULTS

State of advancement

Planning and preliminary work for the demonstration test started in 1985. The preparation of the test field including the instrumentation of drifts and boreholes and the backfilling of the drifts was completed in August 1990. Heating started on September 25, 1990 and is still continuing.

Until the end of 1993 the electrical heaters operated quite well apart from several short breakdowns without an impact on the thermomechanical behaviour of the rock. Different kinds of problems at the heater control system led to a higher thermal power output in 1994, resulting in increasing temperatures both at the surface and around the heater casks.

Progress and results

C.1 Thermomechanical effects in the backfill

A maximum temperature of approximately 210 °C at the surface of the casks is reached after five months. Since then improving heat conductivity due to increasing compaction of the backfill causes continuously decreasing temperatures at the surface of the casks. The temperature distribution in the heated area of the test drifts depends on the distance of the measuring position from the heaters. Temperatures in the warm backfill range up to 135 °C approaching a steady state after three years of heating. With increasing distance from the heaters a steady state in the rock has not been reached yet. By the TSS experiment a large number of data are available now for the validation of constitutive models used to predict the thermomechanical behaviour of rock salt and salt backfill. Measured temperatures in the test drifts fit quite well with theoretical calculations.

Gradual closure of the drifts causes an increasing compaction of the backfill. This process is accelerated considerably by heating. Convergence rates in the heated area rise by a factor of ten immediately after the start of heating. Three months later the rates are decreasing indicating the beginning support by the backfill. The growing resistance of the backfill to drift closure caused by its increasing density and rigidity reduces the convergence rates more and more. Current rates amount to about 0.75 %/a and 0.9 %/a in horizontal and vertical direction respectively, which is still three times the rate prior to heating. The drift convergence in the heated area is considerably lower than calculated. After four years of heating vertical convergence reaches only two thirds of the predicted value (Fig. 2).

In the not heated sections convergence rates remain unchanged at first. With some delay, temperatures start to rise in the cold sections as well reaching about 45 °C up to now. Drift closure subsequently accelerates to double the amount. Two years later, the convergence rates begin to decrease again and are currently still one and a half times of the initial closure rate.

As a result of drift closure the initial backfill porosity of about 35 % has been reduced to 27.5 % to 29 % in the heated area after four years of heating. The decrease of porosity is taking place much slower than predicted due to the lower convergence rates. In the not heated sections the actual backfill porosity ranges between 32.5 % and 33.5 %.

After backfilling of a drift the primary settling of the backfill due to gravity leads to the opening of a gap between the roof and the top of the backfill. The gap opens up to 25 mm in the different sections depending on the local density of the backfill and the local drift convergence. In the heated area the acceleration of drift closure induces the closing of the gap within about four to seven weeks after the start of heating. In the cold sections the closing of the gap takes much longer and lasts up to two years.

Backfill compaction does not start before the gap at the roof is closed. During the first months mainly the upper part of the heated backfill is compacted. Subsequently, increasing portions of the lower part are involved. After two years of heating the vertical distribution is approximately balanced with hardly any change up to now. The highest values of backfill compaction are recorded around the central heaters. Compaction decreases with increasing distance from the heaters.

In the cold sections primary settling continues after the heaters have been switched on, affecting mainly the lower section of the backfill. The upper part, however, remains almost unchanged in the beginning. As a result of the accelerated drift closure following the gradual temperature increase in the cold area, the gap at the roof gets closed and the backfill is compacted more and more in the upper part now.

The compaction of the backfill due to drift closure is causing an increasing pressure between backfill and surrounding rock. In the heated area the backfill pressure starts to rise immediately after the beginning of heating. The pressure increases continuously reaching a maximum of 2.5 MPa at the roof after four years of heating. This value corresponds to approximately 20 % of the initial vertical stress, which has been estimated at about 12 MPa in the test field. Some short drops in pressure are caused by short heater breakdowns resulting in a thermal induced relaxation of stress. An increasing sensitivity of the backfill to power failures in the course of time implies a rising rigidity of the backfill starting from its upper part. The pressure in the cold backfill begins to rise slowly about one year after the start of heating and reaches 0.1 MPa on average up to now.

C.2 Gas components in the backfill

Rock salt contains small amounts of gas and water which can be released into the emplacement drifts due to the heat production of the fuel elements. Gases can also be released by radiolytic impact of gamma radiation on rock salt. Gases and water cause corrosion of the waste canisters and thus induce the generation of hydrogen and the release of radioactive material.

Gas samples are taken from the backfill both in the northern and the southern drift of the test field and analyzed by chromatography in the underground laboratory. Already at the ambient temperature of approximately 36 °C on the 800 m level H_2, CH_4 and CO_2 were detected in the backfill in concentrations of 28 to 44 vpm, ≤ 4 vpm and 35 to 75 vpm respectively. Significant gas release starts immediately after the heaters are switched on. Within six months the concentrations of the major gas components H_2, CH_4 and CO_2 increase up to 550 vpm, 40 vpm and 3000 vpm respectively.

As the backfill is comparatively porous and permeable, the concentration of the released gases is constantly diluted due to pressure variations by mine ventilation as well as by long term atmospheric pressure changes.

The gas measurements were stopped due to financial cuts by the end of 1992. They were resumed in August 1994 with the support of the European Community.

In order to determine the total amount of gas generation, works are in progress to seal one of the drifts at its entrance. The air pressure before and behind the seal will be measured to estimate the tightness of the seal and the loss in gases.

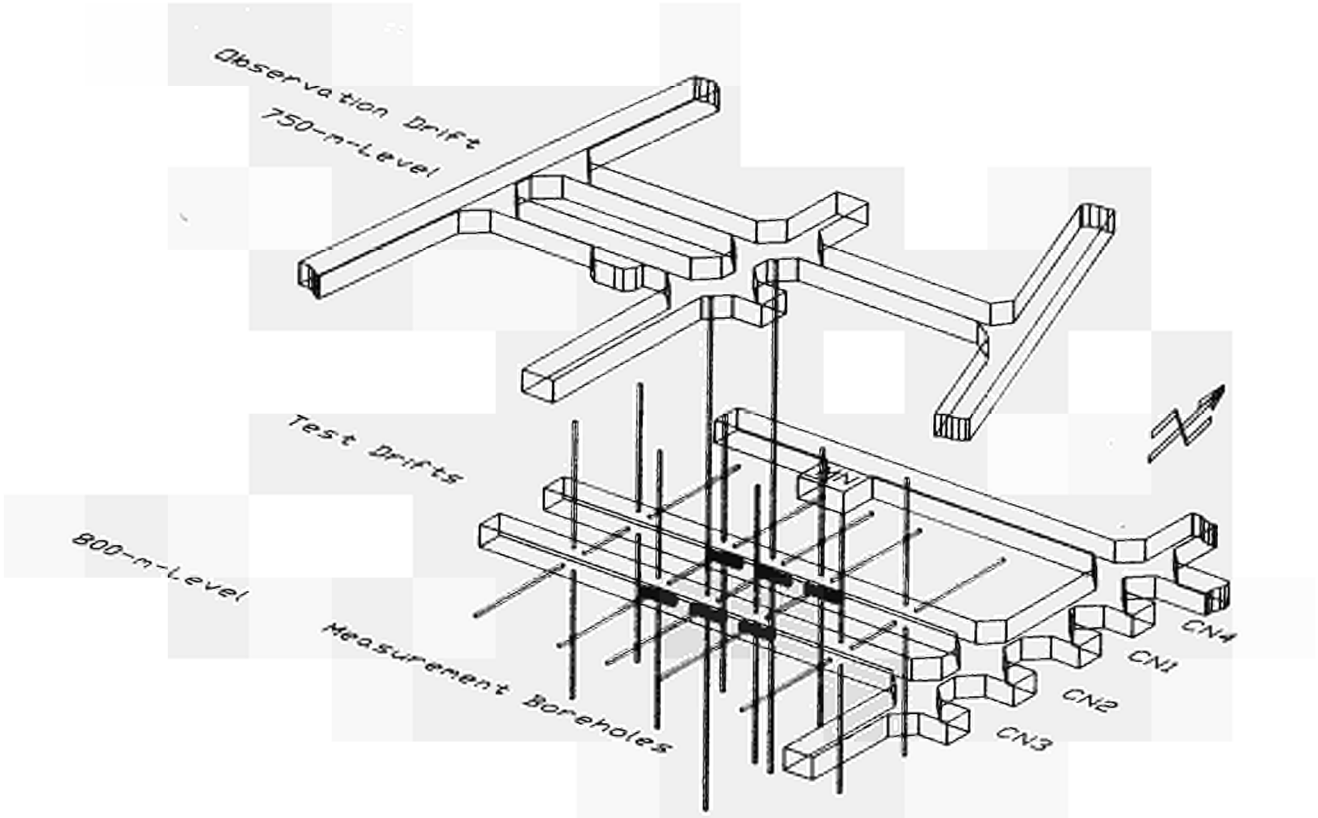

Fig. 1: General View of the Test Field

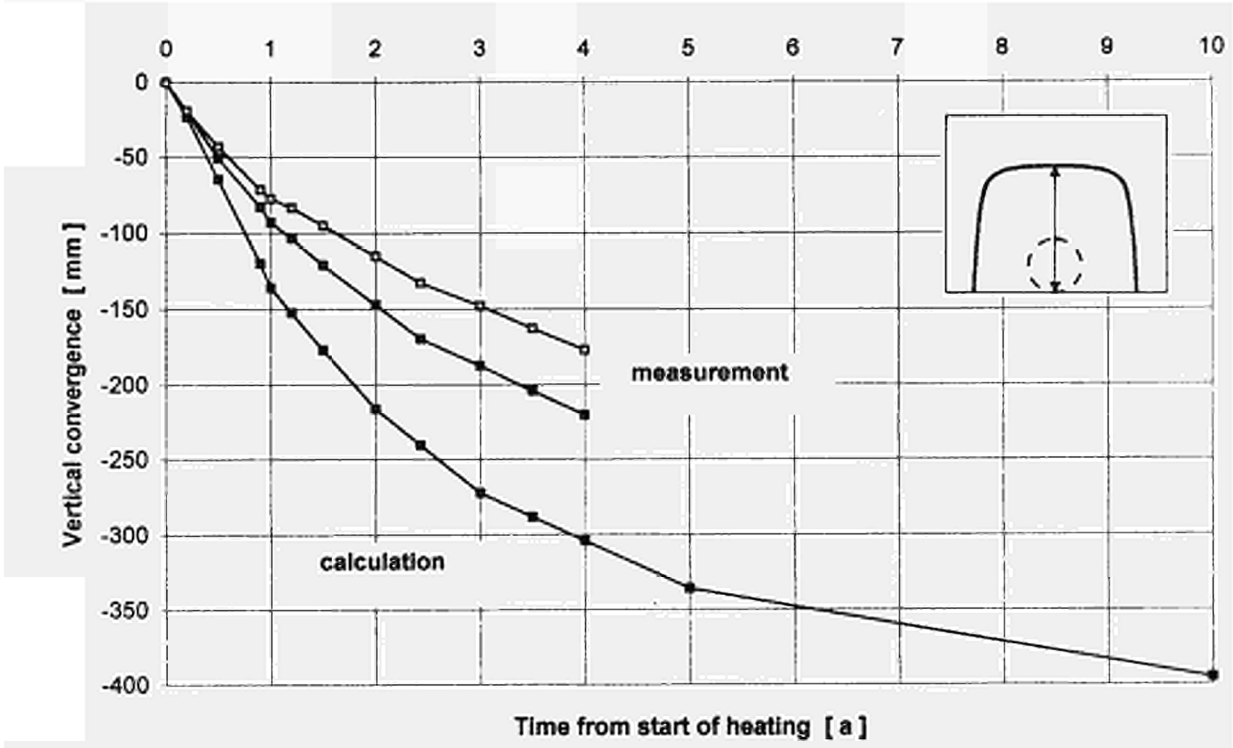

Fig. 2: Range of Vertical Convergences Measured in the Heated Area in Comparison with Calculated Values

Title :	Preliminary Demonstration Test for Disposal of High level Radioactive Waste in Clay (CERBERUS).
Contractors :	ONDRAF/NIRAS, B ; CEN/SCK, B
Contract N° :	FI2W-CT90-0003 b
Duration of contract :	July 1990 - December 1994
Period covered :	January 1994 - December 1994
Project Leaders :	De Preter P. (ONDRAF/NIRAS, Coordinator) B. Neerdael and L. Noynaert (CEN/SCK).

A. OBJECTIVES AND SCOPE.

The CERBERUS test (Control Experiment with Radiation of the Belgian Repository for Underground Storage) is aimed at simulating the near-field effects in an argillaceous environment of a Cogema HLW-canister after 50 years cooling time.
It mainly consists of a mock-up containing a ^{60}Co source of 397 TBq and 2 electrical heating elements each dissipating 365 W placed in the Boom clay from the Underground Research Facility located at Mol.
A monitoring of the thermo-hydro-mechanical fields and the chemical in situ conditions is foreseen.
It allows to launch various validation exercises of computer codes such as the program DOSEGEO (computation of dose rate), the program SOURCE (computation of pore water pressure around drilling and digging works) and the program TEMPPRES (computation of the thermo-mechanical behaviour of the Boom clay).

B. WORK PROGRAMME.

The work programme can be subdivided in 2 main items, the monitoring programme and the validation of existing codes.
The monitoring programme consists in the measurement of :

- dose rate ;
- temperature and heat transfer parameters ;
- pore water pressure and hydraulic conductivity and diffusivity ;
- total stress ;
- pH/Eh ;
- radiolysis effects ;

The codes involved in the validation and interpretation trials are :

- the model DOSEGEO which allows to compute the dose rate around a shielded γ source ;
- the model SOURCE which allows to compute the pore water pressure evolution around a piezometer screen at a constant temperature ;
- the thermo-hydro-mechanical model TEMPPRES.

C. PROGRESS OF WORK AND OBTAINED RESULTS.

State of advancement.

The test is fully operational since the end of November 1989. At the end of October 1994, the heaters have been switched off and the ^{60}Co source has been retrieved, bringing the test in phase 3.

Progress and results.

radiation field
The measurements of the dose rate have been performed almost every month by means of an ionisation chamber. The measured values remain in good agreement with the results obtained with the model DOSEGEO. After compensation for the decrease of the ^{60}Co source and of the iron shielding thickness, no significant change in the measured dose rate has been highlighted.

thermal field
Due to the decrease of the ^{60}Co source the temperature at all thermocouples and Pt100 probes is decreasing according to the values predicted by the model TEMPPRES. Two months after the end of the second phase of the test all the temperature probes indicate almost the same temperature i.e. 30°C.

hydrological field
The hydraulic conductivity values, compensated to take into account the in situ temperature, remain almost constant and range between 2.10^{-12} and 4.10^{-12} $m.s^{-1}$.

thermo-hydro-mechanical field
During the heating and irradiation phase we observed an increase of the pore water pressure, followed by a decrease and a stabilisation above the initial value as a consequence of the near field effects of the Test Drift.

chemical field
The main result are :
- the pH has reached a constant value of 7.3 (22°C) ;
- the Eh still remains reducing (-279 mV versus SHE) ;

Analysis of the irradiated clay water samples shows the presence of thiosulphates (influencing the corrosion of steel), organic sulphur, and organic complexing agents (influencing the migration of radionuclides).
Concentrations between 0.15 and 3 μg H_2/kg H_2O have been detected during the five years irradiation period.

Title :	Mine-by-Test
Contractor :	NIRAS/ONDRAF
Contract N° :	FI2W/CT90/0003 c
Duration of contract :	from 1 July 1990 to 31 December 1994
Period covered :	from 1 January 1994 to 31 December 1994
Project leader Niras :	J. Van Miegroet up to 18 December 1994
:	L. Van Cauteren from 19 December 1994
Project leader SCK :	M. Put and D. De Bruyn.

A. OBJECTIVES AND SCOPE.

The Mine-by-Test deals with the long-term behaviour of the so called Test Drift of the HADES Underground Research Facility. Follow-up and monitoring of the concrete lining and of the terminal shotcreted front ensure the Test Dirft stability. Monitoring of the surrounding clay mass gives reliable data for assessing its rheological behaviour.

B. WORK PROGRAMME.

Acquisition of field measurements and interpretation exercises are the two main items of the programme.

- Measurements in the clay mass around the Test Drift are gathered from :
  - one settlingmeter and one inclinometer devices installed above the Test Drift before the 1987 construction phase ;
  - six piezometer nests, one series of pore water pressure cells and one multiple-point extensometer installed from the Test-Drift.
- Monitoring of the concrete lining is ensured by :
  - 34 load cells installed between the liners and 42 total pressure cells embedded in these liners ;
  - diametrical convergence measurements of seven instrumented sections.
- Follow-up of the terminal shotcreted front occurs through :
  - one multiple-point extensometer installed from the front up to 10 m depth in the clay mass ;
  - 15 reflectors installed on the surface of the shotcreted shell.
- Interpretation of the collected data occurs with simple analytical elasto-plastic models or with finite-element analysis.

C. PROGRESS OF WORK AND OBTAINED RESULTS.

State of advancement.

The Mine-by-Test is in a phase of long term survey.

Progress and results.

Measurements in and around the Test-Drift do not show major differences since the last annual report :

- the total pressure on the lining still ranges from 1.7 to 2.4 MPa when calculated from load-cell measurements, pressure-cell measurements showing more scattering (from 0.5 to 3.3 MPa) ; several problems occurred at the measurement system :
  a new pumping device had to be installed, the calibration sheets had to be corrected. Moreover the mechanical part of all the cells have been checked one by one with a manual testing unit and the quality of the oil outflow was checked. Several sources of impurities were detected : water, white-coloured suspension, rust-like powder and even mercury. For each of the cells presenting some impurity, a special filter will be installed at the outflow to quarantee the pureness of the oil coming back to the acquisition unit ;

- the series of piezometer screens are still working satisfactorily ;

- the manual readings (convergence, pore pressure) are performed in a satisfactory way ;

Fracturing in the shotcreted shell was still increasing. The shell was in contact with the last concrete rings on the whole circumference, what could affect the stability of the sliding ribs part of the Test-Drift. The easiest safe solution was to replace the old shotcreted shell. A pilot gallery was created in the centre top part of the old shell over 1 m depth. The new front was then extended from this gallery, and shotcreted over a minimal thickness of 10 cm. New convergence points have been installed.

Title	Demonstration of the in situ application of an industrial clay-based backfill material (BACCHUS 2)
Contractors	SCK/CEN, ANDRA, ENRESA
Contract N°	FI2W-CT91-0098
Duration of contract	1 October 1991 - 31 May 1995
Period covered	1 January 1994 - 31 December 1994
Project leader	G. Volckaert(SCK/CEN, coordinator), C. Mayor (ANDRA), B. Vignal (ENRESA)

A. OBJECTIVES AND SCOPE

The BACCHUS 2 experiment aims at the optimization and the demonstration of an installation procedure for a clay based backfill material. The installation procedure, materials and techniques have to be as close as possible to realistic industrial processes and capabilities.
The backfill material consist of a mixture of high density clay pellets and clay powder. The experiment is developed in cooperation with ENRESA and ANDRA/CEA.

The instrumentation of the experiment must be optimized in such a way that it can be used as a validation experiment for the hydro-mechanical model developed under CEC contract FI2W-CT90-0033.

The BACCHUS 2 project also includes the characterisation of the granular backfill, and the retrieval and the expertise of the BACCHUS 1 test mock up.

B. WORK PROGRAMME

The work programme consists in the three following points:

1. Study and optimization of the backfill material

The sealing material consist in a mixture of clay pellets and clay powder. The ratio powder/pellets and the density, size and water content of the pellets will be used as parameters in the optimization process.

Fundamental properties of this mixture such as the hydraulic conductivity and the swelling pressure will be measured.

2. Recuperation of the BACCHUS 1 experiment

The BACCHUS 1 mock-up installed in '88 will be retrieved by overcoring. The aspects and hydro-mechanical properties of the retrieved Boom clay seal and the FoCa-bentonite buffer will be studied.

3. In-situ demonstration of the application of the backfill material

The demonstration will consist in the sealing of the large borehole (50 cm diameter) left after the retrieval of the BACCHUS 1 mock-up. The backfill material described under point 1 will be installed around a central filter tube which will be used as support and access tube for the instrumentation.

Probes for water content measurement, based on the experience gained by CEA in the BACCHUS 1 project, will be embedded in the backfill material. Also the instrumentation installed previously in the host clay around the BACCHUS 1 mock-up, can be further used to monitor the host clay behaviour.

C. PROGRESS OF WORK AND RESULTS

State of advancement

The drilling works for the retrieval of the BACCHUS 1 experiment were started in May 1993 and, on the 29th of June 1993, BACCHUS 1 was achieved successfuly. The remaining borehole was immediately cleaned and the BACCHUS 2 mock up installed.

The expertise of the retrieved BACCHUS 1 mock up allowed to determine the cause of the early breakdown of the heater and to check the quality of the hydrated buffer material.

The characterisation of the granular backfill was completed. The hydraulic conductivity and swelling pressure have been measured as a function of the dry density. X-ray tomography has been applied successfully to measure the evolution of the density distribution during hydration.

The evolution of the total stress and the pore water pressure in the host clay around the BACCHUS 2 experiment and in the backfill of the BACCHUS 2 experiment was closely monitored. The state of hydration of the BACCHUS 2 backfill was followed using the thermal shock system. As the natural hydration of the backfill material is a very slow process, we have started the artificial hydration on the 25 th. of November 1994.

Progress and results

X-ray tomography

X-ray tomography technic has been used by the CEA to study quantitatively the evolution of the hydraulical properties of the backfill material (a mixture of high density Boom clay pellets and powder) during the saturation process. X-ray tomography technic allows dynamic studies, is suitable for diffusion kinetic problems and to study the hydration kinetic of clay.

The experimental set-up (see Fig. 1) consists of a hydration system injecting water, by a peristaltic pump, through a steel porous filter placed on one face of the backfill sample (10 cm of diameter, and 16 cm height). The total volume of the water injected in the backfill sample is measured by a graduated burette connected on the hydraulical circuit. The backfill sample is characterised by X-ray tomography technic at initial state and during 5 months after the start of the hydration process.

Figure 2 shows the scanning of a section of the backfill sample at the initial state and after 25.7, 45.4 and 3501 hours. The contrasts between the pellets and the powder are very strong at the initial state and diminish progressively with the saturation process. This demonstrates the homogenisation of the backfill material with hydration.

The initial density profile and the evolution of the saturation process can be obtained from the X-ray scan of the backfill sample. Figure 3 shows the initial density profile and the water content profile at saturation. The backfill sample has a mean density of 1.62 g/cm^3 with a standard deviation of 0.05. The dispersion is due to the heterogeneity of the backfill material. Nevertheless we can assume that in a section of 2 cm thick the dry density of the backfill material remains constant during hydration.

The measurements of the water volume injected in the backfill sample realised by lecture on the graduated burette and by X-ray tomography technic are very close (see Fig. 4). Figure 5 shows the saturation evolution for the different sections (2cm thick) of the backfill sample as a function of the time. The saturation factor tends one (except for the first section in contact with the porous filter). After 3500 hours the backfill sample reaches saturation. The flux was also determined and is greater near the hydration face.

Results on BACCHUS 2

As the natural hydration of the backfill material is a very slow process, we have started the artificial hydration on the 25th. of November 1994. The artificial hydration has been performed by injecting water in the filters on the central tube (see Fig. 6). These filters have been connected to a water reservoir installed in the gallery. The injection pressure thus corresponds to the height of the water column between the filter and the gallery i.e. between 11 and 15 m. Initially the rate of water uptake is about 50 ml/min, but decreases quickly. After two weeks, the rate is reduced to about 1ml/min.

The change in water content in the backfill material is assessed directly with a neutron-gamma probe and indirectly by the interpretation of the measured temperature profile in the backfill material submitted to a thermal load, then evaluating the thermal conductivity and finally the water content.

The measurements before the artificial hydration indicates that the progress of the natural hydration approached the central part of the backfill very slowly. Just after the start of the artificial hydration, we observe a fast increase of the water content around the central tube.

Up to now, a total of 14 thermal campaigns were performed. The data can only be interpreted relatively since the calibration for the conversion of the thermal conductivity in terms of humidity has not yet been supplied by the CEA. As expected, the thermal conductivity increases due to the hydration of the backfill material. If we consider one level and one direction, during the natural hydration phase, the conductivity increases with the radius, which shows the hydration from the clay to the centre. During the artificial hydration, we observe that the radial distribution of the conductivity is inverted. The conductivity is now higher near the central tube where the water is injected.

The conductivity is higher on the south side than on the north side. This observation corresponds with the greater values of the total stress recorded on the south side than on the north side resulting from a consolidation anisotropy.

During the natural hydration, no water pressure increase was observed in the backfill, indicating that the saturation was not yet completed. Since the beginning of the artificial hydration, we record a pore water pressure increase of 1.5 bar on the central part of the bottom flange, corresponding with the pressure of the water column (see Fig. 8).

The total stress measurements are higher on the south side than on the north side. After the start of the artificial hydration, the total stresses increase fast (due to the swelling) while they showed a slow evolution during the natural hydration. For the sensors placed on the vertical plates (see Fig. 9), the increase of the total stress is preceded by a pressure drop, which is larger and faster where the consolidation is less important. This can be explained by the increase of the backfill material plasticity with the fast increase of the water content. Deformation is then possible at lower stresses and thus the total stresses decreases.

The water content measurements performed in the clay massif show after 530 days no evolution. The water content remains around 40 % vol.

We observe higher pore water pressure values at ring 11 than at ring 12. This difference can be explained by the location of the two devices. Indeed, as the piezometers placed at ring 12 are closer to the experiment than those placed at ring 11, the influence of the draining (resulting in lower pore water pressures) caused by the hydration of the backfill material is more important at ring 12.

The piezometer screens placed at the bottom are less influenced by the draining and therefore reacts first. The upper piezometer screens do not react because the saturation is not completed. The effect of the artificial hydration can not yet be detected on the evolution of the pore water pressure.

The total stress (radial, tangential and vertical) recorded in the clay remains almost constant. These stresses seem not to be influenced by the hydration of the backfill material.

Conclusion

X-ray tomography has been used to study quantitatively the evolution of the hydraulical properties of the backfill material (a mixture of high density Boom clay pellets and powder) during the saturation process.

The results on BACCHUS 2 observed this year concern the natural hydration phase of the backfill material and the beginning of the artificial hydration phase. The hydration implies an increase of the thermal conductivity inside the backfill material and low pore water pressure around the experiment. The total stress measurements are higher at the south side than at the north side. These results agree with lower thermal conductivity at the north side than at the south side. These observations show a stronger consolidation on the south side. The measurements realised during more than one year show that the natural hydration of the backfill material is a very slow process.

We have started the artificial hydration on the 25th. of November. The measured parameters in the backfill show clearly the hydration effect i.e. a strong increase in water content, pore water pressure and a redistribution of the mechanical stresses.

At the moment, the effect of the artificial hydration is not yet detectable in the surrounding clay massif.

During next year the interpretation of the results of the artificial hydration of BACCHUS 2 will be continued.

List of publications

/1/ G. Volckaert, B. Neerdael, M. Dardaine (CEA)
Demonstration of the in situ application of an industrial clay-based backfill material: Bacchus 2.
Prog. Report 1-10-1991/30-6-1992
CEC contract FI2W-CT91-0098
Ed.: SCK, R-2951, 1992

/2/ G. Volckaert, M. Dardaine (CEA)
Demonstration of the in situ application of an industrial clay-based backfill material : Bacchus 2
Annual Progress Report 1992
CEC contract FI2W-CT91-0098
Ed. : SCK, R-2953, 1993.

/3/ G. Volckaert, B. Neerdael, M. Dardaine (CEA)
Demonstration of the in situ application of an industrial clay-based backfill material: Bacchus 2.
Prog. Report first semester 1993
CEC contract FI2W-CT91-0098
Ed.: SCK, R-2973, 1993

/4/ G. Volckaert, F. Bernier, M. Dardaine (CEA)
Demonstration of the in situ application of an industrial clay-based backfill material : Bacchus 2
Annual Progress Report 1993
CEC contract FI2W-CT91-0098
Ed. : SCK, R-3011, 1994.

/5/ G. Volckaert, F. Bernier, E. Alonso, A. Gens, M. Dardaine
BACHUS 2: An In Situ Backfill Hydration Experiment for Model Validation.
GEOVAL '94
Paris, France, 11-14 October 1994.

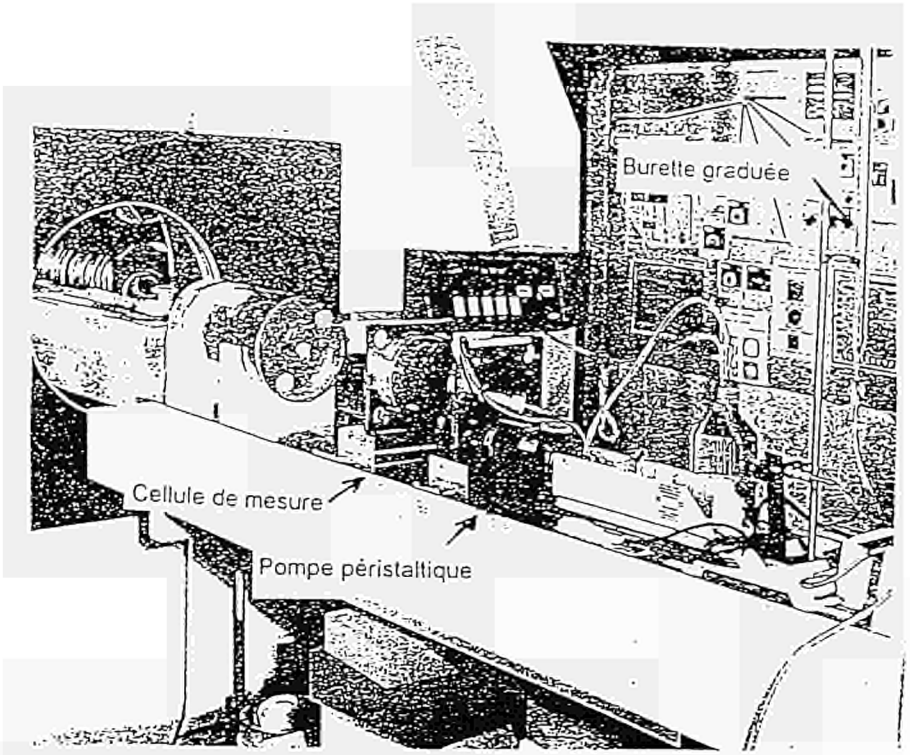

Fig. 1: Experimental set-up for X-ray tomography

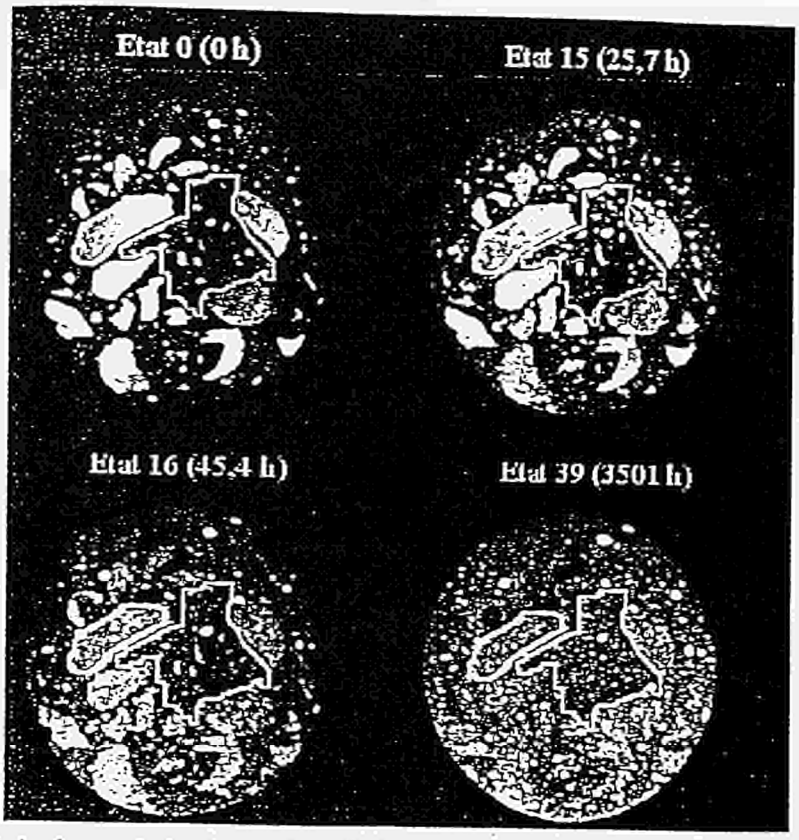

Fig. 2: Hydration evolution for section of a backfill sample after 0,25.7, 45.4 and 3501 hours.

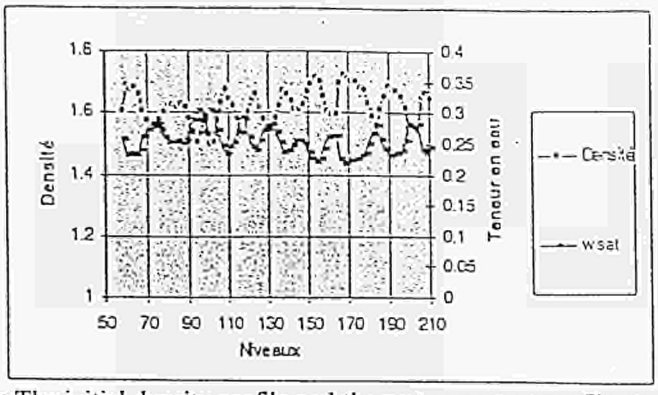

Fig. 3: The initial density profile and the water content profile at saturation.

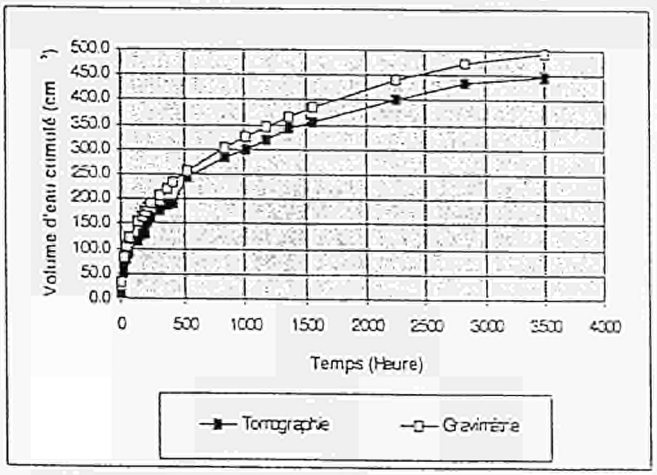

Fig. 4: Injected water volume in the backfill sample.

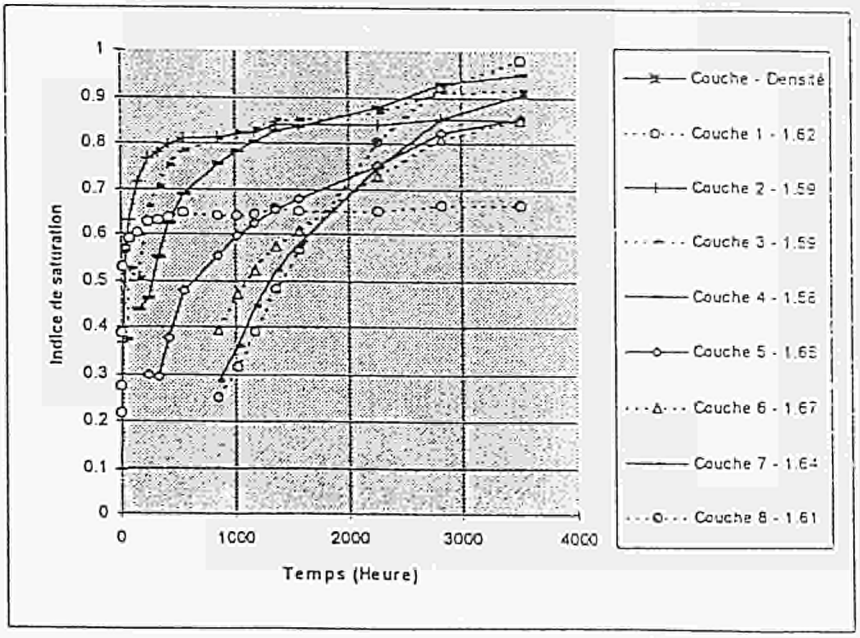

Fig. 5: Saturation evolution in function of time.

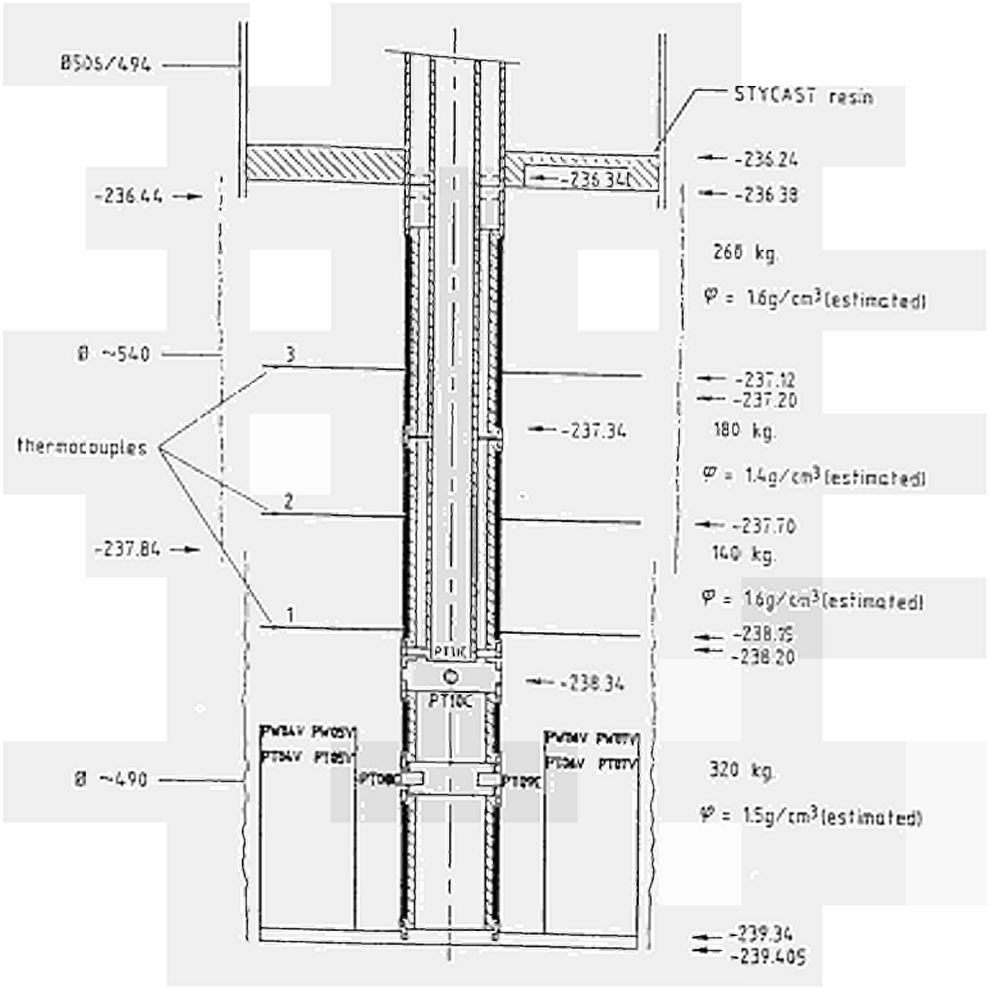

Fig. 6: Experimental set-up.

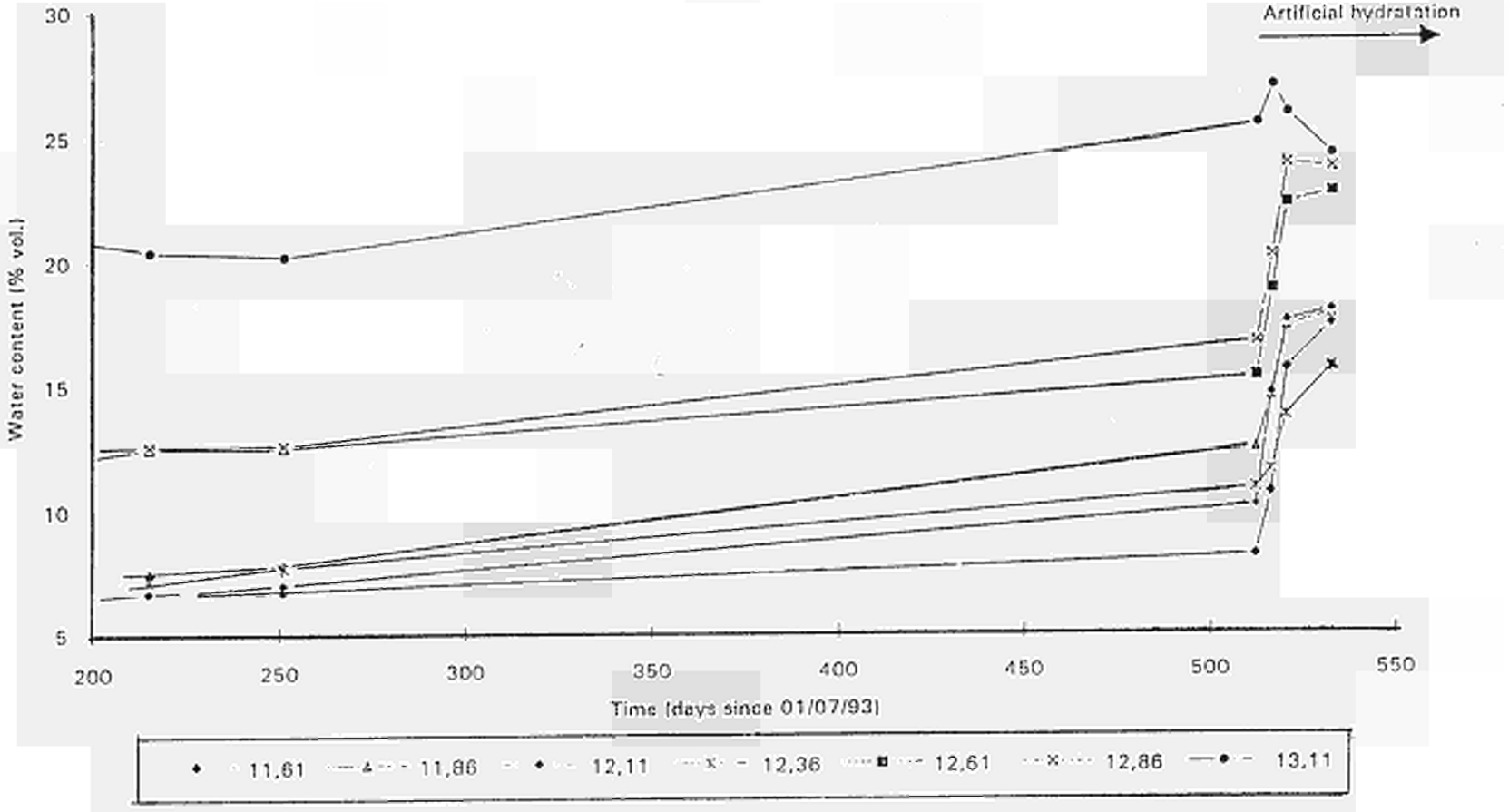

Fig. 7: Water content evolution around the central steel frame (neutron-gamma measurements)

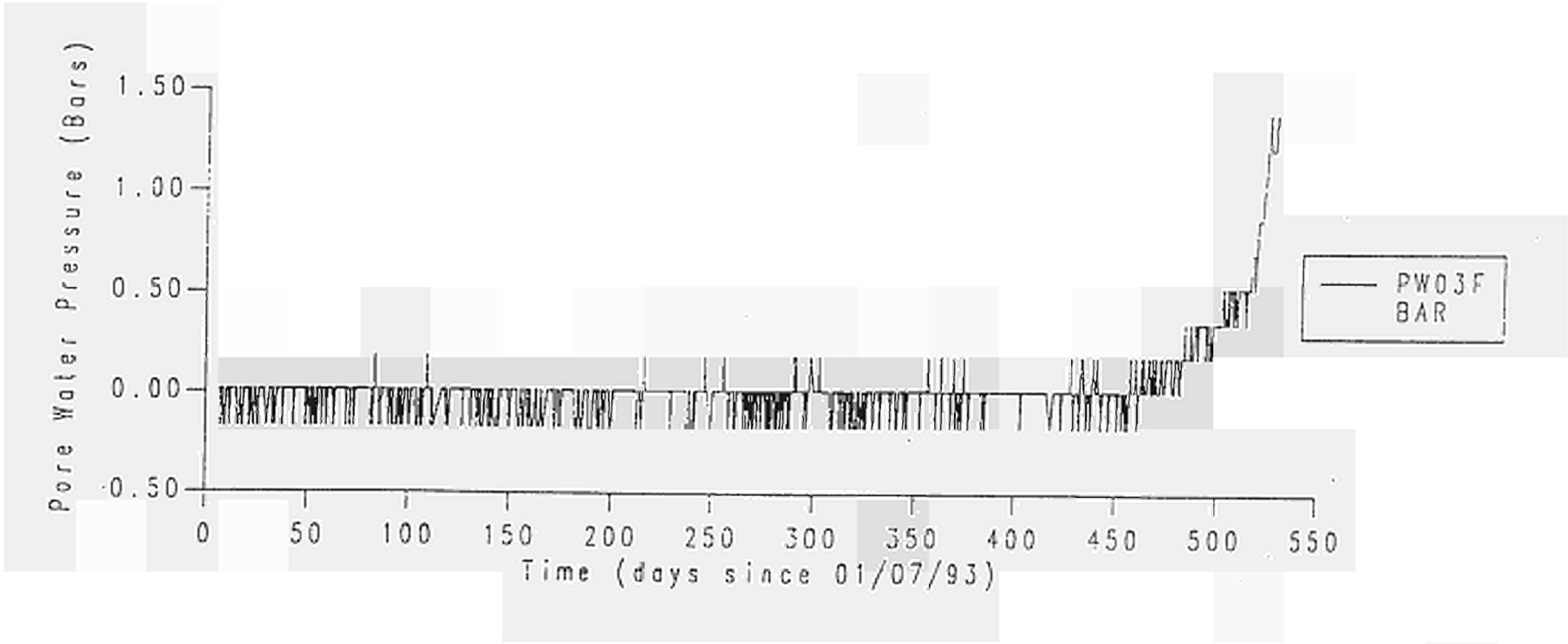

Fig. 8: Pore water pressure on the vertical plates of the BACCHUS 2 mock up.

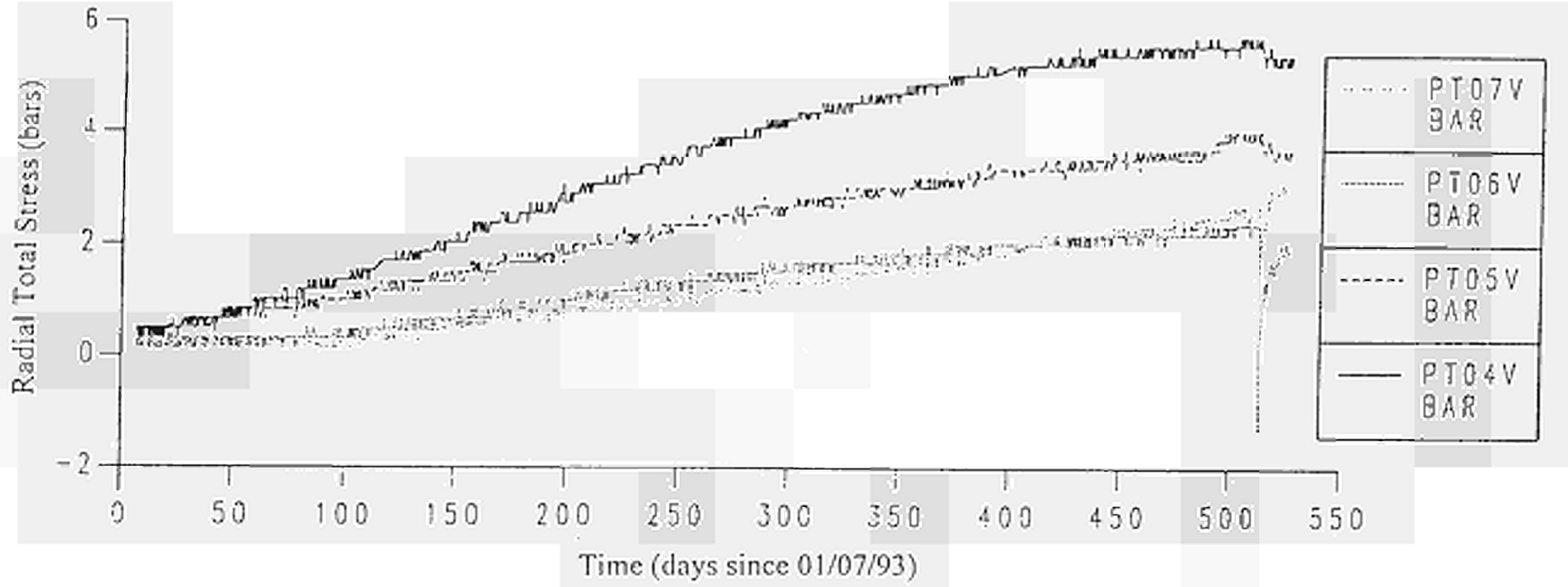

Fig. 9: Total stress on the vertical plates of the BACCHUS 2 mock up.

Title	Modelling and validation of the thermal-hydraulic-mechanical and geochemical behaviour of the clay barrier
Contractors	SCK/CEN, ENRESA, CEA, CIEMAT, UPC, UWCC
Contract N°	FI2W-CT91-0102 AND 0033
Duration of contract	1 October 1991 - 31 December 1994
Period covered	1 January 1994 - 31 December 1994
Project leader	G. Volckaert (coordinator), C. Mayor, E. Alonso, J. Samper, M. Villar, H. Thomas

A. *OBJECTIVES AND SCOPE*

The objective of the study is to analyze and model the behaviour of a clay based engineered barrier during its hydration phase under real repository conditions. The hydro-mechanical and thermo-hydraulical models will be coupled to describe stress/strain behaviour, moisture migration and heat transfer. The thermo-hydraulic model will also be coupled to a geochemical code to describe the migration and formation of chemical species.

Current models are not able to describe the irreversible volumetric strain (swelling or collapse) or the evolution of the mechanical property limits due to changes in the water content. In the case of partly saturated clay materials the suction phenomena, which have a strong influence on the hydraulic, mechanical and thermal properties of the material, are to be considered. To assess the overall performance of a clay barrier also the combined effect of temperature on the hydromechanical and geochemical field needs to be evaluated.

In this project the CEA, CIEMAT, ENRESA and SCK•CEN are responsible for the main experimental work and the research groups at the universities of Cardiff (UWCC) and Catalunya (UPC) are performing the modelling work.

B. *WORK PROGRAMME*

Hydration experiments

Uniaxial experiments determining the influence of the suction potential on the hydration rate, swelling or swelling pressure, will be performed. The progression of the hydration front will be followed by X-ray tomography.

Hydro-mechanical experiments

These experiments will determine the mechanical characteristics of a clay base backfill as a function of the water content and thus the suction potential. In these experiments the suction potential will be imposed. The relation between water content and suction potential will be measured. Also the relation between suction potential, vertical stress and strain will be determined.

Thermo-hydro-mechanical and geochemical experiments

Tests will be carried out in ad hoc designed cells to determine the evolution of temperature, pressure and fluid concentration fields, produced in the clay barrier by heating of the central zone and by injection of water.

Modelling

First the existing models of UPC and UWCC will be adapted for the modelling of the behaviour of dense, swelling clays. In the heat and moisture transfer model, strain and deformation effects will be included as independent variables, while in the moisture migration and stress/strain model, expansive soil effects will be included. A geochemical database will be built including thermal dependencies of thermodynamic constants and reaction rate constant. Finally two types of coupled codes will be made operational i.e. a coupled flow-chemical speciation code and an unsaturated flow code coupled with an elasto-plastic code.

Model application

The thermo-mechanical and thermo-chemical models will be used in the interpretation of the above experiments and experiments carried out in complementary CEC programs e.g. contract n° FI2W-CT90-0033 BACCHUS 2.

C. PROGRESS OF WORK AND OBTAINED RESULTS

State of advancement

Experiments

CIEMAT has completed a series of thermo-hydraulic experiments studying coupled heat and moisture transport and a series of suction controlled oedometer experiments. These experiments were performed on S2 Almeria bentonite. A series of hydrothermal alteration experiments on the S2 Almeria bentonite and a smaller series on Boom clay have been completed. In these experiments they studied the influence of heat on the distribution of moisture, chemical species and physical parameters such as the specific surface.

CEA, SCK•CEN and UPC-geomechanics group have concentrated their experiments on the hydro-mechanical and thermo-hydro-mechanical behaviour of unsaturated clay. UPC and SCK•CEN has performed suction and temperature controlled experiments on Boom clay measuring the water retention curve at different temperatures and swelling/collapse at different stresses and temperatures (UPC only). UPC has also performed suction controlled experiments on a mixture of Boom clay pellets and powder as used in the BACCHUS 2 experiment. CEA has performed oedometer experiments on saturated and unsaturated FoCa and Boom clay. CEA compared the compression/swelling behaviour of FoCa clay with Boom clay and tested the influence of the loading-hydration path on the swelling collapse behaviour.

The UPC-La Coruña geochemistry group has finished the smectite dissolution experiments at 80 °C.

Model development

Thermo-hydro-mechanical

Both UPC and UWCC has developed, verified and tested fully coupled thermo-hydro-mechanical codes for unsaturated swelling clay. Elastic, non-linear elastic (state surfaces), elasto-plastic and thermo-plastic versions of the fully coupled code are now available in 1D and 2D.

UWCC has applied the codes to several laboratory experiments e.g. SCK•CEN's X-ray tomography hydration experiment and CIEMAT's hydro-thermal experiments. UPC has applied their coded for the simulation of the BACCHUS 2 in situ demonstration test performed in the HADES underground research facility at Mol.

Thermo-hydro-chemical

The geochemical code has been further extended to redox reactions, ion exchange and sorption. The code has been verified and successfully compared with the well known geochemical code PHREEQM. A fully coupled thermo-hydro-chemical code has been developed and verified. This code has been applied to simulate the smectite dissolution experiments.

Progress and results

CEA

The CEA has compared the results of a loading-unloading oedometer experiment performed on saturated FoCa clay in which first an unsaturated sample was loaded, saturated at maximum load and then unloaded. In a void ratio (or strain) versus stress diagram the two unloading curves are parallel but the void ratio of the initially unsaturated sample is larger. The two samples have the same swelling coefficient but a different preconsolidation pressure. These observations corresponds with the model of Alonso and Gens.

An oedometer experiment has been performed on saturated and unsaturated Boom clay. In Fig. 1 the results of both tests are shown together with the results of similar tests on FoCa clay. When comparing these results it should be reminded that FoCa clay has a much larger smectite content than Boom clay and thus has a much larger water retention and swelling capacity. Although these important differences, the mechanical behaviour of these two clays is very similar and obeys the same physical model.

CIEMAT

The series of thermo-hydraulic experiments was completed by performing three long term (1 to 4 months) experiments. From these experiments we conclude that the initial water content does not only influence the water uptake rate but also the density and soluble species distribution. The lower the initial water content, the larger and faster is the water uptake and the larger are the density changes and the larger is the mobility of dissolved species in the clay sample. The combination of a low initial water content with a large thermal gradient (about 10 °C/cm) leads to a high salt concentration close to the heater, which strongly influences the physico-chemical and mechanical behaviour of the clay.

In the hydro-thermal alteration cells in total 11 experiments were performed on S2 Almeria bentonite and 2 on Boom clay. These experiments show an increase of sulphates close to the heated end together with a decrease in specific surface area (BET method). The mercury porosimetry data show a general increase in pore volume but with a decrease for the small pore diameter fraction. No significant migration of free silica was observed.

CIEMAT has finalised a series of suction controlled oedometer experiments on the S2 Almeria bentonite using the sulphuric acid and the air pressure technique. The observed swelling/collapse behaviour as well as the results of the mercury porosimetry confirm the validity of the Alonso and Gens model for this very strongly swelling clay.

UPC (main sub-contractor to ENRESA) - geomechanics

Development of the numerical codes

The development of numerical codes within the framework of the project have followed two main directions: coding and testing of the fully coupled 2D code (NOSAT II). Development, testing and use of a coupled 1 D auxiliary code.

The coding of NOSAT II, the 2D coupled thermo-hydro-mechanical code, has been completed and the program has undergone a first stage of testing using simple problems. The main areas of development as far as coding is concerned have been:

- introduction of non-linearity for the mechanical behaviour in the solution scheme for the equilibrium equation;
- introduction of a range of mechanical constitutive laws including an elasto-plastic law for unsaturated material;
- coding of the energy balance equation and coupling to the rest of equations, with temperature as a basic variable;
- introduction of a range of hydraulic and thermal constitutive laws (retention curves, permeability variations with porosity and suction, thermal conductivity laws);
- coding of the unsaturated level terms in the mechanical and hydraulic equations;
- rearrangement of the code referring to the organization of time integration schemes;
- organization of output files for compatibility with the DRAC-VIU post-processor.

The resulting code has been successfully verified in relation with saturated consolidation (Terzaghi), for which an analytical solution exists, and unsaturated consolidation considering a state surface. The results obtained coincide exactly with the analytical results or those computed using an independent code.

Regarding the 1 D coupled code, it has been fully developed for coupled hydro-mechanical cases. The energy balance (thermal) equation has not been implemented yet. The mechanical behaviour of unsaturated soils can be described by a range of constitutive laws including elastic behaviour, non-linear elastic behaviour (state surfaces) and elasto-plastic behaviour.

The code has been successfully verified for a range of sample 1 D cases including saturated consolidation, unsaturated consolidation and swelling pressure tests, against analytical solutions or results from other codes. The 1 D code has been used to perform an analysis of the BACCHUS 2 experiment using the elasto-plastic constitutive law to model the hydromechanical behaviour of the backfill. The results are being analyzed at present.

Modelling of BACCHUS 2

The accumulation of new laboratory data concerning the compacted backfill and a more detailed evaluation of the "in situ" instrumentation located in the natural clay in the vicinity of the emplacement borehole made a new modelling of the test with NOSAT possible. A new set of parameters and constitutive relations were derived from experimental data. In addition, boundary and initial conditions were also reviewed and adapted. It should be recalled that the first analysis reported in the 1992 Annual Progress Report was based on very limited information. The new data set is significantly different from the first one.

The new analysis has followed the organization of the previous one. Elastic and no tension solutions have been obtained. Pore water pressure, air pressure, suction, degree of saturation, water permeability, volumetric strain, radial displacements, radial stress and circumferential stress have been calculated and compared to the measured values. Also, stress paths in the (p, s) and (p, q) planes have been obtained to gain some insight into the mechanical phenomena taking place during hydration of the backfill. As the computed saturation time and stress levels correspond rather well with the experimental results, this updated analysis constitutes clearly an improved prediction of "in situ" behaviour.

Laboratory work

The following basic equipment has become operational:

- Suction controlled oedometers with suction control.

Main characteristics: suction applied by excess nitrogen pressure; vertical load applied by air or water pressure; temperature controlled by an electric heater submerged in an oil bath which surrounds the cell.

- Suction controlled oedometric cell with measurement of horizontal stresses.

Main characteristics: equipment based on existing suction controlled oedometers. Lateral stresses are controlled in a ring wall whose deformations are counterbalanced by oil pressure in a confining chamber.

- Suction-controlled isotropic cell.

Main characteristics: Air and water pressure are jointly imposed at the bottom of the specimen. Volumetric strain is measured by controlling volume change in water inside the cell.

- Suction controlled triaxial apparatus.

Main characteristics: Self-contained applications of vertical and horizontal loads (stress path Bishop cell philosophy); chamber pressure and deviatoric stresses applied by means of air pressure; internal measurement of deviatoric loads and vertical strains; radial strains measured by two external travelling laser beams.

This equipment has been used to obtain the following results concerning Boom clay:

- water retention properties of compacted Boom clay at different temperatures;
- volumetric strains upon wetting as a function of initial dry density and confining stress;
- suction controlled oedometer tests at different temperatures;
- suction controlled oedometer tests on aggregates of highly compacted Boom clay pellets;
- swelling tests on mixtures of clay pellets and powder.

UPC (main sub-contractor to ENRESA) - geochemistry

Experiments

Laboratory smectite dissolution experiments have been completed. Dissolution rates obtained at 80 °C and pH=8.8 have been complemented with the determination of the solubility constant Ksp.

Hydro-chemical model development

As part of the development of the hydrochemical solver/assembler, the chemical model has been improved by incorporating redox reactions, ion exchange reactions and sorption processes. The latter are represented using the constant capacitance model. All these reactions are considered at chemical equilibrium. Other reactions, such as precipitation processes, are usually kinetically controlled. To cope with this, a chemical model for mineral precipitation has been developed, tested and partially validated with a dedolomitization case study.

Most of the computing CPU time required by reactive solute transport models is taken by the solution of the nonlinear chemical equations. In order to improve the overall efficiency of the solution process, a detailed numerical analysis of different solution schemes has been carried out. This includes: (1) working with relative concentration increments, (2) decoupling the pH equation, and (3) assuming a diagonal Jacobian matrix J. The results of the comparison analysis indicate that working with relative concentration increments results in a much better conditioned Jacobian matrix and much faster convergence rates.

Heat Transport

Heat transport through porous media obeys similar laws and principles to those of solute transport. Once the analogy between both phenomena is established, it is straightforward to modify the solute transport equations in order to represent and model heat transport. Using this analogy, currently developed solute transport models have been modified to account for heat transport. In this way, these models can simulate simultaneously heat and solute transport.

Coupling solute transport and geochemical models

The transport of a reactive multicomponent system is characterized by a set of partial differential equations (transport equations) coupled to a set of nonlinear algebraic equations (chemical equations). Their solution can be addressed by: direct substitution, sequential iteration or coupling of an existing geochemical code to a solute transport code.

All three approaches were implemented during 1993 for one dimensional transport. During 1994 they have been extended to 2-D problems. Current codes can handle acid-base, complexation, dissolution-precipitation, ion exchange, redox and sorption reactions. At the current stage of development, problems dealing with kinetically controlled processes have to be solved using the direct substitution method while under equilibrium conditions all three approaches can be used. Under equilibrium conditions, the sequential iteration approach is always the more efficient.

All codes have been extensively verified using analytical solutions (when available), and reported literature solutions. In other cases their solutions have been verified against public domain codes such as PHREEQM. Attempts have been made to validate some aspects of the codes with laboratory experiments. Smectite dissolution experiments performed on Spanish clays have been modelled. Application of the models to simulate CIEMAT's hydro-thermal alteration experiments has not been pursued because these experiments were conducted under partially saturated conditions which can not yet be handled by the current models.

UWCC

Development of computer software

The overall objective is the production of software for the thermo-hydro-mechanical behaviour of unsaturated soil. To this end solutions are sought to four independent variables: temperature, capillary potential (soil suction), air pressure and deformation.

To achieve this aim, bearing in mind the complexity of the problem, it was decided to adopt a step-by-step approach to model development, according to the following strategy:

- The development of software which can solve the three variable formulation mentioned above i.e. temperature, capillary potential (soil suction) and air pressure, in absence of deformation.
- The development of software which can solve the hydro-mechanical behaviour and provide solutions to soil suction and deformation in absence of temperature.
- The development of a comprehensive model which will provide coupled solutions of temperature, soil suction, air pressure and deformation.

This systematic approach has led to the development of the COMPASS software package in which different thermo-hydro-mechanical models have been incorporated (see Table 1). All these codes have been verified to analytical solutions or other codes.

Table 1 Overview of the COMPASS software developed by UWCC

COMPASS	
Version	**Purpose**
HM	Coupled heat and moisture transfer in unsaturated soil
HMA	Coupled heat, moisture and air transfer in unsaturated soil
HMAE	Coupled heat, moisture, air and deformations in unsaturated soil, with deformations calculated by elasticity theory, combined with a state surface approach
HMAEP	Coupled heat, moisture, air and deformations in unsaturated soil, with deformations calculated by an elasto/plastic theory
HMATP	Coupled heat, moisture, air and deformations in unsaturated soil, with deformations calculated by a thermo/plasticity theory

Model applications

The hydration experiments on compacted Boom clay performed by SCK•CEN were simulated and the calculated saturation profiles were compared to those measured by X-ray tomography. The theoretical formulation for the analysis of coupled heat, moisture and air transfer, applicable to non-deformable unsaturated soils, was applied for the simulation of this experiment. Good correlation between the numerical and experimental results was obtained. The HMAE code was applied to simulate a laboratory heating experiment performed by CIEMAT on the Almeria bentonite. The theoretical formulation accommodates liquid flow, vapour flow, bulk air flow and heat transfer as the transport processes, with deformation described by a non-linear elastic stress/strain model based on a state surface approach. Encouraging correlation was obtained between experimental and numerical results indicating a qualitatively correct overall modelling approach. For temperature and moisture content quantitatively correct results were obtained. For stress and strain correct qualitative results were obtained, though for these variables it is much more difficult to obtain quantitatively correct results both numerically and experimentally.

Suction controlled oedometer experiments were performed on Boom clay compacted to a dry density of 1.7 g/cm^3. A constant vertical stress of 0.5 and 4 MPa was applied on the sample. The deformation of the sample was measured while the suction was gradually decreased. The suction in the sample was controlled by circulating air with a constant relative humidity on both the bottom and top of the sample. The relative humidity of the circulating air was controlled by the use of saturated salt solutions. The observed swelling collapse behaviour is in agreement with the model of Alonso and Gens. For the test with a constant vertical stress of 0.5 MPa a complete wetting/drying cycle was performed.

Swelling pressure tests were also performed with oedometer under suction control. Boom clay samples were compacted to a dry density of 1.7 g/cm^3. Sample deformation was maintained to zero at all stages during the wetting and the vertical stress was measured. This test was realised with two different initial vertical stresses: 0.125 and 0.48 MPa.

A series of compression tests on unsaturated Boom clay were performed to measure the measure the consolidation pressure. Boom clay powder was compacted to a dry density of 1.7 g/cm^3 for different initial water content (0, 1, 2.4, 3, 4.4, 6, 8.5 and 11.2% of the dry weight). The force required to reach a density of 1.7 g/cm^3 was recorded to determine the preconsolidation stress as function of the initial water content.

The water content suction relationship for Boom clay measured by SCK•CEN was compared with the results of CIEMAT and UPC for an initial dry density of 1.7 g/cm^3 at 25 °C. We can see on Fig. 2. that the results are very close. Thus equivalent results are obtained with the different oedometer designs and different suction control techniques used by the three institutes.

D. CONCLUSION

We have shown that the three techniques used to control suction i.e. salt solutions, sulphuric acid solutions and air pressure, lead to comparable results. The suction controlled hydro-mechanical tests have shown the general validity of the Alonso and Gens model to describe the swelling collapse behaviour of clays with low to very high swelling ability. The large experimental effort has led to an extended data base with thermal, hydraulic, suction, hydro-mechanical, thermo-hydro-mechanical and chemical properties for Boom clay, FoCA clay and S2 Almeria bentonite.

Fully coupled thermo-hydro-mechanical and thermo-hydro-chemical codes have been developed and verified. Elastic, non-linear elastic, elasto-plastic and thermo-plasticity models have been incorporated in the codes. The codes have been applied to a wide variety of experiments either published in literature or resulting from this research project or other EC projects such as BACCHUS 2. The data base was used for these simulations. The codes allow to simulate the spacial distribution and evolution of the following variables (in increasing order of degree of difficulty): temperature, water content, suction potential, stress, strain and chemical species concentration. To allow quantitative correct simulations of stress, strain and chemical species distribution and evolution, a very important experimental effort is required to obtain the model parameters. Otherwise only qualitative correct simulations can be obtained.

Further research is required to complete the data base and to determine the sensitivity of the parameters in the coupled models. To increase confidence in the model capabilities, the codes should be applied to large scale radioactive waste disposal demonstration tests.

List of publications

G. Volckaert, F. Bernier, E. Alonso, A. Gens, J. Samper, M. Villar, P.L. Martin-Martin, J. Cuevas, R. Campos, H. Thomas, C. Imbert, V. Zingarelli
Model development and validation of the thermo-hydraulic-mechanical and geochemical behaviour of the clay barrier.
Annual progress report 1993, CEC contract FI2W-CT91-0102 and FI2W-CT90-0033
SCK•CEN, Mol, R 3025

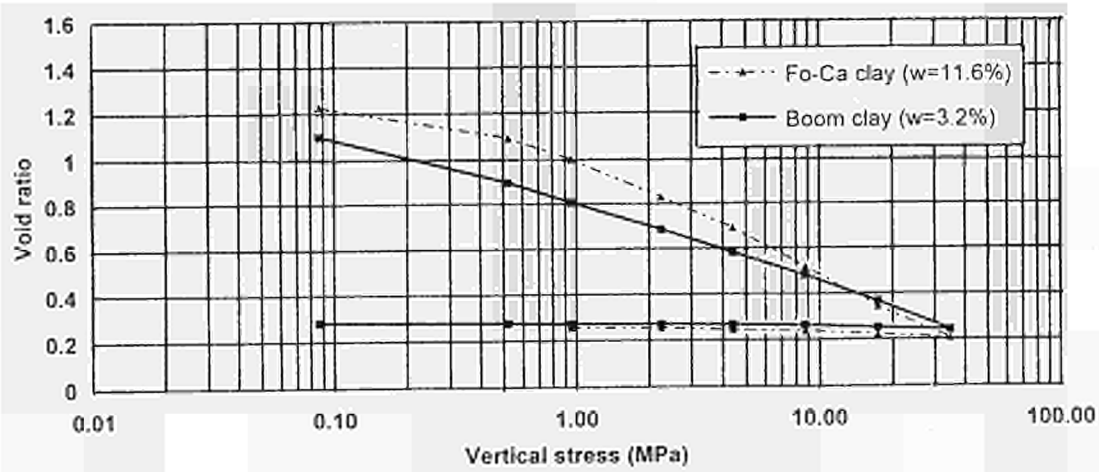

Figure 1: Comparison between the unsaturated behaviour of Boom clay and Fo-Ca clay.

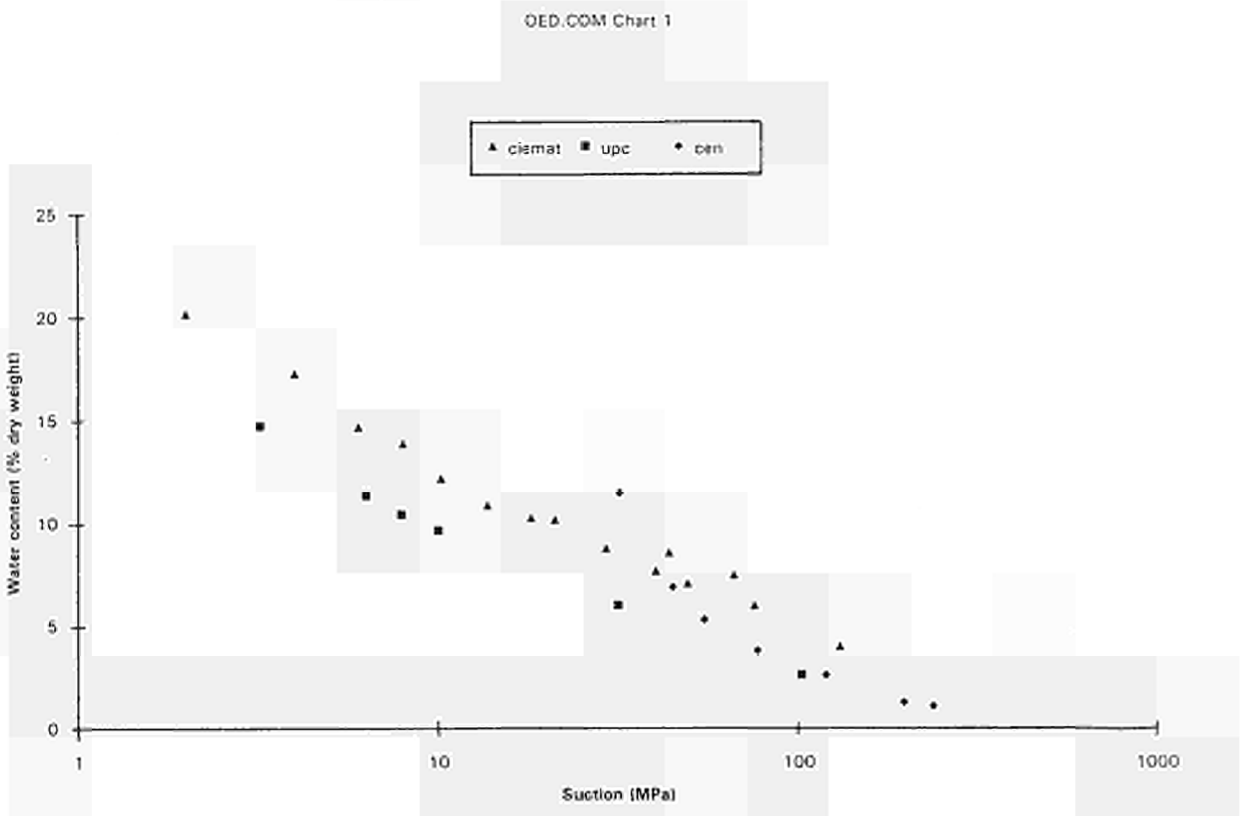

Figure 2: Comparison of the water-retention curves for Boom clay at 25°C as measured by CIEMAT, UPC and SCK.CEN.

Title	Acquisition and Regulation of Water chemistry in an argillaceous medium (ARCHIMEDE)
Contractors	ANDRA (F); BRGM (F); SCK/CEN (B)
Contract N°	FI2W-CT92-0117
Duration of contract	1 January 1992 - 31 December 1994
Period covered	1994
Project leader	T. Merceron (coordinator, ANDRA)

A OBJECTIVES AND SCOPE

Clay is a candidate environment to host highly radioactive waste disposal. Understanding the behaviour of natural elements in clay formations is necessary a step towards understanding of the fate of potentially released radionuclides into the host rock

The ARCHIMEDE Argile project aims at three major goals : i.) understanding the mechanisms of acquisition and regulation of formation water chemistry in clay environment, as a result of water-rock interactions ; ii.) testing and validating physico-chemical parameters that describe the clay formation and its properties, and that feed geochemical models ; iii.) applying these results at modelling a real clay environment : the Boom Clay Formation.

Sampling techniques usually applied can geochemically and microbially disturb the original state of the sediment. Special attention has been paid to prevent such drawback : the Boom clay formation (solid, fluid and gaseous phases) has been sampled from the Underground Research Facility in Mol (Belgium) under anaerobic and aseptic conditions, and experimental works were designed in order to measure non conservative or potentially versatile parameters (pH, Eh). Microbiological techniques have been developped in order to complement conventional microbial ecology studies.

Four scientific teams are in charge of the different phases of the project, under the coordination of ANDRA - DEEC (France) : SCK/CEN (Belgium), CEA-DSD (France), BRGM (France) and GRAM SA with the collaboration of CNRS (France). The ARCHIMEDE project will be achieved within three years (1992-1994).

B. WORK PROGRAMME

The four main topics of the project are as follows :

1. fluid and solid sampling, in situ measurements : all teams are involved in this topic which is planned over 1992 for sampling and over 1993 for in situ measuring ;

2. fluid (CEA-DSD) and solid (BRGM) characterization. The main step of the project is planned over 1993 ;

3. microbial investigations (GRAM SA) will spread over three years (1992-1994) ;

4. fluid-rock interaction modelling (CEA-DSD and BRGM) will integrate the result obtained after the characterization step and has started in late 1993.

C. PROGRESS WORK AND OBTAINED RESULTS

State of advancement

The ANDRA/CCE "ARCHIMEDE - Argile" project made it possible to precisely characterize both microbially and geochemically the Boom Clay Formation.

Conventional microbial ecology studies have demonstrated that bacteria concentration in clay is low, sometimes below detection threshold, apart from the first metre of rock from the underground gallery onwards, where not only bacterial population is abundant, but also very diversified. Most of the fauna identified is not autochthonous, but has been brought in but human activity during Underground Research Facility digging and running. Genetic sequencing of strains has been applied to solid sample populations. The results obtained rend it possible to distinguish between bacterial strains brought into the formation by human activities or through materials used for building the underground gallery. Comparison between phenotypic and genotypic results shows a very good agreement between the two approaches : 62 % out of 81 identified strains, have yield concordent results with both techniques. Discrepency has been recorded for only 23 % of the population, whereas for 15 % contamination problems or loss of strains have been encountered. Both techniques appear complementary : phenotypic studies allow us insight into the knowledge of the metabolic and catabolic activity of the fauna, whereas the phenotypic approach permits quick and objective determination of the strains.

- In geochemistry, two approaches aiming at modelling fluid chemistry acquisition and regulation have been investigated. The first approach, developped by CEA follows a global path at the basin scale, based on the study of the relationship between interstitial fluid and the surrounding aquifers chemistry. The second approach, developped by BRGM relies on the knowledge of clay/water interaction mechanisms in small (local) scale equilibria. Both approaches lead to a model demonstrating that it is now possible to realistically forecast the behaviour of a rock/water system in clay based upon a few geochemical relationships

Progress and results

C.1 Fluid and solid sampling, and in situ experiments.

C.1.1 Fluid and solid sampling

SCK/CEN was in charge of organizing sampling campaingns and on site experiments throughout the project. Sample collection was of prime importance for the project, because of the special requierements for sterility and oxydation prevention. Special training of drilling staff has been necessary, and special cleansing procedures of equipment have been defined in order to collect as undisturbed as possible solid and fluid samples for bacterial and geochemical investigations. 7 horizontal drillholes have been completed for the project. Hole reference A50001 has been drilled sterile to 15 metre depth as a piezometre to collect fluid samples at 3, 7, 8, 14 and 15 metres. The outlet of the different piezometric filtres were connected to sterile flask kept refrigerated. A second piezometre referenced A50005 also 15 metre long was drilled to place piezométric filtres at the same depths to complement fluid collection. In addition, it has been specially arranged to be fitted with a pH sensitive optic fiber in its terminal chamber 15 metre depth. Fluid sampling was performed in controlled conditons throughout the project in order to prevent from any external contamination, for bacteriological and geochemical investigations. More than 26 litres of sterile fluid have been collected from the two piezometres.

Hole A50002 was the deepest (20 metres) and was entierly cored using sterile cutting edges pushed into the clay. Twenty nine fifty centimetre long cores have been collected and stored refrigerated after packaging into nitrogen filled sterile aluminum polythene bags.

C.1.2 On site experiments

Hole A50003 was a test hole for a non metallic tubing experiment designed for collection of fluid in dialysis cells for trace metal analyses. The reinforced rubber tubing tested proved unsuccesful and collapsed due to natural convergence of clay. A new synthetic tubing has been later successfully implanted to hold dialysis cells (hole reference A50008). Hole A50004 has been realized after freezing of a cubic volume of the formation about 2 metre wide. Two small diametre cores about 2 metre long have been collected for fluid extraction experiments. The 2 last works were devoted to on site experiments aiming at testing pH and Eh determination by micro-electrodes (A50006) and cobaltohexamine chloride recirculation (A50007). On site experiments developped for the ARCHIMEDE argile project were :

i. on site measurement of pH using an optic fiber (in collaboration with CEA) ;

ii. elaboration and setting of a dialysis device to collect uncontaminated fluid for trace metal analysis (in collaboration with CEA) ;

iii. active geochemistry experiment aiming at determining pH and Eh using on site microelectrodes and at evaluating cation exchange property of clay.

C.2 Fluid phase characterisation

Interstitial fluids have been collected with the help of the SCK/CEN staff in stainless steel cells, directly connected to the piezometers. Attention has been focused on a good conservation of samples without oxidant contamination. Fluids were fractionated, filtered and conditionned in the laboratory for analysis. Anions were determined on a 0.45µm filtered and non acidified subfraction, and cations on a 0.45µm filtered and acidified (pH: 2-3) aliquote. Trace elements and particularly metal ions were measured from an ultrafiltered and acidified fraction in order to tentatively prevent from any particular contribution. As for fluids from aquifer, filtration and acidification were made directly in the field and sequential filtering (0.45 µm, 0.1µm and 0.01µm) in argon atmosphere was specially used for trace analysis.. In situ measurements or analyses were also required for some parameters such as pH, Eh, alkalinity and sulfide. Fluids were kept under N_2 flow during titration of sulfide by potentiometric measurement with $HgCl_2$. Analyses of fluids have been carried out using ion chromatography (major anions and cations), polarography (Cu, Co, Ni), atomic absorption spectrometry (Fe, Mn, Al), laser spectrofluorometry (U). Trace elements (Rb,Sr, Cs, Ba) analyses were carried out by ICP-MS.

Specific devices have been tested during this project : a specific system to sample interstitial fluids for transition metals analysis has been connected to a dialysis cell, especially designed in synthetic material to prevent from metal contamination ; fiber optics has been successfully tested on site to measure pH with a precision of around 0.05 pH unit.

Groundwaters were sampled from different boreholes, reaching the rupelian aquifer at different depths from 50 to 530 m. The sampling system was set downhole at the required depth and a column of water was moved to the surface by a N_2 flow under pressure, after several flushes.

C.2.1 Interstitial fluids

The chemical composition of interstitial fluids was found to be broadly homogeneous and independent of the distance from the main gallery. Bicarbonate is the major anion ($1.25\ 10^{-2}$ M) and Na the major cation ($1.2\ 10^{-3}$ M), pH is alkaline (8.5) as measured on sampled fluids, to be compared to 8.2 as measured on site, using the optic fibre. This slight difference is due to partial CO_2 degassing during sample collection. Eh is typical of reducing conditions (Eh = -310mV versus H^+/H_2, Cerberus data). The Cerberus test carried out by SCK/CEN produced remarkably stable Eh values over all the campaign (Eh = -310 mV). On site measurments carried out for the Archimede-Argile project never allowed to reach equilibrium. Accurate Eh measurment requires to be performed on fluid still in contact with the formation, in order to maintain redox potential equilibrium. Generally, natural solutions

exhibit mixed redox potentials, which are impossible to relate to a single dominating redox couple in solution.

The comparison of interstitial fluids with those obtained by squeezing fresh cores (collaboration with BGS Keyworth) has shown that the chemical compositions are very similar in absence of oxidation (Table I). In other cases, an oxidising perturbation is evidenced by high sulphate concentration, originating from pyrite oxidation. Isotopic determinations carried out by BGS on squeezing fluids have demonstrated that this oxidation most probably proceedes via porewater oxygen rather than atmospheric oxygen. In this case atmospheric oxygen is therfore not the main oxidizing agent capable of altering sulphides in these sediments, and the preservation of solid samples from oxidation over time is very difficult. Pyrite oxidation, which is a common mineral in Boom clay, leads to sulphate and proton release into solution. This oxidation process, combined with ion exchange and mineral dissolution (mainly carbonates), leads to fluids with high pH and high concentrations of SO_4 and Na. In this case, it seems that reactions of ion exchange are largely predominant.

C.2.2 Fluids from Rupelian aquifer

The regional hydrogeological conditions are fundamental to quantify and to predict the possibility of migration of radioelements from waste disposal. Moreover the similarity between the chemical composition of the rupelian aquifer (in Mol) and the interstitial fluid implies to know the relationship between aquifers (particularly Rupelian) and interstitial fluids. These waters evolve from sodium-bicarbonate to sodium-chloride fluids, with Cl concentrations around 100 mM. Generally alkaline pH decreases from 8.5 to 7.0 in Cl rich fluids (located in the northern part of the aquifer), whilst sulfate concentrations increase steadily, from 1.10^{-6} M to a few 10^{-3} M. Bicarbonate concentrations are globally constant. Therefore, the Cl increase is the major trend of evolution of the Rupelian aquifer. O and H isotopes measurements have been performed and showed a marine origin for these waters. According to mixing model with sea-water, the marine contribution is expected to be up to 16% to the north of the area. So, the chemical composition of these fluids is the combined result of mixing with a marine component and water-rock interaction leading to Na, Ca, K, Mg/Cl ratios lower than those obtained by mixing only. This model should be further precised by the study of halogen elements and isotopic measurements (O, S, H)

C.2.3 Modelling global equilibria

The first step concerning global equilibria of the system is based on speciation calculations and saturation indexes of the main minerals. The PHREEQE software /1/ has been used. All the studied samples (interstitial and aquifer) are saturated with respect to chalcedony.

In interstitial fluids, Ca and Mg are controlled by carbonate solubility, but a slight oversaturation is observed in most locations of the Rupelian, except for chlorinated fluids which are near saturation. This oversaturation could be explained by an extra production of CO_2, resulting from the degradation of organic matter. In natural solutions, Fe is generally assumed to be at the valence II, even when positive redox potentials are measured, Fe (III) is rapidly removed from solution, as oxide or oxi-hydroxide mineral phases. In interstitial fluids and in the aquifer, Fe^{++}, $FeCO_3$ and $FeHCO_3^+$ are predominant species and Fe concentrations are also controlled by carbonate solubility. Chlorinated fluids are however undersaturated with respect to siderite and rhodocrosite. The relatively low concentrations of Fe could result from pyrite oxidation, with beginning of oxides and oxi-hydroxide precipitations.

Global geochemical equilibrium modelling is based on the intergration of the geochemical data obtained regionnaly on the rupelian aquifer and the interstitial fluids at Mol. The natural system to be modelled is made up of a solution in contact with a mineralogical assemblage, for which we considere the following species : Al, Si, Na, K, Ca, Mg, H, O, C and Cl. Oxygen is not an independant variable,

as its concentration is imposed by the valence state of the other elements. Oxydo-reduction equilibria are not considered (mainly concerning Fe and S) in this model.

Various dissolution/precipitations have been evidenced : calcite, dolomite, chalcedony and most probably kaolinite, which are the main mineralogical phase in equilibrium with the fluids, and which control respectively Ca, Mg, Si, and Al. Sodium and potassium are controlled by two aluminosilicates, a sodic one and a potassic one, for which the dissolution constants are imposed by the Log(Na)/(H) and Log(K)/(H) obtained from the observed regression over the whole regional fluids. The values obtained (table) allow us to assimilate these two aluminosilicates to albite (Na) and microcline (K) for modelling purpose. C and Cl are considered as external variables to the system. Each element is controlled by a unique mineral phase : elemental concentrations may thus be written for a given organic carbon content as a function of pH. pH in turn must satisfy electroneutrality of the solution.

We have applied the model using the PHREEQE code /1/, with the following thermodynamic database /2/: Calcite : 1.81, Dolomite : 2.49, Chalcedony : -3.71, Kaolinite : -39.16, M1 sodic : -20.3, as observed (albite : -19.98), M2 potassic : -22.3, as observed (microcline : -22.62). Calculation of porewater chemistry using these relationships leads to good fit between analytical data and calculated ones (Table II).

C.3 Solid phase characterisation

Solid phase of the clay sediment is made up of the constitutive minerals and organic matter (Table III). Quantitative determinations have been made based on XRD determination of whole rock and size fraction preparations, complemented with back calculations from wet chemical analyses of whole rock samples and electron micropobe determinations. The main feature of this mineralogy is the absence of vermiculite and the low content in chlorite, which is in better agreement with the low content in magnesium of the clay. Although the estimates made are only approximative, we believe that it is probably well representative of the true mineralogy of this sediment.

Fluid geochemistry can be considered as the consequence of the interaction between interstitial water and minerals, whereas the role of organic matter is not always taken into account. We have studied in detail the organic matter, in particular with respect to its cation exchange capacity. Organic matter exchange capacity account to about 5 miliéquivalent per 100g of dry sediment over about 30 miliéqivalent total exchange capacity. The geochemical mechanisms potentially involved for fluid geochemistry modelling are dissolution-precipitation, ion exchange and organic matter transformation. Thus, solid phase characterisation involves not only mineralogical determination, but also testing for rock properties or the determination of mineral and organic phase evolution state. To achieve this, a set of experiments has been conducted on fresh (i.e. undisturbed) or oxidized (i.e. disturbed) clay, some of them on site just after sampling in order to work on as fresh material as possible, some other in the lab when specific conditions or methods (pH control for instence) were requiered.

C.3.1 Results

The bulk mineralogy of the clay can be summarised as quartz (18.9 %), pyrite, (4.2 %) carbonates (1.0 % calcite, 0.9 % dolomite and 0.4 % siderite) and some feldspar (plagioclase 2.8 % and microcline 6.0 %), in addition to a clayey phase that makes up about 62 % of the sediment. The clay mineralogy is dominated (about 50 % of the clay fraction) by illite smectite mixed layers (randomly interstratified, containing about 55 % illite, and making up 28.5 % of the whole rock mineralogy), micas (mainly biotite and detrital illite and glauconite, making up altogether about 16.7 % of the whole rock fraction), kaolinite (around 10.1 % of the rock) and only 2.1 % of chloritic minerals. Pyrite appears as aggregates of euhedral crystals and framboids. In oxidized samples, this pyrite is partly replaced by anhydrite, and ferric sulfate and jarosite form if intense oxidation is maintained. Carbonates are disseminated in the clay and appear mainly as calcite and dolomite. Mass balance calculation shows that at least during moderate oxidation, only part of the available carbonate is

enough to account for measured alcalinity. After pyrolysis, organic matter shows low maturation (Tmax = 430°C) with high Hydrogen Index (HI = 300 to 330) confirming low maturation. Organic matter is essentially marine in origin (type III to type II), with some detrital organic inputs. Several indices such as XRD pattern evolution after heating, point towards an intimate mixture of organic matter with clay. SEM examination of stained preparations, along with heavy metal mapping have shown that organic matter is homogeneously partitionned within clay.

Total cation exchange capacity (as measured using cobaltohexamine chloride) amounts to about 25 meq/100g dry sediment, 20 of them due to major cation (Na, K, Ca and Mg) exchange with clay minerals, the rest being due to exchangeable protons. After oxidation, the amount of exchanged calcium and magnesium significantly increases, indicating that clay can still incorporate these elements when rendered available by slight oxidation.

C. 3.2 Modelling local equilibria

The model we propose to explain the present porewater chemistry in the undisturbed clay is an attempt to take into account cation exchange by clay mineral. This is based on the fact that cation exchange is very fast and can establish instantly. In addition, the interstitial porewaters of the Boom clay at Mol plot exactly in the trend of 59 soils from the western United States in a SAR/PAR diagram, and for which cation exchange is documented by the US Salinity Laboratory /3/. In this model, the initial marine water is primarily diluted by 1100 times by meteoric water. The redox potential is maintained reducing by organic matter, whereas pH is buffered by carbonate dissolution. Cation exchange with clays is responsible for sodium and potassium control. Clay minerals exchange mainly sodium and a few potassium against protons, and sodium against calcium and magnesium produced by carbonate dissolution. Exchange constants are those measured for illite by Thellier and Sposito /4/. We have verified by back calculating from our experimental data on natural clay that identical constants can be used in our system. Calculation of interstitial porefluids yields very good agreement with analytical results (Table IV).

The geochemical model developped in the ARCHIMEDE argile project has been completed using a new concept in geochemical modeling. In this concept, a simulator generator (NEPTUNIX^{TM}) has in charge code generation (FORTRAN) freeing the geochemist of computer coding task /5/. This allows him focus only on geochemical mechanisms description : the whole system can be reduced to a collection of elementary models, the interconnection of which yields the integrated model. The state of the system is given at various degrees of advancement, making it possible to visualise acquisition of porewater chemistry (Figure 1). Equilibrium is reached when the calculated composition no longer evolves.

C.4 Microbiological study

Bacteria can survive and even proliferate within deep-subsurface conditions /6,7,8/. The opening of a gallery induces drastic modifications to these environments, stimulating or inhibiting microbial activities. The new interface between subsurface sediments and human activity can be a propitious medium for bacteria brought by human activity. A study has thus been undertaken to investigate the nature and numbers of autochthonous bacteria present in the Boom clay deposit before any human processing, and the behaviour of allochthonous bacteria liable to be introduced in the deposit during the human activity in the gallery.

C.4.1 Sampling conditions

Three 40cm long core samples were sterile collected at 1, 10 and 20 meter depth from the gallery respectively, with the help of the SCK/CEN staff. Interstitial fluid microfauna was also recovered from sterile piezometers. Air and tool bacteria were sampled in order to check for allochthonous contamination. We have analyzed the number of bacteria as a function of depth in clay deposit from the

gallery as well as their activities as estimated in situ. Preliminary data of numerical taxonomy coupled with molecular phylogeny have been used in order to assess whether the bacteria isolated from clay samples are indigenous to the geological deposit, or if they are allochthonous organisms recently introduced from the surface. If bacteria do survive in subsurface environments, they can often be present in quite low numbers. In these conditions, and even when the most stringent precautions are taken to work under aseptic conditions (wear of sterile gloves and protective masks by operators, accurate cleaning and sterilisation of all equipment), the bacteria that always contaminate any human or mechanic operation are extremely difficult to distinguish from the true but rare autochthonous bacteria.

C.4.2 Bacteria distribution

Large number of living bacteria (10^6-10^5 CFU g^{-1}) and molds (10^5-10^4 CFU g^{-1}) were characterized within a few centimeters from the gallery wall. Less bacteria were observed as depth increased. Beyond 80 cm very few bacteria (10^1-10^2 CFU g^{-1}) were counted. Highest counts were recorded in aerobic conditions; microaerophilic and anaerobic bacteria were lacking or poorly represented. Two samples of clay collected at 760 cm and 1960 cm from the gallery wall appeared sterile under all culture conditions.In pore water samples collected at 3, 7 and 15 m depth, total counts ranged from 2.4 10^3 to 1.2 10^6 cells ml^{-1}. Viable counts ranged from none to $3x10^2$ colonies ml^{-1}. Bacterial densities in water do not correlate with sampling depth. In clay, bacterial respiration appeared significant only within the outerlayer (less than 80 cm of depth from the gallery wall), decreasing from 92 to 0.2 nanomole CO_2 l^{-1} h^{-1} from the surface to 80 cm depth. Less than 2 picomole CO_2 l^{-1} h^{-1} were produced in deeper samples (15m, 19m). In collected water, bacterial respiration ranged from 3 to 80 picomole CO_2 l^{-1} h^{-1}, assimilation ranged from 0.5 to 230 picoat C l^{-1} h^{-1}.

C.4.3 Assessment of bacterial origin

A total of 163 bacterial strains were isolated. One hundred and six strains were isolated from clay and water samples: 80 from clay samples (gallery surface: 20; 5 cm: 15; 15 cm: 10; 30 cm: 8; 80 cm: 7; 100 cm: 2; 550 cm: 1; 735 cm: 7; 760 cm: 1; 900 cm: 5; 1100 cm: 1; 1780 cm: 2; 1960 cm: 1), and 26 from pore water samples (300 cm: 1; 700 cm: 12; 1500 cm: 13). Forty seven strains were also isolated from different samples of the gallery atmosphere and 10 were collected on the tools. A combined study by numerical taxonomy and molecular phylogeny was used to assess the indigenous or allochthonous origin of these bacteria. For phenotypic identification each strain was described by 107 morphological, physiological and biochemical features /9/. Strains were compared and clustered using KHI2 coefficient and variance analysis. For molecular phylogeny, species identification was obtained by comparing the 16S ribosomal RNA (rRNA) sequence of each species to sequences obtained in an already existing rRNA databank /10,11,12/. Most of the strains isolated from samples collected beyond 80 cm from the gallery wall cluster (phenotypically and genetically) with strains isolated from the gallery atmosphere or from the coring tools. They were considered as contaminants resulting from the processing of the samples. On the other hand, 57 strains (all but three) isolated from the surface of the gallery down to a depth of 80 cm appeared well separated from other strains, and were considered as autochthonous. The phenotypical description allowed us to identify each bacterial strain according to the reference manuals /13,14,15/. This identification was in good agreement with both the above mentionned phenotypical and genetical clusterings. The bacterial strains isolated from the surface of the gallery to a depth of 80 cm were identified as soil bacteria (mostly Nocardioïdes, Alcaligenes, Azotobacter, Acinetobacter, Paracoccus and Pseudomonas). Most bacterial species considered as contaminants belong to taxonomic groups recognized in previous studies as contaminants ordinarily present in a human environment (Staphylococcus, Streptococcus) or as airborne bacteria (Bacillus).

Our analyses clearly demonstrate that there is a gradient of bacteria in the studied sediments. Bacteria proliferate at the interface between the clay sediments and the gallery due to human activity. This fauna might originate primarily from the grouting material used, mainly made up of a mixture of quartz, sand and concrete.

Bacteria are very rare if not nonexisting in the undisturbed deeper depth of the clay sediments. If methods such as numerical taxonomy or molecular phylogeny had not been used to assess for bacterial diversity and identity, the study would have led to a completely false representation of the numbers of bacteria present in the clay, of their nature and geochemical roles.

C.5 References

/1/ PARKURST D.L, THORSTENSSON D.C., PLUMMER L.N., U.S. Geol. Surv. Water Research Invest., 80-96 (1980)

/2/ MICHARD G. EUR 8590FR (1983)

/3/ U. S. SALINITY LABORATORY STAFF (1954) - Diagnosis and improvement of saline and alkali soils. U. S. Dept. Agric. Handb., 60, 160 p.

/4/ THELLIER C. and SPOSITO G. (1988) - Quaternary cation exchange on Silver Hill Illite. Soil Sci. Soc. Am. J., 52, pp. 979-985.

/5/ FABRIOL R, CZERNICHOWSKI-LAURIOL I., WRI symposium, Park City, Utah, USA, 13-18 july 1992. Proceedings.

/6/ BIANCHI A., HINOJOSA M., GARCIN, J. DELEBASSEE M., NORMAND M., RALIJOANA C., SOHIER L., VIANNA-DORIA E., VILLATA M., Le sondage Misedor, PELET R., (Ed.) Technip, Paris (1987).

/7/ KUZNETSOV S.I., IVANOV M.V., LYALIKOVA N.N., Introduction to geomicrobial microbiology. Mc Graw-Hill, New York (1963).

/8/ PEDERSEN K., EKENDAHL S., Microbiol. Ecol., 20-37 (1990).

/9/ Van WAMBEKE F., BIANCHI M., CAHET G., East. coast. Shelf Sci., 19-291 (1984).

/10/ AMANN R., KRUMHOLTZ L., STAHL D.A. ,J. Bacteriol., 172-762 (1990).

/11/ WERNER L., STACKEBRANDT E., J. Bacteriol., 174, (1992).

/12/ STACKEBRANDT E., LIESACK W., GOEBEL B.M., FASEB J., 7, 232 (1993).

/13/ KRIEG N.R., HOLT J.G., Bergey's Manual of systematic bacteriology. Vol.1. Williams & Wilkins, Baltimore (1984).

/14/ STALEY J.T., BRYANT M.V., PFENNIG N., HOLT J.G., Bergey's Manual of systematic bacteriology. Vol.3. Williams & Wilkins, Baltimore (1989).

/15/ STARR M.P., STOLP H., TRÜPPER H., BALOWS A., SCHLEGEL H.G., The prokaryotes. Vol. 1 & 2., Springer Verlag, Berlin (1981).

C.6 Tables

Table I : Chemical composition of interstitial fluids and aquifer.

	(1)	(2)	(3)		(1)	(2)	(3)
pH	8.75	7.65	8.5	**Na**	17	110.2	12.7
Eh (mV)	38	130	-310	**K**	0.25	1.06	0.25
Alkalinity	17.9	13.2	12.5	**Ca**	0.16	0.81	0.06
SO_4	0.013	4.06	0.05	**Mg**	0.04	1.83	0.12
Cl	0.77	92.7	0.5	**NH_4**	N.D	N.D	0.13
SiO_2	0.14	0.21	0.14				

The concentrations are expressed in mM/l; (1) : Mol; (2) : Meer. (3): interstitial fluid. (1) and (2) represent the two end-members of the Rupelian aquifer.

Table II : Comparison between calculated interstitial fluid (left hand side) and measured composition in the Boom Clay at Mol

Calculated porewater	**Measured porewater**
Imposed parametres :	
C = 12 mmmoles/l	
Cl = 0.5 mmol/l	0.5 mmoles/l
calculated parametres :	
pH = 8.5	8.2
Total alcalinity = 11.9 mmoles/l	12 mmoles/l
Ca = 0.04	0.05
Mg = 0.03	0.05
Na = 12.5	12.6
K = 0.17	0.2
Si = 0.2	0.15

Table III : Boom Clay mineralogy.

WHOLE ROCK	**%**		**%**
QUARTZ	18.9	CALCITE	1.0
MICROCLINE	6.0	PLAGIOCLASE	2.8
DOLOMITE	0.9	SIDERITE	0.4
PYRITE	4.2	ORGANIC MATTER	3.0 to 4.6
CLAY FRACTION			57.4
CLAY FRACTION			**%**
IS MIXED LAYERS, RANDOM (R=0)			28.5
IS MIXED LAYERS, ORDERED (R≥3)			Trace
ILLITE + MICA			16.5
KAOLINITE			10.1
CHLORITE			2.1
OXIDES (Ti, Fe, Mn)			

Table IV : Comparison between calculated porewater (left hand side) and reference porewater of Boom clay at Mol, using ion exchange to control sodium and potassium.

Imposed parametres :	Measured parameter
fCO_2 = 4 matm	4 matm
Cl = 0.5 mmol/l	0.5 mmoles/l
CEC = 24.7	24.7
exchangeable Na = 8.7	8.7
exchangeable K = 2.3	2.3
exchangeable Ca = 3.8	3.8
exchangeable Mg = 3.7	3.7
Calculated porewater	**Measured porewater**
pH = 8.22	8.2
Total alcalinity = 12.1 mmoles/l	11.9 mmoles/l
Ca = 0.054	0.047
Mg = 0.063	0.066
Na = 12.3	12.2
K = 0.214	0.212
Si = 0.19	0.15

C.7 Figures

Figure 1 : Summary of the local equilibria model using the new simulator generator. The evolution of calculated porewater chemistry is displayed as a fonction of reaction progress. In this case, dolomite dissolution first increases magnesium concentration in porewater. Reprecipitation of dolomite governs magnesium in solution.

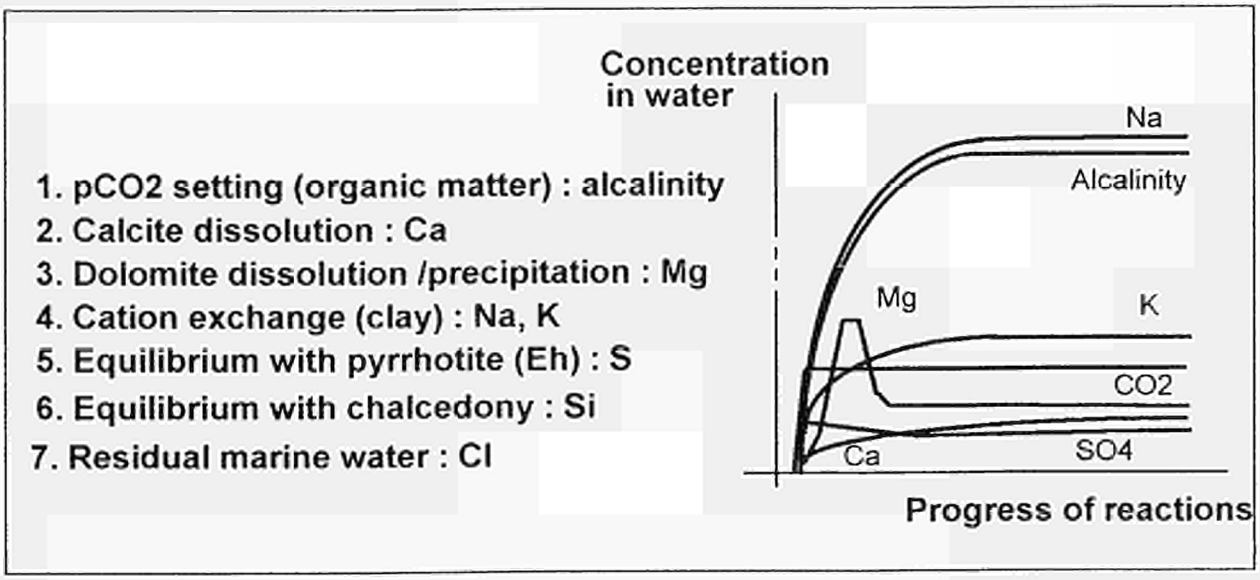

C.8 List of publications

MERCERON T., ANDRE-JEHAN R., FOUILLAC C., SUREAU J.F. ,PETIT P. and TOULHOAT P., 1992. The ARCHIMED-Argile project : acquisition and regulation of the water chemistry in clay formation within the geochemical program of ANDRA for geological disposal of high level radioactive wastes. Int symp. on Geologic disposal of spent fuel, high level and alpha-bearing wastes, Antwerp, Belgium 19-23 october 1992.

MERCERON T., HERMIN M.N., BIANCHI A., BOIVIN V., and CHRISTEN R., 1993. Microbial investigations within the Archimede-Clay project concerning the understanding of the water chemistry in clay environment. Migration'93 congress.

MERCERON T., 1993. ARCHIMEDE-CLAY project : acquisition and regulation of water chemistry in clay. Mirage'93 congress.

SANJUAN B., MOSSMANN J.R., and MERCERON T., 1994. Modelling Boom Clay Formation porewater chemistry : ion exchange versus dissolution precipitation mechanisms. V.M. Goldschmidt Conference, Edinburgh.

In addition, a series of papers is currently being prepared for submission in 1995.

Title	Phenomenology of Hydrical Exchanges Between Underground atmosphere and Storage host-rock (PHEBUS)
Contractors	Agence Nationale pour la gestion des Déchets RAdioactifs (ANDRA)
Contract N°	FI2W-CT91-0116
Duration of contract	January 1992 - December 1995
Period covered	1994
Project leader	J.M. PALUT

A/ OBJECTIVE AND SCOPE

The aim of the PHEBUS project concerns the study of the hydrous behavior of a clay formation around ventilated excavations. It consists of a modelling, a laboratory mock-up and an in situ test carried out at Mol facility in Belgium. Potential effects of clay desaturation around ventilated galleries should be changes in permeability, fissuration or mechanical hardening. These effects may particularly influence lining concepts as well as sealing concepts.

In a first phase, this consists in developing methodological tests not on core samples but on remoulded highly compacted clays. This procedure provides an appropriate control of the hydrical and mechanical history of the sample, making it possible to understand the real hydrous phenomena.

An in situ test will then be carried out in a borehole to validate the mock-up results. Using an appropriate apparatus, this phase will permit to reach some parameters and their time-dependence that can't be measured on a mock-up. It will allow to evaluate the usefulness of a gallery ventilation test and to assess its technical feasibility : ventilation system, lining conception and planning.

B/ WORK PROGRAM

B1. MODELLING

This part consists in developing a simplified model of the hydrical transfer, in isothermal conditions and without mechanical coupling (constant volume and porosity). This allows to study the parameters sensibility and to propose a first evaluation of the hydrical behavior of the clay medium under a ventilation effect (orders of magnitude of water fluxes, desaturation area and phenomenon duration) on the basis of the present data.

B2. MOCK-UP TESTS

The mock-up tests aim to well understand the phenomenology of hydrical exchanges between a controlled humidity air and the initially saturated clay, and to validate the model. It consists to design and manufacture an apparatus to test under high stress a clay with a cylindrical opening in the centre that simulates the ventilated gallery. At the end of each test, the mock-up is dismantled in order to measure the hydrical state around the opening.

B3. IN-SITU TEST

This phase is carried out in an horizontal borehole lined with a porous tubing. This borehole will be ventilated with an air of controlled temperature and relative humidity. The amount of water extracted will be monitored as well as the clay hydrical state around the borehole to evaluate the desaturation line. The experimental results will be compared to the model predictions.

C/ PROGRESS WORK AND RESULTS

State of advancement

The modelling phase has been completed. The main parameters are the relative humidity of the air and the saturated clay permeability. It shows that the desaturation effect will concern a few meters area around the openings, sufficiently to affect the clay mechanical parameters and so the mechanical interaction between the clay and the lining. Under repository conditions the desaturated area should be independent of the radius of the gallery.

The apparatus for mock-up tests basically consists of an oedometer and a ventilation system. Amongst the two experiments scheduled in the contract, the first one carried out with Boom clay was completed successfully in April 1994. Due to an unexpected hydro-mechanical coupling observed during this test, the apparatus has had to be improved by addition of stress measurements. These modifications were implemented in December.

At Mol, the peripheral instrumentation installed in 93 for the in situ phase works in a satisfactory way. The equipment for the main borehole was delivered and installed in October 94. Stabilization of the clay around the probe is under way.

Progress and Results

C.1 MODELLING

The model is based on the analysis of the different types of pore water in clay (free, capillary and adsorbed water). In deep clay most of the water is in adsorbed state. The model considers the specific transfer mechanisms of each type of water. It has been shown that, when the gas phase is under constant pressure, the total water transfer could be addressed with one parameter similar to a diffusion coefficient and function of porosity and water condition. At saturation, this parameter is equal to the permeability. Both mock-up and in situ test have been designed on this basis.

With a permeability of 10^{-12} m/s and for various relative humidities, we calculate the water flux per surface unit, the total water volume and the desaturation front. The water flux decreases rapidly and reaches after two months a pseudo-permanent state independent of the relative humidity. For our experiments that means that it wouldn't be significant to continue after 2 months.

C.2 MOCK-UP TESTS

Procedure

The mock-up apparatus is based on an oedometer for high stress (0-20 MPa) which includes an additional cylindrical hole in the centre (figure 1). Each experiment comprises three steps :

* consolidation of a clay paste to get a highly-compacted remoulded clay,
* ventilation by blowing an air flux of controlled humidity through the central hole, to desaturate the compacted clay. A relative humidity is applied to the air by the mean of saturated salt solutions which capture the water in excess.
* dismantling and sampling of the remoulded clay to measure parameters such as water content *vs* distance to the central ventilated hole.

Results

The first test was performed on a material made from natural Boom clay. This clay was left to soak in slightly mineralized water, then mixed to constitute a fluid paste. The compaction phase lasted five weeks and occurred in three stress levels. The final stress state selected as the reference, i.e. 5 MPa, corresponds to a void index of 0.52. The resulting oedometric curve is given in figure 2.
Once the reference stress state is achieved, the ventilation was started up. It operated continuously for 138 days, was interrupted for 25 days, and was started again for 11 days. The air flow rate was set up to 20 l/sec and its relative humidity was chosen of 33%, corresponding to a potential of 150 Mpa at 20°C. When the ventilation was put on, we observed that the compaction of the clay significantly re-started, then stopped during the interruption of the ventilation and started again with the second ventilation phase (figure 2).
The stoppage of the ventilation was followed by a rapid discharge to exit the clay slab. No significant deformation was observed. Hydrous profiles were measured immediately following several radial directions of the clay slab. The axisymmetric characteristic was validated. The standard profile is shown in figure 4. We observe a very clear desaturation beginning from the central opening with a strong gradient. The periphery is slightly desaturated due to inevitable hydrous exchanges between the dismantling and the sampling.

Interpretation

For the interpretation of the hydrous behavior, the initial modelling was done without taking into account the phase when ventilation was stopped. The difference between the hydrous profile predicted and the experimental data was significant.
During the interruption of the ventilation, the measurement of the relative humidity of the air in the central tube indicated a strong rise from 33% towards 80%. Therefore, a large hydrous re-balancing took place between the clay and the air, on one side, and inside the clay on the other. When the modelling take into account the interruption of the ventilation, its results are consistent with the experimental data (figure 4). The same is true for the quantity of water extracted, as figure 3 shows.

Concerning the hydromechanical behavior, the desaturation of the clay was accompanied by substantial collapse. The material went from a void index of 0.52 to 0.42, or a deformation of around 20%. The stoppage of ventilation showed that the settling was irreversible. The desaturation at a constant total stress therefore translated into a compaction of the material identical to the compaction of a saturated clay by increased mechanical stress. This compaction is identified at the microscopic scale by clay porosity spectra from the central tube to the periphery, which indicates in the most desaturated parts the decrease in the principal porosity mode (100 Å) and the appearance of a smaller mode at 50 Å.

C.3 IN SITU TEST

The principle of this in situ test is to blow a dry air flux into a borehole in order to desaturate the surrounding clay through a porous lining. The water is extracted from the air at the output of the test chamber and measured. Peripheral instrumentation provide data about clay at different distances from the chamber.

Location and dimensions of the test chamber have been defined according to the model calculations (see figure 5). The test zone is located between 11 and 14 meters depth, far enough to reduce the mechanical or hydrical effects of existent excavations. The lining of the test chamber consists of a perforated casing covered with a porous medium of 300 mm in diameter which also supports ground pressure sensors.

The peripheral instrumentation consisting of pore water pressure and stress measurements was installed in three boreholes by the SCK· CEN in 1993. These boreholes are also usable for water content measurements, carried out with the gamma-neutron probe already used in Mol, but accommodate to focus the measurements in one direction. This equipment made it possible to monitor the stabilization of the clay after its installation as well as the drilling of the test chamber one year later (figure 6).

The main borehole was drilled in the middle of the instrumented area in October 1994. The porous chamber was immediately installed in it. The pressure sensors located on the probe body operate properly and denote a slow increase of stress. The ventilation phase will start when stabilization of clay around the chamber is sufficiently advanced, that is expected circa April 1995.

References

"Modèle de transfert de masse dans les argiles à faible porosité. Application à l'effet de la ventilation dans les galeries" JC Robinet, M Al-Mukhtar, M Rhattas, F Plas, P Lebon. Revue Française de géotechnique n°61 pp. 31-43 - décembre 1992.

"Essai PHEBUS : Evaluation des transferts hydriques entre le massif argileux et les excavations" - Contrat CCE N° FI2W-CT91-0116 - Rapport d'avancement n° 5 (Janvier - juin 1994) - JF. Laurens, J.M. Palut, F. Plas

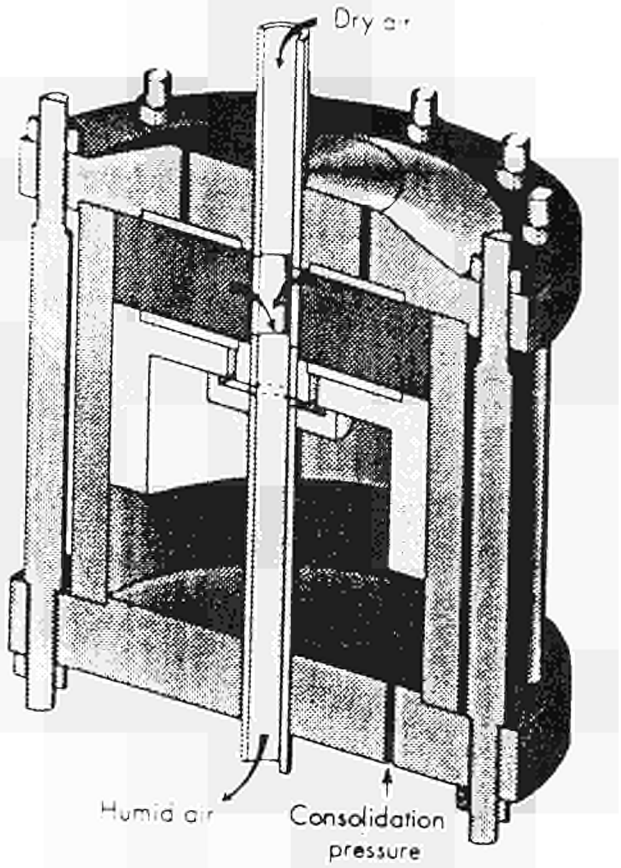

Fig. 1 Experimental setup for mock-up tests

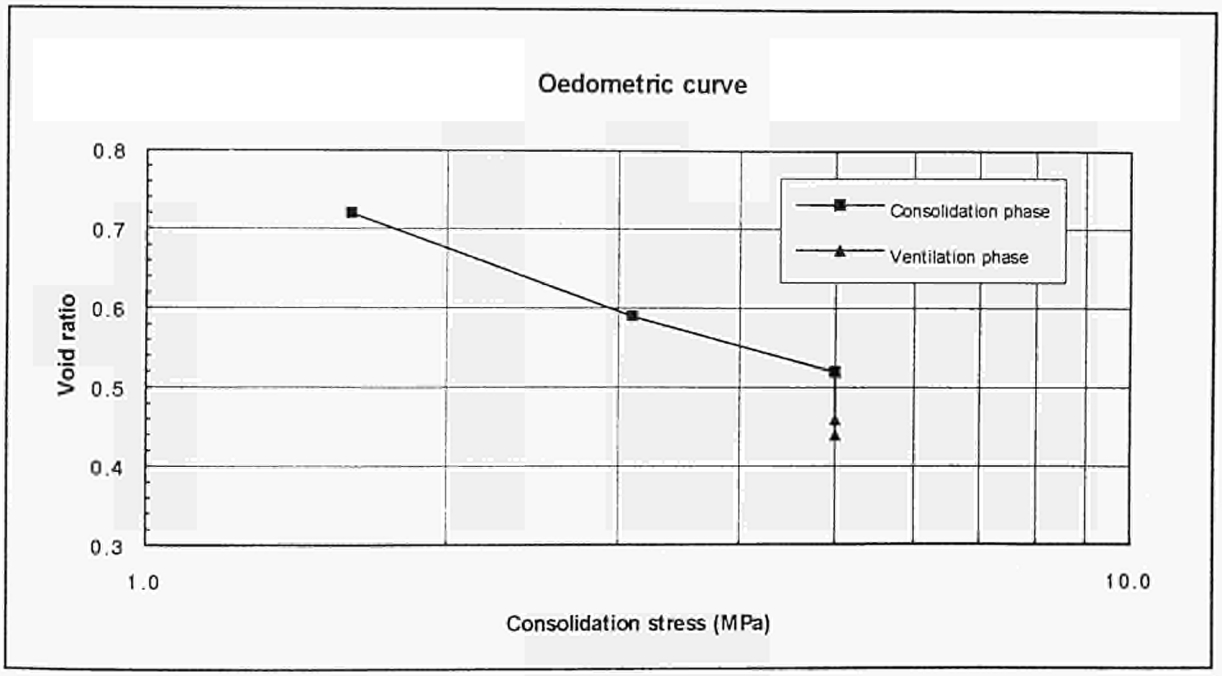

Fig. 2 Oedometric curve recorded during the first test on remoulded Boom clay

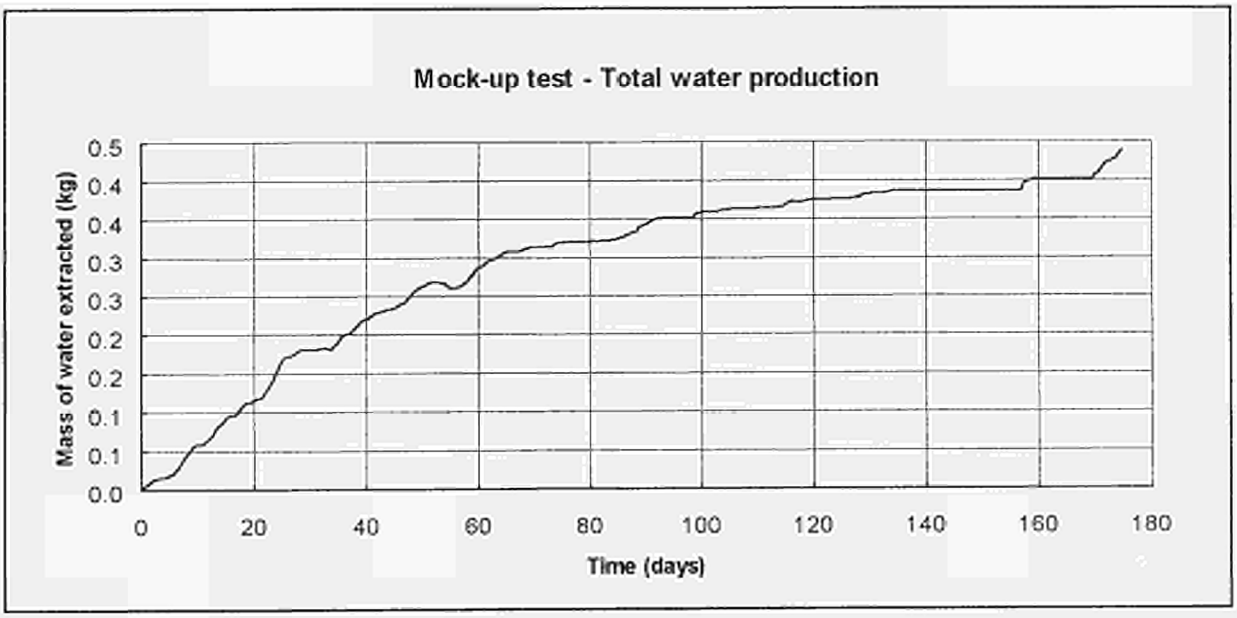

Fig. 3 - Water extracted during the ventilation phase

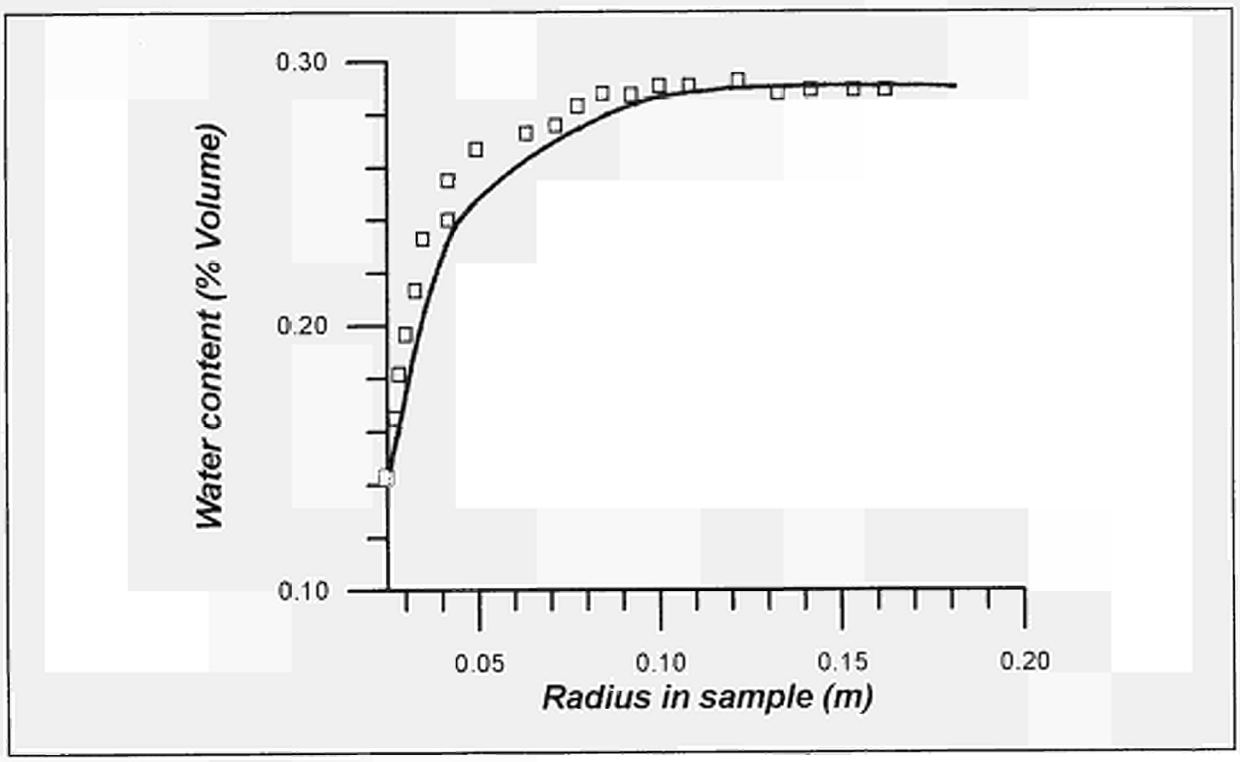

Fig. 4 - 1st mock-up test : hydrous profile in the remoulded clay slab (modelling and experiment data)

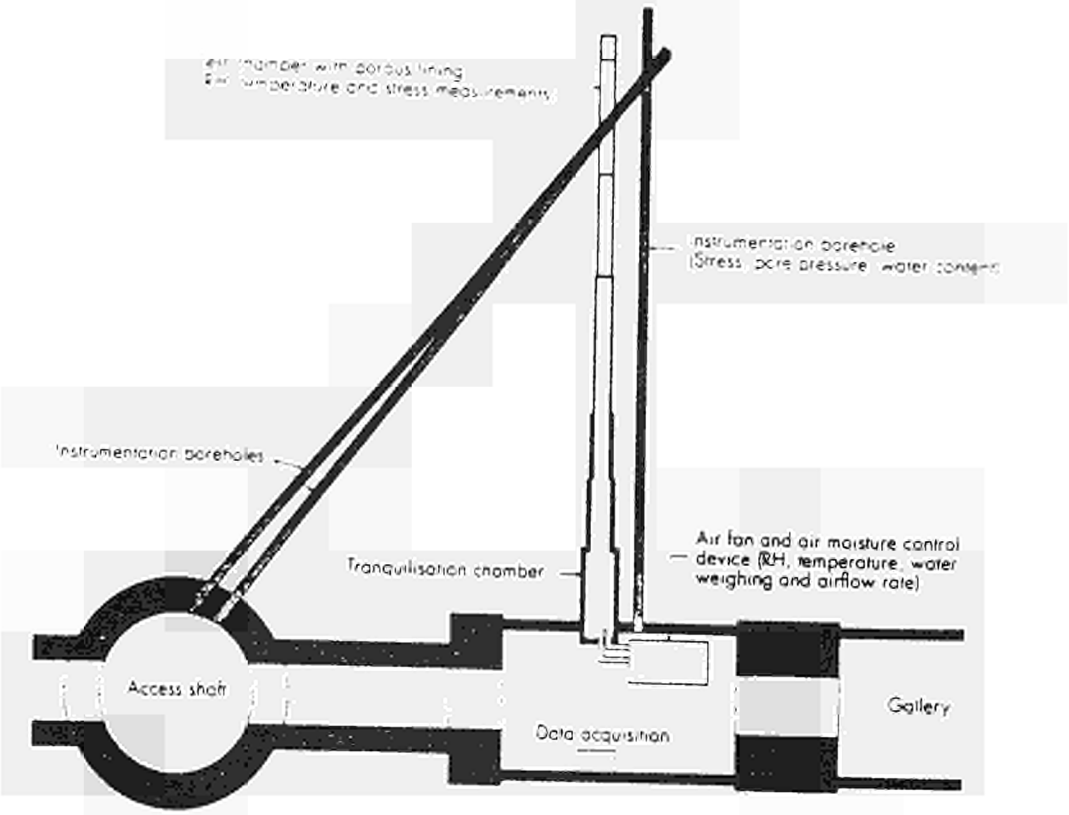

Fig. 5 - Experimental setup for in situ tests

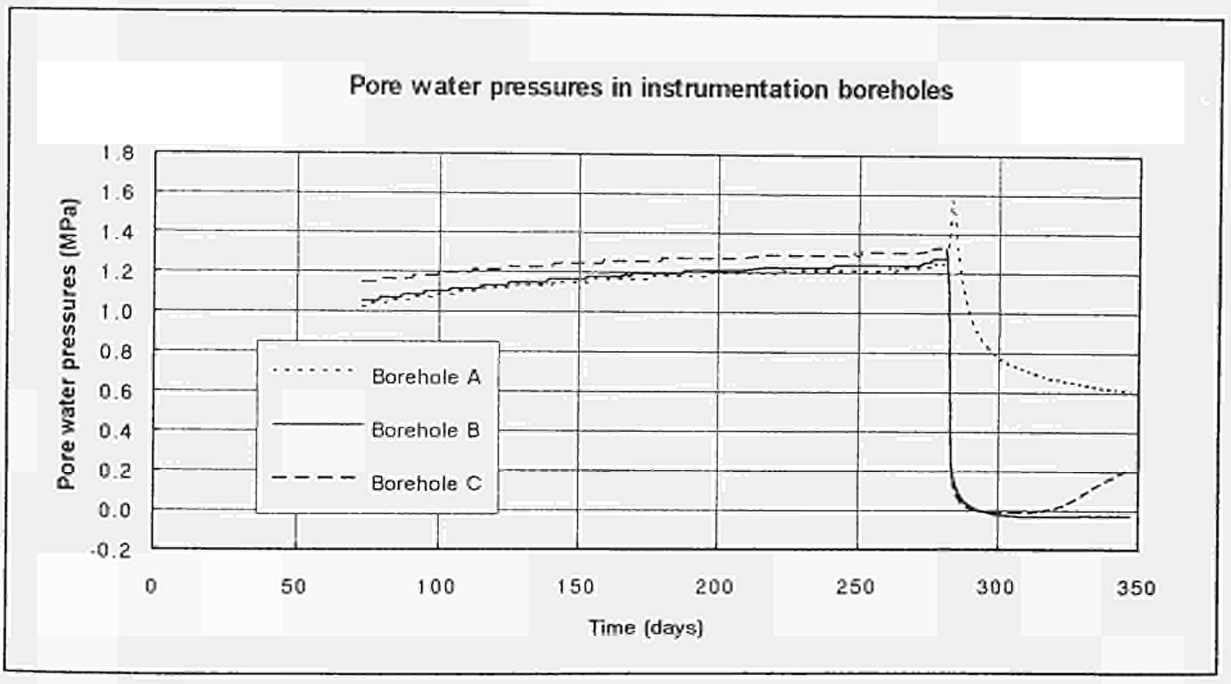

Fig. 6 - Typical results from instrumentation boreholes

Title	Modelling of the thermo-mechanical behaviour of clay (CACTUS test)
Contractors	Agence Nationale pour la gestion des Déchets RAdioactifs (ANDRA)
Contract N°	FI2W-CT94-0129
Duration of contract	August 1994 - January 1996
Period covered	August 1994 - December 1994
Project leader	F. PLAS

A. OBJECTIVES AND SCOPE

As part of the Hades Project and with the support of the Commission of the European Community (CEC contract n° FI2W-001-F), ANDRA developed the Cactus project (Characterization of Clay under Thermal loading for Underground Storage) for the purpose of in situ study of the thermo-hydro-mechanical behavior of a clay massif in the near field of a heater to simulate the thermal release of a stack of vitrified waste packages after 50 years of cooling.

Two separate tests, CACTUS 1 and CACTUS 2, were designed, conducted and evaluated in the Mol underground labaratory by the G.3S from 1989 to 1993, with the technical support of the SCK/CEN (figure 1).

Particular care was taken to ensure accurate of the clay response and reliable measurements. Peripheral instrumentation for each test included thermal probes (temperature), piezometric nests (pore water pressure), Glötzl cells (total stress), extensometers (strain) and a gamma-neutron probe (clay density and water content), as shown on the figure 2.

This instrumentation enable the evolution of the principal physical parameters of the clay massif to be monitored closely throughout all tests, each of which had three phases coresponding to specific thermo-hydro-mechanical loads:

(1) Excavation of the borehole
(2) Installation of the heater and consolidation of the clay massif around the borehole
(3) Heating/cooling cycles (s)

(figure 3)

All design and construction data and experimental results from the two tests were logged in the final CACTUS report (EUR 15482).

The CACTUS tests constitute a rather unique and comprehensive experimental data base that facilitates the overall conduct of modelling from the isothermal phases through thermal cycling. Based on this, ANDRA set up two research teams, that started out with diffrent approaches to the thermo-hydro-mechanical behavior of the saturated clays, particularly Boom clay, and with different modeling tools to conduct the CACTUS tests :

(a) The **G.3S** Research Group on Underground Structures (France)
(b) The **I.S.M.E.S** (Italy)

These two teams were envolved in the CEC projet "INTERCLAY phase II"

B. WORK PROGRAMME

The programme of the study is structured according to following tasks:

B.1 Collection and compilation of the data and characterization of the Boom clay. Review of the in situ (thermo)-(hydro)-mechanical tests at MOL. Preparation of the modelling.
B.2 Modelling of a CACTUS test
B.3 Analysis and synthesis of the modelling results

C. PROGRESS OF WORK AND OBTAINED RESULTS

State of advancement

The preliminary work was conducted as planned, i.e., in accordance with Phase I, modeling preparation. Each research teams conducted a critical review of the data from CACTUS and all data relative to Boom clay from its own perspective.

Progress and results

The main works of G.3S and ISMES were oriented toward the analysis and comparative study of experimental results from various tests performed at Mol (CACTUS 1, CACTUS 2, BACCHUS, CERBERUS) with special attention given to the following:

- The status of in situ stresses and pore water pressure
- The analysis of the hydro-mechanical effects of the borehole excavation
- The analysis of the thermo-hydro-mechanical effects of a thermal loading.

For G.3S the overall in situ experimental results are consistent in terms of stress and pore water pressure (rapid response to loads and higher absolute values), except for the CERBERUS results. However, differences were not explained, although micro cracking of the clay massif in the near field was hypothesized. Concerning the laboratory tests, the main conclusions of G.3S are the following:

- The CamClay model could not be used to describe the behavior of the Boom clay in all the loading directions
- The dependency of the elastic modulus with the temperature could be neglected
- Lastly the principal of the thermal hardening is clearly demonstrated.

ISMES performed two simulations (TESTD31, TESTD33) of the excavation of the test drift of the Underground Laboratory facility at Mol with an elastoplastic hardening material model (Cam Clay) by a finite element model under axisymetric conditions (figure 4). These simulations were calibrated on the basis of two data set obtained from laboratory tests. The comparison with measures of stress taken by pressuremeters within the mine-by experiment, Bonne et Al., 1992, show a satisfactory agreement (figure 5). The comparison with measures of CACTUS tests is not satisfactory; Experimental stress and pore pressure are very low: the average pore pressure ranges between 0.84 MPa (CACTUS 1) and 1.07MPa (CACTUS 2) at distances from the test drift wall ranging from 13 to 15 meters, whereas horizontal total stress, in the same positions, from 0.96 MPa to 1.57 MPa. Two explanations are given:

- the stress re-equilibrium after the excavation of the CACTUS boreholes was not reached;
- unaccuracy of the Glöztl cells used for these measures.

Lastly these first simulations seem to show that the hydro-mechanical effect of the test drift excavation could not be neglected for the simulation of the CACTUS tests.

References

- Essai thermo-hydro-mécanique dans une argile profonde - ESSAI "CACTUS" J.M. PICARD, B. BAZARGAN, G. ROUSSET (G.3S) - CEC Contract n° FI2W-001-F(CD) - Final report Eur 15482

- Modelling of the thermo-mechanical behavior of clay (CACTUS Tests) - CEC Contract n° FI2W-CT94-0129 - 1st progress report - August 1994 to February 1995

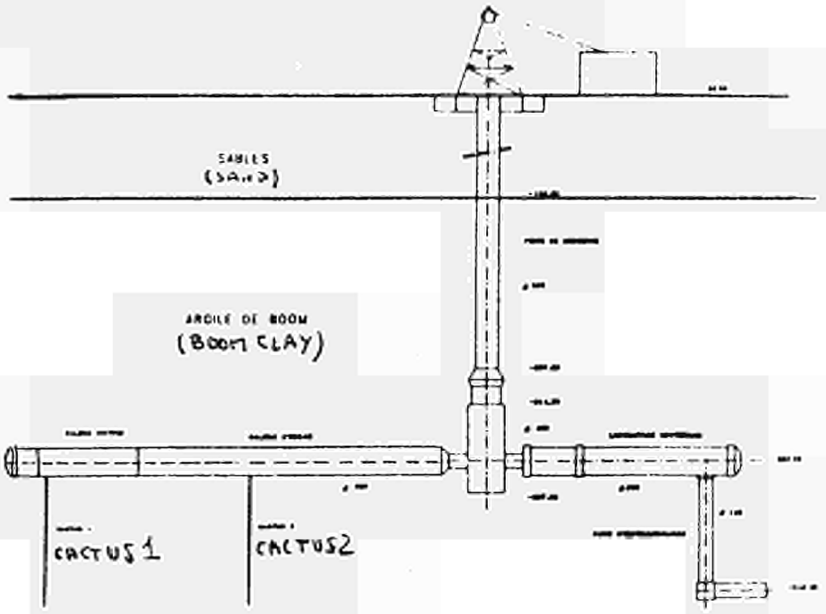

Figure 1 - Emplacement of the CACTUS tests in the Mol Underground facility

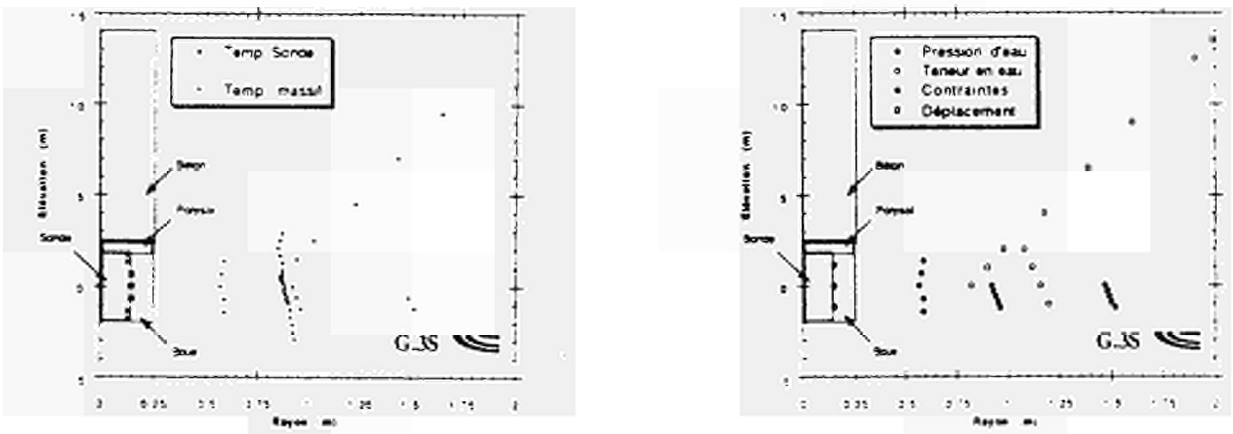

Figure 2 - Peripheral instrumentation of CACTUS 1

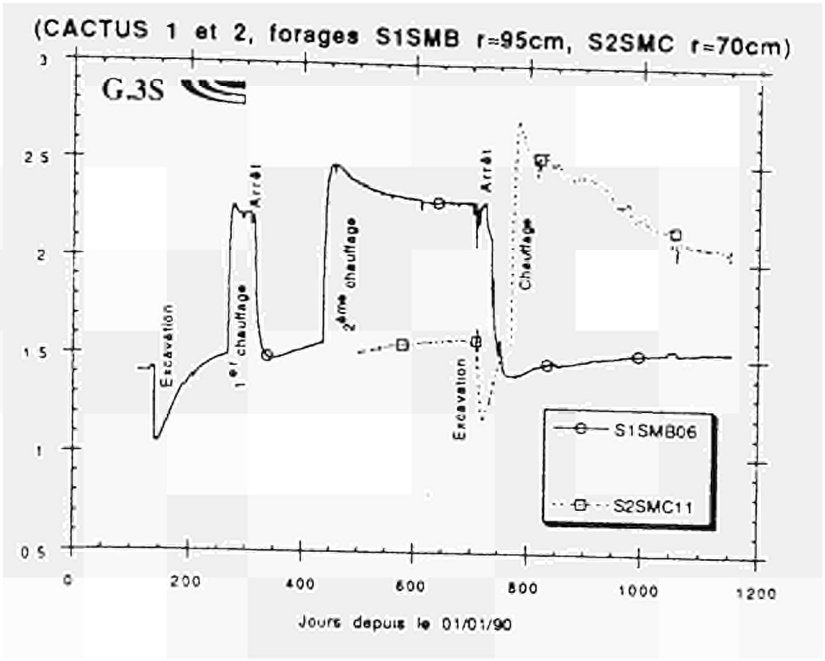

Figure 3 - CACTUS : Radial stress evolution

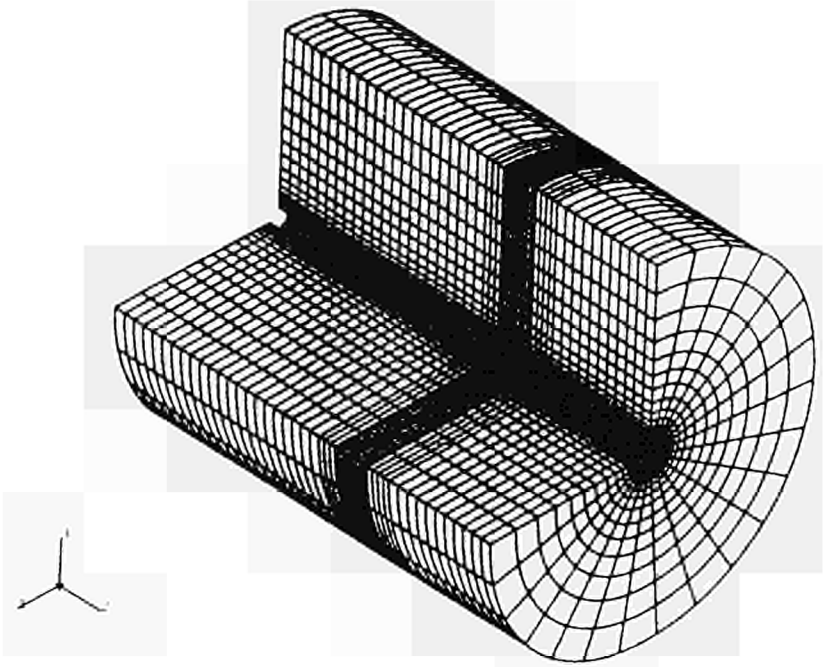

Figure 4 - Finite element mesh used by ISMES to simulate the Test drift excavation

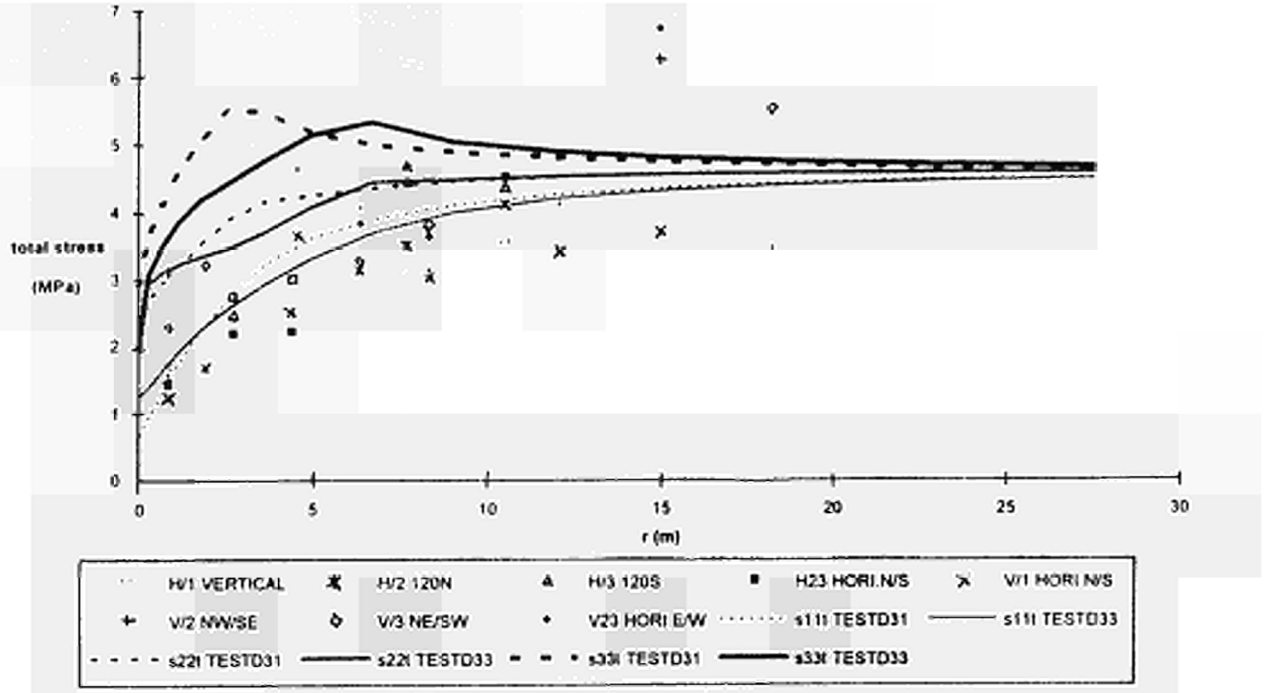

Figure 5 - Comparison between the stress measurements of the mine-by test and the simulated stresses obtained by ISMES

Title :	Hydrogeological characterisation of hard fractured rock at sellafield
Contractor:	United Kingdom Nirex Limited
Contract N°:	FI2W-CT91-0114
Duration of contract:	1 April 1992 - 31 December 1994
Period covered:	January - December 1994
Project leader:	Dr A J Hooper

A. OBJECTIVES AND SCOPE

The overall objective of the project is to decrease uncertainties in the hydrogeological and structural characterisation of a volume of rock at Sellafield in Cumbria. This rock is currently being considered as a potential host for a low and intermediate level solid radioactive waste repository in the United Kingdom.

The specific aims of the work are to perform geophysical and hydrogeological tests in and between two boreholes in a fractured and layered volcanic rock sequence, the Borrowdale Volcanic Group. Geophysical data will be integrated into a model of the rock volume. The results of single and crosshole hydrogeological testing will be used to clarify the lithological and structural features or combination which control groundwater flow in the Borrowdale Volcanic Group. This model will be applied to develop and validate concepts of groundwater flow in the immediate vicinity of the proposed repository.

The work is being performed in conjunction with Sir Alexander Gibb and Partners, acting as Geological Consultant. In addition, the following contractors have been defined: Schlumberger, Golder Associates UK Ltd.

B. WORK PROGRAMME

1. Review methodologies and prepare Design Intent Memorandum.
2. Geophysical testing in Sellafield Borehole n° 4.
3. Cross-borehole geophysical testing.
4. Single borehole hydraulic measurements in Borehole 4.
5. Design of cross-borehole interference testing.
6. Cross-borehole interference testing.

C. PROGRESS OF WORK AND OBTAINED RESULTS

The status of progress has not been forwarded to the Commission for 1994.

ANNEX I: List of organisations participating in the programme during 1994

AEA (UKEA)-Dounreay	AEA (UKEA) Dounreay Nuclear Power UK-THURSO, CAITHNESS KW14 7TZ
AEA Technology - Harwell	AEA (UKAEA) 353 Harwell, Didcot UK-OXFORDSHIRE OX11 0RA
AEA Technology - Windscale	AEA (UKEA) Windscale Seascale UK-CUMBRIA CA20 1PF
AEA Technology - Winfrith	AEA (UKAEA) B44 Winfrith Dorchester UK-DORSET DT2 8DH
ANDRA	Agence Nationale pour la Gestion des Déchets Radioactifs Route du Panorama Robert Schuman B.P. 38 F-92266 FONTENAY-AUX-ROSES Cedex
ARMINES	Association pour la Recherche et le Développement de Méthodes et Processus Industriels Ecole Nationale Supérieure des Mines de Paris Rue Saint Honoré 35 F-77305 FONTAINEBLEAU Cedex
ATKINS	WS Atkins Consultants Limited Woodcote Grove, Ashley Road UK-EPSOM, Surrey KT18 5BW
BAM	Bundesanstalt für Materialforschung-u-Prüfung Unter den Eichen 87 D-12205 BERLIN
BERTIN & CIE	Bertin & Cie Centre de Tarnos Z.I. F-40220 TARNOS

BGR	Bundesanstalt für Geowissenschaften und Rohstoffe Stilleweg 2 Postfach 510153 D-30631 Hannover
BGS (NERC)	British Geological Survey Natural Environment Research Council Kingsley Dunham Centre UK-KEYWORTH, NOTTINGHAM NG12 5GG
BN	Belgonucléaire Avenue Ariane 4 B-1200 BRUXELLES
BNFL	British Nuclear Fuel Plc Risley UK-WARRINGTON, CHESHIRE WA3 6AS
BRGM	Bureau de Recherches Géologiques et Minières Avenue de Concyr B.P. 6009 F-45060 ORLEANS-LA-SOURCE Cédex 2
BS	Brenk Systemplanung Ingenieurbüro für Wissenchaftlich Tech. Umweltschutz Heinrichsallee 38 D-52062 AACHEN
CEA	Commissariat à l'Energie Atomique Rue de la Fédération 31-33 F-75752 PARIS Cédex 15
CEA-CADARACHE	Commissariat à l'Energie Atomique Centre d'Etudes de Cadarache F-13108 ST.PAUL-LEZ-DURANCE Cédex
CEA-FAR	Commissariat à l'Energie Atomique Centre d'Etudes de Fontenay-aux-Roses B.P.6 F-92265 FONTENAY-AUX-ROSES Cédex
CEA-IPSN	Commissariat à l'Energie Atomique Inst. de Protection et de Sûreté Nucléaire Avenue Général Leclerc 60-68 B.P. 6 F-FONTENAY-AUX-ROSE Cédex

CEA-SACLAY	Commissariat à l'Energie Atomique Centre d'Etudes de Saclay F-91191 GIF-SUR-YVETTE Cédex
CEA-VALRHO	Commissariat à l'Energie Atomique Centre d'Etudes de la Vallée du Rhône B.P. 171 F-30207 BAGNOLS-SUR-CEZE Cédex
CEN/SCK	Centre d'Etude de l'Energie Nucléaire Studiecentrum voor Kernenergie Boeretang 200 B-2400 MOL
CIEMAT	Centro de Investigaciones Energeticas Medio Ambientales y Tecnologicas Ministerio de Industria, Comercio y Turismo Avenida Complutense 22 E-28040 MADRID
CIMNE	Centro Intern. de Métodos Numéricos en Ingeniera Jordi Girona Salgado 31 E-08034 BARCELONA
CNRS	Centre Nat. de la Recherche Scientifique Geochimie de la Surface UPR6251 Rue Blessing 1 F-67084 STRASBOURG
CREGU	Centre de Recherche sur la Géologie des Matières Prim. Minérales et Energétiques Rue du Bois de la Champelle 3 F-54501 VANDOEUVRE-LEZ-NANCY
DBE	Deutsche Gesellschaft zum Bau und Betrieb von Endlagern für Abfallstoffe mbH Postfach 1169 D-31201 PEINE
ECN	Stichting Energieonderzoek Centrum Nederland Postbus 1 Westerduinweg 3 NL-1755 ZG PETTEN

EHIC-STRASBOURG	EHICS Lab. de Chimie Phisique - UA CNRS N° 405 1 Rue Blaise Pascal - B.P. N° 296 F-67008 STRASBOURG
ENEA-CASACCIA	Ente per le Nuove tecnologie, l'Energia e l'Ambiente CRE-Cassacia Via Anguillarse 301 I-00060 S. MARIA di GALERIA
ENEA-SALUGGIA	Ente per le Nuove tecnologie, l'Energia e Ambiente Impianto Eurex I-13040 SALUGGIA (Vc)
ENEA-ISPRA	Casella Postale n°37 - c/o CCR Euratom I-21020 ISPRA (Varese)
ENRESA	Empresa National de Residuos Radioactivos S.A. Calle Emilio Vargas 7 E-28043 MADRID
ENSMP	Ecole Nat. Supérieure des Mines de Paris Rue Saint-Honoré, 35 F-77035 FONTAINEBLEAU Cedex
ETSIM	ETSI Minas (Univesidad Politecnica de Madrid) Dpto. de Matematica Aplicada Metodos Informaticas E-28003 MADRID
FPMS	Faculté Polytechnique de Mons Rue de Houdain 9 B-7000 Mons
FRAMATOME	FRAMATOME S.A. Direction Novatome Rue Juliette Récamier 10 F-69006 LYON 03
FZK (former KFK)	Forschungszentrum Karlsruhe GmbH Postfach 3640 D-76021 KARLSRUHE

GCG	Geotechnical Consulting Group Ltd Queensberry Place 1a UK-LONDON SW7 2DL
GCI	GCI GROUP Chelsea Manor Gardens 1 UK-LONDON SW3 5PN
GEOSTOCK	Soc. Française de Stockages Géologiques Geostock/Immeuble Sedgwick Rue Eugène et Arnaud Peugeot 7 F-92563 RUEIL-MALMAISON Cédex
GERMETRAD	Université de Nantes Lab. Biochimie et Radiobiochimie Rue de la Houssinière 2 F-44072 NANTES 03
G.3S	Groupement pour l'Etude des Structures Souterraines de Stockage Route de Saclay F-91128 PALAISEAU
GOLDER ASS.	Goder Associates Ltd. Landmere Lane, Edwalton UK-NOTTINGHAM NG12 4DG
GRAM s.a.	GRAM 10, Rue P. Duhem Z.I. Les Milles F-13856 AIX EN PROVENCE Cedex 3
GRS	Gesellschaft für Reaktorsicherheit mbH Schwertnergasse 1 D-5000 KOELN 1
GSF-IfT	GSF-Forschungszentrum für Umwelt und Gesunheit GmbH Institut für Tieflagerung Theodor Heuss-Strasse 4 D-38122 BRAUNSCHWEIG

GSF	GSF-Forschungzentrum für Umwelt und Gesundheit GmbH Institut für Tieflagerung Schachtanlage Asse D-38319 REMLINGEN
INERIS	Inst. Nat. de l'Environnement industr. et des Risques Lab. Mécanique des Terrains Parc de Saurupt F-54042 NANCY
INFM	Universita di Padova Dip. Fisica Via Marzolo 8 I-35131 PADOVA
INITEC	Empresa Nacional de Ingeneria y Technologica S.A. Padilla 17 E-28006 MADRID
INTAKTA	Intakta France S.a.r.l. Rue des Jeuneurs 21 F-75002 PARIS
INTERA	Intera Information Technologies Ltd. Chiltern House, 45 Station Road Henley-on-Thames UK-OXFORDSHIRE RG9 1AT
ISMES	Instituto Sperimentale Modelli e Strutture SpA Via Giulio Cesare 29 I-24100 BERGAMO
ITGE	Inst. Tecnologio Geominero de Espana Ingeniera Geoambiental Rios Rosas 23 E-28003 MADRID
KEMA	Keuring van Elektrotechnische Materialen N.V. Utrechtseweg 310 NL-6812 AR ARNHEM
KFA	Forschungszentrum Jülich GmbH - ISR D-52425 JÜLICH

KUL	Katholieke Universiteit Leuven Lab. v. Colloidchemie Kardinaal Mercierlaan 92 B-3001 HEVERLEE
LABORELEC	Laboratoire Belge de l'Industrie Electrique Rue de Rhode 125 B-1630 LINKEBEEK
LNETI	Lab. Nacional de Engenharia e tecnol. Industrial Estrade Nacional 10 P-2685 SACAVEM
LUT	Loughborough Univ. of Technology Dept. of Chemistry UK-LOUGHBOROUGH LE11 3TU
MBT	Halesa-MBT SAE Parc Tecnológic del Valles E-08290 CERDANYOLA
MOTT-MACDONALD	MOTT MacDonald Civil Ltd; Foundations & Geotechnics Div. Wellesley Road, 20-26 UK-CROYDON CR9 2UL
NCSR "DEMOKRITOS"	NRCS "DEMOKRITOS" Nuclear Techn. Radiation Protection Aghia Paraskevi, Attikis GR-15310 ATHENS
NERI	National Environment Research Institute Frederiksborgues 399 P.O. Box 358 DK-4000 ROSKILDE
NRI	Nuclear Research Institute CZ-25068 REZ
ONDRAF/NIRAS	Organisme National des Déchets Radioactifs et des Matières Fissiles Enrichies Place Madou 1 (Btes 25) B-1030 BRUSSELS

RGD	Rijks Geologische Dienst-Nederland Richard Holkade 10 NL-2000 AD HAARLEM
RISØ NL	Riso National Laboratory P.O. Box 49 DK-4000 ROSKILDE
RIVM	Rijksinstituut voor Volksgezondheid en Milieuhygiëne Antonie van Leeuwenhoeklaan 9 NL-3720 BA BILTHOVEN
SIEMENS (KWU)	Siemens AG - KWU P.O. Box 1001 00 D-5060 BERGISCH GLADBACH 1
SIF-BACHY	Soc. Sondages Injections Forages de Bachy Rue Ste Claire Deville-lez-Colonnades 4 F-92563 RUEIL-MALMAISON
SIMOCO	Simulation and Model Cons. Ltd. Bank House Merton Road 209 UK-LONDON SW19 1EE
TU MÜNCHEN	Technische Universität München Inst. für Radiochemie Walther-Meissnerstrasse 3 D-85747 GARCHING
UCL/LGC	Université Catholique de Louvain Lab. Génie Civil Place du Levant 1 B-1348 LOUVAIN-LA-NEUVE
UK-NIREX	UK NIREX Ltd Harwell Curie Avenue UK-DIDCOT OX11 ORH
UNIV. ABERDEEN	University of Aberdeen Chemistry Dept. Meston Walk old Aberdeen UK-SCOTLAND AB9 2UE

UNIV.BARCELONA	Universidad de Barcelona Facultad de Quimica Marti I Franques 1-11 E-08028 BARCELONA
UNIV. BELFAST	Queen's University Belfast School of Chemistry UK-BELFAST BT9 5 AG Nothern Ireland
UNIV. BES	Université Franche-Comté de Besançon Fac. Sciences et Techniques Route de Gray 16 F-25030 BESANCON
UNIV. EDINBURGH	University of Edinburgh Old College, South Bridge UK-EDINBURGH EH8 9YL
UNIV. EXETER	University of Exeter - Earth Resource Centre North Park Road UK-EXETER EX4 4QE
UNIV. LA SAPIENZA	Universita degli Studi di Roma "La Sapienza" Dipt. Scienze della Terra Piazza Aldo Moro 5 I-00185 ROMA
UNIV. LIVERPOOL	University of Liverpool Inst. Prehist. Science & Archaelogy Brownlow Street UK-LIVERPOOL L69 3BX
UNIV. MAINZ	J. Gutenberg Universität Mainz Abt. Lehramt Chemie J. Joachim Becher Weg, 345 B1 D-6500 MAINZ
UNIV. NANTES	Université de Nantes Lab. Bio-Radiochimie Rue de la Houssinière 2 F-44072 NANTES
UNIV. OVIEDO	Universidad de Oviedo Depart. de Geologia C. Jesus Arias de Velasco E-33005 OVIEDO

UNIV. OXFORD	University of Oxford Dept. of Materials Parks Road UK-OXFORD OX1 3PH
UNIV. PARMA	Università degli Studi di Parma Istituto chimica organica Viale delle Scienze I-43100 PARMA
UNIV. PERUGIA	Dipartamento di Scienze della Terra dell'Universita di Perugia Piazza Universita I-06100 PERUGIA
UNIV. TWENTE	University of Twente Dept. of Chemistry P.O. Box 217 NL-7500 AE ENSCHEDE
UPC	Universidad Politécnica de Cataluña Dep. Ingenieria del Terreno Jordi Girona Salgado 31 E-08034 BARCELONA
UWCC	University of Wales College of Cardiff Engineering School UK-CARDIFF CF2 1XH

ANNEXII : List of EUR publications of the programme 1990-1994

M.M.R. WILLIAMS
A review of a selection of papers describing the theory of transport in anisotropic porous media
Topical report (contract FI2W-CT91-0087)
EUR-14163 (1993), Euroffice

CEC
Annual progress report 1991
EUR-14418 (1992), Euroffice

L.F.M.HAMILTON,J. PRIJ, B.J.M. BENNEKER
In situ measurements of the mechanical response of rock-salt on variable pressure load
Final report (contract FI2W-CT90-0050)
EUR-14440 (1993), Euroffice

T. ROTHFUCHS, L. VONS, M. RAYNAL,J.C. MAJOR, I. MÜLLER-LYDA
The HAW project - Test disposal of highly radioactive radiation sources in the Asse salt mine
Activity report (contract FI2W-CT90-0002)
EUR-14531 (1993), Euroffice

T.McMENAMIN(Ed.)
The Community's R&D shared-cost action programme on the management and storage of radioactive waste - List of publications - May 1992
EUR-14540 (1993), Euroffice

W. BECHTHOLD,K.D. CLOSS, U. KNAPP,R. PAPP
System analysis for a dual-purpose repository
Final report (contract FI2W-CT90-0038)
EUR-14595 (1993), Euroffice

N. CADELLI,S. ORLOWSKI(Ed.)
Radioactive waste disposal: recommended criteria for siting a repository
Euradwaste series No 6
A guide on siting criteria prepared by a group of experts set up in the framework of the 'Community plan of action in the field of radioactive waste'
EUR-14598 (1992), Euroffice

R.H. LITTLE,C. TORRES, D. CHARLES,H.A. GROGAN, I. SIMON, G.M. SMITH, T.J. SUMERLING,B.M. WATKINS
Post-disposal safety assessment of toxic and radioactive waste: waste types,disposal practices, disposal criteria, assessment methods and post-disposal impacts
Final report (contract FI2W-CT90-0042)
EUR-14627 (1993), Euroffice

M.M.R. WILLIAMS
Methods of handling non-homogeneities at different scales in radionuclide transport
Final report (contract FI2W-CT91-0087)
EUR-14696 (1993), Euroffice

B. HAIJTINK, T. McMENAMIN(Ed.)
Project on effects of gas in underground storage facilities for radioactive waste (Pegasus project)
Proceedings of a progress meeting held in Brussels 11 and 12 June 1992
EUR-14816 (1993), Euroffice

A. GARCIA CELMA,H. DONKER
Stored energy in irradiated salt samples
Topical report (contrat FI2W-CT90-0002)
EUR 14845 (1994), Euroffice

H. VON MARAVIC(Ed.)
Oklo Working Group meeting - Proceedings of the second joint CEC-CEA progress meeting held in Brussels on 6 and 7 April 1992
EUR 14877 (1993), Euroffice

P.D. JACKSON, P.G. GREENWOOD, M.G. RAINES, M.P. RAINSBURY
Seismic tomography investigation of the Down Ampney fault research site
Topical report (contrat FI2W-CT91-0085)
EUR 14918 (1994), Euroffice

D. CHARLES,G.M. SMITH
Waste management study for large volumes of very-low-level waste from decommissioning of nuclear installations
Final report (contrat FI2W-CT90-0041)
EUR 14950 (1993), Euroffice

H.J. WINGENDER,H.J. BECKER,J. DORAN
Study on depleted uranium (tails) and on uranium residues form reprocessing with respect to quantities, characteristics, storage, possible disposal routes and radiation exposure
Final report (contrat FI2W-CT90-0037)
EUR 15032 (1994), Euroffice

P. GOBLET, L.F. DE LOPE, J.M. GOMIT
Study of coupling between "fractured medium" and "porous medium" flow models
Final report (contrat FI2W-CT91-0086)
EUR 15033 (1994), Euroffice

Community's research and development programme on radioactive waste management and storage - Shared-cost action (1990-1994)
Annual progress report, 1992
EUR 15132 (1993), Euroffice

D. READ
Chemval-2 project - Report on Stage 1 : status of six technical areas
Topical report (contrat FI2W-CT90-0065)
EUR 15161 (1994), Euroffice

H. VON MARAVIC, J. SMELLIE(Ed.)
Fifth CEC Natural Analogue Working Group meeting and Alligator Rivers Analogue Project (ARAP) final workshop
Proceedings of an international workshop held in Toledo (Spain) 5 to 9 October 1992
EUR 15176 (1994), Euroffice

H.J. WINGENDER, G.G. SIMON, B. SOHNIUS, J. DORAN, A.W. BRANT, H. CADIOU, S. GOETGHEBEUR
Treatment, disposal, re-use of building demolition and site cleaning wastes from nuclear facilities.
Final report (Contract FI2W-CT90-0044)
EUR 15188 (1994), Euroffice

R.M. JEFFRIES (Ed.)
Interclay II project - A coordinated benchmark exercise on the rheology of clays. Report on Stage 1.
Topical report (Contract FI2W-CT91-0063)
EUR 15285 (1994), Euroffice

ONDRAF/NIRAS
The Praclay project - Demonstration test on the Belgian disposal facility concept for high activity vitrified waste.
Activity report (Contract FI2W-CT90-0003)
EUR 15390 (1994), Euroffice

J. VANDER LEE, E. LEDOUX, G. DE MARSILY, M.D. DE CAYEUX, H. VANDE WEERD, B. FRATERS, J. DODDS, E. RODIER, M. SARDIN, A. HERNANDEZ
A bibliographical review of colloid transport through the geosphere
Topical report (Contract FI2W-CT91-0079)
EUR 15481 (1994), Euroffice

J.M. PICARD, B. BAZARGAN, G. ROUSSET
Essai thermo-hydro-mécanique dans une argile profonde - "Essai Cactus"
Rapport final (contrat FI2W-CT90-0001)
EUR 15482 (1994), Euroffice

J.-M. ASSELINEAU, P. GUETAT, P. RENAUD, L. BAEKELANDT, B. SKA
Propositions de niveaux d'activité pour l'enfouissement de déchets en décharges contrôlées en France et en Belgique
Rapport Phase 1 (contrat FI2W-CT90-0060)
EUR 15483 (1994), Euroffice

R.J. GREATHEAD, D. NICHOLS, A.R. JAMES
Studies of minimizing transport of spent fuel
Final report (contract FI2W-CT90-0067)
EUR 15612 (1994), Euroffice

F. LO GIUDICE, V. PELLECCHIA
Use of methods and programmes developed in the nuclear field for the treatment and disposal of toxic and hazardous wastes.
Final report (Contract FI2W-CT91-0110)
EUR 15624 (1994), Euroffice

P. BERTHIER, J.P. RUTY, C. LADIRAT, R. PICCINATO
Active hulls melting in a cold crucible by high-temperature direct induction technique.
Final report (Contract FI2W-CT90-0052)
EUR 15686 (1994), Euroffice

B. SKA, A. DE GOEYSE
Etude d'évaluation des éléments toxiques présents dans les déchets nucléaires
Rapport final (contrat FI2W-CT90-0045)
EUR 15687 (1995), Euroffice

R. BEAUFAYS,P. DE CANNIERE,A. FONTEYNE,S. LABAT,L. MEYNENDONCKXL. NOYNAERT,G. VOLCKAERT,A. BRUGGEMAN,M. LAMBRECHTS,F. VANDERVOOT
CERBERUS- A demonstration test to study the near-field effects of an HLW canister in an argillaceous formation.
Activity report 1990-92 (Contract FI2W-CT90-0003)
EUR 15718 (1994), Euroffice

R. BEAUFAYS,D. DE BRUYN,K. MOERKENS
Mine-by-test - A long-term monitoring programme around an underground structure in the Boom clay.
Activity report 1990-92 (Contract FI2W-CT90-0003)
EUR 15719 (1994), Euroffice

B. HAIJTINK, T. McMENAMIN(Ed.)
Project on effects of gas in underground storage facilities for radioactive waste (Pegasus project)
Proceedings of a progress meeting held in Cologne (D) 3-4 June 1993.
EUR 15734 (1994), Euroffice

D. NIEPHAUS
Retrievalbe emplacement experiment with ILW and spent HTR fuel elements in the Asse salt mine.
Final report (Contract FI2W-CT90-0006)
EUR 15736 (1994), Euroffice

A. BARBREAU,J.Y. BOISSON
Caractérisation d'une formation argileuse - Synthèse des principaux résultats obtenus à partir du tunnel de Tournemire
Rapport d'activité 1991-1993 (contract FI2W-CT91-0115)
EUR 15756 (1994), Euroffice

Nuclear Fission Safety shared-cost and concerted actions (1989-1994)
Catalogue of research projects, vol. I (Decommissioning nuclear installations, Radioactive Waste Management and Storage, Reactor Safety and Teleman);
vol. II (Radiation protection).
EUR 15796/1-2 (1994), Euroffice

J. BOURGES, M. LECOMTE, J.C. BROUDIC, M. MASSON, D. LALUQUE, J.P. LECOURT
Décontamination de déchets solides contaminés en émetteurs alpha, bêta et gamma, en vue de leur déclassification en termes de stockage
Rapport final (contrat FI2W-CT90-0070)
EUR 15804 (1994), Euroffice

Community's research and development programme on radioactive waste management and storage - Shared-cost action (1990-94).
Annual progress report, 1993
EUR 15853 (1994), Euroffice

J.G. TITLEY, T. CABIANCA, G. LAWSON, S.F. MOBBS, J. SIMMONDS
Improved global dispersion models for iodine-129 and carbon-14
Final report (contract FI2W-CT90-0008)
EUR 15880 (1995), Euroffice

C. LATGE, M. HANEBECK, N. DE SEROUX
Traitement du sodium contaminé provenant du démantèlement des réacteurs à neutrons rapides
Rapport final (contrat FI2W-CT90-0058)
EUR 15881 (1995), Euroffice

P. RIVAS, J. CARRERA, M. IVANOVICH, D. HOLMES, J.M. VINSON, A. AVOGADRO, J. ASTUDILLO, W.M. MILLER(Eds.)
El Berrocal project - Characterization and validation of natural radionuclide migration processes under real conditions on the fissured granitic environment
Summary report of Phase 1 (contract FI2W-CT91-0080)
EUR 15908 (1995), Euroffice

H. VON MARAVIC(Ed.)
Migration of radionuclides in the geosphere (Mirage project - Third phase) - Proceedings of a progress meeting (work period 1992)
EUR 15914 (1995), Euroffice

A. GARCIACELMA, H. DONKER, W.J. SOPPE, L. MIRALLES
Development and anneal of radiation damage in salt
Activity report 1988-93 (contract FI2W-CT90-0002)
EUR 15941 (1995), Euroffice

M.J. HEATH (Ed.)
Rock matrix diffusion as a mechanism for radionuclide retardation : natural radioelement migration in relation to the microfractography and petrophysics of fractured crystalline rock - Phase 1
Topical report (contract FI2W-CT91-0082)
EUR 15977 (1995), Euroffice

B. HAIJTINK, T. McMENAMIN(Ed.)
Project on the effects of gas in underground storage facilities for radioactive waste (Pegasus project)
EUR 16001 (1995), Euroffice

H. VON MARAVIC(Ed.)
OKLOWorking Group - Proceedings of the third joint EC-CEAprogress meeting held in Brussels on 11 and 12 October 1993
EUR 16098 (1995), Euroffice

P.C. ROBINSON, N.S. COOPER (Ed.)
Review on development of methodologies for modelling with uncertainty and variability: Munvar project
Final report (contract FI2W-CT91-0091)
EUR 16174 (1995), Euroffice

J. EISENBLÄTTER
Non-nuclear non-destructive testing methods to determine free water, gas pressure and matrix level in waste drums
Final report (contract FI2W-CT90-0018)
EUR 16190 (1995), Euroffice

A. LUCE, F. TROIANI
Treatment of radioactive solvent waste by catalytic oxidation
Final report (contract FI2W-CT91-0108)
EUR 16196 (1995), Euroffice

J.J. HEIJDRA, J. BEKKERING, J.V.D. GAAG, P.H.V.D.KLEYN, J. PRIJ
Retrievability of radioactive waste from a deep underground disposal facility
Final report (contract FI2W-CT92-0119)
EUR 16197 (1995), Euroffice

O. CAHUZAC,F. ANDALUZ TRUJILLANO
Technical contribution to the definition of incinerator and cement plant acceptance criteria for waste to be incinerated in France and Spain
Final report (contract FI2W-CT90-0066)
EUR 16198 (1995), Euroffice

S. WONNEBERGER,S. KISTINGER,A. DECKERT
Unbiased guess, a concept to cope with fuzzy and random parameters?
Final report (contract FI2W-CT91-0090)
EUR 16199 (1995), Euroffice

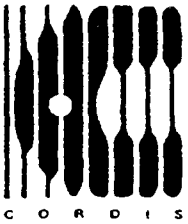

The Communities research and development information service

CORDIS

A vital part of your programme's dissemination strategy

CORDIS is the information service set up under the VALUE programme to give quick and easy access to information on European Community research programmes. It is available free-of-charge online via the European Commission host organization (ECHO), and now also on a newly released CD-ROM.

CORDIS offers the European R&D community:

— a comprehensive up-to-date view of EC R&TD activities, through a set of databases and related services,

— quick and easy access to information on EC research programmes and results,

— a continuously evolving Commission service tailored to the needs of the research community and industry,

— full user support, including documentation, training and the CORDIS help desk.

The CORDIS Databases are:

R&TD-programmes – R&TD-projects – R&TD-partners – R&TD-results
R&TD-publications – R&TD-comdocuments – R&TD-acronyms – R&TD-news

Make sure your programme gains the maximum benefit from CORDIS

— Inform the CORDIS unit of your programme initiatives,

— contribute information regularly to CORDIS databases such as R&TD-news, R&TD-publications and R&TD-programmes,

— use CORDIS databases, such as R&TD-partners, in the implementation of your programme,

— consult CORDIS for up-to-date information on other programmes relevant to your activities,

— inform your programme participants about CORDIS and the importance of their contribution to the service as well as the benefits which they will derive from it,

— contribute to the evolution of CORDIS by sending your comments on the service to the CORDIS Unit.

For more information about contributing to CORDIS, contact the DG XIII CORDIS Unit

Brussels
Ms I. Vounakis
Tel. +(32) 2 299 0464
Fax +(32) 2 299 0467

Luxembourg
M. B. Niessen
Tel. +(352) 4301 33638
Fax +(352) 4301 34989

To register for online access to CORDIS, contact:

ECHO Customer Service
BP 2373
L-1023 Luxembourg
Tel. +(352) 3498 1240
Fax +(352) 3498 1248

If you are already an ECHO user, please mention your customer number.

European Commission

EUR 16548 — Community's research and development programme on radioactive waste management and storage
Shared-cost action (1990-94)

Annual progress report, 1994

Luxembourg: Office for Official Publications of the European Communities

1995 — VIII, 680 pp. — 21.0 x 29.7 cm

Nuclear science and technology series

ISBN 92-827-4632-1

Price (excluding VAT) in Luxembourg: ECU 69.50

In December 1989, the Council of Ministers of the European Communities adopted the fourth R&D programme on the management and storage of radioactive waste for the period 1990-94.

Contract negotiations for selected research proposals led to the signature of contracts with some 120 bodies in charge of carrying out the work programme. This annual report, covering 94 contracts running in 1994, presents, for each contract, the objectives, the whole research programme and a synopsis of progress and results archieved as prepared by the contractor under the responsibility of the project leader.

Part A of the programme deals with the study of management systems, treatment and characterization of waste, general aspects of waste disposal and the safety of geological disposal systems. The running activities on construction and operation of underground facilities in candidated geological media for disposal are presented in Part B.

The previous annual progress reports on the programme are EUR 11089 (for 1986), EUR 11482 (for 1987), EUR 12141 (for 1988), EUR 12761, Volumes 1 and 2 (for 1989), EUR 14418 EN (for 1991), EUR 15132 EN (for 1992) and EUR 15853 EN (for 1993).

The overall results achieved, including the progress of work for 1990, during the programme 1985-89 were presented and discussed at the third European Community Conference on Radioactive Waste Management and Disposal held in Luxembourg from 17 to 21 September 1990 (proceedings published under EUR 13389, Elsevier - applied science publisher).

Venta • Salg • Verkauf • Πωλήσεις • Sales • Vente • Vendita • Verkoop • Venda • Myynti • Försäljning

BELGIQUE / BELGIË

Moniteur belge/
Belgisch Staatsblad

Rue de Louvain 42/Leuvenseweg 42
B-1000 Bruxelles/B-1000 Brussel
Tél. (02) 512 00 26
Fax (02) 511 01 84

Jean De Lannoy

Avenue du Roi 202/Koningslaan 202
B-1060 Bruxelles/B-1060 Brussel
Tél. (02) 538 51 69
Fax (02) 538 08 41

Autres distributeurs/
Overige verkooppunten:

Librairie européenne/
Europese boekhandel

Rue de la Loi 244/Wetstraat 244
B-1040 Bruxelles/B-1040 Brussel
Tél. (02) 231 04 35
Fax (02) 735 08 60

Document delivery:

Credoc

Rue de la Montagne 34/Bergstraat 34
Boîte 11/Bus 11
B-1000 Bruxelles/B-1000 Brussel
Tél. (02) 511 69 41
Fax (02) 513 31 95

DANMARK

J. H. Schultz Information A/S

Herstedvang 10-12
DK-2620 Albertslund
Tlf. 43 63 23 00
Fax (Sales) 43 63 19 69
Fax (Management) 43 63 19 49

DEUTSCHLAND

Bundesanzeiger Verlag

Breite Straße 78-80
Postfach 10 05 34
D-50445 Köln
Tel. (02 21) 20 29-0
Fax (02 21) 2 02 92 78

GREECE/ΕΛΛΑΔΑ

G.C. Eleftheroudakis SA

International Bookstore
Nikis Street 4
GR-10563 Athens
Tel. (01) 322 63 23
Fax 323 98 21

ESPAÑA

Boletín Oficial del Estado

Trafalgar, 27-29
E-28071 Madrid
Tel. (91) 538 22 95
Fax (91) 538 23 49

Mundi-Prensa Libros, SA

Castelló, 37
E-28001 Madrid
Tel. (91) 431 33 99 (Libros)
431 32 22 (Suscripciones)
435 36 37 (Dirección)
Fax (91) 575 39 98

Sucursal:

Librería Internacional AEDOS

Consejo de Ciento, 391
E-08009 Barcelona
Tel. (93) 488 34 92
Fax (93) 487 76 59

Librería de la Generalitat
de Catalunya

Rambla dels Estudis, 118 (Palau Moja)
E-08002 Barcelona
Tel. (93) 302 68 35
Tel. (93) 302 64 62
Fax (93) 302 12 99

FRANCE

Journal officiel
Service des publications
des Communautés européennes

26, rue Desaix
F-75727 Paris Cedex 15
Tél. (1) 40 58 77 01/31
Fax (1) 40 58 77 00

IRELAND

Government Supplies Agency

4-5 Harcourt Road
Dublin 2
Tel. (1) 66 13 111
Fax (1) 47 80 645

ITALIA

Licosa SpA

Via Duca di Calabria 1/1
Casella postale 552
I-50125 Firenze
Tel. (055) 64 54 15
Fax 64 12 57

GRAND-DUCHÉ DE LUXEMBOURG

Messageries du livre

5, rue Raiffeisen
L-2411 Luxembourg
Tél. 40 10 20
Fax 49 06 61

NEDERLAND

SDU Servicecentrum Uitgeverijen

Postbus 20014
2500 EA 's-Gravenhage
Tel. (070) 37 89 880
Fax (070) 37 89 783

ÖSTERREICH

Manz'sche Verlags-
und Universitätsbuchhandlung

Kohlmarkt 16
A-1014 Wien
Tel. (1) 531 610
Fax (1) 531 61-181

Document delivery:

Wirtschaftskammer

Wiedner Hauptstraße
A-1045 Wien
Tel. (0222) 50105-4356
Fax (0222) 50206-297

PORTUGAL

Imprensa Nacional

Casa da Moeda, EP
Rua Marquês Sá da Bandeira, 16-A
P-1099 Lisboa Codex
Tel. (01) 353 03 99
Fax (01) 353 02 94

Distribuidora de Livros
Bertrand, Ld.ª

Grupo Bertrand, SA

Rua das Terras dos Vales, 4-A
Apartado 37
P-2700 Amadora Codex
Tel. (01) 49 59 050
Fax 49 60 255

SUOMI/FINLAND

Akateeminen Kirjakauppa

Akademiska Bokhandeln
Pohjois-Esplanadi 39 / Norra esplanaden 39
PL / PB 128
FIN-00101 Helsinki / Helsingfors
Tel. (90) 121 4322
Fax (90) 121 44 35

SVERIGE

BTJ AB

Traktorvägen 13
S-22100 Lund
Tel. (046) 18 00 00
Fax (046) 18 01 25
30 79 47

UNITED KINGDOM

HMSO Books (Agency section)

HMSO Publications Centre
51 Nine Elms Lane
London SW8 5DR
Tel. (0171) 873 9090
Fax (0171) 873 8463

ICELAND

BOKABUD
LARUSAR BLÖNDAL

Skólavördustíg, 2
IS-101 Reykjavik
Tel. 11 56 50
Fax 12 55 60

NORGE

Narvesen Info Center

Bertrand Narvesens vei 2
Postboks 6125 Etterstad
N-0602 Oslo 6
Tel. (22) 57 33 00
Fax (22) 68 19 01

SCHWEIZ/SUISSE/SVIZZERA

OSEC

Stampfenbachstraße 85
CH-8035 Zürich
Tel. (01) 365 54 49
Fax (01) 365 54 11

BÅLGARIJA

Europress Klassica BK Ltd

66, bd Vitosha
BG-1463 Sofia
Tel./Fax (2) 52 74 75

ČESKÁ REPUBLIKA

NIS ČR

Havelkova 22
CZ-130 00 Praha 3
Tel./Fax (2) 24 22 94 33

HRVATSKA

Mediatrade

P. Hatza 1
HR-4100 Zagreb
Tel. (041) 43 03 92
Fax (041) 45 45 22

MAGYARORSZÁG

Euro-Info-Service

Honvéd Európá Ház
Margitsziget
H-1138 Budapest
Tel./Fax (1) 111 60 61, (1) 111 62 16

POLSKA

Business Foundation

ul. Krucza 38/42
PL-00-512 Warszawa
Tel. (2) 621 99 93, 628 28 82
International Fax&Phone (0-39) 12 00 77

ROMÂNIA

Euromedia

65, Strada Dionisie Lupu
RO-70184 Bucuresti
Tel./Fax 1-31 29 646

RUSSIA

CCEC

9,60-letiya Oktyabrya Avenue
117312 Moscow
Tel./Fax (095) 135 52 27

SLOVAKIA

Slovak Technical
Library

Nàm. slobody 19
SLO-812 23 Bratislava 1
Tel. (7) 52 204 52
Fax (7) 52 957 85

CYPRUS

Cyprus Chamber of Commerce
and Industry

Chamber Building
38 Grivas Dhigenis Ave
3 Deligiorgis Street
PO Box 1455
Nicosia
Tel. (2) 44 95 00, 46 23 12
Fax (2) 36 10 44

MALTA

Miller Distributors Ltd

PO Box 25
Malta International Airport LQA 05 Malta
Tel. 66 44 88
Fax 67 67 99

TÜRKIYE

Pres AS

Istiklal Caddesi 469
TR-80050 Tünel-Istanbul
Tel. (1) 520 92 96, 528 55 66
Fax (1) 520 64 57

ISRAEL

ROY International

31, Habarzel Street
69710 Tel Aviv
Tel. (3) 49 78 02
Fax (3) 49 78 12

Sub-agent (Palestinian authorities):

INDEX Information Services

PO Box 19502
Jerusalem
Tel. (2) 27 16 34
Fax (2) 27 12 19

EGYPT/
MIDDLE EAST

Middle East Observer

41 Sherif St.
Cairo
Tel/Fax (2) 393 97 32

UNITED STATES OF AMERICA/
CANADA

UNIPUB

4611-F Assembly Drive
Lanham, MD 20706-4391
Tel. Toll Free (800) 274 48 88
Fax (301) 459 00 56

CANADA

Subscriptions only
Uniquement abonnements

Renouf Publishing Co. Ltd

1294 Algoma Road
Ottawa, Ontario K1B 3W8
Tel. (613) 741 43 33
Fax (613) 741 54 39

AUSTRALIA

Hunter Publications

58A Gipps Street
Collingwood
Victoria 3066
Tel. (3) 417 53 61
Fax (3) 419 71 54

JAPAN

Procurement Services Int. (PSI-Japan)

Kyoku Dome Postal Code 102
Tokyo Kojimachi Post Office
Tel. (03) 32 34 69 21
Fax (03) 32 34 69 15

Sub-agent:

Kinokuniya Company Ltd
Journal Department

PO Box 55 Chitose
Tokyo 156
Tel. (03) 34 39-0124

SOUTH and EAST ASIA

Legal Library Services Ltd

Orchard
PO Box 0523
Singapore 9123
Tel. 243 24 98
Fax 243 24 79

SOUTH AFRICA

Safto

5th Floor, Export House
Cnr Maude & West Streets
Sandton 2146
Tel. (011) 883-3737
Fax (011) 883-6569

ANDERE LÄNDER
OTHER COUNTRIES
AUTRES PAYS

Office des publications officielles
des Communautés européennes

2, rue Mercier
L-2985 Luxembourg
Tél. 29 29-1
Télex PUBOF LU 1324 b
Fax 48 85 73, 48 68 17

15

CG-NA-16548-EN-C

NOTICE TO THE READER

All scientific and technical reports published by the European Commission are announced in the monthly periodical **'euro abstracts'**. For subscription (1 year: ECU 63) please write to the address below.

Price (excluding VAT) in Luxembourg: ECU 69.50

OFFICE FOR OFFICIAL PUBLICATIONS
OF THE EUROPEAN COMMUNITIES

L-2985 Luxembourg

ISBN 92-827-4632-1